

Olefin Metathesis: A Powerful and Versatile Instrument for Organic Synthesis
Tetrahedron Prize for Creativity in Organic Chemistry 2003
R. H. Grubbs

Guest editors: Stephen F. Martin^a and Harry H. Wasserman^b

^aChemistry and Biochemistry Department, The University of Texas, 1 University Station A5300, Austin, TX 78712-0165, USA

^bDepartment of Chemistry, Yale University, New Haven, CT 06511, USA

Contents

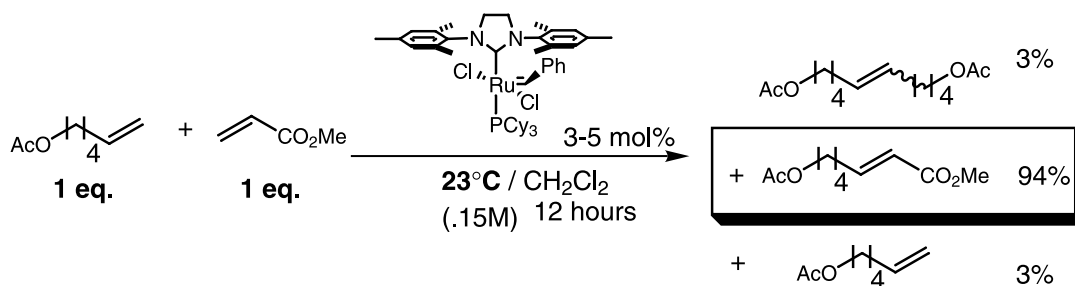
Announcement: Tetrahedron Symposia-in-Print
Preface
Biographical Sketch: Professor R. H. Grubbs

pp 7109–7111
p 7113
p 7115

ARTICLES

Olefin metathesis
 Robert H. Grubbs

pp 7117–7140

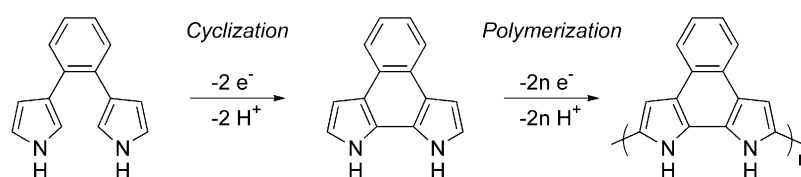


Cross metathesis of Electron Deficient olefins

New β-linked pyrrole monomers: approaches to highly stable and conductive electrochromic polymers

pp 7141–7146

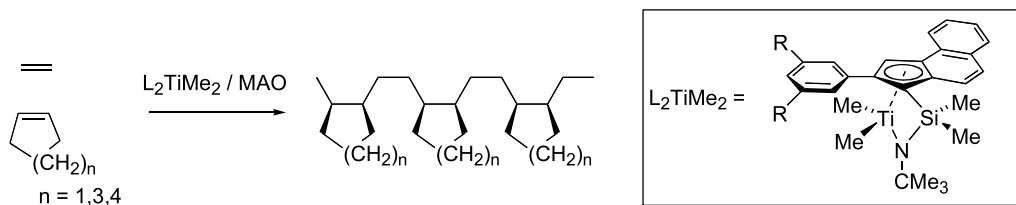
Jocelyn M. Nadeau and Timothy M. Swager*



Catalytic syntheses of alternating, stereoregular ethylene/cycloolefin copolymers

pp 7147–7155

Adrien R. Lavoie and Robert M. Waymouth*



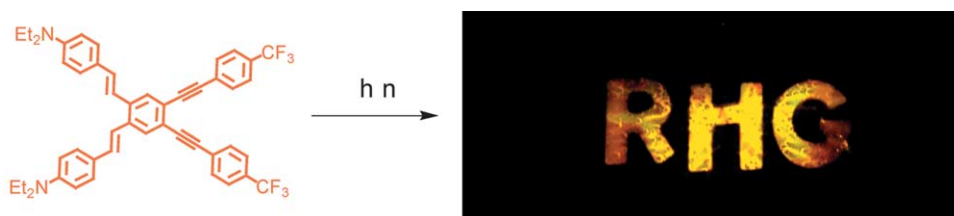
The stereospecific alternating copolymerization of ethylene and cyclopentene, cycloheptene and cyclooctene was carried out with a series of constrained geometry titanium complexes to give new crystalline alternating copolymers.

**Synthesis and electronic properties of bis-styryl substituted trimeric arylenethylenes.**

pp 7157–7167

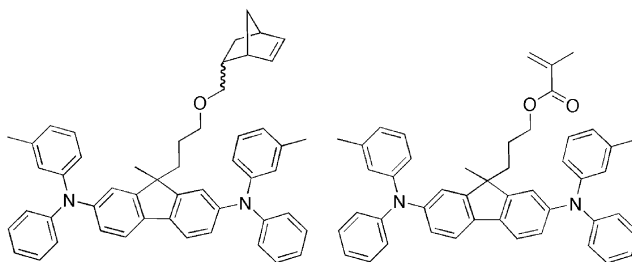
Comparison of cruciforms with *iso*-cruciforms

James N. Wilson, Kenneth I. Hardcastle, Mira Josowicz and Uwe H. F. Bunz*

**Synthesis of acrylate and norbornene polymers with pendant 2,7-bis(diarylamino)fluorene hole-transport groups**

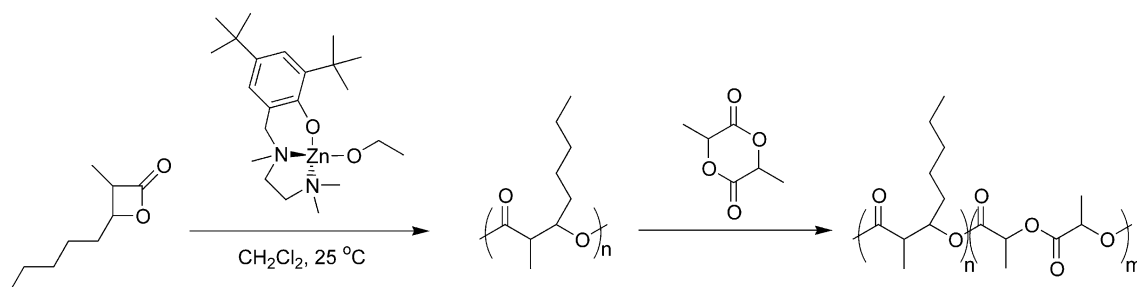
pp 7169–7176

Richard D. Hreha, Andreas Haldi, Benoit Domercq, Stephen Barlow, Bernard Kippelen* and Seth R. Marder*

**Controlled polymerization of α -methyl- β -pentyl- β -propiolactone by a discrete zinc alkoxide complex**

pp 7177–7185

Kathleen M. Schreck and Marc A. Hillmyer*



***ortho*-Tetraaryls as helical building blocks: a study of structure, theory, electrochemistry, and optical properties**

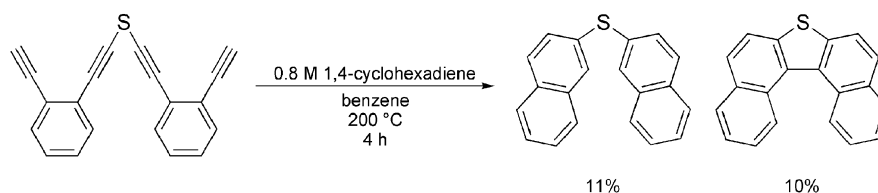
pp 7187–7190

Adah Almutairi, Fook S. Tham and Michael J. Marsella*

**Ethynyl sulfides as participants in cascade cycloaromatizations**

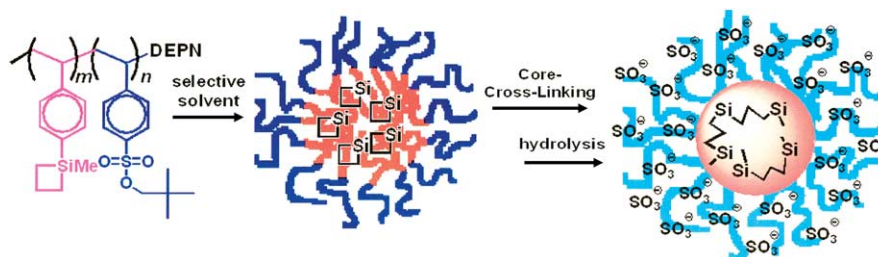
pp 7191–7196

Kevin D. Lewis, Michael P. Rowe and Adam J. Matzger*

**Synthesis of sodium-polystyrenesulfonate-grafted nanoparticles by core-cross-linking of block copolymer micelles**

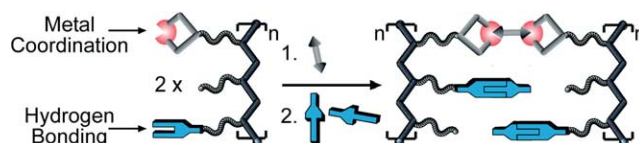
pp 7197–7204

Kozo Matsumoto,* Hirohiko Hasegawa and Hideki Matsuoka

**Cross-linked and functionalized ‘universal polymer backbones’ via simple, rapid, and orthogonal multi-site self-assembly**

pp 7205–7215

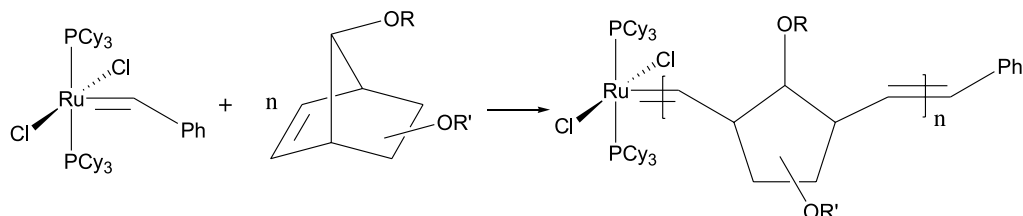
Joel M. Pollino, Kamlesh P. Nair, Ludger P. Stubbs, Jacob Adams and Marcus Weck*



Ring opening metathesis polymerisations of norbornene and norbornadiene derivatives containing oxygen: a study on the regeneration of Grubbs catalyst

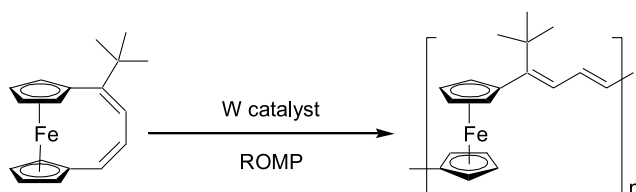
pp 7217–7224

David M. Haigh, Alan M. Kenwright and Ezat Khosravi*


ROMP of *t*-butyl-substituted ferrocenophanes affords soluble conjugated polymers that contain ferrocene moieties in the backbone

pp 7225–7235

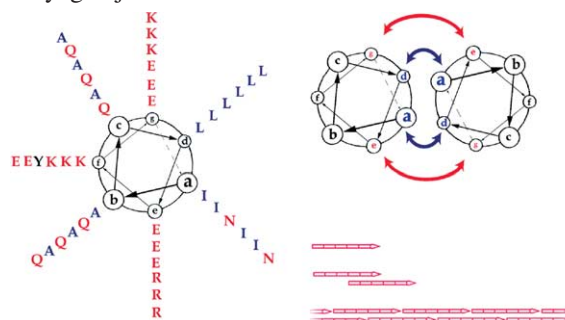
Richard W. Heo, Joon-Seo Park, Jason T. Goodson, Gil C. Claudio, Mitsuru Takenaga, Thomas A. Albright and T. Randall Lee*


Rational design of a nanoscale helical scaffold derived from self-assembly of a dimeric coiled coil motif

pp 7237–7246

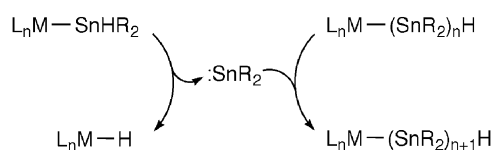
Yuri Zimenkov, Vincent P. Conticello,* Liang Guo and Pappannan Thiyagarajan

A model is described for the design of synthetic α -helical peptides that are competent for self-assembly into structurally defined supra-molecular fibrils. Peptide **YZ1** (see figure at right) was synthesized to test the validity of the model and was shown to self-assemble into long aspect-ratio, α -helical fibrils composed of dimeric coiled coil sub-units.


Reactions of hafnocene stannyl complexes with stannanes: implications for the mechanism of the metal-catalyzed dehydropolymerization of secondary stannanes

pp 7247–7260

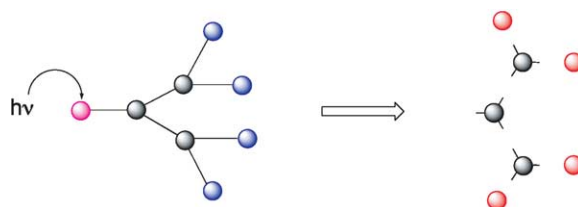
Nathan R. Neale and T. Don Tilley*



Phototriggering of geometric dendrimer disassembly: an improved synthesis of 2,4-bis(hydroxymethyl)phenol based dendrimers

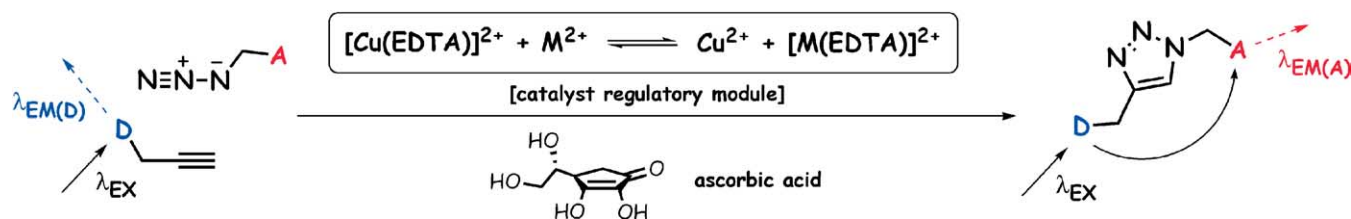
pp 7261–7266

Michael L. Szalai and Dominic V. McGrath*


FRET induced by an ‘allosteric’ cycloaddition reaction regulated with exogenous inhibitor and effectors

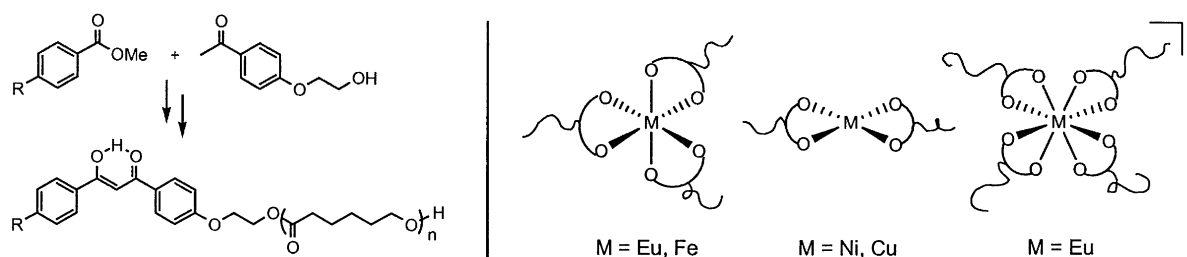
pp 7267–7275

Lei Zhu, Vincent M. Lynch and Eric V. Anslyn*


Poly(ε-caprolactone) macroligands with β-diketonate binding sites: synthesis and coordination chemistry

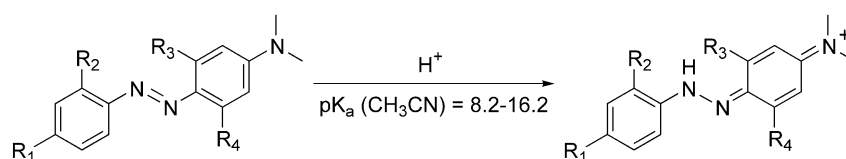
pp 7277–7285

Jessica L. Bender, Qun-Dong Shen and Cassandra L. Fraser*


A novel indicator series for measuring pK_a values in acetonitrile

pp 7287–7292

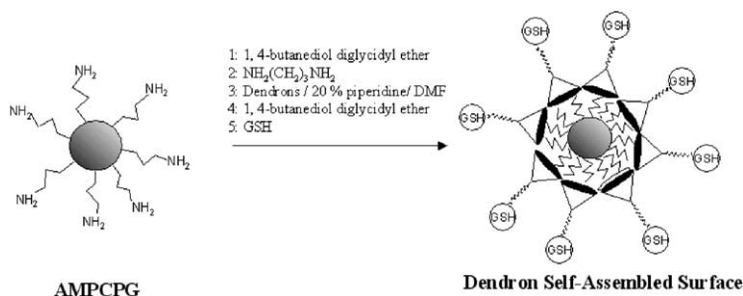
Jennifer M. Heemstra and Jeffrey S. Moore*

Azobenzene indicators facilitate the measurement of pK_a values for neutral organic bases in acetonitrile.

Interaction between glutathione and glutathione-*S*-transferase on dendron self-assembled controlled pore glass beads

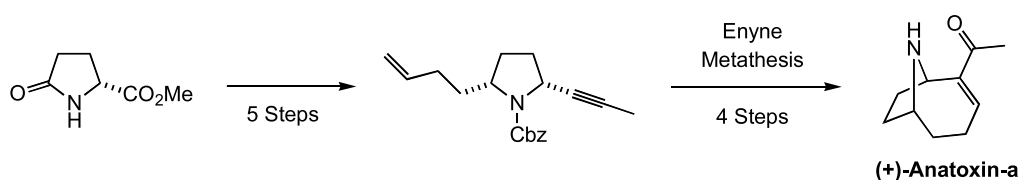
pp 7293–7299

Li-Hua Chen, Young-Seo Choi, Joseph Kwon, Rong-Shun Wang, Taehoon Lee, Sung Ho Ryu and Joon Won Park*


Enantioselective synthesis of (+)-anatoxin-a via enyne metathesis

pp 7301–7314

Jehrod B. Brenneman, Rainer Machauer and Stephen F. Martin*


(*E*)-Cycloalkenes and (*E,E*)-cycloalkadienes by ring closing diyne- or enyne-yne metathesis/semi-reduction

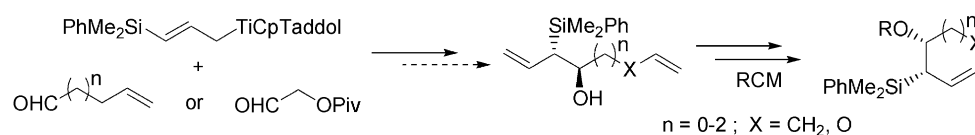
pp 7315–7324

Fabrice Lacombe, Karin Radkowski, Günter Seidel and Alois Fürstner*


Asymmetric synthesis of cyclic β -hydroxyallylsilanes via sequential allyltitanation-ring closing metathesis

pp 7325–7344

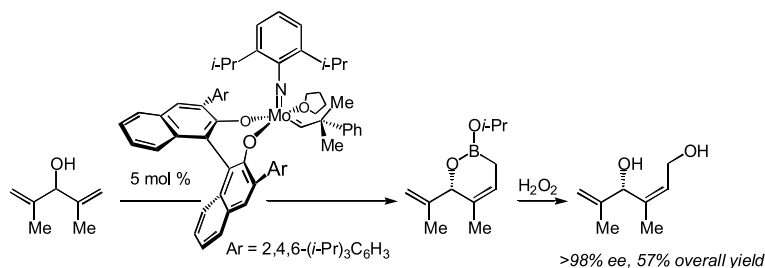
Jean-Michel Adam, Laurence de Fays, Michel Laguerre and Léon Ghosez*



Enantioselective synthesis of cyclic allylboronates by Mo-catalyzed asymmetric ring-closing metathesis (ARCM). A one-pot protocol for net catalytic enantioselective cross metathesis

pp 7345–7351

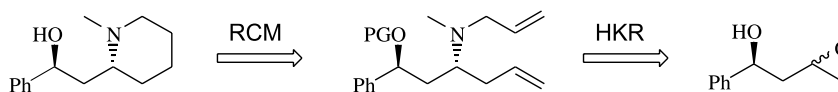
Jesper A. Jernelius, Richard R. Schrock and Amir H. Hoveyda*



A facile synthetic route to (+)-allosedamine via hydrolytic kinetic resolution and olefin metathesis

pp 7353–7359

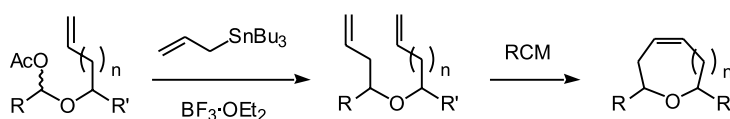
Byungman Kang and Sukbok Chang*



A new approach to the synthesis of cyclic ethers via the intermolecular allylation of α -acetoxy ethers and ring-closing metathesis

pp 7361–7365

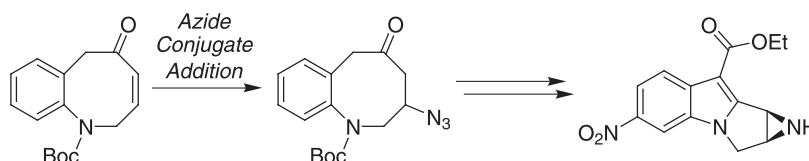
Isao Kadota,* Hiroshi Uyehara and Yoshinori Yamamoto*



Synthesis of aziridinomitosenes through base-catalyzed conjugate addition

pp 7367–7374

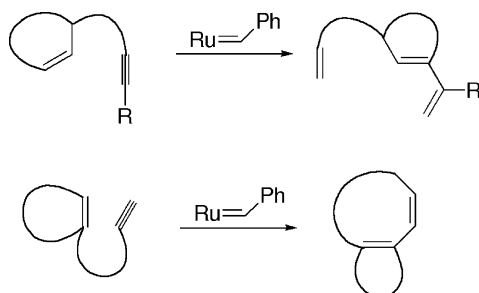
Kazunari Tsuboike, David J. Guerin, Steven M. Mennen and Scott J. Miller*



ROM-RCM of cycloalkene-yne

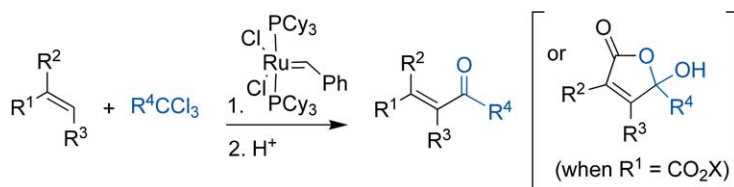
pp 7375–7389

Tsuyoshi Kitamura, Yuichi Kuzuba, Yoshihiro Sato, Hideaki Wakamatsu, Reiko Fujita and Miwako Mori*

**(PCy₃)₂Cl₂Ru=CHPh Catalyzed Kharasch additions. Application in a formal olefin carbonylation**

pp 7391–7396

Belinda T. Lee, Thomas O. Schrader, Belén Martín-Matute, Christopher R. Kauffman, Peng Zhang and Marc L. Snapper*

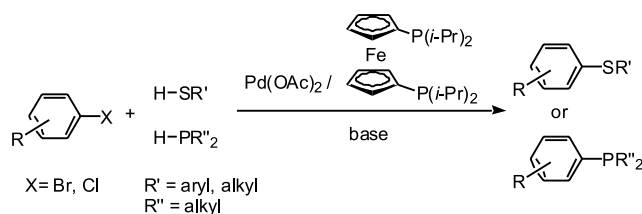


Ruthenium-catalyzed Kharasch additions of alkyltrichlorides to olefins provide polyhalogenated adducts, which upon hydrolysis furnish α,β -unsaturated ketones and aldehydes (when R^1 =aryl and R^2, R^3 =H), or γ -hydroxybutenolides (when R^1 =CO₂X). The two-step process represents an overall acylation or carbonylation of an olefin.

A general and efficient method for the palladium-catalyzed cross-coupling of thiols and secondary phosphines

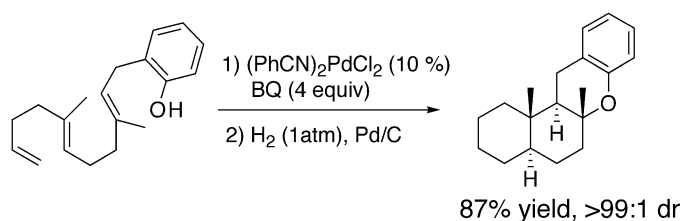
pp 7397–7403

Miki Murata and Stephen L. Buchwald*

**Pd(II)-Catalyzed cyclogeneration of carbocations: subsequent rearrangement and trapping under oxidative conditions**

pp 7405–7410

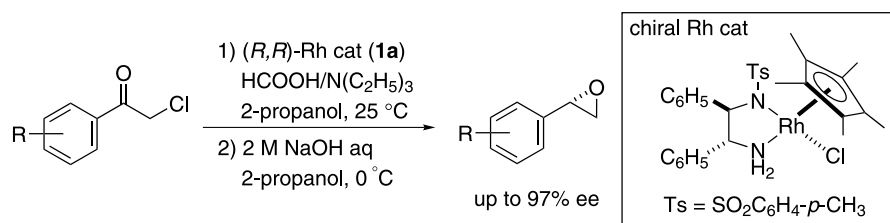
Jeong Hwan Koh, Cheryl Mascarenhas and Michel R. Gagné*



A practical synthesis of optically active aromatic epoxides via asymmetric transfer hydrogenation of α -chlorinated ketones with chiral rhodium–diamine catalyst

pp 7411–7417

Takayuki Hamada, Takayoshi Torii, Kunisuke Izawa and Takao Ikariya*

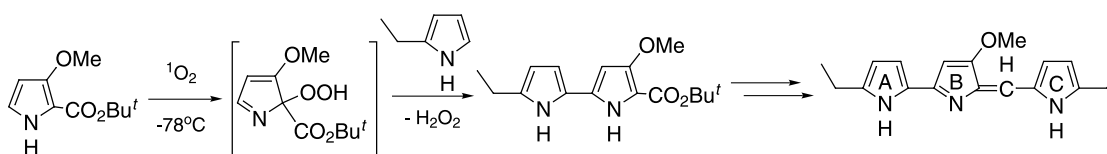


Singlet oxygen reactions of 3-methoxy-2-pyrrole carboxylic acid *tert*-butyl esters.

pp 7419–7425

A route to 5-substituted pyrrole precursors of prodigiosin and analogs

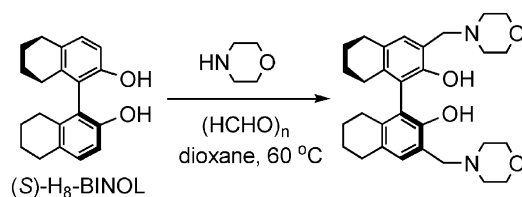
Harry H. Wasserman,* Mingde Xia, Jianji Wang, Anders K. Petersen, Michael Jorgensen, Patricia Power and Jonathan Parr



3,3'-Functionalized octahydro-BINOL: a facile synthesis and its high enantioselectivity in the alkyne addition to aldehydes

pp 7427–7430

Lan Liu and Lin Pu*

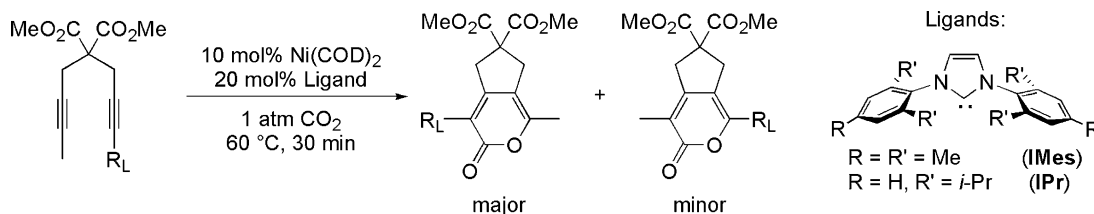


A highly enantioselective catalyst for the alkyne addition to aldehydes.

Regioselectivity in nickel(0) catalyzed cycloadditions of carbon dioxide with diynes

pp 7431–7437

Thomas N. Tekavec, Atta M. Arif and Janis Louie*




OTHER CONTENTS

Contributors to this issue
Instructions to contributors

p I
pp III–VI

*Corresponding author

+ Supplementary data available via ScienceDirect



Full text of this journal is available, on-line from **ScienceDirect**. Visit www.sciencedirect.com for more information.

CONTENTS
direct

This journal is part of **ContentsDirect**, the *free* alerting service which sends tables of contents by e-mail for Elsevier books and journals. You can register for **ContentsDirect** online at: <http://contentsdirect.elsevier.com>

Indexed/Abstracted in: AGRICOLA, Beilstein, BIOSIS Previews, CAB Abstracts, Chemical Abstracts. Current Contents: Life Sciences, Current Contents: Physical, Chemical and Earth Sciences, Current Contents Search, Derwent Drug File, Ei Compendex, EMBASE/Excerpta Medica, Medline, PASCAL, Research Alert, Science Citation Index, SciSearch



ISSN 0040-4020

Tetrahedron Symposia-in-Print

Series Editor

Professor H. H. Wasserman, Department of Chemistry, Yale University, P.O. Box 208107, New Haven, CT 06520-8107, U.S.A.

Tetrahedron Symposia-in-Print comprise collections of original research papers covering timely areas of organic chemistry.

Each symposium is organized by a Symposium Editor who will invite authors, active in the selected field, to submit original articles covering current research, complete with experimental sections. These papers will be rapidly reviewed and processed for publication by the Symposium Editor under the usual refereeing system.

Authors who have not already been invited, and who may have obtained recent significant results in the area of the announced symposium, may also submit contributions for Editorial consideration and possible inclusion. Before submitting such papers authors should send an abstract to the Symposium Editor for preliminary evaluation. Firm deadlines for receipt of papers will allow sufficient time for completion and presentation of ongoing work without loss of the freshness and timeliness of the research results.

Symposia-in-Print—already published

1. Recent trends in organic photochemistry, Albert Padwa, Ed. *Tetrahedron* **1981**, *37*, 3227–3420.
2. New general synthetic methods, E. J. Corey, Ed. *Tetrahedron* **1981**, *37*, 3871–4119.
3. Recent developments in polycyclopentanoid chemistry, Leo A. Paquette, Ed. *Tetrahedron* **1981**, *37*, 4357–4559.
4. Biradicals, Josef Michl, Ed. *Tetrahedron* **1982**, *38*, 733–867.
5. Electron-transfer initiated reactions, Gary B. Schuster, Ed. *Tetrahedron* **1982**, *38*, 1025–1122.
6. The organic chemistry of animal defense mechanisms, Jerrold Meinwald, Ed. *Tetrahedron* **1982**, *38*, 1853–1970.
7. Recent developments in the use of silicon in organic synthesis, Hans Reich, Ed. *Tetrahedron* **1983**, *39*, 839–1009.
8. Linear tetrapyrroles, Ray Bonnett, Ed. *Tetrahedron* **1983**, *39*, 1837–1954.
9. Heteroatom-directed metallations in heterocyclic synthesis, George R. Newkome, Ed. *Tetrahedron* **1983**, *39*, 1955–2091.
10. Recent aspects of the chemistry of β -lactams, J. E. Baldwin, Ed. *Tetrahedron* **1983**, *39*, 2445–2608.
11. New spectroscopic techniques for studying metabolic processes, A. I. Scott, Ed. *Tetrahedron* **1983**, *39*, 3441–3626.
12. New developments in indole alkaloids, Martin E. Kuehne, Ed. *Tetrahedron* **1983**, *39*, 3627–3780.
13. Recent aspects of the chemistry of nucleosides, nucleotides and nucleic acids, Colin B. Reese, Ed. *Tetrahedron* **1984**, *40*, 1–164.
14. Bioorganic studies on receptor sites, Koji Nakanishi, Ed. *Tetrahedron* **1984**, *40*, 455–592.
15. Synthesis of chiral non-racemic compounds, A. I. Meyers, Ed. *Tetrahedron* **1984**, *40*, 1213–1418.
16. Control of acyclic stereochemistry, Teruaki Mukaiyama, Ed. *Tetrahedron* **1984**, *40*, 2197–2344.
17. Recent aspects of anthracycline chemistry, T. Ross Kelly, Ed. *Tetrahedron* **1984**, *40*, 4537–4794.
18. The organic chemistry of marine products, Paul J. Scheuer, Ed. *Tetrahedron* **1985**, *41*, 979–1108.
19. Recent aspects of carbene chemistry, Matthew Platz, Ed. *Tetrahedron* **1985**, *41*, 1423–1612.
20. Recent aspects of singlet oxygen chemistry of photooxidation, Isao Saito and Teruo Matsuura, Eds. *Tetrahedron* **1985**, *41*, 2037–2236.
21. Synthetic applications of dipolar cycloaddition reactions, Wolfgang Oppolzer, Ed. *Tetrahedron* **1985**, *41*, 3447–3568.
22. Selectivity and synthetic applications of radical reactions, Bernd Giese, Ed. *Tetrahedron* **1985**, *41*, 3887–4302.
23. Recent aspects of organoselenium chemistry, Dennis Liotta, Ed. *Tetrahedron* **1985**, *41*, 4727–4890.
24. Application of newer organometallic reagents to the total synthesis of natural products, Martin Semmelhack, Ed. *Tetrahedron* **1985**, *41*, 5741–5900.
25. Formal transfers of hydride from carbon–hydrogen bonds, James D. Wuest, Ed. *Tetrahedron* **1986**, *42*, 941–1208.
26. Synthesis of non-natural products: challenge and reward, Philip E. Eaton, Ed. *Tetrahedron* **1986**, *42*, 1549–1916.
27. New synthetic methods—II, F. E. Ziegler, Ed. *Tetrahedron* **1986**, *42*, 2777–3028.
28. Structure and reactivity of organic radical ions, Heinz D. Roth, Ed. *Tetrahedron* **1986**, *42*, 6097–6350.
29. Organic chemistry in anisotropic media, V. Ramamurthy, J. R. Scheffer and N. J. Turro, Eds. *Tetrahedron* **1987**, *43*, 1197–1746.
30. Current topics in sesquiterpene synthesis, John W. Huffman, Ed. *Tetrahedron* **1987**, *43*, 5467–5722.
31. Peptide chemistry: design and synthesis of peptides, conformational analysis and biological functions, Victor J. Hruby and Robert Schwyzer, Eds. *Tetrahedron* **1988**, *44*, 661–1006.
32. Organosilicon chemistry in organic synthesis, Ian Fleming, Ed. *Tetrahedron* **1988**, *44*, 3761–4292.
33. α -Amino acid synthesis, Martin J. O'Donnell, Ed. *Tetrahedron* **1988**, *44*, 5253–5614.
34. Physical-organic/theoretical chemistry: the Dewar interface, Nathan L. Bauld, Ed. *Tetrahedron* **1988**, *44*, 7335–7626.
35. Recent developments in organocopper chemistry, Bruce H. Lipshutz, Ed. *Tetrahedron* **1989**, *45*, 349–578.
36. Organotin compounds in organic synthesis, Yoshinori Yamamoto, Ed. *Tetrahedron* **1989**, *45*, 909–1230.

37. Mycotoxins, Pieter S. Steyn, Ed. *Tetrahedron* **1989**, *45*, 2237–2464.
38. Strain-assisted syntheses, Léon Ghosez, Ed. *Tetrahedron* **1989**, *45*, 2875–3232.
39. Covalently linked donor–acceptor species for mimicry of photosynthetic electron and energy transfer, Devens Gust and Thomas A. Moore, Eds. *Tetrahedron* **1989**, *45*, 4669–4912.
40. Aspects of modern carbohydrate chemistry, S. Hanessian, Ed. *Tetrahedron* **1990**, *46*, 1–290.
41. Nitroalkanes and nitroalkenes in synthesis, Anthony G. M. Barrett, Ed. *Tetrahedron* **1990**, *46*, 7313–7598.
42. Synthetic applications of anodic oxidations, John S. Swenton and Gary W. Morrow, Eds. *Tetrahedron* **1991**, *47*, 531–906.
43. Recent advances in bioorganic chemistry, Dale L. Boger, Ed. *Tetrahedron* **1991**, *47*, 2351–2682.
44. Natural product structure determination, R. B. Bates, Ed. *Tetrahedron* **1991**, *47*, 3511–3664.
45. Frontiers in natural products biosynthesis. Enzymological and molecular genetic advances, D. E. Cane, Ed. *Tetrahedron* **1991**, *47*, 5919–6078.
46. New synthetic methods—III, S. E. Denmark, Ed. *Tetrahedron* **1992**, *48*, 1959–2222.
47. Organotitanium reagents in organic chemistry, M. T. Reetz, Ed. *Tetrahedron* **1992**, *48*, 5557–5754.
48. Total and semi-synthetic approaches to taxol, J. D. Winkler, Ed. *Tetrahedron* **1992**, *48*, 6953–7056.
49. Synthesis of optically active compounds—prospects for the 21st century, Kenji Koga and Takayuki Shioiri, Eds. *Tetrahedron* **1993**, *49*, 1711–1924.
50. Peptide secondary structure mimetics, Michael Kahn, Ed. *Tetrahedron* **1993**, *49*, 3433–3689.
51. Transition metal organometallics in organic synthesis, Anthony J. Pearson, Ed. *Tetrahedron* **1993**, *49*, 5415–5682.
52. Palladium in organic synthesis, Jan-E. Bäckvall, Ed. *Tetrahedron* **1994**, *50*, 285–572.
53. Recent progress in the chemistry of enediyne antibiotics, Terrence W. Doyle and John F. Kadow, Eds. *Tetrahedron* **1994**, *50*, 1311–1538.
54. Catalytic asymmetric addition reactions, Stephen F. Martin, Ed. *Tetrahedron* **1994**, *50*, 4235–4574.
55. Mechanistic aspects of polar organometallic chemistry, Manfred Schlosser, Ed. *Tetrahedron* **1994**, *50*, 5845–6128.
56. Molecular recognition, Andrew D. Hamilton, Ed. *Tetrahedron* **1995**, *51*, 343–648.
57. Recent advances in the chemistry of zirconocene and related compounds, Ei-ichi Negishi, Ed. *Tetrahedron* **1995**, *51*, 4255–4570.
58. Fluoroorganic chemistry: synthetic challenges and biomedical rewards, Giuseppe Resnati and Vadim A. Soloshonok, Eds. *Tetrahedron* **1996**, *52*, 1–330.
59. Novel applications of heterocycles in synthesis, A. R. Katritzky, Ed. *Tetrahedron* **1996**, *52*, 3057–3374.
60. Fullerene chemistry, Amos B. Smith III, Ed. *Tetrahedron* **1996**, *52*, 4925–5262.
61. New synthetic methods—IV. Organometallics in organic chemistry, István E. Markó, Ed. *Tetrahedron* **1996**, *52*, 7201–7598.
62. Cascade reactions, Ron Grigg, Ed. *Tetrahedron* **1996**, *52*, 11385–11664.
63. Applications of solid-supported organic synthesis in combinatorial chemistry, James A. Bristol, Ed. *Tetrahedron* **1997**, *53*, 6573–6706.
64. Recent applications of synthetic organic chemistry, Stephen F. Martin, Ed. *Tetrahedron* **1997**, *53*, 8689–9006.
65. Chemical biology, Gregory L. Verdine and Julian Simon, Eds. *Tetrahedron* **1997**, *53*, 11937–12066.
66. Recent aspects of S, Se, and Te chemistry, Richard S. Glass and Renji Okazaki, Eds. *Tetrahedron* **1997**, *53*, 12067–12318.
67. Modern organic chemistry of polymerization, H. K. Hall Jr., Ed. *Tetrahedron* **1997**, *53*, 15157–15616.
68. New synthetic methods—V, John L. Wood, Ed. *Tetrahedron* **1997**, *53*, 16213–16606.
69. New developments in organonickel chemistry, Bruce H. Lipshutz and Tien-Yau Luh, Eds. *Tetrahedron* **1998**, *54*, 1021–1316.
70. Solution phase combinatorial chemistry, David L. Coffen, Ed. *Tetrahedron* **1998**, *54*, 3955–4150.
71. Heterocycles in asymmetric synthesis, Alexandre Alexakis, Ed. *Tetrahedron* **1998**, *54*, 10239–10554.
72. Recent advances of phase-transfer catalysis, Takayuki Shioiri, Ed. *Tetrahedron* **1999**, *55*, 6261–6402.
73. Olefin metathesis in organic synthesis, Marc L. Snapper and Amir H. Hoveyda, Eds. *Tetrahedron* **1999**, *55*, 8141–8262.
74. Stereoselective carbon–carbon bond forming reactions, Harry H. Wasserman, Stephen F. Martin and Yoshinori Yamamoto, Eds. *Tetrahedron* **1999**, *55*, 8589–9006.
75. Applications of combinatorial chemistry, Miles G. Siegel and Stephen W. Kaldor, Eds. *Tetrahedron* **1999**, *55*, 11609–11710.
76. Advances in carbon–phosphorus heterocyclic chemistry, François Mathéy, Ed. *Tetrahedron* **2000**, *56*, 1–164.
77. Transition metal organometallics in organic synthesis, Kenneth M. Nicholas, Ed. *Tetrahedron* **2000**, *56*, 2103–2338.
78. Organocopper chemistry II, Norbert Krause, Ed. *Tetrahedron* **2000**, *56*, 2727–2904.
79. Carbene complexes in organic chemistry, James W. Herndon, Ed. *Tetrahedron* **2000**, *56*, 4847–5044.
80. Recent aspects of the chemistry of β -lactams—II, Marvin J. Miller, Ed. *Tetrahedron* **2000**, *56*, 5553–5742.
81. Molecular assembly and reactivity of organic crystals and related structures, Miguel A. Garcia-Garibay, Vaidhyanathan Ramamurthy and John R. Scheffer, Eds. *Tetrahedron* **2000**, *56*, 6595–7050.
82. Protein engineering, Richard Chamberlin, Ed. *Tetrahedron* **2000**, *56*, 9401–9526.
83. Recent advances in peptidomimetics, Jeffrey Aubé, Ed. *Tetrahedron* **2000**, *56*, 9725–9842.
84. New synthetic methods—VI, George A. Kraus, Ed. *Tetrahedron* **2000**, *56*, 10101–10282.
85. Oxidative activation of aromatic rings: an efficient strategy for arene functionalization, Stéphane Quideau and Ken S. Feldman, Eds. *Tetrahedron* **2001**, *57*, 265–424.
86. Lewis acid control of asymmetric synthesis, Keiji Maruoka, Ed. *Tetrahedron* **2001**, *57*, 805–914.
87. Novel aromatic compounds, Lawrence T. Scott and Jay S. Siegel, Eds. *Tetrahedron* **2001**, *57*, 3507–3808.
88. Asymmetric synthesis of novel sterically constrained amino acids, Victor J. Hruby and Vadim A. Soloshonok, Eds. *Tetrahedron* **2001**, *57*, 6329–6650.
89. Recognition-mediated self-assembly of organic systems, Vincent M. Rotello, Ed. *Tetrahedron* **2002**, *58*, 621–844.
90. Synthesis of marine natural products containing polycyclic ethers, Masahiro Hirama and Jon D. Rainier, Eds. *Tetrahedron* **2002**, *58*, 1779–2040.

91. Fluorous chemistry, John A. Gladysz and Dennis P. Curran, Eds. *Tetrahedron* **2002**, 58, 3823–4132.
92. Recent developments in chiral lithium amide base chemistry, Peter O'Brien, Ed. *Tetrahedron* **2002**, 58, 4567–4734.
93. Beyond natural product synthesis (Tetrahedron Prize for Creativity in Organic Chemistry 2001 - Yoshito Kishi), Harry H. Wasserman and Stephen F. Martin, Eds. *Tetrahedron* **2002**, 58, 6223–6602.
94. Strained heterocycles as intermediates in organic synthesis, Amy R. Howell, Ed. *Tetrahedron* **2002**, 58, 6979–7194.
95. Molecular design of Lewis and Brønsted acid catalysts—the key to environmentally benign reagents (Tetrahedron Chair 2002), Hisashi Yamamoto, Ed. *Tetrahedron* **2002**, 58, 8153–8364.
96. Recent developments in dendrimer chemistry, David K. Smith, Ed. *Tetrahedron* **2003**, 59, 3787–4024.
97. Art, science and technology in total synthesis (Tetrahedron Prize for Creativity in Organic Chemistry 2002 - K. C. Nicolaou), Stephen F. Martin and Harry H. Wasserman, Eds. *Tetrahedron* **2003**, 59, 6667–7070.
98. New synthetic methods—VII, Brian M. Stoltz, Ed. *Tetrahedron* **2003**, 59, 8843–9030.
99. Oxiranyl and aziridinyli anions as reactive intermediates in synthetic organic chemistry, S. Florio, Ed. *Tetrahedron* **2003**, 59, 9683–9864.
100. Recent advances in rare earth chemistry, Shū Kobayashi, Ed. *Tetrahedron* **2003**, 59, 10339–10598.
101. Biocatalysts in synthetic organic chemistry, S. M. Roberts, Ed. *Tetrahedron* **2004**, 60, 483–806.
102. Recent advances in the chemistry of zirconocenes, Keisuke Suzuki and Peter Wipf, Eds. *Tetrahedron* **2004**, 60, 1257–1424.
103. Atropisomerism, Jonathan Clayden, Ed. *Tetrahedron* **2004**, 60, 4325–4558.
104. Chemistry of biologically and physiologically intriguing phenomena, Daisuke Uemura, Ed. *Tetrahedron* **2004**, 60, 6959–7098.
105. Olefin metathesis: a powerful and versatile instrument for organic synthesis (Tetrahedron prize for creativity in organic chemistry 2003 – R. H. Grubbs), Stephen F. Martin and Harry H. Wasserman, Eds. *Tetrahedron* **2004**, 60, 7099–7438.



Preface

Tetrahedron Prize for Creativity in Organic Chemistry

The Executive Board of Editors for *Tetrahedron* Publications and Elsevier Ltd. is pleased to dedicate this special Symposium-in-Print issue to Professor Robert H. Grubbs of the California Institute of Technology, a co-recipient of the Tetrahedron Prize for 2003 with Professor Dieter Seebach. Professor Grubbs is being recognized for his ground-breaking work in the field of olefin metathesis including fundamental studies in organometallic chemistry leading to the rational design of new polymerization catalysts.

Robert Grubbs' research in the fields of organometallic chemistry and catalysis represents some of the most creative contributions to the field of organic chemistry during the past three decades. Starting with his interest in the mechanistic aspects of the olefin metathesis reaction in the early 70's, Grubbs has been a primary driving force in the development of olefin metathesis and in the discovery that the reaction could be harnessed for the controlled formation of polymeric materials and for the synthesis of functionalized carbocycles and heterocycles. In the ensuing years, olefin metathesis reactions have played a major part in synthetic applications ranging from the petrochemical industry to the synthesis of complex molecules. A measure of the importance of this work is the widespread adoption of olefin metathesis using Grubbs' catalysts or variants thereof in designing strategies for the syntheses of materials ranging from nucleic acids to saccharides, natural products, and polymers. Bringing olefin metathesis into the everyday arsenal of synthetic methods has truly changed the face of

chemistry and opened up access to a wide range of useful and worthwhile chemistry.

The papers collected in this symposium include examples of syntheses inspired by Grubbs' work either directly, as in the exploration of the activity of ruthenium catalysts in ring opening–ring closing metatheses, or indirectly, as exemplified by the related metathetic reactions of organometallic reagents including the molybdenum-catalyzed enantioselective synthesis of cyclic allyl boronates and the nickel-catalyzed addition of carbon dioxide to diynes. Also evident from a number of these papers is Grubbs' influence in areas related to material science.

It is clear that Robert Grubbs' has been a pioneer in changing the face of organic chemistry with consequences beneficial to society and these are the achievements that the Tetrahedron Prize is proud to recognize.

Harry H. Wasserman
*Department of Chemistry, Yale University,
New Haven, CT 06511, USA*
E-mail address: harry.wasserman@yale.edu

Stephen F. Martin
*Chemistry and Biochemistry Department,
The University of Texas,
1 University Station A5300,
Austin, TX 78712-0165, USA*
E-mail address: sfmartin@mail.utexas.edu

Biographical sketch: Professor Robert Howard Grubbs



Born February 27, 1942, Kentucky. BS, Chemistry, University of Florida, Gainesville, Florida, 1963; MS, M. Battiste, 1965. PhD, R. Breslow, Chemistry, Columbia University, New York, NY, 1968. NIH Postdoctoral Fellow, J. P. Collman, Chemistry, Stanford University, 1968–69.

Dr. Robert H. Grubbs is the Victor and Elizabeth Atkins Professor of Chemistry at the California Institute of Technology, Pasadena, CA, USA, where he has been a faculty member since 1978. Before moving to Caltech, he was at Michigan State University from 1969 to 1978 achieving the rank of Associate Professor.

The research group of Grubbs is involved in the design, synthesis, and mechanistic studies of complexes that catalyze basic organic transformations. The major focus of the group over the past few years has been on the olefin metathesis reaction. To optimize the utility of this reaction, new catalysts have been developed that are extremely tolerant of organic functional groups. Due to their high-activity, functional group tolerance, and ease of use, these ruthenium based catalysts have found wide applications in organic and polymer synthesis. He has 400+ publications and 60+ patents.

Professor Grubbs awards have included: ACS National Award in Organometallic Chemistry (1988), the Arthur C. Cope Scholar Award (1990), the ACS Award in Polymer Chemistry (1995), the Nagoya Medal of Organic Chemistry (1997), the Fluka Reagent of the Year (1998), the Mack Memorial Award (1999), the Benjamin Franklin Medal in Chemistry (2000), the ACS Herman F. Mark Polymer Chemistry Award (2000), the ACS Herbert C. Brown Award for Creative Research in Synthetic Methods (2001), the ACS Arthur C. Cope Award (2002), the ACS Award for Creative Research in Homogeneous or Heterogeneous Catalysis (2003), The Richard C. Tolman Medal (2003), the ACS Tetrahedron Prize for Creativity in Organic Chemistry (2003), The Pauling Award Medal (2003) and the Bristol-Myers Squibb Distinguished Achievement Award in Organic Synthesis (2004). He was elected to the National Academy of Sciences in 1989, and a Fellow of the American Academy of Arts and Sciences in 1994.

Olefin metathesis

Robert H. Grubbs*

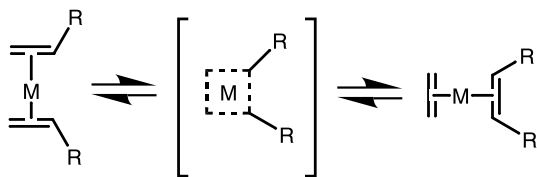
*The Arnold and Mabel Beckman Laboratory of Chemical Synthesis, Division of Chemistry and Chemical Engineering,
California Institute of Technology, Pasadena, CA 91125, USA*

Received 10 May 2004; accepted 11 May 2004

Abstract—Olefin metathesis has become a tool for synthetic organic and polymer chemists. Well-defined, functional group tolerant catalysts have allowed these advances. A discussion of the evolution of mechanistic understanding and early catalyst developments is followed by a description of recent advances in ruthenium based olefin metathesis catalysts. Catalyst improvements have led to new applications in ring closing metathesis, cross metathesis and materials synthesis.

© 2004 Published by Elsevier Ltd.

As with most catalytic processes, olefin metathesis was found by accident. It was discovered as an outgrowth of the study of Ziegler polymerizations with alternate metal systems.¹ By the late 60's, the Phillips group developed a commercial process—the triolefin process—and made the scientific community aware of this unique reaction.² My introduction to olefin metathesis occurred during a group meeting while I was a postdoctoral fellow in Jim Collman's group at Stanford. It became obvious at that meeting that the mechanism of the metathesis reaction would require new intermediates and mechanistic pathways unlike any known at the time. In addition to the intellectual challenge, understanding the mechanism would allow for the development of better catalysts.³ The initially proposed mechanism was that of a pair-wise exchange of alkylidenes through a 'quasicyclobutane' mechanism in which two olefins coordinated to the metal and exchanged alkylidene groups through a symmetrical intermediate. With a few assumptions, this mechanism could account for most of the basic metathesis transformations.⁴ In addition, other mechanisms⁵ were proposed for the isomerization of metal diolefin complexes including metallacyclopentane rearrangements (Scheme 1).⁶



Scheme 1.

Keywords: Olefin metathesis; Polymerization; Carbene.

* Tel.: +1-626-395-6003; fax: +1-626-564-9297;
e-mail address: rhg@caltech.edu

Chauvin proposed a new mechanism to explain a surprising set of observations.⁷ He observed that in some cases where a pair-wise mechanism such as the 'quasicyclobutane' mechanism, predicted only the two olefins resulting from pair-wise exchange of the two ends of the starting olefins, the olefins resulting from cross products were observed very early in the reaction. Although some assumptions would allow the pair-wise mechanism to account for this result, Chauvin proposed a mechanism that involved the fragmentation of the olefin (a non-pairwise mechanism) through what has become known as the 'carbene' mechanism (Scheme 2).

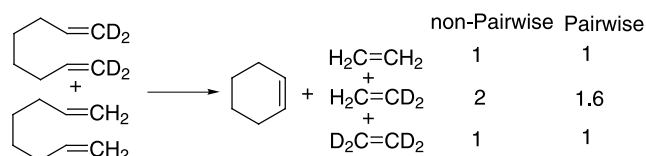


Scheme 2.

Independent of the metathesis mechanism research, considerable progress was being made in the development of metal carbene (alkylidene) complexes. Work by Casey that demonstrated a metathesis like exchange between a Fischer carbene and an electron rich olefin⁸ and the demonstration by Schrock⁹ that metal alkylidenes could be formed under 'metathesis like' conditions made this mechanism even more appealing. Katz, in experiments similar to that of Chauvin, defined the basic assumptions and further strengthened the arguments against the pair-wise mechanism. He demonstrated that the cross-over products were formed even at 'zero' time.¹⁰

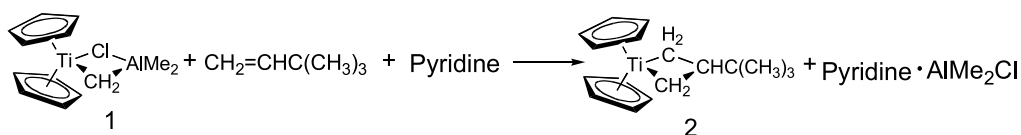
On returning from a meeting in December 1974, where I had discussed the mechanism of metathesis with Chuck Casey, a mechanistic study involving a ring closing metathesis

reaction with deuterium labeling was designed which would allow a distinction to be drawn between pair-wise and non-pairwise mechanisms. With in a couple of months, 1,1,8,8-tetradeutero-1,7-octadiene had been prepared and mixed with the non-deuterated analog and allowed to undergo metathesis with catalysts known at the time to produce cyclohexene (not reactive in metathesis) and deuterated ethylenes. Since unreactive cyclohexene is formed, the system allows the fate of the ends of the olefins to be precisely defined and the expected product mixtures to be calculated for pair-wise or non-pairwise exchange of the terminal methylene groups. The statistical mixture of labeled ethylenes (1:2:1 ratio starting with a 1:1-mixture of $D_4:D_0$ -1,7-octadiene) was formed as the kinetic products instead of the ratio of 1:1.6:1 calculated for a pair-wise mechanism.¹¹ To explain this experiment by the pair-wise mechanism required unreasonable assumptions (Scheme 3).



Scheme 3.

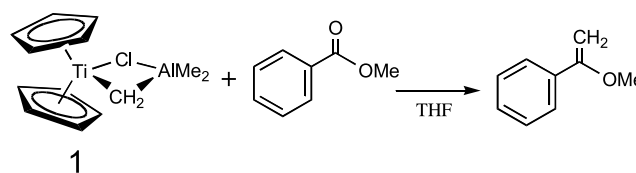
Katz reported a similar ring closing experiment in which phenanthrene was the ring closed product. He carried out a precise analysis of the isotope effect and an alternate analysis of the expected mechanism for the pair-wise mechanism.¹² The key feature of these experiments was the determination that the observed products were not scrambled in a secondary reaction. Although these experiments strongly supported the non-pairwise mechanism, the experiments that demonstrated that the initial products observed did not arise from a secondary scrambling mechanism required several assumptions. I was not totally convinced until, we completed one of my favorite (but probably least read) mechanistic studies using *cis*, *cis*-1,1,1,10,10,10-hexadeutero-2,8-decadiene in place of labeled 1,7-octadiene. In this experiment, the labeled product was cyclohexene and *cis* and *trans* 2-butene. By coupling an isotopic label with a stereochemical label, we could demonstrate that the unfavored *cis* isomer of the product 2-butene was completely scrambled as required for non-pairwise mechanisms.¹³ Katz presented a complete analysis of the Chauvin type of experiment and demonstrated that the ratios of observed products were inconsistent with a pair-wise mechanism.¹⁴ Although these experiments did not prove the Chauvin mechanism, the approach of using ring closing reactions to produce 6-membered rings and labeled acyclic olefins finally discredited the pair-wise mechanism and most researchers quickly considered variations of the basic Chauvin mechanism as the most reasonable.



Scheme 5.

Although some catalysts with activity limited to strained olefin polymerization were prepared from late metal precursors,¹⁵ the most active catalysts were prepared by the alkylation of high oxidation state early metal halides. The first high oxidation state alkylidene complexes of Schrock did not induce olefin metathesis.¹⁶ The Fischer carbenes, which are low oxidation state carbenes, were shown to be olefin metathesis catalysts of low activity.¹⁷ Although fragments of the initiation carbene were later observed as end groups on the polymers produced by such catalysts, the intermediates in the reaction could not be observed.^{18,19} The high oxidation state, late metal complexes of Tebbe,²⁰ Schrock²¹ and Osborn²² provided the transition to the synthesis of well-defined catalysts. In contrast to 'classical' catalysts, well-defined catalysts are those where the propagating species can be observed and controlled. Such systems represent the transition to modern metathesis catalysis.

Fred Tebbe demonstrated that a titanium methylene complex would catalyze the non-productive metathesis exchange of the methylenes between two terminal olefins. Although the catalyst was not particularly active, it served as an excellent model system since the complex was very stable and the propagating methylenide could be observed and studied.²³ We developed two areas of work based on the Tebbe observations. With Dave Evans, we initiated an investigation of this complex, now known as the 'Tebbe Reagent', in a 'Wittig type' reaction for the conversion of esters to vinyl ethers' (Scheme 4).²⁴



Scheme 4.

A second project involved the synthesis of unsymmetrical Tebbe complexes for use in a mechanistic study to determine the structure of the metallacycle intermediate. Much to our surprise, when Tom Howard added pyridine to the reaction, a metallacycle (**2**) was formed as a stable complex whose structure was determined.²⁵ A number of detailed studies demonstrated that this metallacycle was a competent intermediate for the Tebbe metathesis mechanism (Scheme 5).²⁶

These experiments established the metallacyclobutane as a viable intermediate in olefin metathesis. Osborn and Ivin found a catalyst system that showed both the propagating carbene and the metallacycle.²⁷ Schrock²⁸ and later Basset²⁹ developed early metal complexes that were single component and showed useful levels of activity. However, the break through came with the Schrock group's development of tungsten and molybdenum alkylidene complexes that

contained bulky imido ligands.³⁰ These complexes showed high activity, could be prepared on moderate scales and were sufficiently stable to study in detail. These catalysts provided the first efficient and controlled catalysts for metathesis and were the basis for our initial work in organic and controlled polymer synthesis.³¹ For example, the high activity of the tungsten-based systems allowed for the polymerization of cyclooctatetraene to polyacetylene³² and benzvalene to polybenzvalene,³³ work that opened our continuing studies of conjugated polymers.

In a continuation of the Tebbe mechanistic studies, Laura Gilliom found that the Tebbe complex would form a stable metallacycle with norbornene.³⁴ When this complex was heated with more norbornene, a polymer was formed. The polydispersity of the resulting polymer was unusually narrow. Further studies demonstrated that reactions, which utilized these complexes, would polymerize norbornene at higher temperature but would be inactive for polymerization when cooled to room temperature. The resulting polymer contained an active titanacyclobutane at the end of the polymer that could be reactivated on heating. The polydispersity could be further narrowed by the design of a metallacyclic initiator based on diphenylcyclopropene³⁵ that was more reactive than the propagating species (Scheme 6).³⁶

It has become apparent that most stable well-defined initiators of metathesis give 'living' polymerizations with norbornenes. In many cases, techniques must be developed to produce favorable initiation/propagation rates to produce narrow dispersity polymers.

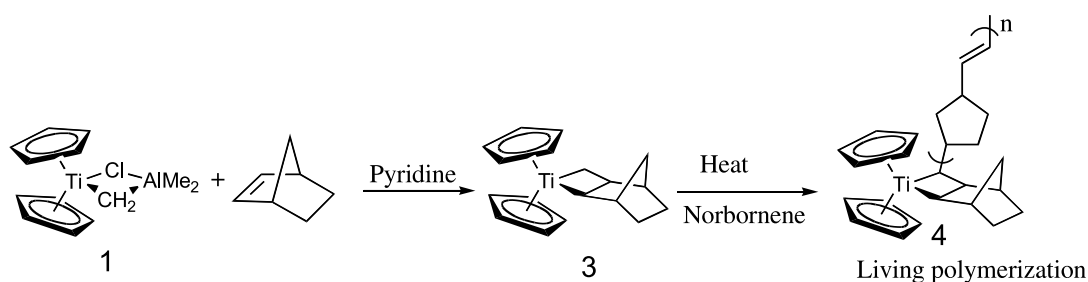
To fully exploit the polymer chemistry of the well-defined metathesis catalysts, part of my group turned almost full time to the study of polymer chemistry and a course in polymer chemistry was initiated at Caltech. Wilhelm Risse

and Lou Cannizzo developed a variety of techniques for the precise synthesis of low dispersity block and star polymers.³⁷ Most of the techniques, which are now used with better catalysts were developed during these studies.

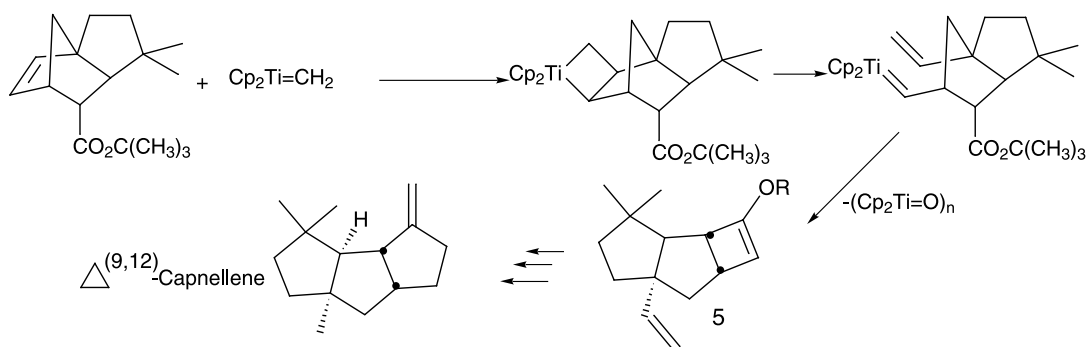
John Stille combined the olefin metathesis activity of the Tebbe reagent with its 'Wittig' nature to produce a key intermediate (**5**) for the synthesis of Capnellene (Scheme 7).³⁸

The availability of well-defined catalysts from the Schrock group provided the opportunity to start applying olefin metathesis to the synthesis of functionalized small molecules. When Greg Fu arrived at Caltech as a postdoctoral fellow, he accepted the challenge of demonstrating the application of well-defined olefin metathesis catalysts (that were being explored as polymerization initiators) to the synthesis of small molecules. In a reasonably short period of time, he demonstrated that the tungsten and molybdenum alkylidenes would induce the ring closing metathesis for the formation of 5, 6 and 7 membered rings.³⁹ The molybdenum system was particularly active and tolerated a range of functionality. This work introduced olefin metathesis to the synthetic organic chemist.⁴⁰ The full value of this reaction was not realized until catalysts⁴¹ were available that could be used with standard organic techniques and tolerated a broad range of functional groups.

During the mid '80's, research that led to the development of ruthenium-based catalysts was initiated. Based on models, it was proposed that the polymers prepared from 7-oxonorbornene derivatives might be good ionophores. Bruce Novak set out to prepare such systems using the titanium and tungsten catalysts available at the time. After finding that none of the known catalysts worked for these systems, he explored the ill-defined catalysts that were



Scheme 6.



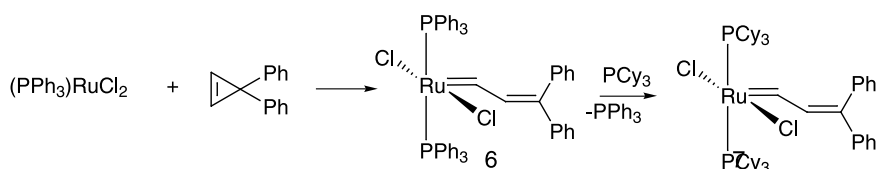
Scheme 7.

prepared from late metal salts. He found that ruthenium trichloride polymerized olefins and would even generate high molecular weight polymers in water.⁴² It was assumed that these catalyst systems operated by the same mechanism as the early metal cases and, therefore, had to involve a metal carbene. If this were the case it would have to be different from the alkylidene complexes known at the time and be stable both in water and show low sensitivity to oxygen. Novak's mechanistic studies demonstrated that a strained olefin and ruthenium(II) were the keys to the formation of an active catalyst. These were the important observations that were essential for the later synthesis of a well-defined catalyst.⁴³

Sonbihn Nguyen took on the challenge of determining whether a well-defined, active ruthenium carbene catalyst could be prepared. Combining the need for ruthenium(II) observed by Novak with the experience of Lynda Johnston in developing routes to the formation of tungsten carbenes⁴⁴ using cyclopropenes, Nguyen reacted a ruthenium(II) complex with diphenylcyclopropene. This reaction resulted in a stable $16 e^-$ ruthenium carbene complex that was not only active towards the polymerization of norbornene but was also stable in the presence of protic solvents!⁴⁵ The basic structure of the active bis(triphenylphosphine)-dichlororuthenium alkylidene complex has remained the same in even the most recent highly active catalysts. The bis(triphenylphosphine) complex (**6**) was only active for metathesis with strained and electron rich olefins. It would not polymerize *cis*-cyclooctene although it would polymerize *trans*-cyclooctene. In order to increase the activity of the catalysts, ligand exchanges were carried out. The lessons learned from the Schrock group suggested that activity increased as the metal center became more electrophilic.⁴⁶ Consequently, the anionic ligands were modified or ionized to form cationic complexes in an attempt to afford more active systems.⁴⁷ In frustration, Nguyen carried out the opposite ligand exchange and substituted the more basic cyclohexylphosphine ligand.⁴⁸ This change produced the desired reactivity (Scheme 8).

The complex with the more basic ligand (**7**) would now polymerize unstrained olefins and induce reactions with acyclic olefins.⁴⁹

Greg Fu demonstrated that these ruthenium-based systems (**7**) would promote many of the same reactions as the Schrock molybdenum-based alkylidene complexes but had greater functional group tolerance and could be handled using standard organic techniques.⁵⁰ The early transition metal-based catalysts required vacuum line and dry box conditions for efficient use in organic reactions whereas the ruthenium catalysts could be handled in air as solids and the reactions were carried out under a nitrogen atmosphere in standard flasks. Although there have been many demonstrations of the



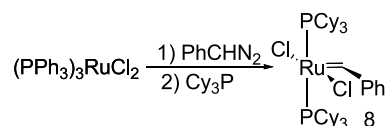
Scheme 8.

tolerance of these catalysts to functional groups, the ring closing reactions of highly functionalized polypeptides by Miller and Blackwell⁵¹ provide some of the most striking examples. In contrast to the usual direction of technology flow, this is a case where a reaction developed for polymerization chemistry became important in organic synthesis.

The ability to promote metathesis polymerization without the processing concerns of the early 'classical' catalysts opened a number of new applications. One group initiated studies of the ruthenium-based catalysts in the polymerization of dicyclopentadiene. Polydicyclopentadiene is a commercial material that is made by a reaction injection molding (RIM) process from tungsten and molybdenum complexes that are combined with alkylaluminums. These processes required protection from air and water, and did not tolerate impurities and additives in the monomer. The ruthenium systems allowed many of these problems to be overcome.⁵²

After the early papers on the ruthenium chemistry, a number of researchers inquired about obtaining samples of the complex. Until a commercial source could be developed, limited samples were provided to the community for testing. John Birmingham of Boulder Scientific obtained the license for the manufacture of the catalyst and aided in the development of the technology by providing substantial volumes of catalyst to organic and polymer chemists. The technology was subsequently licensed to Materia, Inc., who now exclusively manufactures the catalysts and distributes them through Sigma-Aldrich.

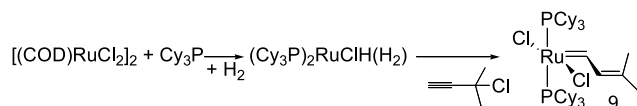
As the need for larger quantities of catalyst grew, more efficient methods for its synthesis were required. The cyclopropene route was useful for the preparation of the catalyst on the gram scale but was very difficult to scale-up. Marcia France initiated work on the use of diazo compounds as initiators for the ill-defined catalysts and demonstrated that stable ruthenium complexes could be prepared by such reactions. Peter Schwab developed an excellent route to the preparation of the ruthenium benzylidene complexes and demonstrated the high activity and rapid initiation of this family of catalysts.⁵³ These complexes have served as the basis for the development of the ruthenium metathesis technology (Scheme 9).



Scheme 9.

Key to their commercialization was the development of a method to safely and efficiently scale-up the diazo route by Mike Giardello. A one pot synthesis of an active derivative

was later developed by Tomas Belderrain and Tom Wilhelm (Scheme 10).⁵⁴



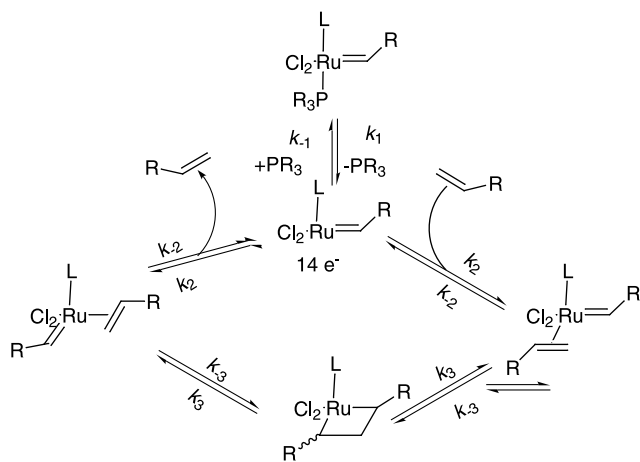
Scheme 10.

This route, which produces catalyst in over 90% yields from ruthenium chloride, has been used to prepare many kilos of the catalyst.

The commercial availability of the ruthenium catalyst made its widespread use possible. Recent reviews⁵⁵ describe a wide variety of applications that range from the synthesis of pharmaceutical intermediates to the production of a variety of polymer composites.⁵⁶

As had been demonstrated earlier, the ruthenium systems derived from ruthenium salts were active in water. By designing the appropriate water soluble ligands, an active water soluble ruthenium based olefin metathesis catalyst was prepared that produced living polymers in water.⁵⁷ The instability of these systems limited their activity in reactions involving unstrained olefins.⁵⁸

Essential for all of our work has been the understanding of the fundamental reaction pathways for catalysis. Eric Dias initiated a detailed study of the mechanism of metathesis using ruthenium catalysts.⁵⁹ The key finding was that the reaction proceeded by the loss of one of the neutral ligands to produce a 14 e⁻ species. It was proposed that the higher activity of the more basic phosphine was a result of stabilization of the intermediate metallacycle since progressing from the carbene olefin complex to the metallacycle involved oxidation of the metal center in addition to favoring the addition of a π -acidic olefin (Scheme 11).



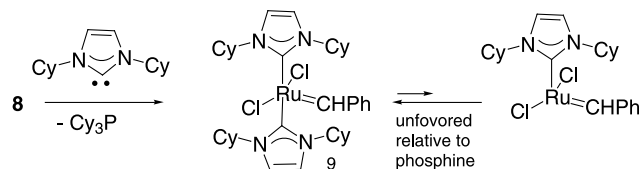
Scheme 11.

Less bulky basic phosphines coordinated too strongly to the metal and were not susceptible to dissociation/initiation. Phosphines with a larger cone angle than cyclohexylphosphine were too labile to produce a stable complex.

In a number of difficult ring-closing reactions, the lifetime

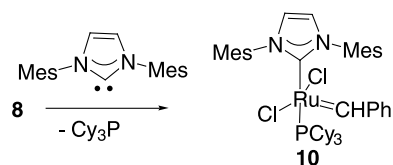
of the catalyst was insufficient to give high yields of products with reasonable catalyst loadings. A study of the thermal reactions of ruthenium alkylidene complexes was initiated to determine the decomposition modes at normal reaction temperatures. Mike Ulman found that substituted alkylidenes decomposed by a bimolecular mechanism that involved the loss of phosphine. Consequently, any technique that increased the rate of phosphine loss would also increase the rate of catalyst decomposition. In fact, productive metathesis is first order while decomposition is second order in the 14 e⁻ species. The parent methylene complex decomposed in a first order phosphine independent mechanism. Under many conditions, the methylene decomposition is the efficiency determining reaction. This set of observations indicated that the tricyclohexylphosphine complex was the optimum phosphine based system. Although a number of techniques utilizing chelating ligands gave some slight improvements in stability,⁶⁰ a new ligand system was required for the next breakthrough.

Herrmann⁶¹ and others demonstrated⁶² that the substitution of phosphines in catalyst systems with stable N-heterocyclic carbenes produced interesting changes in reactivity. In 1998, his group reported that complex (9), in which both phosphines of 8 had been replaced by dialkyl imidazolin-2-ylidene ligands, gave a catalyst with superior activity to that of 8.⁶³ Although these catalysts did not turn out to be more active than the phosphine systems,⁶⁴ the fact that they showed any activity at all even though the NHC ligands were less labile than the phosphines suggested that they might be interesting ligands (Scheme 12).



Scheme 12.

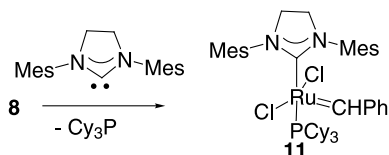
Our group then launched a program to synthesize analogs of 8 by substitution of the phosphines with NHC's. More than 10 different ligand systems were examined. Arduengo's most stable NHC that substituted with mesityl groups, 1,3-dimesitylimidazolin-2-ylidene turned out to be the key ligand. Other alkyl-substituted NHCs or aromatic-substituted NHCs without *ortho* substituents either would not substitute for the phosphine, decomposed rapidly, or gave double substitution. The mesityl substituted ligand—now called Imes—gave a stable system in which only one of the phosphines was substituted by an NHC.⁶⁵ This complex (10), also reported by the Nolan⁶⁶ and the Herrmann⁶⁷ groups, shows high activity and stability. The NHC provided a strong electron donor to stabilize the intermediates and the phosphine provide the labile



Scheme 13.

ligand required for the formation of the $14 e^-$ species (Scheme 13).

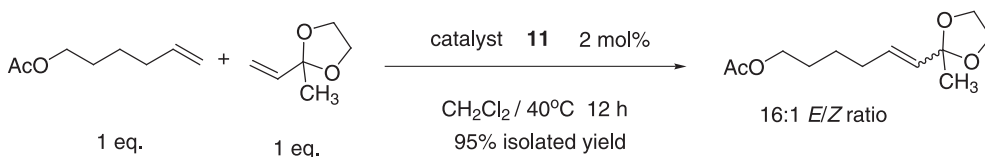
Building on our earlier work on the synthesis of chiral molybdenum⁶⁸ based metathesis catalysts and the outstanding success of the Schrock and Hoveyda groups⁶⁹ with later generation chiral catalysts, Mattias Scholl constructed a chiral NHC using the commercially available (1*R*,2*R*)-diphenylethylenediamine. Palladium coupling with mesityl bromide gave the appropriate precursor for the formation of the dihydro-2-imidazolium salt. The complex that resulted from the substitution of one of the phosphines by this ligand was unusually reactive. The first attempted kinetic resolution was complete in the time period estimated from the reactions with the unsaturated analog. An undergraduate, Sheng Ding, prepared the parent achiral system (**11**) which was more active than **10** in most reactions and was much more stable than the phosphine analogs (Scheme 14).⁷⁰



Scheme 14.

Based on the earlier mechanistic work that demonstrated that activity required the loss of one of the neutral ligands, it was assumed that the increased activity of the NHC systems was a result of the NHC ligands strong σ -donating ability and the resulting strong *trans* effect. Detailed mechanistic studies by Melanie Sanford demonstrated that the rate of formation (k_1) of the $14 e^-$ species was actually 10^2 slower for the NHC systems.⁷¹ The increase in rate was the result of the favored reaction of the π acidic olefin relative to other σ -donors in the system. For example, the reaction of ethylvinyl ether with the intermediate $14 e^-$ complex is 10^4 times faster (k_{-1}/k_2) than with tricyclohexylphosphine. It is this increased reactivity with π acids that accounts for the higher activity of the NHC analogs in olefin metathesis.⁷² Variations on these structures show improved activity for some applications. As will be seen later, the extremely active bispyridine analogs⁷³ have applications in polymer synthesis and it has been found that the chelating ether systems of Hoveyda⁷⁴ have applications in some difficult organic transformations. Although there are now many variations of the catalyst structures, it is interesting that the basic ligand array has remained that initially discovered by Nguyen—two *trans* neutral ligands, two halogens and the alkylidene around a ruthenium center.

Each improvement in catalysts reactivity and selectivity has led to a variety of new applications and synthetic strategies.



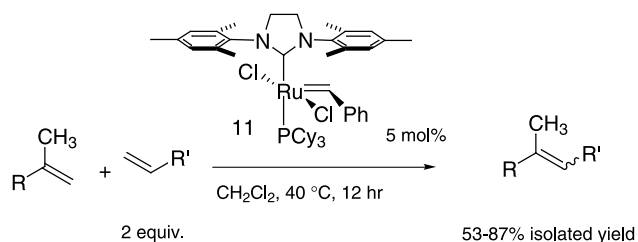
Scheme 15.

The titanium reagents helped to introduce metal alkylidenes to organic and polymer synthesis and served as mechanistic models. However, they were limited by functional group sensitivity and lack of reactivity. The Schrock molybdenum-based systems provided the first catalysts that allowed for the general application of metathesis in organic synthesis and remain key reagents in a number of transformations. However, their sensitivity to air, water and some functional groups limited many of their applications. The initial ruthenium-based catalysts, due to their ease of use and broad functional group tolerance, opened the broad application of metathesis. However, their lack of reactivity limited by their utility. The recently developed NHC systems (**10** and **11** and analogs) have increased reactivity and selectivity. A few of the broadening possibilities opened with recent catalyst developments will be discussed below.

Cross metathesis has seen limited use due to the statistical yield of products observed in cross reactions of simple olefins. The yield of the desired cross product is limited to 50% of a thermodynamic ratio of *E*:*Z* isomers when the olefins are used in a 1:1 ratio.⁷⁵ However, with the more active NHC-substituted catalysts, a number of more highly functionalized olefins were found to undergo clean metathesis reactions. Arnab Chatterjee developed a set of guidelines for the prediction of the outcome of cross metathesis reactions.⁷⁶ Key to this analysis was the finding that there is a wide variety of olefins that will take part in cross metathesis with alkyl-substituted olefins (Type 1) but undergo homometathesis at a much slower rate. Those olefins are classified at Type 2 or 3 depending on the reactivity of the pseudo-dimer. In those circumstances where a Type 1 olefin reacts with a Type 2 or 3 olefin and the reaction is pushed to completion so that all of the methylenes are released as ethylene, the less reactive partner must react with the more reactive partner to give the cross product as the dominate product.

Steric bulk in the allylic position, as well as alkyl substitution directly on the double bond greatly reduces the rate of homodimerization and such olefins are classified as Type 2 or 3. For example, the ketal of methylvinylketone gives a near quantitative yield of the cross product. Steric bulk also favors the *E* isomer (Scheme 15).

In a similar way, isobutylene and other 2-substituted olefins undergo slow dimerization to the tetrasubstituted double bond. When reacted with a terminal olefin, the trisubstituted olefin is favored. To increase the rate of reaction, the 2-substituted olefin is used in large excess. With isobutylene, isoprenoid groups, a general structure in terpenes, is easily installed (Scheme 16).⁷⁷



Scheme 16.

Electron deficient double bonds showed very low reactivity with the bis(phosphine) family of catalysts. For example, the metathesis of a mixture of 6-acetoxy-1-hexene with methylacrylate using **8** as the catalyst gave only the dimer of the hexene. The acrylate neither reacted nor hindered the dimerization reaction. However, Chatterjee found a similar reaction with the NHC catalyst **11** gave a >90% yield of the cross product the substituted acrylate (Scheme 17).⁷⁸

Reaction with electron deficient double bonds is a general feature of these catalysts. The greater electron donating ability of the NHC relative to tricyclohexylphosphine results in excellent reactivity with the more π -acidic acrylates. For example, the reaction of alkyl substituted olefins with crotonaldehyde provides a very efficient route to α,β -unsaturated aldehydes. These products are key intermediates in a variety of transformations including the MacMillan organocatalysis reactions.⁷⁹

The same factors that give high yields of cross products in small molecules, lead to the formation of alternating polymers when a cyclic olefin is reacted with a diacrylate (Scheme 18).

Following the reaction by NMR shows that the cyclic olefin polymerizes first and the electron deficient olefin then

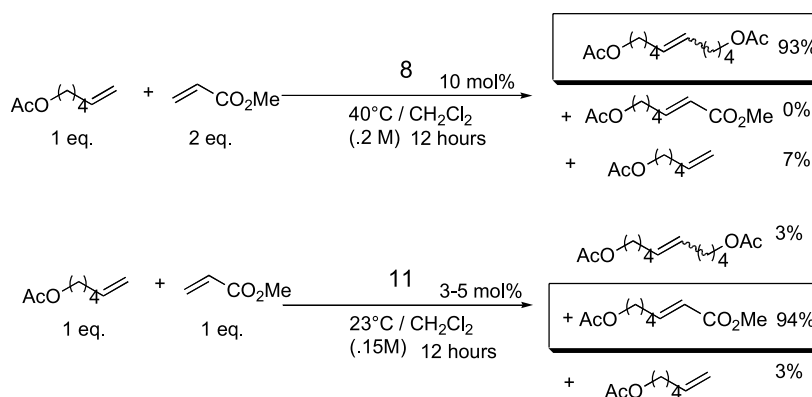
inserts into the polymer chain to release the methylenes as ethylene. The lack of homodimerization of acrylates results in an alternating structure when the monomers are present in precisely a 1:1 ratio.

In addition to the opportunities opened by the functional group and oxygen/water tolerance of the ruthenium catalysts in organic synthesis, these features also provide many new polymer synthesis and processing possibilities.⁸⁰

As with other polymerizations of norbornene with well-defined catalysts, the ruthenium systems are ‘living’. However, in spite of the fact that the growing chains are stable and do not undergo backbiting reactions at a competitive rate, the polydispersity of many of the polymers is broad due to slow initiation of the catalyst. As discussed above, the mechanism of action of these complexes is the loss of one of the neutral ligands. Consequently, the control of the polydispersity is associated with the rate of ligand loss, k_1 , and the rate of propagation k_2 .⁸¹

The polydispersity of the polymers prepared with **8** could be narrowed by adding excess triphenylphosphine, a ligand that has a larger k_1 than the cyclohexylphosphine ligand and also traps the $14 e^-$ species (Scheme 19).⁸²

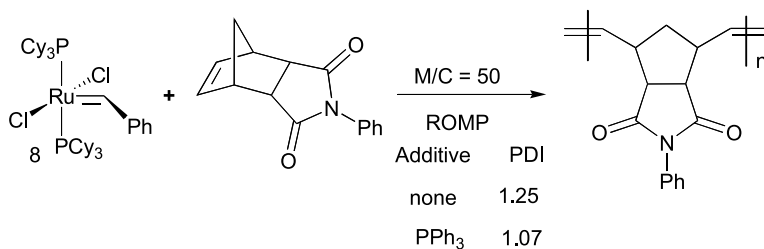
In contrast, the NHC initiator **11** could not be controlled by phosphine addition. As found in the mechanistic studies, the NHC systems showed very high rates of metathesis but unexpectedly low rates of ligand loss—i.e. initiation—to form the $14 e^-$ species. While examining the rates of ligand loss in the mechanistic studies, it was found that the easily formed bispyridine derivatives showed very high exchange rates. These derivatives employ two pyridine ligands on the ruthenium in place of one tricyclohexylphosphine. Their reactivity could be tuned by adding substituents to the pyridine ligands. In the end, the bis(3-bromopyridine)



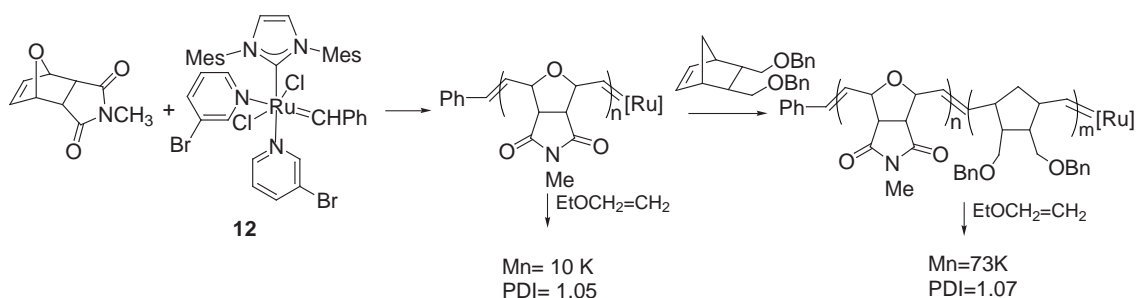
Scheme 17.



Scheme 18.



Scheme 19.



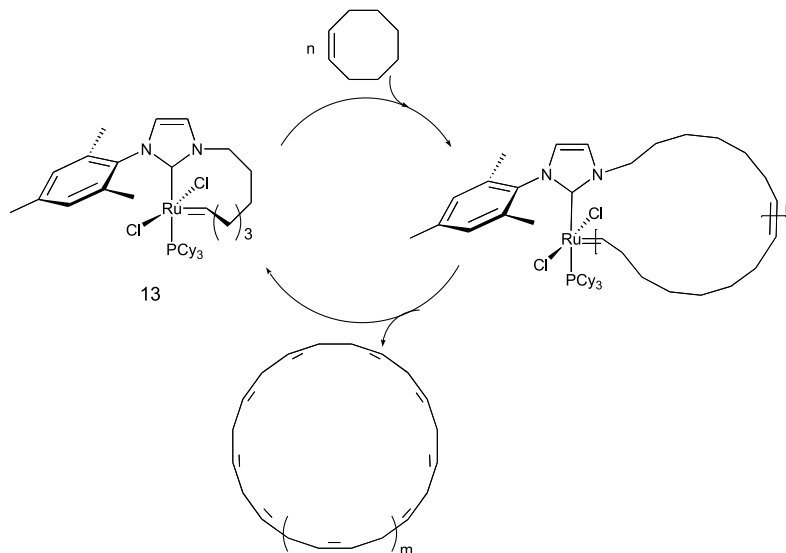
Scheme 20.

adduct (**12**) was found to provide optimum levels of reactivity. The pyridines exchange about 10^3 times faster than the tricyclohexylphosphine ligands. Using the bis(3-bromopyridine) complex as the initiator for the polymerization of a variety of norbornene derivatives produced polymers with narrow polydispersities and allowed the formation of multiblock copolymers. Quenching of the living polymers with ethylvinyl ether resulted in low dispersity homo and block copolymers (Scheme 20).⁸³

The strong complexing ability of the NHC ligand opened the opportunity to prepare a new class of polymers. Cyclic polymers have been of interest for many years. Since the properties of linear polymers are best described using reptation theory, the understanding of mobility of an

endless, cyclic polymer requires a route to prepare pure cycles on a scale large enough for detailed study. Metathesis provides such a possibility. By chelating the carbene to the NHC ligand a catalyst (**13**) is formed that is cyclic. Insertion of a cyclic olefin results in the growth to a larger cycle (Scheme 21).

Backbiting chain transfer can compete with chain growth to bite off a portion of the ring and produce a cycle. It is fortunate that chain growth is much faster than chain transfer and the backbiting appears to occur near the ligand to produce large rings. With cyclooctene as the monomer, polymers with average molecular weights (\bar{M}_n) of >100 K can be produced.⁸⁴ Detailed studies of the physical properties of this fundamentally interesting class of polymers are now being carried out.



Scheme 21.

Following the development of olefin metathesis from an interesting reaction that was only useful for unfunctionalized olefins, used ill-defined catalysts, and proceeded by a totally unknown mechanism to the present highly active, well-defined, functional group tolerant, and mechanistically well understood catalyst systems has been fun. A number of times along the way, I thought the journey was complete. However, the reaction keeps fooling me. It will be interesting to see where it leads next.

References and notes

- Ivin, K. J.; Mol, J. C. *Olefin Metathesis and Metathesis Polymerization*; Academic: New York, 1997.
- Bands, R. L.; Bailey, G. C. *Ind. Eng. Chem., Prod. Res. Dev.* **1964**, 170.
- This is intended to be a personal account and reference will be made to that work that had a major influence on the progress of the research in my group and I apologize for any omissions. A few of the high-light papers that impacted the development of metathesis catalysts in our group will be discussed. I wish to thank the over 200 researchers who have contributed to my work over the years. The major emphasis will be on the path of catalyst development.
- Calderon, N.; Chen, H. Y.; Scott, K. W. *Tetrahedron Lett.* **1967**, 3327.
- Grubbs, R. H.; Brunck, T. K. *J. Am. Chem. Soc.* **1972**, 94, 2538. Lewandos, G. S.; Pettit, R. *J. Am. Chem. Soc.* **1971**, 93, 7087.
- An out growth of our work with metallacyclopentanes lead to the detailed study of metallacyclopentanes of nickel and platinum by Professor Akira Miyashita, deceased November 2003 Grubbs, R. H.; Miyashita, A.; Liu, M.; Burk, P. *J. Am. Chem. Soc.* **1977**, 99, 3863.
- Herisson, J.-L.; Chauvin, Y. *Makromol. Chem.* **1971**, 141, 161.
- Casey, C. P.; Burkhard, T. J. *J. Am. Chem. Soc.* **1973**, 95, 5833–5834. Casey, C. P.; Burkhard, T. J. *J. Am. Chem. Soc.* **1974**, 96, 7808–7809.
- Schrock, R. R. *J. Am. Chem. Soc.* **1974**, 96, 6796–6797.
- Katz, T. J.; McGinnis, J. *J. Am. Chem. Soc.* **1975**, 97, 1592–1594. By measuring the cross over products as a function of time, the ratio of products could be obtained at zero time. In this publication, the mechanism for acetylene metathesis was also proposed.
- Grubbs, R. H.; Burk, P. L.; Carr, D. D. *J. Am. Chem. Soc.* **1975**, 97, 3265. A footnote to the paper in Ref. 10 above was added in proof to this paper.
- Katz, T. J.; Rothchild, R. *J. Am. Chem. Soc.* **1976**, 98, 2519–2526.
- Grubbs, R. H.; Carr, D. D.; Hoppin, C.; Burk, P. L. *J. Am. Chem. Soc.* **1976**, 98, 3478.
- Katz, T. J.; McGinnis, J. *J. Am. Chem. Soc.* **1977**, 99, 1903.
- Michelotti, F. W.; Keaveney, W. P. *J. Polym. Sci.* **1965**, A3, 895.
- Schrock, R. R. *Acc. Chem. Res.* **1979**, 12, 98–104. Alkoxide substitution on the systems converted a number of the early halide complexes into active metathesis catalysts. Schrock, R. R.; Rocklage, S.; Wengrovius, J.; Rupprecht, G.; Fellmann, J. *J. Mol. Catal.* **1980**, 8, 73.
- Katz, T. J.; Lee, S. J.; Acton, N. *Tetrahedron Lett.* **1976**, 47, 4247. See Ref. 6 of Katz, T. J.; Ho, T. H.; Shih, N. Y.; Ying, Y. C.; Stuart, V. *J. Am. Chem. Soc.* **1984**, 106, 2659–2668.
- Lee, S. J.; McGinnis, J.; Katz, T. J. *J. Am. Chem. Soc.* **1976**, 98, 7818.
- Katz, T. J.; Acton, N. *Tetrahedron Lett.* **1976**, 47, 4251–4254.
- Tebbe, F. N.; Parshall, G. W.; Ovenall, D. W. *J. Am. Chem. Soc.* **1979**, 101, 5075.
- Wengrovius, J.; Schrock, R. R.; Churchill, M. R.; Missert, J. R.; Youngs, W. J. *J. Am. Chem. Soc.* **1980**, 102, 4515.
- Kress, J. R. M.; Russell, M. J.; Wesolek, M. G.; Osborn, J. A. *Chem. Commun.* **1980**, 431–432.
- Tebbe, F. N.; Parshall, G. W.; Reddy, G. S. *J. Am. Chem. Soc.* **1978**, 100, 3611.
- Pine, S. H.; Zahler, R.; Evans, D. A.; Grubbs, R. H. *J. Am. Chem. Soc.* **1980**, 102, 3270.
- Howard, T. R.; Lee, J. B.; Grubbs, R. H. *J. Am. Chem. Soc.* **1980**, 102, 6876.
- Lee, J. B.; Ott, K. C.; Grubbs, R. H. *J. Am. Chem. Soc.* **1982**, 104, 7491.
- Kress, J.; Osborn, J. A.; Greene, R. M. E.; Ivin, K. J.; Rooney, J. J. *J. Am. Chem. Soc.* **1987**, 109, 899.
- Wengrovius, J. H.; Schrock, R. R.; Churchill, M. R.; Missert, J. R.; Youngs, W. J. *J. Am. Chem. Soc.* **1980**, 102, 4515–4516.
- Quignard, F.; Leconte, M.; Basset, J.-M. *J. Mol. Catal.* **1986**, 36, 3. Couturier, J. L.; Paillet, C.; Leconte, M.; Basset, J. M.; Weiss, K. *Angew. Chem., Int. Ed. Engl.* **1992**, 31(5), 628–631.
- Schrock, R. R.; DePue, R. T.; Feldman, J.; Schaverien, C. J.; Dewan, J. C.; Liu, A. H. *J. Am. Chem. Soc.* **1988**, 110, 1423–1435.
- Schrock, R. R.; Feldman, J.; Cannizzo, L. F.; Grubbs, R. H. *Macromolecules* **1987**, 20, 1169.
- Klavetter, F. L.; Grubbs, R. H. *J. Am. Chem. Soc.* **1988**, 110, 7807–7813.
- Swager, T. M.; Dougherty, D. A.; Grubbs, R. H. *J. Am. Chem. Soc.* **1988**, 110, 2973–2974.
- Gilliom, L. R.; Grubbs, R. H. *J. Am. Chem. Soc.* **1986**, 108, 733–742. Gilliom, L. R.; Grubbs, R. H.; Gilliom, L. R. *Proceedings of the Fourth International Symposium on Homogeneous Catalysis*, Leningrad, USSR, Sept 24–28, 1984.
- Diphenylcyclopropene would be an important reagent later in our development of the ruthenium based catalysts. My involvement with arylcyclopropenes goes back to my Master's research with Merle Battiste at the University of Florida.
- Gilliom, L. R.; Grubbs, R. H. *Organometallics* **1986**, 5, 721.
- Cannizzo, L. F.; Grubbs, R. H. *Macromolecules* **1987**, 20, 1488–1490. Risse, R. H.; Grubbs, R. H. *Macromolecules* **1989**, 22, 1558–1562.
- Stille, J. R.; Grubbs, R. H. *J. Am. Chem. Soc.* **1986**, 108, 855.
- Fu, G. C.; Grubbs, R. H. *J. Am. Chem. Soc.* **1992**, 114, 5426–5427. Fu, G. C.; Grubbs, R. H. *J. Am. Chem. Soc.* **1992**, 114(18), 7324–7325. Fu, G. C.; Grubbs, R. H. *J. Am. Chem. Soc.* **1993**, 115, 3800–3801.
- Martin, S.; Liao, Y.; Rein, T. *Tetrahedron Lett.* **1994**, 35, 691. Borer, B.; Deerenberg, S.; Bierougel, H.; Pandit, U. K. *Tetrahedron Lett.* **1994**, 35, 3191. Hourii, A.; Xu, Z.; Cogan, D.; Hoveyda, A. *J. Am. Chem. Soc.* **1995**, 117, 2943. Furstner, A.; Langermann, K. *J. Org. Chem.* **1996**, 3942.
- See for early demonstrations of ring closing metathesis using

- 'classical' catalysts Villemin, D. *Tetrahedron Lett.* **1980**, 1715. Tsuji, J.; Hashiguchi, S. *Tetrahedron Lett.* **1980**, 2955.
42. Novak, B. M.; Grubbs, R. H. *J. Am. Chem. Soc.* **1988**, *110*, 960–961.
43. Novak, B. M.; Grubbs, R. H. *J. Am. Chem. Soc.* **1988**, *110*, 7542–7543.
44. Johnson, L. K.; Grubbs, R. H.; Ziller, J. W. *J. Am. Chem. Soc.* **1993**, 8130–8145.
45. Nguyen, S. T.; Johnson, L. K.; Grubbs, R. H.; Ziller, J. W. *J. Am. Chem. Soc.* **1992**, *114*, 3974–3975.
46. Schaverien, C. J.; Dewan, J. C.; Schrock, R. R. *J. Am. Chem. Soc.* **1986**, *108*, 2771–2773.
47. Wu, Z.; Nguyen, S. T.; Grubbs, R. H.; Ziller, J. W. *J. Am. Chem. Soc.* **1995**, *117*, 5503–5511.
48. Nguyen, S. T.; Grubbs, R. H.; Ziller, J. W. *J. Am. Chem. Soc.* **1993**, *115*, 9858–9859.
49. Demonceau, A.; Noels, A. F.; Saive, E.; Hubert, A. J. *J. Mol. Catal.* **1992**, *776*, 123–132, Demonstrated that ruthenium(II) salts mixed with diazo alkanes would yield metathesis products in the presence of tricyclohexylphosphine.
50. Fu, G. C.; Nguyen, S. T.; Grubbs, R. H. *J. Am. Chem. Soc.* **1993**, *115*, 9856–9857.
51. Miller, S. J.; Grubbs, R. H. *J. Am. Chem. Soc.* **1995**, *117*, 5855–5856. Blackwell, H. E.; Grubbs, R. H. *Angew. Chem., Int. Ed.* **1998**, *37*(23), 3281–3284.
52. Charles Woodson started Advanced Polymer Technologies (now Cymetech) to develop ruthenium based polyDCPD technology. Commercial products are now being marketed based on this technology.
53. Schwab and France Schwab, P.; France, M. B.; Ziller, J. W. *Angew. Chem., Int. Ed. Engl.* **1995**, *34*, 2039–2041. *Angew. Chem.* **1995**, *107*, 2179–2181. Schwab, P.; Grubbs, R. H.; Ziller, J. W. *J. Am. Chem. Soc.* **1996**, *118*, 100–110.
54. Wilhelm, T. E.; Belderrain, T. R.; Brown, S. N.; Grubbs, R. H. *Organometallics* **1997**, *16*(18), 3867–3869.
55. *Handbook of Metathesis*; Grubbs, R. H., Ed.; Wiley-VCH: New York, 2003; p 214 Chapter 2.14.
56. Ref. 52, Chapter 3.12. For example a polymer reinforced baseball bat is being marketed by Easton Sports.
57. Lynn, D. M.; Kanaoka, S.; Grubbs, R. H. *J. Am. Chem. Soc.* **1996**, *118*, 784–790. Lynn, D. M.; Mohr, B.; Grubbs, R. H. *J. Am. Chem. Soc.* **1998**, *120*, 1627–1628.
58. Kirkland, T. A.; Lynn, D. M.; Grubbs, R. H. *J. Org. Chem.* **1998**, *63*(26), 9904–9909.
59. Dias, L.; Nguyen, S. T.; Grubbs, R. H. *J. Am. Chem. Soc.* **1997**, *119*, 3887–3897.
60. Chang, S.; Jones, L., II; Wang, C.; Henling, L. M.; Grubbs, R. H. *Organometallics* **1998**, *17*(16), 3460–3465. Dias, E. L.; Grubbs, R. H. *Organometallics* **1998**, *17*(13), 2758–2767.
61. Herrmann, W. A.; Elison, M.; Fischer, J.; Kocher, C.; Artus, G. R. *J. Angew. Chem., Int. Ed. Engl.* **1995**, *21*, 2371–2374.
62. It is interesting that the earliest demonstration of a 'carbene' metathesis mechanism was by M.F. Lappert using N-heterocyclic carbenes Cardin, D. J.; Doyle, M. J.; Lappert, M. F. *Chem. Commun.* **1972**, *16*, 927. He also demonstrated that NHC's were ligands that showed many of the same features as phosphines. Cardin, D. J.; Cetinkay, B.; Lappert, M. F. *Chem. Rev.* **1972**, *5*, 545.
63. Weskamp, T.; Schattenmann, W. C.; Spiegler, M.; Herrmann, W. A. *Angew. Chem., Int. Ed. Engl.* **1998**, *37*, 2490–2493.
64. Herrmann, W. A. *Angew. Chem., Int. Ed. Engl.* **1999**, *38*, 262–262.
65. Scholl, M.; Trnka, T. M.; Morgan, J. P.; Grubbs, R. H. *Tetrahedron Lett.* **1999**, *40*, 2247–2250.
66. Huang, J. K.; Stevens, E. D.; Nolan, S. P.; Petersen, J. L. *J. Am. Chem. Soc.* **1999**, *121*, 2674–2678.
67. Frenzel, U.; Weskamp, T.; Kohl, F. J.; Schattenman, W. C.; Nuyken, O.; Herrmann, W. A. *J. Organomet. Chem.* **1999**, *2*, 263–265.
68. Fujimura, O.; Grubbs, R. H. *J. Am. Chem. Soc.* **1996**, *118*, 2499–2500. Fujimura, O.; Grubbs, R. H. *J. Org. Chem.* **1998**, *63*(3), 824–832.
69. Zhu, S. S.; Cefalo, D. R.; La, D. S.; Jamieson, J. Y.; Davis, W. M.; Hoveyda, A. H.; Schrock, R. R. *J. Am. Chem. Soc.* **1999**, *121*, 8251–8259.
70. Scholl, M.; Ding, S.; Lee, C. W.; Grubbs, R. H. *Org. Lett.* **1999**, *1*(6), 953–956.
71. Sanford, M. S.; Ulman, M.; Grubbs, R. H. *J. Am. Chem. Soc.* **2001**, *123*, 749–750.
72. Sanford, M. S.; Love, J. A.; Grubbs, R. H. *J. Am. Chem. Soc.* **2001**, *123*, 6543–6554.
73. Bielawski, C. W.; Grubbs, R. H. *Angew. Chem., Int. Ed. Engl.* **2000**, *39*(16), 2903–2906. *Angew. Chem.* **2000**, *112*(16) 3025–3028.
74. Kingsbury, J. S.; Harrity, J. P. A.; Bonitatebus, P. J.; Hoveyda, A. H. *J. Am. Chem. Soc.* **1999**, *121*, 791–799.
75. Blackwell, H. E.; O'Leary, D. J.; Chatterjee, A. K.; Washenfelder, R. A.; Busmann, D. A.; Grubbs, R. H. *J. Am. Chem. Soc.* **2000**, *122*, 58–71. O'Leary, D. J.; Blackwell, H. E.; Washenfelder, R. A.; Grubbs, R. H. *Tetrahedron Lett.* **1998**, *39*, 7427–7430.
76. Chatterjee, A. K.; Choi, T.-L.; Sanders, D. P.; Grubbs, R. H. *J. Am. Chem. Soc.* **2003**, *125*, 11360–11370. Chatterjee, A. K.; Grubbs, R. H. *Angew. Chem., Int. Ed. Engl.* **2003**, *41*(17), 3171–3174. *Angew. Chem.* **2002**, *114* (17), 3303–3306.
77. Spessard, S. J.; Stoltz, B. M. *Org. Lett.* **2002**, *1*, 1943–1946.
78. Chatterjee, A. K.; Grubbs, R. H. *Org. Lett.* **1999**, *1*(11), 1751–1753. Chatterjee, A. K.; Morgan, J. P.; Scholl, M.; Grubbs, R. H. *J. Am. Chem. Soc.* **2000**, *122*(15), 3783–3784.
79. Austin, J. F.; MacMillan, D. W. C. *J. Am. Chem. Soc.* **2002**, *124*(7), 1172–1173.
80. Ref. 47, Chapter 3.12.
81. Robson, D. A.; Gibson, V. C.; Davies, R. G.; North, M. *Macromolecules* **1999**, *32*, 6371.
82. Bielawski, C.; Grubbs, R. H. *Macromolecules* **2001**, *34*(26), 8838–8840.
83. Choi, T.-L.; Grubbs, R. H. *Angew. Chem., Int. Ed. Engl.* **2003**, *42*, 1743–1746.
84. Bielawski, C. W.; Benitez, D.; Grubbs, R. H. *Science* **2002**, *297*, 2041–2044.

Publication list of Robert H. Grubbs 1966 to present

1. Battiste, M. A.; Halton, B.; Grubbs, R. Thermal rearrangements in the tetra-arylcyclopropene series. *Chem. Commun.* **1966**, 907.
2. Grubbs, R.; Breslow, R.; Herber, R.; Lippard, S. J. Studies of iron tricarbonyl cyclooctatetraene complexes. *J. Am. Chem. Soc.* **1967**, *89*, 6864.
3. Breslow, R.; Grubbs, R.; Marahashi, S.-I. Electrochemical evidence for the antiaromaticity of cyclobutadiene. *J. Am. Chem. Soc.* **1970**, *92*, 4139.

4. Grubbs, R. H. Cyclobutadienyliron tricarbonyl complexes. *J. Am. Chem. Soc.* **1970**, *92*, 6693.
5. Grubbs, R. H.; Kroll, L. C. Catalytic reduction of olefins with a polymer supported rhodium(I) catalyst. *J. Am. Chem. Soc.* **1971**, *93*, 3062.
6. Grubbs, R. H.; Kroll, L. C. The selectivity of polymer supported homogeneous catalysts. Presented at the 162nd ACS Meeting, Washington, DC, 1971. Special Symposium on Polymers as Reagents. *Polymer Preprints*, 1971.
7. Grubbs, R. H.; Brunck, T. K. A possible intermediate in the tungsten catalyzed olefin metathesis reaction. *J. Am. Chem. Soc.* **1972**, *94*, 2538.
8. Grubbs, R. H. Polymer supported rhodium(I) hydrogenation catalysts: factors controlling substrate selectivity. Presented at the 164th ACS meeting. *Polymer Preprints* **1972**, 46.
9. Grubbs, R.; Grey, R. A. Chiral tricarbonyl cyclobutadienyliron complexes. *Chem. Commun.* **1973**, 76.
10. Grubbs, R.; Gibbons, C.; Kroll, L. C.; Bonds, W. D.; Brubaker, Jr. C. H. Activation of homogeneous catalysis of polymer attachment. *J. Am. Chem. Soc.* **1973**, *95*, 2373.
11. Grubbs, R. H. Polymer attached homogeneous hydrogenation catalysts. *Polym. Prepr.* **1973**, 30.
12. Grubbs, R. H.; Kroll, L. C.; Sweet, E. M. The preparation and selectivity of polymer attached rhodium(I) olefin hydrogenation catalysis. *J. Macromol. Sci. Chem.* **1973**, *A7*, 1047.
13. Grubbs, R. H.; Grey, R. A. Cyclobutadiene as an intermediate in the oxidative decomposition of cyclobutadienyliron tricarbonyl. *J. Am. Chem. Soc.* **1973**, *95*, 5765.
14. Biefield, C. G.; Eick, H. A.; Grubbs, R. H. Crystal structure of bis(triphenylphosphine)tetramethylkene platinum(II). *Inorg. Chem.* **1973**, *12*, 2166.
15. Breslow, R.; Muriyama, D. R.; Murahashi, S. I.; Grubbs, R. H. Quantitative assessment of the antiaromaticity of cyclobutadiene by electrochemical studies on quinone derivatives. *J. Am. Chem. Soc.* **1973**, *95*, 6688.
16. Grubbs, R. H.; Pancoast, T. A.; Grey, R. A. Intramolecular trapping of cyclobutadiene. *Tetrahedron Lett.* **1974**, 2425.
17. Bonds, W. D.; Brubaker, C. H.; Chandrasekaran, E. S.; Gibbons, C.; Grubbs, R. H.; Kroll, L. C. Polystyrene attached titanocene species, preparation and reactions. *J. Am. Chem. Soc.* **1975**, *97*, 23128.
18. Grubbs, R. H.; Burk, P. L.; Carr, D. D. Consideration of the mechanism of the olefin metathesis reaction. *J. Am. Chem. Soc.* **1975**, *97*, 3265.
19. Grubbs, R. H.; Carr, D. D.; Burk, P. L. Metallocycles as intermediates in organotransition-metal reactions. In *Organotransition-metal Chemistry*; Ishii, Y., Tsutsui, M., Eds.; Plenum: New York, NY, 1975; p 135.
20. Grubbs, R. H.; Sweet, E. M. Microprobe analysis of polystyrene-attached catalysts. *Macromolecules* **1975**, *8*, 241.
21. Grubbs, R. H.; Burk, P. L.; Carr, D. D. Consideration of the mechanism of the olefin metathesis reaction. *J. Am. Chem. Soc.* **1975**, *97*, 3265.
22. Grubbs, R. H.; Carr, D. D.; Hoppin, C.; Burk, P. L. Consideration of the mechanism of the metal catalyzed olefin metathesis reaction. *J. Am. Chem. Soc.* **1976**, *98*, 3478.
23. The olefin metathesis reaction; *New applications of organometallic reagents in organic synthesis*. Seyferth, D., Ed.; Elsevier: Amsterdam, 1976; p 423.
24. Grubbs, R. H.; Sweet, E. M.; Phisanbut, S. Polymer attached catalysts. In *Catalysis in Organic Synthesis*; Greenfield, Ed.; Academic, 1976; p 153.
25. Grubbs, R. H.; Chandrasekaran, E. S.; Brubaker, Jr. C. H. Polymer supported organometallic compounds of titanium, zirconium and hafnium as hydrogenation catalyst. *J. Organomet. Chem.* **1976**, *120*, 49.
26. Grubbs, R. H.; Su, S.-C. H. The preparation of polymeric organophosphorus ligands for catalyst attachment. *J. Organomet. Chem.* **1976**, *122*, 151.
27. Grubbs, R. H. Polymer attached homogeneous catalyst. *Strem Chemiker* **1976**, *4*, 3.
28. Grubbs, R. H.; Blackborow, J. R.; Miyashita, A.; Scrivanti, A. Chemical synthesis with metal atoms: the reaction of chromium and nickel atoms with styrene. *J. Organomet. Chem.* **1976**, *120*, C49.
29. Blackborow, J. R.; Grubbs, R. H.; Miyashita, A.; Scrivanti, A.; Koerner von Gustorf, E. A. Chemical synthesis with metal atoms: the reaction of 1,4- and 1,3-cyclohexadiene with chromium atoms and trifluorophosphine. *J. Organomet. Chem.* **1976**, *122*, C6.
30. Grubbs, R. H.; Pancoast, T. A. Intramolecular trapping of cyclobutadiene complexes. *J. Am. Chem. Soc.* **1977**, *99*, 2382.
31. Grubbs, R. H.; Swetnick, S.; Su, S. C.-H. Hybrid catalyst-metathesis catalysts attached to polystyrene copolymer. *Proceedings of CNRS, No. 281 Relations Between Homogeneous and Heterogeneous Catalysis, Lyon* **1977**, *281*, 3–6.
32. Grubbs, R. H.; Swetnick, S.; Su, S.-C. H. Hybrid catalysts-metathesis catalysts attached to polystyrene. *J. Mol. Catal.* **1977**, *3*, 11.
33. Grubbs, R. H.; Hoppin, C. R. Initiation of olefin metathesis: reaction of deca-2,8-diene with catalysts formed from Me₄Sn–WCl₆–(Ph₃P)₂(NO)₂Mo. *J. Chem. Soc., Chem. Commun.* **1977**, 634.
34. Grubbs, R. H.; Miyashita, A.; Liu, M.; Burk, P. The preparation and reactions of nickelocyclopentanes. *J. Am. Chem. Soc.* **1977**, *99*, 3863.
35. Grubbs, R. H.; Miyashita, A. The metallacyclopentane-olefin interchange reaction. *Chem. Commun.* **1977**, 864.
36. Grubbs, R. H.; Su, S.-C. H.; Sweet, E. M. Hybrid catalyst. *Polym. Prepr.* **1977**. Spring ACS meeting.
37. Grubbs, R. H.; Lau, C. P.; Brubaker, C.; Cukier, R. Polymer attached metallocenes. Evidence for site isolation. *J. Am. Chem. Soc.* **1977**, *99*, 4517–4518.
38. Grubbs, R. H. Hybrid phase catalysts. *Chemtech* **1977**, 512.
39. Grubbs, R. H.; DeVries, R. Asymmetric hydrogenation by an atropisomeric diphosphinite rhodium complex. *Tetrahedron Lett.* **1977**, 1879.
40. Blackborow, J. R.; Grubbs, R. H.; Hidenbrand, K.; Koerner von Gustorf, E. A.; Miyashita, A.; Scrivanti, A. Mechanism of the fluxional behavior in (1-5-η-cycloheptadienyl)-1-5-η-cycloheptatrienyliron. *J. Chem. Soc., Dalton Trans.* **1977**, 2205.
41. Grubbs, R. H.; Pancoast, T. A. The mechanism of the oxidative decomposition of cyclobutadienyliron tricarbonyl complexes. *J. Am. Chem. Soc.* **1977**, *99*, 2382.
42. Grubbs, R. H.; Sweet, E. M. Polymer attached catalysts; A comparison between polystyrene attached and homogeneous Rh(I) hydrogenation catalysts. *J. Mol. Catal.* **1977/78**, *3*, 259.
43. Grubbs, R. H. The olefin metathesis reaction; *Progress in Inorganic Chemistry*, Lippard, S. J., Ed.; Wiley: New York, NY, 1978; Vol. 24.
44. Grubbs, R. H.; Miyashita, A. The relationship between metallacyclopentanes and bis-olefin-metal complexes. *J. Am. Chem. Soc.* **1978**, *100*, 1300.

45. Grubbs, R. H.; Miyashita, A. In *Metallacycles in Organotransition Metal Chemistry. 2nd International Symposium on Homogeneous Catalysis, Fundamental Research In Homogeneous Catalysis*; Tsutsui, M., Ed.; 1978; Vol. 2.
46. Grubbs, R. H.; Su, S.-C. H. Organometallic polymers as catalysts. In *Organometallic Polymer*; Sheets, Pittman, Eds.; 1978; p 129.
47. Grubbs, R. H.; Pancoast, T. A. Preparation of cyclobutadienyliron tricarbonyl complexes using disodium tetracarbonyl ferrate (−2). *Synth. React. Inorg. Met.-Org. Chem.* **1978**, *8*, 1.
48. Grubbs, R. H.; Miyashita, A.; Liu, M.; Burk, P. Preparation and reaction of phosphine nickelocyclopentanes. *J. Am. Chem. Soc.* **1978**, *100*, 2419.
49. Grubbs, R. H.; Miyashita, A. Preparation and isomerization reactions of 2-nickelahydrindanes. *J. Organomet. Chem.* **1978**, *161*, 371.
50. Grubbs, R. H.; Miyashita, A. Metallacycles as catalysts for the linear and cyclodimerization of olefins. *J. Am. Chem. Soc.* **1978**, *100*, 7416.
51. Grubbs, R. H.; Miyashita, A. Carbon–carbon bond cleavage reactions in the decomposition of metallacycles. *J. Am. Chem. Soc.* **1978**, *100*, 7418.
52. Grubbs, R. H.; Miyashita, A. *Reactions of metallacycles of nickel, metallacyclopentanes, hexanes and butanes. Proceedings of 1st International Symposium on Homogeneous Catalysis, ACS Meeting, Corpus Christi, Texas; 1978.*
53. Blackburn, J. R.; Feldhoff, U.; Grevels, F.-W.; Grubbs, R. H.; Miyashita, A. Chemical synthesis with metal atoms. Cyclodimerization of norbornadiene via nickela-cyclopentane intermediates. *J. Organomet. Chem.* **1979**, *173*, 253.
54. Grubbs, R. H.; Hoppin, C. Consideration of the mechanism of the transition metal catalyzed olefin metathesis reaction: metathesis of *cis,cis*-2,8-decadiene. *J. Am. Chem. Soc.* **1979**, *101*, 1499.
55. Grubbs, R. H. *Mechanistic studies of olefin metathesis. Lubrizol Award Symposium at the Joint ACS/Chemical Society in Japan, Honolulu, Hawaii; 1979.*
56. Grubbs, R. H. On the mechanism of olefin metathesis and cyclopropanation. *J. Inorg. Chem* **1979**, *18*, 2623.
57. Chang, B.-H.; Grubbs, R. H.; Brubaker, Jr. C. H. The preparation and some catalytic activity of polymer-supported η^5 -cyclopentadienyl-rhodium and -cobalt dicarbonyls. *J. Organomet. Chem.* **1979**, *172*, 81.
58. Grubbs, R. H.; Swetnick, S. J. Mechanism of olefin metathesis over a supported molybdenum catalyst. *J. Mol. Catal.* **1980**, *8*, 25.
59. Pine, S. H.; Zahler, R.; Evans, D. A.; Grubbs, R. H. Titanium-mediated methylene transfer reactions. The direct conversion of esters to vinyl ethers. *J. Am. Chem. Soc.* **1980**, *102*, 3270.
60. Grubbs, R. H.; Hu, S.-C. Polymer-attached homogeneous catalysis. In *Enzymic and Non-enzymic Catalysis*; Dunnill, P., Wiseman, A., Blakebrough, N., Eds.; Ellis Horwood: England, 1980; pp 223–235.
61. Howard, T. R.; Lee, J. B.; Grubbs, R. H. Titana-metalla-carbene-metallacyclobutane reactions: stepwise metathesis. *J. Am. Chem. Soc.* **1980**, *102*, 6876.
62. Lau, C.-P.; Chang, B.-H.; Grubbs, R. H.; Brubaker, Jr. C. H. Polymer-supported metallocenes and their applications to the catalysis of olefin isomerization, oligomerization, epoxidation and dinitrogen fixation reactions. *J. Organomet. Chem.* **1981**, *214*, 325.
63. Lee, J. B.; Gajda, G. J.; Schaefer, W. P.; Howard, T. R.; Ikariya, T.; Grubbs, R. H. Structures of titanacyclobutanes. *J. Am. Chem. Soc.* **1981**, *103*, 7358.
64. Doxsee, K. M.; Grubbs, R. H. Nucleophilic activation of co for reduction by hydrogen. *J. Am. Chem. Soc.* **1981**, *103*, 7696.
65. Ott, K. C.; Grubbs, R. H. 1,3-Dimetallacyclobutanes in metal-methylidene dimerization reactions. *J. Am. Chem. Soc.* **1981**, *103*, 5922.
66. Grubbs, R. H. Metathesis and ring-opening polymerization relationship to Ziegler–Natta polymerization. *Proceedings of the Transition Metal Catalyzed Polymerizations MMI International Symposium, Midland, Michigan* **1981**, 17–21, 1981.
67. Ott, K. C.; Lee, J. B.; Grubbs, R. H. Stereochemical consequence of the interaction of alkylaluminums with titanacyclobutanes and its relationship to the olefin metathesis reaction. *J. Am. Chem. Soc.* **1982**, *104*, 2942.
68. Grubbs, R. H. Alkene and alkyne metathesis reactions. *Comprehensive Organomet. Chem.* **1982**. Chapter 54.
69. Soto, J.; Steigerwald, M.; Grubbs, R. H. Concerning the mechanism of Ziegler–Natta polymerization: isotope effects of propagation rates. *J. Am. Chem. Soc.* **1982**, *104*, 4479.
70. Lee, J. B.; Ott, K. C.; Grubbs, R. H. Kinetics and stereochemistry of the titanacyclobutane-titanamethylene interconversion. Investigation of a degenerate olefin metathesis reaction. *J. Am. Chem. Soc.* **1982**, *104*, 7491.
71. Straus, D. A.; Grubbs, R. H. Preparation and reaction of metal ketene complexes of Zr and Ti. *J. Am. Chem. Soc.* **1982**, *104*, 5499.
72. Ozawa, F.; Yamamoto, A.; Ikariya, T.; Grubbs, R. H. Photolysis and photo-induced isomerization of *cis*- and *trans*-diethyl-bis(tertiary phosphine)palladium(II). *Organometallics* **1982**, *1*, 1481.
73. Straus, D. A.; Grubbs, R. H. Titanacyclobutanes: substitution pattern and stability. *Organometallics* **1982**, *1*, 1658.
74. Moore, E. J.; Straus, D. A.; Armantrout, J.; Santarsiero, B. D.; Grubbs, R. H.; Bercaw, J. E. Synthesis and structure of ketene complexes of permethylzirconocene and their hydrogenation to zirconium enolate hydrides. *J. Am. Chem. Soc.* **1983**, *105*, 2068.
75. Stille, J. R.; Grubbs, R. H. Synthetic applications of titanocene methylene complexes; selective formation of ketone enolates and their reactions. *J. Am. Chem. Soc.* **1983**, *105*, 1664.
76. Buchwald, S. L.; Grubbs, R. H. A titanium vinylidene route to substituted allenes. *J. Am. Chem. Soc.* **1983**, *105*, 5490.
77. Brown-Wensley, K. A.; Buchwald, S. L.; Cannizzo, L. F.; Clawson, L. E.; Ho, S. C. H.; Meinhardt, D. J.; Stille, J. R.; Straus, D. A.; Grubbs, R. H. Cp₂TiCH₂ complexes in synthetic applications. *Pure Appl. Chem.* **1983**, *55*, 1733.
78. Komiya, S.; Katoh, M.; Ikariya, T.; Grubbs, R. H.; Yamamoto, T.; Yamamoto, A. Reverse methyl migration from a methyl-iron complex to trimethyl-aluminum forming an ionic complex [Fe(Dmpe)₂(acac)]⁺AlMe₄[−]. *Organometallics* **1984**, 115.
79. Ott, K. C.; deBoer, E. J. M.; Grubbs, R. H. An investigation of the reaction of bis-cyclopentadienyltitanium dichlorides with trimethylaluminum. Mechanism of an α -hydrogen abstraction reaction. *Organometallics* **1984**, *3*, 223.
80. Mackenzie, P. B.; Ott, K. C.; Grubbs, R. H. Preparation of heteronuclear bridging methylene complexes. *Pure Appl. Chem.* **1984**, *56*, 59.

81. Tilley, T. D.; Grubbs, R. H.; Bercaw, J. E. Halide, hydride, and alkyl derivatives of (pentamethylcyclopenta-dienyl)bis-(triphenylphosphine)ruthenium. *Organometallics* **1984**, *3*, 274.
82. Straus, D. A.; Grubbs, R. H. α,β -Substituted bis(cyclopentadienyl)titanocyclobutanes and their role in productive metathesis. *J. Mol. Catal.* **1985**, *28*, 9. Presented at the International Symposium on Metathesis, France September 22–26, 1983.
83. Doxsee, K. M.; Grubbs, R. H.; Anson, F. C. Decomposition and ligand substitution reaction mechanisms for organometallic radicals. *J. Am. Chem. Soc.* **1984**, *106*, 7819.
84. Ho, S. C. H.; Straus, D. A.; Grubbs, R. H. An alternate path to reductive elimination for group 4B metals: mechanism of cyclopropane formation from titanacyclobutanes. *J. Am. Chem. Soc.* **1984**, *106*, 1433.
85. Ho, S. C. H.; Straus, D. A.; Armantrout, J.; Schaefer, W. P.; Grubbs, R. H. Structure and reactivity of the zirconaenolate anion $[\text{Cp}_2\text{Zr}(\text{C},\text{O}-\eta^2\text{-OCCH}_2\text{CH}_3)\text{-Na}\cdot 2\text{ THF}]$. Synthesis of homo- and heterobinuclear ketene complexes. *J. Am. Chem. Soc.* **1984**, 2210.
86. Clawson, L. E.; Buchwald, S. L.; Grubbs, R. H. The methylenation of enolizable ketones and esters using organotitanium chemistry. *Tetrahedron Lett.* **1984**, 5733.
87. Coolbaugh, T. S.; Santarsiero, B. D.; Grubbs, R. H. Synthesis, characterization and equilibrium studies of group VI-B intramolecular metalloesters: crystal structure of $\text{trans}-(\eta^5\text{-C}_5\text{H}_4)\text{-CH}_2\text{CH}_2\text{-O}_2\text{C-W}(\text{CO})_2\text{PPh}_3$. *J. Am. Chem. Soc.* **1984**, *106*, 6310.
88. Waymouth, R. M.; Santarsiero, B. D.; Grubbs, R. H. A trigonal-bipyramidal methyl group bridging two zirconocene-ketene centers. *J. Am. Chem. Soc.* **1984**, *106*, 4050.
89. Coolbaugh, T. S.; Coots, R. J.; Santarsiero, B. D.; Grubbs, R. H. Transition metal carbonyl compounds containing intramolecular nucleophiles: crystal structure of $[(\eta^5\text{-C}_5\text{H}_4\text{-}(\text{CH}_2)_3(\text{OH})\text{Mo}(\text{CO})_3)_2]$. *Inorg. Chim. Acta* **1985**, *98*, 99.
90. Buchwald, S. L.; Anslyn, E. V.; Grubbs, R. H. The reaction of $\text{Cp}_2\text{Ti}=\text{CH}_2$ with organic electrophiles: evidence for a radical mechanism. *J. Am. Chem. Soc.* **1985**, *107*, 1766.
91. Ikariya, T.; Ho, S. C. H.; Grubbs, R. H. Mechanism of rearrangement of titanacyclobutanes. *Organometallics* **1985**, *4*, 199.
92. Cannizzo, L. F.; Grubbs, R. H. In situ preparation of μ -chloro- μ -methylene-bis(cyclopentadienyl)-titanium dimethylaluminum (Tebbe's reagent). *J. Org. Chem.* **1985**, 2386.
93. Cannizzo, L. F.; Grubbs, R. H. Reactions of ' $\text{Cp}_2\text{Ti}=\text{CH}_2$ ' sources with acid anhydrides and imides. *J. Org. Chem.* **1985**, 2316.
94. Clawson, L. E.; Soto, J.; Buchwald, S. L.; Steigerwald, M. L.; Grubbs, R. H. Olefin insertion in a metal alkyl in a Ziegler polymerization system. *J. Am. Chem. Soc.* **1985**, *107*, 3377.
95. Grubbs, R. H.; Gilliom, L. R. Polymerization of norbornene initiated by cleavage of a titanium metallacyclobutane. Proceedings of the 4th International Symposium on Homogeneous Catalysis, September 24–28, 1984, Leningrad, USSR.
96. Gilliom, L. R.; Grubbs, R. H. Titanacyclobutanes derived from strained, cyclic olefins: the living polymerization of norbornene. *J. Am. Chem. Soc.* **1986**, *108*, 733–742.
97. Meinhart, J. D.; Santarsiero, B. D.; Grubbs, R. H. Carbonylation of titanocenecyclobutenes. Synthesis and characterization of a titanocene vinyl ketene complex. *J. Am. Chem. Soc.* **1986**, *108*, 3318.
98. Waymouth, R. M.; Santarsiero, B. D.; Coots, R. J.; Bronikowski, M. J.; Grubbs, R. H. Trinuclear Zr_2 , Al μ -ketene complexes containing bridging ligands. Implications for transmetalation reactions and CO reduction chemistry. *J. Am. Chem. Soc.* **1986**, *108*, 1427.
99. Gilliom, L. R.; Grubbs, R. H. A titanacyclobutane precursor to alkyl-substituted titanium carbene complexes. *Organometallics* **1986**, *5*, 721.
100. Stille, J. R.; Grubbs, R. H. Synthesis of $(\pm)\Delta^{9,12}$ -Capnellene using titanium reagents. *J. Am. Chem. Soc.* **1986**, *108*, 855.
101. Chang, B. H.; Grubbs, R. H.; Brubaker, Jr. C. H. The preparation and catalytic applications of supported zirconocene and hafnocene complexes. *J. Organomet. Chem.* **1985**, *280*, 365.
102. Swager, T. M.; Grubbs, R. H. Synthesis and properties of the first crossconjugated conductive polymer. *J. Am. Chem. Soc.* **1987**, *109*, 894–896.
103. Waymouth, R. M.; Clauser, K. R.; Grubbs, R. H. Reactivity of group 4 acyl complexes with alkylaluminum reagents: a convenient synthesis of zirconium ketone complexes. *J. Am. Chem. Soc.* **1986**, *108*, 6385–6387.
104. Park, J. W.; Mackenzie, P. B.; Schaefer, W. P.; Grubbs, R. H. Carbon–hydrogen bond activation through a binuclear C–H bond complex. *J. Am. Chem. Soc.* **1986**, *108*, 6402–6404.
105. Tumas, W.; Wheeler, D. R.; Grubbs, R. H. Photochemistry of titanacyclobutanes. Evidence for a metal-centered 1,4-biradical. *J. Am. Chem. Soc.* **1987**, *109*, 6182–6184.
106. Gajda, G. J.; Grubbs, R. H.; Weinberg, W. H. An inelastic electron tunneling spectroscopic investigation of the interaction of molybdenum hexacarbonyl with an aluminum oxide. *J. Am. Chem. Soc.* **1986**, *109*, 66–72.
107. Cannizzo, L. F.; Grubbs, R. H. Endcapping of polynorbornene produced by titanacyclobutanes. *Macromolecules* **1987**, *20*, 1488–1490.
108. Anslyn, E. V.; Grubbs, R. H. The mechanism of titanocene metallacyclobutane cleavage and the nature of the reactive intermediate. *J. Am. Chem. Soc.* **1987**, *109*, 4880–4890.
109. Mackenzie, R. B.; Coots, R. J.; Grubbs, R. H. Synthesis, structure and reactions of heterobinuclear μ -methylene complexes. *Organometallics* **1989**, *8*, 583–589.
110. Anslyn, E. V.; Grubbs, R. H. Dichlorobis(η^5 -chlorocyclopentadienyl)titanium. *Inorganic Synthesis*; Grimes, R. N., Ed.; Wiley: New York, 1992; Vol. 29, pp 198–201.
111. Ho, S. C.; Hentges, S.; Grubbs, R. H. Synthesis and structures of titanaoxacyclobutanes. *Organometallics* **1988**, *7*, 780–782.
112. Schrock, R. R.; Feldman, J.; Cannizzo, L. F.; Grubbs, R. H. Ring-opening polymerization of norbornene by a living tungsten alkylidene complex. *Macromolecules* **1987**, *20*, 1169.
113. Finch, W. C.; Anslyn, E. V.; Grubbs, R. H. Substituent effects on the cleavage rates of titanocene metallacyclobutanes. *J. Am. Chem. Soc.* **1988**, *110*, 2406–2413.
114. Meinhart, J. D.; Grubbs, R. H. Insertion of carbon-heteroatom multiple bonds into bis(η^5 -cyclopentadienyl)-titanacyclobutenes. *Bull. Chem. Soc. Jpn* **1988**, *61*, 171–180.
115. Hawkins, J. M.; Grubbs, R. H. A stereochemical mechanistic probe of substituted α -methylene titanacyclobutane reactivity. *J. Am. Chem. Soc.* **1988**, *110*, 2821–2823.
116. Cannizzo, L. F.; Grubbs, R. H. Block copolymers containing monodisperse segments produced by ring-opening

- metathesis of cyclic olefins. *Macromolecules* **1988**, *21*, 1961–1967.
117. Anslyn, E. V.; Santarsiero, B.; Grubbs, R. H. Synthesis and structures of bimetallic titanium and chromium carbene complexes of the type $\text{Cp}_2\text{Ti}(\text{Cl})\text{O}(\text{CH}_3)\text{CCr}(\text{CO})_5$. *Organometallics* **1988**, *7*, 2137–2145.
118. Klavetter, F. L.; Grubbs, R. H. Polycyclooctatetraene (polyacetylene): synthesis and properties. *J. Am. Chem. Soc.* **1988**, *110*, 7807–7813.
119. Stille, J. R.; Grubbs, R. H. The intramolecular Diels–Alder reaction of α,β -unsaturated ester dienophiles with cyclopentadiene and the dependence on tether length. *J. Org. Chem.* **1989**, *54*, 434.
120. Pranata, J.; Grubbs, R. H.; Dougherty, D. A. Band structures of polyfulvene and related polymers. A new model for the effects of benzannelation on the band structures of polythiophene, polypyrrole and polyfulvene. *J. Am. Chem. Soc.* **1988**, *110*, 3430–3435.
121. Gilliom, L.; Grubbs, R. H. The stereochemistry of norbornene polymerization by titanametalla-cyclobutanes. *J. Mol. Catal.* **1988**, *46*, 255–266.
122. Novak, B. M.; Grubbs, R. H. The ring opening metathesis polymerization of 7-oxabicyclo[2.2.1]hex-5-ene derivatives: a new acyclic polymeric ionophore. *J. Am. Chem. Soc.* **1988**, *110*, 960–961.
123. Waymouth, R. M.; Grubbs, R. H. Facile intramolecular coupling of alkyl and acyl ligands induced by Lewis acids: mechanistic studies on the formation of zirconium ketone complexes. *Organometallics* **1988**, *7*, 1631–1635.
124. Swager, T. M.; Dougherty, D. A.; Grubbs, R. H. Strained rings as a source of unsaturation: polybenzvalene, a new soluble polyacetylene precursor. *J. Am. Chem. Soc.* **1988**, *110*, 2973–2974.
125. Novak, B. M.; Grubbs, R. H. The Design and Synthesis of Novel Polymeric Ionophores by the Ring Opening metathesis Polymerization of 7-Oxabicyclo[2.2.1]hept-5-ene Derivatives. *Polymeric Materials Science and Engineering, Proceedings of the ACS Division of Polymeric Materials, New Orleans, Louisiana*; American Chemical Society, 1987; Vol. 57. p 651.
126. Grubbs, R. H.; Novak, B. M. *Living Polymer Systems: Olefin Metathesis*. 2nd ed. *Encyclopedia of Polymer Science and Engineering*; Wiley: New York, 1989; Suppl. Vol. pp 420–429.
127. Meinhart, J. D.; Anslyn, E. V.; Grubbs, R. H. Synthesis, reactivity and kinetic studies of bis(η^5 -cyclopentadienyl) titanium methylidene phosphine complexes. *Organometallics* **1989**, *8*, 583–589.
128. Klavetter, F. L.; Grubbs, R. H. Kinetic control in the polymerization of a feast monomer: a route into finite polyenes. *Synth. Met.* **1988**, *26*(4), 311–319.
129. Risse, W.; Grubbs, R. H. A novel route to block copolymers by changing from living ring-opening metathesis polymerization of cyclic olefins to Aldol condensation polymerization of silyl vinyl ethers. *Macromolecules* **1989**, *22*, 1558–1562.
130. Novak, B. M.; Grubbs, R. H. Catalytic organometallic chemistry in water: the aqueous ring opening metathesis polymerization of 7-oxanorbornene derivatives. *J. Am. Chem. Soc.* **1988**, *110*, 7542–7543.
131. Swager, T. M.; Grubbs, R. H. New morphologies of polyacetylene from the precursor polymer polybenzvalene. *J. Am. Chem. Soc.* **1989**, *111*, 4413–4422.
132. Risse, W.; Grubbs, R. H. Polynorbornene and poly(*exo*-dicyclopentadiene) with aldehyde end groups. *Die Makromolekulare Chemie* **1989**, *10*, 73.
133. Ozawa, F.; Park, J. W.; Mackenzie, P. B.; Schaefer, W. P.; Henling, L. M.; Grubbs, R. H. Structure and reactivity of titanium/platinum and palladium heterobinuclear complexes with μ -methylene ligands. *J. Am. Chem. Soc.* **1989**, *111*, 1319–1327.
134. Stille, J. R.; Santarsiero, B. D.; Grubbs, R. H. The rearrangement of bicyclo[2.2.1]heptane ring systems by titanocene alkylidene complexes to bicyclo[3.2.1]heptane enol ethers. The total synthesis of (\pm)- $\Delta^9(12)$ -capnellene. *J. Org. Chem.* **1990**, *55*, 843–862.
135. Novak, B. M.; Grubbs, R. H. Polymer Synthesis Using Stable Organometallic Intermediates. In *Encyclopedia of Science and Technology*; 6th ed. 1990 McGraw-Hill Yearbook of Science and Technology, Parker, S. P., Ed.; McGraw-Hill: New York, 1990; pp 258–261.
136. Risse, W.; Wheeler, D. R.; Cannizzo, L. F.; Grubbs, R. H. Di- and tetrafunctional initiators for the living ring-opening olefin metathesis polymerization of strained cyclic olefins. *Macromolecules* **1989**, *22*, 3205–3210.
137. Grubbs, R. H.; Tumas, W. Polymer synthesis and organometallic metal chemistry. *Science* **1989**, *243*, 907–915.
138. Park, J. W.; Schaefer, W. P.; Grubbs, R. H. Mechanism of carbon–hydrogen bond activation through a binuclear CH bond complex. *J. Am. Chem. Soc.* Submitted for publication.
139. Park, J. W.; Henling, L. M.; Schaefer, W. P.; Grubbs, R. H. The structure of a titanium-rhodium heterobinuclear complexes with μ -phenyl ligands. *Organometallics* **1991**, *10*, 171–175.
140. Risse, W.; Grubbs, R. H. Application of wittig-type reactions of titanacyclobutane end groups for the formation of block and graft copolymers. *Macromolecules* **1989**, *22*, 4462–4466.
141. Marder, S. R.; Perry, J. W.; Klavetter, F. L.; Grubbs, R. H. Third-order susceptibilities of soluble polymers derived from the ring opening metathesis copolymerization of cyclooctatetraene and 1,5-cyclooctadiene. *Chem. Mater.* **1989**, *2*, 171–173.
142. Park, J. W.; Henling, L. M.; Schaefer, W. P.; Grubbs, R. H. Structure and reactivity of a titanocene (η^2 -thioformaldehyde) trimethylphosphine complex. *Organometallics* **1990**, *9*, 1650–1656.
143. Perry, J. W.; Stiegman, A. E.; Marder, S. R.; Coulter, D. R.; Beratan, D. N.; Brinza, D. E.; Klavetter, F. L.; Grubbs, R. H. Second and Third Order Nonlinear Optical Properties of Conjugated Molecules and Polymers. In *Proceedings of the International Society for Optical Engineering Meeting on Non-linear Optical Properties of Materials*; Khanarian, G., Ed.; Bellingham: Washington, 1988; p 971.
144. Grubbs, R. H.; Gilliom, L. Metal carbene complexes in polymer synthesis. In *Recent Advances in Mechanistic and Synthetic Aspects of Polymerization*; Fontanille, M., Guyot, A., Eds.; Reidel: Amsterdam, 1987; pp 343–352.
145. Klavetter, F. L.; Grubbs, R. H. Condensed phase route to polyacetylene. *Synth. Met.* **1989**, *28*, D99–D104.
146. Klavetter, F. L.; Grubbs, R. H. Metathesis ‘rainbow’ polymerizations—a systematic route into polyene sequences. *Synth. Met.* **1989**, *28*, D105–D108.
147. Klavetter, F. L.; Grubbs, R. H. Polycyclooctatetraene (a.k.a. polyacetylene): properties and derivatives. *Polym. Mater. Sci. Eng.* **1988**, *58*, 855–885.
148. Marder, S. R.; Perry, J. W.; Klavetter, F. L.; Grubbs, R. H.

- The Synthesis and Third-order Optical Non-linearities of Soluble Polymers Derived from the Ring Opening Metathesis Copolymerization of Cyclooctatetraene and 1,5-Cyclooctadiene. In *Organic Material for Non-Linear Optics*; Hann, R. A., Bloor, D., Eds.; Royal Society of Chemistry, 1989.
149. Ginsburg, E. J.; Gorman, C. B.; Marder, S. R.; Grubbs, R. H. Poly(trimethylsilylcyclooctatetraene): a soluble conjugated polyacetylene via olefin metathesis. *J. Am. Chem. Soc.* **1989**, *111*, 7621–7622.
150. Gorman, C. B.; Ginsburg, E. J.; Marder, S. R.; Grubbs, R. H. Highly conjugated, substituted polyacetylenes via the ring-opening metathesis polymerization of substituted cyclooctatetraenes. *Angew. Chem.* **1989**, *101*, 1603–1606.
151. Swager, T. M.; Rock, M. M.; Grubbs, R. H. Polyquinone Bisketals: Precursors to New Conductive Polymers. *New Polymeric Mater*; Karasz, F. E., Ed.; The Netherlands, 1990; Vol. 2, pp 1–10.
152. Johnson, L. K.; Virgil, S. C.; Grubbs, R. H. Facile tungsten alkylidene synthesis: alkylidene transfer from a phosphorane to a tungsten imido complex. *J. Am. Chem. Soc.* **1990**, *112*, 5384–5385.
153. Grubbs, R. H.; Pine, S. H. Alkene Metathesis and Related Reactions. *Comprehensive Organic Synthesis: Selectivity, Strategy and Efficiency in Modern Organic Chemistry*; Paquette, L. A., Ed.; Pergamon Press: New York, 1991; Vol. 5, pp 1115–1127.
154. Ginsburg, E. J.; Gorman, C. B.; Grubbs, R. H.; Klavetter, F. L.; Lewis, N. S.; Marder, S. R.; Perry, J. W.; Sailor, M. J. Synthesis characterization, and applications of substituted polyacetylenes derived from ring-opening metathesis polymerization of cyclooctatetraenes. In *Conjugated Polymeric Materials: Opportunities in Electronic, Opto-Electronics and Molecular Electronics*; Brédas, J. L., Chance, R. R., Eds.; Kluwer Academic: Netherlands, 1990; pp 65–81.
155. Risse, W.; Grubbs, R. H. Block and graft copolymers by living ring-opening olefin metathesis polymerization. *J. Mol. Catal.* **1991**, *65*, 211–217.
156. Waymouth, R. M.; Potter, K. S.; Schaeffer, W. P.; Grubbs, R. H. Structure of a trinuclear Zr_2Al μ -ketone complex with a bridging trigonal bipyrimidal methyl group. *Organometallic* **1990**, *9*, 2843–2846.
157. McGrath, D. V.; Novak, B. M.; Grubbs, R. H. In *Aqueous Ring-Opening Metathesis Polymerizations of 7-Oxanorbornene Derivatives Using Ruthenium Catalysts*, Proceedings of the NATO ASI in Akcay, Turkey, September, 1989.
158. Gorman, C.; Ginsburg, E.; Marder, S.; Grubbs, R. Soluble, highly conjugated polyacetylenes via the ring-opening metathesis polymerization of cyclooctatetraenes. In *Polymer Preprints, Division of Polymer Chemistry, Inc.*, Proceedings from the ACS Meeting, Boston, MA, Apr 22–27, 1990.
159. Marder, S. R.; Perry, J. W.; Schaefer, W. P.; Ginsburg, E. J.; Gorman, C. B.; Grubbs, R. H. Organic, Organometallic and Polymeric Materials with Nonlinear Optical Properties, Proc. of Materials Res. Soc. Symp. on Multifunctional Materials, Materials Res. Soc. Natl Mtg, Boston, MA, Nov 26–Dec 1, 1989.
160. Tritto, I.; Grubbs, R. H. Conversion of Titanacyclobutane Complexes for Ring Opening Metathesis Polymerization into Ziegler–Natta Catalysts. In *Catalytic Olefin Polymerization*; Keii, T., Soga, K., Eds.; Kodansha-Elsevier: Amsterdam, 1990; pp 301–312.
161. Sailor, M. J.; Ginsburg, E. J.; Gorman, C. B.; Kumar, A.; Grubbs, R. H.; Lewis, N. S. Thin films of *n*-Si/poly-(CH_3)₃Si-cyclooctatetraene: conducting-polymer solar cells and layered structures. *Science* **1990**, *249*, 1146–1149.
162. Grubbs, R. H.; Gorman, C. B.; Ginsburg, E. J.; Perry, J. W.; Marder, S. R. New Polymeric Materials with Cubic Optical Nonlinearities Derived from Ring-Opening Metathesis Polymerization. In *Materials for Nonlinear Optics*; Marder, S. R., Sohn, J. E., Stucky, G. D., Eds.; American Chemical Society: Washington, DC, 1991; pp 672–682.
163. Sailor, M. J.; Klavetter, F. L.; Grubbs, R. H.; Lewis, N. S. Electronic properties of junctions between silicon and organic conducting polymers. *Nature* **1990**, *346*, 155–157.
164. McGrath, D. V.; Novak, B. M.; Grubbs, R. H. Aqueous Ring-Opening Metathesis Polymerizations of 7-Oxanorbornene Derivatives Using Ruthenium Catalysts. In *Olefin Metathesis and Polymerization Catalysts*; Imamoglu, Y., Ed.; Kluwer: The Netherlands, 1990; pp 525–536.
165. Ginsburg, E. J.; Gorman, C. B.; Sailor, M. J.; Lewis, N. S.; Grubbs, R. H. The Application of Ring-Opening Metathesis Polymerization to the Synthesis of Substitute Polyacetylenes. In *Olefin Metathesis and Polymerization Catalysts*; Imamoglu, Y., Ed.; Kluwer: The Netherlands, 1990; pp 537–541.
166. Grubbs, R. H. Polymer Synthesis through Organometallic Intermediates. In *Organic Synthesis via Organometallics*; Dötz, K. H., Hoffman, R. W., Eds.; Vieweg: Braunschweig, 1991; pp 1–14.
167. Moore, J. S.; Gorman, C. B.; Grubbs, R. H. Soluble, chiral polyacetylenes: syntheses and investigation of their solution conformation. *J. Am. Chem. Soc.* **1991**, *113*, 1704–1712.
168. Stelzer, F.; Leitner, O.; Pressl, K.; Leising, G.; Grubbs, R. H. Disordered and oriented polyacetylene-block-poly-norbornene-block-polyacetylene. *Synth. Met.* **1991**, *41–43*, 991–994.
169. Stelzer, F.; Grubbs, R. H.; Leising, G. Synthesis and properties of polyacetylene-poly-norbornene-polyacetylene triblock copolymers. *Polymer* **1991**, *32*(10), 1851–1856.
170. McGrath, D. V.; Grubbs, R. H.; Ziller, J. W. Aqueous ruthenium(II) complexes of functionalized olefins: the X-ray structure of $Ru(H_2O)_2(\eta^2-(O), \eta^2-(C,C'))-OCOCH_2-CH=CHCH_3)_2$. *J. Am. Chem. Soc.* **1991**, *113*, 3611–3613.
171. Jozefiak, T. H.; Ginsburg, E. J.; Gorman, C. B.; Sailor, M. J.; Grubbs, R. H.; Lewis, N. S. *Electrochemical characterization of soluble polyacetylenes from the ring-opening metathesis polymerization (ROMP) of substituted cyclooctatetraenes*. *Proc. Soc. Plastic Eng.*; 1991.
172. Gorman, C. B.; Ginsburg, E. J.; Sailor, M. J.; Moore, J. S.; Jozefiak, T. H.; Lewis, N. S.; Grubbs, R. H.; Marder, S. R.; Perry, J. W. Substituted polyacetylenes through the ring-opening metathesis polymerization (ROMP) of substituted cyclooctatetraenes: a route into soluble polyacetylene. *Synth. Met.* **1991**, *41–43*, 1033–1038.
173. Tritto, I.; Grubbs, R. H. Conversion of Titanacyclobutane Complexes for Ring Opening Metathesis Polymerization into Ziegler–Natta Catalysts, Proceedings from Recent Developments in Olefin Polymerization, Tokyo, Japan, October 1990.
174. Dougherty, D. A.; Grubbs, R. H.; Kaisaki, D. A.; Chang, W.; Jacobs, S. J.; Shultz, D. A.; Anderson, K. K.; Jain, R.; Ho, P. T.; Stewart, E. G. Approaches to Magnetic Organic Materials. In *Magnetic Molecular Materials*; Gatteschi, D., et al. Eds.; Kluwer: The Netherlands, 1991; pp 105–120.
175. Gorman, C. B.; Grubbs, R. H. Conjugated Polymers: The Interplay Between Synthesis Structure, and Properties. In *Conjugated Polymers: The Novel Science and Technology of*

- Conducting and Nonlinear Optically Active Materials*; Brédas, J. L., Silbey, R., Eds.; Kluwer: Dordrecht, 1991; pp 1–49.
176. Hillmyer, M. A.; Lepetit, C.; MacGrath, D. V.; Grubbs, R. H. The Aqueous Ring-Opening Metathesis Polymerization of exo-N-Methyl-7-oxabicyclo[2.2.1]hept-5-ene-2,3-dicarboximide. *Polym. Prepr.* **1991**, *32*, 162–163.
177. Fujiwara, M.; Grubbs, R. H.; Baldeschwieler, J. D. Characterization of pH-dependent poly(acrylic acid) interaction with vesicles. *Polym. Prepr.* **1991**, *32*, 275.
178. Wu, Z.; Johnson, L. K.; Fisher, R. A.; Grubbs, R. H. New applications and control of ring-opening metathesis polymerization: monodispersed polybutadiene and polyethylene from the polymerization of cyclobutene. *Polym. Prepr.* **1991**, *32*, 447–448.
179. Wu, Z.; Wheeler, D. R.; Grubbs, R. H. Living ring-opening metathesis polymerization of cyclobutene: the thermodynamic effect of a reversibly binding ligand. *J. Am. Chem. Soc.* **1992**, *114*, 146–151.
180. Gin, D. L.; Conticello, V. P.; Grubbs, R. H. Transition metal catalyzed polymerizations of heteroatom-substituted cyclohexadienes: precursors to poly(paraphenylene). *Polym. Prepr.* **1991**, *32*, 236–237.
181. Novak, B. M.; Risse, W.; Grubbs, R. H. The Development of Well-Defined Catalysts for Ring-Opening Olefin Metathesis Polymerizations (ROMP). *Advances in Polymer Science*; Kausch, H. H., Ed.; Springer: Berlin, 1992; Vol. 102, pp 48–72.
182. Hillmyer, M. A.; Lepetit, C.; McGrath, D. V.; Novak, B. M.; Grubbs, R. H. Aqueous ring-opening metathesis polymerization of carboximide-functionalized 7-oxanorbornenes. *Macromolecules* **1992**, *25*, 3345–3350.
183. Gin, D. L.; Conticello, V. P.; Grubbs, R. H. Transition-metal-catalyzed polymerization of heteroatom-functionalized cyclohexadienes: stereoregular precursors to poly(paraphenylene). *J. Am. Chem. Soc.* **1992**, *114*, 3167–3169.
184. Nguyen, S. T.; Johnson, L. K.; Grubbs, R. H.; Ziller, J. W. Ring-opening metathesis polymerization (ROMP) of norbornene by a group VIII carbene complex in protic media. *J. Am. Chem. Soc.* **1992**, *114*, 3974–3975.
185. Fu, G. C.; Grubbs, R. H. The application of catalytic ring-closing olefin metathesis to the synthesis of unsaturated oxygen heterocycles. *J. Am. Chem. Soc.* **1992**, *114*, 5426–5427.
186. Benedicto, A. D.; Novak, B. M.; Grubbs, R. H. Microstructural studies of poly(7-oxabicyclo[2.2.1]hept-2-ene) derivatives prepared from selected ruthenium catalysts. *Macromolecules* **1992**, *25*, 5893–5900.
187. France, M. B.; Paciello, R. A.; Grubbs, R. H. Initiation of aqueous ring-opening metathesis polymerization. Extension of $[\text{Ru}(\text{H}_2\text{O})_6]^{2+}$ catalyzed polymerizations to less-strained cyclic monomers. *Macromolecules* **1993**, *26*, 4739–4741.
188. Jozefiak, T. H.; Sailor, M. J.; Ginsburg, E. J.; Gorman, C. B.; Lewis, N. S.; Grubbs, R. H. Soluble polyacetylenes derived from the ring-opening metathesis polymerization (ROMP) of substituted cyclooctatetraenes: electrochemical characterization and Schottky barrier devices. *SPIE* **1991**, *1436*, 8–19.
189. Fu, G. C.; Grubbs, R. H. The synthesis of nitrogen heterocycles via catalytic ring-closing metathesis of dienes. *J. Am. Chem. Soc.* **1992**(18), 7324–7325.
190. Jozefiak, T. H.; Ginsburg, E. J.; Gorman, C. B.; Grubbs, R. H.; Lewis, N. S. Voltammetric characterization of soluble polyacetylene derivatives obtained from the ring-opening metathesis polymerization (ROMP) of substituted cyclooctatetraenes. *J. Am. Chem. Soc.* **1993**, *115*, 4705–4713.
191. Conticello, V. P.; Gin, D. L.; Grubbs, R. H. Ring-opening metathesis polymerization of substituted bicyclo[2.2.2]octadienes: a new precursor route to poly(1,4-phenylenevinylene). *J. Am. Chem. Soc.* **1992**, *114*, 9708–9710.
192. Gorman, C. B.; Ginsburg, E. J.; Grubbs, R. H. Soluble, highly conjugated derivatives of polyacetylene from the ring-opening metathesis polymerization of monosubstituted cyclooctatetraenes: synthesis and the relationship between polymer structure and physical properties. *J. Am. Chem. Soc.* **1993**, *115*, 1397–1409.
193. McGrath, D. V.; Grubbs, R. H. The mechanism of aqueous ruthenium(II)-catalyzed olefin isomerization. *Organometallics* **1994**, *13*, 224–235.
194. Gagne, M. R.; Grubbs, R. H.; Feldman, J.; Ziller, J. W. Catalytic activity of a well defined binuclear ruthenium alkylidene complex. *Organometallics* **1992**, *11*, 3933–3935.
195. Hillmyer, M. A.; Grubbs, R. H. The preparation of hydroxytelechelic poly(butadiene) via ring-opening metathesis polymerization employing a well-defined metathesis catalyst. *Macromolecules* **1993**, *26*, 872–874.
196. France, M. B.; Grubbs, R. H.; McGrath, D. V.; Paciello, R. A. Chain transfer during the aqueous ring-opening metathesis polymerization of 7-oxanorbornene derivative. *Macromolecules* **1993**, *26*, 4742–4747.
197. Grubbs, R. H.; Kratz, D. Highly unsaturated oligomeric hydrocarbons: α -(phenylethynyl)- ω -phenylpoly[1,2-phenylene(2,1-ethynediyl)]. *Chem. Ber.* **1993**, *126*, 149–157.
198. Fu, G. C.; Grubbs, R. H. The synthesis of cycloalkenes via alkylidene-mediated olefin metathesis and carbonyl olefination. *J. Am. Chem. Soc.* **1993**, *115*, 3800–3801.
199. Fisher, R. A.; Grubbs, R. H. Ring-opening metathesis polymerization of exo-dicyclopentadiene: reversible cross-linking by a metathesis catalyst. *Makromol. Chem. Macromol. Symp.* **1992**, *63*, 271–277.
200. Johnson, L. K.; Grubbs, R. H.; Ziller, J. W. Synthesis of tungsten vinyl alkylidene complexes via the reactions of $\text{WCl}_2(\text{NAr})(\text{PX}_3)_3$ ($\text{X}=\text{R}$, OMe) precursors with 3,3-disubstituted cyclopropenes. *J. Am. Chem. Soc.* **1993**, 8130–8145.
201. Johnson, L. K.; Frey, M.; Ulibarri, T. A.; Virgil, S. C.; Grubbs, R. H.; Ziller, J. W. Alkylidene transfer from phosphoranes to tungsten(IV) imido complexes. *J. Am. Chem. Soc.* **1993**, 8167–8177.
202. Wu, Z.; Benedicto, A. D.; Grubbs, R. H. The living ring-opening metathesis polymerization of bicyclo[3.2.0]heptene catalyzed by a ruthenium alkylidene complex. *Macromolecules* **1993**, *26*, 4975–4977.
203. Fu, G. C.; Nguyen, S. T.; Grubbs, R. H. Catalytic ring-closing metathesis of functionalized dienes by a ruthenium carbene complex. *J. Am. Chem. Soc.* **1993**, *115*, 9856–9857.
204. Nguyen, S. T.; Grubbs, R. H.; Ziller, J. W. Syntheses and activities of new single-component, ruthenium-based olefin metathesis catalysts. *J. Am. Chem. Soc.* **1993**, *115*, 9858–9859.
205. Pu, L.; Grubbs, R. H. New syntheses of benzobarrelenes. *J. Org. Chem.* **1994**, *59*, 1351–1353.
206. Benedicto, A. D.; Claverie, J. P.; Grubbs, R. H. On the molecular weight distribution of living polymerization involving chain-transfer agents: computational results, analytical solutions, and experimental investigations using ring-opening metathesis polymerization. *Macromolecules* **1995**, *28*(2), 500–511.

207. Gin, D. L.; Conticello, V. P.; Grubbs, R. H. Stereoregular precursors to poly(*p*-phenylene) via transition-metal-catalyzed polymerization. 1. Precursor design and synthesis. *J. Am. Chem. Soc.* **1994**, *116*, 10507–10519.
208. Gin, D. L.; Conticello, V. P.; Grubbs, R. H. Stereoregular precursors to poly(*p*-phenylene) via transition-metal-catalyzed polymerization. 2. The effects of polymer stereochemistry and acid catalysts on precursor aromatization. *J. Am. Chem. Soc.* **1994**, *116*, 10934–10947.
209. Wu, Z.; Grubbs, R. H. The synthesis of perfect rubber using ring-opening metathesis polymerization of 1-methylcyclobutene. *J. Mol. Catal.* **1994**, *90*, 39–42.
210. Fujimura, O.; Fu, G. C.; Grubbs, R. H. The synthesis of cyclic enol ethers via molybdenum alkylidene-catalyzed ring-closing metathesis. *J. Org. Chem.* **1994**, *59*, 4029–4031.
211. Tritto, I.; Sacchi, M. C.; Grubbs, R. H. From ring-opening metathesis polymerization to Ziegler–Natta polymerization: a method for obtaining polynorbornene–polyethylene block copolymers. *J. Mol. Catal.* **1993**, *82*, 103–111.
212. Flatt, B. T.; Grubbs, R. H.; Blanski, R. L.; Calabrese, J. C.; Feldman, J. Synthesis, structure and reactivity of a rhenium oxo-vinylalkylidene complex. *Organometallics* **1994**, *13*, 2728–2732.
213. France, M. B.; Feldman, J.; Grubbs, R. H. An iridium based catalyst system for metathesis isomerization of acyclic olefins, including methyl oleate. *J. Chem. Soc., Chem. Commun.* **1994**, 1307–1308.
214. Li, R. T.; Nguyen, S. T.; Grubbs, R. H. Reactions of 3,3-diphenylcyclopropene with iridium (I) complexes: probing the mechanism of cyclopropene rearrangements at transition metal centers. *J. Am. Chem. Soc.* **1994**, *116*, 10032–10040.
215. Wu, Z.; Grubbs, R. H. Synthesis of narrow dispersed linear polyethylene and block copolymers from polycyclobutene. *Macromolecules* **1994**, *27*, 6700–6703.
216. Grubbs, R. H. The development of functional group tolerant ROMP catalysts. *Pure Appl. Chem.* **1994**, *A31*(11), 1829–1833.
217. Wu, Z.; Grubbs, R. H. Preparation of alternating copolymers from the ring-opening metathesis polymerization of 3-methylcyclobutene and 3,3-dimethylcyclobutene. *Macromolecules* **1995**, *28*(10), 3502–3508.
218. Kim, S.-H.; Bowden, N.; Grubbs, R. H. Catalytic ring closing metathesis (RCM) of dienyne: construction of fused bicyclic rings. *J. Am. Chem. Soc.* **1994**, *116*, 10801–10802.
219. Chen, Z.-R.; Claverie, J. P.; Grubbs, R. H.; Kornfield, J. A. Modeling ring-chain equilibria in ring-opening metathesis polymerization (ROMP) of cycloolefins. *Macromolecules* **1995**, *28*, 2147–2154.
220. Hillmyer, M. A.; Benedicto, A. D.; Nguyen, S. T.; Wu, Z.; Grubbs, R. H. Ring-opening metathesis copolymerization employing ruthenium-based metathesis catalysts. *Macromol. Symp.* **1995**, *89*, 411–419.
221. Stanton, C. E.; Lee, T. R.; Grubbs, R. H.; Lewis, N. S.; Pudelski, J. K.; Callstrom, M. R.; Erickson, M. S.; McLaughlin, M. L. Routes to conjugated polymers with ferrocenes in their backbones: synthesis and characterization of poly(ferrocenylene divinylene) and poly(ferrocenylene butenylene). *Macromolecules* **1995**, *28*, 8713–8721.
222. Ginsburg, E. J.; Gorman, C. B.; Grubbs, R. H. Polyacetylene. In *Modern Acetylene Chemistry*; Diederich, F. N., Stang, P. J., Eds.; VCH: Weinheim, 1995; pp 353–383.
223. Miller, S. J.; Kim, S.-H.; Chen, Z.-R.; Grubbs, R. H. Catalytic ring closing metathesis (RCM) of dienes: application to the synthesis of eight-membered rings. *J. Am. Chem. Soc.* **1995**, *117*, 2108–2109.
224. Fujimura, O.; Fu, G. C.; Rothermund, P. W. K.; Grubbs, R. H. Hydroxyl-directed, stereoselective olefination of ketones by transition metal alkylidenes. *J. Am. Chem. Soc.* **1995**, *117*, 2355–2356.
225. Fujiwara, M.; Baldeschwieler, J. D.; Grubbs, R. H. Receptor-mediated endocytosis of poly(acrylic acid)-conjugated liposomes by macrophages. *Biochim. Biophys. Acta* **1996**, *1278*, 59–67.
226. Wu, Z.; Nguyen, S. T.; Grubbs, R. H.; Ziller, J. W. Reactions of ruthenium carbenes of the type $(PPh_3)_2(X)_2Ru=CH-CH=CPh_2$ ($X=Cl$ and CF_3COO) with strained acyclic olefins and functionalized olefins. *J. Am. Chem. Soc.* **1995**, *117*, 5503–5511.
227. Pu, L.; Wagaman, M. W.; Grubbs, R. H. Synthesis of poly-(1,4-naphthalene vinylenes): metathesis polymerization of benzobarrelenes. *Macromolecules* **1996**, *29*, 1138–1143.
228. Lynn, D. M.; Kanaoka, S.; Grubbs, R. H. Living ring-opening metathesis polymerization in aqueous media catalyzed by well-defined carbene complexes. *J. Am. Chem. Soc.* **1996**, *118*, 784–790.
229. Kanaoka, S.; Grubbs, R. H. Synthesis of block copolymers of silicon-containing norbornene derivatives via living ring-opening metathesis polymerization catalyzed by a ruthenium carbene complex. *Macromolecules* **1995**, *28*, 4707–4713.
230. Hillmyer, M. A.; Laredo, W. R.; Grubbs, R. H. The ring-opening metathesis polymerization of functionalized cyclooctenes by a ruthenium-based metathesis catalyst. *Macromolecules* **1995**, *28*, 6311–6316.
231. Nguyen, S. T.; Grubbs, R. H. The syntheses and activities of polystyrene-supported olefin metathesis catalysts based on $Cl_2(PR_3)_2 Ru=CH-CH=CPh_2$. *JOMC* **1995**, *497*, 195–200.
232. Miller, S. J.; Grubbs, R. H. Synthesis of conformationally restricted amino acids and peptides employing olefin metathesis. *J. Am. Chem. Soc.* **1995**, *117*, 5855–5856.
233. Fraser, C.; Grubbs, R. H. The synthesis of glycopolymers of controlled molecular weight by ring-opening metathesis polymerization using well-defined functional group tolerant ruthenium carbene catalysts. *Macromolecules* **1995**, *28*, 7248–7255.
234. Grubbs, R. H.; Miller, S. J.; Fu, G. C. Ring-closing metathesis and related processes in organic synthesis. *Acc. Chem. Res.* **1995**, *28*, 446–452.
235. Kim, S.-H.; Zuercher, W. J.; Bowden, N. B.; Grubbs, R. H. Catalytic ring closing metathesis (RCM) of dienyne: construction of fused bicyclic [n.m.0] rings. *J. Org. Chem.* **1996**, *61*, 1073–1081.
236. Hillmyer, M. A.; Grubbs, R. H. Chain transfer in the ring-opening metathesis polymerization of cyclooctadiene using discrete metal alkylidenes. *Macromolecules* **1995**, *28*, 8662–8667.
237. Pangborn, A. B.; Giardello, M. A.; Grubbs, R. H.; Rosen, R. K.; Timmers, F. J. Safe and convenient procedure for solvent purification. *Organometallics* **1996**, *15*(5), 1518–1520.
238. de la Mata, F. J.; Grubbs, R. H. Synthesis and reactions of tungsten oxo vinyl alkylidene complexes: the reactions of $WCl_2(O)(PX_3)_3$ ($X=R, OMe$) precursors with 3,3-diphenylcyclopropene. *Organometallics* **1996**, *15*, 577–584.
239. Fraser, C.; Hillmyer, M. A.; Gutierrez, E.; Grubbs, R. H. Degradable COD/acetol copolymers: versatile precursors to

- 1,4-hydroxytelechelic polybutadiene and hydroxytelechelic polyethylene. *Macromolecules* **1995**, *28*, 7256–7261.
240. Schwab, P.; France, M. B.; Ziller, J. W.; Grubbs, R. H. A series of well-defined metathesis catalysts—synthesis $\text{RuCl}_2(=\text{CHR}')(\text{PR}_3)_2$ and its reactions. *Angew. Chem., Int. Ed. Engl.* **1995**, *34*, 2039–2041, *Angew. Chem.*, 1995, 107, 2179–2181.
241. Schwab, P.; Grubbs, R. H.; Ziller, J. W. Synthesis and applications of $\text{RuCl}_2(=\text{CHR}')(\text{PR}_3)_2$ —the influence of the alkylidene moiety on metathesis activity. *J. Am. Chem. Soc.* **1996**, *118*, 100–110.
242. Weck, M.; Schwab, P.; Grubbs, R. H. Synthesis of ABA triblock copolymers of norbornenes and 7-oxanorbornenes via living ring-opening metathesis polymerization using well-defined, bimetallic ruthenium catalysts. *Macromolecules* **1996**, *29*(5), 1789–1793.
243. Fujimura, O.; de la Mata, F. J.; Grubbs, R. H. Synthesis of new chiral ligand and group VI metal alkylidene complexes. *Organometallics* **1996**, *15*(7), 1865–1871.
244. Fujimura, O.; Grubbs, R. H. Asymmetric ring-closing metathesis: kinetic resolution catalyzed by a chiral molybdenum alkylidene complex. *J. Am. Chem. Soc.* **1996**, *118*, 2499–2500.
245. Lonergan, M. C.; Severin, E. J.; Doleman, B. J.; Beaver, S. A.; Grubbs, R. H.; Lewis, N. S. Array-based vapor sensing using carbon black-polymer, chemically sensitive resistors. *Chem. Mater.* **1996**, *8*(9), 2298–2312.
246. Coates, G. W.; Grubbs, R. H. Quantitative ring-closing metathesis of polyolefins. *J. Am. Chem. Soc.* **1996**, *118*, 229–230.
247. Coates, G. W.; Grubbs, R. H. α -Agostic interactions and olefin insertion in metallocene polymerization catalysts. *Acc. Chem. Res.* **1996**, *29*, 85–93.
248. Wege, V. U.; Grubbs, R. H. Polymer synthesis in confined environments—microemulsion polymerization in monomolecular dendrimeric systems. *Angewandte Chemie*, Submitted for publication.
249. Walba, D. M.; Keller, P.; Shao, R.; Clark, N. A.; Hillmyer, M.; Grubbs, R. H. Main-chain ferroelectric liquid crystal oligomers by acyclic diene metathesis polymerization. *J. Am. Chem. Soc.* **1996**, *118*, 2740–2741.
250. Tasch, S.; Graupner, W.; Leising, W.; Pu, G.; Wagaman, M. W.; Grubbs, R. H. Red-orange electroluminescence with new soluble and air-stable poly(naphthalene-vinylene)s. *Adv. Mater.* **1995**, *7*(11), 903–906.
251. Maughon, B.; Grubbs, R. H. Synthesis and controlled cross-linking of polymers derived from ring-opening metathesis polymerization (ROMP). *Macromolecules* **1996**, *29*, 5765–5769.
252. Li, R. T.; Nguyen, S. T.; Zuercher, W. J.; Grubbs, R. H.; Synthesis and reactivity of iridium and rhodium vinylcarbene complexes: olefin metathesis versus cyclopropanation. *J. Am. Chem. Soc.* Submitted for publication.
253. Li, R. T.; Grubbs, R. H.; Catalytic and stoichiometric cyclopropanation by rhodium complexes: oxidation state effects in reactivity. *J. Am. Chem. Soc.* Submitted for publication.
254. Zuercher, W. J.; Hashimoto, M.; Grubbs, R. H. Tandem ring opening-ring closing metathesis of cyclic olefins. *J. Am. Chem. Soc.* **1996**(28), 6634–6640.
255. Day, M. W.; Wilhelm, T. E.; Grubbs, R. H. A diphenylcyclopropene complex of tungsten, $\text{W}(\text{PMePh}_2)_2\text{Cl}_2\text{O}(\text{C}^2-3$ -3-diphenylcyclopropene), precursor to a tungsten-oxo olefin metathesis catalyst. *Acta Cryst.* **1996**, *C52*, 2460–2462.
256. Maughon, B. R.; Weck, M.; Mohr, B.; Grubbs, R. H. Influence of backbone rigidity on the thermotropic behavior of side-chain liquid crystalline polymers (SCLCPs) synthesized by ring-opening metathesis polymerization (ROMP). *Macromolecules* **1997**, *30*, 257–265.
257. Mohr, B.; Lynn, D. M.; Grubbs, R. H. Synthesis of water-soluble, aliphatic phosphines and their application to well-defined ruthenium olefin metathesis catalysts. *Organometallics* **1996**, *15*(20), 4317–4325.
258. Walba, D. W.; Keller, P.; Shao, R.; Clark, N. A.; Hillmyer, M.; Grubbs, R. H. Main-chain ferroelectric liquid crystal oligomers by acyclic diene metathesis polymerization. *J. Am. Chem. Soc.* **1996**, *118*(11), 2740–2741.
259. Miller, S. J.; Blackwell, H. E.; Grubbs, R. H. Application of ring-closing metathesis to the synthesis of rigidified amino acids and peptides. *J. Am. Chem. Soc.* **1996**(40), 9606–9614.
260. Fujimura, O.; Grubbs, R. H. Asymmetric ring-closing metathesis catalyzed by chiral molybdenum alkylidene complexes. *J. Org. Chem.* **1998**, *63*(3), 824–832.
261. Coates, G. W.; Dunn, A. R.; Henling, L. M.; Dougherty, D. A.; Grubbs, R. H. Phenyl-perfluorophenyl stacking interactions: a new strategy for supramolecular construction. *Angew. Chem., Int. Ed. Engl.* **1997**, *36*, 248–251, *Angew. Chem.*, 1997, 109, 290–293.
262. Wagaman, M. W.; Bellmann, E.; Grubbs, R. H. Photoluminescence properties of polynaphthalenevinylene (PNV) homopolymers and block copolymers by ring-opening metathesis polymerization (ROMP) and study of their photoluminescence properties. *Phil. Trans. R. Soc. Lond. A* **1997**, *355*, 727–734.
263. Wagaman, M. W.; Grubbs, R. H. Synthesis of PNV homo- and copolymers by a ROMP precursor route. *Synth. Met.* **1997**, *84*, 327–328.
264. Hillmyer, M. A.; Nguyen, S. T.; Grubbs, R. H. The utility of a ruthenium metathesis catalyst for the preparation of end-functionalized polybutadiene. *Macromolecules* **1997**, *30*, 718–721.
265. Dias, E. L.; Nguyen, S. T.; Grubbs, R. H. Well-defined ruthenium olefin metathesis catalysts: mechanism and activity. *J. Am. Chem. Soc.* **1997**, *119*, 3887–3897.
266. Fujiwara, M.; Grubbs, R. H.; Baldeschwieler, J. D. Characterization of pH-dependent poly(acrylic acid) complexation with phospholipid vesicles. *J. Colloid Interface Sci.* **1997**, *185*, 210–216.
267. Day, M. W.; Mohr, B.; Grubbs, R. H. (Dicyclohexylphosphine)borane, $\text{BH}_3\text{PH}(\text{C}_6\text{H}_{11})_2$, a precursor to water-soluble phosphine ligands. *Acta Crystallogr.* **1996**, *C52*, 3106–3108.
268. Marsella, M. J.; Maynard, H. D.; Grubbs, R. H. Template-directed ring-closing metathesis: the synthesis polymerization, and subsequent depolymerization of unsaturated crown ether analog. *Angew. Chem., Int. Ed.* **1997**, *36*(10), 1101–1103.
269. Maughon, B. R.; Grubbs, R. H. Ruthenium alkylidene-initiated living ring-opening metathesis polymerization (ROMP) of 3-substituted cyclobutenes. *Macromolecules* **1997**, *30*, 3459–3469.
270. Sauvage, J.-P.; Mohr, B.; Grubbs, R. H.; Weck, M. High yield synthesis of [2]-catenanes via intramolecular ring-closing metathesis. *Angew. Chem.* **1997**, *36*(12), 1308–1310.
271. Wagaman, M. W.; Grubbs, R. H. Synthesis of organic and water soluble poly(1,4-phenylenevinylenes) containing

- carboxyl groups: living ring opening metathesis polymerization (ROMP) of 2,4-dicarboxy barrelenes. *Macromolecules* **1997**, *30*, 3978–3985.
272. Weck, M.; Mohr, B.; Maughon, B. R.; Grubbs, R. H. Synthesis of discotic columnar side-chain liquid crystalline polymers by ring-opening metathesis polymerization (ROMP). *Macromolecules* **1997**, *30*(21), 6430–6437.
273. Chang, S.; Grubbs, R. H. A simple method to polyhydroxylated olefin molecules using ring-closing olefin metathesis. *Tetrahedron Lett.* **1997**, *38*(27), 4757–4760.
274. Wilhelm, T. E.; Belderrain, T. R.; Brown, S. N.; Grubbs, R. H. Reactivity of Ru(H)(H₂)Cl(PCy₃)₂ with propargyl and vinyl chlorides: new methodology to give metathesis-active ruthenium carbenes. *Organometallics* **1997**, *16*(18), 3867–3869.
275. Belderrain, T. R.; Grubbs, R. H. Reaction between Ru(0) or Ru(0) precursor complexes and dihalocompounds. A new method for the synthesis of ruthenium olefin metathesis catalysts. *Organometallics* **1997**, *16*(18), 4001–4003.
276. Lynn, D. M.; Mohr, B.; Grubbs, R. H. Living ring-opening metathesis polymerization in water. *J. Am. Chem. Soc.* **1998**, *120*, 1627–1628.
277. Kirkland, T. A.; Grubbs, R. H. The effects of olefin substitution on the ring-closing metathesis of dienes. *J. Org. Chem.* **1997**, *62*(21), 7310–7318.
278. Wagaman, M. W.; Bellmann, E.; Cucullu, M.; Grubbs, R. H. Synthesis of substituted bicyclo[2.2.2]octatrienes. *J. Org. Chem.* **1997**, *62*(26), 9076–9082.
279. Zuercher, W. J.; Scholl, M.; Grubbs, R. H. Ruthenium-catalyzed polycyclization reactions. *J. Org. Chem.* **1998**, *63*(13), 4291–4298.
280. Grubbs, R. H.; Lynn, D. M. Olefin metathesis. In *Aqueous Phase Organometallic Catalysis*; Cornils, B., Herrmann, W. A., Eds.; VCH: Weinheim, 1998; pp 466–476.
281. Chang, S.; Grubbs, R. H. A highly efficient and practical synthesis of chromene derivatives using ring-closing olefin metathesis. *J. Org. Chem.* **1998**, *63*(3), 864–866.
282. Nolan, S. P.; Belderrain, T. R.; Grubbs, R. H. Convenient synthesis of ruthenium (II) dihydride phosphine complexes H₂Ru(PP)₂ and H₂Ru(PR₃)_x (x=3 and 4). *Organometallics* **1997**, *16*, 5569–5571.
283. Morehead, Jr. A.; Grubbs, R. Formation of bridged bicycloalkenes via ring closing metathesis. *Chem. Commun.* **1998**, 275–276.
284. Grubbs, R. H.; Chang, S. Recent advances in olefin metathesis and its application in organic synthesis. *Tetrahedron* **1998**, *54*, 4413–4450.
285. Dias, E. L.; Grubbs, R. H. Synthesis and investigation of homo- and heterobimetallic ruthenium olefin metathesis catalysts exhibiting increased activities. *Organometallics* **1998**, *17*(13), 2758–2767.
286. Chang, S.; Jones, II., L.; Wang, C.; Henling, L. M.; Grubbs, R. H. Synthesis and characterization of new ruthenium-based olefin metathesis catalysts coordinated with Bidentate Schiff base ligands. *Organometallics* **1998**, *17*(16), 3460–3465.
287. O'Leary, D. J.; Miller, S. J.; Grubbs, R. H. Template-promoted dimerization of C-allylglycine: a convenient synthesis of (S,S)-2,7-diaminosuberlic acid. *Tetrahedron Lett.* **1998**, *39*(13), 1628–1689.
288. Ulman, M.; Grubbs, R. H. Relative reaction rates of olefin substrates with ruthenium (II) carbene metathesis initiators. *Organometallics* **1998**, *17*(12), 2484–2489.
289. Bellmann, E.; Shaheen, S. E.; Thayumanavan, S.; Grubbs, R. H.; Marder, S. R.; Kippelen, B.; Peyghambarian, N. New triarylamine containing polymers as hole transport materials in organic light emitting diodes: effect of polymer structure and crosslinking on device characteristics. *Chem. Mater.* **1998**, *10*(6), 1668–1676.
290. Cucullu, M. E.; Nolan, S. P.; Belderrain, T. R.; Grubbs, R. H. Catalytic dehalogenation of aryl chlorides mediated by ruthenium(II) phosphine complexes. *Organometallics* **1999**, *18*, 1299–1304.
291. Wang, C.; Friedrich, S.; Li, R. T.; Grubbs, R. H.; Bansleben, D. A.; Day, M. W. Neutral Ni(II) based catalysts for ethylene polymerization. *Organometallics* **1998**, *17*(15), 3149–3151.
292. Coates, G. W.; Dunn, A. R.; Henling, L. M.; Ziller, J. W.; Lobkovsky, E. B.; Grubbs, R. H. Phenyl-perfluorophenyl stacking interactions: topochemical [2+2] photodimerization and photopolymerization of olefinic compounds. *J. Am. Chem. Soc.* **1998**, *120*(15), 3641–3649.
293. Doleman, B. J.; Sanner, R. D.; Severin, E. J.; Grubbs, R. H.; Lewis, N. S. Use of compatible polymer blends to fabricate arrays of carbon black-polymer composite vapor detectors. *Anal. Chem.* **1998**, *70*, 2560–2564.
294. Blackwell, H. E.; Grubbs, R. H. Highly efficient synthesis of covalently cross-linked peptide helices by ring-closing metathesis. *Angew. Chem., Int. Ed.* **1998**, *37*(23), 3281–3284.
295. Cucullu, M. E.; Nolan, S. P.; Belderrain, T. R.; Grubbs, R. H. Catalytic dehalogenation of aryl chlorides mediated by ruthenium (II) phosphine complexes. *Organometallics* **1999**, *18*, 1299–1304.
296. Sanford, M. S.; Henling, L. M.; Grubbs, R. H. Synthesis and reactivity of neutral and cationic ruthenium (II) tris(pyrazolyl)borate alkylidenes. *Organometallics* **1998**, *17*(24), 5384–5389.
297. Kirkland, T. A.; Lynn, D. M.; Grubbs, R. H. Ring-closing metathesis in methanol and water. *J. Org. Chem.* **1998**, *63*(26), 9904–9909.
298. Cucullu, M. E.; Li, C.; Nolan, S. P.; Nguyen, S. T.; Grubbs, R. H. Thermochemical Investigation of Phosphine Ligand Substitution Reactions in trans-(PR₃)₂Cl₂Ru=C–C=CPh₂ Complexes. *Organometallics* **1998**, *17*(24), 5565–5568.
299. Grubbs, R. H.; Khosravi, E. Ring-Opening Metathesis Polymerization (ROMP) and Related Processes. In *Material Science and Technology*, Vol., Schmitt, H., Ed., Wiley-VCH: Weinheim.
300. Bellmann, E.; Shaheen, S. E.; Grubbs, R. H.; Marder, S. R.; Kippelen, B.; Peyghambarian, N. Organic two-layer light-emitting diodes based on high T_g hole-transporting polymers with different redox potentials. *Chem. Mater.* **1999**, *11*, 399–407.
301. Weck, M.; Jackiw, J. J.; Rossi, R. R.; Weiss, P. S.; Grubbs, R. H. Ring-opening metathesis polymerization from surfaces. *J. Am. Chem. Soc.* **1999**, *121*(16), 4088–4089.
302. O'Leary, D. J.; Blackwell, H. E.; Washenfelder, R. A.; Grubbs, R. H. A new method for cross-metathesis of terminal olefins. *Tetrahedron Lett.* **1998**, *39*, 7427–7430.
303. O'Leary, D. J.; Blackwell, H. E.; Washenfelder, R. A.; Miura, K.; Grubbs, R. H. Terminal olefin cross-metathesis with acrolein acetals. *Tetrahedron Lett.* **1999**, *40*, 1091–1094.
304. Scholl, M.; Grubbs, R. H. Total Synthesis of (–) and (±)-frontalin via ring-closing metathesis. *Tetrahedron Lett.* **1999**, *40*, 1425–1428.
305. Matzger, A. J.; Lawrence, C. E.; Grubbs, R. H.; Lewis, N. S.

- Combination approaches to the synthesis of vapor detector arrays for use in an electronic nose. *J. Comb. Chem.* **2000**, *2*, 301–304.
306. Scholl, M.; Trnka, T. M.; Morgan, J. P.; Grubbs, R. H. Increased ring closing metathesis activity of ruthenium-based olefin metathesis catalysts coordinated with imidazol-2-ylidene ligands. *Tetrahedron Lett.* **1999**, *40*, 2247–2250.
307. Weck, M.; Dunn, A. R.; Matsumoto, K.; Grubbs, R. H. Influence of perfluoroarene–arene interactions on the phase behavior of liquid crystalline and polymeric materials. *Angew. Chem., Int. Ed. Engl.* **1999**, *38*, 2741–2745.
308. Ulman, M.; Grubbs, R. H. Ruthenium carbene-based olefin metathesis initiators: catalyst decomposition and longevity. *J. Org. Chem.* **1999**, *64*(19), 7202–7207.
309. Weck, M.; Mohr, B.; Sauvage, J.-P.; Grubbs, R. H. Synthesis of catenane structures via ring-closing metathesis. *J. Org. Chem.* **1999**, *64*(15), 5463–5471.
310. Maynard, H. D.; Grubbs, R. H. Purification technique for the removal of ruthenium from olefin metathesis reaction products. *Tetrahedron Lett.* **1999**, *40*, 4137–4140.
311. Bielawski, C. W.; Morita, T.; Grubbs, R. H. Synthesis of ABA triblock copolymers via a tandem ring-opening metathesis polymerization (ROMP)—atom transfer radical polymerization (ATRP) approach. *Macromolecules* **2000**, *33*(3), 678–680.
312. Maughon, B. R.; Morita, T.; Bielawski, C. W.; Grubbs, R. H. Synthesis of cross-linking of telechelic poly(butadiene)s derived from ring-opening metathesis polymerization. *Macromolecules* **2000**, *33*(6), 1929–1935.
313. Maynard, H. D.; Grubbs, R. H. Synthesis of functionalized polyethers by ring-opening metathesis polymerization of unsaturated crown ethers. *Macromolecules* **1999**, *33*(21), 6917–6924.
314. Sotzing, G. A.; Bringlin, S. M.; Grubbs, R. H.; Lewis, N. S. Preparation and properties of vapor detector arrays formed from poly(3,4-ethylenedioxy)thiophene-poly(styrene sulfonate)/insulating polymer composites. *Anal. Chem.* **2000**, *72*, 3181–3190.
315. Shaheen, S. E.; Jabbour, G. E.; Kippelen, B.; Peyghambarian, N.; Anderson, J. D.; Marder, S. R.; Armstrong, N. R.; Bellmann, E.; Grubbs, R. H. Organic light-emitting diode with 20 lm/W efficiency using a triphenyldiamine side-group polymer as the hole transport layer. *Appl. Phys. Lett.* **1999**, *74*(21), 3212–3214.
316. Scholl, M.; Ding, S.; Lee, C. W.; Grubbs, R. H. Synthesis and activity of a new generation of ruthenium-based olefin metathesis catalysts coordinated with 1,3-dimesityl-4,5-dihydro-imidazol-2-ylidene ligands. *Org. Lett.* **1999**, *1*(6), 953–956.
317. Blackwell, H. E.; O'Leary, D. J.; Chatterjee, A. K.; Washenfelder, R. A.; Bussmann, D. A.; Grubbs, R. H. New approaches to olefin cross-metathesis. *J. Am. Chem. Soc.* **2000**, *122*, 58–71.
318. Younkin, T. R.; Connor, E. F.; Henderson, J. I.; Friedrich, S. K.; Grubbs, R. H.; Bansleben, D. A. Neutral single component nickel (II) catalysts that tolerate heteroatoms. *Science* **2000**, *287*, 460–462.
319. Habbour, G. E.; Shalheen, S. E.; Morrell, M. M.; Anderson, J. D.; Lee, P.; Thayumanavan, S.; Barlow, S.; Bellmann, E.; Grubbs, R. H.; Kippelen, B.; Marder, S.; Armstrong, N. R.; Peyghambarian, N. High T_g hole transport polymers for the fabrication of bright and efficient organic light-emitting devices with an air-stable cathode. *IEEE J. Quant. Electron.* **2000**, *36*, 12–17.
320. Sotzing, G. A.; Phend, J. N.; Grubbs, R. H.; Lewis, N. S. Highly sensitive detection and discrimination of biogenic amines utilizing arrays of polyaniline/carbon black composite vapor detectors. *Chem. Mater.* **2000**, *12*, 593–595.
321. Bellmann, E.; Jabbour, G. E.; Grubbs, R. H.; Peyghambarian, N. Hole transport polymers with improved interfacial contact to the anode material. *Chem. Mater.* **2000**, *12*, 1349–1353.
322. Chatterjee, A. K.; Grubbs, R. H. Synthesis of trisubstituted alkenes via olefin cross-metathesis. *Org. Lett.* **1999**, *1*(11), 1751–1753.
323. Morita, T.; Maughon, B. R.; Bielawski, C. W.; Grubbs, R. H. A ring-opening polymerization (ROMP) approach to carboxyl and amino terminated telechelic poly(butadiene)s. *Macromolecules* **2000**, *33*, 6621–6623.
324. Lynn, D. M.; Mohr, B.; Grubbs, R. H.; Henling, L. M.; Day, M. W. Water-soluble ruthenium alkylidenes: synthesis, characterization, and application to olefin metathesis in protic solvents. *J. Am. Chem. Soc.* **2000**, *122*(28), 6601–6609.
325. Chatterjee, A. K.; Morgan, J. P.; Scholl, M.; Grubbs, R. H. Synthesis of functionalized olefins via cross and ring-closing metatheses. *J. Am. Chem. Soc.* **2000**, *122*(15), 3783–3784.
326. Bielawski, C. W.; Grubbs, R. H. Highly efficient ring-opening metathesis polymerization (ROMP) using new ruthenium catalysts containing N-heterocyclic carbene ligands. *Angew. Chem., Int. Ed. Engl.* **2000**, *39*(16), 2903–2906, *Angew. Chem.* **2000**, *112* (16), 3025–3028.
327. Maynard, H. D.; Okada, S. Y.; Grubbs, R. H. Synthesis of norbornenyl polymers with bioactive oligopeptides by ring-opening metathesis polymerization. *Macromolecules* **2000**, *33*(17), 6239–6248.
328. Ulman, M.; Belderrain, T. R.; Grubbs, R. H. A series of ruthenium(II) ester-carbene complexes as olefin metathesis initiators: metathesis of acrylates. *Tetrahedron Lett.* **2000**, *41*, 4689–4693.
329. Bielawski, C. W.; Scherman, O. A.; Grubbs, R. H. Highly efficient syntheses of acetoxyl and hydroxyl terminated telechelic poly(butadiene)s using ruthenium catalysts containing N-heterocyclic ligands. *Polymer* **2001**, *42*, 4939–4945.
330. Louie, J.; Grubbs, R. H. Highly active iron imidazolylidene catalysts for atom transfer radical polymerization. *Chem. Commun.* **2000**, 1479–1480.
331. Bielawski, C. W.; Louie, J.; Grubbs, R. H. Tandem catalysis: ring-opening metathesis polymerization (ROMP), atom transfer radical polymerization (ATRP), and hydrogenation using a single ruthenium complex. *J. Am. Chem. Soc.* **2000**, *122*(51), 12872–12873.
332. Sanford, M. S.; Henling, L. M.; Day, M. W.; Grubbs, R. H. Ruthenium-based four coordinate olefin metathesis catalysts. *Angew. Chem., Int. Ed.* **2000**, *39*(19), 3451–3453, *Angew. Chem.* **2000**, *112* (19), 3593–3595.
333. Lynn, D. M.; Grubbs, R. H. Novel reactivity of ruthenium alkylidenes in protic solvents: degenerate alkylidene proton exchange. *J. Am. Chem. Soc. Commun.* **2001**, *123*(14), 3187–3193.
334. Lee, C. W.; Grubbs, R. H. Stereoselectivity of macrocyclic ring-closing olefin metathesis. *Org. Lett.* **2000**, *2*(14), 2145–2147.
335. Trnka, T.; Grubbs, R. H. The development of $L_2X_2Ru=CHR$

- olefin metathesis catalysts: an organometallic success story. *Acc. Chem. Res.* **2001**, (34), 18–29.
336. Bing, R. J.; Yamamoto, T.; Kim, H.; Grubbs, R. H. The pharmacology of a new nitric oxide donor: B-NOD. *Biochem. Biophys. Res. Commun.* **2000**, 275, 350–353.
337. Matzger, A. J.; Henling, L. M.; Grubbs, R. H. The crystal structures of 1,3,5-tris(phenylethynyl)benzene with its pentadecafluoro derivative and with octafluoronaphthalene: the influence of multiple arene-perfluoroarene interactions. *Chem. Commun.* Submitted for publication.
338. Louie, J.; Grubbs, R. H. Reaction of diazoalkanes with iron phosphine complexes affords novel phosphazine complexes. *Organometallics* **2001**, 20, 481–484.
339. Morgan, J. P.; Grubbs, R. H. In situ preparation of a highly active N-heterocyclic carbene-coordinated olefin metathesis catalyst. *Org. Lett.* **2000**, 2(20), 3153–3155.
340. Louie, J.; Grubbs, R. H. Highly active metathesis catalysts generated in situ from inexpensive and air stable precursors. *Angew. Chem., Int. Ed. Engl.* **2001**, 40, 247–249, *Angew. Chem.* **2001**, 113 (1), 253–255.
341. Maynard, H. D.; Okada, S. Y.; Grubbs, R. H. Inhibition of cell adhesion to fibronectin by oligopeptide substituted polynorbornenes. *J. Am. Chem. Soc.* **2001**, 123, 1275–1279.
342. Sanford, M. S.; Ulman, M.; Grubbs, R. H. New insights into the mechanism of ruthenium catalyzed olefin metathesis reactions. *J. Am. Chem. Soc.* **2001**, 123, 749–750.
343. Choi, T.-L.; Chatterjee, A. K.; Grubbs, R. H. Synthesis of α , β -unsaturated amides by olefin cross-metathesis. *Angew. Chem., Int. Ed. Engl.* **2001**, 40(7), 1277–1279, *Angew. Chem.* **2001**, 113 (7), 1317–1319.
344. Lee, C. W.; Grubbs, R. H. Formation of macrocycles via ring-closing olefin metathesis. A succinct synthesis of (–)-pyrenophorin. *J. Am. Chem. Soc.* Submitted for publication.
345. Scherman, O. A.; Grubbs, R. H. Polycyclooctatetraene (polyacetylene) produced with a ruthenium olefin metathesis catalyst. *Synth. Met.* **2001**, 124, 431–434.
346. Juang, A.; Scherman, O. A.; Grubbs, R. H.; Lewis, N. S. Formation of covalently attached polymer overlayers on Si(111) surfaces using ring-opening metathesis polymerization methods. *Langmuir* **2001**, 17, 1321–1323.
347. Blackwell, H. E.; Sadowsky, J. D.; Howard, R. J.; Sampson, J. N.; Chao, J. A.; Steinmetz, W. E.; O'Leary, D. J.; Grubbs, R. H. Ring-closing metathesis of olefinic peptides: design, synthesis, and structural characterization of macrocyclic helical peptides. *J. Org. Chem.* **2001**, 66(16), 5291–5302.
348. Sanford, M. S.; Love, J. A.; Grubbs, R. H. Mechanism and activity of ruthenium olefin metathesis catalysts. *J. Am. Chem. Soc.* **2001**, 123, 6543–6554.
349. Trnka, T. M.; Henling, L. M.; Day, M. W.; Grubbs, R. H. Novel η^3 -vinylcarbene complexes derived from ruthenium-based olefin metathesis catalysts. *Organometallics* **2001**, 20, 3845–3847.
350. Chatterjee, A. K.; Choi, T.-L.; Grubbs, R. H. Synthesis of vinyl and allylphosphonates by olefin cross-metathesis. *Synlett* **2001**, SI, 1034–1037.
351. Bielawski, C. W.; Benitez, D.; Morita, T.; Grubbs, R. H. Synthesis of end-functionalized poly(norbornene)s via ring-opening metathesis polymerization (ROMP). *Macromolecules* **2001**, 34(25), 8610–8618.
352. Choi, T.-L.; Lee, C. W.; Chatterjee, A. K.; Grubbs, R. H. Olefin metathesis involving ruthenium enoic carbene complexes. *J. Am. Chem. Soc.* **2001**, 123(42), 10417–10418.
353. Lee, C. W.; Grubbs, R. H. Formation of macrocycles via ring-closing olefin metathesis. *J. Org. Chem.* **2001**, 66(21), 5158–5155.
354. Sanford, M. S.; Valdez, M. R.; Grubbs, R. H. Reaction of Tp(PPh₃)Ru(²-O₂CCHPh₂) with carbene and vinylidene precursors. *Organometallics* **2001**, 20(25), 5455–5463.
355. Sanford, M. S.; Love, J. A.; Grubbs, R. H. A versatile precursor for the synthesis of new ruthenium olefin metathesis catalysts. *Organometallics* **2001**, 20(25), 5314–5318.
356. Bielawski, C.; Grubbs, R. H. Increasing the initiation efficiency of ruthenium based ring-opening metathesis polymerization (ROMP) initiators: the effect of excess phosphine. *Macromolecules* **2001**, 34(26), 8838–8840.
357. Trnka, T. M.; Day, M. W.; Grubbs, R. H. Olefin metathesis with 1,1-difluoroethylene. *Angew. Chem., Int. Ed. Engl.* **2001**, 40, 3441–3444.
358. Louie, J.; Bielawski, C. W.; Grubbs, R. H. Tandem catalysis: the sequential mediation of olefin metathesis, hydrogenation, and hydrogen transfer using single component ruthenium complexes. *J. Am. Chem. Soc.* **2001**, 123, 11312–11313.
359. Seiders, T. J.; Ward, D. W.; Grubbs, R. H. Enantioselective ruthenium-catalyzed ring-closing metathesis. *Org. Lett.* **2001**, 3(20), 3225–3228.
360. Schwartz, D. M.; Jethmalani, J. M.; Sandstedt, C. A.; Kornfield, J. A.; Grubbs, R. H. Post implantation adjustable intraocular lenses. No. 2. *Ophthalmology clinics of north america: refractive surgery*; McLeod, S. D., McDonnell, P. J., Eds.; W.B. Saunders: Philadelphia, 2001; Vol. 14, pp 339–345.
361. Morgan, J. P.; Morrill, C.; Grubbs, R. H. Selective ring opening cross metathesis of cyclooctadiene and trisubstituted cycloolefins. *Org. Lett.* **2002**, 4(1), 67–70.
362. Choi, T.-L.; Grubbs, R. H. Tandem ring-closing metathesis reaction with ruthenium catalyst containing N-heterocyclic ligand. *Chem. Commun.* **2001**, 2648–2649.
363. Goldberg, S. D.; Grubbs, R. H. A one-pot cross-metathesis/allylboration reaction; a three component coupling for the synthesis of functionalized homoallylic alcohols. *Angew. Chem., Int. Ed. Engl.* **2002**, 41(5), 807–810, *Angew. Chem.* **2002**, 114 (5), 835–838.
364. Connor, E. F.; Younkin, T. R.; Henderson, J. I.; Hwang, S.; Grubbs, R. H.; Roberts, W. P.; Litzau, J. J. Linear functionalized polyethylene prepared with single component, neutral Ni(II) complexes. *J. Polym. Sci., Part A: Polym. Chem.* **2002**, 40, 2842–2854.
365. Scherman, O. A.; Kim, H. M.; Grubbs, R. H. Synthesis of well-defined poly(vinylalcohol₂-alt-methylene) via ring opening metathesis polymerization (ROMP). *Macromolecules* **2002**, 35(14), 5366–5371.
366. Toste, F. D.; Chatterjee, A. K.; Grubbs, R. H. Functional group diversity by ruthenium catalyzed olefin cross-metathesis. *Pure Appl. Chem.* **2002**, 74(1), 7–10.
367. Louie, J.; Grubbs, R. H. Metathesis of electron rich olefins: structure and reactivity of electron rich carbene complexes. *Organometallics* **2002**, 21(11), 2153–2164.
368. Grubbs, R. H.; Trnka, T. M.; Sanford, M. S. Transition metal-carbene complexes in olefin metathesis and related reactions. In *Fundamentals of Molecular Catalysis*; Yamamoto, A.; Kurosawa, H. Eds.; Elsevier: Amsterdam, Submitted for publication.
369. Koscho, M. E.; Grubbs, R. H.; Lewis, N. S. Properties of vapor detector arrays formed through plasticization of carbon

- black-organic polymer composites. *Anal. Chem.* **2002**, *74*(6), 1307–1315.
370. Kilbinger, A. F. M.; Grubbs, R. H. Arene-perfluoroarene interactions as physical cross-links for hydrogel formation. *Angew. Chem., Int. Ed. Engl.* **2002**, *41*(9), 1563–1566. *Angew. Chem.* **2002**, *114* (9), 1633–1636.
371. Grubbs, R. H. Cross metathesis of functionalized olefins. *Chimia* **2002**, *56*(1–2), 21.
372. Lee, C. W.; Choi, T.-L.; Grubbs, R. H. Ring expansion via olefin metathesis. *J. Am. Chem. Soc.* **2002**, *124*(13), 3224–3225.
373. Chatterjee, A. K.; Grubbs, R. H. Formal vinyl C–H activation and allylic oxidation by olefin metathesis. *Angew. Chem., Int. Ed. Engl.* **2002**, *41*(17), 3171–3174. *Angew. Chem.* **2002**, *114* (17), 3303–3306.
374. Chatterjee, A. K.; Toste, F. D.; Choi, T.-L.; Grubbs, R. H. Ruthenium-catalyzed olefin cross metathesis of styrenes as an alternative to the heck and cross-coupling reactions. *Adv. Synth. Catal.* **2002**, *344*(6+7), 634–637.
375. Chatterjee, A. K.; Sanders, D. P.; Grubbs, R. H. Synthesis of symmetrical trisubstituted olefins by cross metathesis. *Org. Lett.* **2002**, *4*(11), 1939–1942.
376. Grubbs, R. H.; Sanford, M. Mechanism of ruthenium based olefin metathesis catalysts. In *Ring Opening Metathesis Polymerisation and Related Chemistry*; Khosravi, E., Szymanska-Buzar, T., Eds.; Kluwer: The Netherlands, 2002; pp 17–21.
377. Ferguson, M. L.; O'Leary, D. J.; Grubbs, R. H. Ring-closing metathesis synthesis of N-Boc-3-pyrroline. *Org. Synth.* **2003**, *80*, 85–92.
378. Rolle, T.; Grubbs, R. H. Ring closing metathesis in protic media by means of a neutral and polar ruthenium benzyldiene complex. *Chem. Commun.* **2002**, *10*, 1070–1071.
379. Rutenberg, I.; Choi, T. L.; Grubbs, R. H. Synthesis of A,B-alternating copolymers by ring opening insertion metathesis polymerization. *Angew. Chem., Int. Ed. Engl.* **2002**, *41*(20), 3839–3841.
380. Kahnberg, P.; Lee, C. W.; Grubbs, R. H.; Sterner, O. Alternative routes to pterulone. *Tetrahedron* **2002**, *58*(26), 5203–5208.
381. Tran, H. V.; Hung, R. J.; Chiba, T.; Yamada, S.; Mrozek, T.; Hsieh, Y.-T.; Chambers, C. R.; Osborn, B. P.; Trinque, B. C.; Pinnow, M. J.; MacDonald, S. A.; Willson, C. G.; Sanders, D. P.; Connor, E. R.; Grubbs, R. H.; Conley, W. Metal-catalyzed addition polymers for 157 nm resist applications: 2. Fluorinated norbornenes: synthesis, polymerization, and initial imaging results. *Macromolecules* **2002**, *35*(17), 6539–6549.
382. Bielawski, C. W.; Benitez, D.; Grubbs, R. H. An 'endless' route to cyclic polymers. *Science* **2002**, *297*, 2041–2044.
383. Love, J. A.; Morgan, J. P.; Trnka, T. M.; Grubbs, R. H. A practical and highly active ruthenium-based catalyst that effects cross metathesis of acrylonitrile. *Angew. Chem., Int. Ed. Engl.* **2002**, *41*(21), 4035–4037.
384. Trnka, T. M.; Morgan, J. P.; Sanford, M. S.; Wilhelm, T. E.; Scholl, M.; Choi, T.-L.; Ding, S.; Day, M. W.; Grubbs, R. H. Synthesis and activity of ruthenium alkylidene complexes coordinated with phosphine and N-heterocyclic carbene ligands. *J. Am. Chem. Soc.* **2003**, *125*(9), 2546–2558.
385. Chatterjee, A. K.; Toste, F. D.; Goldberg, S. D.; Grubbs, R. H. Synthesis of coumarins by ring-closing metathesis. *Pure Appl. Chem.* **2003**, *75*(4), 421–425.
386. Hejl, A.; Trnka, T. M.; Day, M. W.; Grubbs, R. H. Terminal ruthenium carbido complexes as (-donor ligands. *Chem. Commun.* **2002**, 2524–2525.
387. Love, J. A.; Sanford, M. S.; Day, M. W.; Grubbs, R. H. Synthesis, structure, and activity of enhanced initiators for olefin metathesis reactions. *J. Am. Chem. Soc.* **2003**, *125*, 10103–10109.
388. Tillman, E. S.; Koscho, M. E.; Grubbs, R. H.; Lewis, N. S. Enhanced sensitivity to and classification of volatile carboxylic acids using arrays of linear poly(ethylenimine)-carbon black composite vapor detectors. *Anal. Chem.* **2003**, *75*(7), 1748–1753.
389. Choi, T.-L.; Grubbs, R. H. Controlled living ring-opening metathesis polymerization by fast initiating ruthenium catalyst. *Angew. Chem., Int. Ed. Engl.* **2003**, *42*, 1743–1746.
390. Connor, E. F.; Younkin, T. R.; Henderson, J. I.; Waltman, A.; Henling, L.; Grubbs, R. H. Revealing the role of ligand steric bulk in neutral nickel salicylaldamine polyethylene catalysts. *J. Am. Chem. Soc.* Submitted for publication.
391. Chatterjee, A. K.; Choi, T.-L.; Sanders, D. P.; Grubbs, R. H. A general model for selectivity in olefin cross metathesis. *J. Am. Chem. Soc.* **2003**, *125*, 11360–11370.
392. Bielawski, C. W.; Jethmalani, J. M.; Grubbs, R. H. Synthesis of telechelic polyacrylates with unsaturated end-groups. *Polymers* **2003**, *44*, 3721–3726.
393. Sanders, D. P.; Connor, E. F.; Grubbs, R. H.; Hung, R. J.; Osborn, B. P.; Chiba, T.; MacDonald, S. A.; Willson, C. G.; Conley, W. Metal-catalyzed addition polymers for 157 nm resist applications: synthesis and polymerization of partially fluorinated, ester-functionalized tricyclo[4.2.0²⁻⁵]non-7-enes. *Macromolecules* **2003**, *36*(5), 1534–1542.
394. Bielawski, C. W.; Benitez, D.; Grubbs, R. H. Synthesis of cyclic polybutadiene via ring-opening metathesis polymerization: the importance of removing trace linear contaminants. *J. Am. Chem. Soc.* **2003**, *125*(28), 8424–8425.
395. Kilbinger, A. F. M.; Cantrill, S. J.; Waltman, A. W.; Day, M. W.; Grubbs, R. H. Magic ring rotaxanes via olefin metathesis. *Angew. Chem., Int. Ed. Engl.* **2003**, *42*, 3281–3285.
396. Scherman, O. A.; Rutenberg, I. M.; Grubbs, R. H. Direct synthesis of soluble, end-functionalized polyenes and polyacetylene block-copolymers. *J. Am. Chem. Soc.* **2003**, *125*(28), 8515–8522.
397. Morrill, C.; Grubbs, R. H. Synthesis of functionalized vinyl boronates via ruthenium-catalyzed olefin cross-metathesis and subsequent conversion to vinyl halides. *J. Org. Chem.* **2003**, *68*, 6031–6034.
398. Rutenberg, I. M.; Scherman, O. A.; Bao, Z.; Grubbs, R. H.; Jiang, W. Garfunkel, E. Synthesis of polymer dielectric layers for organic thin film transistors via surface-initiated ROMP. *J. Am. Chem. Soc.* Submitted for publication.
399. Connor, E. F.; Younkin, T. R.; Henderson, J. I.; Waltman, A.; Henling, L.; Grubbs, R. H. Neutral nickel salicylaldamine polyethylene catalysts: the role of ligand steric bulk. *Chem. Commun.* in press.
400. Trinque, B. C.; Chambers, C. R.; Osborn, B. P.; Callahan, R. P.; Lee, G. S.; Kusumoto, S.; Sanders, D. P.; Grubbs, R. H.; Conley, W. E.; Willson, C. G. Vacuum-UV influenced design of polymers and dissolution inhibitors for next generation lithography. *J. Fluorine Chem.* **2003**, *122*, 17.
401. Trnka, T. M.; Dias, E. L.; Day, M. W.; Grubbs, R. H. Ruthenium alkylidene complexes coordinated with tricyclohexylphosphine and heterocyclic N-donor ligands. *ARKI-VOC* **2002**, 28–41, Part 13.

402. Schwartz, D.; Sandstedt, C.; Chang, S.; Kornfield, J.; Jethmalani, J.; Mamalis, N.; Grubbs, R. Materials for remote manipulation in the body: light adjustable intraocular lens. *Nature*, Submitted for publication.
403. Benitez, D.; Bielawski, C. W.; Grubbs, R. H. A ring-opening metathesis polymerization (ROMP) approach to cyclic polyoctenamers. *Macromolecules*, Submitted for publication.
404. Yun, J. -S.; Marinez, E. R.; Grubbs, R. H. New ruthenium-based olefin metathesis catalyst coordinated with 1,3-dimesityl-1,4,5,6-tetrahydropyrimidin-2-ylidene: synthesis, X-ray structure and reactivity. *Organometallics*, Submitted for publication.

Unrefereed Publications

- Grubbs, R. H.; Hillmyer, M.; Benedicto, A.; Wu, Z. Ring-opening metathesis polymerization catalysts. *Polym. Prepr.* **1994**, *35*, 688.
- Chen, Z.; Kornfield, J. A.; Claverie, J. P.; Grubbs, R. H. Ring-chain equilibria in ring-opening metathesis polymerization (ROMP) of cycloolefins. *Polym. Prepr.* **1994**, *35*, 692–693.
- Tritto, I.; Sacchi, M. C.; Grubbs, R. H. From ROMP to Ziegler–Natta polymerization: a study for obtaining poly-norbornene-polyethylene block copolymers. *Polym. Prepr.* **1994**, *35*, 696–697.
- Grubbs, R. H. Transition metal catalyzed reactions of olefins in water: olefin metathesis and isomerization. In *Aqueous Organometallic Chemistry and Catalysis*; Horváth, I. T., Joó, F., Eds.; Kluwer: The Netherlands, 1995; pp 15–22.
- Hillmyer, M. A.; Grubbs, R. H. The ROMP of COD by a well-defined metathesis catalyst in the presence of a difunctional chain transfer agent: the preparation of hydroxy-telechelic 1,4-poly(butadiene). *Polym. Prepr.* **1993**, *34*, 388–389.
- Rock, M. M.; Jozefiak, T. H.; Grubbs, R. H. The design and synthesis of electroactive polymers. *Polym. Prepr.* **1993**, *34*, 358–359.
- Benedicto, A. D.; Claverie, J. P.; Grubbs, R. H. Molecular weight of chain-transferred polymers in living polymerizations: comparison between experiment and theory. *Polym. Prepr.* **1995**, *36*, 172–173.
- Fraser, C.; Hillmyer, M.; Gutierrez, E.; Grubbs, R. H. Degradable cyclooctadiene/acetal copolymers: precursors to 1,4-hydroxytelechelic polybutadiene. *Polym. Prepr.* **1995**, *36*, 237–238.
- Wege, V. U.; Grubbs, R. H. Polymer synthesis in confined environments—microemulsion polymerization in monomolecular dendrimeric systems. *Polym. Prepr.* **1995**, *36*, 239–240.
- Grubbs, R. H.; Hillmyer, M.; Li, R.; Diaz, E.; Nguyen, S. T. Ring opening metathesis polymerization catalysts. *Macromol. Symp.* **1995**, *98*, 43.
- Weck, M.; Maughon, B. R.; Mohr, B.; Grubbs, R. H. Influence of backbone rigidity on the thermotropic behavior of side-chain liquid crystalline (SCLC) polymers synthesized by ring opening metathesis polymerization (ROMP). *Polym. Prepr.* **1996**, *37*(1), 587–588.
- Maughon, B. R.; Grubbs, R. H. Synthesis and characterization of crosslinkable polymers through ring opening metathesis polymerization of cyclooctene-5-methacrylate and cyclooctadiene. *Polym. Prepr.* **1995**, *36*, 471–472.
- Leising, G.; Kopping-Grem, G.; Meghdadi, F.; Niko, A.; Tasch, S.; Fischer, W.; Pu, L.; Wagaman, M. W.; Grubbs, R. H.; et al. Electroluminescence and photoluminescence of conjugated polymers and oligomers. *Prod. SPIE-Int. Soc. Opt. Eng.* **1995**, 307–314.
- Morita, T.; Maughon, B. R.; Grubbs, R. H. Synthesis of cross-linkable telechelic poly(butadiene) via ring-opening metathesis polymerization. *Polym. Prepr.* **1998**, *39*, 226–227, *Abs. Pap. ACS* **1998**, *215*, 231.
- Lynn, D. M.; Mohr, B.; Grubbs, R. H. Living ring-opening metathesis polymerization in water via activation of water-soluble ruthenium alkylidenes. *Polym. Prepr.* **1998**, *39*, 278–279, *Abs. Pap. ACS* **1998**, *215*, 52.
- Grubbs, R. H.; Blackwell, H.; Maughon, B.; Dias, E. Synthesis of organic molecules and materials using ruthenium carbene. *Abs. Pap. ACS* **1997**, *213*, 270.
- Grubbs, R. H.; Bansleben, D. A.; Wang, C. M.; Friedrich, S.; Younkin, T.; et al. The polymerization of ethylene with neutral, late metal catalysts. *Abs. Pap. ACS* **1998**, *215*, 37.
- Kirkland, T. A.; Lynn, D. M.; Grubbs, R. H. Ring-closing metathesis in water and methanol catalyzed by ruthenium alkylidene complexes. *Abs. Pap. ACS* **1998**, *215*, 73.
- Blackwell, H. E.; Grubbs, R. H. Synthesis of constrained cyclic peptide helices by ring closing metathesis. *Abs. Pap. ACS* **1998**, *215*, 72.
- Elder, D. L.; Wagamen, M. W.; Grubbs, R. H. Photoluminescence properties of dialkoxy poly(1,4-naphthalenevinylene) (PNV) homopolymers and copolymers synthesized by ROMP-aromatization route. *Polym. Prepr.* **1998**, *39*(2), 733–734.
- Maynard, H. D.; Grubbs, R. H.; Tandem, A. Approach to the synthesis of functionalized polyethers based on ring-closing metathesis and ring-opening metathesis polymerization. *Polym. Prepr.* **1998**, *39*(2), 523–524.
- Bellmann, E.; Shaheen, S. E.; Marder, S. R.; Kippelen, B.; Grubbs, R. H.; Peyghambarian, N. Synthesis of high- T_g hole-transporting polymers with different redox potentials and their performance in organic two layer LEDs. *SPIE* **1998**. San Diego, CA.
- Morita, T.; Maughon, B. R.; Grubbs, R. H. Synthesis of cross-linkable telechelic poly(butadiene) via ring-opening metathesis polymerization. *Polym. Prepr.* **1998**, *39*(1), 226–227.
- Lynn, D. M.; Mohr, B.; Grubbs, R. H. Living ring-opening metathesis polymerization in water via activation of water-soluble ruthenium alkylidenes. *Polym. Prepr.* **1998**, *39*(1), 278–279.
- Lewis, N. S.; Lonergan, M. C.; Severin, E. J.; Doleman, B. J.; Grubbs, R. H. Array-based vapor sensing using chemically sensitive, carbon black-polymer resistors. *Proc. SPIE—Int. Soc. Opt. Eng.* **1997**, 3079, 660–670.
- Fujimura, O.; Javier De La Mata, F.; Grubbs, R. H. Synthesis of new chiral ligands and their group VI metal alkylidene complexes. *Chemtracts* **1998**, *11*, 143–144.
- Ring-opening metathesis polymerization from surfaces. *Polym. Mater. Sci. Eng.* **1998**, *79*, 72–73.
- Jethmalani, J. M.; Kornfield, J. A.; Grubbs, R. H.; Schwartz, D. M. Photo-induced refractive index modulation of bismethacrylate endcapped siloxane macromer in poly(dimethylsiloxane) (pdms) matrix. *Polym. Prepr.* **1999**, *40*(2), 234–235.
- Jethmalani, J. M.; Kornfield, J. A.; Grubbs, R. H.; Schwartz, D. M. Silicones for photo-induced refractive index modulation: divinyl endcapped /siloxane macromer in

- poly(dimethylsiloxane) matrix. *Polym. Prepr.* **1999**, *40*(2), 271–272.
30. Bielawski, C. W.; Grubbs, R. H. Synthesis of ABA triblock copolymers via a tandem ring-opening metathesis polymerization (ROMP)—atom transfer radical polymerization (ATRP) approach. *Polym. Prepr.* **2000**, *41*(1), 12–13.
 31. Kilbinger, A. F. M.; Grubbs, R. H. Physical polymer networks via perfluoroarene-arene interactions. *Polym. Mater. Sci. Eng.* **2001**, *85*, 350–351.
 32. Grubbs, R. H. Olefin metathesis: a powerful reaction begins to reach its potential. *Adv. Synth. Catal.* **2002**, *344*(6+7), 569.
 33. Maynard, H. D.; Grubbs, R. H.; Hubbell, J. H. Peptide-substituted polymers as synthetic analogs of natural macromolecules. *Polym. Mater. Sci. Eng.* **2002**, *87*, 515.
 34. Pinnow, M. J.; Noyes, III., B. F.; Tran, H. V.; Tattersall, P. I.; Cho, S.; Klopp, J. M.; Bensen, N.; Frechet, J. M. J.; Sanders, D. P.; Grubbs, R. H.; Willson, C. G. Design and syntheses of mass persistent photoresists. *Polym. Mater. Sci. Eng.* **2002**, *87*, 403–404.
 35. Grubbs, R. H. The breadth and depth of olefin metathesis chemistry. *Polym. Mater. Sci. Eng.* **2003**, *88*, 66.
 36. Scherman, O. A.; Walker, R.; Grubbs, R. H. Synthesis of regioregular and stereoregular ethylene vinyl alcohol copolymers via romp of a protected cyclooctene-5,6-(*cis* and *trans*)-diol. *Polym. Prepr.* **2003**, *44*(1), 952–953.
 37. Jordan, J. P.; Scherman, O. A.; Grubbs, R. H. Synthesis of poly(vinylamine) copolymers by the ROMP of temporarily strained cyclic olefins. *Polym. Prepr.* **2003**, *44*(1), 841–842.
 38. Choi, T.-L.; Grubbs, R. H. Controlled living polymerization by fast initiating ruthenium catalyst. *Polym. Prepr.* **2003**, *44*(1), 783–784.
 39. Rutenberg, I. M.; Scherman, O. A.; Bao, Z.; Grubbs, R. H. Synthesis of polymer dielectric layers via romp for use in organic circuit devices. *Polym. Prepr.* **2003**, *44*(1), 566–567.

New β -linked pyrrole monomers: approaches to highly stable and conductive electrochromic polymers[☆]

Jocelyn M. Nadeau and Timothy M. Swager*

Department of Chemistry, Massachusetts Institute of Technology, 77 Massachusetts Avenue, Cambridge, MA 02139, USA

Received 8 May 2004; revised 25 May 2004; accepted 4 June 2004

Available online 2 July 2004

Abstract—An efficient synthetic route to β -linked dipyrrole monomers has been developed. Electrochemical polymerization of these monomers leads to the incorporation of polycyclic aromatic residues into a polymer backbone. The resulting conjugated polymer films are electroactive, robust electrochromic materials that are highly delocalized in their oxidized forms.

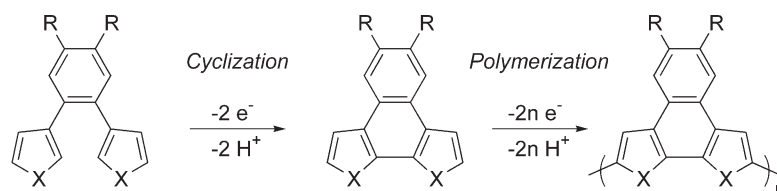
© 2004 Elsevier Ltd. All rights reserved.

1. Introduction

The electron-rich nature of pyrrole typically imparts its polymer derivatives with desirable intrinsic redox properties such as low oxidation potential, high conductivity, and high redox stability. Although there are numerous studies on native polypyrrole,¹ and in contrast to the vast literature on functionalized polythiophenes,² there are relatively few examples of functionalized polypyrrole derivatives.³ Herein we describe our recent progress toward incorporating pyrrole-based polycyclic aromatic units into a polymer backbone using the tandem cyclization/polymerization strategy depicted in **Scheme 1** ($X=NH$; $R=H$). This work was inspired by previous studies in our group, which demonstrated that thiophene-based polycyclic aromatic residues could be incorporated into a conducting polymer backbone using this strategy ($X=S$; $R=$ alkoxy groups).^{4,5} Electrochemical studies of the resulting poly(naphthodithiophene)s revealed a new class of robust, electrochromic conducting polymers. In polymers of this architecture, the polycyclic aromatic core enforces planarity between adjacent heterocycles within the aromatic unit. Increased

planarity leads to better π -overlap in the polymer thereby decreasing the bandgap and increasing conductivity. The β -linkage of the heterocycle to the benzene ring also increases π -overlap in the polymer backbone since fewer if any β -defects would be present due to steric constraints. The incorporation of pyrrole into such a scaffold is highly desirable as polypyrrole is inherently more conductive and better at stabilizing positive charge than simple polythiophene. Including polypyrrole's virtues in new conducting polymers offers potential performance enhancements that are needed in emerging organic electronic technologies. Such polymers could be used as antistatic coatings, in electrochromic devices, and, depending on the optical properties of the resulting polymers, as indium tin oxide replacement materials or optically transparent electrodes.

Herein we report a highly efficient synthetic route to β -linked dipyrrole monomers that can be used to generate families of conducting polymers with selected functionality. Electrochemical and spectroelectrochemical results reveal these materials to be highly electroactive and robust electrochromics.



Scheme 1. Tandem cyclization/polymerization strategy toward conducting polymers.

[☆] Supplementary data associated with this article can be found in the online version, at doi: 10.1016/j.tet.2004.06.016

Keywords: Conducting Polymers; Pyrrole; Electrochromic; Spectroelectrochemistry.

* Corresponding author. Tel.: +1-617-253-4423; fax: +1-617-253-7929; e-mail address: tswager@mit.edu

2. Results and discussion

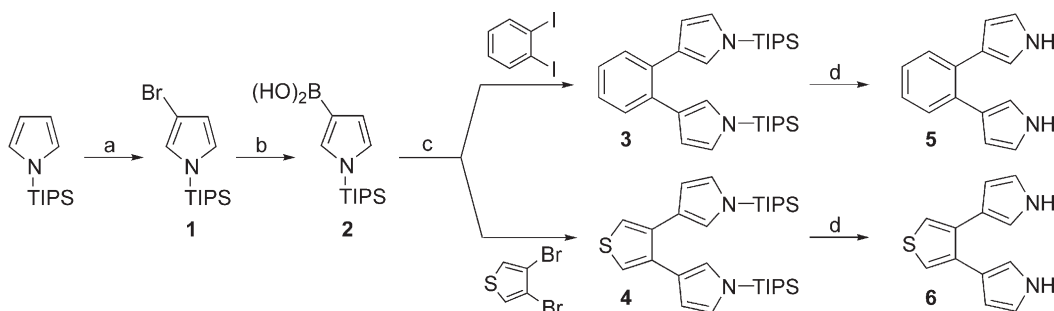
2.1. Synthesis of β -dipyrrole monomers

Suzuki coupling methodology was used to generate new β -linked dipyrrole monomers **5** and **6** from readily available halogenated aromatics (Scheme 2). Palladium coupling methodology was selected for its versatility, as it allows for the generation of families of molecules for comparative studies. Other Pd coupling methods, i.e. Stille and Kumada, were explored, but yields were poor and irreproducible upon scale up. Electrophilic attack on pyrrole occurs preferentially at the α -position, so an indirect strategy developed by Muchowski and co-workers was used to install the boronic acid Pd coupling functionality at the β -position.^{6,7} 1-(Triisopropylsilyl)pyrrole (1-TIPS-pyrrole) was brominated with NBS in THF to give 3-bromo-1-TIPS-pyrrole (**1**) in an 88% yield. Bromination at the β -position is favored because the steric bulk of the TIPS group blocks the more reactive α -sites. Boronic acid **2** was obtained by lithiation of **1** and quenching with $B(OCH_3)_3$ followed by an aqueous MeOH workup. Suzuki coupling of boronic acid **2** with 1,2-

diiodobenzene and 3,4-dibromothiophene gave TIPS-protected β -dipyrrole monomers, **3** and **4**, respectively. The isolated yield of the coupling step was modest (40–80% yield) compared to typical yields observed for thiophene boronic acids.⁴ Removal of the TIPS group with TBAF in THF generated the N–H functionality to give monomers **5** and **6** in 50–70% yield after purification. In addition to **5** and **6**, 1,3-di(pyrrolyl)benzene (**8**)⁸ was synthesized as a model compound to provide a monomer that is capable of electropolymerization but not intramolecular cyclization. Monomer **8** was obtained from 1,3-dibromobenzene in an overall 24% yield using the same methodology described above for **5** and **6** (Scheme 3).

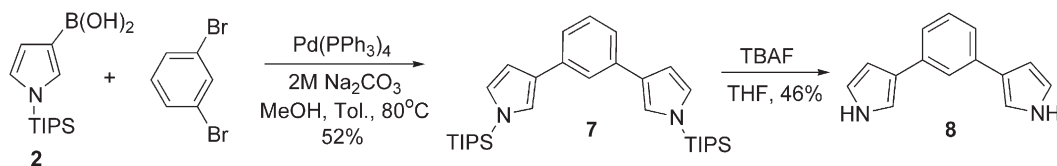
2.2. Electrochemical polymerization of β -dipyrrole monomers **5** and **6**

Electrochemical oxidation of monomer **5** was carried out to determine whether cyclization/polymerization occurs to give poly(**5**) (Scheme 4). Cyclic voltammetry (CV) of an electrolyte solution of dipyrrole monomer **5** and of poly(**5**) in a monomer-free electrolyte solution are shown in

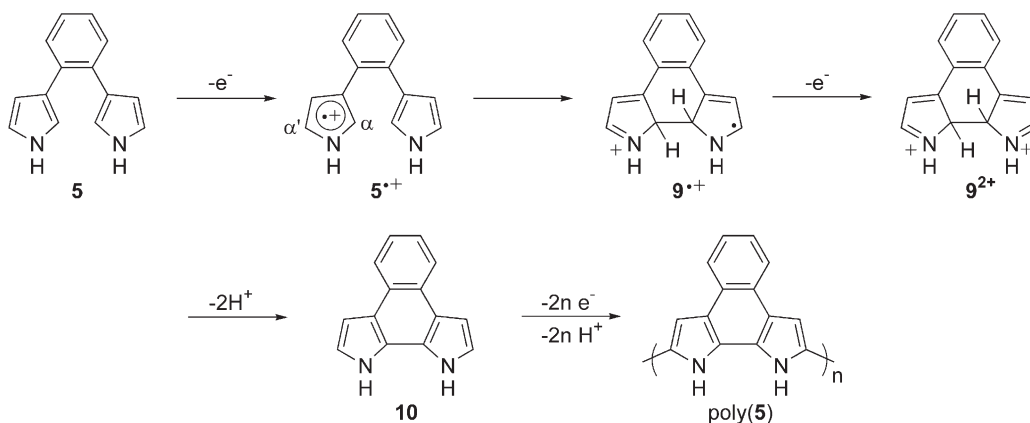


(a) NBS, THF, -78°C ; 88%. (b) (i) *n*-BuLi, THF, -78°C . (ii) $B(OCH_3)_3$. (iii) 50% $\text{MeOH}_{(\text{aq})}$; ~50%. (c) $\text{Pd}(\text{PPh}_3)_4$, 2M Na_2CO_3 , MeOH, Tol., 80°C ; 40–50%. (d) TBAF, THF; 50–75%.

Scheme 2. Synthetic route to β -linked dipyrrole monomers **5** and **6**.



Scheme 3. Synthetic route to model monomer **8**.



Scheme 4. Detailed mechanism proposed for oxidative cyclization/polymerization of monomer **5**.

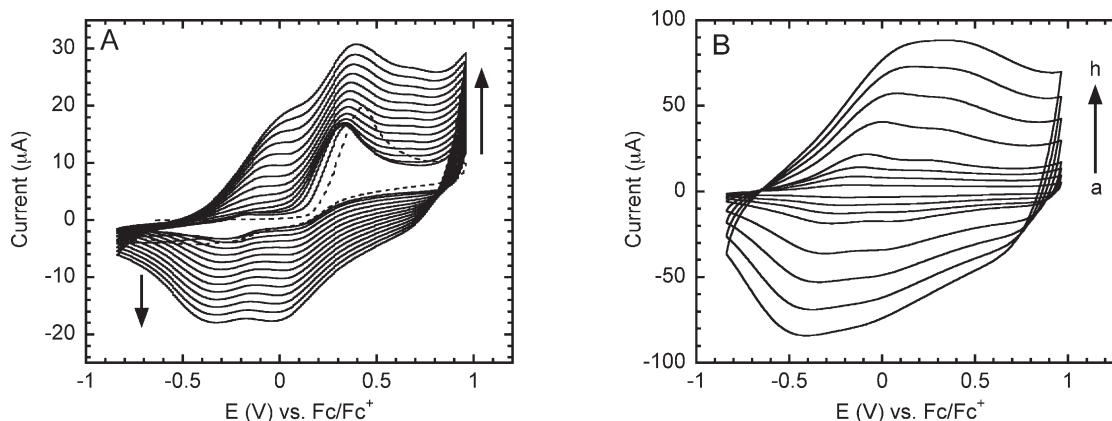


Figure 1. (A) Cyclic voltammetry of monomer **5** (~ 5 mM) in 0.1 M TBAPF₆ (CH₂Cl₂) cycled at 100 mV/s on a Pt button electrode; (B) cyclic voltammetry of resulting poly(**5**) in monomer-free electrolyte solution cycled at: (a) 25; (b) 50; (c) 75; (d) 100; (e) 200; (f) 300; (g) 400; (h) 500 mV/s.

Figure 1. Monomer **5** CV data (Fig. 1; Graph A) show only one distinct, irreversible oxidation wave during the first oxidative scan (dashed line; 0.45 V). Subsequent cycling leads to polymer deposition on the working electrode, as evidenced by the growth of lower-oxidation potential polymer-based redox activity that increases with successive scans. Scan rate dependence studies of poly(**5**) in a monomer-free electrolyte solution demonstrate that oxidation and reduction of the polymer is reversible (i.e., current scales linearly with scan rate) up to 500 mV/s (Fig. 1; Graph B). These results confirm that there is redox-active material confined to the electrode and that there are no significant kinetic barriers to charging and discharging of the film. In situ conductivity measurements for poly(**5**) grown on Pt interdigitated microelectrodes (IMEs) gave values of $0.38\text{--}1.2 \times 10^{-2}$ S cm⁻¹, suggesting that the polymer is highly conducting. Bulk conductivity values reported for polypyrrole are typically $10\text{--}100$ S cm⁻¹,⁹ but in situ IME measurements typically give values that are 4–5 orders of magnitude smaller than bulk values due to the nature of the film coverage on the IME.¹⁰ Conductivity values reported herein represent measurements made on IMEs that were not calibrated for uniform film thickness. Hence, the bulk conductivity of poly(**5**) is likely to actually be on the order of polypyrrole or better, but attempts to grow free-standing films of poly(**5**) to confirm this have yet to be successful.

We propose that oxidation of monomer **5** leads to intramolecular cyclization followed by polymerization to give poly(**5**) according to the mechanism outlined in Scheme 4. Removal of one electron from monomer **5** generates a radical cation on one pyrrole ring to give **5**^{•+}. The pyrrole radical cation reacts with the neighboring pyrrole ring to form a bond between the α -positions. Radical cation **9**^{•+} would readily undergo a one-electron oxidation to give dication **9**²⁺. Subsequent loss of two protons from **9**²⁺ provides the cyclized product **10** that undergoes further oxidation to generate poly(**5**). It is also possible that **9**^{•+} may shed one proton before undergoing additional oxidation; however such deprotonation reactions are generally slower than electron transfer. It could be argued that radical cation **5**^{•+} might undergo reaction at the α' -position with another monomer in solution. However, the intramolecular reaction is likely to be favored entropically and formation of a

polycyclic aromatic residue is likely to provide significant driving force. Moreover, there is some evidence that 3-phenylpyrroles react with electrophiles preferentially at the α -position versus the α' -position, although studies of this nature are limited.¹¹

The CV data for monomer **5** show only one irreversible definable oxidation peak, although we initially expected two peaks representing the independent oxidations of **5** and **10**. However, given the very close potentials for the related oxidations in our earlier thiophene studies,^{4,5} it seems likely that the two waves are simply unresolved. In order to address this issue directly, it would be desirable to synthesize cyclized monomer **10** to verify that its electrochemical behavior as poly(**5**). However, chemical oxidation of monomer **5** with FeCl₃ consistently led to the formation of intractable polymer, even at short reaction times. We further investigated whether treatment of TIPS-protected **3** with FeCl₃ produces the cyclized product since this monomer does not undergo electropolymerization. Only starting material **3** was isolated from the reaction mixture after a reductive anhydrous methanol quench and workup. We attribute this lack of reactivity to the steric bulk of the TIPS groups, which prevents the pyrrole rings from achieving coplanarity.

The cyclization/polymerization mechanism was also explored for monomer **6**. The redox behavior of monomer **6** and poly(**6**) is not as robust as that observed for monomer **5** and poly(**5**) (Fig. 2). The CV data for monomer **6** show a broad, irreversible overlapping oxidative peak in the first scan (dashed line in Fig. 2; Graph A) that is at a higher potential (0.67 V) than the analogous peak seen for monomer **5** (0.45 V). The higher potential is consistent with the larger angle (72°) between the pyrroles in **6**, which would impede its cyclization compared to **5** (60°). Further cycling leads to lower potential polymer-based redox activity. Unlike monomer **5**, successive scans typically leads to film passivation thwarting further polymer growth. Poly(**6**) CV data (Fig. 2; Graph B) show that its redox kinetics are reversible up to 300 mV/s. These results suggest that charge transport in poly(**6**) is not as efficient as in poly(**5**). In situ conductivity measurements on uncalibrated IMEs for poly(**6**) gave values of $0.18\text{--}1.5 \times 10^{-3}$ S cm⁻¹.

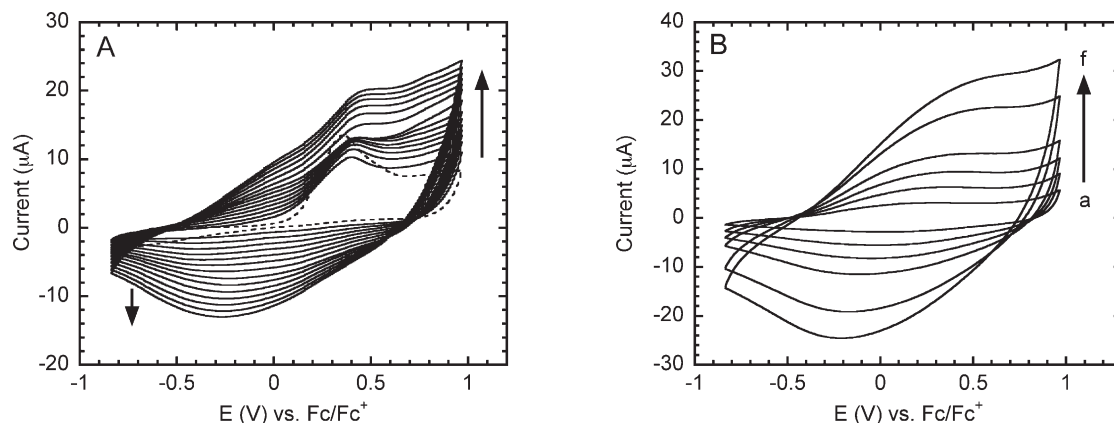


Figure 2. (A) Cyclic voltammetry of monomer **6** (~ 5 mM) in 0.1 M TBAPF₆ (CH₂Cl₂) cycled at 100 mV/s on a Pt button electrode; (B) cyclic voltammetry of resulting poly(**6**) in monomer-free electrolyte solution cycled at: (a) 25; (b) 50; (c) 75; (d) 100; (e) 200; (f) 300 mV/s.

Collectively, these results suggest that poly(**6**) is not as conductive as poly(**5**). It might be that this monomer does not fully cyclize and may also undergo competitive polymerization through the redox-active thiophene, thereby leading to defects in the polymer backbone.

2.3. Spectroelectrochemistry and coulometry

Spectroelectrochemistry is a useful technique for studying conducting polymers, as it allows one to study changes in absorption spectra as a function of applied voltage. This technique was used to evaluate the electrochromicity, charge delocalization and related donor–acceptor transitions that will arise from proximate neutral and oxidized segments in poly(**5**), poly(**6**), and poly(**8**) (Fig. 3; Graphs A, B, and C, respectively). Oxidation of conducting polymers leads to charge delocalization along the polymer backbone,

which gives rise to changes in the polymer's optical transitions. As shown for poly(**5**) in Figure 4, the neutral polymer is composed of isolated aromatic pyrrole units. Oxidation of the polymer leads to a structure with increased quinoidal character, which facilitates charge delocalization along the polymer backbone. This charge delocalization results in a red shift of the polymer's absorption spectrum. The extent of the red shift upon oxidation is a measure of the degree of charge delocalization.

Neutral poly(**5**) is yellow and shows a broad absorption centered at 3.2 eV (Fig. 3; Graph A). Oxidation to its conducting form results in a red shift where an intermediate band at 2.3 eV gives way to a broad band that extends from the visible out into the near-IR region (NIR region < 1.6 eV). Not surprisingly, oxidized poly(**5**) is black, owing to its significant absorption in the visible region.

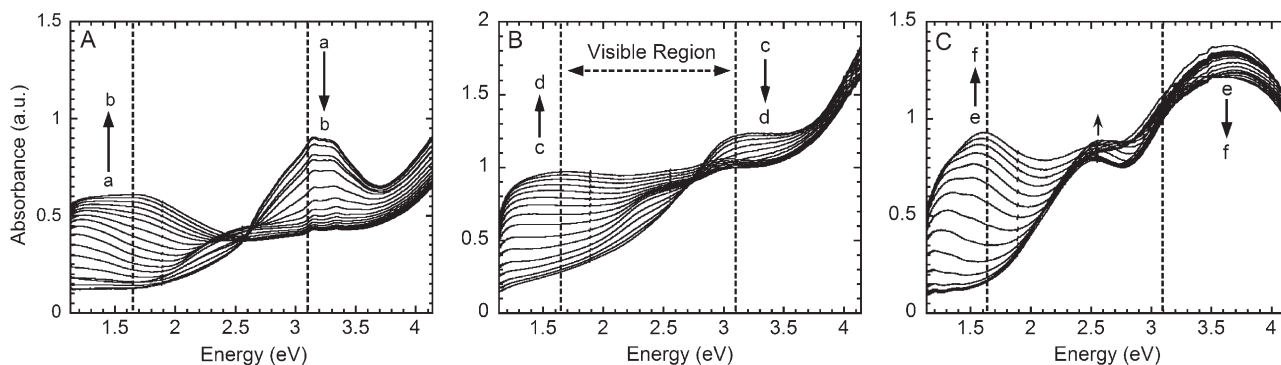


Figure 3. Spectroelectrochemical data for thin polymer films grown on ITO-coated glass. The experiment was conducted in 0.1 M TBAPF₆ (CH₂Cl₂) using 100 mV steps within the following potential windows: (A) poly(**5**) (a and b) -0.93 to $+0.78$ V; (B) poly(**6**) (c and d) -0.83 to $+0.98$ V; and (C) poly(**8**) (e and f) -0.93 to $+0.98$ V.

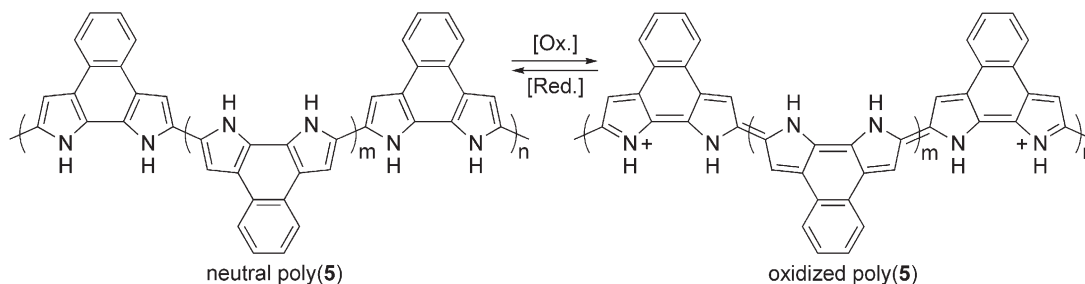


Figure 4. Structures of neutral and oxidized forms of poly(**5**).

Neutral poly(**6**) is yellowish-mauve with a broad absorption at 3.1 eV (Fig. 3; Graph B). Oxidation of poly(**6**) also gives a black film, and the absorption band shifts to a weak intermediate band at 2.3 eV that disappears upon further oxidation to give a broad, lower energy band that spans the visible and extends into the NIR region. The spectroelectrochemical data for poly(**5**) and poly(**6**) are actually quite similar, implying that they have similar structures; however, poly(**5**) is more delocalized as its low-energy band extends further into the NIR region. Poly(**5**) and poly(**6**) both appear to favor a highly delocalized structure in their oxidized forms. Monomer **8** was used as a model because it can electropolymerize, but the pyrrole units are too far apart to undergo intramolecular cyclization (see Supporting information for CV data on monomer **8** and poly(**8**)). Neutral poly(**8**) has two bands centered at 3.7 and 2.6 eVs. Upon oxidation, the former band decreases slightly and the latter increases slightly, which is attended by the appearance of a relatively sharp visible/NIR absorption band that is higher energy than the analogous peak observed for poly(**5**) and poly(**6**). Collectively, these results suggest that the degree of charge delocalization in the polymer backbone decreases in the following order: poly(**5**) > poly(**6**) > poly(**8**). It is likely that poly(**6**) is only partially cyclized within the polymer, which leads to interruption in π -overlap and decreased delocalization.

We were interested to see if our polycyclic pyrrole polymers are capable of displaying improved charge storage capacity relative to polypyrrole. To assess this, we used the amount of irreversible charge integrated through the polymerization to determine the number of moles of monomers deposited on the electrode. Oxidation of polypyrrole leads to one cationic charge for every 3–4 repeating units.¹² We have compared the charge storage capacity of poly(**5**), poly(**6**), and poly(**8**) to that of polypyrrole when oxidized at +0.98 V and find that poly(**5**) and poly(**8**) have equivalent charge storage capacity to polypyrrole determined under identical conditions. Poly(**6**) exhibited a 30% higher charge storage capacity per pyrrole despite its less conductive nature. This improved charge storage capacity reflects the electron rich nature of the thiophene moiety in poly(**6**) relative to the benzene subunit in poly(**5**) and poly(**8**).

3. Conclusions

We have developed an efficient synthetic route to β -linked dipyrrole monomers using Suzuki coupling methodology. Electrochemical oxidation of these monomers leads to the incorporation of polycyclic aromatic residues into a polymer backbone to give highly robust, electrochromic conducting polymers.

4. Experimental

4.1. General comments

¹H and ¹³C NMR spectra were determined at 300 MHz using a Varian Mercury-300 spectrometer and are referenced to residual CHCl₃ (7.27 ppm for ¹H and 77.23 ppm

for ¹³C). Melting points are uncorrected. High-resolution mass spectra (HRMS) were determined at the MIT Department of Chemistry Instrumentation Facility (DCIF) on a Bruker Daltonics APEX II 3 Tesla FT-ICR-MS. Elemental analysis was conducted at Quantitative Technologies, Inc. (Whitehouse, NJ). Compounds **1** and **2** were synthesized according to literature methods.^{6,7} All air and water sensitive synthetic manipulations were performed under an argon atmosphere using standard Schlenk techniques. Tetrahydrofuran (THF), toluene, and dichloromethane (CH₂Cl₂) were passed through activated alumina prior to storage under an inert atmosphere (Innovative Technologies, Inc.). All electrochemical measurements were made with an Autolab II with PGSTAT 30 potentiostat (Eco Chemie). Cyclic voltammetry was performed at a Pt button electrode in an argon-purged, one chamber/three electrode cell. The reference electrode was a quasi-internal Ag wire (BioAnalytical Systems) submersed in 0.01 M AgNO₃/0.1 M TBAPF₆ in anhydrous acetonitrile, and a Pt coil or flag was used as the counter electrode. All potentials are referenced to the Fc/Fc⁺ redox couple. All experiments were conducted in 0.1 M TBAPF₆ in CH₂Cl₂ under ambient laboratory conditions. In situ conductivity measurements were performed on polymer films grown on 5 μ m Pt interdigitated microelectrodes (Abtech Scientific, Inc.) and are uncalibrated. Spectroelectrochemistry was carried out on polymer films deposited on indium-tin oxide (ITO) coated glass, and absorption spectra were determined on an Agilent 8453 diode array spectrophotometer.

4.1.1. 1,2-Di(1-triisopropylsilyl-3-pyrrolyl)benzene (3). A 50 mL Schlenk flask was charged with 1-TIPS-pyrrole-3-boronic acid (**2**) (5.0 g; 19 mmol), 1,2-diodobenzene (627 mg; 1.9 mmol), toluene (10 mL), methanol (10 mL), and 2.0 M Na₂CO₃ (1 mL). The solution was purged with argon for 5 min followed by addition of Pd(PPh₃)₄ (44 mg; 0.038 mmol) under a positive flow of argon. The flask was sealed, and the reaction was heated at 80 °C for 4 h. Upon cooling to room temperature, the reaction mixture was washed with water, and the aqueous layer was extracted with ethyl acetate. The organic layers were combined, dried over MgSO₄, filtered, and concentrated under reduced pressure. The crude product was purified by column chromatography on silica gel (20% CH₂Cl₂ in hexanes) followed by recrystallization from EtOH/H₂O to give a colorless, crystalline solid (420 mg; 42% yield): mp 89–91 °C; ¹H NMR (300 MHz; CDCl₃) δ 1.09 (d, $J=7.5$ Hz, 36H), 1.40 (sept, $J=7.5$ Hz, 6H), 6.26–6.28 (m, 2H), 6.65–6.67 (m, 2H), 6.68–6.69 (m, 2H), 7.20 (dd, $J=3.3, 5.7$ Hz, 2H), 7.42 (dd, $J=3.3, 5.7$ Hz, 2H); ¹³C NMR (300 MHz; CDCl₃) δ 11.86, 18.07, 111.71, 123.21, 123.50, 125.94, 127.11, 130.21, 134.95. MS (ESI) exact mass calculated for C₃₂H₅₂N₂Si₂ [M+Na]⁺ 543.3561, found 543.3576. Repeated attempts to obtain elemental data were unsuccessful as the carbon number was consistently low; however, the hydrogen and nitrogen data were always within the accepted limits (calculated H, 10.06; N, 5.38, found H, 10.15; N, 5.37).

4.1.2. 3,4-Di(1-triisopropylsilyl-3-pyrrolyl)thiophene (4). Prepared as described for **3** from 3,4-dibromothiophene (298 mg; 1.23 mmol) to give a colorless crystalline solid (39% yield): mp 99–101 °C; ¹H NMR (300 MHz; CDCl₃) δ

1.09 (d, $J=7.2$ Hz, 36H), 1.40 (sept, $J=7.5$ Hz, 6H), 6.37–6.38 (m, 2H), 6.70–6.73 (m, 4H), 7.16 (s, 2H); ^{13}C NMR (300 MHz; CDCl_3) δ 11.80, 18.02, 111.29, 120.83, 122.15, 122.75, 123.85, 136.65. MS (EI) exact mass calculated for $\text{C}_{30}\text{H}_{50}\text{N}_2\text{SSi}_2$ $[\text{M}]^+$ 526.3228, found 526.3205. Anal. calculated for $\text{C}_{30}\text{H}_{50}\text{N}_2\text{SSi}_2$: C, 68.38; H, 9.56; N, 5.32; S, 6.08. Found, C, 68.37; H, 9.81; N, 5.21; S, 6.22.

4.1.3. 1,3-Di(1-triisopropylsilyl-3-pyrrolyl)benzene (7).

Prepared as described for **3** from 1,3-dibromobenzene to give a colorless crystalline solid (52% yield): mp 155–156 °C; ^1H NMR (300 MHz; CDCl_3) δ 1.16 (d, $J=7.2$ Hz, 36H), 1.51 (sept, $J=7.5$ Hz; 6H), 6.67–6.69 (m, 2H), 6.83–6.85 (m, 2H), 7.10–7.11 (m, 2H), 7.28–7.39 (m, 3H), 7.72–7.73 (m, 1H); ^{13}C NMR (300 MHz; CDCl_3) δ 11.90, 18.07, 109.04, 120.89, 122.67, 122.79, 125.26, 127.40, 128.88, 136.46. MS (ESI) exact mass calculated for $\text{C}_{32}\text{H}_{52}\text{N}_2\text{Si}_2$ $[\text{M}+\text{H}]^+$ 521.3742, found 521.3724.

4.1.4. 1,2-Di(3-pyrrolyl)benzene (5).

A 1.0 M solution of TBAF in THF (1.7 mL; 1.7 mmol) was added to **3** (420 mg; 0.82 mmol) dissolved in THF. The reaction was stirred at room temperature under argon for 15 min. The solvent was removed under reduced pressure, and the crude product was purified by column chromatography on silica gel (20% hexanes in CH_2Cl_2) to give a colorless oil that crystallized upon standing (132 mg; 78% yield): mp 95–96 °C; ^1H NMR (300 MHz; CDCl_3) δ 6.20–6.22 (m, 2H), 6.65–6.67 (m, 2H), 6.72–6.74 (m, 2H), 7.25 (dd, $J=3.3, 5.4$ Hz, 2H), 7.44 (dd, $J=3.3, 5.4$ Hz, 2H), 8.08 (br s, 2H); ^{13}C NMR (300 MHz; CDCl_3) δ 109.74, 116.86, 117.30, 124.99, 126.24, 130.24, 135.02. MS (ESI) exact mass calculated for $\text{C}_{14}\text{H}_{12}\text{N}_2$ $[\text{M}+\text{Na}]^+$ 231.0893, found 231.0897.

4.1.5. 3,4-Di(3-pyrrolyl)thiophene (6).

Prepared as described for **5** from compound **4** to give a colorless oil (50% yield): ^1H NMR (300 MHz; CDCl_3) δ 6.28–6.31 (m, 2H), 6.73–6.77 (m, 4H), 7.18 (s, 2H), 8.18 (br s, 2H); ^{13}C NMR (300 MHz; CDCl_3) δ 109.34, 116.47, 117.58, 120.11, 121.26, 136.46. MS (ESI) exact mass calculated for $\text{C}_{12}\text{H}_{10}\text{N}_2\text{S}$ $[\text{M}]^+$ 215.0637, found 215.0646.

4.1.6. 1,3-Di(3-pyrrolyl)benzene (8).

Prepared as described for **5** from compound **7** to give a colorless oil (46% yield): ^1H NMR (300 MHz; CDCl_3) δ 6.60–6.62 (m, 2H), 6.85–6.88 (m, 2H), 7.13–7.15 (m, 2H), 7.31–7.40 (m, 3H), 7.72–7.73 (m, 1H), 8.28 (br s, 2H); ^{13}C NMR (300 MHz; CDCl_3) δ 106.91, 114.82, 118.99, 122.64, 122.98, 125.45, 129.07, 136.22. MS (ESI) exact mass calculated for $\text{C}_{14}\text{H}_{12}\text{N}_2$ $[\text{M}]^+$ 209.1073, found 209.1076.

Acknowledgements

The authors are grateful for financial support provided by the Army Research Office's Tunable Optical Polymers MURI program and for the use of resources provided by the Institute for Soldier Nanotechnologies, also funded by the Army Research Office.

References and notes

- (a) In *Handbook of Conducting Polymers*; 2nd ed. Skotheim, T. A., Elsenbaumer, R. L., Reynolds, J. R., Eds.; Marcel Dekker: New York, 1998. (b) Sadki, S.; Schottland, P.; Brodie, N.; Sabouraud, G. *Chem. Soc. Rev.* **2000**, *29*, 283–293.
- (a) Roncali, J. *Chem. Rev.* **1992**, *92*, 711–738. (b) McCullough, R. D. *Adv. Mater.* **1998**, *10*, 93–116.
- (a) Deronzier, A.; Moutet, J. C. *Acc. Chem. Res.* **1989**, *22*, 249–255. (b) Masuda, H.; Kaeriyama, K. *Synth. Met.* **1990**, *38*, 371–379. (c) Chen, J.; Too, C. O.; Wallace, G. G.; Swiegers, G. F.; Skelton, B. W.; White, A. H. *Electrochim. Acta* **2002**, *47*, 4227–4238. (d) Lee, D.; Swager, T. M. *J. Am. Chem. Soc.* **2003**, *125*, 6870–6871. (e) Groenendaal, L.; Zotti, G.; Aubert, P. H.; Waybright, S. M.; Reynolds, J. R. *Adv. Mater.* **2003**, *15*, 855–879. (f) Godillot, P.; Youssoufi, H. K.; Srivastava, P.; El Kassmi, A.; Garnier, F. *Synth. Met.* **1996**, *83*, 117–123.
- Tovar, J. D.; Swager, T. M. *Adv. Mater.* **2001**, *13*, 1775–1780.
- Tovar, J. D.; Rose, A.; Swager, T. M. *J. Am. Chem. Soc.* **2002**, *124*, 7762–7769.
- Bray, B. L.; Mathies, P. H.; Naef, R.; Solas, D. R.; Tidwell, T. T.; Artis, D. R.; Muchowski, J. M. *J. Org. Chem.* **1990**, *55*, 6317–6328.
- Alvarez, A.; Guzman, A.; Ruiz, A.; Velarde, E.; Muchowski, J. M. *J. Org. Chem.* **1992**, *57*, 1653–1656.
- Fumoto, Y.; Uno, H.; Tanaka, K.; Tanaka, M.; Murashima, T.; Ono, N. *Synthesis* **2001**, *3*, 399–402.
- Diaz, A. F.; Castillo, J. I.; Logan, J. A.; Lee, W. Y. *J. Electroanal. Chem.* **1981**, *129*, 115–132.
- Kingsborough, R. P.; Swager, T. M. *Adv. Mater.* **1998**, *10*, 1100–1104.
- Balasubramanian, T.; Strachan, J. P.; Boyle, P. D.; Lindsey, J. S. *J. Org. Chem.* **2000**, *65*, 7919–7929.
- (a) Kanazawa, K. K.; Diaz, A. F.; Geiss, R. H.; Gill, W. D.; Kwak, J. F.; Logan, J. A.; Rabolt, J. F.; Street, G. B. *J. Chem. Soc. Chem. Commun.* **1979**, 854–855. (b) Diaz, A. F.; Castillo, J. I. *J. Chem. Soc. Chem. Commun.* **1980**, 397–398.

Catalytic syntheses of alternating, stereoregular ethylene/cycloolefin copolymers[☆]

Adrien R. Lavoie and Robert M. Waymouth*

Department of Chemistry, Stanford University, Stanford, CA 94305, USA

Received 1 April 2004; revised 26 May 2004; accepted 4 June 2004

Available online 8 July 2004

Dedicated to Professor Robert Grubbs on the occasion of his award of the Tetrahedron Prize

Abstract—The alternating stereospecific copolymerization of ethylene with cycloolefins (cyclopentene, cycloheptene, and cyclooctene) has been investigated with a series of constrained geometry titanium catalysts (CGCs). The metallocene $\text{IndSiMe}_2(\text{tBuN})\text{TiCl}_2$ was found to generate highly alternating and stereoregular cycloolefin-*co*-ethylene polymers while $\text{Me}_4\text{CpSiMe}_2(\text{tBuN})\text{TiCl}_2$ produced alternating atactic polymers. In addition, novel Ti-complexes of the general formula $\text{benz}[6.7]\text{indenylSiMe}_2(\text{tBuN})\text{TiMe}_2$ were synthesized and fully characterized. The chiral indenyl Ti complexes were found to produce exclusive 1,2-enchainment of the cycloolefin to generate highly stereoregular and alternating copolymers.
 © 2004 Elsevier Ltd. All rights reserved.

1. Introduction

Single-component olefin polymerization catalysts have provided new opportunities for the synthesis of novel polymer structures from common olefin feedstocks.^{1–4} The synthesis of new materials from comonomer feedstocks requires catalysts that can simultaneously control the the composition, sequence distribution and stereochemistry of monomer insertion. Cyclo-olefin copolymers (COCs) provide an intriguing target for such molecular engineering as the random copolymers have been recently targeted as a novel class of engineering plastics,^{5–12} with potential optoelectronic applications in data transfer and storage (polymer optical fibers, compact discs).¹³ While ethylene/cycloolefin copolymers with random sequence distributions are typically amorphous glasses, alternating copolymers such as isotactic ethylene/cyclopentene ($T_m=185\text{ }^\circ\text{C}$)^{5,14–16} and ethylene/norbornene ($T_m=295\text{ }^\circ\text{C}$) are semi-crystalline.^{5,12,15–19}

Natta was the first to report on the alternating copolymerization of ethylene and cyclopentene with Ziegler–Natta catalysts.^{14,20} Natta recognized that alternating copolymers

were accessible due to the reticence of many coordination catalysts to homopolymerize cyclopentene. Fractionation of the ethylene/cyclopentene copolymers with boiling solvents yielded a highly crystalline fraction with a melting point of $185\text{ }^\circ\text{C}$, implicating a stereoregular microstructure for these copolymers. Assignment of the material as isotactic was inferred from X-ray diffraction. Natta also disclosed studies on the copolymerization of ethylene with cycloheptene;^{20,21} Kaminsky et al. later described the copolymerization of ethylene with cyclopentene, cycloheptene, and norbornene with homogeneous zirconocene catalysts.^{4,22} For the zirconocene catalysts, copolymerization of ethylene and cyclopentene leads to relatively low incorporation of cyclopentene (up to 37.8% though typically $<20\%$) and as the percent of cyclopentene incorporation increases significant amounts of both 1,2 and 1,3-cyclopentene enchainment are observed.^{23–27} The incorporation of 1,3-enchainment cyclopentane structures has been attributed to initial 1,2-insertion of cyclopentene, followed by β -H elimination, rotation and re-insertion (Fig. 1).^{28–30}

In contrast to the zirconocene catalysts, titanium catalysts exhibit a high selectivity for 1,2-enchainment of cyclopentene. The copolymerization of ethylene and cyclopentene with bis(phenoxyimine) catalysts¹⁶ or constrained geometry

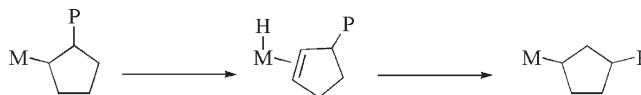


Figure 1. Isomerization mechanism for the generation of 1,3-enchainment CPE units.

[☆] Supplementary data associated with this article can be found in the online version, at doi: 10.1016/j.tet.2004.06.020

Keywords: Alternating copolymers; Cycloolefin; Cyclopentene; Cycloheptene; Cyclooctene; Constrained-geometry; Ziegler–Natta catalysis.

* Corresponding author. Tel.: +1-650-723-4515; fax: +1-650-736-2262; e-mail address: waymouth@stanford.edu

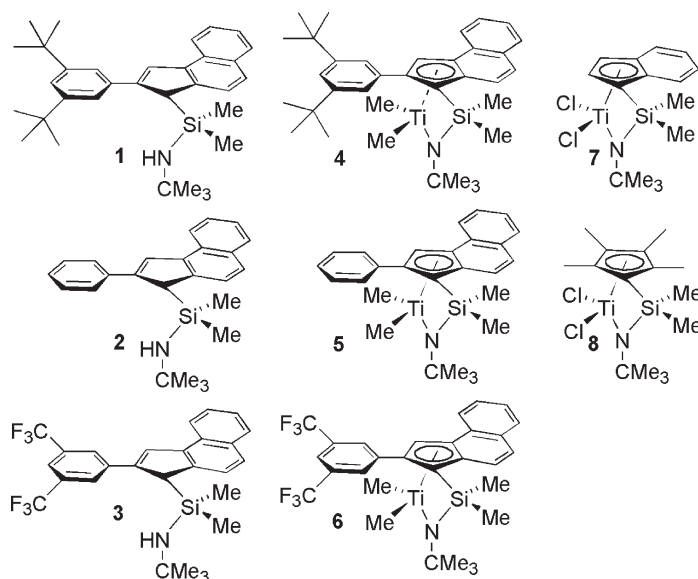


Figure 2. Ligands and precatalysts investigated for ethylene/cycloolefin copolymerization.

monocyclopentadienyl amido catalysts¹⁵ yields highly regioregular alternating ethylene/cyclopentene copolymers. The stereoselectivity of these copolymerizations depends sensitively on the ligand geometry: the bis(phenoxyimine) Ti catalysts¹⁶ and achiral constrained geometry catalysts yield atactic alternating E/cP copolymers, whereas the chiral indenyl constrained geometry catalysts yield stereoregular alternating E/cP copolymers.¹⁵ Here, we report the synthesis of a family of chiral constrained geometry catalysts and their activity for the alternating stereospecific copolymerization of cyclopentene, cyclohexene and cyclooctene.

2. Results and discussion

Alternating copolymers can provide new classes of thermoplastics if both the sequence and stereoselectivity of monomer insertion is controlled.^{5,15,18,19} For example, highly alternating stereoregular ethylene/norbornene copolymers can exhibit melting points as high as 295 °C. For these studies, we focused on the copolymerization of ethylene and cycloalkenes, as ethylene/cyclopentene copolymers crystallize more rapidly from the melt and provide simpler NMR spectra^{15,16} than the ethylene/norbornene copolymers.^{9,17,31} To investigate the influence of ligand structure on ethylene/cycloalkene copolymerizations, we have prepared a family of chiral constrained geometry catalysts with 2-aryl substituted benzannulated indenenes (Fig. 2).^{32,33} Previous studies in our group have shown that bis(2-arylindenyl) metallocene catalysts are

surprisingly effective at incorporating α -olefins and are far superior to bis(indenyl) metallocenes.^{31,34–38}

The synthesis of 2-arylbenz[6.7]indene ligands (1–3) proceeded smoothly by analogy to previously reported literature methods.³⁹ Deprotonation of the 2-arylbenz[6.7]indenenes with *n*-BuLi followed by reaction with Me₂SiCl₂ led to regioselective silylation (See Fig. 3).^{33,40,41} Subsequent Si–Cl metathesis with ^tBuNH₂ generated the desired chiral racemic ligands with concomitant generation of ^tBuNH₃Cl. The regioselectivity of the silylation was confirmed by ¹H NMR (COSY and ROESY) analysis of compound 3. The COSY spectrum revealed that the four aryl protons at 8.24, 7.93, 7.56, and 7.49 ppm were coupled and can thus be assigned to ring A (See Fig. 4). The two aryl protons resonating at 7.78 and 7.72 ppm were coupled and assigned to ring B. A ROESY spectrum indicated a NOE (nuclear overhauser effect) between the Si–CH₃ at 4.41 ppm and cyclopentadienyl Cp–H at 7.77 ppm and the aryl proton at 7.78 ppm of ring B (Fig. 4). These data suggest that silylation occurred predominantly at the sterically less hindered methylenic carbon of the benz[6.7]indene starting material. Given the similarity in ¹H NMR chemical shifts, compounds 1 and 2 were assigned analogous structures.

The syntheses of these Ti-dimethyl complexes^{31,34} were carried using the one-pot procedure described by Resconi et al.⁴¹ where 4 equiv. of MeLi are added to the indenylamido ligand followed by the addition of 1 equiv. of TiCl₄ to give the dimethyl complexes in yields of

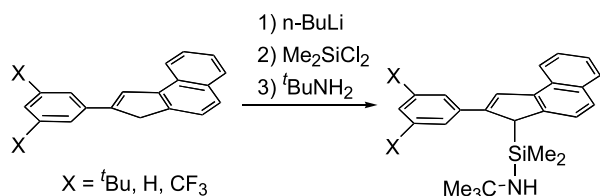


Figure 3. Ligand synthesis.

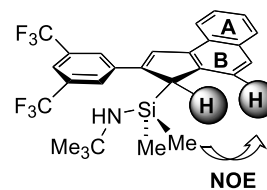


Figure 4. Spectroscopic (COSY/ROESY) isomer-determination for 2-[3,5-(CF₃)₂C₆H₃]-benz[6.7]indeneSiMe₂NH(^tBu) (3).

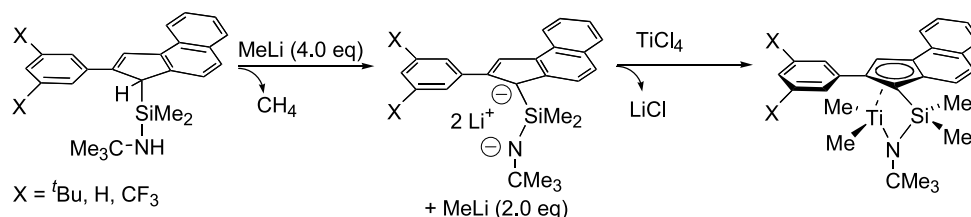


Figure 5. Synthesis of complexes.

21–27%. (Fig. 5). The structure of (2-[CF₃]₂-benz[6.7]-Indenyl)-SiMe₂(^tBuN)TiMe₂, (**6**), was confirmed by ROESY experiments (Fig. 6). In this case, NOEs were observed from the Cp-*H* at 7.95 ppm to both of the diastereotopic TiMe₂ resonances at 0.95 and -0.23 ppm thus implicating a titanium complex in which the concave bay of the benz[6.7]indenyl system was positioned above the TiMe₂ groups. Analogous structures were assigned for compounds **5** and **6** based on their structural and spectroscopic (¹H NMR) similarities.

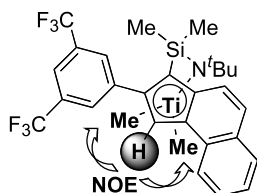


Figure 6. Spectroscopic (COSY/ROESY) isomer-determination for [(2-[CF₃]₂-benz[6.7]Indenyl)SiMe₂(^tBuN)TiMe₂ (**6**).

3. Copolymerization

Copolymerizations were conducted in 150 mL thick-walled glass reactor bottles that were charged with modified methylaluminoxane (MMAO-4, Akzo) toluene, and the desired cycloolefin. Once charged, the bottles were fitted to an airtight reactor-head with a pressure gauge. The

apparatus was charged to 20 psig with the desired ethylene feed (E:Ar dilutions varied between 1:0 and 1:10) followed by equilibration for 30 min. Low concentrations of ethylene were employed in order to obtain high cycloolefin incorporations (50 mol%). The reactions were initiated upon injection of a toluene solution of the precatalyst. This new family of 2-arylbenz[6.7]indenyl catalysts was found to be highly effective for the copolymerization of ethylene with cyclopentene, cycloheptene, and cyclooctene. Attempts to copolymerize cyclohexene were not successful, consistent with previous literature accounts.^{22,42}

Results for the copolymerization of cyclopentene and ethylene with complexes **4–8** are shown in Table 1. Under these conditions, the productivities for E/Cp copolymerization were modest and ranged from 5 to 469 kg/mol h.¹⁵ Copolymers containing close to 50 mol% were obtained under dilute ethylene feeds of 20 psig with E:Ar ratios of 1:6 or 1:10. As the primary focus of these investigations was to generate alternating copolymers, most of the conditions were ‘ethylene-starved’ and thus the productivities are not likely representative of the catalyst activities. Comparison of the different catalysts reveal that the indenyl type catalysts (**4–7**) were better at incorporating cycloolefins and generated higher molecular weight polymers than Me₄CpSiMe₂(^tBuN)TiCl₂ **8** (Table 1, entries 1–2 and 5–9). No clear pattern emerges for the influence of ligand structure on copolymerization behavior: with the

Table 1. Ethylene-cyclopentene copolymerizations with catalysts derived from **4–8** with MMAO-4¹⁵

Entry	Precat ^a	[Ti] M×10 ⁻⁴	T _p (°C)	Time (h)	E:Ar ratio	Yield (g)	Prod ^b	% cP ^c	T _g (°C)	T _m (ΔH _f) ^d	M _w /M _n	M _n ^e
1	7	4.2	25	1.5	1:6	0.49	39	50 ^c	16	183 (36)	1.9	33.9
2	8	5.2	25	4.0	1:6	0.43	10	40 ^c	-22	127 (15)	2.2	8.3
3	7	4.1	60	1.5	1:6	0.31	25	49 ^c	24	175 (36)	2.7	4.6
4	8	5.2	60	4.0	1:6	0.72	17	34 ^c	-18	100 (4)	2.2	7.5
5	7	4.1	25	1.5	1:0	2.91	234	41 ^c	5	123 (12)	1.7	71.7
6	8	5.2	25	1.0	1:0	2.32	225	15 ^c	-27	72 (33)	2.7	5.6
7	4	5.2	25	0.5	1:0	2.43	469	38 ^f	—	—	2.1	65.4
8	5	5.1	25	0.5	1:0	0.35	68	19 ^f	—	—	2.2	47.0
9	6	5.1	25	0.5	1:0	1.45	280	38 ^f	—	—	2.1	35.9
10	4	5.4	25	4.0	1:6	0.31	7	47 ^f	17	152 (26)	2.2	13.3
11	5	5.1	25	4.0	1:6	0.69	17	48 ^f	15	176 (34)	1.8	26.5
12	6	5.3	25	4.0	1:6	0.20	5	48 ^f	18	149 (25)	2.0	16.1

^a Precat ^tBu=**4**; H=**5**; CF₃=**6**; Ind=**7**; Me₄Cp=**8**; E=ethylene; cP=cyclopentene; Ar=argon, total pressure=20 psig. For all experiments, the ratio of Ti:MMAO was 1:400–500 mequiv.

^b Productivity in [kg/(mol Ti·h)].

^c Determined by integration of all ¹³C NMR resonances.¹⁵

^d T_m in °C; ΔH_f in J/g.

^e GPC molecular weights and polydispersities vs. polystyrene standards in units of g/mol×10⁻³.

^f Determined by integration of only the CH₂ and not CH resonances. This method is expected to be slightly more accurate given that relaxation delays (d₁) of the CH₂ nuclei for E and cP should be similar thus leading to more accurate integrals.

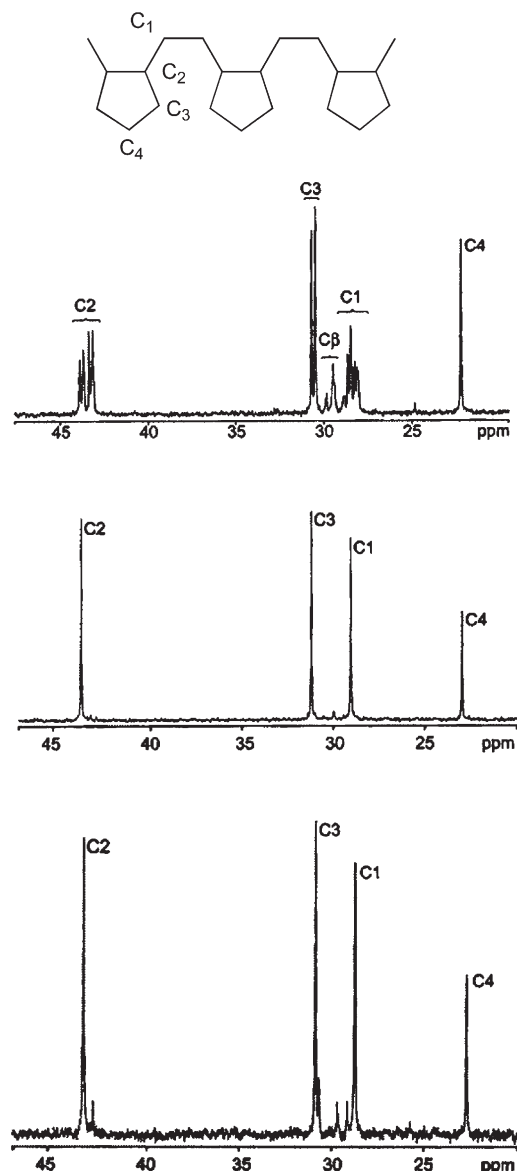


Figure 7. $^{13}\text{C}\{^1\text{H}\}$ NMR spectra of cP-co-E polymers that were generated with $\text{Me}_4\text{CpSiMe}_2(\text{BuN})\text{TiCl}_2$ (**8**, top, Table 1, entry 2), $\text{IndSiMe}_2(\text{BuN})\text{TiCl}_2$ (**7**, middle, Table 1, entry 1), and 3,5-(tBu) $_2$ benz[e]indenyl $\text{SiMe}_2(\text{BuN})\text{TiMe}_2$ (**4**, bottom, Table 1, entry 10) with MMAO-4 as cocatalyst.

exception of **5**, the indenyl catalysts **4–8** showed similar amounts of cyclopentene incorporation.

The indenyl catalysts **4–8** are both highly regio- and stereoselective for the copolymerization of ethylene and cycloolefins. Selected $^{13}\text{C}\{^1\text{H}\}$ NMR spectra of representative ethylene/cyclopentene copolymers are shown in Figure 7. These spectra reveal that for mole fractions of cyclopentene approaching 50%, copolymers derived from catalysts **4–8** are highly alternating and regio-regular,¹⁵ with little evidence for 1,3-enchainment, as commonly observed for zirconocene catalysts.^{23–27} We attribute this selectivity to the lower tendency of these Ti catalysts to undergo β -H elimination in comparison to Zr congeners (see Fig. 1).^{23–25,28,29}

The high stereoselectivity of these catalysts is also evident

from the ^{13}C NMR spectra (Fig. 7). As previously reported, the presence of several resonances corresponding to the C_2 and C_3 carbons is indicative of an atactic alternating microstructure for the copolymer derived from **8**. In contrast, the four sharp resonances evident in Figure 7 are indicative of a highly stereoregular alternating microstructure for copolymers derived from the chiral precursors **7** and **4**. On the basis of model compounds prepared by Fujita and Coates,¹⁶ this microstructure can be assigned as isotactic poly(*cis*-cyclopentene-*alt*-ethylene). Modification of the indene ligands did not lead to significant differences in polymer tacticities as determined by $^{13}\text{C}\{^1\text{H}\}$ NMR, but did have a slight influence on the molecular weight (Table 1, entries 1, 10–12).

The stereospecific copolymerization of ethylene and cyclopentene with metallocenes **4–8** stands in sharp contrast to their behavior with propylene; catalysts derived from **7**/MAO yield only atactic polypropylene.³⁴ These results reveal that the factors which govern stereodifferentiation in ethylene/cyclopentene polymerization are clearly different from those for propylene polymerization. This is also evident from Coates' results, where he demonstrated that the bis phenoxyimine Ti catalysts are stereoselective for propylene (yielding syndiotactic PP) but yield atactic ethylene/cyclopentene copolymers.¹⁶

The origin of the high stereoselectivity for these indenyl catalysts for cyclopentene enchainment is unknown. We believe a chain-end control mechanism to be unlikely. The two heterotopic coordination sites for the indenyl complexes **4–7** could lead to a 'dual-site' mechanism where ethylene inserts at one of the two heterotopic sites and cyclopentene inserts at the other. Similar mechanisms have been proposed for ethylene/ α -olefin and ethylene/norbornene copolymerizations.^{8,43–45} While a dual-site mechanism need not be invoked to explain the sequence alternation, the fact that cyclopentene inserts stereoselectively implies that cyclopentene inserts at only one of the two coordination sites.

These highly alternating copolymers are semi-crystalline. The isotactic *alt*-EcP copolymer derived from **7** exhibits dual melting points at 176 and 183 °C (Table 1, entry 1), consistent with the data reported by Natta and Coates.^{14,16,21} As expected, the melting points of the polymers decrease as the mole fraction of cyclopentene decreases from 0.50 (Table 1, entries 1 vs 5). Some differences were observed in the melting behavior of copolymers derived from catalysts **4–6** (Table 1, entries 10–12), but it is not clear at the moment whether these differences are due to subtle differences in the microstructure or the molecular weight.

Surprisingly, the alternating atactic copolymer derived from **8** is also semi-crystalline with a melting points approaching 127 °C. While the origin for this crystallinity is not fully understood, we suggest that it may be due to the existence of plastic crystals such as those investigated by De Rosa et al. for alternating ethylene-*co*-norbornene copolymers.¹²

The indenyl complexes **4–7** are also effective for the stereospecific alternating copolymerization of ethylene and cycloheptene (Table 2) and cyclooctene (Table 3). As

Table 2. Cycloheptene (cH)/ethylene (E) copolymerization results

Entry	Precat	[Ti] M $\times 10^{-4}$	T_p (°C)	Time (h)	E:Ar ratio ^a	Yield (g)	Prod ^b	% cH ^c	T_g (°C)	M_w/M_n	M_n^d
1	7	10.2	25	0.5	1:0	0.32	62	31	—	—	0.5
2	7	10.2	25	4.0	1:6	0.75	18	45	—	1.73	3.1
3	8	10.3	25	4.0	1:6	0.27	6	34	—	1.64	6.0
4	8	10.3	25	4.0	1:10	0.18	4	47	26	1.94	2.3
5	4	10.4	25	0.5	1:0	2.24	432	35	6	2.12	37.2
6	4	10.3	25	0.5	1:0	1.59	309	28	—	2.34	55.0
7	4	10.4	25	4.0	1:6	0.35	9	50	33	2.18	8.4
8	5	10.3	25	4.0	1:6	0.31	8	42	—	1.93	13.0

^a Precat: ^tBu=**4**; H=**5**; CF₃=**6**; Ind=**7**; Me₄Cp=**8**; E=ethylene; cH=cycloheptene; Ar=argon. Total pressure=20 psig.

^b Productivity in [kg/(mol Ti·h)].

^c Determined by integration of the respective ¹³C NMR resonances. The % cH content was calculated by integration of the downfield cH resonances (corresponding to the two methine resonances)=A_H (between 43.5 and 41.5 ppm) and implementation of the following equations: 3.5 \times A_H=B_H (A_H=integral for the downfield cycloolefin resonances corresponding to two carbon atoms of the cH monomer; B_H=relative integral for all carbons due to cH units); 100-B_H=C_E (C_E=relative integral for inserted ethylene units); B_H/7=X_H (X_H=relative integral for each carbon atom of the inserted cH units); C_E/2=Y_E (Y_E=relative integral for each carbon atom of the inserted E units); X_H/(X_H+Y_E)=% cH. This approximation is considered to be valid given that long delay times (d_1) are used thus leading to accurate ¹³C integrals (in all cases d_1 =9.5 s with acquisition time=4.0 s were applied). For all experiments the ratio of Ti: MMAO was 1:400–500 mequiv.

^d GPC molecular weights and polydispersities vs. polystyrene standards in units of g/mol $\times 10^{-3}$.

Table 3. Cyclooctene (cO)/ethylene (E) copolymerization results

Entry	Precat	[Ti] M $\times 10^{-4}$	T_p (°C)	Time (h)	E:Ar ratio ^a	Yield (g)	Prod ^b [kg/(mol Ti·h)]	% cO ^c	T_g (°C)	M_w/M_n	M_n^d
1	7	9.9	25	1.0	1:0	0.45	44	31	—	2.03	0.3
2	8	10.0	25	1.0	1:0	0.11	10	12	—	3.93	6.5
3	4	10.1	25	0.5	1:0	1.28	249	31	—	2.46	42.6
4	4	10.1	25	4.0	1:6	0.57	14	36	—	1.79	17.1
5	4	10.1	25	4.0	1:10	0.27	6	49	55	1.78	4.2

^a Precat: ^tBu=**4**; H=**5**; CF₃=**6**; Ind=**7**; Me₄Cp=**8**; E=ethylene; cO=cyclooctene; Ar=argon. Total Pressure=20 psig.

^b Productivity in [kg/(mol Ti·h)].

^c Determined by integration of the respective ¹³C NMR resonances. The % cO content was calculated by integration of the downfield cO resonances (corresponding to the two methine resonances)=A_O (between 40.5 and 38.5 ppm) and implementation of the following equations: 4.0 \times A_O=B_O (A_O=integral for the downfield cycloolefin resonances corresponding to two carbon atoms of the cO monomer; B_O=relative integral for all carbons due to cO sequences); 100-B_O=C_E (C_E=relative integral for inserted ethylene units); B_O/8=X_O (X_O=relative integral for each carbon atom of the inserted cO units); C_E/2=Y_E (Y_E=relative integral for each carbon atom of the inserted E units); X_O/(X_O+Y_E)=% cO. This approximation is considered to be valid given that long delay times (d_1) are used thus leading to accurate ¹³C integrals (in all cases d_1 =9.5 s with acquisition time=4.0 s were applied). For all experiments the ratio of Ti:MMAO was 1:400–500 mequiv.

^d GPC molecular weights and polydispersities vs. polystyrene standards in units of g/mol $\times 10^{-3}$.

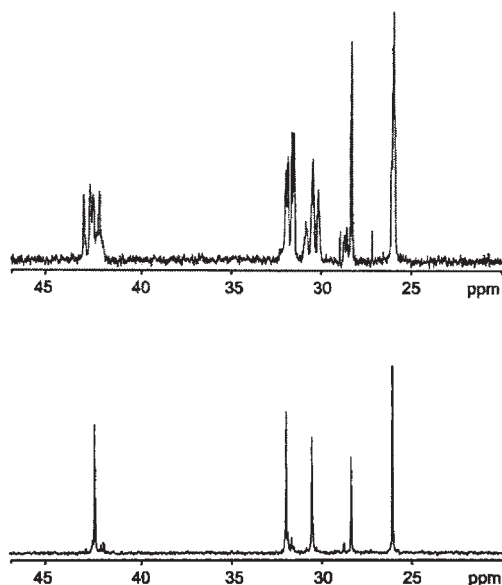


Figure 8. ¹³C{¹H}NMR spectra of cH-co-E polymers that were generated with Me₄CpSiMe₂(^tBuN)TiCl₂ (**8**, top, Table 2, entry 4) or 3,5-(^tBu)₂benz[e]indenyliSiMe₂(^tBuN)TiMe₂ (**4**, bottom, Table 2, entry 7) and MMAO-4 as cocatalyst.

shown in Figure 8, the ¹³C NMR spectra for copolymers derived from **8** are consistent with an alternating atactic microstructure, whereas the spectrum for the copolymer derived from **4** yields only 5 resonances, consistent with a highly regio- and stereoregular alternating copolymer. Isotactic microstructures are tentatively assigned to the stereoregular ethylene/cycloheptene and ethylene/cyclooctene copolymers (Fig. 9) by analogy with the ethylene/cyclopentene copolymers. The stereoregular alternating ethylene/cycloheptene and ethylene/cyclooctene exhibit higher T_g s than the corresponding ethylene/cyclopentene polymers of similar composition (Table 1, entry 10 vs Table 2, entry 4) but did not show any notable crystallinity by DSC.

4. Conclusions

In summary, the alternating stereospecific copolymerization of ethylene with cycloolefins (cyclopentene, cycloheptene, and cyclooctene) can be carried out with a family of chiral indenyl constrained geometry catalysts in the presence of MAO. In contrast, the achiral metallocene Me₄CpSiMe₂(^tBuN)TiCl₂ **8** generates atactic alternating copolymers.

These catalysts exhibit high selectivities for 1,2-enchainment of cycloolefins. Both isotactic and atactic alternating ethylene/cyclopentene copolymers are semi-crystalline, but the isotactic copolymer exhibits a higher melting point (183 °C).

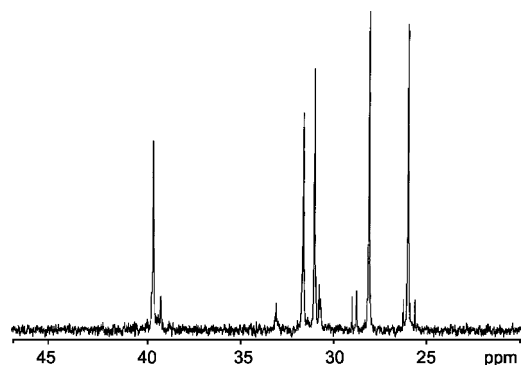


Figure 9. $^{13}\text{C}\{^1\text{H}\}$ NMR spectra of a cO-co-E polymer that was generated with 3,5-(^tBu) $_2$ benz[*e*]indenyliSiMe $_2$ (^tBuN)TiMe $_2$ (**4**, Table 3, entry 5) and MMAO-4 as cocatalyst.

5. Experimental

5.1. General procedures

All synthetic manipulations were carried out using standard Schlenk and/or nitrogen dry-box techniques under an inert atmosphere. Reagent grade solvents including toluene, THF, Et $_2$ O, and pentane were purified by passage through solvent towers of activated alumina and supported copper catalyst. Chloroform-*d* was vacuum-transferred from calcium hydride and benzene-*d* $_6$ was vacuum-transferred from sodium benzophenone. TiCl $_4$, MeLi (1.6 M in Et $_2$ O), and *n*-BuLi (1.6 M in hexanes) were obtained from Aldrich and were used without further purification. Cyclopentene (96%, Aldrich), cycloheptene (90%, Acros), cyclooctene (95%, Acros), SiMe $_2$ Cl $_2$ (Aldrich), and $^t\text{BuNH}_2$ (Aldrich) were dried by stirring over calcium hydride for 24 h, degassed with three freeze-pump-thaw cycles, and vacuum-transferred into teflon-sealed glass ampoules. Modified methylaluminoxane/toluene type 4 (MMAO-4) was obtained from Akzo Nobel (control # 9884) as a solution. It was dried under reduced pressure to remove solvent and residual trimethyl aluminum. The 2-aryl-benz[6.7]indenes: 2-(3',5'-di-*t*-butylphenyl)-benz[6.7]indene (99 +% purity, lot number 19656-125), 2-phenyl-benz[6.7]indene (99 +% purity, lot number 19656-100B), and 2-(3',5'-bis(trifluoromethyl)-phenyl)-benz[6.7]indene (99 +% purity, lot number 19656-108B) were prepared as described in the literature and kindly supplied by B.P. Amoco and were used without further purification.⁴⁶ Compounds IndSiMe $_2$ (^tBuN)TiCl $_2$ (**7**) and Me $_4$ CpSiMe $_2$ (^tBuN)TiCl $_2$ (**8**) were prepared as described in the literature.³⁴ ^1H NMR spectra were recorded on Varian 300, 400, or 500 MHz spectrometers, and chemical shifts are reported in ppm relative to residual solvent resonances (chloroform=7.26 ppm; benzene=7.15 ppm (^1H), 127.5 ppm (^{13}C)). $^{13}\text{C}\{^1\text{H}\}$ NMR spectra of polymer samples (~100 mg) were recorded at 75.4 MHz on a Varian UI300 spectrometer. The samples were dissolved with gentle heating in a 1:3 mixture of benzene-*d* $_6$:1,2,4-trichlorobenzene and spectra were obtained at 100 °C in 10 mm NMR tubes with a spectral

width of 200 ppm, an acquisition time of 4.0 s, and a relaxation delay of 9.5 s. Elemental analyses were carried out by Desert Analytics Laboratory, Tucson, AZ.

5.1.1. Synthesis of 2-[3,5-(^tBu) $_2\text{C}_6\text{H}_3$]-benz[6.7]-indeneSiMe $_2$ NH(^tBu), **1.** A Schlenk flask was charged with 2-(3',5'-di-*t*-butylphenyl)-benz[6.7]indene (1.95 g, 5.5 mmol) and a stir bar. The solid was dissolved in dry THF (10 mL) and was cooled to -78 °C followed by the dropwise addition of 1.6 M *n*-BuLi/hexanes (3.61 mL, 5.78 mmol). The solution was allowed to warm to ambient temperature and was stirred for 18 h. After this time, the solvents were removed under reduced pressure and the resultant yellow oil was dissolved in THF (10 mL). This solution was transferred via cannula to a stirred solution of SiMe $_2$ Cl $_2$ (2.7 mL, 22.25 mmol) in THF (20 mL) at -78 °C and was allowed to warm to ambient temperature. After 18 h, the solvent was removed under reduced pressure and dry pentane (50 mL) was added in order to generate a light yellow slurry which was filtered through Celite and the resultant solution was evaporated under reduced pressure. This material was dissolved in Et $_2$ O (30 mL) and was cooled to 0 °C followed by the dropwise addition of $^t\text{BuNH}_2$ (2.3 mL, 21.9 mmol) and the solution was allowed to warm to ambient temperature. After 20 h, the solvent and excess $^t\text{BuNH}_2$ were removed under reduced pressure and dry pentane (50 mL) was added in order to generate a slurry which was filtered through a Schlenk frit with a pad of Celite. The resultant solution was evaporated under reduced pressure to yield a viscous light brown oil. Yield: 2.43 g, 91%. ^1H NMR (CDCl $_3$, 293 K, δ): compound **1**: ^1H NMR (CDCl $_3$, 293 K, δ): 8.11–7.77 (2H, m, Ar-*H*), 7.66–7.26 (8H, m, Ar-*H*, Cp-*H*), 4.29 (1H, s, SiCH), 1.27 (18H, s, Ar- ^tBu -*H*), 0.86 (9H, s, ^tBuN), 0.45 (1H, s, NH), -0.30 (3H, s, SiCH $_3$), -0.47 (3H, s, SiCH $_3$). $^{13}\text{C}\{^1\text{H}\}$ NMR (C $_6\text{D}_6$, 293 K, δ): 151.59, 150.54, 142.75, 140.58, 137.88, 132.05, 128.34, 128.13, 125.12, 124.35, 123.75, 123.35, 122.57, 122.45, 121.92, 120.92, 119.89, 50.13, 48.88, 33.20, 31.25, 0.07, -0.21 . Anal. Calcd for C $_{33}$ H $_{45}$ NSi: C, 81.92; H, 9.38; N, 2.90; Si, 5.81. Found: C, 82.06; H, 9.31; N, 2.96.

5.1.2. Synthesis of 2-[C $_6$ H $_5$]-benz[6.7]indeneSiMe $_2$ -NH(^tBu), **2.** A Schlenk flask was charged with 2-phenyl-benz[6.7]indene (2 g, 8.3 mmol) and a stir bar. The solid was dissolved in dry THF (15 mL) and was cooled to -78 °C followed by the dropwise addition of 1.6 M *n*-BuLi/hexanes (5.42 mL, 8.7 mmol). The solution was allowed to warm to ambient temperature and was stirred for 5.5 h. After this time, the solvents were removed under reduced pressure and the resultant brown oil was dissolved in THF (10 mL). This solution was transferred via cannula to a stirred solution of SiMe $_2$ Cl $_2$ (4.0 mL, 33.0 mmol) in THF (10 mL) at -78 °C and was allowed to warm to ambient temperature. After 13 h, the solvent was removed under reduced pressure and dry pentane (50 mL) was added in order to generate a light yellow slurry which was filtered through Celite and the resultant solution was evaporated under reduced pressure to yield a white solid. This material was dissolved in Et $_2$ O (30 mL) and was cooled to 0 °C followed by the dropwise addition of $^t\text{BuNH}_2$ (3.5 mL, 33.2 mmol) and the solution was allowed to warm to ambient temperature. After 22 h, the solvent and excess $^t\text{BuNH}_2$ were removed under reduced pressure and dry

pentane (50 mL) was added in order to generate a slurry which was filtered through a Schlenk frit with a pad of Celite. The resultant solution was evaporated under reduced pressure to yield a viscous light brown oil. Yield: 2.33 g, 76%. ^1H NMR (C_6D_6 , 293 K, δ): 8.17 (1H, d, $J=8.2$ Hz, Ar-H), 7.85 (1H, d, $J=8.2$ Hz, Ar-H), 7.77 (1H, d, $J=8.2$ Hz, Ar-H), 7.68 (1H, d, $J=8.2$ Hz, Ar-H), 7.66 (1H, s, Cp-H), 7.47–7.22 (7H, m, Ar-H), 4.23 (1H, s, SiCH), 0.95 (9H, s, ^tBuN), 0.49 (1H, s, NH), -0.19 (6H, s, Si(CH_3) $_2$). $^{13}\text{C}\{^1\text{H}\}$ -NMR (C_6D_6 , 293 K, δ): 150.10, 143.17, 140.41, 137.98, 132.02, 128.36, 128.20, 127.35, 126.93, 126.79, 125.43, 125.22, 124.43, 123.72, 123.47, 122.97, 122.55, 49.90, 33.17, 0.95, -0.90 . Anal. Calcd for $\text{C}_{25}\text{H}_{29}\text{NSi}$: C, 80.81; H, 7.87; N, 3.77; Si, 7.56. Found: C, 81.20; H, 7.86; N, 3.77.

5.1.3. Synthesis of 2-[3,5-(CF_3) $_2\text{C}_6\text{H}_3$]-benz[6.7]-indeneSiMe $_2$ NH(^tBu), 3. A Schlenk flask was charged with 2-(3',5'-di-trifluoromethyl)-benz[6.7]indene (2 g, 5.3 mmol) and a stir bar. The solid was dissolved in dry THF (10 mL) and was cooled to -78 °C followed by the dropwise addition of 1.6 M *n*-BuLi/hexanes (3.47 mL, 5.55 mmol). The reaction was allowed to warm to ambient temperature and was stirred for 18 h thus generating a dark green solution. After this time, the solvents were removed under reduced pressure and the resultant oil was dissolved in THF (20 mL). This solution was transferred via cannula to a stirred solution of SiMe $_2$ Cl $_2$ (2.6 mL, 21.1 mmol) in THF (20 mL) at 0 °C and was allowed to warm to ambient temperature. After 19 h, the solvent was removed under reduced pressure and dry pentane (50 mL) was added in order to generate a brown slurry which was filtered through Celite and the resultant solution was evaporated under reduced pressure. This material was dissolved in Et $_2$ O (30 mL) and was cooled to 0 °C followed by the dropwise addition of $^t\text{BuNH}_2$ (2.2 mL, 21.1 mmol) and the solution was allowed to warm to ambient temperature. After 20 h, the solvent and excess $^t\text{BuNH}_2$ were removed under reduced pressure and dry pentane (50 mL) was added in order to generate a slurry which was filtered through a Schlenk frit with a pad of Celite. The resultant solution was evaporated under reduced pressure to yield a dark brown solid. Yield: 1.87 g, 70%. ^1H NMR (CDCl_3 , 293 K, δ): 8.24 (1H, d, $J=8.9$ Hz, Ar-H), 8.02 (2H, s, Ar-H), 7.93 (1H, d, $J=8.9$ Hz, Ar-H), 7.86 (1H, s, Ar-H), 7.78 (1H, d, $J=8.7$ Hz, Ar-H), 7.77 (1H, s, Cp-H), 7.72 (1H, d, $J=8.7$ Hz, Ar-H), 7.56 (1H, app t, $J=8.7$ Hz, Ar-H), 7.49 (1H, app t, $J=8.7$ Hz, Ar-H), 4.41 (1H, s, Si-CH), 1.09 (9H, s, ^tBuN), 0.46 (1H, s, N-H), -0.10 (3H, s, Si-CH $_3$), -0.18 (3H, s, Si-CH $_3$). $^{13}\text{C}\{^1\text{H}\}$ -NMR (C_6D_6 , 293 K, δ): 145.82, 144.00, 139.82, 139.43, 132.11, 131.46 (CF $_3$, q, $J=32.05$ Hz), 130.40, 128.76, 128.40, 127.61, 126.81, 125.70, 125.63, 124.84, 124.76, 123.58, 122.33, 119.62, 49.93, 32.91, 0.86, -1.15 . Anal. Calcd for $\text{C}_{27}\text{H}_{27}\text{F}_6\text{NSi}$: C, 63.89; H, 5.36; F, 22.46; N, 2.76; Si, 5.53. Found: C, 63.68; H, 5.26; N, 2.74.

5.1.4. Synthesis of [(2-(3,5-(^tBu) $_2\text{C}_6\text{H}_3$)benz[6.7]indenyl)-SiMe $_2$ (^tBuN)TiMe $_2$], 4. A Schlenk flask was charged with 1 (1 g, 2.07 mmol), a stir-bar, and dry/degassed Et $_2$ O (25 mL). This solution was cooled to -78 °C followed by the addition of a 1.6 M Et $_2$ O solution of MeLi (5.3 mL, 8.48 mmol) whereupon the solution became turbid and was allowed to warm to ambient temperature. After stirring for

2 h, a solution of TiCl $_4$ (0.23 mL, 2.07 mmol) in dry/degassed pentane (25 mL) was slowly added via cannula to the MeLi solution. After stirring for 14 h, the resultant black slurry was evaporated under reduced pressure and the material was taken up in pentane (40 mL). This slurry was rinsed through a Schlenk frit containing a pad of Celite to elute a transparent dark green solution while leaving a black chalky substance on the Celite. The resultant filtrate was evaporated to ~ 5 mL and was stored at -20 °C for 2 days leading to precipitation of the desired yellow/brown semi-crystalline solid. Yield: 310 mg, 27%. ^1H NMR (CDCl_3 , 293 K, δ): 7.95 (1H, d, $J=7.9$ Hz, Ar-H), 7.70–7.60 (2H, s, Ar-H, cP-H), 7.58 (2H, d, $J=1.6$ Hz, Ar-H), 7.55–7.52 (2H, m, Ar-H), 7.36–7.24 (3H, m, Ar-H), 1.43 (9H, s, ^tBuN), 1.36 (18H, s, Ar- $^t\text{Bu-H}$), 1.18 (3H, s, TiCH $_3$), 0.63 (3H, s, SiCH $_3$), 0.12 (3H, s, SiCH $_3$), -0.11 (3H, s, TiCH $_3$). $^{13}\text{C}\{^1\text{H}\}$ -NMR (C_6D_6 , 293 K, δ): 149.62, 147.47, 142.87, 136.57, 132.75, 131.90, 130.96, 128.56, 126.93, 126.64, 126.12, 125.14, 124.77, 123.26, 121.48, 112.52, 91.56, 58.30, 58.05, 52.44, 34.55, 33.80, 31.15, 5.36, 5.25. Anal. Calcd for $\text{C}_{35}\text{H}_{49}\text{NSiTi}$: C, 75.10; H, 8.82; N, 2.50; Si, 5.02; Ti, 8.55. Found: C, 75.53; H, 9.19; N, 2.77.

5.1.5. Synthesis of [(2-[C_6H_5]-benz[6.7]indenyl)SiMe $_2$ (^tBuN)TiMe $_2$], 5. A Schlenk flask was charged with 2 (0.92 g, 2.47 mmol), a stir-bar, and dry/degassed Et $_2$ O (25 mL). This solution was cooled to -78 °C followed by the addition of a 1.6 M Et $_2$ O solution of MeLi (6.2 mL, 9.97 mmol) whereupon the solution became turbid and was allowed to warm to ambient temperature. After stirring for 2 h, a solution of TiCl $_4$ (0.27 mL, 2.46 mmol) in dry/degassed pentane (25 mL) was slowly added via cannula to the MeLi solution. After stirring for 19 h, the resultant black slurry was evaporated under reduced pressure and the material was taken up in pentane (40 mL). This slurry was rinsed through a Schlenk frit containing a pad of Celite to elute a transparent yellow/brown solution while leaving a black chalky substance on the Celite. The resultant filtrate was evaporated to ~ 10 mL and was stored at -20 °C for 4 days leading to precipitation of the desired orange semi-crystalline solid. Yield: 230 mg, 21%. ^1H NMR (C_6D_6 , 293 K, δ): 8.00 (1H, d, $J=7.4$ Hz, Ar-H), 7.62 (1H, s, Cp-H), 7.58–7.51 (3H, m, Ar-H), 7.36–7.09 (7H, m, Ar-H), 1.39 (9H, s, ^tBuN), 1.07 (3H, s, TiCH $_3$), 0.64 (3H, s, SiCH $_3$), 0.11 (3H, s, SiCH $_3$), -0.17 (3H, s, TiCH $_3$). $^{13}\text{C}\{^1\text{H}\}$ -NMR (C_6D_6 , 293 K, δ): 145.30, 136.78, 131.83, 130.10, 128.58, 128.37, 127.59, 127.33, 126.91, 126.63, 126.15, 125.48, 125.45, 124.81, 123.25, 120.25, 90.95, 58.39, 58.26, 53.76, 33.73, 5.49, 5.45. Anal. Calcd for $\text{C}_{27}\text{H}_{33}\text{NSiTi}$: C, 72.47; H, 7.43; N, 3.13; Si, 6.28; Ti, 10.70. Found: C, 72.59; H, 7.50; N, 3.04.

5.1.6. Synthesis of [(2-[CF $_3$] $_2$ -benz[6.7]indenyl)SiMe $_2$ (^tBuN)TiMe $_2$], 6. A Schlenk flask was charged with 3 (0.87 g, 1.71 mmol), a stir-bar, and dry/degassed Et $_2$ O (25 mL). This solution was cooled to -78 °C followed by the addition of a 1.6 M Et $_2$ O solution of MeLi (4.3 mL, 6.9 mmol) whereupon the solution became turbid and was allowed to warm to ambient temperature. After stirring for 2 h, a solution of TiCl $_4$ (0.19 mL, 1.71 mmol) in dry/degassed pentane (25 mL) was slowly added via cannula to the MeLi solution. After stirring for 20 h, the resultant black slurry was evaporated under reduced pressure and the material was taken up in pentane (40 mL). This slurry was

rinsed through a Schlenk frit containing a pad of Celite to elute a transparent dark brown solution while leaving a black chalky substance on the Celite. The resultant filtrate was evaporated to ~5 mL and was stored at -20 °C for 10 days leading to precipitation of the desired dark brown semi-crystalline solid. Yield: 252 mg, 25%. ¹H NMR (C₆D₆, 293 K, δ): 8.02 (2H, s, Ar-*H*), 7.95 (1H, s, Cp-*H*), 7.72 (1H, s, Ar-*H*), 7.60–7.22 (6H, m, Ar-*H*), 1.29 (9H, s, ^tBuN), 0.95 (3H, s, TiCH₃), 0.52 (3H, s, SiCH₃), 0.06 (3H, s, SiCH₃), -0.23 (3H, s, TiCH₃). ¹³C{¹H} NMR (C₆D₆, 293 K, δ): 144.00, 141.99, 139.77, 138.93, 133.80, 131.78, 130.83, 130.43, 130.41, 130.12, 128.70, 128.58 (CF₃, *q*, *J*=27.0 Hz), 126.62, 124.85, 124.32, 123.28, 113.05, 91.51, 59.81, 58.56, 54.06, 33.55, 5.11, 5.07. Anal. Calcd for C₂₉H₃₁F₆NSiTi: C, 59.69; H, 5.35; F, 19.54; N, 2.40; Si, 4.81; Ti, 8.20. Found: C, 59.52; H, 5.47; N, 2.51.

5.2. Polymerization procedure (cyclopentene-*co*-ethylene-Table 1)¹⁵

In a nitrogen dry box, a 150 mL thick-walled glass reactor was charged with a teflon stir bar, MMAO-4 (~300 mg, 5.2 mmol), toluene (3 mL) and 15 mL of dried cyclopentene. The glass reactor was affixed with an airtight reactor-head and was removed from the dry-box. The apparatus was pressurized with the desired feed-gas ratio (up to 20 psig) followed by equilibration at the desired reaction temperature for 30 min. During this time, an injection tube was charged with a toluene (2 mL) solution of the desired precatalyst (10.2 μmol). Following equilibration, the precatalyst/toluene solution was injected with a back-pressure of the feed-gas mixture to initiate the reaction. After the desired reaction time, the reactor was vented to atmospheric pressure and methanol (5 mL) was injected to halt the reaction. The resultant slurry was precipitated with acidified methanol (2×300 mL) and the polymer was stirred for several hours followed by filtration to remove residual monomer and Al. The polymer was dried in a vacuum oven at 50 °C over-night. Typically, the procedure yields 0.1–3.0 g of polymer. ¹³C{¹H}NMR spectra of poly(cP-*co*-E) samples (~100 mg) were recorded at 75.4 MHz on a Varian UI300 spectrometer. The samples were dissolved with gentle heating in a 1:3 mixture of d₆-benzene:1,2,4-trichlorobenzene and spectra were obtained at 100 °C in 10 mm NMR tubes with a spectral width of 200 ppm, an acquisition time of 4.0 s, and a relaxation delay of 9.5 s.

5.3. Polymerization procedure (cycloheptene-*co*-ethylene) and (cyclooctene-*co*-ethylene)

These were carried out according to the procedure for cyclopentene-*co*-ethylene. For cycloheptene copolymerizations the bottle was charged with 5.0 mL (38.4 mmol) of cycloheptene and for cyclooctene polymerizations the bottle was charged with 5.3 mL (38.4 mmol) of cyclooctene. ¹³C{¹H}NMR spectra of the resultant polymer samples (~100 mg) were recorded at 75.4 MHz on a Varian UI300 spectrometer. The samples were dissolved with gentle heating in a 1:3 mixture of d₆-benzene:1,2,4-trichlorobenzene and spectra were obtained at 100 °C in 10 mm NMR tubes with a spectral width of 200 ppm, an acquisition time of 4.0 s, and a relaxation delay of 9.5 s.

Acknowledgements

We thank B. P. Amoco for supplying the 2-arylbenz[6.7]-indene starting materials. Financial support of this research has been provided by the NSF and the NIH (ARL postdoctoral research fellowship GM 66597-01). The authors thank Dr. Peter A. Fox (Dupont Dow Elastomers L.L.C., Freeport, TX) for thermal analyses.

References and notes

- Brintzinger, H. H.; Fischer, D.; Mülhaupt, R.; Rieger, B.; Waymouth, R. M. *Angew. Chem., Int. Ed. Engl.* **1995**, *34*, 1143.
- Coates, G. W. *Chem. Rev.* **2000**, *100*, 1223–1252.
- Resconi, L.; Cavallo, L.; Fait, A.; Pietmontesi, F. *Chem. Rev.* **2000**, *100*, 1253–1345.
- Scheirs, J.; Kaminsky, W. *Metallocene-based Polyolefins: Preparation, Properties, and Technology*; Wiley: Chichester, 2000; Vols. 1 and 2.
- Kaminsky, W.; Beulich, I.; Arndt-Rosenau, M. *Macromol. Symp.* **2001**, *173*, 211–225.
- Yoshida, Y.; Saito, J.; Mitani, M.; Takagi, Y.; Matsui, S.; Ishii, S.; Nakano, T.; Kashiwa, N.; Fujita, T. *Chem. Commun.* **2002**, 1298–1299.
- Ruchatz, D.; Fink, G. *Macromolecules* **1998**, 4669–4673.
- Ruchatz, D.; Fink, G. *Macromolecules* **1998**, 4674–4680.
- Ruchatz, D.; Fink, G. *Macromolecules* **1998**, 4681–4683.
- Ruchatz, D.; Fink, G. *Macromolecules* **1998**, 4684–4686.
- Benedikt, G.; Elce, E.; Goodall, B. L.; Kalamarides, H. A.; McIntosh, L. H.; Rhodes, L. F.; Selvy, K. T.; Andes, C.; Oyler, K.; Sen, A. *Macromolecules* **2002**, *35*, 8978–8988.
- De Rosa, C.; Corradini, P.; Buono, A.; Auremma, F.; Grassi, A.; Altamura, P. *Macromolecules* **2003**, *36*, 3789–3792.
- Kaminsky, W.; Engehausen, R.; Kopf, J. *Angew. Chem., Int. Ed. Engl.* **1995**, *3*, 2273–2275.
- Natta, G.; Dall'asta, G.; Mazzanti, G.; Pasquon, I.; Valvassori, A.; Zambelli, A. *Makromol. Chem.* **1962**, *54*, 95–101.
- Lavoie, A.; Ho, M. H.; Waymouth, R. M. *Chem. Commun.* **2003**, *104*, 864–865.
- Fujita, M.; Coates, G. W. *Macromolecules* **2002**, *35*, 9640–9647.
- Tritto, I.; Boggioni, L.; Jansen, J. C.; Thorshaug, K.; Sacchi, M. C.; Ferro, D. R. *Macromolecules* **2002**, 616–623.
- Harrington, B. A.; Crowther, D. J. *J. Mol. Catal. A-Chem.* **1998**, 79–84.
- Cherdron, H.; Brekner, M. J.; Osan, F. *Angew. Makromol. Chemie* **1994**, *223*, 121–133.
- Natta, G.; Dall'Asta, G.; Donegani, G.; Mazzanti, G. *Angew. Chem., Int. Ed. Engl.* **1964**, *3*, 723–729.
- Natta, G.; Dall'Asta, G.; Mazzanti, G. *Chimica e Industria* **1962**, *44*, 1212–1216.
- Kaminsky, W.; Spiehl, R. *Makromol. Chem., Macromol. Chem. Phys.* **1989**, 515–526.
- Naga, N.; Imanishi, Y. *Macromol. Chem. Phys.* **2002**, 159–165.
- Naga, N.; Tsubooka, M.; Suehiro, S.; Imanishi, Y. *Macromolecules* **2002**, *9*, 3041–3047.
- Naga, N.; Tsubooka, A.; Sone, M.; Tashiro, K.; Imanishi, Y. *Macromolecules* **2002**, *31*, 9999–10003.

26. Jerschow, A.; Ernst, E.; Hermann, W.; Muller, N. *Macromolecules* **1995**, 7095–7099.
27. Kelly, W. M.; Wang, S. T.; Collins, S. *Macromolecules* **1997**, 3151–3158.
28. Collins, S.; Kelly, W. M. *Macromolecules* **1992**, 233–237.
29. Keaton, R. J.; Sita, L. R. *J. Am. Chem. Soc.* **2002**, 7, 9070–9071.
30. McLain, S. J.; Feldman, J.; McCord, E. F.; Gardner, K. H.; Teasley, M. F.; Coughlin, E. B.; Sweetman, B. J.; Johnson, L. K.; Brookhart, M. *Macromolecules* **1998**, 6705–6707.
31. McKnight, A. L.; Waymouth, R. M. *Macromolecules* **1999**, 32, 2816.
32. Spaleck, W.; Antberg, M.; Rohrmann, J.; Winter, A.; Bachmann, B.; Kiprof, P.; Behm, J.; Herrmann, W. A. *Angew. Chem., Int. Ed. Engl.* **1992**, 31, 1347–1350.
33. Dietrich, U.; Hackmann, M.; Rieger, B.; Klinga, M.; Leskela, M. *J. Am. Chem. Soc.* **1999**, 12, 4348–4355.
34. McKnight, A. L.; Masood, M. A.; Waymouth, R. M.; Straus, D. A. *Organometallics* **1997**, 2879–2885.
35. Reybuck, S.; Meyer, A.; Waymouth, R. M. *Macromolecules* **2002**, 35, 637–643.
36. Lehtinen, C.; Lofgren, B. *Eur. Polym. J.* **1997**, 33, 115–120.
37. Kravchenko, R.; Waymouth, R. M. *Macromolecules* **1998**, 31, 1–6.
38. Coates, G.; Waymouth, R. M. *Science* **1995**, 267, 217–219.
39. McKnight, A.; Waymouth, R. M. *Chem. Rev.* **1998**, 98, 2587–2598.
40. Xu, G. X.; Ruckenstein, E. *Macromolecules* **1998**, 28, 4724–4729.
41. Resconi, L.; Camurati, I.; Grandini, C.; Rinaldi, M.; Mascellani, N.; Traverso, O. *J. Organomet. Chem.* **2002**, 16, 5–26.
42. Dragutan, V.; Streck, R. *Studies in Surface Science and Catalysis*; Delmon, B., Yates, J. T., Eds.; Elsevier: Amsterdam, 2000; Vol. 131, pp 942–965.
43. Choo, T. N.; Waymouth, R. M. *J. Am. Chem. Soc.* **2002**, 4188–4189.
44. Fan, W.; Leclerc, M.; Waymouth, R. M. *J. Am. Chem. Soc.* **2001**, 9555–9563.
45. Arndt, M.; Kaminsky, W.; Schauwienold, A. M.; Weingarten, U. *Macromol. Chem. Phys.* **1998**, 199, 1135–1152.
46. Ernst, A. B.; Moore, E. J.; Myers, C. L.; Quan, R.W. U.S. Patent 6,479,424.



Synthesis and electronic properties of bis-styryl substituted trimeric arylenethynylenes. Comparison of cruciforms with *iso*-cruciforms

James N. Wilson,^a Kenneth I. Hardcastle,^b Mira Josowicz^a and Uwe H. F. Bunz^{a,*}

^a*School of Chemistry and Biochemistry, Georgia Institute of Technology, 770 State Street, Atlanta, GA 30332, USA*

^b*Department of Chemistry, Emory University, 1515 Pierce Drive, Atlanta, GA 30322, USA*

Received 4 May 2004; revised 27 May 2004; accepted 4 June 2004

Dedicated to Professor Robert H. Grubbs on the occasion of the Tetrahedron prize

Abstract—Four 1,2-distyryl-4,5-bis(phenylethynyl)benzenes are described. A two step synthesis, a combination of Horner and Sonogashira methods is utilized. The targets and their *para* isomers were examined by UV–vis and fluorescence spectroscopies as well as by cyclic voltammetry. They show solvatochromic behavior and are easily oxidized if the styryl units carry dialkylamino substituents. Single crystal structures of three derivatives have been obtained.

© 2004 Elsevier Ltd. All rights reserved.

1. Introduction

Conjugated organic materials are—generally speaking—wide bandgap semiconductors.¹ Their band gap and their emissive properties are primarily manipulated by choice of the covalently assembled chemical structure. This approach leads to an inexhaustible variability of chromophores. Upon combination of two or more organic modules this variability increases if their connection takes place in topologically different ways; absorption and emission will change as a result.

Contrary to inorganic semiconductors that only exist in the solid state, as covalent assemblies,² most organic semiconductors are soluble and processible from solution into amorphous or crystalline films.¹ The processing aspect adds a further layer of complexity to the behavior of most organic semiconductors, with the optical properties being dependent upon solid-state ordering and concomitant aggregation phenomena.³ As a consequence, organic semiconductors might be compared to proteins where primary, secondary and tertiary structures are present and critically important for the correct function. While organic semiconductors are much less complex than proteins, higher order structures—as in the case of nature's polymers—often define the organic semiconductor's electronic properties.

There has been considerable interest in poly(*paraphenyl*-eneethynylene)s (PPE)³ as active layers in light emitting devices.⁴ And while several encouraging reports have appeared in the literature, the hole injecting properties of PPEs present a problem in their use as OLED materials. The difficulty in hole injection is due to the electron withdrawing quality of the alkyne groups. It would be of interest, while preserving the PPE skeleton, to improve the hole injection capabilities of these polymers.⁵ As a consequence, a series of PPEs with styryl side chains was synthesized.⁶ These materials are more electron rich and showed electrooptical properties that were different from those displayed by the PPEs. To understand the properties of these polymers better, cruciform models **1–5** were prepared and their emission and absorption were recorded both in solution and in the solid state.^{7,8}

We describe the electronic effects of different topological arrangements of two phenylethynyl and two styryl groups around a central benzene ring. We compare two series of emissive oligomers, the cruciforms **A (1–5)** and the *iso*-cruciforms **B (6–9)** with respect to their optical, electronic, and electroactive properties in solution and in the solid state; we present single crystal X-ray structures of **6–8**.

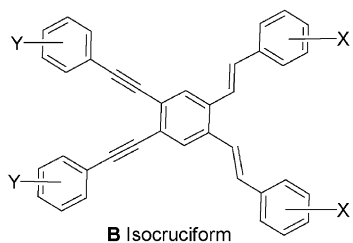
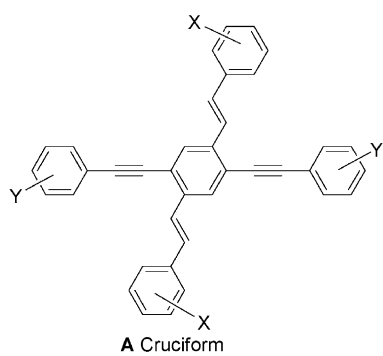
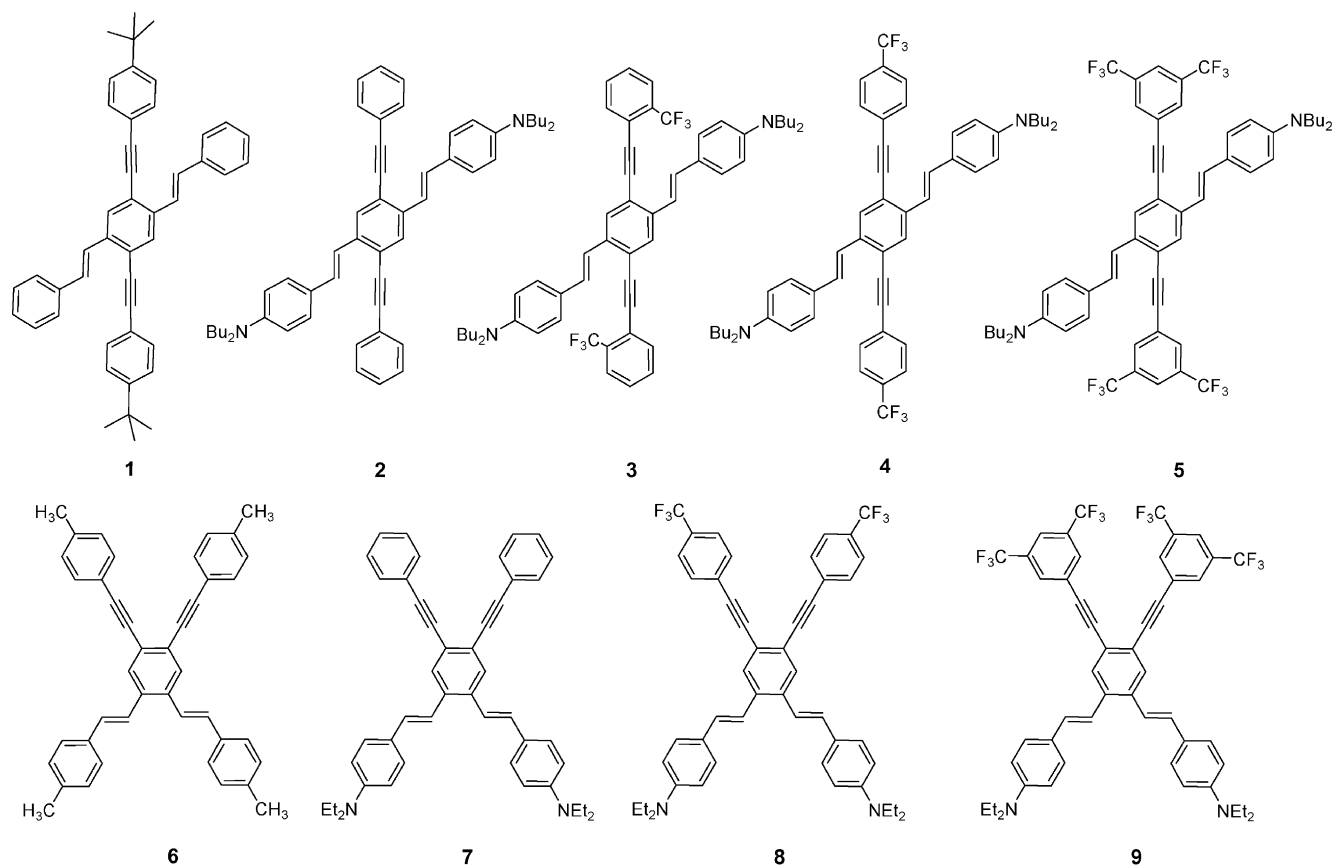
2. Results

2.1. Synthesis

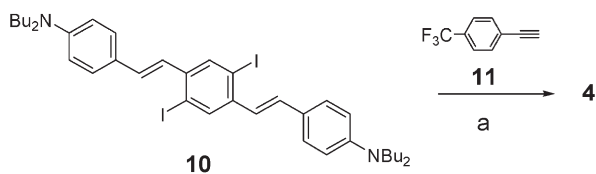
The synthesis of the cruciforms **1–3** and **5** has been

Keywords: Organic semiconductors; Distyrylbenzenes; Alkynes; Cruciforms; Solvatochromicity; Bandgap.

* Corresponding author. Tel./fax: +1-404-385-1795; e-mail address: uwe.bunz@chemistry.gatech.edu

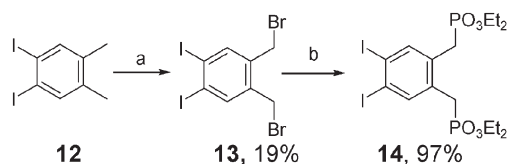


described elsewhere.⁷ The cruciform **4** and the isocruciforms **6–9** were prepared utilizing a similar route. Starting from the known diiodide **10** a Heck–Cassar–Sonogashira–Hagihara coupling with the alkyne **11** furnished the

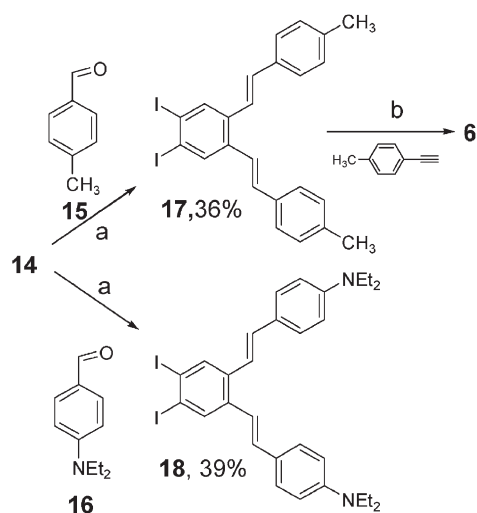


Scheme 1. (a) $(\text{Ph}_3\text{P})_2\text{PdCl}_2$, CuI, piperidine, THF.

cruciform **4** (**Scheme 1**) in high yield and purity after chromatography and crystallization from hexanes.⁹ For the isocruciforms **6–9** (**Schemes 2 and 3**) the central intermediates **17** and **18** were prepared. Starting from the



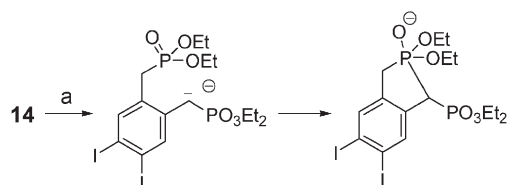
Scheme 2. (a) *N*-Bromo succinimide, sun lamp, CHCl_3 , 6 h. (b) Triethylphosphite (solvent), reflux 8 h.



Scheme 3. (a) NaH, heat; slow addition of either **15** or **16**. (b) $(\text{Ph}_3\text{P})_2\text{PdCl}_2$, CuI, piperidine.

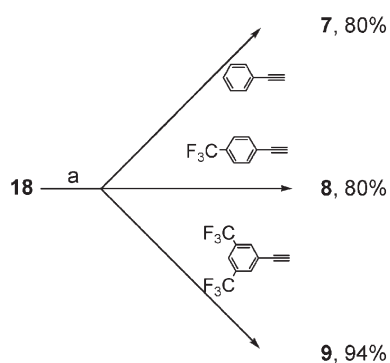
compound **12** photochemical bromination furnished the tetrahalide **13** after multiple recrystallizations in 19% yield.

An Arbuzov reaction transformed **13** into the phosphonate **14**, which in the presence of sodium hydride was subjected to the conditions of a Horner¹⁰ olefination utilizing the aldehydes **15** and **16** to give the intermediates **17** and **18**. The yields in these reactions were considerably lower than those obtained in an analogous coupling for molecules of the type **10**. This is probably due (Scheme 4) to intramolecular ring closure of the sodium salt of **14**. The ring closed species may then decompose into further unidentified products. And indeed, this Horner reaction was always accompanied by the formation of polar, but hard to identify, spectra side products that gave rise to a forest of signals in their proton NMR spectra. In the bisphosphonate precursor to **10** and similar *para*-distyrylbenzenes this intramolecular ring closure is sterically not possible and the yields of those double Horner reactions are considerably higher.⁷



Scheme 4. (a) NaH in mineral oil.

The intermediate **17** (Scheme 3) is coupled to 4-methyl(phenylacetylene), and gave **6** in 46% yield. The intermediate **18** was subjected to a similar Heck–Cassar–Sonogashira–Hagihara⁹ coupling utilizing phenylacetylene, 4-trifluoromethylphenylacetylene and 3,5-bis(trifluoromethyl)(phenylacetylene) (Scheme 5). This reaction



Scheme 5. (a) (Ph₃P)₂PdCl₂, CuI, piperidine.

furnished the isocruciforms **7–9** in yields between 80 and 94% after crystallization and chromatography. All of the isolated materials are yellow to yellow–orange solids, freely soluble in non-polar organic solvents and stable crystalline materials in the solid state.

2.2. Optical and photochemical properties; comparison of cruciforms with the isocruciforms

The optical properties of **1–9** are listed in Table 1. The absorption spectra of the conjugated crosses are unremarkable and their bandgap decreases with increasing donor–acceptor quality of the styryl and phenylethynyl side chains. As a consequence, **1** and **6** show the highest band gaps in solution and in the solid state, while **5** and **9** show the smallest ones. The isocruciforms show a somewhat larger band gap than the cruciforms, suggesting that conjugation is attenuated. In the isocruciforms all of the conjugative interactions of one type of substituent (either styryl or phenylethynyl) are of *ortho*- instead of the *para*-directionality.

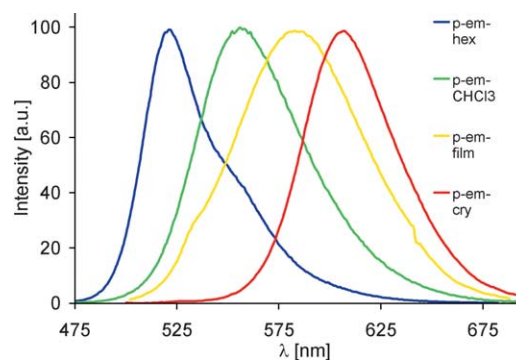


Figure 1. Emission spectra of compound **5** in different solvents and in the solid state. The emission maximum of **5** varies from 521 to 608 nm depending upon the environment.

The tetrasubstituted benzenes **1–9** are emissive in the solid state and in solution. Figure 1 shows the emission spectra of **5** in different solvents. The emission in **5** ranges from 521 to 608 nm. It is instructive to note that the emission of the pure hydrocarbon crosses **1** and **6** do not show any appreciable dependence on solvent (Fig. 2, Table 1).

In Figure 2 a colored bar representation of all of the fluorescence data of **1–9** is displayed to give an overview of their emissive properties in different solvents and in the solid state.

Some general trends can be gleaned. (1) The position of the

Table 1. Absorption and emission data for the cruciforms and isocruciforms **1–9**

Substituents compound	Absorption (nm)			Emission (nm)						
	CHCl ₃	Film	Hex.	CHCl ₃	THF	Acetone	EtOAc	MeOH	Film	Crystal
<i>tert</i> -Butyl, H; 1	369	405 sh	411	421	418	418	415	416	491	487
Me, Me; 6	366	397 sh	426 sh 433	433	430	431	429	430	479	497
H, Nbu ₂ ; 2	442	474	471	510	515	535	510	532	560	603
H, Net ₂ ; 7	410	451	455	518	521	540	514	536	539	535
<i>o</i> -CF ₃ , Nbu ₂ ; 3	440	486 sh	501	542	548	562	546	554	573	595
<i>p</i> -CF ₃ , Nbu ₂ ; 4	441	480 sh	492	539	549	564	546	555	584	594
<i>p</i> -CF ₃ , Et ₂ ; 8	424 sh	462 sh	472	530	545	564	541	555	543	549
M, <i>m</i> -(CF ₃) ₂ , Nbu ₂ ; 5	470 sh	518 sh	521	558	573	591	568	583	585	608
M, <i>m</i> -(CF ₃) ₂ , NEt ₂ ; 9	437 sh	484 sh	484	539	562	591	556	580	566	581

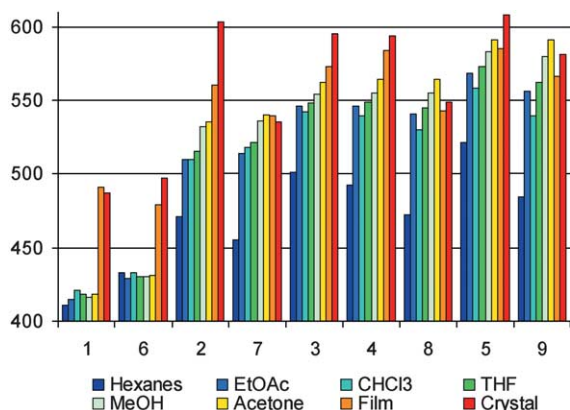


Figure 2. Bar graph of the emission spectra of 1–9. The compounds are grouped according to their substituent patterns. y-axis is the emission maximum in nm.

CF₃-group on the phenylethynyl substituent (*ortho* or *para* with respect to the alkyne group) in 3 and 4 does not have a significant influence on their emission spectra. That is not unexpected, because the CF₃-groups have an inductive effect. Their position should not be critical. (2) The emission of the isocruciforms is blue shifted with respect to that of their cruciform isomers. (3) In thin film and in the crystalline state the emission of 1–9 is bathochromically shifted, probably due to the formation of excimers. This red shift, when going from solution into the crystalline state is significantly larger in the cruciforms when compared to their isocruciforms. Similar trends are observed in thin films, but the emission is generally less red-shifted. (4) The more polar the solvent, the more bathochromically shifted the emission for the donor–acceptor substituted oligomers. The distinct solvatochromicity of the emission is easily understood in terms of the stabilization of the excited state. The more donor–acceptor substituted the oligomer is, the more its excited state is charge-separated, and the more red-shifted the observed emission is. In the compounds 3–5, 8 and 9 these effects are most strongly developed, due to the presence of both a donor (dialkylamino) and one or two acceptor groups (CF₃).

The quantum yields of 1, 2 and 4–9 were determined in hexanes and in chloroform (Fig. 3). Overall the quantum yields tend to be higher in hexanes than in chloroform, but there is no obvious correlation of the quantum efficiency with the structure or with the solvent utilized. The cruciforms 1–5 are photostable and do not bleach after

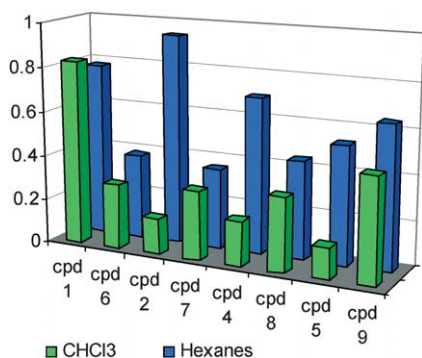


Figure 3. Quantum yield (y-axis) of 1, 2 and 4–9 in hexanes and in chloroform.

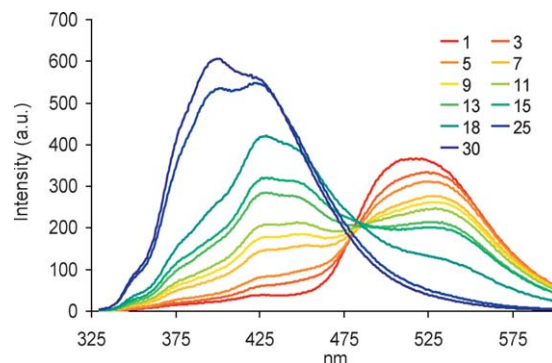


Figure 4. Emission spectra of 8 under irradiation in hexanes after 1, 3, 5, ..., 30 min. After 30 min the spectrum of 8 has disappeared, instead a broad emission centered at 401 nm has developed.

prolonged exposure to UV light in a fluorometer at 315 nm. In the case of the isocruciforms 6–9 fast bleaching in dilute solution and in thin films is observed via an isosbestic point (Fig. 4). Attempts to perform the irradiation in synthetically useful concentrations led to the isolation of an unidentified brownish polymeric-insoluble residue that resisted attempts of a meaningful spectroscopic characterization. Müllen et al. had observed similar behavior when irradiating simple 1,2-distyrylbenzenes.¹¹ A mass spectrum taken from a very dilute sample of 8, irradiated in chloroform, showed the presence of a molecular ion at 794 amu suggesting the uptake of a chlorine atom under the reaction conditions. We speculate that this is a photo-induced radical process, possibly involving a Bergman-type reaction of the enediyne moieties of the isocruciforms. Further investigations of this interesting process are ongoing.

In the solid state the bleaching process can be utilized to irreversibly etch patterns into thin films of 8. Figure 5 shows such a pattern ‘RHG’ etched into a thin film of 8.



Figure 5. Thin film of 8 irradiated through an RHG mask at 315 nm. Irradiated areas are non-fluorescent.

2.3. Electrochemistry of the isocruciforms 6–9

The electrochemistry of the isocruciforms 6–9 was examined by cyclic voltammetry to correlate 6–9’s redox properties to their structure. Table 2 shows the electrochemical potentials of 6–9 for oxidation and for reduction. Comparison of the oxidation potentials of 6–9 reveals that 6 is oxidized at 1.27 V but 7–9 are oxidized at a considerably lower potential, that is, at 0.52–0.57 V. The CF₃-groups in 8 or 9 do not seem to play a role in the determination of the oxidation potential; the diethylamino groups have the determining influence on the oxidation potential. The positive charge of the oxidized species—we speculate—is

Table 2. Reduction and oxidation potentials of **6–9** versus standard hydrogen electrode, HOMO and LUMO positions of **6–9** calculated from oxidation and reduction potentials as well as by SPARTAN with B3LYP utilizing the 6-31G** basis set

	6	7	8	9
	Oxidation (V)			
$E_{1/2}$	1.27	0.52	0.57	0.55
Peak	1.35	0.56	0.62	0.63
HOMO	-5.77	-5.02	-5.07	-5.05
	Reduction (V)			
$E_{1/2}$	-1.77	-1.83	-1.61	-1.62
Peak	-1.86	-1.94	-1.71	-1.70
LUMO	-2.73	-2.67	-2.89	-2.88
Band gap	3.04	2.35	2.18	2.17
	Quantum Chemical Calculations (eV)			
HOMO	-5.16	-4.74	-4.96	-5.04
LUMO	-2.04	-1.68	-2.05	-2.20
Band gap	3.12	3.06	2.91	2.84

located on the distyrylbenzene branch of **7–9**. That is reasonable, because the presence of the diethylamino group pumps electron density into the already electron rich π -system. The phenyleneethynylene branch does not seem to be involved in the reversible electrochemical oxidation event.

The isocruciforms **6** and **7** are reduced between -1.63 and -1.70 V while **8** and **9** are reduced at around -1.47 V, at significantly lower negative potential than **6** and **7**. This is easily understood, because the LUMO of **6–9** should be located on the electron deficient bis(phenylethynyl)benzene branch of the molecules. The electron accepting trifluoromethyl substituents help to accommodate the negative charge on this branch leading to a lower reduction potential.

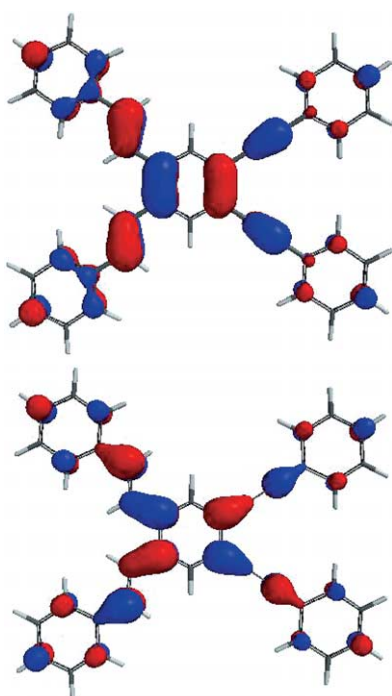


Figure 6. HOMO (top) and LUMO (bottom) of **6**. The methyl groups are omitted to minimize the time to calculate the structures.

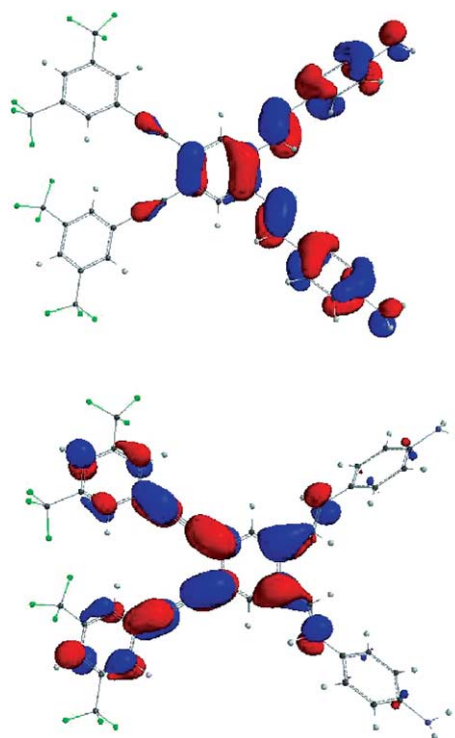


Figure 7. HOMO (top) and LUMO (bottom) of **9**. The diethylamino groups are substituted by simple NH_2 groups to decrease the time to calculate the structures.

2.4. Quantum chemical calculations

To understand the optical (i.e., band gap, solvatochromicity) and the redox properties of **6–9**, quantum chemical calculations (B3LYP utilizing 6-31G** basis set; SPARTAN) were performed. Table 2 contains the results of the calculations for **6–9**. In Figures 6 and 7 the calculated HOMOs and LUMOs of **6** and **9** are shown. The values in Table 2 demonstrate the decreasing band gap when going from the hydrocarbon **6** to the donor–acceptor substituted arene **9**. The localization of the HOMO and the LUMO of **6** and of **9** are critical to understand the solvatochromic behavior of the isocruciforms. In **6** the HOMO as well as the LUMO are spread out over the whole π -system. Both orbitals are decidedly delocalized (Fig. 6). In **9** that is not the case (Fig. 7). Instead the HOMO is mostly located on the distyrylbenzene branch of the molecule, while the LUMO resides mostly on the aryleneethynylene branch of the isocruciform **9**. The central ring is an integral part of both orbitals. Upon photonic excitation, an electron from the HOMO will be advanced into the LUMO to give a highly polarized state. This polarized excited state should be significantly stabilized by polar solvents, as observed (Table 1). Increasing solvent polarity leads to a significantly red shifted emission but only to a small change in absorption as expected for an excited state effect. As a means of comparison we have calculated the structure and the energetics of **5** (B3LYP; 6-31G** basis set). In Figure 8 the HOMO and the LUMO of **5** are shown. The calculated band gap of **5** is 2.7 eV.

The band gap of **5** is lower than that of **9**, which is 2.91 eV. The HOMO and the LUMO of **5** (Fig. 8) are even more

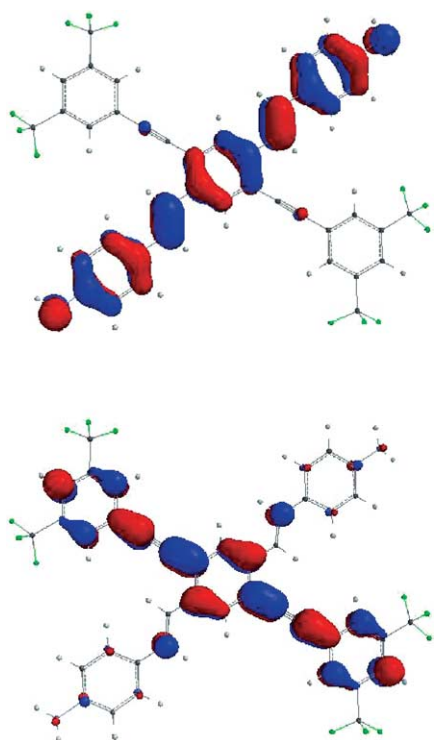


Figure 8. Calculated (B3LYP, 6-31G^{**}, SPARTAN 04) HOMO (top, -4.98 eV) and LUMO (bottom, -2.28 eV) of **5**. The calculated band gap is 2.70 eV.

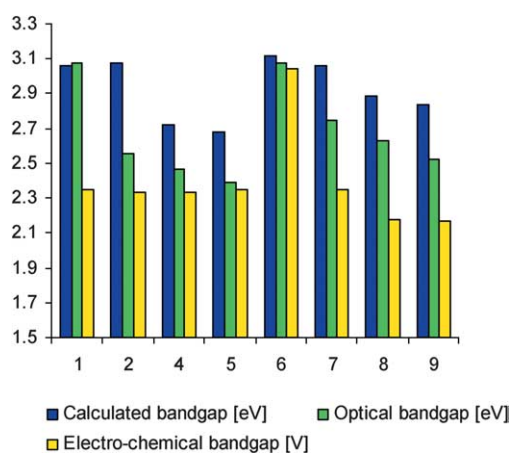


Figure 9. Comparison of the calculated and experimental band gaps of the compounds **1**, **2** and **4–9**. The values are taken from Table 3.

Table 3. Band gap of **1,2** and **4–9** calculated from oxidation and reduction potentials, from the optical band gap as well as by SPARTAN with B3LYP utilizing the 6-31G^{**} basis set. Electrochemical band gaps of **1–5** are from Ref. 7

	Calculated bandgap (eV)	Optical bandgap (eV)	Electro-chemical bandgap (V)
1	3.06	3.08	2.35
2	3.08	2.56	2.33
4	2.72	2.47	2.33
5	2.70	2.39	2.35
6	3.12	3.08	3.04
7	3.06	2.75	2.35
8	2.89	2.63	2.18
9	2.84	2.52	2.17

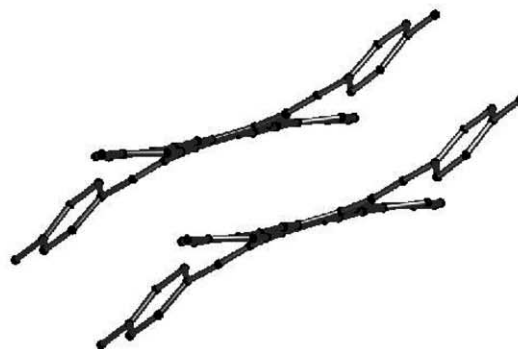
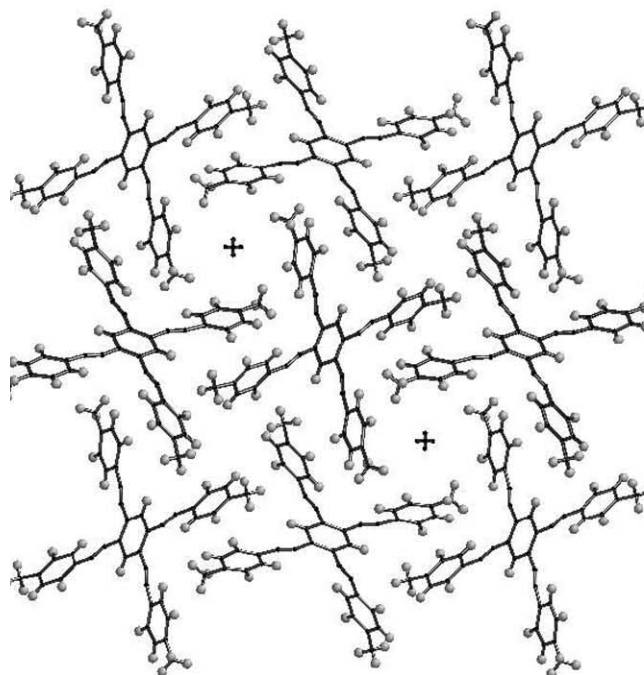
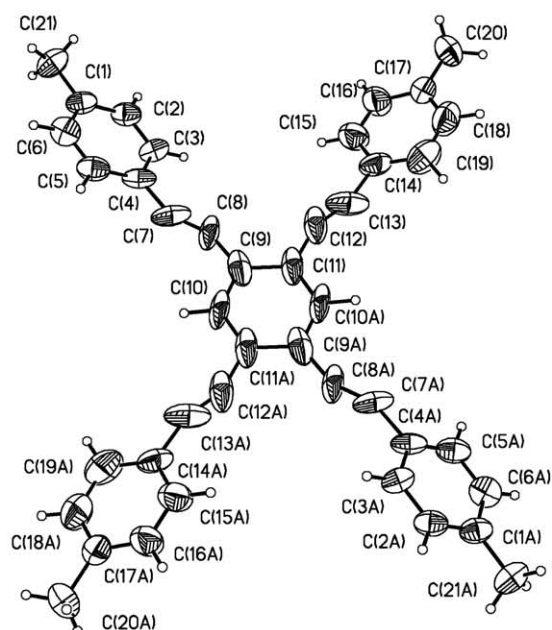


Figure 10. Top: ADP plot representation of **6**. Notable is the disorder, that renders alkyne and alkene units identical in the solid state. Middle, bottom: tetragonal packing of **6**. The molecules of **6** are packed in tilted stacks.

localized on their relative branches than the HOMO and the LUMO of **9** (Fig. 9, Table 3).

The quantum chemical calculations support a self-consistent picture that explains the decreased band gap when going from **6** to **9** as well the increased solvatochromicity. Both effects are due to the increased localization of the HOMO and the LUMO respectively on the distyrylbenzene and the aryleneethynylene branches in **9**. When the HOMO and the LUMO of **9** are compared to the frontier orbitals of **5**⁷ one can see that the geometrical separation of HOMO and LUMO (Figs. 7 and 8) is even more succinct in **5**. So is **5**'s solvatochromicity. The herein presented calculations are in good qualitative agreement with the experimental band gap data obtained from fluorescence spectroscopy and from cyclic voltammetry and explain the observed solvatochromicity.

2.5. X-ray crystal structures of the isocruciforms **6**, **7**, and **8**

To get a better feel for the structures and the conformations of the isocruciforms in the solid state, single crystalline specimen of **6–8** were grown and their structures solved (Figs. 10–12). Compound **9** did not form single crystals but a microcrystalline powder. However, **6–8** are quite disordered in the solid state. The compound **6** crystallizes in an unusual tetragonal space group. That is due to the structural similarity of the styryl and the phenylethynyl substituents that are completely disordered in the solid state. In Figure 10 the ADP plot of **6** and two views of its packing

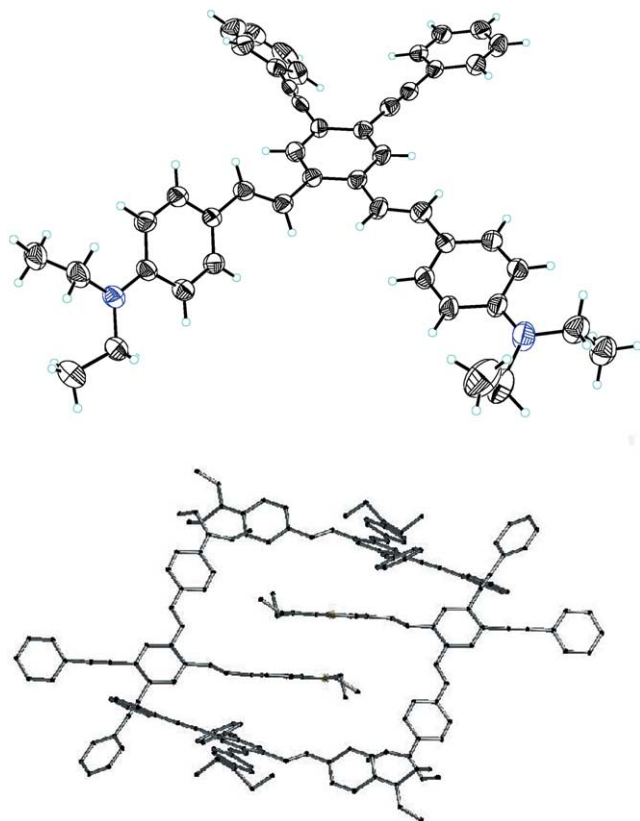


Figure 11. Top: ADP plot representation of **7**. Bottom: packing diagram of **7**. Distance between two layers is 3.596 Å.

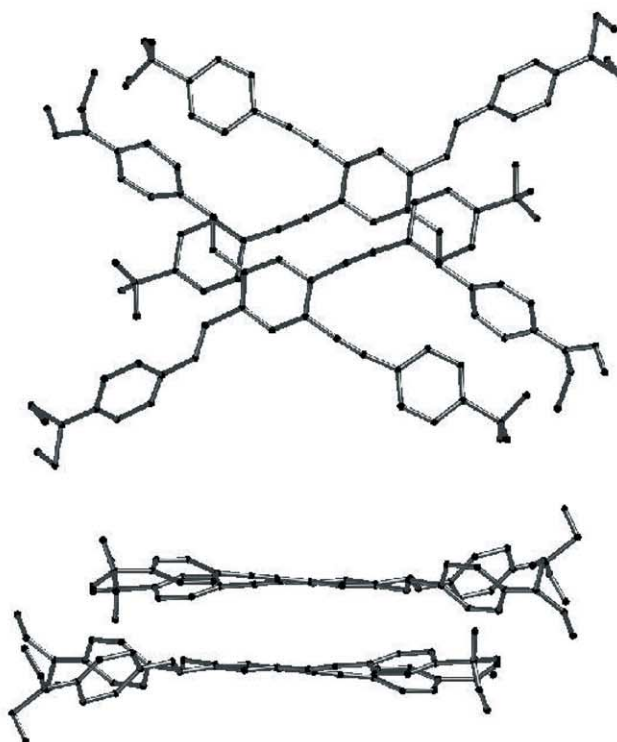
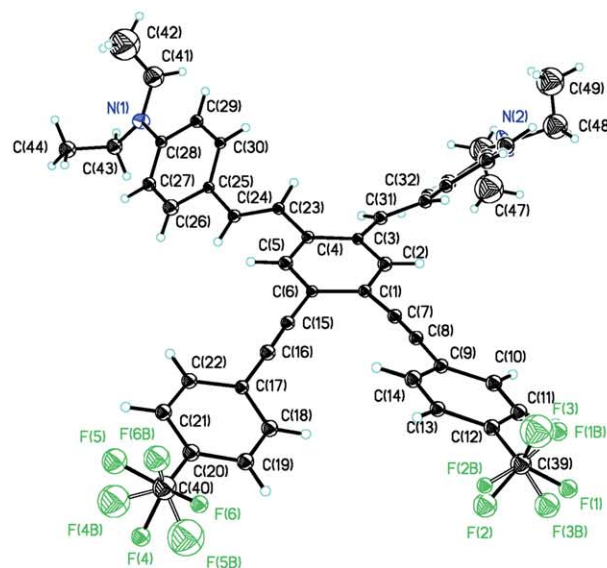


Figure 12. Top: ADP plot representation of a representative molecule of **8**. The trifluoromethyl groups are rotationally completely disordered. Middle, bottom: packing diagram of **8**. Distance between two layers is 3.51 Å.

in the solid state are shown. The alkyne/alkyne connectors are indistinguishable in the solid state. The arene rings are somewhat twisted with respect to each other. The twist angles between the central benzene and the outer rings vary from 12 to 32°. Interestingly, pairs of oppositely located 'arms' show similar torsion angles. The molecules are packed in tilted stacks with an interstack distance of approx. 3.6 Å, the van der Waals radius of carbon.

An ADP plot representation and views of the packing of **7** are shown in Figure 11. The ethyl groups of the amine substituents in **7** are disordered, and the outer rings are twisted with respect to the central one. One of the

Table 4. X-ray data of 6–8

	6	7	8
Empirical formula	C ₄₂ H ₃₀	C ₄₆ H ₄₄ N ₂	C ₄₈ H ₄₂ F ₆ N ₂
Formula weight	534.66	624.83	760.84
Temperature	173(2) K	173(2) K	173(2) K
Wavelength	0.71073 Å	1.54178 Å	1.54178 Å
Crystal system	Tetragonal	Monoclinic	Triclinic
Space group	P4/n	P2(1)/c	P-1
Unit cell dimensions	$a=23.809(2)$ Å, $\alpha=90^\circ$. $b=23.809(2)$ Å, $\beta=90^\circ$. $c=5.8229(8)$ Å, $\gamma=90^\circ$.	$a=8.3889(9)$ Å, $\alpha=90^\circ$. $b=31.632(3)$ Å, $\beta=92.992(5)^\circ$. $c=13.489(1)$ Å, $\gamma=90^\circ$.	$a=10.0454(7)$ Å, $\alpha=91.787(1)^\circ$. $b=13.88826(7)$ Å, $\beta=101.471(4)^\circ$. $c=15.3(10)$ Å, $\gamma=107.723(4)^\circ$.
Volume	3300.8(6) Å ³	3574.4(6) Å ³	1981.7(2) Å ³
Z	4	4	2
Density (calculated)	1.076 Mg/m ³	1.161 Mg/m ³	1.275 Mg/m ³
Absorption coefficient	0.061 mm ⁻¹	0.505 mm ⁻¹	0.775 mm ⁻¹
F(000)	1128	1336	794
Crystal size	0.75×0.12×0.12 mm ³	0.40×0.20×0.17 mm ³	0.57×0.12×0.10 mm ³
Theta range for data collection	1.71–21.24°	2.79–66.69°	2.96–38.07°
Index ranges	–24≤h≤24, –24≤k≤24, –5≤l≤5	–9≤h≤7, –37≤k≤25, –13≤l≤16	–8≤h≤, –11≤k≤11, –12≤l≤12
Reflections collected	23096	12497	18747
Independent reflections	1825 (R(int)=0.0457)	4226 (R(int)=0.0644)	8695 (R(int)=0.0000)
Completeness to theta	99.9%	67.0%	99.9%
Absorption correction	Semi-empirical from equivalents		
Max. and min. transmission	1.000 and 0.757805	Nd	1.000 and 0.425485
Refinement method	Full-matrix least-squares on F ²		
Data/restraints/parameters	1825/0/194	4226/0/438	8695/0/252
Goodness-of-fit on F ²	2.227	1.069	1.180
Final R indices (I>2σ(I))	R1=0.1489, wR2=0.4577	R1=0.0980, wR2=0.2759	R1=0.139, wR2=0.3246
R indices (all data)	R1=0.1567, wR2=0.4654	R1=0.1692, wR2=0.3198	R1=0.1815, wR2=0.3481
Extinction coefficient	Nd	0.0045(8)	Nd
Largest diff. peak and hole	0.786, –0.323 e Å ⁻³	0.371, –0.311 e Å ⁻³	0.710 and –0.573 e Å ⁻³

phenyleneethynylene units is twisted around 13°, while the other one is twisted around 37°. The degree of twisting with respect to the central core ranges from 11 to 58°. In **7** two of the substituents are almost coplanar with the central ring, while the other two show a significant twist. There are four independent molecules in the unit cell and each of them has a set of somewhat different twist angles of the benzene rings with respect to the center ring.

In the crystals of the compound **8** (Fig. 12) the situation is similar to that of **7**. Here as well two out of the four substituents are more twisted than the other two. An additional feature is the rotational disorder of the CF₃ groups that is not unexpected in this type of structures.

In all of the cases, the π-systems are packed closely and in a herringbone or a modified herringbone pattern. The distances between the π-systems are in the range of the van der Waals distance of carbon, that is, between 3.5 and 3.8 Å. The close proximity of the π-systems leads to their interaction in the solid state, and we interpret the observed bathochromic emissions of crystalline or microcrystalline species of **6–9** as a sign of excimer formation of the isocruciforms in the solid state (Table 4).

3. Conclusions

In conclusion we have prepared the isocruciforms **6–9** by a combination of Horner and Heck–Cassar–Sonogashira–Hagihara reactions. The optical and electrochemical properties of the isocruciforms are similar to those of the cruciforms **1–5**, however, their emission spectra are somewhat blue shifted, due to the decreased conjugative

pathways in the *ortho* connected isocruciforms. The electrochemical oxidation and reduction of the isocruciforms combined with the quantum chemical calculations and the emission data in a series of different solvents shows that HOMO and LUMO of the isocruciforms are located on the distyrylbenzene and the bisphenylethynyl branch of the molecules respectively, similar to those observed for **1–5**. This trend is pronounced in the donor–acceptor substituted isocruciforms **8** and **9** where an electronic decoupling of HOMO and LUMO is more prevalent. The cruciforms and the isocruciforms are cross conjugated molecules, even though in a non-classical sense.^{12,13} The large bathochromic shift in emission of **1–9** in the crystalline state can be explained by the packing of the π-systems that leads to strong electronic interactions in the excited state.¹⁴ The presence of the 1,2-distyrylbenzene unit in **6–9** makes them potentially attractive as materials for photopatterning. In future we will report single crystal reactivity of **6–9** and their incorporation into polymers. These materials are interesting for third order NLO-phores and similar applications.

4. Experimental

4.1. General

4.1.1. 1,2-Bis-bromomethyl-4,5-diiodo-benzene (13). A round bottom flask with a stirbar was charged with 50.0 g (0.140 mol) of **12**, 120 g (0.667 mol) of *N*-bromosuccinimide, 1.3 L of chloroform and 1.00 g (6.85 mmol) of *t*-butyl peroxide. A reflux condenser was placed atop the flask and the reaction mixture was irradiated with a sun lamp (120 W, General Electric 120R40/P1) while refluxing for 6 h. The

reaction mixture was allowed to cool to room temperature and crystals of succinimide formed which were filtered off. The chloroform solution was washed three times with 500 mL of 5% sodium sulfite solution followed by two washes with 500 mL of water. The chloroform was removed by roto-vap and the resulting solid was crystallized from hexane. Yield: 14.0 g, 19.4%. Mp: 98 °C. ^1H NMR (CDCl_3) δ 7.79 (s, 2H), 4.47 (s, 4H). ^{13}C NMR (CDCl_3) δ 141.1, 137.6, 108.7, 28.0. IR (cm^{-1}): 3014.5, 2896.9, 2849.6, 2735.4, 2660.1, 2408.9, 2291.3, 1992.3, 1972.1, 1777.8, 1729.6, 156.5, 1451.8, 1432.1, 1341.9, 1268.1, 1212.2, 1168.3, 1142.3, 1098.4, 898.8, 877.1.

4.1.2. [2-(Diethoxy-phosphorylmethyl)-4,5-diiodo-benzyl]-phosphonic acid diethyl ester (14). A 250 mL round bottom flask was charged with a stirbar, 23.2 g (45.0 mmol) of **13**, and 100 mL of triethylphosphite. A condenser column was placed atop the reaction vessel and the reaction refluxed for 8 h. The reaction was allowed to cool briefly before the excess triethylphosphite was distilled off. The product was crystallized from hexane to offer clear crystalline cubes. Yield: 27.5 g, 97%. Mp: 115 °C. ^1H NMR (CDCl_3) δ 7.70 (d, 2H, $J_{\text{H,P}}=1.9$ Hz), 4.06–3.97 (m, 8H), 3.31–3.24 (d, 4H, $J_{\text{H,P}}=20.33$ Hz), 1.28–1.23 (t, 12H, $J_{\text{H,H}}=7.1$ Hz). ^{13}C NMR (CDCl_3) δ 141.6, 133.1, 105.7, 62.3, 31.5–29.6 (d, $J_{\text{IP,C}}=137.4$ Hz), 16.5. IR (cm^{-1}): 2978.4, 2909.9, 2863.1, 2828.9, 2810.1, 1748.5, 1733.4, 1569.5, 1476.4, 1452.3, 1408.9, 1394.0, 1366.5, 1341.9, 1249.8, 1221.8, 1202.5, 1160.1, 1099.4, 1047.3, 1019.3, 893.0, 864.5.

4.1.3. 1,2-Diiodo-4,5-bis-(2-p-tolyl-vinyl)-benzene (17). A 500 mL Schlenk flask was charged with a stirbar and 5.40 g (8.57 mmol) of **14** while under nitrogen purge. Dry THF (250 mL) was added followed by 1.2 g (50 mmol) of NaH. A reflux condenser was placed atop the reaction vessel and capped with a balloon. The Schlenk cock closed and the stem was capped with a septum. The reaction mixture was heated to reflux for 30 min at which point it had turned yellow. Toluene **15** (2.57 g, 21.4 mmol) was added via a syringe in approximately 10 0.25 mL aliquots every 5 min. The reaction was allowed to cool to room temperature. The crude reaction mixture was poured slowly into a 2 L Erlenmeyer flask filled with 1 kg of ice. The product was extracted with hexane (2×200 mL), reduced and run over a fritted funnel with a silica plug. The product was obtained as a pale yellow solid (1.72 g, 36% yield). Mp: 150 °C. ^1H NMR (CDCl_3) δ 8.01 (s, 2H), 7.41–7.39 (d, 4H, $J_{\text{H,H}}=7.69$ Hz), 7.21–7.14 (m, 6H), 6.97–6.92 (d, 2H, $J_{\text{H,H}}=15.9$ Hz), 1.53 (s, 6H). ^{13}C NMR (CDCl_3) δ 138.2, 137.2, 136.7, 132.5, 129.4, 126.6, 123.1, 106.0, 99.3, 21.4. IR (cm^{-1}): 3045.9, 3040.1, 3017.9, 3006.8, 2965.8, 2917.1, 2853.0, 1628.3, 1624.0, 1607.6, 1568.0, 1508.7, 1456.6, 1448.0, 1436.9, 1409.4, 1376.6, 1354.9, 1325.5, 1300.4, 1281.6, 1279.2, 1262.3, 1229.5, 111.81.3, 1118.2, 1108.5, 1040.0, 1038.3, 1016.9, 949.9, 847.2.

4.1.4. 1,2-Bis-(3,5-bis-trifluoromethyl-phenylethynyl)-4,5-bis(4-diethylaminostyryl)benzene (18). A 500 mL Schlenk flask was charged with a stirbar and 3.70 g (5.87 mmol) of **14** while under nitrogen purge. Dry THF (250 mL) was added followed by 1.2 g (50 mmol) of NaH. A reflux condenser was placed atop the reaction vessel and

capped with a balloon. The Schlenk cock was closed and the stem was capped with a septum. The reaction mixture was heated to reflux for 30 min at which point it had turned yellow. Diethylaminobenzaldehyde **16** (2.30 g, 12.9 mmol) was dissolved in the minimum volume of dry THF (~8 mL) and was added via a syringe in 8 aliquots every 5 min. The reaction was allowed to cool to room temperature. The crude reaction mixture was poured slowly into a 2 L Erlenmeyer flask filled with 1 kg of ice. This mixture was separated with the addition of NaCl and the THF portion was extracted then reduced. The crude product was redissolved in 50 mL of hexane with 10 mL of dichloromethane. This solution was run over a fritted funnel with a silica plug in the same solvent mixture. The product proceeded as a yellow band, was collected and the solution was evaporated and further purified by crystallization from hexane/dichloromethane mixture. The product was obtained as large yellow crystals (1.55 g, 39% yield). Mp: 175 °C. ^1H NMR (CDCl_3) δ 7.94 (s, 2H), 7.36–7.35 (d, 4H, 8.24 Hz), 7.01–6.96 (d, 2H, $J_{\text{H,H}}=15.9$ Hz), 6.89–6.86 (d, 2H, $J_{\text{H,H}}=15.9$ Hz), 3.41–3.34 (q, 8H, $J_{\text{H,H}}=7.1$ Hz), 1.52–1.14 (t, 12H, $J_{\text{H,H}}=7.1$ Hz). ^{13}C NMR (CDCl_3) δ 147.9, 138.0, 136.5, 132.5, 128.4, 124.5, 119.4, 111.8, 104.9, 44.7, 13.0. IR (cm^{-1}): 3039.1, 3006.3, 2959.6, 2923.4, 1601.8, 1596.0, 1576.2, 1557.9, 1512.6, 1495.7, 1490.4, 1479.3, 1464.8, 1441.2, 1429.6, 1373.7, 1357.8, 1355.4, 1265.2, 1200.1, 1236.6, 1138.4, 1092.1, 1078.1, 1070.4, 1025.1, 947.0, 930.1.

4.1.5. 1,2-Bis-p-tolyethynyl-4,5-bis-(2-p-tolyl-vinyl)-benzene (6). 1.00 g (1.78 mmol) of **17** were placed into a Schlenk tube with a stirbar under nitrogen purge. To this was added 5.0 mL of THF and 3.0 mL of piperidine. This solution was allowed to stir vigorously for 10 min. 10 mg (14 μmol) of $\text{Pd}(\text{PPh}_3)_2\text{Cl}_2$ and 5.0 mg (26 μmol) of CuI were added and the tube was fitted with a septum. With a syringe, 516 mg (4.45 mmol) of 4-methyl-1-ethynylbenzene were added. The reaction was allowed to proceed at room temperature for 48 h. The crude reaction mixture was diluted with hexane and run through a silica plug on a fritted funnel with hexane (100 mL) as an eluent. The hexane solution was collected and discarded. A 50:50 dichloromethane:hexane mixture (250 mL) was then passed through the silica plug and collected. This solution was reduced to yield 437 mg (46% yield) of a green crystalline solid. To obtain crystals for XRD analysis 100 mg were dissolved in approximately 10 mL of dichloromethane. Aliquots of this solution (2–3 mL) were placed in the bottom of a test tube filled with hexane and capped with a septum. Mp: 233 °C. ^1H NMR (CDCl_3) δ 7.78, 7.51–7.48 (d, 4H, $J_{\text{H,H}}=7.97$ Hz), 7.46–7.43 (d, 4H, $J_{\text{H,H}}=7.97$ Hz), 7.38–7.33 (d, 2H, 15.9 Hz), 7.21–7.16 (m, 8H), 7.09–7.03 (d, 2H, $J_{\text{H,H}}=15.9$ Hz), 2.37 (s, 12H). ^{13}C NMR (CDCl_3) δ 138.4, 137.9, 135.6, 134.3, 132.1, 131.5, 129.5, 129.4, 129.1, 126.6, 124.5, 124.1, 120.2, 94.0, 87.9, 21.7, 21.4. IR (cm^{-1}): 3024.2, 2918.1, 2855.4, 2731.0, 2203.0, 1905.1, 1792.2, 1656.7, 1629.3, 1605.6, 1512.6, 1481.7, 1447.5, 1412.3, 1377.1, 1302.3, 1281.1, 1264.7, 1209.8, 1181.8, 1118.2, 1104.7, 1039.6, 1033.3, 1016.9, 970.1, 962.4, 816.8, 806.7.

4.1.6. 1,2-Bis-phenylethynyl-4,5-bis(4-diethylamino)-styryl-benze (7). 520 mg (0.769 mmol) of **18** were placed into a Schlenk tube with a stirbar under nitrogen purge. To

this was added 5.0 mL of THF and 3.0 mL of piperidine. This solution was allowed to stir vigorously for 10 min. 10 mg (14 μmol) of $\text{Pd}(\text{PPh}_3)_2\text{Cl}_2$ and 5.0 mg (26 μmol) of CuI were added and the tube was fitted with a septum. With a syringe, 500 mg (4.9 mmol) of phenylacetylene were added. The reaction was allowed to proceed at room temperature for 48 h. The crude reaction mixture was diluted with hexane and run through a silica plug on a fritted funnel with hexane (100 mL) as an eluent. The hexane solution was collected and discarded. A 50:50 dichloromethane:hexane mixture (250 mL) was then passed through the silica plug and collected. This solution was reduced to 25 mL and poured into 200 mL of methanol. The precipitate was collected to yield 384 mg (80%) of a yellow crystalline solid. To obtain crystals for XRD analysis 100 mg were dissolved in approximately 10 mL of dichloromethane. Aliquots of this solution (2–3 mL) were placed in the bottom of a test tube filled with methanol and capped with a septum. Mp: 191–193 °C. ^1H : δ 7.88 (s, 2H), 7.64–7.61 (m, 4H), 7.46–7.43 (d, 4H, $J_{3\text{H,H}}=8.5$ Hz), 7.41–7.35 (m, 6H), 7.24–7.19 (d, 2H, $J_{3\text{H,H}}=15.9$ Hz), 7.06–7.00 (d, 2H, 16.2 Hz), 6.71–6.68 (d, 4H, 8.5 Hz), 3.44–3.37 (q, 8H, $J_{3\text{H,H}}=6.9$ Hz), 1.23–1.18 (t, 12H, $J_{3\text{H,H}}=6.9$ Hz) ^{13}C : δ 147.8, 136.5, 132.3, 131.8, 129.5, 128.5, 128.4, 124.9, 123.8, 123.6, 120.4, 111.8, 93.5, 89.3, 44.8, 13.1. IR (cm^{-1}): 3061.8, 3017.9, 2977.4, 2965.8, 2001.5, 1951.4, 1876.6, 1597.4, 1583.9, 1552.1, 1511.1, 1462.9, 1441.2, 1426.7, 1396.4, 1393.0, 1371.3, 1293.2, 1250.8, 1219.4, 1176.5, 1156.7, 1139.9, 1092.1, 1070.9, 1064.2

4.1.7. 1,2-Bis(4-diethylaminostyryl)-4,5-bis-(4-trifluoromethyl-phenylethynyl)benzene (8). 510 mg (0.754 mmol) of **18** were placed into a Schlenk tube with a stirbar under nitrogen purge. To this was added 5.0 mL of THF and 3.0 mL of piperidine. This solution was allowed to stir vigorously for 10 min. 10 mg (14 μmol) of $\text{Pd}(\text{PPh}_3)_2\text{Cl}_2$ and 5.0 mg (26 μmol) of CuI were added and the tube was fitted with a septum. With a syringe, 3.00 g (17.6 mmol) of 4-trimethylfluoromethylethynylbenzene were added. The reaction was allowed to proceed at room temperature for 48 h. The crude reaction mixture was diluted with hexane and run through a silica plug on a fritted funnel with hexane (100 mL) as an eluent. The hexane solution was collected and discarded. A 50:50 dichloromethane:hexane mixture (250 mL) was then passed through the silica plug and collected. This solution was reduced to 25 mL and poured into 200 mL of methanol. The precipitate was collected to yield 457 mg (80%) of a yellow crystalline solid. To obtain crystals for XRD analysis 100 mg were dissolved in approximately 10 mL of dichloromethane. Aliquots of this solution (2–3 mL) were placed in the bottom of a test tube filled with methanol and capped with a septum. Mp: 220 °C. ^1H NMR (CDCl_3) δ 7.73 (s, 2H), 7.64–7.57 (m, 8H), 7.41 (d, 4H, $J_{3\text{H,H}}=8.24$ Hz), 7.18 (d, 2H, $J_{3\text{H,H}}=15.9$ Hz), 7.01 (d, 2H, $J_{3\text{H,H}}=15.9$ Hz), 6.66 (d, 4H, $J_{3\text{H,H}}=8.24$ Hz), 3.40–3.37 (q, 8H, $J_{3\text{H,H}}=6.87$ Hz), 1.21–1.17 (t, 12H, $J_{3\text{H,H}}=6.59$ Hz). ^{13}C NMR (CDCl_3) δ 137.05, 132.67, 131.90, 130.67–129.37 (q, $J_{2\text{C,F}}=33.2$ Hz), 129.68, 129.56–118.76 (q, $J_{1\text{C,F}}=271.4$ Hz), 128.47, 127.53, 125.54, 124.7, 122.82, 120.09, 111.76, 92.03, 91.51, 44.76, 13.03. IR (cm^{-1}): 2967.3, 2866.0, 2207.9, 1873.7, 1616.9, 1601.8, 1576.2, 1475.9, 1456.6, 1448.0, 1428.2, 1398.8, 1358.3, 1349.6, 1310.1, 1297.0, 1267.6,

1154.3, 1120.1, 1104.2, 1064.6, 1013.5, 1001.5, 966.8, 955.2, 931.1.

4.1.8. 1,2-Bis-(3,5-bis-trifluoromethylphenylethynyl)-4,5-bis(4-diethylaminostyryl)benzene (9). 520 mg (0.769 mmol) of **18** were placed into a Schlenk tube with a stirbar under nitrogen purge. To this was added 5.0 mL of THF and 3.0 mL of triethylamine. This solution was allowed to stir vigorously for 10 min. 10 mg (14 μmol) of $\text{Pd}(\text{PPh}_3)_2\text{Cl}_2$ and 5.0 mg (26 μmol) of CuI were added and the tube was fitted with a septum. With a syringe, 3.00 g (12.6 mmol) of 3,5-bistrifluoromethylethynylbenzene were added. The reaction was allowed to proceed at room temperature for 48 h. The crude reaction mixture was diluted with hexane and run through a silica plug on a fritted funnel with hexane (100 mL) as an eluent. The hexane solution was collected and discarded. A 50:50 dichloromethane:hexane mixture (250 mL) was then passed through the silica plug and collected. This solution was reduced to 25 mL and poured into 200 mL of methanol. The precipitate was collected to yield 646 mg (94% yield) of a yellow crystalline solid. To obtain single crystalline specimen 100 mg were dissolved in approximately 10 mL of dichloromethane. Aliquots of this solution (2–3 mL) were placed in the bottom of a test tube filled with methanol and capped with a septum. Mp: 207 °C. ^1H NMR (CDCl_3) δ 7.97 (s, 4H), 7.82 (s, 2H), 7.80 (s, 2H), 7.45 (d, 4H, $J_{3\text{H,H}}=8.79$ Hz), 7.21 (d, 2H, $J_{3\text{H,H}}=15.9$ Hz), 7.06 (d, 2H, $J_{3\text{H,H}}=15.9$ Hz), 6.70 (d, 4H, $J_{3\text{H,H}}=8.80$ Hz), 3.44–3.37 (q, 8H, $J_{3\text{H,H}}=7.12$ Hz), 1.22–1.18 (t, 12H, $J_{3\text{H,H}}=7.13$ Hz). ^{13}C NMR (CDCl_3) δ 148.0, 137.6, 133.2, 133.0–131.6 (q, $J_{2\text{C,F}}=33.2$ Hz), 131.4, 129.9, 128.5, 128.5–117.6 (q, $J_{\text{C,F}}=272.6$ Hz), 125.8, 124.5, 122.2, 121.2, 119.7, 111.8, 92.7, 90.5, 44.8, 13.0. IR (cm^{-1}): 2967.8, 2207.4, 1605.2, 1576.2, 1521.3, 1517.4, 1487.0, 1466.3, 1429.6, 1398.8, 1390.1, 1349.1, 1296.6, 1284.5, 1279.7, 1267.6, 1245.9, 1176.5, 1169.3, 1105.6, 1097.9, 1077.2, 1074.3, 959.5, 937.8.

4.2. Cyclic voltametry

Electrochemical experiments were carried out with CH Instruments model 660 electrochemical workstation. Cyclic voltammograms (CV) were obtained by using a conventional three-electrode system. A platinum foil was used as the counter electrode. A platinum disk electrode ($\phi=1.2$ mm) from Bioanalytical Systems serves as a working electrode. Reference electrode **A**, $\text{Ag}/0.1\text{M}$ AgNO_3 in acetonitrile, was separated from the test by a fritted bridge containing the background electrolyte (0.1 M Bu_4NPF_6 in acetonitrile). The reference electrode was calibrated before each experiment with the ferrocene/ferrocenium (Fc/Fc^+) redox system. The $E_{1/2}$ of 5 mM of Fc/Fc^+ in 0.1 M Bu_4NPF_6 in acetonitrile was 0.37 V. The standard redox potential of the Fc/Fc^+ system has been determined to be 0.190 V (Bard, A. J.; Faulkner, L. R. *Electrochemical Methods*; Wiley: New York, 1980, p 701). Therefore, the potential of our reference electrode **A** was 0.227 V versus S.H.E. All solutions were purged prior to electrochemical measurements using nitrogen gas. All solvents were dried with molecular sieves (3 Å). All the salts were used as received from Aldrich.

4.3. Quantum chemical calculations

The program SPARTAN 04 was implemented on a Windows XP platform (Dell, 3.0 GHz processor speed). The geometries were first determined utilizing an AM1 calculation. The obtained geometries were utilized in a second set of minimizations to determine the equilibrium structure utilizing B3LYP with a 6-31G** basis set.

4.4. Single crystal structure determination^{15–20}

Suitable crystals of **6**, **7** and **8** were coated with Paratone N oil, suspended in a small fiber loop and placed in a cooled nitrogen gas stream at 173 K on a Bruker D8 SMART APEX CCD graphite monochromated Mo K α (0.71073 Å) diffractometer for **6** and a D8 SMART 1000 CCD graphite monochromated Cu K α (1.5418 Å) diffractometer for **7** and **8**. Data were measured using a series of combinations of phi and omega scans with 20 s frame exposures and 0.3° frame widths. Data collection, indexing and initial cell refinements were all carried out using SMART software. Frame integration and final cell refinements were done using SAINT software. The final cell parameters were determined from least-squares refinement on 2911, 3793 and 3786 reflections for **6**, **7** and **8**, respectively. The SADABS program was used to carry out absorption corrections. The structure was solved using Direct methods and difference Fourier techniques (SHELXTL, V6.12). Hydrogen atoms were placed their expected chemical positions using the HFIX command and were included in the final cycles of least squares with isotropic U_{ij} 's related to the atom's riddon upon. The C–H distances were fixed at 0.93 Å (aromatic and amide), 0.98 Å (methine), 0.97 Å (methylene), or 0.96 Å (methyl). All non-hydrogen atoms were refined anisotropically. Scattering factors and anomalous dispersion corrections are taken from the International Tables for X-ray Crystallography.¹⁹ Structure solution, refinement, graphics and generation of publication materials were performed by using SHELXTL, V6.12 software. Additional details of data collection and structure refinement are given in Table 4.

Acknowledgements

U. Bunz and J. Wilson thank the National Science Foundation (DMR 0138948) for generous support.

References and notes

1. *Electronic Materials, the Oligomers Approach*; Müllen, K., Wegner, G., Eds.; Wiley-VCH: Weinheim, 1998.
2. Ball, P. *Made to Measure*; Princeton: Paperback, Princeton, 1999.
3. (a) Bunz, U. H. F. *Chem Rev.* **2000**, *100*, 1603–1644. (b) Halkyard, C. E.; Rampey, M. E.; Kloppenburg, L.; Studer-Martinez, S. L.; Bunz, U. H. F. *Macromolecules* **1998**, *31*, 8655–8659. (c) Miteva, T.; Palmer, L.; Kloppenburg, L.; Neher, D.; Bunz, U. H. F. *Macromolecules* **2000**, *33*, 652–654. (d) Scherf, U. *Top. Curr. Chem.* **1999**, *201*, 163–222.
4. (a) Schmitz, C.; Posch, P.; Thelakkat, M.; Schmidt, H. W.; Montali, A.; Feldman, K.; Smith, P.; Weder, C. *Adv. Funct. Mater.* **2001**, *11*, 41–46. (b) Kokil, A.; Shiyonovskaya, I.; Singer, K. D.; Weder, C. *Synth. Met.* **2003**, *138*, 513–517.
5. Pschirer, N. G.; Miteva, T.; Evans, U.; Roberts, R. S.; Marshall, A. R.; Neher, D.; Myrick, M. L.; Bunz, U. H. F. *Chem. Mater.* **2001**, *13*, 2691–2696.
6. Wilson, J. N.; Windscheif, P. M.; Evans, U.; Myrick, M. L.; Bunz, U. H. F. *Macromolecules* **2002**, *35*, 8681–8683.
7. Wilson, J. N.; Josowicz, M.; Wang, Y. Q.; Bunz, U. H. F. *Chem. Commun.* **2003**, 2962–2963.
8. Wilson, J. N.; Smith, M. D.; Enkelmann, V.; Bunz, U. H. F. *Chem. Commun.*, in press.
9. (a) Yamamoto, T. *Synlett* **2003**, 425–450. (b) Yamamoto, T. *Bull. Chem. Soc. Jpn* **1999**, *72*, 621–638. (c) Sonogashira, K. *J. Organomet. Chem.* **2002**, *653*, 46–49. (d) Sonogashira, K.; Tohda, Y.; Hagihara, N. *Tetrahedron Lett.* **1975**, 4467–4470. (e) Negishi, E.; Anastasia, L. *Chem. Rev.* **2003**, *103*, 1979–2017.
10. (a) Horner, L.; Hoffmann, H.; Wippel, H. G. *Chem. Ber.* **1958**, *91*, 61. (b) Horner, L.; Klink, W. *Tetrahedron Lett.* **1964**, *36*, 2467.
11. (a) Böhm, A.; Adam, M.; Mauermann, H.; Stein, S.; Müllen, K. *Tetrahedron Lett.* **1992**, *33*, 2795–2798. (b) Böhm, A.; Müllen, K. *Tetrahedron Lett.* **1992**, *33*, 611–614. (c) Müller, M.; Mauermann-Düll, H.; Wagner, M.; Enkelmann, V.; Müllen, K. *Angew. Chem., Int. Ed.* **1995**, *34*, 1583–1586.
12. (a) Tykwinski, R. R.; Zhao, Y. M. *Synlett* **2002**, 1939–1953. (b) Zhao, Y. M.; McDonald, R.; Tykwinski, R. R. *J. Org. Chem.* **2002**, *67*, 2805–2812. (c) Tykwinski, R. R.; Schreiber, M.; Carlon, R. P.; Diederich, F.; Gramlich, V. *Helv. Chem. Acta* **1996**, *79*, 2249–2281. (d) Tykwinski, R. R.; Diederich, F. *Liebigs Ann.-Recueil* **1997**, 649–661.
13. (a) Hagen, S.; Hopf, H. *Top. Curr. Chem.* **1998**, *196*, 45–89. (b) Hopf, H.; Kreuzer, M.; Jones, P. G. *Chem. Ber.* **1991**, *124*, 1471–1475.
14. (a) Cao, J.; Curtis, M. D. *Chem. Mater.* **2003**, *15*, 4424–4430. (b) Koren, A. B.; Curtis, M. D.; Francis, A. H.; Kampf, J. W. *J. Am. Chem. Soc.* **2003**, *125*, 5040–5050. (c) Koren, A. B.; Curtis, M. D.; Kampf, J. W. *Chem. Mater.* **2000**, *12*, 1519–1523.
15. SMART Version 5.628, Bruker AXS, Inc Analytical X-ray Systems, 5465 East Cheryl Parkway, Madison WI 53711, 55373, 2003.
16. SAINT Version 6.36A, Bruker AXS, Inc, Analytical X-ray Systems, 5465 East Cheryl Parkway, Madison, WI 53711, 55373, 2002.
17. SADABS Version 2.08, George Sheldrick, University of Göttingen, 2003.
18. SHELXTL V6.12, Bruker AXS, Inc, Analytical X-ray Systems, 5465 East Cheryl Parkway, Madison, WI 53711, 55373, 2002.
19. *International Tables for X-ray Crystallography, Volume C*; Wilson, A. J. C., Ed.; Kynoch, Academic: Dordrecht, 1992; p 500 Tables 6.1.1.4 (pp 500–502) and 4.2.6.8 (pp 219–222).
20. CCDC reference numbers for **6–8** are 238654–6.



Synthesis of acrylate and norbornene polymers with pendant 2,7-bis(diarylamino)fluorene hole-transport groups

Richard D. Hreha,^a Andreas Haldi,^b Benoit Domercq,^{b,c,d} Stephen Barlow,^{a,c,e}
Bernard Kippelen^{b,c,d,*} and Seth R. Marder^{a,b,c,e,*,†}

^aDepartment of Chemistry, University of Arizona, Tucson, AZ 85721, USA

^bOptical Sciences Center, University of Arizona, Tucson, AZ 85721, USA

^cCenter for Organic Photonics and Electronics, Georgia Institute of Technology, Atlanta, GA 30332-0400, USA

^dSchool of Electrical and Computer Engineering, Georgia Institute of Technology, Atlanta, GA 30332-0250, USA

^eSchool of Chemistry and Biochemistry, Georgia Institute of Technology, Atlanta, GA 30332-0400, USA

Received 29 March 2004; revised 4 June 2004; accepted 14 June 2004

Available online 2 July 2004

In honor of Prof. Bob Grubbs on his receipt of the Tetrahedron Prize for Creativity in Organic Chemistry

Abstract—New hole-transport monomers have been synthesized in which a 2,7-(diarylamino)fluorene hole-transport functionality is linked through the 9-position of the fluorene bridge to a polymerizable acrylate or norbornene group; these monomers have been polymerized under free-radical and ring-opening metathesis polymerization (ROMP) conditions, respectively. The norbornene monomer has also been copolymerized with a cinnamate-functionalized norbornene; this copolymer can be rendered insoluble through photo-crosslinking of the cinnamate groups under UV irradiation, thus permitting the use of the polymer in organic electronic devices based upon multiple polymer layers. The norbornene monomer has also been copolymerized with dicyclopentadiene to afford insoluble crosslinked films. Time-of-flight studies indicate that the norbornene polymer has a higher hole mobility than the analogous acrylate material, consistent with the predictions of the disorder formalism.

© 2004 Elsevier Ltd. All rights reserved.

1. Introduction

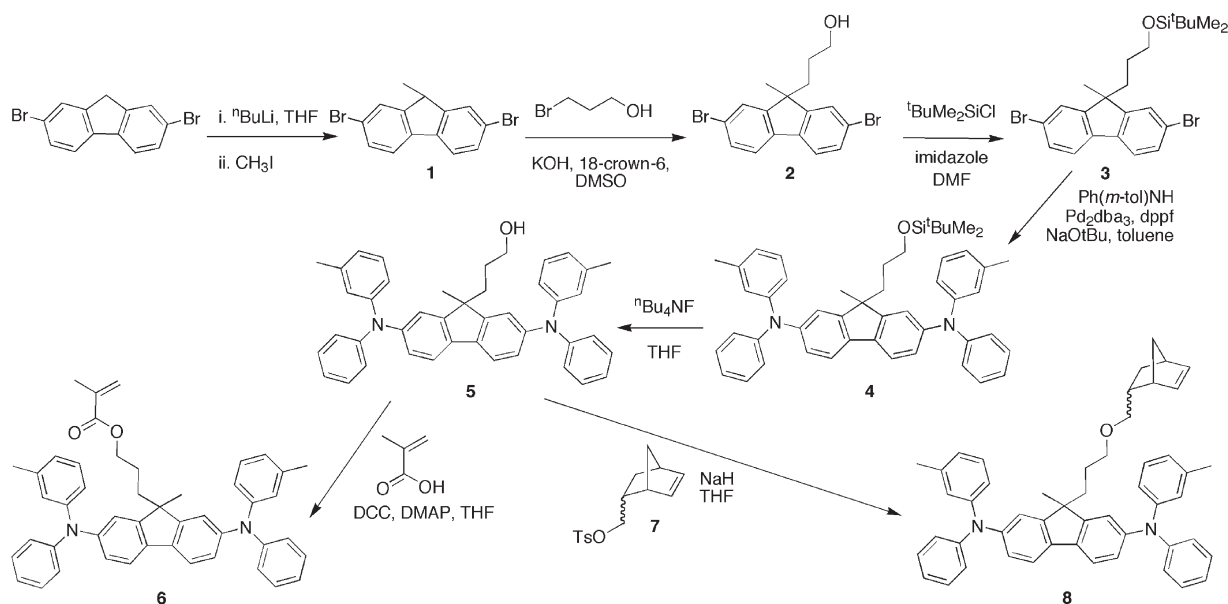
Organic light-emitting diodes (OLEDs) are typically based upon vacuum-deposited small molecules or upon solution-processible conjugated polymers. We have been interested in a third strategy in which devices are based upon solution-processible side-chain polymers in which the side-chains are functionalized with small molecules with transport or luminescent properties.^{1–21} Here the ease of solution processing is retained, whilst the electronic properties of materials can be tuned through the choice of small molecule from among the wide range of well-studied examples. The rheological properties of the polymer may be tuned through the choice of polymer backbone, and through copolymerization with other monomers. In particular, we have focused on polyacrylates: copolymerization of monomers functionalized with 4,4'-bis(diarylamino)biphenyl ('TPD') hole-transport (HT) groups with those bearing photo-

crosslinkable groups has led to polymers that can be rendered insoluble after processing from solution, thus permitting photo-patterning by UV irradiation through a photolithographic mask and fabrication of devices incorporating multiple solution-processible polymer layers.^{15–19,22} OLEDs based on small-molecule 2,7-bis(diarylamino)-9,9-dimethylfluorenes as the HT material have recently been shown to have similar performance to those based upon TPD species with comparable ionization potential (the fluorene species are ca. 0.11–0.14 V more readily oxidized than their biphenyl analogues).²³ Here, we report on the synthesis of bis(diarylamino)fluorene HT polymers with backbones based on (i) radical-polymerized methacrylate groups and (ii) on the ring-opening metathesis polymerization (ROMP) of norbornene. We were particularly interested in norbornene-based polymers, since, according to the disorder formalism of Bäessler, Borsenberger and co-workers,^{24–27} the relatively non-polar main chain should have less adverse effect on the hole mobilities of the material than polar ester groups of poly(acrylate)s, the dipole moments associated with which being anticipated to lead to increased energetic disorder in the HT manifold.²² Moreover, ROMP offers possibilities to obtain polymers with narrow molecular-weight distributions, to control the nature of the end groups, to obtain well-defined block

Keywords: Hole-transport; Organic light-emitting diode; Ring-opening metathesis polymerization.

* Corresponding authors. Tel.: +1-404-385-6048; fax: +1-404-385-6057 (S.R.M.); e-mail addresses: kippelen@ece.gatech.edu; seth.marder@chemistry.gatech.edu

† Present address: School of Chemistry and Biochemistry, Georgia Institute of Technology, Atlanta, GA 30332-0400, USA.



Scheme 1. Synthesis of bis(diarylamino)fluorene-based monomers.

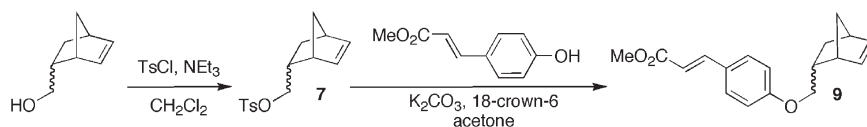
copolymers, and to incorporate a wide range of other chemical functionalities into polymers.^{28–32} We also report the incorporation of our norbornene HT monomer into a photocrosslinkable copolymer with a new cinnamate-functionalized norbornene monomer, and into a cross-linked copolymer with dicyclopentadiene. Finally, we compare the hole mobilities of the acrylate and norbornene polymers measured using the time-of-flight technique.

2. Results and discussion

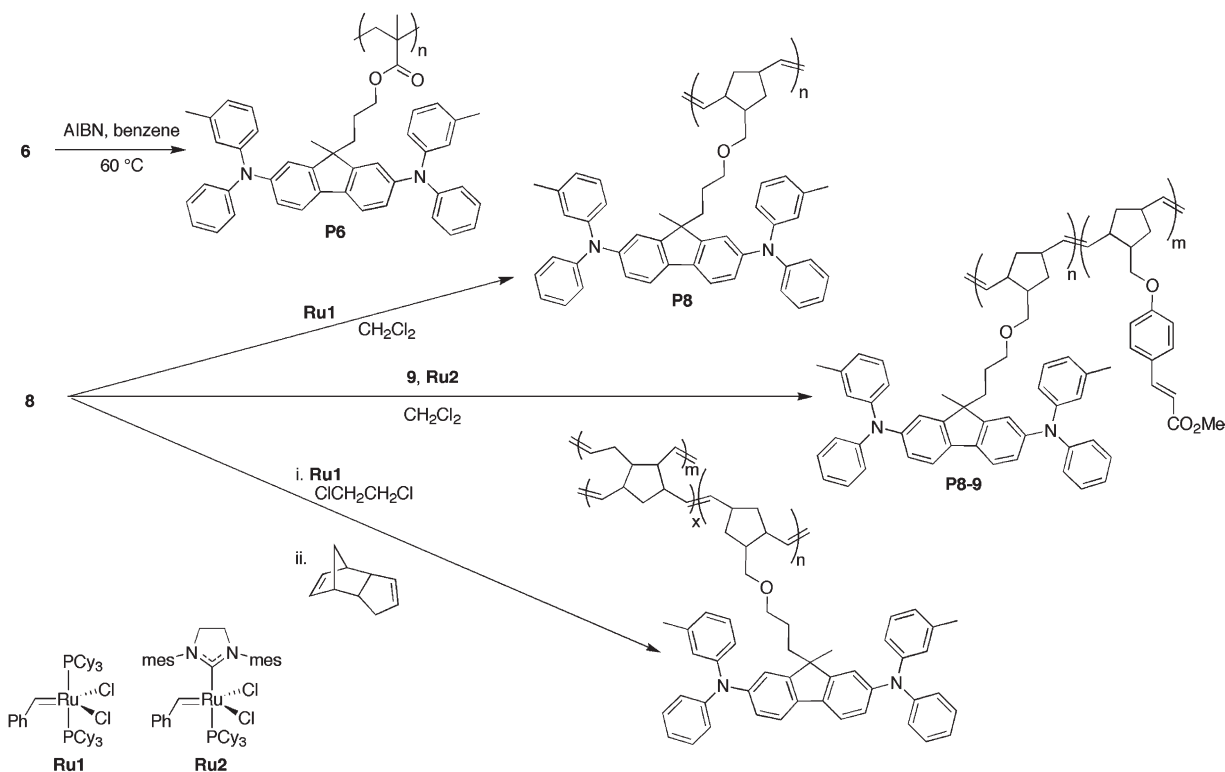
Our synthetic route to bis(diarylamino)fluorene monomers (Scheme 1) takes advantage of the ease with which fluorene may be alkylated in the 9-position. Thus, 2,7-dibromo-9-methylfluorene, **1**, was obtained by lithiation of 2,7-dibromofluorene with $^n\text{BuLi}$, followed by treatment with methyl iodide (**1** has previously been obtained by bromination of 9-methylfluorene³³). The protected-hydroxyl-functionalized 2,7-dibromofluorene, **3**, was then obtained by alkylation with *tert*-butyldimethylsilyl-protected 3-bromopropanol using potassium hydroxide as a base. Alternatively, alkylation can be carried out using unprotected 3-bromopropanol under the same conditions, with subsequent protection of the hydroxy group using *tert*-butyldimethylchlorosilane. The fluorene core, **3**, was then coupled with phenyl-*m'*-tolylamine using the palladium-catalyzed coupling reaction developed by Buchwald and Hartwig,^{34,35} specifically using tris(dibenzylideneacetone)dipalladium (Pd_2dba_3) and 1,1'-bis(diphenylphosphino)ferrocene (dppf) as the catalyst system in the presence of sodium *tert*-butoxide.³⁶ After deprotection of the alcohol using tetra-*n*-

butylammonium fluoride in tetrahydrofuran, the hydroxyl-functionalized bis(diarylamino)fluorene, **5**, can potentially be attached to a variety of polymerizable groups. The methacrylate monomer, **6**, was obtained by condensation of **5** with methacrylic acid using 1,3-dicyclohexylcarbodiimide (DCC) as a dehydrating agent and 4-(dimethylamino)pyridine (DMAP) as a catalyst. The norbornene monomer, **8**, was synthesized under Williamson ether synthesis conditions (Scheme 1); the norbornene tosylate used, **7**, was synthesized in a modification of a literature procedure (Scheme 2).³⁷ Compound **7** was also used to synthesize a cinnamate monomer, **9**, as a photocrosslinking group suitable for copolymerization with **8** (Scheme 2).

The methacrylate monomer, **6**, was polymerized to give **P6** under free-radical conditions using 2,2'-azobisisobutyronitrile (AIBN) as an initiator (Scheme 3); GPC analysis in THF was used to estimate the molecular weight distribution of **P6** and suggested $M_n=17,000$ and $M_w=59,000$, corresponding to $\text{PDI}=3.5$. The norbornene monomer, **8**, was polymerized to give **P8** using the Grubbs catalyst, **Ru1** (Scheme 3). As expected, the ROMP process gave polymer with a much lower polydispersity than the radical polymerization; GPC suggested $M_n=13,000$, $M_w=16,000$ and $\text{PDI}=1.2$. A copolymer, **P8–9**, was synthesized from a 7:3 ratio of **8** and **9** using the Grubbs' second-generation catalyst, **Ru2** (Scheme 3). All three polymers were readily soluble in a range of organic solvents including THF, chloroform, toluene, benzene and dichloromethane. Differential scanning calorimetry (DSC) showed the glass-transition temperatures (T_g) of **P8** and **P8–9** to be 97 and 120 °C, respectively, with no evidence of other thermal



Scheme 2. Synthesis of a norbornene monomer functionalized with a cinnamate crosslinking group.



Scheme 3. Polymerization reactions of the bis(diarylamino)fluorene monomers, **6** and **8**, and structures of the ROMP initiators used (mes=2,4,6-trimethylphenyl; Cy=cyclohexyl).

process in the temperature range investigated (25–250 °C), suggesting these polymers are amorphous.

Crosslinking of **P8–9** under UV irradiation was monitored by UV spectroscopy. In initial experiments, thin films of **P8–9** were obtained on a glass substrate by spin-coating at 1600 rpm from THF solution (20.0 mg in 1 ml). The polymer films were irradiated using an unfiltered hand-held UV source (365 nm, 7 W, UVGL-25, for visualizing thin-layer chromatography plates). The films were kept 6.1 cm from the UV lamp. The progress of the crosslinking was monitored by UV–vis spectroscopy; the absorbance at 310 nm, attributed to the cinnamate group, was found to decrease, whilst that at 377 nm, attributed to the bis(diarylamino)fluorene moiety, remained constant, consistent with the cinnamate groups undergoing 2+2 cycloaddition reactions without photo-induced damage to the HT groups occurring.

The insolubility of the UV-irradiated **P8–9** films on glass substrates was demonstrated by dipping the films in THF for increasing lengths of time and monitoring the UV spectra of the films. For the films that were exposed to 365 nm light from 3 to 6 min, only a small decrease (<5% change) in absorbance was observed, even after soaking the films for up to 120 min, suggesting that the polymers were largely crosslinked. In comparison, the bis(diarylamino)fluorene absorbances of non-irradiated films of **P8–9** on glass were found to decrease dramatically, even after soaking the films in THF for less than 1 min. These findings are entirely analogous to those we have previously reported for bis(diarylamino)biphenyl/cinnamate acrylate-based copolymers,¹⁵ clearly showing the general applicability of the

photocrosslinking of cinnamate side chains as a means to render polymer films insoluble, and suggesting that it should be possible to incorporate norbornene HT polymers into devices based on the processing of more than one layer from solution.

Whilst **P8–9** contains considerably fewer polar groups than our previous crosslinkable acrylate polymers, there are still polar ester groups associated with the crosslinking groups. To further reduce the polarity of our crosslinked polymers, we investigated the copolymerization of **8** with dicyclopentadiene (**Scheme 3**). At room temperature this copolymerization resulted in the formation of an insoluble, presumably crosslinked, material. To create films of the insoluble material, we first initiated the polymerization of **8** using **Ru1** and allowed it to proceed for 2.5 h to obtain active oligomers; these were then spin-cast with dicyclopentadiene and the polymerization allowed to proceed to form insoluble films. The film-forming properties of these solutions rapidly deteriorated as the viscosity of the solution increased and the solution eventually gelled. The films that were applied to a glass substrate were soaked in THF and the UV absorption was monitored. Initially a large decrease in the UV absorption was observed in all the films indicating that a large fraction of the material was not incorporated in a crosslinked film. The film that remained after the first soaking was found to be completely insoluble indicating that a portion of the material was crosslinked.

Hole mobilities have been measured for **P6** and **P8** using the time-of-flight method according to methods we have previously described.^{15,23,38} **Figure 1** compares the room-temperature hole mobilities of the two polymers as a

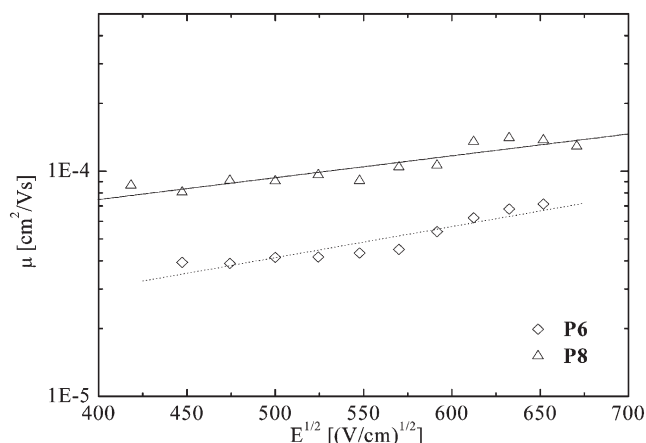


Figure 1. Electric-field dependence of the hole mobilities measured for **P6** and **P8** measured as a function of electric field at 299 K; symbols represent experimental data, lines are linear fits according to the disorder formalism.

function of electric field; the mobilities are comparable to those of blends composed of TPD or bis(diarylamino)fluorene small molecules and polystyrene. The norbornene polymer, **P8**, does indeed show higher hole mobility than its polyacrylate analogue, **P6**, consistent with a reduction in the energetic disorder due to use of a non-polar backbone.^{24–27} We have also demonstrated that OLEDs can be fabricated based upon **P8**. Details of the device work, along with a detailed study of the hole mobilities of **P6**, **P8** and related compounds, will be published elsewhere.

3. Summary

Bis(diarylamino)fluorene hole-transport groups can readily be attached to polymerizable groups through the 9-position of the fluorene. We have synthesized both acrylate and norbornene-based polymers, and have found a higher hole mobility in the latter material, consistent with the disorder formalism, which predicts polar polymer backbones should adversely affect the mobility. Cross-linked films based upon the norbornene-bis(diarylamino)fluorene monomer can be obtained either through photocrosslinking a copolymer with a cinnamate–norbornene monomer, or through copolymerizing active norbornene-bis(diarylamino)fluorene oligomers with dicyclopentadiene.

4. Experimental

4.1. General

Chemicals received from commercial sources were used without further purification. Norbornene-based materials are all derived from (5-norbornen-2-yl)methanol obtained from Aldrich as a mixture (ca. 1:1) of *endo* and *exo* isomers; no attempt was made to separate the isomers for any of our norbornene compounds and so the reported data, therefore, represents the isomeric mixture. Column chromatography was performed using silica gel (200–400 mesh, 60 Å); columns were typically ca. 15–25 cm in length and with a cross-sectional area ca. 10 cm² per 1 g of material to be purified. NMR spectra were internally referenced relative to tetramethylsilane (TMS; $\delta(^1\text{H})=0$ ppm; $\delta(^{13}\text{C})=0$ ppm)

using either the TMS ¹H resonance or the ¹³C resonance of the solvent. UV–vis spectra of thin films on quartz substrates were recorded with a Hewlett Packard 8453 spectrometer. GC–MS data were acquired on a Hewlett Packard HP6890 GC with a Hewlett Packard 5973 mass spectrometer. Glass-transition temperatures were determined using a Shimadzu DSC-50 differential scanning calorimeter run at 10 °C min^{−1}. Gel-permeation chromatography (GPC) was performed at 30 °C in THF using American Polymer Standards columns (100 Å, 1000 Å, 10⁵ Å, 5 μm), a Waters WAT038040 column heater, and a Waters 410 RI detector. Calibration was performed using Polymer Laboratories narrow polystyrene standards (580–350×10⁶).

4.2. 2,7-Dibromo-9-methylfluorene, **1**³³

To a dry 250 ml round-bottomed flask containing a magnetic stir bar was added 2,7-dibromofluorene (19.03 g, 58.7 mmol) and 100 ml of dry THF under argon. The solid was dissolved and the temperature of the reaction mixture was lowered to −78 °C in a dry ice/acetone bath. A 1.6 M solution of ⁿBuLi (40 ml, 64.0 mmol) in hexanes was added over a period of 5 min. The reaction was stirred for 5 min and methyl iodide (9.1 g, 64.0 mmol) was added. The reaction mixture was stirred for 2 h and then carefully poured into a 1000 ml separatory funnel containing 200 ml of dichloromethane and 100 ml of water. The organic layer was collected and the water layer was extracted with dichloromethane (3×50 ml). The organic layers were combined and the solvent was removed under reduced pressure to yield the crude product as a white powder. The product was obtained in pure form as white crystals after recrystallization from hot hexanes (14.0 g, 39.1 mmol, 70.4%). ¹H NMR (500 MHz, CDCl₃) δ 1.50 (d, *J*=8 Hz, 3H), 3.92 (q, *J*=8 Hz, 1H), 7.49 (d, *J*=8 Hz, 2H), 7.57 (d, *J*=8 Hz, 2H), 7.62 (s, 2H). ¹³C NMR (125 MHz, CDCl₃) δ 17.9, 42.4, 121.9, 121.2, 127.4, 130.3, 138.5, 150.6. The ¹H NMR data are consistent with the literature.³³

4.3. 2,7-Dibromo-9-(3-hydroxypropyl)-9-methylfluorene, **2**

To a 500 ml round-bottomed flask equipped a magnetic stir bar was added **1** (33.17 g, 98.1 mmol) and 150 ml of DMSO. After the solid had dissolved, potassium hydroxide (12.8 g, 119 mmol), 18-crown-6 (0.1 g), water (5 ml), and 3-bromopropan-1-ol (16.3 g, 117.0 mmol) were added and the reaction was stirred while the progress of the reaction was followed by GC/MS. Upon disappearance of the starting material, the reaction mixture was carefully poured into a 1000 ml separatory funnel containing 300 ml of dichloromethane and the solution was washed a saturated aqueous solution of sodium chloride (3×50 ml) and with distilled water (2×100 ml). The organic layer was collected and the solvent was removed under reduced pressure. The resulting material was purified by column chromatography eluting with dichloromethane to give a pale yellow oil (28.9 g, 73.4 mmol, 74.8%). ¹H NMR (300 MHz, CDCl₃) δ 0.88 (m, 2H), 1.24 (s, 1H), 1.46 (s, 3H), 2.02 (dt, *J*=3.9 Hz, 2H), 3.39 (t, *J*=6.6 Hz, 2H), 7.45 (dd, *J*=2.1, 7.8 Hz, 2H), 7.50 (d, *J*=2.1 Hz, 2H), 7.53 (d, *J*=7.8 Hz, 2H). ¹³C NMR (75 MHz, CDCl₃) δ 26.72, 27.77, 36.73, 51.18, 62.98,

121.63, 121.85, 126.45, 130.70, 138.35, 153.63. Anal. Calcd for $C_{17}H_{16}Br_2O$: C, 51.55; H, 4.07. Found: C, 51.56; H, 4.03. HRMS: Calcd for $C_{17}H_{16}Br_2O$ 393.9548, found 393.9574.

4.4. 2,7-Dibromo-9-[3-(*tert*-butyldimethylsilyloxy)-propyl]-9-methylfluorene, **3**

To a 500 ml round-bottomed flask equipped a magnetic stir bar was added **2** (28.9 g, 73.1 mmol) and 50 ml of DMF. After the solid had dissolved, *tert*-butyldimethylchlorosilane (14.4 g, 95.6 mmol) and imidazole (6.5 g, 95.6 mmol) were added and the reaction mixture was stirred while the progress of the reaction was followed by thin-layer chromatography (TLC). Upon the disappearance of the starting material, the reaction mixture was poured into a 1000 ml separatory funnel containing 100 ml of diethyl ether and 100 ml of ice-cold water and the solution was extracted with diethyl ether (3×50 ml). The organic layer was collected and the solvent was removed under reduced pressure. The product was isolated as a pale yellow oil by column chromatography, eluting with 4:1 hexanes/dichloromethane (30.4 g, 59.5 mmol, 81.4%). 1H NMR (500 MHz, $CDCl_3$) δ -0.05 (s, 6H), 0.82 (m, 2H), 0.85 (s, 9H), 1.46 (s, 3H), 2.03 (dt, $J=5$ Hz, 2H), 3.36 (t, $J=6$ Hz, 2H), 7.46 (dd, $J=2$, 8 Hz, 2H), 7.49 (d, $J=2$ Hz, 2H), 7.54 (d, $J=8$ Hz, 2H). ^{13}C NMR (125 MHz, $CDCl_3$) δ -1.42, 22.23, 29.87, 30.62, 31.55, 40.41, 54.94, 66.78, 125.25, 125.48, 130.20, 134.28, 142.05, 157.52. Anal. Calcd for $C_{23}H_{30}Br_2OSi$: C, 54.13; H, 5.92. Found: C, 54.30; H, 5.80. HRMS: Calcd for $C_{23}H_{30}Br_2OSi$ 509.0511, found 509.0503.

4.5. 2,7-Bis(phenyl-*m'*-tolylamino)-9-(3-hydroxypropyl)-9-methylfluorene, **5**

To a 250 ml round-bottomed flask equipped with a magnetic stir bar was added phenyl-*m'*-tolylamine (12.5 g, 68.2 mmol), $Pd_2(dba)_3$ (0.94 g, 1.0 mmol), dppf (1.1 g, 2.0 mmol), **3** (14.5 g, 28.4 mmol), and 100 ml of toluene under argon. The reaction mixture was allowed to stir for 10 min and sodium *tert*-butoxide (8.5 g, 88.0 mmol) was added. The reaction was stirred at 110 °C, while the progress of the reaction was monitored by TLC. Upon the disappearance of **3** the reaction mixture was cooled to room temperature and the solvent was removed under reduced pressure. The product was purified by column chromatography on silica gel eluting with 4:1 hexanes/dichloromethane. The solvent was removed under reduced pressure and the material (**4**) was deprotected without further characterization: to the 250 ml round-bottomed flask containing the material and a magnetic stir bar were added THF (30 ml) and a solution of tetra-*n*-butylammonium fluoride (1.0 M in THF, 100 ml). The mixture was stirred while the reaction was followed by TLC. Upon the disappearance of the protected alcohol, the solution was poured into a 500 ml separatory funnel containing 100 ml of water. The product was extracted with diethyl ether (3×50 ml). The organic layers were combined and the solvent was removed under reduced pressure. The product was isolated as a pale yellow glassy solid after flash chromatography, eluting with dichloromethane (9.31 g, 54.6%). 1H NMR (300 MHz, $CDCl_3$) δ 0.94 (quint, $J=4.5$ Hz, 2H), 1.33 (s, 3H), 1.87 (t, $J=8.1$ Hz, 2H), 2.22 (s, 6H), 3.28 (t, $J=5.1$ Hz, 2H), 3.29 (s 1H), 6.85 (m, 4H), 6.97

(m, 6H), 7.07 (dd, $J=1.2$, 8.1 Hz, 4H), 7.14 (t, $J=7.5$ Hz, 2H), 7.19 (d, $J=2.1$ Hz, 2H), 7.25 (m, 4H), 7.58 (d, $J=8.1$ Hz, 2H). ^{13}C NMR (75 MHz, $(CD_3)_2CO$) δ 22.35, 27.74, 29.90, 38.32, 51.96, 63.60, 119.59, 120.82, 121.74, 123.22, 124.12, 124.24, 124.45, 125.14, 129.84, 129.95, 135.76, 139.63, 147.49, 148.69, 148.78, 153.92. HRMS: Calcd for $C_{43}H_{40}N_2O$ 600.3141, found 600.3137. Anal. Calcd for $C_{43}H_{40}N_2O$: C, 85.96; H, 6.71; N, 4.66. Found: C, 85.54; H, 6.69; N, 4.62.

4.6. 2,7-Bis(phenyl-*m'*-tolylamino)-9-[3-(methacryloyloxy)propyl]-9-methylfluorene, **6**

To a dry 250 ml round-bottomed flask under argon were added **5** (1.69 g, 2.8 mmol), dicyclohexylcarbodiimide (1.22 g, 5.9 mmol), methacrylic acid (0.31 g, 3.6 mmol), and 50 ml of THF. The solution was cooled to 0 °C and 4-(dimethyl-amino)pyridine (0.2 g, 1.7 mmol) was added. The temperature was allowed to rise to room temperature while the progress of the reaction was followed by TLC. Upon the disappearance of the starting material the solvent was removed under reduced pressure. The brown solid was dissolved in 100 ml of dichloromethane and washed with 3×50 ml portions of water. The solvent was removed under reduced pressure. The product was purified by flash chromatography, eluting with 7:3 hexanes/dichloromethane. The solvent was removed under reduced pressure to give a pale yellow glassy solid (1.42 g, 2.12 mmol, 75.7%). 1H NMR (300 MHz, $(CD_3)_2CO$) δ 1.09 (quint., $J=7.2$ Hz, 2H), 1.84 (s, 3H), 1.96 (t, $J=7.8$ Hz, 2H), 2.23 (s, 6H), 3.85 (t, $J=6.6$ Hz, 2H), 5.53 (d, $J=1.8$ Hz, 1H), 5.96 (d, $J=1$ Hz, 1H), 6.85 (d, $J=8.4$ Hz, 3H), 6.91 (d, $J=7.5$ Hz, 3H), 7.00 (m, 4H), 7.08 (d, $J=7.8$ Hz, 4H), 7.16 (t, $J=7.8$ Hz, 2H), 7.20 (s, 2H), 7.27 (t, $J=7.5$ Hz, 4H), 7.62 (d, $J=7.8$ Hz, 2H). ^{13}C NMR (75 MHz, $(CD_3)_2CO$) δ 18.42, 21.39, 24.87, 26.97, 36.98, 50.98, 65.13, 119.71, 121.05, 121.89, 123.34, 124.37, 124.43, 124.54, 125.28, 125.42, 129.95, 130.06, 135.85, 137.32, 139.75, 147.81, 148.82, 148.91, 153.60, 167.21. Anal. Calcd for $C_{47}H_{44}N_2O_2$: C, 84.40; H, 6.63; N, 4.19. Found: C, 84.44; H, 6.68; N, 4.17. HRMS: Calcd for $C_{47}H_{44}N_2O_2$ 668.3403, found 668.3395.

4.7. (5-Norbornen-2-yl)methyl *p*-toluenesulfonate, **7**^{37,39,40}

To a 250 ml round-bottomed flask equipped with a magnetic stir bar was added *p*-toluenesulfonyl chloride (33.7 g, 177 mmol), (5-norbornen-2-yl)methanol (20.0 g, 161 mmol) and 80 ml of dichloromethane. After the solid had dissolved, the temperature of the solution was lowered to 0 °C in an ice bath and triethylamine (18.0 g, 177 mmol) was added. The reaction was stirred, and its progress was monitored by TLC. Upon the disappearance of the *p*-toluenesulfonyl chloride, the reaction mixture was poured into a 1000 ml separatory funnel containing 200 ml of dichloromethane and 100 ml of water. The organic layer was collected and subsequently washed with distilled water (3×50 ml). The solvent was removed under reduced pressure and the product was isolated as a colorless oil after purification by flash chromatography eluting with 8:2 hexanes/dichloromethane (33.0 g, 118.6 mmol, 73.7%). 1H NMR (300 MHz, $CDCl_3$) δ 0.42 (ddd, $J=2.4$, 4.5, 11.7 Hz, 0.5H), 1.05 (dt, $J=4.5$, 11.7 Hz, 0.5H), 1.14 (d, $J=9.0$ Hz, 0.5H), 1.21 (d, $J=8.4$ Hz, 1H), 1.28 (m, 0.5H), 1.42 (dd,

$J=2.1, 8.1$ Hz, 0.5H), 1.77 (m, 1H), 2.38 (m, 0.5H), 2.44 (s, 3H), 2.68 (s, 0.5H), 2.78 (s, 1H), 2.87 (s, 0.5H), 3.55 (t, $J=9.6$ Hz, 0.5H), 3.79 (dd, $J=6.3, 9.3$ Hz, 0.5H), 3.90 (t, $J=9.3$ Hz, 0.5H), 4.07 (dd, $J=6.3, 9.6$ Hz, 0.5H), 5.67 (dd, $J=3.0, 6.0$ Hz, 0.5H), 6.04 (s, 0.5H), 6.08 (dd, $J=3.0, 5.7$ Hz, 0.5 Hz) 7.34 (d, $J=8.1$ Hz, 2H), 7.77 (d, $J=5.4, 8.4$ Hz, 2H). ^{13}C NMR (75 MHz, CDCl_3) δ 21.59, 28.59, 29.28, 37.95, 38.13, 41.51, 42.11, 43.29, 43.56, 44.76, 49.23, 73.72, 74.34, 127.82, 129.74, 129.79, 131.71, 133.91, 135.92, 137.01, 137.92, 144.57, 144.64. Anal. Calcd for $\text{C}_{15}\text{H}_{19}\text{O}_3\text{S}$: C, 64.72; H, 6.52. Found: C, 64.88; H, 6.37. HRMS: Calcd for $\text{C}_{15}\text{H}_{19}\text{O}_3\text{S}$ 279.1055, found 279.1049. The ^1H NMR data are consistent with the literature.³⁹

4.8. 2,7-Bis(phenyl-*m'*-tolylamino)-9-[3-[(5-norbornen-2-yl)methoxy]propyl]-9-methylfluorene, **8**

To a 250 ml round-bottomed flask equipped with a reflux condenser and a magnetic stir bar was added 60% sodium hydride in mineral oil (0.7 g, 17.6 mmol) and 50 ml of dry THF under a nitrogen atmosphere. The mixture was heated to 60 °C and a solution of **7** (7.0 g, 11.7 mmol) and **5** (4.90 g, 7.6 mmol) in 50 ml of THF was added over 20 min. The reaction was stirred, while its progress was monitored by TLC. Upon the disappearance of **5**, the reaction was quenched with 10 ml of water. The reaction mixture was poured into a separatory funnel containing 50 ml of dichloromethane and 50 ml of water. The organic layers were combined and the solvent was removed under reduced pressure. The product was obtained as a white powder (7.22 g, 10.2 mmol, 87.2%) after column chromatography eluting with 7:3 hexanes/dichloromethane, followed by reprecipitation in methanol from THF. ^1H NMR (300 MHz, CDCl_3) δ 0.44 (m, 0.5H), 0.91 (t, $J=7.2$ Hz, 0.5H), 1.04 (m, 2.5H), 1.30 (m, 3H), 1.37 (s, 3H), 1.60 (m, 1H), 1.82 (m, 2H), 2.28 (s, 6H), 2.68 (s, 0.5H), 2.78 (s, 1H), 2.85 (s, 0.5H), 2.89 (t, $J=9.0$ Hz, 0.5H), 3.02 (dd, $J=6.6, 9.3$ Hz, 0.5H), 3.16 (m, 2H), 3.35 (dd, $J=6.6, 9.3$ Hz, 0.5H), 5.88 (dd, $J=2.4, 5.7$ Hz, 0.5H), 6.08 (m, 1.5H), 6.84 (d, $J=7.2$ Hz, 2H), 6.97 (m, 8H), 7.15 (m, 6H), 7.26 (t, $J=7.0$ Hz, 4H), 7.49 (d, $J=7.8$ Hz, 2H). ^{13}C NMR (75 MHz, CDCl_3): δ 21.40, 24.89, 26.48, 29.13, 29.69, 36.80, 38.69, 38.77, 41.47, 42.13, 43.62, 43.90, 44.93, 49.36, 50.33, 71.22, 71.31, 74.36, 75.29, 118.99, 119.85, 121.12, 122.29, 123.37, 123.59, 124.59, 128.92, 129.07, 132.43, 135.02, 136.53, 136.60, 137.03, 138.92, 146.65, 147.76, 152.97. HRMS: Calcd for $\text{C}_{51}\text{H}_{50}\text{N}_2\text{O}$ 706.3923, found 706.3937. Anal. Calcd for $\text{C}_{51}\text{H}_{50}\text{N}_2\text{O}$: C, 86.65; H, 7.13; N, 3.96. Found: C, 86.39; H, 6.97; N, 4.30.

4.9. Methyl 4-[(5-norbornen-2-yl)methoxy]cinnamate, **9**

To a 500 ml round-bottomed flask was added methyl 4-hydroxycinnamate (5.66 g, 38.2 mmol), **7** (10.6 g, 38.2 mmol), acetone (50 ml), 18-crown-6 (0.10 g) and potassium carbonate (5.80 g, 42.1 mmol). The reaction was stirred at reflux while being followed by TLC. Upon the disappearance of methyl 4-hydroxycinnamate, the mixture was poured into a separatory funnel containing 100 ml of water. The product was extracted into diethyl ether (3×50 ml) and the organic layer was washed with cold water (3×50 ml) and 1 M NaOH (50 ml). The solvent was removed under reduced pressure. The material was obtained

as a white powder after three reprecipitations into methanol from THF (4.50 g, 15.8 mmol, 49.8%). ^1H NMR (300 MHz, CDCl_3) δ 0.58 (ddd, $J=2.4, 11.7$ Hz, 0.5H), 1.24 (m, 3H), 1.45 (dd, $J=2.1, 7.8$ Hz, 0.5H), 1.87 (m, 1H), 2.51 (m, 0.5H), 2.82 (s, 1.5H), 3.20 (s, 0.5H), 3.51 (t, $J=9.0$ Hz, 0.5H), 3.67 (dd, $J=3.0, 6.3$ Hz, 0.5H), 3.74 (s, 3H), 3.80 (t, $J=9.0$ Hz, 0.5H), 3.97 (dd, $J=3.0, 6.3$ Hz, 0.5H), 5.96 (dd, $J=2.4, 3.0$ Hz, 0.5H), 6.10 (m, 1.5H), 6.26 (dd, $J=2.4, 15.9$ Hz, 1H), 6.84 (dd, $J=2.4, 8.7$ Hz, 2H), 7.40 (dd, $J=4.2, 8.7$ Hz, 2H), 7.60 (dd, $J=2.1, 15.6$ Hz, 1H). ^{13}C NMR (75 MHz, CDCl_3) δ 28.84, 29.45, 38.10, 38.32, 41.43, 42.07, 43.51, 43.70, 44.86, 49.25, 51.31, 71.36, 72.15, 114.66, 114.84, 114.92, 126.64, 126.74, 129.49, 129.53, 132.06, 136.19, 136.69, 137.45, 144.36, 1454.39, 160.82, 160.85, 167.51. HRMS: Calcd for $\text{C}_{18}\text{H}_{20}\text{O}_3$ 284.1412, found 284.1417. Anal. Calcd for $\text{C}_{18}\text{H}_{20}\text{O}_3$: C, 76.05; H, 7.09. Found: C, 75.73; H, 7.04.

4.10. Poly{2,7-bis(phenyl-*m'*-tolylamino)-9-[3-(methacryloyloxy)propyl]-9-methylfluorene}, **P6**

To a thick-walled glass tube containing an argon atmosphere and a stir bar was added 0.35 g (0.75 mmol) of **6** and 0.0006 g (0.0075 mmol) of AIBN. The tube was pump-filled with argon and 5 ml of deoxygenated dry benzene was added. The tube was sealed and heated at 60 °C for 60 h. The reaction mixture was allowed to cool and was poured into 100 ml of methanol. The white solid was collected by vacuum filtration and was dissolved in THF followed by reprecipitation in methanol. The process was repeated three times. The product isolated as a white powder was collected vacuum filtration (0.27 g, 77.1%). ^1H NMR (300 MHz, CDCl_3) δ 1.05 (m, broad overlapping, 10H), 2.06 (s, broad, 8H), 3.36 (m, broad overlapping, 2H), 6.97 (m, broad overlapping, 24H). Anal. Calcd for poly($\text{C}_{47}\text{H}_{44}\text{N}_2\text{O}_2$): C, 84.40; H, 6.63; N, 4.19. Found: C, 84.22; H, 6.64; N, 4.17.

4.11. Poly{2,7-bis(phenyl-*m'*-tolylamino)-9-[3-(5-norbornen-2-yl)methoxypropyl]-9-methylfluorene}, **P8**

To a Kontes tube containing a nitrogen atmosphere and a stir bar was added 1.00 g **8** in 1.5 ml of dichloromethane and 0.023 g (0.0028 mmol) of $[\text{Ru}(\text{PCy}_3)_2(=\text{CHPh})\text{Cl}_2]$ {Cy = cyclohexyl}, **Ru1**. The tube was sealed and the reaction was stirred for 35 min. The reaction mixture was quenched by stirring for 1 h with 5 ml of ethyl vinyl ether. The reaction mixture was poured into 100 ml of methanol. The white solid was collected by vacuum filtration and was dissolved in THF and then precipitated into methanol. The process was repeated twice. The product was collected as a white powder by vacuum filtration (0.76 g, 74.3%). ^1H NMR (300 MHz, THF- d_8) δ 0.93 (s, broad, 4H), 1.23 (m, broad overlapping, 6H), 1.73 (m, broad overlapping, 4H), 2.15 (s, broad, 5H), 2.44 (m, broad overlapping, 1H), 3.02 (m, broad overlapping, 5H), 5.12 (m, broad overlapping, 2H), 6.89 (m, broad overlapping, 22H), 7.44 (s, broad, 2H). Anal. Calcd for poly($\text{C}_{51}\text{H}_{50}\text{N}_2\text{O}$): C, 86.65; H, 7.13; N, 3.96. Found: C, 86.39; H, 6.93; N, 4.26.

4.12. Copolymer (7:3) of **8** and **9**, **P8-9**

To a Kontes tube containing a nitrogen atmosphere and a stir bar was added 0.25 g (0.35 mmol) **8** in 4.0 ml of

dichloromethane, 0.059 g (0.0069 mmol) of [RuL(PCy₃)₂(=CHPh)Cl₂] {L=1,3-bis(mesityl)-2-imidazolidinylidene, Cy=cyclohexyl}, **Ru2**, and 0.04 g (0.15 mmol) of **9**. The tube was sealed and the reaction was stirred for 6 h. The reaction mixture was quenched with 5 ml of ethyl vinyl ether and was poured into 100 ml of methanol. The white solid was collected by vacuum filtration and was dissolved in THF and then precipitated in methanol. The process was repeated twice. The product was collected as a white powder by vacuum filtration (0.17 g, 58.0%). *T*_g=113 °C. ¹H NMR (300 MHz, THF-*d*₈) δ 0.42 (m, broad overlapping 3H), 1.25 (m, broad overlapping, 6H), 1.78 (m, broad overlapping, 6H), 2.16 (m, broad overlapping, 4H), 2.44 (m, broad overlapping, 6H), 3.16 (m, broad overlapping, 3H), 5.24 (m, broad overlapping, 3H), 6.28 (m, broad overlapping, 26H). Anal. Calcd: C, 85.08; H, 7.12; N, 3.38. Found: C, 84.34; H, 7.01; N, 3.32.

4.13. Copolymerization of **8** and dicyclopentadiene

To a Kontes tube containing an nitrogen atmosphere and a stir bar was added 0.21 g (0.30 mmol) of **8** in 25.0 ml of 1,2-dichloroethane and 0.005 g (0.006 mmol) of [Ru(PCy₃)₂(=CHPh)Cl₂] {Cy=cyclohexyl}, **Ru1**. The tube was sealed and stirred for 2.5 h at 60 °C. 1 ml of this oligomer solution was mixed with 1 ml of a crosslinker solution composed of 0.48 g (3.6 mmol) of dicyclopentadiene dissolved in 20 ml of 1,2-dichloroethane. The solution was mixed for either 90, 150 or 180 s, and then applied by spin-coating at 1000 rpm to glass slides. At times longer than 3 min the viscosity had increased too much for the solution to be spin-coated.

4.14. Time-of-flight mobility measurements

Samples were prepared by melting a small amount of material between two ITO-coated glass slides at a temperature between 130 and 140 °C. Calibrated glass spacers (20 μm) were used to ensure a uniform sample thickness. Finally samples were sealed with quick-setting epoxy adhesive. The measurements were conducted as described elsewhere.³⁸

Acknowledgements

This material is based upon work supported in part by the STC Program of the National Science Foundation under Agreement Number DMR-0120967. We also gratefully acknowledge Durel Corporation, the Office of Naval Research, NASA (through the University of Alabama at Huntsville), and the National Science Foundation for other financial support. We also thank Amy Meyers for GPC measurements.

References and notes

- Slovik, J. *Bull. Am. Phys. Soc.* **1977**, *22*, 434.
- Stolka, M.; Pai, D. M.; Renfer, D. S.; Yanus, J. F. *J. Polym. Sci., Polym. Chem. Ed.* **1983**, *21*, 969.
- Cicalli, F.; Li, X. C.; Friend, R. H.; Moratti, S. C.; Holmes, A. B. *Synth. Met.* **1995**, *75*, 161.
- Bisberg, J.; Cumming, W. J.; Gaudiana, R. A.; Hutchinson, K. D.; Ingwall, R. T.; Kolb, E. S.; Mehta, P. G.; Minns, R. A.; Peterson, C. P. *Macromolecules* **1995**, *28*, 396.
- Kolb, E. S.; Gaudiana, R. A.; Mehta, P. G. *Macromolecules* **1996**, *29*, 2359.
- Lee, J. I.; Kang, I. N.; Hwang, D. H.; Shim, H. K.; Jeung, S. C.; Kim, D. *Chem. Mater.* **1996**, *8*, 1925.
- Peng, J.; Yu, B. Y.; Pyun, C. H.; Jin, J. I. *Jpn. J. Appl. Phys.* **1996**, *35*, 4379.
- Bouche, C. M.; Berdague, P.; Facchetti, H.; Robin, P.; Barny, P. L.; Schott, M. *Synth. Met.* **1996**, *81*, 191.
- Son, J. M.; Sakaki, Y.; Ogino, K.; Sato, H. *IEEE Trans. Electron Devices* **1997**, *44*, 1307.
- Antoniadis, H.; Miller, J. N.; Roitman, D. B.; Campbell, I. H. *IEEE Trans. Electron Devices* **1997**, *44*, 1289.
- Hochfilzler, C.; Tasch, S.; Winkler, B.; Huslage, J.; Leising, G. *Synth. Met.* **1997**, *85*, 1271.
- Bellmann, E.; Shaheen, S. E.; Thayumanavan, S.; Barlow, S.; Marder, S. R.; Kippelen, B.; Peyghambarian, N. *Chem. Mater.* **1998**, *10*, 1668–1676.
- Bellmann, E.; Shaheen, S. E.; Grubbs, R. H.; Marder, S. R.; Kippelen, B.; Peyghambarian, N. *Chem. Mater.* **1999**, *11*, 399–407.
- Bacher, A.; Erdelen, C. H.; Paulus, W.; Ringsdorf, H.; Schmidt, H. W.; Schuhmacher, P. *Macromolecules* **1999**, *32*, 4551.
- Zhang, Y.-D.; Hreha, R. D.; Marder, S. R.; Jabbour, G. E.; Kippelen, B.; Peyghambarian, N. *J. Mater. Chem.* **2002**, *12*, 1703–1708.
- Domercq, B.; Hreha, R. D.; Larribeau, N.; Haddock, H. N.; Marder, S. R.; Kippelen, B. *Proc. SPIE* **2002**, 4642.
- Hreha, R. D.; Zhang, Y.-D.; Domercq, B.; Larribeau, N.; Haddock, J. N.; Kippelen, B.; Marder, S. R. *Synthesis* **2002**, 1201–1212.
- Domercq, B.; Hreha, R. D.; Zhang, Y.-D.; Larribeau, N.; Haddock, J. N.; Schultz, C.; Marder, S. R.; Kippelen, B. *Chem. Mater.* **2003**, *15*, 1491–1496.
- Domercq, B.; Hreha, R. D.; Zhang, Y.-D.; Haldi, A.; Barlow, S.; Marder, S. R.; Kippelen, B. *J. Polym. Sci.* **2003**, *B41*, 2726–2732.
- Meyers, A.; Weck, M. *Macromolecules* **2003**, *36*, 1766–1768.
- A related approach uses dendrimers rather than polymers as a macromolecular scaffold for electroactive groups. For example, see: Markham, J. P. J.; Lo, S. C.; Magennis, S. W.; Burn, P. L.; Samuel, I. D. W. *Appl. Phys. Lett.* **2002**, *80*, 2645–2647. Furuta, P.; Brooks, J.; Thompson, M. E.; Fréchet, J. M. J. *Am. Chem. Soc.* **2003**, *125*, 13165–13172.
- We have also previously reported crosslinkable polymers based upon triarylamine-functionalized norbornenes. In these systems, crosslinking requires long exposure times and is accompanied by significant deterioration in device performance (Ref. 12).
- Hreha, R. D.; George, C. P.; Haldi, A.; Domercq, B.; Malagoli, M.; Barlow, S.; Brédas, J.-L.; Kippelen, B.; Marder, S. R. *Adv. Funct. Mater.* **2003**, *13*, 967–973.
- Borsenberger, P. M.; Weiss, D. S. *Organic Photoreceptors for Xerography*; Marcel Dekker: New York, 1998.
- Bässler, H. *Phys. Status Solidi* **1993**, *B175*, 15–56.
- Borsenberger, P. M.; Magin, E. H.; van der Auweraer, M.; de Schryver, F. C. *Phys. Status Solidi* **1993**, *A140*, 9.
- Bässler, H. *Mol. Cryst. Liq. Cryst.* **1994**, *252*, 11.
- Feast, W. J. *Makromol. Chem., Macromol. Symp.* **1992**, *53*, 317–326.

29. Grubbs, R. H.; Miller, S. J.; Fu, G. C. *Acc. Chem. Res.* **1995**, *28*, 446–452.
30. Schrock, R. R. *Top. Organomet. Chem.* **1998**, *1*, 1–36.
31. Grubbs, R. H.; Khosravi, E. *Mater. Sci. Tech.* **1999**, *20*, 65–104.
32. Buchmeiser, M. R. *Chem. Rev.* **2000**, *100*, 1565–1604.
33. Bordwell, F. G.; Hughes, D. L. *J. Org. Chem.* **1980**, *45*, 3314–3320.
34. Baranano, D.; Mann, G.; Hartwig, J. F. *Curr. Org. Chem.* **1997**, *1*, 287–305, and references therein.
35. Yang, B. H.; Buchwald, S. L. *J. Organomet. Chem.* **1999**, *576*, 125–146, and references therein.
36. The palladium-catalyzed coupling reaction was unsuccessful when the hydroxyl group attached to the 9-position of the fluorene was not protected.
37. Leung, W.-H.; Lai, W.; Williams, I. D. *J. Organomet. Chem.* **2000**, *604*, 197–201.
38. Maldonado, J.-L.; Bishop, M.; Fuentes-Hernandez, C.; Caron, P.; Domercq, B.; Zhang, Y.-D.; Barlow, S.; Thayumanavan, S.; Malagoli, M.; Brédas, J.-L.; Marder, S. R.; Kippelen, B. *Chem. Mater.* **2003**, *15*, 994–999.
39. Ashby, E. C.; Pham, T. N. *Tetrahedron Lett.* **1984**, *25*, 4333–4336.
40. Polonski, T.; Dauter, Z. *J. Chem. Soc., Perkin Trans.* **1986**, 1781–1788.

Controlled polymerization of α -methyl- β -pentyl- β -propiolactone by a discrete zinc alkoxide complex

Kathleen M. Schreck and Marc A. Hillmyer*

Department of Chemistry, University of Minnesota, 207 Pleasant St. SE, Minneapolis, MN 55455-0431, USA

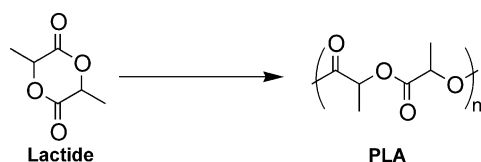
Received 2 April 2004; revised 1 June 2004; accepted 4 June 2004

Abstract—We report the zinc(II) alkoxide-mediated ring opening polymerization of α -methyl- β -pentyl- β -propiolactone. The polymerization proceeds to high conversion and in the absence of significant transesterification to yield polymers with narrow molecular weight distributions. Poly(α -methyl- β -pentyl- β -propiolactone), PMPP, is an amorphous, low glass transition material that forms immiscible blends with polylactide (PLA). PMPP-*b*-PLA diblock copolymers, for use as potential blend compatibilizers, were synthesized in a controlled manner by sequential monomer addition.

© 2004 Elsevier Ltd. All rights reserved.

1. Introduction

Polylactide is a biodegradable, aliphatic polyester obtained by the ring opening polymerization of lactide (Scheme 1). Available entirely from renewable feedstocks,¹ lactide contains two stereogenic centers, which allows for tacticity in the resulting polymer backbone. For example, atactic, amorphous polylactide (PLA) can be obtained by polymerization of D,L-lactide (*R,S*). Stereoregular, semi-crystalline poly(L-lactide) (PLLA), accessed by polymerization of L-lactide (*S,S*), is especially desirable for commercial use, exhibiting improved mechanical properties and higher end-use temperatures relative to its amorphous counterpart.² Initially employed in biomedical applications such as resorbable sutures and degradable implants, polylactide has, of late, gained favor as an environmentally benign thermoplastic well-suited for commercial fiber and packaging products. Fibers produced from polylactide exhibit low odor retention and excellent moisture wicking properties.^{3,4}



Scheme 1. Ring opening polymerization of lactide.

Keywords: Substituted β -lactones; Synthetic polyhydroxyalkanoates; Polylactide block copolymers; Ring opening polymerization; Poly(2-methyl-3-hydroxyoctanoate).

* Corresponding author. Tel.: +1-612-625-7834; fax: +1-612-624-7029; e-mail: hillmyer@chem.umn.edu

Additionally, polylactide bottles, films, and thermoformed containers are becoming increasingly popular for food packaging because of their resistance to fats and oils, as well as their ability to block flavors and aromas.⁵

One drawback of polylactide is the inherent brittleness of the polymer,⁶ which limits its use in applications where mechanical toughness is required. In order for polylactide materials to be suitable for these types of applications, toughening schemes must be employed. One common method is through blending of an appropriate rubber into the thermoplastic matrix.^{6–9} The resulting binary blends are generally immiscible and typically require the addition of an appropriate compatibilizer for good dispersion, strong interfacial adhesion, and optimal toughening. We have demonstrated this strategy in melt blends of PLA with linear low density polyethylene (LLDPE), an economical toughening agent.¹⁰ While a binary 80:20 PLA/LLDPE blend did not show significant toughening compared to homopolymer PLA, addition of 5 wt% of a PLLA-PE block copolymer compatibilized the blend resulting in better PLA/LLDPE interfacial adhesion, better dispersion of the LLDPE in the PLA matrix, and a significant increase in impact resistance.¹⁰ While these ternary blends do show significant toughening with respect to PLA homopolymer, addition of petrochemically based polymers like LLDPE results in blends that are only partially degradable and partially derived from renewable resources. Therefore, we have been pursuing alternative toughening materials that retain the benefits of biodegradability and renewable origins. Promising candidates are the polyhydroxyalkanoates (PHAs).

PHAs are a class of biodegradable polyesters produced naturally by microorganisms as cellular energy sources. As a result of the biosynthetic pathway involved in their formation, natural PHAs (Fig. 1) are generally optically active, isotactic polymers, owing to the *R*-configuration of the β -carbon side-chain.^{11,12} For PHAs with short side-chains, such as poly(3-hydroxybutyrate) (PHB, Fig. 1), this stereoregularity leads to high levels of crystallinity, resulting in material that is brittle and not mechanically useful.¹³ The properties of PHB can be improved, however, by the formation of copolymers of PHB and poly(3-hydroxyvalerate) (PHV, Fig. 1).^{12,14} Typically the degree of crystallinity of a PHA is modulated by increasing the length of the pendant chain (e.g., poly(3-hydroxyoctanoate) (PHO) is a thermoplastic elastomer with $\sim 30\%$ crystallinity¹⁵). However, amorphous, atactic materials of these structures are not generally available through microbial means. Rather, they are prepared synthetically by the ring opening polymerization of β -lactones.

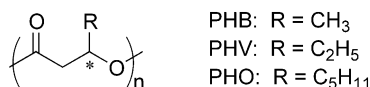


Figure 1. Structures of natural PHAs.

This ring opening strategy has been utilized previously, especially in the case of PHB, whose atactic, synthetic analog poly(β -butyrolactone) (PBL) can be obtained from a commercially available monomer, β -butyrolactone. Preparation procedures for PBL are widely reported,^{12,16–20} although the ability to reach higher molecular weights ($>20,000$ g/mol) with low polydispersities has generally been a more recent development.^{21–23}

Ring opening routes to synthetic medium-chain-length PHAs, while reported,²⁴ are far less common, perhaps because the requisite lactones often have not been commercially or readily available.[†] However, one group has reported the synthesis of poly(α -methyl- β -pentyl- β -propiolactone) (PMPP) from α -methyl- β -pentyl- β -propiolactone (MPP), a β -lactone obtained in two steps from propionic acid and hexanal (Scheme 2).²⁵ While the

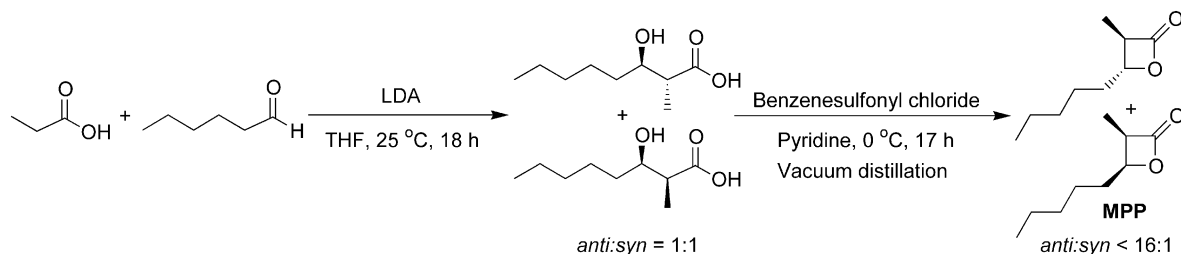
polymerization, initiated by crown ether/KOH or CH₃OK complexes, proceeded only to oligomers in this case, we hypothesized that the material at a higher molecular weight could be used as an LLDPE substitute for PLA toughening. Although the properties of PMPP had not been investigated, we speculated that the glass transition temperature would be below room temperature, and the polyester backbone would be degradable. Additionally, the starting materials for the synthesis, propionic acid and hexanal, can be obtained from renewable sources,^{26,27} thus fulfilling another targeted design criterion.

In this report, we detail our synthesis of MPP according to the previously mentioned route,²⁵ and include additional information regarding product characterization, diastereomeric ratios, and monomer purification and stability. Additionally, we report the successful ring opening polymerization of MPP by a recently reported, high activity lactide polymerization catalyst, LZnOEt (L = 2,4-di-*tert*-butyl-6-[[2'-dimethylaminoethyl]-methylamino]methyl]-phenol),²⁸ yielding an amorphous, high molecular weight polymer not readily available through microbial means. Diblock copolymers of PMPP-*b*-PLA were also prepared and the thermal properties and miscibility of the resulting materials were examined.

2. Results and discussion

2.1. Monomer synthesis

MPP was prepared according to a literature procedure,²⁵ through cyclization of the appropriate β -hydroxy acid. LDA-mediated aldol condensation of commercially available propionic acid and hexanal gave the β -hydroxy acid, 3-hydroxy-2-methyloctanoic acid, in 97.6% yield after extraction and solvent evaporation. Without further purification, the product was cyclized to give crude MPP in 50% yield (Scheme 2). Vacuum distillation (64 °C, 342 mTorr, distilled twice) yielded pure MPP in an overall yield of 20.5%. After drying over CaH₂ for 48 h, MPP was suitable for polymerization and stable (>3 months) when stored at 25 °C under dry nitrogen atmosphere.



Scheme 2. MPP synthesis.

[†] Excellent catalytic methodologies that provide efficient, one-step access to a variety of β -lactones have been reported in recent years, and could prove instrumental in filling this void. See (a) Lee, J. T.; Thomas, P. J.; Alper, H. *J. Org. Chem.* **2001**, *66*, 5424–5426; (b) Schmidt, J. A. R.; Mahadevan, V.; Getzler, Y. D. Y. L.; Coates, G. W. *Org. Lett.* **2004**, *6*, 373–376; (c) Nelson, S. G.; Zhu, C.; Shen, X. *J. Am. Chem. Soc.* **2004**, *126*, 14–15, and references therein.

No specific reagents were introduced in the synthetic route to control the stereochemistry of the reactions, thus products were recovered as mixtures of diastereomers. One-dimensional ¹H–¹H total correlation NMR spectroscopy (¹H–¹H TOCSY),[‡] which indicates both short and long-range proton

[‡] See Section 4 for details.

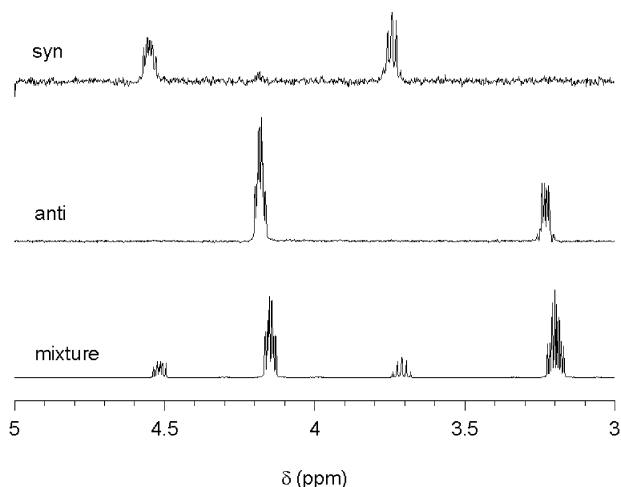


Figure 2. ^1H - ^1H TOCSY NMR spectra of MPP depicting separately the resonances of the *syn* and *anti* diastereomers and actual ^1H NMR of MPP as a diastereomeric mixture (see Section 4 for details).

coupling, enabled independent analysis of each diastereomer spectrum without chromatographic separation (Fig. 2). For both reactions, the diastereomers were assigned by resonances based on published values for the *anti* β -hydroxy acid²⁹ and *anti* MPP.³⁰

The aldol reaction to form 3-hydroxy-2-methyloctanoic acid proceeded with a 1:1 *anti*:*syn* ratio, as expected. However, cyclization to MPP resulted in ratios up to 3:1 *anti*:*syn*. Subsequent study revealed that the enrichment was not due to inherent diastereoselectivity of the reaction, but rather because of the lower stability of the *syn* β -lactone in the presence of nucleophiles or heat.³¹ The ^1H NMR spectrum of the crude cyclization reaction mixture indicated significant amounts of oligomerization, primarily of the *syn* lactone (Fig. 3). Oligomerization was even more pronounced after distillation, in some cases leading to purified MPP with *anti*:*syn* ratios up to 16:1. However, optimization of the distillation (minimizing heating) yielded MPP of

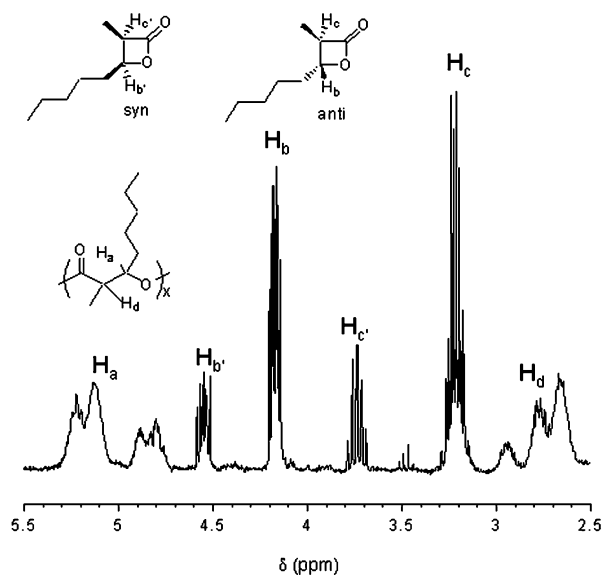
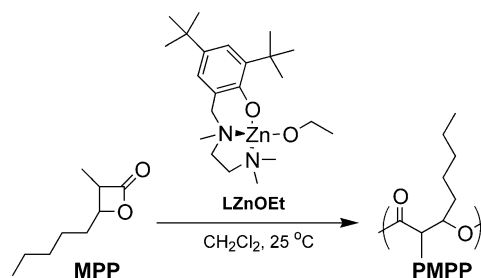


Figure 3. ^1H NMR resonances of MPP and oligomer.



Scheme 3. MPP polymerization.

sufficient purity with a significantly reduced *anti*:*syn* ratio of 4.8:1.

2.2. Polymerization

MPP was successfully polymerized using LZnOEt (Scheme 3) to give polymers with number average molecular weights (M_n) ranging from 10 to 40 kg/mol. Previously reported to be an extremely fast and well controlled catalyst for lactide polymerization,²⁸ LZnOEt has proven effective for MPP polymerization at varying monomer/catalyst ratios (Table 1). MALDI mass spectrometry of the lowest molecular weight sample (Table 1, entry 1) confirmed the incorporation of the ring-opened MPP repeat unit (156.22 g/mol).

Molecular weight determination using the high molecular weight region shown in Figure 4, yielded $M_n = 9.0$ kg/mol with a polydispersity index (PDI) equal to 1.02.[§] End group calculations (i.e., $\text{CH}_3\text{CH}_2\text{O} + (\text{C}_9\text{H}_{16}\text{O}_2)_n + \text{H} + \text{Na}$) gave agreement to integer repeat units values (n) within ± 0.02 , confirming the incorporation of an ethoxide from the zinc catalyst. Methylene ($-\text{OCH}_2\text{CH}_3$) resonances in the ^1H NMR spectrum (Fig. 5) also indicated alkoxide insertion. These resonances at 4.12 ppm integrated in a 2:1 ratio with resonances at 3.63 ppm ($-\text{CHOH}$), consistent with ester and hydroxyl end groups resulting from cleavage of the acyl-oxygen bond. M_n (8.7 kg/mol) calculated for this sample by ^1H NMR spectroscopy using either peak also showed reasonable agreement with predicted and MALDI-calculated values.

Although there is literature precedent for related catalyst systems polymerizing both lactide and β -lactones effectively,^{22,32} LZnOEt polymerization behavior for lactide is quite different than for MPP. Polymerization of lactide occurs very quickly, reaching conversions of >93% after several minutes.²⁸ The polydispersity also increases with time as is typical for an equilibrium polymerization. Meanwhile, MPP polymerization is relatively slow (up to 100 h or more until, in the ^1H NMR spectrum, all monomer resonances were consumed) and the polydispersity is narrow even at high conversion (Table 1). Although

[§] Molecular weight and polydispersity were calculated using all peaks above 6000 g/mol in the MALDI spectrum. Accordingly, matrix and other lower molecular weight peaks were excluded from the analysis. Although some of the lower molecular weight peaks had mass differences corresponding to the polymer repeat unit (156.22 g/mol), such oligomers were not present in the SEC chromatogram, thus we propose these peaks are due to fragmentation of the polyester backbone during the MALDI experiment.

Table 1. MPP polymerization data, CH₂Cl₂, 25 °C

Entry	[MPP] ₀ /[LZnOEt] ₀	[MPP] ₀ (M)	<i>t</i> (h)	<i>M_n</i> (Th) ^a (kg/mol)	<i>M_n</i> ^b (kg/mol)	PDI	Conversion ^c (%)
1	59:1	2.3	18	9.2	10.1	1.07	>99
2	146:1	2.3	72	22.8	13.2	1.07	>99
3	264:1	1.4	52	41.2	25.7	1.07	>99
4	392:1	2.5	100	61.2	39.8	1.09	>99
5	393:1	2.5	75	54.4	38.5	1.11	89

^a Calculated from [MPP]₀/[LZnOEt]₀ × fractional conversion.

^b Determined by SEC relative to polystyrene standards.

^c From NMR integration of polymer and monomer resonances upon quenching.

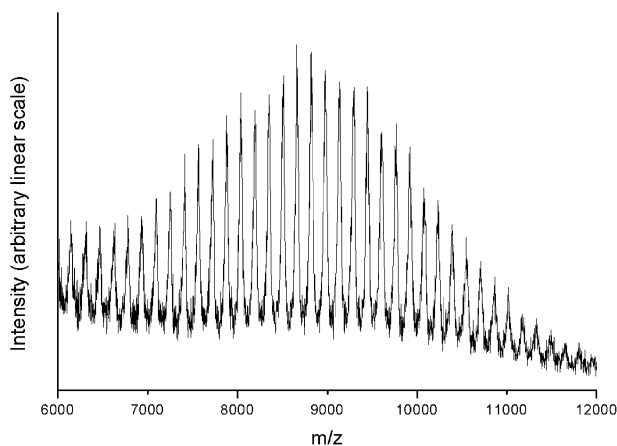


Figure 4. Selected region of the MALDI-TOF spectrum of PMPP (Table 1, entry 1, *M_n*(Th)=9.2 kg/mol): *M_n*(MALDI)=9.0 kg/mol, PDI=1.02.

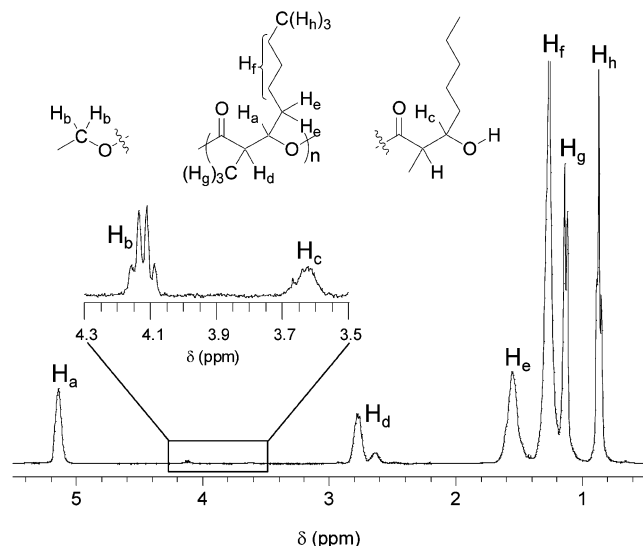


Figure 5. ¹H NMR spectrum of PMPP (Table 1, entry 1, *M_n*(Th)=9.2 kg/mol): *M_n*(NMR)=8.7 kg/mol.

measured molecular weights (determined by size exclusion chromatography (SEC)) deviate from the theoretical values predicted from initial monomer to catalyst ratios, the molecular weights attained are consistent and the polymerization is free of side reactions. The apparent molecular weight deviation may result from the relative SEC calibration (based on polystyrene standards) or perhaps due to the presence of an impurity that serves as a chain transfer agent.²⁸

Table 2. Relative MPP diastereomeric ratios with polymerization time

<i>t</i> (h)	<i>anti:syn</i> ^a
0	4.8:1
0.7	5.5:1
17.5	34:1
22.5	47:1
42.5	<i>syn</i> completely reacted
187	<i>anti</i> completely reacted

^a Determined by ¹H NMR spectrum integrations.

During the polymerizations, the *syn* diastereomer of MPP was consumed markedly faster than the *anti* (Table 2), with $k_{\text{rel}} (k_{\text{obs}}^{\text{syn}}/k_{\text{obs}}^{\text{anti}}) \approx 4.0$.[†] Given the close proximity of the methyl and pentyl substituents and the rigid conformation of the 4-membered ring, the energy of the sterically crowded ring opening of *syn* MPP relative to *anti* MPP, resulting in the observed behavior.³¹ This assertion is further supported by the relative tendencies of the diastereomers to oligomerize upon heating (observed during MPP distillation; Section 2.1).

We also investigated the kinetics of MPP polymerization by LZnOEt. A polymerization was performed in an air-free NMR tube ([MPP]₀/[LZnOEt]₀=272:1, [MPP]₀=0.83 M, [LZnOEt]₀=0.0031 M) and the decrease in total monomer concentration (monitored by ¹H NMR spectroscopy) as a function of reaction time, yielded the data in Figure 6. The decay of monomer showed very good agreement when fit to $[MPP]_t = [MPP]_0 \exp(-k_{\text{obs}}t)$, indicating that the polymerization is first order in monomer, with $k_{\text{obs}} = 1.25 \times 10^{-5} \text{ s}^{-1}$ ($t_{1/2} = 15.4 \text{ h}$ under these conditions).

Polydispersity broadening can occur at high conversion in ring opening polymerizations, and has been reported for both β-butyrolactone³³ and lactide.²⁸ The broadening can be due to side reactions such as transesterification, which occurs when the propagating metal center complexes and inserts a repeat unit from a polymer chain, instead of free monomer. This type of process compromises the control of the polymerization and presents a specific challenge with respect to the preparation of polyester block copolymers due to interblock transesterification. A typical way to circumvent this problem is to terminate the homopolymerization at

[†]This result was corroborated by a separate kinetics experiment with additional data points at early conversions. For this experiment, with [MPP]₀=1.93 M and [LZnOEt]₀=0.00658 M, a k_{rel} of 4.1 was calculated.

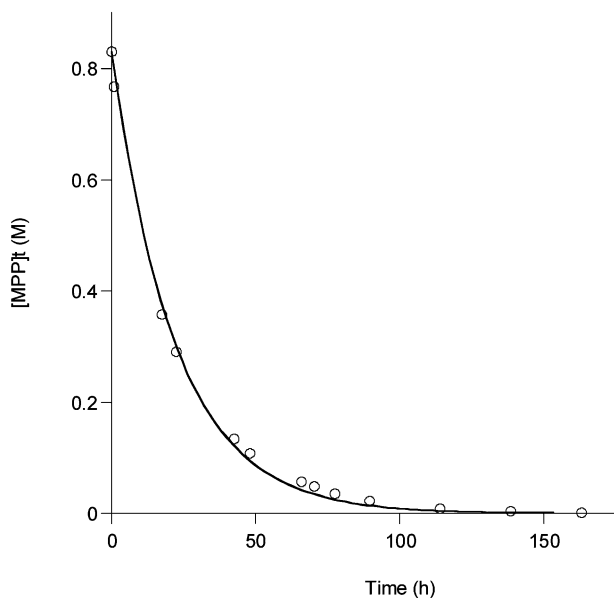


Figure 6. Kinetic data for MPP polymerization ($[LZnOEt]_0 = 0.0031$ M): Data was fit by $[MPP]_t = [MPP]_0 \exp(-k_{obs}t)$ (solid line: $[MPP]_0 = 0.83$ M) indicating the reaction is first order in monomer. k_{obs} was calculated to be $1.25 \times 10^{-5} \text{ s}^{-1}$.

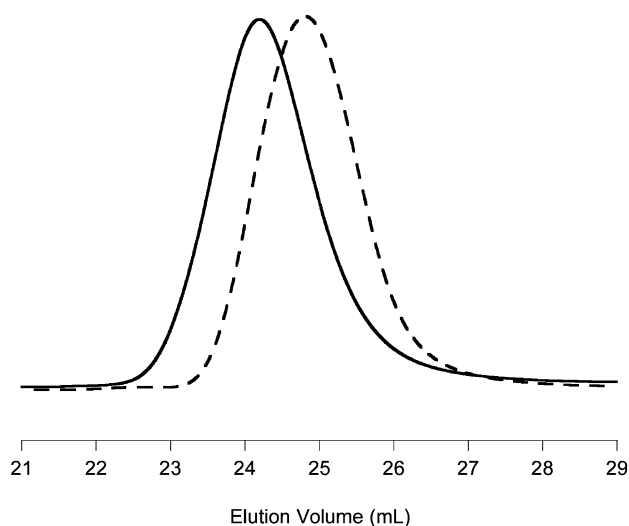


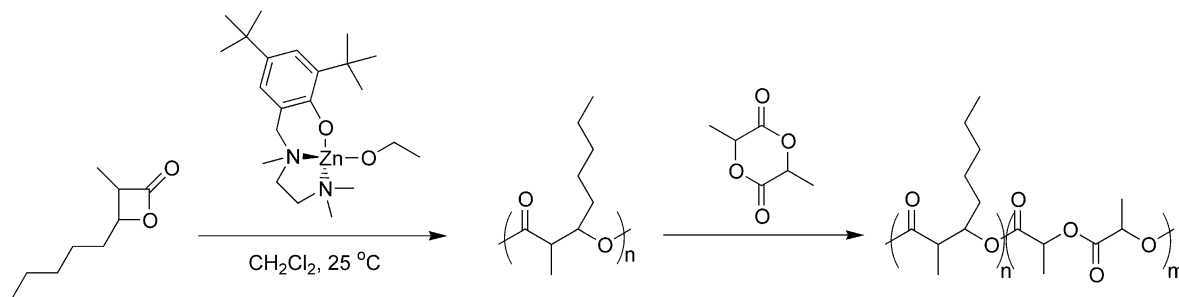
Figure 7. Size exclusion chromatography data for sequential MPP addition: First addition (dashed line) $M_n = 15.3$ kg/mol, PDI = 1.10; second addition (solid line) $M_n = 18.9$ kg/mol, PDI = 1.11.

a lower conversion before the polydispersity begins to broaden. The resulting homopolymer can then be used as a macroinitiator for polymerization of the second block, using a catalyst system that will not participate in transesterification reactions with the first block.³⁴ While this method can be used to synthesize block copolymers, it is not the ideal strategy for cases where both monomers can be polymerized by the same mechanism. In this situation, it is desirable to form diblock copolymers by sequential monomer addition.^{35,36} Since data for LZnOEt polymerization of MPP indicated that the reaction proceeded to >99% conversion with narrow polydispersities (PDI < 1.11), we hypothesized that sequential monomer addition for the formation of block copolymers might be possible with this system. To investigate this, MPP and LZnOEt were allowed to react for 8 days (CD_2Cl_2 , 25 °C), after which SEC indicated $M_n = 15.3$ kg/mol and PDI = 1.10 (Fig. 7). An additional aliquot of neat MPP was then added to the reaction mixture, resulting in a molecular weight increase ($M_n = 18.9$ kg/mol) without significant broadening of the polydispersity (PDI = 1.11) (Fig. 7). This ability to ‘reinitiate’ polymerization with the apparent absence of transesterification suggested that PMPP could be used as a ‘living’ first block, from which lactide could be polymerized in order to prepare diblock copolymers. We therefore, proceeded to access PMPP-*b*-PLA materials in this manner (Scheme 4).

Two PMPP-*b*-PLA diblock copolymers were synthesized using the following procedure. MPP homopolymer polymerization was carried out as previously described (LZnOEt, CH_2Cl_2 , 25 °C), until monomer resonances were absent from the 1H NMR spectrum of the reaction mixture. Solid D,L-lactide was then added and allowed to react before the polymerization was quenched and precipitated into cold methanol. 1H NMR spectroscopy of the precipitated and dried polymers indicated the incorporation of PLA resonances. Additionally, a shift in the SEC chromatograph to lower elution volume demonstrated an increase in molecular weight compared to the PMPP precursor (Fig. 8). Block copolymer SEC traces were also broader than those of the PMPP homopolymer, possibly due to slow initiation or transesterification of the PLA by the propagating alkoxide. Based on the thermal analysis data (detailed in the following section), we do not believe inter-block transesterification is significant.

2.3. PMPP thermal transitions and miscibility with PLA

In order to evaluate PMPP’s potential to serve as an LLDPE replacement in polylactide blends, both its thermal behavior



Scheme 4. Polymerization of PMPP-*b*-PLA diblock copolymers.

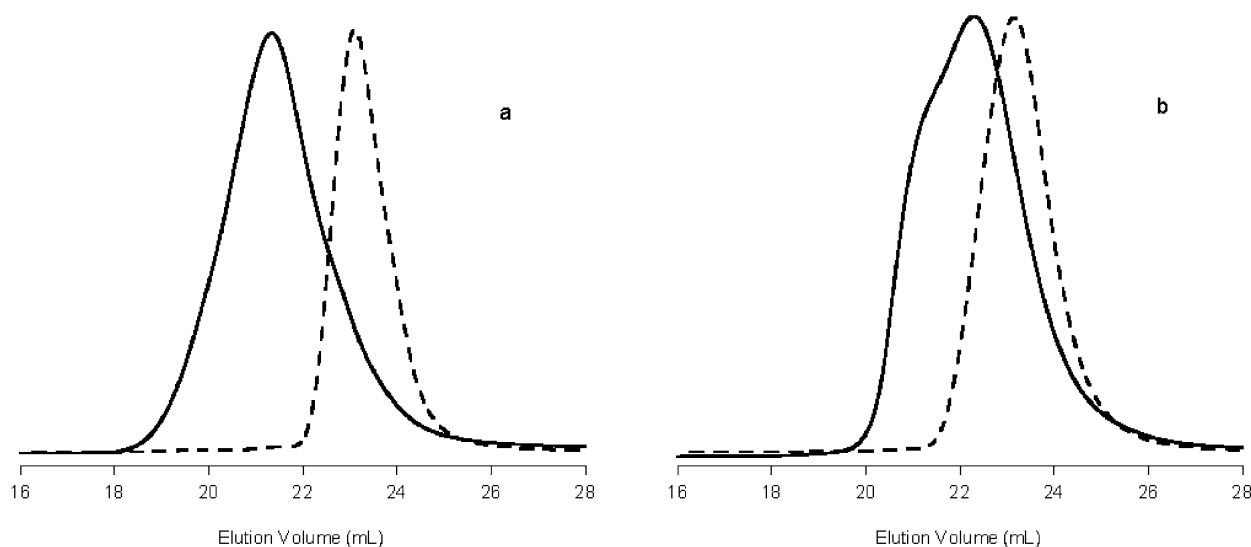


Figure 8. Size exclusion chromatography data for diblock copolymers (solid lines) and PMPP precursors (dashed lines): (a) PMPP(26 K)-*b*-PLA(26 K), PDI = 1.46; PMPP(26 K), PDI = 1.07 (b) PMPP(26 K)-*b*-PLA(10 K), PDI = 1.27; PMPP(26 K), PDI = 1.11.

Table 3. Glass transition temperatures by differential scanning calorimetry

Composition (M_{nSEC})	T_g (°C)
PMPP (39 K)	-18
PLA (72 K)	56
PMPP(39 K)/PLA(72 K) ^a	-16, 57
PMPP(26 K)- <i>b</i> -PLA (10 K)	-17, 55
PMPP(26 K)- <i>b</i> -PLA (26 K)	-16, 54

^a A 50/50 w/w blend.

and miscibility with PLA were investigated (Table 3). The glass transition temperature (T_g) of polylactide is above room temperature (56 °C for 72 kg/mol PLA, Fig. 9a), thus a polymer with a lower T_g is desirable for toughening purposes. The T_g of PMPP (M_{nSEC} = 39 kg/mol) was found by differential scanning calorimetry (DSC) to be -18 °C, with no other observable transitions (Fig. 9e). A 50/50 w/w blend of PMPP and PLA was prepared by co-dissolving the polymers in CH_2Cl_2 , followed by precipitation in methanol. After drying (24 h, 60 °C), DSC of the blend exhibited two T_g 's at -16 and 57 °C (Fig. 9b). The

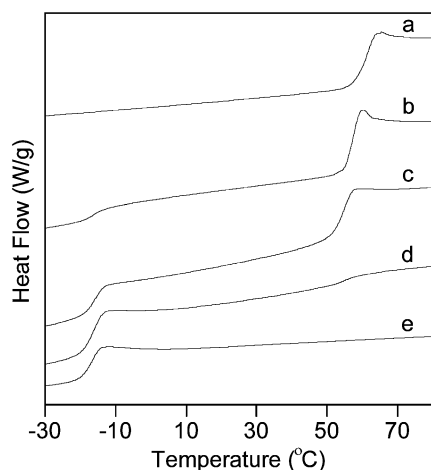


Figure 9. Thermal analysis of: (a) PLA (b) PMPP/PLA (50/50 w/w blend) (c) PMPP(26 K)-*b*-PLA(26 K) (d) PMPP(26 K)-*b*-PLA(10 K) (e) PMPP.

retention of the two T_g 's, similar to those of the respective homopolymers, indicates that segregated regions of each polymer exist. DSC analysis of two PMPP-*b*-PLA diblock copolymers was also consistent with this conclusion (Fig. 9c and d). Each diblock exhibited two glass transition temperatures, confirming the immiscibility of PMPP and PLA. This data indicates that PMPP behaves in a similar manner as LLDPE when combined with PLA, and may serve as a viable substitute for toughening schemes. Blending studies with PMPP and PLA are currently underway, and the effect of PMPP-*b*-PLA copolymer addition is being investigated.

3. Conclusion

We have accessed PMPP, a synthetic polymer similar in structure to PHO, by the zinc alkoxide-mediated ring opening polymerization of α -methyl- β -pentyl- β -propiolactone. The polymerization exhibits good molecular weight control and proceeds without transesterification, yielding an amorphous, low T_g polyester that is immiscible with PLA. Diblock copolymers of PMPP and PLA can be obtained in a controlled manner by sequential monomer addition, and may be useful as additives to alter the properties of PMPP/PLA binary blends. Since MPP can be synthesized from renewable resource starting materials, PMPP/PLA composites may form the basis for mechanically useful materials with the desirable characteristics of complete degradability and renewable origins.

4. Experimental

4.1. Materials and methods

NMR spectra were acquired using a Varian INOVA 300 or 500 spectrometer in either $CDCl_3$ or CD_2Cl_2 , as indicated. Chemical shifts are referenced to residual proteo solvent or the ^{13}C resonance of the solvent. IR spectra were collected on a Nicolet Magna-IR Spectrometer 550 with NaCl plates.

High-resolution mass spectra were obtained on a Finnigan MAT 95 high-resolution instrument using chemical ionization with 4% NH₃ in CH₄ as the reagent gas. MALDI mass spectrometry was performed on a Bruker Reflex III instrument. Samples were prepared in THF with dithranol matrix and sodium counterion. Elemental analyses were performed by Atlantic Microlab, Inc., Norcross, GA. All polymerizations were carried out in an Mbraun glovebox with nitrogen atmosphere. SEC data were obtained using a Hewlett–Packard 1100 series liquid chromatograph with three Jordi polydivinylbenzene columns (10,000, 1000, and 500 Å), a Hewlett–Packard 1047A refractive index detector, and tetrahydrofuran (40 °C, 1 mL/min) mobile phase. SEC values are reported relative to polystyrene calibration standards (Polymer Laboratories). All DSC analyses were performed using a TA Instruments Q1000 differential scanning calorimeter with nitrogen as the purge gas. An indium standard was used for calibration, and the scan rate was 10 °C/min. Samples of known masses (8–15 mg) were placed in hermetic aluminum pans and sealed prior to measurements.

All chemicals, unless otherwise noted, were purchased from Aldrich Chemical Company (Milwaukee, WI). LZnOEt was prepared according to a published procedure²⁸ using ligand supplied by one of the co-authors of that publication. Diisopropylamine was distilled from CaH₂ immediately prior to use. D,L-lactide was recrystallized from toluene followed by vacuum sublimation (2–3×). High molecular weight PLA (used for PMPP/PLA solution blending) was supplied by Cargill Dow LLC (Minnetonka, MN). THF was purified through an alumina column in a home-built solvent purification line.³⁷ Dichloromethane was obtained from purification columns (Glass Contour, Laguna, CA). All other chemicals were used as received.

4.1.1. 3-Hydroxy-2-methyloctanoic acid. Under argon atmosphere, a solution of diisopropylamine (23.0 mL, 16.6 g, 0.164 mol) in THF (200 mL) was prepared in a flame-dried, three-neck flask equipped with calibrated addition funnel. Upon cooling to –10 °C, *n*-butyllithium in hexanes (1.60 M, 100 mL, 0.160 mol) was added dropwise via addition funnel. After stirring at room temperature for 1 h, the resulting solution was cooled to –10 °C, and propionic acid (5.50 mL, 5.46 g, 0.0737 mol), as a 1.0 M solution in THF, was added. After stirring for one hour at room temperature, the reaction was replaced in the –10 °C bath prior to addition of hexanal (11.5 mL, 9.59 g, 0.0958 mol) as a 2.0 M solution in THF. After stirring overnight at room temperature, the reaction was quenched by pouring onto several volumes of ice-cold water. The resulting layers were extracted with diethyl ether, after which the aqueous layer was acidified to a pH of 1 with 6 M hydrochloric acid. After ether extraction of the acidified layer, the ethereal extracts were dried with sodium sulfate and concentrated by rotary evaporation to yield 3-hydroxy-2-methyloctanoic acid as a light yellow oil (12.5 g, 97.6%). ¹H NMR (500 MHz, CDCl₃) (* denotes *syn* diastereomer resonances) δ 7.10–6.30 (broad), 3.96 (m, 1H*), 3.71 (m, 1H), 2.59 (dq, 1H*, *J* = 3.5, 7.0 Hz), 2.56 (m, 1H), 1.57–1.28 (m, 8H, 8H*), 1.24 (d, 3H, *J* = 7.0 Hz), 1.20 (d, 3H*, *J* = 7.0 Hz), and 0.90 (t, 3H, 3H*, *J* = 7.2 Hz); ¹³C NMR (125 MHz, CDCl₃) δ 181.3, 73.5, 72.0, 45.4, 44.3, 34.7,

33.8, 31.9, 25.8, 25.3, 22.8, 14.4, 14.2, and 10.5; IR (NaCl, neat) 3420, 2933, 2860, 1710, 1461, 1410, and 1379 cm⁻¹; HRMS (CI, NH₃/CH₄): Calcd for C₉H₁₈O₃ (M + NH₄)⁺ 192.1600 g/mol, found 192.1604 g/mol.

4.1.2. α -Methyl- β -pentyl- β -propiolactone (MPP). Pyridine (390 mL, 378 g, 4.78 mol) was added to a cooled flask containing crude 3-hydroxy-2-methyloctanoic acid (32.8 g, 0.188 mol). After swirling to dissolve the acid, benzenesulfonyl chloride (42.5 mL, 58.7 g, 0.332 mol) was added. The flask was sealed with a septum and placed in the freezer. After 17 h, the reaction was poured into several volumes of ice-cold, distilled water. The mixture was extracted with diethyl ether, and the resulting ethereal layers were washed with sodium bicarbonate and water, before drying with sodium sulfate. Solvent was removed by rotary evaporation to yield a brown oil. Vacuum distillation (64 °C, 342 mTorr) of the oil yielded α -methyl- β -pentyl- β -propiolactone as a clear, colorless liquid (6.85 g, 23.3%). ¹H NMR (500 MHz, CDCl₃) (* denotes *syn* diastereomer resonances) δ 4.55 (ddd, 1H*, *J* = 4.5, 6.5, 9.0 Hz), 4.17 (ddd, 1H, *J* = 4.5, 6.5, 7.5 Hz), 3.74 (dq, 1H*, *J* = 6.5, 8.0 Hz), 3.22 (dq, 1H, *J* = 4.0, 7.5 Hz), 1.90–1.71 (m, 2H, 2H*), 1.39 (d, 3H, *J* = 7.5 Hz), 1.37–1.31 (m), 1.28 (d, 3H*, *J* = 8.0 Hz), and 0.91 (t, 3H, 3H*, *J* = 7.5 Hz); ¹³C NMR (75 MHz, CDCl₃) δ 172.4, 79.8, 50.9, 34.3, 31.6, 24.8, 22.7, 14.1, and 12.7; IR (NaCl, neat) 2932, 2861, 1825 cm⁻¹; HRMS (CI, NH₃/CH₄): Calcd for C₉H₁₆O₂ (M + NH₄)⁺ 174.1494 g/mol, found 174.1502 g/mol. Anal. Calcd for C₉H₁₆O₂: C, 69.19%; H, 10.32%; O, 20.48%. Found: C, 69.19%; H, 10.42%; O, 20.29%.

4.1.3. ¹H–¹H TOCSY of MPP. A ¹H–¹H TOCSY spectrum exhibits only those resonances that are in the same spin system as an irradiated peak selected by the researcher. Thus, using this technique, one can effectively obtain the ¹H spectrum of a specific molecule that is present in the NMR sample as a mixture (in this case a mixture of diastereomers). An NMR sample was prepared (~5 mg MPP/1 mL CD₂Cl₂) and the experiment was run on a 500 MHz Varian spectrometer at 25 °C. After calibrating the 90° pulse, the mixing time was arrayed (0.0 s–0.015 s), and the resonance for the β -proton of one diastereomer of MPP (*syn*: 4.55 ppm, *anti*: 4.17 ppm) was selectively irradiated. The resulting spectrum showed only those resonances spin coupled (either short- or long-range) to the irradiated proton. The requisite absence of residual proteo solvent resonances in the TOCSY spectra made exact referencing to the original ¹H NMR spectrum difficult, resulting in the slight offset of the resonances seen in Fig. 2.

4.1.4. Poly(α -methyl- β -pentyl- β -propiolactone). MPP was stirred over calcium hydride for 48 h, then degassed with three freeze/pump/thaw cycles. Under nitrogen atmosphere, MPP was filtered through Celite with CH₂Cl₂ rinse, until all calcium hydride was removed. The CH₂Cl₂ was removed *in vacuo*. A 0.038 M catalyst solution of LZnOEt in CH₂Cl₂ was made and stored at –35 °C. (All catalyst solutions were used within 4 h of preparation, as the catalyst seems ineffective after being stored as a solution for extended times.) MPP (0.151 g, 0.969 mmol) was added to an oven-dried vial and diluted with CH₂Cl₂ (0.320 mL). Catalyst solution (0.065 mL, 1.06 mg, 0.00247 mmol) was

added, and the reaction was left to stir. The reaction was quenched by exposure to air, and precipitated into cold methanol. The resulting polymer was dried for 24 h at 40 °C. ^1H NMR (500 MHz, CDCl_3) (* denotes end group resonances) δ 5.15 (m, 1H) 4.12 (q, 2H*), 2.78–2.62 (m, 1H), 1.55 (m, 2H), 1.26 (m, 6H), 1.13 (d, 3H), and 0.86 (m, 3H); ^{13}C NMR (75 MHz, CDCl_3) δ 172.8, 74.6, 43.0, 31.9, 30.7, 25.3, 22.7, 14.2, and 12.3; SEC: M_n = 39.8 kg/mol, PDI = 1.09.

4.1.5. Kinetic studies. Data for the polymerization of MPP by LZnOEt were obtained by in situ ^1H NMR monitoring of monomer and polymer resonances. Reactions were prepared in an Mbraun glovebox as described below and sealed for the remainder of the experiment. A 0.018 M catalyst solution of LZnOEt in CD_2Cl_2 was prepared and stored briefly at -35 °C. MPP (0.192 g, 1.23 mmol) was added to a J. Young NMR tube and diluted with CD_2Cl_2 (1.00 mL). Catalyst solution (0.250 mL, 1.95 mg, 0.00453 mmol) was added, and the ^1H NMR spectrum of the reaction was taken at the indicated times to determine the percent conversion of the polymerization.

4.1.6. PMPP-*b*-PLA diblock copolymers. A 0.039 M catalyst solution of LZnOEt in CH_2Cl_2 was made and briefly stored at -35 °C. MPP (0.0794 g, 0.508 mmol) was added to an oven-dried vial and diluted with CH_2Cl_2 (0.0273 mL). Catalyst solution (0.050 mL, 0.828 mg, 0.00193 mmol) was added, and the reaction was left to stir at 25 °C. ^1H NMR of an aliquot removed at 52 h indicated all MPP had been converted to polymer (SEC: M_n = 25.7 kg/mol, PDI = 1.07). D_3L -lactide (0.075 g, 0.520 mmol) was then added and the reaction was shaken. After 2 min, the polymerization was quenched by exposure to air, then precipitated into cold methanol. The resulting polymer was dried for 24 h at 60 °C. ^1H NMR (500 MHz, CDCl_3) (* denotes PLA resonances) δ 5.20 (m, 1H*), 5.15 (m, 1H), 2.78–2.62 (m, 1H), 1.55 (m, 2H, 3H*), 1.26 (m, 6H), 1.13 (d, 3H), and 0.86 (m, 3H); SEC: M_n = 51.7 kg/mol, PDI = 1.46.

4.1.7. PMPP/PLA solution blending. Blends were prepared by mixing PMPP (30 mg) and PLA (30 mg), followed by addition of CH_2Cl_2 . Polymers were allowed to dissolve completely, then left to stir for no less than 1.5 h. Following precipitation in cold methanol, samples were dried in a vacuum oven (60 °C, 24 h).

4.1.8. DSC measurements. A known mass of polymer was placed in a hermetic aluminum pan. The temperature was then ramped from 50 °C and held at 120 °C to erase the thermal history. After cooling to -100 °C at 10 °C/min, the sample was next heated 10 °C/min to 120 °C. The glass transition temperature (T_g) was determined from this second heating scan. The T_g was calculated at the midpoint of half extrapolated tangents from either side of the transition.

Acknowledgements

This work was supported by the David and Lucile Packard Foundation and the Toyota Motor Corporation. The authors thank Professor William Tolman for generous access to his laboratories, Dr. Letitia Yao for assistance and helpful

conversation regarding NMR experiments, Dr. Dana Reed for assistance with MALDI measurements, and Laurie Breyfogle for supplying ligand for LZnOEt synthesis.

References

1. Drumright, R. E.; Gruber, P. R.; Henton, D. E. *Adv. Mater.* **2000**, *12*, 1841–6.
2. Perego, G.; Cella, G. D.; Bastioli, C. *J. Appl. Polym. Sci.* **1996**, *59*, 37–43.
3. Tullo, A. *Chem. Eng. News* **2000**, *78*, 13.
4. Gross, R. A.; Kalra, B. *Science* **2002**, *297*, 803–7.
5. Tullo, A. *Chem. Eng. News* **2002**, *80*, 13–19.
6. Hiljanen-Vainio, M.; Varpomaa, P.; Seppälä, J.; Törmälä, P. *Macromol. Chem. Phys.* **1996**, *197*, 1503–23.
7. Loyens, W.; Groeninckx, G. *Polymer* **2002**, *43*, 5679–91.
8. Kayano, Y.; Keskkula, H.; Paul, D. R. *Polymer* **1998**, *39*, 2835–45.
9. Paul, D. R.; Bucknall, C. B.; *Polymer Blends*, Vol. 1; Wiley: New York, 2000 p 7.
10. Anderson, K. S.; Lim, S. H.; Hillmyer, M. A. *J. Appl. Polym. Sci.* **2003**, *89*, 3757–68.
11. Brandl, H.; Gross, R. A.; Lenz, R. W.; Fuller, R. C. *Adv. Biochem. Eng. Biotechnol.* **1990**, *41*, 77–93.
12. Müller, H. M.; Seebach, D. *Angew. Chem., Int. Ed. Engl.* **1993**, *32*, 477–502.
13. Anderson, A. J.; Dawes, E. A. *Microbio. Rev.* **1990**, *54*, 450–72.
14. Kelley, A. S.; Jackson, D. E.; Macosko, C.; Srienc, F. *Polym. Degrad. Stab.* **1998**, *59*, 187–90.
15. Mallardé, D.; Valière, M.; David, C.; Menet, M.; Guérin, P. *Polymer* **1998**, *39*, 3387–92.
16. Jedliński, Z.; Kowalczyk, M.; Glówkowski, W.; Grobelny, J. *Macromolecules* **1991**, *24*, 349–52.
17. Kurcok, P.; Dubois, P.; Jérôme, R. *Polym. Int.* **1996**, *41*, 479–85.
18. Jedliński, Z.; Kowalczyk, M.; Kurcok, P.; Adamus, G.; Matuszowicz, A.; Sikorska, W.; Gross, R. A.; Xu, J.; Lenz, R. W. *Macromolecules* **1996**, *29*, 3773–7.
19. Jedliński, Z.; Kurcok, P.; Lenz, R. W. *Macromolecules* **1998**, *31*, 6718–20.
20. Wu, B.; Lenz, R. W. *Macromolecules* **1998**, *31*, 3473–7.
21. Kurcok, P.; Śmiga, M.; Jedliński, Z. *J. Polym. Sci., Part A: Polym. Chem.* **2002**, *40*, 2184–9.
22. Rieth, L. R.; Moore, D. R.; Lobkovsky, E. B.; Coates, G. W. *J. Am. Chem. Soc.* **2002**, *124*, 15239–48.
23. Hori, Y.; Hagiwara, T. *Int. J. Biol. Macromol.* **1999**, *25*, 237–45.
24. Peres, R.; Lenz, R. W. *Macromolecules* **1993**, *26*, 6697–701.
25. Arkin, A. H.; Hazer, B.; Adamus, G.; Kowalczyk, M.; Jedliński, Z.; Lenz, R. *Biomacromolecules* **2001**, *2*, 623–7.
26. Huang, Y. L.; Wu, Z.; Zhang, L.; Cheung, C. M.; Yang, S. *Bioresour. Technol.* **2002**, *82*, 51–9.
27. Aldrich Chemical Company, personal communication.
28. Williams, C. K.; Breyfogle, L. E.; Choi, S. K.; Nam, W.; Young, V. G.; Hillmyer, M. A.; Tolman, W. B. *J. Am. Chem. Soc.* **2003**, *125*, 11350–9.
29. Heathcock, C. H.; Pirrung, M. C.; Montgomery, S. H.; Lampe, J. *Tetrahedron* **1981**, *37*, 4087–95.
30. Romo, D.; Harrison, P. H. M.; Jenkins, S. I.; Riddoch, R. W.;

- Park, K.; Yang, H. W.; Zhao, C.; Wright, G. D. *Bioorg. Med. Chem.* **1998**, *6*, 1255–72.
31. This lower *syn* stability has also been observed in synthesis of other β -lactones. See: Schmidt, J. A. R.; Mahadevan, V.; Getzler, Y. D. Y. L.; Coates, G. W. *Org. Lett.* **2004**, *6*, 373–6.
32. Chamberlain, B. M.; Cheng, M.; Moore, D. R.; Ovitt, T. M.; Lobkovsky, E. B.; Coates, G. W. *J. Am. Chem. Soc.* **2001**, *123*, 3229–38.
33. Möller, M.; Kånge, R.; Hedrick, J. L. *J. Polym. Sci., Part A: Polym. Chem.* **2000**, *38*, 2067–74.
34. Hiki, S.; Miyamoto, M.; Kimura, Y. *Polymer* **2000**, *41*, 7369–79.
35. Kanaoka, S.; Grubbs, R. H. *Macromolecules* **1995**, *28*, 4707–13.
36. Odian, G. *Principles of Polymerization*. 3rd ed.; Wiley: New York, 1991 p 425.
37. Pangborn, A. B.; Giardello, M. A.; Grubbs, R. H.; Rosen, R. K.; Timmers, F. J. *Organometallics* **1996**, *15*, 1518–20.



ortho-Tetraaryls as helical building blocks: a study of structure, theory, electrochemistry, and optical properties

Adah Almutairi, Fook S. Tham and Michael J. Marsella*

Department of Chemistry, University of California at Riverside, Riverside, CA 92521-0403, USA

Received 6 April 2004; revised 25 May 2004; accepted 15 June 2004

Dedicated to Professor Robert H. Grubbs on the occasion of this Special Symposium issue

Abstract—(*ortho*)-3,3'-Diphenyl-2,2'-bithiophene is shown to exhibit a solid-state helical conformation that is consistent with MMFF predictions of structure. The optical, electronic, and conformational properties of this compound are examined, and the results are commensurate with a helical building block capable of exhibiting redox-induced conformational changes along the long molecular axis. Such a property demonstrates promise for this tetramer to function as building block for a spring-like electromechanical actuator.
© 2004 Elsevier Ltd. All rights reserved.

1. Introduction

Helical oligomers and polymers can be principally split into two groups: conformationally rigid or conformationally flexible backbones (i.e., helicenes¹ and polyisonitriles,² respectively). The latter group requires that an external and/or internal force bias the conformational dynamics of the molecule to favor a helical conformation over all other possibilities.³ Recently, we reported *ortho*-sexithiophene **1**,⁴ an oligomer that utilizes internal forces (*torsional strain*) to bias helical conformations in both the solid-state (X-ray) and gas phase (molecular modeling). Herein, we report our efforts to retain a helical conformational bias while simplifying from a parent hexamer to a parent tetramer. Structure, theory, electrochemistry and optical properties are reported for the parent tetramer, compound **2**, and the corresponding polymer, poly(**2**).

2. Design and synthesis

During the course of our studies directed at identifying *ortho*-oligoaryls that adopt a helical conformation, we learned that the strong, helical, conformational bias observed for *ortho*-sexithiophene **1** does not necessarily translate to shorter *ortho*-oligothiophenes. Specifically, X-ray analysis of *ortho*-tetrathiophene **3** reveals a co-crystallization of the three possible C–S regioisomers

(Fig. 1). Given the paucity of related *ortho*-oligoaryl X-ray structures reported to date, we relied on MMFF conformer searches⁵ to assist in our design of a helical tetramer analogous to compound **1**. Note that we have had excellent success in predicting solid-state conformers of *ortho*-oligothiophenes using this level of theory.⁴ In further support, the three lowest energy MMFF conformers of tetramer **3** are in complete agreement with that established from reported X-ray analysis.⁶

Guided by MMFF conformational searches, our screening of candidates revealed that simply replacing the two terminal α -thienyl groups of compound **3** with phenyl rings (compound **2**) fulfils three of our desired goals. First, it removes the asymmetry of the terminal α -thienyl rings, thereby reducing the number of conformational isomers otherwise associated with C–S isomerization (Fig. 1). Second, the replacement of a 5-membered thienyl ring by a 6-membered phenyl ring creates a higher barrier of rotation about the central bithiophene bond (ca. 2 kcal/mol). Third, it decreases the number of available α -thienyl positions from four to two, thus establishing a monomer conducive to electrochemical polymerization of linear α,α' -polythiophene.

Although a search of the Cambridge Structural Database revealed no crystal structure corresponding to compound **2**, the synthesis and electrochemistry of compound **2** has been previously reported by others.⁷ Specifically, the previous study emphasized spectroscopic and charge storage properties of poly(**2**) and related monomers. However, the focus of this prior report did not provide a detailed property analysis of monomer **2**, nor was the electrical conductivity profile of

Keywords: Helicity; Thiophene; Oligomers; Polymers; Molecular modeling; Electrochemistry; Actuation.

* Corresponding author. Tel.: +1-909-787-7223; fax: +1-909-787-2435; e-mail address: michael.marsella@ucr.edu

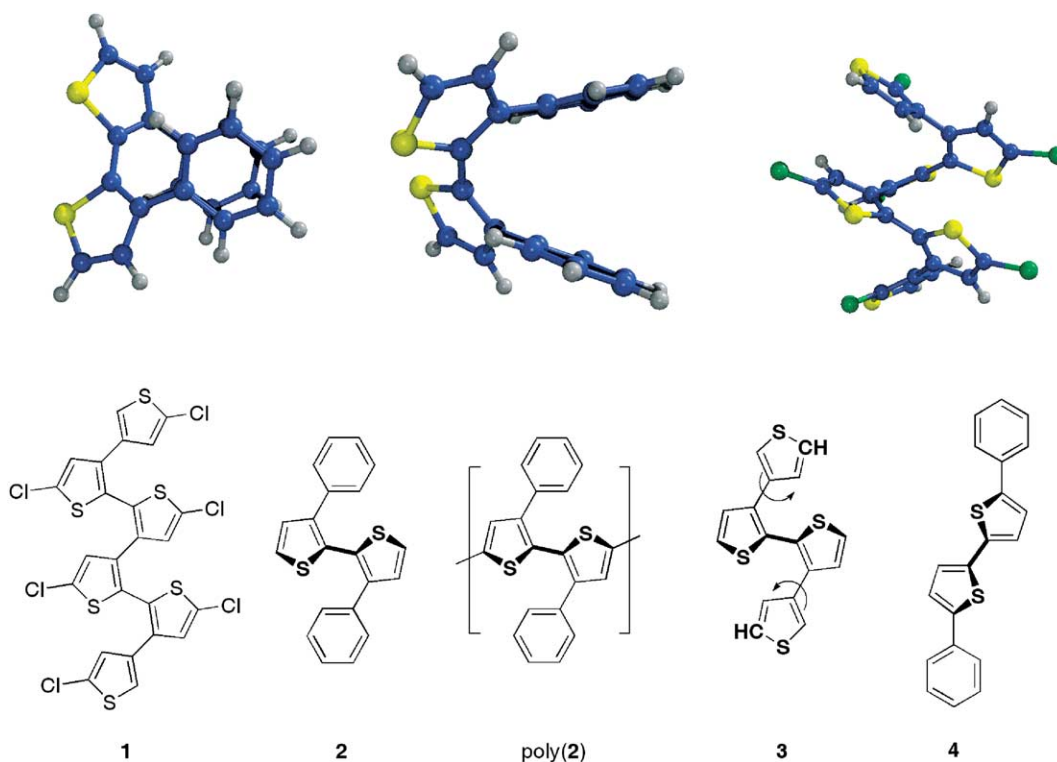


Figure 1. X-ray structures of compounds **1** (two views) and **2** are shown in color. The chemical structures of compounds **1**, **2**, poly(**2**), **3**, and **4** are shown below the crystal structures. The curved arrows shown in compound **3** illustrate the rotation leading to C–S conformer interconversion as described in the text.

poly(**2**) reported. Furthermore, the helical conformation of monomer **2** was discounted based on molecular modeling analysis, and an *anti*-conformation was assumed as the minimum energy conformer (a non-helical conformer with an S–C–C–S dihedral angle of 147.9°).

Our efforts to solve the X-ray structure of compound **2** were successful revealing that the actual S–C–C–S dihedral angle is 69.1° (*syn*-conformation; Fig. 1) is in near complete agreement with MMFF gas-phase predictions (69.8°). A further investigation of these three items (electrochemistry, conductivity, and conformation) would establish a more thorough analysis of compound **2** and related analogs. As such, the previous report of compound **2** and poly(**2**) did not preclude the studies reported herein.

Compound **2** was synthesized as previously reported.⁷ Interestingly, the stability of the 2^{1+} can be gleaned from the fact that FAB-MS reveals an M^+ molecular ion (as opposed to MH^+). For comparative purposes, the linear analog, 5,5'-biphenyl-2,2'-bithiophene (compound **4**) was also prepared using a similar Kumada⁸ coupling strategy.⁹ Gross differences between the two isomers included a dramatic red-shift in absorbance for the linear system (orange versus colorless), and significant solubility differences (**2** is readily soluble in most organic solvents; linear analog **4** is not). Unfortunately, the insolubility of the linear isomer precluded its further analysis.

3. Molecular modeling

The conformations of **2**, 2^{1-} , and 2^{1+} were predicted using a

two-step approach. First, an energy profile corresponding to 180° rotation about the S–C–C–S dihedral of **2** was determined using the semi-empirical level of theory (PM3, C_1 symmetry, tight convergence criterion). Next, the structure corresponding to the global minima was geometry optimized without constraints, using the same level of theory and symmetry. Given that a qualitative assessment of conformation is sufficient at this time, PM3 is a more than adequate level of theory. In all cases, the helical motif is favored over the non-helical, *anti*-conformer (Table 1). With regard to the neutral conformer, PM3 predicts a ca. 6° difference in the S–C–C–S dihedral angle of the most stable conformer relative to that found from MMFF calculations and observed in the X-ray structure of **2**. Given the similarity of the gross topology, we do not find this difference significant for these studies. Note that oxidation and reduction both result in a tighter winding of the helix (i.e., reduction in the S–C–C–S dihedral angle from that observed in the neutral state). This can be directly related to adopting a structure with greater pi-orbital overlap along the helically twisted backbone—particularly with regard to the sp^2 carbons of the internal bithiophene moiety.

Table 1. S–C–C–S dihedral angle for three oxidation states of tetramer **2**, calculated using geometry optimized structures (PM3)

Dihedral/charge	2^{1-}	2	2^{1+}
S–C–C–S	40.93°	76.26°	37.34°

The conformers, mapped with spin density for the 2^{1+} and 2^{1-} case, are shown in Figure 2. The spin density located on the two terminal α -thienyl positions of 2^{1+} is consistent

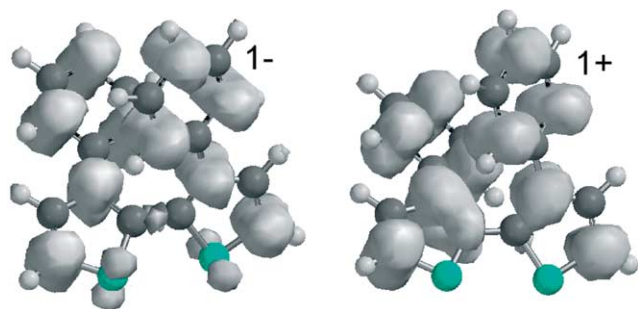


Figure 2. Map of spin density onto (PM3) ground state conformers 2^{1-} and 2^{1+} .

with its known ability to undergo a regiospecific electrochemical polymerization to yield an α,α' -linked polythiophene.^{7,10}

4. Electrochemical properties

Electrochemical examinations of **2** and its corresponding polymer, poly(**2**) reveal distinctive and intriguing properties. As previously detailed, electrochemical oxidation of monomer **2** yields deposition of poly(**2**) onto the surface of the working electrode. Both the anodic and cathodic electrochemistry associated with poly(**2**) are shown in Figure 3.

When poly(**2**) is deposited across two interdigitated microelectrodes (IMEs), and the IME is then configured as a transistor, a profile of relative conductivity as a function of oxidation state can be recorded.¹¹ Significant electrochemical conductivity was only found during the oxidation of poly(**2**). The profile of relative conductivity as a function of oxidation state is also given in Figure 3, with the y -axis labeled I_d (drain current) indicating electrical conductivity when $I_d > 0$. Despite the fact that poly(**2**) can be both n - and p -doped, the conductivity profile is not symmetrical.

Reduction of monomer **2** results not in polymer formation, but highly reversible electrochemistry. Specifically, three overlapping redox couples are observed. A near mirror-image quality square wave voltammogram (Fig. 4) reveals three redox couples likely corresponding to the 1-, 2-, and 3-oxidation states of **2**. However, when analyzed in the presence of an internal ferrocene standard (as shown), it is determined that the three reduction peaks account for a total

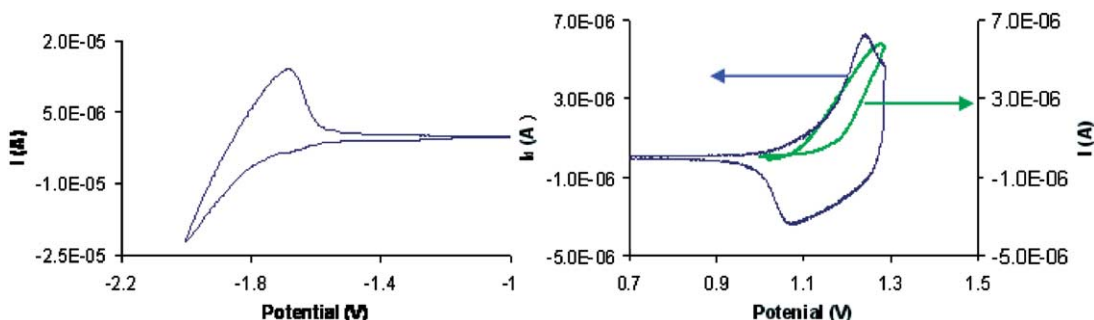


Figure 3. Cyclic voltammetry (blue) and relative electrical conductivity (green) of poly(**2**) are shown. Electrochemical reduction and oxidation were performed in 0.1 M TBAPF₆ THF and MeCN, respectively. Potentials are reported in V versus a Ag/AgCl reference electrode. Scan rates correspond to 100 mV/s for cyclic voltammetry and 5 mV/s for the corresponding transistor experiment (50 mV offset potential; see text).

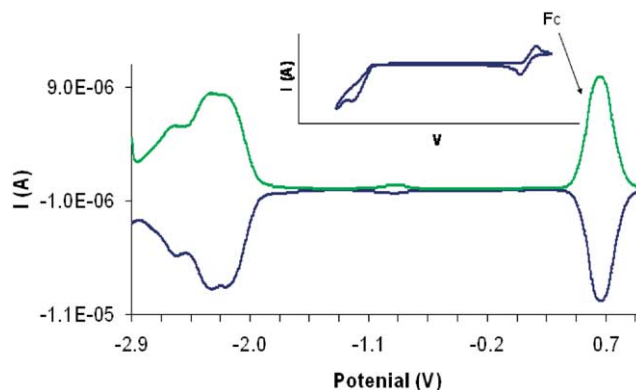


Figure 4. Showing the square wave voltammetry of monomer **2** in 0.1 M TBAPF₆ THF. Potentials are reported as V versus Ag/AgCl reference electrode, and the scan rate is 100 mV/s. The inset is the corresponding cyclic voltammogram. In both cases, an equimolar amount of ferrocene was added as an internal standard, and is shown in both voltammograms.

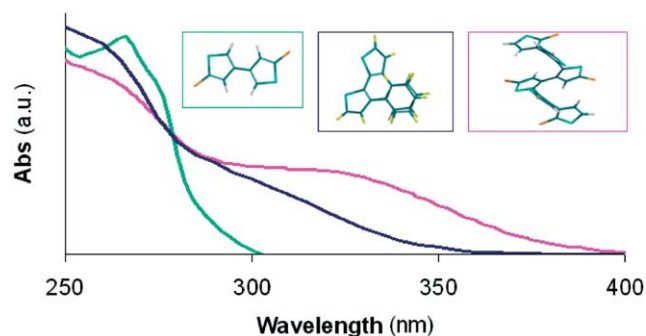
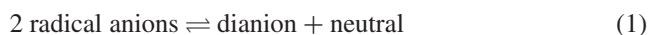


Figure 5. UV–vis absorption of compounds BT, **1**, and **2** in CH₂Cl₂.

of 2.2 e⁻/monomer, not the anticipated value of 3 e⁻/monomer. Discounting instability, the deficiency of 0.8 e⁻/monomer can be rationalized by the well-documented fact that reduction of similar organic compounds readily disproportionate¹² according to Eq. 1:



As such, our observed value of reduction by 2.2 electrons falls within the 1.5- to 3-electron window corresponding to the two kinetic extremes of disproportionation.

5. Optical properties

Figure 5 reports the UV–visible absorption spectra of **1**, **2**

and 5,5'-dichloro-3,3'-bithiophene (**BT**). The latter compound is displayed as a point of reference as it represents the central bithiophene moiety of compound **1**. Although the distribution of conformers in solution has not yet been established, internal torsional strain in **1** and **2** restricts the adoption of planar conformers, and long-range pi-orbital overlap is thus diminished. Regardless, a red-shift is observed as the number of aryl moieties increases from **BT** (two) to compound **2** (four) to **1** (six). The origin of the broad shoulder that first appears in the spectrum of compound **2** and increases in intensity with compound **1** is not yet determined, but internal charge transfer can be ruled out. Specifically, spectra measured across a wide range of solvent polarities resulted in no change in absorption profile. It is also noteworthy to comment that although the onset of absorption increases minimally upon progression from **2** to **1**, the λ_{\max} of the low-energy broad shoulder increases in intensity. This may correspond to the additive effect of a chromophore with a fixed degree of effective conjugation. If the latter hypothesis holds true, the absorption in question may correlate with helical structure. Further investigations of this observation are underway.

Soluble fractions of electrochemically prepared poly(**2**) could be desorbed from the IME using CH_2Cl_2 , yielding a colored solution having a λ_{\max} of 420 nm (Fig. 6). Interestingly, this absorption peak matches the λ_{\max} reported previously for a solid-state film of poly(**2**) on ITO.⁷

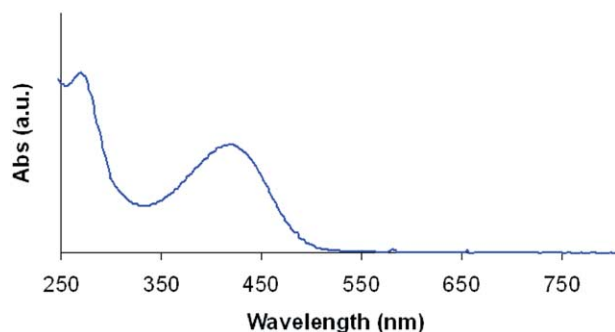


Figure 6. UV-vis absorption of poly(**2**) in CH_2Cl_2 .

6. Discussion and summary

We have previously described the significance of redox-induced dimensional changes in polymer repeat units as the key element in novel electromechanical actuator (EMA) materials.^{13–15} In the course of designing new EMA polymers, the helical motif is particularly interesting given its potential to mimic spring-like behavior, with extension and contraction governed by oxidation state. The first requirement of a spring-like EMA is establishing a reliable helical motif.

In this regard, we have been successful with compound **1**-type systems with regard to gas phase structure (molecular modeling) correlating with solid-state structure (X-ray). Although solution state structure remains uncertain, the physical forces driving helicity in these systems (torsional

strain) are intrinsic, and may be little impacted by medium alone. Having established the X-ray structure of compound **2** is indeed helical, and that geometry optimizations of the electrochemically observed redox species, 2^{1-} , and 2^{1+} , both favor a helical conformation, compound **2**-type tetrameric systems emerge as a candidate of interest for our goals. Favorable qualities that were reported herein include: (i) an intrinsic, torsion-biased helical conformation; (ii) solubility of a tetraaryl in the absence of alkane solubilizing groups; (iii) extended conjugation; (iv) redox activity, including stable redox couples and an ability to support electrical conductivity; and (v) theoretical predictions supporting spring-like behavior that is perturbed as a function of oxidation state. Regarding the latter, perturbations observed in the S–C–C–S dihedral angle of the neutral, 1^- , and 1^+ states of compound **2** (Table 1), translate directly into displacement along the long molecular axis (i.e., spring-like actuation). Further studies of this class of compounds are both warranted and underway.

Acknowledgements

This work is supported by the National Science Foundation (CHE-0138143). M.J.M. congratulates Professor Robert H. Grubbs for his accomplishments, and thanks him for providing a valuable postdoctoral experience.

References and notes

- Paruch, K.; Vyklicky, L.; Katz, T. J.; Incarvito, C. D.; Rheingold, A. L. *J. Org. Chem.* **2000**, *65*, 8774–8782.
- Green, M. M.; Park, J. W.; Sato, T.; Teramoto, A.; Lifson, S.; Selinger, R. L. B.; Selinger, J. V. *Angew. Chem., Int. Ed. Engl.* **1999**, *38*, 3138–3154.
- Review: Hill, D. J.; Mio, M. J.; Prince, R. B.; Hughes, T. S.; Moore, J. S. *Chem. Rev.* **2001**, *101*, 3893–4011.
- Marsella, M. J.; Yoon, K.; Almutairi, A.; Butt, S. K.; Tham, F. S. *J. Am. Chem. Soc.* **2003**, *125*, 13928–13929.
- Spartan 04, Wavefunction, Inc., Irvine, CA, 92612, USA.
- Jayasuriya, N.; Kagan, J.; Huang, D. B.; Teo, B. K. *Heterocycles* **1988**, *27*, 1391–1394.
- Naudin, E.; El Mehdi, N.; Soucy, C.; Breau, L.; Belanger, D. *Chem. Mater.* **2001**, *13*, 634–642.
- Tamao, K.; Kodama, S.; Nakajima, I.; Kumada, M. *Tetrahedron* **1982**, *38*, 3347–3354.
- Marsella, M. J.; Grubbs, R. H. Unpublished results.
- Roncali, J. *Chem. Rev.* **1992**, *92*, 711–738.
- Kittleson, G. P.; White, H. S.; Wrighton, M. S. *J. Am. Chem. Soc.* **1984**, *106*, 7389–7396.
- Rajca, A.; Safronov, A.; Rajca, S.; Wongsriratanakul, J. *J. Am. Chem. Soc.* **2000**, *122*, 3351–3357, and references therein.
- Marsella, M. J.; Piao, G. Z.; Tham, F. S. *Synthesis* **2002**, 1133–1135.
- Marsella, M. J. *Acc. Chem. Res.* **2002**, *35*, 944–951.
- Marsella, M. J.; Reid, R. J. *Macromolecules* **1999**, *32*, 5982–5984.

Ethynyl sulfides as participants in cascade cycloaromatizations

Kevin D. Lewis, Michael P. Rowe and Adam J. Matzger*

Department of Chemistry and the Macromolecular Science and Engineering Program, University of Michigan, 930 N. University Ave., Ann Arbor, MI 48109-1055, USA

Received 8 April 2004; revised 31 May 2004; accepted 4 June 2004

Available online 25 June 2004

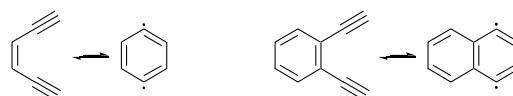
To Robert H. Grubbs for his many contributions to chemistry and his receipt of the Tetrahedron Prize

Abstract—Isomerization of soluble precursor compounds to produce fused-ring systems is an attractive approach for preparing conjugated polymers and oligomers. Cycloaromatization chemistry has previously been explored in this capacity employing reactions based on the Bergman cyclization. Using ethynyl sulfides with a terminal *o*-diethynylbenzene unit, an alternative strategy is demonstrated that offers selectivity advantages in the kinetically controlled radical cyclizations. The products are acene-fused thiophenes in which the diethynylsulfide acts as a relay for the diradical produced in a Bergman cyclization.
 © 2004 Elsevier Ltd. All rights reserved.

1. Introduction

Some of the most interesting properties of conjugated materials arise from molecules with high degrees of planarity and/or ring fusion. However, these structural features are often associated with poor solubility, hampering purification and application of these materials. A common strategy to avoid this problem is to add substituents, such as alkyl chains, that promote solubility.¹ The electronic properties of the compound in the solid state can be altered dramatically by such a perturbation because substituents often radically affect crystal packing. Alternative strategies that circumvent this concern employ soluble precursor routes such as Diels–Alder adducts^{2–4} or silyl substituents on aromatic rings^{5,6} during synthesis, purification, and sometimes deposition. Less well explored is the approach of producing conjugated materials by isomerization of a suitable precursor.^{7–11} With this objective in mind, we explored cycloaromatization routes for the production of fused, conjugated molecules.

Cascade variants of the Bergman cyclization, a unique isomerization of an enediyne to a 1,4-didehydroarene^{12,13} (Scheme 1), are a particularly intriguing route to conjugated oligomers and polymers and have attracted the attention of several groups.^{8,9,14,15} The precursors are *cis*-substituted polyenyne or *ortho*-substituted arylene ethynylenes with generally good solubility, raising the expectation that fused



Scheme 1. Examples of the Bergman cyclization.

conjugated materials can be obtained from thermal isomerization either in solution or the solid state. The first examples of this approach concentrated on hydrocarbon systems. For example, Grubbs and Kratz constructed a precursor for a zipper reaction with the potential to lead to decorated graphite ribbons (Fig. 1).⁸ However, differential scanning calorimetry indicated that a somewhat less exothermic reaction occurred than is expected for full aromatization. A related approach was pursued by Youngs and co-workers employing a cyclyne¹⁶ (dehydrobenzoannulene with no alkenyl ring carbons) precursor with the potential to terminate the radical production intramolecularly to form a cyclic graphite ribbon (Fig. 1).⁹ Neither of these approaches was reported to exclusively produce the desired cascade products.

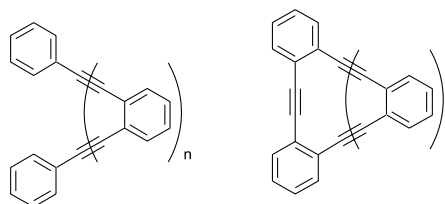


Figure 1. Oligomeric *ortho*-substituted arylene ethynylenes prepared by Grubbs (left)⁸ and Youngs (right).⁹ These compounds are potential precursors to fused acenes through a Bergman multicyclization.

Keywords: Bergman cyclization; Cycloaromatization; Cascade; Enediyne; Thiophene; Ethynyl sulfide; Diradical; Conjugated materials.

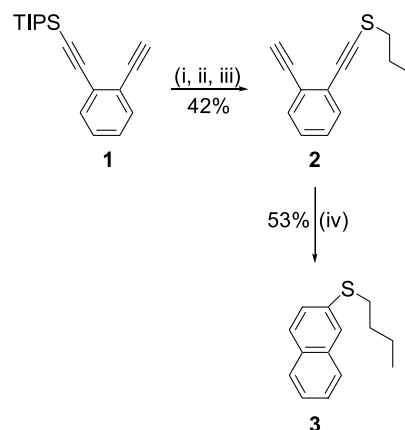
* Corresponding author. Tel.: +1-734-615-6627; fax: +1-734-615-8553; e-mail address: matzger@umich.edu

The failure of these synthetic routes to efficiently yield polyacenes can be traced to the tendency of five-membered cyclizations to proceed competitively with the desired six-membered ring formation. Model studies have shown, both experimentally¹⁷ and theoretically,¹⁸ that five-membered ring formation is favored over cyclization to produce six-membered rings. However, we hypothesized that if instead of the Bergman cyclization a five-membered ring cycloaromatization is employed, the competing four-membered ring cyclization would be much less favorable than the desired pathway. We have recently described the first five-membered ring cycloaromatization¹⁹ involving the photochemical conversion of diethynyl sulfides to thiophenes through the presumed intermediacy of a thiophene-2,5-diyl. Although the reaction does not proceed well under thermal conditions the prospect of using a Bergman cyclization to trigger the five-membered ring cycloaromatization by a cascade reaction is an intriguing route to fused conjugated oligothiophenes.²⁰

2. Approach

The Bergman cyclization of compounds with substituted ethynyl groups has been studied extensively.^{21–24} In many cases the barrier for thermal reaction is substantially increased as a result of steric hindrance in the transition state. However, halogens and some other substituents lower the barrier for thermal reaction. Chlorine or bromine atoms on both triple bonds lower the temperatures required for cyclization and result in yields of 90 and 85%, respectively.²⁵ Surprisingly, little or no data exists for other chalcogenide-substituted ethynyl groups taking part in a Bergman cyclization. For example, attempts at the cycloaromatization of enediynyl ethyl ethers leads to retro-ene reactions to form enyne ketenes which further undergo the Moore cyclization.²⁶ Data have not been reported for sulfur, selenium, or tellurium.

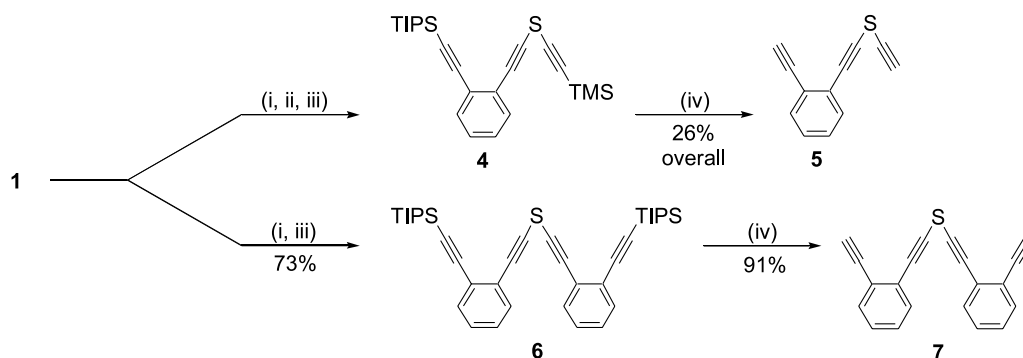
One aspect of concern, in the case of sulfur, is the potential for loss of the heteroatom from the 1,4-didehydroarene to produce an *o*-aryne radical. Accordingly, our initial investigation led us to determine the effect of sulfur on the Bergman cyclization for a simple model ethynyl sulfide: butyl *o*-diethynylbenzene sulfide **2**. The synthesis of this compound in protected form was achieved by treating mono TIPS-protected *o*-diethynylbenzene (**1**)²⁷ with excess butyllithium followed by quenching with SCl₂ (Scheme 2). One



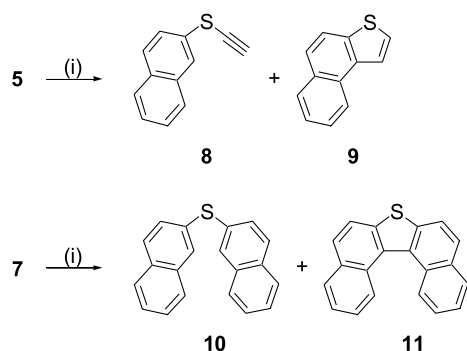
Scheme 2. Reagents and conditions: (i) BuLi, ether, -78 °C; (ii) SCl₂, ether, -78 °C; (iii) TBAF, THF, EtOH; (iv) benzene, CHD, 200 °C, 4 h.

equivalent of alkyllithium generates the acetylide and the remainder reacts with SCl₂ to attach a butyl chain. Treatment of this product with tetrabutylammonium fluoride (TBAF) leads to precursor **2**. Gratifyingly, the cyclization of this compound, effected by heating at 200 °C in benzene with 6 M 1,4-cyclohexadiene (CHD) as trapping agent, proceeded smoothly to afford 2-naphthyl butyl sulfide (**3**) in 53% yield. Competition experiments between **2** and *o*-diethynylbenzene²⁸ indicate that the presence of the sulfur atom increases the barrier to cyclization as evidenced by the decreased conversion of **2** relative to *o*-diethynylbenzene.²⁹ These observations are in agreement with computational predictions for an enediyne bearing an SH group attached to the triple bond.²⁴

Having demonstrated the compatibility of ethynyl sulfides with the Bergman cyclization, the first cascade reaction was attempted. The precursor **4** was synthesized via deprotonation of a mixture of **1** and excess trimethylsilylacetylene using butyllithium followed by quenching with SCl₂ (Scheme 3). Deprotection with TBAF (Scheme 3) yielded *o*-diethynylbenzene ethynyl sulfide **5**. This compound, like many hydrogen-terminated ethynyl sulfides, is particularly prone to decomposition upon exposure to heat and light. Heating **5** to 200 °C for 4 h in the presence of CHD (0.10–10.5 M in benzene) afforded a mixture of naphthalenes (Scheme 4). Surprisingly, the major compound was not the expected naphtho[2,1-*b*]thiophene (**9**), but rather ethynyl 2-naphthyl sulfide (**8**). This indicates that cyclization of the initially formed arene radical onto the triple bond is not fast



Scheme 3. Reagents and conditions: (i) BuLi, ether, -78 °C; (ii) trimethylsilylacetylene; (iii) SCl₂, ether, -78 °C; (iv) TBAF, THF, EtOH.



Scheme 4. Reagents and conditions: (i) benzene, CHD, 200 °C, 4 h.

compared to intermolecular trapping by CHD under these conditions. Although decreasing the concentration of trapping agent led to the expected shift in product ratio towards the thiophene product (**9**), **8** was always the overwhelmingly preferred isomer. Increasing the yield of **9** by using much lower concentrations of CHD was not successful as a result of the tendency of polymerization to compete with small molecule production.³⁰ Indeed a challenge with **2** and related substrates is the poor thermal stability of the free ethynyl sulfide as evidenced by rapid darkening of the pure substances at room temperature.

In order to circumvent the stability problems associated with free ethynyl sulfides, a cyclization precursor was employed lacking this reactive functionality. The cascade cyclization of bis(*o*-diethynylbenzene)sulfide **7**³¹ was expected to afford dinaphtho[2,1-*b*:1',2'-*d*]thiophene (**11**) through an initial 1,4-diradical followed by cyclization onto the ethynyl sulfide and subsequent naphthalene ring formation (Scheme 4). This last step might also be expected to proceed with five-membered ring formation to create a terminal benzofulvene which would presumably further react under the conditions employed.¹⁷ Performing experiments on **7** under the same conditions as **5** led to the cascade product **11** which was obtained in 10% yield with 0.8 M CHD after heating to 200 °C for 4 h. The yield of **11** is remarkable considering the fact that there is substantial steric interaction between hydrogens in the 'bay region' of this compound.³² In contrast to **5**, cyclization onto the ethynyl sulfide competes more equally with intermolecular trapping as evidenced by the 11% yield of bis(2-naphthyl)sulfide (**10**) under these conditions. Although product **10** is expected to arise from independent cyclization and trapping of each *o*-diethynylbenzene unit, cascade reaction is a more energetically viable approach to **11** in order to avoid invoking a tetradical intermediate. At lower concentrations of CHD, formation of **11** is favored over that of **10**. However, once the concentration of CHD is greater than ~0.6 M, **10** is trapped preferentially (Tables 1 and 2).

3. Conclusions

Ethynyl sulfides are compatible with the Bergman cyclization as demonstrated by reactions in which one, two or three rings are formed through cycloaromatization. As demonstrated in the synthesis of dinaphthylthiophene, conjugated compounds can be produced by this route. The potential to extend these studies to longer oligoethynylsulfides³³

Table 1. Yields and relative ratios of products **8** and **9** from the cyclization of **5** at 200 °C

[CHD] (M)	Yield 8 (%)	Yield 9 (%)	8/9
0.1	3.9	1.0	3.7
0.2	8.2	1.9	4.4
0.4	11	2.3	4.7
0.6	14	2.0	6.9
0.8	16	2.1	7.4
1	18	1.9	9.5
2	18	1.3	14
4	18	0.68	27
8	12	0.67	18
10.5	9.4	0.52	18

Table 2. Yields and relative ratios of products **10** and **11** from the cyclization of **7** at 200 °C

[CHD] (M)	Yield 10 (%)	Yield 11 (%)	10/11
0.1	0.96	3.2	0.30
0.2	1.9	5.1	0.38
0.4	3.6	7.2	0.50
0.6	7.4	8.6	0.86
0.8	11	9.9	1.2
1	13	9.0	1.5
2	22	9.2	2.4
4	33	8.1	4.1
8	38	4.5	8.4
10.5	41	3.4	12

suggests a promising entry to fused conjugated materials including higher thienoacenes.²⁰

4. Experimental

4.1. General

Cycloaromatizations employed solutions of the cyclization precursors (3.5 mM) in benzene with CHD. Aliquots (0.5 mL) of the stock solutions were degassed with three freeze/pump/thaw cycles and sealed in glass tubes under vacuum. Reactions were performed in a Parr Reactor, containing benzene to balance the internal pressure of the tubes, equipped with a 4835 control unit. Yields were measured by gas chromatography employing *m*-terphenyl as an internal standard on a Shimadzu GC-17A gas chromatograph equipped with a flame ionization detector. Product identity was confirmed by GC–MS using a ThermoQuest Trace GC equipped with a Finnigan Polaris/GCQ Plus Ion Trap MS by comparison of retention times and mass fragmentation patterns to those of authentic samples prepared by independent routes (vide infra). ¹H NMR spectra were referenced to residual CHCl₃ at 7.26 ppm. Infrared absorption spectra were collected on a Nicolet Avatar 360 IR spectrometer. Elemental analysis and high-resolution mass spectrometry data were provided by the University of Michigan Analytical Laboratory. Ether and THF were dried by passage through activated alumina. CHD was filtered through silica gel prior to use. All other reagents were used as received. All reactions were conducted under nitrogen atmosphere. Compounds **1**,²⁷ **3**,³⁴ **9**,³⁵ **10**,³⁶ and **11**³⁵ were synthesized as described in the literature.

4.1.1. Butyl *o*-diethynylbenzene sulfide 2. A solution of **1** (382 mg, 1.35 mmol) in ether (30 mL) was cooled to -78°C . BuLi (1.6 M in hexanes, 9.50 mL, 15.2 mmol) was added dropwise and allowed to stir for 1 h. A solution of SCl_2 (0.440 mL, 6.93 mmol) in ether (10 mL) cooled to 0°C was added dropwise via cannula. The mixture was allowed to stir for 1 h and then warmed over 2 h. Quenching with water (75 mL) was followed by extraction with hexanes (3 \times 50 mL). The organic layers were combined, washed with brine (2 \times 150 mL), and dried over anhydrous Na_2SO_4 . Flash chromatography on silica gel (hexanes) yielded **2** with the triple bond protected as the ethynyl triisopropylsilyl group (241 mg of a pale yellow oil, 48%). ^1H NMR (400 MHz, CDCl_3) δ 7.47–7.43 (m, 1H), 7.41–7.37 (m, 1H), 7.25–7.17 (m, 2H), 2.82 (t, $J=7.3$ Hz, 2H), 1.78 (tt, $J=7.4$, 7.4 Hz, 2H), 1.48 (qt, $J=7.4$, 7.3 Hz, 2H), 1.16 (s, 21H), 0.96 (t, $J=7.4$ Hz, 3H); ^{13}C NMR (100 MHz, CDCl_3) δ 132.62, 131.85, 127.93, 127.38, 126.37, 125.53, 105.33, 94.85, 91.59, 84.19, 35.59, 31.39, 21.38, 18.64, 13.51, 11.26; GC–MS (EI) m/z (% relative intensity) 370 (42, M^+), 327 (100), 303 (8), 285 (10), 271 (8), 257 (16), 247 (19), 229 (41), 219 (28), 201 (52), 195 (28), 181 (33), 167 (14), 141 (14); IR (film) 3060, 2958, 2941, 2891, 2864, 2160, 1475, 1464, 1440, 1382, 1365, 1272, 1232, 1203, 1159, 1099, 1072, 1016, 995, 946, 918, 883, 814, 756, 677, 665, 636 cm^{-1} . Anal. Calcd for $\text{C}_{23}\text{H}_{34}\text{SSi}$: C, 74.53; H, 9.35. Found: C, 74.11; H, 9.11.

Removal of the TIPS group from the above sulfide (153 mg, 0.411 mmol) was achieved by stirring in THF (2.5 mL) with TBAF (1.0 M in THF, 0.81 mL, 0.81 mmol) and EtOH (0.05 mL) until starting material was consumed as indicated by TLC analysis. The mixture was added to water (10 mL) and extracted with hexanes (3 \times 10 mL). The organic layers were combined, washed with brine (2 \times 30 mL), and dried over anhydrous Na_2SO_4 . Flash chromatography (9:1, hexanes/ CH_2Cl_2), yielded **2** as a pale yellow oil (88.2 mg, 87%). ^1H NMR (500 MHz, CDCl_3) δ 7.49–7.46 (m, 1H), 7.40–7.37 (m, 1H), 7.29–7.25 (m, 1H), 7.24–7.20 (m, 1H), 3.27 (s, 1H), 2.83 (t, $J=7.3$ Hz, 2H), 1.85 (tt, $J=7.4$, 7.4 Hz, 2H), 1.49 (qt, $J=7.5$, 7.4 Hz, 2H) 0.96 (t, $J=7.3$ Hz, 3H); ^{13}C NMR (100 MHz, CDCl_3) δ 132.58, 131.20, 128.53, 127.32, 126.73, 123.86, 91.55, 84.71, 80.72, 80.69, 35.63, 31.29, 21.38, 15.53; GC–MS (EI) m/z (% relative intensity) 214 (51, M^+), 184 (9), 158 (100), 114 (33); IR (film) 3300, 3286, 3061, 2958, 2929, 2872, 2168, 2108, 1475, 1438, 1379, 1255, 1225, 1159, 1095, 1036, 935, 916, 874, 756, 650 cm^{-1} . HRMS–EI (m/z): M^+ calcd for $\text{C}_{14}\text{H}_{14}\text{S}$, 214.0816; found, 214.0822.

4.1.2. Triyne 4. A solution of **1** (694.1 mg, 2.46 mmol) in ether (80 mL) was cooled to -78°C . BuLi (2.5 M in hexanes, 9.65 mL, 24.1 mmol) was added dropwise followed by slow addition of trimethylsilylacetylene (3.10 mL, 22.4 mmol). After stirring 2 h, a solution of SCl_2 (0.770 mL, 12.1 mmol) in ether (30 mL) cooled to 0°C was added dropwise via cannula. The mixture was allowed to stir for 2 h and then warmed over 2 h. Quenching with water (150 mL) was followed by extraction with hexanes (3 \times 100 mL). The organic layers were combined, washed with brine (2 \times 150 mL), and dried over anhydrous Na_2SO_4 . Flash chromatography on silica gel (hexanes) yielded **4** (567 mg, 56%) as a yellow oil. ^1H NMR (500 MHz, CDCl_3)

δ 7.48–7.46 (m, 2H), 7.29–7.23 (m, 2H), 1.16 (s, 21H), 0.20 (s, 9H); ^{13}C NMR (100 MHz, CDCl_3) δ 132.45, 132.38, 128.60, 127.96, 126.47, 125.10, 104.69, 103.24, 95.75, 93.82, 86.03, 75.34, 18.64, 11.22, -0.46 ; GC–MS (EI) m/z (% relative intensity) 410 (1.3, M^+) 367 (34), 325 (75), 299 (50), 283 (100), 251 (61), 235 (85), 223 (41), 219 (31), 209 (31), 195 (36), 191 (15), 165 (13), 149 (7), 115 (6); IR (film) 3063, 2958, 2943, 2891, 2866, 2160, 2104, 1475, 1464, 1441, 1383, 1365, 1252, 1234, 1203, 1159, 1099, 1072, 1037, 1016, 995, 949, 920, 871, 845, 812, 758, 700, 677, 665, 635 cm^{-1} . Anal. Calcd for $\text{C}_{24}\text{H}_{34}\text{SSi}_2$: C, 70.18; H, 8.34. Found: C, 69.92; H, 8.21.

4.1.3. *o*-Diethynylbenzene ethynyl sulfide 5. The compound was more conveniently prepared by the same method as **4** without isolation of the deprotected intermediates; **1** (609 mg, 2.16 mmol), trimethylsilylacetylene (2.62 mL, 18.9 mmol), BuLi (2.5 M in hexanes, 8.50 mL, 21.3 mmol), and SCl_2 (0.675 mL, 10.6 mmol). After removal of the trimethylsilyl group by stirring in ether (2.5 mL) and MeOH (2.5 mL) with K_2CO_3 (6 mg) until starting material was consumed as indicated by TLC analysis, the crude material was poured into water (10 mL) and extracted with hexanes (3 \times 10 mL). The organic layers were combined, washed with brine (2 \times 10 mL), and dried over anhydrous Na_2SO_4 . The solvent and diethynylsulfide byproduct were removed by rotary evaporation. The triisopropylsilyl group was removed by dissolution of the crude material in THF (5 mL) and stirring with TBAF (8.4 mL, 8.4 mmol) and EtOH (0.20 mL) until all starting material was consumed as indicated by TLC analysis. The mixture was added to water (20 mL) and extracted with hexanes (3 \times 20 mL). The organic layers were combined, and washed with brine (2 \times 60 mL), and dried over anhydrous Na_2SO_4 . Flash chromatography on silica gel (9:1, hexanes/ CH_2Cl_2) yielded **5** (103 mg, 26%) as an unstable yellow oil. ^1H NMR (500 MHz, CDCl_3) δ 7.54–7.44 (m, 2H), 7.35–7.27 (m, 2H), 3.33 (s, 1H), 3.02 (s, 1H); ^{13}C NMR (125 MHz, CDCl_3) δ 132.55, 131.93, 128.64, 128.49, 124.98, 124.71, 93.72, 84.13, 81.57, 81.46, 75.04, 67.50; IR (film) 3288, 3063, 2177, 2108, 2054, 1963, 1917, 1475, 1441, 1095, 1036, 953, 876, 758, 690, 656, 625 cm^{-1} . HRMS–EI (m/z): M^+ calcd for $\text{C}_{12}\text{H}_6\text{S}$, 182.0190; found, 182.0194.

4.1.4. Tetrayne 6. A solution of **1** (952.2 mg, 3.37 mmol) in ether (50 mL) was cooled to -78°C . BuLi (1.6 M in hexanes, 2.10 mL, 3.36 mmol) was added dropwise and the reaction mixture allowed to stir for 2 h. A solution of SCl_2 (0.110 mL, 1.73 mmol) in ether (10 mL) cooled to 0°C was added dropwise via cannula. The mixture was allowed to stir for 1 h and then warmed over 2 h. Quenching with water (100 mL) was followed by extraction with hexanes (3 \times 100 mL). The organic layers were combined, washed with brine (2 \times 150 mL), and dried over anhydrous Na_2SO_4 . Flash chromatography on silica gel (9:1, hexanes/ CH_2Cl_2) yielded **6** (731 mg, 73%) as a viscous yellow oil. ^1H NMR (500 MHz, CDCl_3) δ 7.50–7.44 (m, 4H), 7.26 (td, $J=7.5$, 2.1 Hz, 4H), 1.15 (s, 42H); ^{13}C NMR (100 MHz, CDCl_3) δ 132.38, 132.06, 128.37, 127.87, 126.20, 125.10, 104.65, 95.68, 93.40, 75.82, 18.68, 11.31; MS (EI, 70 eV) m/z (% relative intensity) 594 (35, M^+) 551 (17), 509 (34), 467 (27), 425 (21), 321 (14), 239 (26), 157 (67), 115 (100); IR (film)

3061, 2956, 2943, 2891, 2864, 2160, 1558, 1475, 1464, 1441, 1383, 1365, 1275, 1234, 1203, 1159, 1097, 1072, 1036, 1016, 995, 949, 920, 883, 845, 812, 756, 677, 665, 636 cm⁻¹; HRMS-EI (*m/z*): M⁺ calcd for C₃₈H₅₀SSi₂, 594.3172; found, 594.3157. Anal. Calcd for C₃₈H₅₀SSi₂: C, 76.60; H, 8.47. Found: C, 76.74; H, 8.37.

4.1.5. Bis(*o*-diethynylbenzene)sulfide 7. Removal of the triisopropylsilyl group from **6** (405 mg, 0.681 mmol) was achieved by stirring in THF (10 mL) with TBAF (1.0 M in THF, 2.70 mL, 2.70 mmol) and EtOH (0.80 mL) until TLC analysis indicated complete consumption of **6**. The mixture was added to water (20 mL) and extracted with ether (3×20 mL). The organic layers were combined, washed with brine (2×60 mL), and dried over anhydrous Na₂SO₄. Flash chromatography on silica gel (9:1, petroleum ether/CH₂Cl₂) yielded **7** (175 mg, 91%) as an unstable yellow solid. ¹H NMR (500 MHz, CDCl₃) δ 7.52–7.46 (m, 4H), 7.33–7.27 (m, 4H), 3.33 (s, 2H); ¹³C NMR (125 MHz, CDCl₃) δ 132.81, 132.16, 128.76, 128.75, 125.50, 124.91, 93.41, 81.90, 81.82, 76.49; IR (KBr) 3286, 3059, 2168, 2112, 1446, 1439, 1332, 1275, 1252, 1203, 1194, 1165, 1095, 1038, 955, 870, 771, 762, 665, 650, 631, 575, 555, 532, 509, 463 cm⁻¹. HRMS-EI (*m/z*): M⁺ calcd for C₂₀H₁₀S, 282.0503; found, 282.0509.

4.1.6. Ethynyl 2-naphthyl sulfide (8). A solution of 2-bromonaphthalene (531 mg, 2.56 mmol) in ether (20 mL) was cooled to 0 °C. *t*-BuLi (1.5 M in pentane, 3.40 mL, 5.44 mmol) was added dropwise and stirred five minutes. Trimethylsilylacetylene (0.175 mL, 1.27 mmol) was added slowly and stirred 30 min. SCl₂ (0.080 mL, 1.126 mmol) was added dropwise and stirred 1 h. After quenching with NH₄Cl (sat, 3 mL), the mixture was poured into water (40 mL) and extracted with hexanes (3×20 mL). The combined organic layers were washed with brine (2×60 mL) and dried over anhydrous Na₂SO₄. Flash chromatography on silica gel (hexanes) yielded 2-naphthyl trimethylsilylacetylene sulfide (37.5 mg, 15%) as an orange-yellow oil. ¹H NMR (500 MHz, CDCl₃) δ 7.90–7.88 (m, 1H), 7.84–7.80 (m, 2H), 7.78–7.75 (m, 1H), 7.52–7.44 (m, 3H), 0.30 (s, 9H); ¹³C NMR (100 MHz, CDCl₃) δ 133.77, 132.09, 129.65, 128.97, 127.87, 127.15, 126.88, 126.03, 124.63, 124.09, 106.63, 90.21, -0.17; GC-MS (EI) *m/z* (% relative intensity) 256 (100, M⁺), 243 (30), 241 (24), 225 (21), 165 (20), 127 (5), 115 (5), 75 (18); IR (film) 3057, 2958, 2926, 2899, 2852, 2096, 1626, 1587, 1502, 1452, 1410, 1342, 1250, 1132, 1070, 964, 951, 883, 843, 818, 760, 743, 700, 627 cm⁻¹.

Removal of the trimethylsilyl group from 2-naphthyl trimethylsilylacetylene sulfide (24.5 mg, 0.956 mmol) was achieved by stirring in ether (2 mL) and MeOH (2 mL) with K₂CO₃ (5 mg) until all starting material was consumed as indicated by TLC analysis. The mixture was poured into water (10 mL) and extracted with hexanes (3×10 mL). The organic layers were combined and dried over anhydrous Na₂SO₄. (16.2 mg, 92%). ¹H NMR (500 MHz, CDCl₃) δ 7.94–7.92 (m, 1H), 7.84–7.77 (m, 3H), 7.53–7.46 (m, 3H), 3.33 (s, 1H); ¹³C NMR (100 MHz, CDCl₃) δ 133.67, 132.08, 129.00, 128.69, 127.79, 127.11, 126.87, 126.11, 125.05, 124.28, 87.06, 71.06; GC-MS (EI) *m/z* (% relative intensity) 184 (100, M⁺), 152 (51), 139 (25), 126 (11), 115

(8); IR (KBr) 3259, 3053, 2955, 2924, 2852, 2037, 1622, 1587, 1483, 1271, 1240, 1196, 1132, 1063, 960, 941, 891, 858, 812, 748, 714, 584, 563, 478, 467, 457 cm⁻¹. HRMS-EI (*m/z*): M⁺ calcd for C₁₂H₈S, 184.0346; found, 184.0344.

Acknowledgements

The authors would like to thank the ACS-PRF, the Oak Ridge Associated Universities (Ralph E. Powe Award), and the University of Michigan for funding. K. D. L. is a fellow of the NSF sponsored IGERT program for Molecular Designed Electronic, Photonic, and Nanostructured Materials at the University of Michigan.

References and notes

- For examples of this and related strategies successfully applied to the important small molecule semiconductor pentacene see: Hart, H.; Lai, C.; Nwokogu, G. C.; Shamouilian, S. *Tetrahedron* **1987**, *43*, 5203–5224. Takahashi, T.; Kitamura, M.; Shen, B. J.; Nakajima, K. *J. Am. Chem. Soc.* **2000**, *122*, 12876–12877. Meng, H.; Bendikov, M.; Mitchell, G.; Helgeson, R.; Wudl, F.; Bao, Z.; Siegrist, T.; Kloc, C.; Chen, C. H. *Adv. Mater.* **2003**, *15*, 1090–1093. Anthony, J. E.; Brooks, J. S.; Eaton, D. L.; Parkin, S. R. *J. Am. Chem. Soc.* **2001**, *123*, 9482–9483. Sheraw, C. D.; Jackson, T. N.; Eaton, D. L.; Anthony, J. E. *Adv. Mater.* **2003**, *15*, 2009–2011.
- Herwig, P. T.; Mullen, K. *Adv. Mater.* **1999**, *11*, 480–483.
- Afzali, A.; Dimitrakopoulos, C. D.; Breen, T. L. *J. Am. Chem. Soc.* **2002**, *124*, 8812–8813.
- Afzali, A.; Dimitrakopoulos, C. D.; Graham, T. O. *Adv. Mater.* **2003**, *15*, 2066–2069.
- Yassar, A.; Garnier, F.; Deloffre, F.; Horowitz, G.; Ricard, L. *Adv. Mater.* **1994**, *6*, 660–663.
- Mustafa, A. H.; Shepherd, M. K. *Chem. Commun.* **1998**, 2743–2744.
- Goldfinger, M. B.; Swager, T. M. *J. Am. Chem. Soc.* **1994**, *116*, 7895–7896.
- Grubbs, R. H.; Kratz, D. *Chem. Ber.-Recl.* **1993**, *126*, 149–157.
- Baldwin, K. P.; Bradshaw, J. D.; Tessier, C. A.; Youngs, W. J. *Synlett* **1993**, 853–855.
- Lamba, J. J. S.; Tour, J. M. *J. Am. Chem. Soc.* **1994**, *116*, 11723–11736.
- Knoll, K.; Schrock, R. R. *J. Am. Chem. Soc.* **1989**, *111*, 7989–8004.
- Jones, R. R.; Bergman, R. G. *J. Am. Chem. Soc.* **1972**, *94*, 660–661.
- Bergman, R. G. *Acc. Chem. Res.* **1973**, *6*, 25–31.
- Bradshaw, J. D.; Solooki, D.; Tessier, C. A.; Youngs, W. J. *J. Am. Chem. Soc.* **1994**, *116*, 3177–3179.
- Chow, S. Y.; Palmer, G. J.; Bowles, D. M.; Anthony, J. E. *Org. Lett.* **2000**, *2*, 961–963.
- Youngs, W. J.; Tessier, C. A.; Bradshaw, J. D. *Chem. Rev.* **1999**, *99*, 3153–3180.
- Matzger, A. J.; Vollhardt, K. P. C. *Chem. Commun.* **1997**, 1415–1416.
- Olivella, S.; Sole, A. *J. Am. Chem. Soc.* **2000**, *122*, 11416–11422.

19. Lewis, K. D.; Wenzler, D. L.; Matzger, A. J. *Org. Lett.* **2003**, *5*, 2195–2197.
20. Zhang, X.; Matzger, A. J. *J. Org. Chem.* **2003**, *68*, 9813–9815.
21. Lockhart, T. P.; Mallon, C. B.; Bergman, R. G. *J. Am. Chem. Soc.* **1980**, *102*, 5976–5978.
22. Rawat, D. S.; Zaleski, J. M. *Chem. Commun.* **2000**, 2493–2494.
23. König, B.; Pitsch, W.; Klein, M.; Vasold, R.; Prall, M.; Schreiner, P. R. *J. Org. Chem.* **2001**, *66*, 1742–1746.
24. Prall, M.; Wittkopp, A.; Fokin, A. A.; Schreiner, P. R. *J. Comput. Chem.* **2001**, *22*, 1605–1614.
25. Bowles, D. M.; Palmer, G. J.; Landis, C. A.; Scott, J. L.; Anthony, J. E. *Tetrahedron* **2001**, *57*, 3753–3760.
26. Tarli, A.; Wang, K. K. *J. Org. Chem.* **1997**, *62*, 8841–8847.
27. Haley, M. M.; Bell, M. L.; English, J. J.; Johnson, C. A.; Weakley, T. J. R. *J. Am. Chem. Soc.* **1997**, *119*, 2956–2957.
28. Thoen, K. K.; Thoen, J. C.; Uckun, F. M. *Tetrahedron Lett.* **2000**, *41*, 4019–4024.
29. Grissom, J. W.; Calkins, T. L.; McMillen, H. A.; Jiang, Y. H. *J. Org. Chem.* **1994**, *59*, 5833–5835.
30. Johnson, J. P.; Bringley, D. A.; Wilson, E. E.; Lewis, K. D.; Beck, L. W.; Matzger, A. J. *J. Am. Chem. Soc.* **2003**, *125*, 14708–14709.
31. Zhang, H.; Lam, K. T.; Chen, Y. L.; Mo, T.; Kwok, C. C.; Wong, W. Y.; Wong, M. S.; Lee, A. W. M. *Tetrahedron Lett.* **2002**, *43*, 2079–2082.
32. Fabbri, D.; Dore, A.; Gladiali, S.; DeLucchi, O.; Valle, G. *Gazz. Chim. Ital.* **1996**, *126*, 11–18.
33. Lee, A. W. M.; Yeung, A. B. W.; Yuen, M. S. M.; Zhang, H.; Zhao, X.; Wong, W. Y. *Chem. Commun.* **2000**, 75–76.
34. Bates, C. G.; Gujadhur, R. K.; Venkataraman, D. *Org. Lett.* **2002**, *4*, 2803–2806.
35. Imamura, K.; Hirayama, D.; Yoshimura, H.; Takimiya, K.; Aso, Y.; Otsubo, T. *Tetrahedron Lett.* **1999**, *40*, 2789–2792.
36. Argüello, J. E.; Schmidt, L. C.; Peñeñory, A. B. *Org. Lett.* **2003**, *5*, 4133–4136.



Synthesis of sodium-polystyrenesulfonate-grafted nanoparticles by core-cross-linking of block copolymer micelles

Kozo Matsumoto,* Hirohiko Hasegawa and Hideki Matsuoka

Department of Polymer Chemistry, Kyoto University, Katsura, Nishikyo-ku, Kyoto 615-8510, Japan

Received 6 March 2004; revised 21 May 2004; accepted 21 May 2004

Available online 11 June 2004

This paper is dedicated to Professor Robert H. Grubbs on the occasion of his receipt of the 2003 Tetrahedron Prize

Abstract—Sodium poly(styrenesulfonate)(polySSNa)-grafted polymer nanoparticles were synthesized by core-cross-linking of block copolymer micelles and subsequent chemical transformation. Block copolymers, poly(*p*-((1-methyl)silacyclobutyl)styrene-*block*-poly(neopentyl *p*-styrenesulfonate)s, polySBS-*b*-polySSPen, were synthesized by nitroxy-mediated living radical polymerization. The block copolymers formed micelles ($R_h=15-23$ nm, where R_h represents the hydrodynamic radius) with a polySBS core and polySSPen shell in acetone. The micelle core was cross-linked by ring-opening polymerization of silacyclobutyl groups in polySBS. Hydrolysis of the neopentyl groups provided polySSNa-grafted nanoparticles. The R_h of the particles before the hydrolysis ranged from 12 to 21 nm in acetone, while they varied to the range from 50 to 110 nm in water after the hydrolysis.

© 2004 Elsevier Ltd. All rights reserved.

1. Introduction

Block copolymers self-assemble to form micelles in solvents selective for one of the blocks. The core of the micelle consists of an insoluble block, and the shell, which is often called corona, consists of both a soluble block and the solvent.^{1,2} Such micelle formation has attracted much attention for industrial and biomedical applications. Consequently, many block copolymer micelles have been studied not only for use as surfactants such as lubricant, dispersant, and emulsifier, but also as additives in cosmetics or drug carriers for drug delivery systems.^{3,4} Compared with the micelles of low molecular weight surfactants, the block copolymer micelles are generally larger, ranging from several nanometers to tens of nanometers. Additionally, they are more stable due to their slow exchange between associated and non-associated molecules (micelle-unimer exchange). These properties are quite advantageous in constructing nano-scale materials. By cross-linking the core of the micelle, we can obtain nanoparticles with shell-forming polymers grafted from the particle surface.^{5–20} In this study, we synthesized strong-ionic-polymer-grafted nanoparticles, using a styrene-based block copolymer, in which one segment has cross-linkable silacyclobutyl groups and the other has potentially ionic sulfonate ester groups. The precursor block copolymer was prepared by nitroxy-radical-

mediated living polymerization, and its micelle was formed in acetone. Then, the core of the micelle was cross-linked by ring-opening polymerization of silacyclobutyl groups, and finally the ester groups on the grafting polymers were hydrolyzed to obtain sodium poly(styrene sulfonate)-grafted nanoparticles. The outline of this study is shown in Figure 1. The particles synthesized here are expected as new materials in wide variety of applications from industrial surfactants to nano-capsules for biomedical usage. They may also attract fundamental scientific attention as academic samples, since the particle has a well-defined strong polyelectrolyte brush layer on the surface with high grafting density.

2. Experimental

2.1. Materials

Neopentyl *p*-styrenesulfonate (SSPen)²¹ and *N*-*t*-butyl-1-diethylphosphono-2,2-dimethylnitroxyl radical (DEPN)²² were prepared as reported. Benzoyl peroxide (BPO) was purchased from Nacalai Tesque (Kyoto, Japan), 2,2'-azobisisobutyronitrile (AIBN) and chloroplatinic acid hexahydrate ($H_2PtCl_6 \cdot 6H_2O$) were purchased from Wako Pure Chemicals (Osaka, Japan), iodotrimethylsilane was purchased from Tokyo Chemical Industries (Tokyo, Japan), and they were used as delivered. Tetrahydrofuran (THF) and benzene was distilled over sodium benzophenone ketyl under an argon atmosphere. Acetone was purified by distillation over MS-4A. Carbon tetrachloride was distilled over CaH_2 . Water used for dialysis and polymer sample

Keywords: Living radical polymerization; Polymer micelle; Cross-linking; Nanoparticle; Surface-graft; Sodium polystyrenesulfonate.

* Corresponding author. Tel.: +81-75-383-2597; fax: +81-75-383-2599; e-mail address: matsumo@star.polym.kyoto-u.ac.jp

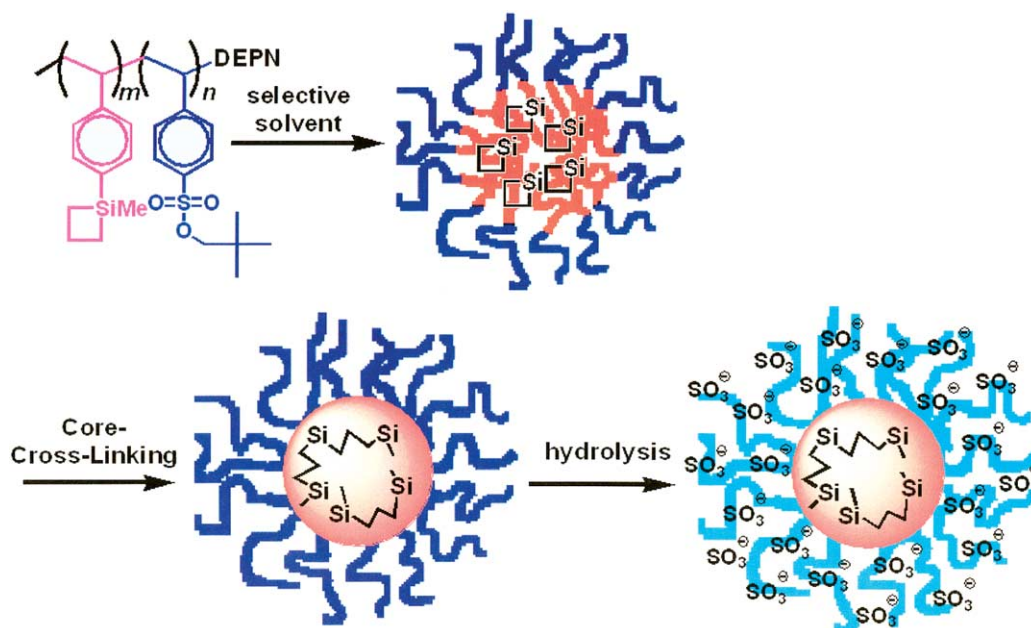


Figure 1. Schematic explanation of synthesis of sodium-polystyrenesulfonate-grafted nanoparticle.

preparation was obtained by a Milli-Q system (Millipore, Pittsburgh, PA) whose resistance was more than 18 M Ω cm.

2.1.1. Synthesis of *p*-(1-methylsilylacyclobutyl)styrene (SBS). A THF solution of 1-chloro-1-methylsilylacyclobutane was prepared as follows. First, 1,2-dibromoethane (0.3 mL) was added to a suspension of magnesium (1.9 g, 80 mmol) in THF (5 mL) to activate the magnesium. Then a THF solution (45 mL) of 3-chloropropylmethylchlorosilane (9.5 mL, 60 mmol) was added dropwise over a period of 10 min. Then the reaction mixture was heated at 50 °C for 2 h. A THF solution of *p*-styrylmagnesium bromide was prepared as follows. First, 1,2-dibromoethane (0.3 mL) was added to a suspension of magnesium (1.5 g, 60 mmol) in THF (5 mL) to activate the magnesium. Then a THF (50 mL) solution of *p*-bromostyrene (6.5 mL, 50 mmol) was added dropwise over a period of 10 min, and the solution was stirred for 2 more hours. The *p*-styrylmagnesium bromide solution thus prepared was slowly added to the 1-chloro-1-methylsilylacyclobutane solution prepared above at an ambient temperature over a period of 10 min. Then the mixture was heated at 40 °C over night. The resulting solution was poured into 1 M aq. HCl, and the product was extracted with hexane. The organic layer was washed twice with water, dried with anhydrous Na₂SO₄, and concentrated. The residual oil was purified by silica-gel column chromatography to give the title compound (29 mmol, 5.4 g) in 57% yield. IR (neat) 3062, 2927, 2855, 1629, 1597, 1543, 1389, 1249, 1105, 1028, 989, 907, 866, 828, 770, 720 cm⁻¹; ¹H NMR (CDCl₃) δ 0.58 (s, 3H), 1.21 (dt, $J=8.4$, 8.4 Hz, 2H), 1.33 (dt, $J=8.4$, 8.4 Hz, 2H), 2.22 (tt, $J=8.4$, 8.4 Hz, 2H), 5.30 (d, $J=10.8$ Hz, 1H), 5.83 (d, $J=17.6$ Hz, 1H), 6.75 (dd, $J=10.8$, 17.6 Hz, 1H), 7.46 (d, $J=12.0$ Hz, 2H), 7.62 (d, $J=12.0$ Hz, 2H); ¹³C NMR (CDCl₃) δ -1.68, 14.46, 18.31, 114.38, 125.61, 133.67, 136.70, 138.16, 138.45. Found: C, 76.74; H, 8.72%. Calcd for C₁₂H₁₆Si: C, 76.51; H, 8.58%.

2.1.2. Synthesis of 1-methyl-1-phenylsilylacyclobutane. A

THF solution of 1-chloro-1-methylsilylacyclobutane was prepared from 22.3 mL of 1-chloro-1-methylsilylacyclobutane (140 mmol) and magnesium (4.13 g, 170 mmol) as described above. Then the solution was cooled to 0 °C and a phenylmagnesium bromide (1.0 mol/L THF solution, 200 mmol, 200 mL) was slowly added. The mixture was stirred at room temperature over night. The resulting solution was poured into 1 M aq. HCl, and the product was extracted with hexane. The organic layer was washed twice with water, dried with anhydrous Na₂SO₄, and concentrated. Distillation of the residual oil over calcium hydride under reduced pressure gave the title compound (15.2 g, 94 mmol) in 67% yield. Bp, 87–89 °C/15 Torr; IR (neat) 3067, 3050, 2927, 2855, 1589, 1487, 1428, 1396, 1300, 1249, 1184, 1112, 998, 925, 899, 866, 772, 732 cm⁻¹; ¹H NMR (CDCl₃) δ 0.55 (s, 3 H), 1.16 (dt, $J=8.4$, 8.4 Hz, 2H), 1.30 (dt, $J=8.4$ Hz, 2H), 2.19 (tt $J=8.4$ Hz, 2H), 7.33–7.43 (m, 3H), 7.57–7.66 (m, 2H); ¹³C NMR (CDCl₃) δ -1.69, 14.42, 18.31, 127.83, 129.32, 133.39, 138.57. Found: C, 73.90; H, 8.91%. Calcd for C₁₀H₁₄Si: C, 73.99; H, 8.71%.

2.2. Polymerization

DEPN-capped SBS₁₁₃ was prepared as follows. A mixture of SBS (3.80 g, 20.1 mmol), BPO (13.6 mg, 0.04 mmol), DEPN (30.1 mg, 0.10 mmol), and benzene (3 mL) was charged in a glass tube equipped with a Teflon screw cock, degassed, and sealed under argon. The Teflon screw cock was used to seal the tube easily and surely. The mixture was kept at 115 °C for 2.5 h. Reprecipitation with a toluene/methanol system, followed by vacuum drying gave DEPN-capped polySBS (2.96 g, 78% SBS conversion) in quantitative yield. $M_n=21,700$, $M_w/M_n=1.31$.

The block copolymer, SBS₁₁₃-*b*-SSPen₂₀₈, was prepared as follows. A mixture of SSPen (2.21 g, 8.70 mmol), DEPN-capped SBS₁₁₃ ($M_n=21,700$, 0.65 g) prepared above, 1.5 mg of DEPN, and benzene (2.5 mL) was charged in a

glass tube equipped with a Teflon cock, degassed, and sealed under argon. The mixture was kept at 115 °C for 2.0 h. Reprecipitation with a chloroform/hexane system, followed by vacuum drying gave SBS₁₁₃-*b*-SSPen₂₀₈ (1.08 g, 62% SSPen conversion) in 54 wt% yield. $M_n=50,500$, $M_w/M_n=1.59$.

2.3. Core-cross-linking of the block copolymer micelle

A core-cross-linked (CCL) block copolymer, CCL-(SBS₁₁₃-*b*-SSPen₂₀₈), was synthesized. About 20 mg of H₂PtCl₆·6-H₂O was placed in a two-necked 500 mL-round bottomed flask equipped with a reflux condenser, and the flask was filled with argon. Then an acetone (100 mL) solution of SBS₁₁₃-*b*-SSPen₂₀₈ (1.0 g) was added, and the mixture was heated at 55 °C for 3 h. The resulting solution was filtrated and concentrated to about 1/5 in volume by evaporation. Then 1,4-dioxane (200 mL) was added and the solution was freeze-dried to give a powdered CCL polymer CCL-(SBS₁₁₃-*b*-SSPen₂₀₈) (1.0 g) in quantitative yield.²³

2.4. Hydrolysis of neopentyl sulfonate

A CCL SBS₁₁₃-*b*-(sodium styrenesulfonate)₂₀₈ (CCL-(SBS₁₁₃-*b*-SSNa₂₀₈)) was synthesized. Trimethylsilyl iodide (1.5 mL, 10 mmol) was added to a solution of CCL-(SBS₁₁₃-*b*-SSPen₂₀₈) (900 mg) in carbon tetrachloride (30 mL), and the mixture was stirred at 50 °C for 15 h. The mixture was concentrated, and the neopentyl and the resulting residue was dissolved in 200 mL of methanol/HCl (1 mol/L) mixture, then aqueous NaOH (1 mol/L) was added to neutralize the solution. The solution was filtrated and dialyzed against deionized water for a week. The dialysate was diluted with water to afford 0.1 wt% aqueous solution of CCL-(SBS₁₁₃-*b*-SSNa₂₀₈) (780 mL).

2.5. Measurements

Gel permeation chromatography (GPC) was carried out in THF on a JASCO PU-980 chromatograph (JASCO Engineering, Tokyo, Japan) equipped with two polystyrene gel columns (Shodex KF804L; separation range in molecular weight of polystyrene: 100 to 4×10⁵) and JASCO RI-930 refractive index detector. The averaged polymerization degree of polySBS and molecular weight distributions were determined relative to polystyrene standards. Proton NMR spectra were recorded on a JEOL AL-400 spectrometer in CDCl₃, acetone-d₆, and D₂O. The averaged polymerization degree of polySSPen segment in polySBS-*b*-polySSPen was calculated from the polymerization degree of SBS pre-polymer (by GPC) and composition of the block copolymer estimated from ¹H NMR measurement. IR spectra were measured on a Shimadzu FTIR-8400 spectrometer. The elemental analyses were carried out at the Elemental Analysis Center of Kyoto University. The dynamic light scattering (DLS) measurements were performed on a DLS apparatus of Photal SLS-6000HL (Otsuka Electric, Osaka, Japan) equipped with a correlator (Photal GC-1000). He-Ne laser (the wavelength of 632.8 nm) was used for the measurements. Sample solutions (1–0.1 wt%) were filtrated through a membrane (Millex-HN, Millipore, pore-size of 0.45 μm). The measurements were performed at 20 °C at

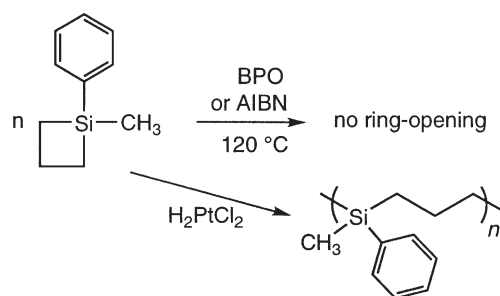
scattering angle of 90°. AFM measurements were performed by SPI3800 probe station and SPA300 unit system of Scanning Probe Microscopy System SPI3800 series (Seiko Instruments, Tokyo, Japan). The cantilever was made of silicon (Olympus, Tokyo, Japan) and its spring constant was 2 N/m. The measurements were performed in Dynamic Force Mode (non-contact mode). For sample preparation, a THF or aqueous solution (ca.0.1 wt%) of the polymer was dropped on a microslide glass (IWAKI, Japan) and air-dried.

3. Results and discussion

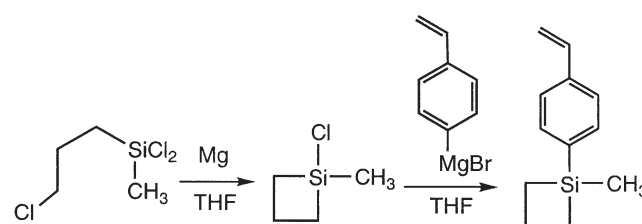
3.1. Block copolymer synthesis

Controlled radical polymerization of vinyl compounds has resulted in a wide variety of well-defined block copolymers.^{24–26} Okamura and co-workers reported a quite sophisticated method of synthesizing polystyrene-*block*-polySSNa by a nitroxyl-radical-mediated living polymerization of styrene with styrene having neopentyl sulfonate group at the *para*-position (SSPen) and a successive hydrolysis of neopentyl ester.²¹ On the other hand, it has been well-known for a long time that silacyclobutanes can be readily polymerized in the presence of platinum catalyst,²⁷ while the four-membered ring is tolerant under radical conditions as shown in Scheme 1. We confirmed that no consumption of 1-methyl-1-phenylsilacyclobutane occurs in heating a bulk 1-methyl-1-phenylsilacyclobutane in the presence of AIBN or BPO at 120 °C. This suggests that styrene derivatives having silacyclobutanes might be radically polymerized without affecting the cyclic group in one step, whereas the resulting styrenic polymer can be cross-linked by ring-opening polymerization in the later step.

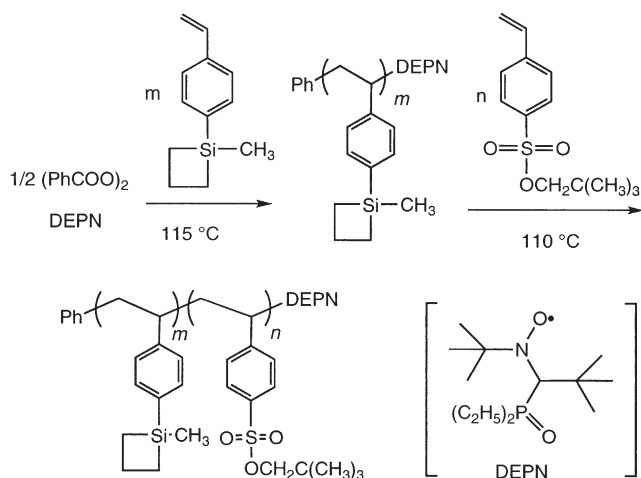
In this study, we used styrenes having a silacyclobutyl group at the *para*-position (SBS) and SSPen as monomers for a



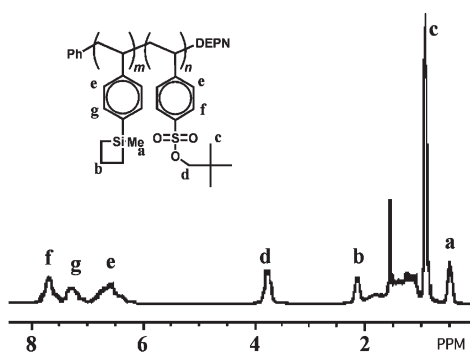
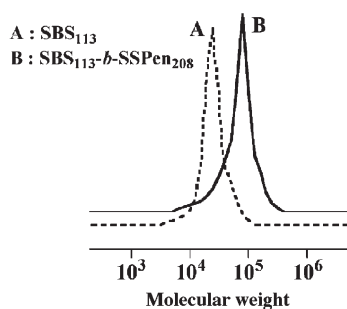
Scheme 1.



Scheme 2.



Scheme 3.

Figure 2. ^1H NMR spectrum of $\text{SBS}_{113}\text{-}b\text{-SSPen}_{208}$ in CDCl_3 .Figure 3. GPC charts for (A) DEPN end-capped SBS_{113} and (B) $\text{SBS}_{113}\text{-}b\text{-SSPen}_{208}$.

block copolymer synthesis. The SBS monomer was readily prepared by treatment of 1-chloro-1-methylsilacyclobutane with *p*-styrylmagnesium bromide as shown in Scheme 2.

The desired block copolymer, polySBS-*b*-polySSPen, was synthesized by nitroxyl-radical-mediated living polymerization as shown in Scheme 3. In the first step, we prepared a nitroxyl-capped polySBS with narrow molecular weight distributions by polymerization of SBS using benzoyl peroxide (BPO) as a radical initiator and DEPN²² as a radical mediator. Then SSPen was polymerized using polySBS as a macro initiator. A representative ^1H NMR spectrum and GPC charts of the obtained polymer are given in Figures 2 and 3. The ^1H NMR spectrum indicates the existence of both polySBS and polySSPen. The peak on the GPC charts shifted to the higher molecular weight region after polymerization of SSPen, which indicates formation of a block copolymer. In the first polymerization step, three polySBS samples having different polymerization degrees were synthesized by tuning the molar ratio of BPO and SBS, while the molar ratio of the radical mediator to the radical initiator was kept constant ($[\text{DEPN}]/[\text{BPO}]=2.5$) in all cases. In the second polymerization step, five different samples were prepared by tuning the molar ratio of SBS prepolymer and SSPen. The polymerization results are summarized in Table 1. The polymerization degree of the polySBS (m) was estimated by GPC measurements relative to polystyrene standard, and the polymerization degree (n) of polySSPen was estimated by ^1H NMR spectra of the block copolymers, thus the m and n are not absolute values. It is also true that the products were contaminated with a trace amount of ‘dead’ polySBS prepolymer as detected by GPC, which broadened the molecular weight distribution, although most of the products were block copolymers. However, we used the crude products in the later experiments without further purification, because the homopolymer was solubilized in the core of the block copolymer micelle and did not pose a crucial problem in the cross-linking step.

3.2. Micelle formation

PolySBS is nonpolar and soluble in nonpolar solvent such as hexane, toluene, chloroform, and THF, while it is insoluble in polar solvent such as acetone, dimethylsulfoxide (DMSO), and *N,N*-dimethylformamide (DMF). On the other hand, polySSPen is moderately polar and insoluble in hexane but soluble in all the other solvents described above. Thus the block copolymers were soluble in chloroform, which is a good solvent for both blocks, and we could see ^1H NMR signals of both polySBS and polySSPen in CDCl_3 as shown in Figure 2. In the meanwhile, the block copolymers were also soluble in acetone, which is a selective solvent for polySSPen. In this case, however, the signals only for polySSPen were observed but the signals for polySBS were

Table 1. Polymerization results of SBS and SSPen

$[\text{BPO}]_0/[\text{SBS}]_0$	Conv. (%) of SBS	m	M_w/M_n of polySBS	$[\text{polySBS}]_0/[\text{SSPen}]_0$	Conv. (%) of SSPen	n	M_w/M_n of block copolymer
1/256	75	64	1.36	1/122	50	70	1.38
1/348	82	89	1.23	1/137	57	97	1.62
—	—	89	1.23	1/251	60	163	1.56
1/480	78	113	1.31	1/194	64	134	1.52
—	—	113	1.31	1/290	62	208	1.59

$[\text{BPO}]_0/[\text{SBS}]_0$: initial molar ratio of BPO and SBS. $[\text{polySBS}]_0/[\text{SSPen}]_0$: initial molar ratio of SBS prepolymer and SSPen. m was determined by GPC relative to polystyrene standard. n was determined by ^1H NMR using the value of m . M_w/M_n was determined by GPC relative to polystyrene standard.

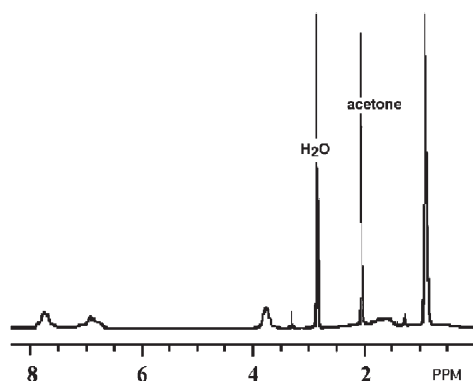


Figure 4. ^1H NMR spectrum of $\text{SBS}_{113}\text{-}b\text{-SSPen}_{208}$ in acetone- d_6 .

acetone-soluble polySSPen and the solvent. To examine more about the micelle formation, we measured the DLS of the block copolymer solutions. In all cases, strong light scattering intensity was observed, which suggested the existence of block copolymer micelles. Hydrodynamic radius (R_h) of the block copolymer micelles in acetone for all the samples examined here are summarized in Table 2. The R_h ranged from 15 to 23 nm, all of which are reasonable values for the block copolymer micelles, and they increased as the total chain length of the block copolymer increased.

3.3. Micelle core cross-linking

It is well-known that silacyclobutanes can be readily polymerized by a hexachloroplatinic acid (H_2PtCl_6).²⁷ We

Table 2. Hydrodynamic radius of $\text{SBS}_m\text{-}b\text{-SSPen}_n$ micelle and $\text{CCL-(SBS}_m\text{-}b\text{-SSPen}_n)$ evaluated by DLS measurement

n	m	Hydrodynamic radius, R_h (nm)				
		$\text{SBS}_m\text{-}b\text{-SSPen}_n$ in acetone	$\text{CCL-(SBS}_m\text{-}b\text{-SSPen}_n)$ in acetone	$\text{CCL-(SBS}_m\text{-}b\text{-SSPen}_n)$ in THF	$\text{CCL-(SBS}_m\text{-}b\text{-SSNa}_n)$ in water	$\text{CCL-(SBS}_m\text{-}b\text{-SSNa}_n)$ in 0.3 M NaCl aq.
64	70	15	12	13	50	40
89	97	17	15	13	82	66
89	163	19	19	19	87	66
113	134	17	21	20	90	63
113	208	23	19	19	110	70

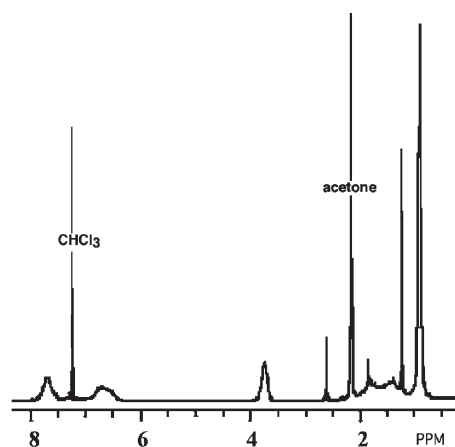
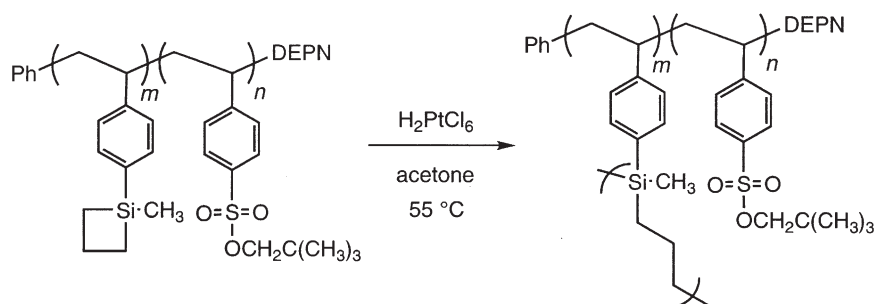


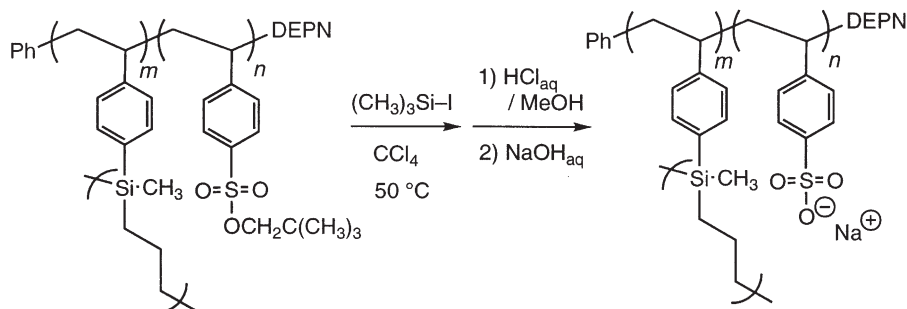
Figure 5. ^1H NMR spectrum of $\text{CCL-(SBS}_{113}\text{-}b\text{-SSPen}_{208})$ in CDCl_3 .

not observed as shown in the spectrum of the block copolymer in acetone- d_6 (Fig. 4). This suggested that micelles were formed in acetone, whose core consists of acetone-insoluble polySBS and the shell consists of

utilized this reaction to a CCL of the block copolymer micelle. The micelle solution in acetone was heated at $55\text{ }^\circ\text{C}$ in the presence of catalytic amount of H_2PtCl_6 . Figure 5 shows ^1H NMR spectrum of the products obtained by treatment with Pt catalyst in acetone and redissolved in CDCl_3 . The four-membered ring methylene signals at 2.2 ppm (observed in Figure 2) completely disappeared and signals of the methyl group on the silicon atom at 0.4 ppm (observed in Figure 2) were detected as significantly broad signals in Figure 5, indicating the occurrence of ring-opening reactions (Scheme 4). Particle size in the acetone solution was examined by DLS measurement. The R_h values for the samples evaluated here are summarized in Table 2. R_h of the obtained particles ranges from 12 to 21 nm in acetone, which are in good agreement with those of the block copolymer micelles before the ring opening reaction. The DLS measurement was also carried out in the THF solution. Light scattering were observed even in THF, which is a good solvent for both polySBS and polySSPen, evidenced the formation of CCL micelles. In addition, the hydrodynamic sizes of the particles evaluated in THF were analogous to those in acetone (Table 2), suggesting that the



Scheme 4.



Scheme 5.

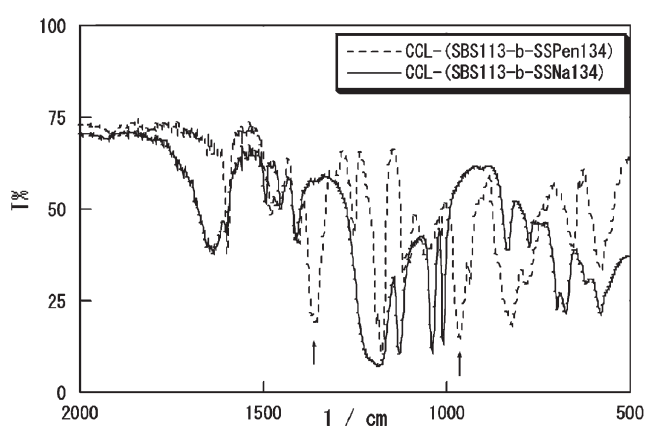


Figure 6. IR-spectra of CCL-(SBS₁₁₃-*b*-SSPen₁₃₄) and CCL-(SBS₁₁₃-*b*-SSNa₁₃₄).

cross-linking proceeded so enough that the core was not swollen even by good solvent. These results clearly indicate the formation of the CCL micelles.

3.4. Synthesis of polySSNa-grafted particle

The neopentyl sulfonates of the grafting chains were transformed into trimethylsilyl sulfonates by treatment with trimethylsilyl iodide in carbon tetrachloride, and the silyl sulfonates were further transformed to sodium sulfonates by sequential exposure to HCl_{aq} and NaOH_{aq} (Scheme 5). Completion of the hydrolysis was confirmed by IR measurements (Fig. 6). Absorption at 1350 and

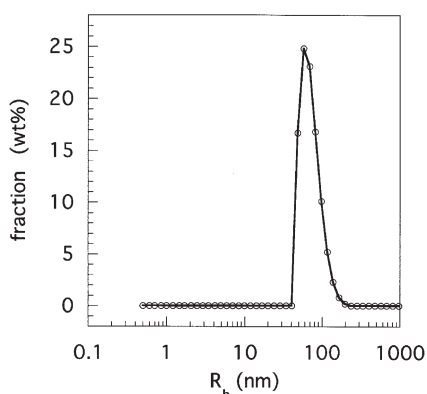


Figure 7. Distribution of hydrodynamic radius (R_h) of CCL-(SBS₁₁₃-*b*-SSNa₁₃₄) in water evaluated by DLS CONTIN analysis. Scattering angle: 90°.

950 cm^{-1} typical for sulfonate ester, which were observed in the case of CCL-(polySBS-*b*-polySSPen), completely disappeared in the spectra for products after hydrolysis.

The hydrolyzed products were soluble in water. DLS analysis of the particles was performed in aqueous solutions. The size distribution of CCL-(SBS₁₁₃-*b*-SSNa₁₃₄) in water is given in Figure 7, which shows narrow size distribution. The R_h values for all the samples are summarized in Table 2. The R_h of the hydrolyzed CCL-micelles ranged from 50 to 110 nm. The size of these particles was about four times larger than that of the esterified particles in organic media. This increase in R_h is probably caused by the drastic conformation change of the grafted polymer chains. The non-ionic polySSPen chain took a corona conformation in the organic solvent, while the ionic polySSNa chains adopted a stretched conformation due to the electrostatic repulsion between the ionic groups. DLS measurement was carried out in salt-added aqueous solutions to confirm this effect. The R_h values for the hydrolyzed particles in 0.3 M NaCl solutions are given in Table 2. The particle sizes were reduced by salt addition in all cases. We consider this to be because the electrostatic interaction in the polySSNa chains is screened by the added ions. Another significant characteristics of this material is that the CCL-(polySBS-*b*-polySSNa) aqueous solution was very stable even in a salted water, that is no flocculation or precipitation of the polymer particles was observed in 0.5 mol/L NaCl aqueous solution at room temperature even after one week. We consider that a high steric stabilization effect of grafting polySSNa chains might play an important role in this phenomenon.

The obtained polymer nanoparticles before and after the hydrolysis were further investigated by AFM. Figure 8 shows typical AFM images for CCL-(SBS₁₁₃-*b*-SSPen₁₃₄) and CCL-(SBS₁₁₃-*b*-SSNa₁₃₄). Many protubances of ca.70 nm in diameter were observed for CCL micelles both before and after hydrolysis, suggesting the existence of spherical particles. The height profiles for the images were also given in the figure. The height of the protubances is ca.6 nm for a particle before hydrolysis, while that for a particle after hydrolysis is ca.30 nm. Because of the convolution effect of a silicon probe used in the AFM measurement, horizontal size is always larger than the real one. Therefore, we estimated the particle size from the height profiles. By AFM analysis, the diameters of the particles were determined at 6 and 30 nm before and after hydrolysis, respectively. These results also suggest that the polySSNa chains in the hydrolyzed particles have a more

stretched conformation than polySSPen in the particles before hydrolysis. However, it should be noted that the particles evaluated here are significantly smaller than those obtained by DLS. This is because the structures of the particles observed by AFM are in a dry state and different from those in a wet state evaluated by DLS. Nevertheless, the AFM observation clearly revealed that spherical nanoparticles could be synthesized by core-cross-linking of block copolymer micelles.

4. Conclusions

A well-defined styrene-based block copolymer having the cross-linkable silacyclobutane and sulfonate groups, polySBS-*b*-polySSPen, was synthesized by nitroxyl-mediated 'living' radical polymerization. The block copolymer formed a micelle whose R_h ranged from 15 to 23 nm in acetone, and the core of the micelle was cross-linked to provide polySBS nanoparticles with polySSPen grafting from the surface. Hydrolysis of the neopentyl ester in polySSPen gave ionic poly(styrene sulfonate)-grafted polySBS nanoparticles. The R_h of the particle with ester-protected graft chains was 12–21 nm in acetone, while that of the particle with ionic polySSNa chains was 50–110 nm in water. This size difference is induced by electrostatic repulsion between ions on the polymer chains. The electrostatic interaction in the grafting polySSNa chains is currently being investigated in detail.

Acknowledgements

This work was financially supported by a Grant-in-aid (A15205017) and 21st century COE program, COE for a United Approach to New Materials Science, of the Ministry

of Education, Culture, Sports, Science, and Technology, Japan.

References and notes

1. Hamley, I. W.; 3rd ed. *Encyclopedia of Polymer Science and Technology*, Mark, H. F., Ed.; Wiley: New Jersey, 2003; Vol. 1, pp 457–482.
2. Hadjichristidis, N.; Pispas, S.; Floudas, G. *Block Copolymers*; Wiley: New Jersey, 2003; pp 203–231.
3. Piirma, I. *Polymeric Surfactants. Surfactant Science Series*; Marcel Dekker: New York, 1992; Vol. 42.
4. Lindman, B.; Alexandridis, P. In *Amphiphilic Block Copolymers*; Lindman, B., Alexandridis, P., Eds.; Elsevier: Amsterdam, 2000.
5. Procházka, K.; Baloch, M. K.; Tuzar, Z. *Makromol. Chem.* **1979**, *180*, 2521.
6. Wilson, D. J.; Riess, G. *Eur. Polym. J.* **1988**, *24*, 617.
7. Ishizu, K.; Onen, A. *J. Polym. Sci., Part A: Polym. Chem.* **1989**, *27*, 3721.
8. Saito, R.; Ishizu, K.; Fukutomi, T. *Polymer* **1990**, *31*, 679.
9. Saito, R.; Ishizu, K.; Fukutomi, T. *Polymer* **1991**, *32*, 531.
10. Saito, R.; Ishizu, K.; Fukutomi, T. *Polymer* **1991**, *32*, 2258.
11. Saito, R.; Ishizu, K.; Fukutomi, T. *Polymer* **1992**, *33*, 1712.
12. Guo, A.; Liu, G.; Tao, J. *Macromolecules* **1996**, *29*, 2487.
13. Henselwood, F.; Liu, G. *Macromolecules* **1997**, *30*, 488.
14. Saito, R.; Ishizu, K. *Polymer* **1997**, *38*, 225.
15. Wang, G.; Henselwood, F.; Liu, G. *Langmuir* **1998**, *14*, 1554.
16. Henselwood, F.; Liu, G. *Macromolecules* **1998**, *31*, 4213.
17. Saito, R.; Akiyama, Y.; Ishizu, K. *Polymer* **1999**, *40*, 655.
18. Saito, R.; Akiyama, Y.; Tanaka, M.; Ishizu, K. *Colloids Surf., A* **1999**, *153*, 305.
19. Won, Y.; Davis, H. T.; Bates, F. S. *Science* **1999**, *283*, 960.
20. Liu, G.; Zhou, J. *Macromolecules* **2003**, *36*, 5279.
21. Okamura, H.; Takatori, Y.; Tsunooka, M.; Shirai, M. *Polymer* **2002**, *43*, 3155.



Cross-linked and functionalized ‘universal polymer backbones’ via simple, rapid, and orthogonal multi-site self-assembly

Joel M. Pollino, Kamlesh P. Nair, Ludger P. Stubbs, Jacob Adams and Marcus Weck*

School of Chemistry and Biochemistry, Georgia Institute of Technology, Atlanta, GA 30332-0400, USA

Received 11 April 2004; revised 22 May 2004; accepted 24 May 2004

Available online 19 June 2004

Abstract—A novel route to cross-linked and functionalized random copolymers using a rapid, one-step, and orthogonal copolymer cross-linking/functionalization strategy has been developed. Random terpolymers possessing high concentrations of pendant alkyl chains and either (1) palladated-pincer complexes and diaminopyridine moieties (DAD hydrogen-bonding entities) or (2) palladated-pincer complexes and cyanuric wedges (ADAADA hydrogen-bonding entities) have been synthesized using ring-opening metathesis polymerization. Non-covalent cross-linking of the resultant copolymers using a directed functionalization strategy leads to dramatic increases in solution viscosities for cross-linked polymers via metal-coordination while only minor changes in viscosity were observed when hydrogen-bonding motifs were employed for cross-linking. The cross-linked materials could be further functionalized via self-assembly by employing the second recognition motif along the polymeric backbones giving rise to highly functionalized materials with tailored cross-links. This novel non-covalent polymer cross-linking/functionalization strategy allows for rapid and tunable materials synthesis by overcoming many difficulties inherent to the preparation of covalently cross-linked polymers.

© 2004 Elsevier Ltd. All rights reserved.

1. Introduction

Cross-linked polymeric materials have important advantages over their non-cross-linked analogues such as superior mechanical and chemical properties, higher thermal stability, and lower temperature dependence on viscosity.^{1,2} Conventional cross-linked materials are prepared via covalent bond formation using curing agents, irradiation, or use of polyfunctional monomers.^{1,2} While successful, these methods are not fully controlled and are often irreversible, which limits the extent of cross-linking and results in the loss of important polymer properties such as thermoplasticity.^{1,2} Furthermore, the preparation of covalently cross-linked materials requires extensive synthesis in order to tune the properties of the final materials. Replacement of covalent cross-linking strategies with non-covalent self-assembly methodologies offers one possible solution to these problems by allowing for simple and rapid preparation of elaborate cross-linked materials with high control over the extent of cross-linking.^{3–6}

A number of non-covalent interactions including hydrogen-bonding and metal-coordination have been used in the fabrication of cross-linked materials via self-assembly. In

particular hydrogen-bonding has been reported widely by a variety of authors.^{3–11} Impressive examples include the work by Stadler and co-workers who reported reversible polymer network formation via intermolecular hydrogen bonding of urazoylbenzoic acid groups situated at the chain ends of polyisobutylene^{12,13} and Coates and co-workers who synthesized reversible thermoplastic elastomers using self-dimerizing ureidopyrimidone units.⁷ Furthermore, Rotello and co-workers have exploited thymine-diaminopyridine interactions to prepare micron-sized aggregates via simple mixing of bsthymine cross-linking agents and diaminopyridine functionalized poly(styrene).⁴ The second class of non-covalent interactions that have been employed in cross-linking studies is metal-coordination, which holds a number of important advantages and differences to its hydrogen-bonding analog.¹⁴ First, metal-coordination is among the strongest non-covalent interaction used in self-assembly.¹⁵ Second, while hydrogen-bonding is generally thermo reversible,^{4,6,15,16} metal-coordination is essentially chemo reversible, i.e. cross-linking by metal-coordination can be reversed by a chemical species.^{15,17,18} A strategy that uses modular cross-linking via the combination of hydrogen-bonding and metal-coordination self-assembly motifs would be highly desirable because it could allow for tuning of important physical properties such as cross-linking strength and reversibility. Ultimately, this approach enables rapid prototyping and facile modification of the physical properties of cross-linked materials, which gives rise to a novel class of designer cross-linked materials

Keywords: Self-assembly; Metathesis; Polymers; Cross-linking.

* Corresponding author. Tel.: +1-404-385-1796; fax: +1-404-894-7452; e-mail address: marcus.weck@chemistry.gatech.edu

formed simply and spontaneously via orthogonal non-covalent side-chain modification.

Even though both covalent and non-covalent cross-linking strategies have been used in the literature, preparation of elaborately constructed and densely functionalized cross-linked polymeric materials remains challenging due to functional group incompatibilities of most polymerization techniques.² One possible solution to these difficulties is the employment of an orthogonal functionalization and cross-linking strategy using self-assembly. Recently, we reported a modular polymer functionalization strategy using pre-fabricated ‘universal polymer backbones’ (UPB) possessing pendant hydrogen-bonding and metal-coordination units.¹⁹ With this system, we have shown that a variety of materials stemming from a single polymer backbone can be prepared rapidly and quantitatively with desirable properties via an orthogonal self-assembly approach.¹⁹ Here, we extend this strategy to the fabrication of non-covalently cross-linked polymers prepared from single universal polymer scaffolds via highly directional self-assembly processes using either metal-coordinating or hydrogen-bonding recognition motifs. Furthermore, we report a novel one-step functionalization/cross-linking strategy where the polymeric scaffold can be non-covalently cross-linked using one of the self-assembly motifs while the other recognition unit operates independently to selectively bind small molecules (Fig. 1). These methodologies offer new possibilities for simple and rapid formation of a variety of functionalized and cross-linked polymeric materials.

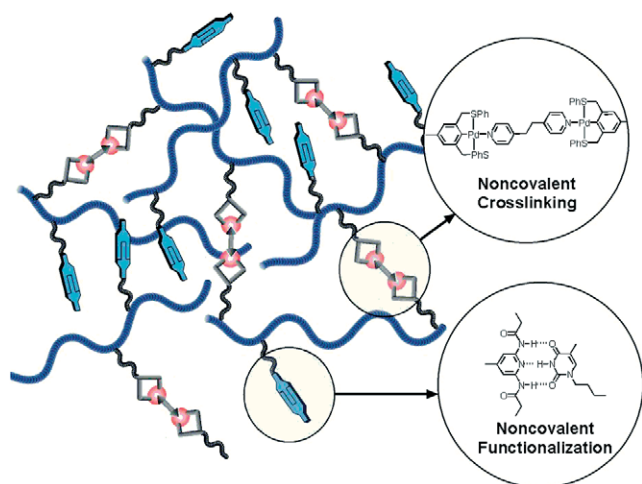


Figure 1. A cartoon depicting multi-step self-assembly via metal-coordination based cross-linking and polymer functionalization via hydrogen-bonding.

2. Research design

Previously reported ‘universal polymer backbones’ are based on random copolymers composed of two monomer units that contain hydrogen-bonding or metal-coordination recognition motifs for self-assembly.¹⁹ Here we incorporate a third, non-functionalized monomer into the copolymer design that is able to dilute and space-out the molecular recognition containing monomers. Terpolymers for the present study were designed to possess low concentrations of both, hydrogen-bonding and metal-coordination recog-

nition motifs, in order to study cross-linking and functionalization, while simultaneously maintaining good polymer properties including solubility. Norbornene was chosen as polymerizable unit since it can be polymerized via ring-opening metathesis polymerization (ROMP), a highly functional group tolerant polymerization technique, in a living fashion.^{20–22} All monomers were designed to contain alkyl spacers to decouple the polymer backbones from the recognition units and to aid in solubility.^{23,24} The two terminal molecular recognition units that were employed are based either on palladated sulfur–carbon–sulfur (SCS) pincer complexes,^{17,25} diaminopyridines,^{16,26,27} or cyanuric wedges.^{28,29}

Palladated sulfur–carbon–sulfur (SCS) pincer complexes are tridentate, square planar coordination spheres that are particularly useful in molecular recognition because they possess only one coordination site accessible for self-assembly.^{17–19,25,30,31} Furthermore, these units are known to undergo fast and quantitative self-assembly which has resulted in their previous employment for the synthesis of supramolecular main-chain polymers³² and metallo-dendrimers.^{17,30}

The hydrogen-bonding units employed in these studies are capable of multiple hydrogen bond formation.⁶ We decided to synthesize two different universal polymer backbones each possessing a unique hydrogen-bonding motif in order to examine how varying hydrogen-bond strength influences cross-linking. In particular, we explored (i) diaminopyridine–thymine complexes that are able to undergo acceptor–donor–acceptor (ADA) to donor–acceptor–donor (DAD) triple hydrogen bonds (K_a = approx. $500–600 \text{ M}^{-1}$)^{4,19,26,27} and (ii) and cyanuric wedges (ADA–ADA arrays) that bind to isophthalamide receptors (DAD–DAD arrays) via six hydrogen bonds (K_a = approx. 10^6 M^{-1}).^{28,29,33}

Non-covalent cross-linkers are made from alkyl chains containing pyridine, uracil derivatives,^{4,34} or isophthalamide derivatives at each terminus. These recognition units bind palladated pincer complexes,^{17,19,25,31} diaminopyridine moieties,^{26,27} or cyanuric wedges, respectively.^{28,29} We chose to employ structurally simple non-covalent cross-linkers to facilitate ease in cross-linker synthesis and polymer characterization. Soluble perylene moieties bis-functionalized with ADA recognition counterparts were also prepared.^{35–37} We rationalized that this unique class of functional compounds, commonly employed in the design of electro-optical materials could serve two purposes: (i) as hydrogen-bonding cross-linking agents and (ii) as photo-luminescent chromophores.^{35–37}

For small molecule functionalization studies, pyridine, *N*-butyl thymine, and isophthalamides were employed. These compounds possess so called anchoring sites²⁵ where advanced functional entities may be attached using an alkyl tether (Fig. 2). Furthermore, these molecules are intentionally structurally simple to facilitate ease in characterization while simultaneously allowing us to fully demonstrate the potential of our one-step, non-covalent approach to functionalized and cross-linked polymeric materials.

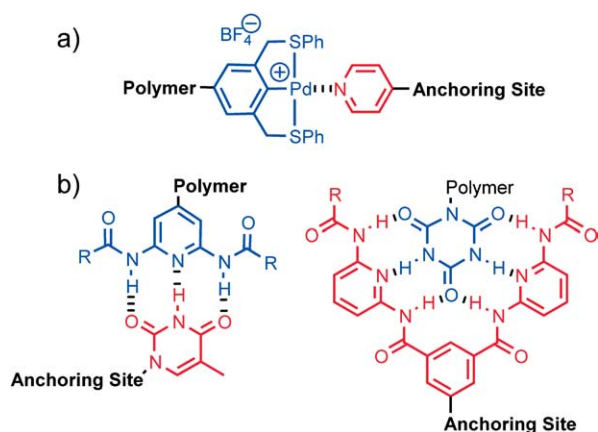
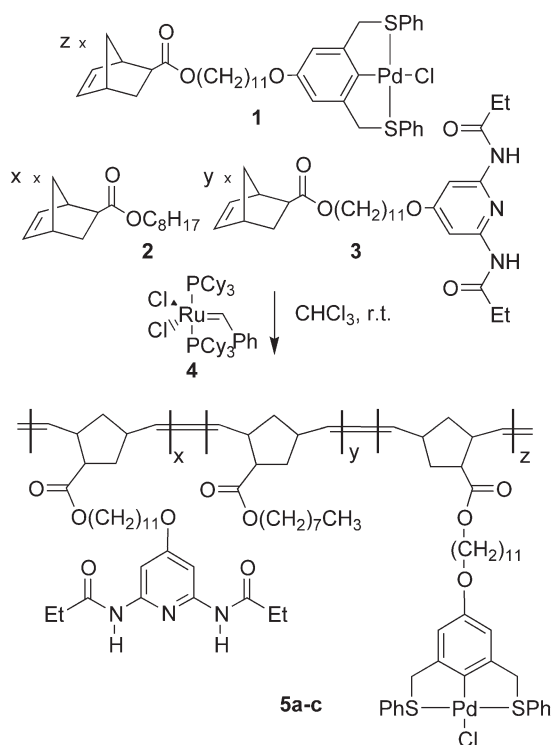


Figure 2. Non-covalent recognition motifs. (a) Metal-coordination, (b) hydrogen-bonding.

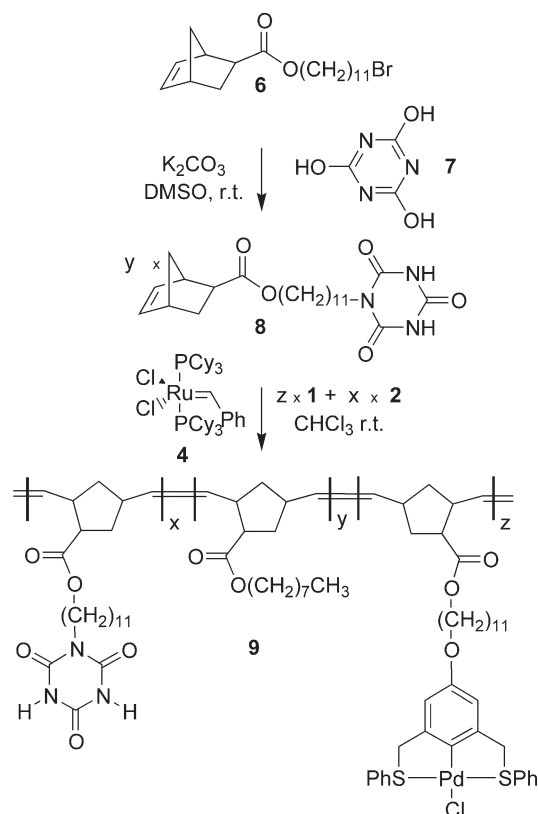
3. Results and discussion

3.1. Synthesis

All monomers were derived from isomerically pure *exo*-norbornene-2-carboxylic acid.^{22,38,39} Monomers **1**, **2**, and **3** were synthesized as previously reported.²² Cyanuric acid functionalized monomer **8** was prepared from bromoester **6** in one step. ROMP was carried out in chloroform using Grubbs' first generation initiator **4**.^{20,21} Monomers **1**, **2**, and **3** or **1**, **2**, and **8** yielded random terpolymers **5a–c** and **9**, respectively (Schemes 1 and 2). In all cases, monomer to catalyst ratios of 200:1 were employed and complete conversion was observed within 6 h at ambient temperatures. The resultant copolymers possessed low polydispersities and molecular weights independent of monomer composition (Table 1) as determined by gel-permeation



Scheme 1. Terpolymer **5** synthesis.



Scheme 2. Terpolymer **9** synthesis.

Table 1. Copolymer characterization data

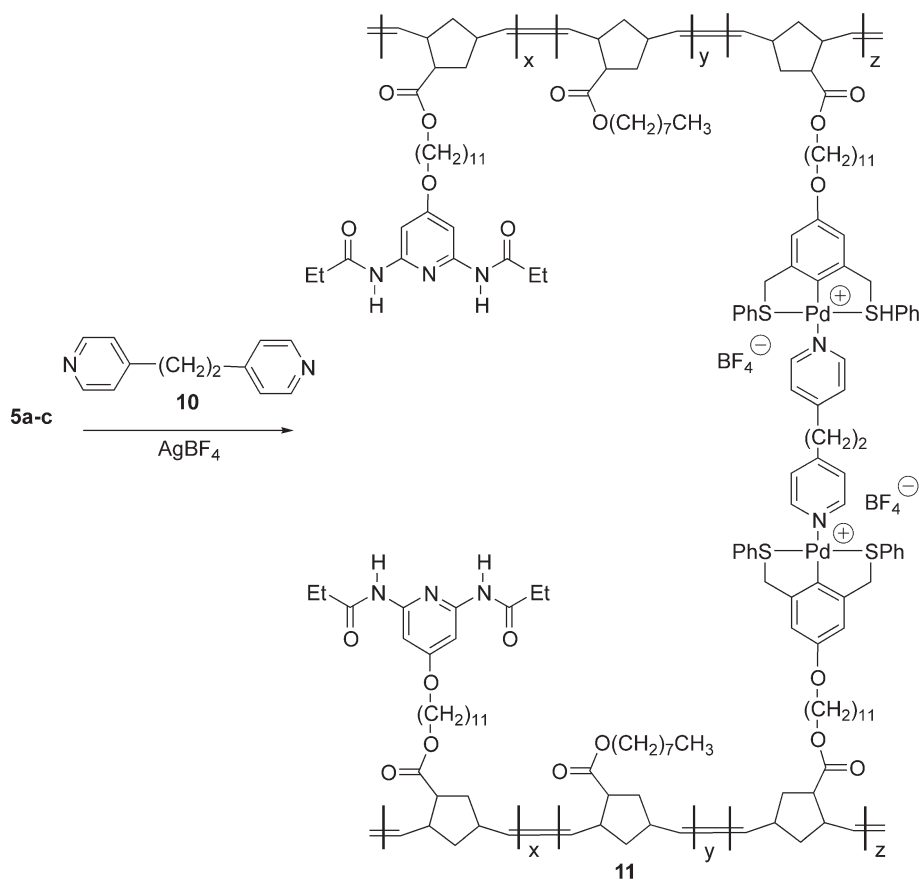
Entry ^a	Composition (%)			M_n	M_w	PDI
	x	y	z			
5a	97	1.5	1.5	40,000	52,000	1.28
5b	95	2.5	2.5	41,000	50,000	1.22
5c	90	5	5	44,000	55,000	1.26
9	95	2.5	2.5	41,000	52,000	1.25

^a [M]/[I]=200:1.

chromatography. Cross-linking agent **10** was commercially available, whereas **12a–b**^{34–37} and **14**²⁸ were synthesized according to literature protocols.

3.2. Directed self-assembly: non-covalent cross-linking

After synthesis, copolymers **5a–c** and **9** were non-covalently cross-linked using a directed self-assembly strategy.¹⁹ This methodology allows for a single interaction, metal-coordination or hydrogen-bonding, to be individually and selectively addressed. The objective of these preliminary studies was to explore the versatility and limitations of the universal polymer backbone concept by rapidly and quantitatively creating cross-linked materials via self-assembly. Cross-linking copolymers **5a–c** and **9** with **10**, **12**, and **14** allowed us to probe how (i) the density of recognition motifs located in the UPB, (ii) the different types of interactions, metal-coordination versus hydrogen-bonding, and (iii) the strength of various hydrogen-bonding motifs and/or cross-linkers effect the cross-linking by studying solution viscosities.



Scheme 3. Directed cross-linking via metal-coordination.

Initially, we explored metal-coordination based cross-linking through the study of palladium–pyridine metal–ligand interactions.^{17,18,25} Copolymers **5a–c** were functionalized using 1 equiv. of **10** to yield polymeric networks **11a–c** containing 1.5, 2.5, and 5% cross-links, respectively. In each case, cross-linking was selective, quantitative, and instantaneous as determined by NMR (Scheme 3).^{19,25}

Viscosity is an excellent indicator for the degree of cross-linking and is highly dependent upon the solution concentration.^{1,2} At constant polymer concentrations cross-linking leads to dramatic increases in solution viscosities when compared to non-cross-linked polymer solutions.^{1,2,7} In order to carry out comparisons between metal-coordinated and hydrogen-bonded polymers we had to identify a concentration region for each polymeric network (**11a–c**) that falls between gel formation and non-viscous flow. To accomplish this goal copolymers **11a–c** were dissolved in chloroform at variable concentrations and ‘time of flows’ were measured relative to pure chloroform using a Cannon-Fenske viscometer.¹ Relative viscosities, presented in Figure 3, show a strong dependence on both, the amount of cross-linker contained within the UPB backbone and the solution concentration. As depicted, the concentration curve for **11a**, possessing 1.5% cross-links gradually rose to high viscosities reaching gelation at approximately 45 g/L whereas **11c**, containing 5% cross-links sharply increased in viscosity becoming a gel at lower concentrations of 20 g/L. Compound **11b**, containing 2.5%

cross-links fell between these two extremes gelling at approximately 27 g/L (Fig. 3).

All polymers were activated prior to coordination by removal of the chloride from the palladium metal center using AgBF_4 , resulting in the formation of highly charged polymeric species containing BF_4^- counter ions **5a–c–Cl** (Scheme 4).^{19,22,25,31} Upon removal of the chloride, notice-

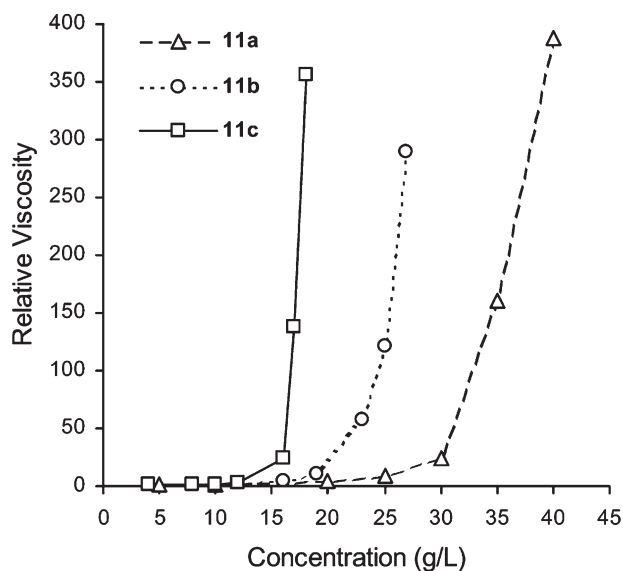
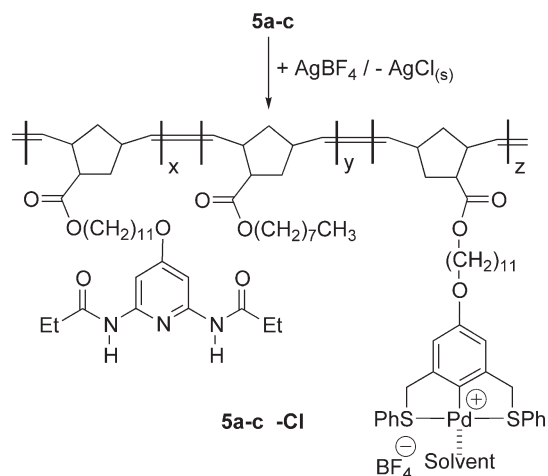


Figure 3. Plot of relative viscosity as a function of solution concentration.



Scheme 4. Preparation of activated polymer **5a-c-Cl**.

able increases in viscosity were visually observed for chloroform solutions of **5a-c-Cl**. One explanation for this phenomenon could be competitive intra/intermolecular coordination of the diaminopyridine moieties to the palladated metal centers. To probe this theory, a series of viscosities at variant solution concentrations were measured for neutral polymer **5b**, activated polymer **5a-c-Cl**, and bispyridine cross-linked polymeric network **11b** (Fig. 4). While slight increases in solution viscosities were observed when comparing **5a-c-Cl** to **5b**, these changes are negligible when compared to the viscosity changes measured for **11b**. Thus, increases in viscosity upon activation of **5b** are most likely not due to intra/intermolecular palladium-diaminopyridine cross-linking but probably arise as consequence of ionic aggregate formation in non-polar solvents.¹

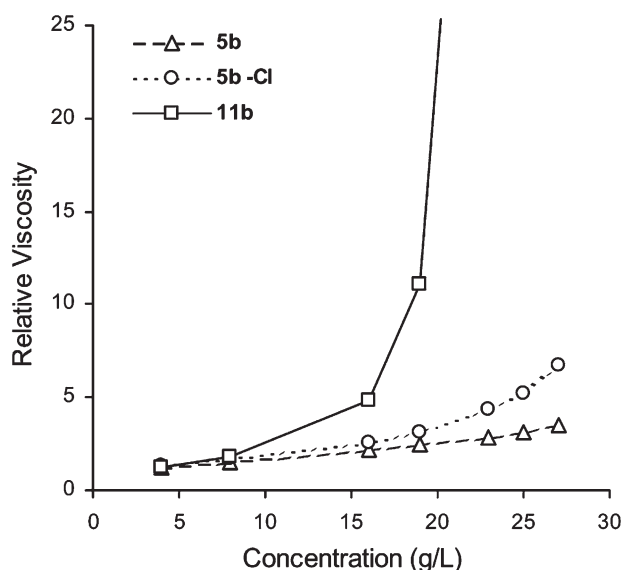


Figure 4. Plot of relative viscosity as a function of solution concentration.

Solution viscosities can also be easily tuned through alteration of the amount of cross-linker added.^{1,7} Indeed, titration of **5b** with **10** at a concentration of 30 g/L resulted in exponential growth of viscosity as a function of added equivalents of cross-linker leading to gelation at less than

1 equiv. (Fig. 5). Addition of more than 1 equiv. of cross-linker leads to decreases in viscosity due to the formation of palladium–pyridine complexes possessing a terminal uncoordinated pyridine as excess pyridine complexes become available.

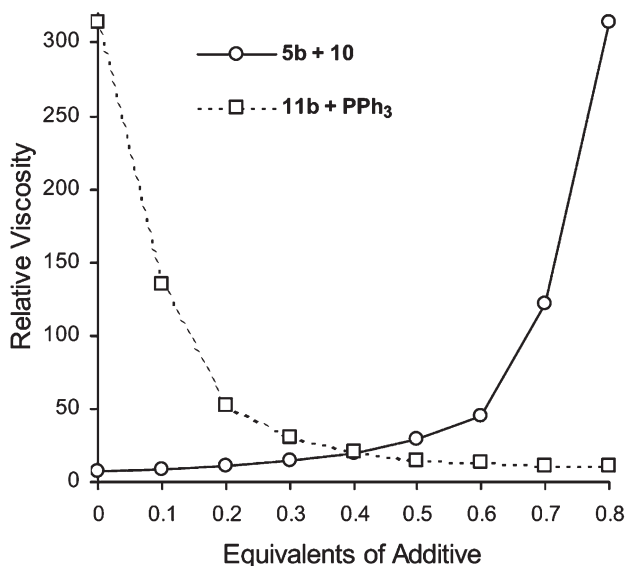
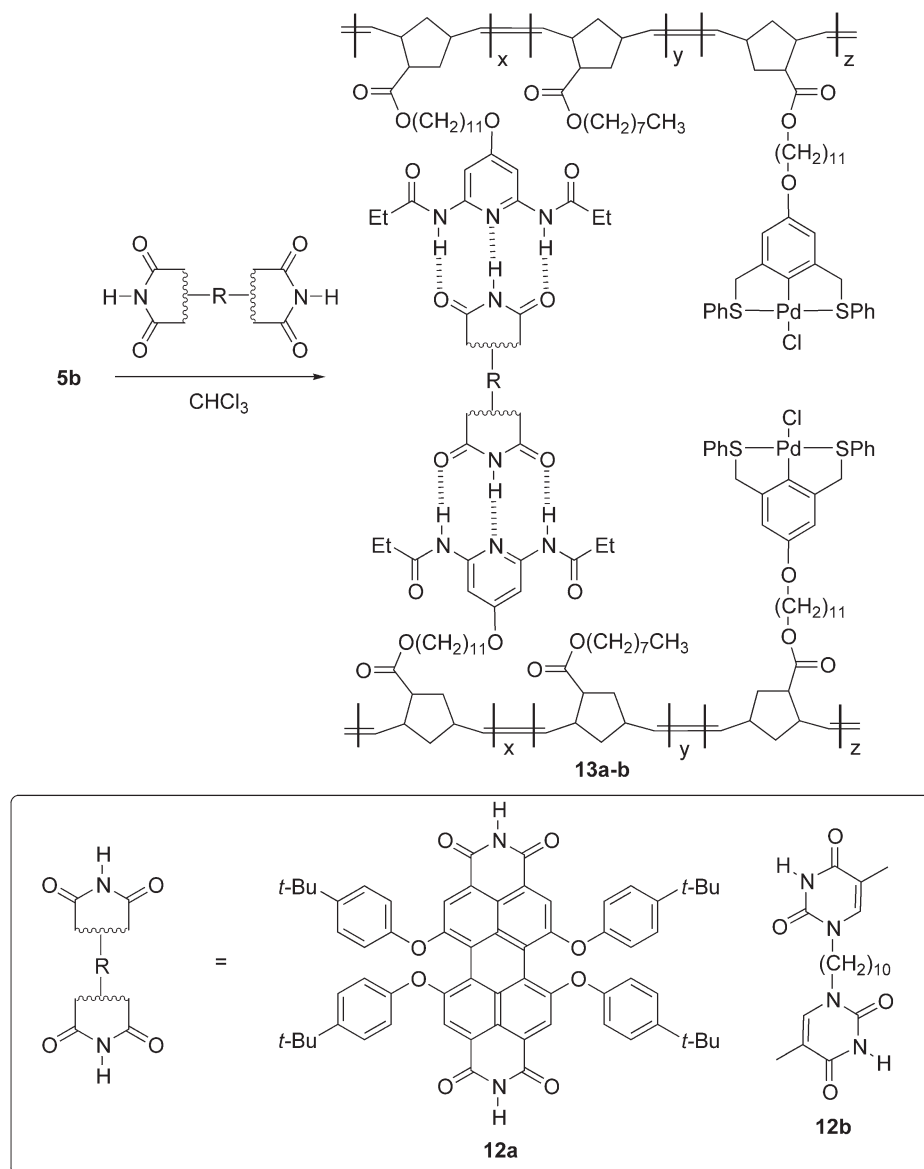


Figure 5. Plot of relative viscosity as a function of added mole equivalents of cross-linker (based on percentage of monomer **1** contained in the backbone) and the same polymer solution following titration with PPh₃.

Another possibility to tailor the degree of cross-linking of **11** is by addition of compounds such as PPh₃ that compete for the coordination onto the metal center. It is known that some ligands on functionalized palladated SCS pincer complexes such as nitriles and pyridines can be quantitatively displaced by stronger ones.^{17,18} For example, in metallo-dendrimer chemistry, Reinhoudt and co-workers reported the quantitative displacement of pyridine ligands bound to palladated SCS pincer complexes by the addition of phosphines.¹⁷ Thus, we reasoned that subjecting cross-linked polymers **11a-c** to PPh₃ would provide a simple method to deconstruct non-covalently cross-linked polymers and to tailor viscosities. To investigate this approach, cross-linked polymer **11b** was titrated with PPh₃. The resulting titration curve depicts an exponential decrease in viscosity, giving merit to the concept of chemo-reversible cross-linking (Fig. 5).

After establishing basic cross-linking conditions using metal-coordination, we investigated the use of hydrogen-bonding as cross-linking interaction. UPB **5b**, containing 2.5% cross-links was employed for these studies. Scheme 5 presents the use of thymine/diaminopyridine complementary pairs used in cross-linking. Copolymer **5b** was functionalized with either bis-perylene **12a** or bis-thymine derivative **12b** by simple 1:1 mixing of the two components (based on the number of recognition motifs) in anhydrous chloroform to form hydrogen-bonded polymers **13a** and **13b**, respectively (Scheme 5).

The strength of the hydrogen-bonding based cross-linking was examined using solution viscosity titration experiments, identical to those described for **11b**. In contrast to **11b**, upon titration of **5b** with **12a** or **12b** at a concentration



Scheme 5. Directed cross-linking via triple hydrogen-bonded diaminopyridine–thymine complexes.

of 30 g/L only minor increases in viscosity were observed (Fig. 6). In comparison to their metal-coordinated analog **11b**, hydrogen-bonded complexes **13a–b** showed almost a 100 times less change in relative viscosities upon cross-linking. Albeit, it is well known that hydrogen bonds are significantly weaker than metal-coordination bonds,^{15,40} such a dramatic difference in solution viscosities was unexpected and may be due in part to shear forces acting upon the relatively weak hydrogen-bonding interactions.¹

In an effort to implement stronger hydrogen-bonding motifs, terpolymer **9** was prepared possessing palladated pincer ligands and cyanuric wedges which are able to form six hydrogen bonds when complexed with tetra diaminopyridine moieties (**14**) giving rise to association constants as high as 10^6 M^{-1} .^{28,29} Terpolymer **9** was cross-linked with **14** via simple 1:1 mixing of the two components in chloroform (Scheme 6). Titration of **9** with **14** at a concentration of 30 g/L led to a large increase in viscosity when compared with **13a** and **13b** (Fig. 6). However, this

system remains inferior when compared to its metal-coordinated analog **11b**, showing 33 times lower viscosities upon cross-linking.

In addition to studying solution viscosities, all copolymers were characterized using differential scanning calorimetry (DSC) and thermal gravimetric analysis (TGA) to determine glass-transition temperatures (T_g) and decomposition onsets (T_{dec}), respectively. Table 2 summarizes this data. In general, polymeric networks synthesized by the cross-linking via metal-coordination displayed higher glass-transition temperatures than their hydrogen-bonding analogs. However, all cross-linked polymers show higher decomposition temperatures when compared to their non-cross-linked counterparts.

3.3. One-step orthogonal self-assembly: cross-linking and small molecule functionalization

The ultimate goal of this study, the design and rapid

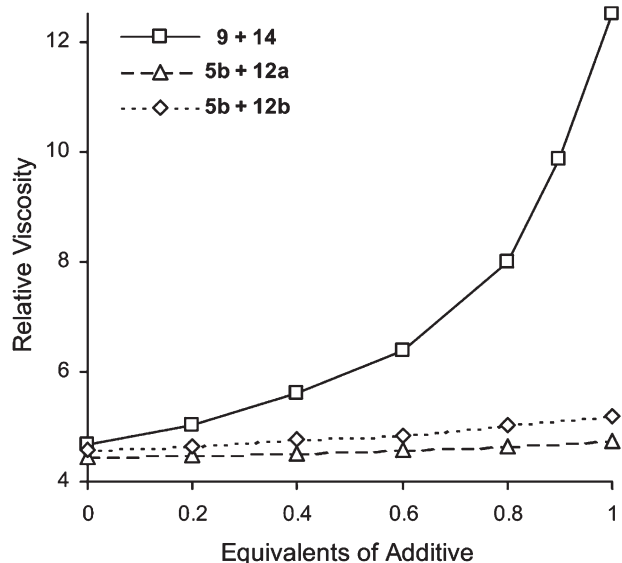
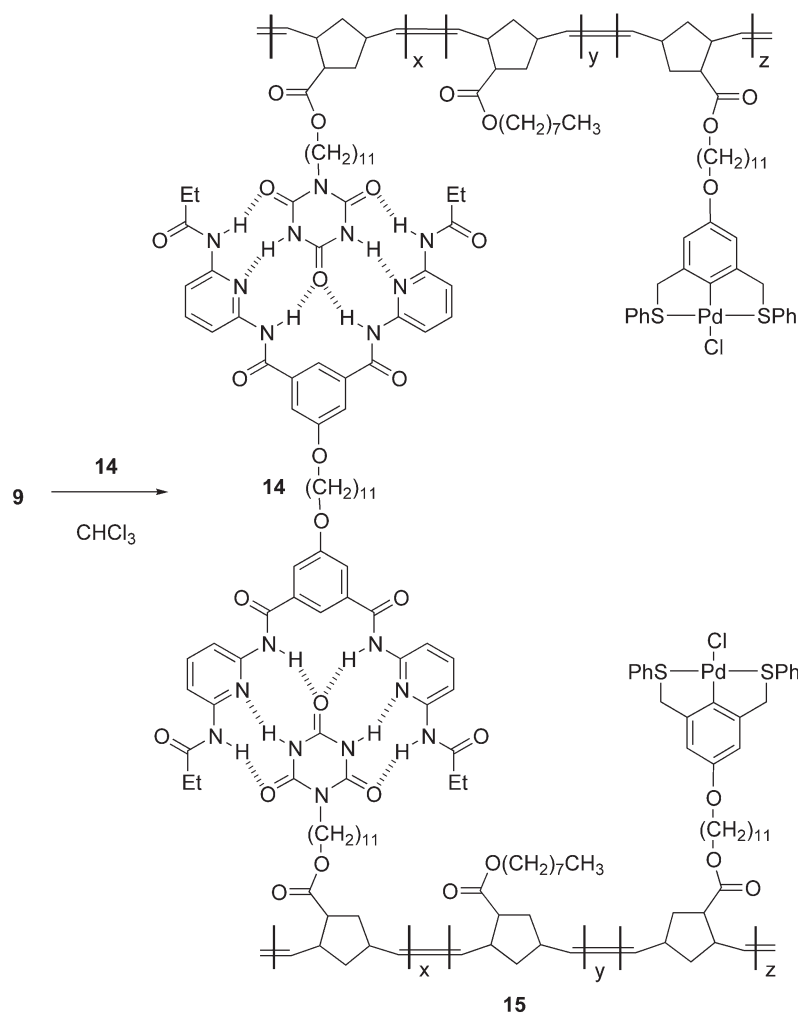


Figure 6. Plot of relative viscosity as a function of added equivalents of cross-linker for hydrogen-bonding.

synthesis of functionalized and cross-linked polymeric materials using selective, non-covalent interactions was accomplished by combining the cross-linking strategies



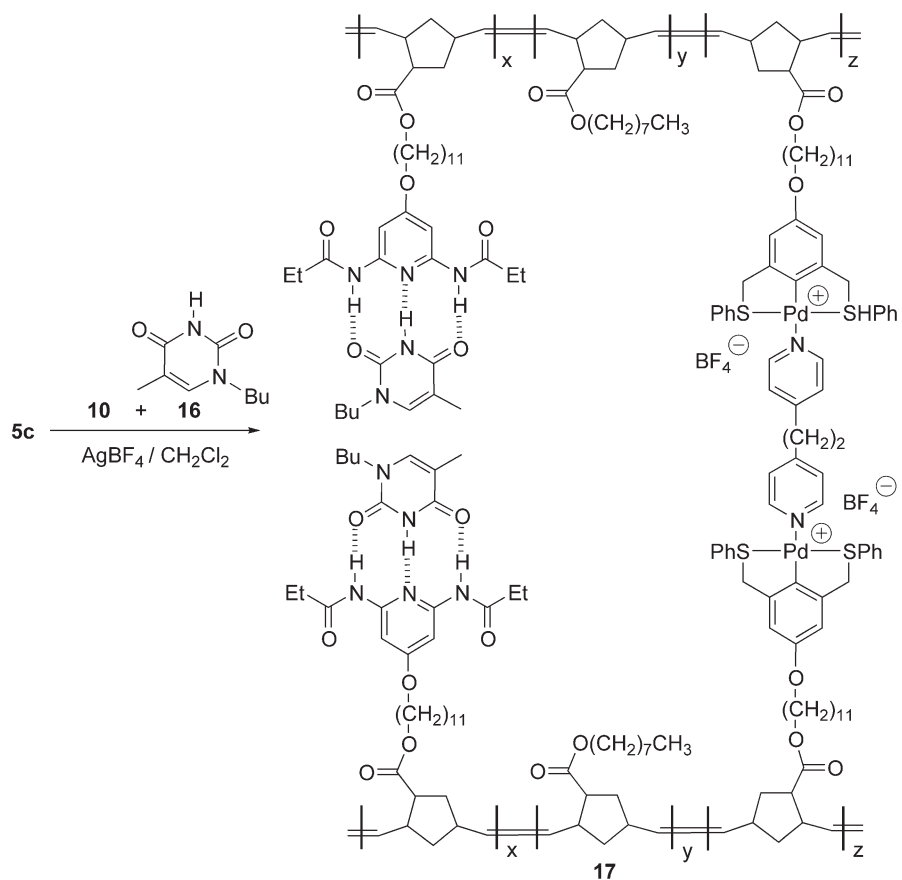
Scheme 6. Directed cross-linking via cyanuric wedges (ADA–ADA arrays) that bind to isophthalamide receptors (DAD–DAD arrays).

Table 2. Thermal characterization data

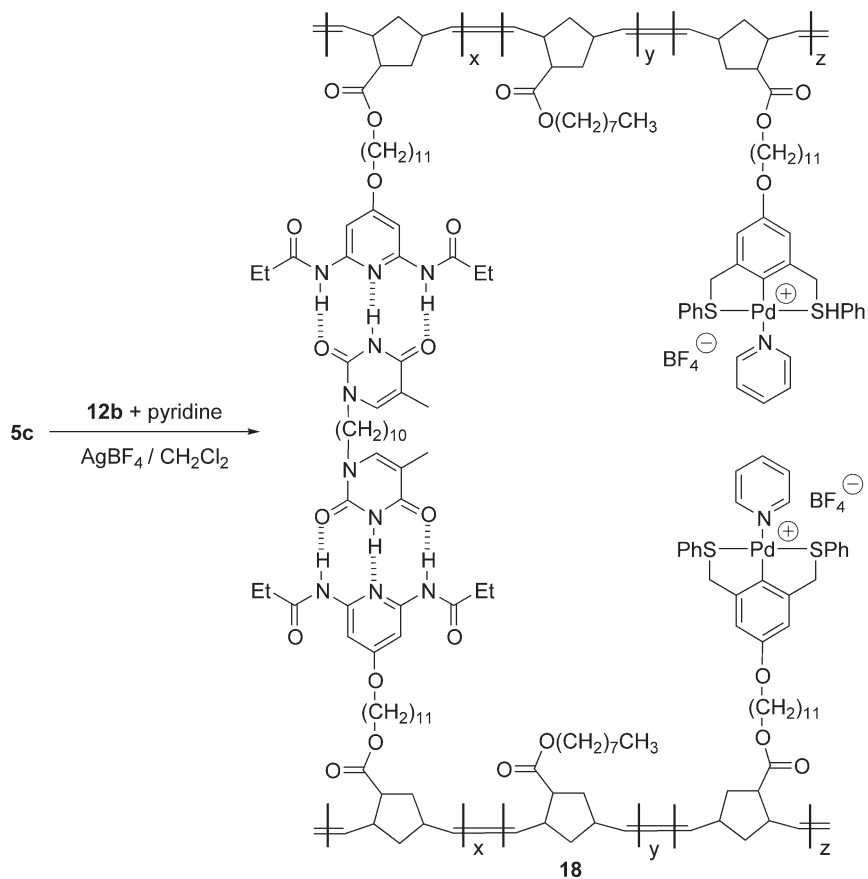
Entry	Composition (%)			T_g (°C)	T_{dec} (°C)
	x	y	z		
5a	97	1.5	1.5	–42	393
5b	95	2.5	2.5	–38	395
5c	90	5	5	–32	381
9	95	2.5	2.5	–37	388
11a	97	1.5	1.5	–42	418
11b	95	2.5	2.5	–26	415
13a	95	2.5	2.5	–40	394
13b	95	2.5	2.5	–74	405
15	95	2.5	2.5	–43	433

described above with small molecule self-assembly. Polymer **5c** was functionalized in one-step by mixing metal cross-linker **10** with *N*-butylthymine (**16**) in CH_2Cl_2 , which instantaneously yielded **17** (Scheme 7). Likewise, combining hydrogen-bonding cross-linker **12b**, polymer **5c** and pyridine in CH_2Cl_2 quantitatively provided **18** (Scheme 8).

The one-step functionalization/cross-linking of **5c** was evaluated by ^1H NMR spectroscopy. For example, a large number of significant chemical shifts are visible for the orthogonal transformation of **5c** to **18**. Three diagnostic



Scheme 7. One-step self-assembly with metal-coordination cross-linking and hydrogen-bonding functionalization.



Scheme 8. One-step self-assembly with hydrogen-bonding cross-linking and metal-coordination functionalization.

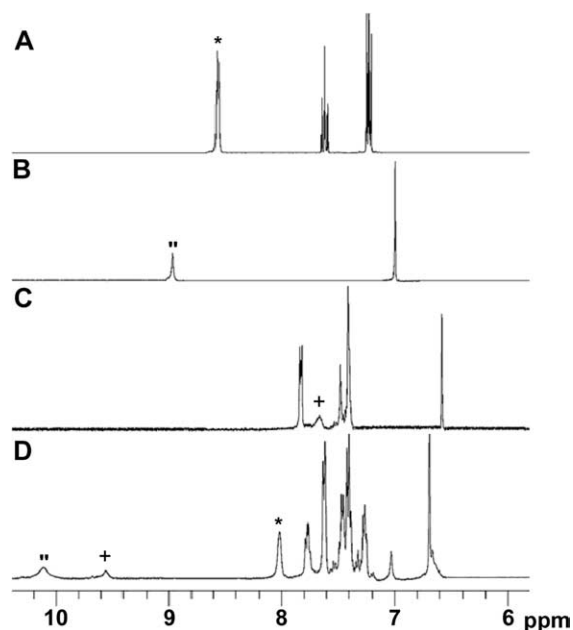


Figure 7. The aromatic region of the ^1H NMR spectra showing one-step multi-functionalization of **5c** with hydrogen-bonding cross-linker **12b** and pyridine. (A) Pyridine (*= α -pyridyl protons); (B) cross-linker **12b** (**=imide proton); (C) terpolymer **5c** (+=amide protons); and (D) cross-linked and functionalized copolymer **18**.

shifts take place when comparing Figure 7A, B, and C to Figure 7D: (1) the α -pyridyl signals of pyridine at 8.58 ppm (Fig. 7A) show a characteristic up-field shift to 8.01 ppm (Fig. 7D)^{19,25} upon coordination, (2) the amide signals of the diaminopyridine moiety at 7.68 ppm (Fig. 7C) give a down-field shift to 9.56 ppm (Fig. 7D) upon hydrogen-bonding,^{19,27} and (3) a large down-field shift from 8.75 ppm (Fig. 7B) to 10.10 ppm (Fig. 7D) is observed for the imide signal for bis-thymine **12b** upon association.^{19,27} Similar diagnostic shifts were observed when following the ^1H NMR signals arising from bis-pyridine **10** (from 8.47 to 8.02 ppm) and *N*-butylthymine **16** (from 10.04 to 10.43 ppm) during the preparation of **17**. Thus, ^1H NMR spectroscopy provides strong evidence for selective, non-covalent polymer cross-linking and small molecule self-assembly clearly demonstrating the proposed orthogonal cross-linking/functionalization scheme is a viable option for fast and easy functionalized polymeric network formation.

4. Conclusion

In this contribution we report the orthogonal cross-linking and functionalization of the universal polymer backbone based on substituted norbornene monomers containing hydrogen-bonding and metal-coordination motifs. Cross-linking or functionalization can be carried out via a modular approach using either metal-coordination or hydrogen-bonding. Furthermore, through choice of the cross-linking motif and agent and its concentration, the strength of the cross-linked polymeric network can be tailored towards potential applications. This strategy allows for (1) functionalization directed by self-assembly of one recognition unit via hydrogen-bonding or metal-coordination, (2) non-covalent cross-linking by metal-coordination or hydrogen-bonding, and ultimately (3) one-step functional-

ization and cross-linking in which both recognition motifs are spontaneously self-assembled in the presence of complementary recognition units. This novel non-covalent polymer cross-linking/functionalization strategy allows for rapid and tunable materials synthesis thereby overcoming many problems inherent to covalently cross-linked polymers.

5. Experimental

5.1. Materials

All chemicals were reagent grade and used without further purification unless otherwise indicated. CDCl_3 was distilled from calcium hydride and degassed prior to use. CH_2Cl_2 was dried via passage through copper oxide and alumina columns. Cyanuric acid **7** and bispyridine **10** were purchased from Acros Organics and Aldrich, respectively. $\text{Ru}(\text{=Ph})\text{Cl}_2(\text{PCy}_3)_2$ **4** was purchased from Strem. Monomers **1** and **3**,²² cross-linkers **12a**,^{35–37} **12b**,³⁴ and **14**,²⁸ bromoester **6**,²² and *N*-butylthymine **16**,²⁷ were prepared as previously reported.

5.2. General methods

NMR spectra were taken using either a 300 MHz Varian Mercury spectrometer or a 400 MHz Bruker AMX 400 spectrometer. All spectra were referenced to residual proton solvent. Mass spectral analysis was kindly provided by the Georgia Tech Mass Spectrometry Facility using a VG-70se spectrometer. Elemental analyses were performed by Atlantic Microlabs, Norcross GA. Solution viscosity was measured using a size 100 Cannon-Fenske viscometer (Cannon Instrument Co., State College, PA, USA). The time of fall was recorded with a stopwatch reading to 0.1 s. GPC analyses were carried out using a waters 510 binary pump coupled to a Waters 410 differential refractometer with THF as an eluant on an American Polymer Standards column set (100, 1000, 100,000 Å, linear mixed bed). All GPCs were calibrated using polystyrene standards. Differential scanning calorimetry (DSC) was performed under nitrogen using a Mettler Toledo DSC 822e. The temperature program provided heating and cooling cycles between -100 and 200 °C at 10 °C/min. Thermal gravimetric analysis (TGA) was performed under nitrogen using a Shimadzu TGA-50 and all samples were heated from 25 to 450 °C at a rate of 10 °C/min.

5.2.1. Exo-Bicyclo[2.2.1] hept-5-ene-2-carboxylic acid octyl ester (2). *Exo*-bicyclo[2.2.1] hept-5-ene-2-carboxylic acid^{38,39} (2.1 g, 0.015 mol) and octan-1-ol (2.0 g, 0.015 mol) were combined, dissolved in anhydrous CH_2Cl_2 (20 mL), and placed under an atmosphere of argon. To the stirred solution, dicyclohexyl-carbodiimide (3.2 g, 0.015 mol) and dimethyl-pyridin-4-yl-amine (cat. amt.) in CH_2Cl_2 (20 mL) were added at 25 °C. Immediately, the solution became turbid with formation of a white precipitate. Following stirring at reflux for 16 h, the mixture was cooled, diluted with CH_2Cl_2 (200 mL), and the precipitate filtered off. The filtrate was dried (MgSO_4) and the solvent removed to give a solid residue that was further purified by column chromatography (SiO_2 , eluant: 1:1

CH₂Cl₂/hexanes). Drying provided pure **2** (3.5 g, 92%) as a colorless oil. ¹H NMR (300 MHz CDCl₃): δ=6.12 (m, 2H, CH=CH), 4.07 (t, 2H, *J*=6.6 Hz, CH₂O), 3.03 (m, 1H), 2.92 (m, 1H), 2.21 (m, 1H), 1.92 (m, 1H), 1.68–1.49 (m, 3H), 1.41–1.24 (m, 12H), 0.88 (t, 3H, *J*=7.1 Hz, CH₂CH₃). ¹³C NMR (300 MHz CDCl₃): δ=176.1, 137.8, 135.6, 64.6, 46.6, 46.3, 43.2, 41.6, 31.8, 30.4, 29.3, 28.7, 25.9, 22.7, 14.2. Anal. calcd for C₁₆H₂₆O₂: C, 76.75; H, 10.47; Found: C, 76.69; H, 10.51.

5.2.2. Terpolymer (5c). Monomers **1** (171 mg, 0.22 mmol, 5%), **2** (1.0 g, 4.0 mmol, 90%), and **3** (117 mg, 0.22 mol, 5%) were weighed, placed under an atmosphere of argon and dissolved in anhydrous, degassed CDCl₃ (10 mL). A stock solution of catalyst **4** (36.6 mg/mL) in CDCl₃ was prepared and 0.5 mL (18.3 mg, 0.022 mmol) was added in one portion to the vigorously stirred monomer solution. Upon complete polymerization (ca. 6 h), 10 drops of ethyl vinyl ether were added to terminate the polymerization. Subsequent precipitation from cold methanol and prolonged drying on high vacuum gave polymers **5a–c** (isolated yield=1.2 g, 93%). ¹H NMR (300 MHz CD₂Cl₂): δ=7.84 (m, 4H, SPh), 7.68 (br s, 2H, CONH), 7.49 (m, 2H, Pyr_βH), 7.42 (m, 6H, SPh), 6.58 (s, 2H, ArH), 5.48–5.15 (m, 6H, CH=CH), 4.58 (br s, 4H, CH₂S), 4.01 (m, 8H, CH₂O), 3.85 (br t, 2H, *J*=6.7 Hz, CH₂O), 3.2–1.0 (m, 73H), 1.14 (br t, *J*=7.4 Hz, 6H, CH₂CH₃), 0.86 (t, 3H, *J*=7.1 Hz, CH₂CH₃). ¹³C NMR (300 MHz CD₂Cl₂): δ=175.4, 172.1, 168.6, 156.9, 151.2, 150.6, 149.9, 134.2, 132.4, 132.0, 131.2, 129.7, 129.4, 108.7, 95.4, 68.5, 68.1, 64.3, 51.8, 50.2, 49.8, 49.6, 47.7, 47.4, 43.1, 42.5, 42.1, 41.8, 41.1, 37.2, 36.9, 36.2, 31.9, 30.6, 29.6–28.7, 27.0, 26.9, 26.4, 26.0, 22.7, 14.0, 9.2.

5.2.3. Exo-Bicyclo[2.2.1] hept-5-ene-2-carboxylic acid 11-(2,4,6-trioxo-[1,3,5] triazinan-1-yl)-undecyl ester (8). Anhydrous K₂CO₃ (1.5 g, 11 mmol) was added to a stirred solution of bromoester **6** (2.0 g, 5.4 mmol) and cyanuric acid **7** (6.9 g, 54 mmol) in DMSO (60 mL). The reaction mixture was allowed to stir at ambient temperature for 48 h, and was subsequently poured into a saturated solution of NaHSO_{3(aq)} (500 mL), extracted with a 1:1 mixture of CH₂Cl₂/diethyl ether (3×200 mL), dried (MgSO₄), and the solvent removed in vacuo. The residue was purified by column chromatography (SiO₂, elutant: 1:1 EtOAc/hexanes) and dried on high vacuum to yield **8** (1.3 g, 58%) as a white solid. ¹H NMR (300 MHz CDCl₃): δ=9.55 (br s, 2H, NH), 6.11 (m, 2H, CH=CH), 4.07 (t, 2H, *J*=6.6 Hz, CH₂O), 3.88 (t, 2H, *J*=7.7 Hz, CH₂N), 3.03 (m, 1H), 2.91 (m, 1H), 2.22 (m, 1H), 1.91 (m, 1H), 1.69–1.49 (m, 5H), 1.41–1.24 (m, 18H). ¹³C NMR (300 MHz CDCl₃): δ=176.2, 149.1, 148.3, 137.8, 135.6, 64.6, 46.6, 46.4, 43.2, 42.0, 41.6, 30.3, 29.4, 29.3, 29.2, 29.1, 28.7, 27.7, 26.6, 25.9. MS (EI): *m/z* (%)=419.24100 (M⁺, 419.24202 calcd). Anal. calcd for C₂₂H₃₃N₃O₅: C, 62.99; H, 7.93; N, 10.02; Found: C, 63.07; H, 7.98; N, 10.00.

5.2.4. Terpolymer (9). Monomers **1** (81 mg, 0.11 mmol, 2.5%), **2** (1.0 g, 4.0 mmol, 95%), and **8** (44 mg, 0.11 mol, 2.5%) were weighed, placed under an atmosphere of argon and dissolved in anhydrous, degassed CDCl₃ (10 mL). A stock solution of catalyst **4** (34.6 mg/mL) in CDCl₃ was prepared and 0.5 mL (17.3 mg, 0.02 mmol) was added in

one portion to the vigorously stirred monomer solution. Upon complete polymerization (ca. 6 h), 10 drops of ethyl vinyl ether were added to terminate the polymerization. Subsequent precipitation from cold methanol and prolonged drying on high vacuum gave terpolymer **9** (isolated yield=1.1 g, 98%). ¹H NMR (300 MHz CD₂Cl₂): δ=7.80 (m, 4H, SPh), 7.40 (m, 6H, SPh), 6.56 (s, 2H, ArH), 5.50–5.07 (m, 6H, CH=CH), 4.55 (br s, 4H, CH₂S), 4.09–3.9 (m, 6H, CH₂O), 3.8–3.7 (m, 4H, CH₂O, CH₂N), 3.2–1.0 (m, 69H), 0.86 (t, 3H, *J*=7.1 Hz, CH₂CH₃). ¹³C NMR (400 MHz CD₂Cl₂): δ=174.0, 156.7, 151.6, 150.3, 149.9, 148.8, 133.5, 132.7, 131.9, 131.0, 129.6, 108.9, 67.7, 64.0, 50.8, 49.8, 49.2, 47.5, 41.7, 38.3, 37.0, 35.9, 35.2, 34.6, 31.6, 29.2–28.2, 27.7, 26.7–25.8, 22.8, 22.4, 14.1.

5.2.5. Metal coordination cross-linked polymers (11a–c). Polymers **5a–c** (300 mg) were dissolved in CHCl₃ (10 mL) and 1 equiv. of AgBF_{4(aq)} (based on Pd–Cl content) was added. Immediately, the solution changed color from green to yellow and an increase in viscosity was observed. Following removal of the precipitated silver salts via filtration over cotton, 1 equiv. of bispyridine (**10**) was slowly added to the vigorously stirred solutions. Subsequent removal of the solvent and prolonged drying on high vacuum provided **11a–c** as a green solid in quantitative yield. ¹H NMR (400 MHz CD₂Cl₂): δ=8.08 (s, 2H, Pyr_αH), 7.75 (m, 4H, SPh), 7.68 (br s, 2H, CONH), 7.51–7.41 (br m, 8H, SPh and Pyr_βH), 7.23 (m, 2H, Pyr_βH), 6.68 (s, 2H, ArH), 5.48–5.15 (m, 6H, CH=CH), 4.72 (br s, 4H, CH₂S), 4.04 (m, 8H, CH₂O), 3.87 (br t, 2H, *J*=6.7 Hz, CH₂O), 3.2–1.0 (m, 75H), 1.14 (br t, *J*=7.4 Hz, 6H, CH₂CH₃), 0.86 (t, 3H, *J*=7.1 Hz, CH₂CH₃).

5.2.6. Hydrogen-bonding cross-linked polymers (13a–b and 14). To a stirred solution of polymer **5b** or **9** (300 mg) in anhydrous CHCl₃ (10 mL), 1 equiv. of **12a–b** or **14** (based on hydrogen-bonding motif content) was added, respectively. The mixtures were then allowed to stir for 5 min, followed by removal of the solvent. Subsequent drying on high vacuum afforded polymers **13a–b** and **14** in quantitative yields.

5.2.7. Polymer 13a. ¹H NMR (400 MHz CD₂Cl₂): δ=9.27 (br s, 1H, CONHCO), 8.14 (s, 2H, ArH_{peryl}), 7.83 (m, 4H, SPh), 7.52 (m, 2H, Pyr_βH), 7.42 (m, 6H, SPh), 7.29 (d, 4H, *J*=8.9 Hz, *t*-BuArH), 6.86 (d, 4H, *J*=8.9 Hz, OArH), 6.58 (s, 2H, ArH), 5.50–5.18 (m, 6H, CH=CH), 4.61 (br s, 4H, CH₂S), 4.03 (m, 8H, CH₂O), 3.87 (br t, 2H, *J*=6.7 Hz, CH₂O), 3.4–1.2 (m, 91H), 1.16 (br t, *J*=7.4 Hz, 6H, CH₂CH₃), 0.88 (t, 3H, *J*=7.1 Hz, CH₂CH₃).

5.2.8. Polymer 13b. ¹H NMR (400 MHz CD₂Cl₂): δ=10.10 (br s, 1H, CONHCO), 9.56 (br s, 2H, CONH), 7.84 (m, 4H, SPh), 7.57 (m, 2H, Pyr_βH), 7.42 (m, 6H, SPh), 7.05 (s, 1H, CH=CCH₃), 6.58 (s, 2H, ArH), 5.48–5.15 (m, 6H, CH=CH), 4.58 (br s, 4H, CH₂S), 4.01 (m, 8H, CH₂O), 3.85 (br t, 2H, *J*=6.7 Hz, CH₂O), 3.70 (br t, 2H, *J*=7.4 Hz, CH₂N), 3.2–1.0 (m, 84H), 1.14 (br t, *J*=7.4 Hz, 6H, CH₂CH₃), 0.88 (t, 3H, *J*=7.1 Hz, CH₂CH₃).

5.2.9. Polymer 15. ¹H NMR (400 MHz CD₂Cl₂): δ=9.87 (br s, 2H, CONH), 9.51 (br s, 2H, CONH), 8.11–7.93 (br m, 7H, PyrH, ArH), 7.84 (m, 4H, SPh), 7.67 (s, 2H, ArH), 7.42

(m, 6H, SPh), 6.58 (s, 2H, ArH), 5.50–5.07 (m, 6H, CH=CH), 4.55 (br s, 4H, CH₂S), 4.09–3.9 (m, 8H, CH₂O), 3.8–3.7 (m, 4H, CH₂O, CH₂N), 3.2–1.0 (m, 81H), 1.18 (t, 6H, 0.86 *J*=7.5 Hz, CH₂CH₃) (t, 3H, *J*=7.1 Hz, CH₂CH₃).

5.2.10. Metal-coordination cross-linking and *N*-butylthymine hydrogen-bonding polymer (17). One equivalent of **10**, AgBF_{4(s)}, and *N*-butylthymine (**16**) were added to a stirred solution of polymer **5c** (100 mg) in anhydrous CH₂Cl₂ (10 mL), which instantaneously and quantitatively yielded polymer **17**. ¹H NMR (400 MHz CD₂Cl₂): δ=10.43 (br s, 1H, CONHCO), 9.43 (br s, 2H, CONH), 8.02 (s, 2H, Pyr_αH), 7.75 (m, 4H, SPh), 7.53–7.37 (br m, 8H, SPh and Pyr_βH), 7.23 (m, 2H, Pyr_βH), 7.05 (s, 1H, CH=CCH₃), 6.68 (s, 2H, ArH), 5.48–5.15 (m, 6H, CH=CH), 4.70 (br s, 4H, CH₂S), 4.04 (m, 8H, CH₂O), 3.87 (br t, 2H, *J*=6.7 Hz, CH₂O), 3.68 (br t, 2H, *J*=7.4 Hz, CH₂N), 3.2–1.0 (m, 82H), 1.14 (br t, *J*=7.4 Hz, 6H, CH₂CH₃), 0.95 (t, *J*=7.4 Hz, 3H, CH₂CH₃), 0.86 (t, 3H, *J*=7.1 Hz, CH₂CH₃).

5.2.11. Hydrogen-bonding cross-linking and pyridine metal-coordination polymer (18). One equivalent of **12b**, pyridine, and AgBF_{4(s)}, were added to a stirred solution of polymer **5c** (100 mg) in anhydrous CH₂Cl₂ (10 mL) to instantaneously yield polymer **18** in quantitative yield. ¹H NMR (400 MHz CD₂Cl₂): δ=10.10 (br s, 1H, CONHCO), 9.56 (br s, 2H, CONH), 8.01 (s, 2H, Pyr_αH), 7.77 (m, 1H, Pyr_γH), 7.62 (m, 6H, SPh and Pyr_β), 7.49–7.37 (br m, 6H, SPh), 7.27 (m, 2H, Pyr_β), 7.03 (m, 1H, CH=CCH₃), 6.69 (s, 2H, ArH), 5.48–5.15 (m, 6H, CH=CH), 4.58 (br s, 4H, CH₂S), 4.01 (m, 8H, CH₂O), 3.85 (br t, 2H, *J*=6.7 Hz, CH₂O), 3.70 (br t, 2H, *J*=7.4 Hz, CH₂N), 3.2–1.0 (m, 84H), 1.14 (br t, *J*=7.4 Hz, 6H, CH₂CH₃), 0.88 (t, 3H, *J*=7.1 Hz, CH₂CH₃).

Acknowledgements

Financial support has been provided by The Petroleum Research Fund administered by the ACS, the National Science Foundation (ChE-0239385), the Office of Naval Research (MURI, Award No. N00014-03-1-0793), and DuPont. M. W. gratefully acknowledges a 3M Untenured Faculty Award and an Oak Ridge Associated University Junior Faculty Enhancement Award. J. A. acknowledges support from the NSF funded REU program.

References and notes

- Rosen, S. L. *Fundamental Principles of Polymeric Materials*; 2nd ed. Wiley: New York, 1993.
- Odian, G. *Principles of Polymerization*; 3rd ed. Wiley: New York, 1991.
- Kato, T.; Kihara, H.; Kumar, U.; Uryu, T.; Fréchet, J. M. J. *Angew. Chem. Int. Ed. Engl.* **1994**, *33*, 1644–1645.
- Thibault, R. J.; Hotchkiss, P. J.; Gray, M.; Rotello, V. M. *J. Am. Chem. Soc.* **2003**, *125*, 11249–11252.
- Lange, R. F. M.; van Gurp, M.; Meijer, E. J. *Polym. Sci., Part A, Polym. Chem.* **1999**, *37*, 3657–3670.
- Brunsveld, L.; Folmer, B. J. B.; Meijer, E. W. *MRS Bull.* **2000**, 49–53.
- Rieth, L. R.; Eaton, R. F.; Coates, G. W. *Angew. Chem. Int. Ed.* **2001**, *40*, 2153–2156.
- Tessa ten Cate, A.; Sijbesma, R. P. *Macromol. Rapid Commun.* **2002**, *23*, 1094–1112.
- Thibault, R. J.; Galow, T. H.; Turnberg, E. J.; Gray, M.; Hotchkiss, P. J.; Rotello, V. M. *J. Am. Chem. Soc.* **2002**, *124*, 15249–15254.
- Zhao, Y.; Yuan, G.; Roche, P. *Polymer* **1999**, *40*, 3025–3031.
- Loontjens, T.; Put, J.; Coussens, B.; Lange, R.; Palmen, J.; Sleijpen, T.; Plum, B. *Macromol. Symp.* **2001**, *174*, 357–371.
- Hilger, C.; Dräger, M.; Stadler, R. *Macromolecules* **1992**, *25*, 2498–2501.
- Müller, M.; Dardin, A.; Seidel, U.; Balsamo, V.; Iván, B.; Spiess, H. W.; Stadler, R. *Macromolecules* **1996**, *29*, 2577–2583.
- Schmatloch, S.; Schubert, U. S. *Macromol. Symp.* **2003**, *199*, 483–497.
- Lehn, J.-M. *Supramolecular Chemistry*; Wiley-VCH: Weinheim, 1995.
- Ilhan, F.; Gray, M.; Rotello, V. M. *Macromolecules* **2001**, *34*, 2597–2601.
- Albrecht, M.; van Koten, G. *Angew. Chem. Int. Ed. Engl.* **2001**, *40*, 3750.
- Albrecht, M.; Lutz, M.; Antoine, M. M.; Lutz, E. T. H.; Spek, A. L.; van Koten, G. *J. Chem. Soc., Dalton Trans.* **2000**, 3797–3804.
- Pollino, J. M.; Stubbs, L. P.; Weck, M. *J. Am. Chem. Soc.* **2004**, *126*, 563–567.
- Fürstner, A. *Angew. Chem. Int. Ed.* **2000**, *39*, 3012–3043.
- Trnka, T. M.; Grubbs, R. H. *Acc. Chem. Res.* **2001**, *34*, 18.
- Pollino, J. M.; Stubbs, L. P.; Weck, M. *Macromolecules* **2003**, *36*, 2230–2234.
- Finkelmann, H.; Happ, M.; Portugall, M.; Ringsdorf, H. *Makromol. Chem.* **1978**, *179*, 2541–2544.
- Portugall, M.; Ringsdorf, H.; Wendorf, J. H. *Makromol. Chem.* **1978**, *179*, 273–276.
- Pollino, J. M.; Weck, M. *Synthesis* **2002**, 1277–1285.
- Dewey, V. C.; Kidder, G. W. *J. Med. Chem.* **1968**, *11*, 126–129.
- Stubbs, L. P.; Weck, M. *Chem. Eur. J.* **2003**, *9*, 992–999.
- Berl, V.; Schmutz, M.; Krische, M. J.; Khoury, R. G.; Lehn, J.-M. *Chem. Eur. J.* **2002**, *8*, 1227–1244.
- Binder, W. H.; Kunz, M. J.; Kluger, C.; Hayn, G.; Saf, R. *Macromolecules* **2004**, *37*, 1749–1759.
- Huck, W. T. S.; Hulst, R.; Timmerman, P.; van Veggel, F. C. J. M.; Reinhoudt, D. N. *Angew. Chem. Int. Ed. Engl.* **1997**, *36*, 1006.
- Pollino, J. M.; Weck, M. *Org. Lett.* **2002**, *4*, 753–756.
- Loeb, S. J.; Shimizu, G. K. H. *J. Chem. Soc., Chem. Commun.* **1993**, 1395.
- Tecilla, P.; Jubian, V.; Hamilton, A. D. *Tetrahedron* **1995**, *51*, 435–448.
- Itahara, T. *Bull. Chem. Soc. Jpn* **1997**, *70*, 2239–2248.
- Dobrawa, R.; Würthner, F. *Chem. Commun.* **2002**, 1878–1879.
- Würthner, F.; Thalacker, C.; Sautter, A.; Schaertl, W.; Ibach, W.; Hollricher, O. *Chem. Eur. J.* **2000**, *6*, 3871–3886.
- Würthner, F.; Sautter, A.; Thalacker, C. *Angew. Chem. Int. Ed.* **2000**, *39*, 1243–1245.
- Roberts, J. D.; Trumbull, E. R.; Bennett, W.; Armstrong, R. *J. Am. Chem. Soc.* **1950**, *72*, 3116–3124.
- Ver Nooy, C. D.; Rondestvedt, C. S. *J. Am. Chem. Soc.* **1955**, *77*, 3583–3586.
- Brunsveld, L.; Folmer, B. J. B.; Meijer, E. W.; Sijbesma, R. P. *Chem. Rev.* **2001**, *101*, 4071–4097.



Ring opening metathesis polymerisations of norbornene and norbornadiene derivatives containing oxygen: a study on the regeneration of Grubbs catalyst

David M. Haigh, Alan M. Kenwright and Ezat Khosravi*

Department of Chemistry, Interdisciplinary Research Centre in Polymer Science and Technology, University of Durham, South Road, Durham DH1 3LE, UK

Received 18 May 2004; revised 11 June 2004; accepted 14 June 2004

Abstract—Ring opening metathesis polymerisation (ROMP) of norbornene and norbornadiene derivatives containing oxygen are investigated using Grubbs well-defined ruthenium initiator. A series of 7-alkoxy norbornadiene monomers (**2b–d**), containing alkoxy groups with decreasing steric hindrance in the 7-position have been prepared. The ROMP reactions of monomers showed that as the reaction proceeds the initiator is consumed first and then is partially regenerated at the expense of the propagating species. A small amount of another carbene species X, giving a broad signal at 17.44 ppm, is also formed which is extremely stable in solution. The species X is an active metathesis species and is able to perform ROMP on strained cyclic olefins. ROMP of monomers without alkoxy groups in the 7-position (**3**, **4a**, **4b**, **5a** and **5b**) and also monomers with alkoxy groups in the 5 and/or 6 positions of norbornene (**6** and **7**) have been performed under similar conditions. None of these systems exhibited regeneration of the initiator and no resonances due to species X can be seen in the ¹H NMR spectra. The results confirm that the presence of oxygen in the 7-position of the norbornadiene monomer plays an important role in the process of regeneration of the initiator. It is found that the steric bulk and the position of substituents of the monomer have a pronounced influence on the extent of regeneration of the initiator.

© 2004 Elsevier Ltd. All rights reserved.

1. Introduction

The olefin metathesis reaction has become an invaluable synthetic tool for chemists. The ability to simultaneously cleave and reform carbon–carbon double bonds has led to its widespread use in the design of useful organic molecules¹ and polymers.²

Although olefin metathesis was discovered as early as 1955,³ it has only achieved a leading role in synthetic methodology in the last decade. This is mainly attributed to advances in the field of catalysis and organometallic chemistry, which have been heavily influenced by the work of Grubbs^{4–6} and Schrock⁷ in developing well-defined transition metal carbene complexes. This new generation of catalysts are powerful tools in the field of organic reactions¹ such as ring opening metathesis (ROM), ring closing metathesis (RCM)⁸ and cross metathesis (CM), and in polymerisation reactions such as ring opening metathesis polymerisations (ROMP)² and acyclic diene metathesis

(ADMET).⁹ They have also found many applications in the synthesis of natural products.^{10–12}

Schrock introduced well-defined molybdenum initiators with bulky alkoxide and arylimido ligands of the type Mo(CHR)(NAr)(OR')₂ [R=–CMe₃ and R'=–CMe₃ or –C(CF₃)₂Me] which allowed a high degree of control of molecular weight, polydispersity, *cis/trans* content and, in favourable cases, tacticity.^{13–16} The key to controlled polymerisation is that while the molybdenum initiators are inactive towards double bonds in the polymer chain, they react rapidly with the strained double bonds in the monomer to give a linear polymer. However, these catalysts are limited by the high oxophilicity of the metal centres, which renders them extremely sensitive to oxygen and moisture. As a result of this, they show limited tolerance towards functional groups, reducing the number of potential monomers.

The key to improved functional group tolerance was the development of catalysts that react preferentially with olefins in the presence of heteroatoms. Grubbs et al.⁶ synthesised ruthenium alkylidene complexes of the type RuCl₂(PCy₃)₂(=CHPh) [**1**], which are tolerant to a wide range of functional groups such as acids, alcohols,

Keywords: NMR; Ring opening metathesis polymerisation; Ruthenium; Regeneration; Norbornenes; Norbornadienes.

* Corresponding author. Tel.: +44-191-3342014; fax: +44-191-3342051; e-mail address: ezat.khosravi@durham.ac.uk

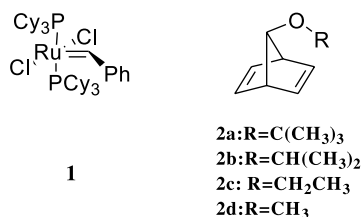


Figure 1. Grubbs ruthenium benzylidene initiator and 7-alkoxy norbornadienes.

aldehydes, esters and amides.⁶ Kinetic studies on these catalysts revealed that catalyst **1** is an efficient initiator for the ROMP of strained cyclic olefins, permitting the incorporation of high degrees of functionality into the resulting polymers.

ROMP reactions using well-defined initiators result in polymers with a narrow polydispersity index (PDI~1.05–1.2). Generally, the initiator is totally consumed and the disappearance of the initiator alkylidene proton and the appearance of the propagating alkylidene protons can be seen in ¹H NMR spectra. In this paper we report the ROMP of 7-alkoxynorbornadienes, in which the initiator is first consumed and then regenerated at the expense of the living propagating species.

2. Results and discussions

We recently made a remarkable observation when catalyst **1** was used to initiate the polymerisation of 7-*t*-butoxynorbornadiene **2a** (Fig. 1) using a monomer–initiator ratio ($[\text{M}]_0/[\text{I}]_0$) of 50.¹⁷ The reaction proceeds rapidly in CDCl_3 with almost complete consumption of initiator to form propagating ruthenium alkylidene species which are then converted slowly, but not completely, back to initiator,

implying a secondary metathesis reaction. The stack plot of the alkylidene proton region at intervals over a 12 h period for this ROMP reaction, Fig. 2, shows these extraordinary features, and it clearly exhibits the presence of three distinct signals. Resonances due to alkylidene protons of **1** appear at 19.9 ppm, a propagating species (P_n) has signals at 19.38, 19.36, 19.33 ppm, and a species X appears at 17.44 ppm. The three propagating signals (P_n) are believed to arise due to the sensitivity of the chemical shift to the *cis/trans* isomerism of the adjacent double bond and to the *meso/racemic* isomerism of the adjacent dyad.¹⁸ The initiator is visibly regenerated at the expense of the propagating species as the reaction proceeds. This can only occur by a secondary metathesis reaction by either an intra- or intermolecular reaction at the living chain ends of the propagating species, Fig. 3. In the intramolecular reactions, (Fig. 3, route a), the end groups of a chain react to form a macrocycle, regenerating the initiator. Whereas, in the intermolecular reactions, (Fig. 3, route b), the end groups from two chains react, resulting in regeneration of the initiator and a new propagating species, which has a combined molecular weight of the original propagating chains. GPC measurements have previously been carried out to investigate this process and unambiguously demonstrate that one or both of these secondary metathesis reactions must take place.¹⁸ Another consequence of these intra and/or intermolecular reactions is a decrease in the proportion of end groups in the polymer. As expected, analysis of the resulting polymers using ¹³C NMR revealed that polymer terminated with ethyl vinyl ether after 24 h had fewer vinylic end groups than that of polymer terminated in the same manner immediately after all of the monomer had been consumed.¹⁸ A small amount of another carbene species, labelled X, giving a broad signal at 17.44 ppm, (Fig. 2), is also formed which is extremely stable in solution. This observation of regeneration of the initiator during a ROMP reaction was the first of its kind and it has not been observed in any other systems. In particular, it has not been observed in the ROMP of 7-alkyl derivatives of norbornadiene.

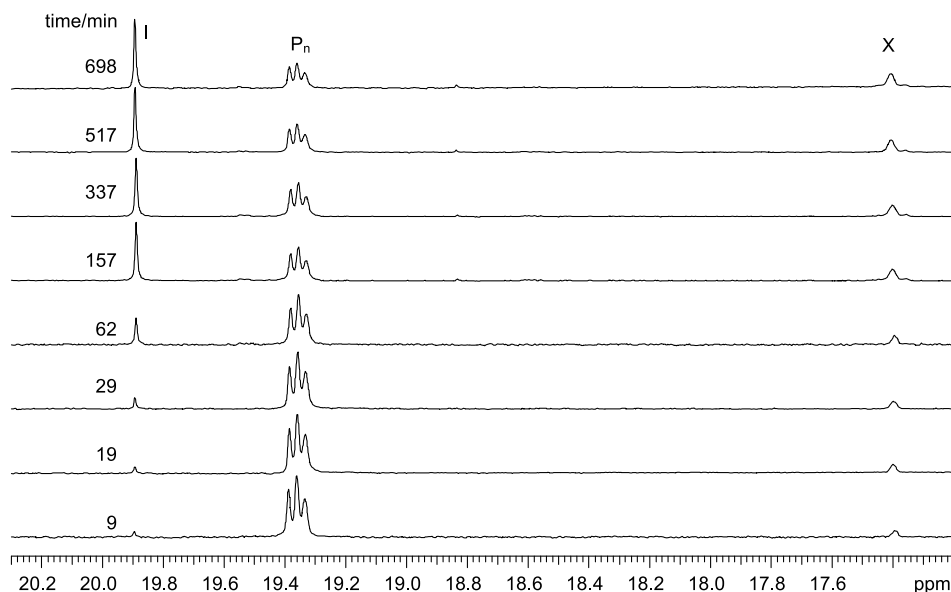


Figure 2. Stack plot showing the alkylidene region of the ¹H NMR spectra for the first 12 h of the ROMP reaction of **2a** initiated by **1** in CDCl_3 system ($[\text{M}]_0/[\text{I}]_0=50$).

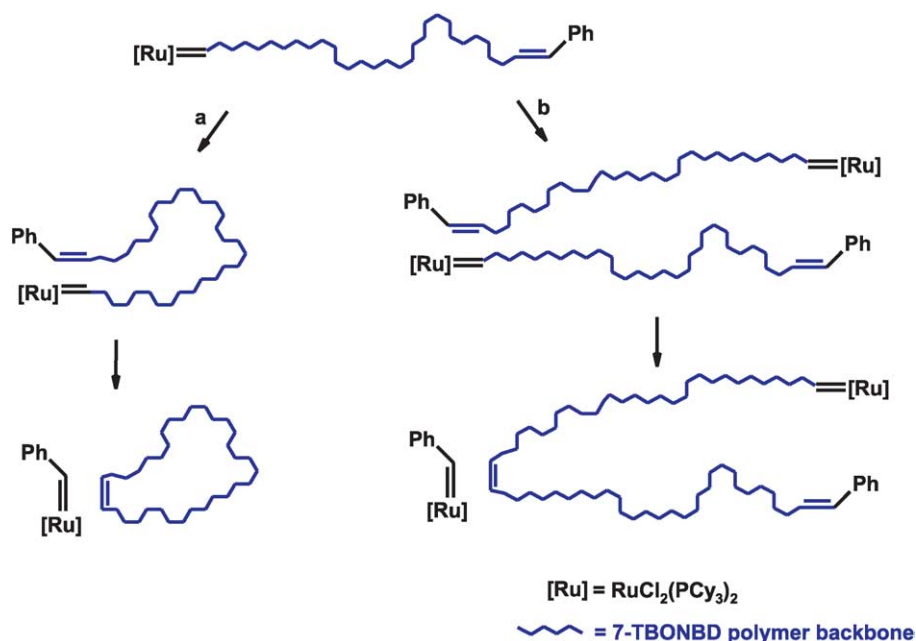


Figure 3. Schematic showing that secondary metathesis leads to regeneration of the initiator by (a) intramolecular cyclisation, or (b) intermolecular reactions.

2.1. The effect of the nature of the substituents on the regeneration of the initiator

In an attempt to probe the parameters which govern the process of regeneration of the initiator, we have investigated whether regeneration is apparent in any other ROMP systems mediated by initiator **1**. Polymerisations of norbornene and the oxygen-containing norbornene deriva-

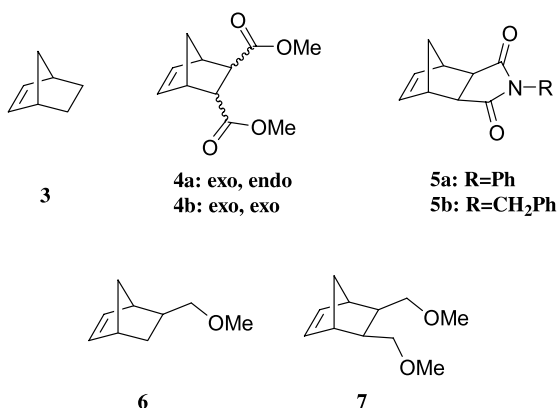


Figure 4. Various strained bicyclic monomers.

Table 1. ROMP of monomers **3**, **4a**, **4b**, **5a**, **5b**^a

Monomer	Monomer consumption (h)	Initiator consumption (%)
3	<0.3 ^b	34
4a	14	83
4b	1	95
5a	0.8	69
5b	<0.3 ^b	91

^a Polymerisations were performed in CDCl₃ at ambient temperature and were initiated by **1** using a ratio of [M]₀/[I]₀=50. [I]₀=15 mM. The reactions were followed by ¹H NMR spectroscopy. None of the reactions exhibited regeneration of the initiator.

^b The monomer is completely consumed before the first ¹H NMR of reaction mixture is taken.

tives **3**, **4a**, **4b**, **5a** and **5b**, shown in Figure 4, have been performed under similar conditions to those described for the ROMP of **2a** initiated by **1**, and the results are shown in Table 1. The reactions were followed by ¹H NMR and, although they behaved differently in terms of the rate of monomer consumption and the amount of initiator consumed, none of these systems exhibited regeneration of the initiator. The alkylidene region (21–16 ppm) of the ¹H NMR spectra when monomers **3**, **4a**, **4b**, **5a** and **5b** are subjected to ROMP by **1** are shown in Figure 5, and it is clear that no resonances due to species X (~17.5 ppm) can be seen during the polymerisation of any of these monomers.

2.2. The effect of the steric bulk of alkoxy substituents in the 7-position of norbornadiene monomers on the process of regeneration of the initiator

The results discussed above suggest that the presence of oxygen in the 7-position of the norbornadiene monomer plays an important role in the process of regeneration for the ROMP of **2a** using initiator **1**. To investigate this effect, a series of new monomers, **2b–d** (Fig. 1), containing alkoxy groups with decreasing steric hindrance in the 7-position have been prepared. The ROMP reactions of monomers **2a–d** initiated by **1** in CDCl₃ were monitored by ¹H NMR spectroscopy. A spectrum was recorded every 15 min for the first 3 h and then at appropriate periods until it was clear that no further reaction was taking place. The alkylidene region (21–16 ppm) of these spectra are shown in Figure 6 and they all exhibit a resonance for the residual initiator (I), the propagating species (P_n) and the stable species X at 19.98, 19.50–18.50, and 17.5 ppm, respectively. Regeneration of the initiator is observed in all of these ROMP reactions, Table 2, and the extent of regeneration is found to increase as the steric bulk of the substituent in the 7-position increases. The regeneration of the initiator is believed to be facilitated by the co-ordination of oxygen from the propagating polymer backbone to the active ruthenium

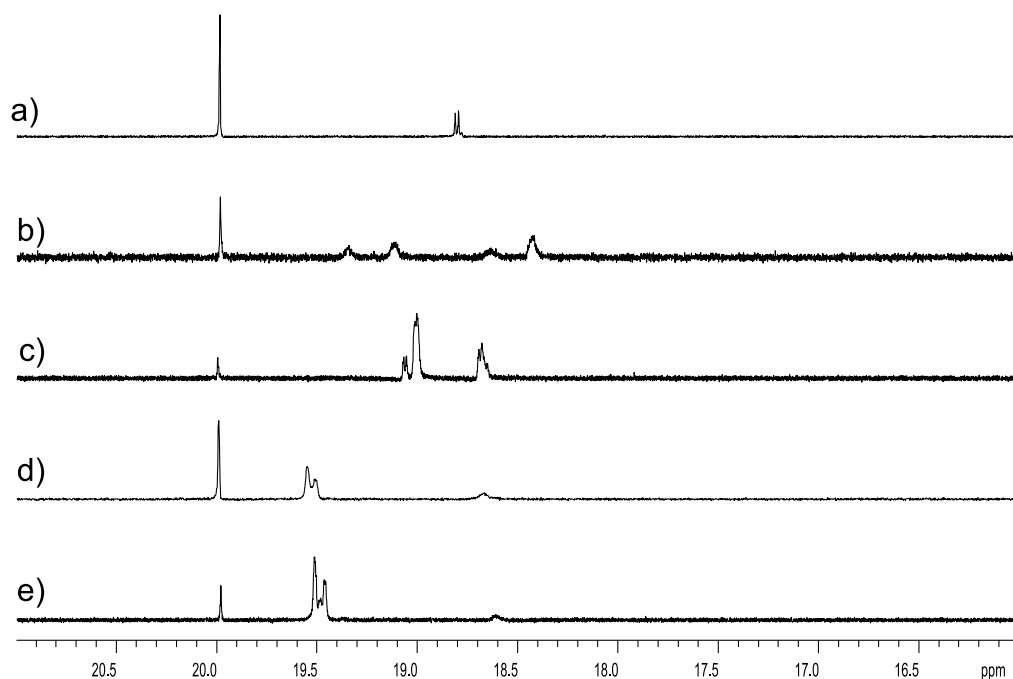


Figure 5. The alkylidene region (21–16 ppm) of the ^1H NMR spectra when monomers (a) **3**, (b) **4a**, (c) **4b**, (d) **5a** and (e) **5b** are subjected to ROMP by **1** using a ratio of $[\text{M}]_0/[\text{I}]_0=50$, $[\text{I}]_0=15$ mM at ambient temperature.

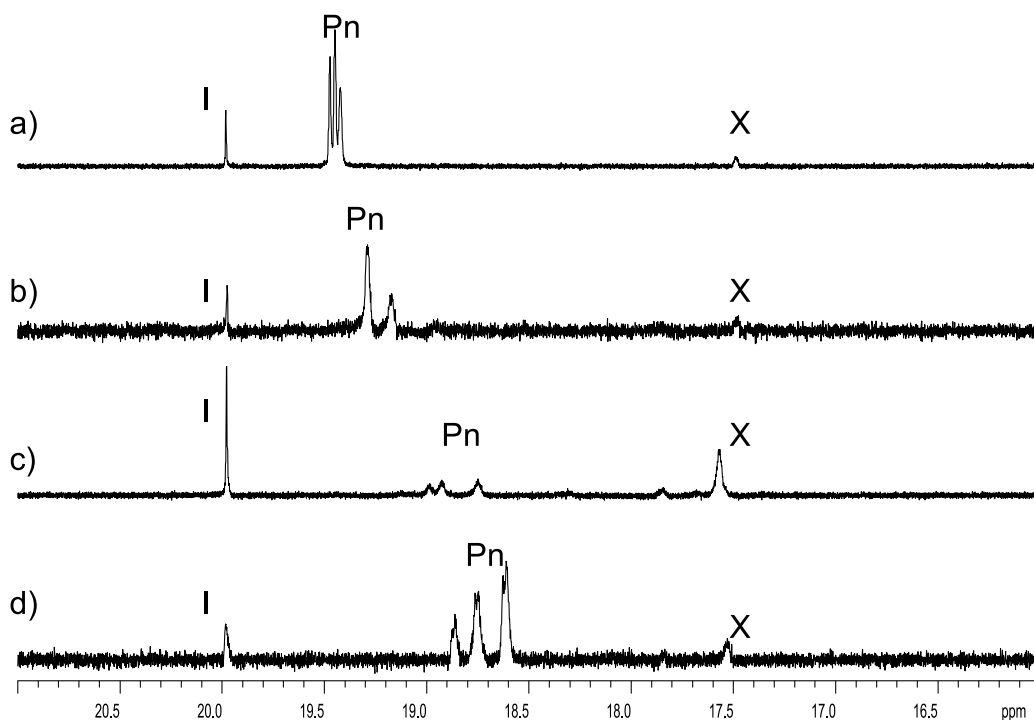


Figure 6. The alkylidene region (21–16 ppm) of the ^1H NMR spectra when monomers (a) **2a**, (b) **2b**, (c) **2c** and (d) **2d** are subjected to ROMP by **1** using a ratio of $[\text{M}]_0/[\text{I}]_0=50$, $[\text{I}]_0=15$ mM at ambient temperature.

metal centre.¹⁸ If the chelating oxygen atom is at the chain end of either the same (Fig. 7, route a) or a different propagating species (Fig. 7, route b), then the terminal double bond is brought into close proximity with the ruthenium carbene and a subsequent secondary metathesis reaction may result in the formation of macrocycles or a polymer of increased molecular weight and regeneration of the initiator. At the moment our hypothesis is that the presence of bulky alkyl groups in the alkoxy substituent in

the 7-position of the monomer makes the oxygen atom more electron rich, and hence a better electron donating moiety.¹⁹

As shown in Table 2, the polymerisation reactions of monomers **2a–d** initiated by **1** also provide information on how the steric bulk of the substituent in the 7-position of the norbornadiene unit affects other aspects of the polymerisation process such as the rate of monomer consumption and the consumption of initiator at the start of the reaction.

Table 2. ROMP of monomers **2a–d**^a

Monomer	$[M]_0/[I]_0$	Monomer consumption (h)	Initial consumption of initiator ^b (%)	Extent of regeneration ^c (%)
2a	50	1	99	29
2a	25	0.5	93	27
2a	10	0.25	81	23
2b	50	2	98	15
2b	25	1	92	18
2b	10	0.5	75	13
2c	50	5	98	6
2c	25	3	92	8
2c	10	0.75	71	10
2d	50	5.5	97	8
2d	25	1	88	3
2d	10	0.5	65	1

^a Polymerisations were performed in $CDCl_3$ at ambient temperature and were initiated by **1** with $[I]_0=15$ mM.

^b Based on the 1H NMR spectrum recorded after 15 min of reaction.

^c The error associated with the extent of regeneration of the initiator is estimated to be $\pm 5\%$ of the quoted value. The reactions were followed by 1H NMR spectroscopy.

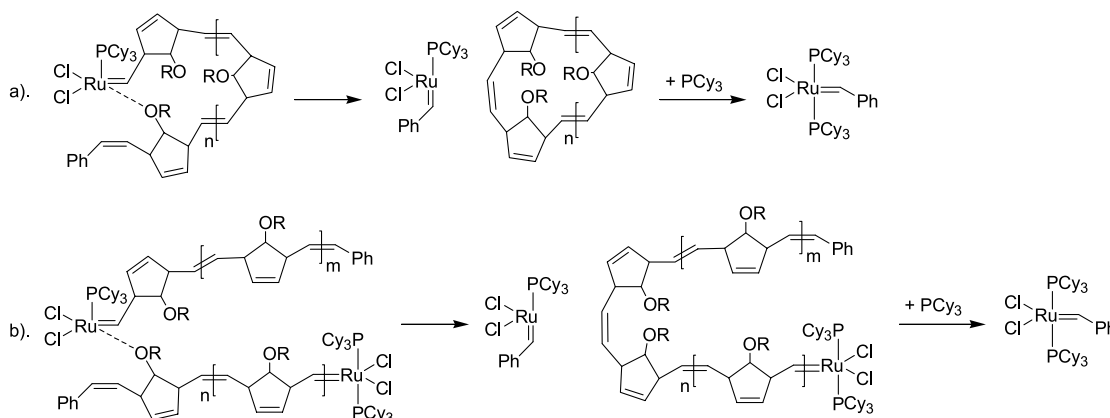


Figure 7. A schematic showing that secondary metathesis reactions at the propagating chain ends can result in regeneration of the initiator. This can be enhanced by (a) intra-, or (b) intermolecular chelation of an oxygen atom from the propagating chain end to the ruthenium metal centre. Species X does not figure in this scheme.

It is now well established that one of the phosphine ligands must dissociate from the ruthenium metal centre if initiation and propagation are to occur in ROMP reactions mediated by Grubbs catalyst.²⁰ This dissociation makes the metal carbene bond accessible for olefins to undergo the necessary [2+2]cyclo-addition reaction. The inserted monomer unit is in close proximity to the active ruthenium carbene centre, and its steric bulk can have a pronounced influence on the ability of the free PCy_3 ligand to re-associate to the metal centre. One possibility is that an increase in the steric bulk in the 7-position of the most recently inserted monomer unit will impede the re-association of the PCy_3 ligand, and hence the active site is more accessible for subsequent addition of monomer units. It may be for this reason that the monomer is consumed faster when the steric bulk in the 7-position is increased.

The amount of initiator consumed at the start of the reaction decreases when the steric bulk of the alkoxy substituent within the monomer is reduced. This is consistent with a decrease in the steric bulk at the 7-position of the monomer enhancing the rate of propagation relative to the rate of initiation compared with a more sterically hindered substituent.

2.3. The effect of the $[M]_0/[I]_0$ ratio on the process of the regeneration of the initiator

The effect of the magnitude of the $[M]_0/[I]_0$ ratio on the regeneration of the initiator for the ROMP of monomers **2a–d** by **1** in $CDCl_3$ has also been studied. **Table 2** shows the results of the ROMP reactions performed on these monomers using $[M]_0/[I]_0=50, 25$ and 10 .

The process of regeneration observed in these ROMP systems is believed to be in competition with other secondary metathesis reactions such as backbiting, involving internal double bonds along the backbone chains.^{18,20} The general trend for the ROMP reactions described in **Table 2**, shows that as the $[M]_0/[I]_0$ ratio is reduced the extent of regeneration of the initiator decreases. Although the reason for this observation is not fully understood, it could be due to the fact that decreasing the length of the propagating polymer chain leads to an enhancement of the secondary metathesis reactions discussed earlier.

In these systems, the rate of propagation is faster than that of initiation.²⁰ Therefore, with a lower concentration of monomer in the system, less of the initiator will be

consumed before propagation becomes the dominant process.

2.4. Species X

We have already discussed in detail the observation of regeneration of the initiator at the expense of the propagating living chains when 7-substituted alkoxy norbornadiene monomers are subjected to ROMP initiated by **1**,^{17,18} and we now consider the appearance of species X in the alkylidene region of the ¹H NMR's. The presence of species X during the ROMP of monomers **2a–d** is clearly shown in Figure 6. In all cases species X is stable and long-lived.

When **2d** is subjected to ROMP using **1** with the ratio of $[M]_0/[I]_0=50$, species X is still visible in the ¹H NMR spectra one month after the start of the polymerisation, and it is the only observable alkylidene species remaining in solution. The disappearance of the initiator and propagating species is consistent with the known rates of decomposition of ruthenium alkylidene species as reported by Grubbs and co-workers,²¹ and it is remarkable that species X still remains in solution after this time. When a second batch of **2d** (18 equiv.) is added to the solution, the monomer is consumed very slowly (20 days), but the appearance of the alkylidene region in ¹H NMR remains unchanged i.e. only species X is observed. This observation implies that X is an active metathesis species, which is able to perform ROMP on strained cyclic olefins.

2.5. The effect of the solvent on the regeneration of the initiator

The effect of the solvent on the rate of regeneration of the initiator for the ROMP of **2a** using $[M]_0/[I]_0=50$, has been studied by performing the polymerisations in CDCl₃,

CD₂Cl₂ and C₆D₆ with $[M]_0/[I]_0=50$ and the results are presented in Table 3. The polarity indices of the solvents according to Allerhand and Schleyer's polarity scale, G, are 106, 100, and 80 respectively.²² A reduction in the polarity of the solvent has no significant effect on the amount of **1** initially consumed by **2a** or on the extent of regeneration of the initiator, but the overall kinetics for the polymerisation process are retarded (i.e. rate of consumption of the monomer is reduced and the time period over which regeneration was observed is extended). Monomer consumption was fastest in CDCl₃ and slowest in C₆D₆. This trend indicates that an increase in the polarity index of the solvent increases the rate at which the ROMP of **2a** occurs. It also reveals that the media in which the polymerisation of **2a** is initiated by **1** plays no role in the regeneration process itself, and that regeneration is solely due to the nature of the monomer and the initiator present.

2.6. ROMP of 5 and/or 6 substituted norbornene monomers

We discussed earlier that norbornadiene monomers with alkoxy functionalities in the 7-position have been found to facilitate the regeneration of initiator **1**. We also showed that the steric bulk of the alkoxy substituent in the monomer unit plays a crucial role in the regeneration process. In order to establish whether the specific position of the alkoxy functionality within the monomer unit has any influence on the process of regeneration of the initiator, monomers with alkoxy groups in the 5 and/or 6 positions of norbornene have been prepared (**6**, **7**, Fig. 4) and subjected to ROMP initiated by **1** in CDCl₃. The polymerisations were monitored by ¹H NMR spectroscopy in the manner described previously. The alkylidene region of the ¹H NMR spectra, shown in Figure 8, indicate that the reactions exhibit similar behaviour to the ROMP reactions of

Table 3. Solvent effects on the ROMP of monomer **2a**^a

Solvent	Regeneration time (days)	Monomer consumption (h)	Initiator consumption (%)	Extent of regeneration ^b (%)
CDCl ₃	1.2	1	99	29
CD ₂ Cl ₂	2.5	3.5	97	29
C ₆ D ₆	3	4.5	100	28

^a Polymerisations were performed at ambient temperature and were initiated by **1** using a ratio of $[M]_0/[I]_0=50$. $[I]_0=15$ mM.

^b The error associated with the extent of regeneration of the initiator is estimated to be $\pm 5\%$ of the quoted value. The reactions were followed by ¹H NMR spectroscopy.

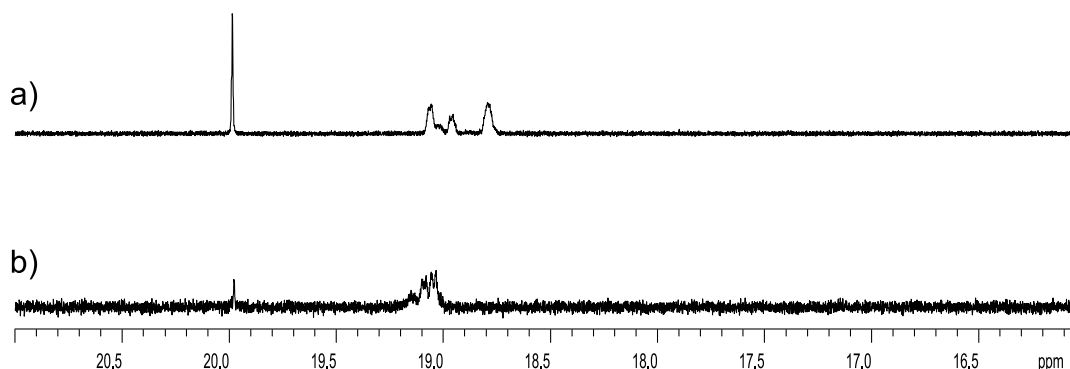


Figure 8. The alkylidene region (21–16 ppm) of the ¹H NMR spectra when monomers (a) **6** and (b) **7** are subjected to ROMP by **1** using a ratio of $[M]_0/[I]_0=50$, $[I]_0=15$ mM at ambient temperature.

monomers **3**, **4a**, **4b**, **5a** and **5b** initiated by **1**. There is no regeneration of the initiator, and no species X is observed. This suggests that the specific position of the alkoxy functionality plays a vital role in the regeneration of the initiator and on the formation of species X when alkoxy norbornadiene monomers are subjected to ROMP.

3. Conclusions

The ROMP reactions of 7-alkoxy norbornadiene monomers (**2b–d**), using Grubbs well-defined ruthenium initiator showed that as the reaction proceeds the initiator is consumed first and then is partially regenerated at the expense of the propagating species. This is believed to occur by either an intra- or intermolecular secondary metathesis reaction at the living chain ends of the propagating species. A small amount of another carbene species X giving a broad signal at 17.44 ppm, is also formed which is extremely stable in solution. The species X is found to be an active metathesis species and is able to perform ROMP on strained cyclic olefins. The extent of regeneration is found to increase as the steric bulk of the substituent in the 7-position increases.

ROMP of oxygen-containing norbornene monomers without alkoxy groups in the 7-position (**4a**, **4b**, **5a** and **5b**) and also monomers with alkoxy groups in the 5 and/or 6 positions of norbornene (**6** and **7**) have been performed under similar conditions. None of these systems exhibited regeneration of the initiator and no resonances due to species X can be seen in the ¹H NMR spectra. This suggests that the specific position of the alkoxy functionality plays a vital role in the regeneration of the initiator and that it has a pronounced influence on the formation of species X.

A change in the polarity of the solvent has no significant effect on the amount of initiator initially consumed or on the extent of regeneration of the initiator, but the overall kinetics for the polymerisation process are retarded.

It is concluded that regeneration of the initiator and the formation of stable ROMP active alkylidene species is dependent on the position of the alkoxy functionality within the monomer unit. This could be attributed to the ability of the oxygen to coordinate efficiently to the ruthenium metal centre when it is specifically situated in the 7-position of the norbornadiene monomers.

We are currently trying to elucidate the chemical structure of species X and the mechanism by which it performs ROMP. The results of these studies will be published elsewhere.

4. Experimental

4.1. General

All reagents used were of standard reagent grade and purchased from Aldrich or Lancaster and used as supplied unless otherwise stated. THF and CDCl₃ (99.9%D, 0.03% v/v TMS) were dried over sodium/benzophenone and P₂O₅,

respectively and distilled prior to use. All other solvents were used without prior purification.

Norbornene [**3**] was dried over sodium and distilled under vacuum prior to use. Grubbs ruthenium initiator⁶ [**1**], 7-*t*-butoxynorbornadiene²³ [**2a**], 7-methoxynorbornadiene²⁴ [**2d**], 5-*exo*,6-*endo*-dicarbomethoxynorbornene²⁵ [**4a**], 5-*exo*,6-*exo*-dicarbomethoxynorbornene^{26,27} [**4b**], *exo*,*exo*-N-phenyl-5,6-dicarboxyimidonorbornene²⁸ [**5a**] and *exo*,*exo*-N-phenylmethyl-5,6-dicarboxyimidonorbornene²⁸ [**5b**], and *exo*,*exo*-5,6-bis(methoxymethyl)norbornene²⁹ [**7**] were synthesized according to literature procedures.

¹H NMR spectra were recorded on a Varian Mercury 400 or a Varian Inova 500. Chemical shifts are quoted in ppm, relative to tetramethylsilane (TMS), using TMS as the internal reference. ¹³C NMR were recorded using broad band decoupling on a Varian Mercury 400 or Varian Inova 500 at 100 and 125 MHz, respectively. Electron impact (EI) mass spectra were recorded on a Micromass Autospec spectrometer operating at 70 eV with the ionisation mode as indicated.

Elemental analyses were obtained on an Exeter Analytical Inc. CE-440 elemental analyser.

4.2. General procedure for ¹H NMR scale ROMP reactions

All ROMP reactions were prepared in a Braun glove box under an inert atmosphere. Initiator **1** (10 mg) was dissolved in deuterated solvent (0.4 mL) and stirred for 5 min. The relevant monomer was dissolved in deuterated solvent (0.4 mL). The monomer solution was injected into the initiator solution and stirred for 5 min. The solution was transferred to an NMR tube fitted with a Young's tap, which allowed the vessel to be closed under a nitrogen atmosphere. The reactions were monitored by ¹H NMR spectroscopy every 15 min for the first 3 h and then at longer periods until no further reaction was observed. In all cases the integrated intensities of the alkylidene signals were compared to that of the TMS signal, which was assumed to remain constant throughout each experiment.

4.2.1. Preparation of 7-*iso*-propoxynorbornadiene [**2b**].

Compound **2a** (6.94 g, 42.3 mmol) was dissolved in propan-2-ol (50 mL) under an inert atmosphere and sulphuric acid (7 mL) dissolved in propan-2-ol (50 mL) was added dropwise with stirring. The solution was heated to 40 °C and stirred for 3 days. The reaction mixture was poured onto ice (75 g) and extracted with dichloromethane (3×25 mL). The combined organic layers were washed successively with saturated solutions of NaHCO₃ (3×50 mL) and NaCl (3×50 mL). After drying over MgSO₄ and filtering, the solvent was removed under vacuum and the residue was purified by fractional distillation under reduced pressure to afford 2.68 g (52–54 °C/18 mbar) of **2b** (yield 42.3%). ¹H NMR (400 MHz, CDCl₃): δ 6.64 (t, 2H, *J*=2.4 Hz), 6.56 (t, 2H, *J*=1.6 Hz), 3.70 (s, 1H), 3.51 (m, 1H, *J*=6.4 Hz), 3.48 (m, 2H, *J*=2.0 Hz), 1.10 (d, 6H, *J*=6.4 Hz) ppm. ¹³C NMR (100 MHz, CDCl₃): δ 139.9, 137.4, 108.0, 70.4, 54.1, 22.7 ppm. Anal. calcd for C₁₀H₁₄O: C, 79.96; H, 9.39.

Found: C, 79.79; H, 9.33. MS (EI): $m/z=149.0$ [M-H]⁺, 135.0 [M-CH₃]⁺, 106.9 [M-CH(CH₃)₂]⁺, 91.2 [M-OCH(CH₃)₂]⁺.

4.2.2. Preparation of 7-ethoxynorbornadiene [2c]. Compound **2a** (20.6 g, 0.125 mol) was dissolved in ethanol (200 mL) under an inert atmosphere and sulphuric acid (14 mL) was added dropwise. The solution was heated to 30 °C and stirred for 5 h. The reaction mixture was poured onto ice (150 g) and extracted with dichloromethane (4×25 mL). The combined organic layers were washed successively with saturated solutions of NaHCO₃ (3×50 mL) and NaCl (3×50 mL). After drying over MgSO₄ and filtering, the solvent was removed under vacuum and the residue was purified by fractional distillation under reduced pressure to afford 2.75 g (48–50 °C/18 mbar) of **2c** (yield 16.1%). ¹H NMR (400 MHz, CDCl₃): δ 6.63 (m, 2H, $J=1.2$ Hz), 6.57 (m, 2H, $J=1.2$ Hz), 3.65 (m, 1H, $J=0.8$ Hz), 3.52 (m, 2H, $J=2.0$ Hz), 3.37 (q, 2H, $J=7.2$ Hz), 1.13 (t, 3H, $J=7.2$ Hz) ppm. ¹³C NMR (100 MHz, CDCl₃): δ 140.1, 137.3, 109.1, 64.0, 53.1, 28.5, 15.4 ppm. Anal. calcd for C₉H₁₂O: C, 79.37; H, 8.88. Found: C, 79.21; H, 8.63. MS (EI): $m/z=136.0$ [M]⁺, 106.9 [M-CH₂CH₃]⁺, 91.3 [M-OCH₂CH₃]⁺.

4.2.3. Preparation of *exo*-5-methoxymethylnorbornene [6]. Under an inert atmosphere, *exo*-5-methanolnorbornene (3.20 g, 25.8 mmol) dissolved in dry THF (10 mL) was added dropwise to a stirred solution of NaH (0.77 g, 32.2 mmol) in dry THF (30 mL). After complete addition, the solution was stirred for 30 min. Methyl iodide (9.14 g, 64.4 mmol) was added dropwise to the solution and a slight exotherm was observed. The reaction was stirred at room temperature for 2 h. Water (~5 mL) was added dropwise to quench any remaining NaH. The solution was poured onto ether (250 mL) and filtered. It was then washed with water (4×100 mL) and dried over MgSO₄. After filtration, the solvent was removed under vacuum to yield the crude product (3.88 g) as a yellow oil. The residue was purified by fractional distillation under reduced pressure to afford 1.81 g (68–72 °C/45 mbar) of **6** (yield 50.8%). ¹H NMR (400 MHz, CDCl₃): δ 6.10 (dd, 1H, $J=5.6, 2.8$ Hz), 6.05 (dd, 1H, $J=5.6, 2.8$ Hz), 3.42 (dd, 1H, $J=9.2, 6.4$ Hz), 3.36 (s, 3H), 3.29 (t, 1H, $J=8.8$ Hz), 2.80 (br. s, 1H), 2.73 (br. s, 1H), 1.68 (m, 1H), 1.31 (q, 2H, $J=4.4$ Hz), 1.24 (dt, 1H, $J=11.6, 2.0$ Hz), 1.11 (dt, 1H, $J=11.6, 4.0$ Hz) ppm. ¹³C NMR (100 MHz, CDCl₃): δ 136.8 (2), 136.8 (0), 77.8, 59.0, 45.2, 43.9, 41.7, 39.1, 29.9 ppm. Anal. calcd for C₉H₁₄O: C, 78.21; H, 10.21. Found: C, 77.83; H, 10.04. MS (EI): $m/z=138.0$ [M]⁺, 123.0 [M-CH₃]⁺, 107.0 [M-OCH₃]⁺, 90.9 [M-CH₂OCH₃]⁺.

Acknowledgements

We thank EPSRC for financial support (D.M.H.) and Catherine Heffernan for her help in obtaining NMR spectra.

References and notes

- Furstner, A. *Alkene Metathesis in Organic Synthesis*; Springer: Berlin, 1998.
- Ivin, K. J.; Mol, J. C. *Olefin Metathesis and Metathesis Polymerisation*; Academic: San Diego, 1997.
- Anderson, A. W.; Merklung, N. G. US Patent 2,721,189, 1955.
- Nguyen, S. T.; Johnson, L. K.; Grubbs, R. H. *J. Am. Chem. Soc.* **1992**, *114*, 3974.
- Schwab, P.; France, M. B.; Ziller, J. W.; Grubbs, R. H. *Angew. Chem., Int. Ed. Engl.* **1995**, *34*, 2039.
- Schwab, P. E.; Grubbs, R. H.; Ziller, J. W. *J. Am. Chem. Soc.* **1996**, *118*, 100.
- Schrock, R. R.; Murdzek, J. S.; Bazan, G. C.; Robbins, J.; DiMare, M.; O'Regan, M. *J. Am. Chem. Soc.* **1990**, *112*, 3875.
- Furstner, A.; Liebl, M.; Lehmann, C. W.; Picquet, M.; Kunz, R.; Bruneau, C.; Touchard, D.; Dixneuf, P. H. *Chem. Eur. J.* **2000**, *6*, 1847.
- Schwendeman, J. E.; Church, A.; Wagener, K. B. *Adv. Synth. Catal.* **2002**, *344*, 597.
- Leeuwenburgh, M. A.; van der Marel, G. A.; Overkleeft, H. S. *Curr. Opin. Chem. Biol.* **2003**, *7*, 757.
- Manning, D. M.; Hu, X.; Beck, P.; Kiessling, L. L. *J. Am. Chem. Soc.* **1997**, *119*, 3161.
- Biagini, S. C. G.; Gibson, V. C.; Giles, M. R.; Marshall, E. L.; North, M. *Chem. Commun.* **1997**, 1097.
- Schrock, R. R.; Feldman, J.; Grubbs, R. H.; Cannizzo, L. *Macromolecules* **1987**, *20*, 1169.
- Murdzek, J. S.; Schrock, R. R. *Macromolecules* **1987**, *20*, 2640.
- Bazan, G. C.; Schrock, R. R.; Khosravi, E.; Feast, W. J.; Gibson, V. C. *Polym. Commun.* **1989**, *30*, 258.
- Bazan, G. C.; Khosravi, E.; Schrock, R. R.; Feast, W. J.; Gibson, V. C.; O'Regan, M. B.; Thomas, J. K.; Davis, W. M. *J. Am. Chem. Soc.* **1990**, *112*, 8378.
- Ivin, K. J.; Kenwright, A. M.; Khosravi, E. *Chem. Commun.* **1999**, 1209.
- Ivin, K. J.; Kenwright, A. M.; Khosravi, E.; Hamilton, J. G. *Macromol. Chem. Phys.* **2001**, *202*, 3624.
- McMurry, J. *Organic Chemistry*; 4th ed.; Cole: Brooks, 1998; p 204.
- Bielawski, C. W.; Grubbs, R. H. *Macromolecules* **2001**, *34*, 8838.
- Ulman, M.; Grubbs, R. H. *J. Org. Chem.* **1999**, *64*, 7202.
- Allerhand, A.; Schleyer, P. v. R. *J. Am. Chem. Soc.* **1963**, *86*, 371.
- Story, P. R. *J. Org. Chem.* **1961**, *26*, 287.
- Lustgarten, R. K.; Richey, H. G. *J. Am. Chem. Soc.* **1974**, *96*, 6393.
- Feast, W. J.; Hesselink, J. L.; Khosravi, E.; Rannard, S. P. *Polym. Bull.* **2002**, *49*, 135.
- Castner, K. F.; Calderon, N. *J. Mol. Catal.* **1982**, *15*, 47.
- Miller, R. D.; Dolce, D. L.; Merritt, V. Y. *J. Org. Chem.* **1976**, *41*, 1221.
- Khosravi, E.; Al-Hajaji, A. A. *Eur. Polym. J.* **1998**, *34*, 153.
- Lynn, D. M.; Kanaoka, S.; Grubbs, R. H. *J. Am. Chem. Soc.* **1996**, *118*, 784.



ROMP of *t*-butyl-substituted ferrocenophanes affords soluble conjugated polymers that contain ferrocene moieties in the backbone

Richard W. Heo, Joon-Seo Park, Jason T. Goodson, Gil C. Claudio, Mitsuru Takenaga, Thomas A. Albright and T. Randall Lee*

Department of Chemistry, University of Houston, 4800 Calhoun Road, Houston, TX 77204-5003, USA

Received 17 April 2004; revised 7 June 2004; accepted 14 June 2004

Available online 8 July 2004

Abstract—A substituted ferrocenophane, 1,1'-((1-*tert*-butyl)-1,3-butadienylene)ferrocene, was synthesized and polymerized via ring-opening metathesis polymerization (ROMP) to give soluble high molecular weight polymers with ferrocenylene units in the backbone. The monomer readily underwent polymerization upon exposure to a tungsten-based metathesis initiator, $W(=CHC_6H_4-o-OMe)(=NPh)[OCMe(CF_3)_2]_2$ (THF), to give high molecular weight polymers (M_w =ca. 300,000). The molecular weights could be varied systematically by adjusting the monomer-to-catalyst ratio. UV/vis spectra revealed a bathochromic shift for the polymer, consistent with enhanced conjugation compared to the monomer. The polymer exhibited thermal properties similar to oligomeric poly(ferrocenylene). Cyclic voltammetry of the polymer suggested that the iron centers are coupled electronically. Upon doping with I_2 vapor, the polymers displayed semiconducting properties ($\sigma=10^{-5}$ S cm^{-1}). Theoretical calculations were used to evaluate the nature of the bonding in these and related polymers.

© 2004 Elsevier Ltd. All rights reserved.

1. Introduction

Conjugated polymers have been widely studied because of their potential use as lightweight and flexible substitutes for metals in a variety of applications.^{1–13} Materials based on conjugated polymers function as conductors of electricity because of electron delocalization through their planar π -system. Interest in conjugated polymers that contain transition metal backbones has been sparked by the promise of a new class of material that will combine the attractive electrical properties of metals with the strength, flexibility, and processability of organic polymers.⁶ Previous attempts, however, to synthesize 'organometallic' polymers have typically afforded poorly conducting and poorly soluble oligomeric materials that are of dubious practical use.^{14,15} The planar π -system that gives conjugated polymers their desired electrical conductivities also causes them to be intractable and infusible. These latter characteristics contribute to a decrease in mechanical strength and processability, which have slowed the incorporation of conjugated polymers in device applications. Sensitivity to ambient conditions (e.g. oxygen, heat, and light) has also

limited the widespread use of conjugated polymers. Overcoming these limitations will be necessary before conjugated polymers will be of practical utility in all but highly specialized technologies.

In an effort to generate a new type of conjugated material, we are exploring the development of organometallic polymers that will be both (1) good conductors of electricity and (2) readily soluble in common organic solvents. Our strategy, which has been reported in preliminary form,^{16,17} involves the synthesis of specifically designed ferrocene-containing monomers that undergo facile polymerization to yield conjugated polymers that contain ferrocenyl units in the polymer backbone. Ferrocenes are attractive building blocks for conjugated polymers for at least three reasons: (1) the ferrocene linkages can act as rotatable π - π -bonds,¹⁸ lending solubility (and thus processability) to the resultant materials, (2) the functionalization of ferrocenes has been well developed, offering a variety of substituted ferrocene-based monomers for the purpose of generating chemically and structurally well-defined ferrocene-containing polymers,¹⁹ and (3) the remarkable air stability and thermal stability (>500 °C) of ferrocenes can be expected to lend enhanced stability to the resultant polymers.²⁰

A wide variety of ferrocene-based organometallic polymers are known. In one particularly successful system,

Keywords: Ring-opening metathesis polymerization (ROMP); Soluble conjugated polymers; Ferrocenophane.

* Corresponding author. Tel.: +1-713-743-2724; fax: +1-281-754-4445; e-mail address: trlee@uh.edu

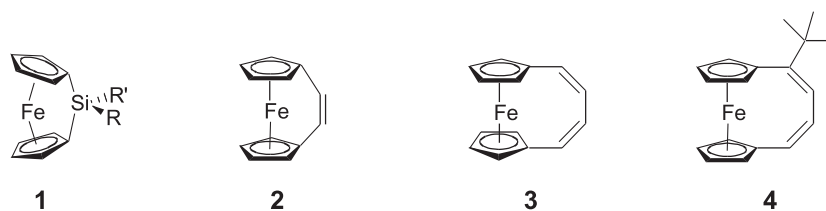


Figure 1. Selected ferrocenophane monomers used in various polymerization trials.

[1]ferrocenophanes bridged by heteroatoms such as germanium, silicon, and phosphorus (e.g. **1** in Fig. 1) have been synthesized.^{21–27} The strain in these ferrocenophanes serves as a destabilizing factor, which leads to facile thermal ring-opening polymerization (ROP).^{24–28} This strategy can be used to generate ferrocene-based materials possessing high molecular weights. The high molecular weight polymers are readily soluble when specifically designed solubilizing functional groups are incorporated in the monomers. Although high molecular weight poly(ferrocenylsilanes) are insulating ($\sigma=10^{-14}$ S cm⁻¹), amorphous samples act as weak semiconductors ($\sigma=10^{-8}$ to 10^{-7} S cm⁻¹) upon doping with I₂.^{14,24} These values of conductivity, however, are still lower than those reported for well known π -conjugated organic polymers, such as polyacetylene ($\sigma=10^5$ S cm⁻¹)²⁹ and poly(phenylenevinylene) ($\sigma=10^3$ S cm⁻¹).³⁰ It is believed that upon polymerization, the heteroatoms lack the necessary π -overlap to afford high electrical conductivities. It is our belief that electronic conjugation would be optimized by incorporating π -conjugated organic spacers between the ferrocene units. Electronic conjugation through the M(d π) of ferrocene and (p π) of the organic spacers would be optimized to give higher electronic conductivity values. The increased conductivity along with the attractive properties afforded by ferrocene should lead to soluble conducting polymers with attractive thermal and air stabilities.

Previous attempts have been made to synthesize highly conjugated ferrocene-based polymers.^{12,13,16,17,31–37} In one study particularly relevant to our work, Tilley and co-workers synthesized *ansa*-(vinylene)[2]ferrocenophane (**2** in Fig. 1) in moderate yield from the McMurry coupling of 1,1'-ferrocenedicarbaldehyde.³¹ The highly strained molecule **2** was targeted as a monomer for ring opening metathesis polymerization (ROMP) to give poly(ferrocenylenevinylene). Indeed, the polymerization using a molybdenum-based ROMP initiator³⁸ yielded poly(ferrocenylenevinylene). However, due to its poor solubility, characterization of this conjugated oligomer was limited. Prior to the work involving **2**, 1,4-(1,1'-ferrocenediyl)-1,3-butadiene (**3** in Fig. 1) was explored as a precursor for the synthesis of poly(ferrocenylenedivinylene) via ROMP.³² Similarly, this polymerization strategy afforded oligomers that were poorly soluble in organic solvents.

In our research,^{16,17} we have adopted this latter type of strategy, but we have modified the monomer structure in efforts to enhance the solubility of the resultant polymers. We believed that judicious structural modification could

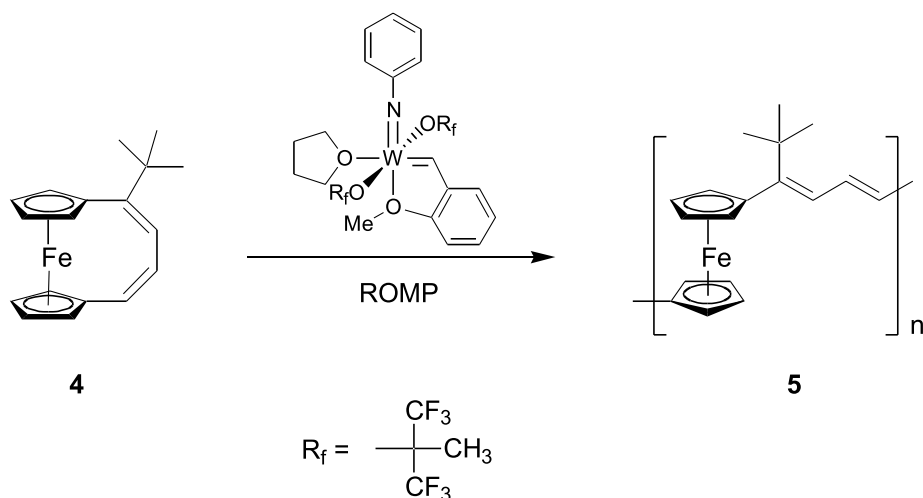
lend enhanced solubility to conjugated polymers. Since the attachment of alkyl groups to the backbones of polymer chains is known to afford organic-soluble polymers,^{39–41} we have designed versions of the monomer with a single alkyl substituent attached to the olefinic bridge (see **4** in Fig. 1). For example, the attachment of bulky pendant alkyl chains to rigid backbones has been shown to increase the solubility of poly(phenylenevinylene),⁴² poly(*p*-phenylene),⁴³ and polypyrrole.⁴⁴ Similarly, substituted polyacetylenes produced from the ROMP of monosubstituted cyclooctatetraenes are soluble in organic solvents when the substituents consist of bulky alkyl groups.³⁹ Furthermore, the incorporation of polar functional groups has permitted the synthesis of water-soluble versions of polythiophene⁴⁰ and polyaniline.⁴¹ When we initially undertook this strategy, we believed that the ROMP of bridge-alkylated derivatives would afford readily soluble versions of polymer. We wished to enhance the solubility in order to facilitate polymer synthesis, characterization, evaluation, and manipulation (i.e. processing).

At least four factors motivated us to choose ROMP as the methodology for synthesizing conjugated organometallic polymers. First, ROMP conserves the number of double bonds (i.e. the degree of unsaturation) of the monomer upon its conversion to the polymer (see Scheme 1), which is a useful feature for the synthesis of conjugated materials. Second, the molecular weight distribution of ROMP-derived polymers is typically narrow, permitting the synthesis of conjugated polymers having well-defined conjugation lengths.^{45–47} Third, certain ROMP initiators can tolerate a wide range of chemical functionalities and reaction conditions,⁴⁸ permitting the incorporation of functional groups that can be used to tune the electrical properties of conjugated polymers. Finally, ROMP can be used to prepare block copolymers having specific segments and/or end group compositions.^{49,50} Based on a previous report of the ROMP of 1,4-(1,1'-ferrocenediyl)-1,3-butadiene **3**,³² we chose the highly reactive tungsten-based metathesis initiator, W(=CHC₆H₄-*o*-OMe)(=NPh)[OCMe(CF₃)₂]₂(THF),⁵¹ (see Scheme 1) as the ROMP initiator in the studies reported here.

2. Results and discussion

2.1. Synthetic approach

Scheme 2 highlights our strategy for preparing unsaturated alkyl-substituted ferrocenophanes. The cornerstone of our approach is the butenone-bridged ferrocenophane **9** first synthesized by Pudelski and Callstrom.^{52,53} We targeted



Scheme 1. ROMP of **4** gives *tert*-butyl substituted poly(ferrocenylenedivinylene) **5**.

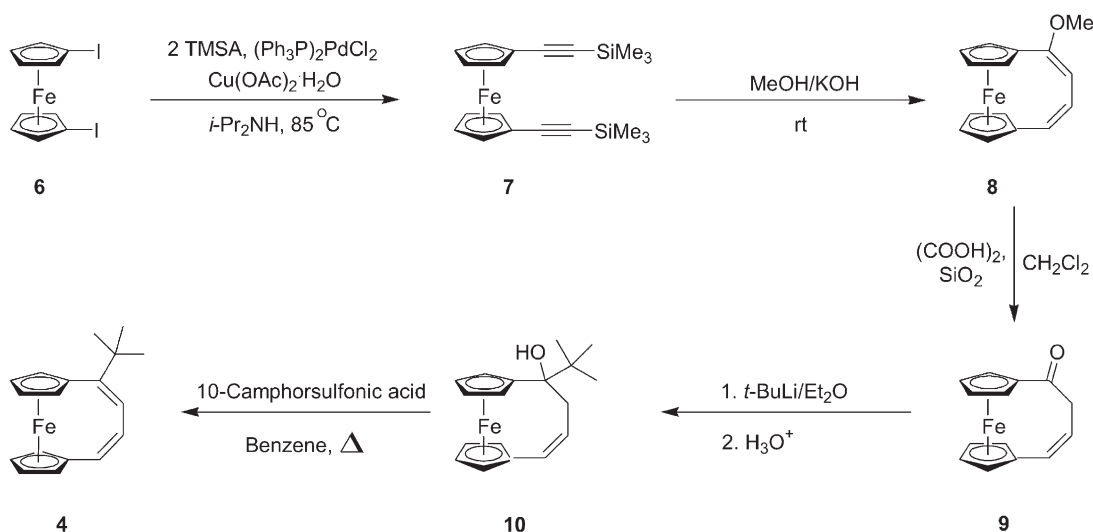
carbon-1 (C-1) on the bridge of **9** as the site for the attachment of a pendant alkyl group. This strategy requires the use of an alkylating agent having no α -hydrogens, since the subsequent dehydration step will thus be restricted to form an endocyclic rather than an exocyclic double bond; the latter would likely predominate if α -hydrogens were available.⁵⁴

2.2. Synthesis of 1,1'-((1-*tert*-butyl)-1,3-butadienylene)ferrocene **4**

As illustrated in **Scheme 2**, alkylation at the C-1 position of **9** was achieved by the use of *tert*-butyllithium. Ferrocenophane **4** was synthesized successfully in two steps from 1,1'-(4-oxo-1-butenylene)ferrocene **9** in 43% overall yield. The crude product was purified by column chromatography followed by recrystallization from hexanes to give large orange needles of **4** that are stable in air and soluble in common organic solvents such as hexane, benzene, methylene chloride, toluene, and tetrahydrofuran (THF).

2.3. X-ray diffraction of 1,1'-((1-*tert*-butyl)-1,3-butadienylene)ferrocene **4**

Although the single crystal X-ray structure of **4** has been reported,¹⁶ we wish to highlight here certain structural features that illustrate the influence of the bulky substituent on the strain and consequent reactivity of **4**. The two Cp rings of **4** lie in a nearly eclipsed conformation and are almost parallel to each other. In contrast, the Cp groups of the parent unsubstituted 1,4-(1,1'-ferrocenediyl)-1,3-butadiene **3** (shown in **Fig. 1**) and the methoxy-substituted 1,1'-(1-methoxy-1,3-butadienylene)ferrocene **8** (shown in **Scheme 2**) lie in a staggered conformation and are substantially more tilted than those of **4**.^{53,55} Moreover, the torsion angle of the butadiene bridge of the parent compound **3** is substantially larger ($\sim 42^\circ$) than that in **4** ($\sim 2^\circ$), further suggesting a relatively constrained geometry for **4**. Apparently, the steric bulk of the *tert*-butyl group gives rise to this constrained geometry, given that the smaller methoxy group in **8** exerts no similar effect. Concrete evidence of strain in **4** is most readily apparent



Scheme 2. Synthesis of 1,1'-((1-*tert*-butyl)-1,3-butadienylene)ferrocene **4**.⁵³

Table 1. Comparison of the solubility of selected olefinic ferrocenylene polymers

Compound	Benzene	CH ₂ Cl ₂	Toluene	THF
Poly(acetylene) ^a	×	×	×	×
Poly(ferrocenylene divinylene) ^b	×	×	×	×
Poly(ferrocenylene <i>tert</i> -butyldivinylene) 5 ^c	√	√	√	√

^a From Ref. 15.^b From Ref. 32.^c From the present study.

as bond-angle strain in the sp² hybridized carbon atoms of the bridge, where the average C–C–C bond angle is 133°. ¹⁶

2.4. Polymerization of 1,1'-((1-*tert*-butyl)-1,3-butadienylene)ferrocene **4**

The strained structure of **4**, when coupled with the increased solubility afforded by the incorporation of the *tert*-butyl group, suggested to us that **4** should be a viable candidate for ROMP. Indeed, as shown in Scheme 1, ferrocenophane **4** readily undergoes ROMP to give the conjugated polymer **5**.^{16,17} The polymerization was monitored in situ both visually and by ¹H NMR spectroscopy (see Fig. 2). Visible color and viscosity changes were detected in the polymer/catalyst solutions with time: the initially orange monomeric solution turned deep red and became more viscous as the reaction proceeded. As illustrated in Figure 2, analysis by ¹H NMR spectroscopy showed the disappearance of the sharp olefinic resonances at δ 5.82 and 6.37, and the appearance of broader olefinic resonances at δ 6.33, 7.03, and 7.68, respectively.

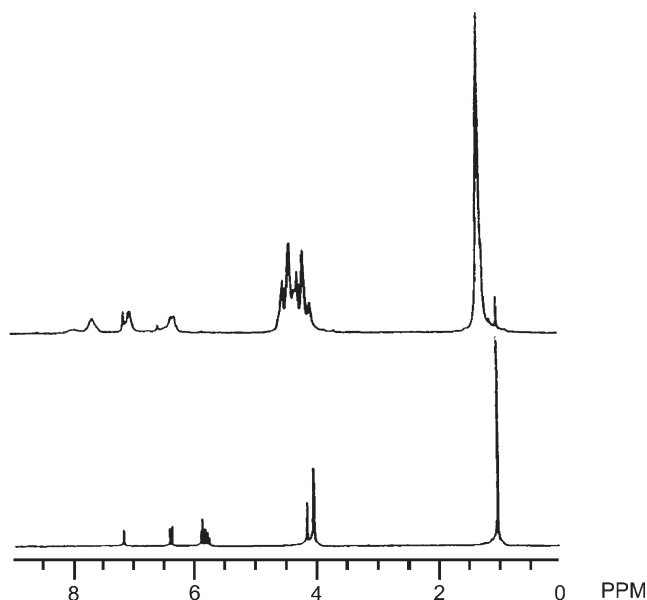


Figure 2. ¹H NMR spectra in C₆D₆ of the monomer **4** (lower) and its nearly complete ROMP to yield polymer **5** (upper).

The polymerization was terminated by the addition of benzaldehyde, which cleaves the polymer chain from the metal center.³² The polymer was purified by precipitation into methanol and then repeatedly into hexanes from CH₂Cl₂ until the solution containing the precipitate became clear (typically 4 precipitations into hexanes). These steps serve to narrow the molecular weight distribution by

removing trace amounts of unreacted monomer and low molecular weight oligomers. After reprecipitation, the overall yields of purified high molecular weight polymer were typically 60%. In the formation of high polymer, the lack of quantitative conversion coupled with the observation of low molecular weight oligomers suggests that the polymerization proceeds by a combination of living and nonliving polymerization mechanisms.⁵⁶ Removal of the solvent gave polymers that were stable to the atmosphere and could be stored for months under ambient conditions without detectable degradation. Polymers having $M_w \leq 100,000$ are brittle, while those with $M_w \geq 300,000$ are flexible, and can be readily peeled from glass slides. It is also noteworthy that these polymers are soluble in most common organic solvents (Table 1), which is rare for conjugated organometallic polymers having high molecular weights.¹⁵

Molecular weights of the polymer were measured by gel permeation chromatography (GPC) using THF as the eluant. Several polymerization trials were attempted to vary the molecular weights of the polymer by controlling the ratio of monomer to catalyst. The data in Figure 3 show that the molecular weights increase qualitatively as the ratio is increased, indicating that a moderate degree of control over the molecular weight can be achieved using this approach. We note further that the values of the polydispersity index are moderately low and fall within a narrow range (1.57–2.34). Importantly, the high molecular weights obtained here are unprecedented for soluble conjugated polymers with ferrocenylene units in the backbone, and rare for conjugated organometallic polymers as a whole.^{14,15}

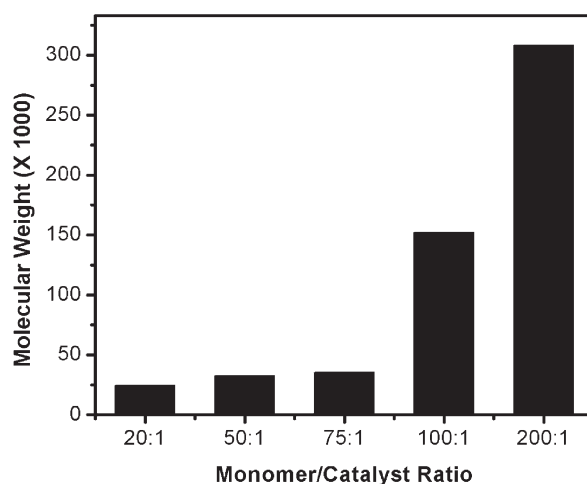


Figure 3. Molecular weight of polymer **5** as a function of monomer/catalyst ratio.

2.5. Spectroscopic characterization of monomer **4** and polymer **5**

2.5.1. Analysis of the ^1H and ^{13}C NMR spectra. As shown in Figure 2, the ^1H NMR spectra of monomer **4** and the corresponding polymer **5** exhibit changes consistent with polymerization. Upon polymerization, for example, the ^1H NMR resonances become broader and shift downfield. The downfield shifts are consistent with an increase in electron delocalization for the polymer relative to the monomer.⁴²

To a first approximation, the chemical shift difference between the H_α and H_β protons attached to the Cp rings of ferrocenophanes can be used to predict qualitatively the tilt of the Cp ring planes relative to each other.^{21,24,31} Consequently, analysis of the chemical shifts of the Cp hydrogens in the ^1H NMR spectrum of **4** can be used to provide an indirect measure of the ferrocenophane ring strain arising from non-coplanarity of the Cp rings.^{21,24,31} In the nonbridged 1,1'-divinylferrocene, for example, the difference between these chemical shifts is 0.18 ppm.²⁴ In the highly tilted *ansa*-(vinylene)ferrocene **2**, however, the separation is 0.79 ppm.²⁴ In contrast, the separation in monomer **4** is 0.11 ppm, which is consistent with little or no strain. While this interpretation is supported by the X-ray crystallographic data,¹⁶ we reiterate that there is strong evidence of bond-angle strain in the sp^2 hybridized carbon atoms of the bridge of **4** (vide supra).

The ^{13}C NMR spectra of monomer **4** and the corresponding polymer **5** exhibited primary resonances consistent with their proposed structures (Fig. 4). Monomer **4** and crude polymer **5** displayed resonances between δ 65 and 75 arising from the carbons of the cyclopentadienyl (Cp) rings. The resonances associated with the corresponding carbons on polymer **5** were shifted slightly downfield and broadened compared to those of the monomer. For monomer **4**, the

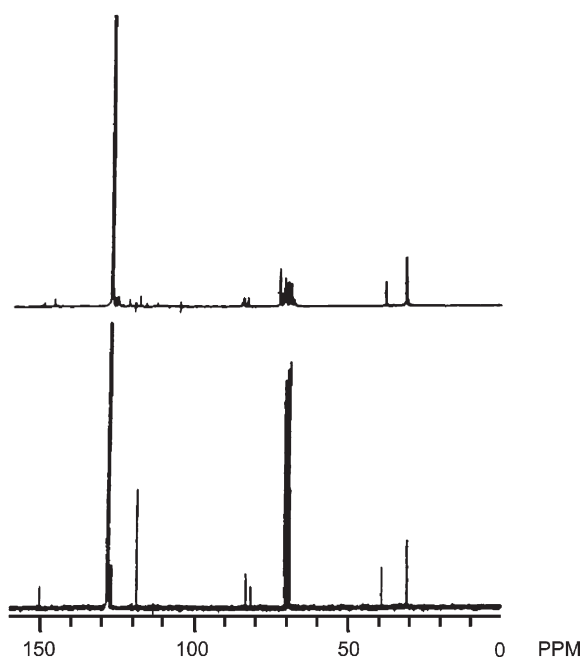


Figure 4. ^{13}C NMR spectra in C_6D_6 of the monomer **4** (lower) and polymer **5** (upper).

resonances associated with the olefinic carbons were observed between δ 125 and 130; for polymer **5**, these peaks were also broadened and shifted downfield relative to those of the monomer. The appearance of several resonances in the δ 120 region of the spectrum for polymer **5** is consistent with the presence of repeat units other than butadienes. Assuming that metal-mediated metathesis takes place solely at the unsubstituted double bond of **4**,^{39,57} we believe a random combination of head-to-tail (see Scheme 1) and head-to-head/tail-to-tail polymerization mechanisms gives rise to the various olefinic carbon species. In our terminology, the head-to-head mechanism would afford ferrocene groups linked by a single unsubstituted olefin ($\text{Fc}-\text{CH}=\text{CH}-\text{Fc}$), and the tail-to-tail mechanism would afford ferrocene groups separated by a tri-olefin in which the *tert*-butyl groups are separated in a sequence of $\text{Fc}-\text{C}(t\text{-Bu})=\text{CH}-\text{CH}=\text{CH}-\text{CH}=\text{C}(t\text{-Bu})-\text{Fc}$.

2.5.2. Ultraviolet/visible spectra. We measured the UV/vis spectra of both **4** and **5** in the range of 300–600 nm to examine the degree of electron delocalization in polymer **5** (See Fig. 5). As shown in the X-ray single crystal structure,¹⁶ for monomer **4**, the π -orbitals in the bridge are perpendicular to those of the Cp groups, which significantly reduces conjugation. The polymer **5**, however, can adopt a conformation in which the π -orbitals in the bridge are nearly parallel to those of the Cp rings; thus, extended overlap between two sets of π -orbitals is possible. As noted above, visual inspection revealed that the solution turned from orange to deep red during the polymerization. Correspondingly, analysis of the UV/vis spectra for **4** and **5** revealed a bathochromic shift of λ_{max} upon polymerization characteristic of absorptions due to π to π^* transitions of ethylenic chromophores: λ_{max} for **4**=444 nm; λ_{max} for **5**=472 nm (Fig. 5). Furthermore, while the monomer exhibited moderately intense absorptions ($\epsilon=4.5\times 10^3 \text{ M}^{-1} \text{ cm}^{-1}$), the polymeric samples showed stronger absorptions ($\epsilon=1.2\times 10^4 \text{ M}^{-1} \text{ cm}^{-1}$). These results are consistent with a moderate degree of conjugation for polymer **5**.⁵⁸

It has also been shown that bathochromic shifts of the λ_{max} value of ferrocenophanes with respect to that of ferrocene reflect the degree of Cp-ring tilt (and thus ring strain) of the

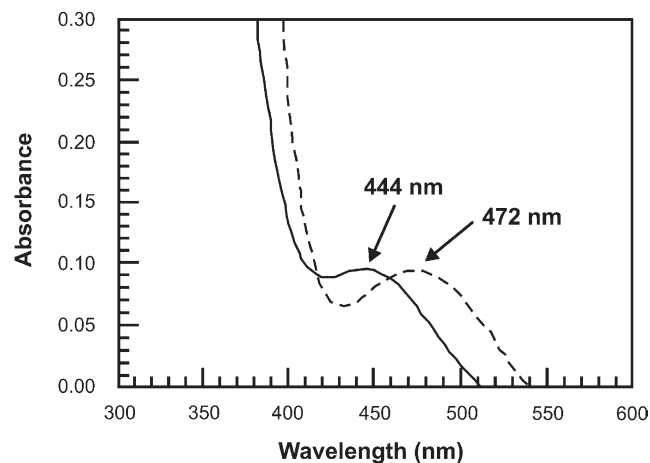


Figure 5. UV/vis spectra of monomer **4** (—, $2.1\times 10^{-4} \text{ M}$) and polymer **5** (- - -, $5.8\times 10^{-5} \text{ M}$).

former.²² For example, Tilley's *ansa*-(vinylene)ferrocene **2** has a λ_{max} value (470 nm) that is red-shifted from that of ferrocene (440 nm);³¹ this red shift is consistent with a substantial degree of ring tilt.^{24,31} In contrast, however, our monomer **4** in which the Cp rings are nearly coplanar, displays a λ_{max} value of 444 nm—an absorption that is red-shifted with respect to that of ferrocene but less so than that of Tilley's monomer **2**. Consequently, given the known Cp ring tilts of the ferrocenophane monomers as determined by X-ray crystallography, the relationships outlined here are also consistent with the predicted relationship between the λ_{max} values and the relative Cp-ring tilts of ferrocenophanes.²⁴

2.6. Thermal analysis of polymer **5**

2.6.1. Thermal gravimetric analysis (TGA) of polymer **5**.

Examination of polymer **5** ($M_w \approx 240,000$) by TGA showed onsets of degradation at ca. 100 and 300 °C with substantial mass loss occurring above 550 °C (Fig. 6). The degree of thermal stability observed for this polymer is consistent with that reported for the structurally similar oligomeric poly(ferrocenylenebutenyne).³² The thermal stability of polymer **5** is also comparable to other conjugated polymers in their undoped-states.⁵⁹ For example, polyacetylene, the simplest and most studied conjugated polymer, was shown by Ito and co-workers to be stable up to 300 °C in an inert atmosphere.⁶⁰ Moreover, poly(*p*-phenylene) was shown to be stable up to 400 °C in air and 550 °C in an inert atmosphere.⁶¹ The thermal stability of polymer **5** reported here suggests that these new materials might find use in materials for solar energy conversion, organic semiconductors, and batteries where elevated temperatures are routinely encountered.⁷

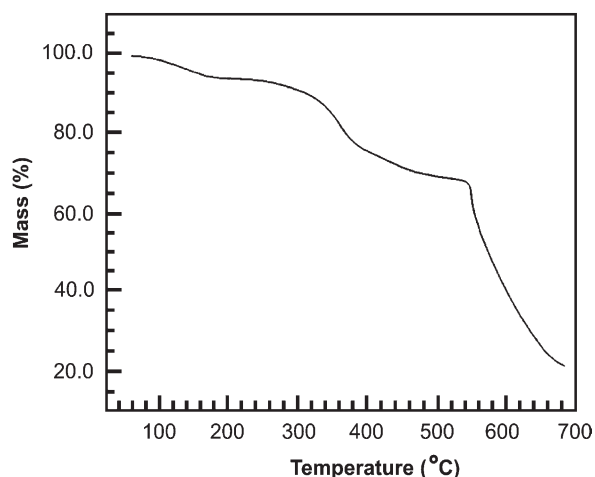


Figure 6. TGA plot for polymer **5** obtained under nitrogen.

2.6.2. Differential scanning calorimetry (DSC) of polymer **5**.

Examination of polymer **5** ($M_w \approx 240,000$) by DSC showed an endothermic transition at 110–120 °C followed by a large exothermic transition at 110–120 °C (Fig. 7). By analogy to the thermal characterization of aryl-linked poly(ferrocenylenes),³⁴ it is possible that the observed exothermic transition arises from a recrystallization process. Furthermore, the observed endothermic transition occurs at a temperature similar to that found for the endothermic

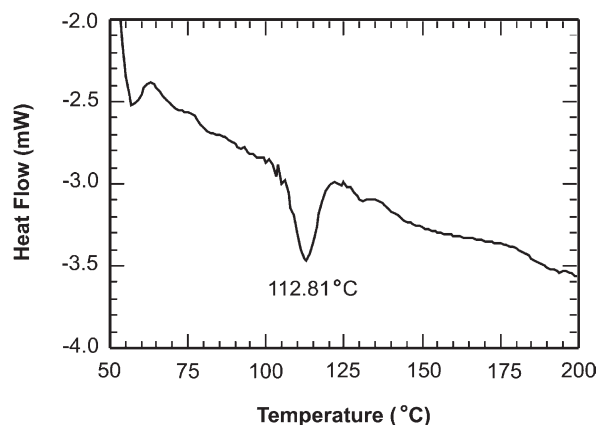


Figure 7. DSC plot for polymer **5** obtained under nitrogen.

transitions of structurally related derivatives of poly(1,1'-ferrocenylene-*alt-p*-oligophenylene).³⁴ We were unable to compare our data with that of the structurally similar oligomeric poly(ferrocenylenevinylene) because no DSC data were reported.³¹ However, analysis by DSC of oligomeric poly(ferrocenylenebutenyne) reported no heat flow change until 385 °C.³² Given that thermal phase behavior can be strongly influenced by (1) the degree of crystallinity and (2) minor physical variations such as small differences in molecular weight and/or the length of side chains,³⁴ it is unsurprising that distinct heat flow characteristics were observed for *tert*-butyl-substituted polymer **5** when compared to the unsubstituted parent oligomer.

The presence of aromatic moieties in conjugated polymer chains has been correlated with increased chain stiffness, T_g , and decomposition temperature.⁵⁹ Reahn, and co-workers explored the thermal phase behavior of poly(1,1'-ferrocenylene-*alt-p*-oligophenylene) derivatives and the poly[2,9-(*o*-phenanthroline)-*alt-p*-oligophenylenes], which possesses no ferrocene moieties along the backbone.³⁴ While the latter polymers exhibit an endothermic transition at 190 °C, the former ferrocene-containing polymers, which are structurally related to our polymer **5**, show strong endothermic transitions at either 65 °C (*n*-dodecyl side chains) or 110 °C (*n*-hexyl side chains). It is possible that the reduction from 190 °C can be attributed to the considerably enhanced conformational freedom of the ferrocene-containing polymers.³⁴

2.7. Electrochemistry

We performed electrochemical measurements of 1 mM CH_2Cl_2 solutions of ferrocene, the unsubstituted ferrocenophane **3**, the *tert*-butyl substituted ferrocenophane **4**, and the ROMP-generated polymer **5** (see Fig. 8). Tetrabutylammonium hexafluorophosphate (TBAHFP) was used as the electrolyte in these experiments in which the data were collected at a scan rate of 200 mV s^{-1} and the electrochemical potentials are reported relative to the standard calomel electrode (SCE). The cyclic voltammetry (CV) of solutions of ferrocene yielded a peak-to-peak separation of ~ 85 mV. The electrochemistry of ferrocene, **3**, and **4** were completely reversible between potentials of 0.00 and +1.00 V using the stated acquisition parameters. The measured electrochemical potentials for both **3** and **4** were

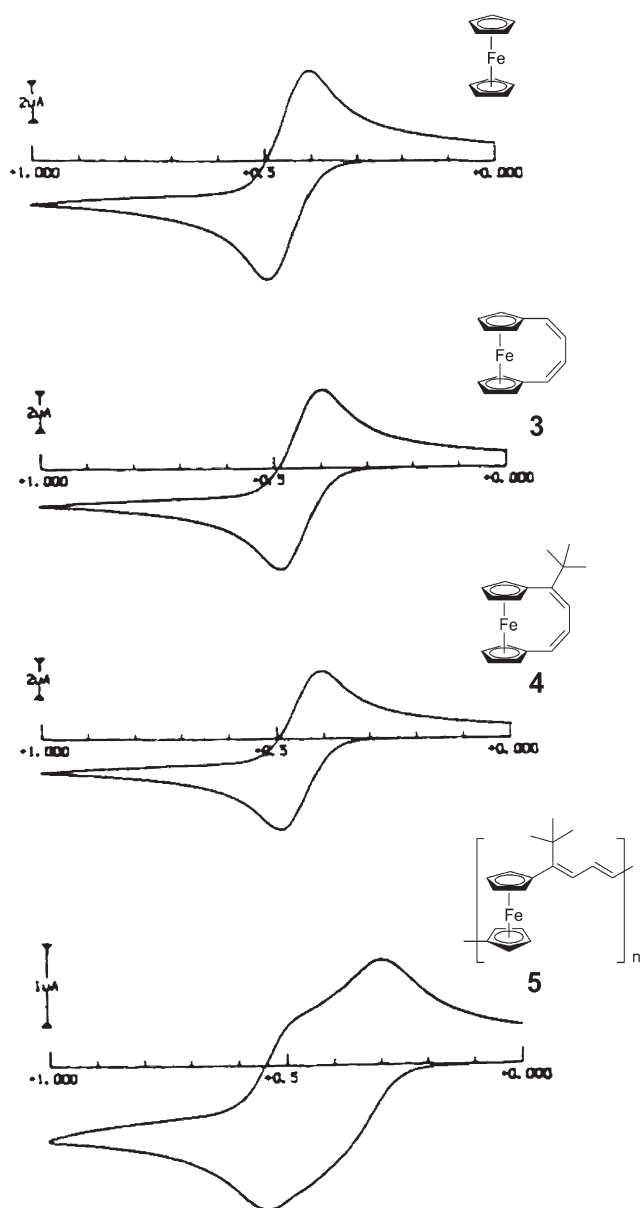


Figure 8. Cyclic voltammograms of 1 mM solutions of ferrocene, **3**, **4**, and **5** in 0.1 M TBAHFP-CH₂Cl₂.

$E^\circ=0.45$ V, which is comparable to that measured for ferrocene ($E^\circ=0.44$ V). Thus, the electrochemical potentials of the monomers were indistinguishable and within experimental error of that of ferrocene. These observations indicate that the presence of the four-carbon bridge (and alkyl substituents on the bridge) fail to influence the electrochemical potential of the ferrocene center. This conclusion is also supported by the ratio of anodic peak current to the cathodic peak current of the molecules. For example, at a scan rate of 200 mV s^{-1} , the ratio of anodic peak current to cathodic peak current was measured to be 0.96 and 0.99 for ferrocene and **4**, respectively.

Electrochemical methods were further used to probe the interaction between the iron centers in **5** (see Fig. 8). The redox waves for the polymer are reversible with a separation (ΔE) of 230 mV ($M_w \approx 240,000$, PDI=2.2). There was no apparent difference in redox properties found for polymers

of low molecular weight vs. those of high molecular weight. The oxidation of the first electron in the polymeric system has a lower oxidation potential than that found for monomer **4** and, as expected, the removal of the second electron is more difficult than the first. The two-wave pattern and the magnitude of ΔE are characteristic of a chain possessing interacting metal centers.^{62,63} Indeed, polymers having non-interacting centers would be expected to show only a single wave.⁶⁴ For example, saturated-hydrocarbon bridged [2]ferrocenophane were found to undergo ROP at high temperatures to give poly(ferrocenylethylenes).⁶⁵ Due to the more insulating characteristics of the saturated-hydrocarbon, the electrochemistry of poly(ferrocenylethylenes) showed the presence of only a single reversible oxidation wave, which indicates that the ferrocene groups interact to a lesser extent than in our polymer **5**. Furthermore, the observed magnitude of ΔE is comparable to that found for related ferrocenyl polymers that exhibit electronic communication between the iron centers, such as poly(ferrocenylenevinylene) ($\Delta E=250$ mV)³³ and the heteroatomic polymers reported by Manners ($\Delta E \sim 210\text{--}290$ mV).²⁴ Unfortunately, no data for poly(ferrocenylenevinylene) were available due to the insolubility of the polymers and the lack of integrity of the polymer films during the collection of cyclic voltammograms in CH₃CN solutions.³²

2.8. Doping and conductivity

Spin-coated samples of polymer **5**, which were highly resistive before doping ($10^{11} \Omega$), were dried under vacuum on a Schlenk line equipped with an attachment for introducing I₂ vapor. After drying, the samples were treated with ca. 200 mm Hg of I₂ at ambient temperature. Instantly, the red translucent films became black. The films were exposed to vacuum for 30 min to ensure the removal of excess I₂ vapor from both the chamber and the film. The conductivity was measured with respect to the doping time as described in the Section 4. Films of polymer **5** ($M_w \approx 240,000$) that were treated in this manner exhibited maximum conductivities on the order of $10^{-5} \text{ S cm}^{-1}$ (Fig. 9).

The measured conductivity of **5** is lower than that reported for either poly(ferrocenylenevinylene) ($10^{-3} \text{ S cm}^{-1}$)³¹ or poly(ferrocenylenevinylene) ($10^{-4} \text{ S cm}^{-1}$).³² Incorporation of

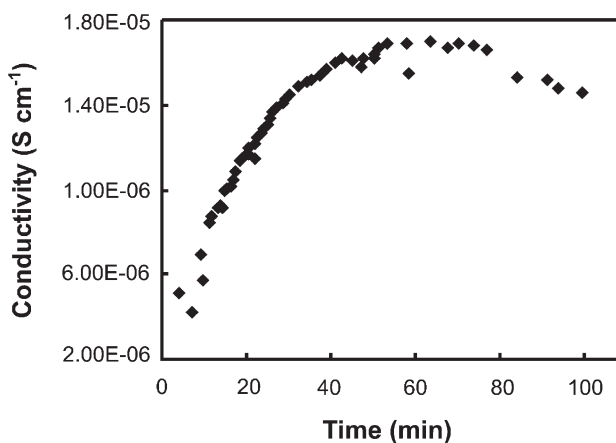


Figure 9. Vacuum conductivity of **5** as a function of the duration of exposure to I₂.

the sterically demanding *tert*-butyl group might plausibly lower the conductivity of **5**. Studies have shown, for example, that the introduction of a *tert*-butyl moiety along the backbone of polyacetylene causes a twisting from planarity of the chain, which partially interrupts the π -conjugation and thereby lowers the conductivity.³⁹ It is also possible that the steric bulk of the *tert*-butyl group lowers the conductivity via an alternative mechanism. If, for example, the major contributing pathway of electronic conduction in these polymers is due to interchain hopping rather than intrachain conduction via the polymer backbone, the bulky *tert*-butyl group might serve to hinder closest packing of the polymer chains and thereby inhibit hole transport.³⁹ Alternatively, the relatively low conductivity observed for **5** might be due to experimental artifact arising from differences in laboratory doping procedures and/or the manner in which the conductivity data were collected (e.g. the use of I₂-treated pressed pellets of the unsubstituted poly(ferrocenylenedivinylene)³² vs. I₂-treated spin-coated films of **5**). On the whole, however, the data reported here provide further support that conjugated polymers with π -electron delocalization through ferrocenyl units are poorer electrical conductors than structurally related conjugated organic polymers such as poly(phenylenevinylene) ($\sigma=10^3$ S cm⁻¹).³⁰

2.9. Bonding in poly(ferrocenylenedivinylene)

Tight binding calculations with an extended Hückel Hamiltonian^{66,67} were used to provide a qualitative assessment of the bonding in the ferrocenyl polymers and to examine why the poly(ferrocenylenedivinylene) derivatives are rather poor conductors. The parameters used for these calculations are the standard ones in CAESAR⁶⁸ and the geometry was adapted from the X-ray structure of **4**.¹⁶ An one-dimensional band model was used for the computations. The density of states (DOS) for the parent poly(ferrocenylenedivinylene) is shown in Figure 10. Here, ϵ_F indicates the position of the Fermi level. A 1.8 eV gap was

found for this polymer. In contrast, the band gap for polyacetylene itself was computed (at the same level) to be 0.7–0.9 eV.⁶⁹ In other words, the introduction of a ferrocenyl unit substantially increases the band gap. Consistent with this result is the fact that the band gap in poly(ferrocenylenedivinylene) was calculated to be 2.0 eV.

The band structure plot for poly(ferrocenylenedivinylene) is shown on the upper right side of Figure 10. There is some dispersion calculated for the valence and conduction bands, both of which contain substantial butadienyl π character. In other words, the valence band can be identified with the HOMO π orbital of butadiene and the conduction band with the LUMO of butadiene. The coordinate system for poly(ferrocenylenedivinylene) is given at the top center of Figure 10. The p_z AOs on carbon are then used for the π -bonding. The dashed line in the DOS plot refers to the projection of carbon p_z for the butadiene linkage. If the ferrocenyl unit were highly conjugating, then the valence band would be more destabilized and the conduction band more stabilized at the zone edge. At the k=X point, the LUMO of butadiene interacts primarily with a higher-lying Cp π combination antibonding to Fe d_{yz}. This interaction stabilizes the conduction band; however, the lower-lying Cp π combination bonding to Fe d_{yz} also mixes into the band and destabilizes it. It is this competition between the two ferrocenyl MOs that keeps the conduction band at high energy for the k=X point. Basically, the same situation applies for the valence band. At k=X, the butadiene HOMO is destabilized by a rather low-lying Cp π combination and stabilized by a Cp π^* MO.

One can also see from both the DOS and band structure plots that the conduction band lies close in energy to a number of states that are highly localized at Fe. These can be associated with the z², xy, and x²-y² d AOs of ferrocene.⁷⁰ Our calculations are insufficiently accurate to distinguish whether the butadiene π band lies just above or within the highly localized Fe d states. The electrochemical

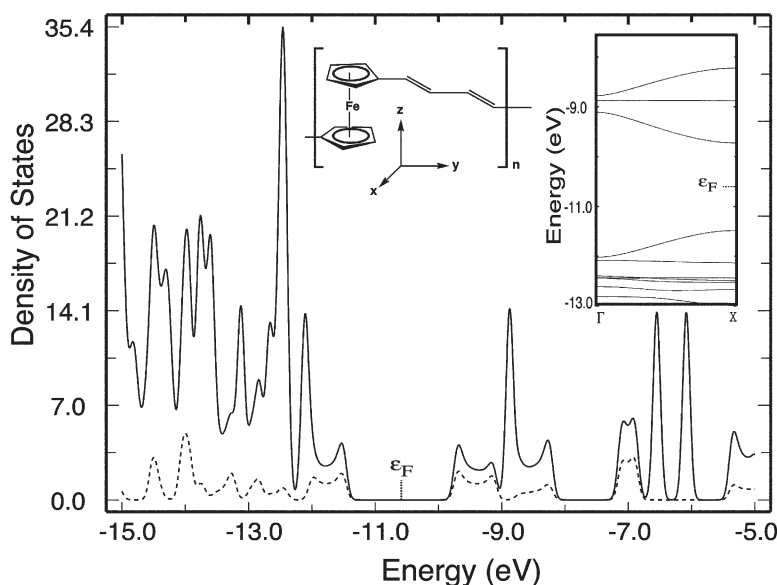


Figure 10. The DOS plot (solid line) for poly(ferrocenylenedivinylene). The dashed line indicates the projection of the butadienyl p_z AOs. The inset on the upper right side shows the band structure for this compound around the Fermi level, ϵ_F .

data presented above would tend to support the latter. Notice, however, that even if the former is true, the density of states at the top of the conduction band is rather low.

An alternative way to view the nature of the bonding is to note that the ferrocenyl unit is 'saturated'. All filled MOs are Cp–Fe bonding and lie at low energies or are highly localized at the metal (note: the z^2 , xy and x^2-y^2 d AOs of ferrocene can be viewed as the t_{2g} set of an octahedral complex).⁷⁰ The empty MOs are Fe–Cp antibonding or Cp– π^* and are at high energies. A similar situation applies for poly(ferrocenylenevinylene). Because of the parity difference in the HOMO and LUMO of a vinyl group compared to that in a divinyl group, the zone center ($k=\Gamma$) now serves to position the band gap. Putting more unsaturated units between the ferrocenes will decrease the gap, which is consistent with the greater conductivity of doped polyacetylene compared to that of the ferrocenyl-containing polymers. There are two plausible scenarios to generate a smaller band gap. The substitution of π -donors on the unsaturated chains will raise the energy of the valence band. The problem with this strategy is that it should also raise the energy of the conduction band, albeit to a lesser extent. Alternatively if there are an odd number of unsaturated carbon atoms between the ferrocene units, then there will be a non-bonding π level at moderate energies that will interact strongly with the metal. The simplest example would be a fulvene-metal-cyclopentadienyl complex. These compounds have been investigated extensively.⁷¹ Calculations on a poly(ferrocenylenevinylene) model show the presence of a band at moderate energy that lies just above and below the valence and conduction bands in the previous systems.

3. Conclusions

We explored the ring-opening metathesis polymerization of **4** to give organometallic polymer **5** that is fully conjugated and contains repeat units of ferrocene in the polymer backbone. The synthetic strategy outlined here offers a general route to the synthesis of high-molecular weight (e.g. $M_w > 300,000$) conjugated organometallic polymers that are soluble in common organic solvents. The unprecedented solubility of these compounds permitted the successful characterization of polymer **5**. Analysis by UV/vis spectroscopy revealed bathochromic shifts for polymer **5**, indicating extended conjugation, which is necessary to facilitate electron conduction through the π -conjugated backbone of the polymer. Some degree of electron delocalization through the backbone was also supported by electrochemical measurements, which revealed the presence of two reversible oxidation waves for polymer **5**. The presence of multiple redox waves indicates that the ferrocene nuclei communicate with each other electronically. The similarity of our measured conductivities to those of oligomeric poly(ferrocenylenevinylene)³¹ and poly(ferrocenylenebutadiene)³² suggests that interchain hopping might be the dominant mechanism of transport found in our polymeric system. Incorporation of the *tert*-butyl group lends solubility to polymer **5**, which facilitates the synthesis of high molecular weight materials. The steric bulk of this substituent might, however, play a

role in lowering the electric conductivity through various mechanisms. Calculations suggest, however, that the ferrocene group itself is primarily responsible for lowering the conductivity. Future studies will explore the incorporation of alternative side groups and linkages to explore these issues in greater detail.

4. Experimental

4.1. General

Reactions sensitive to air and/or water were performed under an inert atmosphere (N_2 or Ar) using either standard Schlenk techniques or an Innovative Technologies glove box. All bulk polymerizations were performed in the glove box. Hydrocarbon solvents were dried by passage through a column of activated alumina; trace amounts of oxygen were removed with a Cu-based catalyst (Q-5, Englehard). Etheral and halogenated solvents were dried by passage through a column of activated alumina. All solvents were degassed using freeze-pump-thaw cycles before use. The tungsten-based metathesis initiator, $W(=CHC_6H_4-o-OMe)(=NPh)[OCMe(CF_3)_2]_2$ (THF), was prepared as described elsewhere.³⁹

4.2. Synthesis and polymerization of 1,1'-(1-*tert*-butyl)-1,3-butadienylene)ferrocene **4**

The monomer used in these studies, 1,1'-(1-*tert*-butyl-1,3-butadienylene)ferrocene **4**, was synthesized via the strategy outlined in Scheme 2. The key intermediate, 1,1'-(4-oxo-1-butenylene)ferrocene **9**, was synthesized using methodology developed by Pudelski and Callstrom (see Scheme 2).⁵³ The procedures for the synthesis and polymerization of 1,1'-(1-*tert*-butyl-1,3-butadienylene)ferrocene **4** have been described in detail in our previous report.¹⁶ Complete analytical data were previously reported for the monomer **4** and the polymer **5**.¹⁶

4.3. Nuclear magnetic resonance (NMR) spectroscopy

NMR spectra were recorded with a General Electric QE-300 (300.2 MHz, 1H ; 75.5 MHz, ^{13}C) spectrometer equipped with a dual probe. Data were collected as indicated in either benzene- d_6 , methylene chloride- d_2 , or chloroform- d . Chemical shifts were referenced to the residual proton or carbon signal of the deuterated solvents.

4.4. Ultraviolet–visible (UV–vis) absorption spectroscopy

Ultraviolet–visible absorption spectra were collected on a Varian Cary 3-Bio UV–visible spectrophotometer. The compounds were dissolved in THF or CH_2Cl_2 , and the data were collected over the range of 300–600 nm in a standard quartz cell $1 \times 1 \times 4$ cm³.

4.5. Thermal gravimetric analysis (TGA)

The thermal degradation of polymer **5** was evaluated using a TA Instrument Hi-Res TGA 2950 Thermogravimetric Analyzer. An aliquot of the polymer sample (~12 mg)

was heated at 0.5 °C/min under a flow of N₂ gas. The percent weight loss of the sample vs. temperature was recorded.

4.6. Differential scanning calorimetry (DSC)

DSC data were collected using a TA Instrument DSC 2010 in a sealed aluminum pan. The sample was heated from 50 to 250 °C at a rate of 10 °C/min under a flow of nitrogen. Conventional heat flow vs. temperature was obtained using a Universal V2.5H TA Instruments program.

4.7. Gel permeation chromatography (GPC)

GPC was used to determine the molecular weights of polymer samples. The GPC system consisted of a Waters 510 pump and a Waters 410 differential refractive index detector. The column set included three Waters Styragel HR columns (Styragel HR 5E, 4E, and 1 in series). THF was used as the eluant, and the flow rate was 1.0 mL/min. The column set was calibrated with narrow molecular weight polystyrene standards purchased from Polysciences. The polymer samples (3–5 mg mL⁻¹) were filtered through a 0.45 μm Millipore, Millex FH 13 mm filter prior to analysis.

4.8. Spin-casting and doping of thin polymer films

A sample of polymer (20 mg) was dissolved in benzene (1 mL) and filtered through a 0.45 μm Millipore, Millex FH 13 mm filter. The solution was cast dropwise onto a glass substrate mounted on Headway Research Spin-Coater. The translucent red films were spun dry and then further dried under vacuum. Doping was accomplished by exposing the polymer films to iodine vapor (200 mm Hg) in an evacuated Schlenk flask for selected intervals of time (typically 2–5 h). The initially translucent red films became black upon exposure to iodine. Before measuring the conductivity, the sample was placed under vacuum for ~30 min to remove any excess iodine.

4.9. Measurements of electrical conductivity

In order to eliminate contact resistance, the conductivities were measured using the four-point probe method.^{11,14} Our homemade four-point probe system consists of four-in-line heads (Keithley), an autoranging digital multimeter (Keithley Model 2001), a picoammeter (Keithley Model 487), and software programmed to measure the voltage and resistivity of the sample (Keithley TestPoint). Four thin gold wires (0.05 mm thick and 99.9% pure) were attached in parallel on the film surface with colloidal silver liquid (Ted Pella, Inc.) for enhanced electrode contact. Conductivity values (σ) were obtained by connecting the four probes to four gold wires on the surface of the doped film, applying a potential via the power source, and measuring the resulting current (i) and the voltage drop (v) between the four probes.

The conductivities were calculated according to the van der Pauw Eq. (1), which applies for a sample in which the thickness (d) is less than the probe spacing. The values of conductivity reported in the text were obtained from the average of a series of multiple current and voltage measurements. To confirm the accuracy of the detection

circuit, measurements were performed on standard resistors prior to collecting the data on the doped samples.

$$\sigma = i(\ln 2)/(\pi dv) \quad (1)$$

Using the apparatus, the electrical conductivities of the polymer samples were measured in an inert atmosphere or in air. Inert atmosphere measurements were performed in a glove box or in Schlenk reaction vessels sealed with rubber septa. Conductivity measurements in air of doped films gave sporadic data, representative of oxidative degradation of the conducting films. Therefore, the reported conductivities of all doped material were collected under an inert atmosphere. Measurements in air were only performed for undoped samples, which were found to be stable in air.

Acknowledgements

Generous support for this research was provided by the Robert A. Welch Foundation (Grants E-0705 and E-1320) and the Texas Institute for Intelligent Bio-Nano Materials and Structures for Aerospace Vehicles, funded by NASA Cooperative Agreement No. NCC-1-02038.

References and notes

1. Arimoto, F. S.; Haven, A. C., Jr. *J. Am. Chem. Soc.* **1955**, *77*, 6295.
2. Chen, Y.-H.; Fernandez-Refojo, M.; Cassidy, H. G. *J. Polym. Sci.* **1959**, *40*, 433.
3. Pittman, C. U., Jr.; Lai, J. C.; Vanderpool, D. P.; Good, M.; Prado, R. *Macromolecules* **1970**, *3*, 746.
4. Cowan, D. O.; Park, J.; Pittman, C. U., Jr.; Sasaki, Y.; Mukherjee, T. K.; Diamond, N. A. *J. Am. Chem. Soc.* **1972**, *94*, 5110.
5. Pittman, C. U., Jr.; Sasaki, Y.; Grube, P. L. *J. Macromol. Sci.-Chem.* **1974**, *A8*, 923.
6. Marks, T. J. *Science* **1985**, *227*, 881.
7. *Handbook of Conducting Polymers*, Skotheim, T. A., Ed.; Marcel Dekker: New York, 1986; Vols. 1 and 2.
8. Sailor, M. J.; Ginsberg, E. J.; Gorman, C. B.; Kumar, A.; Grubbs, R. H.; Lewis, N. S. *Science* **1990**, *249*, 1146.
9. Allcock, H. R. *Science* **1992**, *3*, 381.
10. Bunz, U. H. F. *Angew. Chem., Int. Ed. Engl.* **1996**, *35*, 969.
11. Much recent interest has focused on a family of non- π -conjugated polymers that contain ferrocenylene units in the backbones. See, for example: Manners, I. *Angew. Chem., Int. Ed. Engl.* **1996**, *35*, 1602. and Pannell, K. H.; Dementiev, V. V.; Li, H.; Cervantes-Lee, F.; Nguyen, M. T.; Diaz, A. F. *Organometallics* **1994**, *13*, 3644.
12. Brizius, G.; Pschirer, N. G.; Steffen, W.; Stitzer, K.; zur Loye, H.-C.; Bunz, U. H. F. *J. Am. Chem. Soc.* **2000**, *122*, 12435.
13. Morisaki, Y.; Chujo, Y. *Macromolecules* **2003**, *36*, 9319.
14. For reviews, see: Nguyen, P.; Gomez-Elipe, P.; Manners, I. *Chem. Rev.* **1999**, *99*, 1515.
15. For reviews of inorganic and organometallic polymers, see: Mark, J. E.; Allcock, H. R.; West, R. *Inorganic Polymers*. Prentice Hall: New Jersey, 1992. *Inorganic and Organometallic Polymers II; ACS Symposium Series 572*, Wisian-Neilson, P., Allcock, H. R., Wynne, K. J., Eds.; American Chemical Society: Washington, DC, 1994.

16. Heo, R. W.; Somoza, F. B.; Lee, T. R. *J. Am. Chem. Soc.* **1998**, *120*, 1621.
17. Heo, R. W.; Lee, T. R. *Polym. Prepr.* **1998**, *39*, 169.
18. Gooding, R.; Lillya, C. P.; Chien, J. C. W. *J. Chem. Soc., Chem. Commun.* **1983**, 151.
19. Scholl, H.; Sochaj, K. *Electrochim. Acta* **1991**, *36*, 689.
20. Cotton, F. A.; Wilkinson, G. *Basic Inorganic Chemistry*; Wiley: New York, 1987; p 622.
21. Osborne, A. G.; Whiteley, R. H.; Meads, R. E. *J. Organomet. Chem.* **1980**, *193*, 345.
22. Butler, I. R.; Cullen, W. R.; Einstein, F. W. B.; Rettig, S. J.; Willis, A. J. *Organometallics* **1983**, *2*, 128.
23. Herberhold, M. *Angew. Chem., Int. Ed. Engl.* **1995**, *34*, 1837.
24. Manners, I. *Adv. Organomet. Chem.* **1995**, *37*, 131.
25. Berenbaum, A.; Braunschweig, H.; Dirk, R.; Englert, U.; Green, J. C.; Jakle, F.; Lough, A. J.; Manners, I. *J. Am. Chem. Soc.* **2000**, *122*, 5765.
26. Temple, K.; Dziadek, S.; Manners, I. *Organometallics* **2002**, *21*, 4377.
27. Berenbaum, A.; Lough, A. J.; Manners, I. *Organometallics* **2002**, *21*, 4415.
28. Foucher, D. A.; Tang, B. Z.; Manners, I. *J. Am. Chem. Soc.* **1992**, *114*, 6246.
29. Naarmann, H.; Theophilou, N. *Synth. Met.* **1987**, *22*, 1.
30. Murase, I.; Ohnishi, T.; Noguchi, T.; Hirooka, M. *Polym. Commun.* **1994**, *25*, 327.
31. Buretea, M. A.; Tilley, T. D. *Organometallics* **1997**, *16*, 1507.
32. Stanton, C. E.; Lee, T. R.; Grubbs, R. H.; Lewis, N. S.; Pudelski, J. K.; Callstrom, M. R.; Erickson, M. S.; McLaughlin, M. L. *Macromolecules* **1995**, *28*, 8713.
33. Itoh, T.; Saitoh, H.; Iwatsuki, S. *J. Polym. Sci., Polym. Chem.* **1995**, *33*, 1589.
34. Knapp, R.; Velten, U.; Rehahn, M. *Polymer* **1998**, *39*, 5827.
35. Bochmann, M.; Lu, J.; Cannon, R. D. *J. Organomet. Chem.* **1996**, *518*, 97.
36. Ingham, S. L.; Khan, M. S.; Lewis, J.; Long, N. J.; Raithby, P. R. *J. Organomet. Chem.* **1994**, *470*, 153.
37. Buchmeiser, M. R.; Schuler, N.; Kaltenhauser, G.; Ongania, K. H.; Lagoja, I.; Wurst, K.; Schottenberger, H. *Macromolecules* **1998**, *31*, 3175.
38. Schrock, R. R.; Murdzek, J. S.; Bazan, G. C.; Robbins, J.; DiMare, M. R. *J. Am. Chem. Soc.* **1990**, *112*, 3875.
39. Gorman, C. B.; Ginsburg, E. J.; Grubbs, R. H. *J. Am. Chem. Soc.* **1993**, *115*, 1397, and references therein.
40. Hotta, S.; Rughooputh, S. D. D. V.; Heeger, A. J.; Wudl, F. *Macromolecules* **1987**, *20*, 212.
41. MacIness, D., Jr.; Funt, B. L. *Synth. Met.* **1988**, *25*, 235.
42. Elsenbaumer, R. L.; Jen, K.; Miller, G. G.; Eckhardt, H.; Shacklette, L. W.; Jow, R. *Electronic Properties of Conjugated Polymer*; Kuzmany, H., Mehrring, M., Roth, S., Eds.; Springer: Berlin, 1987; Vol. 76, pp 400–406.
43. Rehahn, M.; Schluter, A. D.; Wegner, G.; Feast, W. J. *Polymer* **1989**, *30*, 1060.
44. Havinga, E. E.; van Korssen, L. W. *Polym. Bull.* **1988**, *18*, 2777.
45. Grubbs, R. H.; Tumas, W. *Science* **1989**, *243*, 907.
46. Schrock, R. R. *Acc. Chem. Res.* **1990**, *23*, 158.
47. Gilliom, L. R.; Grubbs, R. H. *J. Am. Chem. Soc.* **1986**, *108*, 733.
48. Novak, B. M.; Grubbs, R. H. *J. Am. Chem. Soc.* **1988**, *110*, 7542.
49. Cannizzo, L. F.; Grubbs, R. H. *Macromolecules* **1988**, *21*, 1961.
50. Risse, W.; Wheeler, D. R.; Cannizzo, L. F.; Grubbs, R. H. *Macromolecules* **1989**, *22*, 3205.
51. Johnson, L. K.; Virgil, S. C.; Grubbs, R. H.; Ziller, J. W. *J. Am. Chem. Soc.* **1990**, *112*, 5384.
52. Pudelski, J. K.; Callstrom, M. R. *Organometallics* **1992**, *11*, 2757.
53. Pudelski, J. K.; Callstrom, M. R. *Organometallics* **1994**, *13*, 3095.
54. March, J. *Advanced Organic Chemistry*; Wiley: New York, 1992; Chapter 17.
55. Erickson, M. S.; Fronczek, F. R.; McLaughlin, M. L. *Tetrahedron Lett.* **1992**, *2*, 197.
56. Odian, G. *Principles of Polymerization*; Wiley: New York, 1991.
57. Similar steric constraints have been observed in ring-closing metathesis (RCM) reactions: Kirkland, T. A.; Grubbs, R. H. *J. Org. Chem.* **1997**, *62*, 7310.
58. Scott, A. I. *Interpretation of the Ultra-violet Spectra of Natural Products*; MacMillan: New York, 1964.
59. Mohammad, F. Degradation and Stability of Conductive Polymers. In: *Handbook of Organic Conductive Molecules and Polymers*; Wiley: New York, 1996, Vol. 3, Chapter 16.
60. Ito, T.; Shirakawa, H.; Ikeda, S. *J. Polym. Sci. Chem.* **1975**, *13*, 1943.
61. Kovacic, P.; Kyriakis, A. *J. Am. Chem. Soc.* **1963**, *85*, 454.
62. Nguyen, M. T.; Diaz, A. F.; Dement'ev, V. V.; Pannell, K. H. *Chem. Mater.* **1993**, *5*, 1389.
63. Nguyen, M. T.; Diaz, A. F.; Dement'ev, V. V.; Pannell, K. H. *Chem. Mater.* **1994**, *6*, 952.
64. Flanagan, J. B.; Margel, S.; Bard, A. J.; Anson, F. C. *J. Am. Chem. Soc.* **1978**, *100*, 4248.
65. Nelson, J. M.; Rengel, H.; Manners, I. *J. Am. Chem. Soc.* **1993**, *115*, 7035.
66. Hoffmann, R. *J. Chem. Phys.* **1963**, *39*, 1397.
67. Whangbo, M.-H.; Hoffmann, R. *J. Am. Chem. Soc.* **1978**, *100*, 6093.
68. Whangbo, M.-H.; Ren, J.; Weigen, L. *CAESAR*; North Carolina State University: Raleigh, 1998.
69. Whangbo, M.-H.; Hoffmann, R.; Woodward, R. B. *Proc. R. Soc. London A* **1979**, *366*, 23.
70. Albright, T. A.; Burdett, J. K.; Whangbo, M. H. *Orbital Interactions in Chemistry*; Wiley: New York, 1985.
71. See for example, Barlow, S.; Cowley, A.; Green, J. C.; Brunker, T. J.; Hascall, T. *Organometallics* **2001**, *20*, 5351, and references therein.



Rational design of a nanoscale helical scaffold derived from self-assembly of a dimeric coiled coil motif

Yuri Zimenkov,^a Vincent P. Conticello,^{a,*} Liang Guo^b and Pappannan Thiagarajan^b

^aDepartment of Chemistry and Center for the Analysis of Supramolecular Self-assembly, Emory University, 1515 Dickey Drive, Atlanta, GA 30322, USA

^bIntense Pulsed Neutron Source, Argonne National Laboratory, Argonne, IL 60439, USA

Received 5 April 2004; revised 7 June 2004; accepted 14 June 2004

Abstract—We describe a model for the design of synthetic α -helical peptides that are competent for self-assembly into structurally defined supramolecular fibrils on the basis of architectural features that have been programmed into the peptide sequence. In order to test the validity of this experimental model, we have synthesized an oligopeptide **YZ1** that was designed to conform to this model and to self-assemble into an α -helical fibril in which the structural sub-units that comprise the fibril corresponded to coiled coil dimers. Peptide **YZ1** was prepared via conventional solid-phase peptide synthesis and was composed of 42 amino acid residues such that the sequence defined six distinct heptad repeats of a coiled coil structure. The sequence of **YZ1** was designed to adopt an α -helical conformation in which the helical protomers self-associate in a parallel orientation with a staggered orientation between adjacent peptides that corresponded to an axial displacement of three heptads. The self-assembly of peptide **YZ1** was examined at varying levels of structural hierarchy for compliance of the observed structures with the experimental model. Circular dichroism spectroscopy provided evidence for an α -helical coiled coil structure for **YZ1** in aqueous solution, which could be reversibly denatured through thermal methods. TEM measurements indicated the formation of long aspect-ratio fibers of uniform diameter from aqueous solutions of **YZ1**, however the dimensions of the fibers suggested that lateral association occurred between the fibrils corresponding to the 2-stranded helical bundles. The α -helical coiled coil structure was confirmed in the solid-state for fibers derived from self-assembly of **YZ1** by a combination of wide-angle X-ray diffraction and ¹³C CP/MAS NMR spectroscopy. SANS and synchrotron SAXS measurements on dilute aqueous solutions of **YZ1** provided a fibril diameter that corresponded to the lateral dimensions estimated for a dimeric coiled coil assembly on the basis of structural determinations of model peptides.

© 2004 Elsevier Ltd. All rights reserved.

1. Introduction

One of the most promising approaches to the fabrication of multi-functional nano-scale devices involves the self-assembly of molecular components to form ordered arrays on the nanometer to micrometer length scale. However, a critical challenge to this process lies in the rational design of synthetic materials that can self-assemble into structurally defined supramolecular aggregates that are capable of functioning as the components of these devices. In contrast, biological macromolecules routinely operate within the nano-scale size regime to create the complex supramolecular machinery that performs the chemical, electrical, and mechanical functions associated with cellular metabolism, communication, and differentiation.¹ These complex biological machines arise from self-assembly on the basis of structural features programmed into polypeptide and

polynucleotide sequences at the molecular level. As a consequence of the near-absolute control of macromolecular architecture that results from such sequence specificity, biological structural platforms may have advantages for the creation of well-defined supramolecular assemblies in comparison to synthetic polymers. Thus, the conceptual design of synthetic nano-scale devices can derive significant information from structural investigations of biologically derived supramolecular assemblies and, conversely, biological structural motifs present an attractive target for the synthesis of artificial nano-scale systems on the basis of relationships between sequence and supramolecular structure that have been established for native biological assemblies. One can envision that the structural principles implicit in biological systems can be employed for the design and construction of non-native, nano-scale materials that display the structural specificity and the chemically and spatially unique functional group presentation of native biomolecular assemblies. We describe a model for the construction of nano-scale scaffolds derived from α -helical structural motifs and demonstrate that a synthetic

Keywords: Self-assembly; Peptide chemistry; Nanotechnology.

* Corresponding author. Tel.: +1-4047272779; fax: +1-4047276586; e-mail address: vcontic@emory.edu

oligopeptide can be designed to self-assemble into macroscopic fibril as a consequence of structural features programmed into its sequence at the molecular level using the criteria of this model.

Within the last few years, synthetic peptides based on α -helix and β -strand sequence motifs have been described that self-assemble into structurally defined supramolecular aggregates in which the thermodynamics of self-assembly of the peptides has been exploited for the creation of novel nano-scale materials.^{2–12} Although self-assembling β -sheet peptides derived from amyloid and similar synthetic amino acid sequences are being actively scrutinized as functional nanoscale materials,^{2–8} the design of self-assembled fibrils derived from α -helical protomers has not advanced to a similar extent. Helical scaffolds differ in critical structural features from β -sheet assemblies, including the periodicity of the structural repeat and the peptide orientation relative to the long axis of the fibril, which suggests that helical protomers may be effectively considered as complementary modules to β -strands for the construction of functional nanoscale materials. Moreover, in contrast to amyloidogenic peptides, the principles that govern the association of helical protomers into discrete coiled coil assemblies¹³ have been elucidated in detail on the basis of structural studies of model peptides such as leucine zippers.^{14–16} However, the potential of these helical peptides for the construction of well-defined protein fibrils remains largely untapped, despite the fact that prototypes for fibrils derived from α -helical coiled coil motifs occurs widely in native biological systems such as cytoskeleton and extracellular matrix.¹⁷ Thus, α -helical proteins are an attractive target for de novo engineering of structurally-defined fibrils from self-assembly of synthetic helical protomers.

Potekhin, et al.¹⁰ recently proposed a structural model for the rational design of α -helical fibril assemblies to account for the formation of a five-stranded coiled coil¹⁸ fiber from self-assembly of a thirty-four residue oligopeptide, $[Q_cL_dA_eR_fE_gL_a(Q_bQ_cL_dA_eR_fE_gL_a)_4]$,¹⁹ derived from the heptad repeat sequence (a-b-c-d-e-f-g) of a leucine zipper motif. On the basis of this model, an oligopeptide with a heptad repeat sequence can assemble into an ' n '-stranded, α -helical fibril if the axial stagger between adjacent helices (Δl) is equivalent to an integral number of heptads (Fig. 1). Thus, an oligopeptide consisting of thirty-five residue equivalents (thirty-four amino acids and a one-residue spacer) can self-assemble into a five-stranded helical fibril with an axial stagger equivalent to a single heptad (seven residues) as shown in Figure 1. A set of magic numbers for the self-assembly of α -helical fibrils of variable degree of oligomerization was defined by Eq. (1) as follows:

$$(L + \delta l)/n = \Delta l \quad (= 7, 14, 21, \text{etc.}) \quad (1)$$

where n =degree of oligomerization of the helical bundle (typically 2, 3, 4, or 5), L =amino acid residues comprising the oligopeptide (generally 25–50), δl =residue equivalents (usually 0 or 1, for a single space between successive helices), Δl =axial stagger in residues between adjacent helices in the bundle.

The implications of this model may be extended to include coiled coil fibers with different degrees of oligomerization

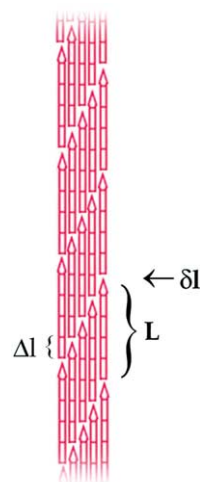


Figure 1. Schematic representation of the self-assembly of an α -helical protomer into a five-stranded fibril according to the model of Potekhin, et al.¹⁰ in which the axial stagger between successive peptides in the fibril corresponds to a single heptad repeat.

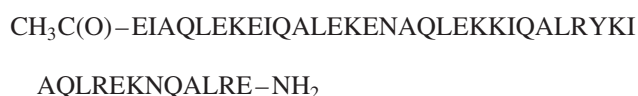
by incorporation of design principles initially determined from model studies of short leucine zipper domains. The oligopeptide described in the latter study assembled into a five-stranded, α -helical fibril despite the fact that its sequence lacked design elements previously postulated to critically influence the formation of specific helical associations in leucine zipper peptides.¹⁰ For example, the core residues at the a- and d-positions of the helicogenic peptide were composed entirely of leucine residues, which have been shown to be compatible with helical oligomerization states from two through five. In addition, the usual electrostatic interactions between e and g residues on adjacent helices were clearly precluded in the sequence of the peptide by the absence of basic residues at the e positions. Not surprisingly, fibril formation occurred only at relatively low pH (≤ 5) in which the partially buried glutamic acid residues at the g positions in the sequence would be protonated and uncharged at the helical interface.²⁰ The coiled coil domains in native proteins usually display precise registration of adjacent helices and a defined oligomerization state, which may be necessary for appropriate function in their specific biological role. These functional considerations may impose stringent requirements on the sequence of the native heptad repeats to impart the necessary structural specificity. In contrast, α -helical fibril formation may have more relaxed constraints as sequences that do not fulfill the criteria of Eq. (1) would be de-stabilized relative to those that do, and, consequently, would not be capable of forming thermodynamically stable fibrils. Moreover, the sequences of potential fibrillogenic peptides could be chosen such that the hydrophobic interactions between the core a and d residues and the electrostatic interactions between proximal e and g residues would reinforce the preferred oligomerization state and the staggered orientation of adjacent helices implicit in the magic number formalism of Eq. (1). Thus, from a consideration of the proposed model and the known structural preferences of coiled coils, it is envisioned that heptad sequences can be designed that would strongly favor particular oligomerization states upon self-assembly of the peptide.

2. Results and discussion

2.1. Design criteria

Several critical structural features must be considered in the design of peptide sequences that are competent for self-assembly into helical fibrils of defined strandedness (n). These design parameters can be inferred from the model of Potekhin, et al.¹⁰ and include the coiled coil oligomerization state, the relative orientation between adjacent helices, and the potential for lateral association between coiled coil assemblies. Rational design of α -helical fibrils was predicated on the assumption that the sequence-structure correlations deduced from model studies of native coiled coil proteins can be extended to fibril-forming peptide systems. We hypothesized that the structural criteria that influence formation of parallel, in-register coiled coils can be re-defined to accommodate the formation of helical fibril assemblies with staggered orientation between adjacent peptides as in Figure 1. In order to explore the implications of this hypothesis in the context of the model of Figure 1, we have synthesized an oligopeptide, **YZ1**, which, on the basis of our initial design, should self-assemble into α -helical fibrils derived from a dimeric coiled coil structural unit.

YZ1



The sequence of peptide **YZ1** comprised six heptad repeats and was compatible with the design rules previously described for the engineering of supramolecular assemblies of α -helical coiled coils.¹⁰ The initial design focused on a coiled coil dimer due to the ubiquitous occurrence of these structures in native α -helical fibrils such as tropomyosin.²¹ The core residues of **YZ1** were chosen to favor the formation of a dimeric assembly under the structural

formalism of the Potekhin model. Structural studies of oligopeptides based on the coiled coil domain of GCN4 indicated that dimer formation was thermodynamically favored for heptad sequences in which isoleucine and leucine occupied the a- and d-positions, respectively, of the repeat unit. However several ancillary features were introduced into the peptide to reinforce the formation of a staggered helical array, while preventing the formation of alternative (non-productive) topologies using a negative design strategy (Fig. 2).²² The choice of these elements provides an illustration of the critical structural features involved in the de novo design of α -helical fibrils. For example, the formation of a parallel, in-register homodimer was disfavored by repulsive electrostatic interactions between charged residues at the e'+1 and g positions that would reside at the helical interface.^{23,24} The formation of anti-parallel dimers was anticipated to be energetically unfavorable, as it would result in burial of polar asparagine residues at the dimeric interface such that they are juxtaposed against hydrophobic leucine or isoleucine residues. In the staggered heterodimer, the asparagine residues would occur at the helical interface in apposition, which should result in the formation of a buried hydrogen bond between the amide side chains.^{25–27} However, in a staggered parallel orientation, the N- and C-terminal halves of the adjacent protomers should align against each other across the helical interface since the critical structural interactions have been designed to reinforce this orientation within a dimeric coiled coil structural unit. Thus, self-assembly of **YZ1** should afford a dimeric helical fibril in which adjacent protomers are packed such that an axial stagger corresponding to three heptads occurs between successive peptides in the supramolecular assembly (Fig. 2).

2.2. Structural analysis

Ultimately, the success of this approach to the synthesis of supramolecular helical assemblies depended on the ability to analyze the implications of the peptide design in terms of

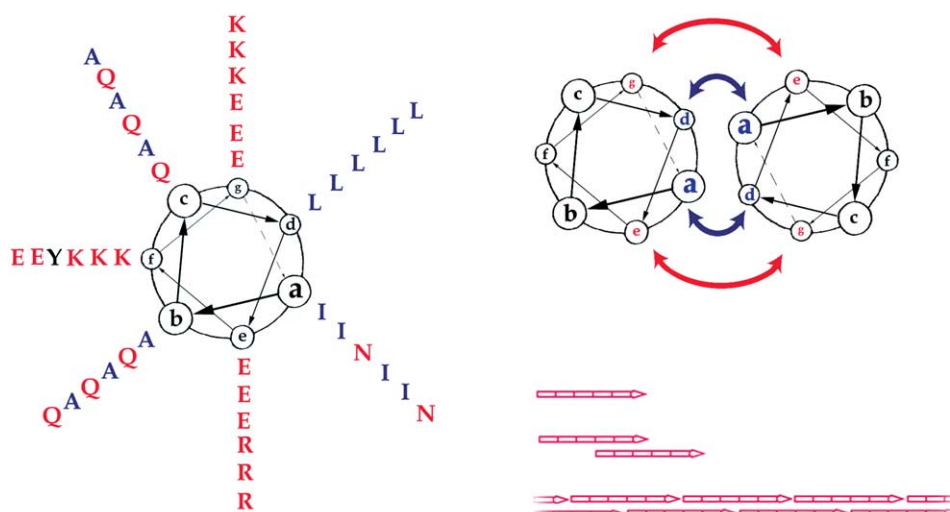


Figure 2. (A) Helical wheel projection of the **YZ1** sequence. (B) Schematic representation of the critical interactions that determine inter-helix alignment in the dimeric coiled coil assembly. Blue arrows indicate hydrophobic and buried polar interactions between core (a,d) residues, while the red arrows indicate electrostatic interactions between proximal (e,g) residues. (C) Schematic representation of the packing arrangement of adjacent helical protomers corresponding to **YZ1**. Note that in a parallel orientation the combination of buried polar interactions and electrostatic interactions should enforce a staggered alignment between helical protomers in which the axial displacement corresponds to three heptads ($\Delta l=21$).

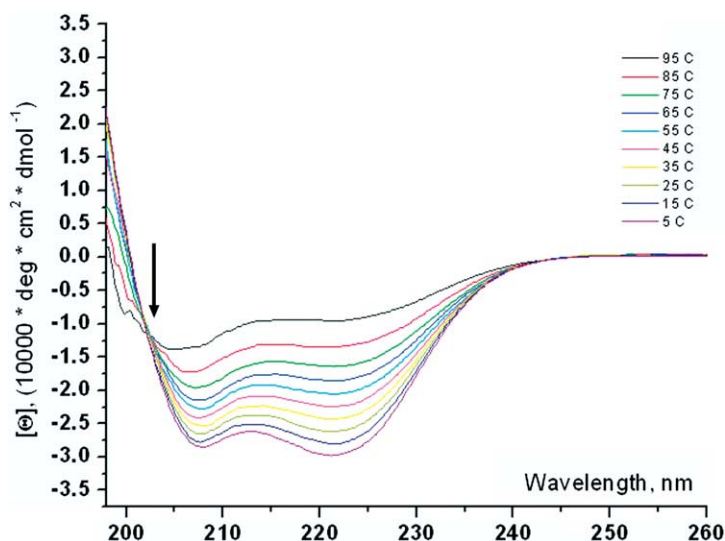


Figure 3. Temperature dependence of the circular dichroism spectra of peptide **YZ1** (82.78 μM) in 10 mM MOPS buffer. The arrow indicates the presence of an isodichroic point in the thermal unfolding curve of **YZ1** ($\lambda=202.3$ nm; $[\Theta]=-11700$ deg cm^2 dmol^{-1}).

the fibril structure at different levels of structural hierarchy. The use of analytical techniques that interrogated structural detail on a variety of length scales was required to develop a complete picture of fibril self-assembly and validate the structural model employed for design of the peptides. The application of these techniques is summarized in the context of the structural information that they provided with respect to the formation and stability of the protein fibril derived from self-assembly of **YZ1**. Note that, in these investigations, we use terminology in which fibril corresponds to a single '*n*'-stranded helical rope and fiber corresponds to bundles that arise from lateral association of these fibrils.

2.2.1. Solution peptide conformation and thermodynamics of self-assembly. Circular dichroism (CD) spectroscopy is a critical tool for structural investigation of polypeptide conformation in solution and for the correlation of the solution thermodynamics and kinetics of self-assembly with secondary structure development within the peptide. The CD signature for α -helices is distinctive with characteristic minima at 208 and 222 nm. The ratio of the mean residue ellipticity of these two signals provides information regarding the presence of a coiled coil structure with respect to unassociated α -helices.²⁸ The CD spectra of **YZ1** clearly indicated the formation of an α -helical coiled coil structure in aqueous solution (Fig. 3). The stability of the helical assembly demonstrated a marked temperature dependence in which the fractional helicity approached uniformity at 4 °C. The ratio of the mean residue ellipticity ($\theta_{222}/\theta_{208}$) was consistent with a coiled coil structure at lower temperatures. The maximal value of 1.04 at 4 °C was within the expected range for coiled coil structures on the basis of CD studies of model peptides. Moreover, a melting transition was observed at 83 °C, which suggested that thermal denaturation of the helical structure occurred at elevated temperature. In support of this hypothesis, an isodichroic point was observed in the CD manifold at a wavelength of 202 nm, which has been implicated as indicative of a two-state transition between a folded helical state and an unfolded random coil state.^{29,30} The CD melting behavior showed a strong concentration depen-

dence (data not shown), in which the T_m increased with increasing peptide concentration as would be expected for a self-association phenomenon. The melting transition of the supramolecular assembly was confirmed via differential scanning calorimetry (DSC) measurements on aqueous solutions of **YZ1** under similar conditions to the CD melting experiment. The DSC data indicated a reversible endothermic transition that correlated with the CD melting behavior and ascertained that thermal denaturation of **YZ1** occurred at elevated temperature (Fig. 4). The observed melting temperatures from DSC measurements of **YZ1** ($T_m=93.6$ °C at 132 μM and 101.1 °C at 680 μM of peptide, respectively) were higher than that observed via CD melting behavior, although this was attributed to the higher concentrations of the peptide employed in the DSC experiment. Notably, a heat capacity increment (positive ΔC_p) was associated with the DSC melting transition, which suggested that thermal denaturation resulted in disruption of non-covalent interactions.³¹ Although the ΔC_p could not be

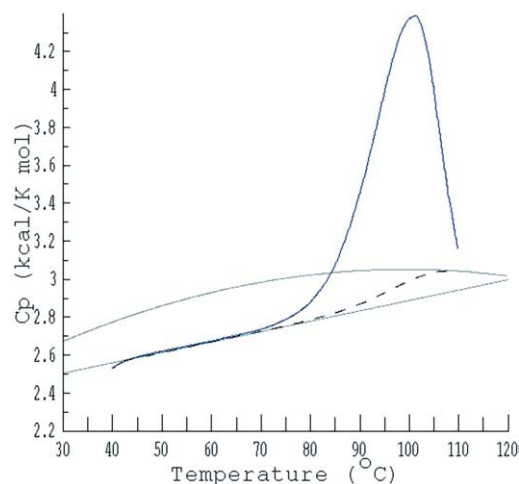


Figure 4. DSC data for endothermic thermal transition of a dilute aqueous solution of peptide **YZ1** (680 μM peptide in 10 mM MOPS pH 7.0 and $P=3$ atm). The dashed line indicates the change in baseline as a function of the transition and provides an estimate of the value of the ΔC_p .

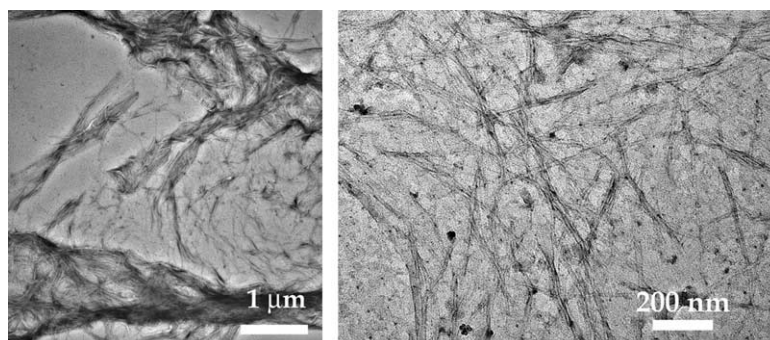


Figure 5. TEM images of fibrils derived from self-assembly of **YZ1** (1 mg/mL) in 10 mM MOPS buffer. The solution of the peptide was heated to 100 °C to denature the nascent structure and slowly cooled over a period of 3 h to the annealing temperature of 4 °C. Fibers were visualized through negative staining with 1% uranyl acetate.

measured accurately due to the absence of a stable baseline in the DSC measurements subsequent to the melting transition, the estimated value of ΔC_p was within the range reported for thermal denaturation of dimeric coiled coil structures.³² Thus, both CD and DSC measurements provided evidence that peptide **YZ1** folds into a coiled coil assembly and can be reversibly denatured through thermal methods.

2.2.2. Fiber assembly and morphology. The design of **YZ1** was based on the structural criteria of Potekhin, et al.¹⁰ in which the molecular level features of the sequence were chosen to favor self-assembly of the peptide into a 2-stranded helical fibril with a staggered orientation between adjacent protomers corresponding to three heptads (Fig. 2). We anticipated that the observation of a stable α -helical signature in the solution CD spectra of **YZ1** implied the formation of a fibrous morphology as a consequence of the structural model that formed the basis of the sequence design. However, neither CD spectroscopy nor DSC measurements were capable of providing direct evidence for fibril formation. Transmission electron microscopy (TEM) was employed to investigate the morphology of aggregates that might result from self-assembly of dilute aqueous solutions of **YZ1**. Counter to our expectations, TEM studies uncovered no evidence for fibril formation from nascent specimens of **YZ1** from aqueous solution, despite the fact that a stable α -helical signature was observed in the CD spectra that was consistent with coiled coil formation. However, if the peptide solution was heated above the melting temperature of the helical bundle and slowly cooled to 4 °C, TEM studies indicated the presence of long aspect-ratio fibers that displayed a uniform diameter and the absence of branch formation (Fig. 5). The diameter of the fibers varied as a function of the temperature and time associated with the annealing process, as has been previously observed for other synthetic fibrillogenic peptide systems,^{9,11} and usually ranged from approximately 20–50 nm under the conditions employed in these studies. We noted that the diameters of the fibrils observed in the TEM measurements of **YZ1** in Figure 5 were at least an order of magnitude larger than the expected diameter for a dimeric coiled coil (vide infra), which suggested the possibility that fibrils that arise from self-assembly of **YZ1** undergo lateral association to form larger fibers. This process may be facilitated through electrostatic interactions between charge-complementary

(Lys/Glu) residue pairs that occupy the f-positions of the heptad repeats within the **YZ1** sequence. This situation is consistent with a model in which lateral association occurred as a result of multiple, non-covalent interactions between residues at non-core positions in adjacent fibrils. However, alternative explanations were also possible for the discrepancy between the observed and expected diameters of the fibrils, in particular, the formation of alternative peptide architectures; the most likely of which correspond to amyloid-like fibrils derived from self-association of β -strands.

2.2.3. Solid-state peptide structure. Supramolecular assemblies display correlation times that are inaccessible for conventional solution-phase NMR and their paracrystalline nature renders such structures equally unsuitable for single crystal X-ray structural determinations. Nonetheless, the solid-state structural information that these techniques provide is vital to assess the validity of the structural model for self-assembly that was originally proposed as the basis of fibril formation and to rule out alternative structural arrangements. In particular, the formation of protein fibrils has been closely associated with the self-assembly of amyloid-like structures that consist of hydrogen-bonded β -sheet subunits. As these fibrils can result from the misfolding of highly α -helical proteins,³³ it was necessary to ascertain that the protein fibrils described herein retain the α -helical structure of the protomers within the supramolecular aggregate. While CD spectroscopy can interrogate for α -helical structure of the peptides in solution, it does not preclude an α -helix-to β -sheet structural rearrangement that would result in the formation of a self-assembled amyloid-like fibril.^{34–36}

Wide-angle X-ray scattering (WAXS) measurements were employed to investigate the structure of the fibril in the solid state and verified the presence of an α -helical coiled coil structure. Concentrated peptide solutions (50–100 mg/mL of **YZ1** in 10 mM MOPS buffer) were thermally denatured and slowly cooled to ambient temperature to form an extremely viscous solution. Large diameter peptide fibers could be prepared from these solutions via extrusion through a syringe under electric field alignment to promote orientation of the protomers within the specimen. The fibers prepared under these conditions displayed diffraction patterns that were characteristic of oriented specimens in which the observed lattice spacings were consistent with a

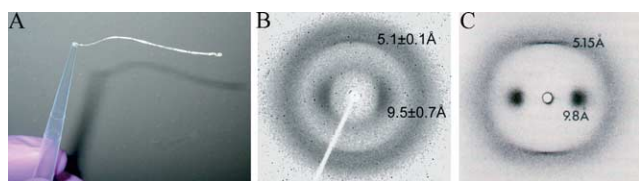


Figure 6. (A) A fibrous specimen of **YZ1** prepared via extrusion of a concentrated solution of annealed peptide under electric field alignment. (B) Fiber diffraction pattern and associated lattice spacings for the oriented fiber derived from **YZ1**. (C) Fiber diffraction pattern and associated lattice spacings for a specimen of alpha keratin derived from porcupine quill (reproduced with permission from Ref.37).

coiled coil structure (Fig. 6).³⁷ A fingerprint reflection at approximately 5.1 Å was observed on the meridian with vertical alignment of the fiber relative to the X-ray beam. This spacing is directly related to the pitch projection of an α -helix along the coiled coil axis, and contrasts with the 5.4 Å spacing that is associated with non-coiled α -helices. In addition, an equatorial reflection was observed at ca. 9.5 Å for the oriented specimen, which corresponded to the mean distance between the axes of adjacent α -helices in the bundle (usually 9.3–9.8 Å for α -helical coiled coil structures). The observed diffraction pattern for the oriented fibers were in agreement with diffraction patterns previously reported for native α -helical assemblies based on coiled coil structural motifs such as the alpha keratin signature of porcupine quill (Fig. 6).³⁸ Note that the fiber diffraction patterns derived from α -helices and β -sheets can be easily distinguished due to difference in the metrical parameters associated with the structural repeat and the peptide orientation with respect to the fibril axis.³⁸ For example, the beta keratin pattern that arises from mechanical deformation of alpha keratin differs dramatically with respect to the position and orientation of the lattice spacings.

Although WAXS data provide information on the peptide conformation within the fiber, alternative approaches that do not rely on mechanical fabrication or macroscopic orientation of concentrated specimens could facilitate investigation of structural development within the fiber under different preparative conditions. High-resolution solid state NMR has revolutionized the structural investigation of paracrystalline assemblies,³⁹ and offers a complementary approach to X-ray fiber diffraction studies for the analysis of peptide conformation and orientation within fibrillar structures. The local conformation of specific amino acid residues in the solid state can be deduced from the ¹³C or ¹⁵N CP/MAS NMR chemical shifts of appropriately labeled amino acids that have been incorporated at specific sites in the sequence during peptide synthesis.⁴⁰ The position of the chemical shift is often diagnostic for a particular secondary structure (α -helix, β -sheet, or random coil) although the observed shift often depends on the atomic position (N, CO, C α , C β) at which the isotopic substitution occurs within the labeled amino acid. In order to investigate the local conformation of the core residues, a variant of **YZ1** was prepared in which the core leucine residue at position 19 was labeled at the structurally sensitive carbonyl carbon with the ¹³C isotope. Concentrated peptide specimens (50–100 mg/mL) were prepared in aqueous buffer (10 mM MOPS, pH 7.0) and thermally denatured and annealed at 25 °C. The aqueous solvent was removed in vacuo to afford

the solid specimen. Solid-state ¹³C CP/MAS NMR spectroscopy of the labeled specimen of **YZ1** indicated a chemical shift of 177.2 ppm for the labeled carbon atom of Leu(19). This resonance was shifted significantly downfield with respect to the average random coil chemical shift of the leucine carbonyl group (mean value of 174.7 ppm) into the expected range for an α -helical conformation (mean value of ca. 176.6 ppm).⁴⁰ The ¹³C chemical shift of the carbonyl group of the Leu(19) residue can be compared with the chemical shift of the corresponding resonances in the ¹³C CP/MAS NMR spectra of the α -helical and β -sheet forms of poly(leucine), which are observed at 175.8 and 171.3 ppm, respectively.^{41,42} Using the poly(leucine) resonances as benchmarks, the ¹³C chemical shift of the carbonyl group of Leu(19) clearly suggested that this residue, and, by implication, the **YZ1** peptide, adopted an α -helical conformation in the solid state. Thus, the WAXS and ssNMR data were consistent with an α -helical coiled coil structure within the fibrils of **YZ1**, however these experimental methods could not distinguish between alternative coiled coil oligomerization states, i.e. dimer, trimer, tetramer, or pentamer, to determine the fundamental building block of the ordered assembly.

2.2.4. Determination of fibril dimension. The design of **YZ1** was based on a dimeric coiled coil sequence motif, which implied that the fundamental structural sub-unit of the peptide assembly corresponded to a 2-stranded helical fibril derived from staggered self-assembly of **YZ1**. However, the TEM evidence suggested that lateral association of the helical fibrils must occur during self-assembly as the diameters of the fibers exceeded those expected for a hypothetical 2-stranded helical fibril by at least an order of magnitude. These measurements provided little information regarding the internal structure of the fibers and, consequently, could not be employed to determine the nature of the structural sub-units from which the fiber was composed. Small-angle neutron scattering (SANS) and synchrotron small-angle X-ray (SAXS) scattering experiments⁴³ were employed to ascertain the identity of the structural sub-unit within the fibers in aqueous solution. These techniques provide direct low resolution information on the size, morphology and composition of macromolecular complexes in solution under realistic conditions of concentration and temperature. The maximum sensitivity of these techniques lies within the size regime from 1 to 50 nm, which corresponds to the expected lateral dimension of the self-assembled fibrils.^{8,44–49}

SANS and synchrotron SAXS data were collected for dilute aqueous solutions of **YZ1** under similar conditions of concentration and temperature. The differential neutron and X-ray scattering cross-sections for the peptide assemblies were interpreted using a modified Guinier analysis for a rod-like particle (Fig. 7).⁴⁴ Two distinct slopes were observed in the modified Guinier plot of the synchrotron SAXS data for aqueous solutions of **YZ1** in which the slope at higher values of Q (data not shown) corresponded to that observed in the corresponding plot of the SANS data in Figure 7 (A). The scattering data in this region can be interpreted in terms of a uniform cylinder in which the cylindrical cross-sectional diameter was on the approximate length scale corresponding to the expected diameter of the 2-stranded

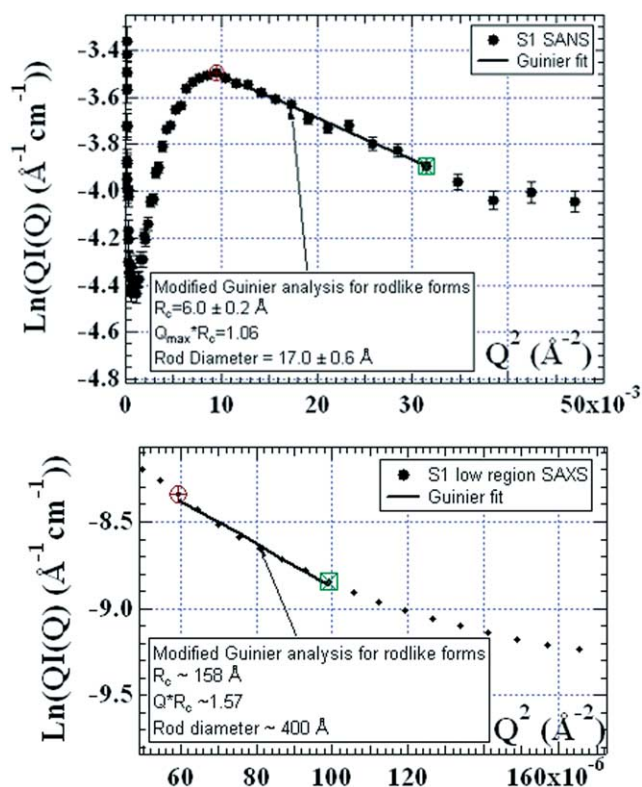


Figure 7. (A) Modified Guinier plot of SANS scattering data in the mid-Q (fibril) region for a D₂O solution of **YZ1** (10 mg/mL in 10 mM MOPS buffer, pH 7.0). (B) Modified Guinier plot of the synchrotron SAXS scattering data in the low-Q (fiber) region for an aqueous solution of **YZ1** (1 mg/mL in 10 mM MOPS buffer, pH 7.0).

helical fibril that was envisioned as the fundamental structural sub-unit of the assembly. The cross-sectional radius of gyration was calculated from this analysis and employed to determine the average diameter of the fibril, which was compared to values derived from the crystallographically determined structures of dimeric helical bundles. A minimal diameter of 14.8 Å was estimated for a coiled coil dimer based on the sum of the average diameters of an α -helix (5.04 Å) and the super-helix of the coiled coil dimer (9.8 Å), which were determined from the Crick parameterization³⁷ of the dimeric coiled coil structure and the average metrical values extracted from the structural database.⁵⁰ As these diameters are calculated from the C α trajectory of the polypeptide chain, they represent a lower limit for the diameter of the structure as they do not account for steric contributions from the amino acid side chains. The estimated diameter for a dimeric coiled coil structure was compared to the calculated diameters derived from the modified Guinier analyses of the small-angle neutron and X-ray scattering data for **YZ1**, $17.0 \pm 0.6 \text{ \AA}$ and $17.1 \pm 0.2 \text{ \AA}$, respectively. The correspondence between these theoretical and observed diameters suggested that the fundamental structural sub-unit of the fiber was compatible with a 2-stranded helical fibril derived from a dimeric coiled coil assembly, which was in agreement with the sequence-structure correlations that formed the basis of the design of peptide **YZ1**. In addition, the large slope in the low-Q region of the SAXS data indicated the existence of a distribution of higher-order assemblies with lateral dimensions corresponding to tens of nanometers (Fig. 7 (B)). The

modified Guinier analysis of the small-angle X-ray scattering cross sections at lower values of Q could be fit to a model for a cylindrical rod and was employed to estimate the average diameter of the larger assemblies. Although a single effective cross-sectional diameter could not be extracted from the low Q data, the average diameter of 40 nm for the assembly agreed substantively with the diameters of the fibers calculated from TEM measurements. These data support a structural model in which the fibers that are observed in TEM measurements and inferred from the low- Q synchrotron SAXS data arise from lateral association of the 2-stranded helical fibrils that were detected from SANS and SAXS measurements in the mid- Q region.

3. Conclusion

This investigation constituted an experimental verification of the Potekhin model¹⁰ as a structural guide for the de novo design of α -helical peptide sequences that were capable of self-assembly into structurally defined protein fibrils. We observed the formation of long aspect-ratio helical fibers of uniform diameter from self-assembly of the synthetic peptide **YZ1** upon thermal annealing of aqueous solutions under controlled conditions. The structural data supported the hypothesis that the fibers arose from lateral association of fibrils in which the fundamental structural sub-unit corresponded to a dimeric α -helical coiled coil assembly that formed the basis for the original design of **YZ1**. This initial research effort was directed toward elucidation of the sequence-structure relationships that define the scope of the self-assembly process in terms of the supramolecular architecture of the aggregates in a single model system derived from a dimeric coiled coil. However, several key challenges remain in the extension of this process to more structurally complex assemblies based on coiled coil trimers, tetramers, and pentamers, particularly with regard to defining unique interactions that specify registration between adjacent helical protomers in the bundle. Therefore, the scope of the self-assembly process remains to be established with regard to the range of accessible supramolecular structures. However, the successful accomplishment of this process would provide a versatile manifold of helical scaffolds that may be employed as components of nano-scale devices. We envision that the self-assembly of synthetic α -helical fibrils derived from oligopeptide modules can serve as a test bed to evaluate the potential of de novo design for the construction of functional supramolecular structures. Ultimately, this process would facilitate the creation of novel, functional nano-scale materials that could take advantage of the structural definition implicit in the self-assembly of these unique, biomimetic materials.

4. Experimental

4.1. Materials and methods

Peptide **YZ1** and the [¹³C]-Leu(19) analogue were prepared via automated solid phase peptide synthesis on a Tenta-Gel RAM resin (Rapp Polymere, GmbH) using a

Rink amide linker. Standard Fmoc protection chemistry⁵¹ was employed with coupling cycles based on HBTU/NMM-mediated activation protocols and base-induced deprotection (20% piperidine in DMF or NMP) of the Fmoc group. The N-terminus of the peptides was capped with acetic anhydride prior to cleavage from the resin. The oligopeptide was isolated from the resin as C-terminal amides after acidic cleavage of the side chain protecting groups and purified via reverse phase high performance liquid chromatography on a C18 column with a gradient of water–acetonitrile (0.1% trifluoroacetic acid). The purity was assessed to be above 97% as demonstrated by MALDI-TOF MS and analytical HPLC. The peptides were lyophilized, sealed, and stored at $-20\text{ }^{\circ}\text{C}$. **YZ1** samples for analytical studies were prepared by dissolving the peptide at the appropriate concentration in aqueous MOPS buffer (10 mM 3-[*N*-morpholino]propane-sulfonic acid, pH 7.0). Annealed specimens were prepared from aqueous solutions of the peptide via thermal denaturation at $100\text{ }^{\circ}\text{C}$ using either a water bath or an automated thermal cycler, followed by slow cooling of the specimen to the annealing temperature, usually 4 or $25\text{ }^{\circ}\text{C}$, over a period of at least 3 h. MALDI-TOF mass spectrum (*m/z*): calcd, 5049; obsd, 5048.

4.2. Physical and analytical measurements

4.2.1. Circular dichroism spectroscopy. CD spectra were recorded on a Jasco J-810 CD spectropolarimeter equipped with a PFD-425S Peltier temperature control unit in 1 mm sealed quartz cells at a concentration of $82.78\text{ }\mu\text{M}$ **YZ1** in MOPS buffer (10 mM, pH 7.0). Spectra were recorded from 260 to 190 nm at a scanning rate of 100 nm/min and a resolution of 0.2 nm. For thermal denaturation studies, the temperature was increased by $2\text{ }^{\circ}\text{C}/\text{min}$ with an equilibration time of 1 min prior to acquisition of each CD trace. The CD data are reported as an average of 10 scans. The peptide concentration was determined spectroscopically by measuring the absorbance at 280 nm (A_{280}). For peptides containing Tyr, Trp or Cys residues, the peptide concentration can be calculated from Eq. (2):

$$MW \times A_{280}/c[\text{mg/mL}] = 1280n_Y + 5690n_W + 120n_C \quad (2)$$

in which n_Y , n_W and n_C are the numbers of tyrosine, tryptophan and cysteine residues, respectively, in the peptide sequence.⁵² As peptide **YZ1** contains only a single tyrosine residue per molecule, then $c = MW \times A_{280}/1280$. To eliminate error in determination of absorbance that could arise as a result of UV light scattering due to peptide self-assembly, aqueous solutions of peptide were mixed with 6 M guanidinium chloride in 1:9 v/v ratio and briefly heated $100\text{ }^{\circ}\text{C}$ in sealed tubes to completely denature the sample prior to performing the absorbance measurements.

4.2.2. Differential scanning calorimetry. DSC studies were conducted on aqueous solution of **YZ1** in MOPS buffer (10 mM, pH 7.0) using a Nano II Model 6100 differential scanning calorimeter (Calorimetry Sciences Corp.) An elevated pressure of 3 atm was used during the sample measurement prevent solvent loss due to evaporation at elevated temperatures. Data were acquired within a scanning range of $20\text{--}110\text{ }^{\circ}\text{C}$ at a scanning rate of $1\text{ }^{\circ}\text{C}/\text{min}$ and represent an average of 8 scans. The DSC data were

processed by the program CPcalc ver 2.1 (Applied Thermodynamics, Inc.).

4.2.3. Transmission electron microscopy. TEM specimens were prepared from annealed solutions of **YZ1** (1 mg/mL) in aqueous MOPS buffer (10 mM, pH 7.0). The samples were deposited onto 200 mesh plasma-etched, carbon-coated, copper grids (Structure Probe, Inc.). After a 1–2 min incubation period, excess liquid was wicked away and the specimens were washed and stained with 0.5–1% uranyl acetate in MOPS buffer. The samples were dried overnight and stored in desiccator. TEM measurements were acquired on a JEOL 1210 instrument with a LaB₆ emission filament at an accelerating voltage of 90 kV. Negatives were scanned at 2,000 dpi resolution on a Agfa DuoScan Flatbed Scanner to provide digital versions of the corresponding TEM images for data analysis.

4.2.4. X-ray fiber diffraction. Concentrated solutions (50–100 mg/mL) of **YZ1** were prepared in aqueous MOPS buffer (10 mM, pH 7.0) and were thermally annealed as described above to afford the thermodynamic product. The viscous solution was transferred to a syringe in which an 18 gauge needle was connected to the positive electrode of an electrospinning device. The peptide solution was slowly extruded through the syringe needle under the influence of an electric field formed between the syringe needle and a grounded piece of aluminum foil (15 kV, 20 cm separation distance) to yield macroscopic fibers up to 5 cm in length. The fibers were detached from the device and dried in a desiccator prior to X-ray diffraction analysis. Fiber diffraction patterns were obtained on a Bruker D8 SMART diffractometer (Cu K α X-ray source) with a Hi-STAR area detector, which was calibrated with respect to corundum prior to data acquisition. The intensity of diffraction as a function of the angle 2θ was integrated using the program GADDS version 4.1.15 (Bruker, Inc.). The distances were obtained using Bragg's law, $d = \lambda/(2 \sin \theta)$, where $\lambda = 1.54178\text{ nm}$ is the X-ray wavelength (Cu K α average).

4.2.5. Solid-state NMR spectroscopy. Concentrated solutions (50–100 mg/mL) of $1\text{-}^{13}\text{C}$ -Leu(19)-**YZ1** in aqueous MOPS buffer (10 mM, pH 7.0) were thermally denatured and slowly cooled to ambient temperature over a period of three hours. Solvent was removed at ambient temperature in vacuo to afford a colorless solid. The sample was packed into a standard 4 mm ceramic rotor. The magic angle spinning (MAS) frequency was set at 6 kHz and the frequencies of the observe and the decouple channels were set to 100.5496 MHz (^{13}C) and 399.8403 MHz (^1H), respectively. The spectra were externally referenced to the signal of the glycine carbonyl carbon at 176.03 ppm, which served as a secondary calibrant with respect to tetramethylsilane (TMS) at 0 ppm. Since only one ^{13}C label was introduced, the carbonyl peak at 178.58 ppm was interpreted as primarily arising from the [$1\text{-}^{13}\text{C}$] Leu19 residue. Chemical shift values were obtained for the α -helix and β -sheet forms of polyleucine versus tetramethylsilane (TMS) from Kricheldorf and Muller.^{41,42} Standard chemical shifts for leucine residues in different conformations were recalculated versus TMS by subtraction of an increment of 1.7 ppm from the reported chemical shift values for the respective resonances relative to the solution biomolecular

NMR standard sodium 2,2-dimethyl-2-silapentane-5-sulfonate (DSS).⁵³

4.2.6. SANS/SAXS measurements. SANS experiments were performed at the SAND instrument of the intense pulsed neutron source (IPNS) and synchrotron SAXS were performed at 12-ID of Advanced Photon Source at Argonne National Laboratory. SANS and SAXS measurements were done at **YZ1** concentrations of 10 and 1 mg/mL, respectively, in aqueous (D₂O or H₂O) MOPS buffer (10 mM, pH 7.0) at 25 °C. Peptide specimens were thermally annealed as described above prior to conducting the measurements. The scattering data were corrected for the background scattering from the solvent and the instrument. The scattering data from SAXS and SANS measurements were analyzed as described below. In a dilute system small angle scattering intensity $I(Q)$ can be described as

$$I(Q) = I_0 n(\Delta\rho)^2 V^2 P(Q) + I_b \quad (3)$$

In Eq. (3), I_0 is an instrument constant, n is the number density of particles, $\Delta\rho$ (contrast) is the difference between scattering length densities of particles and the solvent, V is the volume of particles, I_b is the flat background intensity and $P(Q)$ is the particle form factor. Momentum transfer, $Q = (4\pi/\lambda)\sin(\theta/2)$ where λ is the wavelength of neutron or X-rays, and θ is the scattering angle. Significant scattering intensity in the low- Q region provides evidence for the presence of relatively large objects that can be used to determine the length scales of the assemblies of **YZ1** into fibrillar structures. Since $I(Q)$ varies as Q^{-1} for a long infinitely thin rod at low Q the scattering Eq. (3) can be modified as in Eq. (4).

$$I(Q) = \pi M_w C(\rho_p - \rho_s)^2 / (1000 N_A d^2 L) \exp(-Q^2 R_C^2 / 2) \quad (4)$$

Here L is the length of the rod, M_w is the mass per unit length, C is the concentration of the peptide in mg/mL, N_A is Avogadro's number and d is the inverse of the partial specific volume of **YZ1**. The cross-sectional dimensions of the fibrils can be extracted from the modified Guinier analysis for a rod-like form. If the scattering data is available on an absolute scale from a modified Guinier plot $\ln(Q \times I(Q))$ versus Q^2 it is possible to determine both the cross-sectional radius of gyration R_C from the slope of a line fit in a Q region where $Q_{\max} \times R_C \leq 1$ and the mass per unit length of the **YZ1** fibrils from the y-intercept. For a circular cylinder the radius can be obtained from $\sqrt{2}R_C$. Since the system is highly aggregated as a consequence of lateral association, the mass per unit length of the fibrils could not be reliably determined from the scattering data.

Acknowledgements

We acknowledge financial support from NSF (CHE-9875776) and the DOE (ER-15377) grants. We thank Professor David Lynn for helpful discussions, suggestions and peptide synthesis equipment and Dr David Morgan for assistance in peptide synthesis. We are grateful to Dr Robert Apkarian for assistance with transmission electron microscopy (TEM) measurements. We thank Dr Soenke Seifert for assistance with SAXS experiments. This work benefited from the use of IPNS and APS funded by US DOE

Office of Basic Energy Sciences, Division of Material Sciences, under contract W-31-109-Eng-38. The circular dichroism spectropolarimeter was obtained from funds derived from an NSF grant (CHE-0131013).

References and notes

- Ghadiri, M. R.; Tirrell, D. A. *Curr. Opin. Chem. Biol.* **2000**, *4*, 661–662.
- Burkoth, T. S.; Benzinger, T. L. S.; Gregory, D.; Urban, V.; Botto, R.; Thiyagarajan, P.; Meredith, S. C.; Lynn, D. G. *J. Am. Chem. Soc.* **2000**, *122*, 7883–7889.
- Aggeli, A.; Bell, M.; Boden, N.; Keen, J. N.; Knowles, P. F.; McLeish, T. C.; Pitkeathly, M.; Radford, S. E. *Nature* **1997**, *386*, 259–262.
- Aggeli, A.; Nyrkova, I. A.; Bell, M.; Harding, R.; Carrick, L.; McLeish, T. C.; Semenov, A. N.; Boden, N. *Proc. Natl. Acad. Sci. U.S.A.* **2001**, *98*, 11857–11862.
- Choo, D. W.; Schneider, J. P.; Graciani, N. R.; Kelly, J. W. *Macromolecules* **1996**, *29*, 355–366.
- Janek, K.; Behlke, J.; Zipper, J.; Fabian, H.; Georgalis, Y.; Beyermann, M.; Bienert, M.; Krause, E. *Biochemistry* **1999**, *38*, 8246–8252.
- Schneider, J. P.; Pochan, D. J.; Ozbas, B.; Rajagopal, K.; Pakstis, L.; Kretsinger, J. *J. Am. Chem. Soc.* **2002**, *124*, 15030–15037.
- Lu, K.; Jacob, J.; Thiyagarajan, P.; Conticello, V. P.; Lynn, D. G. *J. Am. Chem. Soc.* **2003**, *125*, 6391–6393.
- Pandya, M. J.; Spooner, G. M.; Sunde, M.; Thorpe, J. R.; Rodger, A.; Woolfson, D. N. *Biochemistry* **2000**, *39*, 8728–8734.
- Potekhin, S. A.; Melnik, T. N.; Popov, V.; Lanina, N. F.; Vazina, A. A.; Rigler, P.; Verdini, A. S.; Corradin, G.; Kajava, A. V. *Chem. Biol.* **2001**, *8*, 1025–1032.
- Ogihara, N. L.; Ghirlanda, G.; Bryson, J. W.; Gingery, M.; DeGrado, W. F.; Eisenberg, D. *Proc. Natl. Acad. Sci. U.S.A.* **2001**, *98*, 1404–1409.
- Ghadiri, M. R.; Granja, J. R.; Milligan, R. A.; McRee, D. E.; Khazanovich, N. *Nature* **1993**, *366*, 324–327.
- Burkhard, P.; Strelkov, S. V.; Stetefeld, J. *Trends Cell. Biol.* **2001**, *11*, 82–88.
- O'Shea, E. K.; Klemm, J. D.; Kim, P. S.; Alber, T. *Science* **1991**, *254*, 539–544.
- Harbury, P. B.; Kim, P. S.; Alber, T. *Nature* **1994**, *371*, 80–83.
- Harbury, P. B.; Zhang, T.; Kim, P. S.; Alber, T. *Science* **1993**, *262*, 1401–1407.
- Beck, K.; Brodsky, B. *J. Struct. Biol.* **1998**, *122*, 17–29.
- Malashkevich, V. N.; Kammerer, R. A.; Efimov, V. P.; Schulthess, T.; Engel, J. *Science* **1996**, *274*, 761–765.
- One letter abbreviations for amino acids: A, Ala; E, Glu; G, Gly; H, His; I, Ile; K, Lys; L, Leu; M, Met; N, Asn; Q, Gln; R, Arg; T, Thr; V, Val; and Y, Tyr.
- Substitution of glutamine residues for the glutamic acid residues of the peptide shifted the pH range for self-assembly of the fiber toward neutral pH Melnik, T. N.; Villard, V.; Vasiliev, V.; Corradin, G.; Kajava, A. V.; Potekhin, S. A. *Protein Eng.* **2003**, *16*, 1125–1130.
- Brown, J. H.; Kim, K.-H.; Jun, G.; Greenfield, N. J.; Dominguez, R.; Volkmann, N.; Hitchcock-DeGregori, S. E.; Cohen, C. *Proc. Natl. Acad. Sci. U.S.A.* **2001**, *98*, 8496–8501.

22. Bryson, J. W.; Betz, S. F.; Lu, H. S.; Suich, D. J.; Zhou, H. X.; O'Neil, K. T.; DeGrado, W. F. *Science* **1995**, *270*, 935–941.
23. Marti, D. N.; Jelesarov, I.; Bosshard, H. R. *Biochemistry* **2000**, *39*, 12804–12818.
24. McClain, D. L.; Binfet, J. P.; Oakley, M. G. *J. Mol. Biol.* **2001**, *313*, 371–383.
25. Lumb, K. J.; Kim, P. S. *Biochemistry* **1995**, *34*, 8642–8648.
26. Oakley, M. G.; Kim, P. S. *Biochemistry* **1998**, *37*, 12603–12610.
27. Akey, D. L.; Malashkevich, V. N.; Kim, P. S. *Biochemistry* **2001**, *40*, 6352–6360.
28. O'Shea, E. K.; Rutkowski, R.; Kim, P. S. *Science* **1989**, *243*, 538–542.
29. Walliman, P.; Kennedy, R. J.; Miller, J. S.; Shalongo, W.; Kemp, D. S. *J. Am. Chem. Soc.* **2003**, *125*, 1203–1220.
30. Holtzer, M. E.; Holtzer, A. *Biopolymers* **1992**, *32*, 1675–1677.
31. Cooper, A. *Biophys. Chem.* **2000**, *85*, 25–39.
32. Ibarra-Molero, B.; Makhatazde, G. I.; Matthews, C. R. *Biochemistry* **2001**, *40*, 719–731.
33. Fandrich, M.; Fletcher, M. A.; Dobson, C. M. *Nature* **2001**, *410*, 165–166.
34. Qu, Y.; Payne, S. C.; Apkarian, R. P.; Conticello, V. P. *J. Am. Chem. Soc.* **2000**, *122*, 5014–5015.
35. Zhang, S.; Rich, A. *Proc. Natl. Acad. Sci. U.S.A.* **1997**, *94*, 23–28.
36. Ciani, B.; Hutchinson, E. G.; Sessions, R. B.; Woolfson, D. N. *J. Biol. Chem.* **2002**, *277*, 10150–10155.
37. Crick, F. H. C. *Acta Crystallogr.* **1953**, *6*, 689–697.
38. Fraser, R. D. B.; MacRae, T. P.; Rogers, G. E. *Keratins: Their Composition, Structure, and Biosynthesis*; Charles C. Thomas: Springfield, IL, 1972.
39. Tycko, R. *Annu. Rev. Phys. Chem.* **2001**, *52*, 575–606.
40. Wishart, D. S.; Nip, A. M. *Biochem. Cell Biol.* **1998**, *76*, 153–163.
41. Kricheldorf, H. R.; Muller, D. *Int. J. Biol. Macromol.* **1983**, *5*, 171–178.
42. Kricheldorf, H. R.; Muller, D. *Macromolecules* **1983**, *16*, 615–623.
43. Guinier, A.; Fournet, G. *Small-Angle Scattering of X-rays*; Wiley-Interscience: New York, 1955.
44. Lynn, D. G.; Meredith, S. C. *J. Struct. Biol.* **2000**, *130*, 153–173.
45. Burkoth, T. S.; Benzinger, T. L. S.; Urban, V. S.; Meredith, S. C.; Lynn, D. G.; Thiyagarajan, P. *J. Am. Chem. Soc.* **1999**, *121*, 7429–7430.
46. Thiyagarajan, P.; Burkoth, T. S.; Urban, V. S.; Seifert, S.; Benzinger, T. L. S.; Morgan, D. M.; Gordon, D.; Meredith, S. C.; Lynn, D. G. *J. Appl. Cryst.* **2000**, *33*, 535–539.
47. Yonezawa, Y.; Tanaka, S.; Kubota, T.; Wakabayashi, K.; Yutani, K.; Fujiwara, S. *J. Mol. Biol.* **2002**, *323*, 237–251.
48. Zhu, L.; Kihara, H.; Kojima, M.; Zhou, J. M.; Perrett, S. *Biochem. Biophys. Res. Commun.* **2003**, *311*, 525–532.
49. Yong, W.; Lomakin, A.; Kirkitadze, M. D.; Teplow, D. B.; Chen, S. H.; Benedek, G. B. *Proc. Natl. Acad. Sci. U.S.A.* **2002**, *99*, 150–154.
50. Harbury, P. B.; Tidor, B.; Kim, P. S. *Proc. Natl. Acad. Sci. U.S.A.* **1995**, *92*, 8408–8412.
51. Chan, W. C.; White, P. D. *Fmoc Solid Phase Peptide Synthesis*; Oxford University Press: New York, NY, 2000.
52. Gill, S. C.; Vonhippel, P. H. *Anal. Biochem.* **1989**, *182*, 319–326.
53. Wishart, D. S.; Bigam, C. G.; Yao, J.; Abildgaard, F.; Dyson, H. J.; Oldfield, E.; Markley, J. L.; Sykes, B. D. *J. Biomol. NMR* **1995**, *6*, 135–140.



Reactions of hafnocene stannyl complexes with stannanes: implications for the mechanism of the metal-catalyzed dehydropolymerization of secondary stannanes

Nathan R. Neale and T. Don Tilley*

Department of Chemistry, Center for New Directions in Organic Synthesis, University of California, Berkeley, CA 94720-1460, USA

Received 22 April 2004; accepted 14 June 2004

Available online 4 July 2004

Dedicated to Bob Grubbs, mentor and friend, in recognition of his many seminal contributions to chemistry

Abstract—Reactions of the hydrostannyl complexes $\text{CpCp}^*\text{Hf}(\text{SnHMes}_2)\text{Cl}$ (**2**), $[\text{Me}_2\text{C}(\text{C}_5\text{H}_4)_2]\text{Hf}(\text{SnHMes}_2)\text{NMe}_2$ (**3**) and $\text{CpCp}^*\text{Hf}(\text{SnHMes}_2)\text{OMe}$ (**4**) with Ph_2SnH_2 or $^t\text{Bu}_2\text{SnH}_2$ afforded poly- and oligostannanes of varying molecular weights. The reaction of **2** with 1.2 equiv. of Ph_2SnH_2 produced the oligostannyl complexes $\text{CpCp}^*\text{Hf}(\text{SnPh}_2\text{SnHMes}_2)\text{Cl}$ (**6**, 68%), $\text{CpCp}^*\text{Hf}(\text{SnPh}_2\text{SnHPh}_2)\text{Cl}$ (**7**, 15%), and $\text{CpCp}^*\text{Hf}(\text{SnPh}_2\text{SnPh}_2\text{SnHPh}_2)\text{Cl}$ (**8**, 7%), which may be intermediates in the dehydropolymerization process. Compounds **7** and **8** were observed in higher yields in the reaction of $\text{CpCp}^*\text{Hf}(\text{H})\text{Cl}$ (**1**) with 2 equiv. of Ph_2SnH_2 . Possible mechanisms for the formation of **6**, **7**, and **8** are discussed. Two trialkylstannyl complexes, $\text{CpCp}^*\text{Hf}(\text{SnMe}_3)\text{Cl}$ (**11**) and $\text{CpCp}^*\text{Hf}(\text{Sn}^t\text{Bu}_3)\text{Cl}$ (**12**), were synthesized in good yields from the reaction of **1** with R_3SnH ($\text{R}=\text{Me}$, ^tBu). When a solution of **11** was heated to 100 °C for 1 h, $\text{CpCp}^*\text{Hf}(\text{SnMe}_2\text{SnMe}_3)\text{Cl}$ (**13**) and $\text{CpCp}^*\text{Hf}(\text{SnMe}_2\text{SnMe}_2\text{SnMe}_3)\text{Cl}$ (**14**) were formed, probably via Me_2Sn insertion into Hf–Sn bonds. Based on the known influence of catalyst structure on the molecular weight of polystannanes, and the observations reported herein, it is proposed that the Sn–Sn bond-forming mechanism may involve R_2Sn insertions into M–Sn bonds.

© 2004 Elsevier Ltd. All rights reserved.

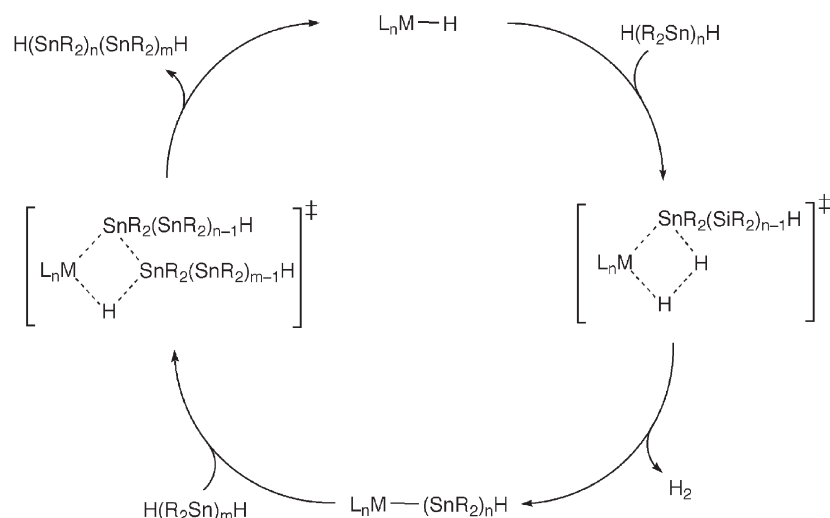
1. Introduction

Polysilanes, $(-\text{RR}'\text{Si}-)_n$, the silicon analogs of polyalkenes, have attracted considerable interest due to their commercial potential. These silicon polymers possess useful electronic properties and have been extensively studied with respect to applications as electro-optical coatings on semiconductor substrates and as photoresists in microlithography.^{1,2} Polymers with heavier atoms (e.g., germanium, tin, and lead) in the backbone are expected to lead to higher photochemical reactivity and narrower band gaps.³ The successful synthesis of high molecular weight polystannanes has recently facilitated the examination of their structural and electronic properties. For example, we have shown that the $\sigma-\sigma^*$ transitions for poly(dialkyl)stannanes are red-shifted by ca. 30–70 nm with respect to those for comparable polysilanes.⁴ Although a number of synthetic methods have been used to access polystannanes,⁵ the highest molecular weight samples (M_w up to 66,000) are prepared by the metal-catalyzed dehydropolymerization of secondary stannanes.^{5k,6}

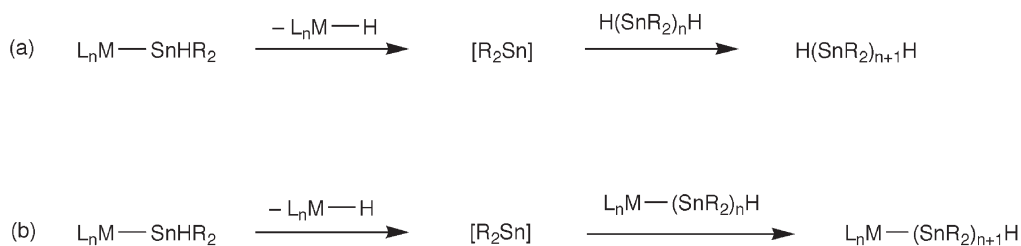
Investigations on the dehydropolymerization of hydro-silanes, as catalyzed by zirconocene and hafnocene derivatives, have implicated a mechanism involving σ -bond metathesis steps for Si–H bond cleavage and Si–Si bond formation.⁷ Thus, a similar mechanism may operate for the metal-catalyzed dehydropolymerization of unhindered secondary stannanes (Scheme 1). In this context, the chemistry of several hafnium hydrostannyl complexes has been investigated,⁸ and most information was obtained from the dehydromerization of Mes_2SnH_2 to $\text{Mes}_2\text{HSnSnHMes}_2$ by the hafnocene hydride $\text{CpCp}^*\text{Hf}(\text{H})\text{Cl}$ (**1**). The reaction of Mes_2SnH_2 with **1** produces an intermediate hydrostannyl complex, $\text{CpCp}^*\text{Hf}(\text{SnHMes}_2)\text{Cl}$ (**2**), which was found to undergo facile α -H-elimination of Mes_2Sn to regenerate **1**. A deuterium labeling experiment provided evidence that the Sn–Sn bond-forming mechanism occurs via Mes_2Sn insertion into the Sn–H bond of Mes_2SnH_2 . This α -H-elimination chemistry may result from the sterically hindered nature of the stannane and the catalyst. However, since α -elimination appears to represent a common decomposition mode for group 4 stannyl complexes,⁹ the stannylene insertion process might be important in the dehydropolymerization of less hindered stannanes (Scheme 2, Eq. a). A second possible mechanism for Sn–Sn bond formation involves stannylene insertion into a M–Sn bond (Scheme 2, Eq. b),

Keywords: Stannyl; Early metal; Dehydropolymerization; Stannane.

* Corresponding author. Tel.: +1-510-642-8939; fax: +1-510-642-8940; e-mail address: tdtilley@socrates.berkeley.edu



Scheme 1.



Scheme 2.

which has not previously been proposed in reactions of this type.

In this report we present experiments that provide evidence for the mechanism of the metal-catalyzed dehydropolymerization of secondary stannanes. Based on the known influence of catalyst structure on the molecular weight of polystannanes^{6a} and the observations reported herein, it is proposed that the Sn–Sn bond-forming mechanism may involve by R_2Sn insertion into a M–Sn bond. The factors that influence the ratio of linear to cyclic polystannanes is also discussed.

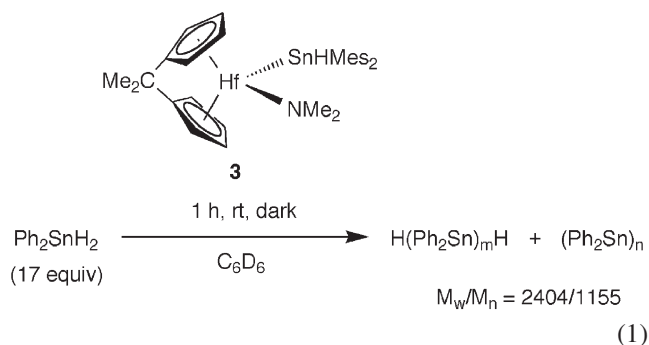
2. Results and discussion

Investigations into the mechanism of stannane dehydropolymerization focused on reactions of isolable hafnium hydrostannyl complexes with secondary stannanes. Hafnium hydrostannyl complexes were employed, since such compounds have been observed to undergo slower reaction (vs. analogous zirconium complexes), thus allowing the observation or isolation of intermediates.^{7b,8} Of particular interest were reactions of hafnocene hydrostannyl complexes with Ph_2SnH_2 and tBu_2SnH_2 , since these monomers give polystannanes in the presence of zirconocene catalysts.^{5k,6}

2.1. Dehydrocoupling reactions catalyzed by $[Me_2C(C_5H_4)_2]Hf(SnHMe_2)NMe_2$ (**3**)

The reaction of $[Me_2C(C_5H_4)_2]Hf(SnHMe_2)NMe_2$ (**3**) with

1 equiv. of Ph_2SnH_2 in benzene- d_6 solution immediately produced a deep yellow color and caused vigorous hydrogen gas evolution to occur. After 2 h, the Ph_2SnH_2 was completely consumed, and a small amount (4%) of an unidentified Hf species was evident in addition to unreacted **3** (96%). Vigorous H_2 evolution was observed upon addition of more Ph_2SnH_2 (17 equiv.), and after 1 h at room temperature the mixture contained a significant amount of precipitate. The formation of an insoluble product suggests the presence of higher molecular weight Sn oligomers, since polymers formed from Ph_2SnH_2 are known to exhibit low solubility.^{6a} A GPC trace of the THF-soluble fraction from this reaction mixture showed a bimodal distribution consistent with formation of small oligomers $H(Ph_2Sn)_mH$ and $(Ph_2Sn)_n$ ($M_w/M_n=2404/1155$) (Eq. 1). Therefore, it appears that with Ph_2SnH_2 , the hydrostannyl complex **3** is a moderately efficient polymerization catalyst and provides soluble Sn–Sn coupling products that are similar to those derived from zirconocene complexes (cf. $M_w/M_n=2200/930$ with $CpCp^*Zr[Si(SiMe_3)_3]Me$).^{6a}

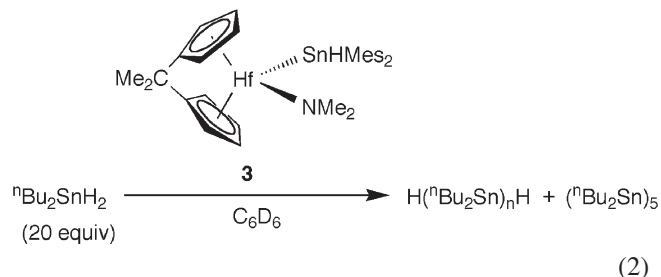


Reaction of **3** with 20 equiv. of ${}^n\text{Bu}_2\text{SnH}_2$ in benzene- d_6 solution gave no visual indication of a reaction after 15 min (the solution color remained pale yellow, and no H_2 gas bubbles were evolved). However, a ${}^1\text{H}$ NMR experiment (20 min) revealed a high concentration of hydrogen gas and moderate conversions of ${}^n\text{Bu}_2\text{SnH}_2$ (32%) and the hydrostannyl complex **3** (16%). The conversion slowly progressed over 100 min, at which point ${}^n\text{Bu}_2\text{SnH}_2$ (22%), **3** (59%), and many unidentified Hf species were observed. In addition, a new hydrostannane (6%) was identified by a Sn–H resonance at δ 4.80 (${}^1J_{117/119\text{Sn}}=1378, 1444$ Hz; cf. 1596 and 1670 for ${}^n\text{Bu}_2\text{SnH}_2$). The chemical shift of this resonance in the ${}^1\text{H}$ NMR spectrum and the high ${}^1J_{\text{SnH}}$ values are not consistent with a hydrostannyl complex such as $[\text{Me}_2\text{C}(\text{C}_5\text{H}_4)_2]\text{Hf}(\text{Sn}^n\text{Bu}_2)\text{NMe}_2$, since such species should exhibit a Sn–H resonance at higher field and with ${}^1J_{\text{SnH}}$ values that are about half that of the corresponding, free stannane.⁸ This species was also observed in reactions of other hafnocene catalysts with ${}^n\text{Bu}_2\text{SnH}_2$ (vide infra), which suggests that it is not an oligostannyl complex of the type $\text{Hf}-(\text{Sn}^n\text{Bu}_2)_n\text{SnH}^n\text{Bu}_2$. Therefore, although unequivocal identification of the new hydrostannane, hereafter referred to as intermediate **A**, was not possible because of its low concentration in solution, this species is likely an intermediate short-chain oligostannane $\text{H}(\text{Sn}^n\text{Bu}_2)_x\text{H}$ (e.g., ${}^n\text{Bu}_2\text{HSnSnH}^n\text{Bu}_2$). A ${}^{119}\text{Sn}$ NMR experiment detected ${}^n\text{Bu}_2\text{SnH}_2$ (δ -202.0), linear polystannanes $\text{H}({}^n\text{Bu}_2\text{Sn})_n\text{H}$ (δ -189.6),^{6a} a weak resonance at δ 13.0, and another slightly more intense peak (δ -206.3) assigned to intermediate **A**. The peak at δ -206.3 is in the expected range for hydrostannanes and is therefore consistent with the assignment of intermediate **A** as a short-chain oligostannane $\text{H}(\text{Sn}^n\text{Bu}_2)_x\text{H}$. Since ${}^{119}\text{Sn}$ NMR shifts of $\text{Hf}-\text{SnR}_3$ ($\text{R}\neq\text{H}$) species are observed $\geq\delta$ 0,⁹ the weak resonance at δ 13.0 could be due to the Hf–Sn group of a growing chain (i.e., $\text{Hf}-\text{Sn}^n\text{Bu}_2(\text{Sn}^n\text{Bu}_2)_n\text{SnH}^n\text{Bu}_2$), but in the absence of observable Sn satellites and other Sn resonances consistent with such a species, a definitive determination is not possible. Note that new CpCp^*Hf species were observed by ${}^1\text{H}$ NMR spectroscopy.

This reaction was monitored over 36 h, at which point $[\text{Me}_2\text{C}(\text{C}_5\text{H}_4)_2]\text{Hf}(\text{SnHMe}_2)\text{NMe}_2$ (**3**) was still observed as 51% of the total hafnocene species. A trace (3%) of a new hafnium hydride species having a downfield resonance for the Hf–H group at δ 8.98 was also detected (by ${}^1\text{H}$ NMR spectroscopy). This species has previously been observed in the photolytic decomposition of **3**, and likely corresponds to $[\text{Me}_2\text{C}(\text{C}_5\text{H}_4)_2]\text{Hf}(\text{H})\text{NMe}_2$.⁸ This hafnium hydride could be the result of α -H-elimination or σ -bond metathesis. As has been shown before,^{6a} d^0 metal hydrides react rapidly with secondary stannanes, and thus $[\text{Me}_2\text{C}(\text{C}_5\text{H}_4)_2]\text{Hf}(\text{H})\text{NMe}_2$ may be the catalytically active species in this system.

The ${}^{119}\text{Sn}$ NMR spectrum of this reaction mixture revealed the presence of four species in solution: a trace of the unidentified product (δ 13.0), **3**, linear polystannanes $\text{H}({}^n\text{Bu}_2\text{Sn})_n\text{H}$, and a small amount of $({}^n\text{Bu}_2\text{Sn})_5$ (Eq. 2).^{6a,10} It is interesting to note that the ratio of linear polystannanes to $({}^n\text{Bu}_2\text{Sn})_5$ is 1:0.01 (by integration of ${}^{119}\text{Sn}$ resonances), whereas dehydropolymerization reactions of zirconocene catalysts with ${}^n\text{Bu}_2\text{SnH}_2$ give a typical

linear/cyclics ratio of 1:0.20.^{6a} Thus, this reaction appears to be unusually selective toward the production of linear polystannanes.



After work-up as described for other soluble polystannanes,^{6a} the GPC trace of the yellow solid isolated from this reaction mixture showed a bimodal pattern indicating the presence of both linear polymers ($M_w/M_n=20118/9050$) and cyclic oligomers ($M_w/M_n=1021/983$). Despite efforts to avoid light during polystannane purification and sample preparation, some exposure to ambient room light was necessary during these manipulations. It is known that linear polystannanes are highly light sensitive and depolymerize rapidly under photolysis (e.g., $\text{H}({}^n\text{Bu}_2\text{Sn})_n\text{H}$ decomposes completely to $({}^n\text{Bu}_2\text{Sn})_5$ and $({}^n\text{Bu}_2\text{Sn})_6$ under ambient room lighting after 2 h).^{6a} Therefore, the higher fraction of cyclic species observed by GPC likely results from the photochemical depolymerization of linear chains during sample manipulation.

2.2. Dehydropolymerization reactions catalyzed by $\text{CpCp}^*\text{Hf}(\text{SnHMe}_2)\text{OME}$ (**4**)

In contrast to the relatively rapid reaction of $[\text{Me}_2\text{C}(\text{C}_5\text{H}_4)_2]\text{Hf}(\text{SnHMe}_2)\text{NMe}_2$ (**3**) with Ph_2SnH_2 , the reaction of $\text{CpCp}^*\text{Hf}(\text{SnHMe}_2)\text{OME}$ (**4**) with Ph_2SnH_2 (1 equiv., benzene- d_6 solution, room temperature) occurred very slowly over days. After 10 min, a trace of hydrogen gas, $\text{CpCp}^*\text{Hf}(\text{H})\text{OME}$ (**5**), and a new peak at δ 6.46 assigned to the Sn–H group of the distannane $\text{Ph}_2\text{HSnSnHPh}_2$ ¹¹ were observed by ${}^1\text{H}$ NMR spectroscopy. Only 2% of Ph_2SnH_2 had been converted at this time, and upon full conversion of Ph_2SnH_2 (3 days), the species remaining in solution were **4** (22%), the hydride **5** (78%), and a number of unidentified Sn species ($\text{Ph}_2\text{HSnSnHPh}_2$ was no longer observed). When **4** was combined with 20 equiv. of ${}^n\text{Bu}_2\text{SnH}_2$ (benzene- d_6 solution), slow conversion of the stannane was observed over 5 days at room temperature. After 3 h, complex **4** had been completely converted to the hydride **5**. A new Sn–H resonance at δ 4.80 (9%, m, ${}^1J_{117/119\text{SnH}}=1378, 1444$ Hz) corresponds to intermediate **A** observed in the reaction of the amido hydrostannyl complex **3** with ${}^n\text{Bu}_2\text{SnH}_2$. The presence of the same intermediate in both of these reactions suggests that these two catalysts may operate by the same mechanism. Thus, the catalytically active species in this dehydropolymerization is likely the hydride $\text{CpCp}^*\text{Hf}(\text{H})\text{OME}$ (**5**).¹²

After 24 h the Sn species in solution were ${}^n\text{Bu}_2\text{SnH}_2$ (21%), intermediate **A** (40%), and at least seven other hydrostannanes (25%, identified by their Sn–H resonances). A ${}^{119}\text{Sn}$ NMR spectrum contained resonances attributed to at least eight different hydrostannanes (δ -223.9 to -201.1 ,

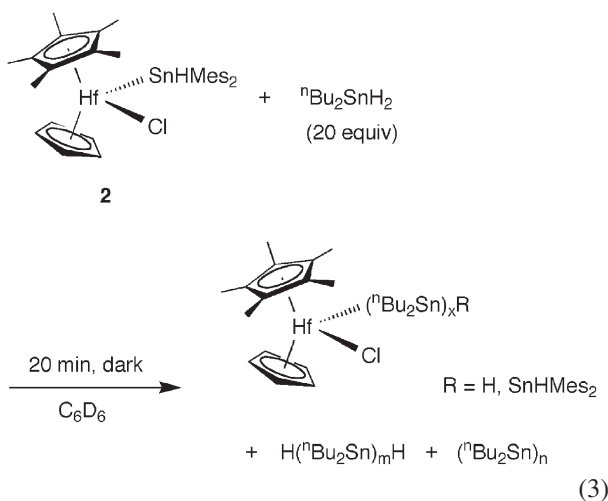
moderate intensity), intermediate **A** (major), $(^n\text{Bu}_2\text{Sn})_6$ (minor), $(^n\text{Bu}_2\text{Sn})_5$ (moderate intensity), and linear polystannanes $\text{H}(^n\text{Bu}_2\text{Sn})_n\text{H}$ (minor). The numerous resonances observed for the other hydrostannanes precluded identification of $^{117/119}\text{Sn}$ satellites from the peak for intermediate **A**, and so definitive identification of this species was not possible. However, since only a trace amount of linear polystannanes $\text{H}(^n\text{Bu}_2\text{Sn})_n\text{H}$ and many hydrostannanes were observed, it appears that the hydrostannyl compound **4** (or the active species **5**) primarily gives short-chain oligomeric species $\text{H}(^n\text{Bu}_2\text{Sn})_m\text{H}$ and cyclic oligomers $(^n\text{Bu}_2\text{Sn})_n$. A possible explanation for this low activity and limited conversion to linear polystannanes is the sterically hindered nature of the CpCp^* ligand set, which should slow the polymerization process.

2.3. Dehydrocoupling reactions catalyzed by $\text{CpCp}^*\text{Hf}(\text{SnHMes}_2)\text{Cl}$ (**2**)

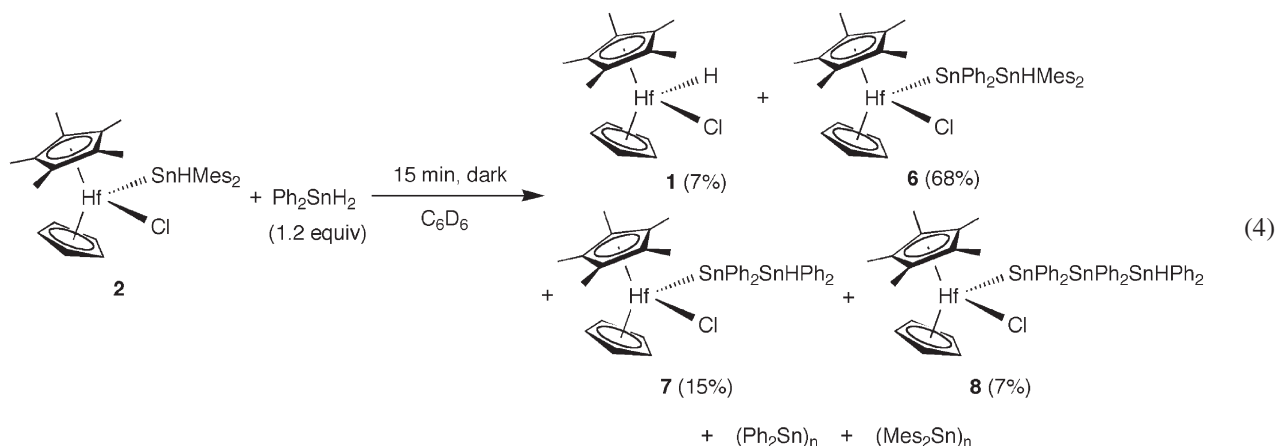
The reaction of $\text{CpCp}^*\text{Hf}(\text{SnHMes}_2)\text{Cl}$ (**2**) with 20 equiv. of $^n\text{Bu}_2\text{SnH}_2$ at room temperature converted 89% of the stannane after 20 min at room temperature. Many Sn–H resonances were observed in the ^1H NMR spectrum at this time, including that for intermediate **A** in high yield (57%). The hafnium hydrostannyl complex **2** was completely converted to four new species, as evidenced by new C_5H_5

resonances in the ^1H NMR spectrum. A ^{119}Sn NMR experiment revealed three major downfield peaks (δ 61.6, 87.9, and 129.6) in the distinctive region for hafnium stannyl species,¹³ as well as a major resonance for intermediate **A** (δ –206.3) and other peaks in the $^n\text{Bu}_2\text{SnRR}'$ region of δ –193 to –224. Thus, it appears that $^n\text{Bu}_2\text{SnH}_2$ undergoes dehydrocoupling to give hafnium oligostannyl species $\text{CpCp}^*\text{Hf}(\text{Cl})\text{Hf}-(\text{Sn}^n\text{Bu}_2)_x\text{R}$ ($\text{R}=\text{H}, \text{SnHMes}_2$) and small oligomers $\text{H}(^n\text{Bu}_2\text{Sn})_m\text{H}$ and $(^n\text{Bu}_2\text{Sn})_n$ as shown in Eq. 3. Furthermore, the absence of $\text{CpCp}^*\text{Hf}(\text{H})\text{Cl}$ (**1**) in this reaction mixture suggests that an oligostannyl complex $\text{CpCp}^*\text{Hf}(\text{Cl})\text{Hf}-(\text{Sn}^n\text{Bu}_2)_x\text{R}$ may be a ‘resting state’ for the catalytically active hydride **1**.

The reaction of $\text{CpCp}^*\text{Hf}(\text{SnHMes}_2)\text{Cl}$ (**2**) with 1.2 equiv. of Ph_2SnH_2 completely consumed both **2** and Ph_2SnH_2 after 15 min. The C_5H_5 region in the ^1H NMR spectrum showed that the hydrostannyl complex **2** had been converted to $\text{CpCp}^*\text{Hf}(\text{H})\text{Cl}$ (**1**, 7%) and three new hafnium oligostannyl complexes, $\text{CpCp}^*\text{Hf}(\text{SnPh}_2\text{SnHMes}_2)\text{Cl}$ (**6**, 68%), $\text{CpCp}^*\text{Hf}(\text{SnPh}_2\text{SnHPh}_2)\text{Cl}$ (**7**, 15%), and $\text{CpCp}^*\text{Hf}(\text{SnPh}_2\text{SnPh}_2\text{SnHPh}_2)\text{Cl}$ (**8**, 7%) (Eq. 4). These oligostannyl species are stable in solution for over one week (dark, room temperature), and thus are much more stable than their hydrostannyl analogs. Observation of the hydride **1** in this case is presumably made possible by the relatively low concentration of Ph_2SnH_2 . In the experiment described above, with a large excess of $^n\text{Bu}_2\text{SnH}_2$, this hydride appears to be fully converted to hafnium oligostannyl complexes.



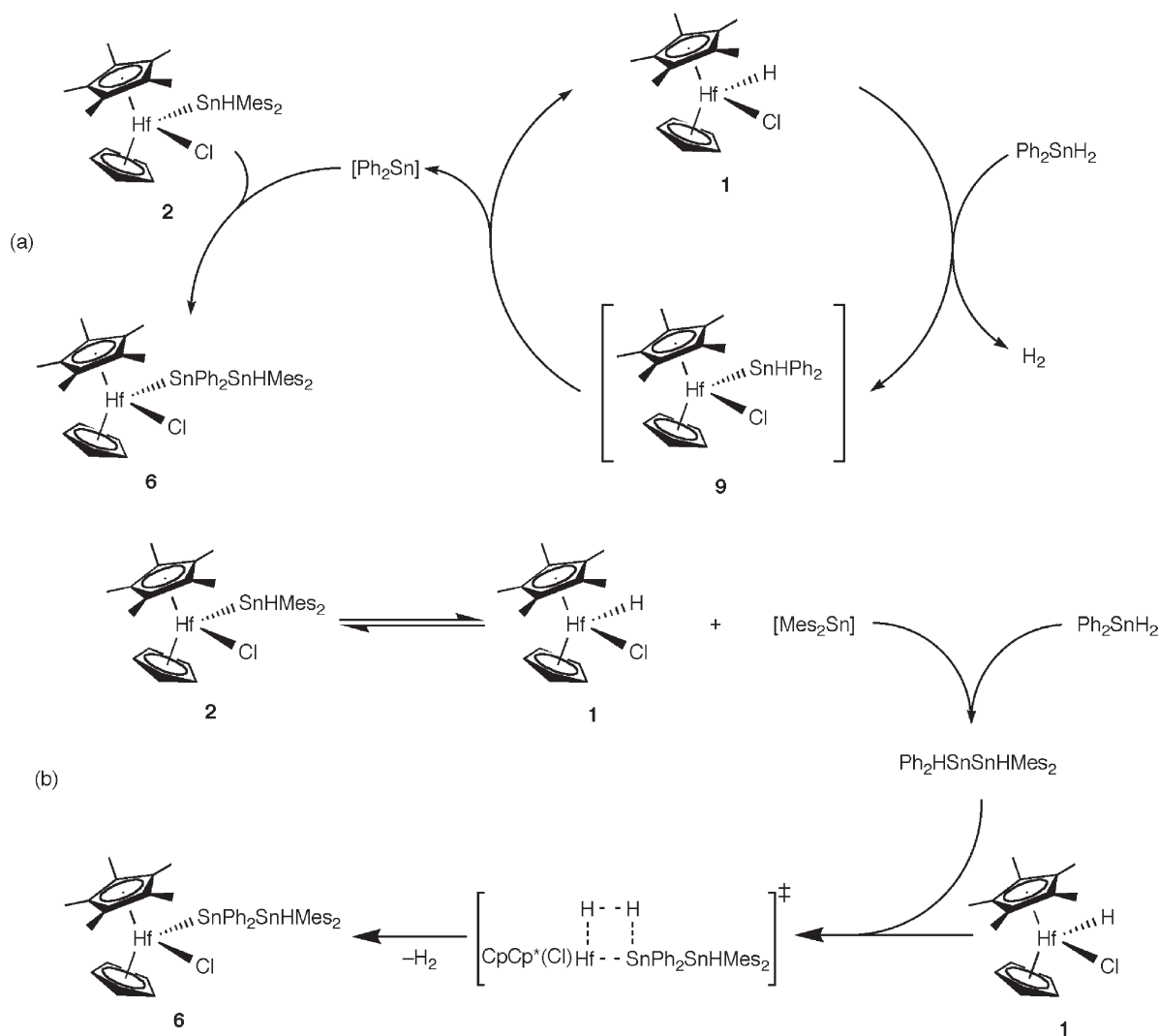
The major product $\text{CpCp}^*\text{Hf}(\text{SnPh}_2\text{SnHMes}_2)\text{Cl}$ (**6**) was identified by NMR spectroscopy. The ^1H NMR spectrum contains a C_5H_5 resonance for **6** (δ 5.88) with Sn–H satellites ($^3J_{\text{SnH}}=7.0$ Hz) that are indicative of a stannyl complex.^{8,9} The Sn–H peak for this species was detected at δ 6.76 and has Sn satellites due to both one-bond ($^1J_{117/119\text{SnH}}=1213, 1269$ Hz) and two-bond ($^2J_{117/119\text{SnH}}=108, 112$ Hz) coupling interactions. Observation of satellites due to both $^1J_{\text{SnH}}$ and $^2J_{\text{SnH}}$ demonstrates that the $-\text{SnHMes}_2$ group is bonded to another Sn atom. Additional evidence for **6** was found from a ^{119}Sn NMR experiment, which showed two major resonances at δ –289.9 and 44.2. The resonance at δ –289.9 has Sn satellites ($^1J_{117/119\text{Sn}-119\text{Sn}}=185$ Hz) that integrate to 9.0 and 7.3% of the parent peak, and that at δ 44.2 has Sn satellites ($^1J_{117/119\text{Sn}-119\text{Sn}}=185$ Hz) that



integrate to 7.0 and 10.0% of the parent peak. These integrations are closest to the theoretical value corresponding to one adjacent, magnetically inequivalent Sn atom (9.7%).¹⁴ Thus, these resonances appear to correspond to an unsymmetrical species with a single Sn–Sn bond. Further, the ¹¹⁹Sn NMR shifts observed in this experiment correlate very well with what is expected for a distannyl complex of this type. Since d⁰ Hf–SnR₃ (R≠H) complexes are characterized by ¹¹⁹Sn NMR shifts downfield of δ 0,^{8,9} the resonance at δ 44.2 is assigned to the SnPh₂ group bonded to Hf, Hf–SnPh₂SnHMes₂. The shift at δ –288.9 is therefore assigned to the dimesitylhydrostannyl end group, Hf–SnPh₂SnHMes₂, which is in a similar region as the shift of δ –320.1 for the distannane Mes₂HSnSnHMes₂. Finally, one-bond Sn–Sn coupling values (¹¹⁷Sn–¹¹⁹Sn and ¹¹⁹Sn–¹¹⁹Sn) are often observed between 2500 and 4200 Hz (e.g., 4211 Hz for Me₆Sn₂), which would seem to contradict the assignment of one-bond coupling of 185 Hz in complex **6**. However, coupling constants for the compounds R₃SnSnR'₃ are known to vary widely with the substituents (e.g., 730 Hz for ⁱPr₃SnSnⁱBu₃),¹⁵ and the CpCp*(Cl)Hf group on one of the Sn atoms likely causes this deviation from more typical values.

Attempts were made to isolate **6** from the preparatory scale reaction of **2** and 1 equiv. of Ph₂SnH₂ in toluene. Repeated crystallizations of the desired distannyl compound from Et₂O at –30 °C did not separate this species from the cyclic polystannanes (Ph₂Sn)_n and (Mes₂Sn)_n (14 mol% total) that are side-products in the reaction.

Two possible mechanisms for the formation of CpCp*-Hf(SnPh₂SnHMes₂)Cl (**6**) are shown in Scheme 3. It has previously been established that the equilibration of **2** with **1** and Mes₂Sn occurs at room temperature to give 20% of **1** after 10 min.⁸ Thus, hydride **1** formed by this equilibration process can react with Ph₂SnH₂ to give the hydrostannyl complex CpCp*Hf(SnHPh₂)Cl (**9**; Scheme 3a). The resulting hydrostannyl species **9** is presumably more unstable than **2** toward α-elimination, since the steric bulk of the R groups on Sn appear to have a drastic effect on the rate of this decomposition pathway.⁸ The rapid decomposition of **9** would regenerate the hydride **1** and produce Ph₂Sn. Thus, Ph₂Sn may be generated from a catalytic cycle involving **1** and the stannane Ph₂SnH₂ (Scheme 3a). The stannylene generated from this process might then insert into the Hf–Sn bond of **2** to produce **6**.



Scheme 3.

A second possible mechanism for the formation of $\text{CpCp}^*\text{-Hf}(\text{SnPh}_2\text{SnHMes}_2)\text{Cl}$ (**6**) involves Mes_2Sn insertion into the Sn–H bond of Ph_2SnH_2 to give the distannane $\text{Ph}_2\text{HSnSnHMes}_2$ (Scheme 3b). Although the equilibration of $\text{CpCp}^*\text{-Hf}(\text{SnHMes}_2)\text{Cl}$ (**2**) with **1** and Mes_2Sn occurs at room temperature to give 20% of **1** after 10 min, the rate of formation of **1** and Mes_2Sn is greatly enhanced in the presence of stannylene traps.⁸ If Ph_2SnH_2 is a good trap for Mes_2Sn , the distannane $\text{Ph}_2\text{HSnSnHMes}_2$ would be generated very rapidly. The hydride **1** might then be expected to react with $\text{Ph}_2\text{HSnSnHMes}_2$ via σ -bond metathesis to form the observed product **6** (Scheme 3b). Selective reaction at the less hindered tin center of $\text{Ph}_2\text{HSnSnHMes}_2$ would produce the observed regioisomer.

To determine which of these two mechanisms is operative, a deuterium labeling study was undertaken. By using $\text{CpCp}^*\text{-Hf}(\text{SnDMes}_2)\text{Cl}$ (**2-d**₁) in place of **2**, a Ph_2Sn insertion mechanism by way of the steps in Scheme 3a should give $\text{CpCp}^*\text{-Hf}(\text{SnPh}_2\text{SnDMes}_2)\text{Cl}$ (**6-d**₁). On the other hand, if the mechanism in Scheme 3b is at work, α -elimination of **2-d**₁ would produce **1-d**₁ and Mes_2Sn . The stannylene Mes_2Sn could then insert into the Sn–H bond of Ph_2SnH_2 to generate $\text{Ph}_2\text{HSnSnHMes}_2$, and reaction of **1-d**₁ with this distannane should eliminate HD and produce **6**.

The reaction of **2-d**₁ with Ph_2SnH_2 (1 equiv.) in benzene-*d*₆ fully converted both **2-d**₁ and Ph_2SnH_2 after 10 min (by ¹H NMR spectroscopy). The resonance for the Sn–H group in **6** was observed as 67% of the expected value for **6**. In addition, a deuterium NMR experiment in C_6H_{12} detected a peak at δ 7.21 that may be assigned to the Sn–D group in **6-d**₁. Thus, it appears that this reaction produced $\text{CpCp}^*\text{-Hf}(\text{SnPh}_2\text{SnHMes}_2)\text{Cl}$ (**6**) and $\text{CpCp}^*\text{-Hf}(\text{SnPh}_2\text{SnDMes}_2)\text{Cl}$ (**6-d**₁) in 67 and 33% yields, respectively. The observed scrambling may be due to the competing reaction between **2-d**₁ and $\text{Mes}_2\text{Sn}(\text{H/D})_2$, which would form via equilibria in this system.⁸ Other H/D exchange processes are also possible.

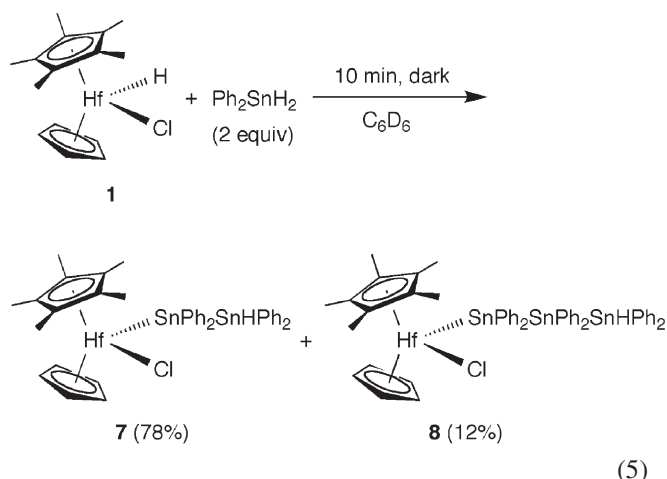
Likewise, by using Ph_2SnD_2 in place of Ph_2SnH_2 , Ph_2Sn insertion by way of the steps in Scheme 3a should give $\text{CpCp}^*\text{-Hf}(\text{SnPh}_2\text{SnHMes}_2)\text{Cl}$ (**6**). If the mechanism in Scheme 3b is operative, the distannane $\text{Ph}_2\text{DSnSnDMes}_2$ should be produced, and reaction of this distannane with **2** should liberate HD and give **6-d**₁. The reaction between **2** and Ph_2SnD_2 (1 equiv.) also resulted in complete conversion of the starting materials after 10 min (by ¹H NMR spectroscopy). Integration of the Sn–H resonance in the ¹H NMR spectrum showed that the distannyl complexes $\text{CpCp}^*\text{-Hf}(\text{SnPh}_2\text{SnHMes}_2)\text{Cl}$ (**6**) and $\text{CpCp}^*\text{-Hf}(\text{SnPh}_2\text{-SnDMes}_2)\text{Cl}$ (**6-d**₁) were formed in 44 and 56% yields, respectively. The deuterium NMR spectrum of this reaction mixture also showed the presence of the peak assigned to **6-d**₁. Although these studies did not provide definitive evidence for either stannylene insertion mechanism, the reaction of **2** and Ph_2SnH_2 provided a number of species that may be relevant to the dehydropolymerization mechanism.

The two other oligostannyl complexes formed from this reaction were tentatively identified as $\text{CpCp}^*\text{-Hf}(\text{SnPh}_2\text{-SnHPh}_2)\text{Cl}$ (**7**) and $\text{CpCp}^*\text{-Hf}(\text{SnPh}_2\text{SnPh}_2\text{SnHPh}_2)\text{Cl}$ (**8**) (vide infra). It is likely that these species resulted from the

reaction of $\text{CpCp}^*\text{-Hf}(\text{H})\text{Cl}$ (**1**) with Ph_2SnH_2 to produce Ph_2Sn by the catalytic cycle shown in Scheme 3a. Reactions similar to those described above could then lead to the observed products. Given the observation of these short oligostannyl species, it seemed that the reaction of Ph_2SnH_2 with **1** might represent a good model system for investigation of the metal-catalyzed dehydropolymerization of secondary stannanes.

2.4. Dehydrocoupling reactions catalyzed by $\text{CpCp}^*\text{-Hf}(\text{H})\text{Cl}$ (**1**)

The reaction of $\text{CpCp}^*\text{-Hf}(\text{H})\text{Cl}$ (**1**) with 2 equiv. of Ph_2SnH_2 in benzene-*d*₆ solution immediately resulted in a deep orange color and vigorous hydrogen gas evolution. After 10 min a ¹H NMR experiment revealed that Ph_2SnH_2 was fully converted to $\text{CpCp}^*\text{-Hf}(\text{SnPh}_2\text{SnHPh}_2)$ (**7**, 78%), $\text{CpCp}^*\text{-Hf}(\text{SnPh}_2\text{SnPh}_2\text{SnHPh}_2)\text{Cl}$ (**8**, 12%), and trace amounts of at least eight other products (10% total) (Eq. 5).



The distannyl complex **7** is characterized by a ¹H NMR shift for the C_5H_5 peak at δ 5.750 (³*J*_{SnH} = 7.0 Hz) and a Sn–H resonance at δ 6.91 (¹*J*_{117/119SnH} = 1329, 1392 Hz; ²*J*_{117/119SnH} = 88, 92 Hz). A ¹¹⁹Sn NMR experiment revealed resonances consistent with this distannyl structure (δ 66.2 and –172.1). Comparison of these shifts to those observed for $\text{CpCp}^*\text{-Hf}(\text{SnPh}_2\text{SnHMes}_2)\text{Cl}$ (**6**) and other hafnium stannyl species^{8,9} leads to an assignment of the resonance at δ 66.2 to the SnPh_2 group bonded to Hf, Hf– $\text{SnPh}_2\text{SnHPh}_2$, and the shift at δ –172.1 to the diphenylhydrostannyl end group, Hf– $\text{SnPh}_2\text{SnHPh}_2$. Compound **8** is characterized by a similar C_5H_5 resonance in the ¹H NMR spectrum, at δ 5.746, but the Sn satellites for this peak were not observed due to overlap with the C_5H_5 resonance for **7**. The Sn–H resonance was not definitively identified for this species, presumably due to its overlap with phenyl resonances, and thus the structure assigned to **8** is tentative. However, the ¹¹⁹Sn NMR spectrum contained three resonances that are consistent with the structure proposed for **8** (δ 76.2, –180.3, and –208.8). The high field peak at δ –208.8 is assigned to the internal SnPh_2 group, Hf– $\text{SnPh}_2\text{-SnPh}_2\text{SnHPh}_2$, by comparison to other internal SnPh_2 groups (e.g., δ –205.9 for $(\text{Ph}_2\text{Sn})_5$ and δ –217.2 for $(\text{Ph}_2\text{Sn})_6$).⁹ The shift at δ 76.2 is assigned to the SnPh_2 group bonded to Hf, Hf– $\text{SnPh}_2\text{SnPh}_2\text{SnHPh}_2$, and the shift at δ –180.3 to the diphenylhydrostannyl end group,

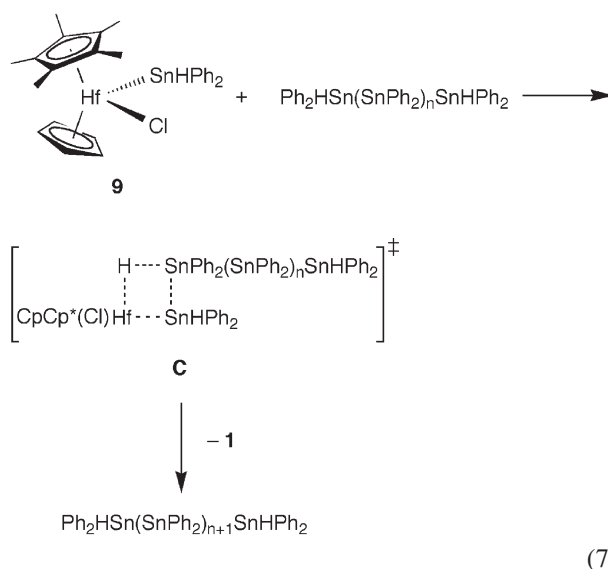
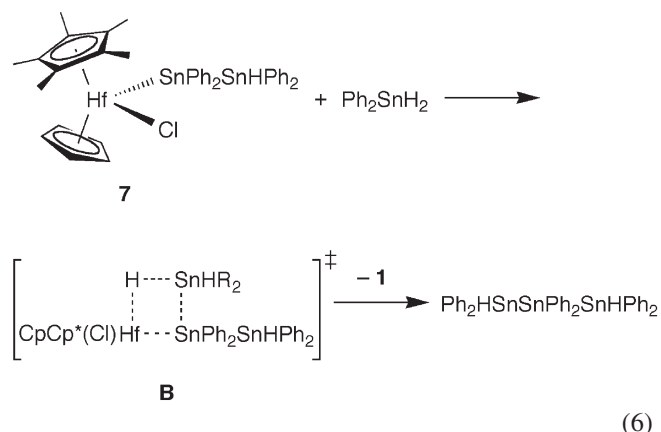
Hf–SnPh₂SnPh₂SnHPh₂. Note also that this latter resonance corresponds well with the shift assigned to the –SnHPh₂ end group in **7**.

The reaction of CpCp*Hf(H)Cl (**1**) with a slightly larger excess of Ph₂SnH₂ (4.3 equiv.) in benzene-*d*₆ solution converted 84% of the stannane after 10 min (by ¹H NMR spectroscopy). The distannane Ph₂HSnSnHPh₂ (1.5%), the distannyl complex CpCp*Hf(SnPh₂SnHPh₂)Cl (**7**; 79%), the tristannyl species CpCp*Hf(SnPh₂SnPh₂SnHPh₂)Cl (**8**; 8%), and a small amount of yellow precipitate (presumably high molecular weight polymers) were observed at this time. After 18 h, 97% of Ph₂SnH₂ had been consumed, and a similar ratio of products was observed. This retardation of the rate of stannane conversion is presumably due to formation of the relatively stable oligostannyl complexes **7** and **8**. Such species may represent intermediates in the dehydropolymerization process, but they could also be side products in the catalysis (e.g., resting states for an active hydride catalysts). To learn more about the interaction of such species with stannane monomer, an attempt was made to isolate **7**.

The distannyl complex CpCp*Hf(SnPh₂SnHPh₂)Cl (**7**) may be isolated in moderate yield (58%) and 91% purity from the preparatory scale reaction of **1** with 2 equiv. of Ph₂SnH₂. The moderate yield of this species was due to the numerous crystallizations performed in an effort to separate **7** from the impurities CpCp*(Cl)Hf(μ-O)Hf(Cl)Cp* Cp and CpCp*-HfCl₂ (from decomposition of the starting hydride **1**; 4% each). These species are unreactive toward stannanes, and so the following reactions of **7** with Ph₂SnH₂ appeared to be unaffected by the impurities.

The reaction of CpCp*Hf(SnPh₂SnHPh₂)Cl (**7**) with 2.5 equiv. of Ph₂SnH₂ did not produce any new species after 3 days at room temperature (dark, benzene-*d*₆ solution). However, addition of a catalytic amount of CpCp*Hf(H)Cl (**1**; 0.13 equiv.) converted 33% of the stannane after 10 min, and the hafnium products remaining in solution were **7** (79%), **8** (13%), and a number of unidentified species (8% total). No further reaction was observed after 2 days, suggesting that the hydride **1** is the active catalyst in the conversion of Ph₂SnH₂. Thus, it appears that compound **7** does not undergo concerted, σ-bond metathesis with Ph₂SnH₂ (to produce the hydride **1** and Ph₂HSnSnPh₂SnHPh₂) under conditions which lead to Sn–Sn bond formation (Eq. 6). This result is consistent with a polymerization mechanism involving the selective coupling of monostannyl species (e.g., CpCp*(Cl)HfSnHPh₂ (**9**)) with the end group of a polystannane chain, as has been proposed for the dehydropolymerization of PhSiH₃ (Eq. 7).⁹ This selectivity would presumably relate to the greater steric crowding in transition state **B** (vs. **C**). Alternatively, the primary Sn–Sn bond-forming process may involve the CpCp*Hf(H)Cl-catalyzed decomposition of Ph₂SnH₂ (via α-H-elimination) to diphenylstannylylene, which then inserts into a Sn–H or a Hf–Sn bond (cf. Scheme 3).

Interestingly, heating a mixture of **7** and 2.3 equiv. of Ph₂SnH₂ to 60 °C for 1 h resulted in a 30% conversion of Ph₂SnH₂, and the hafnium species in solution were **7** (48%),



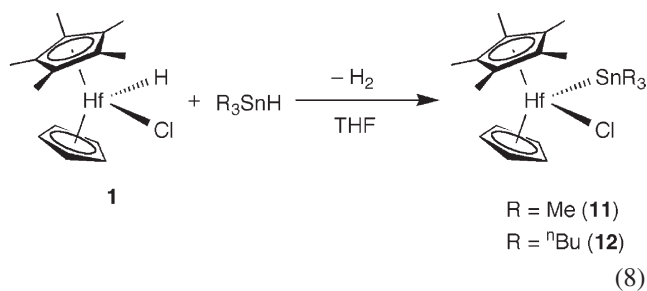
CpCp*Hf(SnPh₂SnPh₂SnHPh₂)Cl (**8**, 41%), and trace amounts of a number of other unidentified products (11% total). Additional heating for 16 h led to a complex mixture of products including **8** (31%) and five unidentified hafnium species (69%). The stannane was completely converted (98%) at this time, and a yellow precipitate was also observed, suggesting the presence of higher molecular weight oligomers. The unidentified Hf products are presumably other oligostannyl complexes of the type CpCp*(Cl)Hf–SnPh₂(SnPh₂)_mH. Under these more forcing conditions, couplings of the type described by Eq. 6 may be possible. Alternatively, thermal decomposition of **7** may produce a catalytically active hydride species.

2.5. Synthesis of hafnocene trialkylstannyl complexes

In an initial attempt to prepare a hafnocene trialkylstannyl complex by salt metathesis, the reaction of CpCp*HfCl₂ with 1 equiv. of LiSnMe₃ (prepared from MeLi and Me₃SnMe₃)¹⁶ in THF solution at –78 °C produced CpCp*Hf(Me)₃Cl (**10**, 68%) and CpCp*HfMe₂ (15%) (the hafnium methyl compounds were independently prepared from CpCp*HfCl₂ and MeLi). Interestingly, the major product from this reaction is that expected from α-elimination of the presumed initial product, CpCp*Hf(SnMe₃)Cl

(**11**). However, it has been shown that LiSnMe_3 exists in equilibrium with MeLi and Me_2Sn .¹⁷ Thus, **10** and $\text{CpCp}^*\text{-HfMe}_2$ may form via the direct reaction of MeLi with $\text{CpCp}^*\text{HfCl}_2$.

A number of hafnium stannyl derivatives have been successfully prepared by the reaction of a hafnium hydride with a stannane,^{8,9} so this method was employed in the syntheses of $\text{CpCp}^*\text{Hf}(\text{SnMe}_3)\text{Cl}$ (**11**) and $\text{CpCp}^*\text{Hf}(\text{Sn}^n\text{Bu}_3)\text{Cl}$ (**12**). The trimethylstannyl complex **11** was prepared from the reaction of $\text{CpCp}^*\text{Hf}(\text{H})\text{Cl}$ (**1**) and HSnMe_3 in THF solution, and was isolated as red–orange crystals from pentane solution in 63% yield (Eq. 8). The tributylstannyl derivative, **11**, was isolated from a similar reaction as red crystals in 68% yield (Eq. 8). These two complexes exhibit downfield ^{119}Sn NMR resonances (δ 147.9 for **11** and 154.4 for **12**) that are characteristic of Hf-SnR_3 ($\text{R}\neq\text{H}$) compounds.^{8,9} The tributyl species **12** is highly soluble in pentane, whereas the trimethyl derivative **11** is reasonably so, and both compounds give orange solutions despite appearing red in the crystalline state.



2.6. Evidence for Me_2Sn insertion into a Hf-Sn bond

Triarylstannyl complexes of hafnium undergo clean thermal decompositions via α -aryl elimination of a Ar_2Sn stannylene.⁹ The thermal decomposition of **12** was found to proceed to 90% conversion at 100 °C over 12 days to give a complex mixture of products. This process does not follow first-order kinetics, but this is perhaps not surprising since the α -butyl-elimination of ${}^n\text{Bu}_2\text{Sn}$ would produce $\text{CpCp}^*\text{Hf}({}^n\text{Bu})\text{Cl}$, which should be prone to β -H-elimination.¹⁸ Under these reaction conditions this secondary process, and others involving $\text{CpCp}^*\text{Hf}(\text{H})\text{Cl}$ (**1**) and butene, may lead to a more complex kinetic behavior.

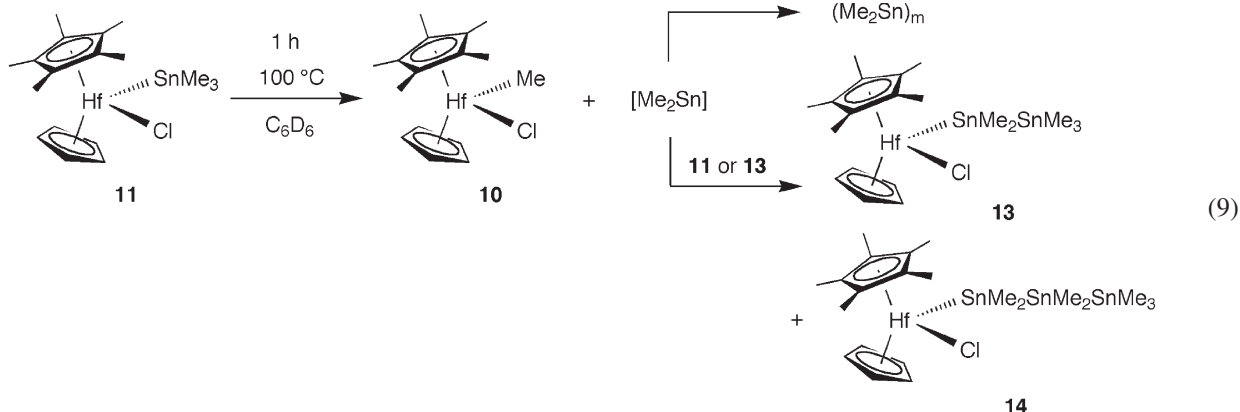
The trimethylstannyl derivative **11** undergoes first-order decomposition to $\text{CpCp}^*\text{Hf}(\text{Me})\text{Cl}$ (**10**) in 98% yield (24 h) with a rate constant k (100 °C) = $2.4 \times 10^{-4} \text{ s}^{-1}$. Interestingly, in addition to the expected product from α -elimination (**10**), there are other metal species observed during the course of the reaction. After heating a concentrated ($[\text{11}]_0 = 80 \text{ mM}$) benzene- d_6 solution for 1 h at 100 °C, the major species observed by ^1H NMR spectroscopy were **10** (37%), unreacted **11** (29%), two intermediates **13** (17%) and **14** (7%), and three other minor products (10% total). Continued heating at 100 °C for 24 h completely converted **13**, **14**, and the three minor products previously observed to $\text{CpCp}^*\text{Hf}(\text{Me})\text{Cl}$ (**10**), presumably via ‘chain-terminating’ α -Me-elimination processes. The major intermediates in this mixture have been identified as the di- and tristannyl

complexes $\text{CpCp}^*\text{Hf}(\text{SnMe}_2\text{SnMe}_3)\text{Cl}$ (**13**) and $\text{CpCp}^*\text{Hf}(\text{SnMe}_2\text{SnMe}_2\text{SnMe}_3)\text{Cl}$ (**14**), respectively. These intermediates are characterized by ^1H NMR shifts that are remarkably similar to those for **11**, which has resonances at δ 0.461 (Hf-SnMe_3), 1.792 (Cp^*), and 5.760 (Cp), due to their related structure. Compound **13** has ^1H NMR shifts of δ 0.467 ($\text{Hf-SnMe}_2\text{SnMe}_3$), 1.796 (Cp^*), and 5.766 (Cp), and **14** has peaks at δ 1.801 (Cp^*) and 5.773 (Cp) (the SnMe_3 resonance was not definitively identified).

More conclusive data in support of these assignments were obtained from a ^{119}Sn NMR spectrum of the reaction mixture. In addition to the resonance assigned to **11** (δ 147.9), two other sets of resonances were observed. The first of these sets is assigned to **13** and is comprised of two peaks (δ 38.6 and -76.0). As with $\text{CpCp}^*\text{Hf}(\text{SnPh}_2\text{SnHMe}_2)\text{Cl}$ (**6**), these resonances have tin satellites with identical coupling constants ($^1J_{117/119\text{Sn}-119\text{Sn}} = 448, 468 \text{ Hz}$). Further, the satellites about the peak at δ 38.6 integrate to 4.16 and 9.49% of the parent peak and those about the peak at δ -76.0 integrate to 8.58 and 8.18%, which indicates that these Sn atoms are adjacent to only one Sn atom.¹⁴ Since Hf-SnR_3 ($\text{R}\neq\text{H}$) compounds appear to be characterized by ^{119}Sn NMR resonances downfield of δ 0,^{8,9} the resonance at δ 38.6 is assigned to the SnMe_2 group bonded to Hf ($\text{Hf-SnMe}_2\text{SnMe}_3$), and that at δ -76.0 to the terminal SnMe_3 group ($\text{Hf-SnMe}_2\text{SnMe}_3$). Further support for this latter assignment is found by comparing these ^{119}Sn NMR shifts to those of tristannanes with the structure $\text{Me}_3\text{Sn}(\text{SnR}_2)\text{-SnMe}_3$. These tristannanes are characterized by a resonance at ca. δ -100 for the terminal SnMe_3 groups, and by resonances at δ -200 to -270 (depending on R) for the internal SnR_2 atom.¹⁹ Thus, the resonance assigned to the terminal $-\text{SnMe}_3$ group is in the range for ^{119}Sn NMR shifts for trimethylstannyl end groups in oligostannyl compounds.

The second set of resonances in the ^{119}Sn NMR spectrum (δ 57.0, -97.2 , and -211.9) is assigned to **14**. These resonances were not sufficiently intense to allow observation of distinct Sn satellites, but the similarity of the ^1H NMR resonances and two of the ^{119}Sn NMR shifts to those of complex **13** suggest that this species is the tristannyl complex $\text{CpCp}^*\text{Hf}(\text{SnMe}_2\text{SnMe}_2\text{SnMe}_3)\text{Cl}$ (**14**). The resonance at δ 57.0 is assigned as the SnMe_2 group bonded to Hf ($\text{Hf-SnMe}_2\text{SnMe}_2\text{SnMe}_3$), and the resonance at δ -97.2 appears to correspond to the terminal SnMe_3 group ($\text{Hf-SnMe}_2\text{SnMe}_2\text{SnMe}_3$). These assignments leave δ -211.9 as the shift assigned to the internal SnMe_2 group ($\text{Hf-SnMe}_2\text{SnMe}_2\text{SnMe}_3$), which falls in the range established for internal SnR_2 groups in $\text{Me}_3\text{Sn}(\text{SnR}_2)\text{SnMe}_3$ compounds.¹⁹

The presence of these di- and tristannyl complexes in this reaction mixture suggests that Me_2Sn inserts into the Hf-Sn bonds of stannyl complexes to give oligostannyl species (Eq. 9). Also, the three other minor products observed by ^1H NMR spectroscopy indicate that higher oligostannyl species (likely $\text{CpCp}^*(\text{Cl})\text{Hf}(\text{SnMe}_2)_m\text{SnMe}_3$ with $m \geq 3$) may be present. These species could result from additional Me_2Sn insertions into Hf-Sn bonds. Indeed, Hf-Sn bonds appear to be more effective than 2,3-dimethylbutadiene as a stannylene trap. This is indicated by an experiment in which **11** was allowed to decompose in the presence of



2,3-dimethylbutadiene (9 equiv., benzene- d_6 solution, 100 °C), which is known to be an efficient stannylene trap.²⁰ The reaction mixture produced by this thermolysis was indistinguishable from that of the reaction in the absence of added trap.

2.7. Reaction of CpCp*Hf(SnMe₃)Cl (11) with stannanes

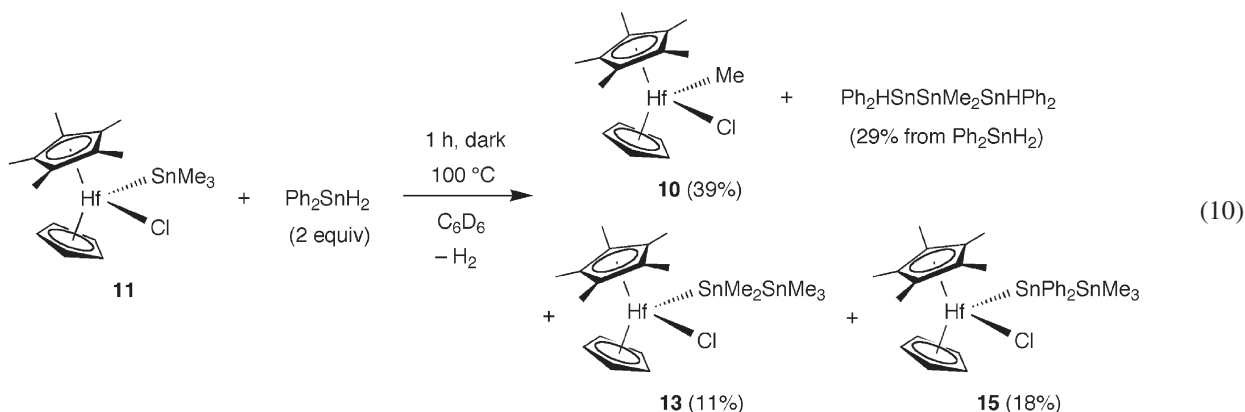
The results presented above indicate that the stannylene Me₂Sn readily inserts into a Hf–Sn bond. Earlier studies implicated the insertion of a stannylene into a Sn–H bond in the dehydrodimerization of Me₂SnH₂.⁸ Both types of insertions represent possible Sn–Sn bond-forming steps for the metal-catalyzed dehydropolymerization of secondary stannanes to polystannanes. In an attempt to assess the relative importance of stannylene insertions into Sn–H and Hf–Sn bonds, the α -methyl-elimination of **11** was examined in the presence of hydrostannanes.

A benzene- d_6 solution of CpCp*Hf(SnMe₃)Cl (**11**) and 2 equiv. of Ph₃SnH remained unchanged after 30 min at room temperature. Heating this mixture to 100 °C for 1 h resulted in the formation of **10**, **13** and **14**, along with other minor species, and the Ph₃SnH had not reacted. Thus, this reaction was indistinguishable from that in the absence of Ph₃SnH, suggesting that stannylene insertion preferentially occurs into Hf–Sn bonds. However, since Ph₃SnH is considerably more sterically hindered than the secondary stannanes Ph₂SnH₂ and ⁿBu₂SnH₂, insertion into the Sn–H bond of Ph₃SnH may not be favored.

Reaction of **11** with 2 equiv. of Ph₂SnH₂ at 100 °C for 1 h converted 87% of the stannane, primarily to the tristannane Ph₂HSnSnMe₂SnHPh₂ (29%; the theoretical yield for this species is 50%). The tristannane is characterized by a ¹H NMR shift at δ 6.90 (¹J_{117/119SnH}=1848, 1934 Hz) for the Sn–H group and a shift at δ 0.47 for the SnMe₂ group. This compound is further characterized by ¹¹⁹Sn NMR resonances at δ –161.4 and –232.8. These resonances have satellites with identical coupling values (¹J_{SnSn}=1280 Hz; the ¹¹⁷Sn and ¹¹⁹Sn satellites were not resolved), indicating that they are due to adjacent Sn atoms. Further, the satellites about the resonance at δ –232.8 integrate to 19.02 and 18.99% of the parent peak. The theoretical value for this integration from two magnetically equivalent Sn atoms is 19.1%.¹⁴ Therefore, this peak is assigned to the internal SnMe₂ group, Ph₂HSnSnMe₂SnHPh₂, which is in the

expected region for internal SnR₂ groups of the tristannanes Me₃Sn(SnR₂)SnMe₃.¹⁹ The satellites about the resonance at δ –161.4 integrate to 6.61 and 7.97% of the parent peak (the theoretical value for this coupling is 9.66%),¹⁴ suggesting that this species has only one neighboring Sn atom. Further, this shift is in a similar region as that observed for the –SnHPh₂ end group in CpCp*Hf(SnPh₂SnHPh₂) (**7**; δ –172.1). Therefore, the peak at δ –161.4 is assigned to the diphenylhydrostannyl end groups, Ph₂HSnSnMe₂–SnHPh₂.

The Hf compounds remaining in solution at this time were **11** (19%), CpCp*Hf(Me)Cl (**10**, 38%), CpCp*Hf(SnMe₂–SnMe₃)Cl (**13**, 11%), CpCp*Hf(SnPh₂SnMe₃)Cl (**15**, 18%), and at least five other minor products (14% total; Eq. 10). The new hafnium distannyl complex **15** was identified by the C₅H₅ resonance in the ¹H NMR spectrum, which has Sn–H coupling constants (³J_{SnH}=7.0 Hz) typical of stannyl complexes of this type (vide supra). Further, the peak for the SnMe₃ group (δ 0.51) exhibits Sn satellites due to both two- and three-bond coupling (²J_{117/119SnH}=42, 44 Hz; ³J_{SnH}=7.9 Hz), confirming that this group is bonded to another Sn atom. A ¹¹⁹Sn NMR experiment revealed the presence of a number of peaks including those for **11** (δ –147.9) and **13** (δ 38.6 and –76.0). Two other intense resonances (δ 63.5 and –67.4) are assigned to the new distannyl complex CpCp*Hf(SnPh₂SnMe₃)Cl (**15**). These resonances have Sn satellites with identical coupling constants (¹J_{117/119Sn–119Sn}=456, 478 Hz), indicating that they are due to adjacent Sn atoms. The resonance at δ 63.5 is assigned to the SnPh₂ group bonded to Hf, Hf–SnPh₂–SnMe₃, by comparison to values of other stannyl complexes (vide supra). The shift of δ –67.4 is in the range expected for XR₂Sn–SnMe₃ species,¹⁹ and is very similar to that for CpCp*Hf(SnMe₂SnMe₃)Cl (**13**; δ –76.0). Therefore, this resonance is assigned to the SnMe₃ end group of **15**. Although the products of this reaction indicate that α -methyl-elimination occurred, these results do not allow a determination of the relative importance of insertions into Hf–Sn and Sn–H bonds. First, it has not been possible to identify all the products of this reaction. Also, whereas certain products (**13** and **15**) suggest that stannylene insertions into Hf–Sn bonds occurred, it is unclear whether or not insertions into the Sn–H bonds of Ph₂SnH₂ took place. For example, Ph₂HSnSnMe₂SnHPh₂ could form via Me₂Sn insertion into Ph₂HSn–H, with the resulting Ph₂HSnSnHMe₂ intermediate undergoing dehydrocoupling



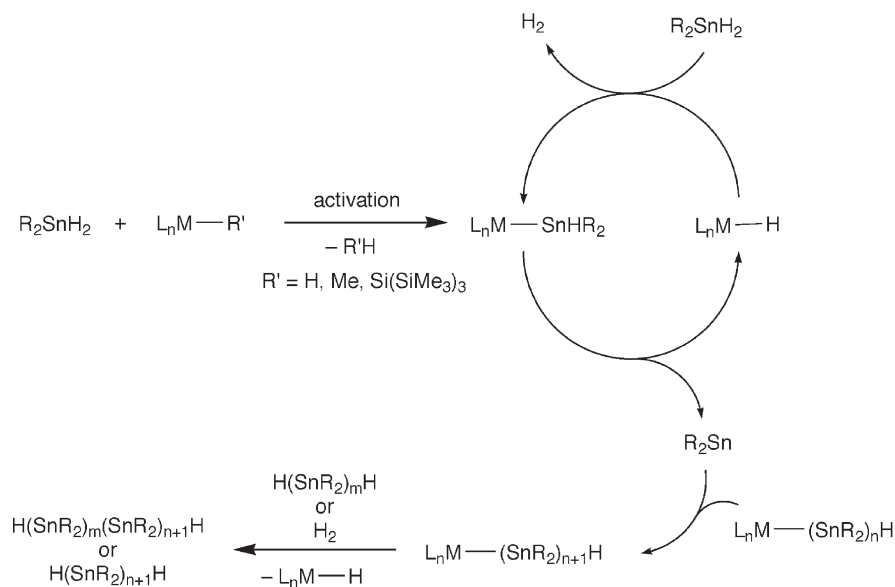
with Ph_2SnH_2 (via σ -bond metathesis) to form the product. Alternatively, this product could form via the initial condensation of Ph_2SnH_2 with $\text{CpCp}^*\text{Hf}(\text{Me})\text{Cl}$ (**10**) to form $\text{CpCp}^*\text{Hf}(\text{SnHPh}_2)\text{Cl}$ and methane (observed in trace quantities by ^1H NMR spectroscopy). The latter hafnium complex could then undergo insertion of Me_2Sn to give $\text{CpCp}^*(\text{Cl})\text{Hf}-\text{SnMe}_2\text{SnHPh}_2$, which could then couple with Ph_2SnH_2 to produce the product. Interestingly, a recent report of R_2Sn ($\text{R}=\text{Me}, \text{Et}, \text{Ph}$) insertion into the $\text{Pt}-\text{Cl}$ bond of the platinum(II) complexes $[\text{Pt}(\text{X})(\text{Cl})\text{L}_2]$ ($\text{X}=\text{Cl}, \text{Me}, \text{Ph}$; $\text{L}=\text{PEt}_3$) to give $[\text{Pt}(\text{X})(\text{SnR}_2\text{Cl})\text{L}_2]$ suggests that stannylene insertion into a metal–ligand bond may be a viable mechanism for this transformation.²¹

2.8. Proposed dehydropolymerization mechanism

The results presented here, and those described earlier,⁸ strongly suggest that the metal-catalyzed dehydropolymerization of secondary stannanes may occur via a mechanism involving α -H-elimination and stannylene insertion. A possible scenario is outlined in Scheme 4. Initially, a catalyst precursor is believed to interact with substrate (R_2SnH_2) via elimination of a small molecule (e.g., H_2 , CH_4 , $\text{HSi}(\text{SiMe}_3)_3$, etc.) via σ -bond metathesis. This produces a hydrostannyl intermediate, which is unstable

toward the α -H-elimination of stannylene. This process appears to be quite facile, and can result in an equilibrium between the hydrostannyl complex and a metal hydride and stannylene.⁸

The $\text{Sn}-\text{Sn}$ bond-forming step proposed in Scheme 4 involves insertion of free stannylene into a metal–tin bond. As mentioned above, insertion may occur into either a $\text{M}-\text{Sn}$ or a $\text{Sn}-\text{H}$ bond. However, without the action of a metal complex, long chains are not the expected product of a dehydrocoupling reaction involving stannylene intermediates. This point is illustrated by amine-catalyzed dehydrocouplings of secondary stannanes, which are known to give only small cyclic species (Eq. 11).²² The mechanism for this transformation is thought to involve stannylene intermediates, and preferential stannylene condensation to small cyclics occurs rather than insertion of the stannylene into the $\text{Sn}-\text{H}$ bonds that are present in the reaction mixture. Note that Sita has invoked stannylene insertion into $\text{Sn}-\text{H}$ bonds to form $\text{H}(\text{Bu}_2\text{Sn})_m\text{H}$ chains up to fifteen Sn atoms in length.⁵¹ However, in the synthesis of these linear species, the $m=3, 4,$ and 5 oligomers predominate, suggesting that low molecular weight oligomers are the kinetic products of stannylene insertion into $\text{Sn}-\text{H}$ bonds. Therefore, if stannylene insertion into $\text{Sn}-\text{H}$ bonds were operative in



Scheme 4.

the metal-catalyzed dehydropolymerization of stannanes, then a distribution of low molecular weight oligomers should be observed. Since the synthesis of polystannanes using d^0 metal catalysts produces primarily long chains, stannylene insertion into Sn–H bonds is highly unlikely for significant chain growth. We therefore propose that the metal-catalyzed dehydropolymerization of secondary stannanes involves insertion of free stannylene species into the Hf–Sn bond of a growing polymer chain (Scheme 4).



3. Concluding remarks

The results presented here suggest the operation of a new type of polymerization mechanism for the metal-catalyzed dehydrocoupling of secondary stannanes to polystannanes. This mechanism features σ -bond metathesis, α -H-elimination, and stannylene insertion into a metal-tin bond as the key, fundamental steps. Whereas this mechanism has not been previously proposed, there has been considerable speculation regarding the possible role of silylenes, or silylene complexes, in the dehydrocoupling of silanes to polysilanes. For example, Yamamoto et al. suggested that a platinum silylene intermediate of the type $(Et_3P)_2PtSiMe_2$ facilitates the dehydrocoupling of $Me_3SiSiHMe_2$ by $(Et_3Pt)_2PtCl_2$. In this case, the silylene Me_2Si was trapped from the reaction mixture with diphenylacetylene.²³ Harrod's original mechanistic proposal for the dehydrocoupling of primary silanes by Cp_2TiMe_2 involves elimination of hydrogen from $Cp_2Ti(H)SiH_2Ph$, with formation of $Cp_2Ti=SiHPh$. The Si–Si bond-forming step would then occur by addition of an Si–H bond across the Ti=Si double bond.²⁴ Finally, Hengge and co-workers have proposed a silylene complex as an intermediate in the Ti- and Zr-catalyzed polymerization of $Me_3SiSiHMe_2$. In the suggested mechanism, a disilyl complex, $L_nM(R)SiMe_2SiMe_3$, undergoes ' β^* -bond elimination' to produce $RSiMe_3$ and $L_nM=SiMe_2$. Dissociation of the silylene ligand then produces the free silylene Me_2Si , which inserts into both Si–H and Si–Si bonds to give the observed oligosilane products.²⁵

We have previously proposed a mechanism for the dehydropolymerization of $PhSiH_3$ by zirconocene and hafnocene catalysts that involves only σ -bond metathesis steps analogous to that in Scheme 1.^{7b} Based on the available facts it is difficult to completely rule out an analogous mechanism for the dehydropolymerizations of secondary stannanes, for all cases. However, the observed α -elimination/stannylene insertion chemistry strongly implicates a mechanism involving these steps. At this time, it is difficult to evaluate the possible role of analogous elimination/insertion steps in the dehydropolymerization of silanes. More generally, the new mechanism outlined in Scheme 4 represents a viable approach for designing catalytic systems for dehydrocouplings and element–element bond formations.

The hafnocene/stannane systems that have been studied in

the context of α -elimination have revealed certain structure–reactivity correlations. For example, it has been observed that π -donating ancillary ligands slow the rate of α -elimination.⁹ Thus, $CpCp^*Hf(SnHMes_2)OMe$ (**4**) is less active as a stannane dehydrocoupling catalyst than is $CpCp^*Hf(SnHMes_2)Cl$ (**2**). In addition, $[Me_2(C_5H_4)_2]Hf(SnHMes_2)NMe_2$ (**3**) is more active than **2** in the dehydrocoupling of Ph_2SnH_2 despite have a stronger π -donating ligand. In this case, the *ansa*-cyclopentadienyl ligand system in **3** seems to provide this catalyst with enhanced activity over the more sterically hindered $CpCp^*$ ligand set. These results suggest that a highly active catalyst for the conversion of stannanes to polystannanes requires an electrophilic metal center with limited steric constraints. Note that these observed effects are consistent with both a purely σ -bond metathesis mechanism, and a mechanism incorporating σ -bond metathesis, α -elimination and stannylene insertion steps.

Finally, the identification of a catalyst, $[Me_2(C_5H_4)_2]Hf(SnHMes_2)NMe_2$ (**3**), which gives unusually high selectivity for dehydrocoupling of nBu_2SnH_2 to linear (vs. cyclic) polystannanes (99/1) provides some potentially useful insight into factors that control this selectivity. Since complex **3** is thermally stable up to 60 °C,^{8b} it can be assumed that stannyl complexes of the type $[Me_2(C_5H_4)_2]Hf(SnHR_2)NMe_2$ undergo relatively slow α -H-elimination reactions. Also, because of the open, *ansa*-bis(cyclopentadienyl) ligand framework, such species are expected to undergo rapid insertions of stannylene (e.g., nBu_2Sn) into the Hf–Sn bond. If the Hf–Sn bond in this system is indeed an efficient trap for nBu_2Sn , and if α -H-elimination to produce stannylene is slow, there would be no significant build-up in the stannylene concentration. The low concentration of stannylene should limit the rate of stannylene condensation to cyclic oligomers, and lead to a high ratio of linear $H(nBu_2Sn)_nH$ polymers to cyclic $(nBu_2Sn)_m$ oligomers. These considerations suggest that good stannane dehydropolymerization catalysts should be based on metal–ligand fragments that (1) have M–Sn bonds that are reactive toward stannylene insertions, and (2) provide hydrostannyl complexes L_nMSnHR_2 that undergo relatively slow decompositions via α -H-elimination.

4. Experimental

4.1. General

All manipulations were carried out under a nitrogen atmosphere using standard Schlenk techniques or a nitrogen-filled glovebox. Dry, oxygen-free solvents were employed throughout. Pentane, diethyl ether and tetrahydrofuran were distilled from sodium/benzophenone, benzene was distilled from potassium, toluene and tetraglyme (0.005 mm Hg, 100 °C) were distilled from sodium, and benzene- d_6 and toluene- d_8 were dried over NaK alloy and Na, respectively, vacuum transferred and then stored over 4 Å molecular sieves. Chloroform was purified by shaking with several small portions of conc. H_2SO_4 , washing with several portions water, and then drying over $CaCl_2$ before distillation. Trimethylsilyl chloride (Gelest or Aldrich) was distilled prior to use. The compounds

CpCp*Hf(H)Cl (**1**),^{7b} CpCp*Hf(SnHMes₂)Cl (**2**),⁸ [Me₂C-(C₅H₄)₂]Hf(SnHMes₂)NMe₂ (**3**),⁸ CpCp*Hf(SnMes₂)OMe (**4**),⁸ and CpCp*Hf(H)OMe (**5**)⁸ were prepared according to literature procedures. The stannanes Ph₂SnH₂, ⁿBu₂SnH₂, and ⁿBu₃SnH were prepared by reducing the corresponding organotin chlorides with LiAlH₄ in Et₂O. The deuterated stannane Ph₂SnD₂ was prepared by using LiAlD₄ in place of LiAlH₄. 2,3-Dimethylbutadiene was purchased from Aldrich and distilled from CaH₂ prior to use. For NMR tube kinetic measurements and all reactions involving a hafnium hydride, glassware was silylated with Me₃SiCl/chloroform solution (1:9, v/v), washed three times with acetone, then once each with distilled water and ethanol before oven-drying.

NMR spectra were recorded in benzene-*d*₆ solutions at 300, 400, or 500 MHz (¹H) with Bruker AMX-300, AVB-400, and DRX-500 spectrometers, at 125.76 MHz (¹³C{¹H}) or at 186.5 MHz (¹¹⁹Sn{¹H}) with a DRX-500 spectrometer at ambient temperature (unless otherwise noted). Elemental analysis was carried out by the Microanalytics Laboratory at the University of California, Berkeley. IR samples of solid materials were prepared as Nujol mulls between two KBr plates unless otherwise noted. All IR absorptions are reported in cm⁻¹ and were recorded with a Mattson Infinity 60 MI FTIR spectrometer.

Kinetic measurements of the decomposition of **11** and **12** were performed using a temperature-controlled oil bath (temperature variation ≤ 1.0 °C). Data points were collected by removing the tubes from the oil and immediately cooling to room temperature. The tubes were typically at room temperature for about 15 min before being returned to the oil bath. The interim time at ambient temperature was not included in the data analysis. Data points were gathered by ¹H NMR spectroscopy, and the rate of disappearance of hafnium stannyl species was monitored by integrating the C₅H₅ peak relative to Cp₂Fe. The rate constant was calculated from first-order plots using data from the first 3–5 half lives.

4.1.1. CpCp*Hf(SnPh₂SnHMes₂)Cl (6**).** The hydrostannyl complex **2** (0.179 g, 0.232 mmol) was dissolved in toluene (5 mL), and a solution of Ph₂SnH₂ (0.064 g, 0.23 mmol) in toluene (5 mL) was added. After 1 h, solvent was removed, and the red–orange residue was washed with pentane (30 mL). The remaining yellow solid was extracted with Et₂O (35 mL), and the yellow solution was filtered via cannula, concentrated to ca. 7 mL, and cooled to –30 °C. A small amount of yellow powder (the desired product **6** and CpCp*(Cl)Hf(μ-O)Hf(Cl)Cp*Cp in a 1.5:1 ratio) was separated via cannula filtration, and the deep yellow filtrate was concentrated to ca. 1 mL and cooled to –30 °C. A small amount of yellow, crystalline solid (0.025 g) was isolated that contained **6**, CpCp*(Cl)Hf(μ-O)Hf(Cl)Cp*Cp (3 mol%), and the cyclic oligostannanes (Ph₂Sn)_n and (Mes₂Sn)_n (14 mol%). ¹H NMR: δ 1.78 (s, 15H, C₅Me₅), 2.11 (s, 6H, *p*-C₆H₂Me₃), 2.41 (s, 6H, *o*-C₆H₂Me₃), 2.49 (s, 6H, *o*-C₆H₂Me₃), 5.88 (s, ³J_{SnH}=7.2 Hz, 5H, C₅H₅), 6.76 (s, ¹J_{117/119SnH}=1213, 1269 Hz, ²J_{117/119Sn-H}=108, 112 Hz, 1H, Sn–H), 6.78 (s, 2H, C₆H₂Me₃), 6.79 (s, 2H, C₆H₂Me₃), 7.14–7.17 (m, overlapping with C₆D₅H resonance, *p*-C₆H₅), 7.22–7.25 (m, 4H, *m*-C₆H₅), 7.83–7.92 (m, 4H,

o-C₆H₅). ¹³C{¹H} NMR: δ 13.19 (s, ³J_{SnC}=12.3 Hz, C₅Me₅), 21.45 (s, *p*-C₆H₂Me₃), 21.46 (s, *p*-C₆H₂Me₃), 27.58 (s, ²J_{SnC}=34.5 Hz, *o*-C₆H₂Me₃), 28.01 (s, ²J_{SnC}=34.2 Hz, *o*-C₆H₂Me₃), 112.6 (s, C₅H₅), 121.5 (s, C₅Me₅), 127.52 (s, *p*-C₆H₅), 127.58 (s, *p*-C₆H₅), *m*-C₆H₂Me₃ not observed (these resonances are often coincident with that of C₆D₆),⁸ 128.75 (s, *m*-C₆H₅), 128.79 (s, *m*-C₆H₅), 137.72 (s, *p*-C₆H₂Me₃), 137.74 (s, *p*-C₆H₂Me₃), 139.32 (s, *o*-C₆H₅), 139.38 (s, *o*-C₆H₅), 141.58 (s, *ipso*-C₆H₅), 142.01 (s, *ipso*-C₆H₅), 145.59 (s, ²J_{SnC}=31.4 Hz, *o*-C₆H₂Me₃), 145.61 (s, ²J_{SnC}=32.4 Hz, *o*-C₆H₂Me₃), 149.81 (s, *ipso*-C₆H₂Me₃), 150.00 (s, *ipso*-C₆H₂Me₃). ¹¹⁹Sn{¹H} NMR: δ –288.9 (s, ¹J_{SnSn}=185 Hz, Hf–SnPh₂SnHMes₂), 44.2 (s, ¹J_{SnSn}=185 Hz, Hf–SnPh₂SnHMes₂). IR (KBr): 3057 (m), 3041 (m), 3009 (m), 2955 (s), 2914 (s), 2859 (s), 2728 (w), 1766 (s, ν_{SnH}), 1596 (w), 1572 (w), 1543 (w), 1476 (m), 1441 (s), 1426 (s), 1402 (m), 1379 (m), 1289 (w), 1258 (w), 1114 (vw), 1062 (m), 1017 (s), 846 (m), 815 (s), 724 (s), 699 (s), 627 (m), 589 (s), 541 (m), 486 (w), 447 (s).

4.1.2. CpCp*Hf(SnPh₂SnHPh₂)Cl (7**).** A solution of Ph₂SnH₂ (0.265 g, 0.964 mmol, 2.04 equiv.) in toluene (2 mL) was added to a solution of **1** (0.196 g, 0.472 mmol) in toluene (8 mL). This mixture was stirred at room temperature for 15 min, and solvent was removed in vacuo to leave a red–orange foam. The foam was extracted with pentane (35 mL) and filtered via cannula, and the resulting red–orange solution was concentrated to ca. 15 mL and cooled to –30 °C. A yellow powder was isolated that was recrystallized two times to give the product in 91% purity and 58% yield (0.229 g, 0.272 mmol). ¹H NMR: δ 1.75 (s, 15H, C₅Me₅), 5.745 (s, ³J_{SnH}=9.5 Hz, 5H, C₅H₅), 6.91 (s, ¹J_{117/119SnH}=1329, 1392 Hz, ²J_{117/119Sn-H}=88, 92 Hz, 1H, Sn–H), 7.09–7.14 (m, 4H SnH(*m*-C₆H₅)₂), 7.14–7.16 (m, overlapping with C₆D₅H resonance, Sn(*p*-C₆H₅)₂ and SnH(*m*-C₆H₅)₂), 7.19–7.24 (m, 4H, Sn(*m*-C₆H₅)₂), 7.71–7.85 (m, 4H, SnH(*o*-C₆H₅)₂), 7.89–7.99 (m, 4H, Sn(*o*-C₆H₅)₂). ¹³C{¹H} NMR: δ 13.16 (s, ³J_{SnC}=13.2 Hz, C₅Me₅), 112.4 (s, C₅H₅), 121.2 (s, C₅Me₅), 127.79 (s, Sn(*p*-C₆H₅)₂), 127.83 (s, Sn(*p*-C₆H₅)₂), SnH(*p*-C₆H₅)₂ not observed (presumably coincident with the C₆D₆ resonance), 129.01 (s, SnH(*p*-C₆H₅)₂), 129.03 (s, Sn(*m*-C₆H₅)₂), 129.06 (s, Sn(*m*-C₆H₅)₂), 139.10 (s, Sn(*o*-C₆H₅)₂), 139.23 (s, Sn(*o*-C₆H₅)₂), 139.53 (s, ²J_{SnC}=21.0 Hz, SnH(*o*-C₆H₅)₂), 141.95 (s, Sn(*ipso*-C₆H₅)₂), 142.42 (s, Sn(*ipso*-C₆H₅)₂), 148.81 (s, SnH(*ipso*-C₆H₅)₂), 149.30 (s, SnH(*ipso*-C₆H₅)₂). ¹¹⁹Sn{¹H} NMR: δ –172.1 (s, Hf–SnPh₂SnHPh₂), 66.2 (s, Hf–SnPh₂SnHPh₂). IR: 3057 (s), 3041 (s), 1770 (s, ν_{Sn-H}), 1573 (m), 1427 (s), 1329 (v. w), 1297 (v. w), 1257 (v. w), 1189 (w), 1156 (v. w), 1066 (m), 997 (m), 819 (s), 725 (s), 699 (s), 569 (s), 547 (s), 447 (s). Mp 65 °C (dec).

4.1.3. Observation of CpCp*Hf(SnPh₂SnPh₂SnHPh₂)Cl (8**).** A solution of Ph₂SnH₂ (0.021 g, 0.075 mmol, 2.0 equiv.) in benzene-*d*₆ (0.2 mL) was added to a solution of **1** (0.015 g, 37 mmol) in benzene-*d*₆ (0.3 mL). Vigorous hydrogen evolution was observed, and a deep orange color developed. The tristannyl complex **7** was observed as 12% of the Hf species in solution. ¹H NMR: δ 1.71 (s, 15H, C₅Me₅), 5.737 (s, 5H, C₅H₅). ¹¹⁹Sn{¹H} NMR: δ –208.8 (s, Hf–SnPh₂SnPh₂SnHPh₂), –180.3 (s, Hf–SnPh₂SnPh₂–SnHPh₂), 76.2 (s, Hf–SnPh₂SnPh₂SnHPh₂).

4.1.4. Observation of CpCp*Hf(Me)Cl (10). Complex **11** (0.0088 g, 0.015 mmol) and ferrocene (0.0025 g, 0.013 mmol) were weighed in a 1.00 ± 0.01 mL volumetric flask, and toluene-*d*₈ was added to make 1.00 mL. A portion of this solution was transferred to a J. Young NMR tube, which was wrapped in aluminum foil to protect the solution from light. After heating the solution to 100 °C for 24 h, the mixture contained **10** in 98% yield. ¹H NMR (toluene-*d*₈): δ -0.05 (s, 3H, Hf-Me), 1.75 (s, 15H, C₅Me₅), 5.71 (s, 5H, C₅H₅).

4.1.5. CpCp*Hf(SnMe₃)Cl (11). The stannane Me₃SnH was prepared in tetraglyme from ClSnMe₃ (0.11 g, 0.57 mmol) and LAH (0.019 g, 0.50 mmol, 0.88 equiv.) according to the literature procedure.²⁶ The stannane was vacuum transferred onto a frozen solution of CpCp*Hf(H)Cl (0.21 g, 0.51 mmol) in THF (10 mL). The mixture was allowed to come to room temperature, and after 30 min an orange color had developed. The solution was stirred for 12 h in the dark, at which point solvent was removed in vacuo from the resulting yellow–orange solution, leaving an orange–yellow residue. The residue was extracted with pentane (20 mL), and the resulting orange solution was filtered via cannula, concentrated to ca. 5 mL and cooled to -30 °C. The product was isolated as red crystals in 63% yield (0.18 g, 0.32 mmol). ¹H NMR: δ 0.46 (s, ²J_{SnH}=31 Hz, 9H, SnMe₃), 1.79 (s, 15H, C₅Me₅), 5.76 (s, ³J_{SnH}=7.1 Hz, 5H, C₅H₅). ¹³C{¹H} NMR: δ -1.24 (s, ¹J_{SnC}=106 Hz, SnMe₃) 12.8 (s, ³J_{SnC}=12.5 Hz, C₅Me₅), 111.2 (s, C₅H₅), 119.8 (s, C₅Me₅). ¹¹⁹Sn{¹H} NMR: δ 147.9 (s). Anal. Calcd. for C₁₈H₂₉ClSnHf: C, 37.40; H, 5.06. Found: C, 37.72; H, 5.00. IR: 3090 (m), 2729 (w), 1734 (v. w), 1653 (v. w), 1559 (v. w), 1177 (v. w), 1161 (w), 884 (m, br), 826 (s), 785 (w), 749 (m), 676 (w), 652 (w), 549 (v. w), 533 (w), 493 (m). Mp 112–113 °C.

4.1.6. CpCp*Hf(SnBu₃)Cl (12). A solution of Bu₃SnH (0.071 g, 0.244 mmol) in THF (5 mL) was added to a solution of CpCp*Hf(H)Cl (0.100 g, 0.241 mmol) in THF (15 mL) at -78 °C. With stirring in the dark, the mixture was allowed to come to room temperature, and the stirring was continued for 12 h. Solvent was removed in vacuo from the resulting red–orange solution, leaving a sticky, red–orange residue. The residue was extracted with pentane (20 mL), and the resulting orange solution was filtered via cannula, concentrated to ca. 1 mL and cooled to -80 °C. The product was isolated as a red–orange solid in 68% yield (0.120 g, 0.124 mmol). ¹H NMR: δ 1.18 (t, ³J_{HH}=7.5 Hz, 9H, SnCH₂CH₂CH₂CH₃), 1.20–1.30 (m, 6H, SnCH₂CH₂CH₂CH₃), 1.68 (d of quin, ³J_{HH}=15 Hz, ³J_{SnH}=15 Hz, 6H, SnCH₂CH₂CH₂CH₃), 1.84–1.91 (m, 6H, SnCH₂CH₂CH₂CH₃), 1.93 (s, 15H, C₅Me₅), 5.96 (s, ³J_{SnH}=6.5 Hz, 5H, C₅H₅). ¹³C{¹H} NMR: δ 12.9 (s, ³J_{SnC}=10.1 Hz, C₅Me₅), 14.5 (s, SnCH₂CH₂CH₂CH₃), 16.1 (s, SnCH₂CH₂CH₂CH₃), 29.5 (s, ¹J_{SnC}=39.8 Hz, SnCH₂CH₂CH₂CH₃), 31.7 (s, ²J_{SnC}=12.5 Hz, SnCH₂CH₂CH₂CH₃), 111.0 (s, C₅H₅), 119.9 (s, C₅Me₅). ¹¹⁹Sn{¹H} NMR: δ 154.4 (s). Anal. Calcd. for C₂₇H₄₇ClSnHf: C, 46.04; H, 6.73. Found: C, 46.18; H, 6.71. IR: 3117 (w), 2730 (w), 1718 (v. w), 1700 (v. w), 1684 (v. w), 1652 (v. w), 1635 (v. w), 1558 (v. w), 1540 (v. w), 1488 (m), 1339 (w), 1282 (w), 1181 (v. w), 1136 (v. w), 1063 (m), 961 (w), 906 (v. w), 857 (w), 816 (s), 767 (v. w), 730 (m), 655 (m), 624 (w), 571 (m). Mp 57–59 °C.

4.1.7. Observation of CpCp*Hf(SnMe₂SnMe₃)Cl (13). A solution of **11** (0.047 g, 0.080 mmol) in benzene-*d*₆ was heated to 100 °C for 1 h. After cooling to room temperature, complex **13** was observed in a yield of 17%. ¹H NMR: δ 0.467 (s, 9H, SnMe₃), SnMe₂ not definitively identified (this resonance presumably overlaps with those from (Me₂Sn)_{*n*}), 1.792 (s, 15H, C₅Me₅), 5.766 (s, 5H, C₅H₅). ¹¹⁹Sn{¹H} NMR: δ -76.0 (s, ¹J_{117/119Sn-119Sn}=448, 468 Hz, Hf-SnMe₂SnMe₃), 38.6 (s, ¹J_{117/119Sn-119Sn}=448, 468 Hz, Hf-SnMe₂SnMe₃).

4.1.8. Observation of CpCp*Hf(SnMe₂SnMe₂SnMe₃)Cl (14). A solution of **11** (0.047 g, 0.080 mmol) in benzene-*d*₆ was heated to 100 °C for 1 h. After cooling to room temperature, complex **14** was observed in a yield of 7%. ¹H NMR: SnMe₃ and SnMe₂ not definitively identified (these resonances presumably overlap with those from **11**, **13**, and (Me₂Sn)_{*n*}), δ 1.801 (s, 15H, C₅Me₅), 5.773 (s, 5H, C₅H₅). ¹¹⁹Sn{¹H} NMR: δ -211.9 (s, Hf-SnMe₂SnMe₂SnMe₃), -97.2 (s, Hf-SnMe₂SnMe₂SnMe₃), 57.0 (s, Hf-SnMe₂SnMe₂SnMe₃).

4.1.9. Observation of Ph₂HSnSnMe₂SnHPh₂. A solution of **11** (0.010 g, 0.017 mmol) and Ph₂SnH₂ (0.0095 g, 0.035 mmol, 2 equiv.) in benzene-*d*₆ (0.5 mL) was heated to 100 °C for 1 h. After cooling to room temperature, the tristannane was observed in a yield of 29% from the stannane (the theoretical yield for this species is 50%). ¹H NMR: δ 0.47 (s, 4H, SnMe₃), 6.90 (s, ¹J_{117/119SnH}=1848, 1934 Hz, 1H, Sn-H), 7.13–7.15 (m, 12H, *m*- and *p*-C₆H₅), 7.49–7.52 (m, ³J_{SnH}=50 Hz, *o*-C₆H₅). ¹¹⁹Sn{¹H} NMR: δ -232.8 (s, ¹J_{117/119Sn-119Sn}=1264, 1284 Hz, Ph₂-HSnSnMe₂SnHPh₂), -161.4 (s, ¹J_{117/119Sn-119Sn}=1264, 1284 Hz, Ph₂HSnSnMe₂SnHPh₂).

4.1.10. Observation of CpCp*Hf(SnPh₂SnMe₃)Cl (15). A solution of **11** (0.010 g, 0.017 mmol) and Ph₂SnH₂ (0.0095 g, 0.035 mmol, 2 equiv.) in benzene-*d*₆ (0.5 mL) was heated to 100 °C for 1 h. After cooling to room temperature, **15** was observed in a yield of 18%. ¹H NMR: δ 0.51 (s, ²J_{117/119SnH}=42, 44 Hz, ³J_{SnH}=7.9 Hz, 9H, SnMe₃), 1.785 (s, 15H, C₅Me₅), 5.80 (s, ³J_{SnH}=7.0 Hz, 5H, C₅H₅), *p*-C₆H₅ resonance not observed (presumably overlaps with resonances for Ph₂HSnSnMe₂SnHPh₂), 7.26–7.29 (m, 4H, *m*-C₆H₅), 7.80–7.85 (m, 4H, *o*-C₆H₅). ¹¹⁹Sn{¹H} NMR: δ -67.4 (s, ¹J_{117/119Sn-119Sn}=456, 478 Hz, Hf-SnPh₂-SnMe₃), 63.5 (s, ¹J_{117/119Sn-119Sn}=456, 478 Hz, Hf-SnPh₂-SnMe₃).

Acknowledgements

Acknowledgment is made to the National Science Foundation for their generous support of this work.

References and notes

- (a) West, R. J. *Organomet. Chem.* **1986**, *300*, 327. (b) Miller, R. D.; Michl, J. *Chem. Rev.* **1989**, *89*, 1259.
- Miller, R. D.; MacDonald, S. A. *J. Imaging Sci.* **1987**, *31*.
- Pitt, C. G. In *Homoaromatic Rings, Chains and*

- Macromolecules of Main-Group Elements*; Rheingold, A. L., Ed.; Elsevier: New York, 1977; Chapter 8.
- Lu, V. Y.; Tilley, T. D. *Macromolecules* **2000**, *33*, 2403.
 - (a) Neumann, W. P.; König, K. *Angew. Chem., Int. Ed.* **1962**, *1*, 212. (b) Sawyer, A. K.; Kuivila, H. G. *J. Am. Chem. Soc.* **1963**, *85*, 1010. (c) Neumann, W. P.; Pedain, J. *Liebigs Ann. Chem.* **1964**, *672*, 34. (d) Neumann, W. P.; Pedain, J. *Liebigs Ann. Chem.* **1964**, *677*, 1. (e) Sawyer, A. K. *J. Am. Chem. Soc.* **1965**, *87*, 537. (f) Neumann, W. P.; Pedain, J.; Sommer, R. *Liebigs Ann. Chem.* **1966**, *694*, 9. (g) Ritter, H.-P.; Neumann, W. P. *J. Organomet. Chem.* **1973**, *56*, 199. (h) Jousseaume, B.; Chanson, E.; Bevilacqua, M.; Saux, A.; Pereyre, M.; Barbe, B.; Petraud, M. *J. Organomet. Chem.* **1985**, *294*, C41. (i) Zou, W. K.; Yang, N.-L. *Polym. Prepr. (Am. Chem. Div. Polym. Chem.)* **1992**, *33*, 188. (j) Sita, L. R. *Organometallics* **1992**, *11*, 1442. (k) Imori, T.; Tilley, T. D. *J. Chem. Soc., Chem. Commun.* **1993**, *21*, 1607. (l) Sita, L. R.; Terry, K. W.; Kazusato, S. *J. Am. Chem. Soc.* **1995**, *117*, 8049.
 - (a) Imori, T.; Lu, V.; Cai, H.; Tilley, T. D. *J. Am. Chem. Soc.* **1995**, *117*, 9931. (b) Lu, V.; Tilley, T. D. *Macromolecules* **1996**, *29*, 5763.
 - (a) Woo, H.-G.; Tilley, T. D. *J. Am. Chem. Soc.* **1989**, *111*, 8043. (b) Woo, H.-G.; Walzer, J. F.; Tilley, T. D. *J. Am. Chem. Soc.* **1992**, *114*, 7047. (c) Tilley, T. D. *Acc. Chem. Res.* **1993**, *26*, 22.
 - (a) Neale, N. R.; Tilley, T. D. *J. Am. Chem. Soc.* **2002**, *124*, 3802. (b) Neale, N. R.; Tilley, T. D. Submitted for publication. (c) Neale, N. R. PhD Thesis, University of California: Berkeley, 2003.
 - Neale, N. R.; Tilley, T. D. Submitted for publication.
 - Jousseaume, B.; Noiret, N.; Pereyre, M.; Saux, A.; Francès, J.-M. *Organometallics* **1994**, *13*, 1034.
 - The low yield (<2%) of this species in solution precluded observation of Sn–H satellites ($^1J_{\text{SnH}}$ and $^2J_{\text{SnH}}$). However, the downfield shift of the Sn–H group in the ^1H NMR spectrum is consistent with the distannane structure (cf. δ 6.49 for $\text{Mes}_2\text{HSnSnHMes}_2$)⁸.
 - Compound **5** has previously been prepared in situ for use in preparatory scale reactions,^{8,9} but since it could not be isolated in pure form, it was not suitable for use in this mechanistic study.
 - Hafnocene stannyl complexes are characterized by ^{119}Sn NMR shifts of ca. δ 100,^{8,9} whereas hydrostannanes exhibit shifts that are well upfield of δ 0. In *Chemistry of Tin*; Harrison, P. G., Ed.; Blackie: New York, 1989; Chapter 2.
 - Holt, M. S.; Wilson, W. L.; Nelson, J. H. *Chem. Rev.* **1989**, *89*, 11.
 - Mitchell, T. N. *J. Organomet. Chem.* **1974**, *70*, C1.
 - Davies, A. G. *Organotin Chemistry*; VCH: New York, 1997; p 253.
 - Kobayashi, K.; Kawanisi, M.; Hitomi, T.; Kozima, S. *J. Organomet. Chem.* **1982**, *233*, 299.
 - Crabtree, R. H. *The Organometallic Chemistry of the Transition Metals*; 2nd ed.; Wiley: New York, 1994; Section 7.2.
 - Mitchell, T. N.; Walter, G. *J. Chem. Soc. Perkins Trans. 2* **1977**, 1842.
 - Neumann, W. P. *Chem. Rev.* **1991**, *91*, 311.
 - Al-Allaf, T. A. K. *J. Organomet. Chem.* **2002**, *654*, 21.
 - Neumann, W. P. *The Organic Chemistry of Tin*; Wiley: New York, 1970.
 - Yamamoto, K.; Okinoshima, H.; Kumada, M. *J. Organomet. Chem.* **1971**, *27*, C31.
 - Harrod, J. F.; Yun, S. S. *Organometallics* **1987**, *6*, 1381.
 - Hengge, E.; Weinberger, M. *J. Organomet. Chem.* **1993**, *443*, 167.
 - Kuivila, H. G.; Dixon, J. E.; Maxfield, P. L.; Scarpa, N. M.; Topka, T. M.; Tsai, K.-H.; Wursthorn, K. R. *J. Organomet. Chem.* **1975**, *86*, 89.

Phototriggering of geometric dendrimer disassembly: an improved synthesis of 2,4-bis(hydroxymethyl)phenol based dendrimers

Michael L. Szalai and Dominic V. McGrath*

Department of Chemistry, University of Arizona, Rm 221, PO Box 210041, Tucson, AZ 85721-0041, USA

Received 27 May 2004; accepted 14 June 2004

Abstract—Dendrimers capable of phototriggered disassembly were prepared up to the second-generation using an improved synthesis of 2,4-bis(hydroxymethyl)phenol based dendrimers. It was found that disassembly proceeds to 75–80% completion after 2 h of irradiation at 310 nm for all molecules studied. The lack of complete reaction is attributed to an inefficient photochemical deprotection process rather than the disassembly itself.

© 2004 Elsevier Ltd. All rights reserved.

1. Introduction

Dendrimers are a class of polymeric materials characterized by their highly globular nature.^{1,2} Though normally prepared as stable covalent structures, dendritic materials with stimuli responsive linkages present attractive possibilities for controlled alteration of the properties of a system, including solubility, energy harvesting, or insulating capabilities. Accordingly, development of methods for the controlled degradation of dendrimers and dendritic macromolecules into discrete subunits is a primary goal of our research program. Recently, we^{3,4} and others^{5,6} have reported the fragmentation of dendrimers whereby each cleavable unit requires 1 equiv. of a triggering stimulus in order to proceed (i.e., stoichiometric degradation). Envisioning a more efficient approach where multiple cleavage events are triggered by a single stimulus, we demonstrated the first dendritic system capable of disassembly into its constituent parts along a linear cleavage vector.⁷ To expand upon this concept, we⁸ and others^{9–11} reported the preparation of dendrimers containing multiple disassembly pathways within the dendritic subunit itself, namely geometric disassembly.

Our dendrimer subunit, 2,4-bis(hydroxymethyl)phenol, contains both *ortho* and *para* disassembly pathways (Fig. 1).⁸ Removal of the trigger group (TG) in **A** generates phenoxide **B**. This vinylogous hemiacetal anion rapidly undergoes cleavage to yield an alkoxide ([−]OR) as well as

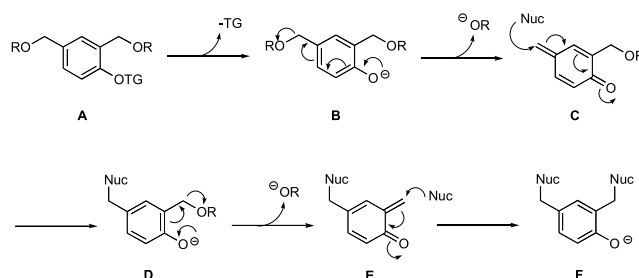


Figure 1. Geometric dendrimer disassembly process illustrating two subsequent cleavages proceeding via intermediate quinone methides.

quinone methide **C**. In the presence of a nucleophile (Nuc), the quinone methide is rapidly trapped to generate a new vinylogous hemiacetal anion **D**. Again, rapid cleavage occurs, releasing a second equivalent of alkoxide ([−]OR) and a new quinone methide **E**. Nucleophilic trapping results in phenoxide **F**. Within a disassembling dendrimer, released alkoxides ([−]OR) are analogous in structure to **B** and disassemble similarly. For a single triggering event at the focal point of a dendron, the total number of periphery and branching subunits released in a geometric disassembly is:

$$\text{released subunits} = \underbrace{N_b^G}_{\text{\# periphery subunits}} + \underbrace{\left(\frac{N_b^G - 1}{N_b - 1} \right)}_{\text{\# branching subunits}}$$

where N_b is the branching multiplicity and G is the generation.

In a previous report,⁸ we demonstrated that the allyl group was an effective trigger albeit under relatively harsh

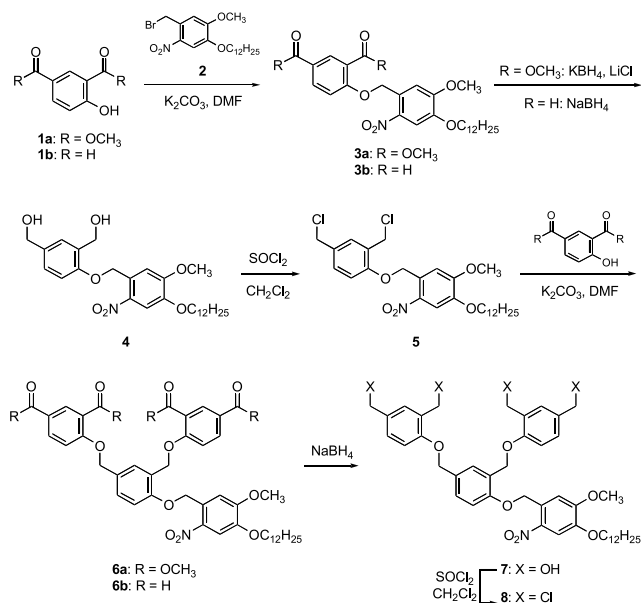
Keywords: Dendrimers; Disassembly; Tetrahydrofuran.

* Corresponding author. Tel.: +1-520-626-4690; fax: +1-520-621-8407; e-mail address: mcgrath@u.arizona.edu

conditions ($\text{Pd}(\text{PPh}_3)_4/\text{NaBH}_4$). Herein we report the preparation and disassembly of dendrons that require only light and mild base to trigger disassembly. This current preparation also improves significantly on our previous synthesis of geometric disassembling dendrimers.⁸

2. Synthesis

To prepare the target dendrons it was first necessary to attach a photolabile group to the dendrimer subunit and proceed by a divergent synthetic strategy. We chose to use an *o*-nitrobenzyl derivative owing to its well-understood and relatively clean photodegradation.¹² Our initial plan was to proceed through the synthesis utilizing dimethyl 4-hydroxyisophthalate (**1a**) as the generational building block as we previously reported.⁸ Indeed, alkylation of **1a** with photolabile benzyl bromide trigger **2** (Scheme 1) proceeded smoothly to give diester **3a**. However, selective reduction of the ester moieties of **3a** gave diol **4** in only poor to moderate yields (maximum 45%), presumably complicated by the presence of the nitro group.

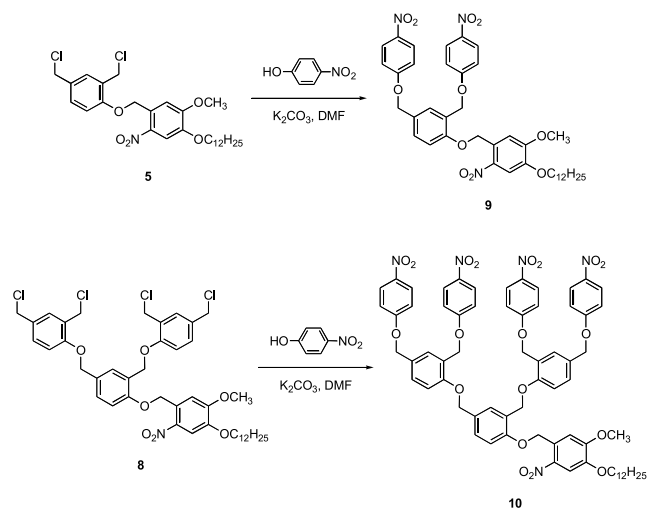


Scheme 1.

Despite these troubling results in the early stages of the synthesis, we chose to proceed using **1a** as the building block. Chlorination of **4** using thionyl chloride provided dichloride **5** in excellent yields and its coupling with 2 equiv. of **1a** gave tetraester **6a** in 73% yield. However, selective reduction of **6a** to tetraalcohol **7** proved problematic. We attempted this reduction using: KBH_4/LiCl in THF or THF–MeOH both at room temperature and at reflux;¹³ $\text{NaBH}_4/\text{THF}/\text{MeOH}$ at reflux;¹⁴ $\text{LiBH}_4/\text{THF}/\text{MeOH}$ both at room temperature and at 60 °C; LAH/THF at room temperature; and LAH/ SiO_2 in Et_2O ¹⁵ at room temperature. Only $\text{LiBH}_4/\text{THF}/\text{MeOH}$ at 60 °C provided the desired product albeit with a small amount of incomplete reduction products that were not easily removed.

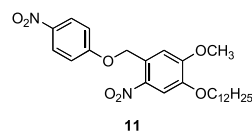
In order to bypass this ester reduction step, we attempted to use 2,4-bis(hydroxymethyl)phenol¹⁶ as our generational building block. Reaction of this compound with **5** in DMF/ K_2CO_3 at 60 °C resulted in decomposition to lower molecular weight compounds (GPC). Lowering the temperature to 40 °C did not improve these results.

More successful were our attempts to use the corresponding phthalaldehyde derivative as a building block. Specifically, reaction of 4-hydroxy isophthalaldehyde (**1b**)¹⁷ with **2** gave dialdehyde **3b** in good yields, and subsequent reduction of **3b** with sodium borohydride proceeded smoothly to give bis(benzyl alcohol) **4** in 93% yield, a significant improvement over the diester reduction (Scheme 1). Chlorination of **4** using thionyl chloride yielded **5** and subsequent coupling with 2 equiv. of **1b** gave first-generation tetraaldehyde **6b**. To our delight, selective reduction of **6b** using relatively mild conditions (NaBH_4/THF at RT) gave tetraalcohol **7** in good yields. Chlorination with thionyl chloride proceeded smoothly resulting in tetrachloride **8**.



Scheme 2.

The *p*-nitrophenoxide ion exhibits a strong absorption band (430 nm) and a distinctive ^1H NMR signal. Thus, in order to easily monitor the disassembly of these dendrons, *p*-nitrophenoxy moieties were installed at the periphery of both dendrons to indicate the extent of disassembly. Accordingly, reaction of **5** and **8** with a slight excess of *p*-nitrophenol (Scheme 2) gave the first generation (**9**) and second generation (**10**) reporter labeled dendrons, respectively, in good yields. Coupling of *p*-nitrophenol with the *o*-nitrobenzyl bromide trigger **2** furnished control compound **11** consisting of the reporter moiety directly attached to the photolabile trigger group.



3. Disassembly studies

3.1. UV–Vis spectroscopy

Compounds **9–11** were thermally stable yet upon release of the photolabile group with irradiation (310 nm) under basic conditions, dendrimer disassembly occurs. Because of the liberation of the strongly absorbing (430 nm) *p*-nitrophenoxide ion, we were able to monitor this process by UV–Vis spectroscopy. Irradiation of DMF solutions (NaBH₄, 1 mg/mL) of **9–11** at 310 nm for increasing time intervals resulted in a decrease of the absorbance band at 310 nm with a concomitant increase of the band at 430 nm (Fig. 2). Substrate concentrations were adjusted such that the final *p*-nitrophenoxide ion absorbance would equal 1.0 upon complete disassembly based on the absorptivity of the ion. Thus, we observed approximately 80% *p*-nitrophenoxide liberation for **9–11** and the disassembly process concluded within 2 h of irradiation. Because the control compound **11** releases only 80% of the expected reporter ion, we conclude that non-quantitative reporter ion liberation arises from the photochemical deprotection process of the *o*-nitrobenzyl trigger rather than from the subsequent disassembly that occurs in compounds **9** and **10**.

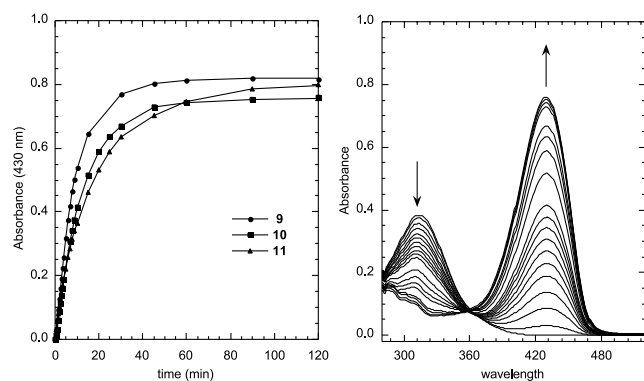


Figure 2. Left: absorbance of *p*-nitrophenoxide ion (430 nm) monitored as a function of 310 nm irradiation time during disassembly of **9–11**. Right: UV–Vis absorption spectra of a solution of **9** containing 1 mg/mL NaBH₄ in DMF after irradiation at 310 nm for various times (0, 1, 2, 3, 4, 5, 6, 7, 8, 9, 10, 15, 20, 25, 30, 45, 60, 90, and 120 min).

3.2. NMR spectroscopy

The photodisassembly of compounds **9–11** was also monitored by ¹H NMR spectroscopy in DMSO-*d*₆ (18 mM) upon irradiation in a Rayonet photochemical chamber (350 nm). The photolabile *o*-nitrobenzyl group is known to cleave at the benzyl ether bond releasing liberated alcohol and the appropriate *o*-nitroso benzaldehyde derivative. Initial NMR spectroscopic studies were carried out on **11** (Fig. 3). After various irradiation times there is clearly

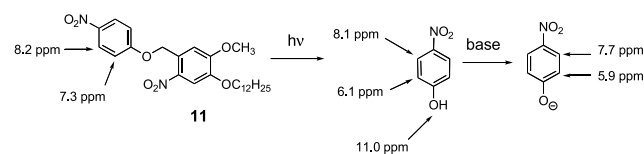


Figure 3. Characteristic ¹H NMR chemical shifts observed while monitoring the disassembly of compound **11**. Conditions: DMSO-*d*₆, 18 mM, 350 nm irradiation.

disappearance of the starting material in the ¹H NMR spectrum with concomitant increase of a new upfield AA'BB' pattern (8.11 and 6.92 ppm) and singlet at 11.0 ppm, indicative of the release of *p*-nitrophenol. However, the aromatic protons of the photocleavable trigger completely disappear and no new corresponding peaks arise. In addition, the methoxy singlet (3.88 ppm) and the methylene triplet (4.06 ppm) decrease in intensity but over 10 h of irradiation this region of the spectra becomes crowded with a multitude of unidentified peaks. It appears that the photocleavage product decomposes over time under the conditions of these experiments. Indeed, we saw similar results in this regard when studying compounds **9** and **10**. This information further confirms that the inefficiency seen in the UV–Vis experiments (80% completion) arises primarily in the photodeprotection process and not in the disassembly itself. Photodecomposition of veratryl based nitrobenzyl ethers are known to be accompanied by complicating side reactions.¹⁸

Addition of sodium borohydride to the sample of **11** after 10 h of irradiation results in the disappearance of the singlet at 11.0 ppm and an upfield shift of the AA'BB' pattern to 7.73 and 5.96 ppm, indicating formation of *p*-nitrophenoxide ion. Performing the irradiation of the sample in the presence of sodium borohydride does not alter the ultimate results but we clearly see generation of the *p*-nitrophenoxide ion over time rather than *p*-nitrophenol. The photochemical process appears to be complete after 6–10 h of irradiation time.

Irradiation of **9** in the absence of base similarly releases the phenolic form of the dendron intact (Fig. 4, center). This is indicated by a new singlet at 10.0 ppm (phenol OH) and an upfield shift of the peaks assigned to the isophthalyl branching subunit. In addition, the three benzyl singlets (5.48, 5.28, and 5.21 ppm) decrease over irradiation time and we observe two new singlets (5.17 and 5.12 ppm) in the benzyl region. Addition of sodium borohydride results in the complete disappearance of phenol (10.0 ppm) and the two new benzyl singlets (5.17 and 5.12 ppm) with the concomitant generation of *p*-nitrophenoxide ion (7.72 and 5.96 ppm) and two new singlets at 2.12 and 2.04 ppm. The upfield singlets are independently confirmed to be the 2,4-dimethylphenoxide ion. Irradiation of the sample in the presence of borohydride ultimately gives the same results but the process is less clean.

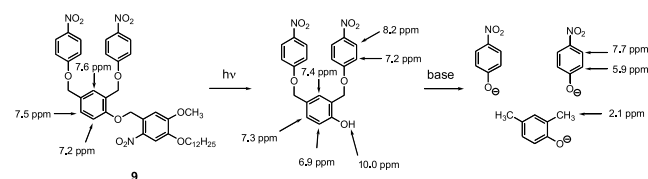


Figure 4. Characteristic ¹H NMR chemical shifts observed while monitoring the disassembly of compound **9**. Conditions: DMSO-*d*₆, 18 mM, 350 nm irradiation.

After 10 h of irradiation of a sample of **10** and the addition of sodium borohydride we see the same ultimate results as with compound **9**, i.e. generation of *p*-nitrophenoxide and

2,4-dimethyl phenoxide. It appears, though, that the photocleavage process for this compound is not complete even after 10 h because we can still see significant amounts of the benzyl peaks of the starting material after the addition of the borohydride. However, the sample irradiated in the presence of borohydride shows complete disappearance of all benzyl peaks after 10 h.

4. Summary

We have prepared dendrimers capable of phototriggered disassembly up to the second generation. During the course of this work it was found that the preferred synthetic route utilizes isophthalaldehyde building blocks rather than isophthalate esters because of the incompatibility of the trigger with the various reaction conditions of the synthesis. The dendrimers are thermally stable but disassemble upon irradiation under basic conditions.

5. Experimental

5.1. General methods

NMR spectroscopy and mass spectrometry (MS) were obtained using commercially available instrumentation. Tetrahydrofuran (THF) was distilled under N₂ from sodium-benzophenone ketyl. Dichloromethane (CH₂Cl₂) was distilled under N₂ from CaH₂. Acetone was dried over crushed 3 Å molecular sieves. All other needed reagents were purchased from commercial suppliers and used as received. Flash chromatography was performed by the method of Still et al. [*J. Org. Chem.* 1978, 43, 2923–2925] using silica gel (40–63 μm, Merck, Darmstadt, Germany). Thin-layer chromatography (TLC) was performed on precoated plates (Silica Gel 60 F₂₅₄, 250 μm, Merck, Darmstadt, Germany). Melting points are uncorrected.

5.1.1. 4-(4-Dodecyloxy-5-methoxy-2-nitrobenzyloxy) isophthalic acid dimethyl ester (3a). A mixture of **2** (4.30 g, 10 mmol), **1a** (2.21 g, 10.5 mmol), K₂CO₃ (4.14 g, 30 mmol), 18-crown-6 (50 mg) and acetone (75 mL) was stirred at room temperature under argon for 2 days. The solvent was removed and the residue was partitioned between CH₂Cl₂ (100 mL) and water (100 mL). The layers were separated and the organic layer was washed with sat. NaHCO₃ (3×50 mL) and brine. The combined aqueous layers were extracted with CH₂Cl₂, the organic layers were combined, dried over MgSO₄, filtered, and concentrated. Recrystallization of the residue from CH₂Cl₂ gave the desired product (**3a**) as a light yellow solid (4.05 g, 72%): ¹H NMR (300 MHz, CDCl₃) δ 8.58 (d, *J*=2.1 Hz, 1H), 8.20 (dd, *J*₁=2.1 Hz, *J*₂=8.4 Hz, 1H), 8.06 (s, 1H), 7.76 (s, 1H), 7.27 (m, 1H), 7.19 (d, *J*=9.0 Hz, 1H), 5.58 (s, 2H), 4.11 (s, 3H), 4.07 (t, *J*=6.9 Hz, 2H), 3.92 (s, 3H), 3.90 (s, 3H), 1.88 (m, 2H), 1.22–1.58 (m, 18H), 0.87 (t, *J*=6.6 Hz, 3H); ¹³C NMR (75 MHz, CDCl₃) δ 165.9, 164.8, 161.1, 154.9, 147.3, 138.2, 135.5, 133.8, 128.3, 122.6, 119.4, 112.7, 110.3, 108.7, 69.5, 67.7, 56.9, 52.2, 51.9, 31.9, 29.63, 29.61, 29.57, 29.5, 29.3, 28.9, 25.9, 22.7, 14.1; MS (FAB⁺) *m/z* 560.4 (M+H⁺, C₃₀H₄₂NO₉ requires 560.3).

5.1.2. 4-(4-Dodecyloxy-5-methoxy-2-nitrobenzyloxy)-isophthalaldehyde (3b). A mixture of **2** (10.2 g, 23.6 mmol), **1b** (3.54 g, 23.6 mmol), K₂CO₃ (6.53 g, 47.2 mmol) and DMF (200 mL) was stirred at 40 °C under argon overnight. The reaction mixture was cooled to room temperature and water (300 mL) was added. After stirring for 10 min the precipitated solid was filtered and washed thoroughly with water. The solid was dissolved in CH₂Cl₂ and the solution was dried (MgSO₄), filtered, and concentrated. Recrystallization of the yellow solid from CH₂Cl₂/hexanes gave the desired product (**3b**) as a light yellow solid (9.87 g, 84%): ¹H NMR (300 MHz, CDCl₃) δ 10.45 (s, 1H), 10.0 (s, 1H), 8.37 (d, *J*=2.1 Hz, 1H), 8.16 (dd, *J*₁=2.1 Hz, *J*₂=8.4 Hz, 1H), 7.79 (s, 1H), 7.66 (s, 1H), 7.32 (d, *J*=8.4 Hz, 1H), 5.68 (s, 2H), 4.10 (t, *J*=6.9 Hz, 2H), 4.07 (s, 3H), 1.90 (m, 2H), 1.22–1.58 (m, 18H), 0.87 (t, *J*=6.6 Hz, 3H); ¹³C NMR (75 MHz, CDCl₃) δ 189.7, 188.4, 163.2, 154.6, 147.8, 138.7, 136.5, 134.3, 130.1, 126.8, 125.2, 113.6, 109.7, 109.0, 69.5, 68.2, 56.7, 31.9, 29.6, 29.59, 29.5, 29.49, 29.3, 28.8, 25.8, 22.6, 14.1; MS (FAB) *m/z* 499.7 (M⁺, C₂₈H₃₇NO₇ requires 499.3).

5.1.3. 1-(4-Dodecyloxy-5-methoxy-2-nitrobenzyloxy)-2,4-bis(hydroxymethyl)benzene (4). To a solution of **3b** (8.6 g, 17.3 mmol), THF (200 mL), and methanol (1.5 mL) was added NaBH₄ (1.95 g, 51.9 mmol) over 5 m. The reaction mixture was stirred at room temperature under argon for 1 h, after which time it was quenched with water (30 mL) and 0.5 N HCl (2 mL) sequentially and stirred for 30 min after the addition of each. CH₂Cl₂ (50 mL) was added to the mixture and the layers were separated. The organic layer was washed with brine, dried over MgSO₄, filtered, and concentrated. Recrystallization of the yellow solid from CH–Cl₃ gave the desired product (**4**) as a light yellow solid (8.11 g, 93%): ¹H NMR (300 MHz, CDCl₃) δ 7.76 (s, 1H), 7.37 (m, 2H), 7.27 (m, 1H), 6.93 (d, *J*=8.1 Hz, 1H), 5.51 (s, 2H), 4.81 (s, 2H), 4.64 (s, 2H), 4.08 (t, *J*=6.6 Hz, 2H), 3.94 (s, 3H), 2.17 (br s, 1H), 1.88 (m, 2H), 1.79 (br s, 1H), 1.22–1.58 (m, 18H), 0.88 (t, *J*=6.3 Hz, 3H); ¹³C NMR (75 MHz, CDCl₃) δ 155.4, 154.4, 147.5, 139.0, 133.9, 129.4, 128.6, 128.1, 128.0, 111.8, 109.4, 109.1, 69.5, 67.1, 64.8, 61.7, 56.4, 31.89, 31.87, 30.9, 29.63, 29.61, 29.6, 29.5, 29.3, 28.9, 25.9, 22.7, 14.1; MS (FAB⁺) *m/z* 503.4 (M⁺, C₂₈H₄₁NO₇ requires 503.3).

5.1.4. 1-(4-Dodecyloxy-5-methoxy-2-nitrobenzyloxy)-2,4-bis(chloromethyl)benzene (5). To a rapidly stirred mixture of **4** (6.23 g, 12.4 mmol) and CH₂Cl₂ (300 mL) under argon at room temperature was added SOCl₂ via syringe over 5 m. After 20 min the reaction was quenched with sat. NaHCO₃ (30 mL) and stirred for an additional 30 m. The layers were separated and the organic layer was washed thoroughly with sat. NaHCO₃, dried over MgSO₄, filtered, and concentrated. Recrystallization of the yellow solid from chloroform/hexanes gave the desired product (**5**) as a light yellow solid (6.38 g, 95%): ¹H NMR (300 MHz, CDCl₃) δ 7.78 (s, 1H), 7.53 (s, 1H), 7.41 (d, *J*=2.4 Hz, 1H), 7.35 (dd, *J*₁=2.4 Hz, *J*₂=8.1 Hz, 1H), 6.96 (d, *J*=8.7 Hz, 1H), 5.57 (s, 2H), 4.75 (s, 2H), 4.57 (s, 2H), 4.09 (t, *J*=6.9 Hz, 2H), 3.98 (s, 3H), 1.89 (m, 2H), 1.22–1.54 (m, 18H), 0.88 (t, *J*=6.9 Hz, 3H); ¹³C NMR (75 MHz, CDCl₃) δ 156.0, 154.6, 147.4, 138.7, 131.3, 130.9, 130.4, 128.5, 126.1, 112.1, 109.4, 109.0, 69.5, 66.9, 56.7, 45.6, 42.1, 31.9,

29.63, 29.62, 29.6, 29.5, 29.3, 28.9, 25.9, 22.7, 14.1; MS (FAB) m/z 540.39 ($M+H^+$, $C_{28}H_{40}NO_5Cl_2$ requires 540.23).

5.1.5. 1-(4-Dodecyloxy-5-methoxy-2-nitrobenzyloxy)-2,4-bis(3,5-carbomethoxyphenoxy)benzene (6a). Compound **5** (2.38 g, 4.40 mmol) was dissolved in 50 mL of DMF with heating (50 °C). **1a** (1.94 g, 9.24 mmol), K_2CO_3 (2.43 g, 17.6 mmol) and 18-crown-6 (20 mg) were added to the solution and the reaction mixture was stirred at 50 °C under argon for 1 day. The reaction mixture was cooled to room temperature and poured into ice water (350 mL). The cloudy mixture was extracted with CH_2Cl_2 (5×100 mL) and the combined organic layers were dried over $MgSO_4$, filtered, and concentrated. Recrystallization of the resulting yellow solid from CH_2Cl_2 /hexanes gave the desired product (**6a**) as an off-white solid (2.86 g, 73%): 1H NMR (300 MHz, $CDCl_3$) δ 8.49 (m, 2H), 8.10 (m, 2H), 7.76 (s, 1H), 7.69 (m, 1H), 7.43 (dd, $J_1=1.7$ Hz, $J_2=8.6$ Hz, 1H), 7.23 (s, 1H), 7.08 (d, $J=8.7$ Hz, 1H), 7.04 (d, $J=9.0$ Hz, 1H), 7.01 (d, $J=7.8$ Hz, 1H), 5.55 (s, 2H), 5.37 (s, 2H), 5.22 (s, 2H), 4.08 (t, $J=6.9$ Hz, 2H), 3.91 (s, 2H), 3.90 (s, 2H), 3.89 (s, 2H), 3.87 (s, 2H), 3.79 (s, 3H), 1.88 (m, 2H), 1.22–1.54 (m, 18H), 0.88 (t, $J=6.9$ Hz, 3H); ^{13}C NMR (75 MHz, $CDCl_3$) δ 166.0, 165.9, 165.6, 165.5, 161.5, 161.4, 155.1, 154.2, 147.6, 139.1, 134.89, 134.86, 133.7, 133.6, 129.1, 128.3, 128.2, 127.7, 124.7, 122.5, 122.4, 120.4, 113.2, 113.0, 112.3, 109.5, 109.2, 70.3, 69.5, 67.7, 66.3, 56.2, 52.1, 52.09, 31.9, 29.63, 29.61, 29.6, 29.5, 29.3, 28.9, 25.9, 22.7, 14.1; MS (FAB $^+$) m/z 886.6 (M^+ , $C_{48}H_{57}NO_{15}$ requires 887.4).

5.1.6. 1-(4-Dodecyloxy-5-methoxy-2-nitrobenzyloxy)-2,4-bis(3,5-diformylphenoxy)benzene (6b). Compounds **5** (5.23 g, 9.68 mmol) and **1b** (3.05 g, 20.3 mmol) were dissolved in 200 mL of DMF with heating at 50 °C. K_2CO_3 (5.35 g, 9.68 mmol) was added to the solution and the reaction mixture was stirred at 50 °C under argon for 2 days. The reaction mixture was cooled to room temperature and poured into water (300 mL). The precipitate was filtered and washed thoroughly with water. The solid was dissolved in CH_2Cl_2 and washed with sat. $NaHCO_3$ and brine. The organic layer was dried over $MgSO_4$, filtered, and concentrated to a yellow solid. Flash chromatography (SiO_2 , gradient CH_2Cl_2 to 5% ethyl acetate in CH_2Cl_2) gave the desired product (**6b**) as a light yellow solid (3.9 g, 52%): 1H NMR (300 MHz, $CDCl_3$) δ 10.48 (s, 1H), 10.45 (s, 1H), 9.95 (s, 1H), 9.94 (s, 1H), 8.322 (d, $J=2.1$ Hz, 1H), 8.315 (d, $J=2.1$ Hz, 1H), 8.09 (overlapping dd, $J_1=2.1$ Hz, $J_2=8.4$ Hz, 2H), 7.73 (s, 1H), 7.58 (d, $J=2.1$ Hz, 1H), 7.48 (dd, $J_1=2.1$ Hz, $J_2=8.7$ Hz, 1H), 7.24 (d, $J=9.3$ Hz, 1H), 7.22 (d, $J=8.7$ Hz, 1H), 7.15 (s, 1H), 7.09 (d, $J=8.1$ Hz, 1H), 5.55 (s, 2H), 5.43 (s, 2H), 5.27 (s, 2H), 4.07 (t, $J=6.6$ Hz, 2H), 3.78 (s, 3H), 1.88 (m, 2H), 1.22–1.54 (m, 18H), 0.88 (t, $J=6.9$ Hz, 3H); ^{13}C NMR (75 MHz, $CDCl_3$) δ 190.1, 190.0, 188.3, 188.2, 164.8, 164.7, 157.1, 156.0, 154.0, 147.9, 139.4, 135.6, 132.0, 131.9, 129.9, 129.8, 129.7, 128.7, 128.1, 127.1, 125.1, 125.0, 124.2, 113.5, 113.47, 112.6, 109.8, 109.2, 70.5, 69.5, 67.9, 66.5, 56.1, 31.8, 29.6, 29.55, 29.5, 29.45, 29.3, 28.8, 25.8, 22.6, 14.1; MS (FAB $^+$) m/z 767.0 (M^+ , $C_{44}H_{49}NO_{11}$ requires 767.3).

5.1.7. 1-(4-Dodecyloxy-5-methoxy-2-nitrobenzyloxy)-

2,4-bis(3,5-bis(hydroxymethyl)phenoxy)benzene (7). To a stirred solution of **6b** (1.07 g, 1.39 mmol), THF (50 mL), and methanol (1 mL) was added $NaBH_4$ (0.42 g, 11.2 mmol) and the reaction mixture was stirred at room temperature under argon for 4 h. The reaction was slowly quenched with water (10 mL) with stirring. A precipitate formed as water was added. The precipitate was filtered and washed thoroughly with water, CH_2Cl_2 , and acetone sequentially. No further purification was required and the product **7** was isolated as a light yellow solid (0.83 g, 77%): 1H NMR (300 MHz, $DMSO-d_6$) δ 7.70 (s, 1H), 7.54 (d, $J=1.8$ Hz, 1H), (dd, $J_1=1.8$ Hz, $J_2=8.4$ Hz, 1H), 7.34 (m, 3H), 7.15 (d, $J=8.4$ Hz, 1H), 7.10 (m, 2H), 6.95 (d, $J=8.4$ Hz, 1H), 6.94 (d, $J=8.4$ Hz, 1H), 5.46 (s, 2H), 5.13 (s, 2H), 4.95 (br s, 4H), 4.51 (s, 4H), 4.41 (s, 4H), 4.04 (t, $J=6.3$ Hz, 2H), 3.64 (s, 3H), 1.71 (m, 2H), 1.18–1.46 (m, 18H), 0.84 (t, $J=6.9$ Hz, 3H); ^{13}C NMR (75 MHz, $DMSO-d_6$) δ 155.1, 153.9, 153.8, 153.4, 147.0, 139.1, 134.4, 134.2, 130.3, 130.3, 129.9, 128.6, 128.3, 127.4, 125.7, 125.66, 125.6, 125.4, 112.1, 111.2, 110.8, 110.3, 108.9, 68.9, 68.7, 66.8, 65.0, 62.9, 58.0, 57.9, 55.7, 31.3, 29.1, 29.05, 29.01, 29.0, 28.74, 28.72, 28.4, 25.4, 22.1, 14.0; MS (MALDI in dithranol) m/z 798.3 ($M+Na$, $C_{44}H_{57}NO_{11}Na$ requires 798.4).

5.1.8. 1-(4-Dodecyloxy-5-methoxy-2-nitrobenzyloxy)-2,4-bis(3,5-bis(chloromethyl)phenoxy)benzene (8). To a stirred solution of **7** (2.64 g, 3.4 mmol) and DMF (100 mL) was added $SOCl_2$ via syringe. After 30 min, CH_2Cl_2 (50 mL) was added, the reaction was quenched slowly with sat. $NaHCO_3$ and stirred for an additional 30 min. The layers were separated and the organic layer was washed thoroughly with sat. $NaHCO_3$, dried over $MgSO_4$, filtered, and concentrated. Flash chromatography (SiO_2 , 2:1 CH_2Cl_2 –hexanes) of the residue gave the desired product (**8**) as a colorless solid (1.73 g, 60%): 1H NMR (300 MHz, $CDCl_3$) δ 7.76 (s, 1H), 7.59 (d, $J=2.1$ Hz, 1H), 7.43 (m, 2H), 7.40 (s, 1H), 7.29 (m, 3H), 7.06 (d, $J=8.4$ Hz, 1H), 6.96 (d, $J=8.4$ Hz, 1H), 6.90 (d, $J=8.4$ Hz, 1H), 5.54 (s, 2H), 5.28 (s, 2H), 5.11 (s, 2H), 4.65 (overlapping s, 4H), 4.56 (s, 2H), 4.55 (s, 2H), 4.09 (t, $J=6.6$ Hz, 2H), 3.67 (s, 3H), 1.89 (m, 2H), 1.22–1.54 (m, 18H), 0.88 (t, $J=6.9$ Hz, 3H); ^{13}C NMR (75 MHz, $CDCl_3$) δ 156.5, 156.3, 155.6, 154.2, 147.5, 138.9, 131.1, 131.0, 130.4, 130.3, 130.1, 129.9, 129.5, 128.8, 128.6, 128.3, 126.6, 126.5, 125.0, 112.3, 112.2, 112.0, 109.2, 109.0, 69.8, 69.5, 67.5, 66.0, 56.0, 45.9, 45.8, 41.4, 41.3, 31.9, 29.63, 29.61, 29.6, 29.5, 29.3, 28.8, 25.9, 22.7, 14.1; MS (FAB $^+$) m/z 846.9 (M^+ , $C_{44}H_{53}NO_7Cl_4$ requires 847.3), 848.9 [$M+2$].

5.1.9. 1-(4-Dodecyloxy-5-methoxy-2-nitrobenzyloxy)-2,4-bis(4-nitrophenoxy)methyl)benzene (9). A mixture of **5** (0.42 g, 0.78 mmol), *p*-nitrophenol (0.23 g, 1.64 mmol), K_2CO_3 (0.32 g, 2.35 mmol), 18-crown-6 (10 mg), acetone (10 mL), and DMF (10 mL) was stirred at reflux under argon for 3 days. The acetone was partially concentrated in vacuo and 1:1 water-brine (60 mL) was added to the remaining DMF with stirring. The resulting precipitate was filtered, washed thoroughly with sat. $NaHCO_3$ and water, redissolved in CH_2Cl_2 , dried over $MgSO_4$, filtered, and concentrated. Flash chromatography (SiO_2 , 2:1 CH_2Cl_2 –hexane) of the residue gave the desired product (**9**) as a colorless solid (0.49 g, 84%): 1H NMR (300 MHz, $CDCl_3$) δ

8.20 (d, $J=8.7$ Hz, 4H), 7.75 (s, 1H), 7.53 (d, $J=1.8$ Hz, 1H), 7.43 (dd, $J_1=2.1$ Hz, $J_2=8.4$ Hz, 1H), 7.06 (d, $J=8.1$ Hz, 1H), 7.04 (d, $J=9.3$ Hz, 4H), 5.56 (s, 2H), 5.29 (s, 2H), 5.12 (s, 2H), 4.07 (t, $J=6.9$ Hz, 2H), 3.74 (s, 3H), 1.89 (m, 2H), 1.22–1.54 (m, 18H), 0.88 (t, $J=6.9$ Hz, 3H); ^{13}C NMR (75 MHz, CDCl_3) δ 163.6, 163.5, 156.0, 154.1, 147.8, 141.74, 141.7, 139.3, 129.8, 129.3, 128.6, 127.7, 126.0, 125.9, 124.4, 114.8, 114.7, 112.5, 109.5, 109.2, 70.1, 69.6, 67.7, 66.2, 56.1, 31.9, 29.63, 29.61, 29.6, 29.5, 29.3, 28.8, 25.9, 22.7, 14.1; MS (FAB) m/z 745.5 (M⁺, $\text{C}_{40}\text{H}_{47}\text{N}_3\text{O}_{11}$ requires 745.3).

5.1.10. 1-(4-Dodecyloxy-5-methoxy-2-nitrobenzyloxy)-2,4-bis(3,5-bis(4-nitrophenoxy)methyl)phenoxybenzene (10).

A mixture of **8** (0.13 g, 0.15 mmol), *p*-nitrophenol (0.1 g, 0.7 mmol), K_2CO_3 (5.35 g, 9.68 mmol), and DMF (10 mL) was stirred at 50 °C under argon for 28 h. The reaction mixture was cooled to room temperature and poured into water (30 mL). The mixture was extracted thoroughly with CH_2Cl_2 and washed with sat. NaHCO_3 and brine. The organic layer was dried over MgSO_4 , filtered, and concentrated to a yellow solid. Flash chromatography (SiO_2 , gradient CH_2Cl_2 to 5% ethyl acetate in CH_2Cl_2) of the yellow solid gave the desired product (**10**) as a light yellow solid (0.14 g, 76%): ^1H NMR (300 MHz, CDCl_3) δ 8.21 (d, $J=9.3$ Hz, 2H), 8.19 (d, $J=9.3$ Hz, 2H), 8.06 (d, $J=9.3$ Hz, 2H), 7.96 (d, $J=9.3$ Hz, 2H), 7.74 (s, 1H), 7.30–7.50 (m, 6H), 7.23 (s, 1H), 7.01 (d, $J=9.3$ Hz, 2H), 7.00 (d, $J=9.3$ Hz, 2H), 6.90–7.05 (m, 3H), 6.95 (d, $J=9.3$ Hz, 2H), 6.88 (d, $J=9.3$ Hz, 2H), 5.48 (s, 2H), 5.20 (s, 2H), 5.15 (s, 2H), 5.13 (s, 2H), 5.10 (s, 2H), 5.08 (s, 2H), 5.00 (s, 2H), 4.08 (t, $J=6.9$ Hz, 2H), 3.68 (s, 3H), 1.88 (m, 2H), 1.22–1.54 (m, 18H), 0.88 (t, $J=6.9$ Hz, 3H); ^{13}C NMR (75 MHz, CDCl_3) δ 163.7, 163.54, 163.52, 163.5, 156.4, 156.2, 155.7, 154.0, 147.7, 141.7, 141.6, 141.5, 139.2, 129.6, 129.5, 129.3, 129.1, 128.8, 128.7, 128.2, 128.16, 127.7, 125.93, 125.9, 125.8, 125.7, 125.1, 124.6, 114.8, 114.73, 114.72, 114.5, 112.2, 111.9, 111.8, 109.4, 109.1, 70.2, 70.16, 69.9, 69.5, 67.6, 65.8, 56.0, 31.9, 29.65, 29.62, 29.57, 29.5, 29.3, 28.9, 25.9, 22.7, 14.1; MS (MALDI in dithranol) m/z 1282.2 (M⁺Na, $\text{C}_{68}\text{H}_{69}\text{N}_5\text{O}_{19}\text{Na}$ requires 1282.4).

5.1.11. 1-(4-Dodecyloxy-5-methoxy-2-nitrobenzyloxy)-4-nitrobenzene (11).

A mixture of *p*-nitrophenol (51 mg, 0.367 mmol), K_2CO_3 (0.145 g, 1.05 mmol), 18-crown-6 (10 mg), and acetone (10 mL) was stirred at room temperature under argon for 30 min. Compound **2** (0.150 g, 0.35 mmol) was then added and the reaction mixture was stirred at room temperature for 2 days. The solvent was removed and the residue was partitioned between CH_2Cl_2 (30 mL) and water (30 mL). The layers were separated and the organic layer was washed with sat. NaHCO_3 (3×30 mL) and brine. The combined aqueous layers were extracted with CH_2Cl_2 , the organic layers were combined, dried over MgSO_4 , filtered, and concentrated to give a deep red oil. This was dissolved in 5 mL of CH_2Cl_2

and slow addition of 50 mL hexanes to this solution afforded the product (**11**) as an off-white precipitate (105 mg, 62%): ^1H NMR (300 MHz, CDCl_3) δ 8.24 (d, $J=8.7$ Hz, 2H), 7.78 (s, 1H), 7.23 (s, 2H), 7.09 (d, $J=9.3$ Hz, 2H), 5.58 (s, 2H), 4.09 (t, $J=6.9$ Hz, 2H), 3.96 (s, 3H), 1.89 (m, 2H), 1.25–1.59 (m, 18H), 0.88 (t, $J=6.3$ Hz, 3H); ^{13}C NMR (75 MHz, CDCl_3) δ 162.9, 154.3, 147.8, 142.1, 139.1, 127.0, 126.0, 114.9, 109.4, 109.2, 69.6, 67.7, 56.4, 31.9, 29.61, 29.6, 29.54, 29.49, 29.31, 29.30, 28.8, 25.8, 22.7, 14.1; MS (FAB⁺) m/z 488.8 (M⁺, $\text{C}_{26}\text{H}_{36}\text{N}_2\text{O}_7$ requires 488.3).

Acknowledgements

This work was supported by the National Science Foundation (CHE-0213537).

References and notes

- Newkome, G. R.; Moorefield, C. N.; Vogtle, F. *Dendrimers and Dendrons: Concepts, Syntheses, Applications*; VCH: New York, 2001.
- Frechet, J. M. J.; Tomalia, D. A. *Dendrimers and Other Dendritic Polymers*; Wiley: New York, 2002.
- Smet, M.; Liao, L.-X.; Dehaen, W.; McGrath, D. V. *Org. Lett.* **2000**, *2*, 511–513.
- Kevwitch, R.; McGrath, D. V. *Synthesis* **2002**, 1171–1176.
- McElhanon, R.; Wheeler, D. R. *Org. Lett.* **2001**, *3*, 2681–2683.
- Sashiwa, H.; Yajima, H.; Aiba, S. *Biomacromolecules* **2003**, *4*, 1244–1249.
- Li, S.; Szalai, M.; Kevwitch, R. M.; McGrath, D. V. *J. Am. Chem. Soc.* **2003**, *125*, 10516–10517.
- Szalai, M.; Kevwitch, R. M.; McGrath, D. V. *J. Am. Chem. Soc.* **2003**, *125*, 15688–15689.
- Amir, R. J.; Pessah, N.; Shamis, M.; Shabat, D. *Angew. Chem. Int. Ed.* **2003**, *42*, 4494–4499.
- de Groot, F. M. H.; Albrecht, C.; Koekkoek, R.; Beusker, P. H.; Scheeren, H. W. *Angew. Chem. Int. Ed.* **2003**, *42*, 4490–4494.
- Shamis, M.; Lode, H.; Shabat, D. *J. Am. Chem. Soc.* **2004**, *126*, 1726–1731.
- Bochet, C. G. *J. Chem. Soc. Perkin Trans. 1* **2002**, 125–142.
- Brown, H.; Narasimhan, S.; Choi, Y. M. *J. Org. Chem.* **1982**, *47*, 4702–4708.
- Soai, K. O. H.; Takase, M.; Ookawa, A. *Bull. Chem. Soc. Jpn* **1984**, *57*, 1948–1953.
- Kamitori, Y.; Hojo, M.; Masuda, R.; Inoue, T.; Izumi, T. *Tetrahedron Lett.* **1983**, *24*, 2575–2576.
- Freeman, J. H. *J. Am. Chem. Soc.* **1952**, *74*, 6257–6260.
- Stille, R.; Ward, J. A.; Leffelman, C.; Sullivan, K. A. *Tetrahedron Lett.* **1996**, *37*, 9267–9270.
- Holmes, C. P.; Jones, D. G. *J. Org. Chem.* **1995**, *60*, 2318–2319. Holmes, C. P. *J. Org. Chem.* **1997**, *62*, 2370–2380.

FRET induced by an ‘allosteric’ cycloaddition reaction regulated with exogenous inhibitor and effectors

Lei Zhu, Vincent M. Lynch and Eric V. Anslyn*

Department of Chemistry and Biochemistry, The University of Texas at Austin, Austin, TX 78712, USA

Received 26 April 2004; accepted 14 June 2004

Dedicated to Robert Grubbs for his mentorship and contributions to organometallic chemistry, and in recognition of his receipt of the Tetrahedron Prize

Abstract—A Cu(I) catalyzed Huisgen cycloaddition was engineered to afford products featuring intramolecular excimer formation (exciplex, **3**) or intramolecular Förster resonance energy transfer (FRET, **6**, **7**). It was further demonstrated that this reaction could be silenced by ethylenediaminetetraacetic acid (EDTA), which prohibited the reduction of copper(II) sulfate to the catalytically active Cu(I) species by sodium ascorbate. Exogenous transition metal ions such as Zn²⁺ and Pb²⁺ were shown to competitively coordinate with EDTA thus releasing free Cu²⁺ for the subsequent reduction, and consequently restoring the reaction. The modulated catalysis showed metal ion concentration dependence and could be monitored by both HPLC and fluorescence. This study is a demonstration of a new sensing paradigm, where a catalytic organometallic reaction can be used as the signal amplifying module of a sensing application by engineering a regulatory element into the reaction process, analogous to an allosteric enzyme or an allosteric ribozyme system.

© 2004 Elsevier Ltd. All rights reserved.

1. Introduction

Sensing applications in a broad sense cover the endeavors of converting selective information in samples to amplifiable signals. The selective information may include the identity (e.g. identification of pathogens),¹ quantity (e.g. pH),² chirality (e.g. enantiomeric excess),³ etc. of a particular substance, or the reactivity of a catalytic system such as in catalysis screening,⁴ enzyme activity probing,⁵ or protein expression/function profiling studies.⁶ The amplifiable signal may originate from a large extinction coefficient (ϵ) in a colorimetric assay, a high quantum yield (ϕ) in a fluorescent assay, accumulating a secondary substance (turnovers) or signal in an analyte-triggered catalysis,⁷ or even differential deflection on microfabricated cantilevers.⁸ Sensing methods most often include analyte-targeting assays or reactivity assays. Particularly interesting to us is the development of analyte-targeting assays with readout signals amplified by advantageous optical properties and/or catalyses. The industrial standard is the enzyme-linked immunosorbent assay (ELISA, Fig. 1).⁹ In ELISA, the analyte (A) is first captured by an analyte-specific antibody (PA) immobilized on a solid surface; then an enzyme-linked secondary antibody (SA) binds with the now surface-bound

analyte through a different epitope; and finally a chromogenic substrate (S) of the enzyme (E) is added so that the color of the product (CP) from the enzyme-catalyzed reaction correlates to the quantity of the analyte. Although ELISA requires extensive washing steps between each binding event, and only multi-epitope analytes are compatible, it still enjoys huge success due to its generality and independent detection and signal amplification steps (favorable for modular design of sensing assays). Many variants of ELISA have also been developed to address specific challenges.¹⁰

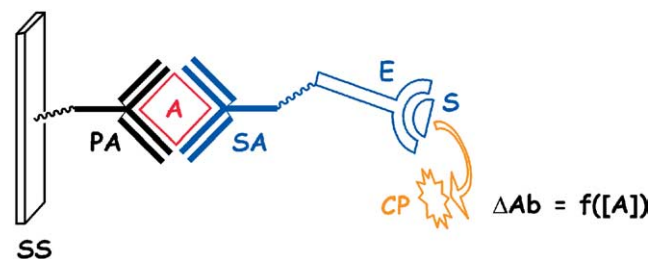
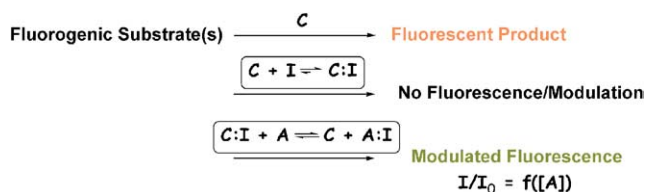


Figure 1. Schematic representation of ELISA. SS—solid support; PA—primary antibody; A—analyte; SA—secondary antibody; E—enzyme; S—substrate; CP—colorimetric product. The absorbance of CP (ΔAb) can be correlated as a function of analyte concentration ($[A]$).

Keywords: ELISA; Förster resonance energy transfer; Allosteric catalysis; Huisgen cycloaddition; T-stack; Zinc; Lead; Metal ion detection; Signal amplification.

* Corresponding author. Tel.: +1-5124710068; fax: +1-5124717791; e-mail address: anslyn@ccwf.cc.utexas.edu

In the course of exploring means to eliminate the stepwise washing maneuvers that are required in ELISA, we envisioned that the aforementioned analyte-targeting assays and reactivity assays were not necessarily independent of



Scheme 1. C—catalyst; I—reversible inhibitor; A—analyte.

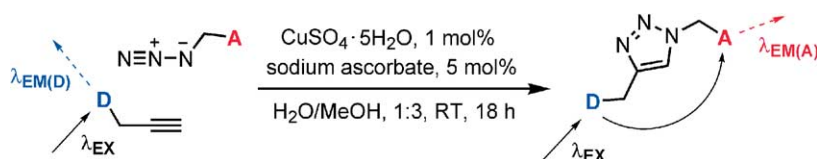


Figure 2. A FRET system constructed through an in situ-generated Cu(I) catalyzed regioselective Huisgen cycloaddition. D—donor; A—acceptor; EM—emission; EX—excitation; catalyst—Cu²⁺/sodium ascorbate (SA); inhibitor—EDTA; effectors—metal ions.

each other. If a regulatory element exists for a given reactivity assay, in principle this reactivity assay can be converted into an analyte assay. For instance, many catalysis assays utilize fluorogenic substrates so that the emission of the products can be used to monitor and to evaluate the catalytic processes.^{4,11} If an inhibitor were found for the catalyst in the assay (Scheme 1), the fluorogenic reaction and subsequent emission could be terminated by introducing the inhibitor.^{11b,d} When the analyte, which happened to be the structural analogue of the catalyst, was added, it would competitively bind with the inhibitor, thus releasing the catalyst to allow the catalysis to proceed. A modulated fluorescence signal would be observed that would correlate to the concentration of the analyte. The cascade of events triggered by analyte addition could combine the signal-amplifying power of both catalysis and fluorescence. Furthermore, it could offer technical advantages over stepwise executed ELISA.

In order to demonstrate this new sensing concept, a suitable reaction needs to meet the following requirements: 1. it is fast and catalytic; 2. it is catalyzed by an analyte analogue; 3. a reversible inhibitor is available; and 4. the reaction conditions are orthogonal to both the sample composition and the usual testing environment (solvent, temperature, etc.). Advances in organic chemistry have offered many opportunities in this regard. For example, our group has utilized a Heck reaction to detect various metal ions by controlling the activity of a palladium catalyst with exogenous inhibitor and activating analytes-metal ions.¹²

In this report, we engineered regulatory elements (e.g. EDTA) into a newly-discovered Cu(I) catalyzed Huisgen cycloaddition reaction (Fig. 2) so that it could be activated by exogenous metal ions and be monitored by a fluorescence modulation. The function and purpose of such designed regulatable catalytic systems is analogous to that of allosteric enzymes¹³ and allosteric ribozymes,¹⁴ where they are only responsive to their effectors. Therefore, this type of organic catalytic system is by analogy, also allosteric.

The Cu(I) catalyzed Huisgen cycloaddition was discovered independently by the Meldal and Fokin/Sharpless groups.¹⁵ The inertness of its carbon azide and terminal alkyne reactants under usual reaction conditions coupled with their high, specific thermodynamic reactivity toward each other makes them selective reaction partners in a sea of most other organic species.^{15b} Because Cu(I) (directly used or in situ generated) was found to greatly accelerate this reaction and provide a regioselective 1,4-substituted triazole product, its applications exploded over the last few years.¹⁶

For our purposes, the in situ method of reduction generated Cu(I) catalyzed version offers two ingredients—copper(II) sulfate and ascorbic acid—that might be regulated through reversible interactions with exogenous species.¹⁷ For example, EDTA can be introduced to bind with Cu²⁺ so that its redox potential is raised to the extent that it will not be reduced by sodium ascorbate (SA), thus halting the reaction. However, if a metal ion is added to competitively displace Cu(II) from its EDTA complex, the reaction will proceed with the available free Cu²⁺ ions, which is controlled by the existing solution equilibrium. Furthermore, this reaction is a conjugate reaction that joins two molecular pieces together. By using a Förster resonance energy transfer (FRET) pair in the reactants,¹⁸ the conjugating cycloaddition can be monitored by a fluorescence modulation (Fig. 2).

2. Results and discussion

2.1. Fluorescence profiles of FRET products

Pyrene and 7-diethylaminocoumarin based carbon azides and terminal alkynes were prepared with known procedures (Section 4.2). The fluorescence profiles of compounds **1** and **5** are shown in Figure 3(A). The emission region of the pyrene-based compound **1** generally covers the excitation area of the coumarin-based **5**. The FRET type energy transfer therefore occurred as predicted in compound **6** when the two pieces joined covalently to within the Förster radius through the Huisgen cycloaddition (Fig. 3(B)). Substantial exciplex emission (487 nm, Fig. 3(C)) was seen with **3**, which features two intramolecular pyrene moieties.¹⁸ FRET was also observed in compound **7** (Fig. 3(D)) which is isomeric to **6**. The X-ray structure analysis of **7** shows the distance between the two α -carbon atoms (C15, C21, Fig. 4(A)) that are attached to the 1,4-positions of the triazole ring to be at 5 Å. The pyrene and coumarin ring systems are perpendicular to each other and at least 9 Å apart, as shown in Figure 4(A). Upon examining the crystal packing in the unit cell (Fig. 4(B)), in the cleft formed

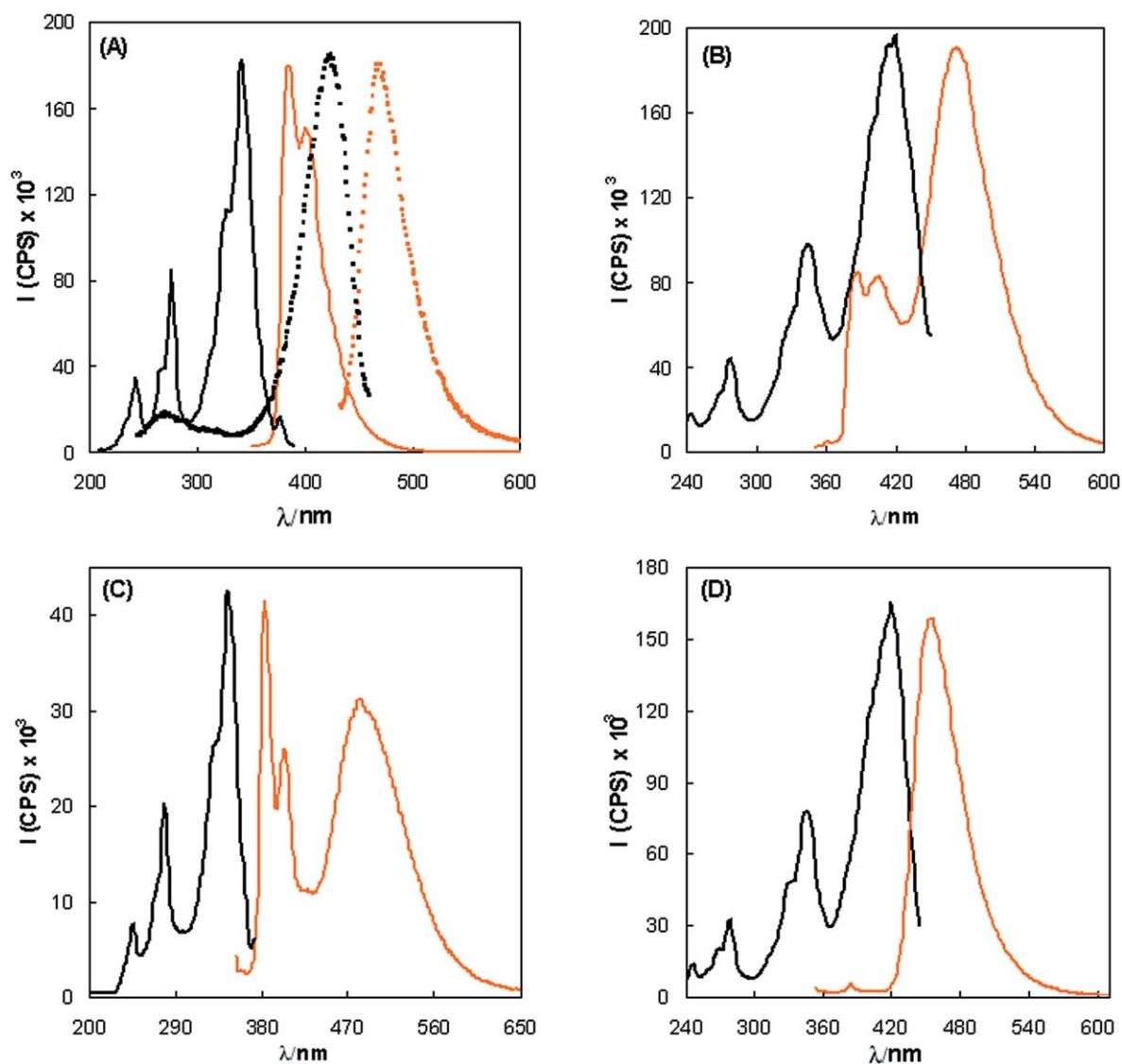


Figure 3. Fluorescence profiles: excitation (black) and emission (orange) spectra of (A) compound **1** (solid line, 0.2 μM in 75% $\text{CH}_3\text{OH}/\text{H}_2\text{O}$, excited at 340 nm); **5** (dotted line, 0.2 μM in 75% $\text{CH}_3\text{OH}/\text{H}_2\text{O}$, excited at 424 nm; spectra normalized to that of **1**); (B) **6** (2 μM in 75% $\text{CH}_3\text{OH}/\text{H}_2\text{O}$, excited at 340 nm, 1 μM was used for excitation spectrum); (C) **3** (0.2 μM in CH_2Cl_2 , excited at 340 nm); (D) **7** (0.2 μM in CH_2Cl_2 , excited at 340 nm, 0.1 μM was used for excitation spectrum). Fluorescence intensity (I) is shown as counts per second (CPS).

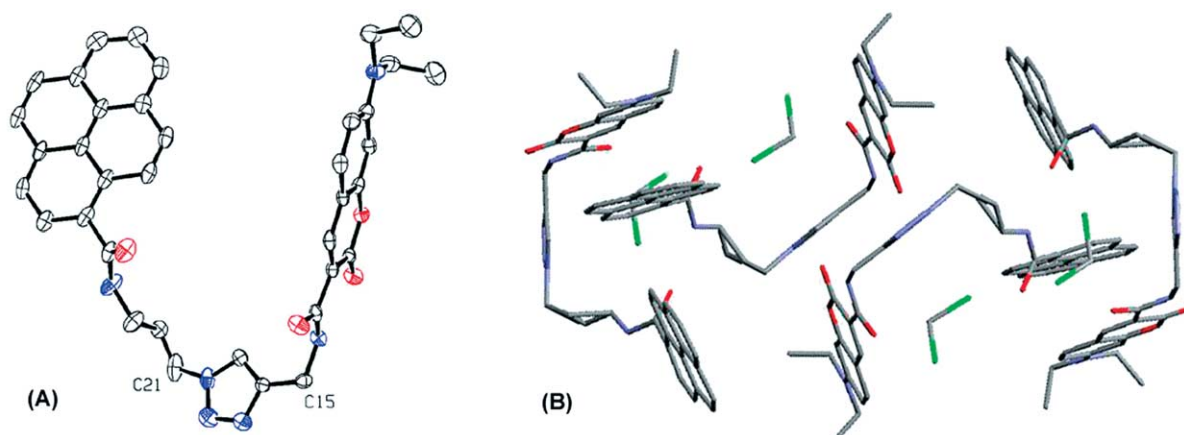
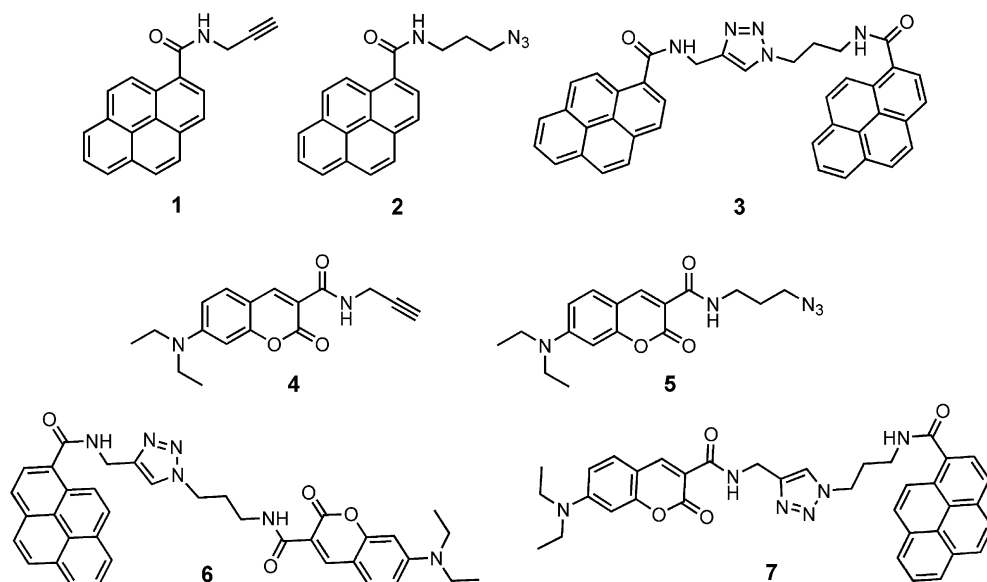


Figure 4. (A) ORTEP diagram (50% probability ellipsoids) of compound **7**. Hydrogen atoms are removed for clarity. (B) The crystal packing structure of compound **7** in a unit cell.

between pyrene and coumarin rings, there is a pyrene moiety from another molecule that is parallel to the coumarin but perpendicular to the pyrene surface. The distance between the parallel coumarin and pyrene is about 3.5 Å, which features a face to face π/π interaction; however, the perpendicular intermolecular pyrene–pyrene interaction is a typical ‘T-stack’ C–H/ π association.¹⁹



2.2. Modulating the Cu(I) catalyzed cycloaddition by EDTA and metal ions

Because the Cu(I) catalyzed cycloaddition generated products with unique fluorescence properties, we set forth to investigate whether this reaction could be regulated through the presence of inhibitors and effectors. A number of reactions were carried out in parallel under different conditions and the aliquots were taken directly after the reactions were terminated for HPLC analysis. As

shown in Figure 5(A1), when the reaction of **1** and **5** proceeded under Fokin–Sharpless conditions,^{15b} product **6** was observed at a retention time of 7.7 min, following the unreacted alkyne (**1**) and azide (**5**) that had eluted out earlier.²⁰ When 1 equiv. of EDTA was present, however, the reaction did not proceed due to the raised redox potential of Cu(II)EDTA complex that prohibited its reduction by

sodium ascorbate to Cu(I) species (Fig. 5(A2)). When metal ions such as Zn²⁺ and Pb²⁺ were present with Cu(II)EDTA, the reaction resumed to yield the triazole product, although to a lesser extent compared to the unencumbered reaction (Fig. 5(A3)). One exception was observed when Hg²⁺ was attempted as a metal ion effector. The reaction did not resume because the Hg²⁺ oxidized sodium ascorbate that was required to reduce Cu²⁺ to yield the active Cu(I) catalytic species. This observation underscores that the effector has to be orthogonal to the

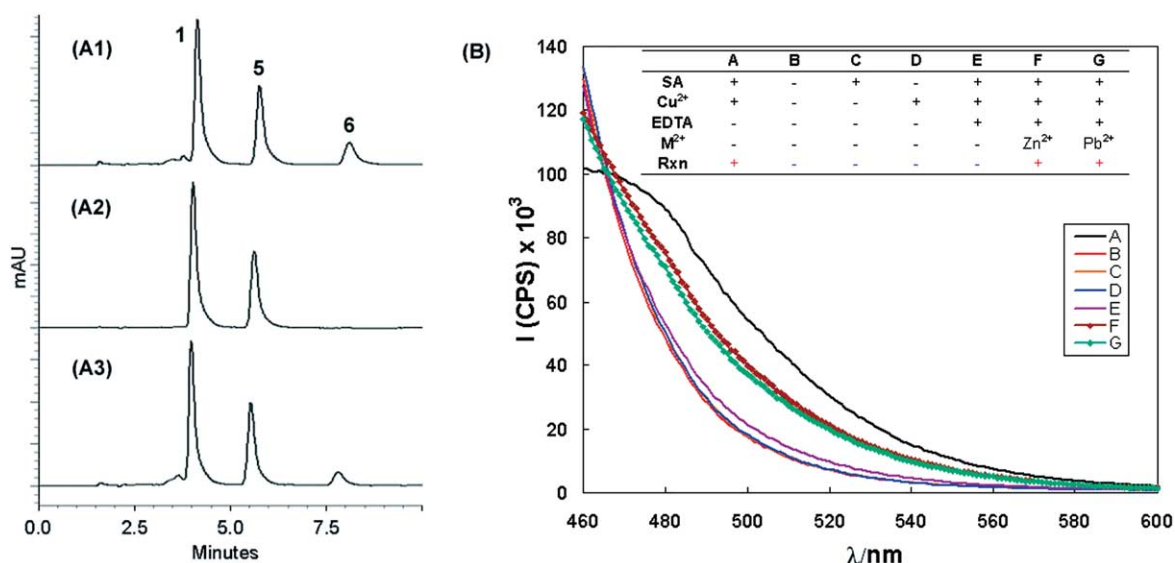


Figure 5. (A) HPLC chromatographs (360 nm) for Cu(I)-catalyzed Huisgen cycloadditions. The aliquots were taken at the end of the reactions and diluted 20 times for injection. Compounds **1** and **5** were 1.0 mM at the inception. A1: sodium ascorbate (SA)—1.0 mM, copper(II) sulfate (CS)—0.1 mM, rt; A2: SA—1.0 mM, Na₂[Cu(II)(EDTA)]—0.1 mM, 50 °C; A3: SA—1.0 mM, Na₂[Cu(II)(EDTA)]—0.2 mM, Pb(OAc)₂—0.2 mM, rt; (B) The fluorescence responses (excited at 340 nm) under various reaction conditions (see inset table).

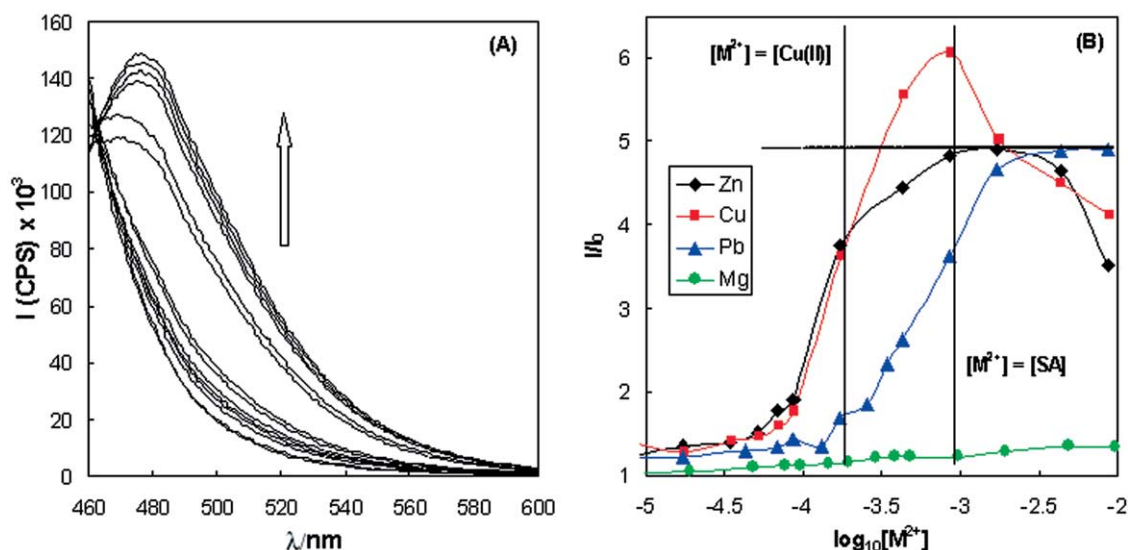


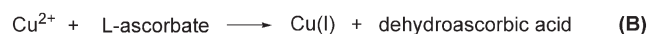
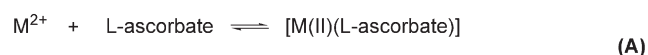
Figure 6. (A) Fluorescence response of EDTA inhibited catalytic Huisgen cycloaddition system to elevated Zn^{2+} concentration (excited at 340 nm); (B) Fluorescence profiles (500 nm) of EDTA inhibited catalytic Huisgen cycloaddition system to various metal ions. I/I_0 : fluorescence increase over inactivated reaction.

reaction conditions, as previously stated. Extensive control reactions showed that the reaction proceeded only when Cu(I) species was available. For example, a Pb^{2+} and sodium ascorbate combination did not promote the reaction. These experiments demonstrated conclusively that the addition of metal ions was the direct and only trigger for the cascade of reactions (from displacing Cu(II) from EDTA, to reducing Cu^{2+} to Cu(I), to the formation of a triazole) to occur.

2.3. Fluorescence modulation as a function of exogenous metal ion concentration

The formation of **6** under different promoting conditions at room temperature was also monitored by fluorescence. Control experiments (Fig. 5(B): (B), (C), (D)) showed that neither Cu^{2+} nor SA by itself promoted the reaction, or had an effect on the resulting fluorescence. Slight background fluorescence fluctuation was observed when Cu^{2+} and EDTA were present in a 1:1 ratio (E). However, the exogenous Zn^{2+} (F) and Pb^{2+} (G) promoted the triazole formation, which resulted in the energy transfer from pyrene to coumarin moieties as evidenced by the increased long wavelength emission. Their FRET effect fell short of the reaction without EDTA and metal ion effectors (A), which was in agreement with the HPLC analysis.

The FRET response also showed metal ion concentration dependence (Fig. 6). The fluorescence intensity due to



Scheme 2. ‘Allosteric’ Cu(I) catalyzed Huisgen reaction process with metal ion (M^{2+}) effectors.

FRET increased until $[\text{Zn}^{2+}]$ went up to 10^{-3} M ($[\text{Na}_2\text{Cu(II)(EDTA)}]$ was kept at 1.9×10^{-4} M). Overall it was responsive to $[\text{Zn}^{2+}]$ from 3.5×10^{-5} to 1.7×10^{-3} M. The inhibited cycloaddition system was less sensitive to activation by Pb^{2+} ion, for it was not responsive until $[\text{Pb}^{2+}]$ was 1.3×10^{-4} M (Fig. 6(B)). Free Cu^{2+} was also tested and FRET intensity increased until the $[\text{Cu}^{2+}]$ was equal to $[\text{SA}]$ when the maximal Cu(I) concentration was reached. The Zn^{2+} and Cu^{2+} profiles overlapped until $[\text{Zn}^{2+}]$ reached the concentration of $\text{Na}_2[\text{Cu(II)(EDTA)}]$.

The entire reaction process can be separated into 3 individual steps (Scheme 2). First, upon addition of metal ions (M^{2+}), the multi-species equilibria (A)²¹ is established to generate free Cu^{2+} , which is rapidly reduced by L-ascorbate in step B. The Cu(I) species then serve as the catalyst for step C to afford triazole **6**. It only takes seconds to complete step B. Therefore, the reaction rate is determined by equilibration step A and triazole formation C. Both Cu^{2+} and Zn^{2+} rapidly coordinate EDTA,²² therefore the step A in Zn^{2+} activated reactions is much faster than step C. The Cu(I) available for catalysis is stoichiometrically equal to the amount of Zn^{2+} that is introduced immediately after the inception of the reaction. However, in Pb^{2+} promoted processes, the relatively slow ligand exchange in step A stymied the generation of Cu^{2+} , thus the available amount of catalytic Cu(I) was always less than the added Pb^{2+} . Therefore, a retardation in its fluorescence profile was observed. As for Mg^{2+} , which barely coordinates with EDTA compared with Zn^{2+} and Pb^{2+} ,²³ the Cu^{2+} producing step A becomes rate-limiting. As a result, the FRET-type fluorescence modulation was barely observed.

Another interesting feature in those fluorescence profiles is that for Zn^{2+} and Pb^{2+} , The fluorescence intensities were continually increasing (to the dotted line, Fig. 6(B)) after the maximal number was reached judged by the Cu^{2+} profile. Besides the identities of the metal ions, the only difference in the Cu^{2+} system and $\text{Zn}^{2+}/\text{Pb}^{2+}$ systems lies in the counter ions: sulfate and acetate, respectively. Therefore,

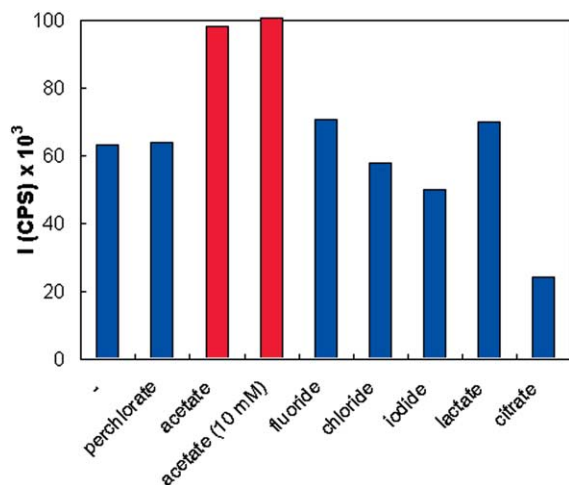


Figure 7. Anion (1.0 mM in the reactions) effects on the Cu(I) catalyzed Huisgen cycloaddition as shown in fluorescence responses (excited at 340 nm, monitored at 500 nm).

the likelihood that acetate anion might have assisted in the catalysis was examined. As shown in Figure 7, reactions were run under standard conditions with different anions as additives. Indeed acetate, at two concentrations (red bars), enhanced the catalysis by Cu(I) by more than 30%. Heavy halides appeared to retard the reaction.²⁴ Citrate inhibited ~70% of the reaction, probably due to its affinity to Cu²⁺ that prevented it from reduction. All other anions tested had no apparent effect on catalysis.

The unexpected fluorescence intensity drop for Cu²⁺ and Zn²⁺ at high concentrations (Fig. 6(B)) may be caused by the disruptive effect of high metal ion concentrations on fluorescence, or originates from their hijacking of some specific transformations in the catalytic cycle. For example, Cu(I) acetylides were proposed as key intermediates.^{15b} However, transition metal ions are known to bind with alkynes.²⁵ Therefore competitive binding from a large excess of metal ions may have disrupted the key Cu(I)

acetylide intermediate formation. A control experiment on high metal ion concentration effect was conducted. High Zn²⁺ and Pb²⁺ concentrations generally resulted in slightly lower fluorescence intensities than reaction without additional transition metal ions (Fig. 8(A)). When [Cu²⁺] increased from 2 to 10 mM, the fluorescence intensity clearly dropped, which is another indication of transition metal ions meddling in the catalytic process. However, when Mg²⁺ ion was present, the fluorescence intensities were unchanged, likely due to its inability to interact with terminal alkynes. Considering the possible interference of high metal ion concentration on fluorescence, a HPLC analysis was carried out to reveal the real relative triazole product concentrations in those reactions. As shown in Figure 8(B), less products were also observed when high concentrations of Zn²⁺ and Pb²⁺ were used. The conclusions from HPLC analysis matched nicely with the fluorescence study.²⁶

3. Conclusions

In the sensing area, analyte targeting and reactivity targeting applications have been mostly independent of each other. This report presents an example of a new paradigm that our group is starting to explore, where the use of an engineered regulatory element in reactivity assays can in principle be converted into an analyte assay. This approach has been adapted recently in several biosensor studies.²⁷ However, organic chemists have yet to take advantage of the repertoire of catalytic organic reactions that can be regulated to assemble such sensing assays by harnessing their signal-amplifying power.

In summation for this study, an example was given in which an in situ generated Cu(I) catalyzed Huisgen cycloaddition was regulated by EDTA and exogenous metal ions. The reaction (silenced by EDTA) was responsive to metal ions that have competitive affinity to EDTA, such as Zn²⁺ and Pb²⁺, relative to Cu²⁺ and it showed exogenous metal ion

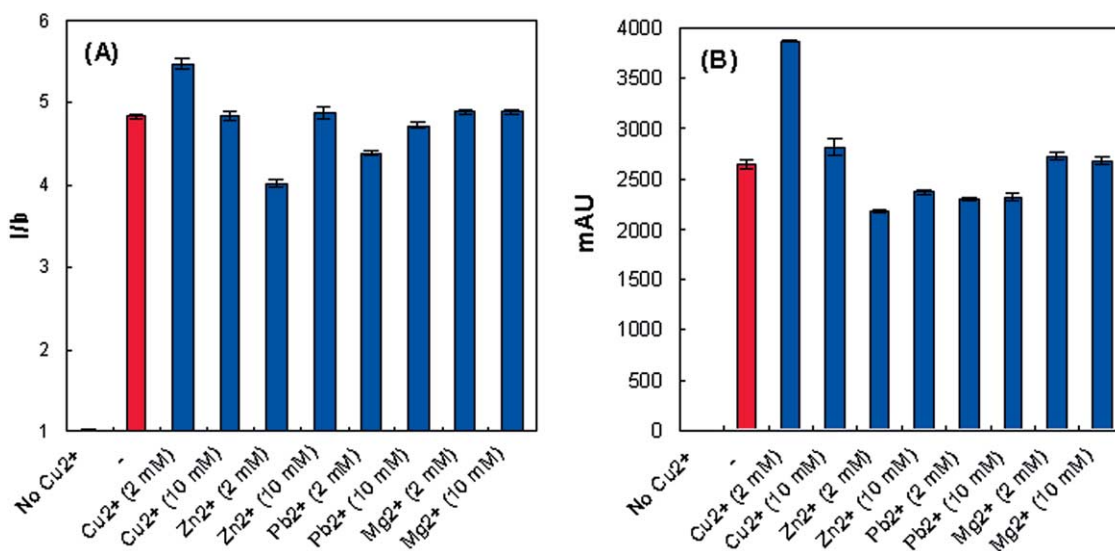


Figure 8. (A) Fluorescence intensities (500 nm, excited at 340 nm) from catalytic Huisgen reaction in the presence of high metal ion concentrations. (B) HPLC readings of the triazole product from the same set of reactions (at 340 nm). All the data are the average of two runs with error shown.

concentration dependence. When a FRET pair of terminal alkyne (**1**) and carbon azide (**5**) were used, the metal ion concentrations could be correlated to the fluorescence intensities that resulted from the energy transfer from the donor pyrene to the acceptor coumarin within the cycloaddition triazole product. A number of complications were also discussed, such as the possible effects of anions and high metal ion concentrations on the catalytic efficiency.

4. Experimental

4.1. General methods

¹H NMR spectra were recorded on a Varian Unity Plus 300 spectrometer. Low resolution and high resolution mass spectra were measured with Finnigan TSQ70 and VG Analytical ZAB2-E instruments, respectively. Reagents were used as purchased from various commercial sources. A Beckman Coulter System Gold 126 Solvent Module coupled to a 168 PDA Detector was used for HPLC analysis. Fluorescence spectra were measured on a PTI (Photon Technology International) Fluorimeter equipped with LPS-220B lamp power supply, a MD-5020 motor driver, and a 814 Photomultiplier Detection System.

4.2. Syntheses

General procedure for compounds 1, 2, 4, 5. 1-Pyrenecarboxylic acid or 7-(diethylamino)-coumarin-3-carboxylic acid (2 mmol) was dissolved in DMF (20 mL). TBUTU (8.0 mmol), HOBt (8.0 mmol) and *N*-methylmorpholine were added sequentially at room temperature. The solution was stirred for 5 min before mono-propargylamine or (3-azidopropyl)amine²⁸ was added slowly. The solution was stirred for 4 h before the solvent was removed under vacuum. The residue was partitioned between EtOAc (100 mL) and 10% NaHCO₃ (50 mL) and the organic layer was washed with another portion of 10% NaHCO₃ (50 mL) and brine (50 mL). After drying over Na₂SO₄ and the removal of solvent, the crude product was chromatographed on silica column eluted with CH₂Cl₂ containing up to 2% EtOAc to afford pure product. The yield was generally over 90%.

General procedure for compounds 3, 6, 7. Terminal alkyne (**1** or **4**, 0.5 mmol) and carbon azide (**2** or **5**, 0.5 mmol) were suspended in 75% methanolic water (5 mL). Copper(II) sulfate (0.1 mmol) and sodium ascorbate (0.5 mmol) were added sequentially and the solution was stirred at room temperature for 24 h (when TLC showed the completion of the reaction). The solvent was then removed under vacuum and the residue was partitioned between CH₂Cl₂ (150 mL) and water (50 mL). The organic layer was washed with brine (50 mL) before dried over Na₂SO₄. The solvent was removed to afford a yellow solid. The solid was washed with hexanes 20 mL×3 and dried under vacuum. The yield was 70%.

4.2.1. Compound 1. ¹H NMR (CDCl₃) δ 8.61 (d, *J*=9.3 Hz, 1H), 8.26–8.05 (m, 8H), 6.37 (s, broad, 1H), 4.46 (dd, *J*=2.7, 5.4 Hz, 2H), 2.37 (d, *J*=2.4 Hz, 1H); MS (CI): calcd (M+H)⁺ 284.1, found 284.1.

4.2.2. Compound 2. ¹H NMR (CDCl₃) δ 8.59 (d, *J*=9.3 Hz, 1H), 8.27–8.08 (m, 8H), 6.37 (s, broad, 1H), 3.77 (m, 2H), 3.57 (t, *J*=6.3 Hz, 2H), 2.06 (m, 2H); MS (CI): calcd (M+H)⁺ 329.1, found 329.3.

4.2.3. Compound 3. ¹H NMR (CDCl₃/CD₃OD) δ 8.30 (d, *J*=9.2 Hz, 2H), 8.05–7.83 (m, 17H), 4.64 (s, 2H), 4.47 (m, 2H), 3.45 (t, *J*=5.6 Hz, 2H), 2.22 (m, 2H); MS (CI): calcd (M+H)⁺ 612.2, found 612.4.

4.2.4. Compound 4. ¹H NMR (CDCl₃) δ 8.99, (s, broad, 1H), 8.70 (s, 1H), 7.42 (d, *J*=6.6 Hz, 1H), 6.64 (d, *J*=6.6 Hz, 1H), 6.50 (s, 1H), 4.23 (s, 2H), 3.45 (q, *J*=5.4 Hz, 4H), 2.23 (s, 1H), 1.24 (t, *J*=5.1 Hz, 6H); MS (CI): calcd (M+H)⁺ 299.1, found 299.1.

4.2.5. Compound 5. ¹H NMR (CDCl₃) δ 8.91 (s, broad, 1H), 8.72 (s, 1H), 7.45 (d, *J*=9.0 Hz, 1H), 6.68 (dd, *J*=2.0, 6.7 Hz, 1H), 6.53 (d, *J*=2.0 Hz, 1H), 3.58–3.41 (m, 8H), 1.93 (m, 2H), 1.26 (t, *J*=7.2 Hz, 6H); MS (CI): calcd (M+H)⁺ 344.2, found 344.3.

4.2.6. Compound 6. ¹H NMR (CDCl₃) δ 8.89 (m, 1H), 8.63 (d, *J*=9.2 Hz, 1H), 8.57 (s, 1H), 8.22–7.97 (m, 9H), 7.27 (d, *J*=9.0 Hz, 1H), 7.23 (m, 1H), 6.56 (dd, *J*=2.3, 9.0 Hz, 1H), 6.37 (d, *J*=2.3 Hz, 1H), 4.95 (d, *J*=5.4 Hz, 2H), 4.51 (t, *J*=6.9 Hz, 2H), 3.54 (m, 2H), 3.40 (q, *J*=7.4 Hz, 4H), 2.28 (m, 2H), 1.22 (t, *J*=7.2 Hz, 6H); HRMS (CI): calcd (M+H)⁺ 627.2720, found 627.2735.

4.2.7. Compound 7. ¹H NMR (CDCl₃) δ 9.42 (s, broad, 1H), 8.55 (d, *J*=9.2 Hz, 1H), 8.39 (s, 1H), 8.19–7.95 (m, 8H), 7.78 (s, 1H), 7.17 (d, *J*=9.0 Hz, 1H), 6.78 (s, broad, 1H), 6.47 (dd, *J*=2.3, 9.0 Hz, 1H), 6.33 (d, 2.3 Hz, 1H), 4.68 (d, *J*=5.6 Hz, 2H), 4.58 (t, *J*=6.7 Hz, 2H), 3.66 (m, 2H), 3.41 (q, *J*=7.2 Hz, 4H), 2.39 (m, 2H), 1.23 (t, *J*=7.2 Hz, 6H); MS (CI): calcd (M+H)⁺ 627.3, found 627.4.

4.3. X-ray crystal structure determination

Crystals grew as very thin, yellow plates by slow evaporation from dichloromethane. The data crystal was broken off a much larger plate and had approximate dimensions; 0.44×0.40×0.04 mm. The data were collected on a Nonius Kappa CCD diffractometer using a graphite monochromator with Mo K α radiation (λ =0.71073 Å). A total of 368 frames of data were collected using ω -scans with a scan range of 1° and a counting time of 156 s per frame. The data were collected at 153 K using an Oxford Cryostream low temperature device. Data reduction was performed using DENZO-SMN. The structure was solved by direct methods using SIR97 and refined by full-matrix least-squares on F² with anisotropic displacement parameters for the non-H atoms using SHELXL-97. The hydrogen atoms on carbon were calculated in ideal positions with isotropic displacement parameters set to 1.2×U_{eq} of the attached atom (1.5×U_{eq} for methyl hydrogen atoms). The hydrogen atoms on the amide nitrogen atoms were observed in a ΔF map and refined with isotropic displacement parameters. One methylene carbon atom, C22, was found to be disordered about two positions of occupancy 75(2)% for C22 and 25(2)% for C22a. Crystallographic data for the structure of compound **7** have been deposited with

the Cambridge Crystallographic Data Centre as supplementary publication number CCDC 236856. Copies of the data can be obtained, free of charge, on application to CCDC, 12 Union Road, Cambridge, CB2 1EZ, UK [fax: +44-1223-336033 or e-mail: deposit@ccdc.cam.ac.uk].

4.4. Typical reaction, HPLC, and fluorescence measurement procedures

Compound **1** (0.7 mM, 400 μ L), **5** (1.2 mM, 600 μ L), Na₂[Cu(II)(EDTA)] (20 mM, 10 μ L), Zn(OAc)₂ (0–1.0 M, 10 μ L), and SA (100 mM, 10 μ L) were added sequentially in a 1.5 mL Eppendorf tube. The final concentrations were: **1**—0.27 mM, **5**—0.70 mM, Na₂[Cu(II)(EDTA)]—0.19 mM, Zn(OAc)₂—(0–9.7 mM), and SA—0.97 mM. The solution was well mixed on a Vortex and incubated in a Thermoline heating block at 50 °C, or at rt for 18 h. After the reaction was terminated by cooling, 50 μ L aliquote was taken and diluted with 1 mL 75% MeOH/H₂O for HPLC injection. A SUPELCO SIL LC-18 HPLC column was used and the elution was initiated with 75% MeOH/H₂O for 5 min. The MeOH gradient was raised to 100% in 3 min followed with 15 min neat MeOH. Fluorescence sample was prepared by diluting 20 μ L aliquot with 4 mL 75% MeOH/H₂O. The sample was excited at 340 nm at rt and its emission was recorded from 460–600 nm.

Acknowledgements

We gratefully acknowledge the National Institute of Health for support of the project (EB-00549-5).

References and notes

- Rider, T. H.; Petrovick, M. S.; Nargi, F. E.; Harper, J. D.; Schwoebel, E. D.; Mathews, R. H.; Blanchard, D. J.; Bortolin, L. T.; Young, A. M.; Chen, J.; Hollis, M. A. *Science* **2003**, *301*, 213–215.
- McQuade, D. T.; Hegedus, A. H.; Swager, T. M. *J. Am. Chem. Soc.* **2000**, *122*, 12389–12390.
- Zhu, L.; Anslyn, E. V. *J. Am. Chem. Soc.* **2004**, *126*, 3676–3677.
- Stauffer, S. R.; Hartwig, J. F. *J. Am. Chem. Soc.* **2003**, *125*, 6977–6985.
- (a) Matayoshi, E. D.; Wang, G. T.; Krafft, G. A.; Erickson, J. *Science* **1990**, *247*, 954–958. (b) Khidekel, N.; Arndt, S.; Lamarre-Vincent, N.; Lippert, A.; Poulin-Kerstien, K. G.; Ramakrishnan, B.; Oasba, P. K.; Hsieh-Wilson, L. C. *J. Am. Chem. Soc.* **2003**, *125*, 16162–16163.
- (a) Pandey, A.; Mann, M. *Nature* **2000**, *405*, 837–846. (b) Speers, A. E.; Adam, G. C.; Cravatt, B. F. *J. Am. Chem. Soc.* **2003**, *125*, 4686–4687.
- (a) Blaedel, W. J.; Boguslaski, R. C. *Anal. Chem.* **1978**, *50*, 1026–1032. (b) Kim, T.-H.; Swager, T. M. *Angew. Chem., Int. Ed.* **2003**, *42*, 4803–4806.
- Fritz, J.; Baller, M. K.; Lang, H. P.; Rothuizen, H.; Vettiger, P.; Meyer, E.; Güntherodt, H.-J.; Gerber, Ch.; Gimzewski, J. K. *Science* **2000**, *288*, 316–318.
- Other amplification modules that have been widely applied include polymerase chain reaction (PCR) Robertson, M. P.; Ellington, A. D. *Nat. Biotechnol.* **1999**, *17*, 62–66.
- Various flavors of ELISA include: (a) catELISA: MacBeath, G.; Hilvert, D. *J. Am. Chem. Soc.* **1994**, *116*, 6101–6106. (b) Open sandwich ELISA: Ueda, H.; Tsumoto, K.; Kubota, K.; Suzuki, E.; Nagamune, T.; Nishimura, H.; Schueler, P. A.; Winter, G.; Kumagai, I.; Mohoney, W. C. *Nat. Biotechnol.* **1996**, *14*, 1714–1718. (c) azido-ELISA: Hang, H. C.; Yu, C.; Pratt, M. R.; Bertozzi, C. R. *J. Am. Chem. Soc.* **2004**, *126*, 6–7. (d) Geymayer, P.; Bahr, N.; Reymond, J.-L. *Chem. Eur. J.* **1999**, *5*, 1006–1012. (e) Taran, F.; Gauchet, C.; Mohar, B.; Meunier, S.; Valleix, A.; Renard, P. Y.; Créminon, C.; Grassi, J.; Wagner, A.; Mioskowski, C. *Angew. Chem., Int. Ed.* **2002**, *41*, 124–127. (f) Weizmann, Y.; Patolsky, F.; Katz, E.; Willner, I. *J. Am. Chem. Soc.* **2003**, *125*, 3452–3454. (g) Oguri, H.; Hiram, M.; Tsumuraya, T.; Fujii, I.; Maruyama, M.; Uehara, H.; Nagumo, Y. *J. Am. Chem. Soc.* **2003**, *125*, 7608–7612.
- Examples of enzyme catalysis: (a) Zlokarnik, G.; Negulescu, P. A.; Knapp, T. E.; Mere, L.; Burres, N.; Feng, L.; Whitney, M.; Roemer, K.; Tsien, R. Y.; Science, . *Science* **1998**, *279*, 84–88. (b) Beekman, B.; Drijfhout, J. W.; Bloemhoff, W.; Ronday, H. K.; Tak, P. P.; te Koppele, J. M. *FEBS Lett.* **1996**, *390*, 221–225. (c) Takakusa, H.; Kikuchi, K.; Urano, Y.; Sakamoto, S.; Yamaguchi, K.; Nagano, T. *J. Am. Chem. Soc.* **2002**, *124*, 1653–1657. (d) Hirata, J.; Ariese, F.; Gooijer, C.; Irth, H. *Anal. Chim. Acta* **2003**, *478*, 1–10. Examples of organic catalysis: Ref. 4; (e) Chatterjee, A. K.; Toste, F. D.; Glodberg, S. D.; Grubbs, R. H. *Pure Appl. Chem.* **2003**, *75*, 421–426. (f) Tanaka, F.; Mase, N.; Barbas, III., C. F. *J. Am. Chem. Soc.* **2004**, *126*, 3692–3693.
- Wu, Q.; Anslyn, E. V. Submitted for publication.
- Stryer, L. *Biochemistry*; 4th ed. Freeman and Company: New York, 1995.
- Soukup, G. A.; Breaker, R. R. *Curr. Opin. Struct. Biol.* **2000**, *10*, 318–325.
- (a) Tornøe, C. W.; Christensen, C.; Meldal, M. *J. Org. Chem.* **2002**, *67*, 3057–3064. (b) Rostovtsev, V. V.; Green, L. G.; Fokin, V. V.; Sharpless, K. B. *Angew. Chem., Int. Ed.* **2002**, *41*, 2596–2599.
- See reviews: (a) Kolb, H. C.; Sharpless, K. B. *Drug Discovery Today* **2003**, *8*, 1128–1137. (b) Breinbauer, R.; Köhn, M. *ChemBioChem* **2003**, *4*, 1147–1149.
- Ascorbate acid activity might be regulated by a saccharide receptor.
- (a) Lakowicz, J. R. *Principles of Fluorescence Spectroscopy*; Plenum: New York, 1999. (b) In *Handbook of Fluorescent Probes and Research Chemicals*; 6th ed. Haugland, R. P., Ed.; Molecular Probes: Eugene, OR, 1996.
- Coates, G. W.; Dunn, A. R.; Henling, L. M.; Dougherty, D. A.; Grubbs, R. H. *Angew. Chem., Int. Ed. Engl.* **1997**, *36*, 215–248, and references therein.
- Although the Cu(I) catalyzed Huisgen cycloaddition is highly efficient, it is after all a bimolecular reaction. The reactants concentrations under this study were ~1 mM, which is 200 times less than reported in the original study (Ref. 15b). Under such conditions the reaction was not completed in 18 h. However, the product abundance is sufficient enough to be monitored by HPLC and have a substantial modulating effect on the fluorescence.
- It is well known that both Zn²⁺ and Pb²⁺ can coordinate with ascorbic acid. (a) Diaz-Arrastia, R.; Hashemi, E. *J. Mol.*

- Neurosci.* **2000**, *14*, 167–173. (b) Pal, D. R.; Chatterjee, J.; Chatterjee, G. C.; *Int. J. Vita. Nutri. Res.* **1975**, *45*, 429–437.
22. Cotton, F. A.; Wilkinson, G. *Advanced Inorganic Chemistry*; 5th ed. Wiley: New York, 1988.
23. Formation constants ($\log K_f$) for metal-EDTA complexes, respectively: Mg^{2+} —8.79; Cu^{2+} —18.80; Pb^{2+} —18.5 (25 °C, $\mu=0.2$); Hg^{2+} —21.7; Zn^{2+} —16.50 Martell, A. E.; Smith, R. M. *Critical Stability Constants*; Plenum: New York, 1974; Vol. 1.
24. In a separate experiment, bromide anion was also shown by fluorescence to slightly slow the reaction down.
25. (a) In *Modern Acetylene Chemistry*; Stang, P. J., Diederich, F., Eds.; VCH: Weinheim, 1995. (b) Sasaki, H.; Boyall, D.; Carreira, E. M. *Helv. Chim. Acta* **2001**, *84*, 964–971.
26. For general practice FRET signal should be denoted as the intensity ratio between acceptor and donor emissions (when donor is excited). However in our case, the donor emission was usually too high to measure, especially when the metal ion effector concentration was low. Therefore, the intensity at 500 nm was used as an alternative measure. That might account for the slight difference between fluorescence and HPLC analysis patterns. HPLC analyses were conducted for other reactions sets as well and they generally match well with the related fluorescence profiles.
27. (a) Hartig, J. S.; Najafi-Shoushtari, S. H.; Grüne, I.; Yan, A.; Ellington, A. D.; Famulok, M. *Nat. Biotechnol.* **2002**, *20*, 717–722. (b) Hartig, J. S.; Grüne, I.; Najafi-Shoushtari, S. H.; Famulok, M. *J. Am. Chem. Soc.* **2004**, *126*, 722–723.
28. Carboni, B.; Benalil, A.; Vaultier, M. *J. Org. Chem.* **1993**, *58*, 3736–3741.



Poly(ϵ -caprolactone) macroligands with β -diketonate binding sites: synthesis and coordination chemistry

Jessica L. Bender, Qun-Dong Shen and Cassandra L. Fraser*

Department of Chemistry, University of Virginia, McCormick Road, PO Box 400319, Charlottesville, VA 22904-4319, USA

Received 3 April 2004; revised 3 June 2004; accepted 4 June 2004

Dedicated to Robert H. Grubbs, in celebration of his many achievements and contributions to chemistry, both as a creative scientist and an inspiring mentor to us all

Abstract—Dibenzoylmethane (dbm) initiators with one and two alcohol sites were used to generate dbm end-functionalized and dbm-centered poly(ϵ -caprolactone) macroligands (dbmPCL and dbmPCL₂) with low polydispersities (~ 1.1). Chelation of polymeric ligands to metal ions (Eu³⁺, Fe³⁺, Ni²⁺ and Cu²⁺) produced metal-centered star polymers, which were characterized by UV–vis and fluorescence spectroscopy, as well as gel permeation chromatography.

© 2004 Elsevier Ltd. All rights reserved.

1. Introduction

Metal β -diketonates are complexes with a wide range of uses, both in materials and catalysis. For example, Europium β -diketonates are finding increasing application in technologies ranging from sensors^{1–3} and molecular probes^{4,5} to OLEDs.^{6–10} Various Eu and other metal diketonates are also commonly used as homogeneous or heterogeneous polymer-bound catalysts for organic reactions.¹¹

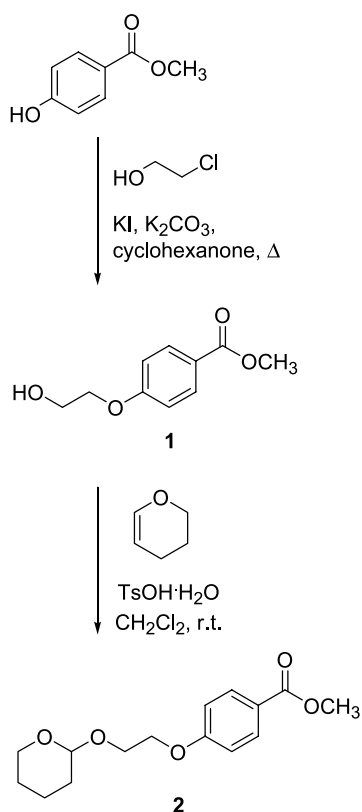
Eu tris(β -diketonates) figure prominently in lanthanide coordination chemistry.^{12,13} Lanthanide metals are characterized by a partially filled 4f electron shell lying within and effectively shielded by lower-lying 5s and 5p shells. Due to this shielding from the surrounding environment, the electronic transitions of the lanthanide ions result in distinct, narrow line emission spectra, unlike the broad peaks arising from electronic transitions of transition metals. Europium itself has a very low molar absorptivity; however, it has been shown that certain ligands can absorb ultraviolet radiation and transfer this energy to the bound lanthanide ion, from which light is emitted.^{14,15} The luminescence intensity of these Europium complexes in solution however, is often diminished due to the easy access of water molecules to the metal center, allowing energy to be dissipated non-radiatively through O–H stretching modes, and decreasing the energy available for radiative decay. The

luminescence of Eu can be enhanced by the presence of a polymeric matrix.^{16,17} Polymers can shield the metal centers from water and solvent molecules and lend processability to the luminescent material. These features make polymeric lanthanide complexes of interest for light-emitting materials.^{8–10,18}

The concept of polymeric metal-centered β -diketonates described herein may also prove useful for supported, site-isolated catalysts in heterogeneous or homogeneous modes, which benefit from greater ease of product isolation. For example, Eu complexes are employed as catalysts for polymerizations,^{19–21} epoxidation of alkenes with O₂,²² and alkyne hydrogenation.²³ Polymer-supported nickel, copper, and iron diketonates have also been utilized in epoxidation reactions,²⁴ and as heterogeneous Lewis acid catalysts for hetero Diels–Alder reactions.²⁵

With these many potential uses in mind, star-shaped polymeric metal β -diketonate complexes have been targeted. Hydroxyl-functionalized dibenzoylmethane (dbm) analogues, dbmOH (**5**) and dbm(OH)₂ (**4**), were prepared for use as initiators in the controlled polymerization of ϵ -caprolactone (CL), producing macroligands dbmPCL (**6**) and dbmPCL₂ (**7**) with dbm binding sites at the end and center of the chains, respectively. To determine the optimal conditions for preparative scale reactions, the polymerization kinetics were explored. Macroligands were chelated to Eu, Fe, Cu and Ni metal ions to produce metal-centered stars of various architectures, the spectroscopic properties of which were compared to non-polymeric M(dbm)_n analogues.^{26,27} This study builds upon prior

Keywords: Metallopolymer; Poly(caprolactone); β -Diketonate; Europium.
* Corresponding author. Tel.: +1-434-9247998; fax: +1-434-9243710; e-mail address: fraser@virginia.edu



Scheme 1. Preparation of THP-protected alcohol ester **2**.

work involving dbm-functionalized poly(lactic acid), dbmPLA, and its Europium complexes, thus expanding the dbm macroligand and polymeric metal complex set to include another biocompatible polyester.¹⁵

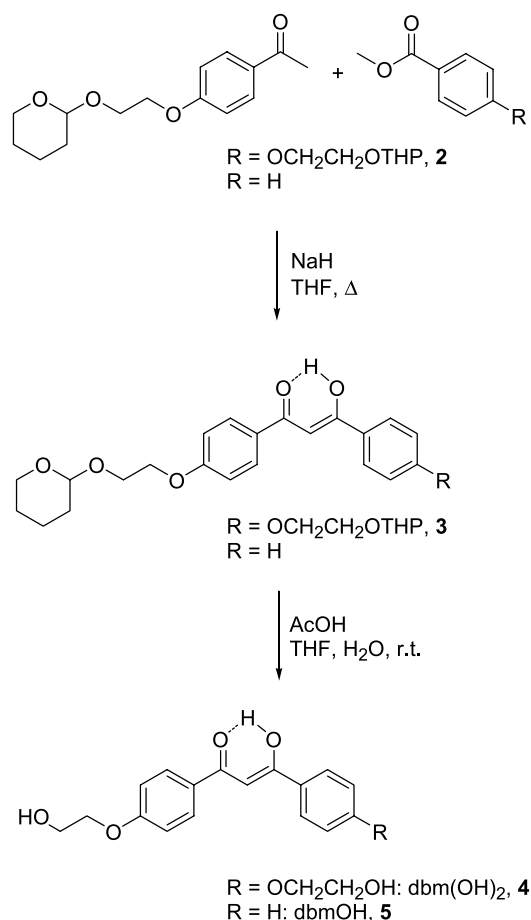
2. Results and discussion

2.1. Ligand initiator synthesis

A condensation reaction between ester and ketone components was used to produce diketones containing primary alcohol groups, which act as initiators for the ring-opening polymerization of ϵ -caprolactone. This modular synthesis allows for variation of the number and placement of initiating sites on the arene rings. Mono- and difunctional ligand initiators **5** and **4** were prepared as shown in Schemes 1 and 2. First, phenol functionalities were converted to primary alcohols by modification with alkyl linkers, as shown for the ester **1**, in Scheme 1. After protection of acidic alcohol sites as tetrahydropyranyl (THP) ethers, β -diketones were generated by condensation of the appropriate ester and ketone. The THP protecting groups were readily removed with acid and the ligand initiators dbm(OH)₂, **4**, and dbmOH, **5** were purified by recrystallization and chromatography, respectively.

2.2. Macroligand synthesis

Macroligands were produced from the diketone alcohol initiators **4** and **5** by controlled polymerization. Living polymerization is a widely-used method for making polymers with discrete architectures, targeted molecular



Scheme 2. Preparation of dibenzoylmethane initiators dbmOH, **5** and dbm(OH)₂, **4**.

weights, and narrow molecular weight distributions (i.e. low polydispersity indices, PDIs).³⁰ Controlled polymerizations feature initiation and propagation; common side reactions such as termination and chain transfer are negligible. Criteria used to test whether a polymerization is living that are relevant to this study include the following: the polymerization proceeds until all monomer is consumed; the number-average molecular weight (M_n) is a linear function of percent monomer conversion; M_n can be predicted in advance based on the monomer to initiator ratio; resulting polymers have narrow PDIs, if initiation is fast relative to propagation; and the overall yield of chain-end functionalized polymers is quantitative.³⁰

Various catalysts were screened to test whether controlled polymerization of ϵ -caprolactone could be achieved with the diketone initiators. Reactions were attempted with Et₃Al, Al(OⁱPr)₃, and Sn(Oct)₂, all common catalysts for the living polymerization of ϵ -caprolactone.^{31–38} Neither Et₃Al nor Al(OⁱPr)₃ produced polymeric products, even after several days. Polymerizations employing Sn(Oct)₂ were successful in generating polymer; thus, further studies focused on this catalyst.

Kinetics studies were performed using Sn(Oct)₂ and bulk ϵ -caprolactone at 110 °C, to determine the optimal reaction conditions for achieving molecular weight control (e.g. low PDI and a linear relationship between M_n and percent

monomer conversion.) Catalyst to initiator ratios of 1/20, 1/40, and 1/60 were screened for the monofunctional initiator **5**. For a 1/20 loading, GPC traces show high molecular weight shoulders and broad PDIs after 1 d, corresponding to only a 10% conversion of monomer. In contrast, a catalyst loading of 1/60 yielded polymer with a low PDI (<1.1) at ~23% monomer conversion, but 3 d were required to achieve this result. With a 1/40 loading, comparable molecular weight control and conversion were achieved after 1 d. Because this loading strikes the best balance between molecular weight control, monomer conversion, and reaction time, the 1/40 ratio was employed in subsequent polymerization studies with initiators **4** and **5**.

Kinetics and molecular weight versus percent conversion plots for polymerizations with dbmOH, **5**, and dbm(OH)₂, **4** are compared in Figures 1 and 2. The rate of polymerization with the difunctional initiator is roughly two times that of

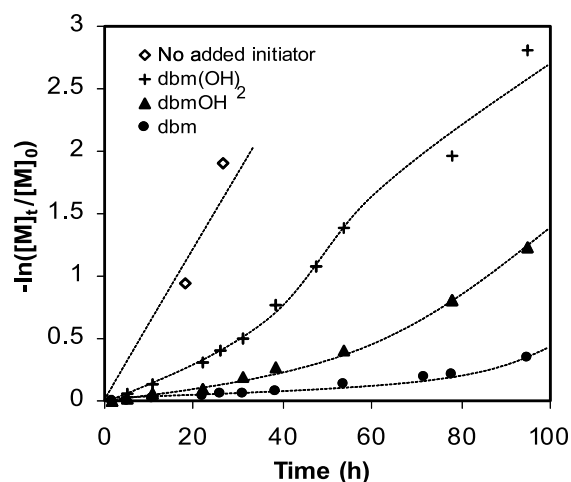


Figure 1. Kinetics plots for the polymerization of ϵ -caprolactone with dbm(OH)₂, **4**, and dbmOH, **5** (Sn(Oct)₂: 1° alcohol=1:40), and control reactions with dbm and no added initiator (curves are drawn through each data set to serve as a guide for the eye).

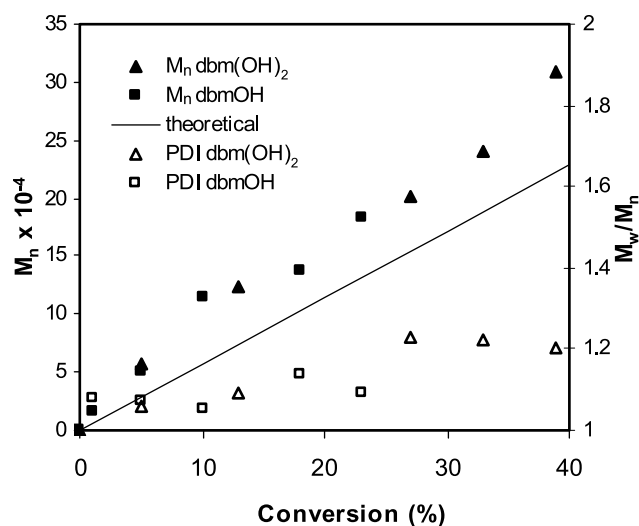


Figure 2. Number-average molecular weight versus percent conversion plots and polydispersity indices for the polymerization of ϵ -caprolactone with the monofunctional and difunctional initiators dbmOH, **5**, and dbm(OH)₂, **4**. (Sn(Oct)₂: 1° alcohol=1:40).

the monofunctional reagent, as expected, and first-order kinetics plots with both **4** and **5** deviate from linearity, after ~11 and 31 h, respectively (Fig. 1). After these time points, GPC analysis reveals high molecular weight shoulders that become increasingly more pronounced over time, correlating with higher PDIs (Fig. 2). M_n versus % conversion plots are essentially linear at low monomer conversion; however, the observed molecular weights are slightly higher than the values that are predicted for a controlled reaction. Unlike lactide polymerizations with the same tin catalyst and initiator **5**, which produce dbmPLA with narrow PDIs up to high monomer conversion,¹⁵ ϵ -caprolactone reactions with **4** and **5** are not controlled.

To account for the diminished control, we first considered the nature of the initiators. Because dbmOH and dbm(OH)₂ are diketones that can tautomerize, it was theorized that the enol form could potentially act as an alcohol initiator for the polymerization of ϵ -caprolactone, perhaps causing the shoulder that is seen in the GPC trace over time. To test this possibility, a polymerization reaction was performed with unmodified dbm, and the reaction mixture became viscous within 1 d. The resulting solid was dissolved in CH₂Cl₂ and precipitated into cold acetone in an attempt to remove any unreacted dbm. Although ¹H NMR analysis of the precipitated polymeric product still showed the presence of poly(ϵ -caprolactone) and dbm resonances, the amount of dbm decreased upon subsequent precipitations. This suggests that the dbm peaks may arise from molecules entrapped within the polymer, and not covalently bound to it as would be the case if dbm were serving as an initiator. Furthermore, the ¹H NMR spectrum of the polymer grown in the presence of unfunctionalized dbm was compared with that of O-acylated diketones.³⁹ The vinyl and enol resonances in the polymer sample correspond to dbm rather than an enol ester, suggesting that the dbm enol is not covalently attached to the end of most polymer chains. However, the possibility of the enol site initiating the polymerization to yield an unstable enol ester that subsequently fragments to reform dbm and a carboxylic acid terminated polymer chain cannot be ruled out on the basis of these findings.

Another control reaction was run to see if polymerization can proceed in the absence of any added initiator. As shown in Figure 1, caprolactone was rapidly polymerized. This is consistent with previous reports that adventitious water from the Sn(Oct)₂, which is present in the catalyst even after multiple distillations,^{31,37,40} can serve as an initiator. This is a negligible problem in most reactions because the Sn hydroxide and oxide initiating species produced from Sn(Oct)₂ and water do not compete effectively with the Sn-alkoxide initiator obtained from primary alcohols.

Although results described above suggest that dbm is not an effective initiator, it may still function as a ligand for the Sn catalyst, thus altering its normal reactivity. To test the effect of dbm on Sn(Oct)₂-catalyzed reactions with primary alcohol initiators, additional controls were run with ethylene glycol, in the presence and absence of dbm. As an example, for a 20:10,000:1 ethylene glycol/ ϵ -caprolactone/Sn(Oct)₂ loading, a polymer with $M_n=25,200$ and PDI=1.14 was produced after 8 h. Under the same conditions, but in the

presence of dbm (1:1 dbm/ethylene glycol), a polymer with $M_n=1000$ and PDI=1.14 was generated. Consistent with data for **4** and **5** shown in Figure 1, polymerization of ϵ -caprolactone is slowed in the presence of dbm.

Although ϵ -caprolactone polymerizations with dbm initiators **4** and **5** are not strictly living, with careful selection of reaction conditions, it is still possible to prepare macroligands with low PDIs and monomodal GPC traces for use in coordination reactions. Based on the kinetics experiments, preparative scale reactions were run using a catalytic loading of 1/40 per primary alcohol initiating site. Polymerizations employing the monofunctional ligand **5** were stopped after 31 h, and polymerizations with the difunctional ligand **4** were stopped after 11 h. The resulting macroligands were analyzed by ^1H NMR and GPC in THF using RI detection. As shown in Figure 3 for dbmPCL, diketone resonances are clearly evident in ^1H NMR spectra. Number-average molecular weights were determined by relative integration of the peak at 4.06 ppm, corresponding to the $-\text{OCH}_2-$ protons of the polymer backbone against a phenyl proton peak at 7.98 ppm. GPC and NMR molecular weight data correlate reasonably well (e.g. dbmPCL: $M_n(\text{NMR})=9700$; $M_n(\text{GPC})=10,000$); however, discrepancies between GPC and ^1H NMR values are not uncommon, since the GPC molecular weights are based on polystyrene standards.^{33,41}

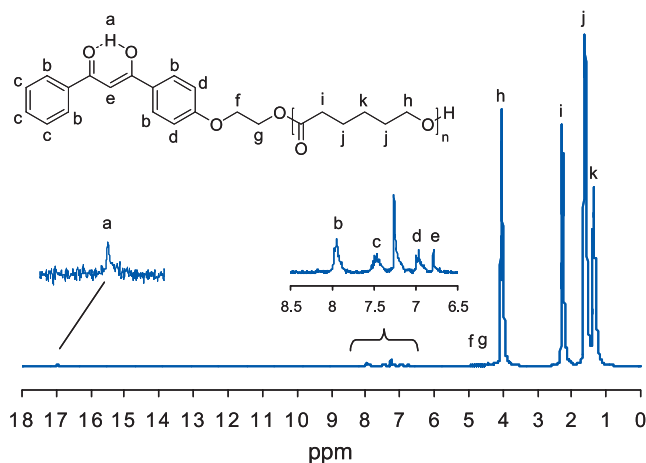


Figure 3. ^1H NMR spectrum of the dibenzoylmethane end-functionalized poly(ϵ -caprolactone) macroligand, dbmPCL **6** in CDCl_3 .

2.3. Synthesis and characterization of Eu-centered polymers

Previously, Eu-centered star polymers based on PLA were synthesized using a mixed solvent system¹⁵ to accommodate the polymer and the metal salt. More recently, it was noted that Eu tris and tetrakis dbm complexes are more conveniently prepared in THF, which solubilizes the macroligand, Et_3N , and anhydrous EuCl_3 reactants. The lability of Europium systems precludes the determination of molecular weight by GPC methods because the complexes fragment into their component parts on the columns. Characterization is accomplished by fluorescence spectroscopy and luminescence lifetime measurements of 1 mM THF solutions. Figure 4 shows representative excitation

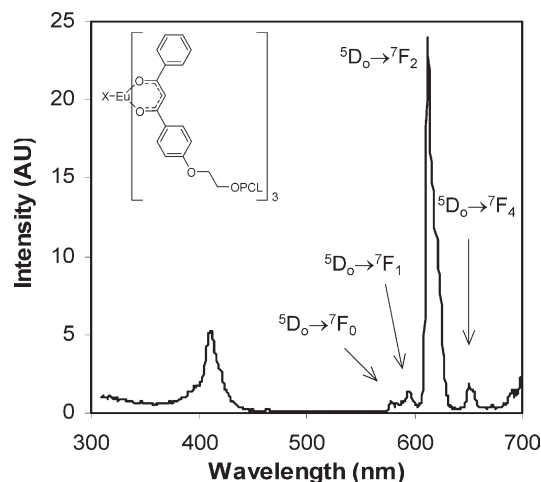


Figure 4. Excitation (~ 300 – 430 nm) and emission (~ 570 – 700 nm) spectra for a 1 mM solution of $\text{Eu}(\text{dbmPCL})_3$ in THF with labeled transitions (X=possible donor ligand, such as H_2O or THF).

and emission spectra of $\text{Eu}(\text{dbmPCL})_3$, the features of which are consistent with the spectra of $\text{Eu}(\text{dbm})_3$. Europium emission spectra vary little with different ligands and solvents because the 4f electrons of the metal are well-shielded by outer-shell electrons; the 4f electronic transitions maintain much of their atomic character in solution.

A titration study was undertaken to compare the relative fluorescence intensities of solutions with different ratios of dbmPCL per Eu ion. Figure 5 shows that the intensity is greatest when 3 equiv of ligand have been added, corresponding to a tris complex, for both the macroligand and dbm. Fluorescence intensities of tris and tetrakis dbmPCL complexes are enhanced relative to the non-polymeric Europium dbm analogues. This is consistent with previous reports describing the protective nature of the polymer shell, diminishing luminescence quenching due to metal–metal encounters and access of water and other donors to the Eu center.^{17,42}

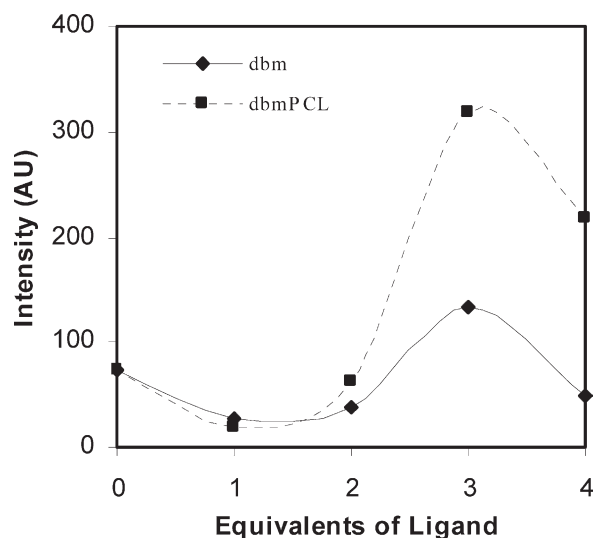


Figure 5. Europium titration experiment. Intensity versus equivalents of dbm and dbmPCL **6** ($M_n(\text{NMR})=7700$) added (per equivalent of EuCl_3). $[\text{Eu}^{3+}]$ held constant at 1 mM.

Luminescence lifetimes provide valuable information about sample homogeneity. In homogeneous samples with only one species emitting, the lifetime decay curve fits a single exponential equation. If, however, the decay curve fits a double or higher exponential equation, the sample may be inhomogeneous, with more than one species emitting. Lifetime data for tris and tetrakis polymeric products as well as the corresponding non-polymeric Eu dbm complexes are presented in Table 1. Tris complexes of dbm, dbmPCL, and dbmPCL₂ all display double exponential lifetime decay curves, as is common for Lewis acidic six-coordinate Eu complexes, with solvent or water occupying remaining binding sites in a fraction of the sample.^{43–45} The data obtained for the tetrakis complexes are consistent with single species in solution.

Table 1. Luminescence lifetimes^a (τ_1 and τ_2) for Europium dibenzoyl-methane complexes

Complex	MW ^b (calcd)	τ_1 (ms)	RW ₁ ^c (%)	τ_2 (ms)	RW ₂ ^c (%)
Eu(dbm) ₃	844	0.02	86	0.30	14
Eu(dbmPCL) ₃	25,000	0.15	94	0.68	6
Eu(dbmPCL ₂) ₃	23,500	0.13	81	0.26	19
Eu(dbm) ₄ ⁻	1068	0.13	100	—	—
Eu(dbmPCL) ₄ ⁻	33,300	0.13	100	—	—
Eu(dbmPCL ₂) ₄ ⁻	31,200	0.13	100	—	—

^a One millimolar THF solutions monitored at 613 nm after excitation at 465 nm.

^b MW (calcd)=calculated molecular weight, determined from M_n (NMR) for polymeric complexes.

^c Relative weighting (RW) of component in double exponential fits.

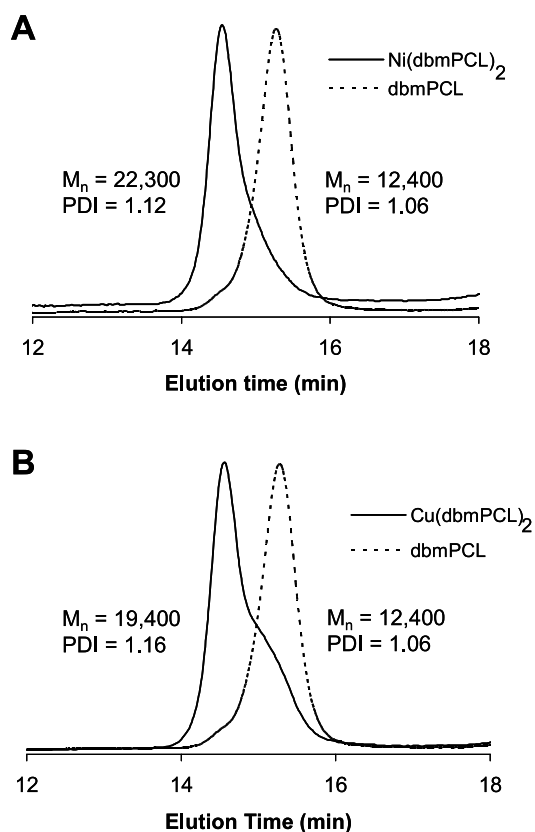


Figure 6. GPC overlay of (A) dbmPCL and a Ni bis dbmPCL complex, and (B) dbmPCL and a Cu bis dbmPCL complex in THF.

Nickel(II) and copper(II) bis β -diketonate complexes are also known^{46,47} and macroligand chelation was explored for these systems as well. Because of differences in solubility between dbm and dbmPCL, literature preparations of Ni and Cu dbm complexes were modified for this study. Both Ni(dbm)₂ and Ni(dbmPCL)₂ were prepared in 1:1 DMF/THF, and copper complexes Cu(dbm)₂ and Cu(dbmPCL)₂ were prepared in THF. During the course of the macroligand chelations, small aliquots of the green Ni and Cu solutions were removed and injected directly onto the GPC for analysis. The GPC overlays of Ni(II) and Cu(II) complexes along with their component macroligands are shown in Figure 6.

The GPC molecular weights of the Ni and Cu species are roughly twice those of the component macroligands, indicative of bis complexes. Unlike the labile Europium systems, both nickel and copper complexes show little fragmentation. Low molecular weight tailing seen for Ni, and the shoulder observed for Cu may be attributed to a small fraction of unreacted, or cleaved macroligand. Sample treatment and also GPC column conditions may affect polymeric Ni and Cu complex fragmentation. Bimodal GPC traces were consistently observed upon analysis of samples that were concentrated in vacuo or isolated after precipitation from THF/hexanes or THF/MeOH. Both Ni and Cu are known to form adducts,^{48,49} and solvato complexes in particular exhibit varying stability.^{50,51} Substitution or removal of donors such as THF, MeOH or Et₃N during precipitation or concentration may account for decreased stability during GPC analysis. Attempts to characterize the Ni and Cu polymeric compounds by UV–vis spectroscopy were also hampered by their sensitivity to fragmentation upon concentration and by insolubility at concentrations required to visualize transitions with low extinction coefficients. Nickel and copper dbm and dbmPCL complexes were analyzed in 1:1 DMF/THF. Green solutions of the polymeric nickel complex show a broad absorbance centered at 620 nm, in accord with the Ni(dbm)₂ complex (λ_{\max} , nm (ϵ , M⁻¹ cm⁻¹)=507 (25sh), 620 (32), 679 (19sh)). Unfortunately, the polymeric Ni complex was insoluble at the concentration required to resolve details of the spectrum that are evident in 20 mM solutions of the Ni dbm complex. Solutions of copper dbm and dbmPCL complexes in 1:1 DMF/THF are both green in color (Cu(dbm)₂: λ_{\max} =656 nm, ϵ =68 M⁻¹ cm⁻¹; Cu(dbmPCL)₂: λ_{\max} =660 nm, ϵ =87 M⁻¹ cm⁻¹). These data compare favorably with literature values for the bis dbm species in dioxane (λ_{\max} =650 nm, ϵ =76 M⁻¹ cm⁻¹).⁵²

The iron complex, Fe(dbmPCL)₃ was also prepared. Because the rates of reaction with polymeric ligands tend to be slower than with small-molecule ligands,⁵³ a chelation kinetics study was performed and the progress of reaction was monitored by UV–vis spectroscopy. After 10 min, the absorbance of the polymeric Fe species had reached a maximum value and plateaued with continued stirring. Thus, preparative scale reactions were run using reaction times of \sim 15 min. UV–vis spectra of Fe(dbmPCL)₃ and Fe(dbm)₃ are compared in Figure 7. Spectral data for Fe(dbm)₃ (λ_{\max} =487 nm, ϵ =4292 M⁻¹ cm⁻¹) and Fe(dbmPCL)₃ (λ_{\max} =485 nm, ϵ =4035 M⁻¹ cm⁻¹) in CH₂Cl₂ correspond reasonably well to the reported value

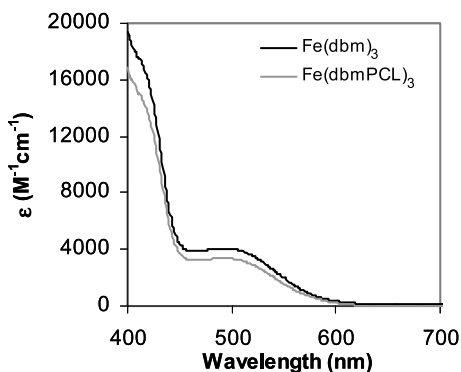


Figure 7. UV-vis spectra of $\text{Fe}(\text{dbmPCL})_3$ ($\lambda_{\text{max}}=485$ nm, $\epsilon=4292$ $\text{M}^{-1} \text{cm}^{-1}$) and $\text{Fe}(\text{dbm})_3$ ($\lambda_{\text{max}}=487$ nm, $\epsilon=4035$ $\text{M}^{-1} \text{cm}^{-1}$) in CH_2Cl_2 .

for the $n \rightarrow d^*$ transition in CHCl_3 ($\lambda_{\text{max}}=500$ nm, $\epsilon=2344$ $\text{M}^{-1} \text{cm}^{-1}$).⁵⁴

3. Conclusions

In summary, the polymerization of ϵ -caprolactone from monofunctional and difunctional alcohol diketonate ligands was explored. Although these reactions do not meet the usual criteria for a living polymerization at high conversions, narrow PDI materials were produced at low monomer conversion. Polymers thus prepared were chelated to a range of metal ions, including Eu, Ni, Cu, and Fe. This approach provides site-isolated polymeric metal complexes with spectroscopic properties that correlate well with non-polymeric analogues. The luminescence intensities of polymeric Europium complexes however, are significantly enhanced relative to Eu dbm species. Further investigation of the properties and reactivities of polymeric β -diketonate complexes will set the stage for their application as new kinds of functional materials and catalysts.

4. Experimental

4.1. Materials

ϵ -Caprolactone (Aldrich) was dried over CaH_2 and distilled prior to use. THF was dried and purified by distillation over sodium benzophenone ketyl. Chloroform-*d* (CDCl_3) was passed through a short plug of dry, activated (Brockman I) basic alumina prior to ^1H NMR spectral analysis of acid sensitive compounds. EuCl_3 (Cerac Inc., 99.9%), Tin(II)2-ethylhexanoate ($\text{Sn}(\text{Oct})_2$, Aldrich) and all other reagents were used as received without further purification. 1-[4-(2-Hydroxyethoxy)-phenyl]-3-phenyl-propane-1,3-dione (dbmOH, **5**), $\text{Eu}(\text{dbm})_3$,¹⁵ and $\text{Fe}(\text{dbm})_3$ ²⁸ were prepared as previously reported.

4.2. Methods

^1H NMR (300 MHz) and ^{13}C NMR (75 MHz) spectra were recorded on a General-Electric QE-300 instrument in CDCl_3 , unless indicated otherwise. ^1H NMR spectra were referenced to the signal for residual chloroform at 7.26 ppm or DMSO at 2.50 ppm. ^{13}C NMR spectra were referenced to

the chloroform signal at 77.0 ppm or the DMSO signal at 39.4 ppm. Analytical thin layer chromatography (TLC) was performed on 0.2 mm silica 60 coated glass plates (Whatman) and spots were visualized by UV light (254 nm). Flash chromatography was carried out on EM Science 40–63 μm silica gel. Deactivation of silica for acid-sensitive samples was performed using 10% Et_3N in hexanes, where indicated. UV-vis spectra were recorded on a Hewlett-Packard 8452A diode-array spectrophotometer. IR spectra of samples as thin films (prepared by evaporation of CH_2Cl_2 solutions onto NaCl plates) were measured using a Nicolet Impact 400D FTIR spectrophotometer. Molecular weights were determined by ^1H NMR and gel permeation chromatography (GPC) (THF, 25 $^\circ\text{C}$, 1.0 mL min^{-1} vs polystyrene standards). Polymer Labs 5 μm -mixed-C columns along with Hewlett-Packard instrumentation (Series 1100 HPLC) and Viscotek software (TriSEC GPC Version 3.0, Viscotek Corp.) were used in the GPC analysis. Emission and excitation spectra were recorded on a SPEX Fluorolog 1680 instrument using right angle illumination. Emission decay curves were recorded using a Tektronix TDS-540 digital oscilloscope, with excitation by a pulsed nitrogen laser (337 nm) and emission monitored at 613 nm.

Thermogravimetric analysis (TGA) was conducted under N_2 using a TA Instruments TGA 2020 thermogravimetric analyzer over a temperature range from 30 to 500 $^\circ\text{C}$ with a heating/cooling rate of 10 $^\circ\text{C min}^{-1}$. Differential scanning calorimetry (DSC) measurements were performed using a TA Instruments DSC 2920 modulated DSC. Analyses were performed in modulated mode under a N_2 atmosphere (amplitude = ± 1 $^\circ\text{C}$; period = 60 s; heating rate = 5 $^\circ\text{C min}^{-1}$; range = -10 to 110 $^\circ\text{C}$). Reported values of thermal events are from the second heating cycle and the reversing heat flow curve (T_g = the midpoint of the change in heat capacity).

4.3. Initiator synthesis

4.3.1. 4-(2-Hydroxyethoxy)-benzoic acid methyl ester (1). Cyclohexanone (20 mL) was added to a mixture of methyl 4-hydroxybenzoate (1.0 g, 6.57 mmol), KI (0.55 g, 3.29 mmol), and K_2CO_3 (1.81 g, 13.1 mmol) under N_2 to produce a yellow suspension. 2-Chloroethanol (1.2 mL, 16.4 mmol) was added and the reaction mixture was stirred at reflux for ~ 1 d or until TLC showed no change. The tan suspension was cooled to room temperature and filtered to remove the solids. The yellow-orange filtrate was concentrated in vacuo to yield a mixture containing a brownish-orange oil and white solid. Addition of CH_2Cl_2 (~ 15 mL) to the mixture produced a cloudy yellow suspension that was gravity filtered, and the filtrate was concentrated in vacuo to yield a light brown solid. The product was purified by column chromatography (1:1 EtOAc/hexanes, $R_f=0.25$) to give the alcohol **1** (1.23 g, 93%) as a white solid. Spectral data corresponds to that previously reported.²⁹

4.3.2. 4-[2-(Tetrahydropyran-2-yloxy)-ethoxy]-benzoic acid methyl ester (2). A solution of **1** (0.50 g, 2.55 mmol), *p*-toluenesulfonic acid monohydrate (2.4 mg, 0.0128 mmol), and 3,4-dihydro-2*H*-pyran (0.35 mL, 3.82 mmol) in CH_2Cl_2 (10 mL) was stirred at room temperature for ~ 2 h or until no starting material was evident by TLC ($R_f=0.81$; 1:1 EtOAc/hexanes). Saturated

NaHCO₃ (aq.) (10 mL) was added, the organic layer was separated, and the aqueous layer was extracted with additional CH₂Cl₂ (3×50 mL). The combined organic fractions were washed with brine (50 mL), dried over sodium sulfate, and then were filtered and concentrated in vacuo. The resulting residue was purified by column chromatography (deactivated silica, 1:1 EtOAc/hexanes, *R_f*=0.79) to afford **2** (0.69 g, 96%) as an orange oil. ¹H NMR δ 7.98 (d, *J*=8.9 Hz, 2H, 2,6-ArH), 6.95 (d, *J*=8.9 Hz, 2H, 3,5-ArH), 4.70 (t, *J*=3.5 Hz, 1H, OCHO (THP)), 4.20 (m, 2H, ROCH₂CH₂OAr), 4.07 (m, 2H, ROCH₂CH₂OAr), 3.88 (s, 3H, CH₃), 3.85 (m, 2H, OCH₂, (THP)), 3.53 (m, 2H, CH₂ (THP)), 1.79 (m, 2H, CH₂ (THP)), 1.59 (m, 2H, CH₂ (THP)). ¹³C NMR δ 131.7, 114.5, 65.9, 62.4, 52.1, 30.7, 25.6, 19.5. Anal. calcd for C₁₅H₂₀O₅: C, 64.27; H, 7.19. Found: C, 64.29; H, 7.20.

4.3.3. 1,3-Bis-[4-[2-(tetrahydropyran-2-yloxy)-ethoxy]-phenyl]-propane-1,3-dione (3). A solution of **2** (1.01 g, 3.68 mmol) and 1-[4-[2-(tetrahydropyran-2-yloxy)-ethoxy]-phenyl]-ethanone (0.95 g, 3.60 mmol) in THF (25 mL) was transferred by cannula to a suspension of sodium hydride (0.21 g, 7.35 mmol) in THF (10 mL) under N₂. The resulting mixture was heated at reflux for ~2.5 d or until TLC (1:1 EtOAc/hexanes) showed complete consumption of the ketone starting material. The resulting brown suspension was cooled to room temperature, and the reaction was quenched by the addition of H₂O (25 mL). EtOAc (50 mL) was added to the solution, and the organic layer was separated. The aqueous layer was extracted with additional EtOAc (3×50 mL). The combined organic fractions were washed with brine (25 mL), dried over sodium sulfate, and concentrated in vacuo to give a yellow-orange solid. The crude product was purified by column chromatography (deactivated silica, 1:1 EtOAc/hexanes, *R_f*=0.50) to give **3** (1.17 g, 63%) as a pale yellow solid. Mp=99–101 °C. ¹H NMR δ 17.11 (s, 1H, enol OH), 7.95 (d, *J*=8.5 Hz, 4H, 2',6'-ArH, 2'',6''-ArH), 7.01 (d, *J*=8.5 Hz, 4H, 3',5'-ArH, 3'',5''-ArH), 6.73 (s, 1H, COCHCO), 4.72 (t, *J*=3.7 Hz, 2H, OCHO (THP)), 4.22 (m, 4H, Ar-O-CH₂), 4.09 (m, 4H, Ar-O-CH₂-CH₂), 3.87 (m, 4H, OCH₂ (THP)), 3.54 (m, 2H, CH₂ diketone form), 1.90–1.46 (m, 12H, CH₂ (THP)). ¹³C NMR δ 19.5, 25.6, 30.7, 62.4, 65.9, 67.8, 91.7, 99.2, 114.8, 128.4, 129.2, 131.5, 162.5, 184.8. Anal. calcd for C₂₉H₃₆O₈: C, 67.95; H, 7.08. Found: C, 67.89; H, 7.08.

4.3.4. 1,3-Bis-[4-(2-hydroxyethoxy)-phenyl]-propane-1,3-dione (4). Acetic acid (40 mL), THF (20 mL), and H₂O (10 mL) were added to **3** (1.12 g, 2.2 mmol), and the mixture was heated at 45 °C under N₂ for 1 d. The reaction was concentrated in vacuo, yielding an off-white solid, which was purified by recrystallization from THF/hexanes to yield the diketone **4** (0.48 g, 1.39 mmol, 58%) as a fluffy white solid. Mp=149–151 °C. ¹H NMR (DMSO-d₆) δ 17.07 (s, 1H, enol OH), 7.96 (d, *J*=8.3 Hz, 4H, 2',6'-ArH, 2'',6''-ArH), 7.00 (d, *J*=8.9 Hz, 4H, 3',5'-ArH, 3'',5''-ArH), 6.73 (s, 1H, COCHCO), 4.17 (t, *J*=4.4 Hz, 4H, HOCH₂-CH₂OAr), 4.01 (t, *J*=4.4 Hz, HOCH₂CH₂OAr), 1.27 (broad s, 2H, HOCH₂CH₂OAr). ¹³C NMR (DMSO-d₆) δ 184.0, 162.4, 129.4, 126.9, 114.5, 91.4, 69.8, 59.3. Anal. calcd for C₁₈H₂₀O₄: C, 66.27; H, 5.84. Found: C, 65.97; H, 5.93.

4.4. Kinetics study of caprolactone polymerization with monofunctional initiator 5

A dry, 50 mL Kontes flask was charged with dbmOH initiator **5** (24.9 mg, 0.088 mmol), and ε-caprolactone (4.8 mL, 44 mmol). The flask was flushed with N₂, sealed, and stirred at 110 °C to ensure a homogeneous mixture, and then an 85 mM solution of Sn(Oct)₂ (26 μL, 2.2 μmol) in hexanes was added under N₂ and the flask was sealed. Small aliquots were removed by pipette under N₂ over a span of 5 d and were transferred to vials and quenched by immediate immersion in an ice bath. Percent monomer conversion was determined by ¹H NMR using relative integrations of the monomer –OCH₂ triplet peak (4.0–4.3 ppm) versus the triplet arising from the –OCH₂– backbone protons of the polymer (3.9–4.1 ppm), which are discrete resonances for individual aliquots. GPC analysis versus polystyrene standards was used to determine molecular weights (*M_n*) and polydispersity indices (PDIs). For comparison, *M_n* was also determined by NMR integration of the polymer –OCH₂– proton peaks (~4.1 ppm) relative to the phenyl initiator peak for the protons adjacent to the diketone moiety (~8.0 ppm).

4.5. Kinetics study of ε-caprolactone polymerization with difunctional initiator 4

A dry, 50 mL Kontes flask was charged with initiator dbm(OH)₂ (**4**) (30 mg, 0.087 mmol) and ε-caprolactone (4.8 mL, 44 mmol). The flask was flushed with nitrogen, sealed and stirred at 110 °C to ensure homogeneity, then an 85 mM solution of Sn(Oct)₂ in hexanes (51 μL, 4.4 μmol) was added under N₂. The flask was resealed and stirring was continued at 110 °C. Aliquots were removed and tested as described for dbmPCL.

4.6. ε-Caprolactone polymerization kinetics control reactions

(1) With dbm

A dry, 50 mL Kontes flask was charged with dibenzoyl-methane (20 mg, 0.088 mmol) and ε-caprolactone (4.8 mL, 44 mmol). The flask was flushed with nitrogen, sealed and stirred at 110 °C until homogeneous, and then an 85 mM solution of Sn(Oct)₂ in hexanes (26 μL, 2.2 μmol) was added under nitrogen. The flask was resealed and stirring was continued at 110 °C. Aliquots were removed and tested as described above for dbmPCL.

(2) With no initiator

This control reaction was run as described above for (1), with the exception that no initiator was added.

(3) With ethylene glycol as initiator

The control reaction with ethylene glycol was run as described in (1), with the exception that ethylene glycol was added instead of dbm. Reagent loadings: ethylene glycol (4.9 μL, 0.087 mmol), ε-caprolactone (4.9 mL, 44 mmol), and Sn(Oct)₂ (49 μL of an 89 mM solution in hexanes).

(4) With ethylene glycol and dbm

The control reaction with ethylene glycol and dbm was run as described above for (3), with the exception that dbm (19.5 mg, 0.087 mmol) was also added.

4.7. Preparative scale reaction with dbm

Polymerizations in the presence of dibenzoylmethane were performed analogous to the corresponding kinetics control described above, but on a larger scale: dbm (50.0 mg, 0.223 mmol), ϵ -caprolactone (12.4 mL, 112 mol) and Sn(Oct)₂ (101 μ L of a 55 mM solution in hexanes). After 12 h, the liquid reaction mixture was added dropwise to cold MeOH (~400 mL), the resulting solid product was collected on a fine frit, and was washed with cold acetone (3 \times 50 mL).

4.8. Macroligand synthesis

4.8.1. Preparative scale synthesis of dbmPCL (6).

A representative procedure is provided. A dry, 50 mL Kontes flask was charged with initiator **5** (24.9 mg, 0.088 mmol) and ϵ -caprolactone (4.8 mL, 44 mmol). The flask was flushed with nitrogen, sealed and stirred at 110 °C until homogenous, then a 69 mM solution of Sn(Oct)₂ in hexanes (32 μ L, 2.2 μ mol) was added under nitrogen. The flask was resealed and stirring was continued at 110 °C for 31 h (i.e. ~30% conversion). The reaction mixture was cooled in an ice bath, dissolved in CH₂Cl₂ (3 mL), and precipitated by dropwise addition to cold stirring MeOH (300 mL). The product was collected on a fine frit, and dried in vacuo. The resulting solid was dissolved in CH₂Cl₂ (2 mL) and precipitated by dropwise addition to cold stirring hexanes (35 mL). The product was collected by centrifugation. The mother liquor was decanted, the solid was washed with additional cold hexanes and then was dried in vacuo to provide **6** as a white solid: 0.55 g (88%; corrected for monomer conversion). *T*_m (DSC)=60.1 °C. ¹H NMR δ 16.96 (s, enol OH), 7.98 (d, *J*=4.6 Hz, 2',6'-ArH, 2'',6''-ArH), 7.49 (m, H-3'', H-4'', H-5''-ArH), 7.00 (d, *J*=4.6 Hz, 3',4'-ArH), 6.81 (s, COCHCO), 4.47 (t, *J*=4.6 Hz, PhOCH₂CH₂), 4.25 (t, *J*=4.6 Hz, PhOCH₂CH₂), 4.06 (t, *J*=6.5 Hz, RCO₂CH₂), 3.65 (m, CH₂OH), 2.30 (t, *J*=7.5 Hz, CH₂CO₂R), 1.64 (m, CH₂), 1.38 (m, CH₂). *M*_n(NMR)=8270; GPC: *M*_n=13,300, *M*_w=14,000, PDI=1.05.

4.8.2. DbmPCL₂ (7). DbmPCL₂ samples were synthesized from **4** and ϵ -caprolactone in the presence of Sn(Oct)₂ according to the procedure for dbmPCL, but with a 1:20 Sn(Oct)₂:**4** loading. The reaction was heated at 110 °C for 9 h (i.e. ~20% conversion). Characterization data for a representative dbmPCL₂ sample is as follows: 0.47 g (69%; corrected for monomer conversion). ¹H NMR δ 17.06 (s, enol H), 7.96 (d, *J*=8.3 Hz, 2',6'-ArH, 2'',6''-ArH), 6.98 (d, *J*=8.3 Hz, 3',5'-ArH, 3'',5''-ArH), 6.74 (s, COCHCO), 4.46 (t, *J*=4.4 Hz, PhOCH₂CH₂), 4.25 (t, *J*=4.4 Hz, PhOCH₂CH₂), 4.06 (t, *J*=6.6 Hz, RCO₂CH₂), 3.65 (m, CH₂OH), 2.30 (t, *J*=7.5 Hz, CH₂CO₂R), 1.64 (m, CH₂), 1.38 (m, CH₂). *M*_n (NMR)=7800; GPC: *M*_n=9700, *M*_w=10,100, PDI=1.05.

4.9. Titration of Eu with dbm and dbmPCL

Dbm (27 mg, 0.12 mmol) was dissolved in THF (10 mL) to produce a 12 mM solution. In a separate volumetric flask, EuCl₃ (26 mg, 100 μ mol) was dissolved in THF (50 mL) to produce a 2 mM solution. The dbm solution (0.5 mL,

6.0 μ mol) and EuCl₃ solution (0.5 mL, 1.0 μ mol) were combined with Et₃N (3 μ L, 20 μ mol) in a fluorescence cuvette equipped with a small stir bar, to produce a 6:1 dbm/Eu solution. After stirring for 30 min, the mixture was centrifuged to settle the fine white solids. The clarified solution was excited at 466 nm in the spectrofluorimeter, the emission was monitored over the range of 500–650 nm, and the maximum intensity at ~612 nm was noted. For a 4:1 dbm/Eu ratio, a second EuCl₃ stock solution was prepared (1 mM, 26 mg in 100 mL THF) and a portion of it (0.5 mL, 0.05 μ mol) was added to the cuvette, which was clarified and analyzed as described above. Ligand to metal ratios of 3:1, 2:1 and 1:1 were prepared and studied in an analogous manner, maintaining a 1 mM Eu concentration throughout so that intensities at different ligand loadings could be compared. A titration of Eu with dbmPCL **6** (*M*_n=13,900) was performed in an analogous manner, starting with a 1 mM solution of EuCl₃ (1 mL, 1 μ mol), solid dbmPCL (83 mg, 6 μ mol), and Et₃N (3 μ L, 20 μ mol) in THF (0.5 mL).

4.10. Synthesis of polymeric metal complexes

4.10.1. Eu(dbmPCL)₃ and Eu(dbmPCL)₂. A representative procedure for Eu(dbmPCL)₃ is provided. DbmPCL **6** (*M*_n(NMR)=9500, 107 mg, 16 μ mol), and Et₃N (10 μ L, 72 μ mol) were dissolved in THF (10 mL), and 0.9 mL of a stock solution of EuCl₃ (23 mg, 3.5 μ mol) in THF (25 mL) was added. The reaction mixture turned pale yellow and a fine white precipitate formed in minutes. The mixture was stirred for 2 h, and then the solid byproduct was removed by centrifugation. The clarified polymer solution was decanted and concentrated in vacuo. The crude product was dissolved in a minimal amount of THF (~2 mL) and added slowly dropwise to stirring cold methanol (35 mL). The mixture was centrifuged, the supernatant was decanted, and the remaining solid was washed with cold methanol (10 mL) and dried in vacuo to give Eu(dbmPCL)₃ as a white powder: 0.100 g (100%).

4.10.2. Ni(dbmPCL)₂. NiCl₂·6H₂O (25.3 mg, 0.106 mmol) was dissolved in DMF (25 mL) to form a 4.3 mM stock solution, and a portion of it (0.5 mL, 2.2 μ mol) was removed and added to a solution of dbmPCL (*M*_n=7100, 31 mg, 4.4 μ mol) in THF (8 mL). Et₃N was added (25 μ L, 17.9 μ mol) to adjust the pH of the solution to ~7. The yellow-green solution was stirred for 2 h before further analysis.

4.10.3. Cu(dbmPCL)₂. CuCl₂·2H₂O (50 mg, 0.29 mmol) was dissolved in THF (50 mL) to form a 5.8 mM stock solution, and a portion of it (0.5 mL, 2.9 μ mol) was removed and added to a solution of dbmPCL (*M*_n=8800, 50 mg, 5.7 μ mol) in THF (5 mL). Et₃N was added (15 μ L, 57 μ mol) and the yellow-green solution was stirred for 2 h before further analysis.

4.10.4. Fe(dbmPCL)₃.

4.10.4.1. Kinetics study. DbmPCL (*M*_n=8300, 13 mg, 1.57 μ mol) and Et₃N (0.2 μ L, 10.53 μ mol) were combined in CH₂Cl₂ (750 μ L) in a sealed cuvette equipped with a small magnetic stir bar. A 2.1 μ M solution of FeCl₃·6H₂O in MeOH was added (250 μ L) and the solution was stirred for

1 min. Absorbance readings at λ_{\max} =480 nm were taken every minute for 0.5 h, then every 2 min for a total of 1 h. An extinction coefficient was calculated as an average of data from three kinetics runs, collected after 10 min of stirring (i.e. after no change in absorbance).

4.10.4.2. Preparative scale. DbmPCL (M_n =10,000, 25 mg, 2.5 μ mol) was dissolved in CH_2Cl_2 (3 mL) and Et_3N (1 μ L, 7.5 μ mol) was added. A 1.71 mM solution of $\text{FeCl}_3 \cdot 6\text{H}_2\text{O}$ (23 mg, 0.085 mmol) in MeOH (50 mL) was added (500 μ L, 0.83 μ mol), along with an additional 500 μ L of MeOH, and the resulting red solution was stirred for 15 min. The reaction mixture was centrifuged to remove solid byproducts, and the clarified solution was added dropwise to cold stirring MeOH (35 mL) to precipitate the polymer product. The mixture was centrifuged, the supernatant was decanted, and the remaining solid was washed with cold methanol (10 mL) and dried in vacuo to give the Fe polymer as a red powder: 25 mg (98%). UV–vis (CH_2Cl_2): λ_{\max} = 485 nm, ϵ =4035 $\text{M}^{-1} \text{cm}^{-1}$.

Acknowledgements

We thank the National Science Foundation and Dupont for support for this research. Prof. James Demas is gratefully acknowledged for the use of his fluorescence equipment, and for invaluable advice and technical assistance.

References and notes

- Best, M. D.; Anslyn, E. V. *Chem. Eur. J.* **2003**, *9*, 51–57.
- Parker, D. *Coord. Chem. Rev.* **2000**, *205*, 109–130.
- Tsukube, H.; Shinoda, S. *Chem. Rev.* **2002**, *102*, 2389–2403.
- Richardson, F. S. *Chem. Rev.* **1982**, *82*, 541–552.
- Elbanowski, M.; Ma, K. *J. Photochem. Photobiol., A* **1996**, *99*, 85–92.
- Jiang, X.; Jen, A. K.-Y.; Huang, D.; Phelan, G. D.; Londergan, T. M.; Dalton, L. R. *Synth. Met.* **2002**, *125*, 331–336.
- Liang, C. J.; Wong, T. C.; Hung, L. S.; Lee, S. T.; Hong, Z. R.; Li, W. L. *J. Phys. D: Appl. Phys.* **2001**, *34*, 61–64.
- Kido, J.; Okamoto, Y. *Chem. Rev.* **2002**, *102*, 2357–2368.
- McGehee, M. D.; Bergstedt, T.; Zhang, C.; Saab, A. P.; O'Regan, M. B.; Bazan, G. C.; Srdanov, V. I.; Heeger, A. J. *Adv. Mater.* **1999**, *11*, 1349–1354.
- Robinson, M. R.; Ostrowski, J. C.; Bazan, G. C.; McGehee, M. D. *Adv. Mater.* **2003**, *15*, 1547–1551.
- Leadbeater, N. E.; Marco, M. *Chem. Rev.* **2002**, *102*, 3217–3273.
- Bauer, H.; Blanc, J.; Ross, D. L. *J. Am. Chem. Soc.* **1964**, *86*, 5125–5131.
- Melby, L. R.; Rose, N. J.; Abramson, E.; Caris, J. C. *J. Am. Chem. Soc.* **1964**, *86*, 5117–5125.
- Lis, S.; Elbanowski, M.; Makowska, B.; Hnatejko, Z. *J. Photochem. Photobiol., A* **2002**, *150*, 233–247.
- Bender, J. L.; Corbin, P. S.; Fraser, C. L.; Metcalf, D. H.; Richardson, F. S.; Thomas, E. L.; Urbas, A. M. *J. Am. Chem. Soc.* **2002**, *124*, 8526–8527.
- Jiang, X.; Jen, A. K.-Y.; Phelan, G. D.; Huang, D.; Londergan, T. M.; Dalton, L. R.; Register, R. A. *Thin Solid Films* **2002**, *416*, 212–217.
- Kawa, M.; Fréchet, J. M. J. *Chem. Mater.* **1998**, *10*, 286–296.
- Kuriki, K.; Koike, Y.; Okamoto, Y. *Chem. Rev.* **2002**, *102*, 2347–2356.
- Yasuda, H. *J. Organomet. Chem.* **2002**, *647*, 128–138.
- Yuan, M.; Li, X.; Xiong, C.; Deng, X. *Eur. Polym. J.* **1999**, *35*, 2131–2138.
- Li, Y.; Ouyang, J. *J. Macromol. Sci., Chem.* **1987**, *A24*, 227–242.
- Yamanaka, I.; Nakagaki, K.; Akimoto, T.; Otsuka, K. *Chem. Lett.* **1994**, *9*, 1717–1720.
- Imamura, H.; Konishi, T.; Sakata, Y.; Tsuchiya, S. *J. Chem. Soc., Faraday Trans.* **1992**, *88*, 2251–2256.
- Nair, V. A.; Sreekumar, K. *J. Polym. Mater.* **2002**, *19*, 155–162.
- Keller, F.; Weinmann, H.; Schurig, V. *Chemische Berichte/Recueil* **1997**, *130*, 879–885.
- Kawaguchi, S. *Coord. Chem. Rev.* **1986**, *70*, 51–84.
- Banu, S.; Tyagi, M. P.; Purohit, D. N. *Acta Ciencia Indica* **1990**, *XVI C*, 102–112.
- Singh, P. R.; Sahai, R. *Inorg. Chim. Acta* **1968**, *2*, 102–106.
- SDSBWeb: [http://www.aist.go.jp/RIODB/SDBS/\(01/04\)](http://www.aist.go.jp/RIODB/SDBS/(01/04)).
- Quirk, R. P.; Lee, B. *Polym. Int.* **1992**, *27*, 359–367.
- Mercerreyes, D.; Dubois, P.; Jérôme, R.; Hedrick, J. L.; Hawker, C. J. *J. Polym. Sci., Part A: Polym. Chem.* **1999**, *37*, 1923–1930.
- Duda, A. *Macromolecules* **1994**, *27*, 576–582.
- Biela, T.; Duda, A.; Penczek, S. *Macromol. Symp.* **2002**, *183*, 1–10.
- Duda, A. *Macromolecules* **1996**, *29*, 1399–1406.
- Kowalski, A.; Duda, A.; Penczek, S. *Macromol. Rapid Commun.* **1998**, *19*, 567–572.
- Lang, M.; Wong, R. P.; Chu, C.-C. *J. Polym. Sci., Part A: Polym. Chem.* **2002**, *40*, 1127–1141.
- Storey, R. F.; Sherman, J. W. *Macromolecules* **2002**, *35*, 1504–1512.
- Corbin, P. S.; Webb, M. P.; McAlvin, J. E.; Fraser, C. L. *Biomacromolecules* **2001**, *2*, 223–232.
- Agoff, J. M.; Cabaleiro, M. C. *Tetrahedron Lett.* **1974**, *39*, 3527–3528.
- Storey, R. F.; Taylor, A. E. *J.M.S.-Pure Appl. Chem.* **1998**, *A35*, 723–750.
- McLain, S. J.; Drysdale, N. E. *Polym. Prepr. (Am. Chem. Soc., Div. Polym. Chem.)* **1992**, *33*, 174–175.
- Kawa, M.; Fréchet, J. M. J. *Thin Solid Films* **1998**, *331*, 259–263.
- Ballard, R. E. *Spectrochim. Acta* **1967**, *24A*, 65–71.
- Brittain, H. G.; Richardson, F. S. *J. Am. Chem. Soc.* **1976**, *98*, 5858–5863.
- Choppin, G. R.; Peterman, D. R. *Coord. Chem. Rev.* **1998**, *174*, 283–299.
- David, L.; Crăciun, C.; Cozar, O.; Chis, V.; Agut, C.; Rusu, D.; Rusu, M. *J. Mol. Struct.* **2001**, *563–564*, 573–578.
- Shcheka, O. L.; Vovna, V. I. *J. Electron. Spectrosc. Relat. Phenom.* **1992**, *60*, 211–223.
- Munakata, M.; Harada, M.; Niina, S. *Inorg. Chem.* **1976**, *15*, 1727–1729.
- Ke, C. H.; Li, N. C. *J. Inorg. Nucl. Chem.* **1969**, *31*, 1383–1393.
- Soldatov, D. V.; Henegouwen, A. T.; Enright, G. D.; Ratcliffe, C. I.; Ripmeester, J. A. *Inorg. Chem.* **2001**, *40*, 1626–1636.
- Lewis, F. D.; Miller, A. M.; Salvi, G. D. *Inorg. Chem.* **1995**, *34*, 3173–3181.
- Singh, P. R.; Sahai, R. *J. Indian Chem. Soc.* **1969**, *46*, 945–952.
- Smith, A. P.; Fraser, C. L. *Macromolecules* **2003**, *36*, 5520–5525.
- Singh, P. R.; Sahai, R. *Aust. J. Chem.* **1969**, *22*, 1169–1175.

A novel indicator series for measuring pK_a values in acetonitrile

Jennifer M. Heemstra and Jeffrey S. Moore*

Departments of Chemistry and Materials Science and Engineering, The University of Illinois at Urbana-Champaign,
600 South Mathews Avenue, Urbana, IL 61801, USA

Received 16 December 2003; revised 15 April 2004; accepted 10 May 2004

Available online 4 June 2004

This article is dedicated to Professor Grubbs, for exploring new frontiers in science and inspiring us to follow

Abstract—A series of substituted azobenzene dyes was found to span a range of 8 pK_a units in acetonitrile. The UV absorption spectra of the dyes are responsive to protonation, changing in both absorption maximum and intensity. These characteristics make the dyes useful as indicators for the measurement of pK_a values of neutral organic bases that absorb in the visible region of the spectrum.

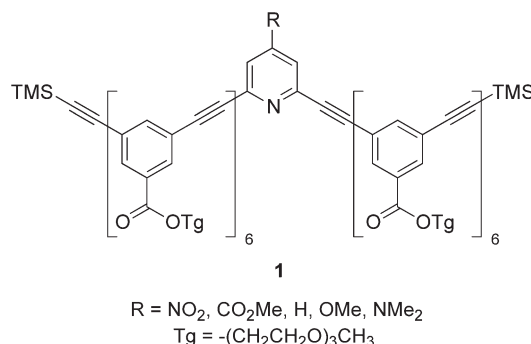
© 2004 Elsevier Ltd. All rights reserved.

1. Introduction

Neutral organic bases play an essential role in a wide range of chemical transformations.¹ The advantages of organic bases over inorganic bases include steric bulk that gives rise to weakly associating ion pairs, enhancing the reactivity of the newly formed anion, increased solubility in organic reaction media, and milder reaction conditions.² The effectiveness of a base in a chemical reaction is largely dependant on its pK_a value, making accurate measurement of pK_a crucial to the successful design of new reaction methods. While the determination of pK_a values in water is straightforward, with extensive quantities of data referenced in the literature,³ many reaction methods employing neutral organic bases are incompatible with aqueous media, creating a demand for improved methods of pK_a determination in aprotic solvents. Here we describe a series of azobenzene indicator dyes that facilitate the accurate measurement of pK_a values in acetonitrile.

The design of supramolecular architectures incorporating neutral organic bases represents one focus of research in our laboratory. These macromolecules have potential to act as enzyme mimics capable of binding substrate molecules and promoting chemical transformations. Toward this goal, we synthesized phenylene ethynylene (PE) oligomers **1**, having a substituted pyridine monomer in the backbone of the oligomer. In acetonitrile, the oligomers adopt a helical conformation with the pyridine nitrogen located on the surface of the interior binding cavity.⁴ Before attempting to use these molecules to promote chemical transformations,

we first wanted to determine the pK_a value of each oligomer in its folded state in acetonitrile.



Measurement of pK_a values in acetonitrile is well documented, with values reported for over 300 compounds.⁵ However, the reliability of much of this data is uncertain, as values reported by different authors often deviate by more than one pK_a unit.⁶ These deviations may arise from difficulties in measuring the acidity in acetonitrile media, accounting for the unreliability of pK_a values determined via direct titration methods. Also, the high concentrations required for some methods can lead to errors resulting from unwanted intermolecular interactions such as homoconjugation between a compound and its ionized species.

Koppel and coworkers have described a method for measuring pK_a values that minimizes these sources of error, and have used this method to measure pK_a values for a wide assortment of compounds in aprotic solvents including acetonitrile.⁶ In this method, UV–vis spectroscopy is used to measure ΔpK_a values for sets of compounds having similar acidities. To obtain a ΔpK_a value for two Brønsted

Keywords: Azobenzene; Indicator; Organic base.

* Corresponding author. Tel.: +1-217-244-4024; fax: +1-217-244-8068; e-mail address: moore@scs.uiuc.edu

bases, substoichiometric portions of strong acid are added to a solution of the two bases, and the resulting changes in the UV spectrum are monitored over the course of the titration.⁷ Thus, the neutral and protonated species of each of the bases must have different molar absorptivities (ϵ) over a given range of wavelengths (λ). After measurements have been made for multiple sets of compounds, an acidity scale is constructed based upon the relative pK_a differences. To assign absolute pK_a values to the acidity scale, a compound for which the pK_a value has been determined reliably is chosen to serve as a reference. By obtaining only the pK_a value of the reference compound using direct titration methods, errors resulting from inaccuracies in measuring the acidity of acetonitrile media are greatly reduced. Also, the use of UV spectroscopy allows ΔpK_a measurements to be carried out at low concentrations, decreasing the possibility of errors arising from unwanted intermolecular interactions. Given that pyridine chromophores are known to undergo a bathochromic shift in UV absorbance upon protonation,⁸ the methods developed by Koppel and coworkers appeared to be suitable for measuring the pK_a values of oligomers **1**.

2. Results and discussion

In the UV spectra of oligomers **1**, the region below 350 nm is dominated by the PE chromophore, so upon protonation of the pyridine moiety, the most easily detectable change occurs at 350–425 nm (Fig. 1). As a result, acquiring ΔpK_a measurements between oligomers **1** and other compounds requires that those compounds likewise have an absorbance band in the region of 350–425 nm that is responsive to changes in protonation state. Unfortunately, only a limited number of compounds having reliably determined pK_a values in acetonitrile meet these criteria,⁵ mandating the design of a new series of indicator compounds that absorb in or near the visible region of the spectrum, undergo a shift in absorbance maximum (λ_{max}) upon protonation, and span the pK_a range that oligomers **1** are expected to occupy ($pK_a=5-14$, based on reported values for substituted pyridine molecules).^{7,9}

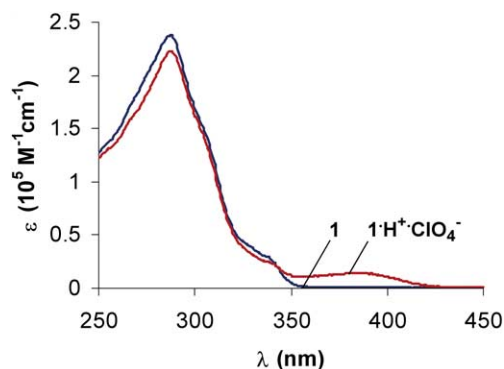


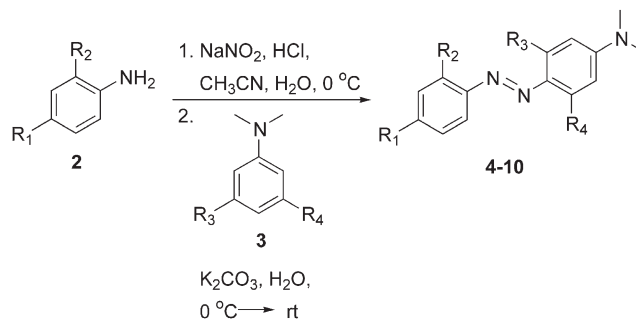
Figure 1. UV spectra of **1** (blue) and $1H^+ClO_4^-$ (red) in acetonitrile ($R=H$). [oligomer] $\sim 3.0 \mu M$.

Substituted azobenzenes possess the needed characteristics to serve as indicator compounds for the oligomer acidity scale. First, their widespread use as dyes is evidence that they absorb strongly in the visible wavelength range. Also,

some azobenzene molecules bearing *N,N*-dimethyl substituents are known to change color upon protonation, indicating a shift in λ_{max} .¹⁰ Furthermore, the basicity of azobenzene molecules can be modulated by addition of electron donating or electron withdrawing substituents to the benzene rings.¹¹ In view of these characteristics, azobenzene was chosen as the framework for the needed indicators, and the synthesis of a series of compounds spanning the pK_a range of 5–14 was initiated.

Synthesis of the azobenzene indicators is shown in Table 1. Reaction of aniline **2** with sodium nitrite under acidic conditions provided the corresponding diazonium salt in situ. Then, nucleophilic attack from *N,N*-dimethylaniline **3**¹² yielded substituted azobenzenes **4-10**. The large number of commercially available anilines and easily accessible *N,N*-dimethylanilines translates into a vast number of potential azobenzene products. However, in the absence of a nitro substituent at the R_1 position, *cis-trans* isomerization about the nitrogen–nitrogen double bond is sufficiently slow as to interfere with pK_a measurements. As a result, the nitro substituent was preserved in all of the azobenzene indicators synthesized.

Table 1. Synthesis of azobenzene indicators



Entry	R_1	R_2	R_3	R_4	Yield (%)
4 ^a	NO ₂	CN	H	H	18
5 ^b	NO ₂	Cl	H	H	82
6 ^c	NO ₂	H	H	H	57
7 ^b	NO ₂	H	Me	H	79
8	NO ₂	H	OMe	H	68
9	NO ₂	OMe	OMe	H	87
10	NO ₂	H	OMe	OMe	99

^a Vaidyanathan, S. *Indian J. Chem.* **1973**, *11*, 400.

^b Nishimura, N.; Kosako, S.; Sueishi, Y. *Bull. Chem. Soc. Jpn.* **1984**, *57*, 1617–1625.

^c Skulski, K. *Bull. Acad. Pol. Sci. Ser. Sci. Chim.* **1973**, *21*, 859–868.

To assess the suitability of azobenzenes **4-10** for use as indicators, UV spectra were acquired for each of the dyes and their conjugate acids. The data in Table 2 reveal that all of the dyes absorb in the visible region of the spectrum and undergo a shift in λ_{max} and intensity (ϵ) upon protonation, fulfilling two of the requirements necessary for the indicator series.

Using the previously described methods,⁷ ΔpK_a values were measured for pairs of indicators having similar acidities ($\Delta pK_a < 2$). These measurements were compiled to form an acidity scale, and absolute pK_a values assigned to each indicator relative to the reference compound of 2,4-dinitrophenol ($pK_a=16.66$).⁶ The pK_a values of indicators

Table 2. UV absorbance of azobenzene indicators and their conjugate acids in acetonitrile

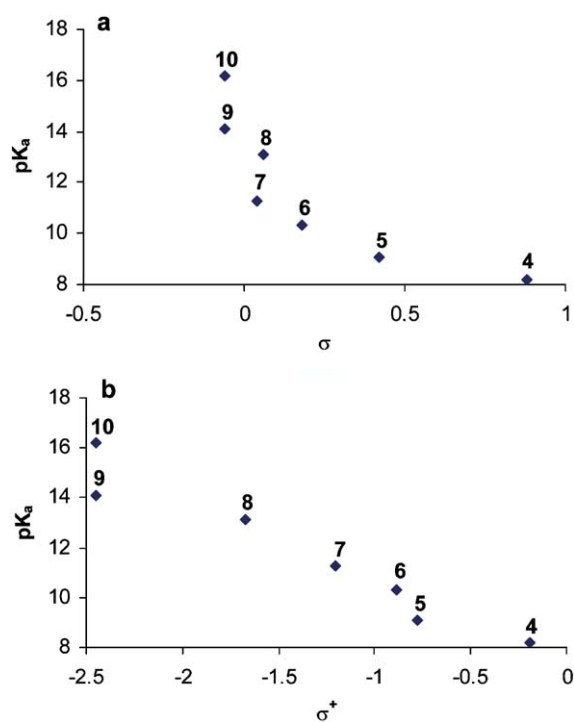
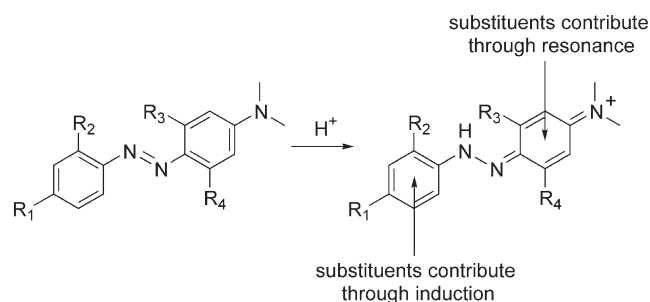
Indicator	λ_{\max} (nm)	ϵ ($M^{-1} \text{ cm}^{-1}$)	Conjugate acid	λ_{\max} (nm)	ϵ ($M^{-1} \text{ cm}^{-1}$)
4	526	36,700	4H⁺	488	43,400
5	499	30,600	5H⁺	495	50,300
6	475	29,800	6H⁺	506	63,300
7	489	30,900	7H⁺	503	64,400
8	497	31,300	8H⁺	475	64,600
9	504	28,600	9H⁺	498	61,700
10	455	25,800	10H⁺	461	59,100

4–10 vary from 8.2 to 16.2 (Table 3), spanning the majority of the expected pK_a range of oligomers **1** and fulfilling the final requirement set forth in the design of the indicator series.

Table 3. pK_a values of azobenzene indicators¹³

Indicator	pK_a (CH_3CN)
4	8.2
5	9.1
6	10.3
7	11.3
8	13.1
9	14.1
10	16.2

In Figure 2, the pK_a values of the indicators are plotted against the sum of the σ or σ^+ values for the substituents located on both benzene rings.¹⁴ We were initially surprised to find such poor correlation in the Hammett plots. However, the primary resonance contributor of the protonated indicators¹⁵ reveals that the substituents on the *N,N*-dimethylaniline ring are in resonance with the positive charge, whereas the substituents on the opposite phenyl ring

**Figure 2.** Correlation between indicator pK_a and σ (a) or σ^+ (b).**Figure 3.** Primary resonance contributor of protonated *N,N*-dimethylazobenzene indicator.

interact with the positive charge solely through induction (Fig. 3). This differentiation between the phenyl rings of the azobenzene indicator provides a likely rationale for the observed inconsistencies.

3. Conclusions

In conclusion, substituted azobenzene dyes were used to generate a novel indicator series. The indicators span a broad range of pK_a values in acetonitrile, and are useful for measuring the basicity of compounds that absorb in the visible region of the spectrum. The basicity data acquired using these indicators may aid in the design of new reaction methods involving neutral organic bases. Future work may include expansion of the indicator series to encompass an increased pK_a range and use of the indicators in a wider variety of aprotic solvents.

4. Experimental

4.1. General

Unless otherwise noted, all starting materials were obtained from commercial suppliers and were used without further purification. Flash column chromatography was carried out with silica gel 60 (230–400 mesh) from EM Science.

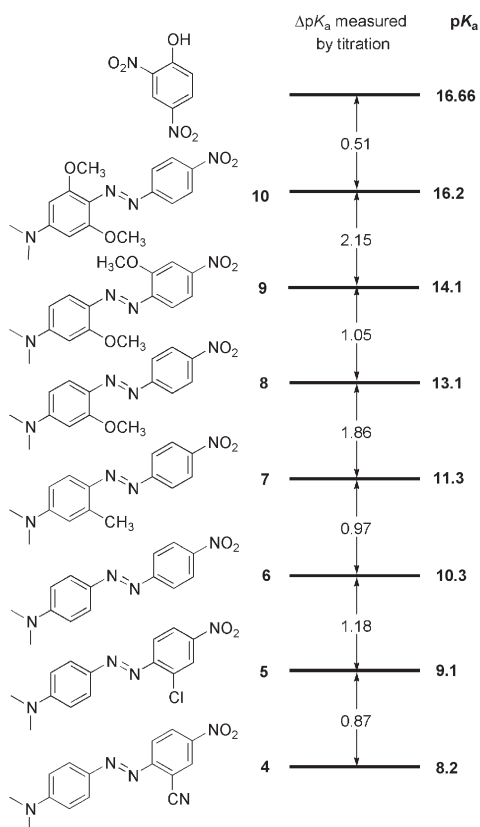
The ^1H and ^{13}C NMR spectra were recorded on a Varian Unity 400, Varian Unity 500, or Varian Narrow Bore 500 spectrometer. Chemical shifts are expressed in parts per million (δ) using residual solvent protons as internal standard (δ 7.26 ppm for CHCl_3). Coupling constants, J , are reported in Hertz (Hz), and splitting patterns are designated as s (singlet), d (doublet), t (triplet), q (quartet), m (multiplet), br (broad), and app (apparent). Mass spectra were obtained through the Mass Spectrometry Facility, School of Chemical Sciences, University of Illinois. Low resolution fast atom bombardment (FAB) and low and high resolution electron impact (EI) mass spectra were obtained on a Micromass 70-VSE spectrometer. High resolution fast atom bombardment (FAB) mass spectra were obtained on a Micromass 70-SE-4F spectrometer. Low resolution matrix assisted laser desorption (MALDI) mass spectra were obtained using a Applied Biosystems Voyager-DE STR spectrometer. Elemental analyses were performed by the University of Illinois Micro Analytical Service Laboratory.

4.2. pK_a measurements using UV–vis spectroscopy

UV absorption spectra were recorded on a Shimadzu (model UV-160A) spectrophotometer using 1-cm quartz cells. For the titration experiments, stock solutions of each of the indicators were prepared using spectrophotometric grade acetonitrile purchased from Fisher Scientific. A UV spectrum of each compound was obtained at a dilution such that the maximum absorbance was <1 . Concentrated HClO_4 was then added, and a UV spectrum of the protonated base acquired. To measure ΔpK_a values, a 1:1 mixture of two indicators was prepared ($c=8\text{--}20\ \mu\text{M}$) in spectrophotometric grade acetonitrile, and small portions of HClO_4 added until no further change was observed in the UV spectrum. The initial concentrations of each indicator were verified using Eq. 1 for the UV spectrum prior to addition of any acid.

$$A^\lambda = \varepsilon_{B_1}^\lambda [B_1] + \varepsilon_{B_2}^\lambda [B_2] \quad (1)$$

ΔpK_a values were then calculated for each of the spectra over the course of the titration using methods outlined by Koppel and coworkers.⁷ The final value of ΔpK_a represents the average of values obtained from spectra where each of the species present meets a threshold concentration. This concentration was typically 10% of the initial concentration, but for $\Delta pK_a > 1.7$, a lower threshold concentration was invoked. Absolute pK_a values were assigned to each compound relative to the 2,4-dinitrophenol reference compound.



4.2.1. Dimethyl-[4-(2-cyano-4-nitro-phenylazo)-phenyl]-amine (4). A 50 mL three-necked round bottom flask equipped with two glass stoppers and a thermometer adapter

was charged with 2-cyano-4-nitroaniline (0.457 g, 2.66 mmol), concd HCl (0.5 mL), and DMF (8 mL), then chilled to $5\ ^\circ\text{C}$ in an ice bath. A solution of NaNO_2 (0.185 g, 2.68 mmol) in 3:1 DMF: H_2O (2 mL) was added, and the reaction mixture stirred at $0\text{--}5\ ^\circ\text{C}$ for 30 min. A second 50 mL three-necked round bottom flask equipped with two glass stoppers and a thermometer adapter was charged with *N,N*-dimethylaniline (0.337 mL, 2.66 mmol), 1 M aq. HCl (8 mL), and DMF (8 mL), then chilled to $5\ ^\circ\text{C}$ in an ice bath. The solution of 2-cyano-4-nitroaniline diazonium salt was transferred to the second flask over 5 min, and the reaction mixture basified with 4 M aq. K_2CO_3 . The solution was warmed to $15\ ^\circ\text{C}$, diluted with 100 mL H_2O , and extracted with $3\times 100\ \text{mL}$ CHCl_3 . The combined organic phase was dried over Na_2SO_4 , filtered, and concentrated to give a purple solid. Recrystallization from EtOAc gave 0.144 g of dark purple solid (18%).¹⁶ Mp $194\text{--}196\ ^\circ\text{C}$. ^1H NMR (400 MHz, CDCl_3) δ 8.62 (dd, $J=2.5, 0.4\ \text{Hz}$, 1H), 8.43 (dd, $J=9.1, 2.5\ \text{Hz}$, 1H), 8.05–7.99 (m, 3H), 6.80 (AA'XX', $J_{AA'}=2.6\ \text{Hz}$, $J_{AX}=9.6\ \text{Hz}$, $J_{AX'}=0.2\ \text{Hz}$, $J_{XX'}=2.6\ \text{Hz}$, 2H), 3.20 (s, 6H). HRMS (EI) m/z 295.1099 (Calcd $[\text{M}]^+=295.1069$).

4.2.2. Dimethyl-[4-(2-chloro-4-nitro-phenylazo)-phenyl]-amine (5). A 50 mL three-necked round bottom flask equipped with two glass stoppers and a thermometer adapter was charged with 2-chloro-4-nitroaniline (0.350 g, 2.03 mmol), 1 M aq. HCl (8 mL), and CH_3CN (4 mL), then chilled to $5\ ^\circ\text{C}$ in an ice bath. A solution of NaNO_2 (0.143 g, 2.07 mmol) in H_2O (1.5 mL) was added dropwise over 2 min, and the reaction mixture stirred at $0\text{--}5\ ^\circ\text{C}$ for 30 min. A second 50 mL three-necked round bottom flask equipped with two glass stoppers and a thermometer adapter was charged with *N,N*-dimethylaniline (0.257 g, 2.03 mmol), 1 M aq. HCl (8 mL), and CH_3CN (8 mL), then chilled to $5\ ^\circ\text{C}$ in an ice bath. The solution of 2-chloro-4-nitroaniline diazonium salt was transferred to the second flask over 5 min, then chilled 4 M aq. K_2CO_3 added to bring to pH 4. The solution was removed from the ice bath and stirred for 1 h. After addition of 100 mL H_2O , the solution was extracted with $3\times 100\ \text{mL}$ CHCl_3 . The combined organic phase was dried over MgSO_4 , filtered, and concentrated to give a dark purple solid. Purification by silica gel chromatography (3:1 hexanes:EtOAc) gave 0.507 g of dark purple solid (82%).¹⁷ Mp $191\text{--}192\ ^\circ\text{C}$. ^1H NMR (400 MHz, CDCl_3) δ 8.40 (dd, $J=2.5, 0.3\ \text{Hz}$, 1H), 8.16 (dd, $J=9.0, 2.4\ \text{Hz}$, 1H), 7.97 (AA'XX', $J_{AA'}=2.6\ \text{Hz}$, $J_{AX}=9.4\ \text{Hz}$, $J_{AX'}=0.1\ \text{Hz}$, $J_{XX'}=2.6\ \text{Hz}$, 2H), 7.79 (d, $J=8.9\ \text{Hz}$, 1H), 6.82 (AA'XX', $J_{AA'}=2.6\ \text{Hz}$, $J_{AX}=9.4\ \text{Hz}$, $J_{AX'}=0.3\ \text{Hz}$, $J_{XX'}=2.6\ \text{Hz}$, 2H), 3.16 (s, 6H). ^{13}C NMR (125.7 MHz, CDCl_3) δ 153.9, 153.3, 147.2, 144.4, 134.0, 126.9, 126.1, 122.7, 118.1, 111.6, 40.4. HRMS (EI) m/z 304.0731 (Calcd $[\text{M}]^+=304.0727$).

4.2.3. Dimethyl-[4-(4-nitro-phenylazo)-phenyl]-amine (6). A 50 mL three-necked round bottom flask equipped with two glass stoppers and a thermometer adapter was charged with 4-nitroaniline (0.258 g, 1.87 mmol), 1 M aq. HCl (8 mL), and CH_3CN (4 mL), then chilled to $5\ ^\circ\text{C}$ in an ice bath. A solution of NaNO_2 (0.135 g, 1.96 mmol) in H_2O (1.5 mL) was added dropwise over 2 min, and the reaction mixture stirred at $0\text{--}5\ ^\circ\text{C}$ for 30 min. A second 50 mL three-necked round bottom flask equipped with two glass stoppers

and a thermometer adapter was charged with *N,N*-dimethylaniline (0.240 g, 1.89 mmol), 1 M aq. HCl (8 mL), and CH₃CN (8 mL), then chilled to 5 °C in an ice bath. The solution of 4-nitroaniline diazonium salt was transferred to the second flask over 5 min, then chilled 4 M aq. K₂CO₃ added to bring to pH 2. The solution was removed from the ice bath and stirred for 2 h. After addition of 100 mL H₂O, the solution was basified with 4 M aq. K₂CO₃ and extracted with 3×100 mL CHCl₃. The combined organic phase was dried over MgSO₄, filtered, and concentrated to give a dark purple solid. The crude product was filtered through a plug of silica gel with 3:1 hexanes:EtOAc, then recrystallized from EtOAc to give 0.289 g of dark purple solid (57%).¹⁸ Mp 229–230 °C. ¹H NMR (400 MHz, CDCl₃) δ 8.32 (AA'XX', J_{AA'}=2.4 Hz, J_{AX}=9.1 Hz, J_{AX'}=0 Hz, J_{XX'}=2.4 Hz, 2H), 8.00–7.92 (m, 4H), 6.78 (d, J=9.3 Hz, 2H), 3.14 (s, 6H). ¹³C NMR (125.7 MHz, CDCl₃) δ 157.0, 153.5, 147.5, 143.9, 126.2, 124.9, 122.8, 111.6, 40.4. HRMS (EI) *m/z* 270.1115 (Calcd [M]⁺=270.1117).

4.2.4. Dimethyl-[3-methyl-4-(4-nitro-phenylazo)-phenyl]-amine (7). A 50 mL three-necked round bottom flask equipped with two glass stoppers and a thermometer adapter was charged with 4-nitroaniline (0.602 g, 4.36 mmol), 1 M aq. HCl (10 mL), and CH₃CN (5 mL), then chilled to 5 °C in an ice bath. A solution of NaNO₂ (0.304 g, 4.40 mmol) in H₂O (1.5 mL) was added dropwise over 2 min, and the reaction mixture stirred at 0–5 °C for 30 min. A second 50 mL three-necked round bottom flask equipped with two glass stoppers and a thermometer adapter was charged with *N,N*-dimethyl-*m*-toluidine (0.590 g, 4.36 mmol), 1 M aq. HCl (10 mL), and CH₃CN (10 mL), then chilled to 5 °C in an ice bath. The solution of 4-nitroaniline diazonium salt was transferred to the second flask over 5 min, at which point a pink precipitate formed. The solution was basified with 4 M aq. K₂CO₃, diluted with 100 mL H₂O, and extracted with 3×100 mL CHCl₃. The combined organic phase was dried over Na₂SO₄, filtered, and concentrated to give a purple solid. Recrystallization from MeOH:EtOAc (15:1, 800 mL) gave 0.984 g of purple solid (79%).⁴ Mp 173–174 °C. ¹H NMR (400 MHz, CDCl₃) δ 8.30 (AA'XX', J_{AA'}=2.3 Hz, J_{AX}=9.1 Hz, J_{AX'}=0.1 Hz, J_{XX'}=2.3 Hz, 2H), 7.90 (AA'XX', J_{AA'}=2.3 Hz, J_{AX}=9.1 Hz, J_{AX'}=0 Hz, J_{XX'}=2.3 Hz, 2H), 7.82 (d, J=8.7 Hz, 1H), 6.60–6.55 (m, 2H), 3.11 (s, 6H), 2.71 (s, 3H). ¹³C NMR (125.7 MHz, CDCl₃) δ 157.3, 153.6, 147.2, 143.2, 142.2, 124.8, 122.7, 117.5, 112.6, 110.2, 40.3, 18.4. HRMS (EI) *m/z* 284.1286 (Calcd [M]⁺=284.1273).

4.2.5. Dimethyl-[3-methoxy-4-(4-nitro-phenylazo)-phenyl]-amine (8). A 50 mL three-necked round bottom flask equipped with two glass stoppers and a thermometer adapter was charged with 4-nitroaniline (0.279 g, 2.02 mmol), 1 M aq. HCl (8 mL), and CH₃CN (4 mL), then chilled to 5 °C in an ice bath. A solution of NaNO₂ (0.140 g, 2.03 mmol) in H₂O (1.0 mL) was added dropwise over 2 min, and the reaction mixture stirred at 0–5 °C for 30 min. A second 50 mL three-necked round bottom flask equipped with two glass stoppers and a thermometer adapter was charged with *N,N*-dimethyl-*m*-anisidine (0.305 g, 2.02 mmol), 1 M aq. HCl (8 mL), and CH₃CN (8 mL), then chilled to 5 °C in an ice bath. The solution of

4-nitroaniline diazonium salt was transferred to the second flask over 5 min, then chilled 4 M aq. K₂CO₃ added to bring to pH 3. The solution was removed from the ice bath and stirred for 30 min. After addition of 100 mL H₂O, the solution was basified with 4 M aq. K₂CO₃ and extracted with 3×100 mL CHCl₃. The combined organic phase was dried over Na₂SO₄, filtered, and concentrated to give a purple solid. Recrystallization from EtOAc gave 0.410 g of dark purple crystals (68%). Mp 169–170 °C. ¹H NMR (400 MHz, CDCl₃) δ 8.28 (AA'XX', J_{AA'}=2.4 Hz, J_{AX}=9.1 Hz, J_{AX'}=0.1 Hz, J_{XX'}=2.4 Hz, 2H), 7.89 (d, J=9.0 Hz, 2H), 7.84 (d, J=9.1 Hz, 1H), 6.35 (dd, J=9.3, 2.4 Hz, 1H), 6.18 (d, J=2.4 Hz, 1H), 4.04 (s, 3H), 3.14 (s, 6H). ¹³C NMR (125.7 MHz, DMSO-*d*₆) δ 160.5, 156.9, 155.6, 146.2, 133.1, 125.0, 122.3, 117.8, 105.3, 94.4, 55.8, 40.0. IR (nujol) 2723, 1601, 1583, 1552, 1509, 1326, 1271, 1189, 1095, 805, 754 cm⁻¹. HRMS (EI) *m/z* 300.1230 (Calcd [M]⁺=300.1222).

4.2.6. Dimethyl-[3-methoxy-4-(2-methoxy-4-nitro-phenylazo)-phenyl]-amine (9). A 50 mL three-necked round bottom flask equipped with two glass stoppers and a thermometer adapter was charged with 2-methoxy-4-nitroaniline (0.256 g, 1.52 mmol), 1 M aq. HCl (6 mL), and CH₃CN (3 mL), then chilled to 5 °C in an ice bath. A solution of NaNO₂ (0.110 g, 1.59 mmol) in H₂O (1.0 mL) was added dropwise over 2 min, and the reaction mixture stirred at 0–5 °C for 30 min. A second 50 mL three-necked round bottom flask equipped with two glass stoppers and a thermometer adapter was charged with *N,N*-dimethyl-*m*-anisidine (0.234 g, 1.55 mmol), 1 M aq. HCl (6 mL), and CH₃CN (6 mL), then chilled to 5 °C in an ice bath. The solution of 2-methoxy-4-nitroaniline diazonium salt was transferred to the second flask over 5 min, then chilled 4 M aq. K₂CO₃ added to bring to pH 3. The solution was removed from the ice bath and stirred for 1 h. After addition of 100 mL H₂O, the solution was basified with 4 M aq. K₂CO₃ and extracted with 3×100 mL CHCl₃. The combined organic phase was dried over MgSO₄, filtered, and concentrated to give a dark green solid. Recrystallization from EtOAc gave 0.439 g of dark green crystals (87%). Mp 177–178 °C. ¹H NMR (400 MHz, CDCl₃) δ 7.88–7.83 (m, 3H), 7.70–7.67 (m, 1H), 6.34 (dd, J=9.4, 2.6 Hz, 1H), 6.17 (d, J=2.6 Hz, 1H), 4.07 (s, 3H), 4.03 (s, 3H), 3.14 (s, 6H). ¹³C NMR (125.7 MHz, DMSO-*d*₆) δ 160.3, 155.3, 155.1, 147.1, 146.9, 133.8, 118.0, 117.0, 116.4, 107.9, 105.2, 94.4, 56.4, 55.7, 40.0. IR (nujol) 2723, 1601, 1326, 1273, 1214, 1124, 1082, 860, 803, 744, 730 cm⁻¹. HRMS (EI) *m/z* 330.1324 (Calcd [M]⁺=330.1328).

4.2.7. Dimethyl-[3,5-dimethoxy-4-(4-nitro-phenylazo)-phenyl]-amine (10). A 50 mL three-necked round bottom flask equipped with two glass stoppers and a thermometer adapter was charged with 4-nitroaniline (0.271 g, 1.96 mmol), 1 M aq. HCl (8 mL), and CH₃CN (4 mL), then chilled to 5 °C in an ice bath. A solution of NaNO₂ (0.136 g, 1.97 mmol) in H₂O (1.5 mL) was added dropwise over 2 min, and the reaction mixture stirred at 0–5 °C for 30 min. A second 50 mL three-necked round bottom flask equipped with two glass stoppers and a thermometer adapter was charged with *N,N*-dimethyl-3,5-dimethoxyaniline (0.355 g, 1.96 mmol), 1 M aq. HCl (8 mL), and CH₃CN (8 mL), then chilled to 5 °C in an ice bath. The solution of

4-nitroaniline diazonium salt was transferred to the second flask over 5 min, and the reaction mixture basified with 4 M aq. K_2CO_3 . The solution was warmed to 25 °C, diluted with 100 mL H_2O , and extracted with 3×100 mL $CHCl_3$. The combined organic phase was dried over Na_2SO_4 , filtered, and concentrated to give a purple solid. Purification by silica gel chromatography (EtOAc) gave 0.645 g of dark purple solid (99%). Mp 191–192 °C. 1H NMR (400 MHz, $CDCl_3$) δ 8.27 (AA'XX', $J_{AA'}=2.4$ Hz, $J_{AX}=9.2$ Hz, $J_{AX'}=0.2$ Hz, $J_{XX'}=2.4$ Hz, 2H), 7.85 (AA'XX', $J_{AA'}=2.4$ Hz, $J_{AX}=9.2$ Hz, $J_{AX'}=0$ Hz, $J_{XX'}=2.4$ Hz, 2H), 5.88 (s, 2H), 3.95 (s, 6H), 3.15 (s, 6H). ^{13}C NMR (125.7 MHz, $DMSO-d_6$) δ 158.5, 157.2, 154.6, 145.8, 124.8, 123.9, 121.7, 88.3, 55.9, 40.0. IR (nujol) 2724, 1602, 1581, 1511, 1320, 1252, 1143, 1099, 871 cm^{-1} . HRMS (EI) m/z 330.1331 (Calcd $[M]^+=330.1328$).

Acknowledgements

This research was funded by the Department of Energy, Division of Materials Sciences (DEFG02-91ER45439) through the Frederick Seitz Materials Research Laboratory at the University of Illinois at Urbana-Champaign and the National Science Foundation (CHE 03-45254). J.M.H. thanks the University of Illinois for a doctoral fellowship.

References and notes

1. *Encyclopedia of Reagents for Organic Synthesis*; Paquette, L. A., Ed.; Wiley: Chichester, 1995.
2. (a) In *Handbook of Reagents for Organic Synthesis: Acidic and Basic Reagents*; Reich, H. J., Rigby, J. H., Eds.; Wiley: Chichester, 1999. (b) Tang, J.; Dopke, J.; Verkade, J. G. *J. Am. Chem. Soc.* **1993**, *115*, 5015–5020. (c) Schwesinger, R.; Schlemper, H.; Hasenfratz, C.; Willaredt, J.; Dambacher, T.; Breuer, T.; Ottaway, C.; Fletschinger, M.; Boele, J.; Fritz, H.; Putzas, D.; Rotter, H. W.; Bordwell, F. G.; Satish, A. V.; Ji, G.-Z.; Peters, E.-M.; Peters, K.; von Schnering, H. G.; Walz, L. *Liebigs Ann.* **1996**, 1055–1081. (d) Sigma-Aldrich Chemfiles. Strong and Hindered Bases in Organic Synthesis. http://www.sigmaaldrich.com/aldrich/brochure/al_chemfile_v3_no1.pdf (accessed Dec 2003).
3. For a comprehensive list of pK_a values, see: Williams, R. pK_a values. http://www.courses.fas.harvard.edu/~chem206/Fall_2001/lectures/18_Acid_Based_Properties_of_Organic_Molecules/pKa_compilation.pdf (accessed Sept 2003).
4. Heemstra, J. M.; Moore, J. S. *Org. Lett.* **2004**, *6*, 659–662.
5. Izutsu, K. *Acid-Base Dissociation Constants in Dipolar Aprotic Solvents. IUPAC Chemical Data Series No. 35*; Blackwell Scientific: Oxford, 1990.
6. Leito, I.; Kaljurand, I.; Koppel, I. A.; Yagupolskii, L. M.; Vlasov, V. M. *J. Org. Chem.* **1998**, *63*, 7868–7874.
7. Kaljurand, I.; Rodima, T.; Leito, I.; Koppel, I. A.; Schwesinger, R. *J. Org. Chem.* **2000**, *65*, 6202–6208.
8. Swain, M.; Woodward, C. F.; Brice, B. A. *J. Am. Chem. Soc.* **1949**, *71*, 1341–1345.
9. Augustin-Nowacka, D.; Makowski, M.; Chmurzynski, L. *Anal. Chim. Acta* **2000**, *418*, 233–240.
10. Fortune, W. B.; Mellon, M. G. *J. Am. Chem. Soc.* **1938**, *60*, 2607–2609.
11. Kurtoğlu, M.; Birbiçer, N.; Kimyonsen, Ü.; Serin, S. *Dyes Pigments* **1999**, *41*, 143–147.
12. Giumanini, A. G.; Chiavari, G.; Musiani, M. M.; Rossi, P. *Synthesis* **1980**, 743–746.
13. pK_a values refer to the dissociation constant of the protonated azobenzene indicator.
14. Carey, F. A.; Sundberg, R. J. *Advanced Organic Chemistry, Part A: Structure and Mechanisms*; 4th ed. Kluwer Academic/Plenum: New York, 2000.
15. Ege, S. N. *Organic Chemistry: Structure and Reactivity*; 3rd ed. DC Heath and Company: Lexington, Massachusetts, 1994.
16. Vaidyanathan, S. *Indian J. Chem.* **1973**, *11*, 400.
17. Nishimura, N.; Kosako, S.; Sueishi, Y. *Bull. Chem. Soc. Jpn* **1984**, *57*, 1617–1625.
18. Skulski, K. *Bull. Acad. Pol. Sci. Ser. Sci. Chim.* **1973**, *21*, 859–868.



Interaction between glutathione and glutathione-*S*-transferase on dendron self-assembled controlled pore glass beads

Li-Hua Chen,^{a,b} Young-Seo Choi,^a Joseph Kwon,^c Rong-Shun Wang,^b Taehoon Lee,^c
Sung Ho Ryu^d and Joon Won Park^{a,*}

^aDepartment of Chemistry, Center for Integrated Molecular Systems, Pohang University of Science and Technology, Pohang 790-784, South Korea

^bFaculty of Chemistry, Institute of Functional Material Chemistry, Northeast Normal University, Changchun 130024, China

^cSigmol Incorporation, Pohang, South Korea

^dDepartment of Life Science, Pohang University of Science and Technology, Pohang 790-784, South Korea

Received 23 March 2004; revised 17 May 2004; accepted 19 May 2004

Available online 7 June 2004

Abstract—Controlled pore glass beads were modified with a conical shaped dendron and interaction between immobilized glutathione on top of the dendron and glutathione-*S*-transferase (GST) in cell lysate was examined. SDS-PAGE chromatogram showed that the dendron modified beads were effective not only in binding the corresponding proteins such as GST and GST-fused proteins but also in suppressing the nonspecific binding of proteins. Dramatic increase of ligand utilization (ca. 30%) was observed in comparison with the conventional approaches. Molecular weight dependence of the beads is comparable to that of Sepharose 4B.
© 2004 Elsevier Ltd. All rights reserved.

1. Introduction

Affinity purification is a well-known technique for the separation and identification of ligand-binding proteins.¹ A unique interaction between a ligand covalently attached to an insoluble matrix and the complementary target protein provides the specificity required for the isolation of biomolecules from complex mixtures. However, its widespread use has been hampered by the limited choice and instability of conventional matrices. Significant nonspecific binding of proteins to many of solid supports has been a persistent problem in establishing new matrices.² It is therefore desirable to find new matrices that are comparable to the traditional matrices in terms of the specificity while exhibiting environmental stability and capability of well-defined and facile attachment of ligands.

Aminopropyl-controlled pore glass (or AMPCPG) that is originally used for the solid-phase peptide synthesis appears to have many of desirable features. However, the controlled pore glass (or CPG) surface is polar and retains partial negative charge even when coated.³ The feature results in significant nonspecific binding of proteins. Therefore,

application on both affinity chromatography and solid-phase peptide synthesis has been limited. Once the obstacles are eliminated, widespread use of the materials can be expected.

Accessibility of ligands is a key factor in determining binding capacity. The traditional approaches are introducing a spacer molecule⁴ and increasing the ligand concentration⁵ for better exposition of the ligand on the surface. The approach works to a certain degree, but insufficient space between the ligands^{5a,b} and random distribution of capture molecules over the surfaces^{5c} are the issues yet to be solved. By far two methods have been employed to improve these shortcomings. One way is to utilize a big molecule such as protein as a placeholder. The protein is conjugated onto the matrix, and the placeholder molecule was cleaved off and washed out. In this way, certain distance between the linkers left on the matrix is secured. Nevertheless, choice of the placeholder molecule and design of the deprotection route have to be elaborately optimized for every different situation.⁶ Another way is to employ a cone-shape dendron that gives a highly ordered self-assembled monolayer and utilize an active functional group at the apex of the dendron.^{5e,7} Whitesell noticed this unique aspect of the dendron and employed it to secure sufficient room for the enhanced helical formation of the tethered peptide.^{7a} Park et al. recently observed remarkable increase of single nucleotide polymorphism discrimination efficiency when he

Keywords: Glutathione; Glutathione-*S*-transferase; Controlled pore glass; Dendron.

* Corresponding author. Tel.: +82-54-279-2119; fax: +82-54-279-0653; e-mail address: jwpark@postech.ac.kr

immobilized oligomeric DNA on the dendron-modified surface.⁸

Here we present modification of AMPCPG with dendrons, further attachment of glutathione (GSH) at the apex of the dendrons, and characteristics of the surface materials in terms of glutathione-*S*-transferase (GST) proteins binding. A dendron featuring three or nine carboxylic acid groups at the termini and one amine group at the apex has been introduced into the matrices. Their carboxylic groups were covalently linked with the solid surface. Due to wide use and understating of GST gene fusion system,⁹ GSH was chosen as a ligand to be tethered on the dendron-treated matrix. Ligand binding property of the matrix has been investigated with GST and two GST-fused proteins (GST-PXP47, GST-Munc-18).

2. Results and discussion

2.1. Synthesis and characterization of GSH immobilized CPG

2.1.1. CPG. Natural polymers such as dextran and agarose are the most frequently utilized chromatography supports for affinity chromatography. Sepharose 6B, 4B, and 2B are chromatographic materials composed of cross-linked agarose, which exhibit extremely low nonspecific adsorption. In spite of their wide use, agarose gel, typically in a bead shape, suffers some drawbacks. For instance, the flow (or elution) rates are moderate due to their soft nature. Also, they cannot be dried or frozen since they shrink severely and irreversibly, and they do not tolerate some organic solvents.^{2,10} In comparison, controlled pore glass (CPG) exhibits many desirable properties as a support: (1) it is mechanically stable, (2) it has a fixed three dimensional structure; it does not swell or shrink upon change of environment, (3) it is chemically stable from pH 1 to pH 14, (4) it is inert to a broad range of nucleophilic and electrophilic reagents, (5) it is stable against heating, (6) it exhibits excellent flow (or elution) properties, (7) it shows less tendency to adhere to surface of containers. In addition, after a modification step, removal of reagents and byproducts through washing is rapid and efficient. All of these characteristics support potential usefulness in many fields such as permeation chromatography, solid phase synthesis, affinity purification, etc.

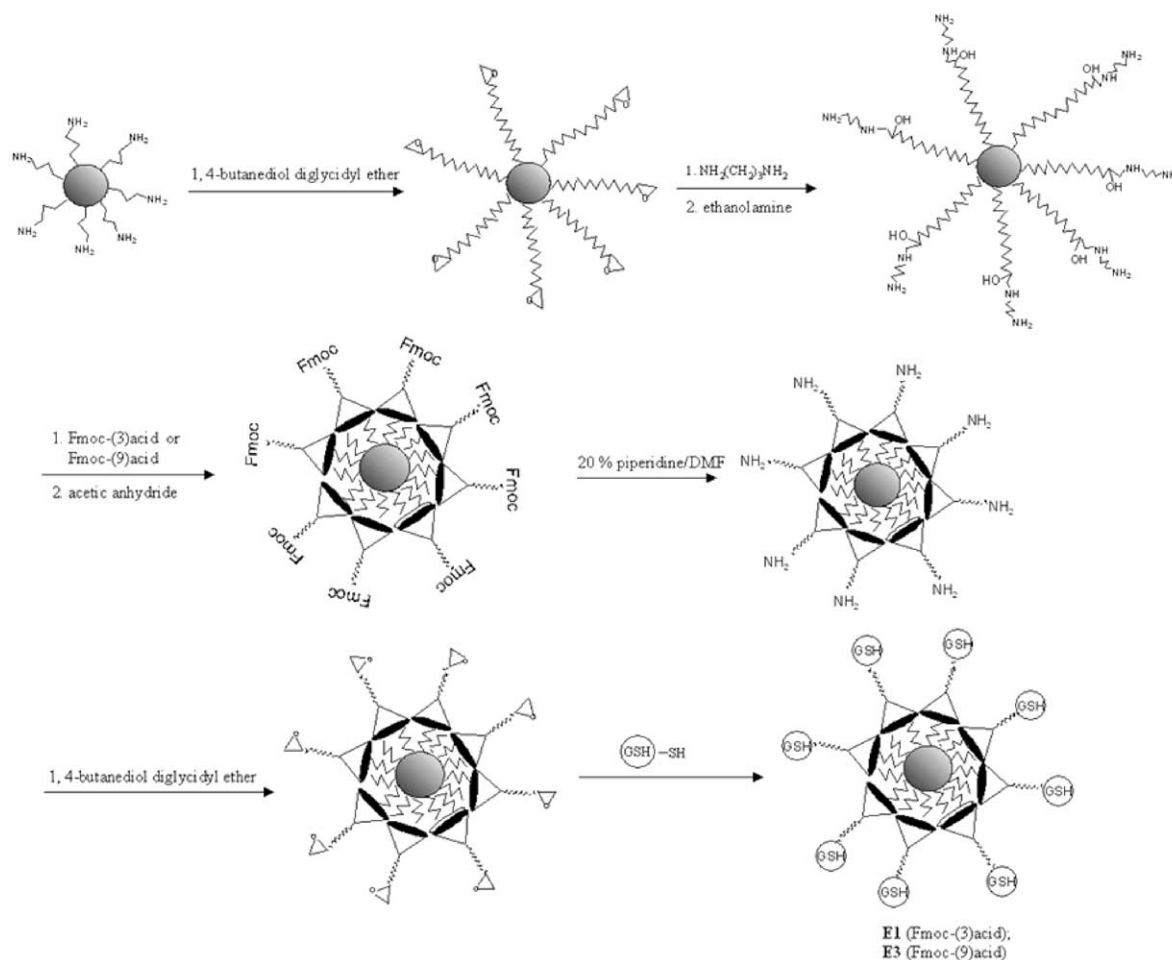
2.1.2. Pore size. Effective porosity of CPG toward an adsorbed molecule is determined by the accessibility of the guest to the host surface. To the first approximation, the accessibility of CPG to a guest depends on geometric factors, which are related to the relative size of the pores of the host compared to the size of the guest. If a guest has a molecular size that is larger than the pore openings leading to the internal surface, adsorption and interactions can only occur with the external surface, which is much smaller than the internal surface area of the investigated porous materials.¹¹ From these considerations, the extent and strength of adsorption of a guest onto CPG is expected to depend on the following parameters: pore size of CPG, the total surface area of the host, and the chemical composition of accessible surface of the host. In our investigation, three

kinds of GST fused protein (GST (28 kDa), GST-PX^{P47} (41 kDa), and GST-Munc18 fragment (98 kDa)) were employed. Molecular dimension of GST-Munc18 should be similar to that of a fused GST of 100 kDa, GST-DREF (140×140×93 Å³).^{12,13} To achieve the balance between pore size and surface area, porosity of the support has to be optimized for each specific protein. Because it is known that CPG with a pore size of approximately 50 nm allows the inclusion of complexes of the complete range of molecular subunits normally found in proteins,¹⁴ our investigation had been carried out with 50 nm CPG. Simultaneously, use of CPG with a larger pore (300 nm) confirmed the effectiveness of the former CPG as far as the above proteins are concerned.

2.1.3. Modification of glutathione CPG (sample E1, E3, A, CS, and CL).

A key concern of affinity matrices is degree of nonspecific binding (or NSB). It is a ubiquitous problem in affinity purification and solid-phase synthesis. In general, key approaches to suppress nonspecific binding are to avoid the hydrogen bond donor groups and increase the hydrophilicity of matrices.¹⁵ CPG surface, even when modified with an aminoalkyl group, is polar and retains partial negative charge.³ Use of a diepoxide as a spacer had been reported to be responsible for the hydrophilic character of the matrix and the minimal nonspecific binding.^{4b,16} Therefore, 1,4-butanediol diglycidyl ether (or BUDGE) was employed for the modification leading to sample E1 and E3. The key features of the incorporation of BUDGE include generation of very stable ethereal bond against hydrolysis, the enhanced flexibility through a long spacer arm, full distance from the surface, and suppression of nonspecific binding to a certain extent. The last advantage can be explained by resembled structural motif with that of polyethylene glycol. Diepoxides can be utilized to link a molecule and a surface having a nucleophile, such as amine and thiol. During the ring opening process, stable carbon-heteroatom bond is generated as well as a β-hydroxy group. Use of the linker before and after the dendron modification guarantees flexibility of the tethered GSH. The summarized modification steps were outlined in Scheme 1. For incorporation of the dendrons on the matrices, common reagents called EDC and NHS were used. After modification with the dendrons, acetic anhydride was introduced into system to cap the remained amine functionality. Finally, matrices were treated by 20% piperidine for 30 min to deblock the Fmoc group of the dendrons for the further modification. After elongation with BUDGE one more time, GSH was immobilized by utilizing reaction between the thiol and the epoxide.

As a control, sample A was prepared. Sequential modification with BUDGE, 1,3-diaminopropane, and BUDGE gave surface materials that is exactly same as E1 and E3 except absence of the dendrons. As before, GSH was immobilized by ring opening reaction between the epoxide and the thiol. Other control beads (sample CL and CS) were prepared by using a heterobiofunctional linker called GMBS to link GSH and AMPCPG or LCAA-CPG. While, AMPCPG has a short arm consisting C3 hydrocarbon at the surface, LCAA-CPG has a long arm of C15 aliphatic chain. After amide formation with GMBS was allowed, the beads



Scheme 1. Schematic presentation of sample **E1** and **E3** preparation with the dendrons on AMPCPG matrices, deprotection of Fmoc group by 20% piperidine in DMF and the incorporation of glutathione.

were treated with GSH. Addition of thiol group into maleimido group generated a covalent bond between carbon and sulfur atoms. The two-step treatment produced GSH-immobilized CPG beads, that is, **CL** and **CS**, through covalent bonds.

2.1.4. Ligand density measurement. Due to the difficulties in measuring amount of immobilized glutathione directly, an indirect method that measured amount of dibenzofulvene released during the deprotection step was employed. 9-Fluorenylmethoxycarbonyl (Fmoc) protecting group at the apex of the dendron is stable against acids but is readily cleaved by a variety of bases. In this study 20% piperidine in DMF is employed to deprotect the Fmoc functional group. Piperidine forms an adduct with the dibenzofulvene, and the adduct absorbs at 301 nm.¹⁷ On the other hand, increased absorbance at the wavelength indicated that the deprotection step proceeded as intended.

Ligand density obtained with this method is 8.3 $\mu\text{mol/g}$ for **E1**, 5.6 $\mu\text{mol/g}$ for **E3**. The density is reduced by a factor of 11.1 upon modification with Fmoc-(3)acid and the value is further reduced by a factor of 1.5 upon use of the larger dendron. Reduction of the density with the smaller dendron is quite effective, but use of the larger dendron shows rather limited success than expected.

2.2. Investigation of interaction between glutathione and glutathione-S-transferase

2.2.1. GST binding assay. Binding characteristics of sample **A**, **E1**, and **E3** were examined using purified GST and cell lysate (lane 2–4 in Fig. 1). Lane 1 shows successful preparation of lysate. It is evident that the three matrices bind purified GST effectively. When cell lysate was introduced into the beads (lane 5–7), a significant difference was observed between **A** and **E1** or **E3**. For sample **A**, in spite of incorporation of BUDGE linkers, serious non-specific binding was observed. Interestingly, when the dendrons were introduced on the matrix, nonspecific protein binding was effectively suppressed. It is noteworthy that self-assembly of either the dendron of the first generation or the second generation dendron effectively suppresses nonspecific binding of the solid support, while an extended spacer between the dendron and GSH retains the activity of the tethered tripeptide.

Whereas the key structural requirements for the minimal nonspecific binding are identified by Whitesides,¹⁵ molecular structure of the employed dendrons (Scheme 2) seems to meet parts of the requirements. Etheral and amide groups constitute the main backbone of the structure, and immobilization of the dendrons generates again amide

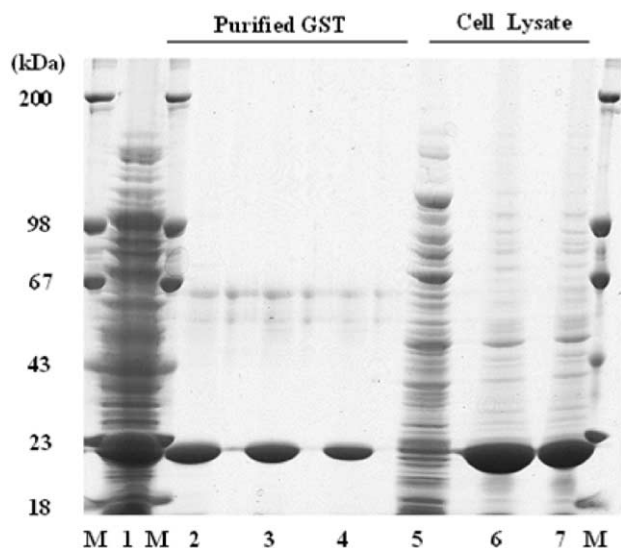
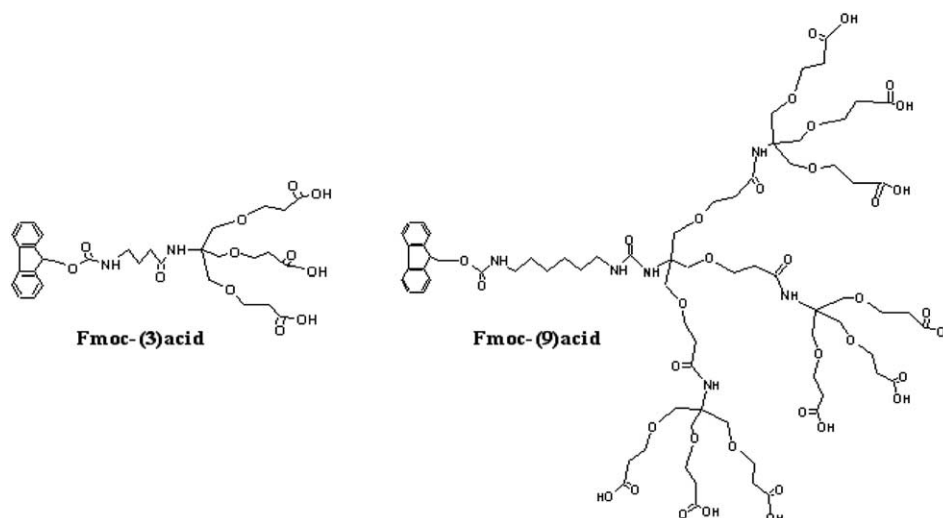


Figure 1. Binding of purified GST and cell lysate using three types of the beads. M: size markers. For comparison, cell lysate is run directly (lane 1). As controls, binding of the purified GST was tested for the matrices (A, E1, and E3) (lane 2–4). Finally, binding of cell lysate was examined to investigate efficiency of the matrices (A, E1, and E3) (lane 5–7).

cases was quite close (29, 31%). The larger spacing of E3 does not enhance the binding efficiency of GST, probably because the examined protein is larger than the spacing of both E1 and E3 anyway. Overall, the ligand utilization is greatly improved with use of the dendrons. Typically, the ligand utilization prepared by conventional immobilization methods and matrices is less than 11%.⁶ The dramatic increase supports that the regular spacing between the ligands plays a key role to enhance the accessibility of proteins to the corresponding ligands.

2.2.2. Control experiment. The measurement showed that density of GSH was 14.5 and 11.9 $\mu\text{mol/g}$ for CS and CL, respectively. To compare efficacy of the beads in terms of specific binding of GST, captured proteins with CS (5.7 mg) and CL (7.0 mg) beads were analyzed along with samples from E1 (10.0 mg) and E3 (14.8 mg) beads. The utilized quantity was adjusted to have the same number of the GSH roughly. It is evident in the chromatogram (Fig. 2) CS and CL beads display poor selectivity as well as low binding capacity. The result stresses again importance of the dendron to guarantee not only improved accessibility of GST towards immobilized GSH but effective suppression of nonspecific binding.



Scheme 2.

bonds. Also, high coverage of the dendron is also an important factor for the success.

The ligand density for E1 is 1.48 times higher than that for E3. In other words, 148% of the ligand concentration was recorded for E1 (Table 1). In order to examine the binding efficiency of both beads, weight of the samples was adjusted to have the same number of GSH in each sample. Densitometer showed that the ligand utilization for both

Table 1. Ligand concentration and ligand utilization of sample E1 and E3

Samples	Ligand density ($\mu\text{mol/g}$)	Ratio of the ligand concentration (%)	Percentage of ligand utilization (%)
E1	8.3	148	29
E3	5.6	100	31

2.2.3. Molecular weight dependence. Because the dendron modification generates a surface of controlled spacing between the immobilized ligands, binding capacity towards proteins of various molecular weights is worth of scrutiny. In particular, it is known that use of the second generation dendron guarantees a spacing over 24 Å.^{7b} For this particular test, GST protein (28 kDa), GST-PX^{P47} (41 kDa), and GST-Munc-18 fragment (98 kDa) from the wild lysate were prepared. As shown in Fig. 3, binding capacity of the beads (E1, E3, and Sepharose 4B) decreases sharply as molecular weight of proteins increases. It is interesting to note the degree of decrease holds same for the three different cases. When binding capacity of E1 is set to be 100% for GST, 92% for GST-PX^{P47} and 22% for GST-Munc-18 are recorded. For E3 bead, 85% for former protein and 23% for the latter protein are recorded. This strong dependence on the protein molecular weight was also observed with glutathione Sepharose-4B. For glutathione

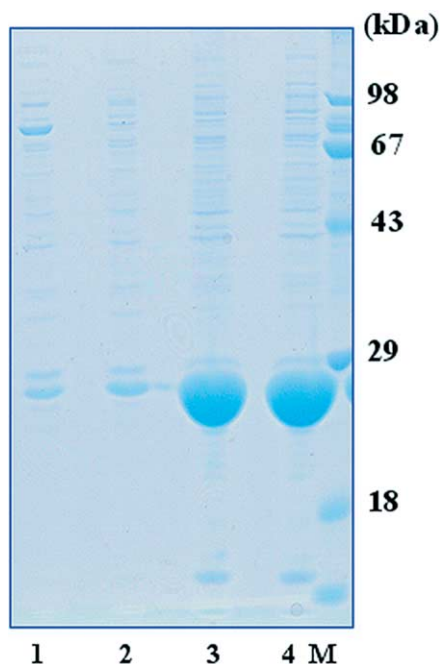


Figure 2. Binding of GST from cell lysate was recorded for two control beads, CL and CS in comparison with E1 and E3. M: size markers; lane 1: CL; lane 2: CS; lane 3: E1; lane 4: E3.

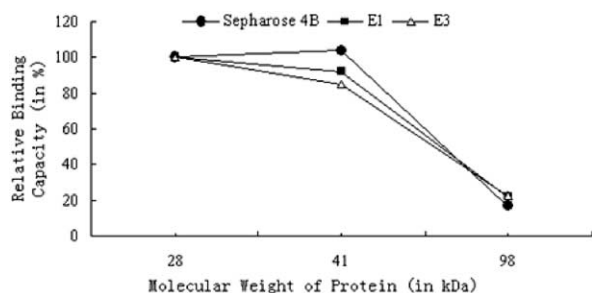


Figure 3. GST (28 kDa) and two GST-fused proteins (GST-PX^{P47} (41 kDa), GST-Munc-18 (98 kDa)) were employed to examine change of the binding capacity. Relative binding capacity of three matrices was measured with a densitometer. Binding capacity of each matrix is set to be 100% for GST. Sepharose-4B (filled circle); E1 (filled square); E3 (open triangle).

Sepharose-4B, the binding efficiencies are 104 and 17% for GST-PX^{P47} and GST-Munc-18, respectively. The only notable difference is a rather constant capacity for GST and GST-PX^{P47} for this commercially available matrix. The difference might reflect heterogeneous spacing in Sepharose 4B. In this material, diverse spacing between GSH exists so that the matrix binds the fused GST proteins as efficiently as the pristine GST. A much bigger protein, GST-Munc-18, is concerned, the spacing should be too small. In this regard, constant decrease of binding capacity of the dendron-treated beads supports again the regular spacing of GSH on the surface.

In summary, the dendron-modified matrix demonstrates selectivity as high as that of the commercial matrix (for example, Sepharose 4B), and almost same molecular weight dependence as the commercial one. The incorporation of the dendrons on AMPCPG matrix not only reduces the

nonspecific binding effectively, but retains binding activity of GSH. Constant decrease of the binding capacity as increase of protein molecular weight was observed, and the phenomenon seems in harmony with the regular spacing between the immobilized GSH. In addition to the well-controlled spacing, favorable aspects such as mechanical stability, wide compatibility with various chemical environment, and easiness to handle promise wider applications.

3. Experimental

3.1. General information

Aminopropyl group tethered controlled pore glass beads (AMPCPG; 80–120 mesh; mean pore diameter, 50 or 300 nm) and controlled pore glass beads modified with a long chain aminoalkyl group (LCAA-CPG; 80–120 mesh; mean pore diameter, 50 nm) were purchased from CPG, Inc. Sepharose 4B was obtained from Amersham Biosciences. 1,4-Butanediol diglycidyl ether, 1,3-diaminopropane, reduced glutathione (GSH), *N*-(3-methylaminopropyl)-*N*'-ethylcarbodiimide (EDC), *N*-hydroxysuccinimide (NHS), *N*-(9-fluorenylmethoxycarbonyloxy)chloride (Fmoc-Cl), piperidine, 4-maleimidobutyric acid *N*-hydroxysuccinimide ester (GMBS), phosphate buffered saline tablets (PBS) were obtained from Sigma-Aldrich. Synthesis of Fmoc-(3)acid and Fmoc-(9)acid was described elsewhere.¹⁸ All other chemicals were of analytical reagent grade and were used without further purification. Deionized water (18 M Ω cm) was obtained by passing distilled water through a Barnstead E-pure 3-Module system. UV-vis spectra were recorded on a Hewlett-Packard diode-array 8453 spectrophotometer.

3.2. Synthesis and characterization of GSH immobilized CPG

3.2.1. Immobilization of glutathione on the dendron-modified CPG (sample E1 and E3). (i) Modification with Fmoc-(3)acid: AMPCPG (dry weight 0.70 g) was washed thoroughly with acetone with a glass filter. After drying in vacuum, a mixture of 1,4-butanediol diglycidyl ether (1.0 mL) and carbonate buffer solution (2.0 mL, pH=11) was added to AMPCPG (surface capacity: 91.8 μ mol/g, surface area: 47.9 m²/g). After shaking for 24 h at room temperature, the resulting beads were separated from the solution by filtration and washed thoroughly with deionized water and subsequently with acetone. Then a vial containing this sample was shaken with a mixture of 1,3-diaminopropane (1.0 mL) and carbonate buffer solution (pH=11) for 24 h at room temperature. After washing thoroughly, a mixture of 2-mercaptoethanol (1.0 mL) and aqueous sodium bicarbonate solution (2.0 mL, pH=8.5) was employed for blocking the residual epoxy group on the surface. Subsequently, an aqueous solution of dimethylformamide (30% DMF (v/v)) dissolving Fmoc-(3)acid (14 mg, 21.3 μ mol), *N*-(3-methylaminopropyl)-*N*'-ethylcarbodiimide (15 mg, 77 μ mol) and *N*-hydroxysuccinimide (9.0 mg, 77 μ mol) was introduced into a vial containing the beads. After shaking for 11 h at room temperature, the beads were washed thoroughly with deionized water and subsequently with acetone. (ii) Capping step: acetic anhydride (1.0 mL) in anhydrous methylene chloride

(2.0 mL) was allowed to react with the residual amine overnight at room temperature. (iii) Deprotection step: after washing the beads with methylene chloride and subsequently with acetone, 20% piperidine in DMF (3.0 mL) was added in a vial holding the beads, and the vial was shaken for 30 min. (iv) Ligand-immobilization step: a mixture of 1, 4-butanediyl diglycidyl ether (1.0 mL) and carbonate buffer solution (2.0 mL, pH=11) was added again into the vial, and the mixture was shaken for another 24 h at room temperature. After washing the beads with deionized water and subsequently with acetone, the reduced glutathione (GSH, 5.4 mg, 17.6 μ mol) in sodium bicarbonate solution (3.0 mL, pH 8.5) was added into a vial containing the beads, and the vial was shaken for 12 h at room temperature. After washing the beads, a mixture of 2-mercaptoethanol (1.0 mL) and aqueous sodium bicarbonate solution (2.0 mL, pH=8.5) was added into the vial containing the beads. Finally, the beads were separated, washed, dried in vacuum, and stored at 4 °C under dry nitrogen atmosphere.

The same steps were followed exactly to prepare the sample **E3** as described above, except that Fmoc-(9)acid was used instead of Fmoc-(3)acid.

3.2.2. Preparation of other GSH tethered matrices for control experiment (sample CS, CL, and A). (i) Sample **CS** and **CL**: GSH was immobilized directly on both AMPCPG and LCAA-CPG through GMBS linker. The beads (0.10 g) were washed thoroughly with acetone with use of a glass filter. After being dried in vacuum, a mixture of DMF and sodium bicarbonate buffer (1.0 mL, 3:7 (v/v), pH=8.5) dissolving 4-maleimidobutyric acid *N*-hydroxy-succinimide ester (GMBS, 3.0 mg, 11 μ mol) was added into a vial containing the beads. After four hours of shaking at room temperature, the resulting beads were separated from the solution by filtration and washed thoroughly with deionized water and subsequently with acetone. Finally, acetic anhydride (1.0 mL) in anhydrous methylene chloride (2.0 mL) was allowed to react with residual amine group on the matrix. After thorough washing, glutathione (GSH, 3.4 mg, 11 μ mol) in PBS buffer (1.0 mL) was added into a vial containing the beads, and the vial was shaken for 12 h at room temperature. After 2-mercaptoethanol (1.0 mL) was used to block the residual maleimido group, the beads were separated, washed, dried in vacuum. (ii) Sample **A**: the same modification steps for **E1** and **E3** were followed to modify AMPCPG with 1,4-butanediyl diglycidyl ether and 1,3-diaminopropane. After the capping with 2-mercaptoethanol, 1,4-butanediyl diglycidyl ether was employed to generate an epoxy group. Finally, glutathione was immobilized, and 2-mercaptoethanol was used to open the remaining epoxy group on the beads.

3.2.3. Determination of amine density on the modified beads. Either modified beads on the way to **E1** (or **E3**) or beads for control experiments (10 mg) were taken into an e-tube. In parallel, 9-fluorenylmethyl chloroformate (Fmoc-Cl, 1.75 mg) and Na₂CO₃ (1.45 mg) were placed into a separate glass vial, and a mixed solvent (2:1 (v/v) 1,4-dioxane and water, 2.5 mL) was added to dissolve the reagents. One fifth of the solution was taken and transferred

into the e-tube containing the beads. The tube was placed into a vial, and the vial was shaken for 12 h at room temperature. The beads were separated with a glass filter, and the porous materials were washed with deionized water and subsequently with acetone. After being dried in vacuum, 20% piperidine in DMF (0.50 mL) was added into an e-tube containing the beads. The beads were allowed to react with piperidine for 30 min. Then the resulting solution from the tube was transferred carefully into a new e-tube, and the beads were washed with 20% piperidine in DMF (0.25 mL) twice. All of the solution was added into the previous e-tube. Then the solution was mixed with a certain volume of methanol to adjust the absorbance. The absorbance at 301 nm was measured using a UV/Vis spectrometer, and a relevant solvent was used for the background correction. To increase reliability, the five experimental runs were carried out in total.

For calibration, series of the solution of *N*-Fmoc-ethanol-amine (or 9-fluorenylmethyl *N*-(2-hydroxyethyl)carbamate) (30–70 μ M) in 20% piperidine/DMF were prepared. After allowing 30 min for the reaction, the solutions containing dibenzofulvene were utilized for measuring absorbance, and calculating the absorption coefficient.

3.3. Preparation of GST fusion protein lysate

GST-fusion proteins were prepared as described before.¹⁹ For large scale cultures, the single colony containing a recombinant pGEX plasmid was incubated into 200 mL of 2X YTA medium. After growing to log phase, gene expression was induced with IPTG for another 6 h. Subsequently, cells were pelleted by centrifugation and washed with 1X PBS. Then *E. coli* was lysed in 10 mL hypotonic buffer (20 mM Tris, 150 mM NaCl, 1.0 mM MgCl₂, 1.0 mM EGTA, pH=7.4) containing 0.50 mM PMSF by a sonicator. The proteins were separated by removal of insoluble material.

3.4. Binding assays

3.4.1. The effect of chain length. The prepared beads **CL** (5.72 mg), **CS** (6.97 mg), **E1** (10.0 mg), and **E3** (14.8 mg) were incubated separately with the mixed solution including GST lysates in 0.8 mL of the incubation buffer (20 mM Tris, 150 mM NaCl, 1.0 mM MgCl₂, 1.0 mM EGTA, 1% TX-100, 0.10 mM PMSF, pH=7.4) for 1 h at 4 °C, washed with ten bed volume of incubation buffer for three times and then 100 μ L of the SDS-sample buffer was added. After the tubes were cooked for 5 min at 95 °C, 20 μ L samples were utilized for SDS-PAGE and the gel was stained by CBB G-250 staining solution.

3.4.2. Selectivity of the dendron-treated matrices. 10 mg of samples **A**, **E1**, and **E3**, as well as 100 μ g of purified GST or GST-fused protein lysate were used in this experiment. The other steps were same as described above.

3.4.3. Elution of GST fusion proteins from glutathione Sepharose-4B, E1 and E3. Glutathione Sepharose-4B, **E1**, and **E3** were processed as described in the above. The amount of the protein bound to beads was determined using Image gauge V3.12 (FUJI PHOTO FILM CO., LTD.). The

same steps were followed for PX domain of p47^{phox} and Munc-18 fragment lysates.

Acknowledgements

This work was supported by the Brain Korea 21 Program of the Ministry of Education and ‘Nanotechnology-based Core Technology Development for Next Generation Businesses’ of MOCIE (00014876).

References and notes

1. Cuatrecasas, P.; Wilchek, M.; Anfinsen, C. B. *Proc. Natl. Acad. Sci. U.S.A.* **1968**, *61*, 636–643.
2. Cuatrecasas, P. *J. Biol. Chem.* **1970**, *245*, 3059–3065.
3. Hudson, D. *J. Comb. Chem.* **1999**, *1*, 403–457.
4. (a) Rusin, K. M.; Fare, T. L.; Stemple, J. Z. *Biosens. Bioelectron.* **1992**, *7*, 367–373. (b) Suen, S. Y.; Lin, S. Y.; Chiu, H. C. *Ind. Eng. Chem. Res.* **2000**, *39*, 478–487. (c) Penzol, G.; Armisén, P.; Fernández-Lafuente, R.; Rodés, L.; Guisán, J. M. *Biotechnol. Bioeng.* **1998**, *60*, 518–523. (d) Spinke, J.; Liley, M.; Schmitt, F. J.; Guder, H. J.; Angermaier, L.; Knoll, W. *J. Chem. Phys.* **1993**, *99*, 7012–7019.
5. (a) Hearn, M. T. W.; Davis, J. R. *J. Chromatogr. A* **1990**, *512*, 23–39. (b) Murza, A.; Fernández-Lafuente, R.; Guisán, J. M. *J. Chromatogr. B* **2000**, *740*, 211–218. (c) Boyer, P. M.; Hsu, J. T. *Chem. Eng. Sci.* **1992**, *47*, 241–251. (d) Houseman, B. T.; Mrksich, M. *Angew. Chem., Int. Ed. Engl.* **1999**, *38*, 782–785. (e) Xiao, Z. D.; Cai, C. Z.; Mayeux, A.; Milenkovic, A. *Langmuir* **2002**, *18*, 7728–7739.
6. Hahn, R.; Berger, E.; Pfelegerl, K.; Jungbauer, A. *Anal. Chem.* **2003**, *75*, 543–548.
7. (a) Whitesell, J. K.; Chang, H. K. *Science* **1993**, *261*, 73–76. (b) Hong, B. J.; Shim, J. Y.; Oh, S. J.; Park, J. W. *Langmuir* **2003**, *19*, 2357–2365.
8. Hong, B. J.; Oh, S. J.; Youn, T. O.; Kwon, S. H.; Park, J. W. *Nature Biotechnology*, manuscript in preparation.
9. (a) Smith, D. B.; Johnson, K. S. *Gene* **1988**, *67*, 31–40. (b) Sebastian, P.; Wallwitz, J.; Schmidt, S. *J. Chromatogr. B* **2003**, *786*, 343–355. (c) Wu, X. Q.; Oppermann, U. *J. Chromatogr. B* **2003**, *786*, 177–185. (d) De Carlos, A.; Montenegro, D.; Alonso-Rodríguez, A.; Páez de la Cadena, M.; Rodríguez-Berrocal, F. J.; Martínez-Zorzano, V. S. *J. Chromatogr. B* **2003**, *786*, 7–15.
10. Amatschek, K.; Necina, R.; Hahn, R.; Schallaun, E.; Schwinn, H.; Josić, D.; Jungbauer, A. *J. High Resolut. Chromatogr.* **2000**, *23*, 47–58.
11. (a) Poschalko, A.; Rohr, T.; Gruber, H.; Bianco, A.; Guichard, G.; Briand, J. P.; Weber, V.; Falkenhagen, D. *J. Am. Chem. Soc.* **2003**, *125*, 13415–13426. (b) Ottaviani, M. F.; Turro, N. J.; Jockusch, S.; Tomalia, D. A. *J. Phys. Chem. B* **2003**, *107*, 2046–2053.
12. Hirose, F.; Yamaguchi, M.; Kuroda, K.; Omori, A.; Hachiya, T.; Ikeda, M.; Nishimoto, Y.; Matsukage, A. *J. Biol. Chem.* **1996**, *271*, 3930–3937.
13. Zhan, Y.; Song, X.; Zhou, G. W. *Gene* **2001**, *218*, 1–9.
14. (a) Collins, R. C.; Haller, W. *Anal. Biochem.* **1973**, *54*, 47–53. (b) Haller, W. *J. Chromatogr.* **1973**, *85*, 129–131.
15. (a) Sigal, G. B.; Mrksich, M.; Whitesides, G. M. *J. Am. Chem. Soc.* **1998**, *120*, 3464–3473. (b) Chapman, R. G.; Ostuni, E.; Yan, L.; Whitesides, G. M. *Langmuir* **2000**, *16*, 6927–6936. (c) Chapman, R. G.; Ostuni, E.; Takayama, S.; Holmlin, R. E.; Yan, L.; Whitesides, G. M. *J. Am. Chem. Soc.* **2000**, *122*, 8303–8304. (d) Holmlin, R. E.; Chen, X. X.; Chapman, R. G.; Takayama, S.; Whitesides, G. M. *Langmuir* **2001**, *17*, 2841–2850. (e) Ostuni, E.; Chapman, R. G.; Liang, M. N.; Meluleni, G.; Pier, G.; Ingber, D. E.; Whitesides, G. M. *Langmuir* **2001**, *17*, 6336–6343. (f) Chapman, R. G.; Ostuni, E.; Liang, M. N.; Meluleni, G.; Kim, E.; Yan, L.; Pier, G.; Warren, H. S.; Whiteside, G. M. *Langmuir* **2001**, *17*, 1225–1233. (g) Ostuni, E.; Chapman, R. G.; Holmlin, R. E.; Takayama, S.; Whitesides, G. M. *Langmuir* **2001**, *17*, 5605–5620.
16. (a) Sundberg, L.; Porath, J. *J. Chromatogr. B* **1974**, *90*, 87–98. (b) Shimizu, N.; Sugimoto, K.; Tang, J. W.; Nishi, T.; Sato, I.; Hiramoto, M.; Aizawa, S.; Hatakeyama, M.; Ohba, R.; Hatori, H.; Yoshikawa, T.; Suzuki, F.; Oomori, A.; Tanaka, H.; Kawaguchi, H.; Watanabe, H.; Handa, H. *Nat. Biotechnol.* **2000**, *18*, 877–881.
17. Øye, G.; Roucoules, V.; Oates, L. J.; Cameron, A. M.; Cameron, N. R.; Steel, P. G.; Badyal, J. P. S.; Davis, B. G.; Coe, D. M.; Cox, R. A. *J. Phys. Chem. B* **2003**, *107*, 3496–3499.
18. Choi, Y. S.; Yoon, C. W.; Lee, H. D.; Park, M. Y.; Park, J. W. *Chem. Commun.* **2004**, 1316–1317.
19. Kim, J. H.; Lee, S.; Kim, J. H.; Lee, T. G.; Hirata, M.; Suh, P.-G.; Ryu, S. H. *Biochemistry* **2002**, *41*, 3414–3421.

Enantioselective synthesis of (+)-anatoxin-a via enyne metathesis

Jehrod B. Brenneman, Rainer Machauer and Stephen F. Martin*

Department of Chemistry and Biochemistry, The University of Texas, 1 University Station A5300, Austin, TX 78712, USA

Received 7 May 2004; revised 28 May 2004; accepted 4 June 2004

Available online 25 June 2004

Dedicated to Professor Robert H. Grubbs in recognition of his many contributions to organic chemistry and his receipt of the Tetrahedron Prize

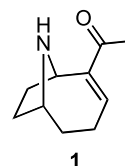
Abstract—A concise synthesis of the potent *n*AChR agonist (+)-anatoxin-a (**1**) has been completed by a series of nine chemical operations and in 27% overall yield from commercially available *D*-methyl pyroglutamate (**12**). The strategy featured the application of a new protocol for the diastereoselective synthesis of *cis*-2,5-disubstituted pyrrolidines bearing unsaturated side chains and an intramolecular enyne metathesis to provide the bridged bicyclic framework of **1**. Thus, *D*-methyl pyroglutamate (**12**) was converted in five steps to **32**, which underwent facile enyne metathesis to deliver the bicyclic diene **33**. Selective oxidative cleavage of the less substituted carbon–carbon double bond in **33** followed by deprotection furnished (+)-anatoxin-a (**1**).
© 2004 Elsevier Ltd. All rights reserved.

1. Introduction

The design and development of general and efficient strategies for alkaloid synthesis has long been a central objective in our laboratories. In that context, we became interested in applying ring-closing metathesis (RCM) to forming nitrogen heterocyclic subunits that are common to different polycyclic alkaloids since the seminal discovery by Grubbs and Fu in 1992¹ that RCM could be applied to the formation of heterocycles.^{2,3} We subsequently established the efficacy of RCM for the facile construction of not only simple fused nitrogen heterocycles,⁴ but of more complex targets such as dihydrocorynantheol⁵ and the anticancer alkaloids manzamine A⁶ and FR900482.⁷ More recently we disclosed a general entry to azabicyclo[*m.n.1*]alkenes (*m*=3–5, *n*=2, 3) by the ring-closing metathesis of *cis*-2,6-dialkenyl-*N*-acyl piperidines.⁸ In a related development, we exploited the RCM of a dialkenyl pyrrolidine as a key step in a concise synthesis of the anticancer alkaloid peduncularine.⁹

It was a logical extension of the aforementioned studies to determine the feasibility of a RCM approach to the unusual azabicyclo[4.2.1]nonene skeleton found in the potent neurotoxic alkaloid anatoxin-a (**1**). (+)-Anatoxin-a (**1**) was isolated from the toxic blooms of the blue–green freshwater algae *Anabaena flos-aquae* (Lyngb.) de Bréb and is one of the most potent nicotinic acetylcholine receptor

(*n*AChR) agonists known.¹⁰ Also referred to as ‘very fast death factor’ (VFDF), **1** has been shown to resist enzymatic degradation by acetylcholine esterase, resulting in respiratory paralysis and eventual death.¹¹ Despite its toxicity, **1** has emerged as a valuable chemical probe for elucidating the mechanism of acetylcholine-mediated neurotransmission and the disease states associated with abnormalities in this important signaling pathway. Consequent to its potent pharmacological profile and unique 9-azabicyclo[4.2.1]nonane skeleton, **1** has remained an attractive synthetic target since its isolation in 1977.¹² A variety of nonlethal analogs that contain the 9-azabicyclo[4.2.1]nonane skeleton have recently been identified as potential therapeutic targets for treating neurological disorders such as Alzheimer’s and Parkinson’s diseases, schizophrenia and depression.¹³ We now report the details of a highly efficient synthesis of **1** employing a strategy that features a new method for the diastereoselective synthesis of *cis*-2,5-disubstituted pyrrolidines and an intramolecular enyne metathesis.^{14–16}



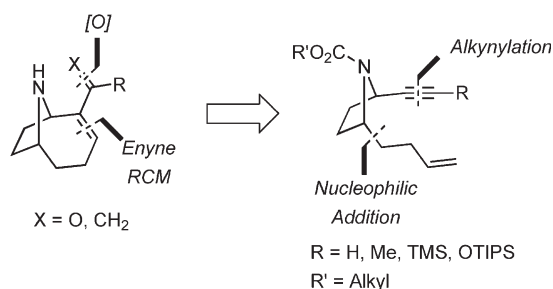
2. Results and discussion

Although we had prepared the five-membered ring of azabicyclo[3.2.1]octenes by the RCM of *cis*-2,6-divinyl piperidines,⁸ the stereoselective synthesis of a suitable

Keywords: Enantioselective synthesis; Ring closing metathesis; Diastereoselective reduction; Pyrrolidine; Iminium ion.

* Corresponding author. Tel.: +1-512-471-3915; fax: +1-512-471-4180; e-mail address: sfmartin@mail.utexas.edu

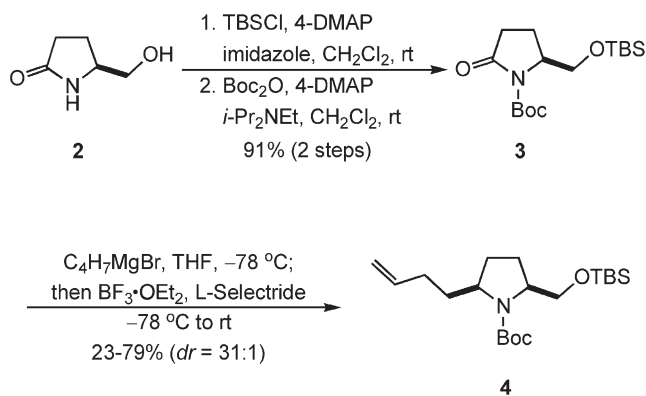
cis-2,7-divinylazepane that would lead to **1** seemed rather daunting. Hence, we were inspired to develop a route to **1** that featured the formation of the seven-membered ring of the bridged bicyclic ring system of **1** by the RCM of an appropriate enyne (Scheme 1). Oxidative cleavage of the pendant olefinic bond would then unveil the α,β -unsaturated ketone moiety of **1**. In order to implement this attractive strategy, it would be necessary to prepare a *cis*-2,5-disubstituted-*N*-acyl pyrrolidine having unsaturated side chains as the prelude to the pivotal RCM.



Scheme 1.

Examination of the literature revealed that the available methods for the efficient and diastereoselective preparation of *cis*-2,5-disubstituted pyrrolidines incorporating unsaturated moieties was limited.¹⁷ Our first task was thus to develop an efficient entry to such pyrrolidines that would provide for the incorporation of butenyl and alkynyl side chains. We reasoned that a one-pot protocol for preparing *cis*-pyrrolidines could be achieved by the reaction of *N*-acyl pyroglutamates, which are readily available in both enantiomeric forms, with an organometallic reagent followed by the stereoselective hydride reduction of the transient iminium ion that would be generated by ionization of the intermediate *N,O*-acetal. Use of a bulky hydride reducing agent would then be expected to preferentially deliver a hydride to the iminium ion from the face opposite the C2-substituent.

In order to test the feasibility of this approach to *cis*-2,5-disubstituted pyrrolidines, a model study was first undertaken employing commercially available L-pyroglutaminol (**2**). In the event, **2** was converted into the imide **3** in excellent overall yield using standard procedures (Scheme 2). We then systematically screened suitable conditions for effecting the one-pot transformation of **3**

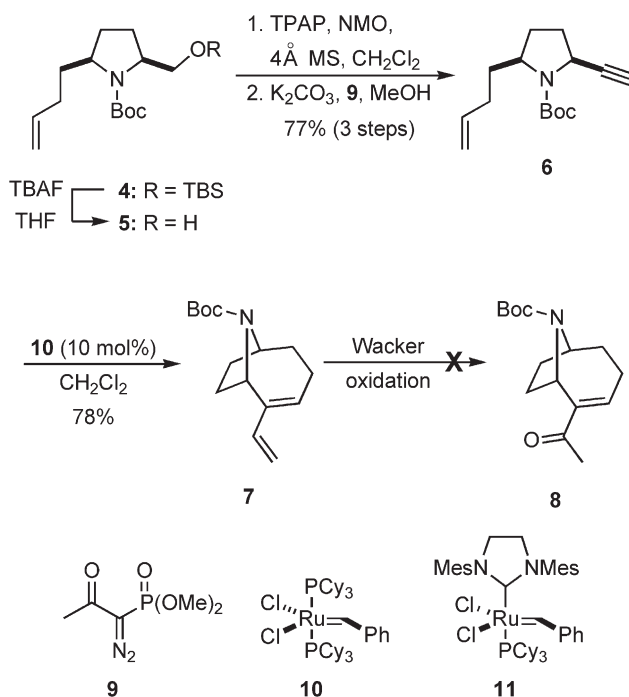


Scheme 2.

into **4**. Thus, reaction of **3** with 3-butenylmagnesium bromide afforded an intermediate alkoxyaminal that was treated in situ with a variety of Lewis acids and sterically demanding hydride donors.¹⁸ We found that the combination of BF₃·OEt₂ and L-Selectride provided the best yields of the desired *cis*-pyrrolidine **4** with excellent diastereoselectivity (*dr*=31:1).

Although this protocol was effective on smaller scales, attempts to increase the scale of the reaction to prepare gram quantities of **4** resulted in drastically reduced yields. The origin of this problem remains unknown, but we speculated that inefficient cooling during premixing of the BF₃·OEt₂ and L-Selectride on larger scales may have resulted in the generation of borane.¹⁹ Despite this drawback, these experiments provided sufficient quantities of **4** to explore the feasibility of an enyne metathesis to form a 9-azabicyclo[4.2.1]nonane skeleton according to Scheme 1. Optimizing the procedure to prepare *cis*-2,5-disubstituted pyrrolidines would wait for another day.

Removal of the silyl ether protecting group from **4** gave the alcohol **5** (Scheme 3). Oxidation of **5** gave the corresponding aldehyde that was transformed to the terminal acetylene **6** in excellent overall yield using Ohira's diazophosphonate (**9**).²⁰ When the enyne **6** was treated with the Grubbs first-generation catalyst **10**, the desired bicyclic intermediate **7** was obtained in good yield. Exposure of **6** to the more reactive Grubbs second-generation catalyst **11** resulted in diminished yields of **7** owing to the formation of increased amounts of dimeric product. On the other hand, reaction of **6** with **11** under an atmosphere of ethylene resulted in a cross-metathesis reaction between ethylene and the alkyne to deliver a C2-butadiene as the major product.²¹



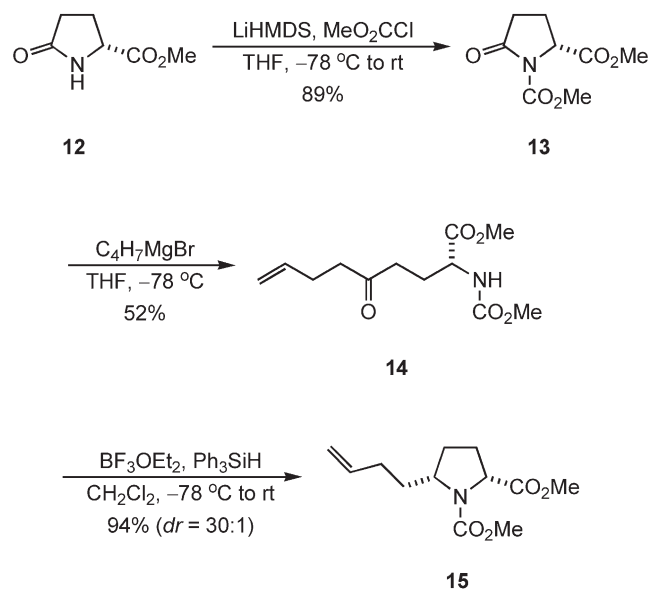
Scheme 3.

We had envisioned that the dienic moiety of **7** would be elaborated into an enone via a Wacker oxidation to deliver

8. However, we recognized that this plan was not supported by a literature precedent as there were no examples of the conversion of conjugated alkenes to enones under Wacker conditions. Rather, in one instance a stable palladium-diene species was isolated and characterized,²² and in another an oxidative cleavage of a carbon–carbon bond was observed.²³ We were unable to oxidize the exocyclic olefin of **7** to a methyl ketone under a number of different reaction conditions; rather **7** (41–63%) was recovered in all instances.²⁴ After conducting these experiments, we concluded that the desired conversion of **7** to **8** via a Wacker oxidation would likely not be possible.²⁵ This realization in conjunction with the variable yields obtained during the one-pot synthesis of the *cis*-pyrrolidine **4** led us to investigate alternative tactics leading to **1**.

Our initial focus was upon developing improved procedures for the synthesis of *cis*-2,5-disubstituted pyrrolidines via the diastereoselective reduction of iminium ions. We were cognizant of several cases wherein the combination of BF₃·OEt₂ and Et₃SiH was employed to effect the selective reduction of Δ^{1,2}-pyrrolinium ions having a bulky group at the C3-position that directed the facial selectivity of the reduction.²⁶ We thus envisioned that use of an even more sterically demanding hydride donor such as Ph₃SiH might reduce 2,5-disubstituted-Δ^{1,2}-pyrrolinium ions in a highly diastereoselective fashion from the face opposite the substituent at C5. Such a reduction protocol might also allow for the selective reduction of an *N*-acyl iminium ion in the presence of a C2-ester moiety, thereby allowing more expeditious assembly of a suitable metathesis precursor.

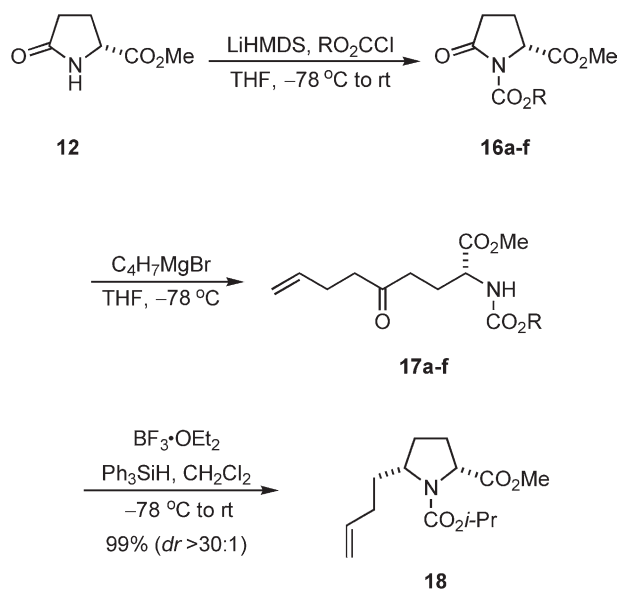
In order to explore the feasibility of the above hypothesis, we directed our attention to preparing **15** according to Scheme 4. D-Methyl-pyrroglutamate (**12**) was first converted to the imide **13**, which underwent addition of 3-butenylmagnesium bromide to provide the keto carbamate **14** in modest yield. The remainder of the mass balance was primarily accounted for by the recovery of **12**, which arose from attack of the Grignard reagent on the carbonyl carbon



Scheme 4.

atom of the carbamate moiety.²⁷ Subsequent treatment of **14** with a premixed solution of BF₃·OEt₂ and Ph₃SiH provided **15** in 94% yield and excellent diastereoselectivity (*dr*=30:1). Efforts to stream-line the conversion of **13** to **15** into a one-pot process proved problematic, resulting in significantly decreased yields. Therefore, **14** was isolated and purified prior to the cyclization-reduction step.

Stimulated by the successful cyclization/reduction of **14**, we wished to improve the yield of the initial addition step by examining carbamate-protecting groups that would be less susceptible to nucleophilic attack by the Grignard reagent. The series of carbamate derivatives of **16a–f** were thus prepared and treated with 3-butenylmagnesium bromide to afford the keto carbamates **17a–f** (Scheme 5) and the results are tabulated in Table 1.



Scheme 5.

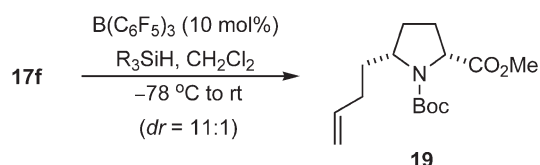
Table 1. Preparation of keto carbamates **17a–f**

Entry	R	Yield (%) 16	Yield (%) 17
a	Cl ₃ (CH ₂) ₂	91	16
b	(Cl ₃ C)CMe ₂	95	34
c	Bn	100	44
d	Cyclopentyl	59	59
e	<i>i</i> -Pr	84	79
f	<i>t</i> -Bu	89	92

As evident by examining Table 1, relatively unhindered or strongly electron withdrawing carbamates were efficiently cleaved in the presence of 3-butenylmagnesium bromide. Only the *i*-propyl and *t*-butyl carbamates **16e,f** gave the keto carbamates **17e,f** in acceptable yields. When **17e** was treated with BF₃·OEt₂ and Ph₃SiH, the *cis*-pyrrolidine **18** was isolated in near quantitative yield and >30:1 diastereoselectivity (Scheme 5).

Initial attempts to induce the cyclization/reduction of **17f** using BF₃·OEt₂ and Ph₃SiH under the same conditions that worked well for transforming **17e** into **18** resulted in extensive loss of the *t*-butyl carbamate moiety. However, we

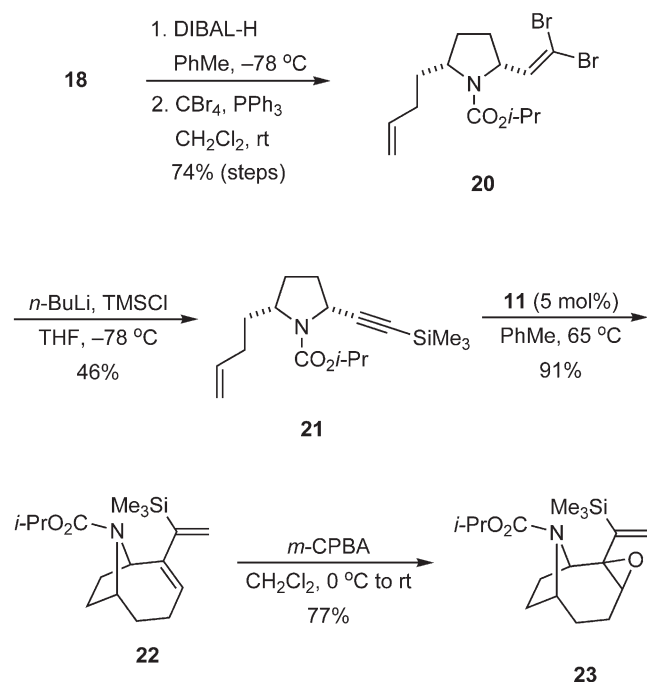
very recently discovered that the cleavage of the *N*-Boc protecting group can be avoided by a modification of our original protocol. Thus, exposure of the keto carbamate **17f** to a premixed solution of Ph_3SiH and $\text{B}(\text{C}_6\text{F}_5)_3$ (10 mol%) afforded **19** in very good diastereoselectivity ($dr=11:1$) and in 98% yield.²⁸ Inasmuch as the putative reducing agent in this process is the bulky hydridoborate $\text{HB}(\text{C}_6\text{F}_5)_3^-$ ion,²⁹ we reasoned that Et_3SiH might be used in place of Ph_3SiH as a less expensive and more atom economical hydride source. Supporting this intriguing hypothesis, we discovered that when **17f** was treated with a mixture of Et_3SiH and $\text{B}(\text{C}_6\text{F}_5)_3$ (10 mol%), **19** was obtained in 80% (unoptimized) yield together with a small amount of a lactone that was produced by reduction/cyclization of **17f** (Scheme 6).



Scheme 6.

Returning to the task at hand, it was necessary to develop an efficient means of converting **18** into a substrate for an intramolecular enyne metathesis that would give a product bearing functionality that could be readily elaborated to introduce the methyl ketone moiety found in **1**. In this regard, we had found a simple acetylenic group wanting (vide supra). We thus envisaged that an enyne metathesis involving a TMS-substituted alkyne would give a vinylsilane that could be unmasked to provide the requisite methyl ketone.³⁰

Toward this end, **18** was converted to the dibromo olefin **20** by reducing the ester to an aldehyde with DIBAL-H, followed by Corey-Fuchs olefination (Scheme 7).³¹ The

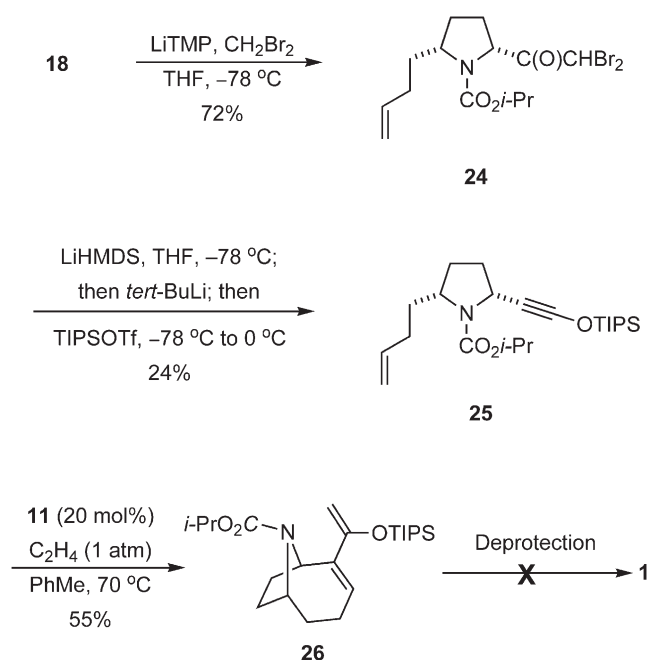


Scheme 7.

dibromide **20** was then converted to the silyl alkyne **21** in modest yield. Exposure of **21** to 5 mol% of **11** provided an excellent yield of the bicyclic vinylsilane **22**.

Unfortunately, our plan to convert the vinylsilane moiety of **22** to a methyl ketone by selective epoxidation, followed by an acid-catalyzed hydrolysis and a Peterson elimination was doomed at the outset. Namely, epoxidation of the pendant olefin of **22** with *m*-CPBA furnished the undesired epoxide **23** as the major product contaminated with smaller quantities of a bis-epoxide in a combined 77% yield (10.4:1 ratio respectively). Although an alternative procedure that was developed by Mukaiyama was considered for the hydrolysis of the vinylsilane to the ketone,³² the operational complexity of the procedure made this option less attractive than a more direct route that we had begun to explore.

During the course of our investigations, Kozmin had reported that the enyne metathesis of siloxy alkynes could be used to synthesize cyclic enones.³³ Encouraged by these results, we queried whether a similar tactic might be employed to provide a silyl enol ether that could be unmasked to reveal the methyl ketone of **1**. We therefore elaborated **18e** to the highly unstable dibromoketone **24** (Scheme 8).



Scheme 8.

Application of the Kowalski protocol for converting **24** to the siloxy alkyne **25** was surprisingly inefficient,³⁴ and all attempts to optimize the procedure were unsuccessful.

Despite the low yields obtained for the conversion of **24** to **25**, we opted to proceed with the enyne metathesis. Thus, when **25** was exposed to 20 mol% of **11** under an ethylene atmosphere, the desired bicyclic intermediate **26** was isolated in 55% yield. In the absence of ethylene, the reactions required longer reaction times (21 h vs. 5 h) and provided **26** in lower yield (44–46%).

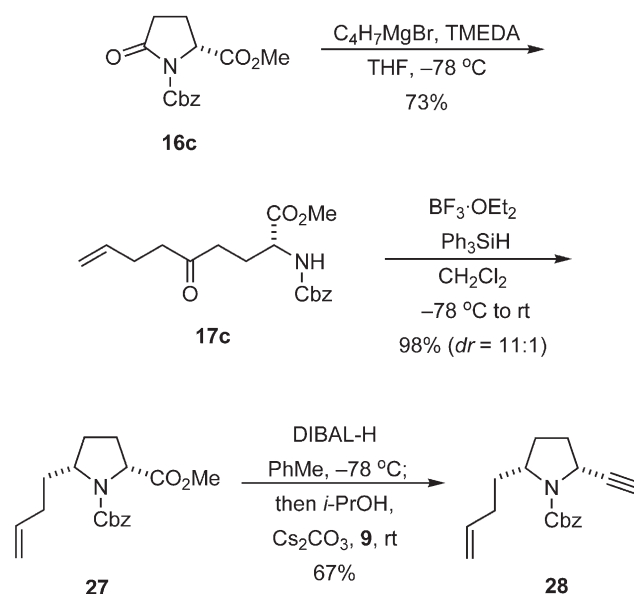
Our intention at this stage was to effect the global deprotection of **26** to arrive at **1**. A survey of the literature revealed but a few examples for removing isopropyl carbamates. The known conditions included exposure to AlCl_3 ,³⁵ gaseous HF ,³⁶ or to mixtures of H_2SO_4 in TFA.³⁷ It seemed reasonable that application of these conditions to **26** might simultaneously cleave both the carbamate and silyl-protecting group. Although the silyl enol ether was readily transformed into a methyl ketone under a variety of conditions, the isopropyl carbamate was stable. Attempts to force the reaction under acidic conditions led to decomposition. We explored several other methods used to deprotect carbamates, including *n*-BuLi, Super-Hydride, and basic hydrolysis. We were again unable to remove the carbamate. Owing to the known stability of tertiary isopropyl carbamates, we had anticipated difficulties, but we had optimistically predicted of an eventual success that was not to be. It was thus evident that a more labile carbamate would be required for the synthesis of **1**. Furthermore, the poor yield obtained for the conversion of **24** to **25** signaled that an alternative strategy for the synthesis of a functionalized bicyclic intermediate suitable for conversion to **1** was essential.

The requirement for a hindered carbamate moiety was dictated by a lack of selectivity in the additions of organometallic reagents to *N*-alkoxycarbonyl pyrrolidone derivatives. A practical solution to that vexing problem was discovered in the context of methodological studies directed toward developing improved routes to *cis*-2,5-disubstituted pyrrolidines. In particular, we discovered that the yields of the additions of Grignard reagents to *N*-alkoxycarbonyl pyrrolidones was significantly improved by premixing the organometallic reagent with an excess of *N,N,N',N'*-TMEDA.³⁸ Under these conditions, competing nucleophilic attack on the carbonyl carbon atom of the carbamate moiety was reduced dramatically. It remained to validate this tactic in our synthesis of (+)-anatoxin-a.

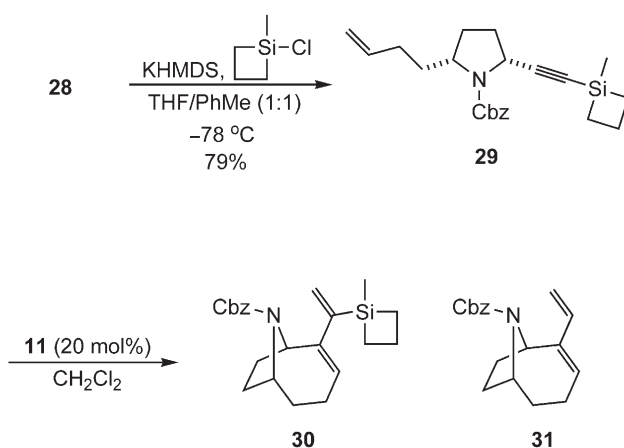
In the event, treating **16c** with a premixed solution of 3-butenylmagnesium bromide and TMEDA afforded the keto carbamate **17c** in 73% yield as contrasted with a yield of 44% in previous experiments (Scheme 9). The **17c** thus obtained was cyclized and reduced with $\text{BF}_3 \cdot \text{OEt}_2$ and Ph_3SiH as before to afford the *cis*-pyrrolidine **27** in 99% yield (*dr*=11:1). A one-pot reduction–homologation procedure, which had been developed within our group,^{8b} was performed to obtain the enyne **28**. At this stage the minor *trans*-diastereomer (6%) was removed by flash chromatography to provide pure **28**.

It was recently reported that vinyl silacyclobutanes may be oxidatively converted to ketones.³⁹ We therefore envisioned a new strategy for the synthesis of **1** that involved the enyne metathesis of an alkynyl silacyclobutane to give a vinyl siletane that could be elaborated to a methyl ketone under mild conditions (Scheme 10). Supporting our idea was an example of a ruthenium catalyzed RCM involving a silacyclobutane.⁴⁰

Encouraged by these findings, we converted **28** to the enyne metathesis precursor **29** (Scheme 10). Attempts to induce



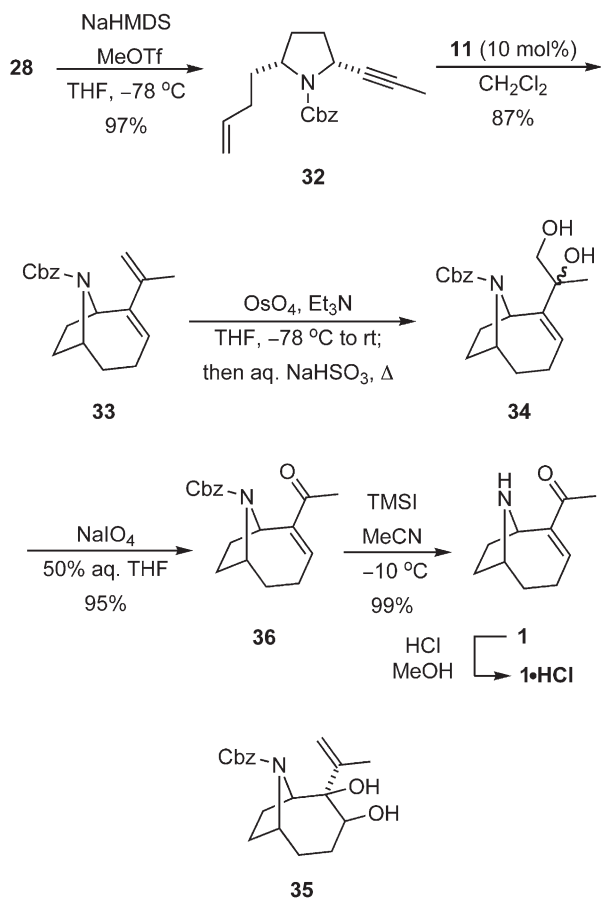
Scheme 9.



Scheme 10.

the enyne metathesis of **29** in the presence of **11** (20 mol%) at room temperature failed to provide any of the desired bicycle **30**; rather **29** (73%) was recovered along with a small amount of the protodesilylated material **31** (4%). When the reaction was performed at 80 °C (sealed tube), **31** (76%) was isolated along with smaller quantities of **29** (8%) and **28** (9%), indicating that the silacyclobutane moiety was labile under these conditions. The mechanistic pathway by which the desilylation occurs is unclear, but it is possible that oxidative insertion of the ruthenium alkylidene species into the silacyclobutane might be responsible.⁴¹

It was again time to explore other variations of an enyne metathesis that would lead to (+)-anatoxin-a (**1**). The plan for what was to be our final attempt was predicated on the hypothesis that it should be possible to induce the selective oxidative cleavage of a diene such as **33** to generate the elusive methyl ketone moiety in **1** (Scheme 11). Toward this end, **29** was first deprotected with LDA and the resulting lithium acetylide was trapped with MeI or MeOTf. However, the yield of **32** was poor owing to competing



Scheme 11.

deprotection of the Cbz-group. This problem was, however, readily circumvented by alkylation of the corresponding sodium acetylide with MeOTf to furnish **32** in excellent yield. When the enyne **32** was exposed to 10 mol% of **11**, the bicyclic diene **33** was obtained in 91% yield.

The critical stage was then set for selectively converting the pendant isopropenyl group present in **33** to a methyl ketone moiety via an oxidative cleavage. Previous work in our laboratories with a related system suggested that a Sharpless asymmetric dihydroxylation⁴² followed by diol cleavage would be superior to ozonolysis for effecting this transformation.^{8b} However, we found that oxidation of **33** using AD-mix β gave a mixture of diols **34** and **35** from which the desired enone **36** was obtained in only 57% yield. Worse yields arose from the use of AD-mix α , presumably because of a chiral mismatch.

We then examined the utility of the complexes generated by mixing OsO_4 with amines. Corey had found that enantioselective dihydroxylations could be induced with OsO_4 in the presence of chiral diamines.⁴³ Even though such a tactic would require use of stoichiometric amounts of OsO_4 , we reasoned that the increased steric bulk about osmium in these complexes would favor dihydroxylating the more accessible isopropenyl group. Although treating **33** with the complex generated from OsO_4 and TMEDA resulted in complete recovery of **33**, reaction of **33** with the complex of OsO_4 and quinuclidine provided **34** in 74% yield along with the regioisomeric diol **35** (11%). Because quinuclidine is

rather expensive, we screened several other tertiary amines and discovered that the complex generated from OsO_4 and Et_3N provided **34** (76%) together with **35** (13%). This mixture of diols was readily separated by flash chromatography to afford pure **34** that was subsequently cleaved by periodate ion to deliver Cbz-anatoxin-a **36**.⁴⁴ *N*-Deprotection of **36** by the action of TMSI at $-10\text{ }^{\circ}\text{C}$ furnished **1** in nearly quantitative yield. The free base thus obtained was then converted into its more stable hydrochloride salt to prevent light-induced decomposition.⁴⁵ The spectral and physical data obtained for synthetic **1** and its hydrochloride salt were consistent with those reported by Rapoport.^{44,46}

3. Conclusions

In summary, we have completed a concise and practical synthesis of the potent neurotoxic alkaloid (+)-anatoxin-a (**1**) in a sequence of only nine chemical operations and in 27% overall yield from commercially available **12**. The strategy featured the application of a new protocol for the diastereoselective synthesis of *cis*-2,5-disubstituted pyrrolidines bearing unsaturated side chains and an intramolecular enyne metathesis to provide the requisite azabicyclo[4.2.1]-nonane skeleton of **1**. We also developed an improvement to our method for the cyclization/reduction of keto carbamates derived from pyroglutamic acid in which catalytic amounts of $\text{B}(\text{C}_6\text{F}_5)_3$ and silanes are employed to reduce transient iminium ions. We are currently exploring the scope of this new reagent combination for the stereoselective reduction of oxonium and iminium ions. Significantly, the approach is versatile and may be applied to the facile preparation of nonlethal analogs of **1** by simply modifying the nature of the unsaturated side-chains at the 2- and 5-positions of the *cis*-pyrrolidine ring prior to metathesis. We are in the process of developing new applications of intramolecular enyne metathesis and related processes for the synthesis of alkaloid natural products, the results of which will be reported in due course.

4. Experimental

4.1. General

Solvents and reagents were reagent-grade and were used without purification, unless otherwise noted. Dichloromethane (CH_2Cl_2), *N,N,N',N'*-tetramethylethylene-diamine (TMEDA), and diisopropylamine were distilled from calcium hydride and stored under nitrogen. Boron trifluoride diethyl etherate ($\text{BF}_3\cdot\text{OEt}_2$) was distilled from calcium hydride. Tetrahydrofuran (THF) and diethyl ether (Et_2O) were passed through two columns of neutral alumina and stored under argon. Methanol (MeOH) and acetonitrile (MeCN) was passed through two columns of molecular sieves and stored under argon. Toluene were first passed through a column neutral alumina, then through a column of Q5 reactant and stored under argon. Iodotrimethylsilane (TMSI) was freshly distilled over flame-dried copper powder onto the same under argon, in the absence of light. All reactions were performed in flame-dried glassware under argon unless otherwise noted. All metatheses were performed in freshly distilled solvent, degassed with a

continuous stream of argon for a minimum of 15 min. All reaction temperatures are reported as the temperature of the surrounding bath. ^1H nuclear magnetic resonance (NMR) spectra were obtained at 500 or 400 MHz as solutions in DMSO- d_6 or CDCl_3 unless otherwise noted. ^{13}C NMR spectra were obtained at 125 MHz or 100 MHz as solutions in DMSO- d_6 or CDCl_3 unless otherwise noted. Chemical shifts are reported in parts per million (ppm, δ) and referenced to the solvent. Coupling constants are reported in Hertz (Hz). Spectral splitting patterns are designated as s: singlet, d: doublet, t: triplet, q: quartet, m: multiplet, comp m: complex multiplet, br: broad. Infrared (IR) spectra were obtained using a Perkin–Elmer FTIR 1600 spectrophotometer. IR spectra were taken neat on sodium chloride plates unless otherwise noted and reported in wave numbers (cm^{-1}). Low-resolution chemical ionization (CI) mass spectra were obtained with a Finnigan TSQ-70 instrument. High-resolution measurements were made with a VG Analytical ZAB2-E instrument. Analytical thin layer chromatography was performed using Merck 250 micron 60F-254 silica gel plates. The plates were visualized with ultraviolet (UV) light, potassium permanganate (KMnO_4), ammonium molybdate ceric ammonium nitrate (AmCAN), or ceric ammonium molybdate (CAM/Hanessians stain). Flash chromatography was performed according to the method of Still⁴⁷ using ICN Silitech 32-63 D 60A silica gel, Aldrich Activated Brockmann I, standard grade, 150 mesh. D-methylpyroglutamate (**12**) was prepared according to the procedure of Pfaltz.⁴⁸ Compound **16f** was prepared from **12** according to the method of Tamm.⁴⁹ Compound **3** was prepared from **2** according to the procedure of Konas.⁵⁰ Compounds **16a–e** were prepared from **12** using the method of Kikugawa.⁵¹ (1-Diazo-2-oxo-propyl)phosphonic acid dimethyl ester (**9**) was prepared according to the procedure of Vandewalle.⁵²

4.1.1. (2S)-But-3-enyl-(5S)-((tert-butyl)dimethylsilanoxy)methylpyrrolidine-1-carboxylic acid tert-butyl ester (4). 4-Bromo-1-butene (18 μL , 0.18 mmol) was added to a stirred mixture of magnesium turnings (26 mg, 1.1 mmol) in THF (1.1 mL) at room temperature. After 20 min, an additional portion of 4-bromo-1-butene (40 μL , 0.35 mmol) was added. The resulting solution was stirred an additional 20 min and then transferred via cannula to a stirred solution of **3** (89 mg, 0.27 mmol) in THF (1.4 mL) at -78°C . The mixture was stirred for 1 h at -78°C , and then a mixture of $\text{BF}_3\cdot\text{OEt}_2$ (0.22 mL, 1.7 mmol) and 1 M L-Selectride in THF (0.57 mL, 0.57 mmol) (mixed at room temperature) was added via syringe. The resulting solution was stirred at -78°C for 1 h, and then the solution was allowed to slowly warm to room temperature before quenching with MeOH (2.5 mL) and H_2O (3 mL). The reaction mixture was then poured into a mixture of saturated NaHCO_3 (30 mL) and Et_2O /pentane (1:1) (10 mL). The layers were separated, and the aqueous layer was extracted with Et_2O /pentane (1:1) (3 \times 15 mL), dried (Na_2SO_4), filtered, and concentrated under reduced pressure to afford a yellow oil. The crude product was purified by flash chromatography (SiO_2) eluting with Et_2O /pentane (1:5) to provide 79 mg (79%) of **4** as a clear oil. ^1H NMR (400 MHz, CDCl_3) δ 5.85–5.75 (m, 1H), 5.00 (dq, $J=17.4$, 1.7 Hz, 1H), 4.94 (app d, $J=9.9$ Hz, 1H), 3.76–3.36 (comp, 4H), 2.14–1.72 (comp, 5H), 1.68–1.52 (m, 1H), 1.44 (s, 9H),

0.87 (s, 9H), 0.03 (d, $J=3.1$ Hz, 6H); ^{13}C NMR (100 MHz, CDCl_3) δ 154.8, 138.6, 114.6, 79.5, 60.4, 57.1, 40.6, 31.6, 29.4, 26.8, 26.5, 19.2, -4.2 ; IR (neat) 3446, 2941, 1696, 1460, 1393, 1365, 1258, 1174, 1101, 837, 776; mass spectrum (CI) m/z 370.2777 [$\text{C}_{20}\text{H}_{40}\text{NO}_3\text{Si}$ (M+1) requires 370.2778], 370, 314, 298, 270 (base), 256.

4.1.2. (2S)-But-3-enyl-(5S)-hydroxymethylpyrrolidine-1-carboxylic acid tert-butyl ester (5). A 1 M solution of TBAF in THF (6.2 mL, 6.20 mmol) was added to a stirred solution of **4** (521 mg, 1.41 mmol) in THF (8 mL). The mixture was stirred for 2 h, and then poured into 10% H_3PO_4 (50 mL) and EtOAc (10 mL). The layers were separated and the aqueous phase was extracted with EtOAc (3 \times 20 mL), and the combined organic extracts were dried (Na_2SO_4), filtered, and concentrated under reduced pressure to give an orange oil that was purified by flash chromatography (SiO_2) eluting with EtOAc/hexanes (2:3) to afford 250 mg (70%) of **5** as a pale-yellow oil. ^1H NMR (500 MHz, CDCl_3) δ 5.79 (ddt, $J=17.1$, 10.2, 6.6 Hz, 1H), 5.00 (dq, $J=15.5$, 1.6 Hz, 1H), 4.94 (br dq, $J=8.4$, 1.8 Hz, 1H), 3.96–3.90 (m, 1H), 3.87–3.81 (m, 1H), 3.65 (br dd, $J=8.6$, 2.4 Hz, 1H), 3.49 (dd, $J=11.2$, 7.9 Hz, 1H), 2.11–1.93 (comp, 3H), 1.90–1.80 (m, 1H), 1.77–1.50 (comp, 3H), 1.45 (s, 9H), 1.42–1.29 (m, 1H); ^{13}C NMR (125 MHz, CDCl_3) δ 138.1, 114.8, 80.4, 68.8, 61.1, 58.8, 34.6, 30.7, 28.9, 28.5, 26.9; IR (neat) 3416, 3074, 2967, 1693, 1661, 1399, 1255, 1170, 1116, 1047, 908, 855, 775, 737 cm^{-1} ; mass spectrum (CI) m/z 256.1919 [$\text{C}_{14}\text{H}_{26}\text{NO}_3$ (M+1) requires 256.1913], 511, 411, 379, 256 (base), 224, 200, 184, 156.

4.1.3. (2S)-But-3-enyl-(5S)-formylpyrrolidine-1-carboxylic acid tert-butyl ester. TPAP (33 mg, 0.094 mmol) was added to a solution of **5** (239 mg, 0.936 mmol), NMO (165 mg, 1.40 mmol), and powdered 4 Å molecular sieves (300 mg) in CH_2Cl_2 (31 mL) at room temperature. The reaction was stirred for 2 h, and then the solvent was removed under reduced pressure to afford a black residue. The residue was suspended in Et_2O (2 mL), and filtered through a short plug of SiO_2 eluting with Et_2O /pentane (2:1) (175 mL). Removal of the solvent under reduced pressure afforded 216 mg (91%) of the aldehyde as a pale-yellow oil. ^1H NMR (500 MHz, $\text{PhMe-}d_8$, 100°C) δ 9.35 (d, $J=2.4$ Hz, 1H), 5.73 (ddt, $J=16.7$, 10.2, 6.3 Hz, 1H), 4.97 (dq, $J=17.1$, 1.7 Hz, 1H), 4.91–4.88 (m, 1H), 3.93–3.90 (m, 1H), 3.78–3.71 (m, 1H), 2.02–1.81 (comp, 3H), 1.60–1.42 (comp, 3H), 1.37 (s, 9H), 1.30–1.19 (comp, 2H); ^{13}C NMR (125 MHz, $\text{PhMe-}d_8$, 100°C) δ 199.1, 154.7, 138.6, 114.8, 80.2, 66.6, 58.8, 35.0, 30.9, 30.0, 28.6, 25.4; IR (neat) 2974, 1739, 1696, 1455, 1382, 1258, 1168, 1112, 910, 776 cm^{-1} ; mass spectrum (CI) m/z 254.1765 [$\text{C}_{14}\text{H}_{24}\text{NO}_3$ (M+1) requires 254.1756], 254, 238, 226, 224, 198 (base), 182, 180, 155, 136, 124.

4.1.4. (2S)-But-3-enyl-(5S)-ethynylpyrrolidine-1-carboxylic acid tert-butyl ester (6). A solution of the preceding aldehyde (207 mg, 0.817 mmol) in anhydrous MeOH (1 mL) was added via syringe to a solution of **9** (188 mg, 0.981 mmol) and K_2CO_3 (226 mg, 1.63 mmol) in anhydrous MeOH (6 mL) at room temperature. The reaction was stirred for 3 h, and then diluted with Et_2O (6 mL) and poured into a mixture of saturated NaHCO_3 (25 mL) and

Et₂O (5 mL). The layers were separated and the aqueous phase was extracted with Et₂O (4×15 mL), and the combined organic extracts were dried (MgSO₄), filtered, and concentrated under reduced pressure to give a pale-yellow oil that was purified by flash chromatography (SiO₂) eluting with Et₂O/pentane (1:6) to afford 155 mg (76%) of **6** as a clear oil. ¹H NMR (500 MHz, DMSO-*d*₆, 100 °C) δ 5.84 (ddt, *J*=16.8, 10.2, 6.5 Hz, 1H), 5.03 (dq, *J*=17.2, 1.7 Hz, 1H), 4.96–4.92 (m, 1H), 4.47–4.43 (m, 1H), 3.77–3.72 (m, 1H), 2.89 (d, *J*=2.1 Hz, 1H), 2.13–1.96 (comp, 4H), 1.93–1.85 (comp, 2H), 1.78–1.71 (m, 1H), 1.57–1.49 (m, 1H), 1.43 (s, 9H); ¹³C NMR (125 MHz, DMSO-*d*₆, 100 °C) δ 152.7, 137.8, 113.8, 84.9, 78.3, 71.0, 57.0, 47.7, 33.4, 31.1, 29.0, 28.9, 27.6; IR (neat) 3302, 3059, 2978, 1685, 1639, 1390, 1263, 1170, 1107, 916, 737, 650 cm⁻¹; mass spectrum (CI) *m/z* 250.1807 [C₁₅H₂₄NO₂ (M+1) requires 250.1807], 499, 444, 399, 343, 250 (base), 194.

4.1.5. 2-Vinyl-9-azabicyclo[4.2.1]non-2-ene-9-carboxylic acid tert-butyl ester (7). To a solution of **6** (18 mg, 72 μmol) in dry degassed CH₂Cl₂ (8 mL) was added **10** (7 mg, 0.008 mmol) in one portion. The mixture was stirred at room temperature for 22 h, and then DMSO (1 mL) was added to decompose the catalyst, and stirring was continued for an additional 2 h. The solvent was removed under reduced pressure, and the residue was purified by flash chromatography (SiO₂) using gradient elution Et₂O/pentane (1:5→1:3) to afford 14 mg (78%) of **7** as a pale-yellow oil. ¹H NMR (500 MHz, CDCl₃) (2 rotamers) δ 6.23 (dd, *J*=17.6, 6.6 Hz, 1H), 5.65–5.60 (m, 1H), 5.14 (t, *J*=17.1 Hz, 1H), 4.98–4.90 (comp, 1.4H), 4.80–4.77 (m, 0.6H), 4.40–4.37 (m, 0.6H), 4.28–4.24 (m, 0.4H), 2.32–2.02 (comp, 5H), 1.77–1.65 (comp, 2H), 1.62–1.51 (comp, 2H), 1.44 (s, 4H), 1.39 (s, 5H); ¹³C NMR (125 MHz, CDCl₃) (2 rotamers) δ 153.5, 153.3, 145.9, 143.8, 139.0, 138.8, 131.2, 130.8, 111.3, 110.5, 79.1, 79.0, 55.2, 54.8, 54.3, 33.9, 31.9, 31.4, 31.0, 30.4, 30.3, 29.6, 28.6, 28.5, 23.8, 23.6; IR (neat) 3437, 2978, 2252, 1683, 1420, 1405, 1367, 1250, 1170, 1116, 994, 908, 737, 652 cm⁻¹; mass spectrum (CI) *m/z* 250.1803 [C₁₅H₂₄NO₂ (M+1) requires 250.1807], 250 (base), 222, 200, 195, 152.

4.1.6. (2R)-Methoxycarbonylamino-5-oxonon-8-enoic acid methyl ester (14). 4-Bromo-1-butene (72 μL, 0.71 mmol) was added to a stirred mixture of magnesium turnings (202 mg, 8.32 mmol) in THF (8.3 mL) at room temperature. The mixture was stirred for 10 min, and an additional portion of 4-bromo-1-butene (350 μL, 3.45 mmol) was added. The resulting mixture was stirred for an additional 15 min and then transferred via syringe to a flask containing TMEDA (3.8 mL, 25 mmol). The initially cloudy suspension was stirred until all precipitate had disappeared (5 min), whereupon the solution was transferred via syringe to a solution of **13** (558 mg, 2.77 mmol) in THF (14 mL) at –78 °C. The reaction mixture was stirred for 1.5 h at –78 °C, and MeOH (5 mL) was added. The reaction mixture was then poured into a mixture of 10% H₃PO₄ (50 mL) and Et₂O (10 mL). The layers were separated, and the aqueous layer was extracted with Et₂O (3×20 mL), dried (MgSO₄), filtered, and concentrated under reduced pressure to afford a yellow oil. The crude product was purified by flash chromatography (SiO₂) eluting with EtOAc/hexanes (2:1) to provide 465 mg (65%) of **14** as a

pale-yellow oil. ¹H NMR (400 MHz, CDCl₃) δ 5.76 (ddt, *J*=16.8, 10.3, 6.5 Hz, 1H), 5.29 (br s, 1H), 5.04–4.93 (comp, 2H), 4.30 (m, 1H), 3.72 (s, 3H), 3.65 (s, 3H), 2.60–2.40 (comp, 4H), 2.34–2.25 (comp, 2H), 2.33–2.26 (m, 1H), 1.96–1.84 (m, 1H); ¹³C NMR (100 MHz, CDCl₃) δ 208.8, 172.5, 156.6, 136.8, 115.2, 53.2, 52.3, 52.2, 41.6, 38.3, 27.5, 26.0; IR (neat) 3345, 2952, 1713, 1640, 1528, 1443, 1359, 1264, 1219, 1062, 1000, 916, 781 cm⁻¹; mass spectrum (CI) *m/z* 258.1348 [C₁₂H₂₀NO₅ (M+1) requires 258.1342], 258, 240 (base), 226, 198.

4.1.7. (2R,5R)-But-3-enylpyrrolidine-1,2-dicarboxylic acid dimethyl ester (15). BF₃·OEt₂ (5.50 mL, 43.2 mmol) was added to a solution of Ph₃SiH (5.63 g, 21.6 mmol) in CH₂Cl₂ (14 mL) at room temperature. The solution was stirred for 5 min, and then transferred via cannula to a stirred solution of **14** (1.85 g, 7.21 mmol) in CH₂Cl₂ (24 mL) at –78 °C. The reaction mixture was stirred at –78 °C for 0.5 h, whereupon the cooling-bath was removed and stirring was continued at room temperature for an additional 2 h. The reaction mixture was recooled to –78 °C and poured into a mixture of sat. aqueous NaHCO₃ (40 mL) and CH₂Cl₂ (10 mL). The layers were separated, and the aqueous phase was extracted with Et₂O (3×20 mL), dried (MgSO₄), filtered, and concentrated under reduced pressure to afford a clear oil. The crude product was purified by flash chromatography (SiO₂) eluting with Et₂O/pentane (3:1) to provide 1.62 g (93%) of **15** as a clear oil (*dr*=16:1)⁵³. ¹H NMR (500 MHz, CDCl₃) (2 rotamers) δ 5.90–5.78 (m, 1H), 5.05 (app dd, *J*=17.3, 1.8 Hz, 1H), 4.96 (br d, *J*=9.8 Hz, 1H), 4.42–4.30 (m, 1H), 4.01–8.85 (m, 1H), 3.77–3.63 (comp, 6H), 2.26–2.16 (m, 1H), 2.14–1.90 (comp, 5H), 1.78–1.68 (m, 1H), 1.58–1.46 (m, 1H); ¹³C NMR (125 MHz, CDCl₃) (2 rotamers) δ 173.4, 155.6, 155.0, 138.1, 137.9, 114.7, 114.6, 60.0, 59.6, 58.8, 58.1, 52.4, 52.1, 33.5, 33.1, 30.5, 30.0, 29.3, 29.1, 28.1; IR (neat) 2955, 1754, 1704, 1450, 1385, 1202, 1175, 1112, 1000, 912, 773 cm⁻¹; mass spectrum (CI) *m/z* 242.1388 [C₁₂H₂₀NO₄ (M+1) requires 242.1392], 242 (base), 210, 186, 168.

4.1.8. (2R)-Isopropoxycarbonylamino-5-oxonon-8-enoic acid methyl ester (17e). 4-Bromo-1-butene (0.70 mL, 6.9 mmol) was added to a stirred mixture of magnesium turnings (1.3 g, 52 mmol) in THF (55 mL) at room temperature. The mixture was stirred for 10 min, and an additional portion of 4-bromo-1-butene was added (2.0 mL, 20 mmol). The resulting mixture was stirred for an additional 1 h, whereupon the solution was transferred via cannula to a solution of **16e** (2.0 g, 8.7 mmol) in THF (65 mL) at –78 °C over a 1 h period. Stirring was continued for an additional 1 h at –78 °C, whereupon a solution of sat. NH₄Cl (10 mL) was added. The reaction mixture was then poured into a mixture of brine (100 mL) and EtOAc (50 mL). The layers were separated, and the aqueous layer was extracted with EtOAc (3×50 mL), dried (MgSO₄), filtered, and concentrated under reduced pressure to afford a yellow oil. The crude product was purified by flash chromatography (SiO₂) eluting with EtOAc/hexanes (1:2) to provide 1.9 g (77%) of **17e** as a pale-yellow oil. ¹H NMR (500 MHz, CDCl₃) δ 5.83–5.75 (ddt, *J*=16.9, 10.2, 6.6 Hz, 1H), 5.22 (br d, *J*=6.6 Hz, 1H), 5.02 (ddd, *J*=17.1, 3.4, 1.6 Hz, 1H), 4.97 (ddd, *J*=10.2, 3.0, 1.4 Hz, 1H), 4.89 (hept, *J*=6.0 Hz, 1H), 4.32 (br d, *J*=5.0 Hz, 1H), 3.74 (s, 3H),

2.59–2.46 (comp, 4H), 2.35–2.30 (comp, 2H), 2.20–2.11 (m, 1H), 1.96–1.88 (m, 1H), 1.23 (d, $J=6.3$ Hz, 3H), 1.21 (d, $J=6.3$ Hz, 3H); ^{13}C NMR (125 MHz, CDCl_3); 208.7, 172.7, 155.8, 136.9, 115.3, 68.6, 53.1, 52.4, 41.8, 38.4, 27.6, 26.4, 22.1, 22.0; IR (neat) 3349, 3077, 2981, 1714, 1642, 1524, 1438, 1375, 1209, 1180, 1112, 1043 cm^{-1} ; mass spectrum (CI) m/z 286.1652 [$\text{C}_{14}\text{H}_{24}\text{NO}_5$ (M+1) requires 286.1654], 286 (base), 268, 244, 226, 200, 182, 144.

4.1.9. (2R,5R)-1-Isopropyl-2-methyl-5-(but-3-enyl)-pyrrolidine-1,2-dicarboxylate (18). A solution of $\text{BF}_3\cdot\text{OEt}_2$ (2.7 mL, 21 mmol) and Ph_3SiH (2.7 g, 11 mmol) in CH_2Cl_2 (5 mL) was added via syringe to a stirred solution of **17e** (1.0 g, 3.5 mmol) in CH_2Cl_2 (25 mL) at -78°C . The reaction mixture was stirred at -78°C for 0.5 h, whereupon the cooling-bath was removed and stirring was continued at room temperature for an additional 2 h. The reaction mixture was recooled to -78°C and poured into a mixture of sat. aqueous NaHCO_3 (20 mL) and CH_2Cl_2 (10 mL). The layers were separated, and the aqueous phase was extracted with CH_2Cl_2 (3 \times 10 mL), dried (MgSO_4), filtered, and concentrated under reduced pressure to afford a clear oil. The crude product was purified by flash chromatography (SiO_2) eluting with EtOAc /hexanes (1:4) to provide 941 mg (99%) of **18** ($dr >30:1$)⁵³ as a clear oil. ^1H NMR (500 MHz, CDCl_3) (2 rotamers) δ 5.86–5.79 (m, 1H), 5.05–5.02 (m, 1H), 5.00–4.85 (comp, 2H), 4.40–4.24 (m, 1H), 3.98–3.83 (m, 1H), 3.72 (s, 3H), 2.27–1.89 (comp, 6H), 1.79–1.72 (m, 1H), 1.59–1.44 (m, 1H), 1.27–1.12 (comp, 6H); ^{13}C NMR (125 MHz, CDCl_3) (2 rotamers) δ 173.7, 173.6, 154.8, 154.1, 138.2, 114.5, 68.7, 68.4, 59.8, 59.7, 59.4, 58.5, 57.8, 52.0, 33.7, 33.0, 30.7, 30.5, 30.1, 29.2, 28.9, 28.1, 22.3, 22.2, 22.1, 21.9; IR (neat) 2978, 2952, 1753, 1699, 1640, 1436, 1404, 1385, 1315, 1202, 1175, 1113, 998 cm^{-1} ; mass spectrum (CI) m/z 270.1709 [$\text{C}_{14}\text{H}_{24}\text{NO}_4$ (M+1) requires 270.1705], 270 (base), 228, 210, 184, 168, 128.

4.1.10. (2R)-1-tert-Butoxycarbonylamino-5-oxonon-8-enoic acid methyl ester (17f). A two-neck flask was charged with magnesium turnings (200 mg, 8.26 mmol) and THF (8 mL). To this stirred mixture was added a portion of 4-bromo-1-butene (0.10 mL, 0.99 mmol) at room temperature. After 15 min, an additional portion of 4-bromo-1-butene (0.32 mL, 3.15 mmol) was added. The resulting yellow solution was stirred for 10 min and then transferred via cannula to a stirred solution of **16f** (502 mg, 2.06 mmol) in THF (14 mL) at -78°C . The mixture was stirred for 3 h at -78°C , and then saturated NH_4Cl (5 mL) was added and the reaction mixture was poured into a mixture of H_2O (60 mL) and Et_2O (10 mL). The layers were separated, and the aqueous layer was extracted with Et_2O (3 \times 20 mL), dried (MgSO_4), filtered, and concentrated under reduced pressure to afford a yellow oil. The crude product was purified by flash chromatography (SiO_2) eluting with EtOAc /hexanes (1:2) to provide 570 mg (92%) of **17f** as a yellow oil. ^1H NMR (300 MHz, CDCl_3) δ 5.83–5.68 (m, 1H), 5.12–4.75 (comp, 3H), 4.28–4.17 (m, 1H), 3.70–3.67 (comp, 3H), 2.57–2.37 (comp, 4H), 2.31–2.24 (comp, 2H), 2.14–2.03 (m, 1H), 1.99–1.78 (m, 1H), 1.40–1.37 (comp, 9H); ^{13}C NMR (75 MHz, CDCl_3) δ 209.0, 173.1, 155.7, 137.2, 115.6, 80.2, 53.1, 52.6, 42.1, 38.7, 28.5, 27.9, 26.7; IR (neat) 3465, 3064, 2984, 1741, 1707, 1392, 1363, 1169, 733 cm^{-1} ; mass

spectrum (CI) m/z 300.1805 [$\text{C}_{15}\text{H}_{26}\text{NO}_5$ (M+1) requires 300.1811], 300, 282, 244 (base), 200, 182.

4.1.11. (2R,5R)-1-tert-Butyl-2-methyl-5-(but-3-enyl)-pyrrolidine-1,2-dicarboxylate (19). $\text{B}(\text{C}_6\text{F}_5)_3$ (8.2 mg, 0.02 mmol) was added to a solution of Ph_3SiH (92 mg, 0.35 mmol) in CH_2Cl_2 (1 mL) at room temperature. The solution was stirred for 10 min, and then added via cannula to a stirred solution of **17f** (48 mg, 0.16 mmol) in CH_2Cl_2 (0.5 mL) at -78°C . The mixture was maintained in a -78°C bath for 0.5 h, whereupon the cooling-bath was removed, and stirring was continued at room temperature for an additional 2 h. The mixture was then recooled to -78°C and an additional 1 mL of a pre-mixed solution of $\text{B}(\text{C}_6\text{F}_5)_3$ (8.2 mg, 0.02 mmol) and Ph_3SiH (92 mg, 0.35 mmol) was added via cannula. The solution was stirred at -78°C for 10 min, and then the cooling bath was removed and stirring was continued at room temperature for 11 h. Et_3N (0.1 mL) was added and stirring was continued for 20 min. The mixture was poured into a solution of 10% H_3PO_4 (20 mL) and Et_2O (5 mL). The layers were separated and the aqueous phase was extracted with Et_2O (3 \times 8 mL). The combined organic layers were dried (MgSO_4), filtered through a 2 cm plug of SiO_2 with Et_2O (40 mL), and concentrated under reduced pressure to afford a pale-yellow oil. The crude product was purified by flash chromatography (SiO_2) eluting with Et_2O /pentane (1:1) to provide 44 mg (97%) of **19** ($dr=11:1$, by ^1H NMR) as a clear oil. ^1H NMR (500 MHz, $\text{DMSO}-d_6$, 100°C) δ 5.84 (ddt, $J=17.0$, 10.2, 6.6 Hz, 1H), 4.98 (app dq, $J=17.2$, 1.7 Hz, 1H), 4.96–4.93 (m, 1H), 4.21 (t, $J=7.5$ Hz, 1H), 3.82–3.77 (m, 1H), 3.65 (s, 2.76H, major diast.), 3.64 (s, 0.24H, minor diast.) 2.20–1.83 (comp, 6H), 1.70–1.65 (m, 1H), 1.52–1.44 (m, 1H), 1.38 (s, 9H); ^{13}C NMR (125 MHz, $\text{DMSO}-d_6$, 100°C) δ 172.6, 152.7, 138.0, 113.8, 78.4, 59.1, 57.3, 50.9, 32.7, 29.4, 28.7, 27.6; IR (neat) 2974, 1754, 1697, 1390, 1172, 1115, 710, 513; mass spectrum (CI) m/z 284.1860 [$\text{C}_{15}\text{H}_{26}\text{NO}_4$ (M+1) requires 284.1862], 284 (base), 228, 184.

4.1.12. (2R,5S)-5-But-3-enyl-2-(2,2-dibromovinyl)-pyrrolidine-1-carboxylic acid isopropyl ester (20). A 1.0 M solution of DIBAL-H in toluene (1.6 mL, 1.6 mmol) was added dropwise to a solution of **18** (393 mg, 1.46 mmol) in toluene (4 mL) at -78°C . After 1 h at -78°C , an additional portion of DIBAL-H (1.6 mL, 1.6 mmol) was added, and the mixture was stirred at -78°C for 15 min. MeOH (0.5 mL) was added, and the mixture was poured into a solution of saturated Rochelle's salt (11 mL) and EtOAc (10 mL). The mixture was stirred at room temperature until the layers separated (1.5 h). The mixture was then poured into brine (20 mL), and the layers were separated. The aqueous layer was extracted with EtOAc (3 \times 15 mL), dried (Na_2SO_4), filtered, and concentrated under reduced pressure to give a yellow oil. The crude product was purified by flash chromatography (neutral Al_2O_3) eluting with EtOAc /hexanes (1:4) to provide 277 mg (79%) of the aldehyde as a pale-yellow oil that was used immediately in the next reaction.

A solution of CBr_4 (420 mg, 1.26 mmol) and PPh_3 (662 mg, 2.52 mmol) in CH_2Cl_2 (3 mL) was cooled to 0°C . After 20 min, a solution of the preceding aldehyde (151 mg, 0.631 mmol) in CH_2Cl_2 (1 mL) was added. The reaction

mixture was stirred with warming to room temperature for 29 h in the dark. The resulting slurry was concentrated in vacuo, diluted in a minimal amount of CH₂Cl₂ (1 mL), and purified by flash chromatography (neutral Al₂O₃) eluting with Et₂O/pentane (1:4) to provide 217 mg (87%) of **20** as a yellow oil. ¹H NMR (300 MHz, CDCl₃) δ 6.44–6.20 (m, 1H), 5.88–5.72 (m, 1H), 5.07–4.82 (comp, 3H), 4.52–4.31 (m, 1H), 3.96–3.76 (m, 1H), 2.25–1.29 (comp, 8H), 1.27–1.18 (comp, 6H); ¹³C NMR (75 MHz, CDCl₃) δ 143.3, 140.9, 138.3, 115.0, 83.3, 68.7, 60.6, 32.3, 30.8, 30.6, 29.4, 22.6, 22.4; mass spectrum (CI) *m/z* 396 (M+1) (base), 382, 354, 340, 294, 210.

4.1.13. (2R,5S)-5-But-3-enyl-2-trimethylsilanylethynylpyrrolidine-1-carboxylic acid isopropyl ester (21). A 2.0 M solution of *n*-BuLi (0.44 mL, 8.8 mmol) in hexanes was added to a solution of **20** (165 mg, 0.418 mmol) in THF (5 mL) at –78 °C. The mixture was stirred for 1.5 h at –78 °C, and then TMSCl (60 μL, 0.46 mmol) was added. The solution was stirred at –78 °C for 4.5 h, and then phosphate buffer (pH 7.4) (1 mL) was added and the reaction was poured into a mixture of brine (10 mL) and Et₂O (5 mL). The layers were separated, and the aqueous layer was extracted with Et₂O (3×15 mL). The combined organic extracts were dried (Na₂SO₄), filtered, and concentrated under reduced pressure to give a dark-yellow oil. The crude product was purified by flash chromatography (SiO₂) eluting with Et₂O/pentane (1:6) to provide 59 mg (46%) of **21** as a yellow oil. ¹H NMR (300 MHz, CDCl₃) δ 5.88–5.74 (m, 1H), 5.06–4.85 (comp, 3H), 4.61–4.42 (m, 1H), 3.89–3.76 (m, 1H), 2.16–1.50 (comp, 8H), 1.25–1.20 (comp, 6H), 0.13–0.09 (comp, 9H); ¹³C NMR (75 MHz, CDCl₃) δ 154.4, 138.4, 114.4, 86.1, 68.3, 57.8, 49.2, 34.1, 32.2, 30.1, 22.3, –0.01; mass spectrum (CI) *m/z* 308 (M+1) (base), 292, 266.

4.1.14. 2-(1-Trimethylsilylvinyl)-9-azabicyclo[4.2.1]non-2-ene-9-carboxylic acid isopropyl ester (22). A solution of **21** (26 mg, 0.085 mmol) in degassed PhMe (0.85 mL) was treated with one portion of solid **11** (4 mg, 4 μmol), and then the solution was sparged for an additional 10 min. The mixture was then heated to 65 °C for 14 h. After cooling to room temperature, the solution was allowed to stir for 2 h exposed to the atmosphere, and then the solvent was removed under reduced pressure to afford a crude brown oil that was purified by flash chromatography (SiO₂) using gradient elution with hexanes and then EtOAc/hexanes (1:5) to afford 24 mg (91%) of **22** as a pale-yellow oil. ¹H NMR (300 MHz, CDCl₃) δ 5.60–5.31 (comp, 2H), 4.97–4.84 (m, 1H), 4.62–4.38 (br m, 1H), 3.92–3.72 (br m, 1H), 2.68–2.45 (m, 1H), 2.34–2.13 (m, 1H), 2.12–1.75 (comp, 4H), 1.66–1.59 (dd, *J*=6.3, 2.1 Hz, 3H), 1.26–1.19 (app dd, *J*=6.4, 3.6 Hz, 9H); ¹³C NMR (75 MHz, CDCl₃) δ 154.8, 154.4, 148.2, 127.6, 126.5, 68.2, 57.3, 49.5, 36.4, 31.3, 29.7, 22.3, 22.2, 18.0, –0.1; mass spectrum (CI) *m/z* 308 (M+1), 292, 264 (base), 238, 179.

4.1.15. (2R,5S)-5-But-3-enyl-2-(triisopropylsilyl-ethynyl)pyrrolidine-1-carboxylic acid isopropyl ester (25). A 2.2 M solution of *n*-BuLi in hexanes (0.83 mL, 1.8 mmol) was added to a solution of 2,2,6,6-tetramethylpiperidine (0.34 mL, 2.0 mmol) in THF (3.4 mL) at 0 °C. The resulting light yellow solution was stirred at 0 °C for

5 min, then transferred dropwise via cannula to a solution of **18** (201 mg, 0.746 mmol) and dibromomethane (0.13 mL, 1.9 mmol) in THF (3.3 mL) at –78 °C. The reaction mixture was stirred at –78 °C for 3 h, whereupon 10% citric acid (1 mL) was added. The reaction was immediately poured into H₂O (15 mL) and Et₂O (5 mL). The layers were separated, and the aqueous layer was extracted with Et₂O (3×10 mL). The combined organic layers were dried (MgSO₄), filtered, and concentrated under reduced pressure to give a crude yellow oil that was purified by flash chromatography (SiO₂) eluting with Et₂O/hexanes (1:3) to afford 220 mg (72%) of **24** as an unstable pale-yellow oil. A portion of the product was immediately dissolved in THF under Ar to avoid decomposition and used in the next reaction.

A solution of 2.2 M *n*-BuLi in hexanes (136 μL, 0.294 mmol) was added to solution of 1,1,1,3,3,3-hexamethyldisilazane (68 μL, 0.321 mmol) in THF (1.6 mL) at 0 °C. The resulting yellow LiHMDS solution was stirred for 10 min at 0 °C, and then transferred via cannula to a solution of **24** (110 mg, 0.268 mmol) in THF (1.4 mL) at –78 °C. The reaction mixture was stirred at –78 °C for 10 min, whereupon a solution of 1.6 M *t*-BuLi in pentane (0.36 mL, 0.56 mmol) was added. The resulting yellow solution was stirred at –78 °C for 1 h, and then freshly distilled TIPSOTf (0.16 mL, 0.59 mmol) was added. After stirring for an additional 10 min, the reaction mixture was diluted with pentane (5 mL) and quenched with saturated NaHCO₃ (1 mL) at –78 °C. After warming to ambient temperature, the reaction mixture was poured into H₂O (15 mL) and Et₂O (5 mL). The layers were separated, and the aqueous layer was extracted with Et₂O (3×15 mL). The combined organic extracts were dried (MgSO₄), filtered, and concentrated under reduced pressure to give a yellow oil that was purified by flash chromatography (SiO₂) eluting with Et₂O/pentane (1:6) to afford 26 mg (24%) of **25** as a pale-yellow oil. ¹H NMR (500 MHz, PhMe-*d*₈, 100 °C) δ 5.87–5.79 (m, 1H), 5.05–4.89 (comp, 3H), 4.68–4.66 (m, 1H), 3.80–3.78 (m, 1H), 2.19–2.01 (comp, 2H), 1.79–1.60 (comp, 4H), 1.37–1.25 (comp, 2H), 1.22–1.05 (comp, 27H); ¹³C NMR (125 MHz, PhMe-*d*₈, 100 °C) δ 154.5, 139.2, 114.4, 89.2, 68.0, 58.4, 49.4, 35.5, 34.0, 33.7, 30.9, 30.8, 22.5, 20.9, 20.7, 20.6, 20.4, 20.2, 20.1, 19.9, 18.1, 17.7, 12.6; IR (neat) 3058, 2944, 2865, 2262, 1688, 1262, 739 cm⁻¹; mass spectrum (CI) *m/z* 408.2935 [C₂₃H₄₁NO₃Si (M+1) requires 408.2934], 408 (base), 366, 279.

4.1.16. 2-(1-Triisopropylsilyloxyvinyl)-9-azabicyclo[4.2.1]non-2-ene-9-carboxylic acid isopropyl ester (26). A screw-capped vial containing **25** (20 mg, 0.049 mmol) and **11** (8 mg, 10 μmol) in PhMe was sparged with ethylene for 10 min. The vial was then heated with stirring under an atmosphere of ethylene (balloon) at 70 °C for 5 h. The mixture was cooled to room temperature, and then DMSO (1 mL) was added. The solution was stirred for 16 h at room temperature, and then concentrated under reduced pressure. The remaining residue was purified by flash chromatography (neutral Al₂O₃) eluting with Et₂O/pentane (1:3) to afford 11 mg (55%) of **26** as a pale-yellow oil. ¹H NMR (500 MHz, PhMe-*d*₈, 2 rotamers) δ 6.37–6.29 (dt, *J*=16.3, 6.0 Hz, 1H), 5.16–5.15 (d, *J*=8.0 Hz, 0.3H), 5.08–4.98 (m, 1H), 4.90–4.88 (d, *J*=7.6 Hz, 0.7H), 4.66 (s, 0.3H),

4.52–4.46 (comp, 1.3H), 4.36 (s, 0.3H), 4.27–4.22 (comp, 1.2H), 2.27–2.12 (comp, 1.3H), 2.11–1.69 (comp, 4H), 1.69–1.62 (m, 1H), 1.42–1.04 (comp, 29H); ^{13}C NMR (125 MHz, PhMe- d_8) δ 156.9, 153.5, 144.2, 127.2, 126.4, 91.0, 89.8, 67.8, 67.5, 57.3, 56.4, 55.7, 55.1, 34.0, 32.5, 32.3, 31.3, 31.1, 29.8, 23.8, 23.6, 22.4, 22.3, 18.4, 13.3; mass spectrum (CI) m/z 408.2933 [$\text{C}_{23}\text{H}_{41}\text{NO}_3\text{Si}$ (M+1) requires 408.2934], 448, 436, 408 (base), 394, 364, 348, 322.

4.1.17. (2R)-Benzyloxycarbonylamino-5-oxonon-8-enoic acid methyl ester (17c). 4-Bromo-1-butene (1.0 mL, 9.9 mmol) was added to a stirred mixture of magnesium turnings (3.8 g, 160 mmol) in THF (160 mL) at room temperature. The mixture was stirred for 20 min, and an additional portion of 4-bromo-1-butene (7.0 mL, 69 mmol) was added. The resulting mixture was stirred for an additional 30 min, and transferred via cannula to a flask containing TMEDA (24 mL, 160 mmol). The initially cloudy suspension was stirred until all precipitate had disappeared (5 min), whereupon the solution was transferred via cannula to a solution of **16c** (14.6 g, 52.7 mmol) in THF (260 mL) at -78°C . The mixture was stirred for 1.5 h at -78°C , and *i*-PrOH (35 mL) was added, and the reaction mixture was warmed to room temperature before pouring into a mixture of 10% H_3PO_4 (300 mL) and Et_2O (100 mL). The layers were separated, and the aqueous layer was extracted with Et_2O (2 \times 100 mL), dried (MgSO_4), filtered, and concentrated under reduced pressure to afford a yellow oil. The crude product was purified by flash chromatography (SiO_2) eluting with Et_2O /pentane (2:1) to provide 11.9 g (73%) of **17c** as a pale-yellow oil. ^1H NMR (500 MHz, DMSO- d_6) δ 7.69 (br d, $J=7.9$ Hz, 0.9H), 7.38–7.24 (comp, 5H), 5.76 (ddt, $J=16.8$, 10.3, 6.5 Hz, 1H), 5.02 (s, 2H), 4.97 (app dq, $J=17.2$, 1.8 Hz, 1H), 4.94–4.90 (m, 1H), 4.01 (m, 1H), 3.62 (s, 2.6H), 3.55 (s, 0.4H), 2.56–2.43 (comp, 4H), 2.20–2.15 (comp, 2H), 1.95–1.88 (m, 1H), 1.76–1.68 (m, 1H); ^{13}C NMR (125 MHz, DMSO- d_6) δ 208.7, 172.5, 156.0, 137.5, 136.9, 128.3, 127.8, 127.7, 115.0, 65.5, 53.1, 51.8, 40.8, 37.9, 27.2, 24.7; IR (neat) 3342, 2954, 2258, 1712, 1518, 1050, 913, 736 cm^{-1} ; mass spectrum (CI) m/z 334.1642 [$\text{C}_{18}\text{H}_{24}\text{NO}_5$ (M+1) requires 334.1655], 334, 316, 290 (base), 272, 182, 119.

4.1.18. (2R,5R)-But-3-enylpyrrolidine-1,2-dicarboxylic acid 1-benzyl ester 2-methyl ester (27). $\text{BF}_3\cdot\text{OEt}_2$ (15.2 mL, 120 mmol) was added to a solution of Ph_3SiH (15.7 g, 60.1 mmol) in CH_2Cl_2 (40 mL) at room temperature. The solution was stirred for 10 min, and then added via cannula to a stirred solution of **17c** (10.0 g, 30.0 mmol) in CH_2Cl_2 (100 mL) at -78°C . The reaction mixture was kept with stirring at -78°C for 0.5 h, whereupon the cooling-bath was removed and stirring was continued at room temperature for an additional 2 h. The reaction mixture was then recooled to -78°C and poured into a solution of sat. aqueous NaHCO_3 (350 mL). The layers were separated and the aqueous phase was extracted with Et_2O (3 \times 75 mL), dried (MgSO_4), filtered, and concentrated under reduced pressure to afford a pale-yellow oil. The crude product was purified by flash chromatography (SiO_2) eluting with Et_2O /pentane (1:1) to provide 9.37 g (98%) of **27** ($dr=11:1$, by ^1H NMR) as a clear oil. ^1H NMR (500 MHz, DMSO- d_6 , 100°C) δ 7.38–7.27 (comp, 5H), 5.81 (ddt, $J=16.9$, 10.3,

6.5 Hz, 1H), 5.15–4.98 (comp, 3H), 4.94–4.91 (m, 1H), 4.36–4.33 (m, 1H), 3.93–3.87 (m, 1H), 3.61 (s, 2.75H, major diast.), 3.57 (s, 0.25H, minor diast.), 2.24–2.17 (m, 1H), 2.14–1.86 (comp, 5H), 1.74–1.66 (m, 1H), 1.56–1.47 (m, 1H); ^{13}C NMR (125 MHz, DMSO- d_6 , 100°C) δ 172.2, 153.4, 137.8, 136.3, 127.6, 127.1, 126.7, 113.8, 65.6, 59.1, 57.8, 51.0, 32.6, 29.2, 28.8, 27.6; IR (neat) 2954, 1752, 1707, 1410, 1204, 1176, 1107, 1005, 913, 748, 696 cm^{-1} ; mass spectrum (CI) m/z 318.1695 [$\text{C}_{18}\text{H}_{24}\text{NO}_4$ (M+1) requires 318.1705], 318 (base), 274, 182.

4.1.19. (2R,5R)-But-3-enyl-2-ethynylpyrrolidine-1-carboxylic acid benzyl ester (28). A solution of 1.0 M DIBAL-H in PhMe (7.4 mL) was added to a solution of **27** (1.4 g, 4.4 mmol) in PhMe (22 mL) at -78°C . The resulting solution was stirred at -78°C for 3 h, whereupon *i*-PrOH (22 mL) was slowly added via cannula. The cooling bath was removed, and the reaction mixture was warmed to room temperature. To the resulting cloudy-white solution was added solid Cs_2CO_3 (8.6 g, 26 mmol) in one portion. After approximately 1 min, a solution of **9** (1.7 g, 8.8 mmol) in *i*-PrOH (13 mL) was added via cannula. The resulting yellow solution was stirred at room temperature for 17 h, whereupon a mixture of sat. aqueous Rochelle's salt solution (50 mL) and EtOAc (30 mL) were added. The reaction mixture was vigorously stirred for 2 h, and then poured into H_2O (50 mL). The resulting layers were separated, and the aqueous layer was extracted with Et_2O (3 \times 30 mL), dried (MgSO_4), filtered, and concentrated under reduced pressure to afford a yellow oil. The crude product was purified by flash chromatography (SiO_2) eluting with Et_2O /pentane (1:2) to provide 826 mg (67%) of **28** as a pale-yellow oil, and 74 mg (6%) of the corresponding *trans*-product. ^1H NMR (500 MHz, DMSO- d_6 , 100°C) δ 7.40–7.27 (comp, 5H), 5.80 (ddt, $J=17.0$, 10.2, 6.5 Hz, 1H), 5.11 (s, 2H), 5.01 (app dq, $J=17.2$, 1.7 Hz, 1H), 4.95–4.91 (m, 1H), 4.58–4.55 (m, 1H), 3.88–3.81 (m, 1H), 2.95 (app d, $J=2.2$ Hz, 1H), 2.17–1.87 (comp, 6H), 1.82–1.75 (m, 1H), 1.60–1.51 (m, 1H); ^{13}C NMR (125 MHz, DMSO- d_6 , 100°C) δ 153.3, 137.6, 136.5, 127.7, 127.0, 126.7, 113.9, 84.5, 71.6, 65.6, 57.4, 48.0, 33.2, 31.2, 28.9; IR (neat) 3307, 2955, 2355, 2250, 1696, 1408, 1355, 1185, 1102 cm^{-1} ; mass spectrum (CI) m/z 284.1639 [$\text{C}_{18}\text{H}_{22}\text{NO}_2$ (M+1) requires 284.1651], 284 (base), 240.

4.1.20. (2R)-But-3-enyl-(5R)-2-(1-methylsiletan-1-ylethynyl)pyrrolidine-1-carboxylic acid benzyl ester (29). A solution of **28** (302 mg, 1.07 mmol) in THF (11 mL) was added via cannula to a solution of KHMDS (4.3 mL, 2.1 mmol, 0.5 M in PhMe) in THF (4.3 mL) at -78°C . The mixture was stirred at -78°C for 10 min, and then 1-chloro-1-methylsilylaclobutane (0.52 mL, 514 mg, 4.3 mmol) was added via syringe. Stirring was continued at -78°C for 5 h, whereupon the reaction was poured into a mixture of 1 N HCl (40 mL) and Et_2O (10 mL). The resulting layers were separated, and the aqueous phase was extracted with Et_2O (2 \times 15 mL). The combined organic layers were dried (MgSO_4), filtered, and concentrated under reduced pressure to provide a crude oil that was purified by flash chromatography (SiO_2) eluting with Et_2O /pentane (1:3) to afford 309 mg (79%) of **29** as a colorless oil along with 15% recovered **28**. ^1H NMR (400 MHz, CDCl_3) δ 7.42–7.25 (comp, 5H), 5.80 (br s, 1H), 5.27–4.88 (comp,

4H), 4.64 (br s, 1H), 3.96–3.80 (m, 1H), 2.18–1.80 (comp, 9H), 1.68–1.56 (m, 1H), 1.24–1.10 (comp, 2H), 1.07–0.96 (comp, 2H), 0.38 (s, 3H); ^{13}C NMR (125 MHz, CDCl_3) δ 153.3, 138.2, 136.9, 128.4, 127.8, 127.7, 127.5, 114.6, 85.1, 76.1, 66.8, 58.3, 49.4, 32.3, 30.3, 30.1, 29.7, 18.3, 15.3, –0.2.; IR (neat) 3067, 3034, 2931, 2711, 1705, 1641, 1496, 1449, 1406, 1355, 1308, 1252, 1184, 1107, 996, 911, 872 cm^{-1} ; mass spectrum (CI) m/z 368.2053 [$\text{C}_{22}\text{H}_{30}\text{NO}_2$ (M+1) requires 368.2046], 368 (base), 324, 284.

4.1.21. (2R)-But-3-enyl-(5R)-prop-1-ynylpyrrolidine-1-carboxylic acid benzyl ester (32). A solution of **28** (765 mg, 2.69 mmol) in THF (13 mL) was added to a solution of 1.0 M NaHMDS in THF (8.0 mL, 8.0 mmol) at -78°C . The resulting solution was stirred for 5 min at -78°C , and then MeOTf (1.53 mL, 13.5 mmol) was added. After stirring for 2 h at -78°C , the reaction mixture was poured into a mixture of sat. aqueous NaHCO_3 (90 mL) and Et_2O (20 mL), and the layers were separated. The aqueous phase was extracted with Et_2O (3 \times 50 mL) and the combined organic extracts were washed with 1 N HCl (2 \times 70 mL), dried (MgSO_4), filtered, and concentrated under reduced pressure to provide a pale-yellow oil that was purified by flash chromatography (SiO_2) eluting with Et_2O /pentane (1:2) to afford 781 mg (97%) of **32** as a pale-yellow oil. ^1H NMR (500 MHz, $\text{DMSO}-d_6$, 100°C) δ 7.39–7.33 (comp, 4H), 7.32–7.27 (m, 1H), 5.80 (ddt, $J=16.9$, 10.2, 6.5 Hz, 1H), 5.10 (dd, $J=24.0$, 12.9 Hz, 1H), 5.03–4.98 (m, 1H), 4.94–4.90 (m, 1H), 4.55–4.51 (m, 1H), 3.85–3.79 (m, 1H), 2.15–1.96 (comp, 4H), 1.95–1.84 (comp, 2H), 1.82–1.72 (comp, 4H), 1.58–1.51 (m, 1H); ^{13}C NMR (125 MHz, $\text{DMSO}-d_6$, 100°C) δ 153.3, 137.7, 136.6, 127.6, 127.0, 126.7, 113.8, 79.8, 77.2, 65.4, 57.3, 48.3, 33.3, 31.5, 29.0, 28.9, 2.3; IR (neat) 2955, 1702, 1402, 1343, 1208, 1097 cm^{-1} ; mass spectrum (CI) m/z 298.1800 [$\text{C}_{19}\text{H}_{24}\text{NO}_2$ (M+1) requires 298.1807], 298 (base).

4.1.22. (+)-(1R)-2-Isopropenyl-9-benzyloxycarbonyl-9-azabicyclo[4.2.1]-2-nonene (33). To a degassed solution of **32** (212 mg, 0.250 mmol) in CH_2Cl_2 (500 mL) was added a solution **11** (744 mg, 2.50 mmol) in degassed CH_2Cl_2 (30 mL). The mixture was stirred under a blanket of argon for 16 h, and then DMSO (0.89 mL) was added to decompose the catalyst. The mixture was stirred for an additional 23 h, whereupon the solvent was removed under reduced pressure and the resulting residue was purified by flash chromatography (SiO_2) eluting with Et_2O /pentane (1:2) to afford 623 mg (84%) of **33** as a yellow oil. ^1H NMR (500 MHz, $\text{DMSO}-d_6$, 100°C) δ 7.36–7.25 (comp, 5H), 5.74–5.71 (m, 1H), 5.10–4.96 (comp, 3H), 4.91–4.84 (comp, 2H), 4.39–4.34 (m, 1H), 2.29–2.16 (comp, 3H), 2.13–1.97 (comp, 2H), 1.82 (s, 3H), 1.77–1.68 (comp, 2H), 1.64–1.57 (m, 1H); ^{13}C NMR (125 MHz, $\text{DMSO}-d_6$, 100°C) δ 152.3, 146.3, 142.4, 136.8, 127.6, 127.0, 126.7, 125.2, 110.5, 65.2, 56.5, 54.7, 31.8, 30.6, 29.2, 22.7, 20.7; IR (neat) 2931, 1701, 1421, 1330, 1107, 1005 cm^{-1} ; mass spectrum (CI) m/z 298.1799 [$\text{C}_{19}\text{H}_{24}\text{NO}_2$ (M+1) requires 298.1807], 298 (base), 254.

4.1.23. (+)-(1R)-2-(1,2-Dihydroxy-1-methylethyl)-9-benzyloxycarbonyl-9-azabicyclo[4.2.1]-2-nonene (34). Et_3N (74 μL , 0.53 mmol) was added to a solution of OsO_4 (108 mg, 0.424 mmol) in THF (2.1 mL) at room tempera-

ture. The resulting brown solution was stirred for 5 min and then cooled to -78°C . To this mixture was added a solution **33** (87 mg, 0.29 mmol) in THF (2 mL). The resulting mixture was allowed to warm slowly to room temperature over 2 h, and stirring was continued for 20 h at room temperature. A solution of sat. aqueous NaHSO_3 (5 mL) was added, and the mixture was heated to reflux for 2.5 h. The resulting black mixture was cooled to room temperature, diluted with EtOAc (10 mL), and then filtered through a plug of SiO_2 , eluting with EtOAc . The filtrate was concentrated under reduced pressure to provide a crude oil that was purified by flash chromatography (SiO_2) eluting with EtOAc /hexanes (3:1) to afford 89 mg (76%) of **34** as a pale-yellow oil and 15 mg (13%) of the undesired cyclic diol **35** (mp $94\text{--}95^\circ\text{C}$). ^1H NMR (**34**) (500 MHz, $\text{DMSO}-d_6$, 100°C) δ 7.36–7.27 (comp, 5H), 5.64–5.61 (m, 1H), 5.06 (app q, $J=12.6$ Hz, 2H), 4.68–4.66 (m, 1H), 4.41–4.37 (m, 1H), 4.02–3.93 (comp, 2H), 3.39–3.25 (comp, 2H), 2.28–2.12 (comp, 3H), 2.03–1.95 (m, 1H), 1.86–1.80 (comp, 2H), 1.73–1.67 (m, 1H), 1.61–1.55 (m, 1H), 1.26–1.15 (comp, 3H); ^{13}C NMR (100 MHz, CDCl_3) δ 152.2, 151.4, 136.7, 127.7, 127.1, 127.0, 122.1, 73.9, 68.0, 65.3, 55.5, 54.9, 31.1, 28.0, 24.2, 22.6; IR (neat) 3401, 2931, 1672, 1426, 1326, 1114, 914, 732 cm^{-1} ; mass spectrum (CI) m/z 332.1854 [$\text{C}_{19}\text{H}_{26}\text{NO}_4$ (M+1) requires 332.1862], 332, 314 (base).

4.1.24. (+)-(1R)-2-Acetyl-9-benzyloxycarbonyl-9-azabicyclo[4.2.1]-2-nonene (36). Solid NaIO_4 (140 mg, 0.655 mmol) was added to a solution of **34** (70 mg, 0.21 mmol) in 50% aqueous THF (4 mL) at room temperature. The reaction mixture was stirred for 1.5 h, and then diluted with H_2O (2 mL). The solution was poured into a mixture of H_2O (15 mL) and Et_2O (5 mL), and the layers were separated. The aqueous phase was extracted with Et_2O (3 \times 10 mL). The combined organic layers were dried (MgSO_4), filtered, and concentrated under reduced pressure to afford a pale-yellow oil. The crude product was purified by flash chromatography (SiO_2) eluting with Et_2O /pentane (8:1) to afford 60 mg (95%) of **36** as a pale-yellow oil. All data in accordance with the literature.⁴⁴ $[\alpha]_D^{26} -36.1$ (c 1.42, CH_3OH) (lit.⁴⁴ $[\alpha]_D^{22} -37.5$ (c 1.12, CH_3OH)). ^1H NMR (400 MHz, CDCl_3) δ 7.38–7.22 (comp, 5H), 6.83–6.75 (m, 1H), 5.27 (d, $J=8.9$ Hz, 1H), 5.16–4.98 (comp, 2H), 4.52–4.38 (m, 1H), 2.47–2.00 (comp, 8H), 1.74–1.61 (comp, 3H); ^{13}C NMR (100 MHz, CDCl_3) δ 197.8, 153.4, 149.3, 142.3, 136.8, 128.4, 127.9, 127.7, 66.3, 56.0, 53.0, 31.6, 30.4, 28.5, 25.3, 24.1; IR (neat) 3538, 2951, 1700, 1665, 1418, 1106 cm^{-1} ; mass spectrum (CI) m/z 300.1587 [$\text{C}_{18}\text{H}_{22}\text{NO}_3$ (M+1) requires 300.1600], 300 (base), 256, 192.

4.1.25. (+)-(1R)-2-Acetyl-9-azabicyclo[4.2.1]-2-nonene (1). Freshly distilled TMSI (122 μL , 0.856 mmol) was added to a solution of **36** (122 mg, 0.408 mmol) in MeCN (1.4 mL) at -10°C . The resulting solution was stirred for 20 min in the absence of light. A solution of 1.25 M methanolic HCl (1 mL) was added and the resulting solution was maintained in the dark while warming to room temperature. The solution was concentrated under reduced pressure, and the resulting solid was dissolved in H_2O (10 mL). The aqueous solution was extracted with CH_2Cl_2 (2 \times 4 mL). The aqueous phase was then basified to pH=12

with NH_4OH and extracted first with CH_2Cl_2 (2×4 mL) and then with 3:1 $\text{CH}_2\text{Cl}_2/i\text{-PrOH}$ (2×5 mL). The combined organics were rapidly dried (MgSO_4), filtered, and concentrated under reduced pressure to afford a pale-yellow oil. The light sensitive free-base was dried at 0.1 mm Hg for 1 h to afford 67 mg (99%) of **1** as a pale-yellow oil. The ^1H and ^{13}C NMR data were consistent with those reported in the literature.^{44,46} ^1H NMR (400 MHz, CDCl_3) δ 6.89–6.84 (m, 1H), 4.66 (app d, $J=8.9$ Hz, 1H), 3.82–3.75 (m, 1H), 3.13 (br s, 1H), 2.52–2.34 (comp, 2H), 2.25 (s, 3H), 2.21–2.09 (m, 1H), 2.01–1.92 (m, 1H), 1.82–1.57 (comp, 4H); ^{13}C NMR (100 MHz, CDCl_3) δ 198.9, 152.4, 143.6, 58.1, 54.3, 33.5, 33.1, 30.5, 25.8, 25.2; IR (neat) 3392, 2933, 1663, 1433, 1397, 1361, 1258, 1228, 847 cm^{-1} ; mass spectrum (CI) m/z 166.1234 [$\text{C}_{10}\text{H}_{16}\text{NO}$ (M+1) requires 166.1232], 166 (base), 149.

4.1.26. (+)-(1R)-2-Acetyl-9-azabicyclo[4.2.1]-2-nonene hydrochloride (1·HCl). A solution of 1.25 M HCl in MeOH (1 mL) was added to a solution of **1** (48 mg, 0.16 mmol) in dry MeOH (1 mL) at 0 °C. The solvent was removed under reduced pressure, and the crude oil was dried under vacuum (0.3 mm Hg) for 15 h. The resulting off-white foam was azeotropically dried with PhH (2×0.3 mL) and then under vacuum (0.3 mm Hg) for 2 h. The resulting foam was dissolved in a solution of 6% MeOH/ Et_2O (2 mL), at 50 °C. The solution was cooled to room temperature and placed in a 4 °C refrigerator for 5 d. The resulting colorless prisms were collected by vacuum filtration, rinsing with cold Et_2O (5 mL), and dried at 0.3 mm Hg for 2 d to afford 32 mg (100%) of **1·HCl**. All spectra in accordance with the literature.⁴⁶ $[\alpha]_D^{27} +37.3$ (c 2.08, abs. EtOH) [(lit.⁴⁶ $[\alpha]_D^{24} +43.2$ (c 0.676, abs. EtOH), (lit.⁵⁴ $[\alpha]_D^{24} +36$ (c 0.85, EtOH)]; mp 151–153 °C (lit.⁴⁶ mp 152–153 °C). ^1H NMR (500 MHz, CDCl_3) δ 10.02 (br s, 1H), 9.42 (br s,), 7.11 (dd, $J=8.2, 3.4$ Hz, 1H), 5.23–5.19 (m, 1H), 4.37–4.29 (m, 1H), 2.65–2.58 (m, 1H), 2.56–2.47 (comp, 2H), 2.42–2.30 (comp, 5H), 1.94–1.78 (comp, 3H); ^{13}C NMR (125 MHz, CDCl_3) δ 196.4, 145.4, 143.9, 58.3, 52.1, 30.2, 27.7, 27.5, 25.2, 23.6; IR (neat) 3417, 2924, 1661, 1471, 1432, 1403, 1364, 1269, 1230, 911, 743 cm^{-1} ; mass spectrum (CI) m/z 200.0835 [$\text{C}_{10}\text{H}_{15}\text{NOCl}$ (M–1) requires 200.0842], 216, 202, 200 (base), 179.

Acknowledgements

We thank the National Institutes of Health, the Robert A. Welch Foundation, Pfizer, Inc., Merck Research Laboratories, and the Alexander von Humboldt Stiftung for their generous support of this research. R. M. gratefully acknowledges a Feodor-Lynen postdoctoral fellowship from the Alexander von Humboldt Foundation. We additionally thank Mr. Alexander Rudolph and Dr. Christopher Straub for helpful discussions. We are also grateful to Dr. Richard Fisher (Materia, Inc.) for catalyst support and helpful discussions.

References and notes

- (a) Grubbs, R. H.; Fu, G. C. *J. Am. Chem. Soc.* **1992**, *114*, 5426–5427. (b) Grubbs, R. H.; Fu, G. C. *J. Am. Chem. Soc.* **1992**, *114*, 7324–7325.
- For a review, see: Martin, S. F. *Handbook of Metathesis*; Grubbs, R. H., Ed.; Wiley–VCH: New York, 2003; Vol. 2, pp 338–352.
- For a recent review of applications of RCM to the synthesis of oxygen and nitrogen heterocycles, see: Deiters, A.; Martin, S. F. *Chem. Rev.* **2004**, *104*, 2199–2238.
- (a) Martin, S. F.; Liao, Y.; Chen, H.-J.; Paetzel, M.; Ramser, M. N. *Tetrahedron Lett.* **1994**, *35*, 6005–6008. (b) Martin, S. F.; Chen, H.-J.; Courtney, A. K.; Liao, Y.; Patzel, M.; Ramser, M. N.; Wagman, A. S. *Tetrahedron* **1996**, *52*, 7251–7264.
- Deiters, A.; Martin, S. F. *Org. Lett.* **2002**, *4*, 3243–3245.
- (a) Martin, S. F.; Liao, Y.; Wong, Y.-L.; Rein, T. *Tetrahedron Lett.* **1994**, *35*, 691–694. (b) Martin, S. F.; Humphrey, J. M.; Ali, A.; Hillier, M. C. *J. Am. Chem. Soc.* **1999**, *121*, 866–867. (c) Martin, S. F.; Humphrey, J. M.; Liao, Y.; Ali, A.; Rein, T.; Wong, Y.-L.; Chen, H.-J.; Courtney, A. K. *J. Am. Chem. Soc.* **2002**, *124*, 8584–8592.
- (a) Martin, S. F.; Wagman, A. S. *Tetrahedron Lett.* **1995**, *36*, 1169–1170. (b) Martin, S. F.; Fellows, I. M.; Kaelin, D. E., Jr. *J. Am. Chem. Soc.* **2000**, *10781*, 10787.
- (a) Martin, S. F.; Neipp, C. E. *Tetrahedron Lett.* **2002**, *43*, 1779–1782. (b) Martin, S. F.; Neipp, C. E. *J. Org. Chem.* **2003**, *68*, 8867–8878.
- Washburn, D. G.; Heidebrecht, R. W., Jr.; Martin, S. F. *Org. Lett.* **2003**, *5*, 3523–3525.
- Devlin, J. P.; Edwards, O. E.; Gorham, P. R.; Hunter, N. R.; Pike, R. K.; Stavric, B. *Can. J. Chem.* **1977**, *55*, 1367–1371.
- (a) Carmichael, W. W.; Biggs, D. F.; Gorham, P. R. *Science* **1975**, *187*, 542–544. (b) Spivak, C. E.; Witkop, B.; Albuquerque, E. X. *Mol. Pharmacol.* **1980**, *18*, 384–394.
- For a review of earlier syntheses of **1** see: (a) Mansell, H. L. *Tetrahedron* **1996**, *52*, 6025–6061. For recent syntheses of **1**, see: (b) Oh, C.-Y.; Kim, K.-S.; Ham, W.-H. *Tetrahedron Lett.* **1998**, *39*, 2133–2136. (c) Trost, B. M.; Oslob, J. D. *J. Am. Chem. Soc.* **1999**, *121*, 3057–3064. (d) Aggarwal, V. K.; Humphries, P. S.; Fenwick, A. *Angew. Chem., Int. Ed.* **1999**, *38*, 1985–1986. (e) Parsons, P. J.; Camp, N. P.; Edwards, N.; Sumoreah, L. R. *Tetrahedron* **2000**, *56*, 309–315. (f) Wegge, T.; Schwarz, S.; Seitz, G. *Tetrahedron: Asymmetry* **2000**, *11*, 1405–1410. See also Refs. 14,15.
- (a) Williams, M.; Arneric, S. P. *Exp. Opin. Invest. Drugs* **1996**, *5*, 1035–1045. (b) Arneric, S. P.; Holladay, M. W.; Sullivan, J. P. *Exp. Opin. Invest. Drugs* **1996**, *5*, 79–100. (c) Sutherland, A.; Gallagher, T.; Sharples, C. G. V.; Wonnacott, S. *J. Org. Chem.* **2003**, *68*, 2475–2478.
- For a preliminary account of some of this work, see: Brenneman, J. B.; Martin, S. F. *Org. Lett.* **2004**, *6*, 1329–1331.
- Subsequent to publication of our synthesis of **1** (Ref. 14), another synthesis has been published in which an enyne RCM was used to construct the bicyclic ring system. See: Mori, M.; Tomita, T.; Kita, Y.; Kitamura, T. *Tetrahedron Lett.* **2004**, *45*, 4397–4399.
- The synthesis of the closely related alkaloid (–)-ferruginine using an enyne RCM to construct the requisite azabicyclo[3.2.1]octane skeleton was recently reported. See: Aggarwal, V. K.; Astle, C. J.; Rogers-Evans, M. *Org. Lett.* **2004**, *6*, 1469–1471.
- (a) Celimene, C.; Dhimane, H.; Le Bail, M.; Lhommet, G. *Tetrahedron Lett.* **1994**, *35*, 6105–6106. (b) Chiesa, M. V.;

- Mazoni, L.; Scolastico, C. *Synlett* **1996**, 441–443. (c) Bubnov, Y. N.; Klimkina, E. V.; Lavrinovich, L. I.; Zykov, A. Y.; Ignatenko, A. V. *Russ. Chem. Bull.* **1999**, 48, 1696–1706. (d) Hong, S.; Marks, T. J. *J. Am. Chem. Soc.* **2002**, 124, 7886–7887.
18. Other Lewis acids screened: Ti(OiPr)₄, TiCl₄, Et₂AlCl, Bu₂BOTf, B(OiPr)₃, LiBr, Sm(OTf)₃, TMSOTf, LiClO₄. Other reducing agents screened: Ph₃SnH, Red-Al, DIBAL-H, NaBH(OAc)₃, PMHS, PhNEt₂-BH₃.
 19. Kanth, J. V.; Brown, H. C. *Inorg. Chem.* **2000**, 39, 1795–1802.
 20. Ohira, S. *Synth. Commun.* **1989**, 19, 561–564.
 21. Kinoshita, A.; Norikazu, S.; Mori, M. *J. Am. Chem. Soc.* **1997**, 119, 12388–12389.
 22. McQuillin, F. J.; Parker, D. G. *J. Chem. Soc., Perkin Trans. 1* **1974**, 809–815.
 23. Mukai, C.; Nomura, I. *J. Org. Chem.* **2004**, 69, 1803–1812.
 24. Oxidation conditions employed: (i) PdCl₂ (10 mol%), Cu(OAc)₂ (20 mol%), *N,N*-dimethylacetamide–H₂O (7:1), O₂, 85 °C; (ii) PdCl₂ (20 mol%), Cu(OAc)₂ (200 mol%), *N,N*-dimethylacetamide–H₂O (7:1), O₂, 85 °C; (iii) PdCl₂ (10 mol%), CuCl (100 mol%), DMF–H₂O (7:1), O₂, 65 °C.
 25. Subsequent to these studies, a successful Wacker oxidation on a related azabicyclic intermediate was reported. See Ref. 16.
 26. (a) Yoda, H.; Yamazaki, H.; Takabe, K. *Tetrahedron: Asymmetry* **1996**, 7, 373–374. (b) Kanazawa, A.; Gillet, S.; Delair, P.; Greene, A. E. *J. Org. Chem.* **1998**, 63, 4660–4663.
 27. For the addition of organometallic nucleophiles to *N*-alkoxycarbonyl lactams, see: (a) Ohta, T.; Hosoi, A.; Kimura, T.; Nozoe, S. *Chem. Lett.* **1987**, 2091–2094. (b) Giovannini, A.; Savoia, D.; Umami-Ronchi, A. *J. Org. Chem.* **1989**, 54, 228–234.
 28. For a review of the use of B(C₆F₅)₃ in organic synthesis see: Ishihara, K.; Yamamoto, H. *Eur. J. Org. Chem.* **1999**, 3, 527–538.
 29. Parks, D. J.; Blackwell, J. M.; Piers, W. E. *J. Org. Chem.* **2000**, 65, 3090–3098.
 30. (a) Groebel, B. T.; Seebach, D. *Angew. Chem.* **1974**, 86, 102–103. (b) Stork, G.; Jung, M. E. *J. Am. Chem. Soc.* **1974**, 96, 3682–3684.
 31. Corey, E. J.; Fuchs, P. L. *Tetrahedron Lett.* **1972**, 3769–3772.
 32. Mukaiyama, T.; Kato, K. *Chem. Lett.* **1989**, 2233–2236.
 33. Kozmin, S. A.; Reddy, D. S.; Schramm, M. P. *Angew. Chem., Int. Ed.* **2001**, 40, 4274–4277.
 34. Kowalski, C. J.; Lal, G. S.; Haque, M. S. *J. Am. Chem. Soc.* **1986**, 108, 7127–7128.
 35. Chee, G.-L. *Synlett* **2001**, 1593–1595.
 36. Sakakibara, S.; Shimonishi, Y.; Kishida, Y.; Okada, M.; Sugihara, H. *Bull. Chem. Soc. Jpn.* **1967**, 40, 2164–2167.
 37. Saito, N.; Yamauchi, R.; Nishioka, H.; Ida, S.; Kubo, A. *J. Org. Chem.* **1989**, 54, 5391–5395.
 38. Rudolph, A.; Machauer, R.; Martin, S. F. *Tetrahedron Lett.* **2004**, 45, 4895–4898.
 39. Sunderhaus, J. D.; Lam, H.; Dudley, G. B. *Org. Lett.* **2003**, 5, 4571–4573, We thank Professor G. B. Dudley for providing us with details prior to publication.
 40. Undheim, K.; Ahmad, I.; Falck-Pederson, M. L. *J. Organomet. Chem.* **2001**, 625, 160–172.
 41. (a) Tanaka, M.; Yamashita, H.; Honda, K. *J. Am. Chem. Soc.* **1995**, 117, 8873–8874. (b) Tilley, T. D.; Campion, B. K.; Heyn, R. H. *J. Am. Chem. Soc.* **1988**, 110, 7558–7560.
 42. Sharpless, K. B.; Kolb, H. C.; VanNieuwenhze, M. S. *Chem. Rev.* **1994**, 94, 2483–2547.
 43. Corey, E. J.; Jardine, P. D.; Virgil, S.; Yuen, P.-W.; Connell, R. D. *J. Am. Chem. Soc.* **1989**, 111, 9243–9244.
 44. Rapoport, H.; Sardina, F. J.; Howard, M. H.; Koskinen, A. M. P. *J. Org. Chem.* **1989**, 54, 4654–4660.
 45. Krieger, R. I.; Stevens, D. K. *Toxicon* **1991**, 29, 167–179.
 46. (a) Rapoport, H.; Fels, G.; Petersen, J. S. *J. Am. Chem. Soc.* **1984**, 106, 4539–4547. (b) Rapoport, H.; Koskinen, A. M. P. *J. Med. Chem.* **1985**, 28, 1301–1309.
 47. Still, W. C.; Kahn, M.; Mitra, A. *J. Org. Chem.* **1978**, 43, 2923–2925.
 48. Pfaltz, A.; Leutenegger, U.; Siegmann, K.; Fritschi, H.; Keller, W.; Krathy, C. *Helv. Chim. Acta* **1988**, 71, 1541–1552.
 49. Tamm, C.; Matthes, M.; Ackermann, J. *Helv. Chim. Acta* **1990**, 73, 122–132.
 50. Konas, D. W.; Coward, J. K. *J. Org. Chem.* **2001**, 66, 8831–8842.
 51. Kikugawa, Y.; Li, H.; Sakamoto, T.; Kato, M. *Synth. Commun.* **1995**, 25, 4045–4052.
 52. Callant, P.; D’Haenens, L.; Vandewalle, M. *Synth. Commun.* **1984**, 14, 155–161.
 53. The diastereoselectivity was determined by GC analysis using a Hewlett Packard 5890 Series II instrument fitted with an Alltech ECONO-CAP SE-54 column (initial Temp=110 °C, final Temp 200 °C at 5 °C/min; retention time=17.1 min for **15** and 21.4 min for **18**).
 54. Campbell, H. F.; Edwards, O. E.; Kolt, R. *Can. J. Chem.* **1977**, 55, 1372–1379.

(*E*)-Cycloalkenes and (*E,E*)-cycloalkadienes by ring closing diyne- or enyne–yne metathesis/semi-reduction

Fabrice Lacombe, Karin Radkowski, Günter Seidel and Alois Fürstner*

Max-Planck-Institut für Kohlenforschung, Kaiser-Wilhelm-Platz 1, D-45470 Mülheim an der Ruhr, Germany

Received 2 April 2004; revised 18 May 2004; accepted 19 May 2004

Available online 9 June 2004

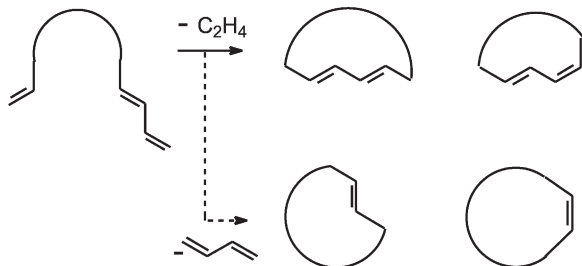
Dedicated with great respect and admiration to Professor R. H. Grubbs as the recipient of the 2004 Tetrahedron Prize

Abstract—A concise, practical and stereoselective entry into macrocyclic (*E*)-alkenes is outlined comprising a sequence of ring closing alkyne metathesis (RCAM), *trans*-selective hydrosilylation of the resulting cycloalkynes catalyzed by $[\text{Cp}^*\text{Ru}(\text{MeCN})_3]\text{PF}_6$, and a protodesilylation of the ensuing vinylsilanes with AgF in aq. THF/MeOH. Moreover, the first examples of intramolecular enyne–yne metathesis reactions catalyzed by the Schrock alkylidyne complex $(\text{tBuO})_3\text{W}\equiv\text{CCMe}_3$ are reported; the resulting cyclic enynes can be converted along similar lines into the corresponding (*E,E*)-configured 1,3-dienes in good overall yields. Cycloalkyne **4** and the (*E*)-configured cyclic olefins **6** and **21** were characterized by X-ray crystallography.
© 2004 Elsevier Ltd. All rights reserved.

1. Introduction

The advent of well defined catalysts for alkene metathesis combining high activity, durability and functional group tolerance has had a tremendous impact on organic chemistry and polymer science during the last decade.¹ One of the very few remaining shortcomings of this method is the lack of stereocontrol over the emerging double bond, especially during the formation of medium- or large rings.

This selectivity issue is augmented when macrocyclic 1,3-dienes (or higher polyenes) are targeted. In this case stereocontrol and a rigorous control over the site of attack by the metathesis catalyst must go hand in hand to avoid the formation of ring contracted products that are difficult to separate from the individual cycloalkadiene isomers (Scheme 1).^{2,3}

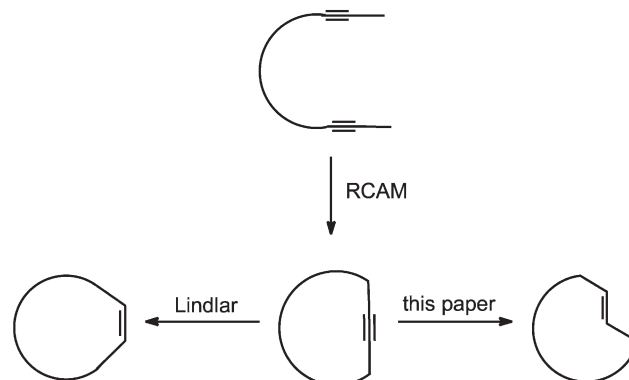


Scheme 1. Possible product spectrum upon ring closure of diene–enes by RCM.

Keywords: Olefins; Cycloalkyne; Enyne; Diene; Metathesis.

* Corresponding author. Tel.: +49-208-306-2342; fax: +49-208-306-2994; e-mail address: fuerstner@mpi-muelheim.mpg.de

Although these problems may eventually be solved by the development of more selective catalysts and/or the implementation of improved retrosynthetic logic,⁴ recourse to alkyne metathesis constitutes a reliable alternative devoid of these shortcomings. Thus, it has been shown that a sequence of ring closing alkyne metathesis (RCAM) followed by Lindlar hydrogenation of the resulting cycloalkynes opens a convenient, reliable and stereoselective route to (*Z*)-cycloalkenes of various ring sizes (Scheme 2).^{5,6} This methodology was scrutinized, inter alia, by many successful implementations into the total synthesis of structurally complex natural products of biological significance.^{7–9} Since an equally convenient and general method for the conversion of alkynes into the corresponding (*E*)-alkenes, however, has been missing until recently, the full potential of RCAM could not be exploited. Outlined



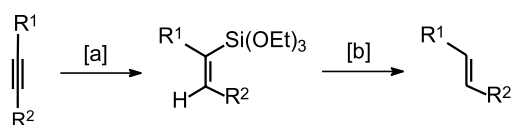
Scheme 2. Preparation of cycloalkenes with defined configuration via ring closing alkyne metathesis (RCAM) followed by semi-reduction.

below are our efforts to fill this gap.¹⁰ Moreover, it will be shown that an alkyne metathesis/semi-reduction sequence is also able to provide (*E,E*)-configured 1,3-dienes with excellent stereochemical and constitutional integrity due to the remarkable ability of the chosen catalysts to distinguish between different π -systems.

2. Results and discussion

While an (*E*)-selective hydrogenation of alkynes as the stereochemical complement to the Lindlar reduction is still elusive,¹¹ the existing methods for the conversion of alkynes to (*E*)-alkenes are rather limited in scope and hardly meet the stringent criteria of selectivity, practicality and functional group tolerance imposed upon advanced organic synthesis. They are either based on the use of metal hydrides,¹² over-stoichiometric amounts of low-valent chromium salts,¹³ or involve dissolving metal reductions.¹⁴

To circumvent the obvious disadvantages associated with any of these protocols, it was envisaged to pursue a sequence of *trans*-selective hydrosilylation of the (cyclo)alkyne substrates followed by a protodesilylation of the resulting vinylsilanes as an inherently catalytic way to transform alkynes into (*E*)-alkenes (Scheme 3). This approach seemed lucrative since *trans*-hydrosilylations are well precedented in the literature.^{15,16} However, most catalyst systems are limited to terminal alkynes as the substrates and are therefore inappropriate for the envisaged application.¹⁷ Only recently has the cationic ruthenium complex $[\text{Cp}^*\text{Ru}(\text{MeCN})_3]\text{PF}_6$ ¹⁸ been shown to effect the chemo- and stereoselective hydrosilylation of internal alkynes with remarkable efficiency.^{19–21} Applications of this new procedure to cyclic alkynes, however, have not been reported.



Scheme 3. Strategy for the preparation of (*E*)-alkenes from alkynes via *trans*-selective hydrosilylation (step [a]) followed by protodesilylation (step [b]).

To probe this aspect, a series of cycloalkynes of different ring size has been prepared in good to excellent yields by RCAM of the corresponding diynes in the presence of the Schrock alkylidyne complex $(\text{tBuO})_3\text{W}\equiv\text{CCMe}_3$ ²² in toluene as the catalyst. Figure 1 depicts the structure of a representative example of this series in the solid state.

These compounds were subjected to hydrosilylation in the presence of catalytic amounts of $[\text{Cp}^*\text{Ru}(\text{MeCN})_3]\text{PF}_6$ in CH_2Cl_2 at ambient temperature. As can be seen from the results compiled in Table 1, the additions proceeded smoothly even with catalyst loadings as low as ≤ 1 mol%, and consistently afforded the desired *trans*-addition products with good to excellent selectivity. It is also important to note that this method tolerates a host of functional groups including ketones, esters, amides, sulfones, and sulfonamides. Although various silanes are amenable to the reaction,¹⁹ $(\text{EtO})_3\text{SiH}$ turned out to be best

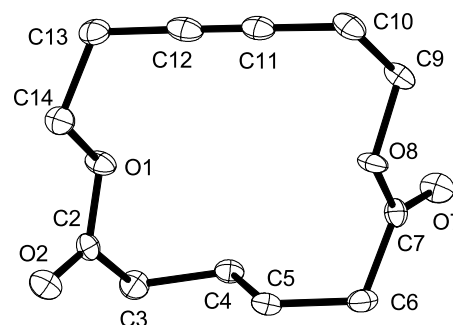


Figure 1. Molecular structure of cycloalkyne **4** in the solid state. Anisotropic displacement parameters are shown at the 50% probability level. Only one of the two independent molecules in the unit cell is depicted.

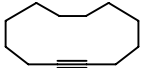
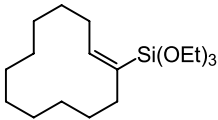
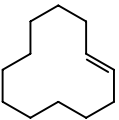
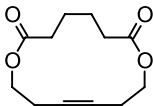
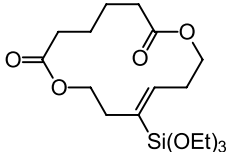
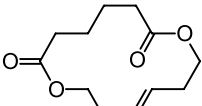
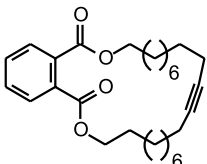
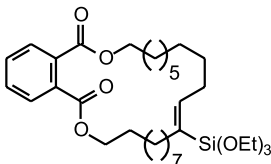
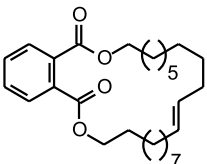
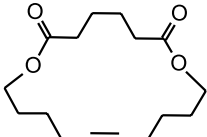
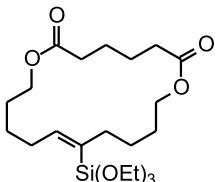
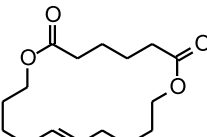
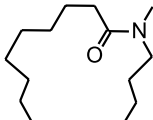
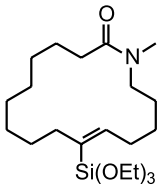
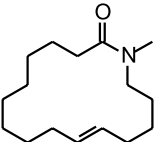
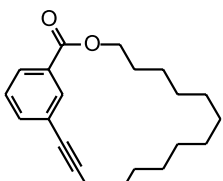
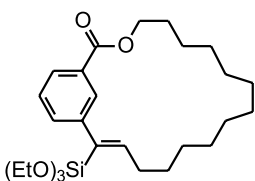
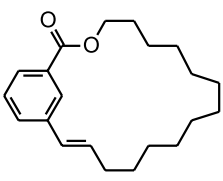
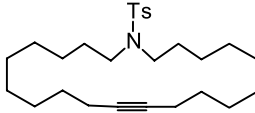
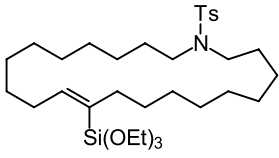
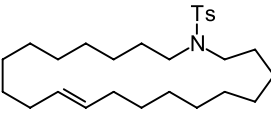
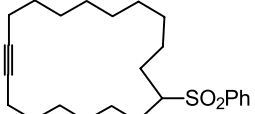
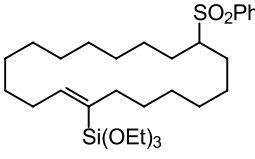
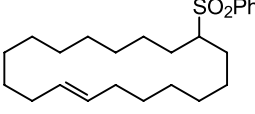
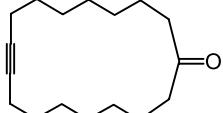
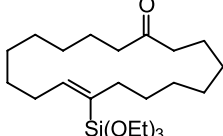
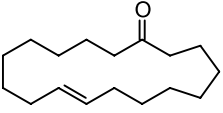
suitable for further elaboration. As expected, the hydrosilylation of unsymmetrical alkynes afforded mixtures of the regioisomeric vinylsilanes which were processed in the next step without further purification.

The subsequent protodesilylation of the vinylsilanes thus formed turned out to be more difficult than anticipated. Although several methods for this seemingly trivial transformation are known in the literature, none of them is particularly attractive from the application point of view. Specifically, simple protonation with strong mineral acids such as HI suffers from a narrow functional group tolerance and possible problems with the configurational stability of the double bond.²⁴ The use of TBAF in various media, on the other hand, requires high temperatures (≥ 80 °C) and was found to be rather unselective even when applied to the bare cyclododecene derivative **2** depicted in entry 1 of Table 1.²⁵

As a consequence, we have carried out a screening of other possible reagents that might effect the desired cleavage under sufficiently mild conditions. While HF–pyridine, NaF, KF, CsF, TBAF, $(\text{Bu}_4\text{N})(\text{Ph}_2\text{SiF}_3)$, ZnF_2 , and FeF_2 in different solvent systems were found unsuitable, AgF promoted the desired transformation and turned out to be compatible with sensitive functional groups. Thus, stirring of a vinylsilane with AgF (1.5–2.0 equiv.) in aq. THF/MeOH in the dark at ambient temperature resulted in a rapid, quantitative and selective protodesilylation without noticeable isomerization of the olefin. The corresponding (*E*)-alkenes were obtained in good to excellent yields (Table 1). AgF can also be used in catalytic amounts (2–20 mol%), provided that TBAF is added to the medium as a stoichiometric fluoride source (Table 2).²⁶ The fact that AgF is far more effective than all other reagents investigated suggests a synergetic mode of action involving the specific affinity of the fluoride anion for silicon and of the silver cation for the π -bond of the substrate. It is assumed that the fluoride initially leads to a pentacoordinate silicate species²⁷ and thereby facilitates transmetalation to a transient vinylsilver intermediate that is immediately trapped to give the alkene product.

The (*E*)-configuration of the resulting olefins can be deduced from their spectroscopic data. Particularly diagnostic are the shifts of the allylic C-atoms in the ¹³C NMR spectra ($\delta \approx 32$ –33 ppm), whereas the corresponding

Table 1. Preparation of cycloalkynes by RCAM followed by conversion into (*E*)-cycloalkenes via the corresponding vinylsilanes

Cycloalkyne	Yield ^a	Vinylsiloxane ^b	Yield (<i>E/Z</i>)	Cycloalkene	Yield (<i>E/Z</i>)
	1		2 (90%) (91:9)		3 (84%) (90:10)
	4 (79%)		5 (93%) (95:5)		6 (92%) (95:5)
	7 (70%)		8 (97%) (98:2)		9 (90%) (98:2)
	10 (80%)		11 (88%)		12 (90%) (>98:2)
	13 (68%)		14 (95%)		15 (82%) (95:5)
	16 (71%)		17 (80%) ^c		18 (74%) (93:7)
	19 (86%)		20 (86%) (>98:2)		21 (85%) (>98:2)
	22 (72%)		23 (92%) (>98:2)		24 (88%) (>98:2)
	25 (65%)		26 (93%) (>98:2)		27 (70%) (>98:2)

^a Yields refer to the product of ring closing alkyne metathesis (RCAM); compound **1** was prepared from cyclododecene in analogy to Ref.²³

^b All hydrosilylation reactions were carried out in CH₂Cl₂ at ambient temperature using 1 mol% of [Cp*₂Ru(MeCN)₃]PF₆ as the catalyst unless stated otherwise. Hydrosilylation of unsymmetrical alkynes provides mixture of regioisomers; only one of them is depicted in the Table.

^c Using 15 mol% of the catalyst.

Table 2. Protodesilylation of representative vinylsilanes to the corresponding (*E*)-alkenes: comparison of the results using stoichiometric and catalytic amounts of AgF

Entry	Substrate	AgF (mol%)	Additive (1 eq.)	Product (Yield)
1	5	200	—	6 (92%)
2	5	20	TBAF	6 (86%)
3	5	10	TBAF	6 (82%)
4	5	2	TBAF	6 (86%)
5	11	200	—	12 (90%)
6	11	20	TBAF	12 (90%)
7	11	20	KF	12 (<20%)

positions of the (*Z*)-isomers are known to be shielded and appear at higher field ($\delta \approx 27$ – 28 ppm).²⁸ To avoid any ambiguity in this regard, however, two representative examples were subjected to X-ray crystallography. The structures of compounds **6** and **21** in the solid state are depicted in Figures 2 and 3 which both clearly feature (*E*)-olefin entities embedded into the macrocyclic rings.

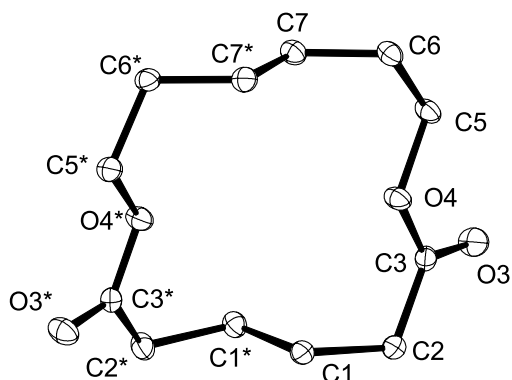


Figure 2. Molecular structure of (*E*)-cycloalkene **6** derived from cycloalkyne **4** in the solid state. Anisotropic displacement parameters are shown at the 50% probability level.

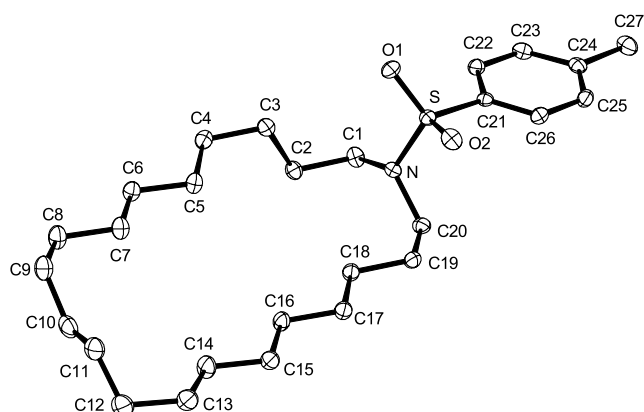
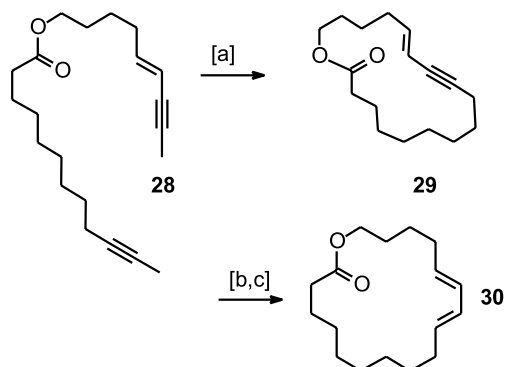
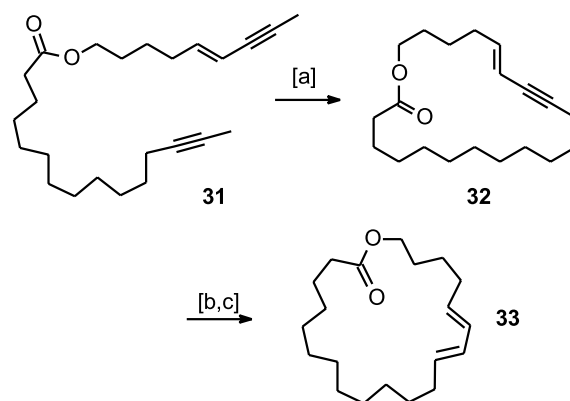


Figure 3. Molecular structure of (*E*)-cycloalkene **21** in the solid state. Anisotropic displacement parameters are shown at the 50% probability level.

Next we investigated if the novel route to (*E*)-cycloalkenes can be extended to the formation of stereodefined cycloalka-1,3-dienes. To this end, suitable substrates were subjected to ring closure by what is believed to be the first examples of intramolecular enyne–yne metathesis reactions.²⁹ As can be seen from Schemes 4 and 5, decent yields of the corresponding cyclic enynes were obtained using the



Scheme 4. Preparation of an 18-membered (*E,E*)-cycloalkadiene by ring closing enyne–yne metathesis followed by *trans*-hydrosilylation and protodesilylation. [a] $(t\text{BuO})_3\text{W}\equiv\text{CCMe}_3$ (10 mol%), toluene, 80 °C, 75%; [b] $(\text{EtO})_3\text{SiH}$, $[\text{Cp}^*\text{Ru}(\text{MeCN})_3]\text{PF}_6$ (8 mol%), neat, 80% (mixture of regioisomers); [c] AgF, aq. THF/MeOH, 79%, *E/Z*=97:3.

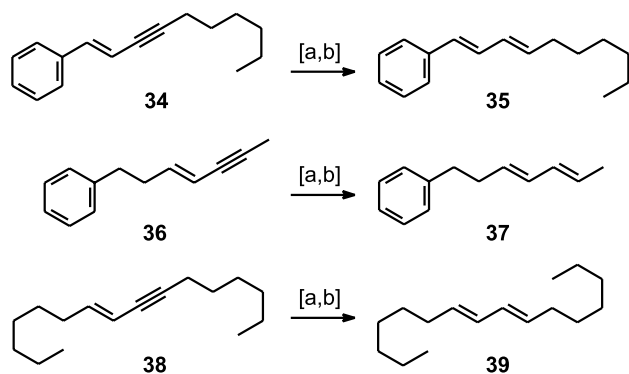


Scheme 5. Preparation of a 21-membered (*E,E*)-cycloalkadiene by ring closing enyne–yne metathesis followed by *trans*-hydrosilylation and protodesilylation. [a] $(t\text{BuO})_3\text{W}\equiv\text{CCMe}_3$ (10 mol%), toluene, 80 °C, 84%; [b] $(\text{EtO})_3\text{SiH}$, $[\text{Cp}^*\text{Ru}(\text{MeCN})_3]\text{PF}_6$ (15 mol%), CH_2Cl_2 , 65% (mixture of regioisomers); [c] AgF, aq. THF/MeOH, 79%, *E/Z*=95:5.

standard Schrock alkylidyne complex $(t\text{BuO})_3\text{W}\equiv\text{CCMe}_3$ as the catalyst in toluene under high dilution conditions (ca. 0.001 M). Attempts to form the analogous 15-membered lactone, however, mainly led to oligomeric products likely due to the ring strain of the cyclic monomer. Despite this limitation, these results highlight the ability of metal alkylidyne complexes to distinguish between the π -systems of alkenes and alkynes even if they are in conjugation, and therefore lend credence to the notion that the metathesis of alkynes is mechanistically closely related yet orthogonal to alkene metathesis from the preparative point of view.^{6,7}

It was gratifying to note that the subsequent hydrosilylation of the cyclic enynes thus formed proceeded chemo-selectively at the alkyne site. The conjugated alkene moiety was not affected to any noticeable extent. The reaction was best performed without solvent, or in case of solid material, in a minimum amount of CH_2Cl_2 as the reaction medium. Higher catalyst loadings than in the case of simple cycloalkynes, however, had to be used to ensure rapid and clean reactions, which usually afforded mixtures of both possible regioisomeric vinylsilanes. Since they converge to the same 1,3-diene product upon protodesilylation, no attempts were made to separate these isomers. The cleavage

of the C–Si bond was carried out with AgF in aq. THF/MeOH following the protocol outlined above. Moreover, Scheme 6 shows that the sequence of hydrosilylation/protodesilylation also applies to acyclic enynes.



Scheme 6. Preparation of acyclic (*E,E*)-configured 1,3-dienes by *trans*-hydrosilylation of enynes followed by protodesilylation. [a] (EtO)₃SiH, [Cp**Ru*(MeCN)₃]PF₆ (15 mol%), CH₂Cl₂, 71–88% (mixture of regioisomers); [b] AgF, aq. THF/MeOH, 79% (35), 78% (37), 91% (39), *E/Z*=98:2.

In summary, a highly stereoselective entry into macrocyclic (*E*)-alkenes and (*E,E*)-configured 1,3-dienes has been developed that relies upon the excellent application profiles of metal-catalyzed alkyne metathesis and hydrosilylation. The implementation of this strategy into target oriented synthesis is actively pursued in this laboratory and will be reported in due course.

3. Experimental

3.1. General

All reactions were carried out under Argon in flame-dried glassware using Schlenk techniques. The solvents were dried by distillation over the indicated drying agents and were stored and transferred under Argon: CH₂Cl₂, Et₃N, DMF (CaH₂), toluene, THF (Na). Flash chromatography: Merck silica gel (230–400 mesh) using either hexanes/ethyl acetate or pentanes/diethyl ether in various proportions as the eluents. NMR: spectra were recorded on a Bruker DPX 300, AMX 400, DMX 600 spectrometer in CDCl₃ or CD₂Cl₂ as indicated. Chemical shifts (δ) are given in ppm relative to the residual peak of CHCl₃ or CHDCl₂, coupling constant (*J*) in Hz. IR: Nicolet FT-7199, wavenumbers in cm⁻¹. MS: Varian CH-5 (70 eV), HRMS: Finnigan MAT SSQ 7000 (70 eV). Elemental analyses: H. Kolbe, Mülheim. Commercially available reagents (Aldrich, Fluka, Strem, Lancaster) were used as received.

3.1.1. Ring closing alkyne metathesis (RCAM). Cycloheptadec-9-yn-1-one (25). A solution of 2,19-heneicosadiyn-11-one (556 mg, 1.80 mmol)^{7d} and (tBuO)₃W≡CCMe₃ (85 mg, 10 mol%)²² in toluene (300 mL) is stirred at 80 °C for 30 min. The reaction mixture is filtered through a pad of silica, the insoluble residues are carefully washed with CH₂Cl₂ (100 mL in several portions), the combined filtrates are evaporated and the residue is purified by flash chromatography (hexane/ethyl acetate, 50/1→30/1) to give cycloalkyne **25** as a

colorless syrup (299 mg, 65%). ¹H NMR (300 MHz, CDCl₃) δ 2.41 (t, *J*=6.9 Hz, 4H), 2.17 (m, 4H), 1.65 (m, 4H), 1.44 (m, 8H), 1.32 (m, 8H). ¹³C NMR (75 MHz, CDCl₃) δ 212.9, 80.5, 42.3, 28.7, 28.6, 28.2, 27.9, 24.0, 18.5. IR (neat): 2928, 2856, 1710, 1460, 1437, 1357, 1331, 1276, 1113, 1053, 722 cm⁻¹. MS (EI) *m/z* (rel. intensity): 248 ([M⁺], 11), 230 (3), 219 (5), 205 (5), 193 (7), 179 (6), 166 (19), 151 (11), 135 (16), 121 (27), 107 (32), 93 (47), 81 (65), 79 (64), 67 (74), 55 (79), 41 (100). Anal. (C₁₇H₂₈O) calcd. C 82.20, H 11.36, found C 82.35, H 11.20.

All other cycloalkynes were prepared analogously. The physical data of compound **4** are reported in the literature,⁶ those of all new cycloalkynes are compiled below:

3.1.2. Benzo-[c]-1,6-dioxo-2,5-dioxocyclooctacos-16-yne (7). ¹H NMR (CDCl₃, 400 MHz) δ 7.66 (m, 2H), 7.51 (m, 2H), 4.29 (t, *J*=6.6 Hz, 4H), 2.16 (m, 4H), 1.72 (m, 4H), 1.21–1.51 (m, 24H). ¹³C NMR (CDCl₃, 100 MHz) δ 167.8, 132.3, 130.9, 128.9, 80.5, 66.0, 29.7, 29.3, 29.2, 28.6, 28.5, 28.3, 26.3, 18.5. IR (KBr) 2926, 2852, 1745, 1735, 1578, 1464, 1450, 1297, 1281, 1133, 1078, 746 cm⁻¹. MS (EI) *m/z* (rel. intensity): 440 [M⁺] (9), 312 (4), 292 (3), 291 (2), 259 (4), 245 (4), 178 (11), 167 (3), 164 (17), 151 (2), 149 (100), 136 (5), 134 (1), 121 (15), 111 (9), 110 (7), 104 (3), 97 (12), 95 (15), 80 (16), 79 (17), 67 (21), 55 (23), 41 (16). HRMS (C₂₈H₄₀O₄) calcd. 440.292660, found 440.293118.

3.1.3. 1,8-Dioxacyclooctadec-13-yn-2,7-dione (10). ¹H NMR (400 MHz, CD₂Cl₂) δ 4.11 (t, *J*=6.7 Hz, 4H), 2.33 (m, 4H), 2.18 (m, 4H), 1.77 (m, 4H), 1.68 (m, 4H), 1.53 (m, 4H). ¹³C NMR (100 MHz, CD₂Cl₂) δ 173.2, 80.3, 64.0, 34.4, 27.8, 25.4, 24.8, 18.4. IR (KBr) 2948, 2866, 2235, 1733, 1245 cm⁻¹. MS (EI) *m/z* (rel. intensity): 280 [M⁺] (2), 252 (2), 179 (5), 151 (19), 134 (82), 119 (36), 106 (46), 91 (77), 79 (65), 67 (45), 55 (100), 41 (58), 29 (27). HRMS (M+H, C₁₆H₂₄O₄) calcd. 281.175285, found 281.175010.

3.1.4. 1-(*N*-Methyl)-azacyclohexadec-11-yn-2-one (13). ¹H NMR (400 MHz, CDCl₃, rotamers) δ 3.39 and 3.28 (m, 2H), 2.97 and 2.86 (s, 3H), 2.51 (m, 2H), 2.16 (m, 4H), 1.51–1.76 (m, 4H), 1.21–1.51 (m, 12H). ¹³C NMR (100 MHz, CDCl₃, rotamers) δ 173.2, 173.1, 81.0, 81.0, 80.2, 50.9, 47.0, 35.9, 33.7, 32.8, 32.6, 28.6, 28.4, 28.4, 28.2, 28.0, 27.8, 27.4, 27.3, 27.0, 26.9, 26.8, 25.9, 25.4, 19.1, 19.0, 18.2. IR (KBr) 2928, 2855, 1641, 1483, 1458, 1437, 1400, 577 cm⁻¹. MS (EI) *m/z* (rel. intensity): 249 [M⁺] (25), 248 (21), 221 (4), 208 (7), 206 (12), 193 (4), 178 (8), 167 (5), 165 (9), 164 (9), 152 (18), 136 (6), 135 (4), 126 (6), 124 (28), 112 (35), 98 (8), 94 (8), 91 (11), 86 (18), 80 (7), 79 (21), 77 (10), 73 (15), 70 (100), 67 (15), 57 (17), 55 (24), 44 (76), 41 (22). HRMS (C₁₆H₂₇NO) calcd. 249.209264, found 249.209070.

3.1.5. 3-Oxabicyclo[16.3.1]docosa-1(22),18,20-trien-16-yn-2-one (16). ¹H NMR (400 MHz, CDCl₃) δ 7.98 (m, 2H), 7.53 (dt, *J*=0.5, 7.7 Hz, 1H), 7.38 (dt, *J*=1.45, 7.7 Hz, 1H), 4.32 (m, 2H), 2.46 (br t, 2H), 1.75 (m, 2H), 1.26–1.66 (m, 18H). ¹³C NMR (100 MHz, CDCl₃) δ 166.1, 135.2, 132.6, 130.7, 128.9, 128.4, 124.5, 91.3, 80.4, 65.7, 29.3, 29.2, 28.4, 28.3, 28.1, 27.9, 27.8, 27.6, 26.9, 19.0. IR (KBr) 2927, 2855, 2228, 1722, 1600, 1580, 1460, 909, 816, 754, 725, 684 cm⁻¹. MS (EI) *m/z* (rel. intensity): 313 (23), 312

[M⁺] (100), 214 (9), 187 (38), 186 (18), 184 (17), 171 (13), 162 (14), 159 (11), 144 (25), 142 (41), 141 (36), 135 (21), 129 (66), 117 (28), 116 (21), 115 (53), 114 (46), 113 (10), 95 (41), 93 (14), 91 (21), 88 (10), 80 (22), 79 (17), 67 (42), 55 (80), 43 (27), 41 (72). HRMS (C₂₁H₂₈O₂) calcd. 312.208930, found 312.208644.

3.1.6. 1-(Toluene-4-sulfonyl)-azacyclohepticos-11-yne (19). Mp=92–94 °C. ¹H NMR (300 MHz, CDCl₃) δ 7.67 (d, *J*=8.3 Hz, 2H), 7.29 (d, 2H), 3.01 (t, *J*=7.5 Hz, 4H), 2.42 (s, 3H), 2.17 (m, 4H), 1.59 (m, 4H), 1.44 and 1.31 (m, 24H). ¹³C NMR (75 MHz, CDCl₃) δ 142.9, 136.2, 129.5, 127.1, 80.4, 50.0, 29.4, 29.18, 29.16, 28.8, 28.6, 28.5, 26.9, 21.4, 18.6. MS: *m/z* (rel. intensity): 445 (7) [M⁺], 290 (100), 262 (2), 198 (6), 155 (13), 91 (37), 81 (8), 67 (10), 55 (11), 44 (16), 41 (10). Anal. (C₂₇H₄₃NO₂S) calcd. C 72.76, H 9.72; found C 72.72, H 9.92.

3.1.7. 9-Benzenesulfonyl-cyclooctadec-1-yne (22). ¹H NMR: δ 7.91–7.86 (m, 2H), 7.69–7.61 (m, 1H), 7.61–7.57 (m, 2H), 2.94 (m, 1H), 2.15 (m, 4H), 1.90–1.60 (m, 4H), 1.45 (m) and 1.31 (m, 22H) ¹³C NMR: δ 138.2, 133.4, 129.0, 128.7, 80.6, 80.4, 63.9, 28.8, 28.6, 28.4 (2C), 28.27, 28.24, 28.0, 27.6, 27.1, 26.8, 25.9, 25.7, 24.6, 18.5, 18.4. MS (EI) *m/z* (rel. intensity): 388 (7) [M⁺], 246 (28), 143 (28), 123 (21), 109 (50), 95 (100), 81 (99), 67 (89), 55 (71), 41 (58). Anal. (C₂₄H₃₆O₂S) calcd. C 74.18, H 9.34, found C 74.29, H 9.16.

3.1.8. Oxacyclooctadec-13-en-11-yn-2-one (29). ¹H NMR (400 MHz, CDCl₃) δ 5.91 (dd, *J*=15.8, 7.3 Hz, 1H), 5.43 (dm, *J*=15.8 Hz, 1H), 4.11 (t, *J*=5.8 Hz, 2H), 2.30 (m, 4H), 2.12 (m, 2H), 1.16–1.76 (m, 16H) ¹³C NMR (100 MHz, CDCl₃) δ 173.7, 142.6, 111.1, 88.9, 80.3, 63.7, 34.7, 31.5, 29.1, 28.3, 28.2, 27.7, 27.4, 25.3, 24.7, 18.9. IR (KBr) 3018, 2930, 2856, 2216, 1735, 1459, 1178, 957 cm⁻¹. MS (EI) *m/z* (rel. intensity): 262 [M⁺] (13), 133 (16), 120 (100), 105 (55), 91 (60), 79 (39), 67 (24), 55 (33), 43 (12), 29 (14). HRMS (C₁₇H₂₆O₂+Na) calcd. 285.183049, found 285.18286.

3.1.9. Oxacyclohepticos-16-en-14-yn-2-one (32). ¹H NMR (300 MHz, CDCl₃) δ 5.99 (dt, *J*=15.8, 7.1 Hz, 1H), 5.44 (dm, *J*=15.8 Hz, 1H), 4.10 (t, *J*=6.0 Hz, 2H), 2.30 (m, 4H), 2.12 (m, 2H), 1.62 (m, 4H), 1.21–1.54 (m, 18H) ¹³C NMR (75 MHz) δ 173.9, 142.4, 110.5, 89.0, 79.7, 63.7, 34.5, 32.1, 29.7, 29.4, 29.1, 28.8, 28.6, 27.9, 27.8, 27.7, 27.5, 25.4, 25.3, 19.1. IR 3016, 2927, 2855, 2202, 1734, 1672, 1460, 1243, 1170, 957, 724 cm⁻¹. MS (EI) *m/z* (rel. intensity): 304 [M⁺] (12), 121 (16), 120 (100), 105 (53), 104 (2), 94 (18), 92 (37), 91 (58), 80 (21), 79 (36), 67 (19), 55 (18), 41 (19). HRMS (C₂₀H₃₂O₂) calcd. 304.240230, found 304.240154.

3.1.10. Representative procedure for the hydrosilylation of cycloalkynes: (Z)-9-[(Triethoxysilyl)-cyclohepta-dec-9-en-1-one (26). To a solution of alkyne **25** (65 mg, 0.262 mmol) and (EtO)₃SiH (51 mg, 0.31 mmol) in CH₂Cl₂ (0.5 mL) is added [Cp*⁺Ru(MeCN)₃]PF₆⁻ (1.3 mg, 1 mol%) and the resulting mixture is stirred for 15 min at ambient temperature. Prior to work-up, P(CH₂OH)₃ (5 mg) is added and stirring is continued for 30 min. The mixture is filtered through a short pad of silica which is carefully rinsed with Et₂O, and the combined filtrates are evaporated to give

26 as a colorless syrup (100 mg, 93%). ¹H NMR (400 MHz, CDCl₃) δ 6.04 (t, *J*=7.4 Hz, 1H), 3.80 (q, *J*=7.0 Hz, 6H), 2.36 (q, *J*=7.1 Hz, 4H), 2.28 (q, *J*=7.1 Hz, 2H), 2.12 (t, *J*=6.3 Hz, 2H), 1.57–1.63 (m, 4H), 1.38–1.43 (m, 4H), 1.26–1.30 (m, 12H), 1.22 (t, *J*=7.0 Hz, 9H). ¹³C NMR (100 MHz, CDCl₃) δ 213.0, 148.7, 132.2, 58.1, 43.1, 42.0, 36.9, 31.4, 29.5, 29.1, 28.7, 28.5, 28.4, 27.9, 27.4, 24.5, 23.6, 18.3. IR (KBr) 1712 cm⁻¹. MS (EI) *m/z* (rel. intensity): 412 ([M⁺], 1.5), 366 (100).

The following compounds were prepared analogously:

3.1.11. 1-(Triethoxysilyl)-cyclododecene (2). ¹H NMR (400 MHz, CDCl₃) δ 6.25 (tt, *J*=7.8, 1.1 Hz, 1H), 3.82 (q, *J*=7.0 Hz, 6H), 2.30 (m, 2H), 2.18 (m, 2H), 1.49–1.52 (m, 4H), 1.41 (m, 2H), 1.34 (m, 2H), 1.26–1.29 (m, 8H), 1.21 (t, *J*=7.0 Hz, 9H) ¹³C NMR (100 MHz, CDCl₃) δ 149.7, 131.4, 58.2, 36.6, 32.1, 27.0, 26.7, 26.2, 26.0, 25.8, 24.4, 24.1, 24.0, 18.2.

3.1.12. 11-(Triethoxysilyl)-1,8-dioxacyclotetradec-11-ene-2,7-dione (5). ¹H NMR (300 MHz, CDCl₃) δ 6.13 (m, 1H), 4.16 (m, 4H), 3.80 (q, *J*=6.9 Hz, 6H), 2.63 (m, 2H), 2.44 (m, 2H), 2.30 (m, 4H), 1.61 (m, 4H), 1.20 (t, *J*=6.9 Hz, 9H) ¹³C NMR (75 MHz, CDCl₃) δ 173.2, 173.0, 146.4, 131.3, 64.1, 63.5, 58.2, 36.9, 35.0, 34.9, 30.7, 24.7, 24.3, 18.1. IR (KBr) 2975, 1727, 1626, 1282, 1082, 787 cm⁻¹. MS (EI) *m/z* (rel. intensity): 388 [M⁺] (0.2), 343 (8), 242 (55), 198 (87), 163 (78), 135 (100), 119 (42), 79 (41), 55 (19). HRMS (C₁₈H₃₂O₇Si+H) calcd. 389.199559, found 389.199279.

3.1.13. 17-(Triethoxysilyl)-6,29-dioxabenzocyclo-octacos-(17Z)-ene-5,30-dione (8). ¹H NMR (CDCl₃, 300 MHz) δ 7.70 (m, 2H), 7.50 (m, 2H), 6.05 (m, 1H), 4.27 (t, *J*=6.6 Hz, 4H), 3.78 (q, *J*=7.0 Hz, 6H), 2.26 (m, 2H), 2.11 (m, 2H), 1.70 (m, 4H), 1.16–1.46 (m, 33H) ¹³C NMR (CDCl₃, 75 MHz) δ 167.8, 148.6, 132.4, 132.3, 131.8, 130.9, 130.9, 129.0, 128.8, 66.0, 58.0, 36.9, 31.5, 29.7, 29.5, 29.5, 29.3, 29.2, 29.0, 28.6, 27.8, 26.2, 18.2. IR (KBr) 2971, 2926, 2854, 1729, 1601, 1580, 1448, 1388, 1289, 1104, 780, 743 cm⁻¹. MS (EI) *m/z* (rel. intensity): 604 [M⁺] (9), 560 (13), 558 (100), 512 (13), 283 (39), 163 (45), 137 (8), 135 (19), 119 (28), 107 (13), 81 (10), 79 (12). HRMS (C₃₄H₅₆O₇Si) calcd. 604.379534, found 604.379109.

3.1.14. 13-(Triethoxysilyl)-1,8-dioxacyclooctadec-(13E)-ene-2,7-dione (11). ¹H NMR (300 MHz, CDCl₃) δ 6.05 (t, *J*=7.5 Hz, 1H) 4.09 (m, 4H), 3.80 (q, *J*=7.0 Hz, 6H), 2.31 (m, 6H), 2.13 (m, 2H), 1.38–1.71 (m, 12H), 1.22 (t, *J*=7.0 Hz, 9H) ¹³C NMR (75 MHz, CDCl₃) δ 173.3, 147.9, 132.2, 64.3, 64.3, 58.1, 36.2, 34.7, 34.6, 31.0, 28.1, 27.6, 26.1, 25.7, 25.0, 24.9, 18.2. MS (EI) *m/z* (rel. intensity): 444 [M⁺] (0.5), 398 (100), 296 (3), 255 (4), 217 (33), 163 (38), 108 (27), 79 (29), 55 (11).

3.1.15. (11Z)-N-Methyl-12-(triethoxysilyl)azacyclo-hexadec-11-en-2-one and isomer (14). ¹H NMR (300 MHz, CDCl₃, rotamers) δ 6.01 (m, 1H), 3.76 (m, 6H), 3.29 (m, 2H), 2.94 and 2.85 (m, 3H), 2.26 (m, 4H), 2.12 (m, 2H), 1.11–1.66 (m, 26H) ¹³C NMR (75 MHz, CDCl₃, rotamers) δ 173.3, 173.2, 173.1, 172.9, 149.6, 149.2, 149.1, 148.1, 133.0, 132.8, 132.7, 131.8, 58.5, 58.4, 58.3, 54.5, 54.2, 53.8,

53.4, 53.1, 51.2, 51.2, 47.4, 47.3, 38.0, 37.6, 37.3, 36.5, 35.8, 35.6, 33.9, 33.7, 32.9, 32.9, 32.6, 32.3, 32.3, 31.9, 31.8, 31.0, 29.7, 29.2, 29.0, 28.9, 28.8, 28.6, 28.5, 28.3, 28.2, 28.1, 28.0, 27.9, 27.85, 27.8, 27.7, 27.3, 27.2, 27.1, 27.0, 26.9, 26.7, 26.4, 26.1, 26.0, 25.8, 25.5.

3.1.16. 17-(Triethoxysilyl)-3-oxa-bicyclo[16.3.1]docosa-1(22),16,18,20-tetraen-2-one and Isomer (17). ^1H NMR (300 MHz, CDCl_3 , data of the major isomer) δ 7.96 (dt, $J=7.7, 1.5$ Hz, 1H), 7.85 (t, $J=1.5$ Hz, 1H), 7.50 (dt, $J=7.7, 1.5$ Hz, 1H), 7.38 (t, $J=7.7$ Hz, 1H), 6.44 (t, $J=7.5$ Hz, 1H), 4.37 (m, 2H), 3.83 (q, $J=7.0$ Hz, 6H), 2.58 (m, 2H), 1.81 (m, 2H), 1.57 (m, 4H), 1.34–1.49 (m, 14H), 1.21 (t, $J=7.0$ Hz, 9H) ^{13}C NMR (75 MHz, CDCl_3 , major isomer) δ 167.0, 153.2, 145.3, 134.5, 132.6, 130.5, 128.1, 127.5, 127.4, 65.2, 58.5, 31.2, 28.9, 28.4, 28.3, 28.4, 28.3, 28.0, 27.9, 27.7, 27.6, 26.7, 18.1. IR (KBr) 2973, 2926, 2856, 1721, 1597, 1582, 1481, 1460, 1442, 1104, 1081, 781, 755, 726, 697, 681 cm^{-1} . MS (EI) m/z (rel. intensity): 476 [M^+] (72), 432 (1), 431 (38), 430 (100), 412 (3), 401 (5), 385 (11), 384 (29), 291 (23), 265 (31), 255 (23), 163 (38), 135 (18), 119 (33), 107 (14), 79 (20), 55 (12). HRMS ($\text{C}_{27}\text{H}_{44}\text{O}_5\text{Si}$) calcd. 476.295804, found 476.296057.

3.1.17. 1-(Toluene-4-sulfonyl)-11-triethoxysilylazacyclohenicos-(11E)-ene (20). ^1H NMR (400 MHz, CDCl_3) δ 7.66 (d, $J=8.3$ Hz, 2H), 7.28 (d, $J=8.1$ Hz, 2H), 6.04 (t, $J=7.3$ Hz, 1H), 3.80 (q, $J=7.1$ Hz, 6H), 3.00 (t, $J=7.1$ Hz, 4H), 2.41 (s, 3H), 2.28 (m, 2H), 2.13 (m, 2H), 1.57 (m, 4H), 1.17–1.45 (m, 24H), 1.22 (t, $J=7.1$ Hz, 9H) ^{13}C NMR (100 MHz, CDCl_3) δ 148.6, 142.9, 136.4, 131.9, 129.5, 127.2, 58.0, 50.2, 50.0, 37.3, 31.7, 29.8, 29.7, 29.5, 29.4, 29.3, 29.2, 29.1, 29.0, 28.9, 28.7, 28.0, 26.9, 26.5, 21.4, 18.2. IR (KAP): 3066, 3026, 2973, 2925, 2854, 1615, 1599, 1494, 1463, 1389, 1343, 1305, 1161, 1103, 1082, 958, 814, 777, 719, 653, 550 cm^{-1} . MS (EI) m/z (rel. intensity): 609 (5, [M^+]), 565 (19), 564 (46), 563 (100), 454 (11), 163 (14).

3.1.18. 1-Benzenesulfonyl-8-triethoxysilylcyclooct-(8E)-ene and Isomer (23). ^1H NMR (300 MHz, CDCl_3) δ 7.88 (d, $J=7.2$ Hz, 2H), 7.60 (m, 3H), 6.03 (m, 1H), 3.79 (q, $J=7.2$ Hz, 3H), 3.78 (q, $J=6.8$ Hz, 3H), 2.93 (m, 1H), 2.19–2.35 (m, 2H), 2.02–2.19 (m, 2H), 1.58–1.86 (m, 4H), 1.14–1.54 (m, 22H), 1.21 (t, $J=7.2$ Hz, 9H) ^{13}C NMR (75 MHz, CDCl_3) δ 148.6, 138.4, 138.3, 133.4, 132.2, 131.8, 129.0, 128.7, 64.1, 64.0, 58.0, 37.0, 36.6, 31.6, 31.2, 29.4, 29.2, 29.1, 28.9, 28.7, 28.6, 28.4, 28.3, 28.0, 27.8, 27.7, 27.5, 27.4, 27.1, 27.0, 26.8, 26.7, 25.9, 25.8, 25.4, 25.0, 18.2. IR (KAP): 3062, 2972, 2926, 2854, 1616, 1586, 1480, 1460, 1446, 1389, 1304, 1145, 1103, 1083, 958, 778, 725, 692, 600 cm^{-1} . MS (EI) m/z (rel. intensity): 506 (51, [M^+]), 261 (10), 260 (18), 259 (100), 195 (17), 163 (60), 119 (25).

3.1.19. Representative procedure for the proto-desilylation reaction. (E)-Cycloheptadec-9-en-1-one (27). A suspension of AgF (1 M in aq. MeOH, 0.47 mL, 0.47 mmol) is added to a solution of vinylsilane **26** (95 mg, 0.23 mmol) in THF (1.2 mL) and the resulting mixture is stirred in the dark for 3h. The insoluble residues are filtered off and are carefully washed with Et_2O and EtOAc (3 mL each), the combined filtrates are evaporated and the residue is purified by flash chromatography (pentane/ Et_2O , 8:1) to give alkene **27** as a colorless syrup

(40 mg, 70%). ^1H NMR (400 MHz, CDCl_3) δ 5.31 (m, 2H), 2.37 (t, $J=7.1$ Hz, 4H), 2.01 (m, 4H), 1.60 (m, 4H), 1.20–1.37 (m, 16H). ^{13}C NMR (100 MHz, CDCl_3) δ 213.0, 131.0, 42.5, 32.0, 28.9, 28.8, 28.4, 27.4, 24.1. IR: 1711 (C=O), 966 ((E)-alkene). MS (EI) m/z (rel. intensity): 250 [M^+], 100. Anal. ($\text{C}_{17}\text{H}_{30}\text{O}$) calcd. C 81.54, H 12.07, found C 81.66, H 12.12.

The following compounds were prepared analogously:

3.1.20. (E)-Cyclododecene (3).³⁰ ^1H NMR (400 MHz, CDCl_3) δ 5.37 (tt, $J=4.1, 1.0$ Hz, 2H), 2.06 (q, $J=6$ Hz, 4H), 1.39–1.47 (m, 4H), 1.25–1.37 (m, 9H), 1.29 (s, 3H) ^{13}C NMR (100 MHz, CDCl_3) δ 131.4, 32.1, 26.3, 25.6, 25.0, 24.6.

3.1.21. 1,8-Dioxacyclotetradec-(11E)-ene-2,7-dione (6). $\text{Mp}=95\text{--}96$ °C. ^1H NMR (300 MHz, CDCl_3) δ 5.46 (tt, $J=3.8, 1.5$ Hz, 1H), 4.14 (dd, $J=6.4, 4.5$ Hz, 2H), 2.29–2.45 (m, 4H), 1.64 (m, 2H). ^{13}C NMR (75 MHz, CDCl_3) δ 173.1, 129.2, 63.1, 35.0, 31.9, 24.7. IR (KBr): 1719, 1284, 961 cm^{-1} . MS (EI) m/z (rel. intensity): 196 (1), 129 (3), 101 (3), 80 (100), 79 (14), 68 (31), 67 (16), 55 (12). Anal. ($\text{C}_{12}\text{H}_{18}\text{O}_4$) calcd. C 63.70, H 8.02, found C 63.81, H 8.09.

3.1.22. 6,29-Dioxabenzocyclooctacos-(17E)-ene-5,30-dione (9). ^1H NMR (CDCl_3 , 400 MHz) δ 7.71 (m, 2H), 7.52 (m, 2H), 5.32 (m, 2H), 4.28 (t, $J=6.6$ Hz, 4H), 2.00 (m, 4H), 1.72 (m, 4H), 1.16–1.46 (m, 24H) ^{13}C NMR (CDCl_3 , 100 MHz) δ 167.7, 132.3, 130.9, 130.7, 128.9, 66.0, 32.0, 29.5, 29.3, 29.2, 28.8, 28.6, 28.0, 26.2. IR (KBr) 3067, 3025, 2925, 2853, 1730, 1600, 1465, 1448, 1288, 1126, 968, 742 cm^{-1} . MS (EI) m/z (rel. intensity): 442 [M^+] (57), 424 (4), 294 (7), 149 (100), 124 (13), 121 (10), 96 (31), 95 (21), 82 (30), 67 (26), 55 (33), 54 (12), 43 (8), 41 (21). HRMS ($\text{C}_{28}\text{H}_{42}\text{O}_4+\text{Na}$) calcd. 465.29808, found 465.29800.

3.1.23. 1,8-Dioxacyclooctadec-(13E)-ene-2,7-dione (12). ^1H NMR (400 MHz, CDCl_3) δ 5.35 (m, 2H), 4.07 (t, $J=6.7$ Hz, 4H), 2.31 (m, 4H), 2.01 (m, 4H), 1.55–1.66 (m, 8H), 1.40 (m, 4H) ^{13}C NMR (100 MHz, CDCl_3) δ 173.2, 130.6, 64.2, 34.5, 31.6, 27.6, 25.4, 24.9. IR (KBr) 3024, 2932, 2858, 1734, 1241, 971 cm^{-1} . MS (EI) m/z (rel. intensity): 282 [M^+] (12), 136 (100), 121 (39), 108 (62), 79 (62), 55 (67), 29 (15). HRMS ($\text{C}_{16}\text{H}_{26}\text{O}_4+\text{Na}$) calcd. 305.172879, found 305.17255.

3.1.24. N-Methylazacyclohexadec-(11E)-en-2-one (15). ^1H NMR (400 MHz, CD_2Cl_2 , rotamers) δ 5.23 (m, 2H), 3.20 and 3.30 (m and t, $J=7.7$ Hz, 2H), 2.80 and 2.90 (s, 3H), 2.20 (m, 2H), 1.92 (m, 4H), 1.00–1.60 (m, 16H) ^{13}C NMR (100 MHz, CD_2Cl_2 , rotamers) δ 173.3, 173.1, 131.6, 131.5, 131.3, 131.1, 51.3, 47.6, 36.0, 34.1, 33.0, 32.6, 32.5, 32.5, 31.3, 28.9, 28.7, 28.5, 28.3, 27.9, 27.5, 27.5, 27.4, 27.1, 27.0, 26.9, 26.2, 25.7. IR (KBr) 3022, 300, 2926, 2853, 1642, 968 cm^{-1} . MS (EI) m/z (rel. intensity): 251 [M^+] (32), 236 (2), 210 (3), 208 (4), 156 (2), 152 (3), 126 (7), 114 (8), 113 (5), 87 (12), 86 (13), 74 (9), 73 (15), 70 (39), 67 (14), 57 (11), 55 (25), 44 (100), 41 (32). HRMS ($\text{C}_{16}\text{H}_{29}\text{NO}$) calcd. 251.224914, found 251.225135.

3.1.25. 3-Oxabicyclo[16.3.1]docosa-1(22),16,18,20-tetraen-2-one (18). ^1H NMR (400 MHz, CDCl_3) δ 8.04

(m, 1H), 7.90 (dt, $J=7.4, 1.6$ Hz, 1H), 7.37 (m, 2H), 6.41 (d, $J=15.8$ Hz, 1H), 6.26 (dt, $J=15.8, 7.0$ Hz, 1H), 4.31 (t, $J=5.3$ Hz, 2H), 2.28 (m, 2H), 1.75 (m, 2H), 1.16–1.66 (m, 18H). ^{13}C NMR (100 MHz, CDCl_3) δ 166.6, 138.3, 132.2, 131.0, 130.8, 129.6, 128.6, 128.1, 125.8, 65.6, 31.6, 29.5, 28.9, 28.8, 28.5, 28.3, 28.2, 28.1, 27.6, 27.1, 26.9. IR (KBr) 3063, 2926, 2854, 1721, 1653, 1600, 1584, 1483, 1460, 965, 816, 748, 686 cm^{-1} . MS (EI) m/z (rel. intensity): 314 [M^+] (52), 188 (13), 174 (10), 162 (13), 148 (100), 129 (42), 115 (84), 109 (18), 95 (30), 82 (41), 67 (34), 55 (75), 41 (64). HRMS ($\text{C}_{21}\text{H}_{30}\text{O}_2$) calcd. 314.224580, found 314.224826.

3.1.26. 1-(Toluene-4-sulfonyl)-azacyclohepticos-(11E)-ene (21). Mp=104–105 °C. ^1H NMR (400 MHz, CDCl_3) 7.66 (d, $J=8.1$ Hz, 2H), 7.28 (d, $J=8.1$ Hz, 2H), 5.31 (m, 2H), 3.01 (m, 4H), 2.41 (s, 3H), 2.00 (m, 4H), 1.52–1.62 (m, 4H), 1.20–1.40 (m, 24H). ^{13}C NMR (100 MHz, CDCl_3) 142.8, 136.4, 130.8, 129.5, 127.2, 50.1, 32.3, 29.6, 29.3, 29.1, 28.9, 28.8, 28.3, 26.6, 21.4. IR (KBr): 3029, 2921, 2851, 1599, 1494, 1465, 1336, 1156, 1090, 967, 816, 697, 651, 551 cm^{-1} . MS (EI) m/z (rel. intensity): 447 [M^+] (16), 293 (22), 292 (100), 155 (11), 91 (22).

3.1.27. 1-Benzenesulfonyl-cyclooct-(8E)-ene (24). Mp=62–63 °C. ^1H NMR (400 MHz, CDCl_3) δ 7.88 (m, 2H), 7.61–7.67 (m, 1H), 7.52–7.59 (m, 2H), 5.30 (m, 2H), 2.93 (m, 1H), 1.99 (m, 4H), 1.61–1.84 (m, 4H), 1.40–1.50 (m, 2H), 1.18–1.39 (m, 20H). ^{13}C NMR (100 MHz, CDCl_3) δ 138.4, 133.4, 130.9, 130.8, 129.0, 128.7, 64.1, 32.1, 31.8, 28.9, 28.8, 28.6, 28.4, 28.2, 28.0, 27.8, 27.3, 27.2, 26.7, 25.9, 25.8, 24.8. IR (KBr): 3053, 2923, 2852, 1584, 1463, 1447, 1305, 1143, 1083, 974, 729 cm^{-1} . MS (EI) m/z (rel. intensity): 248 (100), 143 (96), 111 (15), 109 (11), 97 (35), 96 (10), 95 (20), 94 (17), 83 (36), 82 (12), 81 (26), 80 (33), 69 (32), 67 (27), 55 (50), 54 (11). Anal. ($\text{C}_{24}\text{H}_{38}\text{O}_2\text{S}$) calcd. C 73.80, H 9.81, found C 73.87, H 9.76.

3.1.28. Oxacyclooctadeca-11,13-dien-2-one (30). ^1H NMR (400 MHz, CDCl_3) δ 5.98 (m, 2H), 5.44 (m, 2H), 4.06 (t, $J=7.1$ Hz, 2H), 2.26 (t, $J=6.5$ Hz, 2H), 2.09 (m, 4H), 1.51–1.61 (m, 4H), 1.28–1.42 (m, 4H), 1.13–1.33 (m, 8H). ^{13}C NMR (100 MHz) δ 137.8, 132.5, 132.1, 131.2, 130.6, 63.9, 34.6, 31.9, 31.5, 29.2, 28.3, 28.1, 27.8, 27.5, 26.6, 25.4, 24.5. IR 2929, 2857, 1733, 1460, 1175, 975 cm^{-1} . MS (EI) m/z (rel. intensity): 264 [M^+] (55), 236 (9), 149 (15), 135 (31), 121 (52), 107 (39), 94 (88), 80 (99), 79 (100), 67 (81), 55 (58), 41 (73). HRMS ($\text{C}_{17}\text{H}_{28}\text{O}_2$) 264.208930, found 264.209119.

3.1.29. Oxacyclodocosa-15,17-dien-2-one (33). ^1H NMR (400 MHz, CDCl_3) δ 5.99 (m, 2H), 5.50 (m, 2H), 4.08 (t, $J=6.6$ Hz, 2H), 2.30 (t, $J=6.7$ Hz, 2H), 2.08 (m, 4H), 1.61 (m, 4H), 1.16 (m, 18H). ^{13}C NMR (100 MHz, CDCl_3) δ 173.9, 132.5, 131.2, 130.9 (2 \times), 64.0, 34.5, 31.8, 31.6, 29.5, 29.2, 28.9, 28.7, 28.3, 28.1, 28.0, 27.8, 27.1, 25.4, 25.4. IR (KBr) 3014, 2926, 2854, 1736, 1659, 1623, 1460, 1247, 1169, 987, 725 cm^{-1} . MS (EI) m/z (rel. intensity): 308 [M^+] (4), 278 (11), 149 (12), 135 (31), 121 (48), 107 (32), 94 (68), 80 (100), 67 (58), 55 (46), 41 (40). HRMS ($\text{C}_{20}\text{H}_{34}\text{O}_2$) calcd. 306.255880, found 306.255638.

3.1.30. (1E,3E)-1-Phenyldeca-1,3-diene (35).³¹ ^1H NMR (400 MHz, CD_2Cl_2) δ 7.20 (m, 5H), 6.68 (dd, $J=15.6,$

10.4 Hz, 1H), 6.34 (d, $J=15.6$ Hz, 1H), 6.12 (dd, $J=10.4, 0.7$ Hz, 1H), 5.76 (dt, $J=15.2, 7.0$ Hz, 1H), 2.06 (m, 2H), 1.28 (m, 8H), 0.81 (m, 3H). ^{13}C NMR (100 MHz, CD_2Cl_2) δ 138.2, 136.6, 130.8, 130.2, 130.0, 129.0, 127.5, 126.5, 32.3, 32.2, 29.8, 29.3, 23.1, 14.3.

3.1.31. (2E,4E)-7-Phenylhepta-2,4-diene (37). ^1H NMR (400 MHz, CDCl_3) δ 7.13–7.30 (m, 5H), 6.01 (m, 2H), 5.57 (m, 2H), 2.68 (m, 2H), 2.36 (m, 2H), 1.71 (m, 3H). ^{13}C NMR (100 MHz, CDCl_3) δ 141.9, 131.6, 130.8, 128.4, 128.3, 127.2, 125.8, 35.9, 34.4, 18.0. IR (KBr) 3085, 3063, 3017, 2928, 2853, 1604, 1496, 1453, 1377, 988, 745, 698 cm^{-1} . MS (EI) m/z (rel. intensity): 172 [M^+] (17), 91 (31), 81 (100), 79 (13). HRMS ($\text{C}_{13}\text{H}_{16}$) calcd. 172.125200, found 172.125299.

3.1.32. (7E,9E)-Hexadec-7-9-diene (39).³² ^1H NMR (400 MHz, CDCl_3) δ 5.98 (m, 2H), 5.55 (m, 2H), 2.03 (m, 4H), 1.16–1.46 (m, 16H), 0.87 (m, 6H). ^{13}C NMR (100 MHz, CDCl_3) δ 132.0, 130.0, 32.2, 31.4, 29.0, 28.5, 22.2, 13.7. IR (KBr) 3014, 2957, 2925, 2855, 1622, 1378, 985, 724 cm^{-1} . MS (EI) m/z (rel. intensity): 222 [M^+] (35), 138 (15), 110 (52), 95 (44), 81 (56), 67 (100), 55 (26), 41 (34), 29 (17).

3.2. X-ray crystallographic study

Suitable crystals were obtained by recrystallization from *n*-heptane (4), diethylether (6) and *n*-hexane (21). Data were recorded using an Enraf–Nonius CAD-IV-diffractometer (4) and Enraf–Nonius KappaCCD diffractometer (6 and 21) with graphite-monochromated $\text{Mo K}\alpha$ radiation ($\lambda=0.71073$ Å). The crystal was mounted in a stream of cold nitrogen gas. The structures were solved by direct methods (SHELXS-97)³³ and refined by full-matrix least-squares techniques against F^2 (SHELXL-97).³⁴ Hydrogen atoms were inserted from geometry consideration using the HFIX option of the program. Crystallographic data (excluding structure factors) have been deposited with the Cambridge Crystallographic Data Centre as supplementary publication number CCDC 234489, 234490 and 234491. Copies of the data can be obtained, free of charge, on application to CCDC, 12 Union Road, Cambridge CB2 1EZ, UK (fax: +44-1223-336033 or e-mail: deposit@ccdc.cam.ac.uk).

3.2.1. Selected data for compound 4. $\text{C}_{12}\text{H}_{16}\text{O}_4$, $M_r=224.25$ g mol $^{-1}$, colorless, crystal size 0.64 \times 0.64 \times 0.07 mm, triclinic, PI No. 2], $a=8.542(3)$, $b=11.595(4)$, $c=12.050(5)$ Å, $\alpha=92.96(4)$, $\beta=105.72(3)$, $\gamma=91.15(3)^\circ$, $V=1146.6(7)$ Å 3 , $Z=4$, $D_{\text{calc}}=1.299$ mg m $^{-3}$, $\mu=0.097$ mm $^{-1}$, $T=100$ K, 8942 reflections collected, 5194 independent reflections, 3424 reflections with $I>2\sigma(I)$, $\theta_{\text{max}}=27.47^\circ$, 289 refined parameters, $R=0.086$, $R_w=0.291$, $S=1.074$, largest diff. peak and hole=0.596/−0.602 e Å $^{-3}$.

3.2.2. Selected data for compound 6. $\text{C}_{12}\text{H}_{18}\text{O}_4$, $M_r=226.26$ g mol $^{-1}$, colorless, crystal size 0.20 \times 0.11 \times 0.06 mm, monoclinic, $C2/c$ [No. 15], $a=7.7012(3)$, $b=16.4386(6)$, $c=9.1563(4)$ Å, $\beta=93.009(2)^\circ$, $V=1157.56(8)$ Å 3 , $Z=4$, $D_{\text{calc}}=1.144$ mg m $^{-3}$, $\mu=0.147$ mm $^{-1}$, $T=100$ K, 5442 reflections collected, 2195 independent reflections, 2195 reflections with $I>2\sigma(I)$,

θ_{\max} =27.50°, 109 refined parameters, R =0.045, R_w =0.149, S =1.031, largest diff. peak and hole=0.410/−0.251 e Å^{−3}.

3.2.3. Selected data for compound 21. C₂₇H₄₅NO₂S, M_r =447.70 g mol^{−1}, colorless, crystal size 0.40×0.18×0.09 mm, monoclinic, $P2_1/c$ [No. 14], a =30.7015(3), b =7.57090(10), c =11.21650(10) Å, β =94.65°, V =2598.57(5) Å³, Z =4, D_{calc} =1.298 mg m^{−3}, μ =0.096 mm^{−1}, T =100 K, 55819 reflections collected, 7921 independent reflections, 6699 reflections with $I > 2\sigma(I)$, θ_{\max} =30.59°, 281 refined parameters, R =0.052, R_w =0.119, S =1.078, largest diff. peak and hole=0.466/−0.344 e Å^{−3}.

Acknowledgements

Generous financial support by the Deutsche Forschungsgemeinschaft (Leibniz award to A. F.), the Fonds der Chemischen Industrie, and the Merck Research Council is gratefully acknowledged. We thank Dr. C. W. Lehmann for solving the X-ray structures as well as Dr. R. Mynott and C. Wirtz for their help with some of the NMR spectra.

References and notes

- Reviews: (a) Trnka, T. M.; Grubbs, R. H. *Acc. Chem. Res.* **2001**, *34*, 18–29. (b) Fürstner, A. *Angew. Chem., Int. Ed.* **2000**, *39*, 3012–3043. (c) Grubbs, R.; Chang, S. *Tetrahedron* **1998**, *54*, 4413–4450. (d) Schrock, R. R. *Top. Organomet. Chem.* **1998**, *1*, 1–36. (e) Schuster, M.; Blechert, S. *Angew. Chem., Int. Ed. Engl.* **1997**, *36*, 2037–2056. (f) Fürstner, A. *Top. Catal.* **1997**, *4*, 285–299.
- For leading references on the synthesis of cyclic 1,3-dienes by RCM strategies and illustrations of the selectivity issues related to diene–ene cyclizations see: (a) Wagner, J.; Martin Cabrejas, L. M.; Grossmith, C. E.; Papageorgiou, C.; Senia, F.; Wagner, D.; France, J.; Nolan, S. P. *J. Org. Chem.* **2000**, *65*, 9255–9260. (b) Martin Cabrejas, L. M.; Rohrbach, S.; Wagner, D.; Kallen, J.; Zenke, G.; Wagner, J. *Angew. Chem., Int. Ed.* **1999**, *38*, 2443–2446. (c) Paquette, L.; Basu, K.; Eppich, J. C.; Hofferberth, J. E. *Helv. Chim. Acta* **2002**, *85*, 3033–3051. (d) Garbaccio, R.; Stachel, S. J.; Baeschlin, D. K.; Danishefsky, S. J. *J. Am. Chem. Soc.* **2001**, *123*, 10903–10908. (e) Yamamoto, K.; Garbaccio, R. M.; Stachel, S. J.; Solit, D. B.; Chiosis, G.; Rosen, N.; Danishefsky, S. J. *Angew. Chem., Int. Ed.* **2003**, *42*, 1280–1284. (f) Biswas, K.; Lin, H.; Njardarson, J. T.; Chappell, M. D.; Chou, T.-C.; Guan, Y.; Tong, W. P.; He, L.; Horwitz, S. B.; Danishefsky, S. J. *J. Am. Chem. Soc.* **2002**, *124*, 9825–9832. (g) Dvorak, C. A.; Schmitz, W. D.; Poon, D. J.; Pryde, D. C.; Lawson, J. P.; Amos, R. A.; Meyers, A. I. *Angew. Chem., Int. Ed.* **2000**, *39*, 1664–1666. (h) Bach, T.; Lemarchand, A. *Synlett* **2002**, 1302–1304. (i) Sedrani, R.; Martin Cabrejas, L. M.; Papageorgiou, C. D.; Senia, F.; Rohrbach, S.; Wagner, D.; Thai, B.; Eme, A.-M. J.; France, J.; Oberer, L.; Rihs, G.; Zenke, G.; Wagner, J. *J. Am. Chem. Soc.* **2003**, *125*, 3849–3859.
- See the following for leading references on triene formation by metathesis in which useful levels of regio- and stereocontrol have been attained: (a) Evano, G.; Schaus, J. V.; Panek, J. S. *Org. Lett.* **2004**, *6*, 525–528. (b) Wang, X.; Porco, J. A., Jr. *J. Am. Chem. Soc.* **2003**, *125*, 6040–6041.
- For an example see: Fürstner, A.; Radkowski, K.; Wirtz, C.; Goddard, R.; Lehmann, C. W.; Mynott, R. *J. Am. Chem. Soc.* **2002**, *124*, 7061–7069.
- Fürstner, A.; Seidel, G. *Angew. Chem., Int. Ed.* **1998**, *37*, 1734–1736.
- (a) Fürstner, A.; Guth, O.; Rumbo, A.; Seidel, G. *J. Am. Chem. Soc.* **1999**, *121*, 11108–11113. (b) Fürstner, A.; Mathes, C.; Lehmann, C. W. *J. Am. Chem. Soc.* **1999**, *121*, 9453–9454. (c) Fürstner, A.; Mathes, C.; Lehmann, C. W. *Chem. Eur. J.* **2001**, *7*, 5299–5317.
- (a) Fürstner, A.; Stelzer, F.; Rumbo, A.; Krause, H. *Chem. Eur. J.* **2002**, *8*, 1856–1871. (b) Fürstner, A.; Radkowski, K.; Grabowski, J.; Wirtz, C.; Mynott, R. *J. Org. Chem.* **2000**, *65*, 8758–8762. (c) Fürstner, A.; Rumbo, A. *J. Org. Chem.* **2000**, *65*, 2608–2611. (d) Fürstner, A.; Seidel, G. *J. Organomet. Chem.* **2000**, *606*, 75–78. (e) Fürstner, A.; Castanet, A.-S.; Radkowski, K.; Lehmann, C. W. *J. Org. Chem.* **2003**, *68*, 1521–1528. (f) Fürstner, A.; Mathes, C.; Grela, K. *Chem. Commun.* **2001**, 1057–1059. (g) Fürstner, A.; Grela, K.; Mathes, C.; Lehmann, C. W. *J. Am. Chem. Soc.* **2000**, *122*, 11799–11805. (h) Fürstner, A.; Grela, K. *Angew. Chem., Int. Ed.* **2000**, *39*, 1234–1236. (i) Fürstner, A.; Dierkes, T. *Org. Lett.* **2000**, *2*, 2463–2465. (j) Fürstner, A.; Mathes, C. *Org. Lett.* **2001**, *3*, 221–223. (k) Song, D.; Blond, G.; Fürstner, A. *Tetrahedron* **2003**, *59*, 6899–6904. (l) Fürstner, A.; DeSouza, D.; Parra-Rapado, L.; Jensen, J. T. *Angew. Chem., Int. Ed.* **2003**, *42*, 5358–5360.
- (a) Aguilera, B.; Wolf, L. B.; Nieczypor, P.; Rutjes, F. P. J. T.; Overkleeft, H. S.; van Hest, J. C. M.; Schoemaker, H. E.; Wang, B.; Mol, J. C.; Fürstner, A.; Overhand, M.; van der Marel, G. A.; van Boom, J. H. *J. Org. Chem.* **2001**, *66*, 3584–3589. (b) IJsselstijn, M.; Aguilera, B.; van der Marel, G.; van Boom, J. H.; van Delft, F. L.; Schoemaker, H.; Overkleeft, H. S.; Rutjes, F. P. J. T.; Overhand, M. *Tetrahedron Lett.* **2004**, *45*, 4379–4382.
- For recent applications of RCAM to non-natural products see: (a) Hellbach, B.; Gleiter, R.; Rominger, F. *Synthesis* **2003**, 2535–2541. (b) Brizius, G.; Billingsley, K.; Smith, M.; Bunz, U. H. F. *Org. Lett.* **2003**, *5*, 3951–3954. (c) Bauer, E.; Szafert, S.; Hampel, F.; Gladysz, J. A. *Organometallics* **2003**, *22*, 2184–2186. (d) Miljanic, O.; Vollhardt, K. P. C.; Whitener, G. D. *Synlett* **2003**, 29–34. (e) Grela, K.; Ignatowska, J. *Org. Lett.* **2002**, *4*, 3747–3749. (f) Pschirer, N.; Fu, W.; Adams, R. D.; Bunz, U. H. F. *Chem. Commun.* **2000**, 87–88.
- Preliminary communication: Fürstner, A.; Radkowski, K. *Chem. Commun.* **2002**, 2182–2183.
- For exploratory studies and pertinent discussions see: (a) Burch, R. R.; Muetterties, E. L.; Teller, R. G.; Williams, J. M. *J. Am. Chem. Soc.* **1982**, *104*, 4257–4258. (b) Burch, R.; Shusterman, A. J.; Muetterties, E. L.; Teller, R. G.; Williams, J. M. *J. Am. Chem. Soc.* **1983**, *105*, 3546–3556. (c) Schleyer, D.; Niessen, H.; Bargon, J. *New J. Chem.* **2001**, *25*, 423–426. (d) Tani, K.; Iseki, A.; Yamagata, T. *Chem. Commun.* **1999**, 1821–1822.
- (a) Tsuda, T.; Yoshida, T.; Kawamoto, T.; Saegusa, T. *Org. Chem.* **1987**, *52*, 1624–1627. (b) Jones, T.; Denmark, S. E. *Org. Synth.* **1986**, *64*, 182–188.
- (a) Castro, C.; Stephens, R. D. *J. Am. Chem. Soc.* **1964**, *86*, 4358–4363. (b) Smith, A. B.; Levenberg, P. A.; Suits, J. Z. *Synthesis* **1986**, 184–189. (c) Carreira, E.; DuBois, J. *J. Am.*

- Chem. Soc.* **1995**, *117*, 8106–8125. For a review of Cr(II) see: (d) Fürstner, A. *Chem. Rev.* **1999**, *99*, 991–1045.
14. Brandsma, L.; Nieuwenhuizen, W. F.; Zwikker, J. W.; Mäeorg, U. *Eur. J. Org. Chem.* **1999**, 775–779, and literature cited therein.
 15. Reviews: (a) Ojima, I.; Li, Z.; Zhu, J. *The Chemistry of Organosilicon Compounds*; Rappoport, Z., Apeloig, Y., Eds.; Wiley: Chichester, UK, 1998; Vol. 2, pp 1687–1792. (b) In *Comprehensive Handbook on Hydrosilylation*; Marciniak, B., Ed.; Pergamon: Oxford, 1992. (c) Hiyama, T.; Kusumoto, T. *Comprehensive Organic Synthesis*; Trost, B. M., Fleming, I., Eds.; Pergamon: Oxford, 1991; Vol. 8, pp 763–792.
 16. (a) Takeuchi, R.; Nitta, S.; Watanabe, D. *Org. Chem.* **1995**, *60*, 3045–3051. (b) Mori, A.; Takahisa, E.; Kajiro, H.; Hirabayashi, K.; Nishihara, Y.; Hiyama, T. *Chem. Lett.* **1998**, *27*, 443–444. (c) Tanke, R.; Crabtree, R. H. *J. Am. Chem. Soc.* **1990**, *112*, 7984–7989. (d) Ojima, I.; Clos, N.; Donovan, R.; Ingallina, P. *Organometallics* **1990**, *9*, 3127–3133. (e) Na, Y.; Chang, S. *Org. Lett.* **2000**, *2*, 1887–1889. (f) Faller, J. W.; D'Alliessi, D. G. *Organometallics* **2002**, *21*, 1743–1746.
 17. For an exception see: Sudo, T.; Asao, N.; Gevorgyan, V.; Yamamoto, Y. *J. Org. Chem.* **1999**, *64*, 2494–2499.
 18. (a) Gill, T.; Mann, K. R. *Organometallics* **1982**, *1*, 485–488. (b) Steinmetz, B.; Schenk, W. A. *Organometallics* **1999**, *18*, 943–946. (c) Trost, B.; Older, C. M. *Organometallics* **2002**, *21*, 2544–2546.
 19. (a) Trost, B.; Ball, Z. T. *J. Am. Chem. Soc.* **2001**, *123*, 12726–12727. (b) Trost, B. M.; Ball, Z. T.; Jöge, T. *J. Am. Chem. Soc.* **2002**, *124*, 7922–7923. (c) Trost, B. M.; Ball, Z. T. *J. Am. Chem. Soc.* **2003**, *125*, 30–31. (d) Trost, B. M.; Ball, Z. T.; Jöge, T. *Angew. Chem., Int. Ed.* **2003**, *42*, 3415–3418.
 20. For a somewhat controversial discussion of the mechanism see: (a) Chung, L. W.; Wu, Y.-D.; Trost, B. M.; Ball, Z. T. *J. Am. Chem. Soc.* **2003**, *125*, 11578–11582. (b) Crabtree, R. H. *New J. Chem.* **2003**, *27*, 771–772.
 21. For related studies see: (a) Denmark, S. E.; Pan, W. *Org. Lett.* **2002**, *4*, 4163–4166. (b) Denmark, S.; Pan, W. *Org. Lett.* **2003**, *5*, 1119–1122.
 22. (a) Schrock, R.; Clark, D. N.; Sancho, J.; Wengrovius, J. H.; Rocklage, S. M.; Pedersen, S. F. *Organometallics* **1982**, *1*, 1645–1651. (b) Freudenberger, H.; Schrock, R. R.; Churchill, M. R.; Rheingold, A. L.; Ziller, J. W. *Organometallics* **1984**, *3*, 1563–1573. (c) Listemann, M.; Schrock, R. R. *Organometallics* **1985**, *4*, 74–83. (d) Schrock, R. R. *Polyhedron* **1995**, *14*, 3177–3195.
 23. Brandsma, L. *Synthesis of Acetylenes, Allenes and Cumulenes. Methods and Techniques*; Elsevier: Oxford, 2004.
 24. (a) Fleming, I.; Newton, T.; Roessler, F. *J. Chem. Soc., Perkin Trans. 1* **1981**, 2527–2532. (b) Kaye, A.; Pattenden, G.; Roberts, S. M. *Tetrahedron Lett.* **1986**, *27*, 2033–2036.
 25. Oda, H.; Sato, M.; Morizawa, Y.; Oshima, K.; Nozaki, H. *Tetrahedron* **1985**, *41*, 3257–3268.
 26. For the use of CuI/TBAF to effect protodesilylation of acyclic vinylsilanes see Ref. 19b.
 27. Tamao, K.; Kobayashi, K.; Ito, Y. *Tetrahedron Lett.* **1989**, *30*, 6051–6054.
 28. Breitmaier, E.; Voelter, W. *Carbon-13 NMR Spectroscopy High-Resolution Methods and Applications in Organic Chemistry and Biochemistry*; 3rd ed. VCH: Weinheim, 1987; pp. 192–194.
 29. For intermolecular metathesis of enynes using an in situ catalyst system see: Brizius, G.; Bunz, U. H. F. *Org. Lett.* **2002**, *4*, 2829–2831.
 30. (a) Matsubara, S.; Matsuda, H.; Hamatani, T.; Schlosser, M. *Tetrahedron* **1988**, *44*, 2855–2863. (b) Maercker, A.; Girreser, U. *Tetrahedron* **1994**, *50*, 8019–8034.
 31. Organ, M.; Cooper, J. T.; Rogers, L. R.; Soleymanzadeh, F.; Paul, T. *J. Org. Chem.* **2000**, *65*, 7959–7970.
 32. Negishi, E.; Takahashi, T.; Akiyoshi, K. *J. Organomet. Chem.* **1987**, *334*, 181–194.
 33. Sheldrick, G.M., SHELXS-97, Program for the determination of crystal structures; University of Göttingen, Germany, 1997.
 34. Sheldrick, G.M., SHELXL-97, Program for least-squares refinement of crystal structures; University of Göttingen, Germany, 1997.

Asymmetric synthesis of cyclic β -hydroxyallylsilanes via sequential allyltitanation-ring closing metathesis

Jean-Michel Adam,^a Laurence de Fays,^b Michel Laguerre^b and Léon Ghosez^{b,*}

^aDépartement de Chimie, Université catholique de Louvain, place L. Pasteur, B-1348 Louvain-la-Neuve, Belgium

^bInstitut Européen de Chimie et Biologie, 2 rue Robert Escarpit, 33600 Pessac, France

Received 6 April 2004; revised 19 May 2004; accepted 21 May 2004

Available online 26 June 2004

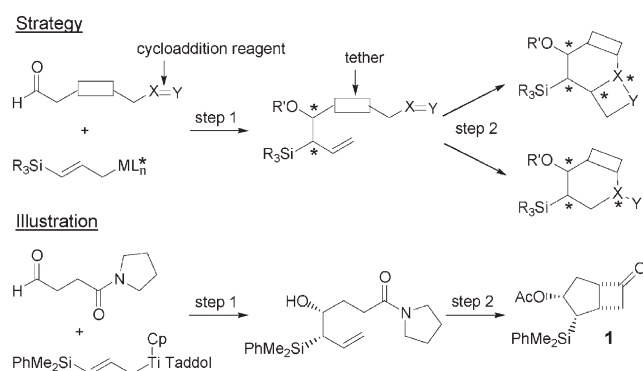
Dedicated to Professor Robert H. Grubbs for his seminal contributions to organic and polymer synthesis

Abstract—Highly enantioenriched cyclic β -hydroxyallylsilanes have been prepared via enantioselective allylation of unsaturated aldehydes using a chiral allyltitanium reagent, followed by a ring-closing metathesis. Functionalized rings of various sizes have been synthesized and the electronic effect of the silicon group in the RCM reaction has been studied. The resulting cyclic β -hydroxyallylsilanes reacted stereoselectively with a variety of electrophilic reagents. A first application of this method to the synthesis of a highly functionalized dihydropyran is reported.

© 2004 Elsevier Ltd. All rights reserved.

1. Introduction

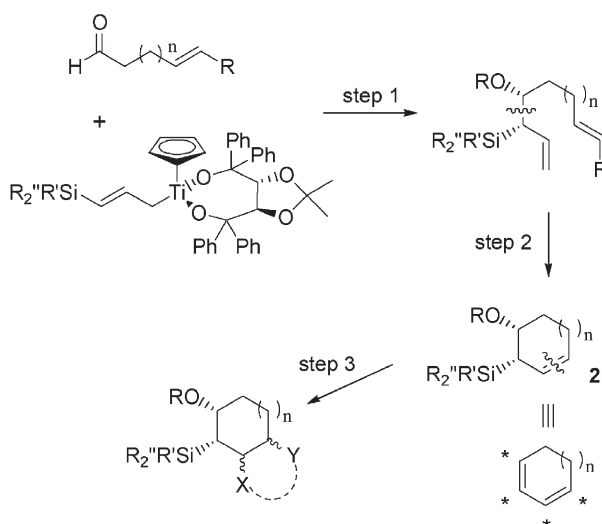
A convergent strategy for the enantioselective synthesis of (poly)cyclic molecules consists of a two-step sequence of reactions starting with an asymmetric allylation of an aldehyde with an organometallic reagent followed by an intramolecular diastereoselective silicon-directed (cyclo)addition reaction (Scheme 1).



Scheme 1.

A first example of this strategy has been reported in 1999 by our group.¹ It involved the reaction of a silyl-substituted allyltitanate reagent with an aldehyde carrying a tertiary amide group at the β -carbon followed by a silicon-directed

intramolecular cycloaddition reaction of the allylsilane to an in situ generated keteniminium reagent. This led to bicyclo[3.2.0]heptan-6-one **1** in good yield and high enantiomeric excess.



Scheme 2.

The combination of step 1 with a ring-closing metathesis (RCM)² was considered as an attractive sequence for the synthesis of β -hydroxyallylsilanes **2** which can be looked upon as chiral equivalents of cyclic conjugated dienes (Scheme 2). The dense functionality of these intermediates should allow to take full benefit of the presence of a silyl

Keywords: Ring closing metathesis; Allyltitanation; β -Hydroxy-allylsilane; Asymmetric synthesis; Dihydropyran.

* Corresponding author. Tel.: +33-5-4000-2217; fax: +33-5-4000-2222; e-mail address: l.ghosez@iecb.u-bordeaux.fr

substituent as control element for further transformations into a variety of enantiopure mono- and polycyclic compounds. In earlier examples of sequential asymmetric allylation-RCM, the olefinic partners for the RCM were always linked by a heteroatom which became part of the newly formed ring.³ A preliminary report on the sequence of **Scheme 2** has been recently published by Roush et al. who elegantly applied it to the synthesis of conduritol and inositols of high enantiomeric purities.⁴ We now wish to report our studies of the scope and limitation of the allylation-RCM sequence and illustrate the synthetic potential of the resulting products **2**.⁵

2. Substrate design

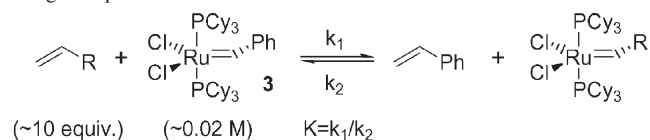
2.1. Carbene-exchange reaction

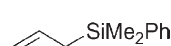
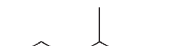
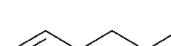
In the sequence described in **Scheme 2**, one of the olefinic partners for the RCM is an allylsilane. In order to optimize the reaction in terms of yields and turnover of the catalyst, we decided to perform some model experiments.

Several examples of RCM of allylsilanes have been reported. Crowe and coworkers assigned the preference of allylsilanes for cross-metathesis to the silicon β -effect.⁶ Doubts about the role of this β -effect arose from a report of Blechert et al.⁷ Based on a competition experiment between TMS-CH₂CH=CH₂ and *t*-Bu-CH₂CH=CH₂, they deduced that the β -effect of silicon did not significantly affect the rate of metathesis. However, since the kinetics of the reaction were not known, the identification of the carbene from which the cross-metathesis mainly occurred was not possible.

We first evaluated the carbene exchange reaction between several olefins and Grubbs' catalyst **3** (**Table 1**). It was possible to determine K and hence k_2 by taking advantage of the higher rate of the carbene exchange reaction as compared to the productive metathesis.⁸ Indeed, equilibrium was reached before a significant amount of

Table 1. Relative second-order rate constants (k_{rel}) for metathesis reactions using 10 equiv. of olefin



Olefin	k_{1rel}^a	K^b	k_{2rel}^a
	0.5	$3.1 \pm 0.2 \times 10^{-3}$	4.8
	0.9	$19 \pm 3 \times 10^{-2c}$	1.6
	1	$32 \pm 4 \times 10^{-2}$	1

^a $k_{1rel} = k_1(\text{olefin})/k_1(\text{hexene})$, $k_{2rel} = k_2(\text{olefin})/k_2(\text{hexene})$.

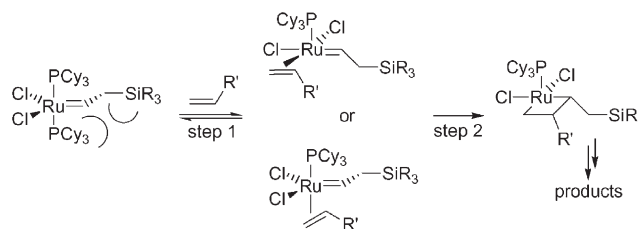
^b $k(K) \pm$ standard deviation.

^c The equilibrium constant ($K=0.32$, rt) for hexene is slightly higher than the previously reported value of 0.2 determined by Grubbs and coworkers for the same reaction at 7 °C.⁸

methylidene carbene was formed. We selected hexene as a reference, 4-methylpentene to evaluate the impact of steric hindrance, and allyldimethylphenylsilane to measure the influence of the silyl substituent.

Examination of k_{1rel} showed that electronic effects mediated by σ -bonds did not strongly influence the reactivity of the olefins. The lower rate observed for the allylsilane was mainly attributed to steric effects since the silicon β -effect should have increased the rate of reaction with the electrophilic carbene complex. The trend in reactivity (k_{2rel}) seems to roughly follow the steric demand of the substituents. The more reactive complex was the allyldimethylphenylsilane-substituted carbene. This could be explained by an increase of phosphine lability as a result of the presence of the bulky silyl group (**Scheme 3**).⁹

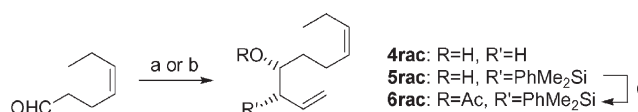
The influence of the silyl group on other parameters such as olefin complexation (step 1) or the rate of the metathesis (step 2) was believed to be limited. First, the geometric requirement for a strong hyperconjugating interaction would be difficult to fulfill and secondly, electronic effects are only slightly influencing step 2 as seen by the small ρ value determined in the gas phase (0.69).⁸ Moreover, if operating, the β -effect is expected to disfavor olefin complexation which should result in a decrease of reactivity. We thus propose that, in carbene exchange reactions, the silicon β -effect is not an important parameter and that steric effects are probably the true reactivity modulators.



Scheme 3.

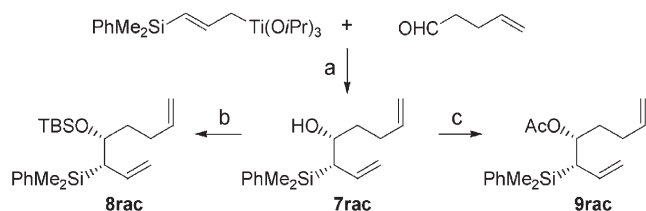
2.2. RCM model experiments

2.2.1. Synthesis of the model substrates. Two types of model substrates were prepared to study the reactivity of the allylsilane. Racemic substrates **4rac** and **5rac** were prepared by allylmetallations of hept-4-enal. Acetylation of **5rac** gave **6rac** (**Scheme 4**).



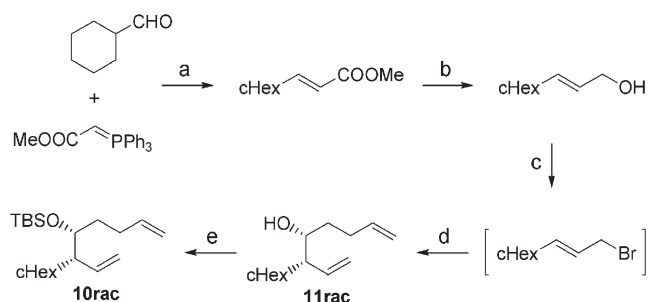
Scheme 4. Reagents and conditions: (a) allylmagnesium bromide (1.1 equiv.), Et₂O, 95%; (b) allyldimethylphenylsilane (1.15 equiv.), THF, *n*-BuLi (1.15 equiv.), 3 h, -78 °C then 40% aqueous NH₄F, 15 h, rt, 87%; (c) pyridine (4 equiv.), CH₃COCl (3 equiv.), CH₂Cl₂, 1.5 h, rt, 95%.

Racemic dienes **7rac-9rac** were prepared by allyltitanation of 4-pentenal followed by protection of the alcohol by either an acetyl or a *t*-butyldimethylsilyl group (**Scheme 5**).



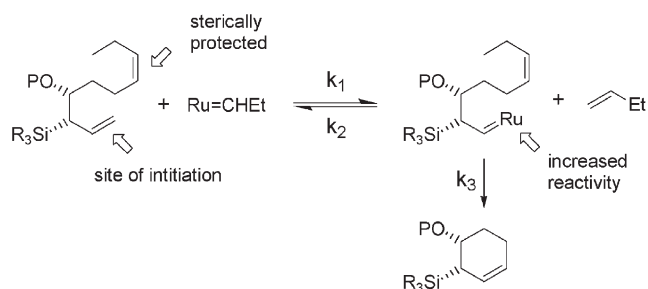
Scheme 5. Reagents and conditions: (a) allyldimethylphenylsilane (1.15 equiv.), *n*BuLi 2.1 M (1.15 equiv.), $\text{ClTi}(\text{O}i\text{Pr})_3$ (1.25 equiv.) to give γ -silylallyltitanate, then 4-pentenal, THF, -78°C , 2 h, 75%; (b) TBSCl (1.2 equiv.), imidazole (1.3 equiv.), 36 h, 50°C , DMF, 83%; (c) pyridine (4 equiv.), CH_3COCl (3 equiv.), CH_2Cl_2 , 30 min, rt, 95%.

Diene **10rac**, bearing a cyclohexyl group at the allylic position was prepared by a simple sequence starting from cyclohexylcarboxaldehyde (Scheme 6). This diene gave us the opportunity to evaluate the accelerating effect due to steric hindrance. The cyclohexyl group was selected since it has an *A* value comparable to that of a TMS group and will induce no electronic effect.¹⁰ Wittig olefination, reduction of the ester, Corey bromination of the allylic alcohol and chromium-mediated allylation¹¹ of pentenal gave the desired homoallylic alcohol **11rac**. Protection of the alcohol by a TBS group yielded **10rac**.



Scheme 6. Reagents and conditions: (a) CHCl_3 , reflux, 87%, 97% of *E* (GC/NMR); (b) DIBAL, >99%; (c) DMS/NBS, 78%; (d) CrCl_2 (2 equiv.), THF, rt, 15 h, 61–71%; (e) TBSCl (1.1 equiv), imidazole (2 equiv), 16 h, 50°C , DMF, 73%.

2.2.2. Ring closing metathesis. We first examined dienes **4rac–6rac**. In this case, we expected the initiation to take place mainly at the allylsilane double bond since the other olefin is sterically protected (Scheme 7).

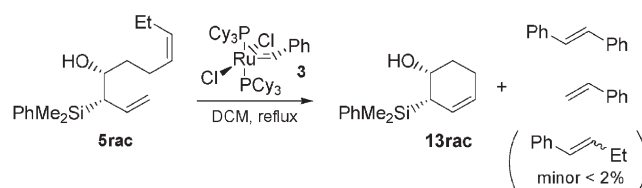


Scheme 7.

On the basis of the results of Section 2.1, we hoped that these carbenes would also be more reactive in the productive metathesis step as a result of increased phosphine lability of the silyl-substituted carbene. In the case described in Scheme 7 the propagating species would be an alkylidene carbene which has been shown to be more

active and decompose more slowly than the corresponding methyldiene.¹²

We checked that the initiation was taking place at the terminal olefin. Diene **5rac** was reacted with 0.8 equiv. of **3** in refluxing CH_2Cl_2 and the crude mixture was analysed by GC-MS (EI and CI). In addition to the starting material and the cyclized product, analyses revealed the presence of tricyclohexylphosphine, styrene, stilbene as well as only trace amounts of 2-ethylstyrene (Scheme 8).



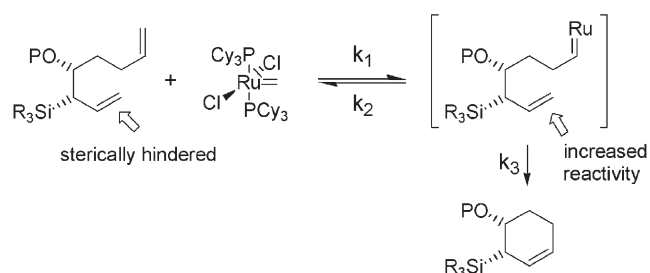
Scheme 8.

The homoallylic alkoxy derivatives **4rac–6rac** were reacted with a catalytic amount of **3**. ^1H NMR and GC analysis of the crude mixtures indicated clean conversions. Table 2 shows that the main influence of the silicon group is to decrease the rate of the RCM due to its steric hindrance.

Table 2.

Diene	R=	R'='	3 (mol%)	Temperature	Time	Product	Yield (%)
4rac	H	H	1.6	rt	1 h	12rac	>95
4rac	H	H	1.6	Reflux	<5 min	12rac	>95
5rac	H	PhMe_2Si	3.2	Reflux	42 h	13rac	86
6rac	Ac	PhMe_2Si	1.6	Reflux	24 h	14rac	91

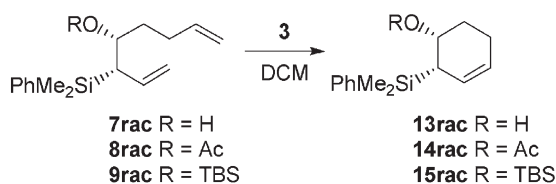
The modification of the initiation site should lead to an increase of reactivity: when the two double bonds are terminal, the carbene complex will react faster at the less hindered double bond, the one without any substituent at the allylic position (Scheme 9).



Scheme 9.

The three dienes **7rac–9rac** were reacted with catalyst **3** with varying efficiency depending on the protecting group (Table 3). With 1.6 mol% of catalyst at room temperature, the homoallylic alcohol **7rac** reacted rapidly up to 40% conversion at which point the reaction nearly stopped (entry

Table 3.

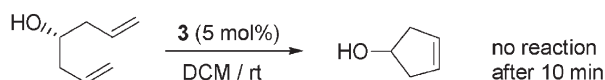


Entry	Diene	R=	3 (mol%)	Temperature	Time	Product	Conv. (%)
1	7rac	H	1.6	rt	3 h ^a	13rac	49
2	7rac	H	1.6	Reflux	1.5 h	13rac	64
3	7rac	H	4.8	Reflux	2 h	13rac	98
4	8rac	Ac	1.6	rt	20 min	14rac	> 99
5	9rac	TBS	1.6	rt	2 min	15rac	> 99
6	9rac	TBS	0.05	Reflux	1 h	15rac	98

^a 40% conversion after 5 min then, the reaction nearly stopped.

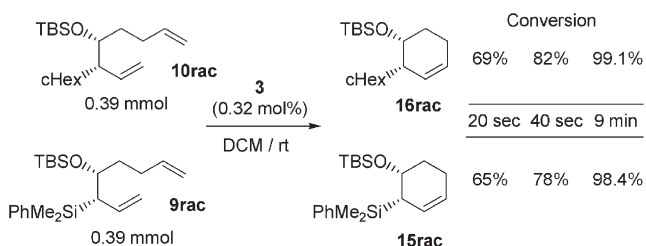
1). Heating at reflux didn't allow complete conversion (entry 2). It was necessary to triple the catalyst concentration to achieve a complete conversion of the starting material (entry 3). The acetyl-protected diene **8rac** gave a 92% conversion after only 4 min and quantitative conversion after 20 min at room temperature (entry 4). More surprising was the fast RCM of the *t*-butyldimethylsilyl ether **9rac**, the reaction being complete within 2 min at room temperature (entry 5). In this case, it was possible to complete the RCM in 1 h in refluxing dichloromethane with as little as 0.05 mol% catalyst (entry 6).

Interestingly, comparison of Table 2 (entry 1) and Table 3 (entry 1) with a previous result on metathesis of hept-1,6-diene-4-ol¹³ (Scheme 10) indicates that proper choice of the site of carbene exchange could prevent formation of unreactive chelates and hence deliver higher possible turnover.



Scheme 10.

The unexpected high reactivity of diene **9rac** could result from the high nucleophilicity of the allylsilane as proposed by Crowe and coworkers.⁶ If the silicon β-effect was responsible for this high reactivity, the replacement of the silyl substituent by a group of comparable steric hindrance but lacking electronic effects such as cyclohexyl, should induce a decrease in reactivity. A competition experiment was performed using equimolar amounts of **9rac** and **10rac** (Scheme 11).



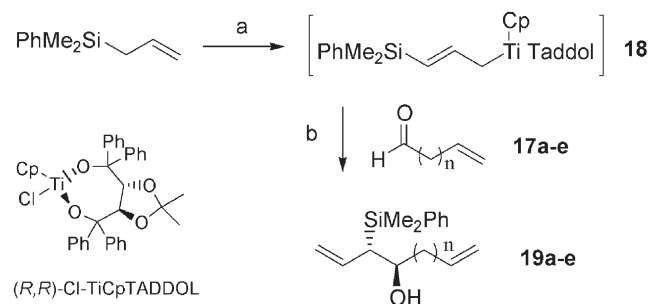
Scheme 11.

GC analysis of the mixture after 20 s, 40 s and 9 min showed no significant difference in reactivity between the two dienes. This was also confirmed in separate experiments. Thus the enhanced reactivity of these dienes is primarily a consequence of the bulk of the substituents which could accelerate the loss of a phosphine ligand but probably also increase the population of the conformation necessary for RCM.

3. Asymmetric allylation-RCM: application to the synthesis of β-hydroxyallylsilanes

3.1. Preparation of chiral diene equivalents via asymmetric allyltitanation

Unlike Roush et al., we performed the asymmetric allylmethylation of the unsaturated aldehydes **17a-e**¹⁴ with (*E*)-γ-dimethylphenylsilyl substituted titanium reagent **18** generated from allyldimethylphenylsilane, *n*-BuLi and (*R,R*)-Cl-TiCpTADDOL at -78 °C (Table 4). These allylmethyl reagents were known to give the *anti*-β-hydroxyallylsilanes in good yields and high enantiomeric purities.¹⁵ This was also the case here. The absolute configurations of **19a-e** were assigned by analogy with previous results.¹ As will be shown later, this was confirmed by analysis of the absolute conformation of the triol derived from **19b** (see Scheme 17).

Table 4. Asymmetric allylmethylation of terminally unsaturated aldehydes **17a-e** with **18**

Entry	Aldehyde	<i>n</i> =	Product	Yield (%)	ee (%)
1	17a	1	19a	68	96
2	17b	2	19b	68	92
3	17c	3	19c	75	90
4	17d	4	19d	67	94
5	17e	8	19e	71	91

Reagents and conditions: (a) *n*-BuLi (1.1 equiv.) in THF, 20 min, rt then (*R,R*)-Cl-TiCpTADDOL (1.15 equiv.), 30 min, -78 °C to give a solution of **18**; (b) aldehyde **17a-e** (1 equiv.), 3 h, -78 °C, 40% aqueous NH₄F, 15 h, rt, flash chromatography, ee determined by HPLC on a Chiralcel AS or OD column, the other diastereoisomer was not detected (de > 98%).

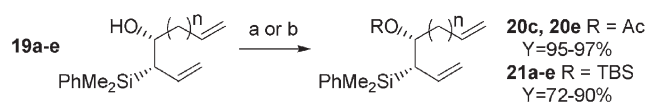
Scheme 12. Reagents and conditions: (a) pyridine (3.5 equiv.), CH₃COCl (2.5 equiv.), CH₂Cl₂, 30 min, rt; (b) TBSCl (1.5 equiv.), imidazole (4 equiv.), 16 h, 50 °C, DMF.

Table 5. Ring-closing metathesis of dienes **19b**, **20** and **21**: assays with different metathesis pre-catalysts and alcohol protecting groups

Entry	Substrate	Catalyst	(mol%)	Solvent	Temperature	<i>t</i>	Product	Yield (%)
1		3	5	CH ₂ Cl ₂	Reflux	2 h		13 13 (87%)
2		3	2	CH ₂ Cl ₂	rt	5 min		22a 22a (98%)
3		3	1.6	CH ₂ Cl ₂	rt	5 min		22b 22b (98%)
4		3	6	CH ₂ Cl ₂	rt	48 h		24 24 (0%)
5		3	7.5	Toluene	60 °C	24 h		24 (66%) ^a
6		3	20	CH ₂ Cl ₂	rt	4 h		22c 22c (70%)
7		3	7.5	Toluene	60 °C	2 h		22c (93%)
8		23	2	Toluene	60 °C	2 h		22c (76%)+ 22b (20%)
9		23	2	CH ₂ Cl ₂	rt	2 h		22c (82%)+ 22b (6%)
10		3	30	Benzene- <i>d</i> ₆	60 °C	24 h		22d —
11		23	20	CH ₂ Cl ₂	rt	72 h		22c (54%) ^a + 21d (42%) ^a
12		23	7.5	Toluene	60 °C	11 h		22c (89%) ^a + 22d (8%) ^a
13		23	7.5	CDCl ₃	60 °C	1 h		22c (42%) ^a + 22d (52%) ^a
14		3	20	CH ₂ Cl ₂	rt	72 h		25 (42%) ^a + 21d (51%) ^a
15		3	20	CH ₂ Cl ₂	rt	72 h	No RCM product	—
16		3	20	Toluene	60 °C	48 h	No RCM product	—

^a Observed conversion by GC-MS, not isolated yield.

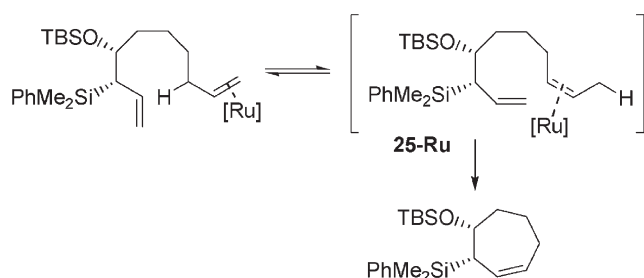
Acetylation or silylation of the alcohols **19a–e** yielded the corresponding esters **20c,e** or silyl ethers **21a–e** (Scheme 12).

3.2. Ring-closing metathesis

RCM of the unprotected alcohol **19b** using Grubbs' catalyst **3** (5 mol%) gave the cyclohexenylsilane **13** in good yield (Table 5, entry 1). *t*-Butyldimethylsilyl ethers **21a–b** underwent an extremely fast RCM reaction in the presence of catalyst **3** (entries 2 and 3). Compounds **22a–b** were obtained in excellent yields and the same enantiomeric purities as the starting dienes. As it could be expected, the formation of the 7-membered ring proved to be more difficult: the RCM of diene **21c** was much slower, requiring higher temperatures and more catalyst (entries 6 and 7). The use of 2 mol% of the 2nd generation Grubbs' catalyst **23**¹⁶ enabled the reaction to take place at room temperature in 2 h (entry 9). However, traces of the 6-membered ring were observed in presence of catalyst **23**. The proportion of **22b** increased when the reaction was conducted in toluene at 60 °C (entry 8). RCM of the acetate **20c** was slower. Heating the dienes at 60 °C in toluene in the presence of 7.5 mol% of **3** gave 66% yield of **24** (entry 5).

The treatment of **20e** and **21e** with **3** didn't give the 12-membered ring (entries 15 and 16). Close NMR observation after adding 1 equiv. of catalyst showed complete conversion of the less hindered terminal olefin into the corresponding ruthenium–carbene complex but no cyclization occurred even after 2 days at 60 °C in toluene. The catalyst **23** didn't give any metathesis product neither.

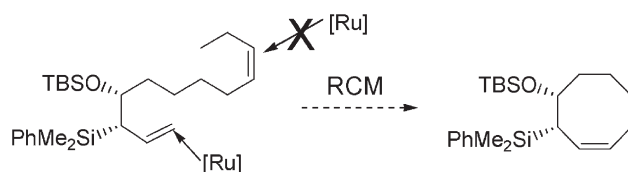
A first attempt to form the 8-membered ring was conducted in boiling deuterated benzene and followed by NMR. Again, the only product was the ruthenium–carbene complex (entry 10). The use of the more reactive catalyst **23** did not give the 8-membered ring. Instead a mixture of the 7-membered ring **22c** and starting diene **21c** was obtained when the reaction was run at room temperature (entry 11). At 60° in toluene (entry 12), the conversion was complete, but gave only a small amount of the 8-membered ring **22d**, the main product being the 7-membered ring **22c**. Surprisingly, in deuterated chloroform at 60 °C, the major product was **22d** as shown by GC-MS analysis (entry 13). Unfortunately this product could not be separated from the lower homologue **22c**. These results can be explained by a ruthenium-catalyzed isomerization of diene **21d** into the more stable internal olefin **25** (Scheme 13).



Scheme 13.

Indeed, a mixture of the terminal **21d** and isomerized olefin **25** was formed when **21d** was exposed to Grubbs catalyst at room temperature for 72 h (entry 14). This type of isomerization is often encountered in RCM involving weakly reactive systems.¹⁷

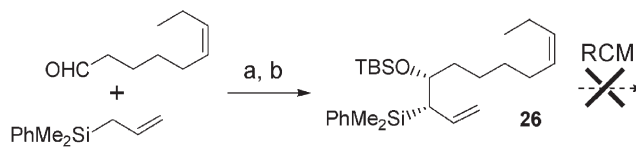
We reasoned that we might avoid olefin isomerization if we could force the catalyst to enter at the allylsilane position. The introduction of an ethyl substituent at the terminal carbon atom of the olefin was expected to slow down carbene formation at that double bond (Scheme 14).



Scheme 14.

Diene **26** was synthesized by the allyltitanation-metathesis sequence and subjected to RCM conditions (Table 6). Unfortunately, at room temperature neither **3** nor **23** were efficient enough to promote the formation of the 8-membered ring (entries 1 and 2). When the reaction was carried out in toluene at 60 °C, no reaction occurred in presence of catalyst **3** (entry 3). With catalyst **23** isomerization preceded RCM, giving again the 7-membered ring **22c** (entry 4).

Table 6. RCM of **26**



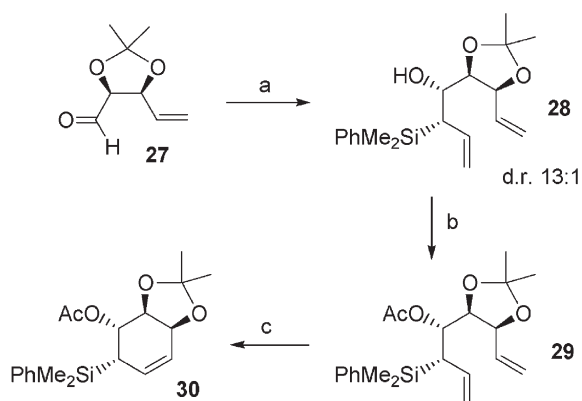
Entry	Catalyst	Conditions	Result
1	3	CH ₂ Cl ₂ , rt, 2 d	No reaction
2	23	CH ₂ Cl ₂ , rt, 2 d	No reaction
3	3	Toluene, 60 °C	No reaction
4	23	Toluene, 60 °C	22c 62% + 22d 12%

Reagents and conditions: (a) *n*-BuLi (1.1 equiv.) in THF, 20 min, rt then (*R,R*)-Cl–TiCpTADDOL (1.15 equiv.), 30 min, –78 °C then *cis*-6-nonenal (1 equiv.), 3 h, –78 °C, 40% aqueous NH₄F, 15 h, rt, 64%; (b) TBSOCl (1.1 equiv.), imidazole (2 equiv.), 16 h, 50 °C, DMF, 63%.

Clearly the synthetic utility of this asymmetric allylmetallation-RCM sequence would be greatly enhanced if it could be successfully applied to substituted aldehydes (Scheme 15). We have therefore examined the allyltitanation of the acetonide-protected aldehyde **27**¹⁸ which proceeded indeed with high diastereoselectivity to give the corresponding *anti*- β -hydroxyallylsilane **28**. The corresponding acetate **29** was subjected to RCM in the presence of catalyst **23** to give 80% yield of cyclohexene **30** in high enantiomeric purity (ee >98%, d.r.: 13:1 determined by chiral HPLC).

3.3. Conformations of the cyclic *cis*- β -hydroxyallylsilanes

The conformations of the cyclic *cis*- β -hydroxyallylsilanes



Scheme 15. Reagents and conditions: (a) n -BuLi (1.1 equiv.) in THF, 20 min, rt then (R,R) -Cl-TiCpTADDOL (1.15 equiv.), 30 min, -78°C then **27** (1 equiv.), 3 h, -78°C , 40% aqueous NH_4F , 15 h, rt, 55%; (b) pyridine (3.5 equiv.), CH_3COCl (2.5 equiv.), CH_2Cl_2 , 4 h, rt, 89%; (c) catalyst **23** (8 mol%), boiling CH_2Cl_2 , 2 h, 80%.

22a-c were examined by correlation of the experimental coupling constants with calculated values obtained by a Monte-Carlo conformational search (Fig. 1). The experimental coupling constants of the ring-protons were compared with the one calculated for the representative structures of each cluster obtained from the conformational search. The existence of second-order effects and long range couplings specific to an allylic system led us to use an iterative procedure to assign all coupling constants values. In all three cases the values of the coupling constants confirmed that the silicon group was pseudo-axial. The preference for a pseudo-axial position of the silyl group can be explained on the basis of a stabilizing ground state interaction between the $\sigma_{\text{C-Si}}$ and the $\pi_{\text{C=C}}$. This kind of interaction has been proposed previously to rationalize the preferred conformation of allylsilanes.¹⁹

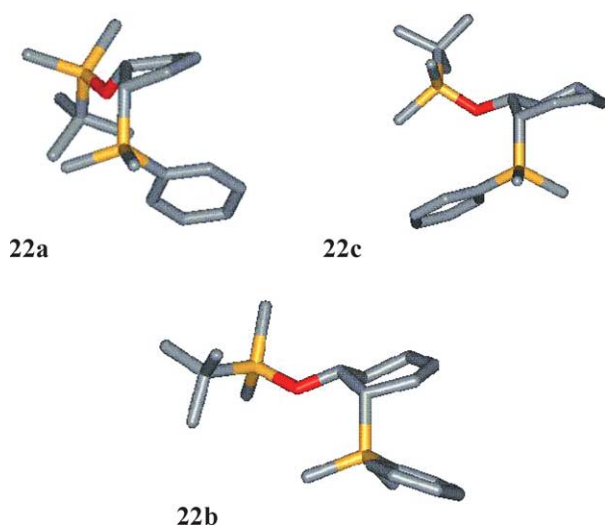


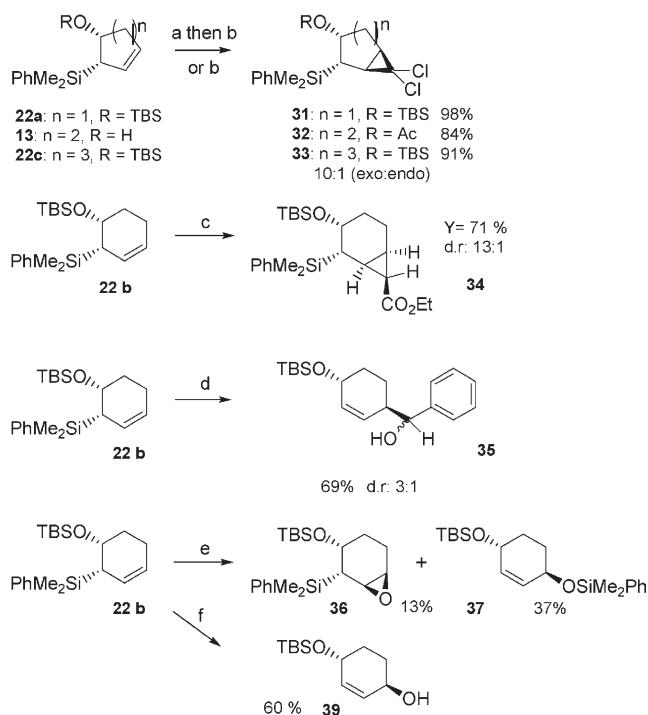
Figure 1. Following the Monte Carlo conformational search—calculations were considered to be convergent when each conformation was found at least three times—a cluster analysis was performed with Xcluster 1.1. The representative conformer of the cluster exhibiting calculated coupling constants consistent with the one observed by ^1H NMR spectrum are shown above. This cluster was also the one containing the conformer with the lowest energy in the three cases.

^1H NMR analysis and molecular modeling⁵ of **30** also suggested a half-chair conformation with a pseudoaxial silyl substituent.

4. Transformations of cyclic β -hydroxyallylsilanes

Compounds **13** and **22a-c** contain a combination of an allyl- and a β -silyloxy-silane which should be prone to undergo interesting transformations leading to a wide variety of enantioenriched, highly functionalized building blocks. Scheme 16 shows an illustrative selection of diastereoselective transformations of **22a-c**. In all cases, the axial silyl group acts as an efficient stereodirecting group, favouring the attack on the opposite face. HPLC analyses showed that the enantiomeric purity of the starting materials was conserved after the transformations.

The cyclohexenylsilanes **13** and **22a,c** were first reacted with dichlorocarbene and the relative configuration of the cycloadducts was ascertained by ^1H NOE experiments. The facial selectivity was excellent for **22a** and **13** (only the *exo* isomer was detected by HPLC) but a 10:1 mixture of *exo* and *endo* was obtained in the case of **33**. The addition of ethyldiazoacetate in presence of $[\text{Rh}(\text{OAc})_2]_2$ yielded 43% of **34** in a 3:1 mixture of epimers but with complete facial selectivity. The use of $\text{Cu}(\text{acac})_2$ instead, as described by Landais et al., gave the cyclopropane with a better yield (71%) and a better epimer ratio (13:1 determined by ^1H NMR).²⁰

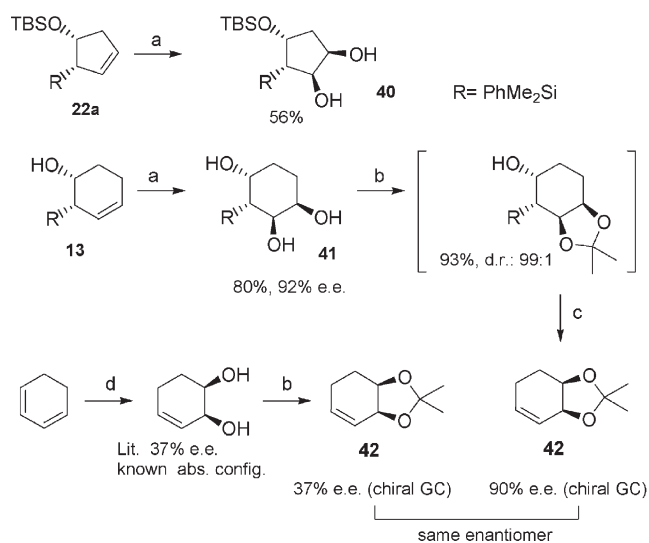


Scheme 16. Reagents and conditions: (a) pyridine (3 equiv.), CH_3COCl (2 equiv.), CH_2Cl_2 , 4 h, rt, 92%; (b) Et_3BnNCl (0.1 equiv.), NaOH 50%, CHCl_3 , rt, 15 h; (c) ethyl diazoacetate (1.2 equiv.), $\text{Cu}(\text{acac})_2$ (2 mol%), toluene, 90°C , 3 h; (d) benzaldehyde (1.1 equiv.), TMSNTf_2 (1.1 equiv.), i -BDMP (1.5 equiv.), CH_2Cl_2 , -78°C , 1 h.; (e) m -cpba (1 equiv.), -20°C , 1 h.; (f) N -methyl-1,2-oxido-1,2,3,4-tetrahydroisquinoline tetrafluoroborate **38** (1 equiv.), CH_2Cl_2 , rt, 30 min.

As the PhMe_2Si group was axial in **22b**, we expected to observe the reactivity typical of an allylsilane and attempted a Sakurai reaction. In the presence of 1.1 equiv. of TMSNTf_2 **22b** reacted with benzaldehyde to yield 69% of **35** as a mixture of epimers (3:1).

Epoxidation proved to be more difficult. Treatment of **22b** at room temperature with *m*-cpba gave a complex mixture probably due to the acidic nature of the oxidant. At -20°C only 13% of epoxide **36** were obtained along with 37% of **37** resulting from the rearrangement of the epoxide. The neutral oxaziridinium salt **38**²¹ directly yielded alcohol **39** in 60% yield.

Dihydroxylation of **22a** yielded the diol **40** with an excellent facial selectivity (only one isomer detected by ^1H NMR of the crude mixture) (Scheme 17). Dihydroxylation of **13** gave the triol **41** in good yield and the reaction was found to be 99% diastereoselective. Only 1% of the *cis*-isomer could be detected by GC-MS after protection of the 1,2-diol. Chiral HPLC analysis showed that **42** was identical to the product resulting from Sharpless dihydroxylation of cyclohexadiene with AD-mix β followed by acetonide protection.²² These data further confirmed the configurational assignment of our RCM products.



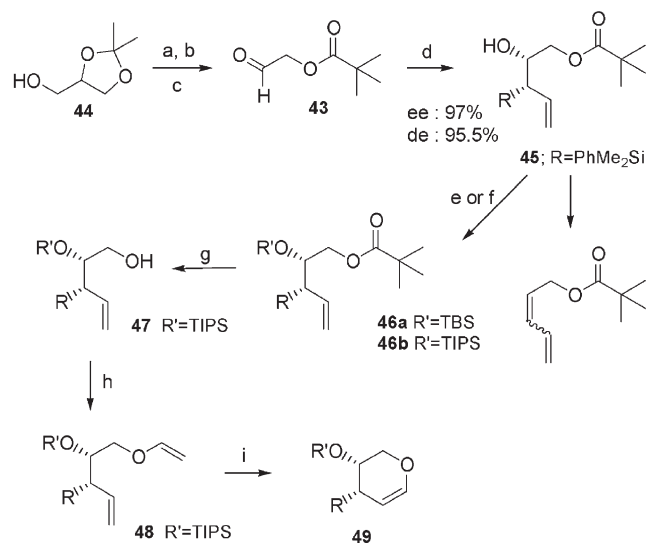
Scheme 17. Reagents and conditions: (a) $\text{K}_2\text{OsO}_4 \cdot 2\text{H}_2\text{O}$ (2 mol%), $\text{NMO} \cdot \text{H}_2\text{O}$ (1.7 equiv.), $\text{H}_2\text{O}/\text{THF}$, rt, 48 h; (b) dimethoxypropane (1.5 equiv.), $\text{PTSA} \cdot \text{H}_2\text{O}$ cat., CH_2Cl_2 , rt, 10 min; (c) NaH (1.3 equiv.), THF , 55°C , 5 h; (d) AD-mix β , MeSO_2NH_2 , *t*-BuOH, H_2O , 3°C , 2.25 h.

5. Conclusions and perspectives

In conclusion, we have demonstrated that the asymmetric allylmethallation-ring-closing metathesis is an efficient sequence to access various polyfunctionalized rings with good enantioselectivities. In this sequence, the bulk of the silyl substituent plays a significant role, favouring the RCM reaction. The silyl group is also a key player in the further transformations of the RCM products. Both the β -effect and bulk of the axial silyl group are responsible for a complete control of the facial selectivity in electrophilic additions to the cyclic allylsilanes. The work of Roush et al. on the total synthesis of conduritols and inositols is undoubtedly a

beautiful illustration of the power of this synthetic strategy for natural products synthesis.

We wanted to find out whether this synthetic strategy could be applied to the synthesis of enantiopure heterocyclic rings such as dihydropyranes which could be useful intermediates for the synthesis of glycomimetics. As a conclusion of these studies, we want to show a first illustration of this new application (Scheme 18).



Scheme 18. Reagents and conditions: (a) pivaloyl chloride (1 equiv.), solketal (1 equiv.), pyridine (1.1 equiv.), CH_2Cl_2 , 48 h, -10°C , 83%; (b) HCl (2 N), THF , 16 h, rt, 98%; (c) NaIO_4 (1.1 equiv.), $\text{water}/\text{CH}_2\text{Cl}_2$, 4 h, rt, 71%; (d) *n*-BuLi (1.1 equiv.) in THF , 20 min, rt then (*R,R*)- Cl-TiCpTADDOL (1.15 equiv.), 30 min, -78°C then **43** (1 equiv.), 3 h, -78°C , 40% aqueous NH_4F , 15 h, rt, 56%; (e) TBSCl (1.5 equiv.), imidazole (3 equiv.), 36 h, 60°C , DMF ; (f) TIPSCl (1.5 equiv.), imidazole (3 equiv.), 36 h, 60°C , DMF ; (g) DIBAL 1.5 M (2 equiv.), CH_2Cl_2 , -78°C , 1 h, 73%; (h) ethylvinyl ether, $\text{Hg}(\text{OAc})_2$ (1.1 equiv.), 48 h, 67%; (i) **23** (25 mol%), CH_2Cl_2 , reflux, 4 h, 93%.

Aldehyde **43** was prepared by standard procedures from (+/−)-solketal **44** and successfully submitted to allyl-methallation. All our attempts to introduce a benzyl protecting group on alcohol **45** failed and gave instead the diene resulting from a Peterson elimination. A TBS group could be easily introduced but, unexpectedly, attempts to cleave the pivaloyl group by LiAlH_4 also gave 2,4-pentadien-1-ol. However the use of a more stable protecting group such as TIPS allowed cleavage of the pivaloyl group with DIBAL . The resulting alcohol **47** was subsequently vinylylated by transesterification in presence of $\text{Hg}(\text{OAc})_2$. 25 mol% of catalyst **23** allowed a clean conversion of the diene **48** into the cyclic vinyl ether **49**.

Further applications of this strategy will be reported in due course.

6. Experimental

6.1. General

^1H NMR spectra and ^{13}C NMR spectra were recorded in CDCl_3 at 400 and 100 MHz on a Bruker Avance 400 instrument or at 300 and 75 MHz on a Varian Gemini

300BB Instrument. Chemical shifts are reported in ppm using residual CHCl_3 (7.26 ppm) and CDCl_3 (77 ppm) as references. HPLC analyses were realized with a Waters Alliance apparatus. The mass spectra under fast atom bombardment (FAB) or chemical ionization (CI) were recorded at 70 eV ionizing potential; $\text{CH}_4\text{-N}_2\text{O}$ were used for CI. The spectra are presented as m/z (% rel. int.). High resolution mass spectra were performed in the laboratory of Prof. Flammang (Université de Mons Hainaut) or at the Cesamo Laboratory (Université Bordeaux I). $[\alpha]$ were measured on a Perkin–Elmer 241 MC polarimeter. Thin-layer chromatographic analyses were performed on MERCK 60 F₂₅₄ silica gel plates (coated on aluminium). Visualization was realized under UV lamp or KMnO_4 revelator. Flash chromatography separations were performed using MERCK 60 40–63 μm silica and technical grade solvents.

Reaction requiring anhydrous conditions were performed using flame-dried glassware under a positive pressure of argon. Dry THF was distilled from potassium and benzophenone under argon, CH_2Cl_2 was distilled from CaH_2 , Et_2O and toluene were distilled from Na, DMF was dried over 3 Å MS. 1st and 2nd generation Grubbs' catalysts **3** and **23** were purchased from Strem Chemicals.

The calculations were performed on a SGI Octane platform running Macromodel version 6.5 (Schrödinger Inc.). Conformational minima were found using the modified MM3* (1991 parameters) or MM2* (1987 parameters) force fields as implemented and completed in the macromodel program. Build structures were minimized to a final RMS gradient $\leq 0.01 \text{ kJ } \text{Å}^{-1} \text{ mol}^{-1}$ via the Truncated Newton Conjugated Gradient (TNCG) method (500 cycles). Coupling constant calculations were performed using Ref. 23 as implemented in Macromodel.

6.2. Reaction rate measurements

For the kinetics, a known amount of catalyst **3** (~10 mg) was weighted in an NMR tube. Deuterated benzene (0.6 mL) was added just before performing the NMR. After addition of 20 μL of olefin (~10 equiv. depending on the olefin) with a calibrated Hamilton syringe, an arrayed ^1H NMR experiment was started taking spectra every 40 or 60 s. The delay between the addition of the olefin and the first ^1H NMR acquisition was measured precisely to be able to consider the point at the origin for the linear regression analysis. Before each set of measurements, an experiment with hexene was performed to ascertain reproducibility and the quality of the catalyst. The experiment was repeated at least two independent times. Pseudo-first order rate constants were measured from the integration of the different $\text{Ru}=\text{CH-X}$ signals. First-order fits were obtained for all experiments under these pseudo-first-order conditions. Second-order rate constants were calculated from pseudo-first-order rate constants, k_1 and k_2 measured were divided by the values obtained for hexene to give $k_{1\text{rel}}$ and $k_{2\text{rel}}$ as listed in Table 1.

6.3. Procedures

6.3.1. cis-Deca-1,7-diene-4-ol (4rac). To allylmagnesium

bromide (1 M in Et_2O , 25 mL, 1.1 equiv.) at 0 °C was added *cis*-hept-4-enal (2.5 g, 22 mmol, 1 equiv.) dropwise. After 15 min at 0 °C and 20 min at rt was added MeOH (1 mL, 1.1 equiv.) to quench excess Grignard reagent. 1.2 N HCl (20 mL) was added and the organic phase was separated. The aqueous phase was extracted with Et_2O . The combined organic phases were dried over MgSO_4 and concentrated under reduced pressure to yield the crude alcohol in quantitative yield (pure by NMR and GC). ^1H NMR (CDCl_3): δ 5.75–5.9 (m, 1H), 5.3–5.5 (m, 2H), 5.1–5.2 (2m, 2H), 3.67 (pseudo q, 1H, $J=6$ Hz), 2–2.4 (m, 6H), 1.64 (br s, 1H), 1.45–1.6 (m, 2H), 0.97 (t, 3H, $J=7.5$ Hz). ^{13}C NMR (CDCl_3): δ 134.8, 132.3, 128.4, 118.2, 70.3, 41.9, 36.4, 23.5, 20.5, 14.4. IR (film) ν_{max} cm^{-1} 3364, 3077, 3006, 2963, 2932, 2874, 1441, 1067. MS(EI, 70 eV): 154 (7), 136 (16), 113 (58), 95 (100), 41 (57). HRMS: Calcd for $\text{C}_{10}\text{H}_{18}\text{O}$: 154.13576 found: M 154.13593.

6.3.2. anti-3-Dimethylphenylsilyl-deca-1,7-diene-4-ol (5rac). To a solution of allyldimethylphenylsilane (3.6 g, 21 mmol, 1.15 equiv.) in THF (100 mL) was added *n*-BuLi 2.2 M in hexane (9.3 mL, 1.15 equiv.) dropwise at room temperature in 15 min. After 15 min, the solution was cooled to -78 °C and a solution of $\text{CITi}(\text{O}i\text{Pr})_3$ (5.8 g, 1.25 equiv.) in THF (8 mL) was added dropwise. After 20 min at -78 °C, was added heptenal (2 g, 18 mmol, 1 equiv.). After 1.5 h of reaction, 45% NH_4F (75 mL) was added and stirring was continued overnight. The reaction mixture was filtered of Celite and the organic phase was separated. The aqueous phase was extracted with AcOEt. The combined organic phases were dried over MgSO_4 and concentrated under reduced pressure. Flash chromatography (SiO_2 : CH_2Cl_2 /hexane: 4:6) gave the homoallylic alcohol as a light yellow oil in 88% yield (pure by NMR, >99% by GC). TLC R_f 0.48 (Et_2O /hexane, 3:17, KMnO_4). ^1H NMR (CDCl_3): δ 7.3–7.6 (m, 5H), 5.83 (ddd, 1H, $J=17$, 10.4, 10.4 Hz), 5.05 (dd, 1H, $J=10.3$, 2 Hz), 4.91 (dd, 1H, $J=17$, 2 Hz), 3.74 (pseudo q, 1H, $J=4.8$ Hz), 1.93–2.1 (m, 4H), 1.9 (dd, 1H, $J=10.7$, 4.4 Hz), 1.4–1.5 (m, 3H), 0.93 (t, 3H, $J=7.4$ Hz), 0.35 (s, 3H), 0.33 (s, 3H). ^{13}C NMR (CDCl_3): δ 137.9, 135.1, 134, 132.2, 129.1, 128.4, 127.7, 115.5, 71.2, 42.1, 37.1, 23.6, 20.5, 14.3, -3.5 , -3.9 . IR (film) ν_{max} cm^{-1} 3570, 3463, 3070, 3004, 2961, 2874, 1248, 1112. MS(CI): 289 (2) $[\text{M}+1]^+$, 271 (24), 137 (67), 135 (100). Elem. Anal. Calcd for $\text{C}_{18}\text{H}_{28}\text{OSi}$ C 74.94, H 9.78 found: C 74.45, H 9.72.

6.3.3. cis-3-Dimethylphenylsilyl-deca-1,7-diene-4-yl acetate (6rac). To a solution of the alcohol **5rac** (2 g, 6.9 mmol, 1 equiv.) and pyridine (2.3 mL, 4 equiv.) in CH_2Cl_2 (50 mL) at 0 °C was added AcCl (1.5 mL, 3 equiv.) dropwise. The suspension was stirred for 1.5 h at rt Et_2O (50 mL) was added and the reaction mixture was filtered; The filtrate was concentrated under reduced pressure and Et_2O (100 mL) was added. The organic phase was washed twice with 1.2 N HCl and once with Na_2CO_3 sat. The crude alcohol was obtained in quantitative yield (pure by NMR, 99% by GC). TLC R_f 0.76 (CH_2Cl_2 , KMnO_4). ^1H NMR (CDCl_3): δ 7.3–7.5 (m, 5H), 5.85 (ddd, 1H, $J=17.1$, 11.3, 11.3 Hz), 5.05 (dd, 1H, $J=10$, 2 Hz), 5.03 (dt, 1H, $J=6.9$, 3.8 Hz), 4.89 (dd, 1H, $J=17$, 1.9 Hz), 1.8–2.1 (m, 4H), 1.82 (s, 3H), 1.4–1.7 (m, 2H), 0.93 (t, 3H, $J=7.5$ Hz), 0.33 (s, 3H), 0.31 (s, 3H). ^{13}C NMR (CDCl_3): δ 170.2, 137.3, 134.6,

133.9, 132.1, 129.1, 127.8, 127.6, 115.6, 73.7, 39.3, 33.9, 23, 20.5, 21.1, 14.3, -3.9, -4. IR (film) ν_{\max} cm^{-1} 3072, 3051, 3007, 2962, 2934, 2874, 1739, 1237; MS(EI, 70 eV): 315 (2), 270 (2), 179 (16), 135 (100), 117 (57). Elem. Anal. Calcd for $\text{C}_{20}\text{H}_{30}\text{O}_2\text{Si}$: C 72.67, H 8.96 found: C 72.57, H 8.96.

6.3.4. anti-3-Dimethylphenylsilyl-oct-1,7-diene-4-ol (7rac). To a solution of the allylsilane (8 g, 45.4 mmol, 1.15 equiv.) in THF (150 mL) at rt was added 2.1 M BuLi (21.6 mL, 1.15 equiv.) dropwise. After 20 min, the orange solution was cooled to -78 °C and a solution of CITi(OiPr)₃ (14.8 g, 1.25 equiv.) in THF (20 mL) was added dropwise over 10 min. After 15 min, the neat aldehyde (3.3 g, 40 mmol, 1 equiv.) was added over 5 min. After 2 h at -75 °C, the cooling bath was removed and 45% NH₄F (160 mL) were added. After 4 h of hydrolysis, Et₂O (100 mL) was added and the crude mixture was filtered of Celite. The solid residue was washed with Et₂O (4×50 mL) and the organic layer was separated. The aqueous phase was extracted once with Et₂O (100 mL). The combined organic phases were dried over MgSO₄ and concentrated under reduced pressure. Flash chromatography (SiO₂; 100% CH₂Cl₂) gave the homoallylic alcohol in 63–75% yield (>99% pure by GC). For characterization see **19b**.

6.3.5. anti-3-Dimethylphenylsilyl-oct-1,7-diene-4-yl *t*-butyl-dimethylsilyl ether (8rac). A solution of the alcohol (2.2 g, 8.5 mmol, 1 equiv.) and TBDMSCl (1.5 g, 1.2 equiv.) in DMF (10 mL) was stirred at 50 °C for 36 h. Water (150 mL) was added and the reaction mixture was extracted with Et₂O. The combined organic layers were dried over MgSO₄ and concentrated in vacuo. Flash chromatography (100%, hexane) gave the silyl ether in 83% yield (>99% d.e. and >99% pure by GC). TLC R_f 0.97 (CH₂Cl₂, KMnO₄). ¹H NMR (CDCl₃): δ 7.3–7.6 (m, 5H), 5.85 (ddd, 1H, $J=17.3$, 10.3, 10.3 Hz), 5.7 (ddt, 1H, $J=17$, 10.5, 6.5 Hz), 4.7–5 (m, 4H), 3.87 (ddd, 1H, $J=8$, 5, 3.3 Hz), 2.03 (dd, 1H, $J=10.4$, 3.3 Hz), 1.8–2.1 (m, 2H), 1.4–1.7 (m, 2H), 0.88 (s, 9H), 0.35 (s, 3H), 0.31 (s, 3H), 0.01 (s, 3H), -0.01 (s, 3H). ¹³C NMR (CDCl₃): δ 138.7, 138.5, 135.8, 134.1, 128.8, 127.5, 114.5, 114.4, 72.8, 40.4, 35.8, 29.8, 26.1, 18.2, -3.1, -3.7, -3.9. MS(EI, 70 eV): 319 (22), 317 (15), 209 (100), 135 (83). IR (film) ν_{\max} cm^{-1} 3072, 3052, 2999, 2956, 2930, 2858, 1254, 1063. Elem. Anal. Calcd for $\text{C}_{22}\text{H}_{38}\text{OSi}_2$ C 70.52, H 10.22 found: C 70.40, H 10.52.

6.3.6. anti-3-Dimethylphenylsilyl-oct-1,7-diene-4-yl acetate (9rac). To a solution of the alcohol (3 g, 11.5 mmol, 1 equiv.) and pyridine (3.65 mL, 4 equiv.) in CH₂Cl₂ (75 mL) at 0 °C was added AcCl (2.46 mL, 3 equiv.) dropwise. After 30 min at rt, Et₂O (75 mL) was added, the reaction mixture was filtered of Celite and concentrated in vacuo. The residue was taken up in Et₂O (150 mL) and was washed twice with 1.2 N HCl and once with Na₂CO₃sat. The organic phase was dried over MgSO₄ and concentrated under reduced pressure to afford the crude acetate (98% by GC) in quantitative yield. Filtration over SiO₂ (CH₂Cl₂ 100%) gave analytically pure acetate in 95% yield (99% pure by GC). TLC R_f 0.8 (CH₂Cl₂, KMnO₄). ¹H NMR (CDCl₃): δ 7.3–7.5 (m, 5H), 5.85 (ddd, 1H, $J=17.2$, 10.4, 10.4 Hz), 5.7 (ddt, 1H, $J=17$, 10.4, 6.4), 4.8–5.1 (m,

5H), 2.03 (dd, 1H, $J=10.7$, 3.9 Hz), 1.85 (m, 2H), 1.85–2 (m, 2H), 1.82 (s, 3H), 1.4–1.7 (m, 2H), 0.33 (s, 3H), 0.31 (s, 3H). ¹³C NMR (CDCl₃): δ 170.2, 137.7, 134.5, 133.9, 129.1, 127.7, 137.3, 115.7, 114.7, 73.4, 39.4, 33.1, 29.6, 21.1, -4. IR (film) ν_{\max} cm^{-1} 3072, 3001, 2956, 2857, 1739, 1237. MS(CI): 243 (40), 179 (23), 135 (68), 117 (100). Elem. Anal. Calcd for $\text{C}_{18}\text{H}_{26}\text{O}_2\text{Si}$ C 71.47, H 8.66 found: C 71.45, H 8.73.

6.3.7. 3-Cyclohexyl-oct-1,7-diene-4-yl *t*-butyldimethylsilyl ether (10rac). A solution of the alcohol **11rac** (594 mg, 2.85 mmol, 1 equiv.), imidazole (388 mg, 2 equiv.) and TBSCl (473 mg, 1.1 equiv.) in DMF (5 mL) was heated overnight at 45–50 °C. Water (50 mL) and Et₂O (40 mL) were added. The organic layer was separated and washed with 1.2 N HCl. Purification by flash chromatography (SiO₂; 100% hexane) gave 73% yield of the silyl ether as a colorless liquid (>99% by GC). TLC R_f 0.79 (hexane, KMnO₄). ¹H NMR (CDCl₃): δ 5.78 (ddt, 1H, $J=17$, 10.2, 6.8 Hz), 5.68 (ddd, 1H, $J=17.5$, 9.9, 9.9 Hz), 3.85 (ddd, 1H, $J=7.9$, 5.5, 2.5 Hz), 0.88 (s, 9H), 0.7–2.1 (m, 16H), 0.05 (s, 6H). ¹³C NMR (CDCl₃): δ 138.7, 138.1, 116.4, 114.4, 71, 54.5, 36.7, 34.7, 31.8, 31.5, 29.7, 26.7, 26.5, 26.4, 25.9, 18.2, -3.8, -4.5. IR (KBr) ν_{\max} cm^{-1} 3074, 2928, 2854, 1254, 1075. MS(EI, 70 eV): 307 (0.5) [M-Me]⁺; 265 (76), 199 (100). HRMS Calcd for $\text{C}_{20}\text{H}_{38}\text{OSi}$ 323.277020 found: M 323.276936. Elem. Anal. Calcd for $\text{C}_{20}\text{H}_{38}\text{OSi}$ C 74.46, H 11.87 found: C 74.54, H 12.00.

6.3.8. 3-Cyclohexyl-oct-1,7-diene-4-ol (11rac). To a green suspension of CrCl₂ (1.23 g, 10 mmol, 2 equiv.) and 4-pentenal (420 mg, 5 mmol, 1 equiv.) in THF (20 mL) was added allylbromide (1.03 g, 5 mmol, 1 equiv.). After 15 h of reaction, 1.2 N HCl (10 mL) and Et₂O (20 mL) were added to the resulting purple reaction mixture. After 30 min of hydrolysis, the organic layer was separated and the aqueous phase extracted with Et₂O. The combined organic phases were dried over MgSO₄ and concentrated in vacuo. Flash chromatography (SiO₂; 100% CH₂Cl₂) gave the homoallylic alcohol in 61–71% yield. TLC R_f 0.5 (CH₂Cl₂, KMnO₄). ¹H NMR (CDCl₃): δ 5.84 (ddt, 1H, $J=17.1$, 10.3, 6.8 Hz), 5.7 (ddd, 1H, $J=17.2$, 10.2, 10.2 Hz), 5.2 (dd, 1H, $J=10.3$, 2.3 Hz), 5–5.1 (m, 2H), 3.74 (d pseudo q, 1H, $J=9.3$, 4.7 Hz), 2–2.2 (m, 2H), 1.41 (d, 1H, $J=4.4$ Hz), 0.8–1.8 (m, 13H). ¹³C NMR (CDCl₃): δ 138.7, 136.9, 118.5, 114.7, 69.9, 56.1, 36.7, 34.4, 31.7, 29.9, 26.6, 26.54, 26.48 (note: the cHex shows diastereotopic carbons giving thus 5 signals instead of 3). IR (film) ν_{\max} cm^{-1} 3385, 3075, 2925, 2853, 1641, 1449, 911. MS(CI): 415 (100) [M+M-1], 359 (12), 307 (48), 291 (72), 151 (40), 99 (10), 83 (28). Elem. Anal. Calcd for $\text{C}_{14}\text{H}_{24}\text{O}$ C 80.71, H 11.61 found: C 80.36, H 11.61.

6.3.9. Cyclohex-3-enol (12rac). To a refluxing solution of the diene **4rac** (120 mg, 0.78 mmol, 1 equiv.), was added **3** (10 mg, 1.6 mol%), in CH₂Cl₂ (0.7 mL). The reaction reached completion after less than 10 min (TLC and GC). The solvent was removed under reduced pressure to give a quantitative yield of crude cyclohexenol **12rac**²⁴ (>99% by GC). ¹H NMR (CDCl₃): δ 5.68 (dm, 1H, $J=11.3$ Hz), 5.56 (dm, 1H, $J=10.6$ Hz), 3.95 (br, 1H), 1.5–2.5 (m, 7H).

6.3.10. *cis*-2-Dimethylphenylsilyl-cyclohexy-3-enol (13rac). To a refluxing solution of the diene (365 mg, 1.27 mmol, 1 equiv.) in CH₂Cl₂ (16 mL) was added **3** (16 mg, 1.6 mol%) in CH₂Cl₂ (1 mL). After 41 h of reaction the solvent was evaporated under reduce pressure. Flash chromatography (SiO₂, hexane/Et₂O, 17:3) gave the cyclohexene in 86% yield (>99% by GC). For characterization see **13ent**.

6.3.11. 3-Dimethylphenylsilyl-deca-1,7-diene-4-yl acetate (14rac). Via RCM of **6rac**. To a refluxing solution of the diene (258 mg, 0.78 mmol, 1 equiv.) in CH₂Cl₂ (10 mL) was added **3** (10 mg, 1.6 mol%) in CH₂Cl₂ (0.7 mL). After 23 h of reaction the solvent was evaporated under reduced pressure. Flash chromatography (SiO₂, hexane/Et₂O, 8:2) gave the acetate in 91% yield (>99% by GC).

Via RCM of **8rac**. To a solution of the diene (1.5 g, 4.96 mmol, 1 equiv.) in CH₂Cl₂ (35 mL) at rt was added **3** (15 mg, 0.3 mol%) in three portions in 20 min intervals. The reaction mixture was concentrated in vacuo and was stirred in MeOH (20 mL) for 45 min. The solvent was evaporated and flash chromatography gave the acetate in 88% yield (>99% yield). TLC R_f 0.45 (hexane/Et₂O, 8:2, KMnO₄). [α]_D²³ = +108 (*c* = 0.64 in CH₂Cl₂). ¹H NMR (CDCl₃): δ 7.3–7.6 (m, 5H), 5.6–5.7 (m, 1H, *J* = 10.1, 3.3, 3.3 Hz), 5.5–5.6 (m, 1H, *J* = 10.1, 3.3 Hz), 5.22 (ddd, 1H, *J* = 8, 5.7, 3 Hz), 2.28 (m, 1H), 2–2.1 (m, 2H), 1.75–1.9 (m, 1H), 1.81 (s, 3H), 1.63 (d pseudo-t d, 1H, *J* = 13, 7, 7, 3 Hz), 0.36 (s, 3H), 0.35 (s, 3H). ¹³C NMR (CDCl₃): δ 170.5, 138.4, 133.7, 128.9, 127.7, 125, 124.6, 71.9, 31.6, 26.4, 22.1, 21.1, –3, –3.2. IR (film) ν_{max} cm^{–1} 3068, 3031, 2962, 2913, 2840, 1732, 1247. MS(CI): 214 (2), 179 (11), 137 (26), 135 (89), 117 (100), 80 (81). Elem. Anal. Calcd for C₁₆H₂₂O₂Si C 70.03, H 8.08 found: C 69.91, H 8.19.

6.3.12. *cis*-2-Dimethylphenylsilyl-cyclohex-3-enyl *t*-butyldimethylphenylsilyl ether (15rac). To a refluxing solution of the diene **9rac** (292 mg, 0.78 mmol, 1 equiv.) in CH₂Cl₂ (1 mL) was added a solution of **3** (1 mL of a 3.2 mg cata/10 mL CH₂Cl₂ solution, 0.05 mol%). After completion, the flask was open to air for 1 h and the reaction mixture was concentrated in vacuo. Flash filtration over SiO₂ (100% hexane) gave **15rac** (98% yield, >99% pure by GC). For analyses see **22b**.

6.3.13. *cis*-2-Cyclohexyl-cyclohex-3-enyl *t*-butyldimethylsilyl ether (16rac). To a solution of the diene (252 mg, 0.78 mmol, 1 equiv.) in CH₂Cl₂ (10 mL) was added Grubbs catalyst (1.6 mol%, 10 mg) in CH₂Cl₂ (0.7 mL). After 5 min of reaction, the solvent was removed under reduced pressure and the residue was chromatographed (SiO₂: 100% hexane) to give **16rac** in 98% yield. ¹H NMR (CDCl₃): δ 5.68 (dm, 1H, *J* = 11 Hz), 5.61 (br d, 1H, *J* = 11 Hz), 4.12 (br, 1H), 2.1–2.3 (m, 1H), 1.4–2 and 0.8–1.3 (m, 15H), 0.89 (s, 9H), 0.07 (s, 3H), 0.06 (s, 3H). ¹³C NMR (CDCl₃): δ 126.7, 126.5, 67.6, 46.3, 37.4, 31.9, 30.8, 29.8, 26.6, 25.9, 21.9, 18.2, –4, –5. IR (film) ν_{max} cm^{–1} 3031, 2926, 2854, 1252, 1079. MS(EI, 70 eV): 279 (1), 237 (100), 219 (12), 161 (24). HRMS: Calcd for C₁₈H₃₄O₂Si 294.237894 found: *M* 294.237078.

6.3.14. Asymmetric allylation: typical procedure A. To a

solution of allyldimethylphenylsilane (5.3 g, 30 mmol, 1.15 equiv.) in THF (40 mL) at rt was added 2.1 M *n*-BuLi (14.3 mL, 1.15 equiv.) dropwise over 10 min. After 20 min, the yellow solution was transferred via canula over 10 min to a suspension of (*R,R*)-TiClCpTADDOL (20 g, 32.6 mmol, 1.25 equiv.) in THF (150 mL) at –78 °C. After 30 min, neat aldehyde (1 equiv.) was added over 4 min. The reaction was continued for 3 h at –78 °C. AcOEt (50 mL) and 45% NH₄F (200 mL) were added and the heterogeneous mixture was filtered of Celite and the solid residue was washed with Et₂O (90 mL). The organic layer was separated and the aqueous phase was extracted twice with Et₂O (70 mL). The combined organic layers were dried over MgSO₄ and concentrated in vacuo. Hexane (300 mL) was added to precipitate (*R,R*)-TADDOL. After 20 min stirring, the mixture was filtered. Evaporation of the solvent followed by flash chromatography gave the enantioenriched homoallylic alcohol.

6.3.15. (3*S*,4*R*)-anti-3-(Dimethyl-phenyl-silanyl)-hepta-1,6-dien-4-ol (19a). Following the typical procedure A. To a solution of allyldimethylphenylsilane (3.8 g, 22 mmol, 1 equiv.) in THF (33 mL) at rt was added 2.1 M *n*-BuLi (12 mL, 1.15 equiv.) dropwise over 10 min. After 20 min, the yellow solution was transferred via canula over 10 min to a suspension of (*R,R*)-TiClCpTADDOL (16.7 g, 27.2 mmol, 1.25 equiv.) in THF (125 mL) at –78 °C. After 30 min, 3-butenal (2 g in solution in 10 mL CH₂Cl₂, freshly synthesized and kept at –78 °C before use, 29 mmol, 1.15 equiv.) was added. Chromatography (SiO₂: CH₂Cl₂/cyclohexane, 3:2) 3.68 g (68% yield). [α]_D²³ = –4.56 (*c* = 1.23 in CHCl₃). TLC R_f 0.57 (CH₂Cl₂: cyclohexane, 3:2, KMnO₄). ¹H NMR (CDCl₃): δ 7.48 (m, 2H), 7.28 (m, 3H), 5.80 (ddd, 1H, *J* = 17.4, 10.5, 10.3 Hz), 5.65 (dddd, 1H, *J* = 17.1, 10.3, 7.6, 6.8 Hz), 4.97 (m, 3H), 4.82 (ddd, 1H, *J* = 17.1, 2.2, 0.7 Hz), 3.69 (m, 1H, *J* = 7.6, 5.4, 3.7, 1.0 Hz), 2.09 (m, 2H), 1.83 (dd, 1H, *J* = 10.5, 3.7 Hz), 1.53 (d, 1H, *J* = 1 Hz), 0.37 (s, 3H), 0.33 (s, 3H). ¹³C NMR (CDCl₃): δ 138.3, 135.6, 135.3, 134.5, 129.5, 128.1, 118.2, 115.9, 70.7, 42.3, 42.0, –3.2, –3.6. IR (film) ν_{max} cm^{–1} 3577, 3464, 3071, 2972, 2902, 1639, 1625, 1427, 1248, 1113. MS(CI): 229 (49) [M–OH]⁺, 209 (8), 205 (22), 135 (100), 127 (16), 94 (33), 79 (23), 75 (27). HRMS Calcd for C₁₅H₂₁Si [M–OH]⁺ 229.141469 found: *M* 229.141254. Elem. Anal. found: C 72.68, H 9.16 Calcd for C₁₅H₂₂O₂Si C 73.11, H 9.00.

6.3.16. (3*S*,4*R*)-anti-3-(Dimethyl-phenyl-silanyl)-octa-1,7-dien-4-ol (19b). Following the typical procedure A. To a solution of allyldimethylphenylsilane (5.3 g, 30 mmol, 1.15 equiv.) in THF (40 mL) at rt was added 2.1 M *n*-BuLi (14.3 mL, 1.15 equiv.) dropwise over 10 min. After 20 min, the yellow solution was transferred via canula over 10 min to a suspension of (*R,R*)-TiClCpTADDOL (20 g, 32.6 mmol, 1.25 equiv.) in THF (150 mL) at –78 °C. After 30 min, neat 4-pentenal (2.2 g, 26.1 mmol, 1 equiv.) was added. [α]_D²³ = –1 (*c* = 1.1 in CH₂Cl₂). TLC R_f 0.55 (CH₂Cl₂, KMnO₄). ¹H NMR (CDCl₃): δ 7.3–7.6 (m, 5H), 5.84 (ddd, 1H, *J* = 17, 10.5, 10.5 Hz), 5.74 (ddt, 1H, *J* = 17, 10, 6.7 Hz), 4.85–5.1 (m, 4H), 3.75 (m, 1H), 2.04 (pseudo q, 2H, *J* = 7 Hz), 1.91 (dd, 1H, *J* = 10.4, 4.4 Hz), 1.49 (pseudo q, 2H, *J* = 6.8 Hz), 1.44 (d, 1H, *J* = 4.1 Hz), 0.36 (s, 3H), 0.34 (s, 3H). ¹³C NMR (CDCl₃): δ 138.4, 135.1, 134.1, 129.1, 127.8, 127.9, 115.6, 114.6, 71, 42.1, 36.2, 30.2, –3.4, –3.9.

IR (film) ν_{\max} cm^{-1} 3582, 3455, 3070, 3051, 2956, 2932, 1428, 1249, 1113. MS(CI): 261 (2) $[\text{M}+1]^+$, 243 (26), 153 (21), 137 (50), 135 (100), 109 (72). Elem. Anal. Calcd for $\text{C}_{16}\text{H}_{24}\text{OSi}$ C 73.79, H 9.29 found: C 73.68, H 9.29.

6.3.17. (3*S*,4*R*)-anti-3-(Dimethyl-phenyl-silanyl)-nona-1,8-dien-4-ol (19c). Following the typical procedure A. To a solution of allyldimethylphenylsilane (6.2 g, 35.2 mmol, 1.15 equiv.) in THF (47 mL) at rt was added 2.3 M *n*-BuLi (15.3 mL, 1.15 equiv.) dropwise over 10 min. After 20 min, the yellow solution was transferred via canula over 10 min to a suspension of (*R,R*)-TiClCpTADDOL (24.4 g, 37.6 mmol, 1.25 equiv.) in THF (175 mL) at -78°C . After 30 min, neat 5-hexenal (3 g, 30.6 mmol, 1 equiv.) was added. Chromatography (SiO_2 : AcOEt/PE, 5:95) 6.25 g (75% yield). TLC R_f 0.45 (CH_2Cl_2 , KMnO_4). ^1H NMR (CDCl_3): δ 7.53 (m, 2H), 7.36 (m, 3H), 5.83 (ddd, 1H, $J=17.1, 10.5, 10.2$ Hz), 5.73 (ddt, 1H, $J=17.0, 10.2, 6.7$ Hz), 5.06 (dd, 1H, $J=10.2, 1.9$ Hz), 4.93 (m, 3H), 3.74 (m, 1H), 1.93 (m, 3H), 1.37 (m, 5H), 0.36 (s, 3H), 0.33 (s, 3H). ^{13}C NMR (CDCl_3): δ 138.7, 137.9, 135.1, 133.9, 129.0, 127.7, 115.6, 114.4, 71.2, 42.1, 36.5, 33.4, 25.0, $-3.4, -4.0$. IR (film) ν_{\max} cm^{-1} 3571, 3449, 3069, 2932, 2858, 1640, 1625, 1427, 1250, 1113, 1053, 998, 908, 832, 814, 733, 700. MS(CI): 257 (10) $[\text{M}-\text{OH}]^+$, 209 (5), 205 (5), 179 (8), 135 (100), 122 (17), 107 (15), 81 (20), 75 (27). HRMS Calcd for $\text{C}_{17}\text{H}_{26}\text{OSi}$ $[\text{M}]^+$ 274.175294 found: *M* 274.174264.

6.3.18. (3*S*,4*R*)-anti-3-(Dimethyl-phenyl-silanyl)-deca-1,9-dien-4-ol (19d). Following the typical procedure A. To a solution of allyldimethylphenylsilane (5.4 g, 30.6 mmol, 1.15 equiv.) in THF (40 mL) at rt was added 2.3 M *n*-BuLi (13.3 mL, 1.15 equiv.) dropwise over 10 min. After 20 min, the yellow solution was transferred via canula over 10 min to a suspension of (*R,R*)-TiClCpTADDOL (21.2 g, 32.6 mmol, 1.25 equiv.) in THF (175 mL) at -78°C . After 30 min, neat 6-heptenal (3 g, 26.7 mmol, 1 equiv.) was added. Chromatography (SiO_2 : AcOEt/PE, 5:95) 5.15 g (67% yield). TLC R_f 0.42 (CH_2Cl_2 , KMnO_4). ^1H NMR (CDCl_3): δ 7.56 (m, 2H), 7.38 (m, 3H), 5.85 (ddd, 1H, $J=17.1, 10.5, 10.3$ Hz), 5.78 (ddt, 1H, $J=17.1, 10.2, 6.7$ Hz), 5.07 (dd, 1H, $J=10.3, 2.1$ Hz), 4.96 (m, 3H), 3.74 (m, 1H), 1.99 (m, 2H), 1.93 (dd, 1H, $J=10.5, 4.5$ Hz), 1.39 (m, 2H), 1.29 (m, 4H), 0.38 and 0.35 (s, 3H). ^{13}C NMR (CDCl_3): δ 139.3, 138.4, 135.6, 134.4, 129.5, 128.2, 116.0, 114.7, 71.8, 42.5, 37.4, 34.1, 29.2, 25.6, $-2.9, -3.5$. IR (film) ν_{\max} cm^{-1} 3582, 3445, 3071, 2930, 2856, 1641, 1625, 1428, 1249, 1113, 1046, 999, 902, 834, 815, 734, 701. MS(CI): 288 (5), 271 (3), 209 (7), 135 (100), 75 (21). HRMS: Calcd for $\text{C}_{18}\text{H}_{27}\text{OSi}$ $[\text{M}-\text{H}]^+$ 287.183119 found: *M* 287.183177.

6.3.19. (3*S*,4*R*)-anti-3-(Dimethyl-phenyl-silanyl)-tetradeca-1,13-dien-4-ol (19e). Following the typical procedure A. To a solution of allyldimethylphenylsilane (0.59 g, 3.36 mmol, 1.15 equiv.) in THF (40 mL) at rt was added 2.2 M *n*-BuLi (1.52 mL, 1.15 equiv.) dropwise over 10 min. After 20 min, the yellow solution was transferred via canula over 10 min to a suspension of (*R,R*)-TiClCpTADDOL (2.33 g, 3.58 mmol, 1.25 equiv.) in THF (175 mL) at -78°C . After 30 min, neat undecylenic aldehyde (0.5 g, 3 mmol, 1 equiv.) was added. Chromatography (SiO_2 : AcOEt/PE, 5:95) gave 0.73 g of colorless oil (71% yield).

TLC R_f 0.61 ($\text{CH}_2\text{Cl}_2/\text{PE}$, 1:1, KMnO_4). $[\alpha]_D^{25} = -0.4$ ($c=1.04$ in CHCl_3). ^1H NMR (CDCl_3): δ 7.56 (m, 2H), 7.38 (m, 3H), 5.86 (ddd, 1H, $J=17.1, 10.5, 10.2$ Hz), 5.82 (ddt, 1H, $J=17.1, 10.2, 6.7$ Hz), 5.08 (dd, 1H, $J=10.2, 2$ Hz), 5.02 (ddt, 1H, $J=17.3, 2, 1.5$ Hz), 4.95 (ddt, 1H, $J=10.2, 2, 1.2$ Hz), 4.94 (dd, 1H, $J=17.1, 2$ Hz), 3.74 (m, 1H, $J=11.7, 4.6$ Hz), 2.06 (td, 2H, $J=7.5, 6.7$ Hz), 1.93 (dd, 1H, $J=10.5, 4.5$ Hz), 1.2 (m, 12H), 0.38 and 0.35 (s, 3H). ^{13}C NMR (CDCl_3): δ 139.6, 138.4, 135.6, 134.4, 129.5, 128.2, 115.3, 114.5, 71.9, 42.5, 37.5, 34.2, 29.89, 29.87, 29.8, 29.5, 29.3, 26.1, $-2.9, -3.1$. IR (film) ν_{\max} cm^{-1} 3573, 3447, 3070, 2920, 2850, 1640, 1625, 1427, 1250, 1113, 1054, 998, 907, 832, 814, 733, 700. MS(CI): 345 $[\text{M}+\text{H}]^+$ (5), 286 (15), 271 (100), 209 (72), 152 (17), 137 (95), 135 (36), 75 (37). HRMS Calcd for $\text{C}_{22}\text{H}_{35}\text{OSi}$ $[\text{M}-\text{H}]^+$ 343.245719 found: *M* 343.244560.

6.4. Protection of the alcohol by an acetyl group: typical procedure B

To solution of the alcohol (1 equiv.) and pyridine (3.5 equiv.) in CH_2Cl_2 (43 equiv.) at 0°C is added dropwise acetyl chloride (2.5 equiv.). The reaction mixture is stirred at room temperature for 4 h. CH_2Cl_2 is added and the organic phase is washed twice with HCl 0.1 N. The aqueous phase is extracted with CH_2Cl_2 and the combined organic layers are washed twice with NH_4Cl sat, dried over MgSO_4 and concentrated in vacuo. Flash chromatography gave the acetyl protected alcohol.

6.4.1. (3*S*,4*R*)-anti-3-Dimethylphenylsilyl-nona-1,8-diene-4-yl acetate (20c). Following the typical procedure B. The reaction was carried out on 0.3 g of **19a** (1.09 mmol). Flash chromatography (SiO_2 : CH_2Cl_2) gave 0.332 g of colorless oil (95% yield). TLC R_f 0.75 (CH_2Cl_2 , KMnO_4). ^1H NMR (CDCl_3): δ 7.46 (m, 2H), 7.34 (m, 3H), 5.82 (ddd, 1H, $J=17.1, 10.5, 10.2$ Hz), 5.71 (ddt, 1H, $J=16.8, 10.2, 7$ Hz), 4.84–5.05 (m, 5H), 2.01 (dd, 1H, $J=10.5, 3.6$ Hz), 1.94 (dt, 2H, $J=7.2, 6.6$ Hz), 1.82 (s, 3H), 1.46 (m, 2H), 1.26 (m, 2H), 0.49 and 0.47 (s, 3H). ^{13}C NMR (CDCl_3): δ 170.4, 138.5, 137.5, 134.8, 134.1, 129.2, 127.8, 115.7, 114.8, 74.0, 39.7, 33.7, 33.6, 24.8, 21.4, $-3.6, -3.7$. MS(CI): 288 (9), 257 (15), 179 (34), 154 (17), 135 (100), 123 (25), 117 (89), 107 (16), 80 (17). HRMS Calcd for $\text{C}_{17}\text{H}_{25}\text{Si}$ $[\text{M}-\text{AcO}]^+$ 257.172554 found: *M* 257.173270.

6.4.2. (3*S*,4*R*)-anti-3-Dimethylphenylsilyl-tetradeca-1,13-diene-4-yl acetate (20e). Following the typical procedure B. The reaction was carried out on 0.5 g of **19e** (1.45 mmol). Flash chromatography (SiO_2 : CH_2Cl_2) gave 0.545 g of colorless oil (97% yield). ^1H NMR (CDCl_3): δ 7.48 (m, 2H), 7.37 (m, 3H), 5.38 (m, 2H), 4.96 (m, 5H), 2.04 (m, 3H), 1.84 (s, 3H), 1.47 (m, 2H), 1.37 (m, 2H), 1.21 (m, 10H), 0.34 and 0.32 (s, 3H). ^{13}C NMR (CDCl_3): δ 170.2, 139.1, 137.6, 134.8, 133.9, 129.1, 127.7, 115.5, 114.1, 74.1, 39.6, 34.0, 33.8, 29.4 (2 carbons), 29.3, 29.1, 28.9, 25.2, 21.1, $-3.8, -3.9$. IR (film) ν_{\max} cm^{-1} 3071, 2921, 2852, 1736, 1640, 1626, 1461, 1427, 1370, 1237, 1113, 1019, 904, 833, 700. MS(CI): 329 (100) $[\text{M}+1-\text{CH}_3\text{CO}-\text{CH}_3]^+$, 327 (33), 192 (8), 179 (10), 135 (39), 117 (41).

6.4.3. Protection of the alcohol by a TBS: typical procedure C. To a solution of TBSCl (1.5 equiv.) in

DMF (12 equiv.) was added imidazole (4 equiv.). The reaction mixture was heated to 60 °C for 1.2 h before to add the alcohol (1 equiv.). The reaction was monitored by GC. After 48 h the reaction was complete and 1/2 volume of NH_4Cl sat were added. The aqueous phase was extracted with pentane (3×1 volume) and the combined organic phase were dried over MgSO_4 and concentrated in vacuo. Flash chromatography gave the TBS-protected alcohol.

6.4.4. (3S,4R)-anti-3-Dimethylphenylsilyl-hepta-1,6-diene-4-yl *t*-butyldimethylsilyl ether (21a). Following the typical procedure C. The reaction was carried out on 1.7 g of **19a** (6.9 mmol). Flash chromatography (SiO_2 : PE) gave 2.12 g of colorless oil (85% yield, >99% pure by GC). $[\alpha]_D^{23} = +2.91$ ($c=0.55$ in CHCl_3). TLC R_f 0.58 (PE, KMnO_4). ^1H NMR (CDCl_3): δ 7.51 (m, 2H), 7.35 (m, 3H), 5.90 (ddd, 1H, $J=17.4, 10.4, 10.2$ Hz), 5.64 (dddd, 1H, $J=17.1, 10.2, 7.5, 6.7$ Hz), 4.99 (m, 3H), 4.77 (dd, 1H, $J=17.4, 1.7$ Hz), 3.91 (ddd, 1H, $J=8.0, 4.8, 2.8$ Hz), 2.32 (m, 1H, $J=13.0, 8.0, 7.5$ Hz), 2.21 (m, 1H, $J=13.0, 6.7, 4.8$ Hz), 2.08 (dd, 1H, $J=10.4, 2.8$ Hz), 0.89 (s, 9H), 0.36 and 0.31 (s, 3H), 0.04 and 0.01 (s, 3H). ^{13}C NMR (CDCl_3): δ 138.9, 135.9, 135.4, 134.5, 129.2, 127.9, 117.5, 115.3, 73.2, 41.9, 40.5, 26.5, 18.6, -2.8, -3.3, -3.4, -3.5. IR (film) ν_{max} cm^{-1} 3072, 2956, 2858, 1626, 1472, 1428, 1361, 1254, 1090, 939, 834, 774, 732. MS(FAB): 359 (2), 345 (1), 319 (14), 303, 251, 209 (24), 193, 147, 135 (100). HRMS: Calcd for $\text{C}_{21}\text{H}_{35}\text{O}_1\text{Si}$ (M-H): 359.22264 found: M 359.22193.

6.4.5. (3S,4R)-anti-3-Dimethylphenylsilyl-octa-1,7-diene-4-yl *t*-butyldimethylsilyl ether (21b). Following the typical procedure C. The reaction was carried out on 6 g of **19b** (23 mmol). Flash chromatography (SiO_2 : PE) gave 7.77 g of colorless oil (90% yield, >99% pure by GC). $[\alpha]_D^{23} = -1.00$ ($c=1.16$ in CHCl_3). TLC R_f 0.46 (hexane, KMnO_4). ^1H NMR (CDCl_3): δ 7.3–7.6 (m, 5H), 5.85 (ddd, 1H, $J=17.3, 10.3, 10.3$ Hz), 5.7 (ddt, 1H, $J=17, 10.5, 6.5$ Hz), 4.7–5 (m, 4H), 3.87 (ddd, 1H, $J=8, 5, 3.3$ Hz), 2.03 (dd, 1H, $J=10.4, 3.3$ Hz), 1.8–2.1 (m, 2H), 1.4–1.7 (m, 2H), 0.88 (s, 9H), 0.35 (s, 3H), 0.31 (s, 3H), 0.01 (s, 3H), -0.01 (s, 3H). ^{13}C NMR (CDCl_3): δ 138.7, 138.5, 135.8, 134.1, 128.8, 127.5, 114.5, 114.4, 72.8, 40.4, 35.8, 29.8, 26.1, 18.2, -3.1, -3.7, -3.9. IR (film) ν_{max} cm^{-1} 3072, 3052, 2999, 2956, 2930, 2858, 1254, 1063. MS(EI, 70 eV): 319 (22), 317 (15), 209 (100), 135 (83). MS(CI): 375 $[\text{M}+\text{H}]^+$ (2), 359 (2), 319 (7), 251 (14), 209 (100), 189 (14), 147 (16), 135 (14). HRMS: Calcd for $\text{C}_{22}\text{H}_{39}\text{OSi}_2$ $[\text{M}+\text{H}]^+$ 375.253948 found: M 375.253989. Elem. Anal. Calcd for $\text{C}_{22}\text{H}_{38}\text{OSi}_2$ C 70.52, H 10.22 found: C 70.40, H 10.52.

6.4.6. (3S,4R)-anti-3-Dimethylphenylsilyl-nona-1,8-diene-4-yl *t*-butyldimethylsilyl ether (21c). Following the typical procedure C. The reaction was carried out on 1.6 g of **19c** (5.8 mmol). Flash chromatography (SiO_2 : PE) gave 1.65 g of colorless oil (72% yield, 98% pure by GC). $[\alpha]_D^{23} = -3.87$ ($c=1.12$ in CHCl_3). TLC R_f 0.53 (PE, KMnO_4). ^1H NMR (CDCl_3): δ 7.52 (m, 2H), 7.36 (m, 3H), 5.86 (ddd, 1H, $J=17.2, 10.5, 10.2$ Hz), 5.74 (ddt, 1H, $J=17.2, 10.2, 6.7$ Hz), 4.95 (m, 3H), 4.77 (dd, 1H, $J=17.2, 1.7$ Hz), 3.86 (m, 1H, $J=7.9, 3.5$ Hz), 2.03 (dd, 1H, $J=10.2, 3.5$ Hz), 1.94 (m, 2H, $J=6.7$ Hz), 1.51 (m, 1H), 1.41 (m,

1H), 1.28 (m, 1H), 1.14 (m, 1H), 0.87 (s, 9H), 0.34 and 0.29 (s, 3H), 0.00 and -0.01 (s, 3H). ^{13}C NMR (CDCl_3): δ 139.3, 139.2, 136.4, 134.5, 129.1, 127.9, 114.84, 114.82, 73.6, 41.1, 36.7, 34.1, 26.5, 25.2, 18.7, -2.6, -3.29, -3.31 and -3.5. IR (film) ν_{max} cm^{-1} 3070, 2927, 2857, 1641, 1625, 1471, 1463, 1427, 1413, 1253, 1112, 1061, 907, 834, 772, 732. MS(CI): 388 (1) $[\text{M}]^+$, 331 (12), 319 (21), 209 (85), 193 (17), 135 (100), 107 (15), 75 (73), 73 (57). HRMS: Calcd for $\text{C}_{23}\text{H}_{40}\text{OSi}_2$ (M-H): 387.25394 found: M 387.25367.

6.4.7. (3S,4R)-anti-3-Dimethylphenylsilyl-deca-1,9-diene-4-yl *t*-butyldimethylsilyl ether (21d). Following the typical procedure C. The reaction was carried out on 1.6 g of **19d** (5.5 mmol). Flash chromatography (SiO_2 : cyclohexane) gave 1.76 g of colorless oil (79% yield, 99% pure by GC). $[\alpha]_D^{23} = -2.53$ ($c=0.83$ in CHCl_3). TLC R_f 0.47 (PE, KMnO_4). ^1H NMR (CDCl_3): δ 7.50 (m, 2H), 7.34 (m, 3H), 5.84 (ddd, 1H, $J=17.1, 10.4, 10.2$ Hz), 5.77 (ddt, 1H, $J=17.1, 10.2, 6.7$ Hz), 4.94 (m, 3H), 4.74 (m, 2H, $J=17.1, 2.2$ Hz), 3.83 (m, 1H, $J=7.9, 4.5, 3.5$ Hz), 1.99 (m, 3H), 1.52 (m, 1H), 1.39 (m, 1H), 1.20 (m, 4H), 0.87 (s, 9H), 0.34 and 0.29 (s, 3H), 0.00 and -0.01 (s, 3H). ^{13}C NMR (CDCl_3): δ 139.3, 139.2, 136.3, 134.4, 129.1, 127.9, 114.8, 114.7, 73.8, 41.1, 37.2, 34.2, 29.4, 26.6, 25.5, 18.8, -2.5, -3.1, -3.2, -3.3. IR (film) ν_{max} cm^{-1} 3070, 2950, 2928, 2855, 1624, 1471, 1462, 1427, 1253, 1111, 1059, 1019, 905, 834, 773, 700. MS(FAB): 425 (3) $[\text{M}+\text{Na}]^+$, 401 (6) $[\text{M}-\text{H}]^+$, 387 (3), 345 (10), 329 (9), 319 (20), 288 (92), 267 (8), 251 (9), 227 (5), 209 (100). HRMS: Calcd for $\text{C}_{24}\text{H}_{42}\text{OSi}_2$ (M-H): 401.26959 found: M 401.26943.

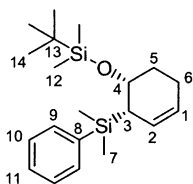
6.4.8. (3S,4R)-anti-3-Dimethylphenylsilyl-tetradeca-1,13-diene-4-yl *t*-butyldimethylsilyl ether (21e). Following the typical procedure C. the reaction was carried out on 2 g of **19e** (5.8 mmol). Flash chromatography (SiO_2 : PE) gave 2.39 g of colorless oil (90% yield, 98% pure by GC). TLC R_f 0.68 (PE, KMnO_4). ^1H NMR (CDCl_3): δ 7.52 (m, 2H), 7.35 (m, 3H), 5.85 (m, 2H), 4.98 (d, 2H, $J=17.1$ Hz), 4.94 (d, 2H, $J=10.2$ Hz), 4.76 (d, 1H, $J=17.1$ Hz), 3.85 (m, 1H, $J=7.5, 3.7$ Hz), 2.05 (m, 3H), 1.40 (m, 2H), 1.25 (m, 12H), 0.89 (s, 9H), 0.37 and 0.32 (s, 3H), 0.02 and 0.01 (s, 3H). ^{13}C NMR (CDCl_3): δ 139.6, 139.3, 136.5, 134.5, 129.1, 127.9, 114.7, 114.5, 73.8, 41.0, 37.3, 34.2, 30.0, 29.9, 29.8, 29.5, 29.3, 26.5, 25.8, 18.6, -2.6, -3.2, -3.3, -3.5. IR (film) ν_{max} cm^{-1} 3070, 2927, 2854, 1640, 1625, 1471, 1462, 1427, 1413, 1252, 1061, 907, 834, 772, 732. MS(CI): 459 (20) $[\text{M}+\text{H}]^+$, 444 (27), 401 (30), 319 (72), 283 (18), 251 (67), 209 (77), 189 (42), 135 (100). HRMS: Calcd for $\text{C}_{28}\text{H}_{50}\text{OSi}_2$ 458.340023 found: M 458.340914.

6.4.9. (1R,2S)-2-(Dimethylphenylsilyl)-cyclohex-3-enol (13ent). To a boiling solution of **19b** (2.5 g, 0.96 mmol, 1 equiv.) in CH_2Cl_2 (120 mL) was added **3** (400 mg, 5 mol%) in CH_2Cl_2 (3 mL). After 2 h of reaction the conversion was complete. The solvent was evaporated under reduced pressure. Flash chromatography (SiO_2 , $\text{CH}_2\text{Cl}_2/\text{EP}$, 1:1) gave 1.92 g of **13ent** (87% yield). $[\alpha]_D^{23} = +81.9$ ($c=0.7$ in CH_2Cl_2). TLC R_f 0.35 ($\text{Et}_2\text{O}/\text{hexane}$, 3:17, KMnO_4). ^1H NMR (CDCl_3): δ 7.3–7.7 (m, 5H), 5.67 (dm, 1H, $J=10.5$ Hz), 5.57 (d, 1H, $J=10.8$ Hz), 4.2 (br s, 1H), 2–2.2 (m, 3H), 1.5–1.8 (m, 2H), 1.44 (d, 1H, $J=6$ Hz), 0.40 and 0.38 (s, 3H). ^{13}C NMR (CDCl_3): δ 138.8,

134, 128.9, 127.7, 125.1, 124.7, 68, 34.3, 29.8, 21.2, –3.1, –3.2. IR (film) ν_{\max} cm^{-1} 3578, 3456, 3068, 3020, 2952, 2921, 2841, 1427, 1247. MS(CI): 215 (32), 155 (20), 137 (61), 135 (100). HRMS: Calcd for $\text{C}_{14}\text{H}_{19}\text{Si}$ ($M+1-\text{H}_2\text{O}$) 215.125604 found: M 215.12500.

6.4.10. (1*R*,2*S*)-2-(Dimethylphenylsilyl)-cyclopent-3-enyl *t*-butyldimethylphenylsilyl ether (22a). To a solution of **21a** (1.6 g, 4.43 mmol, 1 equiv.) in CH_2Cl_2 (215 mL) was added **3** (73 mg, 2 mol%) in CH_2Cl_2 (2 mL). After 5 min of reaction the flask was open to air for 1 h then the solvent was evaporated under reduced pressure. Flash chromatography (SiO_2 : hexane) gave 1.45 g of **22a** (98% yield). $[\alpha]_{\text{D}}^{23} = +94.2$ ($c=0.75$ in CHCl_3). TLC R_f 0.67 (PE, KMnO_4). ^1H NMR (CDCl_3): δ 7.54 (m, 2H), 7.33 (m, 3H), 5.51 (m, 2H), 4.96 (dd, 1H, $J=8.5, 7.3$ Hz), 2.49 (m, 2H, $J=8.5$ Hz), 2.18 (m, 1H, $J=14.9, 7.3, 2.2$ Hz), 0.87 (s, 9H), 0.38 and 0.35 (s, 3H), 0.03 and –0.02 (s, 3H). ^{13}C NMR (CDCl_3): δ 140.5, 134.3, 131.9, 128.8, 127.8, 125.7, 77.5, 42.75, 42.72, 26.5, 18.5, –1.8, –2.7, –4.34, –4.36. IR (film) ν_{\max} cm^{-1} 3053, 2955, 2929, 2857, 1471, 1427, 1362, 1253, 1094, 898, 835, 776, 700. MS(CI): 331 (5) $[\text{M}-\text{H}]^+$, 251 (44), 209 (100), 189 (11), 147 (18), 135 (39).

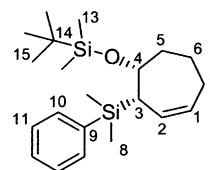
6.4.11. (1*R*,2*S*)-2-(Dimethylphenylsilyl)-cyclohex-3-enyl *t*-butyldimethylphenylsilyl ether (22b). To a solution of **21b** (292 mg, 0.78 mmol, 1 equiv.) in CH_2Cl_2 (10 mL) was added **3** (10 mg, 1.6 mol%) in CH_2Cl_2 (0.7 mL). After 2 min of reaction the flask was open to air then the solvent was evaporated under reduced pressure. Flash chromatography (SiO_2 : hexane) gave 265 mg of **22b** (98% yield). $[\alpha]_{\text{D}}^{23} = +74.1$ ($c=1.35$ in CH_2Cl_2). TLC R_f 0.63 (hexane, KMnO_4). ^1H NMR (CDCl_3): δ 7.53 (m, 2H), 7.33 (m, 3H), 5.47 (m, 1H, $J=9.9, 4.5, 3.1$ Hz), 5.41 (m, 1H, $J=9.9, 4.6, 1.8$ Hz), 4.22 (ddd, 1H, $J=10.5, 6.5, 4.1$ Hz), 2.19 (m, 1H), 2.04 (m, 2H), 1.59 (m, 2H), 0.88 (s, 9H), 0.38 and 0.37 (s, 3H), 0.05 and 0.00 (s, 3H). ^{13}C NMR (CDCl_3): δ 140, 134.2, 128.5, 127.5, 127.2, 123.6, 71.5, 36.1, 30.6, 24.7, 26.2, 18.4, –1.3, –2, –4.3, –4.8. IR (film) ν_{\max} cm^{-1} 3096, 3050, 3024, 2955, 2930, 2857, 1252, 1081. MS(CI): 345 (100) $[\text{M}-\text{H}]^+$, 303 (25), 283 (33), 269 (44), 251 (57), 227 (60), 209 (69), 189 (25), 135 (51), 80 (32). Elem. Anal. Calcd for $\text{C}_{20}\text{H}_{34}\text{OSi}_2$ C 69.10, H 9.89 found: C 69.10, H 9.98.



Measured and calculated 3J values (in Hz) with MM3 force field

H	3J	3J calculated (Hz)	
		Cluster 1	Cluster 2
2-3	4.6	4.6	2.8
3-4	4.1	6.0	2.9
4-5	6.5	3.4	1.8
4-5'	10.5	11.6	4.7
1-6	3.0	3.1	4.6
1-6'	3.5	4.5	3.0
ΔE (kJ/mol)	0		2.25

6.4.12. (1*R*,2*S*)-2-(Dimethylphenylsilyl)-cyclohept-3-enyl *t*-butyldimethylphenylsilyl ether (22c). To a solution of **21c** (200 mg, 0.514 mmol, 1 equiv.) in toluene (30 mL) was added **3** (32 mg, 7.5 mol%) in toluene (1 mL). The reaction mixture was heated at 60 °C for 2 h then the flask was open to air then the solvent was evaporated under reduced pressure. Flash chromatography (SiO_2 : hexane) gave 173 mg of **22c** (93% yield). $[\alpha]_{\text{D}}^{23} = +48.27$ ($c=0.98$ in CHCl_3). TLC R_f 0.5 (Cyclohexane, KMnO_4). ^1H NMR (CDCl_3): δ 7.57 (m, 2H), 7.35 (m, 3H), 5.65 (m, 1H, $J=11.6, 7.39, 4.01$ Hz), 5.53 (m, 1H, $J=11.6, 8.5, 2.5$ Hz), 3.95 (ddd, 1H, $J=11.3, 4.5, 4.1$ Hz), 2.35 (dd, 1H, $J=8.5, 4.1$ Hz), 2.05 (dddd, 1H, $J=16.1, 7.4, 6.7, 2.5$ Hz), 1.88 (m, 1H, $J=13.7, 11.0, 4.0$ Hz), 1.73 (m, 1H, $J=11.0, 4.0$ Hz), 1.67 (m, 1H, $J=16.1, 4.1, 2.5$ Hz), 1.55 (m, 1H, $J=14.0, 6.7, 2.0$ Hz), 1.23 (m, 1H, $J=8.0, 2.5$ Hz), 0.92 (s, 9H), 0.47 and 0.43 (s, 3H), 0.06 and 0.05 (s, 3H). ^{13}C NMR (CDCl_3): δ 140.2, 134.2, 129.5, 128.6, 128.5, 127.4, 75.2, 42.4, 38.9, 28.3, 26.1, 24.4, 18.2, –0.6, –1.1, –4.7, –4.8. IR (film) ν_{\max} cm^{-1} 3070, 2950, 2868, 1471, 1392, 1254, 1141, 1070, 1021, 832, 791. MS(FAB): 360 (1), 303(2), 209 (73), 193 (20), 134.9 (100), 106.8 (11), 93.9 (82), 78.9 (30), 74.9 (30). HRMS: Calcd for $\text{C}_{21}\text{H}_{35}\text{OSi}_2$ ($M-\text{H}$): 359.22264 found: M 359.22213.



Measured and calculated 3J values (in Hz) with MM3 force field

H	measured (Hz)	3J calculated (Hz)				
		Cluster 1	Cluster 2	Cluster 3	Cluster 4	Cluster 5
2-3	8.55	6.0	5.4	4.8	2.7	5.9
3-4	4.1	3.7	0.2	2.9	3.2	1.6
4-5	4.51	2.5	1.9	5.4	5.8	8.9
4-5'	11.29	11.6	4.9	10.5	1.5	6.6
5-6	11.0	5.8	13.5	9.6	5.6	8.3
5-6'	4.00	1.5	2.5	8.7	1.7	0.4
5'-6	4.00	1.7	2.0	8.5	6.0	0.5
5'-6'	11.00	13.4	5.0	0.4	12.0	12.4
6-7	6.7	4.5	12.9	12.9	6.2	1.7
6-7'	2.00	2.4	1.4	1.3	1.2	5.6
6'-7	2.5	2.3	1.3	1.2	1.3	5.5
6'-7'	8.00	13.1	5.9	6.2	12.9	12.0
7-1	7.39	6.3	4.4	2.6	5.4	3.2
7'-1	4.00	2.8	6.6	6.1	2.8	4.5
ΔE (kJ/mol)	0	2.03	5.57	9.51	11.61	

6.4.13. (3*S*,4*R*)-anti-3-Dimethylphenylsilyl-dodeca-1,9-diene-4-yl *t*-butyldimethylsilyl ether (26). (3*S*,4*R*)-anti-3-(Dimethyl-phenyl-silyl)-dodeca-1,9-dien-4-ol. Following the typical procedure A. To a solution of allyldimethylphenylsilyl ether (2 g, 11.3 mmol, 1.1 equiv.) in THF (25 mL) at rt was added 2.2 M *n*-BuLi (5.15 mL, 1.1 equiv.) dropwise over 10 min. After 20 min, the yellow solution was

transferred via canula over 10 min to a suspension of (*R,R*)-TiClCpTADDOL (7.6 g, 11.8 mmol, 1.15 equiv.) in THF (30 mL) at -78°C . After 30 min, neat *cis*-6-nonenal (1.72 mL, 10.3 mmol, 1 equiv.) was added. Chromatography (SiO₂: AcOEt/PE, 4:96) 2.08 g (64% yield). $[\alpha]_{\text{D}}^{23} = +1.36$ ($c = 1.1$ in CHCl₃). TLC R_f 0.54 (CH₂Cl₂, KMnO₄). ¹H NMR (CDCl₃): δ 7.54 (m, 2H), 7.36 (m, 3H), 5.83 (ddd, 1H, $J = 17.2, 10.5, 10.4$ Hz), 5.33 (m, 2H), 5.05 (dd, 1H, $J = 10.4, 2.1$ Hz), 4.91 (dd, 1H, $J = 17.2, 2.1$ Hz), 3.72 (m, 1H), 2.01 (m, 4H), 1.90 (dd, 1H, $J = 10.5, 4.5$ Hz), 1.32 (m, 6H), 0.94 (t, 2H, $J = 7.6$ Hz), 0.36 and 0.33 (s, 3H). ¹³C NMR (CDCl₃): δ 138.0, 135.2, 133.8, 131.7, 129.0 (2 carbons), 127.7, 115.5, 71.5, 42.2, 37.1, 29.7, 27.3, 25.4, 20.5, 14.3, $-3.3, -3.9$. IR (film) ν_{max} cm⁻¹ 3446, 3070, 2969, 2869, 1716, 1625, 1428, 1380, 1250, 1142, 1021, 900, 834, 701. MS(CI): 315 (6) [M-H]⁺, 299 (3), 271 (10), 247 (15), 229 (5), 209 (7), 205 (10), 187 (14), 135 (100), 81 (45). HRMS: Calcd for C₂₀H₃₁OSi [M-H]⁺ 315.214419 found: *M* 315.2144612. (26) Following the typical procedure C. The reaction was carried out on 0.77 g of (3*S*,4*R*)-*anti*-3-(dimethyl-phenyl-silanyl)-dodeca-1,9-dien-4-ol (2.44 mmol). Flash chromatography (SiO₂: cyclohexane) gave 0.67 g of colorless oil (63% yield). ¹H NMR (CDCl₃): δ 7.50 (m, 2H), 7.34 (m, 3H), 5.84 (ddd, 1H, $J = 17.2, 10.4, 10.2$ Hz), 5.32 (m, 2H), 4.94 (dd, 1H, $J = 10.2, 2.1$ Hz), 4.75 (dd, 1H, $J = 17.2, 2.1$ Hz), 3.84 (m, 1H, $J = 8.0, 4.5, 3.2$ Hz), 1.99 (m, 5H, $J = 7.6$ Hz), 1.51 (m, 1H), 1.39 (m, 1H), 1.17 (m, 4H), 0.96 (t, 3H, $J = 7.6$ Hz), 0.88 (s, 9H), 0.35 and 0.30 (s, 3H), 0.01 and -0.01 (s, 3H). ¹³C NMR (CDCl₃): δ 138.8, 135.9, 134.1, 131.6, 129.1, 128.7, 127.5, 114.4, 73.3, 40.6, 36.7, 29.7, 27.1, 26.1, 25.1, 20.5, 18.2, 14.4, $-3.1, -3.6, -3.7, -3.9$. MS(CI): 431 (19) [M+1]⁺, 430 (15) [M], 416 [M-Me]⁺, 373 (44), 319 (100) [M-(CH₂)₄-C=C-Et]⁺, 299 (8), 295 (10), 251 (71), 209 (84), 189 (35), 135 (100). HRMS: Calcd for C₂₆H₄₇OSi₂ [M+H]⁺ 431.316548 found: *M* 431.314734.

6.4.14. 2-(Dimethyl-phenyl-silanyl)-1-(2,2-dimethyl-5-vinyl-[1,3]dioxolan-4-yl)-but-3-en-1-ol (28). Following the typical procedure A. To a solution of allyldimethyl-phenylsilane (2.7 g, 15.5 mmol, 1.1 equiv.) in THF (30 mL) at rt was added 2.2 M *n*-BuLi (7 mL, 1.1 equiv.) dropwise over 10 min. After 20 min, the yellow solution was transferred via canula over 10 min to a suspension of (*R,R*)-TiClCpTADDOL (10.4 g, 16.2 mmol, 1.15 equiv.) in THF (40 mL) at -78°C . After 30 min, the neat alcohol **28** (2.2 g, 14 mmol, 1 equiv.) was added. Chromatography (SiO₂: CH₂Cl₂) 3.1 g (55% yield). $[\alpha]_{\text{D}}^{23} = -33.4$ ($c = 0.99$ in CHCl₃). TLC R_f 0.42 (CH₂Cl₂, KMnO₄). ¹H NMR (CDCl₃): δ 7.52 (m, 2H), 7.36 (m, 3H), 5.99 (ddd, 1H, $J = 17.1, 10.8, 10.2$ Hz), 5.70 (ddd, 1H, $J = 17.1, 10.2, 8.5$ Hz), 5.28 (ddd, 1H, $J = 17.1, 1.6, 0.7$ Hz), 5.22 (ddd, 1H, $J = 10.2, 1.6, 0.7$ Hz), 4.98 (dd, 1H, $J = 10.2, 2.0$ Hz), 4.79 (ddd, 1H, $J = 17.1, 2.0$ Hz), 4.39 (dd, 1H, $J = 8.5, 6.1$ Hz), 4.01 (dd, 1H, $J = 8.5, 6.1$ Hz), 3.69 (ddd, 1H, $J = 8.5, 2.6, 2.5$ Hz), 2.15 (dd, 1H, $J = 2.6, 1.9$ Hz), 1.90 (ddd, 1H, $J = 10.8, 2.5, 1.9$ Hz), 1.44 (s, 3H), 1.32 (s, 3H), 0.37 (s, 3H), 0.31 (s, 3H). ¹³C NMR (CDCl₃): δ 138.1, 134.9, 134.8, 134.5, 129.4, 128.0, 119.2, 115.2, 108.9, 80.7, 78.7, 70.0, 37.9, 28.5, 25.9, $-3.4, -3.7$. IR (film) ν_{max} cm⁻¹ 3490, 3070, 2986, 2902, 1624, 1471, 1427, 1371, 1246, 1114, 1068, 835. MS(CI): 331 (1) [M-H]⁺, 317 (4) [M-Me]⁺, 259 (19), 257 (23), 205 (31), 203 (36), 144 (17), 137 (56), 135 (100), 124 (28), 98 (24), 75

(34), 68 (45). HRMS: Calcd for C₁₉H₂₈O₃SiNa (M+Na) 355.17054 found: *M* 355.17023.

6.4.15. Acetic acid 2-(dimethyl-phenyl-silanyl)-1-(2,2-dimethyl-5-vinyl-[1,3]dioxolan-4-yl)-but-3-enyl ester (29). Following the typical procedure B. The reaction was carried out on 1.2 g of **28** (3.25 mmol). Flash chromatography (SiO₂: CH₂Cl₂/PE, 3:2) gave 1.08 g of colorless oil (89% yield). $[\alpha]_{\text{D}}^{23} = +2.91$ ($c = 0.96$ in CHCl₃). TLC R_f 0.83 (CH₂Cl₂/PE, 3:2, KMnO₄). ¹H NMR (CDCl₃): δ 7.44 (m, 2H), 7.35 (m, 3H), 5.94 (ddd, 1H, $J = 17.1, 10.7, 10.1$ Hz), 5.83 (ddd, 1H, $J = 17.1, 10.1, 9.1$ Hz), 5.05 (dd, 1H, $J = 10.1, 1.7$ Hz), 4.83 (dd, 1H, $J = 17.1, 1.7$ Hz), 4.39 (dd, 1H, $J = 8.5, 5.9$ Hz), 4.19 (dd, 1H, $J = 8.8, 5.9$ Hz), 2.00 (dd, 1H, $J = 10.7, 2.4$ Hz), 1.78 (s, 3H), 1.43 and 1.27 (s, 3H), 0.32 and 0.27 (s, 3H). ¹³C NMR (CDCl₃): δ 170.1, 137.2, 134.9, 134.5, 134.4, 129.6, 128.0, 119.6, 116.4, 109.2, 79.0, 78.7, 70.6, 37.5, 28.3, 26.0, 21.4, $-3.4, -4.2$. IR (film) ν_{max} cm⁻¹ 3071, 2958, 1743, 1626, 1428, 1371, 1233, 1113, 1048, 874, 835, 757, 735. MS(FAB): 397 (100) [M+Na]⁺, 329 (32), 288 (17), 267 (22), 257 (47), 237 (17), 217 (21), 209 (46). HRMS: Calcd for C₂₁H₃₀O₄SiNa 397.18110 found: *M* 397.18095.

6.4.16. Acetic acid 5-(dimethyl-phenyl-silanyl)-2,2-dimethyl-3a,4,5,7a-tetrahydro-benzo[1,3]dioxol-4-yl ester (30). To a solution of **29** (840 mg, 0.22 mmol, 1 equiv.) in CH₂Cl₂ (30 mL) were added 2nd generation Grubbs' catalyst (160 mg, 8 mol%, 0.018 mmol). The reaction mixture was heated at reflux and argon was bubbled for 2 h. Flash chromatography (SiO₂: CH₂Cl₂) gave 632 mg (80% yield) of **30** as a colorless oil. $[\alpha]_{\text{D}}^{23} = +5.32$ ($c = 1.39$ in CHCl₃). TLC R_f 0.19 (CH₂Cl₂, KMnO₄). ¹H NMR (CDCl₃): δ 7.5 (m, 2H), 7.37 (m, 3H), 5.87 (dd, 1H, $J = 9.9, 5.5$ Hz), 5.80 (ddd, 1H, $J = 9.9, 3.4, 1.4$ Hz), 5.07 (dd, 1H, $J = 9.2, 6.4$ Hz), 4.39 (dd, 1H, $J = 6.6, 3.4$ Hz), 4.01 (dd, 1H, $J = 9.2, 6.6$ Hz), 2.63 (dd, 1H, $J = 6.4, 5.5$ Hz), 1.78 (s, 3H), 1.42 (s, 3H), 1.30 (s, 3H), 0.36 (s, 3H), 0.35 (s, 3H). ¹³C NMR (CDCl₃): δ 171.2, 137.6, 134.3, 131.6, 129.8, 128.3, 122.2, 109.4, 75.2, 75.0, 72.8, 41.3, 32.5, 28.4, 26.0, 21.3, $-2.3, -2.6$. IR (film) ν_{max} cm⁻¹ 3069, 2924, 2852, 1744, 1624, 1459, 1369, 1230, 1112, 1049, 1018, 834, 812, 733, 701. MS(FAB): 369 (50) [M+Na]⁺, 355 (10), 341 (11), 329 (100), 288 (29), 280 (23), 271 (14), 267 (13), 245 (11), 229 (19), 226 (17), 223 (27), 209 (97), 207 (36). HRMS: Calcd for C₁₉H₂₆O₄SiNa (M+Na) 369.1498 found: *M* 369.1510.

6.5. Addition of dichlorocarbene: typical procedure D

To a mixture of the cyclic allylsilane (0.62 mmol, 1 equiv.) and Et₃BnNCl (15 mg, 0.065 mmol, 0.1 equiv.) in CHCl₃ (4 mL) was added 50% NaOH (1 mL) under vigorous stirring. After 15 h, water (4 mL) was added and the organic layer was separated. The aqueous phase was extracted with CHCl₃. The combined organic phases were dried over MgSO₄ and concentrated in vacuo. Purification by flash chromatography gave the dichlorocyclopropane.

6.5.1. (1*R*,2*S*,3*R*,5*R*)-3-(*tert*-Butyl-dimethyl-silanyloxy)-6,6-dichloro-2-(dimethyl-phenyl-silanyl)-bicyclo[3.1.0]-hexane (31). Following procedure D, the reaction was carried out on 206 mg (0.62 mmol) of **22a**. Chromatography

(SiO₂: cyclohexane) gave 252 mg of colorless oil (98% yield). $[\alpha]_D^{23} = -10.1$ ($c = 1.3$ in CDCl₃). TLC R_f 0.64 (cyclohexane, KMnO₄). ¹H NMR (CDCl₃): δ 7.56 (m, 2H), 7.36 (m, 3H), 4.60 (ddd, 1H, $J = 7.5, 7.0, 5.3$ Hz), 2.23 (ddd, 1H, $J = 14.3, 7.0, 0.6$ Hz), 2.10 (ddd, 1H, $J = 8.1, 6.5, 0.6$ Hz), 2.05 (dd, 1H, $J = 7.5, 1.5$ Hz), 1.98 (dd, 1H, $J = 8.1, 1.5$ Hz), 1.91 (ddd, 1H, $J = 14.3, 6.5, 5.3$ Hz), 0.85 (s, 9H), 0.41 and 0.39 (s, 3H), 0.01 and -0.06 (s, 3H). ¹³C NMR (CDCl₃): δ 139.7, 134.2, 129.2, 128.2, 78.4, 70.3, 39.6, 38.8, 36.5, 35.9, 26.5, 18.5, -1.2, -2.1, -4.1, -4.3. IR (film) ν_{\max} cm⁻¹ 3071, 2954, 2929, 2857, 1471, 1427, 1361, 1255, 1143, 1110, 1058, 888, 834, 778, 731, 700. MS(CI): 414 (2) [M]⁺, 379 (2) [M-Cl]⁺, 325 (5), 283 (7), 251 (35), 209 (75), 189 (30), 154 (40), 135 (71), 113 (47), 75 (15), 59 (100). HRMS Calcd for C₂₀H₃₂Cl₂O₂Si₂ 414.136878 found: M 414.137426.

6.5.2. (1R,2S,3R,6R)-7,7-Dichloro-2-dimethylphenylsilyl-bicyclo[4.1.0]heptan-3-yl acetate (32). Acetic acid 2-(dimethylphenylsilyl)-cyclohex-3-enyl ester. To a solution of **13ent** (374 mg, 1.6 mmol, 1 equiv.) and pyridine (0.39 mL, 3 equiv.) in CH₂Cl₂ (6 mL) at 0 °C was added AcCl (0.23 mL, 2 equiv.) dropwise. After 1 h at rt, Et₂O (7 mL) was added, the reaction mixture was filtered and concentrated in vacuo. The residue was taken up in Et₂O (12 mL), filtered, washed twice with 1.2 N HCl (3 mL) and once with Na₂CO₃sat (3 mL). The organic phase was dried over MgSO₄ and concentrated under reduced pressure to afford the crude acetate. Filtration over SiO₂ (hexane/Et₂O, 8:2) gave pure acetate in 92% yield (>99% by GC, 92% ee by HPLC) $[\alpha]_D^{23} = +108$ ($c = 0.64$ in CH₂Cl₂). For analyses see **14rac**. (**32**) Following procedure D, the reaction was carried out on 170 mg (0.62 mmol) of acetic acid 2-(dimethylphenylsilyl)-cyclohex-3-enyl ester. Chromatography (SiO₂: hexane 90:10 AcEt) gave **32** in 84% yield (93% ee by HPLC, only one isomer detected by NMR, GC and HPLC). $[\alpha]_D^{23} = -4$ ($c = 0.5$ in CH₂Cl₂). TLC R_f 0.3 (hexane/AcOEt, 9:1, KMnO₄). ¹H NMR (CDCl₃): δ 7.3–7.6 (m, 5H), 4.98 (ddd, 1H, $J = 3.9, 2.5, 2.5$ Hz), 1.92 (s, 3H), 1.3–1.4 and 1.6–1.9 (m, 6H), 1.17 (dd, 1H, $J = 5, 2.8$ Hz), 0.42 (s, 3H), 0.39 (s, 3H). ¹³C NMR (CDCl₃): δ 170.2, 136.7, 133.8, 129.4, 128, 67.9, 67.3, 26, 25.6, 23.7, 23.7, 13.8, 21.2, -3.9, -4. IR (film) ν_{\max} cm⁻¹ 3070, 3049, 3014, 2957, 2861, 1737, 1372, 1239, 1207. MS(EI, 70 eV): 179 (17), 135 (100), 117 (92), 127 (49), 43 (37). Elem. Anal. Calcd for C₁₇H₂₂Cl₂O₂Si 57.14, H 6.21, Cl 19.93 found: C 57.23, H 6.22, Cl 19.93.

6.5.3. (1R,2S,3R,7R)-3-(tert-Butyl-dimethyl-silanyl-oxy)-8,8-dichloro-2-(dimethyl-phenyl-silanyl)-bicyclo[5.1.0]octane (33). Following procedure D, the reaction was carried out on 224 mg (0.62 mmol) of **22c**. Chromatography (SiO₂: cyclohexane) gave 250 mg of colorless oil (98% yield) as a 10:1 mixture of diastereoisomers. $[\alpha]_D^{23} = -12.8$ ($c = 1.1$ in CHCl₃). TLC R_f 0.59 (PE, KMnO₄). ¹H NMR (C₆D₆): δ 7.66 (m, 2H), 7.32 (m, 3H), 4.22 (dd, 1H, $J = 4.8, 1.4$ Hz), 1.99 (m, 1H, $J = 11.6, 11.6$ Hz), 1.99 (m, 1H, $J = 12.6, 6.8$ Hz), 1.82 (m, 1H, $J = 13, 4.8$ Hz), 1.77 (m, 1H, $J = 11.6, 11.6, 6.8$ Hz), 1.72 (m, 1H, $J = 13, 13, 12.7$ Hz), 1.33 (m, 1H, $J = 13, 12.6, 11.6$ Hz), 1.29 (m, 1H, $J = 13, 3.4$ Hz), 1.17 (d, 1H, $J = 11.6$ Hz), 1.01 (s, 9H), 0.9 (m, 1H, $J = 13, 12.7, 3.4, 1.4$ Hz), 0.63 and 0.56 (s, 3H), 0.04 and -0.01 (s, 3H). ¹³C NMR (CDCl₃): δ 138.3, 134.5, 129.4,

128.2, 71.3, 69.8, 42.1, 35.1, 33.4, 32.0, 27.3, 26.6, 21.9, 18.6, -2.5, -2.5, -4.1, -4.3. IR (film) ν_{\max} cm⁻¹ 3069, 2954, 2856, 1471, 1427, 1255, 1089, 1043, 1017, 916, 830, 772, 731, 700, 607. MS(FAB): 441 [M-H]⁺ (1), 385 (1), 327 (2), 307 (2), 288, 255 (6), 251, 228, 209 (65), 193, 179, 147, 135 (95), 105, 93, 73. HRMS: Calcd for C₂₂H₃₆O₂Si₂-Cl₂ 442.168178 found: M 442.167339.

6.5.4. 3-(tert-Butyl-dimethyl-silanyloxy)-2-(dimethyl-phenyl-silanyl)-bicyclo[4.1.0]heptane-7-carboxylic acid ethyl ester (34). Compound **22b** (300 mg, 0.831 mmol, 1 equiv.) was added to a suspension of copper acetylacetonate (4.5 mg, 0.017 mmol, 2 mol%) in freshly dried and degassed toluene (1 mL). The mixture was heated at 90 °C and ethyl diazoacetate (118 mg, 0.998 mmol, 1.2 equiv.) in toluene (2 mL) was added over 3 h thanks to a syringe pump. The brown reaction mixture was cooled to room temperature and the solvent was removed under reduce pressure (temperature of the water bath below 35 °C). The resulting oil was treated with 500 mg of alumine to remove the catalyst. Pentane was added before filtration and concentration. The oil was chromatographed on SiO₂ (AcOEt/PE: 2.5:97.5) to give 266 mg (71% yield) of **34**. $[\alpha]_D^{23} = +44.11$ ($c = 1.33$ in CHCl₃). TLC R_f 0.28 (AcOEt/PE: 3:97, KMnO₄). ¹H NMR (CDCl₃): δ 7.54 (m, 2H), 7.31 (m, 3H), 4.06 (qd, 2H, $J = 7.2, 2.3$ Hz), 3.93 (m, 1H, $J = 6, 3.3, 1.8$ Hz), 2.14 (m, 1H, $J = 13.7, 11.3, 6.5, 1.8$ Hz), 1.70 (m, 1H, $J = 14.4, 6.5$ Hz), 1.70 (m, 1H, $J = 9.7, 5.8, 4.3$ Hz), 1.62 (m, 1H, $J = 13.7, 6, 5.8$ Hz), 1.52 (m, 1H, $J = 9.7, 4.3, 3.3$ Hz), 1.30 (dd, 1H, $J = 4.3, 4.3$ Hz), 1.23 (m, 1H, $J = 3.3, 3.3$ Hz), 1.20 (t, 3H, $J = 7.2$ Hz), 1.14 (m, 1H, $J = 13.7, 11.3, 6.5, 1.8$ Hz), 0.90 (s, 9H), 0.38 and 0.37 (s, 3H), 0.01 and -0.06 (s, 3H). ¹³C NMR (CDCl₃): δ 174.3, 138.9, 133.8, 128.6, 127.6, 66.6, 60.0, 31.5, 28.9, 27.9, 26.1, 21.9, 21.7, 18.2, 17.0, 14.2, -2.9, -3.4, -4.1, -4.4. IR (film) ν_{\max} cm⁻¹ 2954, 2858, 1723, 1427, 1317, 1300, 1255, 1200, 1174, 1113, 1036, 986, 831, 700. MS(FAB): 455 (9) [M+Na]⁺, 431 (5), 387 (9), 355 (7), 345 (6), 301 (16), 288 (10), 251 (13), 223 (7), 209 (100). HRMS: Calcd for C₂₄H₃₉O₃Si₂ (M-H): 431.24377 found: M 431.24350.

6.5.5. (1R,4R)-[4-(tert-Butyl-dimethyl-silanyloxy)-cyclohex-2-enyl]-phenyl-methanol (35). To a solution of 2,6-di-*t*-butyl-4-methylpyridine (266 mg, 1.29 mmol, 1.5 equiv.) and TMSNTf₂ (305 mg, 0.86 mmol, 1 equiv.) in CH₂Cl₂ (5 mL) at -78 °C was added benzaldehyde (97 μL, 0.95 mmol, 1.1 equiv.). After 10 min, **22c** (300 mg, 0.86 mmol, 1 equiv.) was added and the reaction mixture was stirred at -78 °C for 1 h. HCl (5 mL) were added and the organic phase was washed with NaHCO₃sat. The combined organic phases were dried over MgSO₄ and concentrated in vacuo. The oil was purified by chromatography (SiO₂, CH₂Cl₂/EP: 1:1). The product was isolated as a 3:1 mixture of epimers. Analyses of enriched major isomer: TLC R_f 0.18 (CH₂Cl₂/EP, 2:3, KMnO₄). ¹H NMR (CDCl₃): 7.38 (m, 5H), 5.95 and 5.65 (dm, 1H, $J = 10.3, 1.5$ Hz), 4.26 (d, 1H, $J = 8.1$ Hz), 4.18 (m, 1H), 2.44 (m, 1H), 1.85 (m, 1H), 1.40 (m, 1H, $J = 13, 9, 3$ Hz), 1.28 (m, 1H) 1.09 (m, 1H, $J = 13, 10, 3$ Hz), 0.88 (s, 9H), 0.06 and 0.05 (s, 3H). ¹³C NMR (CDCl₃): 143.4, 133.2, 130.2, 129.8, 128.0, 127.6, 79.7, 68.5, 44.3, 32.6, 26.3, 24.6, 18.6, -4.1, -4.3. MS(FAB): 341 (21) [M+Na]⁺, 317 (8), 301 (37), 281 (62), 267 (31), 241 (21), 221 (100), 211 (25).

HRMS Calcd for $C_{19}H_{30}O_2NaSi$ 341.191279 found: *M* 341.192469.

6.5.6. Epoxidation of 22b. To a solution of *m*-cpba (100 mg, 0.57 mmol, 1 equiv.), in CH_2Cl_2 (6 mL) at $-20^\circ C$ was added **22b** (200 mg, 0.57 mmol, 1 equiv.). After 6 h the solvent was evaporated and the solid was taken back in pentane. The solution was filtrated and concentrated before chromatography (SiO_2 , AcOEt/PE: 5:95) to give 78 mg of **37** and 27 mg of **36**. (**36**) TLC R_f 0.4. (AcOEt/PE, 5:95, $KMnO_4$). 1H NMR ($CDCl_3$): δ 7.56 (m, 2H), 7.35 (m, 3H), 4.10 (dd, 1H, $J=4.9, 4.7$ Hz), 3.15 (m, 1H, $J=4.1$ Hz), 3.11 (m, 1H, $J=4.1$ Hz), 2.03 (m, 1H, $J=15.3, 7.3, 2.8$ Hz), 1.94 (m, 1H, $J=15.3, 6$ Hz), 1.84 (d, 1H, $J=4.7$ Hz), 1.49 (ddd, 2H, $J=7.3, 6, 4.9$ Hz), 0.88 (s, 9H), 0.44 and 0.41 (s, 3H), 0.03 and -0.03 (s, 3H). ^{13}C NMR ($CDCl_3$): $\delta=139.01, 134.3, 129.34, 128.21, 67.53, 54.3, 52.65, 32.95, 28.00, 26.61, 20.93, 18.69, -1.63, -1.39, -3.86, -3.96$. MS(FAB): 385, 361, 345, 305, 231, 209, 135 (100). HRMS: Calcd for $C_{20}H_{33}O_2Si_2$ $[M-H]^+$: 361.201912 found: *M* 361.201613. (**37**) TLC R_f 0.64. (AcOEt/PE, 5:95, $KMnO_4$). 1H NMR ($CDCl_3$): δ 7.59 (m, 2H), 7.38 (m, 3H), 5.64 (m, 2H, $J=10.5, 7.5, 2.3$ Hz), 4.09 (m, 2H), 1.77 (m, 2H), 1.62 (m, 2H), 0.88 (s, 9H), 0.395 and 0.392 (s, 3H), 0.05 (s, 6H). ^{13}C NMR ($CDCl_3$): $\delta=138.75, 133.91, 132.93, 131.92, 129.89, 128.17, 66.55, 66.18, 29.07, 28.79, 26.25, -0.61, -0.65, -4.23, -4.24$. MS(FAB): 385, 361, 345, 231, 209, 193, 147, 135 (100). HRMS: Calcd for $C_{20}H_{33}O_2Si_2$ (M-H): 361.201912 found: *M* 361.203290.

6.5.7. (1S,4R)-4-(tert-Butyl-dimethyl-silanyloxy)-cyclohex-2-enol (39). To a suspension of **38** (100 mg, 0.4 mmol, 1 equiv.) in CH_2Cl_2 (2 mL) was added **22b** (138 mg, 0.4 mmol, 1 equiv.) in solution in CH_2Cl_2 (1 mL). After 1 h, the solvent was evaporated and the mixture was taken back in pentane, the precipitate was filtrated and the solvent evaporated. Chromatography (SiO_2 , AcOEt/PE: 25:75) to give **39**²⁶ (55 mg, 60% yield) TLC R_f 0.45 (AcOEt/PE, 25:75, $KMnO_4$). 1H NMR ($CDCl_3$): δ 5.71 (pseudo q, 2H, $J=10.5, 4.8$ Hz), 4.26 (m, 2H, $J=6.2, 1.6$ Hz), 2.12 and 1.99 (m, 1H, $J=12.1, 4.8, 1.3$ Hz), 1.59 (broad s, 1H), 1.49 (m, 2H, $J=12.9, 10.7, 8.3, 1.6$ Hz), 0.89 (s, 9H), 0.07 (s, 6H). ^{13}C NMR ($CDCl_3$): $\delta=134.2, 132.1, 67.4, 66.9, 31.4, 31.3, 26.2, 18.6, -4.3$.

6.5.8. (1R,2R,3R,4R)-4-(tert-Butyl-dimethylsilanyl-oxy)-3-(dimethyl-phenyl-silanyl)-cyclopentane-1,2-diol (40). To a vigorously stirred solution of water (2.5 mL) and $K_2OsO_4 \cdot 2H_2O$ (~8 mg, 2.5 mol%) was added $NMO \cdot H_2O$ (199 mg, 1.7 equiv.). The solution turned yellow. To this mixture was added a solution of **22a** (287 mg, 0.86 mmol, 1 equiv.) in THF (2.5 mL). The solution turned brown. After 8 h at rt, $NaHSO_3$ (100 mg) and magnesol (100 mg) were added to the resulting yellow solution. After stirring for 30 min at rt, the pH was adjusted to 1 with H_2SO_4 and the reaction mixture was filtrated of Celite. The magnesol was washed twice with water and twice AcOEt. The organic phase was separated and the aqueous phase extracted with AcOEt. The combined organic phases were dried over $MgSO_4$ and concentrated in vacuo. Flash chromatography (SiO_2 , PE/AcOEt: 8:2) gave a colorless viscous oil. Traces of solvent were removed and the solid mixture was then triturated in hexane to obtain the diol **40** as a white solid

(180 mg, 56% yield). $[\alpha]_D^{23} = -8.2$ ($c=1.03$ in CH_2Cl_2). TLC R_f 0.64 (cyclohexane, $KMnO_4$). 1H NMR ($CDCl_3$): δ 7.56 (m, 2H), 7.36 (m, 3H), 4.60 (ddd, 1H, $J=7.5, 7.0, 5.3$ Hz), 2.23 (ddd, 1H, $J=14.3, 7.0, 0.6$ Hz), 2.10 (ddd, 1H, $J=8.1, 6.5, 0.6$ Hz), 2.05 (dd, 1H, $J=7.5, 1.5$ Hz), 1.98 (dd, 1H, $J=8.1, 1.5$ Hz), 1.91 (ddd, 1H, $J=14.3, 6.5, 5.3$ Hz), 0.85 (s, 9H), 0.41 and 0.39 (s, 3H), 0.01 and -0.06 (s, 3H). ^{13}C NMR ($CDCl_3$): δ 139.7, 134.2, 129.2, 128.2, 78.4, 70.3, 39.6, 38.8, 36.5, 35.9, 26.5, 18.5, $-1.2, -2.1, -4.1, -4.3$. IR (film) ν_{max} cm^{-1} 2955, 2857, 1471, 1427, 1255, 1110, 1068, 888, 700. MS(CI): 365 (4) $[M-H]^+$, 349 (68), 331 (14), 271 (15), 209 (100), 197 (53), 149 (63), 135 (37), 83 (40). Elem. Anal. Calcd for $C_{19}H_{34}O_3Si_2$ C 62.24, H 9.35 found: C 62.54, H 9.64.

6.5.9. (1R,2R,3R,4R)-2-Dimethylphenylsilylcyclohexa-1,3,4-triol (41). To a vigorously stirred solution (pink colored) of water (3 mL) and $K_2OsO_4 \cdot 2H_2O$ (~8 mg, 2 mol%) was added $NMO \cdot H_2O$ (261 mg, 1.7 equiv.). The solution turned yellow. To this mixture was added a solution of the cyclohexene (260 mg, 1.12 mmol, 1 equiv.) in THF (3 mL). The solution turned brown. After 8 h at rt, $NaHSO_3$ (100 mg) and magnesol (100 mg) were added to the resulting yellow solution. After stirring for 30 min at rt, the pH was adjusted to 1 with H_2SO_4 and the reaction mixture was filtrated of Celite. The magnesol was washed twice with water and twice AcOEt. The organic phase was separated and the aqueous phase extracted with AcOEt. The combined organic phases were dried over $MgSO_4$ and concentrated in vacuo. Flash chromatography (SiO_2 : AcOEt) gave the triol as a colorless viscous oil. Traces of solvent were removed by freeze-pump-thaw cycles. The solid mixture was then triturated in hexane to obtain the triol **41** as a white solid in 80% yield (93% ee by HPLC). Mp $102^\circ C$. $[\alpha]_D^{23} = -62.7$ ($c=0.38$ in CH_2Cl_2). TLC R_f 0.35 (AcOEt, $KMnO_4$). 1H NMR ($CDCl_3$): δ 7.2–7.7 (m, 5H), 3.97 (m, 1H), 3.9 (dd, 1H, $J=11.3, 2.7$ Hz), 3.82 (m, 1H), 1.82–1.96 (m, 1H), 1.6–1.77 (m, 2H), 1.49 (dd, 1H, $J=11.3, 2.8$ Hz), 1.3–1.41 (m, 1H), 0.389 and 0.385 (s, 3H). ^{13}C NMR ($CDCl_3$): δ 141.4, 135.5, 129.5, 128.5, 71.4, 71.2, 69.9, 33.6, 29.1, 27.1, $-1.4, -2.2$. IR (film) ν_{max} cm^{-1} 3547, 3427, 3069, 3023, 2960, 2939, 2897, 1241, 1185, 1069. MS(CI): 417 (89), 399 (10), 265 (100), 247 (16), 151 (24). Elem. Anal. Calcd for $C_{14}H_{22}O_3Si$ C 63.12, H 8.32 found: C 63.01, H 8.34.

6.5.10. Chemical correlation from (1R,2R,3R,3R)-2-dimethylphenylsilyl-cyclohexa-1,3,4-triol: synthesis of (3aR,7aS)-2,2-dimethyl-3a,4,5,7a-tetrahydro-1,3-benzodioxole (42). To a solution of **41** (140 mg, 0.53 mmol, 1 equiv.) and dimethoxypropane (97 μL , 1.5 equiv.) in CH_2Cl_2 (5 mL) was added PTSA- H_2O (cat.). GC analysis indicated completion of the reaction after 10 min at rt. A solution of $NaHCO_3$ sat was added and the organic layer was separated. The aqueous phase was extracted with CH_2Cl_2 . The combined organic phases were dried over $MgSO_4$ and concentrated under reduced pressure to give the crude ketal in 93% yield (99% pure by GC, 1% of the *cis*-isopropylidene ketal was identified by GC/GC-MS). The product was dissolved in THF (5 mL) and NaH (60% dispersion in mineral oil, 25 mg, 1.3 equiv.) was added. The reaction mixture was stirred for 5 h at $55^\circ C$. Water and Et_2O were added and the organic phase was separated. The

aqueous phase was extracted with Et₂O. The combined organic layers were dried over MgSO₄ and concentrated in vacuo. Flash chromatography (SiO₂: hexane 90:10 Et₂O) gave the cyclohexene **42** in 82% yield (91% ee by GC on the crude after chromatography). $[\alpha]_{\text{D}}^{25} = +17.5$ ($c = 0.68$ in CH₂Cl₂). TLC R_f 0.35 (hexane/Et₂O, 9:1 KMnO₄). ¹H NMR (CDCl₃): δ 5.92 (dt, 1H, $J = 10.1, 3.6$ Hz), 5.71 (dm, 1H, $J = 10.1$ Hz), 4.5 (m, 1H), 4.27 (ddd, 1H, $J = 6, 6, 3.8$ Hz), 1.7–2.3 (m, 4H), 1.42 (s, 3H), 1.37 (s, 3H). ¹³C NMR (CDCl₃): δ 131.2, 125.4, 108.3, 73.1, 71.4, 28.1, 26.4, 25.5, 20.8. MS(EI, 70 eV): 233 (28) [M–acetone], 171 (14), 139 (54), 137 (100), 135 (76).

6.5.11. 2,2-Dimethyl-propionic acid 2-oxo-ethyl ester (43). (+/–)-Solketal pyvaloate. Pyvaloyl chloride (44.7 mL, 363 mmol, 1 equiv.) was added dropwise to a gently agitated solution of solketal (48 g, 363 mmol, 1 equiv.) and pyridine (32.3 mL, 399 mmol, 1.1 equiv.) in CH₂Cl₂ (363 mL) at –10 °C. After standing two days at room temperature the solution was washed thoroughly twice with 30 mL of water and dried with MgSO₄. The CH₂Cl₂ was distilled off under normal pressure at the lowest possible bath temperature. The residue was fractionally distilled in vacuo (135–138 °C/60–80 mm Hg) to yield 65.7 g (83%) as a colourless oil. ¹H NMR (CDCl₃): δ 4.3 (m, 1H), 4.15 (dd, 1H, $J = 11.5, 4.6$ Hz), 4.11 (dd, 1H, $J = 11.5, 5.38$ Hz), 4.06 (dd, 1H, $J = 8.3, 6.4$ Hz), 3.76 (dd, 1H, $J = 8.3, 6.1$ Hz), 1.43 (s, 3H), 1.36 (s, 3H), 1.21 (s, 9H).

1-Pivaloyloxypropane-2,3-diol. To a solution of (+/–)-solketal pyvaloate (65 g, 300 mmol, 1 equiv.) in THF (250 mL) was added a solution of HCl 2 N (75 mL). The mixture was then stirred overnight. After the reaction mixture was saturated with NaCl, the products were extracted with AcOEt (×4) and the organic layer was dried over MgSO₄ to give 52 g (98%) of 1-pivaloyloxypropane-2,3-diol²⁵ as colourless oil. ¹H NMR (CDCl₃): δ 4.44 (broad s, 2H), 4.12 (m, 2H), 3.91 (m, 1H), 3.68 (dd, 1H, $J = 11.5, 3.3$ Hz), 3.57 (dd, 1H, $J = 11.5, 6.1$ Hz), 1.19 (s, 9H). (**43**) To a solution of 1-pivaloyloxypropane-2,3-diol (10 g, 56.7 mmol, 1 equiv.) in CH₂Cl₂ (85 mL) was added a solution of sodium periodate (13.3 g, 62.4 mmol, 1.1 equiv.) in water (85 mL). This biphasic solution was stirred for 3–4 h. The organic layer was separated and concentrated to give an oil which was distilled (87 °C/65 mm Hg). The aldehyde was obtained as an colorless oil (8.9 g, 71% yield). ¹H NMR (CDCl₃): δ 9.59 (s, 1H), 4.65 (s, 2H), 1.27 (s, 9H). ¹³C NMR (CDCl₃): δ 195.9, 177.9, 68.5, 38.7, 27.1.

6.5.12. (2R,3S)-2,2-Dimethyl-propionic acid 3-(dimethyl-phenyl-silanyl)-2-hydroxy-pent-4-enyl ester (45). Following the typical procedure A. To a solution of allyldimethylphenylsilane (2.6 g, 15 mmol, 1.1 equiv.) in THF (33 mL) at rt were added 2.3 M *n*-BuLi (6.5 mL, 15 mmol, 1.1 equiv.) dropwise over 10 min. After 20 min, the yellow solution was transferred via canula over 10 min to a suspension of (*R,R*)-TiClCpTADDOL (10 g, 15.6 mmol, 1.15 equiv.) in THF (40 mL) at –78 °C. After 30 min, **43** (2 g, 13.5 mmol, 1 equiv.) was added. Chromatography (SiO₂, CH₂Cl₂/PE: 2:3) gave **45** as a colorless oil: 2.44 g (56% yield). $[\alpha]_{\text{D}}^{25} = -1.6$ ($c = 1$ in CHCl₃). TLC R_f 0.41 (CH₂Cl₂/PE, 2:3, KMnO₄). ¹H NMR (CDCl₃): δ 7.55 (m, 2H), 7.36 (m, 3H), 5.89 (ddd, 1H, $J = 17.1, 10.5,$

10.2 Hz), 5.03 (dd, 1H, $J = 10.2, 1.9$ Hz), 4.89 (dd, 1H, $J = 17.1, 1.9$ Hz), 3.96 (m, 3H), 2.00 (s, 1H), 1.93 (dd, 1H, $J = 10.5, 2.4$ Hz), 1.18 (s, 9H), 0.39 and 0.34 (s, 3H). ¹³C NMR (CDCl₃): δ 178.9, 137.8, 134.4, 134.2, 129.5, 128.1, 116.1, 69.9, 69.1, 39.3, 39.1, 27.5, –3.3, –3.7. IR (film) ν_{max} cm^{–1} 3491, 3071, 2961, 1730, 1625, 1481, 1428, 1399, 1284, 1256, 1160, 815, 734, 700. MS(CI): 319 (4) [M–H]⁺, 209 (10), 177 (46), 175 (72), 168 (54), 159 (100), 137 (53), 135 (94), 115 (38), 85 (31), 75 (86), 67 (88), 57 (61). HRMS: Calcd for C₁₈H₂₇O₃Si [M–H]⁺ 319.172948 found: *M* 319.173362.

6.5.13. (2R,3S)-2,2-Dimethyl-propionic acid 2-(tert-butyl-dimethyl-silyloxy)-3-(dimethyl-phenyl-silanyl)-pent-4-enyl ester (46a). Following the typical procedure C. The reaction was carried out on 1.5 g of **45** (4.7 mmol). Flash chromatography (SiO₂, CH₂Cl₂/PE: 1:4) gave 1.28 g of colorless oil (63% yield). $[\alpha]_{\text{D}}^{25} = -0.5$ ($c = 0.5$ in CHCl₃). TLC R_f 0.73 (CH₂Cl₂/PE: 1:4, KMnO₄). ¹H NMR (CDCl₃): δ 7.84 (m, 2H), 7.34 (m, 3H), 5.88 (ddd, 1H, $J = 17.1, 10.5, 10.2$ Hz), 4.99 (dd, 1H, $J = 10.2, 2.2$ Hz), 4.80 (dd, 1H, $^3J(\text{H,H}) = 17.1, 2.2$ Hz), 4.00 (m, 2H), 3.87 (m, 1H), 2.09 (dd, 1H, $J = 10.5, 2.4$ Hz), 1.18 (s, 9H), 0.87 (s, 9H), 0.36 (s, 3H), 0.31 (s, 3H), 0.04 (s, 3H), –0.01 (s, 3H). ¹³C NMR (CDCl₃): δ 178.5, 138.3, 135.1, 134.4, 129.4, 128.1, 115.9, 70.8, 66.9, 39.7, 39.1, 27.6, 26.3, 18.5, –2.8, –3.5, –3.7, –3.8. IR (film) ν_{max} cm^{–1} 3072, 2958, 2858, 1734, 1480, 1397, 1362, 1255, 1150, 1004, 902, 835, 700. MS(CI): 419 (21) [M–Me]⁺, 377 (67), 333 (21), 319 (60), 275 (25), 233 (51), 199 (47), 159 (100), 135 (47), 67 (60). HRMS: Calcd for C₂₃H₃₉O₃Si₂ [M–Me]⁺ 419.243777 found: *M* 419.243722.

6.5.14. (2R,3S)-2,2-Dimethyl-propionic acid 3-(dimethyl-phenyl-silanyl)-2-triisopropylsilyloxy-pent-4-enyl ester (46b). To a solution of TiPSCl (2 mL, 9.36 mmol, 1.5 equiv.) in DMF (6 mL) was added imidazole (1.7 g, 25 mmol, 4 equiv.). The reaction mixture was heated to 60 °C for 1:2 h before to add **45** (2 g, 6.24 mmol, 1 equiv.). The reaction was monitored by GC. After 48 h NH₄Cl sat (5 mL) were added. The aqueous phase was extracted with pentane (3×5 mL), the combined organic phases were dried over MgSO₄ and concentrated in vacuo. Flash chromatography (SiO₂, CH₂Cl₂/PE, 1:4) gave 1.77 g of **46b** as a colorless oil (59% yield). $[\alpha]_{\text{D}}^{25} = 18$ ($c = 1.11$ in CHCl₃). TLC R_f 0.27 (CH₂Cl₂/PE: 1:4, KMnO₄). ¹H NMR (CDCl₃): δ 7.48 (m, 2H), 7.33 (m, 3H), 5.78 (ddd, 1H, $J = 17.1, 10.5, 10.5$ Hz), 5.11 (ABX system, ddd, 1H, $J = 6.2, 6.2, 4.5$ Hz), 5.01 (dd, 1H, $J = 10.5, 2.1$ Hz), 4.88 (dd, 1H, $J = 17.1, 2.1$ Hz), 3.51 and 3.48 (ABX system, 2dd, 2H, $J = 10, 6.2$ Hz), 2.28 (dd, 1H, $J = 10.5, 4.5$ Hz), 1.1 (s, 9H), 0.985 (s, 21H), 0.323 and 0.318 (2s, 6H). ¹³C NMR (CDCl₃): δ 177.9, 137.8, 134.8, 134.3, 129.5, 128.1, 116.2, 73.7, 64.3, 39.3, 36.8, 27.7, 18.4, 12.3, –3.1, –3.6. IR (film) ν_{max} cm^{–1} 3070, 2958, 2866, 1730, 1626, 1461, 1427, 1279, 1249, 1157, 1113, 1014, 882, 812, 733. MS(CI): 433 (95) [M–(CH₃)₂CH]⁺, 375 (10), 345 (9), 289 (14), 285 (18), 215 (100), 201 (31), 197 (20), 159 (32), 135 (16), 111 (18). HRMS: Calcd for C₂₄H₄₁O₃Si₂ [M–*i*Pr]⁺ 433.259427 found: *M* 433.258928.

6.5.15. (2R,3S)-3-(Dimethyl-phenyl-silanyl)-2-triisopropyl-silyloxy-pent-4-en-1-ol (47). To a solution of

46b (410 mg, 0.85 mmol, 1 equiv.) in CH_2Cl_2 (5 mL) was added DIBAL 1.5 M in toluene (1.15 mL, 2 equiv.) after stirring for 1 h at -78°C the reaction was quenched with methanol (1 mL) and 2 mL of a solution of NH_4Cl sat were added. The mixture was stirred vigorously at rt for 2 h and the whole was extracted with AcOEt (2×5 mL). The combined organic extracts were washed with brine (5 mL) and dried over MgSO_4 . Filtration and evaporation in vacuo furnished the crude product, which was purified by flash chromatography (SiO_2 : $\text{CH}_2\text{Cl}_2/\text{PE}$: 1:4) to give 246 mg of colorless oil (73% yield). $[\alpha]_{\text{D}}^{23} = 11.4$ ($c = 1.02$ in CHCl_3). TLC R_f 0.53 ($\text{CH}_2\text{Cl}_2/\text{PE}$, 2:3, KMnO_4). ^1H NMR (CDCl_3): δ 7.56 (m, 2H), 7.35 (m, 3H), 5.92 (ddd, 1H, $J = 17.1, 10.2, 9.9$ Hz), 4.96 (dd, 1H, $J = 10.2, 2.1$ Hz), 4.82 (dd, 1H, $J = 17.1, 2.1$ Hz), 3.79 (ABX system, ddd, 1H, $J = 10, 3.9, 2.4$ Hz), 3.46 and 3.44 (ABX system, 2dd, 2H, $J = 14, 10, 2.4$ Hz), 2.62 (broad s, 1H), 2.00 (dd, 1H, $J = 9.9, 3.9$ Hz), 1.01 and 1.00 (2s, total 21H), 0.39 and 0.33 (s, 3H). ^{13}C NMR (CDCl_3): δ 138.3, 135.3, 134.4, 129.3, 128.0, 114.7, 71.8, 68.1, 38.5, 18.5, 12.4, $-3.0, -3.7$. IR (film) ν_{max} cm^{-1} 3575, 3069, 2943, 2866, 1624, 1463, 1427, 1247, 1113, 1100, 1017, 882, 807. MS(CI): 391(3) $[\text{M}-\text{H}]^+$, 376 (49), 375 (100) $[\text{M}-\text{OH}]^+$, 315 (20), 307 (15), 239 (57), 231 (65), 205 (58), 197 (65), 157 (15), 135 (68), 67 (100). HRMS: Calcd for $\text{C}_{22}\text{H}_{39}\text{O}_2\text{Si}_2$ $[\text{M}-\text{H}]^+$ 391.248863 found: M 391.252510.

6.5.16. (2R,3S)-3-(Dimethyl-phenyl-silanyl)-2-triisopropylsilanyloxy-1-vinyloxy-pent-4-en-1-yl ether (48). To a solution of **47** (328 mg, 408 μmol , 1 equiv.) in ethyl-vinyl ether (3 mL) was added mercury(II) acetate (143 mg, 448 μmol , 1.1 equiv.) and the resulting mixture was heated at reflux for 48 h. The ethyl-vinyl ether was then removed under reduced pressure. The resulting oil was taken back in pentane and the organic phase was washed with brine, dried over MgSO_4 and concentrated in vacuo. Flash chromatography (SiO_2 , $\text{CH}_2\text{Cl}_2/\text{PE}$: 1:9) gave 240 mg of the vinyl ether **48** (67% yield). $[\alpha]_{\text{D}}^{23} = +12$ ($c = 0.6$ in CDCl_3). TLC R_f 0.9 ($\text{CH}_2\text{Cl}_2/\text{PE}$, 1:4, KMnO_4). ^1H NMR (CDCl_3): δ 7.68 (m, 2H), 7.51 (m, 3H), 6.38 (dd, 1H, $J = 13.8, 6.3$ Hz), 6.03 (ddd, 1H, $J = 17.1, 10.5, 10.2$ Hz), 5.15 (dd, 1H, $J = 10.2, 2.4$ Hz), 5.01 (dd, 1H, $J = 17.1, 2.4$ Hz), 4.39 (dd, 1H, $J = 13.8, 1.5$ Hz), 4.05 (dd, 1H, $J = 6.3, 1.5$ Hz), 3.97 (ddd, 1H, $J = 6.6, 6.3, 2.4$ Hz), 3.83 (dd, 1H, $J = 10.1, 6.6$ Hz), 3.71 (dd, 1H, $J = 10.1, 6.3$ Hz), 2.29 (dd, 1H, $J = 10.5, 2.4$ Hz), 1.17 and 1.16 (2s, total of 21H), 0.52 and 0.47 (s, 3H). ^{13}C NMR (CDCl_3): δ 152.5, 137.6, 134.4, 134.2, 128.9, 127.8, 115.4, 87.4, 80.9, 65.0, 37.3, 17.9, 11.8, $-3.8, -4.5$. IR (film) ν_{max} cm^{-1} 3070, 2943, 2866, 1627, 1463, 1427, 1249, 1186, 1114, 1052, 1004, 882, 812, 699. MS(CI): 391(5) $[\text{M}-\text{CH}=\text{CH}_2]^+$, 377 (55), 375 (100), 353 (10), 315 (20), 241 (20), 239 (55), 231 (61), 205 (57), 197 (53), 157 (15), 135 (55), 67 (85). HRMS: Calcd for $\text{C}_{22}\text{H}_{39}\text{OSi}_2$ $[\text{M}-\text{CH}_2=\text{CH}-\text{O}]^+$ 375.253948 found: M 375.252969.

6.5.17. (3R,4S)-4-(Dimethyl-phenyl-silanyl)-3-triisopropylsilanyloxy-3,4-dihydro-2H-pyran (49). To a solution of **48** (100 mg, 0.229 mmol, 1 equiv.) in CH_2Cl_2 (20 mL) was added **23** (49 mg, 0.057 mmol, 0.25 equiv.) in solution in CH_2Cl_2 (1 mL). The mixture was heated 4 h at reflux until disappearance of the starting compound. The ruthenium catalyst was then oxidized by stirring the mixture at open air

overnight. Concentration in vacuo followed by flash chromatography (SiO_2 : hexane) gave 82 mg of product (93% yield). TLC R_f 0.49 (hexane, KMnO_4). ^1H NMR (CDCl_3): δ 7.48 (m, 2H), 7.34 (m, 3H), 6.19 (dd, 1H, $J = 2.7, 2.4$ Hz), 4.76 (dd, 1H, $J = 2.7, 2.7$ Hz), 4.52 (ddd, 1H, $J = 7.2, 6.3, 4.8$ Hz), 3.63 (dd, 1H, $J = 10.2, 6.3$ Hz), 3.49 (dd, 1H, $J = 10.2, 4.8$ Hz), 2.21 (ddd, 1H, $J = 7.2, 2.7, 2.4$ Hz), 1.01 and 1.00 (2s, total of 21H), 0.29 and 0.28 (2s, total of 6H). ^{13}C NMR (CDCl_3): δ 137.8, 134.3, 134.1, 129.7, 128.4, 97.8, 83.1, 64.9, 23.5, 18.4, 12.4, $-0.9, -2.6$. IR (film) ν_{max} cm^{-1} 3069, 2943, 2866, 1762, 1691, 1463, 1427, 1251, 1113, 1063, 1014, 882. MS(CI): 390 $[\text{M}]^+$ (4), 375 (5), 347 (14), 265 (39), 180 (98), 169 (35), 157 (75), 137 (43), 135 (63), 123 (100), 75 (17). HRMS: Calcd for 391.248863 found: M 391.247701.

Acknowledgements

We warmly thank the FNRS (Belgium) and the Ministry of Research (France) for PhD fellowships to J.M.A. and L.d.F. These studies were supported by grants from the Ministère de l'Éducation et de la Recherche, Communauté française de Belgique (action concertée), the Université catholique de Louvain, the Conseil Régional d'Aquitaine and the Université Bordeaux I. We are also indebted to Prof. E. de Hoffmann and Prof. J.-L. Habib for the mass spectra, Prof. Flammang for the HRMS and Dr. Roland Touillaux for the meticulous measurement and recording of high-field NMR spectra.

References and notes

- Adam, J.-M.; Ghosez, L.; Houk, K. N. *Angew. Chem., Int. Ed.* **1999**, *38*, 2728–2730.
- For reviews see: (a) Grubbs, R. H.; Chang, S. *Tetrahedron* **1998**, *54*, 4413. (b) Fürstner, A. *Angew. Chem., Int. Ed.* **2000**, *39*, 3012–3043.
- (a) Fürstner, A.; Langemann, K. *J. Am. Chem. Soc.* **1997**, *119*, 9130–9136. (b) Cossy, J.; Bauer, D.; Bellosta, V. *Tetrahedron Lett.* **1999**, *40*, 4187–4188. (c) Scholl, M.; Grubbs, R. H. *Tetrahedron Lett.* **1999**, *40*, 1425–1428. (d) Ahmed, M.; Barrett, A. G. M.; Beall, J. C.; Braddock, D. C.; Flack, K.; Gibson, V. C.; Procopriou, P. A.; Slater, M. M. *Tetrahedron* **1999**, *55*, 3219–3232. (e) Mulzer, J.; Hanbauer, M. *Tetrahedron Lett.* **2000**, *41*, 33–36. (f) Ramachandran, P. V.; Reddy, M. R. V.; Brown, H. C. *Tetrahedron Lett.* **2000**, *41*, 583–586. (g) Cossy, J.; Willis, C.; Bellosta, V.; Bouzbouz, S. *Synlett* **2000**, *10*, 1461–1463. (h) Landais, Y.; Surange, S. S. *Tetrahedron Lett.* **2001**, *42*, 581–584. (i) Felpin, F. X.; Girard, S.; Vo-Tham, G.; Robins, R. J.; Villieras, J.; Lebreton, J. *J. Org. Chem.* **2001**, *66*, 6305–6312. (j) Cossy, J.; Willis, C.; Bellosta, V.; Bouzbouz, S. *J. Org. Chem.* **2002**, *67*, 1982–1992. (k) Bouzbouz, S.; Cossy, J. *Tetrahedron Lett.* **2003**, *44*, 4471–4473. (l) Bouzbouz, S.; Cossy, J. *Org. Lett.* **2003**, *5*, 3029–3031. (m) Marco, J. A.; Carda, M.; Rodriguez, S.; Castillo, E.; Kneeteman, M. N. *Tetrahedron* **2003**, *59*, 4085–4101.
- (a) Heo, J.-N.; Micaizio, G. C.; Roush, W. R. *Org. Lett.* **2003**, *5*, 1693–1696. (b) Heo, J.-N.; Holson, E. B.; Roush, W. R. *Org. Lett.* **2003**, *5*, 1697–1700.

5. Preliminary report: de Fays, L.; Adam, J.-M.; Ghosez, L. *Tetrahedron Lett.* **2003**, *44*, 7197–7199.
6. Crowe, W. E.; Golberg, D. R.; Zhang, Z. J. *Tetrahedron Lett.* **1996**, *37*, 2117–2120.
7. (a) Brummer, O.; Rucket, A.; Blechert, S. *Chem. Eur. J.* **1997**, *3*, 441–446. (b) Chatterjee, A. K.; Choi, T.-L.; Sanders, D. P.; Grubbs, R. H. *J. Am. Chem. Soc.* **2003**, *125*, 11360–11370, and references cited therein.
8. Ulman, M.; Grubbs, R. H. *Organometallics* **1998**, *17*, 2484–2489.
9. Dias, E. L.; Nguyen, S. T.; Grubbs, R. H. *J. Am. Chem. Soc.* **1997**, *119*, 3887–3897.
10. Adam, J.-M. PhD Dissertation, Université catholique de Louvain, 2000.
11. For chromium-catalyzed reactions see: Fürstner, A. *Chem. Rev.* **1999**, *99*, 991–1045.
12. (a) Ulman, M.; Grubbs, R. H. *J. Org. Chem.* **1999**, *64*, 7202–7207. (b) Kirkland, T. A.; Lynn, D. M.; Grubbs, R. H. *J. Org. Chem.* **1999**, *63*, 9904–9909.
13. Scholl, M.; Ding, S.; Woo Lee, C.; Grubbs, R. H. *Org. Lett.* **1999**, *1*, 953–956.
14. Synthesis of 3-butenal: (a) Crimmins, M. T.; Kirincich, S. T.; Wells, A. J.; Choy, A. L. *Synth. Commun.* **1998**, *28*, 3675–3679. Synthesis of 5-hexenal: (b) Ikeda, T.; Yue, S.; Hutchinson, C. R. *J. Org. Chem.* **1985**, *50*, 5193–5199. Synthesis of 6-heptenal: (c) Taylor, R. E.; Galvin, G. M.; Hilfiker, K. A.; Chen, Y. *J. Org. Chem.* **1998**, *63*, 9580–9583.
15. (a) Duthaler, R. O.; Hafner, A. *Chem. Rev.* **1992**, *92*, 807–832. (b) Hafner, A.; Duthaler, R. O.; Marti, R.; Rihs, G.; Rothe-Streit, P.; Schwarzenbach, F. *J. Am. Chem. Soc.* **1992**, *114*, 2321–2336.
16. (a) For catalyst **23** see Ref. 13. (b) Sanford, M. S.; Love, J. A.; Grubbs, R. H. *J. Am. Chem. Soc.* **2001**, *123*, 6543–6554.
17. (a) Fürstner, A.; Thiel, O. R.; Ackermann, L.; Schanz, H.-J.; Nolan, S. P. *J. Org. Chem.* **2000**, *65*, 2204–2207. (b) Kinderman, S. S.; van Maarseveen, J. H.; Schoemaker, H. E.; Hiemstra, H.; Rutjes, F. P. J. T. *Org. Lett.* **2001**, *3*, 2045–2048. (c) Bourgeois, D.; Pancrazi, A.; Nolan, S. P.; Prunet, J. *J. Organomet. Chem.* **2002**, *643-644*, 247–252.
18. For synthesis of (4*S*,5*S*)-2,2-dimethyl-5-vinyl-[1,3]-dioxolane-4-carbaldehyde **27** see: Moon, H. R.; Choi, W. J.; Kim, H. O.; Jeong, L. S. *Tetrahedron: Asymmetry* **2002**, *13*, 1189–1193.
19. White, J.-M. *Aust. J. Chem.* **1995**, *48*, 1227–1252.
20. Ethoxycarbonylmethylation: (a) Reissig, H.-U.; Reichelt, I.; Kunz, T. *Org. Synth.* **1993**, *71*, 189–199. (b) Angelaud, R.; Landais, Y.; Parra-Rapado, L. *Tetrahedron Lett.* **1997**, *38*, 8845–8848.
21. Hanquet, G.; Lusinch, X.; Milliet, P. *Tetrahedron* **1992**, *49*, 423–438.
22. Wang, Z.-M.; Kakiuchi, K.; Sharpless, K. B. *J. Org. Chem.* **1994**, *59*, 6895–6897.
23. Haasnoot, C. A. G.; De Leeuw, F. A. A. M.; Altona, C. *Tetrahedron* **1980**, *36*, 2783–2792.
24. Kashiwara, H.; Suemune, H.; Kawahara, K.; Sakai, K. *J. Chem. Soc., Perkin Trans. 1* **1990**, 1663–1667.
25. Balint, J.; Egri, G.; Kolbert, A.; Dianoczky, C.; Fogassy, E.; Novak, L.; Poppe, L. *Tetrahedron: Asymmetry* **1999**, *10*, 4017–4028.
26. Arjona, O.; de Dios, A.; Plumet, J.; Saez, B. *J. Org. Chem.* **1995**, *60*, 4932–4935.



Enantioselective synthesis of cyclic allylboronates by Mo-catalyzed asymmetric ring-closing metathesis (ARCM). A one-pot protocol for net catalytic enantioselective cross metathesis

Jesper A. Jernelius,^a Richard R. Schrock^b and Amir H. Hoveyda^{a,*}

^aDepartment of Chemistry, Merkert Chemistry Center, Boston College, Chestnut Hill, MA 02467, USA

^bDepartment of Chemistry, Massachusetts Institute of Technology, Cambridge, MA 02138, USA

Received 19 April 2004; revised 28 May 2004; accepted 4 June 2004

Available online 25 June 2004

This work is dedicated to our colleague and friend, Professor Robert H. Grubbs, for his groundbreaking contributions to organometallic chemistry and catalytic metathesis

Abstract—Mo-catalyzed asymmetric ring-closing metathesis (ARCM) reactions are used to synthesize cyclic allylboronates of high optical purity (89% ee to >98% ee). A one-pot procedure involving formation of allylboronates, Mo-catalyzed ARCM and functionalization of the optically enriched cyclic allylboronates constitutes net asymmetric cross metathesis (ACM). Structural modification of ARCM products include reactions with aldehydes to afford optically enriched compounds that bear quaternary carbon centers with excellent diastereoselectivity. These studies emphasize the significance of the availability of chiral Mo-based complex as a class of chiral metathesis catalysts that frequently complement one another in terms of reactivity and selectivity.

© 2004 Published by Elsevier Ltd.

1. Introduction

Catalytic enantioselective olefin metathesis allows efficient access to a range of optically enriched organic molecules that cannot be readily synthesized by alternative methods.¹ Accordingly, research in these laboratories has focused on the design and development of effective chiral complexes for asymmetric olefin metathesis.¹ We have disclosed the synthesis, characterization and activity of a number of chiral Mo-based alkylidenes (see [Chart 1](#)) that readily promote asymmetric ring-closing (ARCM)² and ring-opening metathesis (AROM)³ reactions. We recently outlined the synthesis of supported chiral catalysts⁴ (e.g., **5** in [Chart 1](#)) as well as practical procedures involving in situ preparation and use of related Mo complexes.⁵ Applications to enantioselective synthesis of biologically active compounds are beginning to emerge.⁶

One area of research that poses a challenging task, but is of high potential in enantioselective organic synthesis, relates to the development of catalytic asymmetric cross metathesis (ACM) reactions.⁷ Discovery of a direct catalytic ACM

(**i**→**ii**, [Scheme 1](#)) is yet to be realized. However, an alternative approach, one that involves a one-pot operation and the intermediacy of cyclic allylboronates,⁸ is illustrated in [Scheme 1](#). Thus, formation of allylboronate **iii**, followed by catalytic ARCM may afford cyclic **iv** which can then be functionalized to afford net ACM products (e.g., **ii** after oxidation). Such a strategy provides opportunities for stereoselective formation of additional C–C bonds through reaction of **iv** with different electrophiles (e.g., carbonyl-containing compounds).

Herein we report an approach to net ACM which involves the intermediacy of optically enriched cyclic allylboronates formed through Mo-catalyzed ARCM. The present protocol offers an efficient route for the preparation of synthetically versatile organic molecules of high optical purity (up to >98% ee). Research outlined further underlines the significance of the modular character of high oxidation state Mo-based complexes that has led to the availability of a class of chiral catalysts for enantioselective olefin metathesis.^{1a,b,9}

2. Optically pure cyclic allylboronates by Mo-catalyzed kinetic resolution

We began our investigation by examining the possibility of

Keywords: Allylboronates; Asymmetric cross metathesis; Asymmetric ring-closing metathesis.

* Corresponding author. Tel.: +1-617-552-3618; fax: +1-617-552-1442; e-mail address: amir.hoveyda@bc.edu

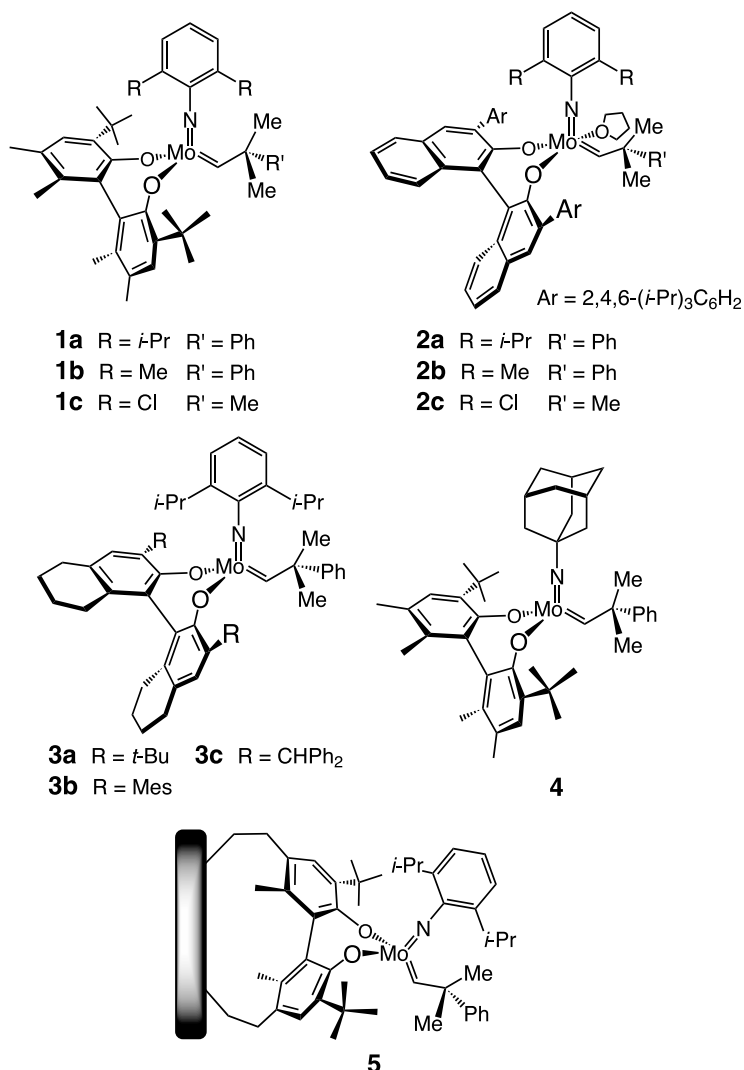
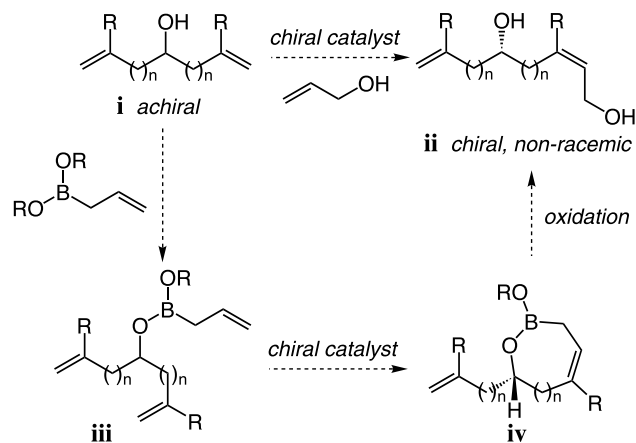


Chart 1. Representative chiral Mo catalysts for olefin metathesis.

the one-pot Mo-catalyzed strategy shown in **Scheme 1** to effect kinetic resolution of dienes **6** and **11** (**Scheme 2**). As illustrated in **Scheme 2**, treatment of *rac*-diene **6** with one equivalent of allyl boronate **7** in benzene at 22 °C results in the smooth formation of a solution of triene **8** (400 MHz ¹H NMR analysis). Since high oxidation state Mo complexes are sensitive to unprotected alcohols, *i*-PrOH generated in

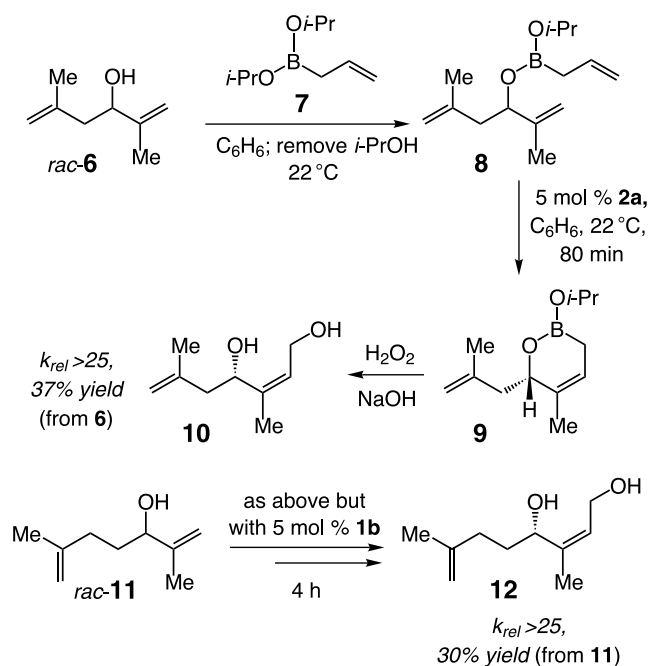


Scheme 1. Catalytic asymmetric CM and a one-pot multistep alternative.

the course of the formation of **8** must be removed in vacuo before the addition of chiral metathesis catalysts. Screening studies indicated that in the presence of 5 mol% **2a** (see **Chart 1**), ARCM proceeds smoothly to afford **9** (~50% conv. after 80 min). The resulting cyclic allylboronate can be directly (not isolated) subjected to oxidation conditions (H₂O₂, NaOH) to afford optically pure **10** in 37% overall isolated yield (>30:1 *Z/E*; maximum theoretical yield=50%). In a similar fashion *rac*-**11** is converted, by the one-pot protocol, to stereoisomerically pure **12** in 35% yield. It should be noted that catalytic ARCM of the allylboronate derived from *rac*-**11** proceeds most selectively in the presence of chiral complex **1b** (vs. **2a** for *rac*-**6**; see below for additional discussion).

3. Enantioselective synthesis of cyclic allylboronates by Mo-catalyzed ARCM

With the feasibility of the general approach described in **Scheme 1** substantiated through our investigation of the Mo-catalyzed kinetic resolutions shown in **Scheme 2**, we turned our attention to the possibility of achieving net ACM through one-pot desymmetrizations of achiral substrates.



^aEnantioselectivities determined through chiral GLC analysis (α -dex)

Scheme 2. Catalytic kinetic resolution through ARCM/oxidation (net asymmetric CM)^a.

The results of these investigations are summarized in **Table 1**. Treatment of diene **13** with 1 equiv. of allylboronate **7** (**Scheme 2**), removal of *i*-PrOH in vacuo and treatment with chiral binaphtholate-based Mo complex **2a**

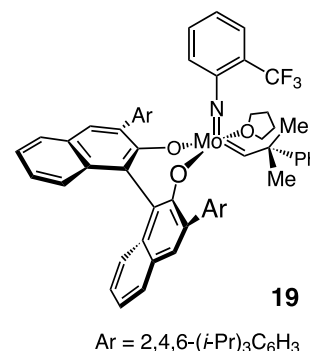
(**Chart 1**) leads to formation of the desired cyclic allylboronate (cf. **9**, **Scheme 2**) which is directly oxidized to afford **14** in >98% ee and 57% overall isolated yield.¹⁰ Catalytic enantioselective desymmetrization of allylic alcohol **15** is promoted by dichloroimido complex **1c** to deliver **16** in optically pure form and 58% yield after silica gel chromatography. As the data in entry 3 of **Table 1** indicate, one-pot desymmetrization of homoallylic alcohol **17** in the presence of 5 mol% *o*-(trifluoromethyl)phenylimido complex **19** leads to the formation of **18** in 89% ee and 64% isolated yield. Net Mo-catalyzed ACM with tertiary homoallylic alcohol **20** is less efficient and proceeds to ~80% conv. in the presence of 5 mol% of a variety of Mo catalysts; the highest enantioselectivity is obtained with adamantylimido complex **4** (**Chart 1**) to generate **21** in >98% ee and 38% isolated yield (from **20**).

Several issues regarding the experiments summarized in **Table 1** are worthy of note:

- (1) An underlining feature of the present catalytic method is that in each of the cases described above a different chiral Mo complex is used to obtain optimal levels of reactivity and selectivity. This should not be viewed as a drawback of the protocol. As we have described in detail elsewhere,^{1a,b} the identity of the optimal chiral metathesis catalyst should not be generalized; the availability of a class of catalysts increases the possibility of obtaining the most desirable conversion and enantioselectivities. If **1a** were the only available chiral complex, high selectivities would be feasible in

Table 1. Mo-catalyzed one-pot net ACM reactions^a

Entry	Substrate	Product	Catalyst	Time (h)	Conv. (%); ^b yield (%) ^c	ee (%) ^d
1			2a	12	78; 57	>98
2			1c	1	90; 58	>98
3			19	14	80; 64	>89
4			4	24	80; 38 ^e	>98



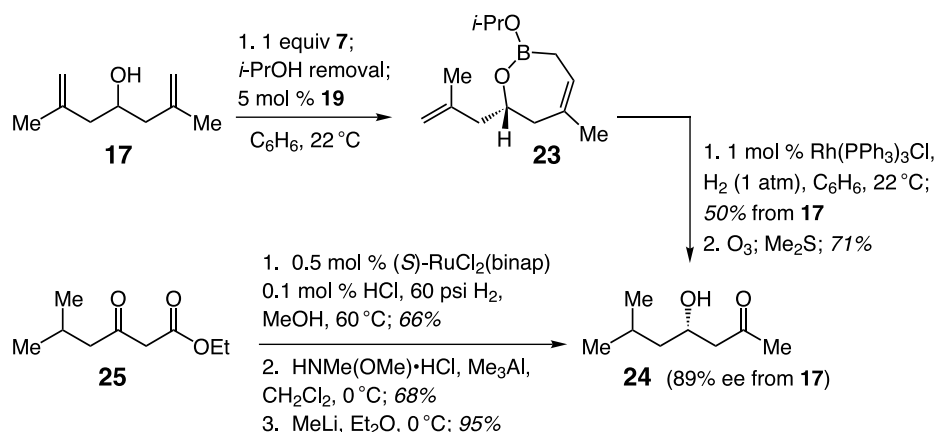
^a Conditions: 5 mol% chiral catalyst, C₆H₆, 22 °C.

^b Conversions determined through 400 MHz ¹H NMR analysis.

^c Isolated yields of purified products (overall from starting diene).

^d Determined by GLC (entries 1–3, α -dex column) and HPLC (entry 4, chiral OJ column).

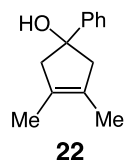
^e 40% of tetrasubstituted olefin **22** also formed.



Scheme 3. Mo-catalyzed conversion of diene **17** to optically pure β -hydroxyketone **24**.

net ACM with *rac*-**11** (Scheme 2); other transformations shown here would proceed with similar levels of efficiency but with significantly lower selectivities.

- (2) The lower efficiency of the catalytic ARCM involving tertiary alcohol **20** is likely due to inefficient formation of the acyclic allylboronate intermediate (cf. **iii** in Scheme 1). As a result, cyclic tertiary alcohol **22**, bearing a tetrasubstituted olefin, is formed as a significant byproduct (40% yield). This observation indicates that not only is chiral alkylimido complex **4** capable of promoting the formation of tetrasubstituted olefins by RCM but also that sterically congested alcohols may be viewed as viable substrates for this class of chiral metathesis catalysts. Studies to investigate and exploit such attributes of chiral Mo complex **4** are underway.



4. Functionalization and synthetic utility of optically enriched allylboronates

The allylboronates obtained in the Mo-catalyzed ARCM reactions discussed above can be functionalized in a variety of manners (in addition to oxidations). One example is shown in Scheme 3. Regioselective Rh-catalyzed hydrogenation¹¹ of cyclic boronate **23** (89% ee; see entry 3 in Table 1), followed by ozonolytic cleavage of the trisubstituted cyclic olefin leads to the formation of the acetate

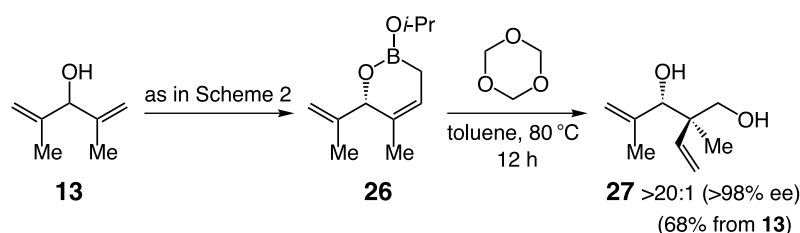
aldol adduct **24**. Conversion of **25** to the same compound based on previously reported protocols,¹² as illustrated in Scheme 3, secures the stereochemical identity of the major enantiomer in the catalytic ARCM.¹³

Optically enriched allylboronates are attractive because they can serve as effective nucleophiles. The example shown in Scheme 4 is illustrative. Treatment of optically pure **26**, obtained from catalytic ARCM of the allylboronate derived from **13**, with trioxane in toluene at 80 °C leads to the formation of diol **27** as a single enantiomer and diastereomer (68% overall yield from **13**). The facile synthesis and stereoselective formation of the quaternary carbon center¹⁴ in **27** augurs well for the utility of cyclic allylboronates generated by catalytic ARCM reactions.^{15,16}

Such C–C bond forming reactions are less feasible with the corresponding cyclic siloxanes that can also be obtained through Mo-catalyzed ARCM reactions.¹⁷ Although Mo-catalyzed ARCM of allylsiloxanes allows access to products shown in Scheme 2 and Table 1 through oxidations of the C–Si bonds, the present method offers a more attractive option. This preference is for two reasons: (i) C–Si oxidation is generally less efficient than those of C–B bonds and with allylsilane compounds such processes can occur with low regioselectivity. (ii) In contrast to the one pot procedure described herein, installation of the silyl ether and its subsequent oxidation must be carried out in separate vessels, thus reducing the efficiency of the overall protocol.

5. Conclusions

In summary, we disclose an efficient catalytic enantioselective method for the preparation of synthetically



Scheme 4. Diastereo- and enantioselective synthesis of quaternary carbons.

versatile cyclic allylboronates through ring-closing metathesis. The products obtained after functionalization of the optically enriched allylboronates can be considered as products of catalytic ACM reactions. Design and development of additional effective catalysts that promote a wide variety of metathesis reactions and applications to the synthesis of biologically active molecules continue in these laboratories.

6. Experimental

6.1. General

Infrared (IR) spectra were recorded on a Nicolet 210 spectrophotometer, ν_{\max} is in cm^{-1} . Bands are characterized as broad (br), strong (s), medium (m), and weak (w). ^1H NMR spectra were recorded on Varian GN-400 (400 MHz), and Varian Gemini 2000 (400 MHz) spectrometers. Chemical shifts are reported in ppm from tetramethylsilane with the solvent resonance as the internal standard (CDCl_3 : δ 7.26, C_6D_6 : δ 7.15). Data are reported as follows: chemical shift, multiplicity (s=singlet, d=doublet, t=triplet, q=quartet, br=broad, m=multiplet), coupling constants (Hz), integration, and assignment. ^{13}C NMR spectra were recorded on Varian GN-400 (100 MHz), and Varian Gemini 2000 (100 MHz) spectrometers with complete proton decoupling. Chemical shifts are reported in ppm from tetramethylsilane with the solvent as the internal reference (CDCl_3 : δ 77.2 ppm, C_6D_6 : δ 128.1 ppm). Enantiomer ratios were determined by chiral GLC (Supelco alphasdex 120 column (30 m \times 0.25 mm)) or chiral HPLC analysis (Chiral Technologies chiracel OJ (0.46 cm \times 25 cm)) in comparison with authentic racemic materials.

All reactions were conducted in oven- (135 °C) and flame-dried glassware under an inert atmosphere of dry nitrogen. Solvents were purified under a positive pressure of dry argon by a modified Innovative Technologies purification system. Benzene and toluene were purged with argon before being passed through activated copper and alumina columns. Tetrahydrofuran, and diethyl ether are purged with Ar before being passed through activated alumina columns. Olefin-free pentane was generated by allowing (commercial grade) pentane to stir in the presence of concentrated sulfuric acid (20 mL per L of pentane) for 24 h. The pentane was poured over fresh concentrated sulfuric acid. The process was repeated until the acid layer remained colorless for 48 h. The pentane was separated, washed with water, dried over Na_2SO_4 , filtered, purged with Ar and then passed through activated copper and alumina columns. All handling of the molybdenum catalysts was performed in a glove box under nitrogen atmosphere. All substrates were rigorously dried by repeated azeotropic distillation using anhydrous benzene (3 times) prior to use.

6.1.1. (4R)-Diol 10. To a round bottom flask was added *rac*-dieneol **6** (150 mg, 1.19 mmol, 1.0 equiv.), diisopropoxyallylboronate **7** (202 mg, 1.19 mmol, 1.0 equiv.) and benzene (12.0 mL) (in a glovebox). The resulting mixture was allowed to stir for 16 h at 22 °C. At this time, benzene was removed in vacuo to afford the desired mixed boronate as a colorless oil (222.0 mg, 0.940 mmol). Analysis of the

^1H NMR spectrum showed complete removal of isopropanol by absence of ^1H resonance at 4.04 ppm. A portion of the resulting oil (11.8 mg, 0.050 mmol) was dissolved in 0.50 mL of benzene and chiral complex (*R*)-**2a** (2.9 mg, 0.03 mmol, 0.05 equiv.) was added. The mixture was allowed to stir at 22 °C for 80 minutes. At this time, the reaction vessel was removed from the glovebox, and the reaction was quenched by exposure of the solution to air.¹⁸ The unpurified mixture was dissolved in THF (500 μL) and ethanol (500 μL). To this stirring solution was added aqueous NaOH (500 μL of a 3.8 M solution) and H_2O_2 (500 μL of a 30% aqueous solution). The mixture was allowed to stir at 22 °C for 2 h during which the solution changed in color from dark brown to light yellow. After 2 h, the solution was washed with 5.0 mL of Et_2O . The organic layer was dried over anhydrous Na_2SO_4 , filtered, and concentrated in vacuo. The resulting light yellow oil was dissolved in 2 mL of hexanes and purified by silica gel chromatography (1:1 hexanes/ Et_2O) to afford diol **10** as a colorless oil (3.7 mg, 0.023 mmol, 46%). $R_f=0.1$ (1:1 hexanes/ Et_2O). IR (neat): 3377 (s), 2974 (m), 2930 (m), 1652 (w), 1445 (m), 1381 (m), 1060 (s), 1023 (s), 872 (m) cm^{-1} ; ^1H NMR (CDCl_3 , 400 MHz): δ 5.55 (t, $J=8.2$ Hz, 1H, $\text{C}=\text{CHCH}_2\text{OH}$), 4.89 (m, 1H, $\text{CH}_A\text{H}_B=\text{C}$), 4.81 (m, 1H, $\text{CH}_A\text{H}_B=\text{C}$), 4.66 (dd, $J=9.2$, 5.1 Hz, 1H, CHOH), 4.26 (dd, $J=12.7$, 8.5 Hz, 1H, $\text{CH}_A\text{H}_B\text{OH}$), 4.08 (dd, $J=12.5$, 6.0 Hz, 1H, $\text{CH}_A\text{H}_B\text{OH}$), 2.36 (dd, $J=13.6$, 8.7 Hz, 1H, $\text{CH}_A\text{H}_B\text{CHOH}$), 2.19 (dd, $J=13.6$, 4.9 Hz, 1H, $\text{CH}_A\text{H}_B\text{CHOH}$), 1.78 (s, 6H, $-\text{CH}_3$). ^{13}C NMR (CDCl_3 , 100 MHz): δ 142.2, 141.0, 126.2, 113.9, 67.7, 58.0, 43.8, 22.5, 18.4; HRMS calcd for $\text{C}_9\text{H}_{16}\text{O}_2\text{Na}$: 179.1048. Found: 179.1046.

6.1.2. (4R)-Diol 12. $R_f=0.1$ (1:1 hexanes/ Et_2O). IR (neat): 3327 (s), 3068 (w), 2943 (s), 1652 (m), 1628 (m), 1451 (s), 1376 (m), 1067 (m), 1004 (s), 891 (m) cm^{-1} ; ^1H NMR (CDCl_3 , 400 MHz): δ 5.54 (dd, $J=6.8$, 6.8 Hz, 1H, $\text{C}=\text{CHCH}_2\text{OH}$), 4.74 (m, 1H, $\text{CH}_A\text{H}_B=\text{C}$), 4.71 (m, 1H, $\text{CH}_A\text{H}_B=\text{C}$), 4.52 (t, $J=6.8$ Hz, 1H, CHOH), 4.25 (dd, $J=12.8$, 8.4 Hz, 1H, $\text{CH}_A\text{H}_B\text{OH}$), 4.06 (ddd, $J=12.8$, 6.4, 1.2 Hz, 1H, $\text{CH}_A\text{H}_B\text{OH}$), 3.70 (br s, 2H, $-\text{OH}$), 2.03 (m, 2H, $\text{CH}_2\text{C}=\text{CH}_2$), 1.81 (m, 1H, $\text{CH}_A\text{H}_B\text{CHOH}$), 1.76 (s, 3H, $-\text{CH}_3$), 1.74 (s, 3H, $-\text{CH}_3$), 1.62 (m, 1H, $\text{CH}_A\text{H}_B\text{CHOH}$); ^{13}C NMR (CDCl_3 , 100 MHz): δ 145.3, 141.4, 126.2, 110.3, 69.7, 58.1, 34.1, 32.9, 22.7, 18.3; HRMS calcd for $\text{C}_{10}\text{H}_{18}\text{O}_2\text{Na}$: 193.1204. Found: 193.1208.

6.1.3. (4R)-Diol 14. $R_f=0.1$ (1:1 hexanes/ Et_2O). IR (neat): 3376 (br s), 2971 (m), 2921 (s), 2853 (m), 1721 (m), 1658 (m), 1449 (m), 1381 (m), 1256 (w), 1230 (w), 1060 (s), 1017 (s), 994 (s), 903 (m) cm^{-1} ; ^1H NMR (CDCl_3 , 400 MHz): δ 5.64 (dd, $J=6.6$, 6.6 Hz, 1H, $\text{C}=\text{CHCH}_2\text{OH}$), 5.10 (s, 1H, $\text{C}=\text{CH}_A\text{H}_B$), 4.95 (s, 1H, $\text{C}=\text{CH}_A\text{H}_B$), 4.91 (s, 1H, CHOH), 4.32 (dd, $J=12.4$, 8.2 Hz, 1H, $\text{CH}_A\text{H}_B\text{OH}$), 4.14 (dd, $J=12.4$, 6.0 Hz, 1H, $\text{CH}_A\text{H}_B\text{OH}$), 2.06 (br s, 2H, $-\text{OH}$), 1.66 (s, 3H, $-\text{CH}_3$), 1.64 (s, 3H, $-\text{CH}_3$); ^{13}C NMR (CDCl_3 , 100 MHz): δ 145.0, 139.4, 127.5, 110.8, 73.4, 58.5, 19.4, 18.4; HRMS calcd for $\text{C}_8\text{H}_{14}\text{O}_2\text{Na}$: 165.0891. Found: 165.0891.

6.1.4. (4R)-Diol 16. $R_f=0.1$ (1:1 hexanes/ Et_2O). IR (neat): 3394 (s), 2953 (s), 2924 (s), 2853 (m), 1729 (m), 1474 (m), 1367 (m), 1099 (s), 1022 (s), 802 (m) cm^{-1} ; ^1H NMR

(CDCl₃, MeOD 400 MHz): δ 5.73–5.68 (m, 2H, C=CHCHOH), 5.64–5.53 (m, 2H, CH=CHCHOH), 4.93 (t, $J=7.6$ Hz, 1H, CHOH), 4.35–4.30 (dd, $J=12.8$, 7.2 Hz, 1H, CH_AH_BOH), 4.23–4.18 (dd, $J=12.8$, 6.4 Hz, 1H, CH_AH_BOH), 1.71 (dd, $J=6.8$ Hz, 3H, –CH₃); ¹³C NMR (CDCl₃, MeOD 100 MHz): δ 133.5, 132.4, 130.0, 127.1, 68.7, 58.2, 18.2; HRMS calcd for C₇H₁₃O₂: 129.0916. Found: 129.0918.

6.1.5. (5R)-Diol 18. $R_f=0.1$ (1:1 hexanes/Et₂O). IR (neat): 3323 (s), 3075 (w), 2967 (s), 2934 (s), 2916 (m), 1658 (w), 1628 (m), 1445 (s), 1376 (m), 1068 (m), 1046 (w), 1024 (s), 997 (s), 890 (m), 669 (w) cm⁻¹; ¹H NMR (CDCl₃, 400 MHz): δ 5.76 (dd, $J=8.2$, 7.1 Hz, 1H, C=CHCH₂OH), 4.92 (m, 1H, CH_AH_B=C), 4.83 (m, 1H, CH_AH_B=C) 4.17 (dd, $J=11.8$, 8.2 Hz, 1H, CH_AH_BOH), 3.92 (dd, $J=11.8$, 7.0 Hz, 1H, CH_AH_BOH), 3.84 (ddt, $J=9.7$, 6.4, 2.7 Hz, 1H, CHOH), 2.51 (dd, $J=13.5$, 9.7 Hz, 1H, CH₂C=CCH_AH_MCHOH), 2.23 (d, $J=6.4$ Hz, 2H, CH₂CHOH), 2.02 (dd, $J=13.5$, 2.7 Hz, 1H, CH₂C=CCH_AH_MCHOH), 1.81 (s, 3H, –CH₃), 1.79 (s, 3H, –CH₃); ¹³C NMR (CDCl₃, 100 MHz): δ 142.5, 127.0, 114.1, 113.4, 65.8, 57.9, 46.7, 39.5, 24.0, 22.5; HRMS calcd for C₁₀H₁₈O₂Na: 193.1204. Found: 193.1205.

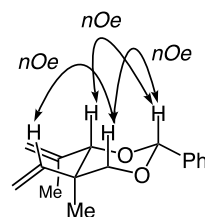
6.1.6. (5R)-Diol 21. $R_f=0.1$ (1:1 hexanes/Et₂O). IR (neat): 3384 (s), 3067 (w), 3027 (w), 2960 (s), 2921 (s), 2869 (m), 1709 (m), 1636 (m), 1446 (s), 1370 (s), 1070 (m), 996 (m), 889 (m) 701 (s) cm⁻¹; ¹H NMR (CDCl₃, 400 MHz): δ 7.42 (d, $J=7.1$ Hz, 2H, Ar–H), 7.31 (dd, $J=7.3$, 7.1 Hz, 2H, Ar–H), 7.22 (dd, $J=7.3$, 7.2 Hz, 1H, Ar–H), 5.63 (dd, $J=6.6$, 6.6 Hz, 1H, C=CHCH₂OH), 4.89 (m, 1H, CH_AH_B=C), 4.77 (m, 1H, CH_AH_B=C), 4.06 (dd, $J=11.7$, 8.1 Hz, 1H, CH_AH_BOH), 3.86 (dd, $J=11.7$, 7.3 Hz, 1H, CH_AH_BOH), 2.82 (dd, $J=13.6$, 3.5 Hz, 2H, CH₂COH), 2.60 (d, $J=13.4$ Hz, 1H, CH_AH_BCOH), 2.51 (d, $J=13.4$ Hz, 1H, CH_AH_BCOH), 1.30 (s, 3H, –CH₃), 1.28 (s, 3H, –CH₃); ¹³C NMR (CDCl₃, 100 MHz): δ 145.8, 142.4, 137.0, 128.5, 128.2, 126.9, 125.7, 116.6, 74.4, 58.5, 51.4, 46.0, 26.1, 24.4; HRMS calcd for C₁₆H₂₂O₂Na: 269.1517. Found: 269.1515.

6.1.7. Diol 27. Paraformaldehyde (42 mg, 1.0 mmol) was added (while stirring) to a solution of boronate **26** (7.8 mg, 0.050 mmol) in toluene (200 μ L). The resulting mixture was placed under nitrogen and heated to 80 °C (temperature controlled oil bath) for 12 h. At this time, the solution was allowed to cool to 22 °C, and volatiles were removed in vacuo to afford a viscous black oil. The resulting black oil was dissolved in MeOH (1.0 mL of a solution of MeOH (5.0 mL) at 0 °C (ice bath) and acetyl chloride (100 μ L, 1.4 mmol)) was added slowly with vigorous stirring (caution: highly exothermic) and then allowed to stand at 22 °C for 5 minutes. Evaporation of volatiles (3 times) resulted in the removal of volatile boron-derived impurities. The resulting black oil was dissolved in a 0.5 mL of 1:1 hexanes/Et₂O and purified by silica gel chromatography (1:1 hexanes/Et₂O) to give **27** as a colorless oil (6.6 mg, 0.043 mmol, 85%). $R_f=0.1$ (1:1 hexanes/Et₂O). IR (neat): 3386 (s), 3075 (w), 2974 (s), 2924 (s), 2873 (m), 1728 (w), 1652 (m), 1457 (m), 1426 (m), 1375 (m), 1161 (w), 1037 (s), 1013 (m), 912 (m) cm⁻¹; ¹H NMR (CDCl₃, 400 MHz): δ 5.92 (dd, $J=17.6$, 11.0 Hz, 1H, CH=CH₂), 5.20 (d, $J=17.2$ Hz, 1H, CH=CH_AH_B), 5.17 (d, $J=12.3$ Hz, 1H, CH=CH_AH_B), 5.00 (s, 2H, CH₃C=CH₂), 4.20 (s, 1H,

CHOH), 3.66 (m, 2H, CH₂OH), 1.79 (s, 3H, CH₃) 1.06 (s, 3H, CH₃); ¹³C NMR (CDCl₃, 100 MHz): δ 146.0, 141.8, 114.9, 113.9, 81.2, 70.4, 46.0, 21.3, 16.3; HRMS calcd for C₉H₁₆O₂Na: 179.1048. Found: 179.1043.

6.1.8. Benzylidene acetal derived from diol **27** (for proof of relative stereochemistry).

To a solution of diol **27** (5.0 mg, 0.032 mmol) in benzene (300 μ L) was added benzaldehyde (16 μ L, 0.16 mmol, 5.0 equiv.) and 100 μ L of a solution consisting of 1.0 mL CH₂Cl₂, 3.0 mg *p*TsOH·H₂O, 0.10 μ L MeOH (to dissolve *p*-TsOH). The resulting mixture was placed under N₂ atmosphere and heated to 100 °C (temperature controlled oil bath) for 10 h. The solution was allowed to cool to ambient temperature and was loaded directly onto a silica gel column (eluted with 100:1 hexanes/Et₂O) to give **28** as a colorless oil (6.8 mg, 0.28 mmol, 87%). $R_f=0.9$ (10:1 hexanes/Et₂O). IR (neat): 3081 (m), 3062 (m), 3024 (m), 2967 (s), 2917 (s), 2848 (s), 1734 (w), 1646 (m), 1457 (s), 1407 (s), 1394 (s), 1350 (s), 1300 (m), 1224 (m), 1174 (m), 1099 (s), 1029 (s), 979 (m), 916 (m), 752 (m), 696 (s), 658 (m) cm⁻¹; ¹H NMR (CDCl₃, 400 MHz): δ 7.53 (dd, $J=8.1$, 1.8 Hz, 2H, Ar–H), 7.37 (m, 3H, Ar–H), 5.74 (dd, $J=17.0$, 11.3 Hz, 1H, CH=CH₂), 5.56 (s, 1H, Ar–CH(O)O), 5.18 (s, 1H, CH_AH_B=CH), 5.14 (dd, $J=7.1$, 1.1 Hz, 1H, CH_AH_B=CH), 5.02 (m, 1H, CH_AH_B=C), 4.96 (m, 1H, CH_AH_B=C), 4.21 (s, 1H, CH–C=CH₂), 3.85 (d, $J=11.4$ Hz, 1H, CH_AH_BO), 3.69 (d, $J=11.2$ Hz, 1H, CH_AH_BO), 1.76 (s, 3H, –CH₃) 1.27 (s, 3H, –CH₃); ¹³C NMR (CDCl₃, 100 MHz): δ 142.3, 140.9, 138.7, 129.0, 128.4, 126.4, 115.5, 113.5, 101.8, 86.1, 77.2, 40.6, 21.9, 15.6; HRMS calcd for C₁₆H₂₀O₂Na: 267.1361. Found: 267.1359.



Acknowledgements

This research was generously supported by the NIH (GM-57212).

References and notes

- (a) Hoveyda, A. H.; Schrock, R. R. *Chem. Eur. J.* **2001**, *7*, 945–950. (b) Schrock, R. R.; Hoveyda, A. H. *Angew. Chem., Int. Ed.* **2003**, *38*, 4555–4708. For general reviews on catalytic olefin metathesis, see: (c) In *Handbook of Olefin Metathesis*; Grubbs, R. H., Ed.; VCH-Wiley: Weinheim, 2003.
- For Mo-catalyzed ARCM, see: (a) Alexander, J. B.; La, D. S.; Cefalo, D. R.; Hoveyda, A. H.; Schrock, R. R. *J. Am. Chem. Soc.* **1998**, *120*, 4041–4142. (b) La, D. S.; Alexander, J. B.; Cefalo, D. R.; Graf, D. D.; Hoveyda, A. H.; Schrock, R. R. *J. Am. Chem. Soc.* **1998**, *120*, 9720–9721. (c) Weatherhead, G. S.; Houser, J. H.; Ford, J. G.; Jamieson, J. Y.; Schrock, R. R.; Hoveyda, A. H. *Tetrahedron Lett.* **2000**, *41*, 9553–9559. (d) Dolman, S. J.; Sattely, E. S.; Hoveyda,

- A. H.; Schrock, R. R. *J. Am. Chem. Soc.* **2002**, *124*, 6991–6997. (e) Teng, X.; Cefalo, D. R.; Schrock, R. R.; Hoveyda, A. H. *J. Am. Chem. Soc.* **2002**, *124*, 10779–10784. (f) Dolman, S. J.; Schrock, R. R.; Hoveyda, A. H. *Org. Lett.* **2003**, *5*, 4899–4902. For Ru-catalyzed ARCM, see: (g) VanVeldhuizen, J. J.; Gillingham, D. G.; Garber, S. B.; Kataoka, O.; Hoveyda, A. H. *J. Am. Chem. Soc.* **2003**, *125*, 12502–12508. For related studies on Ru-catalyzed ARCM, see: (h) Seiders, T. J.; Ward, D. W.; Grubbs, R. H. *Org. Lett.* **2001**, *3*, 3225–3228.
3. For Mo-catalyzed AROM, see: (a) La, D. S.; Ford, J. G.; Sattely, E. S.; Bonitatebus, P. J.; Schrock, R. R.; Hoveyda, A. H. *J. Am. Chem. Soc.* **1999**, *121*, 11603–11604. (b) La, D. S.; Sattely, E. S.; Ford, J. G.; Schrock, R. R.; Hoveyda, A. H. *J. Am. Chem. Soc.* **2001**, *123*, 7767–7778. (c) Weatherhead, G. S.; Ford, J. G.; Alexanian, E. J.; Schrock, R. R.; Hoveyda, A. H. *J. Am. Chem. Soc.* **2000**, *122*, 1828–1829. For Ru-catalyzed AROM, see: (d) Van Veldhuizen, J. J.; Garber, S. B.; Kingsbury, J. S.; Hoveyda, A. H. *J. Am. Chem. Soc.* **2002**, *124*, 4954–4955.
4. Hultsch, K. C.; Jernelius, J. A.; Hoveyda, A. H.; Schrock, R. R. *Angew. Chem., Int. Ed.* **2002**, 589–593.
5. Aeilts, S. L.; Cefalo, D. R.; Bonitatebus, P. J.; Houser, J. H.; Hoveyda, A. H.; Schrock, R. R. *Angew. Chem., Int. Ed.* **2001**, *40*, 1452–1456.
6. (a) Burke, S. D.; Muller, N.; Beudry, C. M. *Org. Lett.* **1999**, *1*, 1827–1829. (b) Cefalo, D. R.; Kiely, A. F.; Wuchrer, M.; Jamieson, J. Y.; Schrock, R. R.; Hoveyda, A. H. *J. Am. Chem. Soc.* **2001**, *123*, 3139–3140. (c) Weatherhead, G. S.; Cortez, A. G.; Schrock, R. R.; Hoveyda, A. H. *Proc. Natl. Acad. Sci.* **2004**, *101*, 5805–5809.
7. For a recent review on catalytic cross metathesis, see: Connon, S. J.; Blechert, S. *Angew. Chem., Int. Ed.* **2003**, *42*, 1900–1923.
8. For previous reports on synthesis of cyclic allylboronates by non-asymmetric catalytic RCM, see: (a) Micalizio, G. C.; Schreiber, S. L. *Angew. Chem., Int. Ed.* **2002**, *41*, 152–154. (b) Micalizio, G. C.; Schreiber, S. L. *Angew. Chem., Int. Ed.* **2002**, *41*, 3272–3276. For one-pot non-asymmetric Ru-catalyzed CM/allylboration, see: (c) Goldberg, S. D.; Grubbs, R. H. *Angew. Chem., Int. Ed.* **2002**, *41*, 807–810.
9. For a detailed discussion regarding catalyst diversity versus specificity, see: Hoveyda, A. H. In *Handbook of Combinatorial Chemistry*; Nicolaou, K. C., Hanks, R., Hartwig, W., Eds.; Wiley-VCH: Weinheim, 2002; pp 991–1016.
10. Isolated yields in this study often suffer from volatility of the desired products.
11. Burgess, K.; Van der Donk, W. A. *Encyclopedia of Reagents for Organic Synthesis*; Paquette, L. A., Ed.; Wiley: New York, 1995; Vol. 2, pp 1253–1261.
12. (a) King, S. A.; Thompson, A. S.; King, A. O.; Verhoeven, T. R. *J. Org. Chem.* **1992**, *57*, 6689–6691. (b) Evans, D. A.; Chapman, K. T.; Carreira, E. M. *J. Am. Chem. Soc.* **1988**, *110*, 3560–3578.
13. All other stereochemical assignments are inferred from this correlation. It is important to note, however, that subtle structural variations can lead to reversal of the identity of the major product enantiomer. In case of application to total synthesis, rigorous determination of the identity of the major enantiomer is thus warranted.
14. For reviews on stereoselective formation of quaternary carbons, see: (a) Corey, E. J.; Guzman-Perez, A. *Angew. Chem., Int. Ed.* **1998**, *37*, 388–401. (b) Christoffers, J.; Mann, A. *Angew. Chem., Int. Ed.* **2001**, *40*, 4591–4597. (c) Denissova, I.; Barriault, L. *Tetrahedron* **2003**, *59*, 10105–10146.
15. For recent studies regarding Lewis acid-catalyzed additions of allylboranes to carbonyl compounds, see: Rauniyar, V.; Hall, D. G. *J. Am. Chem. Soc.* **2004**, *126*, 4518–4519.
16. For a recent review on catalytic enantioselective additions of allylic organometallic reagents to carbonyl compounds, see: Denmark, S. E.; Fu, J. *Chem. Rev.* **2003**, *103*, 2763–2793.
17. Kiely, A. F.; Jernelius, J. A.; Schrock, R. R.; Hoveyda, A. H. *J. Am. Chem. Soc.* **2002**, *124*, 2868–2869.
18. Yields of formation of allylboronates (both precursors and products of ARCM) range from 75–90%. All allylboronates were analyzed by ¹H NMR spectroscopy without purification; these spectra indicated that ARCM products are 90–95% pure. Representative ¹H NMR data for allylboronate precursor to **14** (entry 1, Table 1; derived from catalytic ARCM): (400 MHz, CDCl₃): δ 5.61 (s, 1H), 5.10–4.86 (m, 2H), 4.79 (s, 1H), 4.23–4.18 (m, 1H), 1.90–1.83 (m, 1H), 1.76–1.68 (m, 1H), 1.62 (s, 3H), 1.58 (s, 3H).

A facile synthetic route to (+)-allosedamine via hydrolytic kinetic resolution and olefin metathesis

Byungman Kang and Sukbok Chang*

Department of Chemistry and School of Molecular Science (BK21), Center for Molecular Design and Synthesis (CMDS), Korea Advanced Institute of Science and Technology (KAIST), 373-1, Kusong-dong, Yusong-gu, Daejeon 305-701, South Korea

Received 10 March 2004; revised 22 May 2004; accepted 24 May 2004

Available online 10 June 2004

This paper is dedicated to Professor Robert H. Grubbs of California Institute of Technology on the occasion of his receiving the Tetrahedron Prize

Abstract—A concise synthesis of (+)-allosedamine has been achieved using cobalt-catalyzed hydrolytic kinetic resolution (HKR) and ruthenium-catalyzed ring closing metathesis (RCM) as two key steps, in which HKR was used to introduce both stereogenic centers in the natural compound with a high degree of diastereomeric ratio and cyclization was carried out with the well developed RCM procedure. © 2004 Elsevier Ltd. All rights reserved.

1. Introduction

Lobelia inflata, also known as Indian tobacco, has been used for the treatment of some respiratory illnesses by American settlers. It was later found that a family of piperidine alkaloids including lobeline, lobelanine, lobelanidine and allosedamine are responsible for the therapeutic effects (Fig. 1).¹ Extracts of the plants have been also used for the treatment of narcotic poisoning, coal gas asphyxia, pneumonia and control of anxiety, and it has been revealed that the continual doses of its extracts cause a various side effects.²

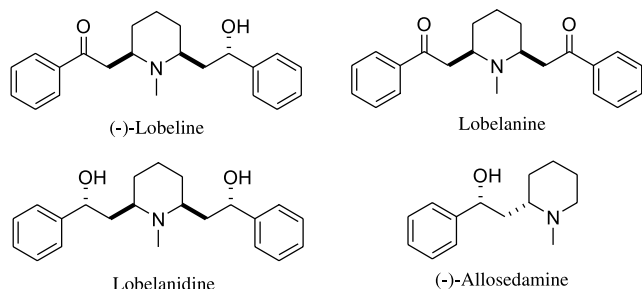


Figure 1. *Lobelia* alkaloids.

We were particularly interested in the development of an efficient asymmetric synthetic route of allosedamine and its diastereomeric isomer (sedamine) among those alkaloids. While numerous approaches have been reported for the

synthesis of sedamine alkaloid in racemic³ and optically active form,⁴ facile and direct application of the approaches on synthesis of allosedamine turned out to be difficult in most cases.⁵ For example, whereas an elegant recent strategy described by Cossy et al. for the synthesis of (+)-sedamine is based on the enantioselective allyltitanation of an aldehyde precursor by chiral titanium complex followed by ring-closing metathesis to provide a *N*-heterocyclic system,^{4c} Lebreton's route for the preparation of (–)-allosedamine relies on Brown's asymmetric allylation and subsequent electrophilic cyclization.^{5c}

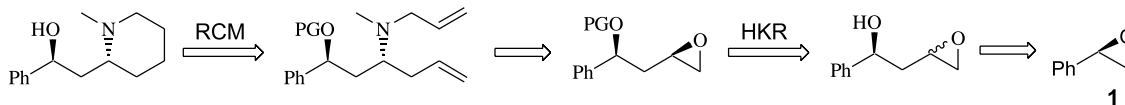
2. Results and discussion

One of the most distinguishing structural features of (+)-allosedamine is the fact that it contains a secondary free benzylic hydroxy group and a piperidine moiety. At the outset of our studies, it was anticipated that both of two stereogenic centers located at β -position each other could be readily introduced by asymmetric catalysis. Our synthetic approach for (+)-allosedamine relies on two metal-catalyzed reactions; hydrolytic kinetic resolution (HKR) and ring-closing metathesis (RCM) (Scheme 1).⁶ Inversion of a hydroxyl group-containing stereogenic center at homoallylic position was envisioned to be another key step for the success in this strategy. (+)-Styrene oxide **1** was chosen as a starting material for providing a stereogenic center at benzylic position because it is readily available in multi gram scale via a hydrolytic kinetic resolution of racemic styrene oxide.⁷

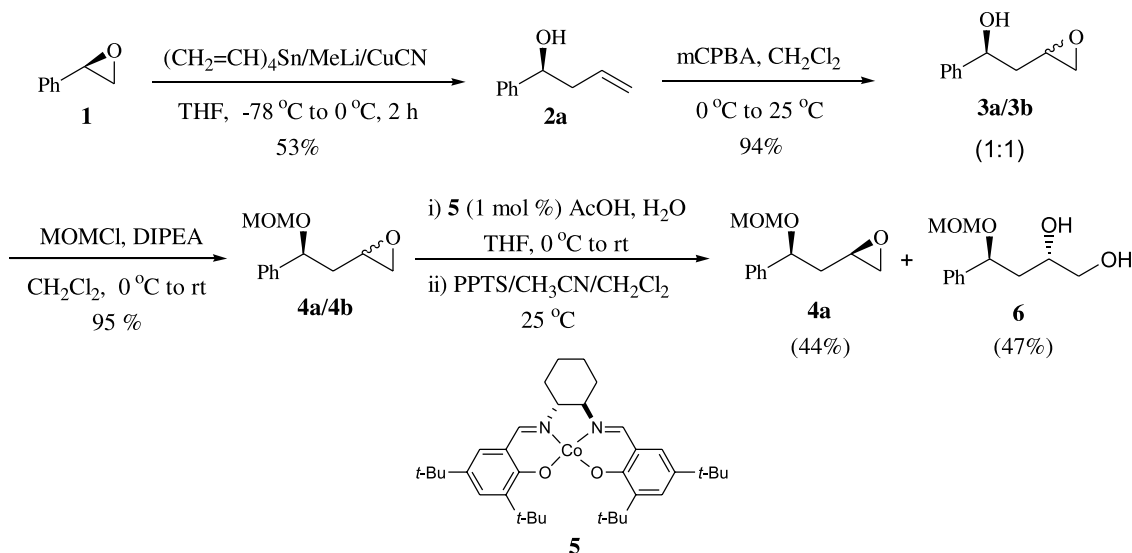
As shown in Scheme 2, regioselective ring opening of

Keywords: Allosedamine; Total synthesis; Hydrolytic kinetic resolution; Ring-closing metathesis.

* Corresponding author. Tel.: +82-428692841; fax: +82-428692810; e-mail address: sbchang@kaist.ac.kr



Scheme 1. Retrosynthetic analysis of (+)-allosedamine.



Scheme 2. Construction of two stereogenic centers.

(+)-styrene oxide **1**⁸ was most efficiently achieved by using cuprate reagents derived from tetravinyltin in THF among a variety of conditions examined leading to a homoallylic alcohol **2a**.⁹ Employment of other sources of vinyl group or use of different solvents resulted in much lower selectivities for the desired secondary alcohol. For example, when vinylmagnesium bromide was used in the presence of Cu(I) salt,¹⁰ almost equal ratio of primary versus secondary alcohol isomer was generated albeit with higher combined yields. In addition, when vinyl bromide was utilized in combination with *t*-BuLi and CuCN, no desired product was obtained from the reaction.

It was expected at the beginning that a directed epoxidation of homoallylic alcohol **2a** would be possible giving practically acceptable diastereoselectivity under certain conditions. Some precedent examples demonstrate that either peroxy acids alone or peracids in combination with

Table 1. Attempts of directed epoxidation of homoallylic alcohol **2a**

Entry	Reaction conditions ^a	Yield (%; 3a:3b) ^b
1	MPPA, NaOH (1 M), rt	NR
2	MPPA, CH ₂ Cl ₂ , 0 °C to rt	80 (1:1)
3	MPPA, THF, 0 °C to rt	63 (1:1)
4	<i>m</i> -CPBA, CH ₂ Cl ₂ , 0 °C to rt	94 (1.1:1)
5	Mo(CO) ₆ , TBHP, C ₆ H ₆ , rt	51 (1.2:1)
6	VO(acac) ₂ , TBHP, C ₆ H ₆ , rt	42 (2.8:1)

^a MPPA: monoperoxyphthalic acid, *m*-CPBA: 3-chloroperbenzoic acid, TBHP: *t*-butyl hydroperoxide.

^b Combined yields, and ratios were determined by ¹H NMR integration of the crude reaction mixture.

certain transition metal species provide high degree of directing effects in the epoxidation of homoallylic alcohols.¹¹ This directed epoxidation is presumed to be operated mainly via hydrogen bonding interactions between the hydroxyl group of substrates and peroxy acids or peracids leading to *syn* epoxy alcohols. As shown in Table 1, a directed epoxidation of **2a** was examined under various conditions on the basis of the reported procedures.

In reality, no measurable diastereoselective induction was observed when the epoxidation of **2a** was carried out with peracid or peroxide in the absence of metal species (entries 1–4). While almost no selectivity was also observed in the presence of a Mo catalyst (entry 5), slightly improved selectivity was induced with the use of a vanadium catalyst albeit in lower yield (entry 6). The unexpectedly low diastereoselectivity would be probably derived from weak hydrogen bonding interactions between peracid oxygen and homoallylic alcohol **2a**. This result led us to employ a two-step pathway for the preparation of an optically active epoxy alcohol **3a** from **2a**: non-selective epoxidation of **2a** with *m*-CPBA and subsequent kinetic resolution of the resulting epoxy alcohol moiety.

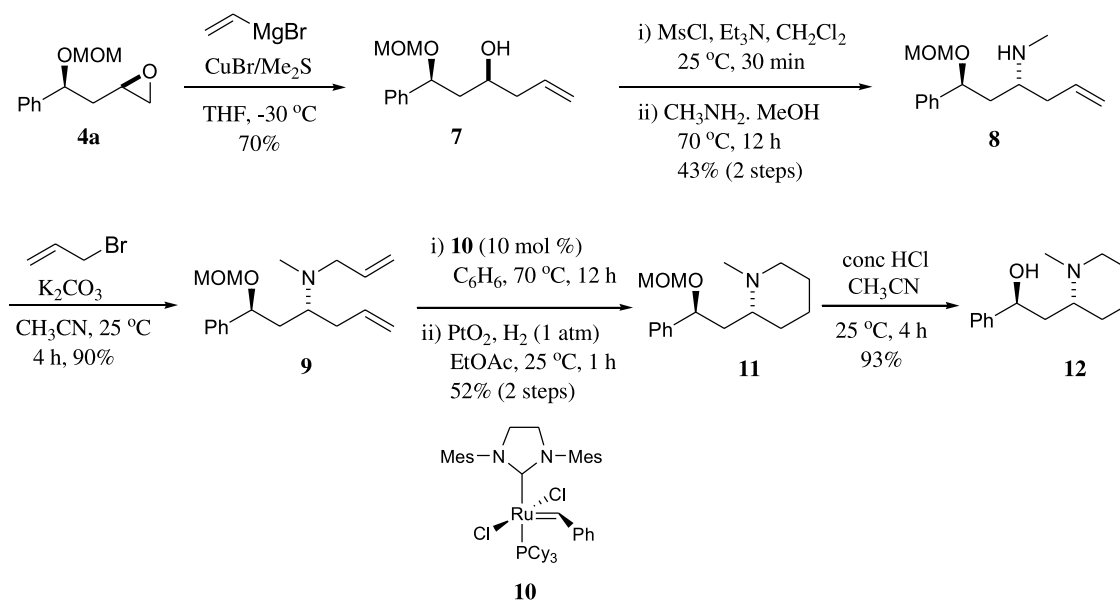
Protection of free hydroxyl group of **3a/3b** was carried out in high yield (95%) with chloromethyl methyl ether in CH₂Cl₂ at 0 °C giving the corresponding MOM ethers **4a/4b** in the same ratio.¹² In order to perform a kinetic resolution of the diastereomeric epoxide mixture **4a/4b**, Jacobsen's (*R,R*)-(–)-Co(salen) catalyst (**5**) was employed under the optimized conditions.⁷ Treatment of a mixture of **4a/4b** (~1:1) with **5** (1 mol%), acetic acid (4 mol%), and H₂O (0.55 equiv.) in THF at room temperature provided **4a** in 44% yield with >98% de. In the resolution reaction, diol **6** was isolated in 47% yield as a single diastereomer

determined by ^1H NMR. It is noteworthy that synthetic utility of the ring-opened diol **6** could be readily found in other syntheses because it is highly functionalized compound with well-defined stereochemistry. Designation of the absolute stereochemistry in the resolved epoxide, (1*S*,3*R*)-**4a**, was ensured by comparing it with that of an authentic sample which was prepared independently by a literature procedure.^{4d} Residual amounts of the used cobalt catalyst in the product was completely removed by the use of pyridinium *p*-toluene sulfonate (PPTS) during workup processes.^{7c} It should be particularly mentioned that the present synthetic route can be also applied to the synthesis of optically active sedamine, a diastereomer of allosedamine by the choice of the Jacobsen's Co catalyst. With the use of (*S,S*)-(+)-Co(salen) catalyst instead of (*R,R*)-isomer, a diastereomeric epoxide **4b** would be obtained with the same efficiency and selectivity eventually leading to (–)-sedamine. It should be mentioned that this synthetic route uses two resolution reactions to obtain the key epoxide intermediate **4a** starting from a readily available racemic styrene epoxide. Both resolutions proceed with an excellent selectivity under mild conditions making the present synthesis highly efficient and practical.

Epoxide opening of an oxirane **4a** with vinyl Grignard reagent underwent smoothly in the presence of copper additives in THF affording another homoallylic alcohol **7** in 70% yield (Scheme 3). Initially, the Mitsunobu's inversion protocol was investigated to introduce the required amino group at the homoallylic position using allylamine and its derivatives as a nucleophile.¹³ However, a variety of attempts with several amino groups were unsuccessful presumably because of steric hindrance around the alcohol substrate. This led us to employ a two-step alternative: conversion of the homoallylic alcohol **7** into its corresponding mesylate followed by amination with methylamine to provide an amino ether adduct **8** (43% over two steps). The fact that configuration of the free hydroxyl containing carbon in **7** was completely inverted in the substituted product **8** was readily confirmed by ^1H NMR. Allylation of

the secondary amino moiety **8** was carried out efficiently under normal conditions to afford a diene compound **9**, a precursor for ring-closing metathesis.

Efficiency of the ring-closing metathesis reaction of **9** was examined with the use of several catalyst systems under various conditions.¹⁴ The best result was obtained when diene **9** was reacted with the Grubbs' second generation catalyst (Im) $\text{Cl}_2\text{PCy}_3\text{RuCHPh}$ **10** (10 mol%) in benzene under N_2 atmosphere to generate an olefinic piperidine moiety in 54% yield. Other ruthenium carbene catalysts gave a rather reduced activity and lower yields under otherwise same conditions; $\text{Cl}_2(\text{PCy}_3)_2\text{RuCHPh}$ (40%) and (3-bromopyridine) $\text{Cl}_2(\text{Im})\text{RuCHPh}$ (47%).¹⁵ No significant improvement was observed when the cyclization was carried out under ethylene atmosphere instead of N_2 . In addition, when ammonium salts of diolefinic amine **9** were subjected to the metathesis conditions, noticeable improvements in chemical yields were not observed compared to free amino substrate **9**. For example, RCM of ammonium salts of **9** of trifluoroacetic acid, *p*-toluenesulfonic acid, and 10-camphorsulfonic acid afforded the cyclized product in 54, 43, and 43% isolated yields under identical conditions, respectively.¹⁶ While tandem hydrogenation of the olefinic intermediate into a saturated piperidine adduct **11** was initially tried in the absence of additional metal catalysts,¹⁷ no desired activity of the ruthenium carbene precursor was observed for the reduction step. This led us to use another one-pot procedure: addition of platinum oxide catalyst (0.1 equiv.) after the metathesis reaction for the subsequent hydrogenation.¹⁸ Hydrogenation underwent almost quantitatively in the presence of PtO_2 catalyst giving a protected allosedamine **11** in 52% yield (two steps starting from **9**). To remove the residual ruthenium by products from the product, various known purification procedures were examined.¹⁹ Whereas simple silica gel column chromatography left significant amounts of residual ruthenium in the desired product, treatment of the crude reaction mixture with either lead tetraacetate (1.5 equiv. to catalyst)^{19a} or tris(hydroxymethylphosphine) (100 equiv. to catalyst)^{19b}



Scheme 3. Final stages in the synthesis of (+)-allosedamine.

resulted in only marginal improvement in purity and brown color was still seen from the isolated product. Most effective removal of ruthenium residues from the reaction mixture was achieved according to a recently published protocol, in which the reaction mixture was treated with activated charcoal (50 equiv. to the crude product in wt)^{19c} for 12 h followed by a silica gel column chromatography. Subsequent deprotection of MOM group by conc. HCl in acetonitrile¹² provided (+)-allosedamine **12** in high yield, spectral data of which are identical to those of the reported literature ones.⁵

3. Conclusion

A concise synthesis of (+)-allosedamine has been achieved using cobalt-catalyzed hydrolytic kinetic resolution (HKR) and ruthenium-catalyzed ring closing metathesis (RCM) as two key steps. HKR was used to introduce both stereogenic centers in the natural compound with a high degree of diastereomeric ratio. Cyclization was carried out with the well-developed RCM procedure and the desired piperidine moiety was isolated after tandem hydrogenation in one-pot. With the present synthetic approach, optically active sedamine, a diastereomeric isomer of allosedamine, could be also readily accessed by a simple choice of enantiomeric cobalt catalyst via HKR.

4. Experimental

4.1. General methods

Oxygen or moisture sensitive reactions were conducted in oven- or flame-dried glassware under nitrogen. Unless otherwise specified, materials were purchased from commercial supplier and used without further purification. Solvents were dried and purified prior to use. Benzene, acetonitrile, and dichloromethane were distilled from calcium hydride under argon or nitrogen atmosphere. THF was distilled from sodium metal and benzophenone. Analytical thin layer chromatography (TLC) was performed on Merck precoated silica gel 60 F254 plates. Purification by column chromatography was carried out using silica gel 60 (230–400 mesh, ASTM, Merck). Proton nuclear magnetic resonance spectra were recorded on a Bruker AVANCE 400 (400 MHz) spectrometer. Chemical shifts are reported in delta (δ) units, parts per million (ppm) downfield from internal standard (tetramethylsilane), or in ppm relative to the singlet at 7.26 ppm of chloroform-*d*₁. Splitting patterns are designated as follows: s; singlet, d; doublet, t; triplet, q; quintet, m; multiplet, dd; doublet of doublet, ddd; doublet of doublet of doublet, bs; broad singlet. HRMS spectra were recorded on a VG AUTOSPEC ULTIMA spectrometer.

4.1.1. (1S)-1-Phenylbut-3-en-1-ol (2a). A solution of tetravinyltin (0.46 mL, 2.45 mmol) in THF (7 mL) was cooled to 0 °C and methylolithium (1.4 M in Et₂O, 6.1 mL, 8.57 mmol) was added. The colorless solution was stirred for 1 h and cooled to –78 °C. To a stirred heterogeneous solution of CuCN (392 mg, 4.37 mmol) in THF (2 mL), the colorless vinylolithium solution was added dropwise via

cannula at –78 °C. The mixture was allowed to warm slowly to –30 °C with stirring and then a heterogeneous solution changed into a homogeneous yellow solution. After cooling to –78 °C, a solution of (+)-styrene oxide (0.20 mL, 1.75 mmol) in THF (1 mL) was added dropwise to the above solution. After stirring for 2 h at –30 °C, the mixture was allowed to warm slowly to room temperature. The reaction was quenched by addition of saturated NH₄Cl and filtered through celite. The organic phase was washed with brine, dried over MgSO₄ and concentrated in vacuo. The crude residue was purified on silica gel (EtOAc/*n*-hexane, 1:5) to afford **2a** as a colorless oil (137 mg, 53%): *R*_f=0.52 (EtOAc/*n*-hexane, 1:3); [α]_D = –50.2 (*c* 1.45, C₆H₆); IR (KBr) 3386, 1640, 1603, 1493, 1453 cm^{–1}; ¹H NMR (400 MHz, CDCl₃) δ 2.09 (d, 1H, *J*=3.3 Hz), 2.51 (m, 2H), 4.72 (m, 1H), 5.11–5.17 (m, 2H), 5.80 (m, 1H), 7.24–7.34 (m, 5H); ¹³C NMR (100 MHz, CDCl₃) δ 43.7, 73.2, 118.4, 125.8, 127.5, 128.4, 134.4, 143.8; HRMS (EI) calcd for C₁₀H₁₂O [M⁺] 148.0888, found 148.0899.

4.1.2. (1S)-2-Oxiranyl-1-phenylethanol (3a, 3b). The mixture of olefin **2a** (500 mg, 3.37 mmol), *m*-chloroperbenzoic acid²⁰ (983 mg, 4.38 mmol) in CH₂Cl₂ (12 mL) was stirred at 0 °C for 30 min. The mixture was stirred for 12 h at room temperature and was then diluted with dichloromethane. The organic phase was extracted with saturated NaHCO₃ twice. The organic phase was washed with brine, dried over MgSO₄ and concentrated in vacuo. The crude residue was purified on silica gel (EtOAc/*n*-hexane, starting from 1/6 to 1/1) to afford product as a colorless oil (521 mg, 94%) with a diastereomeric ratio of 1:1 (**3a:3b**, determined by ¹H NMR): *R*_f=0.20 (EtOAc/*n*-hexane, 1:3); IR (KBr) 3423, 1494, 1454, 1410 cm^{–1}.

3a: ¹H NMR (400 MHz, CDCl₃) δ 1.90 (dd, 1H, *J*=14.1, 6.5 Hz), 2.02 (dd, 1H, *J*=9.5, 4.4 Hz), 2.48 (dd, 1H, *J*=4.8, 2.8 Hz), 2.74 (t, 1H, *J*=4.1 Hz), 2.99 (m, 1H), 4.89–4.96 (m, 1H), 7.25–7.39 (m, 5H); ¹³C NMR (100 MHz, CDCl₃) δ 41.3, 46.7, 49.8, 71.8, 125.5, 127.6, 128.5, 143.8.

3b: ¹H NMR (400 MHz, CDCl₃) δ 1.80 (ddd, 1H, *J*=14.4, 6.7, 3.5 Hz), 2.13 (ddd, 1H, *J*=17.0, 9.0, 4.0 Hz), 2.59 (dd, 1H, *J*=5.5, 3.5 Hz), 2.81 (t, 1H, *J*=4.4 Hz), 3.16 (m, 1H), 4.89–4.96 (m, 1H), 7.25–7.39 (m, 5H); ¹³C NMR (100 MHz, CDCl₃) δ 41.8, 46.9, 50.1, 72.7, 125.7, 127.7, 128.5, 144.1; HRMS (EI) calcd for C₁₀H₁₂O₂ [M⁺] 164.0837, found 164.0836.

4.1.3. (1S)-Methoxymethyl-(2-oxiranyl-1-phenylethyl)-ether (4a, 4b). To a solution of a mixture of alcohol **3a** and **3b** (506 mg, 3.08 mmol) in CH₂Cl₂ (8 mL) at 0 °C were added diisopropylethylamine (2.15 mL, 12.3 mmol), chloromethyl methyl ether (0.70 mL, 9.24 mmol). After being stirred at room temperature for 6 h, the resulting mixture was diluted with dichloromethane and quenched with water. The aqueous phase was extracted with dichloromethane. The combined extracts were washed with brine, dried over MgSO₄, and filtered. Removal of solvent left an oil which was purified by column chromatography (EtOAc/*n*-hexane, 1:9), affording product (604 mg, 95%) as a colorless oil: *R*_f=0.55 (EtOAc/*n*-hexane, 1:3); IR (KBr) 2925, 2887, 1494, 1454, 1408 cm^{–1}.

4a: ^1H NMR (400 MHz, CDCl_3) δ 1.91 (ddd, 1H, $J=14.0$, 6.5, 5.0 Hz), 2.09 (m, 1H), 2.44 (dd, 1H, $J=5.0$, 2.7 Hz), 2.70 (t, 1H, $J=4.1$ Hz), 2.90 (m, 1H), 3.37 (s, 3H), 4.54 (s, 2H), 4.79 (t, 1H, $J=6.8$ Hz), 7.25–7.36 (m, 5H); ^{13}C NMR (100 MHz, CDCl_3) δ 40.9, 46.7, 49.6, 55.5, 75.7, 93.9, 126.8, 127.8, 128.5, 141.0.

4b: ^1H NMR (400 MHz, CDCl_3) δ 1.80 (ddd, 1H, $J=14.1$, 7.1, 3.9 Hz), 2.13 (m, 1H), 2.59 (dd, 1H, $J=5.0$, 2.7 Hz), 2.81 (t, 1H, $J=4.0$ Hz), 3.16 (m, 1H), 3.38 (s, 3H), 4.56 (s, 2H), 4.84 (dd, 1H, $J=9.4$, 3.8 Hz), 7.25–7.39 (m, 5H); ^{13}C NMR (100 MHz, CDCl_3) δ 41.4, 47.5, 49.6, 55.6, 75.2, 94.0, 126.6, 127.9, 128.5, 141.4.

4.1.4. (1S,3R)-Methoxymethyl-(2-oxiranyl-1-phenylethyl)ether (4a). A 25 ml round bottom flask equipped with a stirring bar was charged with (*R,R*)-Co(salen) catalyst (**5**, 16.8 mg, 27.8 μmol). The catalyst was treated with a solution of **4a/4b** mixture (~1:1, 580 mg, 2.78 mmol), acetic acid (6.4 μL , 111 μmol) in THF (0.2 mL). The solution was cooled to 0 °C, and H_2O (27 μL , 1.53 mmol) was added. The reaction mixture was allowed to warm to room temperature and stirred for 16 h. Pyridinium *p*-toluenesulfonate (28 mg, 4.0 equiv. based on catalyst) and 1 mL of $\text{CH}_3\text{CN}/\text{CH}_2\text{Cl}_2$ (1:1, v/v) were added, and the reaction mixture was applied to a pad of silica gel. The pad was washed with EtOAc. After the mixture was concentrated under reduced pressure, the residue was purified on silica gel (EtOAc/*n*-hexane, 1:6) to afford **4a** as a colorless oil (255 mg, 44%, 98% de based on the ^1H NMR): $[\alpha]_{\text{D}}^{25} = -121.1$ (*c* 1.0, CHCl_3); ^1H NMR (400 MHz, CDCl_3) δ 1.91 (ddd, 1H, $J=14.0$, 6.5, 5.0 Hz), 2.09 (q, 1H, 7.0 Hz), 2.44 (dd, 1H, $J=4.9$, 2.6 Hz), 2.70 (t, 1H, $J=4.1$ Hz), 2.90 (m, 1H), 3.37 (s, 3H), 4.54 (s, 2H), 4.79 (t, 1H, $J=6.8$ Hz), 7.25–7.35 (m, 5H); ^{13}C NMR (100 MHz, CDCl_3) δ 40.9, 46.7, 49.6, 55.5, 75.7, 93.9, 126.8, 127.9, 128.5, 141.0; HRMS (EI) calcd for $\text{C}_{12}\text{H}_{16}\text{O}_3$ [M^+] 208.1099, found 208.1097.

4.1.5. (1S,3S)-1-Methoxymethoxy-1-phenylhex-5-en-3-ol (7). To a solution of $\text{CuBr}/\text{Me}_2\text{S}$ (246 mg, 1.2 mmol) in THF (4 mL) cooled to -30 °C was added vinyl magnesium bromide (3.6 mL, 3.6 mmol, 1.0 M in THF). The resulting mixture was allowed to warm slowly to -0 °C and a solution of epoxide **4a** (250 mg, 1.2 mmol) in THF (2 mL) was added at -60 °C. After being stirred at -30 °C for 1 h, the mixture was allowed to warm slowly to room temperature. The reaction was quenched with saturated NH_4Cl solution and extracted with Et_2O . The combined extracts were washed with brine, dried over MgSO_4 , filtered, and concentrated in vacuo. The crude residue was purified on silica gel (EtOAc/*n*-hexane, 1:6) to afford **7** as a colorless oil (198 mg, 70%): $R_{\text{f}}=0.42$ (EtOAc/*n*-hexane, 1:3); $[\alpha]_{\text{D}}^{25} = -159.5$ (*c* 1.0, CHCl_3); IR (KBr) 3447, 2943, 1638 cm^{-1} ; ^1H NMR (400 MHz, CDCl_3) δ 1.81 (ddd, 1H, $J=14.4$, 4.6, 2.4 Hz), 1.97 (m, 1H), 2.24 (m, 1H), 3.25 (d, 1H, $J=1.7$ Hz), 3.39 (s, 3H), 3.83 (m, 1H), 4.45 (s, 2H), 4.84 (dd, 1H, $J=9.5$, 4.7 Hz), 5.06 (d, 1H, $J=2.3$ Hz), 5.10 (d, 1H, $J=7.0$ Hz), 5.82 (m, 1H), 7.25–7.35 (m, 5H); ^{13}C NMR (100 MHz, CDCl_3) δ 41.9, 44.1, 55.9, 70.3, 78.0, 93.7, 117.6, 126.8, 127.9, 128.5, 134.5, 140.9; HRMS (EI) calcd for $\text{C}_{14}\text{H}_{20}\text{O}_3$ [M^+] 236.1412, found 236.1462.

4.1.6. (1S,3R)-(1-(2-(Methoxymethoxy)-2-phenylethyl)-but-3-enyl)methylamine (8). To a solution of alcohol **7** (188 mg, 0.79 mmol) in CH_2Cl_2 (5 mL) at 0 °C were added triethylamine (0.22 mL, 1.59 mmol), methanesulfonylchloride (0.12 mL, 1.59 mmol). After 30 min, the mixture was diluted with dichloromethane, washed with brine, dried over MgSO_4 , and concentrated to afford the crude mesylate. The crude mesylate was taken up in a methanolic solution of methylamine (14.6 mL, 39.2 mmol, 2.0 M in MeOH). The resulting solution was heated to 70 °C for 12 h. After cooling to room temperature, the solution was concentrated. Then it was diluted with Et_2O , washed with brine, dried over MgSO_4 , and concentrated in vacuo. The crude residue was purified on silica gel (starting from EtOAc/*n*-hexane, 1:3 to MeOH/ CH_2Cl_2 , 1:12) to afford **8** as a yellow oil (86 mg, two steps 43%): $R_{\text{f}}=0.67$ (MeOH/ CH_2Cl_2 , 1:8); $[\alpha]_{\text{D}}^{25} = -123.0$ (*c* 1.0, MeOH); IR (KBr) 3354, 2936, 1638, 1493, 1454 cm^{-1} ; ^1H NMR (400 MHz, CDCl_3) δ 1.76 (ddd, 1H, $J=14.0$, 8.1, 4.5 Hz), 1.91 (ddd, 1H, $J=13.3$, 8.9, 4.4 Hz), 2.11 (bs, 1H), 2.28 (m, 1H), 2.41 (s, 3H), 2.75 (m, 1H), 3.39 (s, 3H), 4.54 (s, 2H), 4.82 (dd, 1H, $J=8.8$, 4.4 Hz), 5.11 (d, 1H, $J=11.9$ Hz), 5.77 (m, 1H), 7.28–7.35 (m, 5H); ^{13}C NMR (100 MHz, CDCl_3) δ 32.8, 37.6, 41.9, 55.1, 55.7, 75.4, 94.2, 117.4, 126.6, 127.5, 128.4, 134.9, 142.0; HRMS (EI) calcd for $\text{C}_{15}\text{H}_{23}\text{NO}_2$ [M^+] 249.1729, found 249.1716.

4.1.7. (1S,3R)-N-Allyl-(1-(2-(methoxymethoxy)-2-phenylethyl)but-3-enyl)methylamine (9). To a solution of amine **8** (63 mg, 0.25 mmol) in acetonitrile (3 mL) was added powder K_2CO_3 (105 mg, 0.76 mmol). The mixture was stirred for 30 min at room temperature, and then allylbromide (32.8 μL , 0.38 mmol) was added. After stirring for 4 h at room temperature, the resulting mixture was diluted with Et_2O and quenched with water. The aqueous phase was extracted with Et_2O . The extracts were washed with brine, dried over MgSO_4 , and concentrated in vacuo. The crude residue was purified on silica gel (EtOAc/*n*-hexane, 1:5) to afford **9** as a pale yellow oil (66 mg, 90%): $R_{\text{f}}=0.57$ (EtOAc/*n*-hexane, 1:3); $[\alpha]_{\text{D}}^{25} = -104.2$ (*c* 1.0, CHCl_3); IR (KBr) 2942, 1639, 1493, 1452 cm^{-1} ; ^1H NMR (400 MHz, CDCl_3) δ 1.64 (ddd, 1H, $J=14.4$, 9.6, 3.4 Hz), 1.80–1.93 (m, 2H), 2.19 (s, 3H), 2.90 (m, 1H), 3.01 (dd, 1H, $J=13.7$, 6.1 Hz), 3.11 (dd, 1H, $J=13.8$, 6.1 Hz), 3.32 (s, 3H), 4.53 (dd, 2H, $J=14.8$, 6.6 Hz), 4.85 (dd, 1H, $J=9.6$, 3.3 Hz), 5.02 (d, 2H, $J=14.2$ Hz), 5.04 (d, 1H, $J=17.2$ Hz), 5.15 (dd, 2H, $J=12.9$, 1.3 Hz), 5.79 (m, 1H), 7.28–7.35 (m, 5H); ^{13}C NMR (100 MHz, CDCl_3) δ 33.1, 36.1, 39.8, 55.5, 56.5, 59.1, 75.3, 94.5, 116.1, 126.6, 127.2, 128.3, 137.0, 137.1, 143.1; HRMS (EI) calcd for $\text{C}_{18}\text{H}_{27}\text{NO}_2$ [M^+] 289.2042, found 289.2036.

4.1.8. (2R)-2-((2S)-2-(Methoxymethoxy)-2-phenylethyl)-N-methylpiperidine (11). To a solution of diene **9** (178 mg, 0.61 mmol) in anhydrous benzene (28 mL) was added a solution of the Grubbs ruthenium catalyst (Im) Cl_2PCy_3 -RuCHPh (**10**, 52 mg, 0.06 mmol) in benzene (2 mL) at room temperature. The mixture was refluxed at 70 °C for 12 h. It was cooled to room temperature and was concentrated in vacuo. Then, to a solution of crude metathesis product in EtOAc (8 mL) was added PtO_2 (14 mg, 0.06 mmol). After 1 h under H_2 (1 atm), the mixture was filtered through celite and concentrated in vacuo. The crude residue in CH_2Cl_2 (5 mL) was added to a solution of

activated charcoal (10.0 g, 50 equiv. wt of the crude product) in CH_2Cl_2 (95 mL) and stirred for 12 h. After the carbon was filtered, the filtrate was concentrated in vacuo and purified on a silica gel column chromatography (MeOH/ CH_2Cl_2 , starting from 1:8 to 1:3) to provide **11** as a colorless oil (84 mg, two steps 52%): $R_f=0.37$ (MeOH/ CH_2Cl_2 , 1:12); $[\alpha]_D=-101.1$ (c 0.5, MeOH); IR (KBr) 2943, 1631, 1454, 1376 cm^{-1} ; ^1H NMR (400 MHz, CDCl_3) δ 1.36 (m, 1H), 1.73 (m, 3H), 1.93 (m, 2H), 2.09 (m, 1H), 2.26 (m, 1H), 2.56 (s, 3H), 2.62 (m, 2H), 3.13 (m, 1H), 3.31 (s, 3H), 4.47 (dd, 2H, $J=9.7, 6.6$ Hz), 4.68 (t, 1H, $J=6.9$ Hz), 7.23–7.35 (m, 5H); ^{13}C NMR (100 MHz, CDCl_3) δ 21.6, 22.5, 29.2, 38.2, 40.3, 54.9, 55.8, 61.5, 75.7, 94.1, 126.7, 128.3, 128.7, 139.9; HRMS (EI) calcd for $\text{C}_{16}\text{H}_{25}\text{NO}_2$ [M^+] 263.1885, found 263.1848.

4.1.9. (2R)-2-((2S)-2-Hydroxy-2-phenylethyl)-N-methylpiperidine (12). A solution of piperidine **11** (50 mg, 0.19 mmol) in CH_3CN (2 mL) was treated with conc. HCl (0.02 mL). After being stirred at room temperature for 4 h, the solution was diluted with EtOAc/isopropanol mixture and basified with aqueous NaHCO_3 until pH 9–10. The aqueous layer was extracted with ethyl acetate. The organic extracts were dried over MgSO_4 , filtered, and evaporated under reduced pressure. The crude residue was purified on silica gel (MeOH/ CH_2Cl_2 , 1:6) to afford **12** (38 mg, 93%): $R_f=0.37$ (MeOH/ CH_2Cl_2 , 1:6); IR (KBr) 3363, 2943, 2692, 1453 cm^{-1} ; ^1H NMR (400 MHz, CDCl_3) δ 1.47 (m, 1H), 1.73–1.78 (m, 2H), 1.85 (m, 1H), 1.93–2.01 (m, 3H), 2.11 (m, 1H), 2.77 (s, 3H), 2.84 (m, 1H), 3.16 (br, 1H), 3.30 (m, 1H), 5.11 (dd, 1H, $J=9.5, 3.2$ Hz), 7.18–7.35 (m, 5H); ^{13}C NMR (100 MHz, CDCl_3) δ 21.3, 22.4, 27.6, 38.7, 40.7, 55.7, 62.0, 68.7, 125.5, 127.3, 128.4, 144.1; HRMS (EI) calcd for $\text{C}_{14}\text{H}_{21}\text{NO}$ [M^+] 219.1623, found 219.1624.

Acknowledgements

This work was supported by a grant of the Korea Health 21 R and D Project, Ministry of Health and Welfare, Republic of Korea (01-PJ1-PG1-01CH12-0002).

References and notes

- Dwoskin, L. P.; Crooks, P. A. *Biochem. Pharmacol.* **2002**, *63*, 89–98.
- Fodor, G. B.; Colasanti, B. *Alkaloids: Chemical and Biological Perspectives*; Pelletier, S. W., Ed.; Wiley: New York, 1985; Vol. 3, pp 41–63.
- (a) Shono, T.; Matsumura, Y.; Tsubata, K. *J. Am. Chem. Soc.* **1981**, *103*, 1172–1176. (b) Tirel, P.-J.; Vaultier, M.; Carrié, R. *Tetrahedron Lett.* **1989**, *30*, 1947–1950. (c) Pilli, R. A.; Dias, L. C. *Synth. Commun.* **1991**, *21*, 2213. (d) Ozawa, N.; Nakajima, S.; Zaoya, K.; Hamaguchi, F.; Nagasaka, T. *Heterocycles* **1991**, *32*, 889–894.
- (a) Comins, D. L.; Hong, H. *J. Org. Chem.* **1993**, *58*, 5035–5036. (b) Yu, C.-Y.; Meth-Cohn, O. *Tetrahedron Lett.* **1999**, *40*, 6665–6668. (c) Cossy, J.; Willis, C.; Bellostia, V.; BouzBouz, S. *J. Org. Chem.* **2002**, *67*, 1982–1992. (d) Felpin, F.-X.; Lebreton, J. *J. Org. Chem.* **2002**, *67*, 9192–9199.
- (a) Wakabayashi, T.; Watanabe, K.; Kato, Y.; Saito, M. *Chem. Lett.* **1977**, 223–228. (b) Liguori, A.; Ottana, R.; Romeo, G.; Sindona, G.; Uccella, N. *Chem. Ber.* **1989**, *122*, 2019–2020. (c) Oppolzer, W.; Deerberg, J.; Tamura, O. *Helv. Chim. Acta* **1994**, *77*, 554–560. (d) Meth-Cohn, O.; Yau, C. C.; Yu, C.-Y. *J. Heterocyclic Chem.* **1999**, *36*, 1549–1554. (e) Felpin, F.-X.; Lebreton, J. *Tetrahedron Lett.* **2002**, *43*, 225–227.
- For recent examples of metathesis-based synthesis from this laboratory, see: (a) Jo, E.; Na, Y.; Chang, S. *Tetrahedron Lett.* **1999**, *40*, 5581–5582. (b) Lee, W.-W.; Chang, S. *Tetrahedron: Asymmetry* **1999**, *10*, 4473–4475. (c) Lee, W.-W.; Shin, H. J.; Chang, S. *Tetrahedron: Asymmetry* **2001**, *12*, 29–31. (d) Park, S.-H.; Kang, H. J.; Ko, S.; Park, S. Y.; Chang, S. *Tetrahedron: Asymmetry* **2001**, *12*, 2621–2624. (e) Chang, S.; Na, Y.; Shin, H. J.; Choi, E.; Jeong, L. S. *Tetrahedron Lett.* **2002**, *43*, 7445–7448. (f) Kang, B.; Kim, D.-h.; Do, Y.; Chang, S. *Org. Lett.* **2003**, *5*, 3041–3043.
- (a) Tokunaga, M.; Larrow, J. F.; Kakiuchi, F.; Jacobsen, E. N. *Science* **1997**, *277*, 936–938. (b) Jacobsen, E. N. *Acc. Chem. Res.* **2000**, *33*, 421–431. (c) Ready, J. M.; Jacobsen, E. N. *J. Am. Chem. Soc.* **2001**, *123*, 2687–2688. (d) Schaus, S. E.; Brandes, B. D.; Larrow, J. F.; Tokunaga, M.; Hansen, K. B.; Gould, A. E.; Furrow, M. E.; Jacobsen, E. N. *J. Am. Chem. Soc.* **2002**, *124*, 1307–1315.
- It was obtained in high enantiomeric purity (>98% ee) using the Jacobsen's protocol (Ref. 7) in multi gram scales from racemic epoxide.
- (a) Lipshutz, B. H.; Wilhelm, R. S.; Kozlowski, J. A. *J. Org. Chem.* **1984**, *49*, 3938–3942. (b) Lipshutz, B. H.; Wilhelm, R. S. *J. Am. Chem. Soc.* **1981**, *103*, 7672–7674.
- Smith, J. G. *Synthesis* **1984**, 629–656.
- (a) Hoveyda, A. H.; Evans, D. A.; Fu, G. C. *Chem. Rev.* **1993**, *93*, 1307–1370. (b) Mihelich, E. D.; Daniels, K.; Eickhoff, D. J. *J. Am. Chem. Soc.* **1981**, *103*, 7690–7692. (c) Fringuelli, F.; Germani, R.; Pizzo, F.; Santinelli, F.; Savelli, G. *J. Org. Chem.* **1992**, *57*, 1198–1202.
- (a) Stork, G.; Takahashi, T. *J. Am. Chem. Soc.* **1977**, *99*, 1275–1276. (b) Greene, T. W.; Wuts, P. G. M.; 3rd ed. *Protective Groups in Organic Synthesis*; Wiley: New York, 1999. (c) Seto, H.; Mander, L. N. *Synth. Commun.* **1992**, *22*, 2823–2828. (d) Yang, W.-Q.; Kitahara, T. *Tetrahedron* **2000**, *56*, 1451–1461, pp 27–33.
- (a) Mitsunobu, O. *Synthesis* **1981**, 1–28. (b) Edwards, M. L.; Stemerick, D. M.; McCarthy, J. R. *Tetrahedron Lett.* **1990**, *31*, 3417–3420. (c) Fukuyama, T.; Jow, C.-K.; Cheung, M. *Tetrahedron Lett.* **1995**, *36*, 6373–6374. (d) Nikam, S. S.; Kornberg, B. E.; Rafferty, M. F. *J. Org. Chem.* **1997**, *62*, 3754–3757.
- For recent reviews on olefin metathesis, see: (a) Schuster, M.; Blechert, S. *Angew. Chem., Int. Ed.* **1997**, *36*, 2036–2056. (b) Grubbs, R. H.; Chang, S. *Tetrahedron* **1998**, *54*, 4413–4450. (c) Fürstner, A. *Angew. Chem., Int. Ed.* **2000**, *39*, 3012–3043. (d) Connon, S. J.; Blechert, S. *Angew. Chem., Int. Ed.* **2003**, *42*, 1900–1923. (e) In *Handbook of Metathesis*; Grubbs, R. H., Ed.; Wiley-VCH: Weinheim, 2003.
- Love, J. A.; Morgan, J. P.; Trnka, T. M.; Grubbs, R. H. *Angew. Chem., Int. Ed.* **2002**, *41*, 4035–4037.
- For some selected examples of RCM using ammonium salts as a substrate, see: (a) Wright, D. L.; Schutle, J. P., II; Page, M. A. *Org. Lett.* **2000**, *2*, 1847–1850. (b) Salim, S. S.; Bellingham, R. K.; Satcharoen, V.; Brown, R. C. D. *Org. Lett.* **2003**, *5*, 3403–3406. (c) Verhelst, S. H. L.; Martinez, B. P.; Timmer,

- M. S. M.; Lodder, G.; van der Marel, G. A.; Overkleeft, H. S.; van Boom, J. H. *J. Org. Chem.* **2003**, *68*, 9598–9603.
17. For some examples of tandem RCM and hydrogenation with a common ruthenium carbene precursor, see: (a) Louie, J.; Bielawski, C. W.; Grubbs, R. H. *J. Am. Chem. Soc.* **2001**, *123*, 11312–11313. (b) Sutton, A. E.; Seigal, B. A.; Finnegan, D. F.; Snapper, M. L. *J. Am. Chem. Soc.* **2002**, *124*, 13390–13391.
18. For some examples of tandem RCM and other catalytic reactions by the addition second catalysts, see: (a) Alexakis, A.; Croset, K. *Org. Lett.* **2002**, *4*, 4147–4149. (b) Cossy, J.; Bargiggia, F.; BouzBouz, S. *Org. Lett.* **2003**, *5*, 459–462.
19. (a) Paquette, L. A.; Schloss, J. D.; Efremov, I.; Fabris, F.; Gallou, F.; Mendez-Andino, J.; Yang, J. *Org. Lett.* **2000**, *2*, 1259–1261. (b) Maynard, H. D.; Grubbs, R. H. *Tetrahedron Lett.* **1999**, *40*, 4137–4140. (c) Cho, J. H.; Kim, B. M. *Org. Lett.* **2003**, *5*, 531–533. (d) Ahn, Y. M.; Yang, K. L.; Georg, G. I. *Org. Lett.* **2001**, *3*, 1411–1413.
20. The calculated molarity of the *m*-chloroperbenzoic acid was based on the 77% purity of the commercial peracid.

A new approach to the synthesis of cyclic ethers via the intermolecular allylation of α -acetoxy ethers and ring-closing metathesis

Isao Kadota,^{a,*} Hiroshi Uyehara^b and Yoshinori Yamamoto^{b,*}

^aResearch and Analytical Center for Giant Molecules, Graduate School of Science, Tohoku University, Sendai 980-8578, Japan

^bDepartment of Chemistry, Graduate School of Science, Tohoku University, Aramaki, Aoba-ku, Sendai 980-8578, Japan

Received 17 March 2004; revised 17 May 2004; accepted 19 May 2004

Available online 7 June 2004

This paper is dedicated to Professor R. H. Grubbs on the occasion of his receipt of the 2003 Tetrahedron Prize

Abstract—A concise synthesis of the isolaurepinnacin skeleton **6** was achieved via the intermolecular allylation of the α -acetoxy ether **3** followed by ring-closing metathesis. This methodology was successfully applied to the convergent synthesis of the oxocene **15**, an advanced synthetic intermediate for the total synthesis of laurencin.

© 2004 Elsevier Ltd. All rights reserved.

1. Introduction

Red algae and marine organisms which feed on *Laurencia* species have produced a variety of medium ring ethers such as isolaurepinnacin,¹ laurencin,² and obtusenyne³ (Fig. 1). The unique structural features of these C15 metabolites have attracted the attention of synthetic chemists, and a number of strategies have been investigated.⁴

We recently developed a convergent method for the synthesis of polycyclic ether frameworks by the *intra-molecular* allylation of α -acetoxy ether and ring-closing metathesis.⁵ It was thought that the *intermolecular* version of this methodology would provide an efficient route to the construction of medium ring ethers. Crimmins et al. have reported similar approaches via asymmetric aldol- or alkylation followed by ring-closing metathesis.^{6,7} In this paper, we wish to report concise syntheses of seven- and

eight-membered ring ethers by the intermolecular allylation of α -acetoxy ethers and ring-closing metathesis.

2. Results and discussion

For an initial study, we examined the synthesis of the seven-membered cyclic ether **6** as shown in Scheme 1.⁸ Reaction of the homoallylic alcohol **1**⁹ with butyryl chloride and pyridine gave **2** in 99% yield. The ester **2** was then subjected to the Rychnovsky acetylation. Partial reduction of **2** with DIBAL-H followed by trapping of the resulting aluminium hemiacetal with acetic anhydride/pyridine/DMAP afforded the α -acetoxy ether **3** in 78% yield.¹⁰ Treatment of **3** with allyltrityl tin and BF₃·OEt₂ gave the allylated product **4** as a 1:1 mixture of diastereoisomers in 85% yield.¹¹ Finally, the diene **4** obtained was subjected to ring-closing metathesis.¹² Thus, treatment of **4** with the first generation

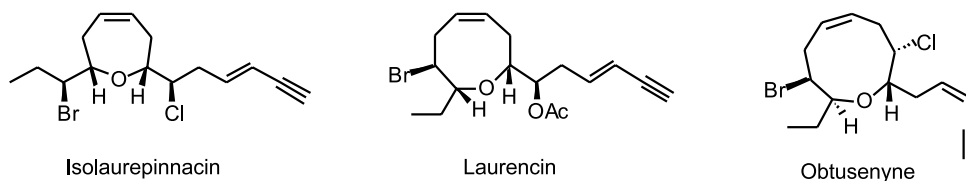
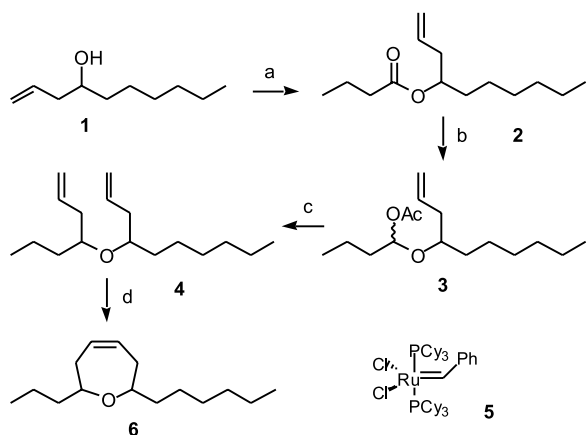


Figure 1. Representative marine medium ring ethers.

Keywords: Polycyclic ether; Allylation; RCM; Lewis acid; Marine natural product.

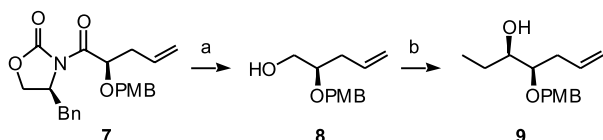
* Corresponding authors. Tel.: +81-22-217-6581; fax: +81-22-217-6784; e-mail addresses: yoshi@yamamoto1.chem.tohoku.ac.jp; ikadota@mail.tains.tohoku.ac.jp



Scheme 1. Reagents and conditions: (a) C_3H_7COCl , pyridine, CH_2Cl_2 , $0^\circ C$, 99%; (b) DIBAL-H, CH_2Cl_2 , $-78^\circ C$, then Ac_2O , pyridine, DMAP, $-78^\circ C$ to rt, 78%; (c) allyltributyltin, $BF_3 \cdot OEt_2$, CH_2Cl_2 , $0^\circ C$ to rt, 85%; (d) **5**, CH_2Cl_2 , $35^\circ C$, 100%.

Grubbs catalyst **5**¹³ provided the oxepene **6**, corresponding to the isolaurepinnacin skeleton, in quantitative yield. Although the target molecule **6** was obtained as a mixture of diastereoisomers, the methodology employed allowed us to construct the seven-membered cyclic ether **6** in only four steps from the known alcohol **1**.

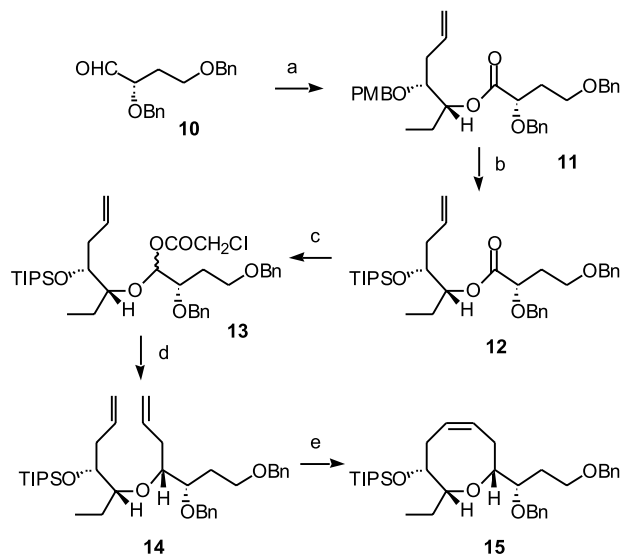
Encouraged by this result, we next examined the synthesis of eight-membered cyclic ether using the methodology described above. **Scheme 2** illustrates the preparation of the alcohol segment **9**. Reduction of **7**¹⁴ with $LiBH_4$ gave the alcohol **8** in 94% yield. Swern oxidation of **8** followed by Grignard reaction in the presence of $ZnBr_2$ afforded **9** as the sole product in 86% yield.¹⁵



Scheme 2. Reagents and conditions: (a) $LiBH_4$, MeOH, $0^\circ C$, 94%; (b) (i) $(COCl)_2$, DMSO, CH_2Cl_2 , $-78^\circ C$, then Et_3N ; (ii) $EtMgBr$, $ZnBr_2$, ether, $0^\circ C$, 86%.

Oxidation of the known aldehyde **10**¹⁶ with Ag_2O generated from $AgNO_3$ and KOH in situ gave the corresponding carboxylic acid, which was subjected to the Yamaguchi esterification with the alcohol **9** obtained above, providing the ester **11** in 94% yield (**Scheme 3**).¹⁷ Removal of the PMB group of **11** with DDQ followed by protection with TIPS group gave **12** in 81% overall yield.¹⁸ The modified Rychnovsky acetylation afforded the α -chloroacetoxy ether **13** in 78% yield.¹⁹ Allylation of **13** using allyltributyltin/ $BF_3 \cdot OEt_2$ gave **14** with high stereoselectivity ($>95:5$) in 64% yield.²⁰ Finally, the diene **14** was subjected to the ring-closing metathesis to provide **15** in 99% yield. The oxocene **15** is an advanced synthetic intermediate for the total synthesis of laurencin.

The α, α' -*cis* stereochemistry of **15** was unambiguously determined by NOE experiment on the acetate derivative **16** as shown in **Figure 2**.



Scheme 3. Reagents and conditions: (a) (i) $AgNO_3$, KOH , MeOH– H_2O , $0^\circ C$; (ii) 2,4,6-trichlorobenzoyl chloride, Et_3N , THF, rt, then **9** DMAP, toluene, rt, 94%; (b) (i) DDQ, $NaHCO_3$, CH_2Cl_2 – H_2O , $0^\circ C$, 91%; (ii) TIPSOTf, 2,6-lutidine, CH_2Cl_2 , rt, 89%; (c) DIBAL-H, CH_2Cl_2 , $-78^\circ C$, then $(CH_2ClCO)_2O$, pyridine, DMAP, $-78^\circ C$ to rt, 78%; (d) allyltributyltin, $BF_3 \cdot OEt_2$, CH_2Cl_2 , $-78^\circ C$, 64%; (e) **5**, CH_2Cl_2 , $35^\circ C$, 99%.

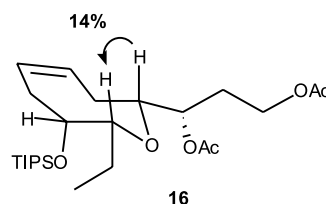


Figure 2. NOE experiment on the acetate **16**.

3. Conclusion

We have developed a new method for the construction of medium ring ethers via the intermolecular allylation of α -acetoxy ethers and ring-closing metathesis. The result described here demonstrates the efficiency and applicability of this methodology, and further studies towards the total synthesis of marine cyclic ethers having a medium ring are in progress.

4. Experimental

4.1. General

All reactions involving air- and/or moisture-sensitive materials were carried out under argon with dry solvents purchased from Wako or Kanto chemicals. On workup, extracts were dried over $MgSO_4$. Reactions were monitored by thin-layer chromatography carried out on 0.25 mm Merck silica gel plates (60F-254). Column chromatography was performed with Kanto Chemical silica gel (60N, spherical, neutral, particle size 0.100–0.210 mm). Yields refer to chromatographically and spectroscopically homogeneous materials.

4.1.1. Ester 2. To a solution of **1** (1.76 g, 11.2 mmol) in

CH₂Cl₂ (110 mL) at 0 °C were added pyridine (1.82 mL, 22.5 mmol) and butyryl chloride (1.39 mL, 13.4 mmol). After stirring for 1 h at the same temperature, the mixture was diluted with ether, then washed with saturated NaHCO₃ and brine. Concentration and chromatography (hexane/EtOAc, 20:1) gave **2** (2.49 g, 99%): oil; *R*_f=0.68 (hexane/EtOAc, 4:1); IR (neat) 1738 cm⁻¹; ¹H NMR (300 MHz, CDCl₃) δ 5.75 (dddd, *J*=17.1, 9.9, 7.2, 7.2 Hz, 1H), 5.10–5.00 (m, 2H), 4.93 (quint, *J*=6.3 Hz, 1H), 2.34–2.24 (m, 2H), 2.26 (t, *J*=7.3 Hz, 2H), 1.73–1.52 (m, 4H), 1.34–1.20 (m, 8H), 0.95 (t, *J*=7.3 Hz, 3H), 0.88 (t, *J*=7.0 Hz, 3H); ¹³C NMR (75 MHz, CDCl₃) δ 173.2, 133.8, 117.4, 72.9, 38.6, 36.4, 33.5, 31.6, 29.0, 25.2, 22.5, 18.5, 13.9, 13.3. Anal. calcd for C₁₄H₂₆O₂: C, 74.29; H, 11.60. Found: C, 73.90; H, 11.52.

4.1.2. α-Acetoxy ether 3. To a solution of **2** (0.57 g, 2.52 mmol) in CH₂Cl₂ (15 mL) at -78 °C was added DIBAL-H (0.93 M in hexane, 5.0 mL, 5.04 mmol), and the mixture was stirred for 1 h at the same temperature. To the mixture, acetic anhydride (1.43 mL, 15.1 mmol), DMAP (0.61 g, 5.04 mmol) in CH₂Cl₂ (8 mL), and pyridine (0.62 mL, 7.5 mmol) were added. After stirring for 24 h at -78 °C, the mixture was allowed to warm to room temperature. The mixture was diluted with ether, then washed with saturated potassium sodium tetrates, saturated NaHCO₃, and brine. Concentration and chromatography (hexane/EtOAc, 40:1 containing 1% Et₃N) gave **3** (0.53 g, 78%) as a mixture of diastereomers: oil; *R*_f=0.57 (hexane/EtOAc 20:1); IR (neat) 1737 cm⁻¹; ¹H NMR (400 MHz, C₆D₆) δ 6.18–6.03 (m, 1H), 5.97–5.73 (m, 1H), 5.09–4.92 (m, 2H), 3.73–3.68 (m, 1H), 2.37–2.18 (m, 2H), 1.76 (s, 1.5H), 1.73 (s, 1.5H), 1.69–1.23 (m, 14H), 0.90–0.81 (m, 6H); HRMS (ESI), calcd for C₁₆H₂₉O₃Na (M+Na): 293.2093. Found: 293.2043.

4.1.3. Diene 4. To a solution of **3** (0.19 g, 0.71 mmol) in CH₂Cl₂ (7 mL) at 0 °C were added allyltributyltin (0.45 mL, 1.42 mmol) and BF₃·OEt₂ (1.0 M in CH₂Cl₂, 1.42 mL, 1.42 mmol). After stirring for 3 h at room temperature, the mixture was diluted with ether, then washed with saturated NaHCO₃ and brine. Concentration and chromatography (hexane/EtOAc, 20:1) gave **4** (2.49 g, 85%) as a 1:1 mixture of diastereoisomers: colorless oil; *R*_f=0.45 (hexane/EtOAc 10:1); IR (neat) 1640 cm⁻¹; ¹H NMR (400 MHz, CDCl₃) δ 5.80–5.68 (m, 2H), 5.03–4.82 (m, 4H), 3.40–3.22 (m, 2H), 2.22–2.00 (m, 4H), 1.54–1.00 (m, 14H), 0.89–0.78 (m, 6H); HRMS (EI), calcd for C₁₇H₃₂O (M⁺): 252.2453. Found: 252.2464.

4.1.4. Oxepene 6. To a solution of **4** (40 mg, 0.16 mmol) in CH₂Cl₂ (16 mL) was added **5** (26 mg, 32 μmol). After stirring for 4 h at 35 °C, the mixture was concentrated and purified by silica gel column chromatography (hexane/EtOAc, 10:1) to give **6** (38 mg, 100%): colorless oil; *R*_f=0.56 (hexane/EtOAc 10:1); IR (neat) 2930, 1460 cm⁻¹; ¹H NMR (400 MHz, CDCl₃) δ 5.74–5.64 (m, 2H), 3.98–3.94 (m, 1H), 3.30–3.25 (m, 1H), 2.37–2.03 (m, 4H), 1.60–1.28 (m, 14H), 0.93–0.87 (m, 6H); HRMS (EI), calcd for C₁₅H₂₈O (M⁺): 224.2140. Found: 224.2130.

4.1.5. Alcohol 8. To a solution of **7** (1.77 g, 4.47 mmol) and methanol (0.22 mL, 5.36 mmol) in ether (45 mL) at 0 °C

was added LiBH₄ (0.12 g, 5.36 mmol), and the mixture was stirred for 1.5 h at the same temperature. The mixture was quenched with aqueous NaOH (10%, 40 mL) and extracted with EtOAc. The organic layer was washed with brine. Concentration and chromatography (hexane/AcOEt=2:1) gave **8** (0.94 g, 94%): oil; *R*_f=0.35 (hexane/AcOEt=2:1); [α]_D²³=-14.1 (*c* 0.94, CHCl₃); IR (neat) 3600–3200, 1612 cm⁻¹; ¹H NMR (400 MHz, CDCl₃) δ 7.27 (d, *J*=8.5 Hz, 2H), 6.89 (d, *J*=8.5 Hz, 2H), 5.81 (ddd, *J*=17.1, 7.1, 2.9 Hz, 1H), 5.14–5.07 (m, 2H), 4.59 (d, *J*=11.2 Hz, 1H), 4.47 (d, *J*=11.2 Hz, 1H), 3.81 (s, 3H), 3.68–3.50 (m, 3H), 2.41–2.26 (m, 2H), 1.94 (m, 1H); ¹³C NMR (100 MHz, CDCl₃) δ 158.6, 133.5, 129.8, 128.8, 117.0, 113.4, 78.4, 70.9, 63.8, 55.1, 35.3; HRMS (ESI), calcd for C₁₃H₁₈O₃Na (M+Na): 245.1148. Found: 245.1154.

4.1.6. Alcohol 9. To a solution of DMSO (0.95 mL, 13.4 mmol) in CH₂Cl₂ (40 mL) at -78 °C was added (COCl)₂ (0.95 mL, 10.9 mmol), and the mixture was stirred for 15 min at the same temperature. A solution of **8** (1.35 g, 6.07 mmol) in CH₂Cl₂ (20 mL) was introduced to the resulting mixture. After stirring for additional 15 min, Et₃N (4.2 mL, 30.4 mmol) was added, and the mixture was allowed to warm to room temperature. The reaction mixture was diluted with ether, then washed with water and brine. After concentration, the residual crude aldehyde was used for next reaction without purification.

To a stirring mixture of anhydrous zinc bromide (1.5 g, 6.70 mmol) in ether (30 mL) at 0 °C were added the alcohol obtained above in ether (30 mL) and EtMgBr (1.0 M in ether, 36 mL, 36 mmol). After stirring for 2 h at the same temperature, the mixture was quenched with saturated NH₄Cl and extracted with ether. The organic layer was washed with saturated NaHCO₃ and brine. Concentration and chromatography (hexane/AcOEt=2:1) gave **9** (1.3 g, 86%): oil; *R*_f=0.57 (hexane/AcOEt=2:1); [α]_D²¹=-17.4 (*c* 0.99, CHCl₃); IR (neat) 3600–3200, 1463 cm⁻¹; ¹H NMR (400 MHz, CDCl₃) δ 7.25 (d, *J*=8.5 Hz, 2H), 6.87 (d, *J*=8.5 Hz, 2H), 5.85 (ddd, *J*=16.3, 10.0, 7.1 Hz, 1H), 5.15–5.06 (m, 2H), 4.62 (d, *J*=11.0 Hz, 1H), 4.41 (d, *J*=11.0 Hz, 1H), 3.79 (s, 3H), 3.44 (ddd, *J*=13.4, 5.1, 5.1 Hz, 1H), 3.32 (dd, *J*=11.1, 5.5 Hz, 1H), 2.49–2.29 (m, 3H), 1.60–1.38 (m, 2H), 0.95 (t, *J*=7.4 Hz, 3H); ¹³C NMR (100 MHz, CDCl₃) δ 159.1, 134.3, 130.4, 129.3, 117.2, 113.7, 80.8, 73.7, 71.8, 55.2, 34.9, 26.2, 10.1; HRMS (ESI), calcd for C₁₅H₂₂O₃Na (M+Na): 273.1461. Found: 273.1467.

4.1.7. Ester 11. To a solution of **10** (2.29 g, 8.06 mmol) in methanol (80 mL) at 0 °C were added KOH (6.78 g, 120 mmol) in water (40 mL) and AgNO₃ (13.7 g, 80.6 mmol) in water (40 mL). After stirring for 20 min at the same temperature, the insoluble material was filtered off through a Celite pad. The filtrate was acidified by 10% H₂SO₄ and extracted with EtOAc. The organic layer was washed with brine and concentrated to give the crude carboxylic acid which was used for next reaction without purification.

To a solution of the carboxylic acid obtained above in THF (80 mL) were added Et₃N (1.12 mL, 8.06 mmol) and 2,4,6-trichlorobenzoyl chloride (1.26 mL, 8.06 mmol). After stirring for overnight, the mixture was concentrated under

reduced pressures and diluted with toluene (80 mL). A solution of **9** (437 mg, 1.05 mmol) and DMAP (4.0 g, 32.2 mmol) in toluene (80 mL) was added, and the mixture was stirred for 3 h at room temperature. The mixture was diluted with ether, then washed with aqueous NH_4Cl , water, and brine. Concentration and chromatography (hexane/EtOAc, 10:1) gave **11** (2.76 g, 77%): oil; $R_f=0.69$ (hexane/AcOEt=2:1); $[\alpha]_D^{25}=-17.4$ (c 0.97, CHCl_3); IR (neat) 1744 cm^{-1} ; $^1\text{H NMR}$ (400 MHz, CDCl_3) δ 7.33–7.23 (m, 12H), 6.83 (d, $J=8.8$ Hz, 2H), 5.82 (dddd, $J=17.1, 10.0, 7.1, 7.1$ Hz, 1H), 5.11–4.95 (m, 2H), 4.68 (d, $J=11.5$ Hz, 1H), 4.58–4.40 (m, 4H), 4.32 (d, $J=11.5$ Hz), 4.16 (dd, $J=10.7, 6.1$ Hz, 1H), 3.75 (s, 3H), 3.66–3.54 (m, 3H), 3.50 (dd, $J=10.7, 6.1$ Hz, 1H), 2.29 (dd, $J=6.8, 6.3$ Hz, 2H), 2.18–1.95 (m, 2H), 1.74–1.53 (m, 2H), 0.86 (t, 3H)HH; $^{13}\text{C NMR}$ (100 MHz, CDCl_3) δ 172.3, 159.0, 138.2, 137.4, 134.9, 134.3, 132.3, 130.2, 129.2, 128.2, 128.0, 127.9, 127.6, 127.4, 117.2, 113.6, 78.1, 75.9, 74.9, 72.9, 72.3, 71.6, 65.8, 55.2, 34.4, 33.2, 22.6, 10.1; HRMS (ESI), calcd for $\text{C}_{33}\text{H}_{40}\text{O}_6\text{Na}$ (M+Na): 555.2723. Found: 555.2705.

4.1.8. TIPS Ether 12. To a solution of **11** (16.8 mg, 38 μmol) in CH_2Cl_2 (0.4 mL) at 0°C were added saturated NaHCO_3 (40 μL) and DDQ (31 mg, 0.13 mmol). After stirring for 5 h at the same temperature, the mixture was diluted with ether, then washed with saturated NaHCO_3 and brine. Concentration and chromatography (hexane/EtOAc, 4:1) gave the corresponding alcohol (11 mg, 91%).

To a solution of the alcohol obtained (9.3 mg, 29 μmol) in CH_2Cl_2 (1 mL) at 0°C were added 2,6-lutidine (7 μL , 58 μmol) and TIPSOTf (11 μL , 41 μmol). After stirring for 4.5 h at room temperature, the mixture was quenched with MeOH, diluted with ether, then washed with water and brine. Concentration and chromatography (hexane/EtOAc, 10:1) gave **12** (12 mg, 89%): oil; $R_f=0.63$ (hexane/AcOEt=4:1); $[\alpha]_D^{25}=-14.3$ (c 1.43, CHCl_3); IR (neat) 1747 cm^{-1} ; $^1\text{H NMR}$ (400 MHz, CDCl_3) δ 7.36–7.23 (m, 10H), 5.85 (dddd, $J=17.1, 10.0, 7.1, 7.1$ Hz, 1H), 5.10–5.00 (m, 2H), 4.88 (ddd, $J=9.3, 3.7, 3.7$ Hz, 1H), 4.73 (d, $J=11.5$ Hz, 1H), 4.48 (d, $J=12.0$ Hz, 1H), 4.42 (d, $J=12.0$ Hz, 1H), 4.37 (d, $J=11.5$ Hz, 1H), 4.15 (dd, $J=9.0, 3.9$ Hz, 1H), 3.97 (dd, $J=10.3, 5.9$ Hz, 1H), 3.69–3.54 (m, 2H), 2.38–1.94 (m, 3H), 1.80 (ddd, $J=14.6, 7.6, 3.3$ Hz, 1H), 1.75–1.50 (m, 2H), 1.16 (m, 2H), 0.89 (t, $J=7.5$ Hz, 1H); $^{13}\text{C NMR}$ (100 MHz, CDCl_3) δ 172.3, 134.8, 128.3, 128.2, 127.9, 127.7, 127.6, 127.5, 117.1, 78.2, 75.1, 73.0, 72.4, 72.2, 65.9, 37.7, 33.3, 21.7, 18.2, 15.4, 12.8, 10.4; HRMS (ESI), calcd for $\text{C}_{34}\text{H}_{52}\text{O}_5\text{SiNa}$ (M+Na): 591.3482. Found: 591.3476.

4.1.9. Diene 14. To a solution of **12** (345 mg, 0.61 mmol) in CH_2Cl_2 (3 mL) at -78°C was added DIBAL-H (0.93 M in hexane, 1.30 mL, 1.21 mmol), and the mixture was stirred for 0.5 h at the same temperature. To the mixture, pyridine (0.15 mL, 1.83 mmol), DMAP (148 mg, 1.21 mmol) in CH_2Cl_2 (1.5 mL), and $(\text{CH}_2\text{ClCO})_2\text{O}$ (626 mg, 3.66 mmol) in CH_2Cl_2 (1.5 mL) were added. After stirring for 1 h at -78°C , the mixture was allowed to warm to room temperature. The mixture was diluted with ether, then washed with saturated potassium sodium tetrates, saturated NaHCO_3 , and brine. Concentration gave the crude α -chloro-

acetoxy ether **13** which was used for next reaction without purification.

To a solution of **13** obtained above in CH_2Cl_2 (6 mL) at -78°C were added allyltributyltin (0.96 mL, 3.10 mmol) and $\text{BF}_3\cdot\text{OEt}_2$ (1.0 M in CH_2Cl_2 , 1.8 mL, 1.8 mmol). After stirring for 3 h at room temperature, the mixture was quenched with Et_3N , diluted with ether, then washed with saturated NaHCO_3 and brine. Concentration and chromatography (hexane/ether, 10:1) gave **14** (230 mg, 64%): oil; $R_f=0.46$ (hexane/AcOEt=10:1); $[\alpha]_D^{25}=+1.0$ (c 1.36, CH_3Cl); IR (neat) 1641 cm^{-1} ; $^1\text{H NMR}$ (400 MHz, CDCl_3) δ 7.34–7.22 (m, 10H), 5.96–5.79 (m, 2H), 5.10–4.99 (m, 4H), 4.69 (d, $J=11.8$ Hz, 1H), 4.49 (d, $J=11.8$ Hz, 1H), 4.45 (d, $J=10.2$ Hz, 1H), 4.42 (d, $J=8.0$ Hz, 1H), 3.95 (dt, $J=8.3, 3.5$ Hz, 1H), 3.71–3.67 (m, 1H), 3.62–3.55 (m, 3H), 3.47 (dt, $J=9.3, 3.2$ Hz, 1H), 2.47–2.06 (m, 4H), 1.93–1.70 (m, 5H), 1.43–1.35 (m, 2H), 1.07–1.00 (m, 2H); $^{13}\text{C NMR}$ (100 MHz, CDCl_3) δ 138.7, 138.4, 136.8, 135.4, 128.1, 128.0, 127.4, 127.3, 127.2, 117.0, 116.0, 84.2, 80.6, 72.7, 72.2, 67.1, 36.2, 36.0, 31.1, 21.8, 18.2, 12.8, 11.7; HRMS (ESI), calcd for $\text{C}_{37}\text{H}_{58}\text{O}_4\text{SiNa}$ (M+Na): 617.4002. Found: 617.3997.

4.1.10. Oxocene 15. To a mixture of **14** (179 mg, 0.303 mmol) in CH_2Cl_2 (60 mL) was added **5** (24 mg, 30 μmol). After stirring for 4 h at 35°C , the mixture was concentrated and purified by silica gel column chromatography (hexane/EtOAc, 10:1) to give **15** (170 mg, 99%): oil; $R_f=0.33$ (hexane/AcOEt, 10:1); $[\alpha]_D^{25}=-15.7$ (c 1.09, CH_3Cl); IR (neat) $3027, 1454\text{ cm}^{-1}$; $^1\text{H NMR}$ (400 MHz, CDCl_3) δ 7.37–7.24 (m, 10H), 5.82–5.65 (m, 2H), 4.81 (d, $J=11.5$ Hz, 1H), 4.59 (d, $J=11.5$ Hz, 1H), 4.48 (d, $J=11.9$ Hz, 1H), 4.42 (d, $J=11.9$ Hz, 1H), 3.91 (ddd, $J=8.8, 5.0, 2.0$ Hz, 1H), 3.77–3.73 (m, 1H), 3.58 (t, $J=7.2$ Hz, 2H), 3.38–3.32 (m, 1H), 3.28 (dd, $J=10.0, 2.6$ Hz), 2.84–2.76 (m, 1H), 2.60–2.52 (m, 1H), 2.27–2.21 (m, 1H), 2.13 (dd, $J=13.9, 8.3$ Hz, 1H), 1.82 (q, $J=6.2$ Hz, 2H), 1.78–1.39 (m, 2H), 1.13–0.87 (m, 2H), 0.90 (t, $J=6.4$ Hz, 3H); $^{13}\text{C NMR}$ (100 MHz, CDCl_3) δ 139.0, 138.5, 130.0, 129.2, 128.2, 128.1, 127.6, 127.4, 127.3, 84.7, 84.3, 79.3, 76.0, 73.0, 72.8, 67.4, 33.9, 32.9, 29.5, 26.1, 18.4, 18.3, 13.2, 12.8, 11.2; HRMS (ESI), calcd for $\text{C}_{35}\text{H}_{54}\text{O}_4\text{SiNa}$ (M+Na): 589.3689. Found: 589.3684.

4.1.11. Acetate 16. Lithium wire (2.3 mg, 330 μmol) was cut into small pieces and added to 10 mL of liquid ammonia at -78°C , and the mixture was stirred for 10 min at the same temperature. To the resulting deep blue mixture, a solution of **15** (19 mg, 33 μmol) was introduced. After stirring for 20 min, the mixture was quenched with a 1:1 mixture of methanol and saturated NH_4Cl . The mixture was extracted with ether, and the organic layer was washed with brine. Concentration and chromatography (hexane/EtOAc, 2:1) gave the corresponding diol (12.8 mg, 100%).

To a solution of the diol obtained (7.5 mg, 19.4 μmol) in CH_2Cl_2 (0.5 mL) were added Ac_2O (11 μL , 116 μmol), pyridine (9.4 μL , 116 μmol), and DMAP (a catalytic amount). After stirring for 16 h, the mixture was concentrated and subjected to a column chromatography (hexane/EtOAc, 10:1 to 4:1) to give **16** (9 mg, 100%): oil; $R_f=0.77$ (hexane/AcOEt, 2:1); $[\alpha]_D^{25}=-12.0$ (c 0.40, CH_3Cl); IR

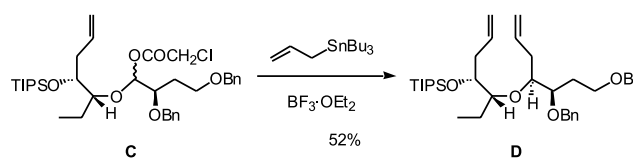
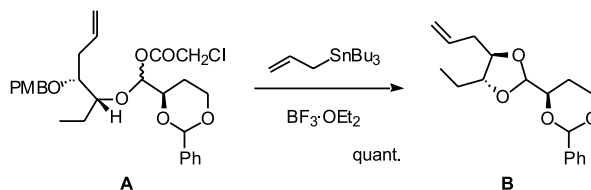
(neat) 2925, 1742 cm^{-1} ; ^1H NMR (500 MHz, C_6D_6) δ 5.61–5.50 (m, 2H), 5.02 (ddd, $J=9.5, 3.4$ Hz, 1H), 4.21–4.01 (m, 2H), 3.79 (ddd, $J=11.0, 4.9, 2.4$ Hz, 1H), 3.34 (dd, $J=10.5, 3.4$ Hz), 3.26–3.22 (m, 1H), 2.84–2.76 (m, 2H), 2.37–1.65 (m, 6H), 1.74 (s, 3H), 1.69 (s, 3H), 1.12–0.94 (m, 21H), 0.96 (t, $J=7.4$ Hz, 3H); ^{13}C NMR (125 MHz, CDCl_3) δ 169.8, 129.6, 129.3, 84.2, 82.5, 76.7, 73.9, 61.0, 34.2, 28.8, 26.5, 20.8, 18.7, 18.6, 18.5, 13.6, 11.1; HRMS (ESI), calcd for $\text{C}_{25}\text{H}_{46}\text{O}_6\text{SiNa}$ (M+Na): 493.2961. Found: 493.2991.

Acknowledgements

This work was financially supported by the Grant-in-Aid for Scientific Research from the Ministry of Education, Culture, Sports, Science and Technology, Japan.

References and notes

- Fukuzawa, A.; Masamune, T. *Tetrahedron Lett.* **1981**, *41*, 4081–4084.
- (a) Irie, T.; Suzuki, M.; Masamune, T. *Tetrahedron Lett.* **1965**, 1091–1099. (b) Irie, T.; Suzuki, M.; Masamune, T. *Tetrahedron Lett.* **1968**, *24*, 4193–4205.
- (a) King, T. J.; Imre, S.; Öztunc, A.; Thomson, R. H. *Tetrahedron Lett.* **1979**, *35*, 1453–1454. (b) Howard, B. M.; Schulte, G. R.; Fenical, W.; Solheim, B.; Clardy, J. *Tetrahedron Lett.* **1980**, *36*, 1747–1751.
- For some examples of the total syntheses of marine medium ring ethers, isolaurepinnacin: (a) Berger, D.; Overman, L. E.; Renhowe, P. A. *J. Am. Chem. Soc.* **1993**, *115*, 9305–9306. (b) Berger, D.; Overman, L. E.; Renhowe, P. A. *J. Am. Chem. Soc.* **1997**, *119*, 2446–2452. Laurencin: (c) Murai, A.; Murase, H.; Matsue, H.; Masamune, T. *Tetrahedron Lett.* **1977**, 2507–2510. (d) Masamune, T.; Matsue, H.; Murase, H. *Bull. Chem. Soc. Jpn* **1979**, *52*, 127–134. (e) Masamune, T.; Murase, H.; Matsue, H.; Murai, A. *Bull. Chem. Soc. Jpn* **1979**, *52*, 135–141. (f) Tsushima, K.; Murai, A. *Tetrahedron Lett.* **1992**, *33*, 4345–4348. (g) Robinson, R. A.; Clark, J. S.; Holmes, A. B. *J. Am. Chem. Soc.* **1993**, *115*, 10400–10401. (h) Bratz, M.; Bullock, W. H.; Overman, L. E.; Takemoto, T. *J. Am. Chem. Soc.* **1995**, *117*, 5958–5966. (i) Burton, J. W.; Clark, J. S.; Derrer, S.; Stork, T. C.; Bendall, J. G.; Holmes, A. B. *J. Am. Chem. Soc.* **1997**, *119*, 7483–7498. (j) Crimmins, M. T.; Emmitte, K. A. *Org. Lett.* **1999**, *1*, 2029–2032. Obtusenyne: (k) Fujiwara, K.; Awakura, D.; Tsunashima, M.; Nakamura, A.; Honma, T.; Murai, A. *J. Org. Chem.* **1999**, *64*, 2616–2617. (l) Crimmins, M. T.; Powell, M. T. *J. Am. Chem. Soc.* **2003**, *125*, 7592–7595. Regioloxepane A: (m) Matsumura, R.; Suzuki, T.; Hagiwara, H.; Hoshi, T.; Anso, M. *Tetrahedron Lett.* **2001**, *42*, 1543–1546. (n) Crimmins, M. T.; DeBaillie, A. C. *Org. Lett.* **2003**, *5*, 3009–3011.
- Kadota, I.; Ohno, A.; Matsuda, K.; Yamamoto, Y. *J. Am. Chem. Soc.* **2002**, *124*, 3562–3566.
- (a) Crimmins, M. T.; Choy, A. L. *J. Org. Chem.* **1997**, *62*, 7548–7549. (b) Crimmins, M. T.; Choy, A. L. *J. Am. Chem. Soc.* **1999**, *121*, 5653–5660. (c) Ref. 4j.
- For a recent review of the synthesis of cyclic ethers via ring-closing metathesis, see: Yet, L. *Chem. Rev.* **2000**, 2963–3007.
- For the stereoselective synthesis of **6**, see: Berger, D.; Overman, L. E. *Synlett* **1992**, 811–813.
- Katzenellenbogen, J. A.; Lenox, R. S. *J. Org. Chem.* **1973**, *38*, 326–335.
- (a) Dahanukar, V. H.; Rychnovsky, S. D. *J. Org. Chem.* **1996**, *61*, 8317–8320. (b) Kopecky, D. J.; Rychnovsky, S. D. *J. Org. Chem.* **2000**, *65*, 191–198. (c) Kopecky, D. J.; Rychnovsky, S. D. *Org. Synth.* **2003**, *80*, 177–183.
- For the intermolecular allylation of α -acetoxy ethers, see Ref. 9a.
- For recent reviews on ring-closing metathesis, see: (a) Grubbs, R.; Miller, S. J.; Fu, G. C. *Acc. Chem. Res.* **1995**, *28*, 446–452. (b) Schmalz, H.-G. *Angew. Chem., Int. Ed. Engl.* **1995**, *34*, 1833–1835. (c) Schuster, M.; Bleichert, S. *Angew. Chem., Int. Ed. Engl.* **1997**, *36*, 2036–2056. (d) Grubbs, R.; Chang, S. *Tetrahedron* **1998**, *54*, 4413–4450. (e) Armstrong, S. K. *J. Chem. Soc., Perkin Trans. 1* **1998**, 371–388.
- (a) Schwab, P.; France, M. B.; Ziller, J. W.; Grubbs, R. H. *Angew. Chem., Int. Ed. Engl.* **1995**, *34*, 2039–2041. (b) Schwab, P.; Grubbs, R. H.; Ziller, J. W. *J. Am. Chem. Soc.* **1996**, *118*, 100–110.
- Crimmins, M. T.; Emmitte, K. A.; Katz, J. D. *Org. Lett.* **2000**, *2*, 2165–2167.
- Asami, M.; Kimura, R. *Chem. Lett.* **1985**, 1221–1222.
- Tadano, K.; Iimura, Y.; Ohmori, T.; Ueno, Y.; Suami, T. *J. Carbohydr. Chem.* **1986**, *5*, 423–435.
- Inanaga, J.; Hirata, K.; Saeki, H.; Katsuki, T.; Yamaguchi, M. *Bull. Chem. Soc. Jpn* **1979**, *52*, 1989–1993.
- In a preliminary experiment, compound A, having a PMB protective group, was treated with allyltributyltin and $\text{BF}_3\cdot\text{OEt}_2$. Unexpectedly, the acetal derivative B was produced via the intramolecular attack of the PMB ether moiety to the resulting oxocarbenium ion. To avoid this undesired reaction, the electron-donating PMB group was replaced by a TIPS group at this stage.
- Kadota, I.; Takamura, H.; Sato, K.; Ohno, A.; Matsuda, K.; Yamamoto, Y. *J. Am. Chem. Soc.* **2003**, *125*, 11893–11899.
- The reaction of the epimeric substrate C gave the diastereoisomer D, selectively (ca. 4:1). These results suggest that the stereoselectivity of the allylation is controlled by the stereochemistry at the β -position.



Synthesis of aziridinomitosenes through base-catalyzed conjugate addition

Kazunari Tsuboike, David J. Guerin, Steven M. Mennen and Scott J. Miller*

Department of Chemistry, Merkert Chemistry Center, Boston College, Chestnut Hill, MA 02467-3860, USA

Received 29 April 2004; revised 27 May 2004; accepted 4 June 2004

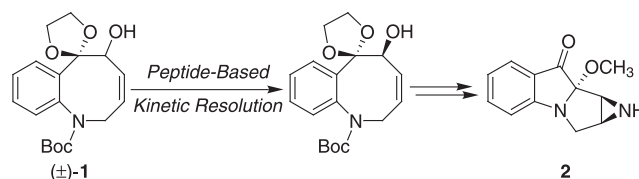
This paper is dedicated to Professor Robert H. Grubbs on the occasion of his receiving the Tetrahedron Prize

Abstract—Synthesis of an aziridinomitosene core structure that relies on a facile tertiary-amine base-catalyzed azide conjugate addition is reported. Straightforward derivatization of the conjugate addition product affords the desired mitomycin ring system. Initial catalyst screens have identified peptides that afford the product with modest enantioselectivities.
© 2004 Elsevier Ltd. All rights reserved.

1. Introduction

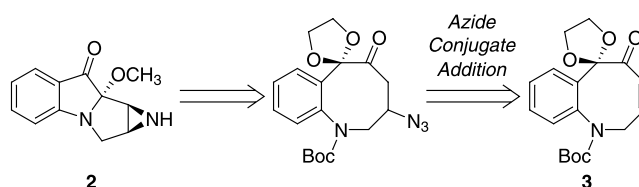
The development of flexible strategies to access biologically relevant classes of molecules is critical for the development of tomorrow's pharmaceuticals. As such, the complex molecular architecture of the mitomycin family of natural products presents a challenge to test the state-of-the-art in synthetic chemistry. In addition, alternative strategies may lead to new possibilities for analog generation, as well as the growing field of diversity-oriented synthesis.¹ Synthetic studies have provided numerous approaches to these and the related FR900482 systems, resulting in total syntheses from the laboratories of Kishi,² Fukuyama,³ Danishefsky,⁴ Martin,⁵ Terashima,⁶ Williams,⁷ Ciufolini⁸ and Rapoport.⁹ Numerous other approaches to various model systems have appeared in the literature as well.¹⁰ Reported herein is the development of a tertiary-amine catalyzed azide conjugate addition approach towards the synthesis of an aziridinomitosene core system. Highlights are the facility of the conjugate addition and efficient conversion to the core system. In addition, we report the results of preliminary attempts to render the sequence enantioselective, employing a peptide-based catalytic, asymmetric azidation strategy.^{11,12}

Recent studies in peptide-based asymmetric acyl transfer led to the synthesis of optically pure mitosane **2**, via a kinetic resolution of racemic allylic alcohol **1** and subsequent conversion to the desired mitosane ring system (Scheme 1).¹³ In search of alternative approaches towards



Scheme 1.

the asymmetric synthesis of mitomycin-like targets not involving a resolution, we were drawn to the possibility of developing a conjugate addition approach involving cyclooctenone **3**, a key intermediate in the synthesis of mitosane **2** (Scheme 2). We proposed that the base-catalyzed conjugate addition of azide¹⁴ to enone **3** could install the nitrogen functionality required for subsequent aziridine formation.



Scheme 2.

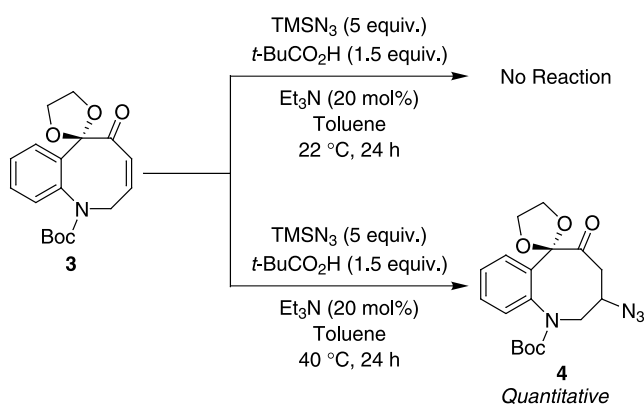
2. Results and discussion

Initial studies were performed to determine if cyclooctenone **3** was a suitable substrate for conjugate addition under the optimized conditions developed previously. However, enone **3** proved to be sluggish towards conjugate addition.

Keywords: Aziridinomitosene; Conjugate addition; Peptide; Organocatalyst.

* Corresponding author. Tel.: +1-6175523620; fax: +1-6175522473; e-mail address: scott.miller.1@bc.edu

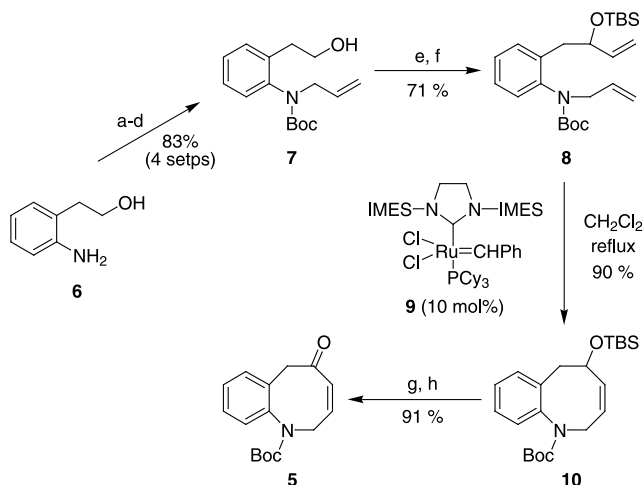
Treatment of **3** with TMSN_3 , $t\text{-BuCO}_2\text{H}$, and Et_3N (20 mol%) did not lead to any of the desired conjugate addition product when the reaction was carried out at ambient temperature (Scheme 3). In fact, careful examination of the X-ray structure of **3** reveals that the carbonyl group and the olefin are twisted approximately 100.4° out of conjugation.¹⁵ This result is also in accordance with the failure of previous efforts to functionalize this system under nucleophilic epoxidation conditions. However, by simply elevating the reaction temperature to 40°C , quantitative conversion to azide **4** was achieved.



Scheme 3.

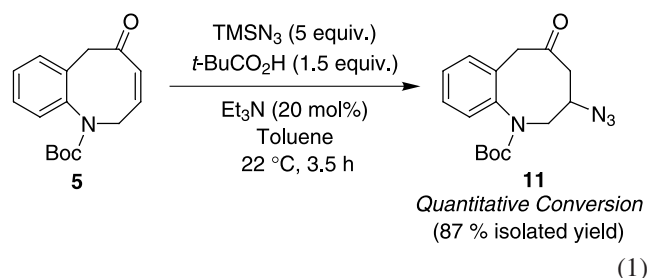
Although efficient conjugate addition could be carried out at elevated reaction temperatures, we desired a room temperature protocol. With this in mind we set out to prepare a more reactive enone substrate that would afford appreciable reactivity at ambient temperatures or below. We postulated that removal of the ketal moiety on enone **3** might lead to a less rigid octacycle **5** (Scheme 4), one whose conformation would allow for the carbonyl and olefin to achieve conjugation at lower temperatures, thereby leading to higher reactivity under conjugate addition conditions.

The synthesis of **5** started from the commercially available



Scheme 4. (a) BOC_2O , NaHCO_3 , dioxane/ H_2O , rt; (b) TBSCl , imid., DMF, rt; (c) allyl bromide, NaH , DMF, 0°C to rt; (d) PPTS , MeOH , rt; (e) $(\text{COCl})_2$, DMSO , Et_3N , THF; then vinyl magnesium bromide -78°C to rt; (f) TBSCl , imid., DMF, rt; (g) PPTS , MeOH , rt; (h) $(\text{COCl})_2$, DMSO , Et_3N , CH_2Cl_2 .

alcohol **6** (Scheme 4). Conversion of the anilinic nitrogen to the BOC-carbamate was achieved using BOC_2O (NaHCO_3 , dioxane/ H_2O). Treatment of the BOC-protected derivative with TBSCl and imidazole affords the corresponding TBS ether. Carbamate N -allylation (NaH , allyl bromide) followed by desilylation using PPTS affords allylated alcohol **7** (83%, four steps). Alcohol **7** was then subjected to a one-pot, two-step Swern oxidation/Grignard addition¹⁶ to afford an intermediate in which the alcohol was protected as its TBS ether to provide **8** in 71% yield (two steps). Ring-closing metathesis of **8** using Ru-alkylidene **9**¹⁷ (CH_2Cl_2 , reflux) affords the known octacycle **10** in 90% yield.^{18,19} Deprotection (PPTS , MeOH) followed by Swern oxidation delivers enone **5** in 91% yield (two steps). Indeed, enone **5** exhibits enhanced reactivity under the azidation conditions in comparison to octacycle **3**. Enone **5**, when treated with TMSN_3 , $t\text{-BuCO}_2\text{H}$, and Et_3N (20 mol%) delivers azide **11** in quantitative conversion (87% isolated yield) after only 3.5 h at 22°C (Eq. 1; cf. quantitative conversion after 24 h at 40°C , Scheme 3). In addition, enone **5** shows appreciable reactivity at temperatures lower than 22°C .



(1)

While our group has been successful in developing peptides for the enantioselective azidation of α,β -unsaturated imide substrates, we felt that it was a likely possibility that an entirely different peptide may turn out to be optimal for enone substrates of general structure **5**. As a starting point, we began our studies with catalysts that had been developed previously for these imide substrates in order to obtain a 'benchmark' to be used for subsequent catalyst development.

Peptide catalyst **12a**, and the rigidified peptide **12b**, were examined under optimized conditions (2.5 mol% peptide, Fig. 1). Peptide **12a** delivers azide **11** in low but measurable ee (12%), while the β -substituted peptide **12b** is slightly more selective, affording product **11** in 21% ee. Knowing that catalysts such as **12** were optimized for a substrate which is significantly different structurally, we sought to examine peptides of different structural types in hopes of increasing selectivity. We thought that enantioselectivity may be increased by developing peptides that incorporate the basic τ -benzyl histidine residue at an internal position, rather than at the N -terminus. We felt that this change may induce a more asymmetric environment around the imidazole moiety, by more effectively surrounding it with the chiral information of the peptide backbone. Peptide **13**, possessing the τ -benzyl histidine residue at the $i+1$ position, is indeed more selective, delivering **11** in 30% ee (22°C). By lowering the reaction temperature, a more selective reaction is achieved whereby **11** is obtained in 35% ee (4°C). Subsequent catalyst development is ongoing in our laboratory. Small peptide libraries (<50 catalysts) based on

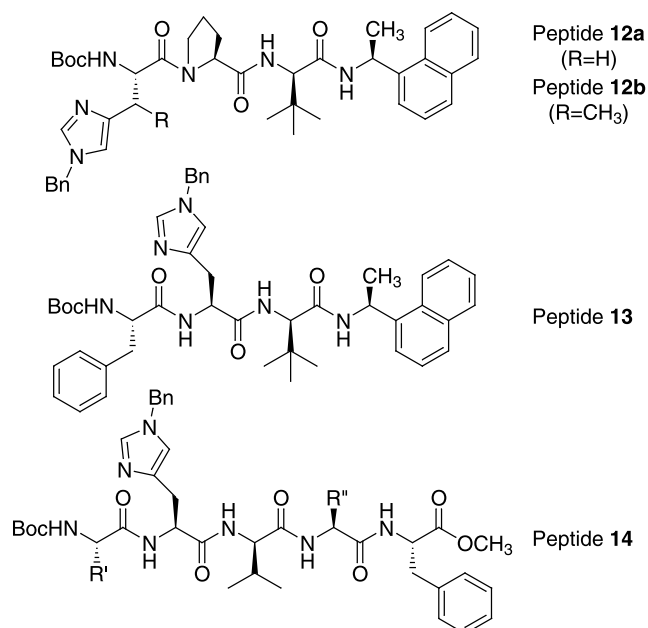
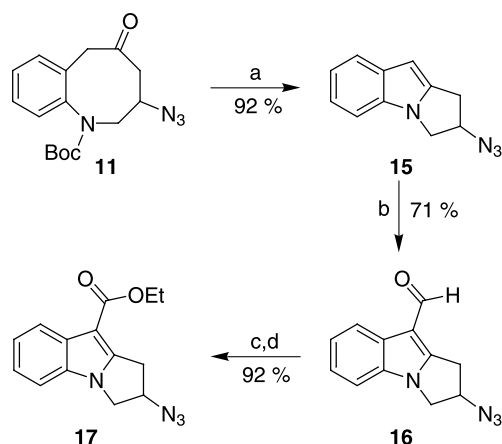


Figure 1. Peptide catalysts used in initial screening.

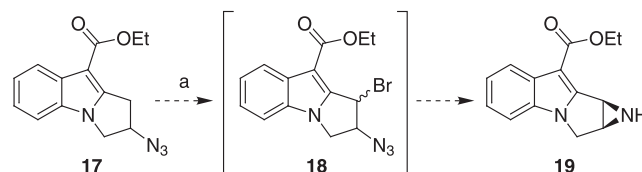
the general structure of peptide **14** were synthesized and screened for enantioselectivity; these catalysts were found to be comparably or less selective than the parent peptide. While these initial results are promising, a better understanding of potential substrate–catalyst interactions will be essential to design more selective catalysts.

With a mild, efficient protocol for the azidation of enone **5** in hand, we turned our attention towards seeing if a synthesis of an aziridinomitosenone was feasible from azide **11** (Scheme 5). Azide **11**, when treated with trifluoroacetic acid (CH₂Cl₂, rt, 5 min) affords indole derivative **15** via a facile tandem deprotection/transannular cyclization/dehydration pathway. Indole **15** was then immediately subjected to Vilsmeier conditions (POCl₃, DMF) to afford aldehyde **16**. Aldehyde **16** was then oxidized (NaClO₂, NaH₂PO₄) to deliver an intermediate acid which was further converted to the corresponding ethyl ester **17** (EtI, *i*-Pr₂NEt) in 92% yield.



Scheme 5. (a) TFA/CH₂Cl₂ 1:1, rt, 5 min; (b) POCl₃, DMF, 0 °C to rt; then aq. NaOAc; (c) NaClO₂, NaH₂PO₄, 2-methyl-2-butene, dioxane/H₂O 0 °C to rt; (d) EtI, Hunig's base, DMF, 50 °C.

We speculated that the required aziridine ring could be constructed via a reductive ring-closure of an azido-bromide intermediate **18** (Scheme 6). However, this reaction sequence turned out to be capricious, and attempts to isolate the desired aziridinomitosenone **19** cleanly met with limited success. This could be due to instability of mitosenone **19** under our conditions, as this is essentially an activated form of a mitomycin core ring system.



Scheme 6. (a) NBS, BPO, benzene, 75 °C, 3 h; then polymer-supported PPh₃, H₂O, Hunig's base, THF, rt.

To circumvent this problem, we decided to install a nitro group on the aromatic ring in an attempt to stabilize the aziridine ring system by decreasing the electron density of the indole moiety. Treatment of azide **17** with copper nitrate (Ac₂O solvent) affords the desired nitrated indole **20** along with regioisomers (regiochemistry of **20** was confirmed by X-ray crystallography, Fig. 2). Indeed, this compound seems to be more stable; bromination of **20** (NBS, cat. benzoyl peroxide) allows the isolation of *trans*-azido bromide **21** after conventional chromatographic purification. Reductive cyclization of **21** under Staudinger conditions (polymer-supported PPh₃, *i*-Pr₂NEt, THF/H₂O)

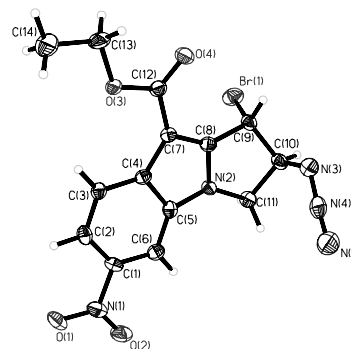
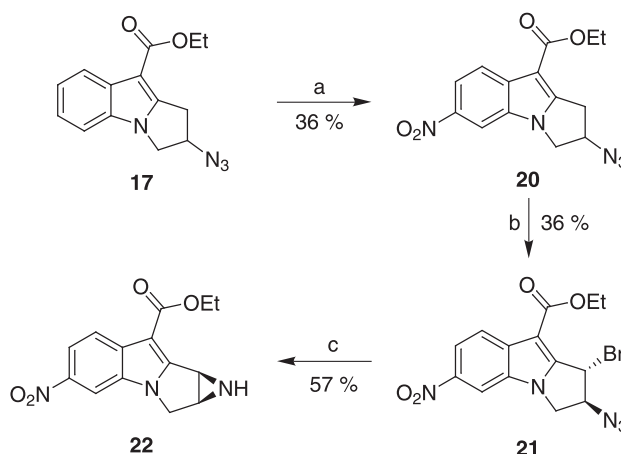


Figure 2. ORTEP drawing for *trans*-azido bromide **21**.



Scheme 7. (a) Cu(NO₃)₂, Ac₂O, -10 °C to rt; (b) NBS, BPO, benzene, 75 °C, 40 h; (c) polymer-supported PPh₃, H₂O, Hunig's base, THF, rt.

provides aziridinomitosenone **22** in 57% isolated yield. The NMR data of **22** is complicated due to slow inversion at the aziridine nitrogen resulting in two sets of the invertomers (Scheme 7).²⁰

3. Conclusions

In summary, we have developed a method to access aziridinomitosenone systems by employing a mild, efficient conjugate addition of azide to an appropriately functionalized eight-membered ring enone substrate. Introduction of the azide functionality allows for rapid entry into mitomycin-like ring systems. Preliminary studies in search of an enantioselective catalyst have identified peptides that afford modest enantioselectivities for this conjugate addition. Studies aimed at developing highly selective peptide catalysts for this transformation are currently underway, for applications in both target- and diversity-oriented synthesis.

4. Experimental

4.1. General

Proton NMR spectra were recorded on Varian 400 or 500 spectrometers. Proton chemical shifts were reported in ppm (δ) relative to internal tetramethylsilane (TMS, δ , 0.0). Spectral data is reported as follows: chemical shift (multiplicity [singlet (s), doublet (d), triplet (t), quartet (q), and multiplet (m)], coupling constants (J) [Hz], integration). Carbon NMR spectra were recorded on a Varian 400 MHz (100 MHz) spectrometer with complete proton decoupling. Carbon chemical shifts are reported in ppm (δ) relative to the residual solvent signal (CDCl₃, δ 77.16). NMR data were collected at 25 °C, unless otherwise indicated. Infrared spectra were obtained on a Perkin–Elmer Spectrum 1000 spectrometer. Analytical thin-layer chromatography (TLC) was performed using Silica Gel 60 F254 pre-coated plates (0.25 mm thickness), TLC R_f values are reported and visualization was accomplished by irradiation with a UV lamp and/or staining with cerium ammonium molybdate (CAM) solutions. Flash column chromatography was performed using Silica Gel 60 Å (40 μ m) from Scientific Adsorbents Inc. High resolution mass spectra were obtained from Mass Spectrometry Facilities of Boston College (Chestnut Hill, MA). The method of ionization is given in parentheses.

All reactions were carried out under a nitrogen atmosphere employing oven- and flame-dried glassware. Solvents were distilled over appropriate drying reagents prior to use.

Caution. Organic azides are potentially explosive compounds and should be handled with great care. However, we encountered no explosive behavior during these studies.

4.2. Preparation of enone 5

4.2.1. Preparation of 6a. The anilinic nitrogen of 2-(2-aminophenyl)ethanol **6** was protected as the BOC-carba-

mate according to the method of Crich.²¹ Protection of the alcohol as its TBS ether **6a** was accomplished using the following procedure. To a solution of 2-(2-((*tert*-butoxycarbonyl)amino)phenyl)ethanol (0.37 g, 1.5 mmol) in anhydrous DMF (5.0 mL) was added imidazole (0.63 g, 9.2 mmol) followed by TBSCl (0.70 g, 4.6 mmol). The reaction was stirred for 18 h, then quenched with aqueous NH₄Cl (10 mL) and partitioned between Et₂O (20 mL) and 10% NH₄Cl (20 mL). The organic layer was washed with aqueous NH₄Cl (2×20 mL), dried over sodium sulfate, filtered and concentrated to an oil that was purified by silica gel chromatography (5% EtOAc/hexane) to provide analytically pure **6a** (quantitative yield).

Data for 6a. ¹H NMR (CDCl₃, 400 MHz) δ 8.07 (br s, 1H), 7.78 (br d, $J=9.6$ Hz, 1H), 7.21 (t, $J=8.0$ Hz, 1H), 7.08 (d, $J=8.0$ Hz, 1H), 7.00 (t, $J=7.2$ Hz, 1H), 3.87 (t, $J=6.0$ Hz, 2H), 2.82 (t, $J=5.6$ Hz, 2H), 1.51 (s, 9H), 0.86 (s, 9H), -0.02 (s, 6H); ¹³C NMR (CDCl₃, 100 MHz) δ 153.3, 137.4, 130.8, 129.9, 126.9, 123.4, 121.9, 79.6, 66.0, 35.5, 28.5, 26.1, 18.5, -5.5; IR (film, cm⁻¹) 3345, 1726; TLC R_f 0.24 (10% EtOAc/hexane). Exact mass calcd for [C₁₉H₃₃NO₃SiNa]⁺ requires m/z 374.2130. Found 374.2127 (ESI).

4.3. Preparation of 6b

To a stirred solution of **6a** (0.54 g, 1.5 mmol) in anhydrous DMF (20 mL) was added allyl bromide (0.40 mL, 4.6 mmol). The solution was cooled to 0 °C (ice bath) and solid NaH (0.059 g, 1.6 mmol) was added slowly in one portion. Vigorous gas evolution ensued, and the resulting reaction mixture was allowed to warm to room temperature and stirred for 3 h. The reaction was quenched with 10% aqueous NH₄Cl (5 mL) and was partitioned between Et₂O (20 mL) and 10% NH₄Cl (20 mL). The organic layer was washed with aqueous NH₄Cl (2×20 mL), dried over sodium sulfate, filtered and concentrated to an oil that was purified by silica gel chromatography (5% EtOAc/hexane) to provide crude product which was carried on without further purification (quantitative yield).

Data for 6b. ¹H NMR (CDCl₃, 400 MHz) not fully coalesced: δ 7.28 (m, 2H), 7.19–7.02 (m, br s, 2H total), 5.93 (complex m, 1H), 5.08 (complex m, 2H), 4.37 (br m, 1H), 3.81 (complex m, 3H), 2.76 (t, $J=7.5$ Hz, 2H), 1.50, 1.32 (br s, 9H total), 0.88 (br s, 9H), 0.03, 0.02 (br s, 6H total); ¹³C NMR (CDCl₃, 100 MHz) major peaks δ 154.6, 136.5, 133.6, 130.0, 128.7, 126.9, 126.5, 117.4, 79.7, 63.3, 53.0, 34.5, 28.4, 26.0, 25.8, 18.4, -5.1; IR (film, cm⁻¹) 1703, 1608, 1583; TLC R_f 0.18 (5% EtOAc/hexane). Exact mass calcd for [C₂₂H₃₇NO₃SiNa]⁺ requires m/z 414.2440. Found 414.2450 (ESI).

4.4. Preparation of 7

To a stirred solution of **6b** (0.60 g, 1.5 mmol) in MeOH (10 mL) was added pyridinium *p*-toluenesulfonate (0.39 g, 1.5 mmol) in one portion. The reaction was stirred for 12 h, and concentrated to a crude oil, which was partitioned between EtOAc (20 mL) and 10% citric acid solution (20 mL). The organic layer was washed with sat. NaHCO₃ (1×20 mL), dried over sodium sulfate, and filtered. Concentration of the filtrate provides crude product that

was purified by silica gel chromatography to afford a clear oil **7** (94% yield).

Data for 7. ^1H NMR (CDCl_3 , 400 MHz) not fully coalesced: δ 7.33–7.03 (br m, s, 4H total), 5.93 (complex m, 1H), 5.11 (br m, 2H), 4.45–4.21 (br m, 1H), 3.88 (br s, 3H), 2.87 (pentet, $J=7.0$ Hz, 1H), 2.78 (br m, 1H), 1.52, 1.34 (br s, 9H total); ^{13}C NMR (CDCl_3 , 100 MHz) major peaks δ 154.7, 141.2, 137.2, 136.2, 133.6, 130.2, 123.0, 128.9, 127.4, 126.9, 117.6, 80.8, 80.2, 62.7, 54.0, 53.1, 34.4, 28.5; IR (film, cm^{-1}) 3440, 1697; TLC R_f 0.35 (30% EtOAc/hexane). Exact mass calcd for $[\text{C}_{16}\text{H}_{23}\text{NO}_3\text{Na}]^+$ requires m/z 300.1570. Found 300.1576 (ESI).

4.5. Preparation of **7a**

Compound **7** was subjected to a one-pot, two step Swern oxidation/Grignard addition sequence according to the method of Martin¹⁶ to afford **7a** after silica gel chromatography (5% EtOAc/hexane, 71% yield).

Data for 7a. ^1H NMR (CDCl_3 , 400 MHz) not fully coalesced: δ 7.42–7.02 (br m, 4H), 6.00–5.86 (overlapping m, 2H), 5.30 (br m, 1H), 5.15–5.06 (br m, 3H), 4.43 (br m, 2H), 4.25–3.50 [4.19 (m), 3.95 (br m), 3.79 (dd, $J=15.4$, 6.6 Hz), 3.57 (m), 3H total], 2.93–2.62 [2.89 (br m), 2.76 (br m), 2.67 (dd, $J=13.6$, 8.8 Hz), 3H total], 1.51, 1.34 (br s, 9H total); ^{13}C NMR (CDCl_3 , 100 MHz) major peaks δ 155.0, 141.4, 140.5, 136.6, 135.6, 133.5, 130.2, 129.3, 128.4, 127.3, 117.7, 114.6, 113.8, 81.2, 80.4, 73.2, 72.0, 54.2, 53.2, 39.3, 39.0, 28.5; IR (film, cm^{-1}) 3465, 1709, 1600, 1579; TLC R_f 0.31 (20% EtOAc/hexane). Exact mass calcd for $[\text{C}_{18}\text{H}_{25}\text{NO}_3\text{Na}]^+$ requires m/z 326.1735. Found 326.1732 (ESI).

4.5.1. Preparation of 8. TBS protection of substrate **7a** was performed in an analogous manner to that described above to afford **8** which was purified by silica gel chromatography (5% EtOAc/hexane, quantitative). Structural characterization for this compound has been reported previously by Grubbs and Miller.¹⁸

4.5.2. Preparation of 10. To a solution of **8** (0.19 g, 0.45 mmol) in CH_2Cl_2 (130 mL) was added ruthenium catalyst **9** (0.038 g, 0.045 mmol) in one portion. The solution was heated under reflux for 24 h. The reaction was cooled to room temperature, then concentrated to a crude oil that was purified by silica gel chromatography (5% EtOAc/hexane) to give the known octacycle **10** in 90% yield.¹⁸

4.5.3. Preparation of 10a. TBS ether cleavage of substrate **10** followed the same procedure using pyridinium *p*-toluenesulfonate as described above to afford **10a**, which was carried on without further purification (quantitative).

Data for 10a. ^1H NMR (CDCl_3 , 400 MHz) not fully coalesced: δ 7.27–7.16 (m, 3H), 7.05 (br s, 1H), 5.53 (br m, 1H), 5.29 (br m, 1H), 5.02 (br m, 1H), 3.86–3.40 [3.80 (br m), 3.60 (br m), 3.46 (br m), 3H total], 1.90 (br s, 1H), 1.53, 1.35 (br s, 9H total); ^{13}C NMR (CDCl_3 , 100 MHz) major peaks δ 154.5, 139.3, 138.0, 135.7, 130.7, 128.2, 127.5, 127.2, 124.0, 80.3, 67.5, 48.6, 42.7, 28.6; IR (film,

cm^{-1}) 3427, 1701, 1601, 1580; TLC R_f 0.26 (20% EtOAc/hexane). Exact mass calcd for $[\text{C}_{16}\text{H}_{21}\text{NO}_3\text{Na}]^+$ requires m/z 298.1420. Found 298.1419 (ESI).

4.6. Preparation of enone **5**

To a stirred solution of $(\text{COCl})_2$ (0.059 g, 0.45 mmol) in anhydrous CH_2Cl_2 (2.5 mL) was added DMSO (0.076 g, 0.97 mmol) at -78°C . The reaction was stirred for 15 min at -78°C , upon which was added a solution of substrate **10a** (0.11 g, 0.39 mmol) in CH_2Cl_2 (1.3 mL) via cannula (followed by a rinse 2×0.50 mL CH_2Cl_2). The reaction was stirred at -78°C for an additional 15 min, followed by the addition of Et_3N (0.32 g, 3.1 mmol) dropwise. The reaction mixture was allowed to warm to room temperature, then partitioned between CH_2Cl_2 (20 mL) and sat. NaHCO_3 (20 mL). The organic layer was then dried over sodium sulfate, filtered, and concentrated to a crude oil that was purified by silica gel chromatography to afford enone **7** in 91% yield.

Data for 5. ^1H NMR (CDCl_3 , 400 MHz) not fully coalesced: δ 7.31 (br pentet, $J=7.6$ Hz, 2H), 7.26 (br t, $J=8.0$ Hz, 1H), 7.16 (br s, 1H), 5.88 (br d, $J=12.4$ Hz, 1H), 5.68 (br m, 1H), 4.37 (br m, 1H), 3.81 (br m, 3H), 1.49, 1.34 (br s, 9H total); ^{13}C NMR (CDCl_3 , 100 MHz) major peaks δ 203.8, 153.9, 140.2, 135.6, 132.4, 129.9, 129.0, 128.9, 128.3, 127.4, 81.2, 50.7, 48.4, 28.6; IR (film, cm^{-1}) 1702, 1501; TLC R_f 0.24 (20% EtOAc/hexane). Exact mass calcd for $[\text{C}_{16}\text{H}_{19}\text{NO}_3\text{Na}]^+$ requires m/z 296.1267. Found 296.1263 (ESI).

4.7. Conversion of enone **5** to ester **17**

4.7.1. Preparation of azide 11. To a stirred solution of enone **7** (0.023 g, 0.084 mmol) in anhydrous toluene (0.50 mL) was added azidotrimethylsilane (0.048 g, 0.42 mmol) dropwise, followed by solid trimethyl acetic acid (0.013 g, 0.13 mmol). To this was added a stock solution of Et_3N in CH_2Cl_2 (0.050 mL, 0.017 mmol). The reaction was allowed to stir at room temperature for 3.5 h, upon which TLC indicated reaction was complete. The crude reaction mixture was applied directly to a short silica gel plug, and filtered using 50% EtOAc/hexane as the eluent. Concentration of the filtrate delivers azide **11** in 87% yield.

Data for 11. ^1H NMR (CDCl_3 , 400 MHz) not fully coalesced: δ 7.33 (br pentet, $J=7.8$ Hz, 2H), 7.22 (m, 1H), 7.13 (d, $J=7.2$ Hz, 1H), 4.40 (br m, 1H), 4.26 (br m, 1H), 3.79 (dd, $J=37.0$, 18.0 Hz, 1H), 3.59 (d, $J=18.0$ Hz, 1H), 2.91–2.64 [2.87 (br t, $J=4.4$ Hz), 2.71 (m), 2H total], 2.46 (br d, $J=12.0$ Hz, 1H), 1.32, 1.24 (s, 9H total); ^{13}C NMR (CDCl_3 , 100 MHz) major peaks δ 204.0, 134.5, 130.3, 130.1, 129.2, 129.0, 128.3, 128.1, 127.6, 60.3, 54.0, 48.9, 42.9, 28.3, 27.1; IR (film, cm^{-1}) 2112, 1709; TLC R_f 0.45 (20% EtOAc/hexane). Exact mass calcd for $[\text{C}_{16}\text{H}_{20}\text{N}_4\text{O}_3\text{Na}]^+$ requires m/z 339.1418. Found 339.1433 (ESI).

4.8. Preparation of indole **15**

To a stirred solution of azide **11** (0.12 g, 0.38 mmol) in

CH₂Cl₂ (1.0 mL) was added trifluoroacetic acid (1.0 mL). The reaction mixture was allowed to stir at room temperature for no more than 5 min. During this time, the solution changed from colorless to a dark purple solution. The reaction was slowly quenched with sat. NaHCO₃ until gas evolution ceased, and the aqueous layer was pH 8 (pH paper). The organic layer was dried over sodium sulfate, filtered, and concentrated to an oil that solidified on high vacuum to give indole derivative **15** (92% yield) that was carried on immediately to the next step (product begins to slowly decompose at room temperature).

Data for 15. ¹H NMR (CDCl₃, 400 MHz) δ 7.56 (d, *J*=8.0 Hz, 1H), 7.23 (d, *J*=8.0 Hz, 1H), 7.15 (t, *J*=7.2 Hz, 1H), 7.09 (t, *J*=7.2 Hz, 1H), 6.24 (s, 1H), 4.77 (septet, *J*=4.0 Hz, 1H), 4.33 (dd, *J*=10.8, 6.6 Hz, 1H), 4.06 (dd, *J*=10.8, 4.0 Hz, 1H), 3.40 (dd, *J*=16.8, 7.2 Hz, 1H), 3.13 (dd, *J*=16.8, 4.2 Hz, 1H); ¹³C NMR (CDCl₃, 100 MHz) δ 140.1, 132.6, 132.4, 120.6, 120.4, 119.4, 109.2, 93.8, 63.0, 49.3, 31.4; IR (film, cm⁻¹) 2106, 1709; TLC *R*_f 0.60 (20% EtOAc/hexane). Exact mass calcd for [C₁₁H₁₀N₄Na]⁺ requires *m/z* 221.0806. Found 221.0803 (ESI).

4.9. Preparation of aldehyde 16

To a stirred round-bottom flask containing anhydrous DMF (0.44 mL) under nitrogen was added POCl₃ (0.18 g, 1.2 mmol) dropwise at 0 °C. Let stir for 30 min at 0 °C. To this was added a solution of substrate **15** in CH₂Cl₂/pyridine (4:1, 2.8 mL) by cannula (followed by a rinse of the same solvent, 3×0.70 mL). The reaction was allowed to slowly warm to room temperature and stirred for an additional 5 h. The reaction was then quenched with aqueous sat. NaOAc (10 mL) at 0 °C, and stirred for 12 h. The reaction mixture was then partitioned between CH₂Cl₂ (30 mL) and brine (30 mL). The organic layer was dried over sodium sulfate, filtered, and concentrated to a crude oil which was purified by silica gel chromatography (30% EtOAc/hexane) to deliver **16** as a reddish solid (71% yield), that was immediately carried on to the next step.

Data for 16. ¹H NMR (CDCl₃, 400 MHz) δ 10.0 (s, 1H), 8.19 (br d, *J*=7.2 Hz, 1H), 7.33–7.27 (m, 3H), 4.94 (septet, *J*=3.6 Hz, 1H), 4.38 (dd, *J*=11.0, 6.4 Hz, 1H), 4.13 (dd, *J*=11.4, 3.8 Hz, 1H), 3.65 (dd, *J*=18.4, 7.2 Hz, 1H), 3.42 (dd, *J*=18.0, 3.6 Hz, 1H); ¹³C NMR (CDCl₃, 100 MHz) δ 182.9, 150.8, 132.7, 129.2, 123.1, 122.8, 121.1, 110.7, 109.9, 62.4, 50.3, 31.8; IR (film, cm⁻¹) 2099, 1659; TLC *R*_f 0.41 (50% EtOAc/hexane). Exact mass calcd for [C₁₂H₁₀N₄O₂Na]⁺ requires *m/z* 249.0760. Found 249.0752 (ESI).

4.9.1. Preparation of acid 16a. To a stirred suspension of **16** (0.15 g, 0.67 mmol) in dioxane (13 mL) and 2-methyl-2-butene (1.0 mL) was added a solution of NaClO₂ (0.54 g) and NaH₂PO₄ (0.54 g) in H₂O (5.0 mL) over 10 min at 0 °C. The reaction was warmed to room temperature, and stirred for an additional 5 h. The reaction mixture was then charged with an additional 0.34 g each of NaClO₂ and NaH₂PO₄, and stirred for an additional 12 h at room temperature. The reaction mixture was partitioned between aqueous 5% NaOH (40 mL) and CH₂Cl₂ (40 mL). The aqueous layer was washed with CH₂Cl₂ (2×20 mL). The combined

organic extracts were then washed with 10% citric acid solution, which was then immediately extracted with copious amounts of CH₂Cl₂. The combined organic extracts were dried over sodium sulfate, filtered, and concentrated to afford a crude solid **16a** that was used to the next step without further purification.

4.9.2. Preparation of ester 17. To a stirred solution of **16a** (0.050 g, 0.21 mmol) in anhydrous DMF (1.0 mL) was added Hunig's base (0.13 g, 1.0 mmol) and ethyl iodide (0.16 g, 1.0 mmol). The reaction was heated at 50 °C for 24 h. The reaction was then cooled to room temperature, and partitioned between 10% NH₄Cl and Et₂O. The organic layer was washed with additional 10% NH₄Cl, dried over sodium sulfate, filtered, and concentrated to a crude solid that was purified by silica gel chromatography (20% EtOAc/hexane) to deliver **17** in 92% yield.

Data for 17. ¹H NMR (CDCl₃, 400 MHz) δ 8.17 (m, 1H), 7.32–7.28 (m, 3H), 4.89 (septet, *J*=3.6 Hz, 1H), 4.42 (q, *J*=13.2, 7.6 Hz, 2H), 4.39 (dd, *J*=11.8, 6.8 Hz, 1H), 4.14 (dd, *J*=11.2, 3.6 Hz, 1H), 3.68 (dd, *J*=18.2, 7.0 Hz, 1H), 3.47 (dd, *J*=17.8, 3.8 Hz, 1H), 1.47 (t, *J*=7.0 Hz, 3H); ¹³C NMR (CDCl₃, 100 MHz) δ 164.7, 148.2, 146.9, 132.4, 130.3, 122.1, 121.7, 121.4, 109.6, 62.3, 59.5, 50.3, 33.3, 14.7; IR (film, cm⁻¹) 2099, 1690; TLC *R*_f 0.33 (20% EtOAc/hexane). Exact mass calcd for [C₁₄H₁₄N₄O₂Na]⁺ requires *m/z* 293.1014. Found 293.1004 (ESI).

4.9.3. Synthesis of peptides. Peptide catalysts were prepared employing standard solution phase coupling techniques, utilizing commercially available amino acid derivatives with EDC (1-(3-dimethylaminopropyl)-3-ethylcarbodiimidehydrochloride) as the coupling agent and HOBt (1-hydroxybenzotriazole) as a racemization suppressant. The resulting peptides were then purified by silica gel flash column chromatography (2–5% MeOH/CH₂Cl₂).

Data for 12a,b. Characterization data for these compounds has been reported previously.¹¹

Data for 13. ¹H NMR (CDCl₃, 400 MHz) δ 8.08 (d, *J*=8.5 Hz, 1H), 7.81 (br m, 1H), 7.77 (d, *J*=8.0 Hz, 1H), 7.71 (d, *J*=7.9 Hz, 1H), 7.55 (br m, 1H), 7.51–7.36 (m, 5H), 7.29–7.26 (m, 2H), 7.21–7.06 (m, 5H), 7.01 (br s, 1H), 6.94 (br m, 1H), 6.82 (br m, 1H), 6.32 (br s, 1H), 5.92 (pentet, *J*=7.0 Hz), 4.97 (br m, 1H), 4.71 (d, *J*=15.0 Hz, 1H), 4.60–4.51 (br m, 2H), 4.43 (br m, 1H), 4.21 (d, *J*=8.7 Hz, 1H), 3.01–2.98 (br m, 2H), 2.90 (dd, *J*=7.6, 13.9 Hz, 1H), 2.76 (dd, *J*=7.0, 14.8 Hz, 1H), 1.58 (d, *J*=6.7 Hz, 3H); ¹³C NMR (CDCl₃, 100 MHz) δ 170.9, 170.8, 169.0, 155.1, 138.9, 137.6, 136.5, 136.2, 135.6, 133.7, 130.8, 129.2, 128.8, 128.6, 128.3, 128.1, 127.9, 127.3, 126.6, 126.2, 125.6, 125.2, 123.3, 122.5, 117.2, 79.8, 61.4, 55.4, 53.6, 50.7, 44.8, 38.9, 34.7, 31.0, 28.5, 27.0, 21.7; IR (film, cm⁻¹) 3298, 2973, 1698, 1674, 1660, 1638; TLC *R*_f 0.25 (5% MeOH/CH₂Cl₂). Exact mass calcd for [C₄₅H₅₄N₆O₅Na]⁺ requires *m/z* 781.4053. Found 781.4051 (ESI).

4.10. Conversion of ester 17 to aziridinomitosenone 22

4.10.1. Preparation of nitrated indole 20. To a stirred solution of **17** (0.050 g, 0.185 mmol) in anhydrous Ac₂O

(1.8 mL) was added cupric nitrate (0.045 g, 0.185 mmol) at $-10\text{ }^{\circ}\text{C}$. The reaction was allowed to slowly warm to room temperature and stirred for 16 h. The reaction mixture was partitioned between sat. NaHCO_3 (20 mL) and EtOAc (40 mL). The aqueous layer was extracted with EtOAc (2 \times 15 mL). The combined organic extracts were dried over sodium sulfate, filtered, and concentrated to a crude mixture of nitrated compounds that was purified by silica gel chromatography (20% EtOAc/hexane) to afford nitrated indole **20** in 36% yield. Recrystallization from Et_2O gave an analytical sample.

Data for 20. ^1H NMR (CDCl_3 , 400 MHz) δ 8.23 (d, $J=2.0$ Hz, 1H), 8.20 (d, $J=8.9$ Hz, 1H), 8.14 (dd, $J=2.0$, 8.9 Hz, 1H), 4.95 (septet, $J=3.3$ Hz, 1H), 4.46 (dd, $J=6.4$, 11.4 Hz, 1H), 4.40 (q, $J=7.1$ Hz, 2H), 4.22 (dd, $J=3.2$, 11.4 Hz, 1H), 3.70 (dd, $J=7.0$, 18.4 Hz, 1H), 3.50 (dd, $J=3.6$, 18.4 Hz, 1H), 1.44 (t, $J=7.1$ Hz, 3H); ^{13}C NMR (CDCl_3 , 100 MHz) δ 163.9, 153.4, 143.1, 135.2, 131.2, 121.5, 117.1, 106.6, 102.0, 62.4, 60.3, 51.2, 34.0, 14.8; IR (film, cm^{-1}) 2114, 1692, 1513, 1337; TLC R_f 0.49 (50% EtOAc/hexane). Exact mass calcd for $[\text{C}_{14}\text{H}_{13}\text{N}_5\text{O}_4\text{Na}]^+$ requires m/z 338.0865. Found 338.0861 (ESI).

4.10.2. Preparation of bromide 21. To a stirred solution of **20** (0.074 g, 0.235 mmol) in anhydrous benzene (6.0 mL) was added *N*-bromosuccinimide (0.125 g, 0.705 mmol) followed by a catalytic amount of benzoyl peroxide. The reaction was heated at $75\text{ }^{\circ}\text{C}$ for 17.5 h. An additional catalytic amount of benzoyl peroxide was added and the reaction was heated at $75\text{ }^{\circ}\text{C}$ for an additional 13.5 h. The reaction mixture was then charged with an additional 0.042 g of *N*-bromosuccinimide and a catalytic amount of benzoyl peroxide, and heated at $75\text{ }^{\circ}\text{C}$ for an additional 8.5 h. The reaction was cooled to room temperature, and partitioned between sat. NaHCO_3 (40 mL) and CH_2Cl_2 (30 mL). The aqueous layer was extracted with CH_2Cl_2 (2 \times 15 mL). The combined organic extracts were dried over sodium sulfate, filtered, and concentrated to a crude product that was purified by silica gel chromatography to afford bromide **21** in 36% yield. Recrystallization from hexane/EtOAc gave an analytical sample for X-ray crystallographic analysis.

Data for 21. ^1H NMR (CDCl_3 , 400 MHz) δ 8.30 (d, $J=2.0$ Hz, 1H), 8.27 (d, $J=9.0$ Hz, 1H), 8.17 (dd, $J=2.0$, 9.0 Hz, 1H), 5.60 (s, 1H), 5.04 (d, $J=4.4$ Hz, 1H), 4.64 (dd, $J=4.4$, 11.8 Hz, 1H), 4.51 (qd, $J=7.1$, 10.8 Hz, 1H), 4.41 (qd, $J=7.1$, 10.8 Hz, 1H), 4.28 (d, $J=11.8$ Hz, 1H), 1.49 (t, $J=7.1$ Hz, 3H); ^{13}C NMR (CDCl_3 , 100 MHz) δ 162.9, 150.6, 144.3, 135.0, 131.4, 122.9, 117.7, 107.2, 103.2, 71.6, 60.8, 49.7, 42.1, 14.8; IR (film, cm^{-1}) 2114, 1703, 1515, 1344; TLC R_f 0.22 (20% EtOAc/hexane). Exact mass calcd for $[\text{C}_{14}\text{H}_{12}\text{N}_5\text{O}_4\text{BrNa}]^+$ requires m/z 415.9970. Found 415.9974 (ESI).

4.10.3. Preparation of aziridinomitosenone 22. To a stirred solution of **21** (0.033 g, 0.084 mmol) in THF (3.0 mL) and water (0.2 mL) was added polymer-supported PPh₃ (0.054 g, 0.168 mmol) and Hunig's base (0.021 g, 0.168 mmol). The reaction mixture was stirred at room temperature for 4 h. The reaction mixture was applied to a short silica gel plug, filtered using EtOAc as the eluent, and

then concentrated to a crude product that was purified by silica gel chromatography (50% EtOAc/hexane to 80% EtOAc/hexane) to afford aziridinomitosenone **22** in 57% yield.

Data for 22. ^1H NMR (CDCl_3 , 500 MHz) δ 8.16 (br d, $J=8.8$ Hz, 1H), 8.14 (br d, $J=1.7$ Hz, 1H), 8.10 (br d, $J=8.8$ Hz, 1H), 4.44 (qd, $J=7.1$, 10.6 Hz, 1H), 4.42 (qd, $J=7.1$, 10.6 Hz, 1H), 4.33 (br d, $J=10.9$ Hz, 1H), 4.21 (br d, $J=10.9$ Hz, 1H), 4.10 (br s, 0.6H), 3.84 (br s, 0.4H), 3.77 (br s, 0.6H), 3.62 (br s, 0.4H), 1.51 (br s, 0.6H), 1.45 (t, $J=7.1$ Hz, 3H), 0.75 (br s, 0.4H); ^{13}C NMR (CDCl_3 , 100 MHz) δ 163.9, 154.0, 143.4, 134.5, 131.7, 121.9, 117.2, 116.9, 106.2, 60.2, 48.0, 40.4, 38.9, 33.3, 32.8, 14.7; IR (film, cm^{-1}) 1696, 1514, 1342; TLC R_f 0.27 (EtOAc). Exact mass calcd for $[\text{C}_{14}\text{H}_{14}\text{N}_3\text{O}_4]^+$ requires m/z 288.0984. Found 288.0980 (ESI).

Acknowledgements

This research is supported by National Science Foundation (CHE-0236591). In addition, we are grateful to support from Ube Industries, Ltd (Japan) for support of K. T. S. J. M. thanks the Merck Chemistry Council and Pfizer Global Research for support. S. J. M. is a Fellow of the Alfred P. Sloan Foundation and a Camille Dreyfus Teacher-Scholar. The authors wish to thank T. J. Paxton for critical assistance in the preparation of intermediates.

References and notes

- Schreiber, S. L. *Science* **2000**, 287, 1964–1969.
- For a review of the Kishi laboratory's studies, see: Kishi, Y. *J. Nat. Prod.* **1979**, 42, 549–568.
- Mitomycin C: (a) Fukuyama, T.; Yang, L. *J. Am. Chem. Soc.* **1989**, 111, 8303–8304. (b) Fukuyama, T.; Yang, L. *J. Am. Chem. Soc.* **1987**, 109, 7881–7882. (c) Fukuyama, T.; Xu, L.; Goto, S. *J. Am. Chem. Soc.* **1992**, 114, 383–385. (d) Suzuki, M.; Kambe, M.; Tokuyama, H.; Fukuyama, T. *Angew. Chem., Int. Ed.* **2002**, 41, 4686–4688.
- Danishefsky, S. J.; Schkeryantz, J. M. *Synlett* **1995**, 475–490. This paper also provides a thorough bibliography to the mitomycin literature.
- Fellows, I. M.; Kaelin, D. E., Jr.; Martin, S. F. *J. Am. Chem. Soc.* **2000**, 122, 10781–10787.
- (a) Katoh, T.; Itoh, E.; Yoshino, T.; Terashima, S. *Tetrahedron* **1997**, 53, 10229–10238. (b) Yoshino, T.; Nagata, Y.; Itoh, E.; Hashimoto, M.; Katoh, T.; Terashima, S. *Tetrahedron* **1997**, 53, 10239–10252. (c) Katoh, T.; Nagata, Y.; Yoshino, T.; Nakatani, S.; Terashima, S. *Tetrahedron* **1997**, 53, 10253–10270.
- Judd, T. C.; Williams, R. M. *Angew. Chem., Int. Ed.* **2002**, 41, 4683–4685.
- Ducray, R.; Ciufolini, M. A. *Angew. Chem. Int. Ed.* **2002**, 41, 4688–4691.
- Paleo, M. R.; Aurrecoechea, N.; Jung, K.-Y.; Rapoport, H. J. *Org. Chem.* **2003**, 68, 130–138.
- For example, see: (a) Vedejs, E.; Little, J. D.; Seanev, L. M. *J. Org. Chem.* **2004**, 69, 1788–1793. (b) Vedejs, E.; Little, J. D. *J. Org. Chem.* **2004**, 69, 1794–1799. (c) Vedejs, E.; Naidu, B. N.; Klapars, A.; Warner, D. L.; Li, V.-S.; Na, Y.;

- Kohn, H. *J. Am. Chem. Soc.* **2003**, *125*, 15796–15806.
- (d) Vedejs, E.; Little, J. *J. Am. Chem. Soc.* **2002**, *124*, 748–749. (e) Vedejs, E.; Klapars, A.; Naidu, B. N.; Piotrowski, D. W.; Tucci, F. C. *J. Am. Chem. Soc.* **2000**, *122*, 5401–5402. (f) Lee, S.; Lee, W. M.; Sulikowski, G. A. *J. Org. Chem.* **1999**, *64*, 4224–4225. (g) Colandrea, V. J.; Rajaraman, S.; Jimenez, L. S. *Org. Lett.* **2003**, *5*, 785–787. (h) Dong, W.; Jimenez, L. S. *J. Org. Chem.* **1999**, *53*, 2520–2523. (i) Wang, Z.; Jimenez, L. S. *J. Org. Chem.* **1996**, *61*, 816–818. (j) Katoh, T.; Yoshino, T.; Nagata, Y.; Nakatani, S.; Terashima, S. *Tetrahedron Lett.* **1996**, *37*, 3479–3482. (k) Shaw, K. J.; Luly, J. R.; Rapoport, H. *J. Org. Chem.* **1985**, *50*, 4515–4523. (l) Ban, Y.; Nakajima, S.; Yoshida, K.; Mori, M.; Shibasaki, M. *Heterocycles* **1994**, *39*, 657–667. (m) Rebeck, J.; Shaber, S. H.; Shue, Y.-K.; Gehret, J.-C.; Zimmerman, S.; *J. Org. Chem.* **1984**, *49*, 5164–5174.
11. (a) Guerin, D. J.; Miller, S. J. *J. Am. Chem. Soc.* **2002**, *124*, 2134–2136. (b) Horstmann, T. E.; Guerin, D. J.; Miller, S. J. *Angew. Chem., Int. Ed.* **2000**, *39*, 3635–3638.
12. For an alternative metal-catalyzed azide conjugate addition, see: Myers, J. K.; Jacobsen, E. N. *J. Am. Chem. Soc.* **1999**, *121*, 8959–8960.
13. (a) Papaioannou, N.; Evans, C. E.; Blank, J. T.; Miller, S. J. *Org. Lett.* **2001**, *3*, 2879–2882. (b) Papaioannou, N.; Blank, J. T.; Miller, S. J. *J. Org. Chem.* **2003**, *68*, 2728–2734.
14. (a) Guerin, D. J.; Horstmann, T. E.; Miller, S. J. *Org. Lett.* **1999**, *1*, 1107–1109. (b) See also: Lakshmipathi, P.; Rama Rao, A. V. *Tetrahedron Lett.* **1997**, *38*, 2551–2552.
15. See Ref. 13 for the X-ray structure and details.
16. Martin, S. F.; Chen, H.-J.; Courtney, A. K.; Liao, Y.; Patzel, M.; Ramser, M. N.; Wagman, A. S. *Tetrahedron* **1996**, *52*, 7251–7264.
17. Trnka, T. M.; Morgan, J. P.; Sanford, M. S.; Wilhem, T. E.; Scholl, M.; Choi, T.-L.; Ding, D.; Day, M. W.; Grubbs, R. H. *J. Am. Chem. Soc.* **2003**, *125*, 2546–2558.
18. Miller, S. J.; Kim, S.-H.; Chen, Z.-R.; Grubbs, R. H. *J. Am. Chem. Soc.* **1995**, *117*, 2108–2109.
19. For a related example, see: Martin, S. F.; Wagman, A. S. *Tetrahedron Lett.* **1995**, *36*, 1169–1170.
20. Han, I.; Kohn, H. *J. Org. Chem.* **1991**, *56*, 4648–4653.
21. Crich, D.; Hao, X. *J. Org. Chem.* **1997**, *62*, 5982–5988.

ROM-RCM of cycloalkene-yne

Tsuyoshi Kitamura,^a Yuichi Kuzuba,^a Yoshihiro Sato,^a Hideaki Wakamatsu,^b Reiko Fujita^b and Miwako Mori^{a,*}

^aGraduate School of Pharmaceutical Sciences, Hokkaido University, Sapporo 060-0812, Japan

^bTohoku Pharmaceutical University, 4-4-1 Komatsushima, Aoba-ku, Sendai 981-8558, Japan

Received 25 March 2004; revised 12 May 2004; accepted 14 May 2004

Available online 24 June 2004

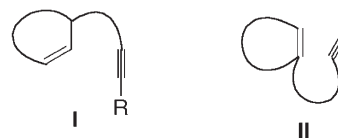
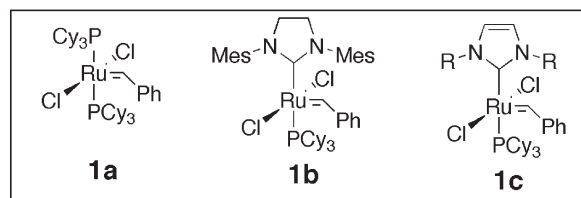
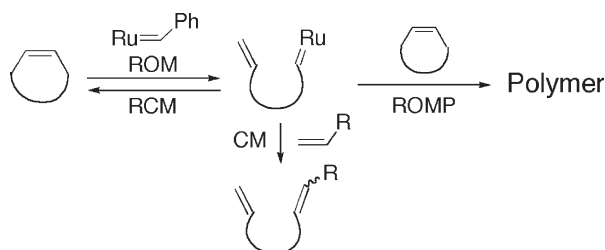
We dedicate this paper to Professor Grubbs on the occasion of his receipt of the Tetrahedron Prize

Abstract—Ring-opening metathesis and ring-closing metathesis (ROM-RCM) of cycloalkene-yne was demonstrated using a first- or second-generation ruthenium complex. When cycloalkenes bearing the alkyne part at the C-3 position were reacted with a first-generation ruthenium–carbene complex under an atmosphere of ethylene, ROM-RCM proceeded smoothly to give skeletal reorganized products in good yields. In this reaction, cycloalkene-yne having terminal alkyne were suitable. On the other hand, when cycloalkenes bearing the alkyne part at the C-1 position were treated with a second-generation ruthenium–carbene complex, ROM-RCM proceeded smoothly to give bicyclic compounds and/or dimeric compounds in good yields.
© 2004 Elsevier Ltd. All rights reserved.

1. Introduction

Transition metals have played an important role in recent synthetic organic chemistry, and they are now important tools for the syntheses of complex molecules, such as natural products and biologically active substances. Olefin metathesis reaction¹ using a metal carbene complex is interesting because formally the carbon–carbon double bonds are cleaved and, at the same time, new carbon–carbon double bonds are formed between the two double bonds. Intramolecular olefin metathesis is a useful methodology in synthetic organic chemistry, since carbocyclic and heterocyclic compounds having various ring sizes can be synthesized. In 1999, second-generation ruthenium–carbene complexes², such as **1b** and **1c**, were developed by Herrmann, Nolan and Grubbs, independently, and metathesis of olefin having substituents could be further developed. On the other hand, intramolecular enyne metathesis^{3–5} is particularly attractive since the double bond of enyne is cleaved and the alkylidene part of alkene migrates to the alkyne carbon to give a cyclized compound having a diene moiety. We have already reported intramolecular enyne metathesis³ using Grubbs' ruthenium carbene complex **1** and the syntheses of five- to nine-membered ring compounds.

The metathesis reaction of cycloalkene did not proceed under the usual reaction conditions, and cyclooctene or norbornene afforded a polymer via ring opening polymerization (ROMP). Recently, ring-opening metathesis of cycloalkene followed by cross-metathesis (ROM-CM⁶) with olefin has been developed.



Scheme 1. Metathesis reaction of alkene.

Keywords: Enyne metathesis; Ring-opening metathesis and ring-closing metathesis; ROM-RCM; Cycloalkene-yne; Pyrrole derivative; Ethylene.

* Corresponding author. Tel./fax: +81-11-706-4982;

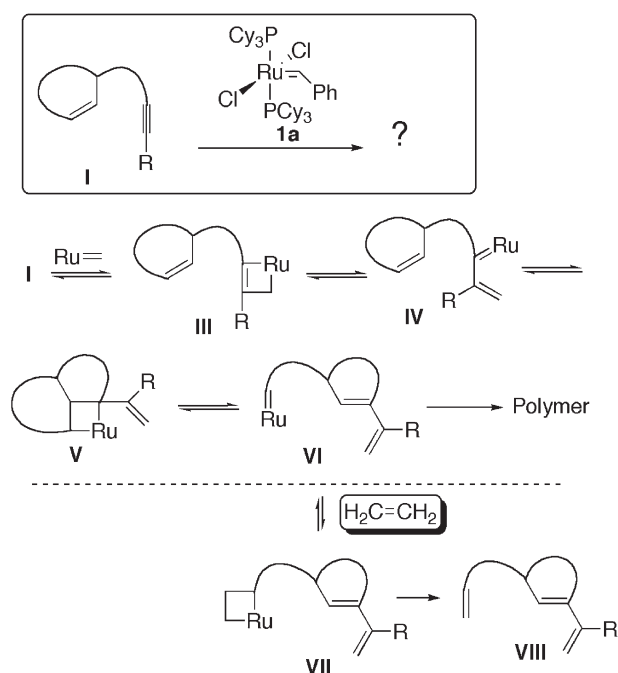
e-mail address: mori@pharm.hokudai.ac.jp

Ring-opening metathesis and ring-closing metathesis⁷ (ROM-RCM) of cycloalkene-yne is also very attractive, but there have been few reports on ROM-RCM in the literature.⁸ Herein, we describe in detail of ROM-RCM of cycloalkene-yne **1** and **II** using ruthenium–carbene complex **1** (Scheme 1).^{3a,b}

2. Results and discussion

2.1. Metathesis of cycloalkene having alkyne in a tether at the C-3 position

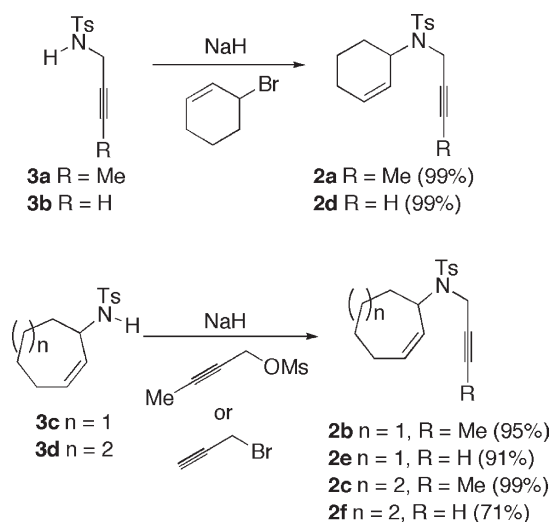
Metathesis of cycloalkene-yne, whose tether having an alkyne part is connected to the C-3 position of cycloalkene, was investigated. If the alkyne part of substrate **I** reacts with a ruthenium complex, ruthenacyclobutene **III** should be formed and it would be converted into ruthenium–carbene complex **IV** by ring-opening. Then, if this carbene complex **IV** reacts with a cycloalkene part intramolecularly, highly strained ruthenium complex **V** would be formed and it should be converted into **VI**. However, this ruthenium carbene complex **VI** cannot react with the diene moiety intramolecularly and would react with another molecule **I** to give a polymer (Scheme 2).



Scheme 2. Our plan for ROM-RCM of cycloalkene-yne **I**.

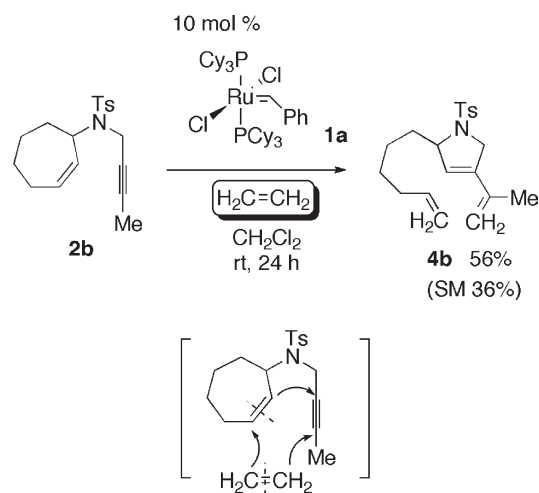
However, if this reaction were carried out under an atmosphere of ethylene,^{3f,9} ruthenium complex **VI** would react with ethylene to give ring-opening metathesis product **VIII** via ruthenacyclobutane **VII**. The chain lengths of the tethers in the products **VIII** would be dependent on the ring-size of cycloalkene.

To examine our plan, various cycloalkene-yne **2** were prepared as shown in Scheme 3. N-Alkylation of *N*-2-butynyl- or *N*-propargyl-*N*-tosylamide **3a** and **3b** with 3-bromocyclohexene gave cyclohexene-yne **2a** and **2d** in



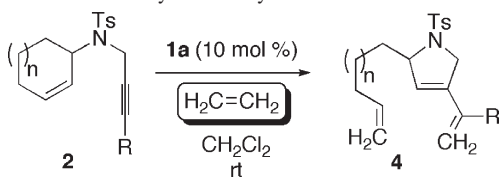
Scheme 3. Synthesis cycloalkene-yne **2**.

quantitative yields. *N*-Alkylation of *N*-cycloheptenyl- or *N*-cyclooctenyl-*N*-tosylamides **3c**¹⁰ and **3d**^{7c} with but-2-ynyl methanesulfonate or propargyl bromide gave cycloalkene-yne **2b**, **2e**, **2c** and **2f**, respectively, in good yields.



Scheme 4. ROM-RCM of cycloalkene-yne **2b**.

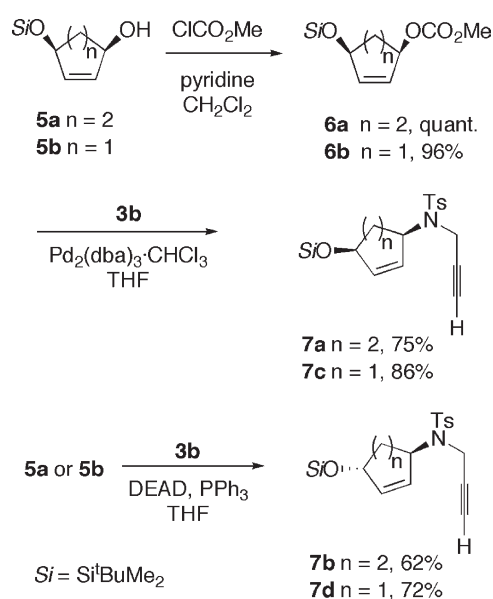
When a CH_2Cl_2 solution of cycloheptene-yne **2b** and 10 mol% of ruthenium complex **1a** was stirred at room temperature for 24 h under an atmosphere of ethylene, we were pleased to find that the desired ring-opening metathesis product **4b** was obtained in 56% yield (Scheme 4). This product **4b** should be obtained through the proposed reaction course. Thus, formally, in this reaction, the double bond of cycloalkene was cleaved, and one alkylidene carbon reacts with an alkyne carbon to form a five-membered ring, while the other alkylidene carbon and alkyne carbon react with methylene parts of ethylene. It is interesting that three new double bonds in **4b** were formed from two double bonds and one triple bond in **2b** in this process. As substrates, **2a** and **2c** were treated in a similar manner, and the desired ROM-RCM products **4a** and **4c** were obtained in 15 and 22% yields, respectively, and the starting materials **2a** and **2c** were recovered in 70 and 75% yields, respectively (Table 1, runs 1 and 3).

Table 1. ROM-RCM of cycloalkene-yne **2**


Run	R	n	Starting material	Time (h)	Yield (%)
1	Me	1	2a	24	4a , 15
2	Me	2	2b	24	4b , 56
3	Me	3	2c	24	4c , 22
4	H	1	2d	4	4d , 78
5	H	2	2e	1	4e , 70
6	H	3	2f	1	4f , 75

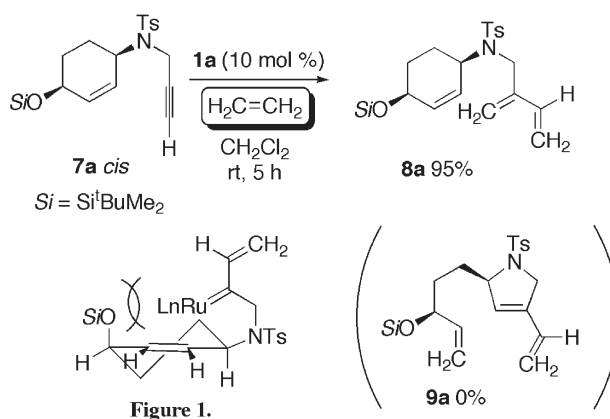
Since this reaction was carried out under ethylene gas, cycloalkene bearing terminal alkyne can be used.^{3f} When a CH_2Cl_2 solution of cyclohexene-yne **2d** and 10 mol% of **1a** was stirred at room temperature under an atmosphere of ethylene, the reaction proceeded smoothly and the desired product **4d** was obtained in 78% yield (run 4). Under similar reaction conditions, metatheses of cycloalkene-ynes **2e** and **2f** were carried out and the desired products **4e** and **4f** were obtained in good yields (runs 5 and 6).

Next, the ROM-RCM reaction of cycloalkene-yne **7** having two substituents on the cycloalkene ring was investigated. These cycloalkene-ynes **7** were synthesized from cycloalkenes **5a** or **5b** as shown in Scheme 5. Cycloalkene-ynes **7a** and **7c** having *cis*-substituents were prepared using palladium-catalyzed allylic substitution of carbonates **6a** and **6b**. Cycloalkene-ynes **7b** and **7d** having *trans*-substituents were prepared from **5a** and **5b** using Mitsunobu reaction.

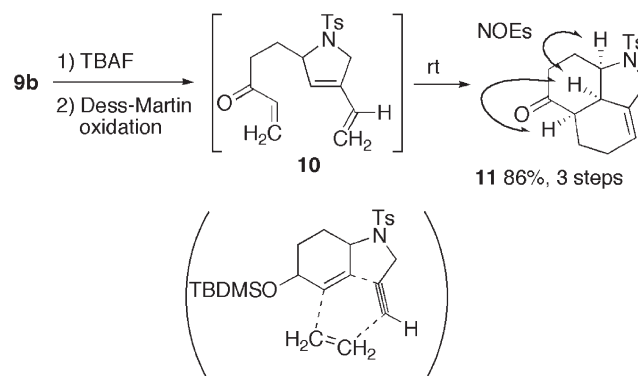
**Scheme 5.** Synthesis of cycloalkene-yne **7** having substituents.

When a CH_2Cl_2 solution of **7a** having *cis*-substituents and 10 mol% of **1a** was stirred at room temperature under an atmosphere of ethylene, the reaction proceeded smoothly to give a single product in high yield. However, this is a cross-

metathesis product **8a** of an alkyne part of **7a** with ethylene. Presumably, the steric hindrance between the intermediate ruthenium–carbene part and the silyloxy group would prevent the intramolecular metathesis reaction (Scheme 1). As a result, the ruthenium–carbene part reacted with ethylene to yield 1,3-diene **8a**. On the other hand, when cyclohexene-yne **7b** having *trans*-substituents was treated in a similar manner, the desired ring-opening metathesis product **9b** was obtained in 90% yield as a single product (Scheme 6).

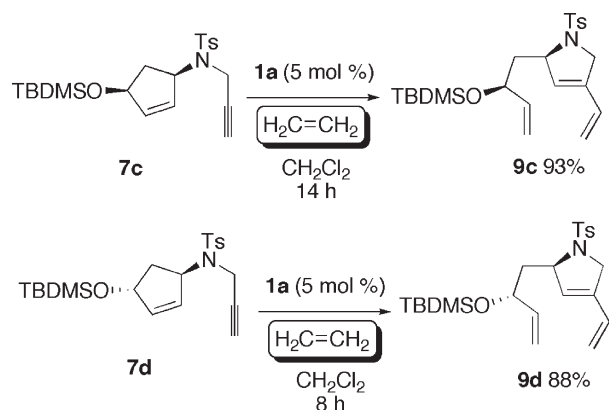
**Scheme 6.** ROM-RCM of cycloalkene-yne bearing substituents.

Since cyclized product **9b** has the diene moiety and an alkene part, cyclization by Diels–Alder reaction would be expected (Scheme 7). Desilylation of **9b** followed by Dess–Martin oxidation¹¹ at room temperature afforded a mixture of the desired ketone **10** and tricyclic compound **11**, which should be produced by Diels–Alder reaction, in 86% yield. The resultant mixture was allowed to stand at room temperature to give tricyclic compound **11** as a single product. The stereochemistry of **11** was determined by an NOESY experiment, and the cross-peaks on NOE were observed between the ring-junction protons. These results

**Scheme 7.** Synthesis of tricyclic compound via Diels–Alder reaction.

indicated, that formally, tricyclic compound **11** was formed via [2+2+2] cocyclization of cycloalkene, alkyne and ethylene.

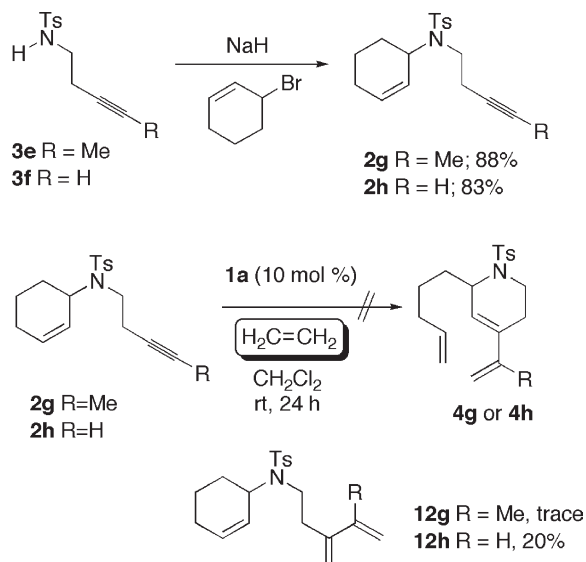
Under similar reaction conditions, metatheses of cyclopentene-yne **7c** and **7d** were carried out. The reaction of each compound having *cis*- or *trans*-substituents proceeded smoothly to afford the desired products **9c** and **9d**, respectively in good yields (Scheme 8). Presumably, steric hindrance between the ruthenium–carbene part and the silyloxy group on the cyclopentene ring in **7c** is not affected by ring-opening metathesis and the desired product **9c** is formed.



Scheme 8. ROM-RCM of cycloalkene-yne **7c** and **7d**.

Subsequently, the construction of a dehydropiperidine skeleton was attempted. For that purpose, one carbon in a tether of cycloalkene-yne should be elongated. Cycloalkene-yne **2g** and **2h** having one-carbon elongated tether were synthesized from **3e** and **3f** by the usual method.

ROM-RCM of these cycloalkene-yne **2g** and **2h** were carried out in a similar manner, but, unfortunately, no ring-opening metathesis products **4g** or **4f** were formed and the starting materials **2g** and **2h** were recovered in 96 and 66% yields, respectively, along with a small amount of cross-

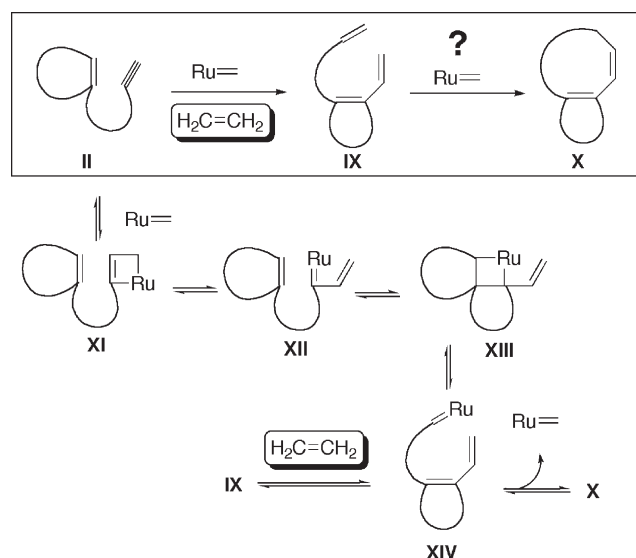


Scheme 9. Attempt to synthesize piperidine-ring.

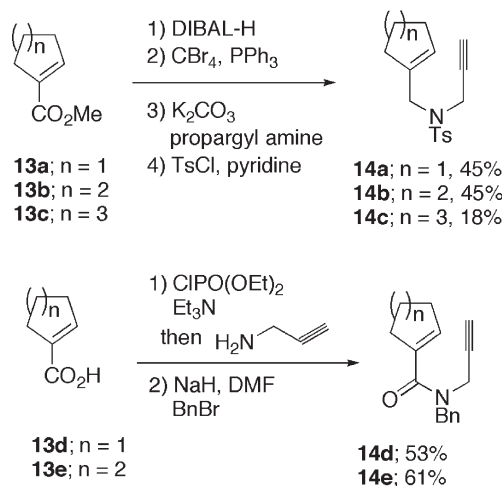
metathesis products **12g** and **12h** with ethylene in each case (Scheme 9). It is not clear why the starting materials were recovered without formation of ROM-RCM products.

2.2. Metathesis of cycloalkene having alkyne in a tether at the C-1 position

Subsequently, metathesis reaction of cycloalkene-yne, whose tether having an alkyne part is connected to the C-1 position of cycloalkene, was investigated (Scheme 10). If the metathesis of cycloalkene-yne **II** proceeds under ethylene gas, the alkyne part of **II** would react with the ruthenium–carbene complex to give ruthenacyclobutene **XI**, which would be converted into ruthenium–carbene complex **XII** by ring opening. Intramolecular [2+2] cycloaddition would occur to afford ruthenacyclobutane **XIII**, which would then be converted into ruthenium–carbene complex **XIV**. This would react with ethylene intermolecularly to afford triene **IX**. On the other hand, if this complex **XIV** can react with an alkene part of the diene moiety intramolecularly, bicyclic compound **X** would be obtained.



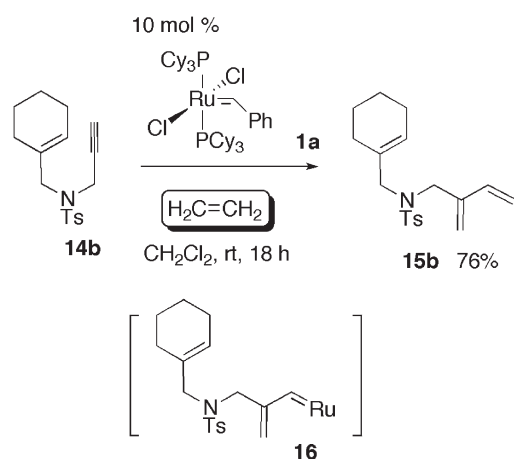
Scheme 10. Plan for ROM-RCM of cycloalkene-yne **II**.



Scheme 11. Synthesis cycloalkene-yne **14**.

Cycloalkene-yne **14** was easily prepared from ester or carboxylic acid **13** as shown in Scheme 11. Reduction of **13a**, **13b** or **13c**¹² with DIBAL-H followed by bromination afforded a corresponding allyl bromide, which was reacted with propargyl amine followed by tosylation to afford cycloalkene-yne **14a**, **14b** or **14c** in moderate yield. Synthesis of cycloalkene-yne **14d** or **14e** was carried out by condensation of carboxylic acid **13d** or **13e** with propargylamine followed by alkylation with benzyl bromide.

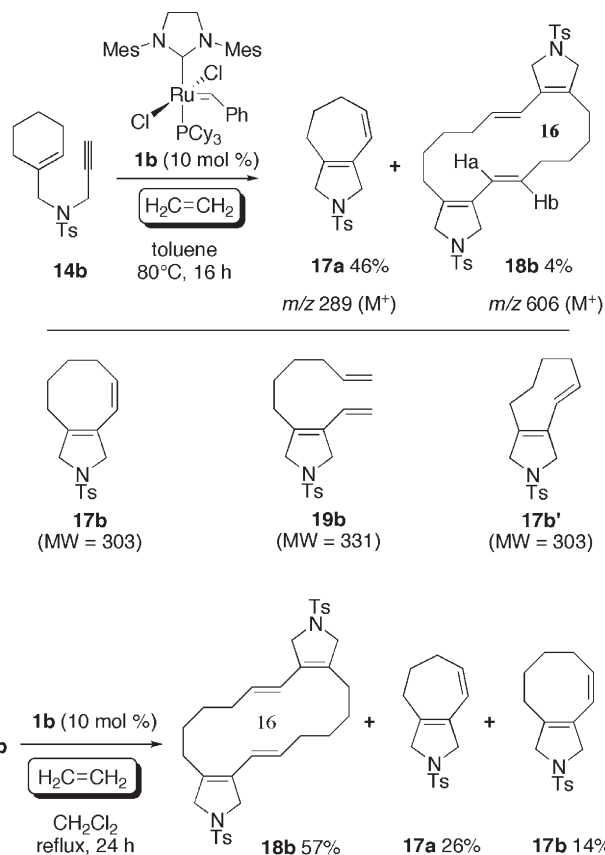
When a CH₂Cl₂ solution of cyclohexene-yne **14b** and 10 mol% of a first-generation ruthenium carbene complex **1a** was stirred at room temperature for 18 h under an atmosphere of ethylene, cross-ene-yne metathesis product **15b** was obtained in 76% yield instead of the ROM-RCM product (Scheme 12). Presumably, carbene complex **16** cannot react with trisubstituted alkene moiety. A second-generation ruthenium carbene complex was therefore used for ROM-RCM of **14b**.



Scheme 12. Reaction of **14b** with **1a**.

When a toluene solution of **14b** and 10 mol% of a second-generation ruthenium carbene complex **1b** was stirred at 80 °C for 16 h under an atmosphere of ethylene, two products were obtained (Scheme 13). Surprisingly, the expected products **17b** and **19b** were not obtained, and ¹H NMR and mass spectra revealed that one is compound **17a** having a 5,7-fused ring system, which was obtained in 46% yield. The structure of **17a** was confirmed by X-ray crystallographic analysis.¹³ The other is 16-membered ring compound **18b**, which was obtained in 4% yield. The structure of **18b** was confirmed as follows. From the coupling constant of Ha and Hb on a ¹H NMR spectrum ($J_{\text{Ha-Hb}}=16.0$ Hz), this compound was first thought to be **17b'** having *trans*-olefin because one set of peaks corresponding to **17b'** were seen on ¹H NMR and ¹³C NMR spectra. However, a mass spectrum of **18b** (m/z 606 [M⁺]) indicated that it is a dimeric compound, formed from intermolecular metathesis of two molecules.

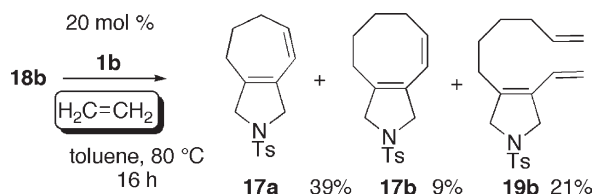
When a solution of **14b** and 10 mol% of **1b** in CH₂Cl₂ was refluxed under an atmosphere of ethylene for 24 h, the yields were improved. Although the expected product **17b** was obtained in 14% yield under these reaction conditions, the main product was dimeric compound **18b** (57% yield)



Scheme 13. ROM-RCM of **14b** using **1b**.

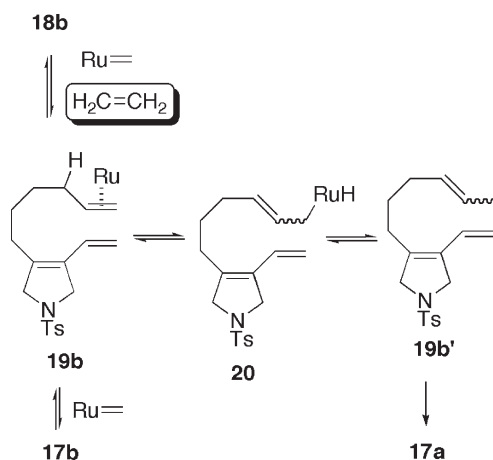
and the yield of 5,7-fused ring compound **17a** was greater than that of 5,8-fused ring compound **17b**.

Next, to examine whether dimeric compound **18b** is converted into a 5,7 or 5,8-fused ring compounds under the metathesis reaction conditions, a solution of **18b** and 20 mol% of **1b** in toluene was stirred at 80 °C for 16 h under an atmosphere of ethylene. Interestingly, **17a**, **17b** and **19b** were obtained in 39, 9 and 21% yields, respectively (Scheme 14). In this case, the yield of **17a** was also higher than that of **17b**. These results suggest that **18b** reacted with ethylene in the presence of ruthenium complex **1b** to afford **19b** and that **17a** and **17b** were then formed.



Scheme 14. ROM of dimeric compound **18b**.

Since ring-closure of **19b** into an eight-membered ring is difficult, olefin migration¹⁴ followed by olefin metathesis would occur to give 5,7-fused ring compound **17a**. Isomerization of the double bond of **19b** should be caused by a ruthenium complex. Coordination of the terminal olefin of **19b** into a ruthenium complex followed by hydrogen elimination and then reductive elimination gives **19b'** via **20**. Olefin metathesis of **19b'** affords 5,7-fused ring compound **17a**. At a higher reaction temperature, **17b** was



Scheme 15. Possible reaction course for formation of **17a**.

not formed because **19b** was easily converted into **19b'** and **17a** should be stable under these reaction conditions (Scheme 15).

Subsequently, ROM-RCM of cyclopentene-yne **14a** was investigated (Table 2). When a CH_2Cl_2 solution of **14a** and 10 mol% of **1b** was refluxed under an atmosphere of ethylene for 2 h, the desired ROM-RCM product **17a** was obtained in 95% yield (run 1). Even in the case of longer reaction time (26 h), **17a** was obtained in a quantitative yield (run 2). The results indicated that ring-closure into a seven-membered ring is easier and that **17a** is stable under these reaction conditions. The use of 5 mol% of **1b** gave similar results (run 3). In this reaction, ethylene was not introduced into the product. Thus, the reaction was carried out in the absence of ethylene to give **17a** in 81% yield, although the yield was slightly decreased (run 4).

Table 2. ROM-RCM of cycloalkene-yne **14a**

Run	Time (h)	Yield (%)
1	2	96
2	26	Quant.
3 ^a	4	90
4 ^b	1	81

^a 5 mol % of **1b** was used.

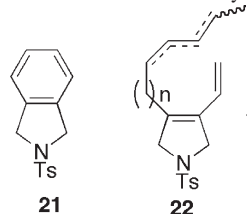
^b Reactions were carried out under an atmosphere of Ar.

Furthermore, ROM-RCM of cycloheptene-yne **14c** was investigated (Table 3). When the reaction of **14c** was carried out in toluene at 80 °C for 21 h, 5,7-fused ring compound **17a**, dimeric compound **18c** and isoindoline derivative **21**¹⁵ were obtained in 36, 8 and 6% yields, respectively, along with an inseparable mixture of **22** (run 1). GC–MS analysis of **22** showed that it is a mixture of dihydropyrrole derivatives having different carbon lengths and/or having olefin at various positions in a tether. On the other hand, when the reaction was carried out in CH_2Cl_2 upon heating

Table 3. ROM-RCM of cycloalkene-yne **14c**

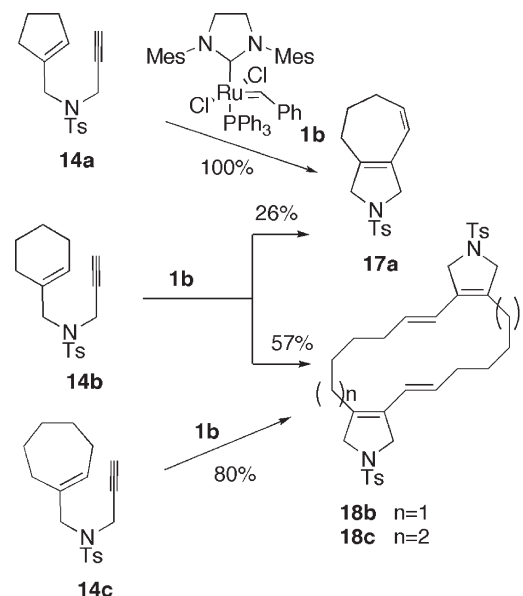
Run	Conditions	Yields (%)	
		17a	18c
1 ^a	Toluene, 80 °C, 21 h	36	8
2	CH_2Cl_2 , reflux, 15 h	Trace	58
3	CH_2Cl_2 , reflux, 1 h	0	80

^a **21** was obtained in 6% yield.



for 15 h, dimerization product **18c** was obtained in 58% yield along with a considerable amount of **22** (run 2). However, when the reaction was quenched after the spot of the starting material **14c** had disappeared on TLC, only **18c** was obtained in 80% yield (run 3).

ROM-RCM of 5-, 6-, and 7-membered cycloalkene-yne **14** are summarized in Scheme 16. When the reaction was carried out in CH_2Cl_2 , cyclopentene-yne **14a** gave 5,7-fused

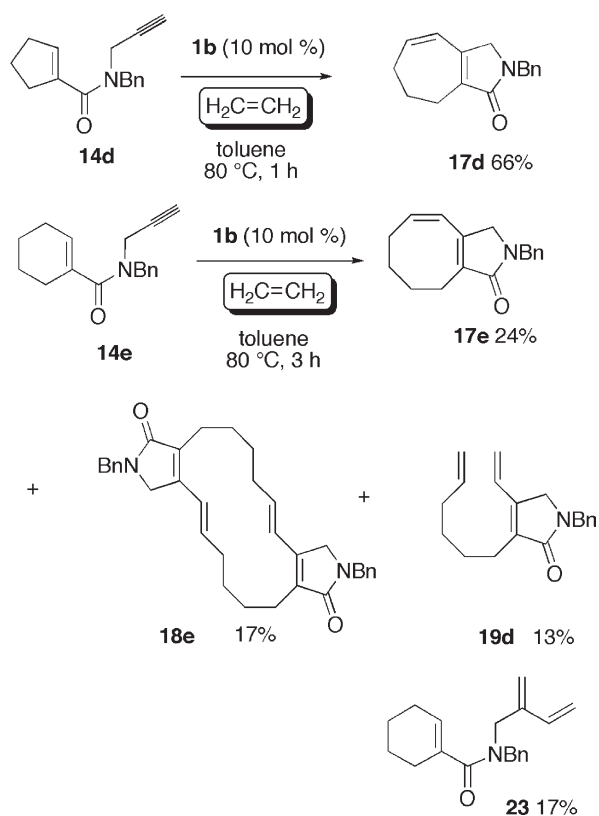


All reactions were carried out in CH_2Cl_2 with 10 mol % of **1b** under an atmosphere of ethylene.

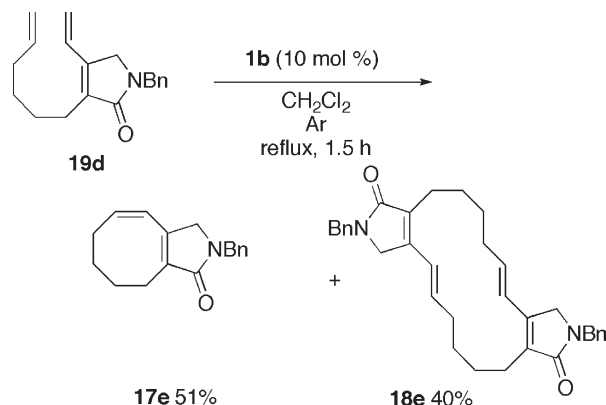
Scheme 16. Summary of ROM-RCM of cycloalkene-yne **14a–14c**.

ring compound **17a** in high yield, but cycloheptene-yne **14c** afforded dimeric compound **18c** in high yield. However, under similar reaction conditions, cyclohexene-yne **14b** gave **17a** and dimeric compound **18b** in 26 and 57% yields, respectively. Since the reaction of **14c** in toluene at 80 °C gave **17a** in good yield, **17a** was obtained in all cases due to the easy isomerization of the terminal olefin in a tether and the easy formation of a seven-membered ring.

Furthermore, ROM-RCM of cycloalkenecarboxamide having an alkyne moiety on nitrogen was carried out. When a toluene solution of **14d** and 10 mol% of **1b** was stirred in toluene at 80 °C for 1 h under an atmosphere of ethylene, the desired 5,7-fused ring compound **17d** was obtained in 66% yield as a single product. On the other hand, when ROM-RCM of cyclohexene-yne **14e** was carried out in a similar manner, 5,8-fused ring compound **17e**, dimeric compound **18e**, pyrrolidine derivative **19d** and cross-metathesis product **23** with ethylene were obtained in 24, 17, 13 and 17% yields, respectively. In this case, it was interesting that 5,7-fused ring compound **17d** was not formed. Presumably, before isomerization of the double bond of **19d**, olefin metathesis should occur to give **17e**, which is stable under the reaction conditions. Although it is not clear why a dimeric compound is formed, a relatively large amount of dimeric compound **18e** was also obtained in this case. Since compound **19d** was thought to be a product of ring-opening metathesis followed by cross-metathesis with ethylene, further treatment of compound **19d** with **1b** was carried out. When a CH₂Cl₂ solution of **19d** and 10 mol% of **1b** was refluxed for 1.5 h under argon gas upon heating, 5,8-fused ring compound **17e** and dimeric



Scheme 17. ROM-RCM of cycloalkene-yne **14d** and **14e**.



Scheme 18. Reaction of **19d** with **1b**.

compound **18e** were obtained in 51 and 40% yields, respectively (Scheme 17 and 18).

3. Conclusions

ROM-RCM of cycloalkene-yne was realized. In the first ROM-RCM of cycloalkene having alkyne in a tether at the C-3 position, the reaction proceeded smoothly and the expected products were obtained in high yields. Ethylene gas is essential for these reactions. Formally, in this reaction, the double bond of cycloalkene was cleaved, and one alkyldiene carbon reacts with an alkyne carbon to form a five-membered ring, while the other alkyldiene carbon and alkyne carbon react with methylene parts of ethylene to form two terminal olefins, respectively. However, in the second ROM-RCM of cycloalkene having alkyne in a tether at the C-1 position, unexpected 5,7-fused ring compound **17a** was formed from all cycloalkene-ynes. Moreover, dimeric compounds **18** were obtained from cyclohexene and cycloheptene derivatives. Presumably, the reaction rate of ROM-RCM of cyclopentene is fast and the expected stable product **17a** would be produced predominantly. However, since ROM-RCM products of cyclohexene and cycloheptene derivatives were unstable under these reaction conditions, further reactions would proceed to give a dimeric compound and the cross-metathesis product with ethylene.

4. Experimental

4.1. General

The metathesis reactions were carried out under an atmosphere of ethylene (1 atm). All other manipulations were carried out under an atmosphere of argon unless otherwise mentioned. Solvents were distilled under an atmosphere of argon from sodium–benzophenone (toluene), or CaH₂ (CH₂Cl₂). Ethylene gas was purified by passage through the aqueous CuCl solution (2 g of CuCl in 180 mL of saturated NH₄Cl aqueous) and concentrated H₂SO₄ and then KOH tubes. Ruthenium complexes were purchased from Strem Chemicals. All other solvents and reagents were purified when necessary using standard procedure.

4.2. Typical procedure for the metathesis reaction

To a solution of enyne **2d** (98.2 mg, 0.34 mmol) in a CH₂Cl₂ solution (11.3 mL) was added **1a** (26.1 mg, 34 μmol), and the solution was degassed through freeze–pump–thaw cycle, and stirred at room temperature under an atmosphere of ethylene for 4 h. To this solution was added an excess of ethyl vinyl ether. After the solvent was removed, the residue was purified by flash column chromatography on silica gel (hexane/ethyl acetate 9:1) to yield **4d** (83.6 mg, 78%) as a colorless solid.

4.3. Spectral data for metathesis products

4.3.1. 4-Isopropenyl-2-pent-4-enyl-1-(toluene-4-sulfonyl)-2,5-dihydro-1H-pyrrole (4a). A colorless oil; IR (neat) ν 1640, 1600, 1346, 1164 cm⁻¹; ¹H NMR (270 MHz, CDCl₃) δ 1.31–1.52 (m, 2H), 1.77–1.86 (m, 2H), 1.83 (s, 3H), 2.07 (dt, $J=6.7$, 7.3 Hz, 2H), 2.41 (s, 3H), 4.19–4.27 (m, 2H), 4.52 (br, 1H), 4.76 (s, 1H), 4.93–5.04 (m, 3H), 5.50 (s, 1H), 5.79 (ddt, $J=17.0$, 10.1, 6.7 Hz, 1H), 7.29 (d, $J=8.3$ Hz, 2H), 7.71 (d, $J=8.3$ Hz, 2H); ¹³C NMR (67.8 MHz, CDCl₃) δ 20.0 (CH₃), 21.5 (CH₃), 24.0 (CH₂), 33.7 (CH₂), 35.6 (CH₂), 55.2 (CH₂), 67.8 (CH), 114.5 (CH₂), 114.7 (CH₂), 125.0 (CH), 127.4 (CH \times 2), 129.7 (CH \times 2), 134.9 (C), 136.6 (C), 138.4 (C), 138.6 (CH), 143.3 (C); LRMS m/z 331 (M⁺), 262, 176, 155, 107, 91; HRMS calcd for C₁₉H₂₅NO₂S (M⁺) 331.1606, found 331.1613.

4.3.2. 2-Hex-5-enyl-4-isopropenyl-1-(toluene-4-sulfonyl)-2,5-dihydro-1H-pyrrole (4b). A colorless oil; IR (neat) ν 1640, 1600, 1346, 1164 cm⁻¹; ¹H NMR (270 MHz, CDCl₃) δ 1.26–1.43 (m, 4H), 1.75–1.87 (m, 2H), 1.83 (s, 3H), 2.04 (dt, $J=6.5$, 6.5 Hz, 2H), 2.41 (s, 3H), 4.19–4.31 (m, 2H), 4.51 (br, 1H), 4.76 (s, 1H), 4.92 (m, 1H), 4.96 (m, 1H), 5.02 (m, 1H), 5.50 (s, 1H), 5.80 (ddt, $J=17.0$, 10.1, 6.7 Hz, 1H), 7.29 (d, $J=8.1$ Hz, 2H), 7.71 (d, $J=8.1$ Hz, 2H); ¹³C NMR (67.8 MHz, CDCl₃) δ 20.0 (CH₃), 21.5 (CH₃), 24.1 (CH₂), 28.9 (CH₂), 33.6 (CH₂), 35.9 (CH₂), 55.2 (CH₂), 67.8 (CH), 114.3 (CH₂), 114.5 (CH₂), 125.1 (CH), 127.4 (CH \times 2), 129.7 (CH \times 2), 134.9 (C), 136.6 (C), 138.3 (C), 138.8 (CH), 143.3 (C); LRMS m/z 345 (M⁺), 262, 155, 107, 91; HRMS calcd for C₂₀H₂₇NO₂S (M⁺) 345.1762, found 345.1752.

4.3.3. 2-Hept-6-enyl-4-isopropenyl-1-(toluene-4-sulfonyl)-2,5-dihydro-1H-pyrrole (4c). A colorless oil; IR (neat) ν 1640, 1598, 1346, 1164 cm⁻¹; ¹H NMR (400 MHz, CDCl₃) δ 1.24–1.86 (m, 8H), 1.82 (s, 3H), 2.03 (dt, $J=6.7$, 6.4 Hz, 2H), 2.41 (s, 3H), 4.20–4.30 (m, 2H), 4.50 (br, 1H), 4.76 (s, 1H), 4.92–5.01 (m, 2H), 4.96 (s, 1H), 5.50 (s, 1H), 5.80 (ddt, $J=16.7$, 10.0, 6.7 Hz, 1H), 7.29 (d, $J=8.3$ Hz, 2H), 7.71 (d, $J=8.3$ Hz, 2H); ¹³C NMR (100 MHz, CDCl₃) δ 20.1 (CH₃), 21.6 (CH₃), 24.5 (CH₂), 28.9 (CH₂), 29.2 (CH₂), 33.8 (CH₂), 36.1 (CH₂), 55.2 (CH₂), 67.9 (CH), 114.2 (CH₂), 114.4 (CH₂), 125.1 (CH), 127.3 (CH \times 2), 129.6 (CH \times 2), 134.8 (C), 136.5 (C), 138.1 (C), 138.9 (CH), 143.2 (C); LRMS m/z 359 (M⁺), 262, 155, 107, 91; HRMS calcd for C₂₁H₂₉NO₂S (M⁺) 359.1919, found 359.1919.

4.3.4. 2-Pent-4-enyl-1-(toluene-4-sulfonyl)-4-vinyl-2,5-dihydro-1H-pyrrole (4d). A colorless solid; IR (nujol) ν 1642, 1598, 1344, 1166 cm⁻¹; ¹H NMR (270 MHz, CDCl₃)

δ 1.24–1.49 (m, 2H), 1.76–1.85 (m, 2H), 2.06 (dt, $J=6.8$, 7.3 Hz, 2H), 2.41 (s, 3H), 4.16–4.28 (m, 2H), 4.50 (br, 1H), 4.92–5.03 (m, 2H), 5.01 (d, $J=17.8$ Hz, 1H), 5.14 (d, $J=10.5$ Hz, 1H), 5.51 (br, 1H), 5.78 (ddt, $J=17.0$, 10.3, 6.8 Hz, 1H), 6.32 (dd, $J=17.8$, 10.5 Hz, 1H), 7.29 (d, $J=8.1$ Hz, 2H), 7.71 (d, $J=8.3$ Hz, 2H); ¹³C NMR (67.8 MHz, CDCl₃) δ 21.5 (CH₃), 23.9 (CH₂), 33.7 (CH₂), 35.5 (CH₂), 54.3 (CH₂), 67.3 (CH), 114.6 (CH₂), 116.7 (CH₂), 127.3 (CH \times 2), 127.8 (CH), 129.7 (CH \times 2), 129.9 (CH), 134.8 (C), 136.6 (C), 138.5 (CH), 143.3 (C); LRMS m/z 317 (M⁺), 248, 155, 91; HRMS calcd for C₁₈H₂₃NO₂S (M⁺) 317.1449, found 317.1455.

4.3.5. 2-Hex-5-enyl-1-(toluene-4-sulfonyl)-4-vinyl-2,5-dihydro-1H-pyrrole (4e). A colorless oil; IR (neat) ν 1640, 1598, 1346, 1162 cm⁻¹; ¹H NMR (270 MHz, CDCl₃) δ 1.23–1.46 (m, 4H), 1.71–1.86 (m, 2H), 2.04 (dt, $J=6.7$, 6.5 Hz, 2H), 2.41 (s, 3H), 4.16–4.28 (m, 2H), 4.49 (br, 1H), 4.91–5.03 (m, 2H), 5.01 (d, $J=17.8$ Hz, 1H), 5.14 (d, $J=11.1$ Hz, 1H), 5.52 (m, 1H), 5.79 (ddt, $J=17.0$, 10.1, 6.7 Hz, 1H), 6.33 (dd, $J=17.8$, 11.1 Hz, 1H), 7.29 (d, $J=8.1$ Hz, 2H), 7.71 (d, $J=8.1$ Hz, 2H); ¹³C NMR (67.8 MHz, CDCl₃) δ 21.4 (CH₃), 24.1 (CH₂), 28.8 (CH₂), 33.6 (CH₂), 35.9 (CH₂), 54.2 (CH₂), 67.4 (CH), 114.3 (CH₂), 116.6 (CH₂), 127.3 (CH \times 2), 127.9 (CH), 129.7 (CH \times 2), 129.9 (CH), 134.5 (C), 136.6 (C), 138.8 (CH), 143.3 (C); LRMS m/z 331 (M⁺), 248, 155, 91; HRMS calcd for C₁₉H₂₅NO₂S (M⁺) 331.1606, found 331.1604.

4.3.6. 2-Hept-6-enyl-1-(toluene-4-sulfonyl)-4-vinyl-2,5-dihydro-1H-pyrrole (4f). A colorless oil; IR (neat) ν 1640, 1598, 1346, 1164 cm⁻¹; ¹H NMR (270 MHz, CDCl₃) δ 1.21–1.39 (m, 6H), 1.73–1.82 (m, 2H), 1.99–2.06 (m, 2H), 2.41 (s, 3H), 4.16–4.29 (m, 2H), 4.49 (br, 1H), 4.90–5.03 (m, 2H), 5.01 (d, $J=17.6$ Hz, 1H), 5.14 (d, $J=10.8$ Hz, 1H), 5.52 (m, 1H), 5.80 (ddt, $J=17.0$, 10.3, 6.8 Hz, 1H), 6.33 (dd, $J=17.6$, 10.8 Hz, 1H), 7.29 (d, $J=8.1$ Hz, 2H), 7.71 (d, $J=8.1$ Hz, 2H); ¹³C NMR (67.8 MHz, CDCl₃) δ 21.5 (CH₃), 24.4 (CH₂), 28.8 (CH₂), 29.0 (CH₂), 33.7 (CH₂), 36.0 (CH₂), 54.3 (CH₂), 67.5 (CH), 114.2 (CH₂), 116.6 (CH₂), 127.3 (CH \times 2), 127.9 (CH), 129.7 (CH \times 2), 123.0 (CH), 134.9 (C), 136.6 (C), 139.0 (CH), 143.3 (C); LRMS m/z 345 (M⁺), 248, 155, 106, 91; HRMS calcd for C₂₀H₂₇NO₂S (M⁺) 345.1762, found 345.1760.

4.3.7. *N*-{(1R*,4S*)-4-(tert-Butyl-dimethylsilyloxy)-cyclohex-2-enyl}-4-methyl-*N*-(2-methylene-but-3-enyl)-benzenesulfonamide (8a). A colorless oil; IR (neat) ν 1638, 1598, 1342, 1253, 1163, 1093 cm⁻¹; ¹H NMR (270 MHz, CDCl₃) δ -0.02 (s, 3H), -0.01 (s, 3H), 0.81 (s, 9H), 1.54–1.66 (m, 3H), 1.79–1.87 (m, 1H), 2.43 (s, 3H), 3.76 (d, $J=17.6$ Hz, 1H), 4.00 (br, 1H), 4.04 (d, $J=17.6$ Hz, 1H), 4.44–4.48 (m, 1H), 5.03–5.09 (m, 2H), 5.17–5.24 (m, 2H), 5.42 (br, 1H), 5.69–5.75 (m, 1H), 6.40 (dd, $J=18.1$, 11.3 Hz, 1H), 7.30 (d, $J=8.4$ Hz, 2H), 7.74 (d, $J=8.4$ Hz, 2H); ¹³C NMR (67.8 MHz, CDCl₃) δ -4.9 (CH₃), -4.6 (CH₃), 17.9 (C), 21.5 (CH₃), 22.9 (CH₂), 25.7 (CH₃ \times 3), 30.4 (CH₂), 45.1 (CH₂), 55.6 (CH), 62.6 (CH), 113.3 (CH₂), 117.4 (CH₂), 127.2 (CH \times 2), 129.0 (CH), 129.7 (CH \times 2), 134.1 (CH), 136.9 (CH), 137.9 (C), 142.5 (C), 143.2 (C); LRMS m/z 447 (M⁺), 390, 248, 132, 91; HRMS calcd for C₂₄H₃₇NO₃SSi (M⁺) 447.2263, found 447.2244.

4.3.8. (2S*)-2-[(3S*)-3-(tert-Butyl-dimethylsilyloxy)-pent-4-enyl]-1-(toluene-sulfonyl)-4-vinyl-2,5-dihydro-1H-pyrrole (9b). A colorless oil; IR (neat) ν 1646, 1598, 1348, 1252, 1163, 1096 cm^{-1} ; ^1H NMR (400 MHz, CDCl_3) δ 0.03 (s, 3H), 0.06 (s, 3H), 0.89 (s, 9H), 1.41–1.57 (m, 2H), 1.76–1.91 (m, 2H), 2.41 (s, 3H), 4.07 (dt, $J=6.4$, 6.0 Hz, 1H), 4.17–4.26 (m, 2H), 4.54 (br, 1H), 4.98 (d, $J=17.6$ Hz, 1H), 5.01 (d, $J=10.4$ Hz, 1H), 5.13 (d, $J=17.2$ Hz, 1H), 5.14 (d, $J=10.8$ Hz, 1H), 5.47 (br, 1H), 5.76 (ddd, $J=17.2$, 10.4, 6.4 Hz, 1H), 6.32 (dd, $J=17.6$, 10.8 Hz, 1H), 7.29 (d, $J=8.4$ Hz, 2H), 7.71 (d, $J=8.4$ Hz, 2H); ^{13}C NMR (100 MHz, CDCl_3) δ -4.7 (CH₃), -4.2 (CH₃), 18.3 (C), 21.6 (CH₃), 25.9 (CH₃×3), 31.7 (CH₂), 32.7 (CH₂), 54.4 (CH₂), 67.3 (CH), 73.7 (CH), 113.7 (CH₂), 116.6 (CH₂), 127.3 (CH×2), 127.7 (CH), 129.6 (CH×2), 129.8 (CH), 134.7 (C), 136.6 (C), 141.5 (CH), 143.3 (C); LRMS m/z 432 (M^+-CH_3), 390, 292, 262, 248, 236, 155, 91; HRMS calcd for $\text{C}_{23}\text{H}_{34}\text{NO}_3\text{SSi}$ (M^+-CH_3) 432.2067, found 432.2048. Anal. calcd for $\text{C}_{24}\text{H}_{37}\text{NO}_3\text{SSi}$: C, 64.39; H, 8.33; N, 3.13; S, 7.16. Found: C, 64.48; H, 8.48; N, 2.91; S, 7.21.

4.3.9. (2S*)-2-[(2R*)-2-(tert-Butyl-dimethyl-silyloxy)-but-3-enyl]-1-(toluene-4-sulfonyl)-4-vinyl-2,5-dihydro-1H-pyrrole (9c). A colorless oil; IR (neat) ν 2954, 2928, 2856, 1646, 1599, 1348, 1163 cm^{-1} ; ^1H NMR (270 MHz, CDCl_3) δ 0.00 (s, 3H), 0.02 (s, 3H), 0.88 (s, 9H), 1.75 (ddd, $J=13.8$, 9.7, 4.3 Hz, 1H), 2.37 (m, 1H), 2.39 (s, 3H), 4.12 (m, 1H), 4.22 (m, 1H), 4.28 (m, 1H), 4.48 (br, 1H), 4.98 (d, $J=17.6$ Hz, 1H), 5.09 (dt, $J=10.8$, 1.6 Hz, 1H), 5.11 (d, $J=10.3$ Hz, 1H), 5.20 (dt, $J=17.8$, 1.6 Hz, 1H), 5.68 (br, 1H), 5.88 (ddd, $J=17.6$, 10.3, 5.7 Hz, 1H), 6.29 (dd, $J=17.8$, 10.8 Hz, 1H), 7.26 (d, $J=9.7$ Hz, 2H), 7.68 (d, $J=9.7$ Hz, 2H); ^{13}C NMR (67.8 MHz, CDCl_3) δ -5.0 (CH₃), -4.3 (CH₃), 18.1 (C), 21.5 (CH₃), 25.8 (CH₃×3), 44.5 (CH₂), 53.9 (CH₂), 64.4 (CH), 71.2 (CH), 114.3 (CH₂), 116.5 (CH₂), 127.5 (CH×2), 128.8 (CH), 129.7 (CH×2), 130.1 (CH), 134.2 (C), 135.6 (C), 140.8 (CH), 143.4 (C); LRMS m/z 432 (M^+-1), 418, 403, 376, 278, 220, 155, 91. Anal. calcd for $\text{C}_{23}\text{H}_{35}\text{NO}_3\text{SSi}$: C, 63.70; H, 8.13; N, 3.23; S, 7.39. Found: C, 63.47; H, 8.07; N, 3.20; S, 7.23.

4.3.10. (2S*)-2-[(2S*)-2-(tert-Butyl-dimethyl-silyloxy)-but-3-enyl]-1-(toluene-4-sulfonyl)-4-vinyl-2,5-dihydro-1H-pyrrole (9d). A colorless solid. Mp 91 °C (ether/hexane); IR (nujol) ν 3088, 1829, 1597, 1343, 1165 cm^{-1} ; ^1H NMR (270 MHz, CDCl_3) δ 0.04 (s, 3H), 0.08 (s, 3H), 0.89 (s, 9H), 1.77–1.85 (m, 1H), 2.25–2.31 (m, 1H), 2.39 (s, 3H), 4.02 (m, 1H), 4.10 (m, 1H), 4.30–4.35 (m, 1H), 4.46 (br, 1H), 4.97 (d, $J=17.8$ Hz, 1H), 5.05 (dt, $J=10.4$, 1.6 Hz, 1H), 5.10 (d, $J=10.4$ Hz, 1H), 5.16 (dt, $J=17.8$, 1.6 Hz, 1H), 5.63 (br, 1H), 5.79 (ddd, $J=17.8$, 10.4, 6.2 Hz, 1H), 6.28 (dd, $J=17.8$, 10.4 Hz, 1H), 7.27 (d, $J=8.2$ Hz, 2H), 7.68 (d, $J=8.2$ Hz, 2H); ^{13}C NMR (67.8 MHz, CDCl_3) δ -4.7 (CH₃), -4.3 (CH₃), 18.2 (C), 21.5 (CH₃), 25.9 (CH₃×3), 45.0 (CH₂), 53.7 (CH₂), 65.2 (CH), 72.0 (CH), 114.3 (CH₂), 116.5 (CH₂), 127.5 (CH×2), 128.8 (CH), 129.7 (CH×2), 130.1 (CH), 134.2 (C), 135.6 (C), 147.4 (CH), 143.4 (C); LRMS m/z 433 (M^+), 418, 376, 278, 248, 220, 155, 91; HRMS calcd for $\text{C}_{22}\text{H}_{32}\text{NO}_3\text{SSi}$ (M^+-Me) 418.1892, found 418.1872. Anal. calcd for $\text{C}_{23}\text{H}_{35}\text{NO}_3\text{SSi}$: C, 63.70; H, 8.13; N, 3.23; S, 7.39. Found: C, 63.68; H, 8.12; N, 3.20; S, 7.29.

4.3.11. N-Cyclohex-2-enyl-4-methyl-N-(3-methylene-pent-4-enyl)-benzenesulfonamide (12h). A colorless oil; IR (neat) ν 2934, 1648, 1595, 1494, 1450, 1392, 1340, 1224, 1160, 1126, 1097, 1019 cm^{-1} ; ^1H NMR (270 MHz, CDCl_3) δ 1.48–1.96 (m, 6H), 2.42 (s, 3H), 2.46–2.82 (m, 2H), 2.99–3.28 (m, 2H), 4.48 (m, 1H), 5.01 (s, 1H), 5.05 (s, 1H), 5.07–5.12 (m, 1H), 5.11 (d, $J=10.8$ Hz, 1H), 5.40 (d, $J=17.3$ Hz, 1H), 5.75–5.80 (m, 1H), 6.33 (dd, $J=10.8$, 17.3 Hz, 1H), 7.28 (d, $J=8.1$ Hz, 2H), 7.72 (d, $J=8.1$ Hz, 2H); ^{13}C NMR (67.8 MHz, CDCl_3) δ 21.5 (CH₃), 21.8 (CH₂), 24.4 (CH₂), 29.0 (CH₂), 34.6 (CH₂), 44.0 (CH₂), 55.4 (CH), 114.2 (CH₂), 117.3 (CH₂), 127.1 (CH), 127.7 (CH×2), 129.7 (CH×2), 132.3 (CH), 138.1 (C), 138.2 (CH), 143.0 (C), 145.9 (C); LRMS m/z 331 (M^+), 316, 288, 364, 351, 184, 176, 155, 91; HRMS calcd for $\text{C}_{19}\text{H}_{25}\text{NO}_2\text{S}$ (M^+) 331.1606, found 331.1605.

4.3.12. N-Cyclohex-1-enylmethyl-4-methyl-N-(2-methylene-but-3-enyl)-benzenesulfonamide (15b). A colorless oil; IR (neat) ν 1597, 1338, 1160 cm^{-1} ; ^1H NMR (400 MHz, CDCl_3) δ 1.46–1.51 (m, 4H), 1.81 (br, 2H), 1.90 (br, 2H), 2.42 (s, 3H), 3.64 (s, 2H), 3.91 (s, 2H), 5.05 (s, 1H), 5.06 (d, $J=10.8$ Hz, 1H), 5.13 (s, 1H), 5.29 (d, $J=18.0$ Hz, 1H), 5.46 (br, 1H), 6.30 (dd, $J=18.0$, 10.8 Hz, 1H), 7.29 (d, $J=8.4$ Hz, 2H), 7.70 (d, $J=8.4$ Hz, 2H); ^{13}C NMR (100 MHz, CDCl_3) δ 21.5 (CH₃), 22.1 (CH₂), 22.5 (CH₂), 25.2 (CH₂), 26.2 (CH₂), 48.6 (CH₂), 54.6 (CH₂), 114.3 (CH₂), 117.6 (CH₂), 126.8 (CH), 127.2 (CH×2), 129.4 (CH×2), 132.3 (C), 136.6 (CH), 137.0 (C), 140.3 (C), 142.9 (C); LRMS m/z 331 (M^+), 316, 302, 290, 276, 264, 249, 236, 198, 184, 176, 155, 148, 133, 119, 106; HRMS calcd for $\text{C}_{19}\text{H}_{25}\text{NO}_2\text{S}$ (M^+) 331.1606, found 331.1606. Anal. calcd for $\text{C}_{19}\text{H}_{25}\text{NO}_2\text{S}$: C, 68.85; H, 7.60; N, 4.23; S, 9.67. Found: C, 68.73; H, 7.61; N, 4.29; S, 9.77.

4.3.13. 2-(Toluene-4-sulfonyl)-1,2,3,4,5,6-hexahydro-cyclohepta[c]pyrrole (17a). A colorless crystals. Mp 111–113 °C (ether); IR (nujol) ν 2924, 2854, 1654, 1344, 1163 cm^{-1} ; ^1H NMR (400 MHz, CDCl_3) δ 1.78 (m, 2H), 2.20 (br, 2H), 2.31 (m, 2H), 2.43 (s, 3H), 4.10 (br, 4H), 5.52 (d, $J=11.6$ Hz, 1H), 5.83 (dt, $J=11.6$, 5.6 Hz, 1H), 7.32 (d, $J=8.0$ Hz, 2H), 7.72 (d, $J=8.0$ Hz, 2H); ^{13}C NMR (100 MHz, CDCl_3) δ 21.6 (CH₃), 23.4 (CH₂), 29.5 (CH₂), 30.6 (CH₂), 58.4 (CH₂), 59.5 (CH₂), 120.3 (CH), 127.2 (C), 127.4 (CH×2), 129.6 (CH×2), 133.9 (C), 134.1 (C), 134.7 (CH), 143.2 (C); LRMS m/z 289 (M^+), 155, 134, 91; HRMS calcd for $\text{C}_{16}\text{H}_{19}\text{NO}_2\text{S}$ (M^+) 289.1136, found 289.1124.

4.3.14. Dimeric compound 18b. A colorless solid; IR (nujol) ν 2924, 2854, 1598, 1348, 1157 cm^{-1} ; ^1H NMR (400 MHz, CDCl_3) δ 1.29–1.39 (m, 8H), 2.05–2.09 (m, 4H), 2.12–2.16 (m, 4H), 2.41 (s, 6H), 4.06 (s, 4H), 4.16 (s, 4H), 5.34 (m, 2H), 6.10 (d, $J=16.0$ Hz, 2H), 7.30 (d, $J=8.0$ Hz, 4H), 7.70 (d, $J=8.0$ Hz, 4H); ^{13}C NMR (100 MHz, CDCl_3) δ 21.5 (CH₃×2), 24.4 (CH₂×2), 25.6 (CH₂×2), 26.8 (CH₂×2), 30.9 (CH₂×2), 55.1 (CH₂×2), 57.5 (CH₂×2), 121.8 (CH×2), 127.4 (CH×4), 129.0 (C×2), 129.7 (CH×4), 131.6 (CH×2), 133.2 (C×2), 134.3 (C×2), 143.4 (C×2); LRMS m/z 606 (M^+), 518, 451, 295, 155, 91; HRMS calcd for $\text{C}_{34}\text{H}_{42}\text{N}_2\text{O}_4\text{S}_2$ (M^+) 606.2586, found 606.2581.

4.3.15. 2-(Toluene-4-sulfonyl)-2,3,4,5,6,7-hexahydro-1H-cycloocta[c]pyrrole (17b). A colorless solid; IR (nujol) ν

2924, 2854, 1654, 1344, 1162 cm^{-1} ; ^1H NMR (270 MHz, CDCl_3) δ 1.45–1.52 (m, 2H), 1.59–1.67 (m, 2H), 2.03–2.07 (m, 2H), 2.13–2.17 (m, 2H), 2.43 (s, 3H), 4.03 (s, 4H), 5.62–5.66 (m, 2H), 7.32 (d, $J=8.1$ Hz, 2H), 7.72 (d, $J=8.1$ Hz, 2H); ^{13}C NMR (67.8 MHz, CDCl_3) δ 21.6 (CH_3), 21.6 (CH_2), 25.4 (CH_2), 27.0 (CH_2), 27.1 (CH_2), 58.2 (CH_2), 59.2 (CH_2), 122.3 (CH), 127.1 (C), 127.5 ($\text{CH}\times 2$), 129.7 ($\text{CH}\times 2$), 132.7 (CH), 132.9 (C), 134.3 (C), 143.3 (C); LRMS m/z 303 (M^+), 155, 148, 91; HRMS calcd for $\text{C}_{17}\text{H}_{21}\text{NO}_2\text{S}$ (M^+) 303.1293, found 303.1299.

4.3.16. 3-Hex-5-enyl-1-(toluene-4-sulfonyl)-4-vinyl-2,5-dihydro-1H-pyrrole (19b). A colorless solid; IR (film) ν 2926, 2855, 1654, 1598, 1347, 1164 cm^{-1} ; ^1H NMR (400 MHz, CDCl_3) δ 1.26–1.40 (m, 4H), 1.98–2.05 (m, 2H), 2.12–2.15 (m, 2H), 2.43 (s, 3H), 4.11 (s, 2H), 4.22 (s, 2H), 4.93–4.99 (m, 3H), 5.12 (d, $J=10.8$ Hz, 1H), 5.74 (m, 1H), 6.43 (dd, $J=17.2$, 10.8 Hz, 1H), 7.32 (d, $J=8.1$ Hz, 2H), 7.73 (d, $J=8.0$ Hz, 2H); ^{13}C NMR (100 MHz, CDCl_3) δ 21.6 (CH_3), 26.0 (CH_2), 27.3 (CH_2), 28.5 (CH_2), 33.4 (CH_2), 54.9 (CH_2), 57.6 (CH_2), 114.7 (CH_2), 115.3 (CH_2), 127.4 ($\text{CH}\times 2$), 129.4 (CH), 129.7 ($\text{CH}\times 2$), 130.8 (C), 133.9 (C), 135.8 (C), 138.3 (CH), 143.4 (C); LRMS m/z 331 (M^+), 248, 176, 155, 91; HRMS calcd for $\text{C}_{19}\text{H}_{25}\text{NO}_2\text{S}$ (M^+) 331.1606, found 331.1592.

4.3.17. Dimeric compound 18c. A colorless solid; IR (nujol) ν 2923, 2854, 1598, 1348, 1157 cm^{-1} ; ^1H NMR (400 MHz, CDCl_3) δ 0.99–1.38 (m, 12H), 2.01–2.14 (m, 8H), 2.42 (s, 6H), 4.05 (s, 4H), 4.19 (s, 4H), 5.33 (m, 2H), 6.02 (d, $J=15.6$ Hz, 2H), 7.32 (d, $J=8.0$ Hz, 4H), 7.73 (d, $J=8.0$ Hz, 4H); ^{13}C NMR (100 MHz, CDCl_3) δ 21.6 ($\text{CH}_3\times 2$), 25.3 ($\text{CH}_2\times 2$), 26.9 ($\text{CH}_2\times 2$), 27.0 ($\text{CH}_2\times 2$), 27.9 ($\text{CH}_2\times 2$), 33.1 ($\text{CH}_2\times 2$), 55.2 ($\text{CH}_2\times 2$), 57.0 ($\text{CH}_2\times 2$), 121.6 ($\text{CH}\times 2$), 127.4 ($\text{CH}\times 4$), 129.5 (C $\times 2$), 129.6 ($\text{CH}\times 4$), 132.1 ($\text{CH}\times 2$), 132.4 (C $\times 2$), 134.1 ($\text{CH}\times 2$), 143.3 (C $\times 2$); LRMS m/z 634 (M^+), 479, 451, 323, 155, 91; HRMS calcd for $\text{C}_{36}\text{H}_{46}\text{N}_2\text{O}_4\text{S}_2$ (M^+) 634.2899, found 634.2902.

4.3.18. N-Benzyl-3,6,7,8-tetrahydro-cyclohepta[c]-pyrrol-1(2H)-one (17d). A colorless liquid; IR (neat) ν 1674 (s), 1495 (m), 1452 (s) cm^{-1} ; ^1H NMR (270 MHz, CDCl_3) δ 1.84–1.92 (m, 2H), 2.47 (dt, $J=5.6$, 5.4 Hz, 2H), 2.63 (br, 2H), 3.71 (t, $J=2.2$ Hz, 2H), 4.63 (s, 2H), 5.78 (dt, $J=11.3$, 2.0 Hz, 1H), 6.10 (dt, $J=11.3$, 5.6 Hz, 1H), 7.23–7.35 (m, 5H); ^{13}C NMR (67.8 MHz, CDCl_3) δ 22.8, 27.3, 31.9, 46.2, 52.4, 121.0, 127.3, 127.9, 128.6, 133.9, 137.4, 139.1, 143.8, 172.0; EI-LRMS m/z 239 (M^+), 162, 148, 105, 91, 77; EI-HRMS m/z calcd for $\text{C}_{16}\text{H}_{17}\text{ON}$ (M^+) 239.1310, found 239.1320.

4.3.19. N-Benzyl-2,3,6,7,8,9-hexahydro-1H-cycloocta[c]-pyrrol-1-one (17e). A colorless liquid; IR (neat) ν 1683 (s), 1636 (m), 1604 (w), 1495 (m), 1453 (s) cm^{-1} ; ^1H NMR (270 MHz, CDCl_3) δ 1.55–1.64 (m, 2H), 1.78–1.87 (m, 2H), 2.27–2.34 (m, 2H), 2.48–2.52 (m, 2H), 3.64 (t, $J=2.1$ Hz, 2H), 4.62 (s, 2H), 5.78–5.95 (m, 2H), 7.22–7.36 (m, 5H); ^{13}C NMR (67.8 MHz, CDCl_3) δ 21.4, 25.0, 25.4, 27.1, 46.3, 52.6, 123.0, 127.3, 128.0, 128.6, 133.0, 135.2, 137.4, 143.5, 172.1; EI-LRMS m/z 253 (M^+), 224, 162, 91; EI-HRMS m/z calcd for $\text{C}_{17}\text{H}_{19}\text{ON}$ (M^+) 253.1467, found 253.1463.

4.3.20. Dimeric compound 18e. A colorless liquid; IR (neat) ν 1678 (s), 1480 (m), 1453 (m), 1410 (m) cm^{-1} ; ^1H NMR (270 MHz, CDCl_3) δ 1.46–1.64 (m, 8H), 2.20–2.29 (m, 4H), 2.36–2.43 (m, 4H), 3.83 (br, 4H), 4.61 (br, 4H), 5.80 (dt, $J=6.6$, 16.0 Hz, 2H), 6.42 (d, $J=16.0$ Hz, 2H), 7.21–7.34 (m, 10H); EI-LRMS m/z 506 (M^+), 415, 368, 304, 227, 91; EI-HRMS m/z calcd for $\text{C}_{34}\text{H}_{38}\text{O}_2\text{N}_2$ (M^+) 506.2933, found 506.2916.

4.3.21. N-Benzyl-3-(hex-5-enyl)-4-vinyl-5-hydro-1H-pyrrol-1-one (19d). A colorless liquid; IR (neat) ν 1681 (s), 1640 (m), 1624 (m), 1452 (m), 1408 (m) cm^{-1} ; ^1H NMR (270 MHz, CDCl_3) δ 1.40–1.64 (m, 4H), 2.03–2.13 (m, 2H), 2.40 (t, $J=7.4$ Hz, 2H), 3.87 (s, 2H), 4.64 (s, 2H), 4.90–5.04 (m, 2H), 5.28 (d, $J=10.9$ Hz, 1H), 5.31 (d, $J=17.6$ Hz, 1H), 5.81 (ddt, $J=10.2$, 17.0, 6.6 Hz, 1H), 6.70 (dd, $J=10.9$, 17.6 Hz, 1H), 7.21–7.38 (m, 5H); EI-LRMS m/z 281 (M^+), 252, 240, 226, 213, 190, 149, 122, 109, 91; EI-HRMS m/z calcd for $\text{C}_{19}\text{H}_{23}\text{ON}$ (M^+) 281.1779, found 281.1755.

4.3.22. N-Benzyl-N-(2-methylene-but-3-enyl)-1-cyclohexene-1-carboxamide (23). A colorless liquid; IR (neat) ν 1658 (m), 1621 (s), 1495 (m), 1453 (s), 1418 (s) cm^{-1} ; ^1H NMR (270 MHz, CDCl_3) δ 1.55–1.72 (m, 4H), 2.02–2.10 (m, 2H), 2.21–2.27 (m, 2H), 4.02–4.22 (m, 2H), 4.58 (s, 2H), 4.88–5.36 (m, 4H), 5.87 (m, 1H), 6.38 (dd, $J=11.0$, 17.7 Hz, 1H), 7.15–7.38 (m, 5H); EI-LRMS m/z 281 (M^+), 240, 214, 190, 172, 109; EI-HRMS m/z calcd for $\text{C}_{19}\text{H}_{23}\text{ON}$ (M^+) 281.1779, found 281.1754.

4.4. Procedure for the Diels–Alder reaction

4.4.1. (2S*)-2-((3S*)-3-Hydroxy-pent-4-enyl)-1-(toluene-sulfonyl)-4-vinyl-2,5-dihydro-1H-pyrrole. A solution of **9b** (55 mg, 0.12 mmol) in THF (1.0 mL) was added TBAF (1.0 M in THF, 0.2 mL, 0.2 mmol) at 0 $^\circ\text{C}$, and the solution was stirred at room temperature for 3 h. To this solution was added saturated NH_4Cl aq., and the aqueous layer was extracted with ethyl acetate. The organic layer was washed with brine, dried over Na_2SO_4 , and evaporated. The residue was purified by column chromatography on silica gel (hexane/ethyl acetate 4:1–1:1) to yield title alcohol (40 mg, 98%) as a colorless oil. IR (neat) ν 3518, 1647, 1598, 1342, 1160 cm^{-1} ; ^1H NMR (400 MHz, CDCl_3) δ 1.45–1.53 (m, 1H), 1.59–1.68 (m, 1H), 1.86 (br, 1H), 1.87–1.92 (m, 2H), 2.41 (s, 3H), 4.13 (dt, $J=6.4$, 6.4 Hz, 1H), 4.17–4.28 (m, 2H), 4.57 (m, 1H), 5.01 (d, $J=17.6$ Hz, 1H), 5.11 (d, $J=10.0$ Hz, 1H), 5.11 (d, $J=10.8$ Hz, 1H), 5.23 (d, $J=17.6$ Hz, 1H), 5.48 (m, 1H), 5.85 (ddd, $J=17.6$, 10.0, 6.4 Hz, 1H), 6.32 (dd, $J=17.6$, 10.8 Hz, 1H), 7.30 (d, $J=8.0$ Hz, 2H), 7.71 (d, $J=8.0$ Hz, 2H); ^{13}C NMR (100 MHz, CDCl_3) δ 21.5 (CH_3), 31.5 (CH_2), 31.5 (CH_2), 54.4 (CH_2), 67.0 (CH), 72.9 (CH), 114.7 (CH_2), 116.8 (CH_2), 127.3 ($\text{CH}\times 2$), 127.5 (CH), 129.6 ($\text{CH}\times 2$), 129.7 (CH), 134.3 (C), 136.6 (C), 140.8 (CH), 143.4 (C); LRMS m/z 315 ($\text{M}^+-\text{H}_2\text{O}$), 248, 178, 155, 91; HRMS calcd for $\text{C}_{18}\text{H}_{21}\text{NO}_2\text{S}$ ($\text{M}^+-\text{H}_2\text{O}$) 315.1293, found 315.1301.

4.4.2. (5aS*,8aS*,8bR*)-1-(Toluene-4-sulfonyl)-2,4,5,5a,7,8,8a,8b-octahydro-1H-benzo[cd]indol-6-one (11). To a suspension of Dess–Martin periodinane (77 mg, 0.18 mmol) in CH_2Cl_2 (0.5 mL) was added a solution of

alcohol (40 mg, 0.12 mmol) in CH_2Cl_2 (0.7 mL) at 0 °C, and the solution was stirred at room temperature for 1 h. To this solution was added saturated NaHCO_3 aq. and saturated $\text{Na}_2\text{S}_2\text{O}_3$ aq., and the aqueous layer was extracted with ether. The organic layer was washed with brine, dried over Na_2SO_4 , and evaporated. The residue was purified by column chromatography on silica gel (hexane/ethyl acetate 3:1) to yield **10** and **11** as an inseparable mixture. This mixture was allowed at room temperature to give **11** (35 mg, 88%) as colorless needles. Mp 136.5–139 °C. (Ethyl acetate/hexane); IR (film) ν 1713, 1598, 1341, 1164 cm^{-1} ; ^1H NMR (400 MHz, CDCl_3) δ 1.24–1.33 (m, 1H), 1.86–1.98 (m, 2H), 2.08–2.16 (m, 2H), 2.24–2.37 (m, 3H), 2.43 (s, 3H), 2.60 (m, 1H), 2.79 (br, 1H), 3.79–3.83 (m, 1H), 3.91 (d, $J=13.2$ Hz, 1H), 4.24 (ddd, $J=13.2$, 8.0, 5.2 Hz, 1H), 5.61 (br, 1H), 7.33 (d, $J=8.0$ Hz, 2H), 7.75 (d, $J=8.0$ Hz, 2H); ^{13}C NMR (100 MHz, CDCl_3) δ 20.9 (CH_2), 21.0 (CH_2), 21.6 (CH_3), 28.5 (CH_2), 36.6 (CH_2), 41.9 (CH), 42.3 (CH), 51.1 (CH_2), 58.2 (CH), 121.6 (CH), 127.4 ($\text{CH}\times 2$), 129.7 ($\text{CH}\times 2$), 134.0 (C), 134.7 (C), 143.6 (C), 209.9 (C); LRMS m/z 331 (M^+), 274, 176, 155, 120, 91; HRMS calcd for $\text{C}_{18}\text{H}_{21}\text{NO}_3\text{S}$ (M^+) 331.1242, found 331.1233. Anal. calcd for $\text{C}_{18}\text{H}_{21}\text{NO}_3\text{S}$: C, 65.23; H, 6.39; N, 4.23; S, 9.68. Found: C, 65.03; H, 6.40; N, 4.22; S, 9.52.

4.5. Typical procedure for the preparation of cycloalkene-yne **2**

To a suspension of NaH (60% oil suspension, 147 mg, 3.6 mmol) in THF/DMF (5 mL each) was added a solution of **3a** (673 mg, 3.0 mmol) in THF/DMF (5 mL each) at 0 °C, and the solution was stirred at room temperature for 60 min. To this solution was added 3-bromocyclohexene (0.4 mL, 3.6 mmol). The whole solution was warmed at 40 °C for 4.5 h. To this solution was added saturated NH_4Cl aq., and the aqueous layer was extracted with ethyl acetate. The organic layer was washed with brine, dried over Na_2SO_4 , and evaporated. The residue was purified by column chromatography on silica gel (hexane/ether 5:1) to yield **2a** (900 mg, quant.) as a colorless solid.

4.6. Spectral data for cycloalkene-yne **2**

4.6.1. N-But-2-ynyl-N-cyclohex-2-enyl-4-methyl-benzenesulfonamide (2a). A colorless solid. Mp 84–86 °C. (Ether/hexane); IR (film) ν 2225, 1647, 1334, 1160 cm^{-1} ; ^1H NMR (270 MHz, CDCl_3) δ 1.68 (t, $J=2.4$ Hz, 3H), 1.74–1.81 (m, 4H), 1.95 (br, 2H), 2.42 (s, 3H), 3.83–4.09 (m, 2H), 4.49 (br, 1H), 5.30–5.33 (m, 1H), 5.83–5.87 (m, 1H), 7.27 (d, $J=8.3$ Hz, 2H), 7.81 (d, $J=8.3$ Hz, 2H); ^{13}C NMR (100 MHz, CDCl_3) δ 3.4 (CH_3), 21.4 (CH_3), 21.4 (CH_2), 24.3 (CH_2), 27.9 (CH_2), 33.1 (CH_2), 54.9 (CH), 75.5 (C), 79.6 (C), 127.1 (CH), 127.2 ($\text{CH}\times 2$), 129.0 ($\text{CH}\times 2$), 132.5 (CH), 138.1 (C), 142.7 (C); LRMS m/z 303 (M^+), 155, 148, 91; HRMS calcd for $\text{C}_{17}\text{H}_{21}\text{NO}_2\text{S}$ (M^+) 303.1293, found 303.1287. Anal. calcd for $\text{C}_{17}\text{H}_{21}\text{NO}_2\text{S}$: C, 67.29; H, 6.98; N, 4.62; S, 10.57. Found: C, 67.22; H, 6.82; N, 4.54; S, 10.56.

4.6.2. N-But-2-ynyl-N-cyclohept-2-enyl-4-methyl-benzenesulfonamide (2b). A colorless solid. Mp 93–96 °C. (Ether/hexane); IR (nujol) ν 2213, 1647, 1596, 1336,

1162 cm^{-1} ; ^1H NMR (270 MHz, CDCl_3) δ 1.26–2.23 (m, 8H), 1.68 (t, $J=2.4$ Hz, 3H), 2.42 (s, 3H), 3.93–4.10 (m, 2H), 4.56 (br, 1H), 5.52 (m, 1H), 5.70–5.79 (m, 1H), 7.27 (d, $J=8.3$ Hz, 2H), 7.77 (d, $J=8.3$ Hz, 2H); ^{13}C NMR (67.8 MHz, CDCl_3) δ 3.5 (CH_3), 21.5 (CH_3), 26.3 (CH_2), 27.6 (CH_2), 28.2 (CH_2), 33.2 (CH_2), 33.7 (CH_2), 59.6 (CH), 75.2 (C), 80.1 (C), 127.5 ($\text{CH}\times 2$), 129.2 ($\text{CH}\times 2$), 132.3 (CH), 133.4 (CH), 138.2 (C), 142.9 (C); LRMS m/z 317 (M^+), 249, 234, 162, 155, 94, 91; HRMS calcd for $\text{C}_{18}\text{H}_{23}\text{NO}_2\text{S}$ (M^+) 317.1449, found 317.1442. Anal. calcd for $\text{C}_{18}\text{H}_{23}\text{NO}_2\text{S}$: C, 68.10; H, 7.30; N, 4.41; S, 10.10. Found: C, 68.08; H, 7.18; N, 4.37; S, 10.15.

4.6.3. N-But-2-ynyl-N-cyclooct-2-enyl-4-methyl-benzenesulfonamide (2c). A colorless solid. Mp 85–87 °C. (Ethyl acetate/hexane); IR (nujol) ν 2214, 1648, 1597, 1333, 1162 cm^{-1} ; ^1H NMR (270 MHz, CDCl_3) δ 1.32–1.77 (m, 8H), 1.67 (t, $J=2.4$ Hz, 3H), 2.11–2.21 (m, 2H), 2.40 (s, 3H), 3.96–4.16 (m, 2H), 4.79–4.88 (m, 1H), 5.54–5.62 (m, 2H), 7.24 (d, $J=8.3$ Hz, 2H), 7.75 (d, $J=8.3$ Hz, 2H); ^{13}C NMR (67.8 MHz, CDCl_3) δ 3.4 (CH_3), 21.5 (CH_3), 24.6 (CH_2), 26.1 (CH_2), 26.2 (CH_2), 29.0 (CH_2), 33.5 (CH_2), 34.5 (CH_2), 55.6 (CH), 75.1 (C), 80.2 (C), 127.6 ($\text{CH}\times 2$), 128.4 (CH), 129.0 ($\text{CH}\times 2$), 130.1 (CH), 138.0 (C), 142.8 (C); LRMS m/z 331 (M^+), 249, 234, 176, 155, 94, 91; HRMS calcd for $\text{C}_{19}\text{H}_{25}\text{NO}_2\text{S}$ (M^+) 331.1606, found 331.1631. Anal. calcd for $\text{C}_{19}\text{H}_{25}\text{NO}_2\text{S}$: C, 68.85; H, 7.60; N, 4.23; S, 9.67. Found: C, 68.87; H, 7.56; N, 4.24; S, 9.66.

4.6.4. N-Cyclohex-2-enyl-4-methyl-N-prop-2-ynyl-benzenesulfonamide (2d). A colorless solid; IR (nujol) ν 2116, 1653, 1596, 1332, 1157 cm^{-1} ; ^1H NMR (270 MHz, CDCl_3) δ 1.52–1.98 (m, 6H), 2.16 (t, $J=2.4$ Hz, 1H), 2.42 (s, 3H), 3.91 (dd, $J=18.4$, 2.4 Hz, 1H), 4.13 (dd, $J=18.4$, 2.4 Hz, 1H), 4.46–4.51 (m, 1H), 5.29–5.33 (m, 1H), 5.86–5.91 (m, 1H), 7.28 (d, $J=8.4$ Hz, 2H), 7.81 (d, $J=8.4$ Hz, 2H); ^{13}C NMR (67.8 MHz, CDCl_3) δ 21.4 (CH_2), 21.5 (CH_3), 24.3 (CH_2), 28.0 (CH_2), 32.6 (CH_2), 55.1 (CH), 72.0 (CH), 80.6 (C), 127.0 (CH), 127.4 ($\text{CH}\times 2$), 129.4 ($\text{CH}\times 2$), 133.2 (CH), 137.9 (C), 143.2 (C); LRMS m/z 289 (M^+), 155, 134, 91; HRMS calcd for $\text{C}_{16}\text{H}_{19}\text{NO}_2\text{S}$ (M^+) 289.1136, found 289.1126. Anal. calcd for $\text{C}_{16}\text{H}_{19}\text{NO}_2\text{S}$: C, 66.40; H, 6.62; N, 4.84; S, 11.08. Found: C, 66.46; H, 6.58; N, 4.89; S, 11.04.

4.6.5. N-Cyclohept-2-enyl-4-methyl-N-prop-2-ynyl-benzenesulfonamide (2e). A colorless oil; IR (neat) ν 2120, 1654, 1598, 1336, 1160 cm^{-1} ; ^1H NMR (270 MHz, CDCl_3) δ 1.30–2.24 (m, 8H), 2.17 (t, $J=2.4$ Hz, 1H), 2.42 (s, 3H), 4.01 (d, $J=2.4$ Hz, 1H), 4.14 (d, $J=2.4$ Hz, 1H), 4.56 (br, 1H), 5.49 (m, 1H), 5.71–5.81 (m, 1H), 7.27 (d, $J=8.1$ Hz, 2H), 7.78 (d, $J=8.1$ Hz, 2H); ^{13}C NMR (67.8 MHz, CDCl_3) δ 21.5 (CH_3), 26.2 (CH_2), 27.3 (CH_2), 28.1 (CH_2), 33.1 (CH_2), 33.2 (CH_2), 59.7 (CH), 72.2 (CH), 80.1 (C), 127.4 ($\text{CH}\times 2$), 129.4 ($\text{CH}\times 2$), 132.7 (CH), 132.9 (CH), 137.8 (C), 143.2 (C); LRMS m/z 303 (M^+), 155, 148, 91; HRMS calcd for $\text{C}_{17}\text{H}_{21}\text{NO}_2\text{S}$ (M^+) 303.1293, found 303.1282. Anal. calcd for $\text{C}_{17}\text{H}_{21}\text{NO}_2\text{S}$: C, 67.29; H, 6.98; N, 4.62; S, 10.57. Found: C, 67.10; H, 6.93; N, 4.60; S, 10.58.

4.6.6. N-Cyclooct-2-enyl-4-methyl-N-prop-2-ynyl-benzenesulfonamide (2f). The title compound was prepared in quantitative yield according to the literature procedure.^{7c}

4.6.7. *N*-Cyclohex-2-enyl-4-methyl-*N*-pent-3-ynyl-benzenesulfonamide (2g). A colorless oil; IR (neat) ν 2934, 1598, 1494, 1448, 1393, 1340, 1233, 1161, 1097, 1044 cm^{-1} ; ^1H NMR (270 MHz, CDCl_3) δ 1.47–1.96 (m, 6H), 1.77 (t, $J=2.4$ Hz, 3H), 2.42 (s, 3H), 2.36–2.70 (m, 2H), 3.01–3.29 (m, 2H), 4.45 (m, 1H), 5.01–5.05 (m, 1H), 5.75–5.80 (m, 1H), 7.29 (d, $J=8.4$ Hz, 2H), 7.73 (d, $J=8.4$ Hz, 2H); ^{13}C NMR (67.8 MHz, CDCl_3) δ 3.4 (CH_3), 21.5 (CH_3), 21.7 (CH_2), 22.3 (CH_2), 24.4 (CH_2), 28.9 (CH_2), 43.6 (CH_2), 55.4 (CH), 76.12 (C), 77.4 (C), 127.1 (CH), 127.4 ($\text{CH}\times 2$), 129.7 ($\text{CH}\times 2$), 132.5 (CH), 137.8 (C), 143.1 (C); LRMS m/z 317 (M^+), 302, 288, 264, 250, 236, 184, 182, 155, 91; HRMS calcd for $\text{C}_{18}\text{H}_{23}\text{NO}_2\text{S}$ (M^+) 317.1449, found 317.1455.

4.6.8. *N*-But-3-ynyl-*N*-cyclohex-2-enyl-4-methyl-benzenesulfonamide (2h). A colorless crystals. Mp 66–67 $^\circ\text{C}$; IR (nujol) ν 3277, 2968, 2867, 1697, 1648, 1597, 1493, 1450, 1336, 1238, 1198, 1162, 1097 cm^{-1} ; ^1H NMR (270 MHz, CDCl_3) δ 1.46–1.62 (m, 2H), 1.75–1.96 (m, 4H), 2.02 (t, $J=2.7$ Hz, 1H), 2.42 (s, 3H), 2.46–2.78 (m, 2H), 3.07–3.34 (m, 2H), 4.45 (m, 1H), 5.03 (m, 1H), 5.76–5.82 (m, 1H), 7.30 (d, $J=8.1$ Hz, 2H), 7.73 (d, $J=8.1$ Hz, 2H); ^{13}C NMR (67.8 MHz, CDCl_3) δ 21.4 (CH_3), 21.6 (CH_2), 21.9 (CH_2), 24.3 (CH_2), 28.8 (CH_2), 43.0 (CH_2), 55.3 (CH), 70.0 (C), 81.3 (CH), 127.0 (CH), 127.1 ($\text{CH}\times 2$), 129.7 ($\text{CH}\times 2$), 132.7 (CH), 137.6 (C), 143.2 (C); LRMS m/z 303 (M^+), 264, 249, 184, 155, 148, 108, 91. Anal. calcd for $\text{C}_{17}\text{H}_{21}\text{NO}_2\text{S}$: C, 67.29; H, 6.98; N, 4.62. Found: C, 67.15; H, 7.08; N, 4.73.

4.7. Synthesis of cycloalkene-yne 7

4.7.1. Carbonic acid (1R*, 4S*)-4-(*tert*-butyl-dimethylsilyloxy)-cyclohex-2-enyl ester methyl ester (6a). A solution of **5a** (789 mg, 3.45 mmol) in CH_2Cl_2 (17 mL) was added pyridine (0.84 mL, 10.4 mmol), methyl chloroformate (0.53 mL, 6.9 mmol) at 0 $^\circ\text{C}$, and the solution was stirred at 0 $^\circ\text{C}$ for 1 h. To this solution was added water, and the aqueous layer was extracted with ethyl acetate. The organic layer was washed with brine, dried over Na_2SO_4 , and evaporated. The residue was purified by column chromatography on silica gel (hexane/ethyl acetate 9:1) to yield **6a** (988 mg, quant.) as a colorless oil. IR (neat) ν 1747, 1472, 1462, 1442, 1395, 1360, 1344, 1321, 1309, 1270, 1224, 1205, 1149, 1094, 1046, 1025, 1005 cm^{-1} ; ^1H NMR (270 MHz, CDCl_3) δ 0.07 (s, 6H), 0.89 (s, 9H), 1.72–2.00 (m, 4H), 3.77 (s, 3H), 4.16 (br, 1H), 5.01 (br, 1H), 5.78 (dd, $J=3.8, 10.3$ Hz, 1H), 5.89 (dd, $J=2.7, 10.3$ Hz, 1H); ^{13}C NMR (67.8 MHz, CDCl_3) δ -4.7 (CH_3), -4.6 (CH_3), 18.0 (C), 25.3 (CH_2), 25.8 ($\text{CH}_3\times 3$), 28.2 (CH_2), 54.5 (CH_3), 66.2 (CH), 70.9 (CH), 125.4 (CH), 136.9 (CH), 155.4 (C); LRMS m/z 229 ($\text{M}^+ - \text{Bu}$), 211, 185, 151, 133; HRMS calcd for $\text{C}_{10}\text{H}_{17}\text{O}_4\text{Si}$ ($\text{M}^+ - \text{Bu}$) 229.0896, found 229.0880. Anal. calcd for $\text{C}_{14}\text{H}_{26}\text{O}_4\text{Si}$: C, 58.70; H, 9.15. Found: C, 58.73; H, 9.20.

4.7.2. Carbonic acid (1R*, 4S*)-4-(*tert*-butyl-dimethylsilyloxy)-cyclopent-2-enyl ester methyl ester (6b). A colorless oil; IR (neat) ν 1748, 1472, 1462, 1443, 1375, 1361, 1335, 1268, 1193, 1132, 1098, 1048, 1007 cm^{-1} ; ^1H NMR (270 MHz, CDCl_3) δ 0.06 (s, 6H), 0.86 (s, 9H), 1.65 (dt, $J=13.9, 7.3$ Hz, 1H), 2.80 (dt, $J=13.9, 7.3$ Hz, 1H), 3.74

(s, 3H), 4.68 (t, $J=5.7$ Hz, 1H), 5.35 (t, $J=5.7$ Hz, 1H), 5.89 (d, $J=5.4$ Hz, 1H), 5.97 (d, $J=5.4$ Hz, 1H); ^{13}C NMR (67.8 MHz, CDCl_3) δ -4.8 (CH_3), -4.7 (CH_3), 18.0 (C), 25.8 ($\text{CH}_3\times 3$), 40.9 (CH_2), 54.5 (CH_3), 74.6 (CH), 80.4 (CH), 130.5 (CH), 139.4 (CH), 155.4 (C); LRMS m/z 271 ($\text{M}^+ - \text{H}$), 215, 197, 171, 151, 133, 125, 111; HRMS calcd for $\text{C}_{13}\text{H}_{23}\text{O}_4\text{Si}$ ($\text{M}^+ - \text{H}$) 271.1365, found 271.1363.

4.7.3. *N*-{(1R*, 4S*)-4-(*tert*-Butyl-dimethylsilyloxy)-cyclohex-2-enyl}-4-methyl-*N*-prop-2-ynyl-benzenesulfonamide (7a). To a solution of **6a** (430 mg, 1.5 mmol), and PPh_3 (37 mg, 0.15 mmol) in THF (15 mL) was added $\text{Pd}_2\text{dba}_3\cdot\text{CHCl}_3$ (37 mg, 0.04 mmol), and the solution was degassed through freeze–pump–thaw cycle. The whole solution was stirred at room temperature for 48 h. The solvent was removed, and the residue was purified by flash column chromatography on silica gel (hexane/ethyl acetate 20:1–10:1) to yield **7a** (471 mg, 75%) as colorless needles. IR (film) ν 2121, 1654, 1598, 1338, 1255, 1163, 1093 cm^{-1} ; ^1H NMR (270 MHz, CDCl_3) δ 0.04 (s, 6H), 0.87 (s, 9H), 1.56–1.72 (m, 3H), 2.01–2.08 (m, 1H), 2.14 (t, $J=2.4$ Hz, 1H), 2.42 (s, 3H), 3.95 (dd, $J=18.4, 2.7$ Hz, 1H), 4.06 (m, 1H), 4.11 (dd, $J=18.4, 2.7$ Hz, 1H), 4.35–4.40 (m, 1H), 5.41 (dd, $J=10.0, 2.4$ Hz, 1H), 5.83–5.89 (m, 1H), 7.28 (d, $J=8.4$ Hz, 2H), 7.81 (d, $J=8.4$ Hz, 2H); ^{13}C NMR (67.8 MHz, CDCl_3) δ -4.8 (CH_3), -4.5 (CH_3), 18.0 (C), 21.5 (CH_3), 22.5 (CH_2), 25.8 ($\text{CH}_3\times 3$), 30.4 (CH_2), 32.9 (CH_2), 54.7 (CH), 63.0 (CH), 72.1 (CH), 80.3 (C), 127.5 ($\text{CH}\times 2$), 129.1 (CH), 129.5 ($\text{CH}\times 2$), 135.0 (CH), 137.9 (C), 143.3 (C); LRMS m/z 404 ($\text{M}^+ - \text{CH}_3$), 362, 266, 155, 132, 117, 91; HRMS calcd for $\text{C}_{18}\text{H}_{24}\text{NO}_3\text{SSi}$ ($\text{M}^+ - \text{Bu}$) 362.1246, found 362.1233. Anal. calcd for $\text{C}_{22}\text{H}_{33}\text{NO}_3\text{SSi}$: C, 62.97; H, 7.93; N, 3.34; S, 7.64. Found: C, 63.05; H, 7.80; N, 3.22; S, 7.59.

4.7.4. *N*-[(1R*, 4S*)-4-(*tert*-Butyl-dimethyl-silyloxy)-cyclopent-2-enyl]-4-methyl-*N*-prop-2-ynyl-benzenesulfonamide (7c). A colorless crystal. Mp 97.5 $^\circ\text{C}$ (EtOAc/hexane); IR (nujol) ν 3261, 2925, 2855, 2120, 1594, 1330, 1154 cm^{-1} ; ^1H NMR (270 MHz, CDCl_3) δ 0.02 (s, 6H), 0.84 (s, 9H), 1.57 (m, 1H), 2.08 (t, $J=2.4$ Hz, 1H), 2.41 (s, 3H), 2.46 (m, 1H), 4.02 (brs, 2H), 4.58 (br, 1H), 4.80 (br, 1H), 5.63 (m, 1H), 5.87 (m, 1H), 7.27 (d, $J=8.6$ Hz, 2H), 7.79 (d, $J=8.6$ Hz, 2H); ^{13}C NMR (67.8 MHz, CDCl_3) δ -4.8 (CH_3), -4.7 (CH_3), 18.0 (C), 21.5 (CH_3), 25.8 ($\text{CH}_3\times 3$), 32.4 (CH_2), 38.7 (CH_2), 61.8 (CH), 71.9 (C), 74.6 (CH), 80.7 (CH), 127.5 ($\text{CH}\times 2$), 129.4 ($\text{CH}\times 2$), 131.6 (CH), 137.5 (C), 138.2 (CH), 143.3 (C); LRMS m/z 405 (M^+), 390, 348, 308, 250, 155, 139, 118, 91. Anal. calcd for $\text{C}_{21}\text{H}_{31}\text{NO}_3\text{SSi}$: C, 62.18; H, 7.70; N, 3.45. Found: C, 61.97; H, 7.69; N, 3.47.

4.7.5. *N*-{(1S*, 4S*)-4-(*tert*-Butyl-dimethylsilyloxy)-cyclohex-2-enyl}-4-methyl-*N*-prop-2-ynyl-benzenesulfonamide (7b). To a solution of **5a** (437 mg, 1.92 mmol), **3b** (570 mg, 2.88 mmol), and PPh_3 (1.03 g, 3.83 mmol) in THF (10 mL) was added DEAD (0.6 mL, 3.83 mmol) at 0 $^\circ\text{C}$, and the solution was stirred at room temperature for 10 h. The solvent was removed, and the residue was purified by flash column chromatography on silica gel (hexane/ethyl acetate 9:1) to yield **7b** (500 mg, 62%) as a colorless oil. IR (neat) ν 2120, 1654, 1598, 1338, 1162 cm^{-1} ; ^1H NMR (400 MHz, CDCl_3) δ 0.05 (s, 6H), 0.87 (s, 9H), 1.47–1.56

(m, 1H), 1.73–1.83 (m, 1H), 1.87–1.91 (m, 1H), 1.97–2.01 (m, 1H), 2.17 (t, $J=2.4$ Hz, 1H), 2.42 (s, 3H), 3.88 (dd, $J=18.4$, 2.4 Hz, 1H), 4.07 (dd, $J=18.4$, 2.4 Hz, 1H), 4.24 (m, 1H), 4.50 (m, 1H), 5.29 (dd, $J=10.4$, 1.6 Hz, 1H), 5.74 (dd, $J=10.4$, 2.0 Hz, 1H), 7.27 (d, $J=8.0$ Hz, 2H), 7.78 (d, $J=8.0$ Hz, 2H); ^{13}C NMR (100 MHz, CDCl_3) δ -4.7 (CH_3), -4.5 (CH_3), 18.2 (C), 21.6 (CH_3), 25.9 ($\text{CH}_3\times 3$), 27.0 (CH_2), 32.5 (CH_2), 32.7 (CH_2), 55.3 (CH), 66.9 (CH), 72.3 (CH), 80.3 (C), 127.3 ($\text{CH}\times 2$), 127.8 (CH), 129.4 ($\text{CH}\times 2$), 137.5 (C), 137.6 (CH), 143.3 (C); LRMS m/z 404 (M^+-CH_3), 362, 288, 264, 155, 132, 91; HRMS calcd for $\text{C}_{18}\text{H}_{24}\text{NO}_3\text{SSi}$ (M^+-Bu) 362.1246, found 362.1230. Anal. calcd for $\text{C}_{22}\text{H}_{33}\text{NO}_3\text{SSi}$: C, 62.97; H, 7.93; N, 3.34; S, 7.64. Found: C, 62.83; H, 7.72; N, 3.16; S, 7.67.

4.7.6. *N*-[(1*S,4*S**)-4-(*tert*-Butyl-dimethyl-silanyloxy)-cyclopent-2-enyl]-4-methyl-*N*-prop-2-ynyl-benzenesulfonamide (7d).** A colorless oil; IR (neat) ν 3277, 2954, 2930, 2856, 2361, 2344, 1598, 1339, 1162 cm^{-1} ; ^1H NMR (270 MHz, CDCl_3) δ 0.02 (s, 6H), 0.84 (s, 9H), 1.84 (m, 1H), 2.07 (t, $J=2.4$ Hz, 1H), 2.13 (m, 1H), 2.41 (s, 3H), 3.78 (dd, $J=18.9$, 2.4 Hz, 1H), 3.97 (dd, $J=18.9$, 2.4 Hz, 1H), 4.98 (m, 1H), 5.20 (m, 1H), 5.55–5.59 (m, 1H), 5.89–5.93 (m, 1H), 7.27 (d, $J=8.4$ Hz, 2H), 7.77 (d, $J=8.4$ Hz, 2H); ^{13}C NMR (67.8 MHz, CDCl_3) δ -4.7 ($\text{CH}_3\times 2$), 18.1 (C), 21.5 (CH_3), 25.8 ($\text{CH}_3\times 3$), 32.5 (CH_2), 38.4 (CH_2), 63.3 (CH), 72.2 (C), 76.3 (CH), 79.9 (CH), 127.5 ($\text{CH}\times 2$), 129.5 ($\text{CH}\times 2$), 131.8 (CH), 137.3 (C), 139.6 (CH), 143.4 (C); LRMS m/z 405 (M^+), 390, 348, 250, 155, 139, 118, 91; HRMS calcd for $\text{C}_{20}\text{H}_{28}\text{NO}_3\text{SSi}$ (M^+-Me) 390.1559, found 390.1547. Anal. calcd for $\text{C}_{21}\text{H}_{31}\text{NO}_3\text{SSi}$: C, 62.18; H, 7.70; N, 3.45; S, 7.91. Found: C, 61.99; H, 7.68; N, 3.42; S, 8.08.

4.8. Typical procedure for the preparation of cycloalkene-yne 14

To a solution of **13a** (2.2 mL, 17.3 μmol) in CH_2Cl_2 (49 mL) was added DIBAL-H (42 mL, 39 mmol, 0.93 M in hexane), and the solution was stirred at -78°C for 1 h. To this solution was added MeOH and 3 N NaOH aq. at -78°C and the aqueous layer was extracted with Et_2O . The organic layer was washed with brine, dried over Na_2SO_4 and evaporated. To a solution of the crude alcohol in CH_2Cl_2 (32 mL) were added CBr_4 (6.5 g, 19.5 mmol) and PPh_3 (5.9 g, 22.5 mmol), and the solution was stirred at room temperature for 2 h. To a solution of propargyl bromide (5.9 mL, 86 mmol) and K_2CO_3 (9.6 g, 69 mmol) in CH_3CN (115 mL) was added the above solution, and the whole solution was stirred at room temperature for 16 h. Then the solution was filtered through Celite. To this mother liquid was added pyridine (15.5 mL, 193 mmol) and *p*-toluenesulfonyl chloride (24.5 g, 130 mmol), and the solution was stirred at room temperature for 25 h. To this solution was added MeOH and the solution was diluted with ethyl acetate. The organic layer was washed with 10% HCl aq., 10% NaOH aq., and brine, dried over Na_2SO_4 and evaporated. After the solvent was removed, the residue was purified by flash column chromatography on silica gel (hexane/ethyl acetate 5:1) to yield **14a** (2.3 g, 45%) as a colorless crystal.

Typical procedure for the preparation of cycloalkene-yne

14d–e. Et_3N (0.30 mL, 2.13 mmol) and $\text{ClPO}(\text{OEt})_2$ (0.17 mL, 1.16 mmol) was added to a solution of **13d** (108.5 mg, 0.97 mmol) in CH_2Cl_2 (5 mL) at 0°C . After stirring for 1 h at the same temperature, propargylamine (0.10 mL, 1.45 mmol) was added. The resulting solution was stirred for 22 h at room temperature. Saturated NaHCO_3 solution was added, and the aqueous phase was extracted with AcOEt. The organic phase was washed with saturated NH_4Cl solution and brine, and dried over MgSO_4 , filtered, and concentrated. The residue was purified by column chromatography on silica gel (hexane/AcOEt 3:2) to afford crude amide (89.7 mg, 62%). A solution of crude amide (260 mg, 1.74 mmol) in DMF (6 mL) was added to a suspension of NaH (85 mg, 2.09 mmol) in DMF (3 mL) at 0°C . After stirring for 1 h at room temperature, BnBr (0.33 mL, 2.79 mmol) was added at 0°C . The resulting solution was stirred for 30 min at room temperature. Saturated NH_4Cl solution was added, and the aqueous phase was extracted with AcOEt. The organic phase was washed with H_2O and brine, and dried over MgSO_4 , filtered, and concentrated. The residue was purified by column chromatography on silica gel (hexane/AcOEt 3:1) to afford **14d** (353 mg, 85%) as a pale yellow oil.

4.9. Spectral data for 14

4.9.1. *N*-Cyclopent-1-enylmethyl-4-methyl-*N*-prop-2-ynyl-benzenesulfonamide (14a). A colorless crystal. Mp 55.5°C . (Ether/hexane); IR (nujol) ν 3259, 2923, 2114, 1654, 1596, 1343, 1160 cm^{-1} ; ^1H NMR (270 MHz, CDCl_3) δ 1.89 (dt, $J=7.3$ Hz, 2H), 1.97 (t, $J=2.4$ Hz, 1H), 2.24–2.36 (m, 4H), 2.42 (s, 3H), 3.86 (s, 2H), 4.04 (d, $J=2.4$ Hz, 2H), 5.69 (brs, 1H), 7.28 (d, $J=8.1$ Hz, 2H), 7.74 (d, $J=8.1$ Hz, 2H); ^{13}C NMR (67.8 MHz, CDCl_3) δ 21.5 (CH_3), 23.4 (CH_2), 32.5 (CH_2), 33.0 (CH_2), 35.6 (CH_2), 46.5 (CH_2), 73.5 (CH), 76.7 (C), 127.8 ($\text{CH}\times 2$), 129.4 ($\text{CH}\times 2$), 130.6 (CH), 136.1 (C), 138.2 (C), 143.4 (C); LRMS m/z 289 (M^+), 155, 134, 91. Anal. calcd for $\text{C}_{16}\text{H}_{19}\text{NO}_2\text{S}$: C, 66.41; H, 6.62; N, 4.84; S, 11.08. Found: C, 66.42; H, 6.73; N, 4.79; S, 11.14.

4.9.2. *N*-Cyclohex-1-enylmethyl-4-methyl-*N*-prop-2-ynyl-benzenesulfonamide (14b). A colorless crystal. Mp 54 – 54.5°C . (Ether/hexane); IR (nujol) ν 3292, 2926, 2853, 1596, 1346, 1158 cm^{-1} ; ^1H NMR (270 MHz, CDCl_3) δ 1.57 (m, 4H), 1.94 (t, $J=2.4$ Hz, 1H), 1.99 (m, 4H), 2.42 (s, 3H), 3.67 (s, 2H), 4.02 (d, $J=2.4$ Hz, 2H), 5.68 (s, 1H), 7.28 ($J=8.4$ Hz, 2H), 7.73 (d, $J=8.4$ Hz, 2H); ^{13}C NMR (67.8 MHz, CDCl_3) δ 21.5 (CH_3), 22.2 (CH_2), 22.5 (CH_2), 25.2 (CH_2), 25.8 (CH_2), 35.2 (CH_2), 52.8 (CH_2), 73.4 (CH), 76.6 (C), 127.6 (CH), 127.8 ($\text{CH}\times 2$), 129.3 ($\text{CH}\times 2$), 131.6 (C), 136.2 (C), 143.3 (C); LRMS m/z 303 (M^+), 288, 222, 155, 148, 91; HRMS calcd for $\text{C}_{17}\text{H}_{21}\text{NO}_2\text{S}$ (M^+) 303.1293, found 303.1303. Anal. calcd for $\text{C}_{17}\text{H}_{21}\text{NO}_2\text{S}$: C, 67.29; H, 6.98; N, 4.62; S, 10.57. Found: C, 67.11; H, 7.13; N, 4.47; S, 10.71.

4.9.3. *N*-Cyclohept-1-enylmethyl-4-methyl-*N*-prop-2-ynyl-benzenesulfonamide (14c). A colorless crystal. Mp 72 – 73°C . (Ether/hexane); IR (nujol) ν 3304, 2922, 2852, 1654, 1597, 1348, 1163 cm^{-1} ; ^1H NMR (270 MHz, CDCl_3) δ 1.48–1.54 (m, 4H), 1.69 (m, 2H), 1.92 (t, $J=2.4$ Hz, 1H), 2.08–2.21 (m, 4H), 2.42 (s, 3H), 3.65 (s, 2H), 4.04 (d,

$J=2.4$ Hz, 2H), 5.79 (m, 1H), 7.28 (d, $J=8.4$ Hz, 2H), 7.74 (d, $J=8.4$ Hz, 2H); ^{13}C NMR (67.8 MHz, CDCl_3) δ 21.5 (CH_3), 26.7 (CH_2), 27.0 (CH_2), 28.5 (CH_2), 30.0 (CH_2), 32.2 (CH_2), 35.1 (CH_2), 54.4 (CH_2), 73.6 (CH), 77.2 (C), 127.9 ($\text{CH}\times 2$), 129.3 ($\text{CH}\times 2$), 132.9 (CH), 136.2 (C), 137.7 (C), 143.3 (C); LRMS m/z 317 (M^+), 162, 155, 91. Anal. calcd for $\text{C}_{16}\text{H}_{19}\text{NO}_2\text{S}$: C, 68.10; H, 7.30; N, 4.41; S, 10.10. Found: C, 68.00; H, 7.28; N, 4.46; S, 10.16.

4.9.4. N-Benzyl-N-(prop-2-ynyl)-1-cyclopentene-1-carboxamide (14d). A pale yellow oil; IR (neat) ν 2120 (w), 1714 (s), 1644 (s), 1606 (s), 1454 (s), 1244 (s) cm^{-1} ; ^1H NMR (270 MHz, CDCl_3) δ 1.93 (tt, $J=7.5, 7.5$ Hz, 2H), 2.25 (br, 1H), 2.43–2.52 (br, 2H), 2.63–2.72 (m, 2H), 4.06–4.14 (br, 2H), 4.75 (s, 2H), 6.08 (br, 1H), 7.24–7.37 (m, 5H); ^{13}C NMR (67.8 MHz, DMSO) δ 21.9, 32.4, 33.6, 35.4, 48.6, 73.7, 78.9, 126.5, 126.7, 127.7, 131.6, 136.4, 137.3, 167.7; EI-LRMS m/z 239 (M^+), 211, 200, 95, 91; EI-HRMS m/z calcd for $\text{C}_{16}\text{H}_{17}\text{ON}$ (M^+) 239.1310, found 239.1297.

4.9.5. N-Benzyl-N-(prop-2-ynyl)-1-cyclohexene-1-carboxamide (14e). A colorless liquid; IR (neat) ν 2118 (w), 1621 (s), 1495 (m), 1451 (s), 1239 (s) cm^{-1} ; ^1H NMR (270 MHz, CDCl_3) δ 1.58–1.75 (m, 4H), 2.07–2.15 (m, 2H), 2.23–2.30 (m, 3H), 4.04–4.10 (br, 2H), 4.73 (s, 2H), 5.99 (br, 1H), 7.23–7.37 (m, 5H); ^{13}C NMR (67.8 MHz, DMSO) δ 20.7, 21.1, 23.6, 24.9, 35.6, 48.5, 73.7, 78.9, 126.6, 126.9, 126.9, 127.9, 133.4, 136.6, 171.3; EI-LRMS m/z 253 (M^+), 214, 109, 91; EI-HRMS m/z calcd for $\text{C}_{17}\text{H}_{19}\text{ON}$ (M^+) 253.1467, found 253.1467.

References and notes

- (a) Grubbs, R. H. *Handbook of Metathesis*; Wiley-VCH: Weinheim, 2003. Recent reviews for olefin metathesis; (b) Grubbs, R. H.; Miller, S. J. *Acc. Chem. Res.* **1995**, *28*, 446. (c) Schuster, M.; Blechert, S. *Angew. Chem. Int. Ed. Engl.* **1997**, *36*, 2036. (d) Schmalz, H.-G. *Angew. Chem. Int. Ed. Engl.* **1995**, *34*, 1833. (e) Fürstner, A. *Topics in Organometallic Chemistry*; Springer: Berlin, 1998; Vol. 1. (f) Grubbs, R. H.; Chang, S. *Tetrahedron* **1998**, *54*, 4413. (g) Armstrong, S. K. *J. Chem. Soc., Perkin Trans. 1* **1998**, 371. (h) Phillips, A. J.; Abell, A. D. *Aldrichim. Acta* **1999**, *32*, 75. (i) Fürstner, A. *Angew. Chem. Int. Ed.* **2000**, *39*, 3013. (j) Trnka, T. M.; Grubbs, R. H. *Acc. Chem. Res.* **2001**, *34*, 18. (k) Schrock, R. R.; Hoveyda, A. H. *Angew. Chem. Int. Ed.* **2003**, *42*, 4592. (l) Connon, S. J.; Blechert, S. *Angew. Chem. Int. Ed.* **2003**, *42*, 1900. Review for enyne metathesis; (m) Mori, M. *Top. Organomet. Chem.* **1998**, *1*, 133. (n) Mori, M. *J. Synth. Org. Chem. Jpn* **1998**, *56*, 115. (o) Poulsen, C. S.; Madsen, R. *Synthesis* **2003**, 1.
- For **1a**: (a) Schwab, P.; France, M. B.; Ziller, J. W.; Grubbs, R. H. *Angew. Chem. Int. Ed. Engl.* **1995**, *34*, 2039. For **1b**: (b) Scholl, M.; Ding, S.; Lee, C. W.; Grubbs, R. H. *Org. Lett.* **1999**, *1*, 953. For **1c**: (c) Weskamp, T.; Schattenmann, W. C.; Spiegler, M.; Herrmann, W. A. *Angew. Chem. Int. Ed.* **1998**, *37*, 2490. (d) Huang, J.; Stevens, E. D.; Nolan, S. P.; Peterson, J. L. *J. Am. Chem. Soc.* **1999**, *121*, 2674. (e) Scholl, M.; Trnka, T. M.; Morgan, J. P.; Grubbs, R. H. *Tetrahedron Lett.* **1999**, *40*, 2247.
- Preliminary reports: (a) Kitamura, T.; Mori, M. *Org. Lett.* **2001**, *3*, 1161. (b) Mori, M.; Kuzuba, Y.; Kitamura, T.; Sato, Y. *Org. Lett.* **2002**, *4*, 3855. For reports from our laboratory; (c) Kinoshita, A.; Mori, M. *Synlett* **1994**, 1020. (d) Kinoshita, A.; Mori, M. *J. Org. Chem.* **1996**, *61*, 8356. (e) Kinoshita, A.; Mori, M. *Heterocycles* **1997**, *46*, 287. (f) Mori, M.; Sakakibara, N.; Kinoshita, A. *J. Org. Chem.* **1998**, *63*, 6082. (g) Kinoshita, A.; Sakakibara, N.; Mori, M. *J. Am. Chem. Soc.* **1997**, *119*, 12388. (h) Kinoshita, A.; Sakakibara, N.; Mori, M. *Tetrahedron* **1999**, *55*, 8155. (i) Mori, M.; Kitamura, T.; Sakakibara, N.; Sato, Y. *Org. Lett.* **2000**, *2*, 543. (j) Mori, M.; Kitamura, T.; Sato, Y. *Synthesis* **2001**, 654. (k) Kitamura, T.; Sato, Y.; Mori, M. *Chem. Commun.* **2001**, 1258. (l) Kitamura, T.; Sato, Y.; Mori, M. *Adv. Synth. Catal.* **2002**, *344*, 678. (m) Mori, M.; Tonogaki, K.; Nishiguchi, N. *J. Org. Chem.* **2002**, *67*, 224. (n) Saito, N.; Sato, Y.; Mori, M. *Org. Lett.* **2002**, *4*, 803. (o) Tonogaki, K.; Mori, M. *Tetrahedron Lett.* **2002**, *43*, 2235.
- Ruthenium carbene systems; (a) Kim, S.-H.; Bowden, N.; Grubbs, R. H. *J. Am. Chem. Soc.* **1994**, *116*, 10801. (b) Stragies, R.; Schuster, M.; Blechert, S. *Angew. Chem. Int. Ed. Engl.* **1997**, *36*, 2518. (c) Barrett, A. G. M.; Baugh, S. P. D.; Braddock, D. C.; Flack, K.; Gibson, V. C.; Giles, M. R.; Marshall, E. L.; Procopiou, P. A.; White, A. J. P.; Williams, D. J. *J. Org. Chem.* **1998**, *63*, 7893. (d) Hoye, R. T.; Donaldson, S. M.; Vos, T. *Org. Lett.* **1999**, *1*, 277. (e) Stragies, R.; Voigtmann, U.; Blechert, S. *Tetrahedron Lett.* **2000**, *41*, 5465. (f) Bentz, D.; Laschat, S. *Synthesis* **2000**, 1766. (g) Bentz, D.; Laschat, S. *Synthesis* **2000**, 1766. (h) Kulkarni, A. A.; Diver, S. T. *Org. Lett.* **2000**, *2*, 2271. (i) Schramm, M. P.; Reddy, D. S.; Kozmin, S. A. *Angew. Chem. Int. Ed.* **2001**, *40*, 4274. (j) Fürstner, A.; Ackermann, L.; Gabor, B.; Goddard, R.; Lehmann, C. W.; Mynott, R.; Stelzer, F.; Thiel, O. R. *Chem. Eur. J.* **2001**, *7*, 3236. (k) Timmer, M. S. M.; Ovaa, H.; Filippov, D. V.; van der Marel, G. A.; van Boom, J. H. *Tetrahedron Lett.* **2001**, *42*, 8231. (l) Yao, Q. *Org. Lett.* **2001**, *3*, 2069. (m) Smulik, J. A.; Giessert, A. J.; Diver, S. T. *Tetrahedron Lett.* **2002**, *43*, 209. (n) Layton, M. E.; Morales, C. A.; Shair, M. D. *J. Am. Chem. Soc.* **2002**, *124*, 773. (o) Poulsen, C. S.; Madsen, R. *J. Org. Chem.* **2002**, *67*, 4441. (p) Micalizio, G. C.; Schreiber, S. L. *Angew. Chem. Int. Ed.* **2002**, *41*, 3272. (q) Hansen, E. C.; Lee, D. *J. Am. Chem. Soc.* **2003**, *125*, 9582. (r) Katritzky, A. R.; Nair, S. K.; Khokhlova, T.; Akhmedov, N. G. *J. Org. Chem.* **2003**, *68*, 5724. (s) Yang, Y.-K.; Tae, J. *Synlett* **2003**, 2013. (t) Lee, H.-Y.; Kim, H. Y.; Tae, H.; K. B. G.; Lee, J. *Org. Lett.* **2003**, *5*, 3439. (u) Kulkarni, A. A.; Diver, S. T. *Org. Lett.* **2003**, *5*, 3463. (v) Giessert, A. J.; Brazis, N. J.; Diver, S. T. *Org. Lett.* **2003**, *5*, 3819.
- Review on cycloisomerization of enynes; (a) Trost, B. M.; Krische, M. J. *Synlett* **1998**, 1. For selected other examples; (b) Katz, T. J.; Sivavec, T. M. *J. Am. Chem. Soc.* **1985**, *107*, 737. (c) Trost, B. M.; Tanoury, G. J. *J. Am. Chem. Soc.* **1988**, *110*, 1636. (d) Mori, M.; Watanuki, S. *J. Chem. Soc., Chem. Commun.* **1992**, 1082. (e) Watanuki, S.; Ochifuji, N.; Mori, M. *Organometallics* **1994**, *13*, 4129. (f) Chatani, N.; Morimoto, T.; Muto, T.; Murai, S. *J. Am. Chem. Soc.* **1994**, *116*, 6049. (g) Fürstner, A.; Szillat, H.; Stelzer, F. *J. Am. Chem. Soc.* **2000**, *122*, 6785. (h) Fürstner, A.; Stelzer, F.; Szillat, H. *J. Am. Chem. Soc.* **2001**, *123*, 11863. (i) Ackermann, L.; Bruneau, C.; Dixneuf, P. H. *Synlett* **2001**, 397. (j) Semeril, D.; Cleran, M.; Bruneau, C.; Dixneuf, P. H. *Adv. Synth. Catal.* **2001**, *343*, 184.
- Examples; (a) Randall, M. L.; Tallarico, J. A.; Snapper, M. L. *J. Am. Chem. Soc.* **1995**, *117*, 9610. (b) Schneider, M. F.;

- Blechert, S. *Angew. Chem. Int. Ed. Engl.* **1996**, *35*, 411.
(c) Michaut, M.; Parrain, J.-L.; Santilli, M. *Chem. Commun.* **1996**, 2567. (d) Schneider, M. F.; Lucas, N.; Velder, J.; Blechert, S. *Angew. Chem. Int. Ed. Engl.* **1997**, *36*, 257. (e) La, D. S.; Ford, J. G.; Sattely, S. E.; Bonitatebus, P. J.; Schrock, R. R.; Hoveyda, A. H. *J. Am. Chem. Soc.* **1999**, *121*, 11603, and references cited therein.
7. Recent application of ROM-RCM; (a) Zuercher, W. J.; Hashimoto, M.; Grubbs, R. H. *J. Am. Chem. Soc.* **1996**, *118*, 6634. (b) Chatani, N.; Furukawa, N.; Sakurai, H.; Murai, S. *Organometallics* **1996**, *15*, 901. (c) Fürstner, A.; Szillat, H.; Gabor, B.; Mynott, R. *J. Am. Chem. Soc.* **1998**, *120*, 8305. (d) Burke, S. D.; Quinn, K. J.; Chen, V. J. *J. Org. Chem.* **1998**, *63*, 8626. (e) Adams, J. A.; Ford, J. G.; Stamatou, P. J.; Hoveyda, A. H. *J. Org. Chem.* **1999**, *64*, 9690. (f) Voigtmann, U.; Blechert, S. *Synthesis* **2000**, 893. (g) Trost, B. M.; Doherty, G. A. *J. Am. Chem. Soc.* **2000**, *122*, 3801. (h) Ova, H.; Stragies, R.; van der Malel, G. A.; van Boom, J. H.; Blechert, S. *Chem. Commun.* **2000**, 1501. (i) Fürstner, A.; Szillat, H.; Stelzer, F. *J. Am. Chem. Soc.* **2000**, *122*, 6785. (j) Stragies, R.; Blechert, S. *J. Am. Chem. Soc.* **2000**, *122*, 9584. (k) Voigtmann, U.; Blechert, S. *Org. Lett.* **2000**, *2*, 3971. (l) Choi, T.-L.; Grubbs, R. H. *Chem. Commun.* **2001**, 2648. (m) Lee, C. W.; Choi, T.-L.; Grubbs, R. H. *J. Am. Chem. Soc.* **2002**, *124*, 3224. (n) Minger, T. L.; Phillips, A. J. *Tetrahedron Lett.* **2002**, *43*, 5357. (o) van Otterlo, W. A. L.; Ngidi, E. L.; de Koning, C. B.; Fernandes, M. A. *Tetrahedron Lett.* **2004**, *45*, 659, and references cited therein.
8. Recently, Blechert et al. reported the similar reaction using ethylene or other alkene. (a) Rückert, A.; Eisele, D.; Blechert, S. *Tetrahedron Lett.* **2001**, *42*, 5245. (b) Randl, S.; Lucas, N.; Connon, J.; Blechert, S. *Adv. Synth. Catal.* **2002**, *344*, 631. (c) Imhof, S.; Blechert, S. *Synlett* **2003**, 609.
9. The effective use of ethylene for metathesis reaction: (a) Harrity, J. P. A.; Visser, M. S.; Gleason, J. D.; Hoveyda, A. H. *J. Am. Chem. Soc.* **1997**, *119*, 1488. (b) Bassindale, M.; Hamley, P.; Harrity, J. P. A. *Tetrahedron Lett.* **2001**, *42*, 9055. (c) Banti, D.; North, M. *Tetrahedron Lett.* **2002**, *43*, 1561. (d) Meng, D.; Parker, D. *Tetrahedron Lett.* **2002**, *43*, 9035.
10. Byström, S.; Aslanian, R.; Bäckvall, J. E. *Tetrahedron Lett.* **1985**, *26*, 1749.
11. Dess, D.; Martin, J. C. *J. Org. Chem.* **1983**, *48*, 4156.
12. Pawlak, L.; Berchtold, G. A. *J. Org. Chem.* **1988**, *53*, 4063.
13. Crystallographic data have been deposited with Cambridge Crystallographic Data Center as supplementary publication No. CCDC 193041.
14. For examples for olefin migration under the metathesis condition; (a) Fürstner, A.; Thiel, O. R.; Ackermann, L.; Schanz, H.-J.; Nolan, S. P. *J. Org. Chem.* **2000**, *65*, 2204. (b) Alcaida, B.; Almendros, P.; Alonso, J. M.; Aly, M. F. *Org. Lett.* **2001**, *3*, 3781. (c) Cadot, C.; Dalko, P. I.; Cossy, J. *Tetrahedron Lett.* **2002**, *43*, 1839. (d) Huang, J.; Hsung, R. P.; Rameshkumar, C.; Mulder, J. A.; Grebe, T. P. *Org. Lett.* **2002**, *4*, 2417, and references cited therein.
15. Compound **21** was reported in the literature and agreed with those of their spectral data; Bottino, F.; Grazia, M. D.; Finocchiaro, P.; Fronczek, F. R.; Mamo, A.; Pappalardo, S. *J. Org. Chem.* **1988**, *53*, 3521.

(PCy₃)₂Cl₂Ru=CHPh Catalyzed Kharasch additions. Application in a formal olefin carbonylation

Belinda T. Lee, Thomas O. Schrader, Belén Martín-Matute, Christopher R. Kauffman,
Peng Zhang and Marc L. Snapper*

Department of Chemistry, Eugene F. Merkert Chemistry Center, Boston College, Chestnut Hill, MA 02467-3860, USA

Received 30 March 2004; revised 8 June 2004; accepted 14 June 2004

Available online 10 July 2004

Contributed in honor of Professor Robert H. Grubbs reception of the Tetrahedron Prize for Creativity in Organic Chemistry

Abstract—(PCy₃)₂Cl₂Ru=CHPh-catalyzed Kharasch additions of trihaloalkanes across olefins provide polyhalogenated adducts, which upon hydrolysis furnish α,β-unsaturated ketones, aldehydes, or γ-hydroxybutenolides. This two-step process represents an overall acylation or carbonylation of an olefin.

© 2004 Elsevier Ltd. All rights reserved.

1. Introduction

Olefin carbonylation is an important bond forming process that continues to draw attention as a developing synthetic methodology.¹ Intramolecular carbonylative Heck² and Phauson-Khand³ reactions, for example, have already found applications in natural product total syntheses. Intermolecular olefin acylations, on the other hand, are less common,⁴ mainly because of the forcing reaction conditions and high carbon monoxide pressures that are often required.⁵ Herein we report a two-step process that represents a relatively mild synthetic alternative to direct olefin carbonylations.

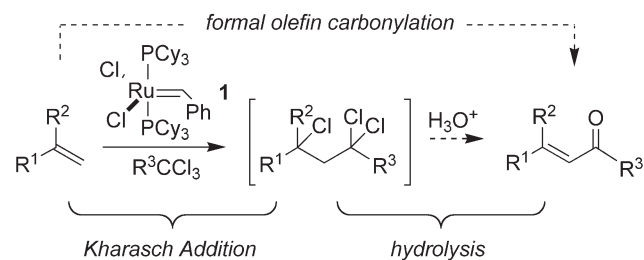
It has been shown that complex **1**, a ruthenium benzylidene well known for its ability to promote olefin metatheses, is also an effective catalyst in radical atom transfer reactions (Kharasch addition, Scheme 1).⁶ We sought to expand the scope of this alkylidene's reactivity by examining the

addition of a variety of trihaloalkanes additions across alkenes. It was also noted that the hydrolysis of the corresponding halogenated adducts could offer novel access to α,β-unsaturated carbonyl-containing compounds. The net result of this two-step sequence would be an overall carbonylation of the olefin. While precedent for the Kharasch addition was strong,⁷ examples of hydrolyses of related halogenated systems were few, but encouraging.⁸

2. Results and discussion

2.1. Kharasch addition

The ability of Grubbs' ruthenium complex **1** to catalyze the addition of several trichloroalkyls⁹ across alkenes is illustrated in Table 1. Typically, the reaction is carried out using 5–10 mol% of benzylidene **1** in the presence of excess trichloroalkanes at 65–80 °C. It is important to note that the reactivity of Grubb's catalyst **1** in these transformations far exceeds other common ruthenium-based Kharasch addition catalysts such as (Ph₃P)₃RuCl₂.^{6a} Substrates that typically fail to undergo Kharasch additions due to harsh conditions will participate effectively in this transformation when catalyzed by **1**. In particular, alkenes less prone to undergo an olefin metatheses, such as styrenes and acrylates, serve as excellent substrates for Kharasch additions, especially with chloroform or 1,1,1-trichloroethane as their reaction partner. On the other hand, similar reaction conditions with 4-vinyl-1-cyclohexene led to significant amounts of cross-metathesis products along with lesser amounts of the Kharasch addition product (data not shown).



Scheme 1. Kharasch addition followed by hydrolysis.

Keywords: Kharasch; Metathesis; Radical; Carbonylation.

* Corresponding author. Tel.: +1-617-5528096; fax: +1-617-5521442; e-mail address: marc.snapper@bc.edu

Table 1. Kharasch additions catalyzed by complex **1**^a

$$\text{R}^1\text{C}(\text{R}^2)\text{CH}=\text{CH}_2 + \text{R}^3\text{CCl}_3 \xrightarrow{\text{cat. } \mathbf{1}} \text{R}^1\text{C}(\text{R}^2)\text{CH}(\text{Cl})\text{CH}_2\text{R}^3$$

Entry	Alkene	Trichloroalkyl	Product	Yield (%) ^c
(1)		CHCl ₃		99 ^b
(2)		MeCCl ₃		96
(3)				57
(4)		MeCCl ₃		>69 ^c
(5)		CHCl ₃		84 ^b
(6)		MeCCl ₃		79
(7)		BnCCl ₃		64 ^d
(8)		MeCCl ₃		91

^a Typical reaction conditions: 5 mol% **1**, 20 equiv. 1,1,1-trichloroalkyl, 65–80 °C.

^b See Ref. 6a.

^c Compound **9** was converted directly to enone **17** in 69% overall yield (see Table 2, entry 5).

^d 10 mol% **1**, 10 equiv. BnCCl₃.

^e Isolated yields.

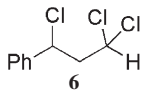
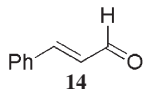
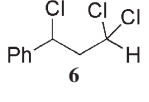
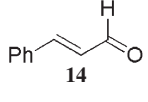
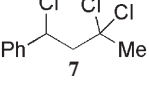
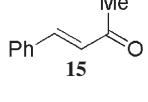
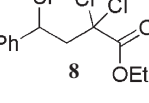
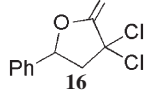
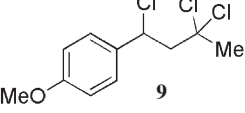
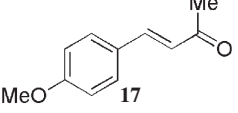
Besides 1,1,1-trichloroethane and chloroform, alkylidene **1** was also effective at promoting the addition of other chlorinated substrates across olefins. Entry 3 illustrates the addition of ethyl trichloroacetate across styrene, while entry 7 shows the benzyl trichloromethane-methyl methacrylate adduct. In regard to diversity-oriented synthesis, these results suggest that a range of useful olefin and trihaloalkane functionalities can be coupled under relatively mild conditions through this ruthenium-catalyzed protocol.

2.2. Hydrolysis

Considering that the resulting dichlorinated carbons in the Kharasch addition products **6–13** are formally in the

carbonyl oxidation state, efforts were turned toward identifying reaction conditions for the hydrolysis of these substrates.⁸ Table 2 summarizes the hydrolysis of some of the styrenyl-derived Kharasch addition products. A silver-assisted hydrolysis of the Kharasch addition product **6** in refluxing H₂O delivers *trans*-cinnamaldehyde **14** in 63% yield (entry 1). Alternatively, adduct **6** can be converted to aldehyde **14** in 77% yield by heating with 10% H₂SO₄ in a sealed reaction vessel for 6.5 h (entry 2). Hydrolysis of compound **7** using silver nitrate produced enone **15** as the *trans* isomer (*trans*:*cis*=11:1) in 76% yield (entry 3). When α -dichloro ester **8** is treated with refluxing 1 M HCl, lactone **16** is produced in 89% yield with no evidence of products resulting from further hydrolysis of the ester's α -chlorides

Table 2. Hydrolyses of styrene-derived Kharasch adducts

Entry	Trichloroalkane	Product	Conditions	Yield (%) ^a
(1)			AgNO ₃ , H ₂ O 100 °C, 72 h	63
(2)			10% H ₂ SO ₄ 180 °C, 6.5 h	77
(3)			AgNO ₃ , H ₂ O 100 °C, 16 h	76
(4)			1 M HCl 100 °C, 72 h	89
(5)			SiO ₂	69 ^b

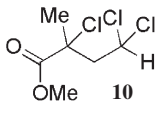
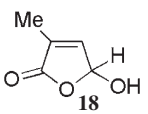
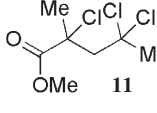
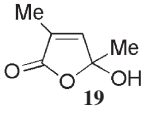
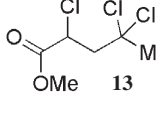
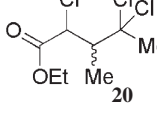
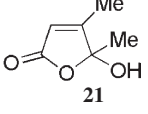
^a Isolated yields.^b Overall yield from *p*-methoxystyrene (3).

(entry 4). These results suggest that the benzylic chloride is more labile to hydrolysis than the dichloride carbon in these systems. In further support, the electron rich aromatic system **9** undergoes a much more facile, room temperature hydrolysis; the *trans*-enone **17** was obtained directly after the Kharasch addition in 69% overall yield by passing the reaction mixture through two successive columns of silica gel (entry 5).

In comparison to the styrenyl substrates, hydrolysis of the

acrylate-derived addition products offered an alternative carbonylation product. **Table 3** illustrates the conversion of the acrylate-derived Kharasch addition products into substituted γ -hydroxybutenolides,¹⁰ an important functionality found in several biologically active natural products.¹¹ As shown in entries 1 and 2, acidic hydrolyses of trichlorinated esters **10** and **11** provides γ -hydroxybutenolides **18** and **19**, in 91 and 65% yield, respectively. On the other hand, hydrolysis of the less substituted Kharasch addition product **13** (entry 3) under similar reaction con-

Table 3. Conversion of acrylate-derived Kharasch addition products to γ -hydroxybutenolides.

Entry	Trichloroalkanel	Product	Conditions	Yield (%) ^a
(1)			HCl, H ₂ O 100 °C	91
(2)			HCl, H ₂ O 100 °C	65
(3)		Mixture		
(4)			10% H ₂ SO ₄ 160 °C, 17 h	58

^a Isolated yields.

ditions gave a complex mixture of products.¹² Hydrolysis of **20** (as a mixture of diastereomers) in 10% H₂SO₄ at 160 °C, however, generates **21** in 58% yield (entry 4) indicating that alkyl substitution at either the α - or β -position of the requisite ester was necessary for effective γ -hydroxybutenolide formation.

3. Summary

Grubbs' ruthenium benzylidene **1** catalyzes a mild radical atom transfer of trichloroalkyl groups across a variety of olefins (Kharasch addition). This transformation can be followed by the hydrolysis of the resulting polychlorinated adducts to provide a viable olefin carbonylation protocol. Hydrolyses of the resulting addition products can lead to various enals, enones, lactones, and γ -hydroxybutenolides. Overall, the two-step sequence represents a convenient method for the attachment of carbonyl functionality to olefins.

4. Experimental

4.1. General methods

Starting materials and reagents were purchased from commercial suppliers and used without purification with the exception of the following: ethyl trichloroacetate and all olefinic substrates were distilled prior to use. Chromatographic solvents such as diethyl ether (Et₂O), pentanes, and hexanes were distilled prior to use. Benzyl trichloromethane [(2,2,2-trichloro-ethyl)-benzene] was prepared according to a literature procedure.¹³

Kharasch addition reactions were carried out under N₂ atm. in flame-dried glassware. Grubbs' catalyst (**1**) and Cl₂Ru(PPh₃)₃ were transferred in a glove box. Heavy walled sealed tubes with Teflon™ screw caps, purchased from Ace Glass Incorporated, were used for all reactions that required heating to ≥ 130 °C. Silica gel chromatography was performed using Baxter brand silica gel 60 Å (230–400 mesh ASTM). Cerium ammonium molybdate and phosphomolybdic acid (PMA, 20%) in ethanol were used as the primary thin layer chromatography (TLC) staining reagents.

Proton nuclear magnetic resonance spectra (¹H NMR) were measured on a Varian Gemini-400 spectrometer (400 MHz). Carbon nuclear magnetic resonance spectra (¹³C NMR) were recorded on a Varian Gemini-400 spectrometer (100 MHz). All ¹H NMR chemical shifts are reported in ppm downfield from tetramethylsilane with the solvent reference as the internal standard (CHCl₃: δ 7.26). ¹³C NMR chemical shifts are referenced to CHCl₃ (δ 77.23). Infrared spectra (IR) were measured on a Perkin–Elmer 1310 Infrared Spectrometer, λ_{\max} in cm⁻¹. Robertson Microlit Laboratories Inc.; Madison, NJ 07940, performed elemental analyses.

4.1.1. (1,3,3-Trichloro-butyl)-benzene (7). To a Schlenk flask equipped with a reflux condenser was added catalyst **1** (395 mg, 0.480 mmol), 1,1,1-trichloroethane (19.1 mL, 20.0 equiv.) and styrene (**2**) (1.0 g, 9.6 mmol). The reaction

was heated to 75 °C under N₂ atm. for 1.5 h. The reaction was concentrated and purified by silica gel chromatography (pentanes) to give compound **7** (2.19 g, 9.2 mmol, 96% yield) as a colorless oil. Compound **7**: ¹H NMR (CDCl₃, 400 MHz): δ 7.49–7.30 (5H, m), 5.26 (1H, t, $J=6.0$ Hz), 3.18 (1H, dd, $J=15.2$, 6.0 Hz), 3.10 (1H, dd, $J=15.2$, 6.0 Hz), 2.08 (3H, s). ¹³C NMR (CDCl₃, 100 MHz): δ 141.5, 129.1, 128.9, 127.3, 88.3, 59.3, 58.7, 38.0. IR (NaCl, thin film): 3063, 30301, 2987, 2937, 1501, 1455, 1388, 1212, 1168, 1068 cm⁻¹. Anal. calcd for C₁₀H₁₁Cl₃: C, 50.56; H, 4.67. Found: C, 50.79; H, 4.73.¹⁴

4.1.2. 2,2,4-Trichloro-4-phenyl-butyric acid ethyl ester (8). To a Schlenk flask was added catalyst **1** (18.0 mg, 0.020 mmol), ethyl trichloroacetate (1.2 mL, 20 equiv.) and styrene (**2**) (46 mg, 0.44 mmol). The reaction was heated to 75 °C under N₂ atm. for 48 h. The reaction was concentrated and purified by silica gel chromatography (pentanes/Et₂O, 4:1) to give compound **8** (73 mg, 0.25 mmol, 57% yield) as a colorless oil. Ester **8**: ¹H NMR (CDCl₃, 400 MHz): δ 7.42–7.31 (5H, m), 5.23, (1H, dd, $J=7.6$, 6.0 Hz), 4.15 (1H, m), 4.05 (1H, m), 3.44 (1H, dd, $J=15.0$, 7.6 Hz), 3.21 (1H, dd, $J=15.0$, 6.0 Hz), 1.30 (3H, t, $J=7.6$ Hz). ¹³C NMR (CDCl₃, 100 MHz): δ 165.0, 139.7, 129.0, 128.8, 127.5, 82.5, 64.3, 58.8, 54.2, 14.0. IR (NaCl, thin film): 3024, 2987, 2936, 1753, 1495, 1451, 1250, 1193, 1029 cm⁻¹. Anal. calcd for C₁₂H₁₃Cl₃O₂: C, 48.76; H, 4.43. Found: C, 49.01; H, 4.24.

4.1.3. 2,4,4-Trichloro-2-methyl-pentanoic acid methyl ester (11). To a Schlenk flask equipped with a reflux condenser was added catalyst **1** (184.0 mg, 0.223 mmol), 1,1,1-trichloroethane (8.4 mL, 20 equiv.) and methyl methacrylate (**5**) (421 mg, 4.21 mmol). The reaction was heated to 75 °C under N₂ atm. for 2 h. The reaction was concentrated and purified by silica gel chromatography (pentanes/Et₂O, 100:1) to give compound **11** (770 mg, 3.30 mmol, 79% yield), as a colorless oil. Ester **11**: ¹H NMR (CDCl₃, 400 MHz): δ 3.81 (3H, s), 3.38 (1H, d, $J=15.4$ Hz), 3.05 (1H, d, $J=15.4$ Hz), 2.23 (3H, s), 2.00 (3H, s). ¹³C NMR (CDCl₃, 100 MHz): δ 171.5, 87.0, 67.0, 59.2, 54.6, 40.1, 28.9. IR (NaCl, thin film): 2999, 2955, 1753, 1451, 1388, 1319, 1243, 1136, 1092 cm⁻¹. Anal. calcd for C₇H₁₁Cl₃O₂: C, 36.00; H, 4.75. Found: C, 36.13; H, 4.76.

4.1.4. 2,4,4-Trichloro-2-methyl-5-phenyl-pentanoic acid methyl ester (12). To a Schlenk flask equipped with a reflux condenser was added catalyst **1** (14.0 mg, 0.017 mmol), benzyl trichloromethane (370 mg, 1.78 mmol, 9.9 equiv.) and methyl methacrylate (**4**) (17.7 mg, 0.177 mmol). The reaction was heated to 75 °C under N₂ atm. for 12 h. The reaction was concentrated and purified by silica gel chromatography (pentanes/Et₂O, 50:1) to give compound **12** (35.0 mg, 0.113 mmol, 64% yield) as a colorless oil. Compound **12**: ¹H NMR (CDCl₃, 400 MHz): δ 7.38 (5H, m), 3.74 (3H, s), 3.56, (2H, s), 3.49 (1H, d, $J=15.2$ Hz), 2.87 (1H, d, $J=15.2$ Hz), 2.05 (3H, s). ¹³C NMR (CDCl₃, 100 MHz): δ 170.8, 133.8, 131.7, 128.2, 128.0, 88.7, 66.2, 55.8, 55.7, 53.6, 27.6. IR (NaCl, thin film): 3024, 2993, 2948, 2357, 1741, 1495, 1451, 1394, 1313, 1237 cm⁻¹. Anal. calcd for C₁₃H₁₅Cl₃O₂: C, 50.43; H, 4.88. Found: C, 50.15; H, 4.95.

4.1.5. 2,4,4-Trichloro-pentanoic acid methyl ester (13).

To a Schlenk flask equipped with a reflux condenser was added catalyst **1** (478 mg, 0.581 mmol), 1,1,1-trichloroethane (25.0 mL, 21.0 equiv.) and methyl acrylate (**5**) (960 mg, 11.2 mmol). The reaction was heated to 75 °C under N₂ atm. for 2 h. The reaction was concentrated and purified by silica gel chromatography (pentanes/Et₂O, 50:1) to give compound **13** (2.23 g, 10.2 mmol, 91% yield) as a colorless oil. Compound **13**: ¹H NMR (CDCl₃, 400 MHz): δ 4.63 (1H, dd, *J*=7.6, 4.2 Hz), 3.82 (3H, s), 3.27 (1H, dd, *J*=15.0, 7.6 Hz), 2.75 (1H, dd, *J*=15.0, 4.2 Hz), 2.21 (3H, s). ¹³C NMR (CDCl₃, 100 MHz): δ 169.7, 86.9, 53.7, 53.6, 52.4, 37.9. IR (NaCl, thin film): 2993, 2949, 1753, 1438, 1275, 1168, 1086, 985 cm⁻¹. Anal. calcd for C₆H₉Cl₃O₂: C, 32.83; H, 4.13. Found: C, 32.97; H, 3.91.

4.1.6. 4-(4-Methoxy-phenyl)-but-3-en-2-one (17). To a Schlenk flask equipped with a reflux condenser was added catalyst **1** (92 mg, 0.11 mmol), 1,1,1-trichloroethane (4.4 mL, 20 equiv.) and *p*-methoxystyrene (**3**) (300 mg, 2.32 mmol). The reaction was heated to 75 °C under N₂ atm. for 2 h. The reaction was concentrated and purified by silica gel chromatography (two successive columns; pentanes/Et₂O, 3:2) to give enone **17** (*E:Z* >20:1, 270 mg, 1.53 mmol, 69% yield) as a white solid. Compound **17** (data for the *trans* isomer is given): ¹H NMR (CDCl₃, 400 MHz): δ 7.49 (2H, d, *J*=8.4 Hz), 7.47 (1H, d, *J*=16.4 Hz), 6.91 (2H, d, *J*=8.8 Hz), 6.60 (1H, d, *J*=16.4 Hz), 3.83 (3H, s), 2.35 (3H, s). ¹³C NMR (CDCl₃, 100 MHz): δ 198.2, 161.6, 143.2, 130.0, 127.1, 125.1, 114.5, 55.6, 27.5. IR (NaCl, thin film): 3011, 2960, 2930, 2855, 1678, 1610, 1525, 1511, 1186, 1036 cm⁻¹. These spectral data are in agreement with the reported literature values for *trans*-**17**.¹⁵

4.1.7. 3-Phenyl-propenal (14). To a round-bottom flask equipped with a reflux condenser was added compound **6** (70 mg, 0.31 mmol), H₂O (2 mL), and AgNO₃ (255 mg, 1.50 mmol). The reaction was stirred at 100 °C for 72 h. After cooling to rt the reaction mixture was extracted with pentanes and the organic layer was concentrated. Purification by silica gel chromatography (pentanes/Et₂O, 5:1) gave *trans*-cinnamaldehyde (**14**) (26 mg, 0.19 mmol, 63% yield) as a yellow oil. The spectral data obtained for **14** was identical to an authentic sample obtained from Aldrich Chemical Co.

4.1.8. Alternative hydrolysis. To a heavy walled reaction tube was added compound **6** (70 mg, 0.31 mmol), and H₂SO₄ (10% aq., 1.0 mL). The tube was sealed with a Teflon™ screw cap and heated to 180 °C (oil bath temp) for 6.5 h. The reaction was partitioned between Et₂O and H₂O. The organic layer was separated, concentrated, and purified by silica gel chromatography (pentanes/Et₂O, 10:1) to give *trans*-cinnamaldehyde (**14**) (31 mg, 0.24 mmol, 77% yield) as a yellow oil.

4.1.9. 4-Phenyl-but-3-en-2-one (15). To a round-bottom flask equipped with a reflux condenser was added compound **7** (70 mg, 0.29 mmol), H₂O (3.0 mL), and AgNO₃ (250 mg, 1.47 mmol). The reaction was stirred at 100 °C for 16 h. After cooling to rt the reaction mixture was extracted with pentanes and the organic layer was concentrated. Purification by silica gel chromatography (pentanes/Et₂O, 5:1) gave enone **15** (*E:Z* >10:1, 32 mg,

0.22 mmol, 76% yield) as a yellow oil. The spectral data obtained for **15** were identical to an authentic sample obtained from Aldrich Chemical Co.

4.1.10. 3,3-Dichloro-5-phenyl-dihydro-furan-2-one (16). To a round-bottom flask equipped with a reflux condenser was added compound **8** (26.0 mg, 0.088 mmol) and HCl (1 M aq., 1 mL). The reaction was stirred at 100 °C for 72 h. After cooling to rt the reaction mixture was extracted with ether and the organic layer was dried over MgSO₄, filtered, and concentrated to give analytically pure lactone **16** (18 mg, 0.078 mmol, 89% yield) as a colorless oil. Compound **16**: ¹H NMR (CDCl₃, 400 MHz): δ 7.47–7.35 (5H, m), 5.62 (1H, dd, *J*=10.1, 5.1 Hz), 3.45 (1H, dd, *J*=14.2, 5.1 Hz), 2.93 (1H, dd, *J*=14.2, 10.1 Hz). ¹³C NMR (CDCl₃, 100 MHz): δ 167.5, 135.6, 129.7, 129.2, 125.9, 82.1, 78.9, 52.6. IR (NaCl, thin film): 3031, 2911, 2848, 1797, 1325, 1199, 1174, 1036, 960 cm⁻¹. Anal. calcd for C₁₀H₈Cl₂O₂: C, 51.98; H, 3.49. Found: C, 51.67; H, 3.42.

4.1.11. 5-Hydroxy-3-methyl-5H-furan-2-one (18). To a round-bottom flask equipped with a reflux condenser was added compound **10** (50 mg, 0.23 mmol) and HCl (6 M aq., 2.3 mL). The reaction was stirred at 100 °C for 48 h. After cooling to rt the reaction mixture was extracted with ether and the organic layer was dried over MgSO₄, filtered, and concentrated. Purification by silica gel chromatography (Et₂O) gave pure compound **18** (24 mg, 0.21 mmol, 91% yield) as a white solid. The spectral data obtained for compound **18** were identical to the reported literature data.¹⁶

4.1.12. 5-Hydroxy-3,5-dimethyl-5H-furan-2-one (19). To a round-bottom flask equipped with a reflux condenser was added compound **11** (80 mg, 0.34 mmol) and HCl (1.2 M aq., 2 mL). The reaction was stirred at 100 °C for 72 h. The water was removed by a lyophilization and the reaction mixture was purified by silica gel chromatography (CH₂Cl₂/MeOH, 20:1) to provide pure **19** (28 mg, 0.22 mmol, 65% yield) as a white solid. The spectral data obtained for compound **19** were identical to the reported literature data.¹⁷

4.1.13. 2,4,4-Trichloro-3-methyl-pentanoic acid ethyl ester (20). To a heavy walled reaction tube was added Cl₂Ru(PPh₃)₃ (37 mg, 0.039 mmol), ethyl crotonate (110 mg, 0.964 mmol), and 1,1,1-trichloroethane (1.50 mL, 18.5 equiv.). The tube was sealed under N₂ with a Teflon™ screw cap and heated to 130 °C (oil bath temperature) for 65 h. The reaction was concentrated and purified by silica gel chromatography (hexanes/Et₂O, 10:1) to give 199 mg of a colorless oil containing a mixture of the diastereomeric ester **20** (86% wt/wt, 171 mg, 0.690 mmol, 72% yield, dr=1.1:1) and a regioisomeric product (14% wt/wt, 28.0 mg, 0.11 mmol, 12% yield, data not shown). Compound **20**: ¹H NMR (CDCl₃, 400 MHz), Major diastereomer: δ 4.83 (1H, d, *J*=5.2 Hz), 4.22 (2H, m), 2.76 (1H, qd, *J*=9.2, 5.2 Hz), 2.25 (3H, s), 1.48 (3H, d, *J*=9.6 Hz), 1.31 (3H, t, *J*=7.2 Hz). Minor diastereomer: δ 5.04 (1H, d, *J*=3.6 Hz), 4.22 (2H, m), 3.08 (1H, qd, *J*=9.2, 3.6 Hz), 2.19 (3H, s), 1.34 (3H, d, *J*=9.2 Hz), 1.29 (3H, t, *J*=7.2 Hz). ¹³C NMR (CDCl₃, 100 MHz) taken as a diastereomeric mixture: δ 162.8, 87.0, 64.8, 57.7, 57.2, 56.6, 54.0, 51.7, 50.1, 31.8, 29.8, 9.2, 9.0, 7.41, 7.40.

4.1.14. 5-Hydroxy-4,5-dimethyl-5H-furan-2-one (21). To a heavy walled reaction tube was added compound **20** (100 mg, 0.40 mmol), and H₂SO₄ (10% aq., 2 mL). The tube was sealed with a Teflon™ screw cap and heated to 160 °C (oil bath temperature) for 17 h. The reaction was neutralized by the drop wise addition of 5% NaOH solution to pH=7. The reaction mixture was concentrated and purified by silica gel chromatography (CH₂Cl₂/MeOH, 20:1) to give compound **21** (29 mg, 0.23 mmol, 58% yield) as a light yellow oil. Compound **21**: ¹H NMR (CDCl₃, 400 MHz): δ 5.74 (1H, q, *J*=1.2 Hz), 4.55 (1H, bs), 2.08 (3H, d, *J*=1.2 Hz), 1.64 (3H, s). ¹³C NMR (CDCl₃, 100 MHz): δ 168.3, 117.1, 107.2, 23.6, 12.8. These spectral data are identical to the reported literature values.¹⁸

Acknowledgements

We thank the National Science Foundation for financial support (CHE-0132221). B. T. L. & C. R. K. acknowledge the Under-graduate Faculty Research Fellows Program at Boston College for summer fellowships. We also thank Bhaumik Pandya for experimental assistance.

References and notes

- (a) Colquhoun, H. M.; Thompson, D. J.; Twigg, M. V. *Carbonylation: Direct Synthesis of Carbonyl Compounds*; Plenum: New York, 1991. (b) Breit, B.; Seiche, W. *Synthesis* **2001**, 1–36. (c) Agbossou, F.; Carpentier, J.-F.; Mortreux, A. *Chem. Rev.* **1995**, *95*, 2485–2506. (d) For a related transformation, see: Kreimeram, S.; Ryu, I.; Minakata, S.; Komatsu, M. *Org. Lett.* **2000**, *2*, 389–391, and references cited therein.
- (a) Artman, III., G.; Weinreb, S. M. *Org. Lett.* **2003**, *5*, 1523–1526. (b) Copéret, C.; Negishi, E. *Org. Lett.* **1999**, *1*, 165–167. (c) Kündig, E.; Ratni, H.; Crousse, B.; Bernardinelle, G. *J. Org. Chem.* **2001**, *66*, 1852–1860. (d) Zhang, Y.; Negishi, E. *J. Am. Chem. Soc.* **1989**, *111*, 3454–3456.
- (a) Gibson, S. E.; Stevenazzi, A. *Angew. Chem. Int. Ed.* **2003**, *42*, 1800–1810. (b) Hicks, F. A.; Buchwald, S. L. *J. Am. Chem. Soc.* **1996**, *118*, 11688–11689, and references cited therein.
- For examples of hydroformylations, see (a) Saraf, S. T.; Leighton, J. L. *Org. Lett.* **2000**, *2*, 3205–3208. (b) Krauss, I. J.; Wang, C. C.-Y.; Leighton, J. L. *J. Am. Chem. Soc.* **2001**, *123*, 11514–11515, and references cited therein.
- For alternative strategies, see: (a) Almtorp, G. T.; Bachmann, T. L.; Torssell, K. B. G. *Acta Chem. Scand.* **1991**, *45*, 212–215. (b) Tsuge, O.; Kanemasa, S.; Suga, H.; Nakagawa, N. *Bull. Chem. Soc. Jpn* **1987**, *60*, 2463–2473.
- (a) Tallarico, A.; Malnick, L. M.; Snapper, M. L. *J. Org. Chem.* **1999**, *64*, 344–345. For similar transformations with Grubbs' metathesis catalysts, see: (b) Simal, F.; Demonceau, A.; Noels, A. F. *Tetrahedron Lett.* **1999**, *40*, 5689–5693. (c) De Clercq, B.; Verpoort, F. *J. Mol. Cat.* **2002**, *180*, 67–76.
- (d) Alcaide, B.; Almendros, P. *Chem. Eur. J.* **2003**, *9*, 1259–1262, and references cited therein. Grubbs' 2nd generation catalyst was not nearly as active in Kharasch additions.
- (a) Kharasch, M. S.; Jensen, E. V.; Urry, W. H. *Science* **1945**, *102*, 128. (b) Kharasch, M. S.; Jensen, E. V.; Urry, W. H. *J. Am. Chem. Soc.* **1945**, *67*, 1864–1865. (c) Kharasch, M. S.; Jensen, E. V.; Urry, W. H. *J. Am. Chem. Soc.* **1946**, *68*, 154–155. (d) Walling, C. *Free Radicals in Solution*; Wiley: New York, 1957; pp 247–272. For transition metal-mediated radical additions, see: (e) Minisci, F. *Acc. Chem. Res.* **1975**, *8*, 165–171. (f) Iqbal, J.; Bhatia, B.; Nayyar, N. K. *Chem. Rev.* **1994**, *94*, 519–564. (g) Curran, D. P. *Synthesis* **1988**, 417–439. (h) Curran, D. P. *Synthesis* **1988**, 489–513. (i) Tsuji, J.; Sato, K.; Nagashima, H. *Chem. Lett.* **1981**, 1169–1170. (j) Matsumoto, H.; Nakano, T.; Nagai, Y. *Tetrahedron Lett.* **1973**, *51*, 5147–5150. (k) Lee, G. M.; Weinreb, S. M. *J. Org. Chem.* **1990**, *55*, 1281–1285. (l) Feng, H.; Kavrakova, I. K.; Pratt, D. A.; Tellinghuisen, J.; Porter, N. A. *J. Org. Chem.* **2002**, *67*, 6050–6054. For a review of transition metal-promoted radical addition reactions, see: (m) Iqbal, J.; Bhatia, B.; Nayyar, N. K. *Chem. Rev.* **1994**, *94*, 519–564.
- For a related study using CCl₄ and styrenes, see: (a) Aslam, M.; Stansbury, W.; Reiter, R.; Larkin, D. *J. Org. Chem.* **1997**, *62*, 1550–1552. (b) Asscher, M.; Vofsi, D. *J. Chem. Soc.* **1963**, 3921–3927.
- For the limited systems examined, similar results were obtained for the corresponding tribrominated alkanes (data not shown).
- Kernan, M.; Faulkner, D. J. *J. Org. Chem.* **1988**, *53*, 2773–2776.
- (a) Cheung, A.; Snapper, M. L. *J. Am. Chem. Soc.* **2002**, *124*, 11584–11585. (b) Brohm, D.; Philippe, N.; Metzger, S.; Bhargava, A.; Muller, O.; Lieb, F.; Waldmann, H. *J. Am. Chem. Soc.* **2002**, *124*, 13171–13178. (c) Demeke, D.; Forsyth, C. *J. Org. Lett.* **2003**, *5*, 991–994. (d) De Silva, E.; Scheuer, P. J. *Tetrahedron Lett.* **1980**, *21*, 1611–1614. (e) Miyaoka, H.; Yamanishi, M.; Kajiwara, Y.; Yamada, Y. *J. Org. Chem.* **2003**, *68*, 3476–3479.
- The *cis-trans* isomerization of β-acetylacrylic acid under acidic conditions was studied previously, see: Seltzer, S.; Stevens, K. D. *J. Org. Chem.* **1968**, *33*, 2708–2711.
- Walling, C.; Lepley, A. R. *J. Am. Chem. Soc.* **1972**, *94*, 2007–2014.
- For previous reports of compound **7**, see: (a) Sato, T.; Seno, M.; Asahara, T. *Seisan Kenkyu* **1972**, *24*, 230–233. (b) Freidlina, R.; Kamyshova, A. A.; Posledova, N. N.; Chukovskaya, E. T.; Freidlina, R. *Izvestiya Akademii Nauk SSSR, Seriya Khimicheskaya* **1979**, 392–395.
- Knölker, H.-J.; Ahrens, B.; Gonser, P.; Heininger, M.; Jones, P. G. *Tetrahedron* **2000**, *56*, 2259–2271.
- Cooper, G. K.; Dolby, L. J. *J. Org. Chem.* **1979**, *44*, 3414–3416.
- Wendler, N.; Slates, H. L. *J. Org. Chem.* **1967**, *32*, 849–851.
- Farrand, C.; Johnson, D. C. *J. Org. Chem.* **1971**, *36*, 3609–3612.



A general and efficient method for the palladium-catalyzed cross-coupling of thiols and secondary phosphines

Miki Murata and Stephen L. Buchwald*

Department of Chemistry, Massachusetts Institute of Technology, 77 Massachusetts Ave. Bldg 18-305, Cambridge, MA 02139, USA

Received 30 March 2004; revised 17 May 2004; accepted 19 May 2004

Available online 7 June 2004

Dedicated to Professor Bob Grubbs in recognition of his continuing contributions to organic chemistry and for his mentoring over the years

Abstract—The general and efficient cross-coupling of thiols with aryl halides was developed utilizing Pd(OAc)₂/1,1'-bis(diisopropylphosphino)ferrocene as the catalyst. The substrate scope is broad and includes a variety of aryl bromides and chlorides, which can be coupled to aliphatic and aromatic thiols. This catalyst system has the widest substrate scope of any reported to date. The present catalyst system also enables the palladium-catalyzed coupling of secondary phosphines with aryl bromides and chlorides.
© 2004 Elsevier Ltd. All rights reserved.

1. Introduction

During the past few years, significant progress in palladium-catalyzed methods for the formation of carbon–nitrogen and –oxygen bonds has been achieved.¹ In particular, by the use of bulky and electron-rich monophosphine ligands, not only aryl bromides and iodides but also aryl chlorides can be used as substrates for palladium-catalyzed cross-couplings.² In contrast, methods for the analogous formation of carbon–sulfur and –phosphorus bonds have lagged behind. In fact, examples of the coupling of aryl chlorides with sulfur-³ and phosphorus-based nucleophiles⁴ are rare. This may be due to the high coordinating abilities of both the substrates and products. In this paper, we wish to report a general protocol for palladium-catalyzed synthesis of aryl sulfides and tertiary phosphines via cross-coupling protocols. Our method overcomes a number of limitations of previous systems and is the most general system that is available to date.

2. Results and discussion

2.1. Palladium-catalyzed carbon–sulfur bond formation

Despite the early work of Migita,⁵ the preparation of aryl sulfides by C–S bond-forming reactions using palladium catalysis has only recently received increased attention.

Keywords: Palladium catalysis; Thiol cross-coupling; Phosphine cross-coupling.

* Corresponding author. Tel.: +1-6172531852; fax: +1-6172533297; e-mail address: sbuchwal@mit.edu

Some success has been realized using bidentate phosphines^{6–8} or dialkylphosphine oxides³ as ligands. These protocols, however, lack generality: electron-rich or sterically-hindered substrates are often problematic.⁹ While the nickel-¹⁰ and copper-catalyzed¹¹ cross-coupling of thiols has been reported, these methods are limited to aryl iodides. Based on our success in related chemistry, we decided to determine whether we could contribute to this area.

In our initial screening experiments, 4-bromoanisole and benzenethiol were used as substrates for discovery of suitable reaction conditions (Fig. 1, series 1). All reagents except for the substrates were stirred together at room temperature for 1 h before the thiol and the aryl bromide were added. If all reaction components were simply mixed together, low conversion to the desired product was observed.⁶ As shown, use of DPPF,⁶ DPEphos⁸ and 1,1'-bis(diisopropylphosphino)ferrocene (DiPPF) as supporting ligand gave the best results. The use of BINAP for this coupling was unsuccessful. This is not unexpected as in previous work on the reaction of aryl triflates with aliphatic thiols using tol-BINAP, the reaction of aromatic thiols were not suitable substrates.⁷ We found that inclusion of 10 mol% PhB(OH)₂¹² in the reaction mixture with BINAP as ligand allowed the reaction to proceed to full conversion. Thus, it appears that reduction from Pd(II) to Pd(0) is slow when BINAP is used with aromatic thiols. This is consistent with the notion that BINAP is bulkier than DPPF and more rigorously η² than DPPF or DPEphos. Our bulky monodentate phosphines were also ineffective under these reaction conditions; inclusion of 10% PhB(OH)₂ with these ligands led to ca. 50% yield (GC analysis). Our supposition is that a chelating ligand is necessary to prevent

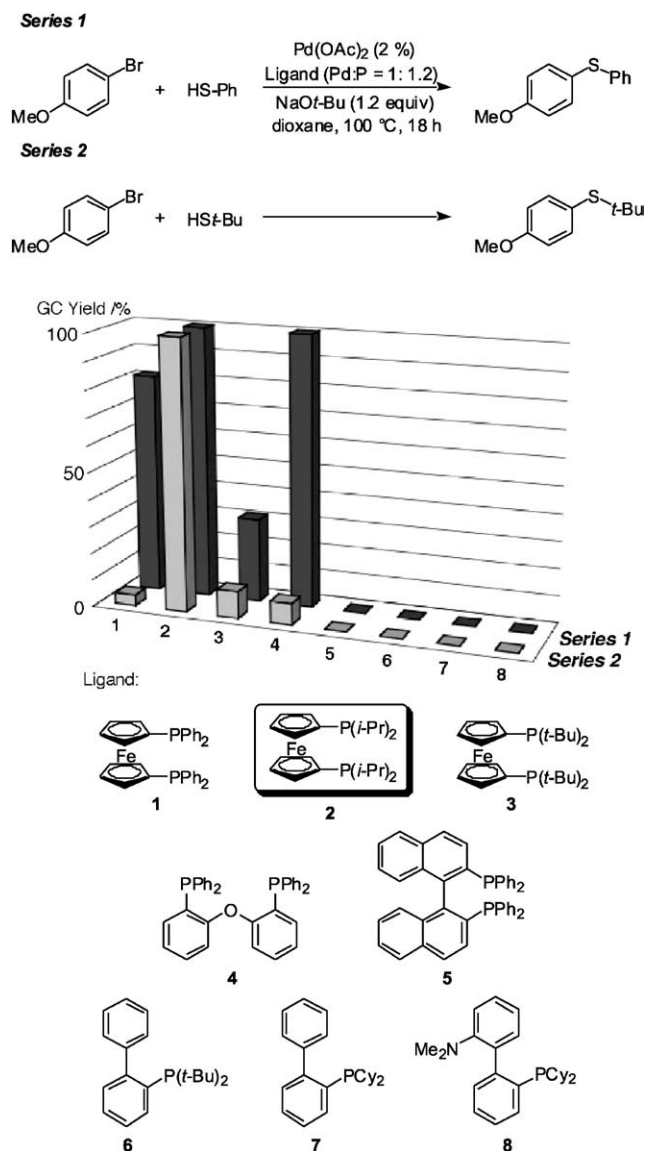


Figure 1. Screen for ligand efficiency in Pd-catalyzed C–S bond-forming reactions. Reaction conditions: ArBr (1.0 mmol), RSH (1.0 mmol), Pd(OAc)₂ (2.0 mol%), Ligand (Pd/P=1.0/1.2), *t*-BuONa (1.2 mmol) in dioxane (2 mL) at 60 °C for 18 h.

binding of more than one substrate that could lead to catalyst deactivation. It must, however, be of a suitable size or flexibility to allow for reduction of Pd(II) to Pd(0) to occur.

We also examined the reaction of 4-chloroanisole with 2-methyl-2-propanethiol (Fig. 1, series 2). DiPPF proved to be the most effective ligand for the coupling of unactivated aryl chlorides. In this case, DPPF and DPEphos were inefficient, as expected. NaOt-Bu proved to be the most generally useful base in these C–S coupling reactions. Tertiary amines were also found to be effective as bases for the reactions of aryl bromides with aliphatic thiols.^{6,7} The use of NaOt-Bu was essential, however, for the reactions of aromatic thiols.⁸ The use of other bases such as Et₃N or Cs₂CO₃ gave no product. Dioxane proved to be the most generally effective solvent, while the use of toluene resulted in slower conversion to product.

The reaction conditions described above were applied to the coupling of a number aryl bromides and chlorides at 100 °C (Table 1). As can be seen, the reactions of both of electron-rich 4-haloanisoles^{3,6,7} and di-*ortho*-substituted halides,⁸ which were problematic substrates in previous catalyst systems, proceeded in high yield (entries 1, 3, 7 and 8). The present technique tolerated a broad range (in terms of size) of aliphatic thiols, including primary, secondary and tertiary thiols. In addition, commercially available¹³ DiPPF provides a general catalyst system for C–S bond formation

Table 1. Pd-catalyzed C–S bond formation

Entry	Product	X of Ar–X	Yield (%)
1		X=Br	98
2		X=Cl	95
3		X=Cl	99
4		X=Cl	95
5 ^a		X=Cl	77
6 ^b		X=Cl	85
7		X=Br	93
8		X=Br	95
9 ^{c,d}		X=Cl	89
10		X=Cl	82
11 ^{c,d,e}		X=Cl	91

Reaction conditions: ArX (1.0 mmol), RSH (1.0 mmol), Pd(OAc)₂ (2.0 mol%), DiPPF (2.4 mol%), *t*-BuONa (1.2 mmol) in dioxane (2 mL) at 100 °C for 18 h.

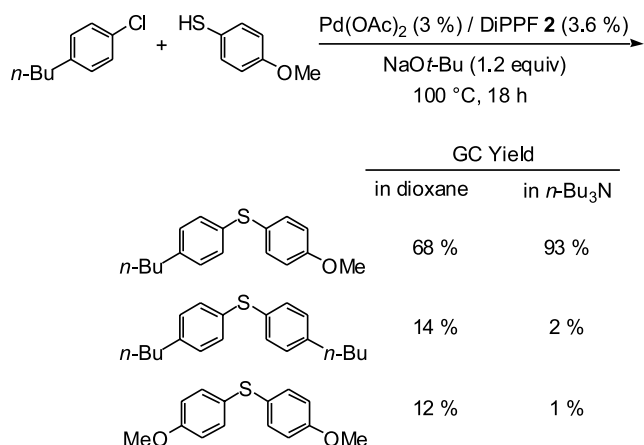
^a 1.02 mmol of *t*-BuONa was used.

^b The reaction was carried out in toluene (2.0 mL).

^c In Bu₃N (2.0 mL).

^d 3.0 mol% of catalyst was used.

^e At 120 °C.



Scheme 1. Coupling of aromatic thiols with aryl chlorides.

for aryl chlorides substrates, even electron-rich 4-chloroanisole can be processed in excellent yield (entry 3). Several functional groups in the starting aryl halides were tolerated, including a nitrile and a methyl ester (entries 5 and 10). In the case of the methyl ester, it was necessary to use a stoichiometric quantity of base; the use of excess amount of base caused the formation of the *t*-butyl ester as a side product. It was also found that triisopropylsilanethiol, an H₂S surrogate, coupled well under these conditions (entry

6).¹⁴ In contrast to the couplings of aliphatic thiols, the reactions of aryl chlorides with aromatic thiols were initially problematic. Under the standard reaction conditions, the desired product was formed along with symmetrical diarylsulfides. For example, the reaction of 4-*n*-butylchlorobenzene and 4-methoxybenzenethiol in dioxane gave the desired product along with 4-*n*-butylphenyl sulfide and 4-methoxyphenyl sulfide (Scheme 1).¹⁰ Several attempts to alleviate this problem including using lower reaction temperatures, or lower quantities of catalyst, or through the use of toluene as solvent resulted in low conversion to product, although the selectivity of the process was increased. We found, however, aryl–aryl scrambling could be prevented by the use of Bu₃N as a solvent, and the products were obtained in high yields (entries 9 and 10).

2.2. Palladium-catalyzed carbon–phosphorus bond formation

The results presented above suggested to us that bidentate ligands having di(*sec*-alkyl)phosphino groups could be highly efficient as supporting ligands for the coupling of aryl bromides and chlorides in situation in which the nucleophile and/or the product could potentially slow the desired catalytic process. In light of our results in C–S coupling reactions, we proceeded to examine the same catalyst system in carbon–phosphorus bond-forming

Table 2. Pd-catalyzed C–P bond formation

Entry	Product	X of Ar–X	Base	Solvent	Temp. (°C)	Yield (%)
1 ^a		X=Br	NaOt-Bu	Toluene	80	87
2		X=Br	Cs ₂ CO ₃	Dioxane	80	82
3		X=I	Cs ₂ CO ₃	Dioxane	80	85
4		X=Br	NaOt-Bu	Toluene	100	76
5 ^b		X=Br	Cs ₂ CO ₃	DMF	120	63
6		X=Cl	Cs ₂ CO ₃	Diglyme	120	75

Reaction condition: ArX (1.0 mmol), R₂PH (1.0 mmol), Pd(OAc)₂ (2.0 mol%), DiPPF (2.4 mol%), base (1.2 mmol) in solvent (1 mL) for 18 h.

^a The reaction was carried out for 6 h.

^b 0.5 mmol of ArBr₂ was used.

reactions (Table 2). The palladium-catalyzed coupling of various phosphorus-based nucleophiles, such as phosphites,¹⁵ phosphine oxides,¹⁶ phosphines,¹⁷ and phosphine–borane complexes,¹⁸ has previously been reported. This has been stimulated by a need to access tertiary phosphines, which are widely used as ligands for transition metal-catalyzed reactions. Secondary phosphines have been employed as coupling partners with transition-metal catalysts based on palladium, nickel¹⁹ or copper complexes.²⁰ Common protocols, however, have been inefficient for the coupling of aryl bromides,²¹ and there has been no report of the coupling of aryl chlorides with secondary phosphines. In addition, previous reports have focused on the reaction of diarylphosphines; the literature on the coupling reactions of dialkylphosphine with aryl halides is sparse.^{20a}

The reaction conditions for the C–P coupling was optimized using 5-bromo-*m*-xylene and dicyclohexylphosphine as substrates. Phosphination proceeded in high yield at 80 °C using the Pd(OAc)₂/DiPPF catalyst system (Table 2, entry 1). In contrast, DPPF and DtBPF proved ineffective as supporting ligands for this coupling process. NaO*t*-Bu/toluene and Cs₂CO₃/dioxane were found to be effective combinations of base and solvent for C–P coupling reactions, whereas tertiary amines, which were used in the previous studies, were ineffective. The coupling of *ortho*-substituted aryl halides could also be accomplished, although a small amount of reduction product was observed in several reactions (entries 2–5). Chemoselective phosphination of 1,2-dihalobenzenes could be successfully carried out to obtain (2-halophenyl)dialkylbenzenes using Cs₂CO₃ as base (entries 2 and 3). Interestingly, the present reaction was selective for the diphosphination of 2,2'-dibromo-1,1'-biphenyl (entry 5).²² Although the crude product was contaminated with reduced (2-biphenyl)dicyclopentylphosphine (25% yield), no monophosphinated 2-bromo-2'-dicyclopentylphosphino-1,1'-biphenyl was observed. The coupling of dicyclohexylphosphine with electron-deficient aryl chlorides could be carried out in good yield, although a reaction temperature of 120 °C was required (entry 6). Unfortunately, the reaction of electron-neutral 4-chlorotoluene with dicyclohexylphosphine resulted in only 36% conversion and GC yield of product under these reaction conditions (120 °C). To the best of our knowledge, this is the first example of a palladium-catalyzed cross-coupling reaction of aryl chlorides with secondary phosphines.

3. Conclusion

We have developed a general method for the cross-coupling of thiols with aryl halides using Pd(OAc)₂/1,1'-bis(diisopropylphosphino)ferrocene (DiPPF) as the catalyst. The substrate scope is significantly broader than previous methods and includes electron-rich and sterically-hindered aryl halides as well as primary, secondary and tertiary and aromatic thiols. In addition, the present system is efficient for the coupling of thiols with unactivated aryl chlorides. The Pd(OAc)₂/DiPPF catalyst system is also effective for the palladium-catalyzed coupling of secondary phosphines with aryl bromides and chlorides.

4. Experimental

4.1. General considerations

Pd(OAc)₂ and 1,1'-bis(diisopropylphosphino)ferrocene (DiPPF) were purchased from Strem Chemical Co. and used without further purification. Anhydrous NaO*t*-Bu was purchased from Aldrich and Cs₂CO₃ was purchased from Chemetall; the bulk of the material was stored under nitrogen in a Vacuum Atmospheres glovebox. Small portions (1–2 g) were removed from the glovebox in glass vials, stored in the air, and weighed in the air. Anhydrous dioxane, diglyme, and DMF were purchased from Aldrich in Sure/Seal[®] bottles and used without further purification. Toluene was purchased from J. T. Baker in CYCLE-TAINER[®] solvent delivery kegs, which were vigorously purged with argon for 2 h, and further purified by passing the solvent through two packed columns of neutral alumina and copper(II) oxide under argon pressure. All other reagents were purchased from Alfa Aesar or Aldrich or Strem Chemical Co., and used without further purification. All reactions were carried out under an argon atmosphere in oven-dried glassware. Melting points were obtained on a Mel-Temp capillary melting point apparatus. IR spectra were obtained by placing neat samples directly on the DiComp probe of an ASI REACTIR in situ IR instrument. ¹H NMR, ¹³C NMR and ³¹P NMR spectra were recorded on a Bruker 400 MHz with chemical shifts reported in ppm relative to the residual deuterated solvent, the internal standard tetramethylsilane, or external 85% H₃PO₄ for ³¹P. Elemental analyses were performed by Atlantic Microlabs, Norcross, GA. Gas chromatography analyses were performed on a Hewlett Packard 6890 instrument with a FID detector and a Hewlett Packard 25 m×0.2 mm i.d. HP-1 capillary column. Mass spectra (GC-MS) were recorded on a Hewlett Packard model G1800B. Flash chromatography was performed on E.M. Science Kieselgel 60 (230–400 mesh). Yields refer to isolated yields of compounds greater than 95% purity as determined by capillary GC and ¹H NMR analysis. Yields reported in Tables 1 and 2 are an average of two independent runs. The procedures described in this section are representative; thus, the yields may differ slightly from those given in Tables. All new compounds were further characterized by elemental analysis.

4.2. General procedure for palladium-catalyzed carbon–sulfur bond formation

Pd(OAc)₂ (0.020 mmol), DiPPF (0.024 mmol), NaO*t*-Bu (1.2 mmol) and the aryl halide (1.0 mmol) (if a solid) were added to an oven-dried re-sealable Schlenk tube (Table 1). The tube was evacuated and backfilled with argon (3 cycles) and then charged with dioxane (2.0 mL). The solution was stirred for 1 h at room temperature. Then aryl halide (1.0 mmol) (if a liquid) and the thiol (1.0 mmol) were added by syringe. The Schlenk tube was sealed with a Teflon valve, heated to 100 °C and stirred for 18 h. The reaction mixture was then allowed to reach room temperature. Ether (ca. 3 mL) was added and an aliquot was removed and analyzed by GC. The reaction mixture was then filtered and concentrated. The crude product was purified by flash column chromatography on silica gel to afford the desired thioether.

4.2.1. 2,6-Dimethylphenyl 2-methyl-2-propyl sulfide (entry 1).²³ Following the general procedure, the coupling of 2-bromo-*m*-xylene and 2-methyl-2-propanethiol afforded 191 mg (99% yield) of the title compound as a colorless oil. ¹H NMR (CDCl₃) δ 1.29 (s, 9H), 2.58 (s, 6H), 7.12 (s, 3H). ¹³C NMR (CDCl₃) δ 23.3, 31.8, 49.4, 128.1, 128.5, 132.4, 145.4. IR (neat, cm⁻¹) 2962, 1578, 1457, 1362, 1165, 1055. MS (EI) *m/z* (relative intensity) 194 (M⁺, 6), 138 (100). Anal. Calcd for C₁₂H₁₈S, C: 74.16, H: 9.34. Found C: 74.20, H: 9.41.

4.2.2. 4-Butylphenyl hexyl sulfide (entry 2). Following the general procedure, the coupling of 4-butylchlorobenzene and hexanethiol afforded 236 mg (95% yield) of the title compound as a yellow oil. ¹H NMR (CDCl₃) δ 0.88 (t, *J*=7.0 Hz, 3H), 0.92 (t, *J*=7.3 Hz, 3H), 1.2–1.7 (m, 12H), 2.57 (t, *J*=7.6 Hz, 2H), 2.88 (t, *J*=7.5 Hz, 2H), 7.09 (d, *J*=8.1 Hz, 2H), 7.25 (d, *J*=8.1 Hz, 2H). ¹³C NMR (CDCl₃) δ 13.9, 13.9, 22.3, 22.5, 28.5, 29.2, 31.4, 33.5, 34.3, 35.1, 128.9, 129.6, 133.5, 140.8. IR (neat, cm⁻¹) 2927, 2858, 1493, 1466, 1092. MS (EI) *m/z* (relative intensity) 250 (M⁺, 53), 207 (54), 166 (27), 123 (100). Anal. Calcd for C₁₆H₂₆S, C: 76.73, H: 10.46. Found C: 76.73, H: 10.51.

4.2.3. 4-Methoxyphenyl 2-methyl-2-propyl sulfide (entry 3). Following the general procedure, the coupling of 4-chloroanisole and 2-methyl-2-propanethiol afforded 194 mg (99% yield) of the title compound as a colorless oil. ¹H NMR (CDCl₃) δ 1.26 (s, 9H), 3.81 (s, 3H), 6.86 (d, *J*=8.7 Hz, 2H), 7.44 (d, *J*=8.7 Hz, 2H). ¹³C NMR (CDCl₃) δ 31.0, 45.7, 55.5, 114.2, 123.9, 139.1, 160.5. IR (neat, cm⁻¹) 2960, 1590, 1492, 1362, 1285, 1245, 1169, 1102, 1032. MS (EI) *m/z* (relative intensity) 196 (M⁺, 11), 140 (100). Anal. Calcd for C₁₁H₁₆OS, C: 67.30, H: 8.22. Found C: 66.51, H: 8.27.

4.2.4. 2,5-Dimethylphenyl 2-methyl-2-propyl sulfide (entry 4).²⁴ Following the general procedure, the coupling of 2-chloro-*p*-xylene and 2-methyl-2-propanethiol afforded 177 mg (91% yield) of the title compound as a colorless oil. ¹H NMR (CDCl₃) δ 1.29 (s, 9H), 2.31 (s, 3H), 2.47 (s, 3H), 7.07 (d, *J*=7.7 Hz, 1H), 7.16 (d, *J*=7.7 Hz, 1H), 7.35 (s, 1H). ¹³C NMR (CDCl₃) δ 20.9, 21.5, 31.3, 47.3, 129.9, 130.4, 132.0, 135.4, 139.7, 140.8. IR (neat, cm⁻¹) 2962, 1488, 1455, 1362, 1158. MS (EI) *m/z* (relative intensity) 194 (M⁺, 11), 138 (100). Anal. Calcd for C₁₂H₁₈S, C: 74.16, H: 9.34. Found C: 74.01, H: 9.24.

4.2.5. Methyl 3-(cyclohexylsulfanyl)benzoate (entry 5). Following the general procedure, slightly modified so that a stoichiometric quantity of NaO^tBu (98 mg, 1.02 mmol) was used, the coupling of methyl 3-chlorobenzoate and cyclohexanethiol afforded 263 mg (82% yield) of the title compound as a yellow oil. ¹H NMR (CDCl₃) δ 1.2–2.0 (m, 10H), 3.14 (br s, 1H), 3.92 (s, 3H), 7.57 (d, *J*=7.8 Hz, 1H), 7.88 (d, *J*=7.8 Hz, 1H), 8.06 (s, 1H). ¹³C NMR (CDCl₃) δ 25.9, 26.2, 33.4, 46.7, 52.5, 127.9, 128.9, 130.9, 132.6, 136.2, 136.3, 166.9. IR (neat, cm⁻¹) 2931, 2854, 1719, 1573, 1436, 1258. MS (EI) *m/z* (relative intensity) 250 (M⁺, 22), 168 (100). Anal. Calcd for C₁₄H₁₈O₂S, C: 67.16, H: 7.25. Found C: 67.41, H: 7.31.

4.2.6. 4-Butylphenyl triisopropylsilyl sulfide (entry 6).

Following the general procedure, slightly modified so that the reaction was carried out in toluene (2 mL), the coupling of 4-butylchlorobenzene and triisopropylsilane-thiol afforded 263 mg (82% yield) of the title compound as a colorless oil. ¹H NMR (CDCl₃) δ 0.91 (t, *J*=7.3 Hz, 3H), 1.07 (d, *J*=7.2 Hz, 18H), 1.1–1.6 (m, 7H), 2.55 (t, *J*=7.6 Hz, 2H), 7.01 (d, *J*=8.1 Hz, 2H), 7.39 (d, *J*=8.1 Hz, 2H). ¹³C NMR (CDCl₃) δ 13.1, 13.9, 18.4, 22.2, 33.5, 35.1, 127.7, 128.7, 135.3, 141.6. IR (neat, cm⁻¹) 2944, 2865, 1492, 1461, 1383. MS (EI) *m/z* (relative intensity) 322 (M⁺, 17), 279 (100). Anal. Calcd for C₁₉H₃₄SSi, C: 70.73, H: 10.62. Found C: 70.51, H: 10.45.

4.2.7. 4-Methoxyphenyl phenyl sulfide (entry 7).²⁵ Following the general procedure, the coupling of 4-bromoanisole and thiophenol afforded 206 mg (95% yield) of the title compound as a colorless oil. ¹H NMR (CDCl₃) δ 3.82 (s, 3H), 6.90 (d, *J*=8.8 Hz, 2H), 7.1–7.3 (m, 5H), 7.42 (d, *J*=8.8 Hz, 2H). ¹³C NMR (CDCl₃) δ 55.7, 115.4, 124.8, 126.2, 128.7, 129.3, 135.7, 139.0, 160.3. IR (neat, cm⁻¹) 3058, 3004, 2941, 2834, 1592, 1492, 1287, 1243, 1171. MS (EI) *m/z* (relative intensity) 216 (M⁺, 100), 201 (53). Anal. Calcd for C₁₃H₁₂OS, C: 72.19, H: 5.59. Found C: 72.31, H: 5.50.

4.2.8. 2,6-Dimethylphenyl phenyl sulfide (entry 8).²⁵ Following the general procedure, the coupling of 2-bromo-*m*-xylene and thiophenol afforded 202 mg (94% yield) of the title compound as a colorless oil. ¹H NMR (CDCl₃) δ 2.42 (s, 6H), 6.9–7.2 (m, 8H). ¹³C NMR (CDCl₃) δ 22.3, 125.1, 126.1, 128.9, 129.3, 129.7, 131.0, 138.5, 144.3. IR (neat, cm⁻¹) 3058, 2975, 1582, 1476, 1461, 1439, 1376. MS (EI) *m/z* (relative intensity) 214 (M⁺, 100), 136 (48). Anal. Calcd for C₁₄H₁₄S, C: 78.46, H: 6.58. Found C: 78.34, H: 6.53.

4.2.9. 4-Butylphenyl 4-methoxyphenyl sulfide (entry 9). The coupling reaction of 4-butylchlorobenzene and 4-methoxybenzenethiol was carried out in Bu₃N (2 mL) using Pd(OAc)₂ (6.8 mg, 0.030 mmol) and DiPPF (15.0 mg, 0.036 mmol). The reaction mixture was heated to 100 °C, stirred for 18 h, then allowed to reach room temperature. After ether (ca. 6 mL) was added, the resulting mixture was washed with 1 M HCl aq. (3×5 mL), dried over Na₂SO₄, and concentrated. The crude product was purified by column chromatography to afford 231 mg (85% yield) of the title compound as a colorless oil. ¹H NMR (CDCl₃) δ 0.93 (t, *J*=7.3 Hz, 3H), 1.3–1.6 (m, 4H), 2.55 (t, *J*=7.8 Hz, 2H), 3.80 (s, 3H), 6.87 (d, *J*=8.9 Hz, 2H), 7.06 (d, *J*=8.3 Hz, 2H), 7.13 (d, *J*=8.3 Hz, 2H), 7.37 (d, *J*=8.9 Hz, 2H). ¹³C NMR (CDCl₃) δ 13.9, 22.3, 33.5, 35.1, 55.3, 114.9, 125.5, 129.1, 129.2, 134.4, 134.6, 141.1, 159.5. IR (neat, cm⁻¹) 2929, 2858, 1592, 1492, 1287, 1245, 1171. MS (EI) *m/z* (relative intensity) 272 (M⁺, 62), 229 (100). Anal. Calcd for C₁₇H₂₀OS, C: 74.96, H: 7.40. Found C: 74.67, H: 7.31.

4.2.10. 3-Cyanophenyl phenyl sulfide (entry 10).²⁶ Following the above procedure, slightly modified so that the reaction was carried out at 100 °C using Pd(OAc)₂ (0.020 mmol) and DiPPF (0.024 mmol), the coupling of 3-chlorobenzonitrile and thiophenol afforded 162 mg (77% yield) of the title compound as a colorless oil. ¹H NMR (CDCl₃) δ 7.3–7.5 (m). ¹³C NMR (CDCl₃) δ 113.3, 118.2,

128.8, 129.5, 129.5, 129.8, 131.6, 132.2, 132.8, 133.3, 140.0. IR (neat, cm^{-1}) 3060, 2231, 1567, 1474, 1439, 1405. MS (EI) m/z (relative intensity) 211 (M^+ , 100), 184 (16). Anal. Calcd for $\text{C}_{13}\text{H}_9\text{NS}$, C: 73.90, H: 4.29. Found C: 73.77, H: 4.26.

4.2.11. 2,5-Dimethylphenyl 4-methoxyphenyl sulfide (entry 11). Following the above procedure, slightly modified so that the reaction was carried out at 120°C , the coupling of 2-chloro-*p*-xylene and 4-methoxybenzenethiol afforded 225 mg (92% yield) of the title compound as a colorless oil. ^1H NMR (CDCl_3) δ 2.20 (s, 3H), 2.32 (s, 3H), 3.79 (s, 3H), 6.8–6.9 (m, 4H), 7.06 (d, $J=7.6$ Hz, 1H), 7.29 (d, $J=8.7$ Hz, 2H). ^{13}C NMR (CDCl_3) δ 19.8, 20.9, 55.3, 114.9, 125.1, 127.3, 130.1, 130.4, 133.9, 134.5, 136.1, 136.1, 159.3. IR (neat, cm^{-1}) 2964, 2834, 1592, 1492, 1287, 1243, 1173. MS (EI) m/z (relative intensity) 244 (M^+ , 100), 229 (17), 136 (49). Anal. Calcd for $\text{C}_{15}\text{H}_{16}\text{OS}$, C: 73.73, H: 6.60. Found C: 73.78, H: 6.61.

4.3. General procedure for palladium-catalyzed carbon–phosphorus bond formation

$\text{Pd}(\text{OAc})_2$ (4.5 mg, 0.020 mmol), DiPPF (10.0 mg, 0.024 mmol), base (1.2 mmol) and the aryl halide (1.0 mmol) (if a solid) were added to an oven-dried resealable Schlenk tube (Table 2). The Schlenk tube was evacuated and backfilled with argon (3 cycles) and then charged with solvent (1.0 mL). The solution was stirred for 1 h at room temperature. Then aryl halide (1.0 mmol) (if liquid) and the secondary phosphine (1.0 mmol) were added by syringe. The Schlenk tube was sealed with a Teflon valve, heated and stirred for 18 h. The reaction mixture was then allowed to reach room temperature. Ether (ca. 3 mL) was added and the aliquot was analyzed by GC. The reaction mixture was then filtered and concentrated. The crude product was purified by flash column chromatography on silica gel to afford the desired tertiary phosphine.

4.3.1. Dicyclohexyl(3,5-dimethylphenyl)phosphine (entry 1). Following the general procedure, the coupling of 5-bromo-*m*-xylene and dicyclohexylphosphine was carried out in toluene (1 mL) at 80°C for 6 h using NaO^tBu (115 mg, 1.2 mmol) as a base to afford 255 mg (84% yield) of the title compound as a white solid, mp $77\text{--}78^\circ\text{C}$. ^1H NMR (C_6D_6) δ 1.0–2.0 (m, 22H), 2.16 (s, 1H), 6.82 (s, 1H), 7.34 (d, $J=7.1$ Hz, 2H). ^{13}C NMR (C_6D_6) δ 21.7, 27.2, 27.8 (d, $J=7$ Hz), 27.9 (d, $J=12$ Hz), 29.8 (d, $J=8$ Hz), 31.1 (d, $J=17$ Hz), 33.7 (d, $J=14$ Hz), 131.3, 133.4 (d, $J=20$ Hz), 135.9 (d, $J=19$ Hz), 137.7 (d, $J=7$ Hz). ^{31}P NMR (C_6D_6) δ 3.62. IR (neat, cm^{-1}) 2921, 2848. MS (EI) m/z (relative intensity) 302 (M^+ , 26), 247 (23), 220 (95). Anal. Calcd for $\text{C}_{20}\text{H}_{31}\text{P}$, C: 79.43, H: 10.33. Found C: 79.29, H: 10.43.

4.3.2. (2-Chlorophenyl)dicyclohexylphosphine (entry 2). Following the general procedure, the coupling of 2-chlorobromobenzene and dicyclohexylphosphine was carried out in dioxane at 80°C using Cs_2CO_3 as a base to afford 259 mg (84% yield) of the title compound as a white solid, mp $82\text{--}83^\circ\text{C}$. ^1H NMR (C_6D_6) δ 1.0–2.0 (m, 22H), 6.82 (t, $J=7.6$ Hz, 1H), 6.91 (t, $J=7.4$ Hz, 1H), 7.2–7.4 (m, 2H). ^{13}C NMR (C_6D_6) δ 26.8, 27.5 (d, $J=8$ Hz), 27.6 (d, $J=12$ Hz), 29.7 (d, $J=7$ Hz), 30.9 (d, $J=18$ Hz), 34.2 (d,

$J=16$ Hz), 126.2, 130.0, 130.4, 134.9, 135.7 (d, $J=25$ Hz), 142.8 (d, $J=26$ Hz). ^{31}P NMR (C_6D_6) δ -4.75 . IR (neat, cm^{-1}) 2921, 2848, 1418, 1034. MS (EI) m/z (relative intensity) 308 (M^+ , 10), 273 (100). Anal. Calcd for $\text{C}_{18}\text{H}_{26}\text{ClP}$, C: 70.00, H: 8.49. Found C: 69.85, H: 8.62.

4.3.3. (2-Bromophenyl)dicyclohexylphosphine (entry 3). Following the general procedure, the coupling of 2-bromiodobenzene and dicyclohexylphosphine was carried out in dioxane (1 mL) at 80°C for 18 h using Cs_2CO_3 (391 mg, 1.2 mmol) as a base to afford 300 mg (85% yield) of the title compound as a white solid, mp $76\text{--}77^\circ\text{C}$. ^1H NMR (C_6D_6) δ 1.0–2.0 (m, 22H), 6.73 (t, $J=7.7$ Hz, 1H), 6.95 (t, $J=7.4$ Hz, 1H), 7.24 (d, $J=7.6$ Hz, 1H), 7.49 (dd, $J=8.0$, 3.1 Hz, 1H). ^{13}C NMR (C_6D_6) δ 27.0, 27.7 (d, $J=8$ Hz), 27.8 (d, $J=12$ Hz), 29.9 (d, $J=10$ Hz), 31.0 (d, $J=17$ Hz), 35.0 (d, $J=17$ Hz), 127.0, 130.5, 134.1 (d, $J=3$ Hz), 134.5 (d, $J=30$ Hz), 134.9, 138.1 (d, $J=23$ Hz). ^{31}P NMR (C_6D_6) δ 2.26. IR (neat, cm^{-1}) 2919, 2848, 1019. MS (EI) m/z (relative intensity) 354 (M^+ , 6), 352 (M^+ , 6), 273 (100). Anal. Calcd for $\text{C}_{18}\text{H}_{26}\text{BrP}$, C: 61.20, H: 7.42. Found C: 60.97, H: 7.40.

4.3.4. 2-(Dicyclopentylphosphino)biphenyl (entry 4). Following the general procedure, the coupling of 2-bromobiphenyl and dicyclopentylphosphine was carried out in toluene at 100°C using NaO^tBu as a base to afford 265 mg (83% yield) of the title compound as a white solid, mp $88\text{--}89^\circ\text{C}$. ^1H NMR (C_6D_6) δ 1.3–2.2 (m, 18H), 7.2–7.4 (m, 6H), 7.48 (d, $J=8.1$ Hz, 2H), 7.55 (d, $J=8.1$ Hz, 1H). ^{13}C NMR (C_6D_6) δ 26.3 (d, $J=7$ Hz), 27.3 (d, $J=8$ Hz), 32.0 (d, $J=24$ Hz), 32.2 (d, $J=15$ Hz), 40.0 (d, $J=14$ Hz), 127.2, 127.7, 128.8, 130.7 (d, $J=5$ Hz), 131.7 (d, $J=4$ Hz), 132.9 (d, $J=3$ Hz), 139.1 (d, $J=20$ Hz), 143.7 (d, $J=6$ Hz), 150.4 (d, $J=28$ Hz). ^{31}P NMR (C_6D_6) δ -12.42 . IR (neat, cm^{-1}) 2944, 2863, 1463. MS (EI) m/z (relative intensity) 321 (M^+ , 97), 253 (20), 183 (100). Anal. Calcd for $\text{C}_{22}\text{H}_{27}\text{P}$, C: 81.95, H: 8.44. Found C: 81.90, H: 8.49.

4.3.5. 2,2'-Bis(dicyclopentylphosphino)-1,1'-biphenyl (entry 5). Following the general procedure, the coupling of 2,2'-dibromo-1,1'-biphenyl (0.5 mmol) and dicyclopentylphosphine (1.0 mmol) was carried out in DMF (1 mL) at 120°C using Cs_2CO_3 (1.2 mmol) as a base. Additional recrystallization from methanol/ CH_2Cl_2 was required to provide the analytically pure product, afforded 159 mg (65% yield) of the title compound as a white solid, mp $158\text{--}159^\circ\text{C}$. ^1H NMR (C_6D_6) δ 1.3–2.2 (m, 36H), 7.3–7.4 (m, 6H), 7.61 (d, $J=6.7$ Hz, 2H). ^{13}C NMR (C_6D_6) δ 26.1 (t, $J=4$ Hz), 26.7 (t, $J=4$ Hz), 26.9 (t, $J=3$ Hz), 28.1 (t, $J=4$ Hz), 31.7 (t, $J=9$ Hz), 32.0 (t, $J=7$ Hz), 32.4 (t, $J=11$ Hz), 32.8 (t, $J=14$ Hz), 37.5 (dd, $J=8$, 5 Hz), 43.0 (dd, $J=8$, 5 Hz), 127.4, 127.8, 132.3 (t, $J=4$ Hz), 132.6, 139.3 (dd, $J=10$, 6 Hz), 150.1 (t, $J=18$ Hz). ^{31}P NMR (C_6D_6) δ -13.01 . IR (neat, cm^{-1}) 2948, 2863, 1426. Anal. Calcd for $\text{C}_{32}\text{H}_{44}\text{P}_2$, C: 78.34, H: 9.04. Found C: 78.51, H: 8.99.

4.3.6. 3-(Dicyclohexylphosphino)benzotrile (entry 6). Following the general procedure, the coupling of 3-chlorobenzotrile and dicyclohexylphosphine was carried out in diglyme (1 mL) at 120°C for 18 h using Cs_2CO_3 as a base to afford 210 mg (70% yield) of the title compound as a white solid, mp $77\text{--}78^\circ\text{C}$. ^1H NMR (C_6D_6) δ 0.9–1.8 (m, 22H),

6.72 (t, $J=7.7$ Hz, 1H), 7.00 (d, $J=7.7$ Hz, 1H), 7.36 (t, $J=6.5$ Hz, 1H), 7.68 (t, $J=5.2$ Hz, 1H). ^{13}C NMR (C_6D_6) δ 26.9, 27.4 (d, $J=7$ Hz), 27.6 (d, $J=12$ Hz), 29.5 (d, $J=8$ Hz), 30.6 (d, $J=17$ Hz), 33.1 (d, $J=14$ Hz), 113.4 (d, $J=7$ Hz), 119.2, 128.8 (d, $J=7$ Hz), 132.5, 138.1 (d, $J=19$ Hz), 138.4 (d, $J=26$ Hz), 139.3 (d, $J=21$ Hz). ^{31}P NMR (C_6D_6) δ 4.28. IR (neat, cm^{-1}) 2923, 2850. MS (EI) m/z (relative intensity) 299 (M^+ , 19), 244 (17), 217 (79). Anal. Calcd for $\text{C}_{19}\text{H}_{26}\text{NP}$, C: 76.22, H: 8.75. Found C: 75.98, H: 8.70.

Acknowledgements

We thank the National Institutes of Health (GM 58160) for supporting this work. We are grateful to Pfizer, Merck, Novartis and Rhodia for additional unrestricted support. We also thank Mr. Eric R. Strieter for help in preparing this manuscript. M.M. was supported by the Ministry of Education, Culture, Sports, Science and Technology, Japan.

References and notes

- For reviews, see: (a) Muci, A. R.; Buchwald, S. L. *Top. Curr. Chem.* **2002**, 219, 131. (b) Hartwig, J. F. In *Handbook of Organopalladium Chemistry for Organic Synthesis*; Negishi, E., Ed.; Wiley: New York, 2002; p 1051. (c) Prim, D.; Campagne, J.-M.; Joseph, D.; Andrioletti, B. *Tetrahedron* **2002**, 58, 2014.
- For a review, see: Littke, A. F.; Fu, G. C. *Angew. Chem., Int. Ed.* **2002**, 41, 4176.
- (a) Li, G. Y. *Angew. Chem., Int. Ed.* **2001**, 40, 1513. (b) Li, G. Y.; Zheng, G.; Noonan, A. F. *J. Org. Chem.* **2001**, 66, 8677. (c) Li, G. Y. *J. Org. Chem.* **2002**, 67, 3643.
- Montchamp, J.-L.; Dumond, Y. R. *J. Am. Chem. Soc.* **2001**, 123, 510.
- (a) Migita, T.; Shimizu, T.; Asami, Y.; Shiobara, J.-I.; Kato, Y.; Kosugi, M. *Bull. Chem. Soc. Jpn* **1980**, 53, 1385. (b) Kosugi, M.; Ogata, T.; Terada, M.; Sano, H.; Migita, T. *Bull. Chem. Soc. Jpn* **1985**, 58, 3657.
- (a) Ciattini, P. G.; Morera, E.; Ortar, G. *Tetrahedron Lett.* **1995**, 36, 4133. (b) Wendeborn, S.; Berteina, S.; Brill, W. K.-D.; DeMesmaeker, A. *Synlett* **1998**, 671.
- (a) Zheng, N.; McWilliams, J. C.; Fleitz, F. J.; Armstrong, J. D., III; Volante, R. P. *J. Org. Chem.* **1998**, 63, 9606. (b) McWilliams, J. C.; Fleitz, F. J.; Zheng, N.; Armstrong, J. D., III. *Org. Synth.* **2002**, 79, 43.
- Schopfer, U.; Schlapbach, A. *Tetrahedron* **2001**, 57, 3069.
- The effect of 4-methoxy and 2,6-dimethyl substrates on the rate of C–S bond-forming processes has been reported. (a) Baranano, D.; Hartwig, J. F. *J. Am. Chem. Soc.* **1995**, 117, 2937. (b) Mann, G.; Baranano, D.; Hartwig, J. F.; Rheingold, A. L.; Guzei, I. A. *J. Am. Chem. Soc.* **1998**, 120, 9205.
- Takagi, K. *Chem. Lett.* **1987**, 2221.
- (a) Kwong, F. Y.; Buchwald, S. L. *Org. Lett.* **2002**, 4, 3517. (b) Bates, C. G.; Gujadhur, R. K.; Venkataraman, D. *Org. Lett.* **2002**, 4, 2803.
- Huang, X.; Anderson, K. W.; Zim, D.; Jiang, L.; Klapars, A.; Buchwald, S. L. *J. Am. Chem. Soc.* **2003**, 125, 6653.
- \$144 for 2 g from Strem Chemical Co.
- Sodium silyliolates have been used as nucleophiles Arnould, J.-C.; Didelot, M.; Pasquet, M.-J.; Cadilhac, C. *Tetrahedron Lett.* **1996**, 37, 4523.
- Hirao, T.; Masunaga, T.; Yamada, N.; Ohshiro, Y.; Agawa, T. *Bull. Chem. Soc. Jpn* **1982**, 55, 909.
- Xu, Y.; Li, Z.; Xia, J.; Guo, H.; Huang, Y. *Synthesis* **1984**, 781.
- (a) Tunney, S. E.; Stille, J. K. *J. Org. Chem.* **1987**, 52, 748. (b) Herd, O.; Hessler, A.; Hingst, M.; Tepper, M.; Stelzer, O. *J. Organomet. Chem.* **1996**, 522, 69. (c) Ager, D. J.; East, M. B.; Eisenstadt, A.; Laneman, S. A. *Chem. Commun.* **1997**, 2359. (d) Martorell, G.; Garcías, X.; Janura, M.; Saá, J. M. *J. Org. Chem.* **1998**, 63, 3463. (e) Kwong, F. Y.; Chan, K. S. *Chem. Commun.* **2000**, 1069. (f) Stadler, A.; Kappe, C. O. *Org. Lett.* **2002**, 4, 3541. (g) Brauer, D. J.; Hingst, M.; Kottsieper, K. W.; Liek, C.; Nickel, T.; Tepper, M.; Stelzer, O.; Sheldrick, W. S. *J. Organomet. Chem.* **2002**, 645, 14.
- (a) Imamoto, T. *Pure Appl. Chem.* **1993**, 65, 655. (b) Lipshutz, B. H.; Buzard, D. J.; Yun, C. S. *Tetrahedron Lett.* **1999**, 40, 201. (c) Al-Masum, M.; Livinghouse, T. *Tetrahedron Lett.* **1999**, 40, 7731. (d) Gaumont, A.-C.; Hursthouse, M. B.; Coles, S. J.; Brown, J. M. *Chem. Commun.* **1999**, 63.
- Synthesis of BINAP has been reported. Cai, D.; Payack, J. F.; Bender, D. R.; Hughes, D. L.; Verhoeven, T. R.; Reider, P. J. *J. Org. Chem.* **1994**, 59, 7180.
- (a) Gelman, D.; Jiang, L.; Buchwald, S. L. *Org. Lett.* **2003**, 5, 2315. (b) Allen, D. V.; Venkataraman, D. *J. Org. Chem.* **2003**, 68, 4590.
- The asymmetric coupling using Pd(Me-Duphos)(Ph)(I) at 50 °C was reported. Only one example of aryl bromide, however, was provided. Moncarz, J. R.; Laritcheva, N. F.; Glueck, D. S. *J. Am. Chem. Soc.* **2002**, 124, 13356.
- The selective monophosphinylation of 1,1'-binaphthyl 2, 2'-ditriflate have been reported. (a) Kurz, L.; Lee, G.; Morgans, D., Jr.; Waldyke, M. J.; Ward, T. *Tetrahedron Lett.* **1990**, 31, 6321. (b) Uozumi, Y.; Tanahashi, A.; Lee, S.-Y.; Hayashi, T. *J. Org. Chem.* **1993**, 58, 1945.
- Davis, F. A.; Jenkins, R. H.; Rizvi, S. Q. A.; Yocklovich, S. G. *J. Org. Chem.* **1981**, 46, 3467.
- Nakazumi, H.; Kitaguchi, T.; Ueyama, T.; Kitao, T. *Synthesis* **1984**, 518.
- Bates, C. G.; Gujadhur, R. K.; Venkataraman, D. *Org. Lett.* **2002**, 4, 2803.
- Kwong, F. Y.; Buchwald, S. L. *Org. Lett.* **2002**, 4, 3517.

Pd(II)-Catalyzed cyclogeneration of carbocations: subsequent rearrangement and trapping under oxidative conditions

Jeong Hwan Koh, Cheryl Mascarenhas and Michel R. Gagné*

Department of Chemistry, University of North Carolina at Chapel Hill, Chapel Hill, NC 27599-3290, USA

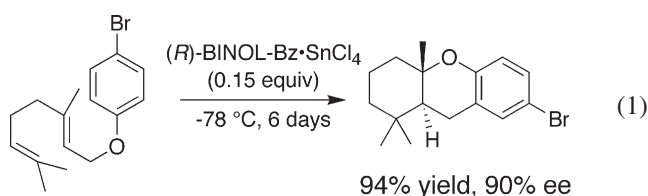
Received 1 April 2004; revised 2 June 2004; accepted 4 June 2004

Dedicated to Professor Robert H. Grubbs in recognition of his receipt of the 2003 Tetrahedron Prize

Abstract—A catalytic oxidative polycyclization reaction initiated by the carbocyclization of 1,5-dienes with Pd(II) is reported. Trapping of a putative carbocation with suitable functional groups (phenols, alkenes, alcohols, sulfonamide), or rearrangement protocols (Pinacol) yields poly-cyclic products in good yields and in excellent diastereoselectivities. Turnover of the intermediate Pd–C bond is via β -H elimination. © 2004 Elsevier Ltd. All rights reserved.

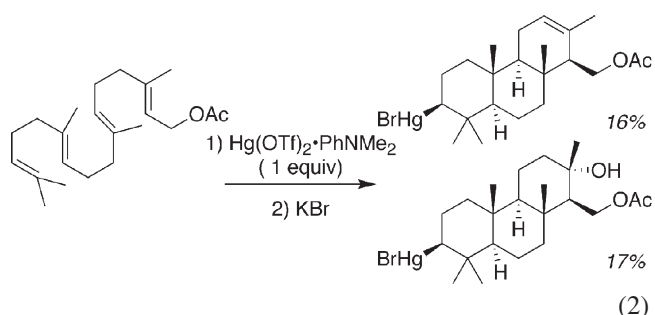
1. Introduction

Carbocations are key intermediates in the biosynthesis of the terpenoid natural products. These reactive intermediates are normally generated by alkene or epoxide protonation, or pyrophosphate elimination followed by trapping or rearrangement under careful enzymatic guidance.¹ Because enantioselective proton delivery is considerably more difficult to control in non-enzymatic situations, their application to synthesis is significantly less developed.² Notable exceptions, however, are Yamamoto's chiral Brønsted Lewis Acid (BLA) catalysts,³ which can deliver H^+ with a preference for one enantioface of a polyene reactant and, thereby, initiate enantioselective cation-olefin polycyclization reactions, in analogy to steroid biosynthesis (e.g., Eq. 1).



The analogy between proton reactivity and electrophiles like Hg(II) and Br^+ has stimulated the development of methods for activating alkenes towards the addition of carbon and hetero-nucleophiles alike.² Similar to H^+ , electrophiles like Hg(II) prefer to coordinate and activate electron rich alkenes and are thus able to initiate steroid-like

cation-olefin cascades of polyprenoids, for example, Eq. 2.⁴ The resulting C–Hg bond is stable and amenable to numerous derivitization protocols.^{5,6}

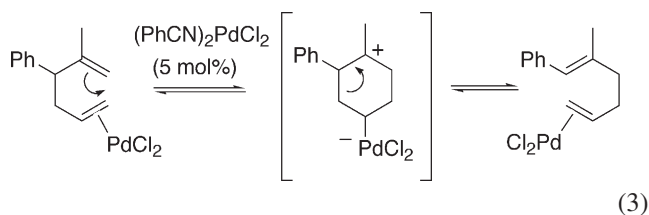


Another electrophilic species that has shown significant utility in the activation of alkenes towards hetero-nucleophiles is Pd(II).⁷ However, few applications of Pd(II) utilize carbon-based nucleophiles,⁸ though several recent publications are demonstrating that this limitation is being solved, especially for enolic nucleophiles.^{9–11} Like the Hg(II)-initiated cascade in Eq. 2, the addition of alkene nucleophiles to Pd(II)-alkene intermediates would be a valuable reaction as the carbocyclic products would contain Pd–C bonds that could be derivitized in situ so that the metal could be used in catalytic quantities (Hg(II) is a stoichiometric reagent).⁶ The first evidence that Pd(II) could catalytically¹² generate cations by the action of an alkene nucleophile on an activated alkene was realized by Overman in the Pd(II)-catalyzed Cope-rearrangement reactions (Eq. 3),¹³ wherein a cyclic cation was proposed as an intermediate in the rearrangement.^{13b} Grob-type fragmentation consumed the cation and led to the diene product; one

Keywords: Polycyclization; Carbocations; Carbocycles; Palladium.

* Corresponding author. Tel.: +1-91-99626341; fax: +1-91-99626342; e-mail address: mgagne@unc.edu

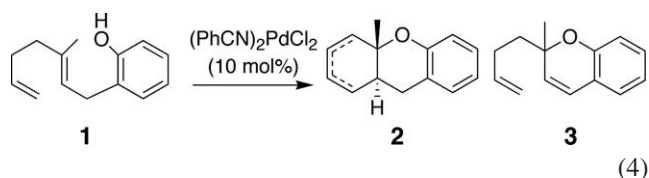
type of diene did provide a cyclic product.¹⁴ More recent studies have shown that carbocycles can be routinely maintained if the carbon nucleophile is an enol,^{9,10} or an indole.¹¹ Two recent intermolecular C–C bond forming reactions that reasonably propose cationic intermediates have been reported by Vitagliano using pincer-ligated Pt-dications¹⁵ and by Wiedenhoefer with PtCl₂.¹⁶



2. Results and discussion

We recently initiated a program to investigate methods for trapping the putative cation generated by the Pd(II)-mediated cycloisomerization of 1,5-dienes.¹⁷ To this end, we examined catalysts for the bicyclization of dienyphenol **1**, which was designed to trap the cation with the heteroatom, followed by proton loss. Since Pd(II) has a strong preference for the less substituted alkenes, the terminal alkene was expected to be the point of initiation. In the case of weakly ligated Pd(II) sources, rapid β -hydride elimination of the Pd–C bond was expected, and several reoxidation (Pd(0) to Pd(II)) procedures were investigated.^{7a}

As shown in Eq. 4, mono- and bicyclic products were obtained when PdCl₂(PhCN)₂ (10 mol%) was reacted with **1** at RT in the presence of 4 equiv. of benzoquinone (BQ). The monocyclic product (**3**) is presumably the result of a Wacker-type cyclization and is well preceded.¹⁸ The desired product (**2**) was formed as a mixture of alkene isomers, and exclusively with a *trans* ring junction. Proof of the ring stereochemistry was obtained by comparison to the known hydrogenation product (**4**).^{17,19}



Attempts to utilize CuCl₂ (Table 1, entry 2) or O₂ (entry 3) as the stoichiometric oxidant were less successful and products incorporating Cl (presumably Cl[−] trapping of the cation) or low conversions were obtained, respectively. The optimum procedure utilized CH₃CN at elevated temperatures and provided the bicycle in 85% yield, free of the Wacker product (entry 5). In contrast to PdCl₂, catalytic Pd(OAc)₂ provided none of **2**, and only the Wacker product **3** in 95% yield (entry 6).²⁰

The optimized protocol was applied to a variety of poly-enyl compounds with traps for the putative cation; the resulting alkene containing products were hydrogenated (H₂, Pd/C) and analyzed. As shown in Table 2 (entry 2), cascade cyclizations were possible from trienylphenol (**5**) to provide tricyclic products in excellent yields (89%), again as a mixture of three alkene isomers (70:17:13). Hydrogenation and NMR analysis showed the product (**6**) to have a *trans*–*trans* ring junction with diaxial methyl groups.¹⁷ When primary alcohols were utilized as the terminal trapping agent both dieny (**7**, entry 3) and trieny (**9**, entry 4) alcohols provided the desired bi-²¹ and tricyclic hydrofurans.²² The bicyclic product (**8**) was obtained as a single isomer after hydrogenation, while the tricycle was a mixture of two (91:9). The major diastereomer (**10a**) was unambiguously assigned to be dinor-ambrox, a compound whose scent has been described as having ‘a strong earthy odor reminiscent of a freshly plowed field’.²² The minor diastereomer (**10b**) was not conclusively identified, but literature data (¹H NMR) was consistent with the C-9 epimer. A sulfonamide (**11**) is also an efficient trap of the cation and annulated pyrrolidine products (**12a**, **12b**) were obtained, again with good stereocontrol of the ring junction (94:6, entry 5).²³ Stimulated by the ring-expanding/contracting pinacol rearrangement reactions reported by Overman,²⁴ we also examined the 1,5-dienyl carbinol (**13**) in entry 6. As expected, the putative tertiary carbocation undergoes a rearrangement to provide a bicyclic ketone as a mixture of two diastereomers, each a 1:1 mixture of alkene isomers. Hydrogenation provided the saturated products as an 85:15 mixture of *cis* (**14a**) and *trans* (**14b**) ring junctions.²⁵ The preference for *cis*-selective migration has been noted in several bicyclic Pinacol rearrangement reactions.^{24,26}

In contrast to the smooth high yielding reactions of 1,5-dienyl compounds, the 1,6-dienyl substrate (**15**) in entry 7 was more capricious. Multiple alkene products were obtained and hydrogenation provided a 68:32 mixture of two identifiable diastereomers (**16a**, **16b**), both of which

Table 1. Optimization of PdCl₂-catalyzed oxidative cyclization reactions

Entry	Catalyst (10 mol%)	Oxidant (equiv.)	Solvent	Temp, time	Conversion ^a (% 2 + 3)	Ratio ^a 2 : 3
1	(PhCN) ₂ PdCl ₂	BQ (4.0)	CH ₂ Cl ₂	RT, 40 h	39	74:26
2	(PhCN) ₂ PdCl ₂	CuCl ₂ (2.5)	DCE	RT, 20 h	59 ^b	72:28
3	(PhCN) ₂ PdCl ₂	O ₂ (1 atm)	THF	60 °C, 40 h	16	75:25
4	(PhCN) ₂ PdCl ₂	BQ (4.0)	THF	60 °C, 40 h	75	90:10
5	(PhCN) ₂ PdCl ₂	BQ (4.0)	CH ₃ CN	80 °C, 15 h	85	>99:1
6	Pd(OAc) ₂	BQ (4.0)	THF	60 °C, 24 h	95	>1:99

^a Determined by GC.

^b 20% of a Cl containing compound (GC-MS) was observed as a byproduct.

Table 2. PdCl₂-catalyzed oxidative cyclization reactions^a

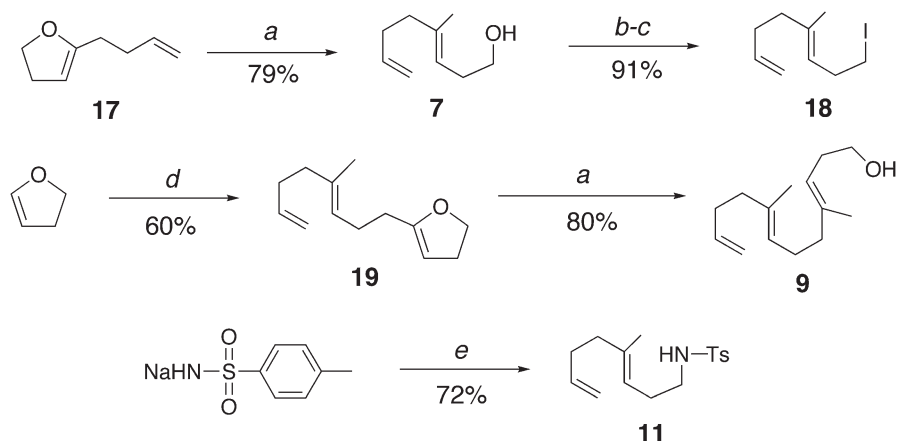
Entry	Substrate	Reaction time (h)	Alkene product (yield, ^b alkene ratio ^c)	Hydrogenated product (yield, ^b dr ^d)	
1		15	 (83%, 68:19:13)	 (98%, >99:1)	
2		48	 (89%, 70:17:13)	 (98%, >99:1)	
3		15	 (80%, >99:1)	 (98%, ^e >99:1)	
4		20	 (80%, 84:8:5:3)	 (98%, 91:9)	 10b
5		40	 (75%, 80:12:8)	 (98%, 94:6) ^f	 12b
6		17	 (85%, 43:43:7:7)	 (98%, 85:15)	 14b
7		60	 (75%, 14:27:17:15)	 (98%, ^g 68:32)	 16b

^a Reaction conditions are as described in Table 1 entry 5.^b Yield after chromatographic purification.^c Determined by GC.^d Determined by GC and ¹H NMR.^e Hydrogenation was carried out in Et₂O.^f The major is assigned the *trans* configuration by analogy.^g Includes 20% of unknown isomers

contained *trans* ring junctions but were epimeric at C-1.²⁷ The major C-1 diastereomer was equatorial, but the natural selectivity of the C–C bond-forming step is not clear since β-H elimination compromises this stereocenter. This compound was contaminated with 20% of several unidentified structural isomers (GC-MS).

3. Conclusions

Based on the precedence established by Overman in the PdCl₂-catalyzed Cope-rearrangement we report herein a PdCl₂-catalyzed cyclization reaction that is consistent with a mechanism involving the cyclo-generation of cyclic



(a) MeMgBr, Ni(0), Toluene; (b) MeSO₂Cl/Et₃N, CH₂Cl₂; (c) NaI, acetone;
 (d) t-BuLi/ Et₂O, **18**; (e) **18**, DMF.

Scheme 1. Synthetic procedure for substrates **7**, **9**, and **11**.

3°-cations from 1,5- and 1,6-dienes.^{†28} When provided with suitable traps for the cation, various poly-cyclization products are formed that are each consistent with an intermediate carbocation. Turnover is achieved by β-hydride elimination to yield cycloalkene products, usually as a mixture of alkene isomers. The resulting Pd(0) is reoxidized under standard benzoquinone oxidation conditions to the reactive Pd(II)-form. Future directions for this work will include developing traps (e.g., CO/MeOH) for the intermediate alkyl, more efficient reoxidation procedures, and asymmetric variants.

4. Experimental

4.1. General

Pd(II)-catalyzed cyclization reactions were performed under a dinitrogen atmosphere using standard Schlenk techniques. NMR spectra were recorded on a Bruker Avance400 spectrometer; chemical shifts are given in ppm and are referenced to residual solvent peaks. Gas chromatography was performed on an HP 6890 gas chromatography equipped with an HP-5 column. GC-MS analysis was performed on an Agilent 5973. High resolution mass spectrum was performed by the Mass Spectrometry Service Laboratory at the University of Minnesota. Synthesis of **1**, **5**, and **15** were performed as previously described,¹⁷ as was **13**.²⁹ Synthesis of **7**, **9**, and **11** were performed by modification of existing literature procedures^{30,31} (Scheme 1). The cyclization products **4**, **6**, and **16** were previously reported,¹⁷ as were **8**,²¹ **10**,²² and **14**.²⁵ All new compounds were determined to be >95% pure by GC and ¹H NMR spectroscopy.

[†] The bicyclization reactions in entries 1, 3, 5 and 7 can also be explained by an initiating oxypalladation of the alkene proximal to the heteroatom,²⁸ followed by a 6-*endo* coordination insertion/β-hydride elimination. The all *trans* ring junctions in the tricyclic products are not consistent with a propagating 6-*endo* cyclization, since this leads to a *cis* A-ring junction. The terminally trisubstituted compound *ortho*-geranylphenol does not react under the standard reaction conditions. A more thorough mechanistic analysis will be published in due course.

4.2. Substrate synthesis

4.2.1. 1,5-Dienyl alcohol (7).³⁰ A solution of methylmagnesium bromide in ether (21 mL, 60 mmol) was added to a stirred suspension of bis(triphenylphosphine)nickel dichloride (650 mg, 1.0 mmol) in dry toluene (45 mL) under dry nitrogen. The resulting red solution was stirred at room temperature for 20 min, and a solution of 5-(3-butenyl)-2,3-dihydrofuran (**17**) (2.5 g, 20 mmol) in toluene (30 mL) was then added. The mixture was heated to 80 °C for 1.5 h, cooled to room temperature, and poured into a saturated ammonium chloride solution (60 mL) with vigorous stirring. The mixture was stirred until decolorized and the organic material was extracted with ether. The combined extracts were dried (MgSO₄) and evaporated to leave a yellow oil. The crude mixture was purified by column chromatography on silica gel (Hexane–EtOAc=2:1) to give the product (**7**) as a colorless oil (2.2 g, 79%). ¹H NMR (400 MHz, CDCl₃) δ 5.76 (m, 1H), 5.11 (t, *J*=6.0 Hz, 1H), 4.96 (dd, *J*=17.2, 1.6 Hz, 1H), 4.92 (dd, *J*=10.0, 1.2 Hz, 1H), 3.59 (q, *J*=6.4 Hz, 2H), 2.27 (q, *J*=6.8 Hz, 2H), 2.09–2.16 (m, 4H), 1.57 (s, 3H); ¹³C NMR (100 MHz, CDCl₃) δ 138.9, 138.6, 120.7, 114.9, 62.7, 39.5, 32.5, 31.8, 16.5; HRMS (CI) [M+H]⁺/*z* Calcd 141.1279, found 141.1279.

4.2.2. 1,5,9-Trienyl alcohol (9).³⁰ 1,5,9-Trienyl alcohol (**9**) was prepared in 80% yield from **19** as described for **7**. ¹H NMR (400 MHz, CDCl₃) δ 5.77 (m, 1H), 5.09 (dd, *J*=8.0, 7.6 Hz, 2H), 4.98 (dd, *J*=16.8, 2.0 Hz, 1H), 4.91 (dd, *J*=10.0, 1.2 Hz, 1H), 3.59 (t, *J*=6.4 Hz, 2H), 2.26 (q, *J*=6.4 Hz, 2H), 2.02–2.16 (m, 8H), 1.65 (s, 3H), 1.58 (s, 3H); ¹³C NMR (100 MHz, CDCl₃) δ 139.2, 139.1, 135.1, 124.6, 120.3, 114.6, 62.8, 40.1, 39.4, 32.7, 31.8, 26.8, 16.5, 16.3; HRMS (CI) [M+NH₄]⁺/*z* Calcd 226.2171, found 226.2178.

4.2.3. 1,5-Dienyl sulfonamide (11). A mixture of 8-iodo-5-methyl-1,5-octadiene (**18**) (0.38 g, 1.54 mmol) and tosylamide monosodium salt³¹ (0.3 g, 1.54 mmol) in DMF (5.0 mL) were stirred at 80 °C for 5 h. The reaction mixture was cooled to room temperature and ether was added. The resulting solution was washed with brine, dried over MgSO₄, and evaporated under vacuum. The crude mixture

was purified by column chromatography on silica gel (Hexene–EtOAc=4:1) to give the product (**11**) as a colorless oil (0.32 g, 72%). ¹H NMR (400 MHz, CDCl₃) δ 7.71 (d, *J*=8.0 Hz, 2H), 7.27 (d, *J*=8.0 Hz, 2H), 5.71 (m, 1H), 4.89–4.99 (m, 3H), 4.61 (t, *J*=6.0 Hz, 1H), 2.91 (q, *J*=6.4 Hz, 2H), 2.39 (s, 3H), 1.98–2.15 (m, 6H), 1.51 (s, 3H); ¹³C NMR (100 MHz, CDCl₃) δ 143.2, 138.5, 138.4, 137.1, 129.6, 127.0, 120.0, 114.6, 42.8, 38.9, 32.0, 27.9, 21.4, 16.0; HRMS (CI) [M+H]⁺/*z* Calcd 294.1528, found 294.1532.

4.3. General procedure for catalytic cyclization

To a solution of (PhCN)₂PdCl₂ (7.1 mg, 18.5 μmol), and benzoquinone (80 mg, 0.74 mmol) in CH₃CN (3.0 mL) was added trienylphenol (**5**) (50 mg, 0.185 mmol). The resulting solution was stirred at 80 °C for 48 h. The reaction mixture was cooled to room temperature, filtered through a plug of silica gel, and eluted with ether. The filtrate was concentrated under vacuum and chromatographed (hexane–EtOAc=9:1) to give a mixture of alkene products (44 mg, 89%, 70:17:13). The colorless oil was taken up in MeOH (2.0 mL), and Pd/C (5 mol%) was added. The resulting slurry was stirred under hydrogen atmosphere (1 atm) at room temperature for 5 h. The reaction mixture was filtered through a plug of Celite, and washed with ether. The filtrate was concentrated under vacuum to give tricyclic product (**6**) as a colorless oil (44 mg, 98%).¹⁷

4.3.1. Trans-fused bicyclic furan (8). ¹H NMR (400 MHz, CDCl₃) δ 3.80 (m, 2H), 1.58–1.86 (m, 7H), 1.35–1.41 (m, 4H), 0.92 (s, 3H); ¹³C NMR (100 MHz, CDCl₃) δ 80.9, 64.7, 47.9, 38.7, 28.9, 26.7, 26.5, 23.7, 17.1; HRMS (CI) [M+H]⁺/*z* Calcd 141.1279, found 141.1280.

4.3.2. Trans-fused bicyclic pyrrolidine (12a). ¹H NMR (400 MHz, CDCl₃) δ 7.71 (d, *J*=8.0 Hz, 2H), 7.24 (d, *J*=8.0 Hz, 2H), 3.43 (td, *J*=9.2, 1.2 Hz, 1H), 3.27 (t, *J*=9.2 Hz, 1H), 2.39 (s, 3H), 1.78 (m, 1H), 1.49–1.71 (m, 4H), 1.47 (dd, *J*=12.8, 4.4 Hz, 1H), 1.15–1.38 (m, 5H), 1.04 (s, 3H); ¹³C NMR (100 MHz, CDCl₃) δ 142.5, 139.1, 129.7, 127.5, 66.5, 49.8, 46.5, 38.4, 30.1, 26.9, 25.8, 22.6, 21.8, 17.3; HRMS (CI) [M+H]⁺/*z* Calcd 294.1528, found 294.1533.

4.3.3. Wacker product (3). ¹H NMR (400 MHz, CDCl₃) δ 7.07 (t, *J*=7.6 Hz, 1H), 6.94 (d, *J*=7.2 Hz, 1H), 6.80 (t, *J*=7.2 Hz, 1H), 6.73 (d, *J*=8.0 Hz, 1H), 6.34 (d, *J*=10.0 Hz, 1H), 5.80 (m, 1H), 5.53 (d, *J*=10.0 Hz, 1H), 4.99 (d, *J*=17.2 Hz, 1H), 4.91 (d, *J*=8.8 Hz, 1H), 2.11–2.70 (m, 2H), 1.69–1.84 (m, 2H), 1.38 (s, 3H); ¹³C NMR (100 MHz, CDCl₃) δ 153.1, 138.5, 129.3, 129.0, 126.3, 122.9, 120.9, 120.5, 116.0, 114.3, 40.5, 28.3, 26.6, 25.2; HRMS (ESI) [M+Na]⁺/*z* Calcd 223.1094, found 223.1091.

Acknowledgements

This work was supported by the NIH (GM-60578), we also thank Ms. Claire Catteral (University of Bristol exchange student) for experimental assistance with compound **13**. MRG is a Camille Dreyfus Teacher Scholar.

References and notes

- Richards, J. H.; Hendrickson, J. B. *The Biosynthesis of Steroids, Terpenes, and Acetogenins*. W.A. Benjamin Inc: New York, 1964; pp 240–288.
- Bartlett, P. A. *Asymmetric Synthesis*, Morrison, J. D., Ed.; Academic: New York, 1984; Vol. 3, pp 341–409.
- (a) Ishihara, K.; Ishibashi, H.; Yamamoto, H. *J. Am. Chem. Soc.* **2002**, *124*, 3647–3655. (b) Nakamura, S.; Ishihara, K.; Yamamoto, H. *J. Am. Chem. Soc.* **2000**, *122*, 8131–8140.
- Nishizawa, M.; Takenaka, H.; Hayashi, Y. *J. Org. Chem.* **1986**, *51*, 806–813.
- Larock, R. C. *Organomercury Compounds in Organic Synthesis*. Springer: Berlin, 1985; pp 155–229.
- Several recent developments in Hg(II) chemistry include (a) enantioselective L*Hg(II) reagents and (b) an enyne carbocyclization that is catalytic in Hg(OTf)₂; (a) Kang, S. H.; Kim, M. *J. Am. Chem. Soc.* **2003**, *125*, 4684–4685. (b) Nishizawa, M.; Yadav, V. K.; Skwarczynski, M.; Imagawa, T. H.; Sugihara, T. *Org. Lett.* **2003**, *5*, 1609–1611.
- (a) Hegedus, L. S. *Transition Metals in the Synthesis of Complex Organic Molecules*. University Science Books: Mill Valley, CA, 1994; pp 199–236. (b) Hegedus, L. S. *Comprehensive Organic Synthesis*, Trost, B. M., Ed.; Pergamon, 1991; Vol. 4, pp 551–569.
- Hegedus, L. S. *Comprehensive Organic Synthesis*, Trost, B. M., Ed.; Pergamon, 1991; Vol. 4, pp 571–583.
- (a) Qian, H.; Widenhoefer, R. A. *J. Am. Chem. Soc.* **2003**, *125*, 2056–2057. (b) Wang, X.; Pei, T.; Han, X.; Widenhoefer, R. A. *Org. Lett.* **2003**, *5*, 2699–2701. (c) Widenhoefer, R. A. *Acc. Chem. Res.* **2002**, *35*, 905–913. (d) Pei, T.; Widenhoefer, R. A. *J. Am. Chem. Soc.* **2001**, *123*, 11290–11291. (e) Yang, D.; Li, J.-H.; Gao, Q.; Yan, Y.-L. *Org. Lett.* **2003**, *5*, 2869–2871.
- Toyota, M.; Rudyanto, M.; Ihara, M. *J. Org. Chem.* **2002**, *76*, 3374–3386.
- Ferreira, E. M.; Stoltz, B. M. *J. Am. Chem. Soc.* **2003**, *125*, 9578–9579.
- For early examples of stoichiometric Pd(II) reactivity see: (a) Trebellas, J. C.; Olechowski, J. R.; Jonassen, H. B. *J. Organomet. Chem.* **1966**, *6*, 412–420. (b) Heimbach, P.; Molin, M. *J. Organomet. Chem.* **1973**, *49*, 477–482. (c) Heimbach, P.; Molin, M. *J. Organomet. Chem.* **1973**, *49*, 483–494. (d) Brown, E. D.; Sam, T. W.; Sutherland, J. K.; Torre, A. *J. Chem. Soc., Perkin Trans. 1* **1975**, 2326–2332. (e) Hegedus, L. S.; Williams, R. E.; McGuire, M. A.; Hayashi, T. *J. Am. Chem. Soc.* **1980**, *102*, 4973–4979.
- (a) Overman, L. E.; Knoll, F. M. *J. Am. Chem. Soc.* **1980**, *102*, 865–867. (b) Overman, L. E.; Jacobsen, E. J. *J. Am. Chem. Soc.* **1982**, *104*, 7225–7231. (c) Overman, L. E.; Renaldo, A. F. *J. Am. Chem. Soc.* **1990**, *112*, 3945–3949.
- Overman, L. E.; Renaldo, A. F. *Tetrahedron Lett.* **1983**, *24*, 235–238.
- Hahn, C.; Cucciolo, M. E.; Vitagliano, A. *J. Am. Chem. Soc.* **2002**, *124*, 9038–9039.
- Wiang, W.; Widenhoefer, R. A. *Chem. Commun.* **2004**, 660–661.
- For examples of non-oxidative Pd(II)- and Pt(II)-mediated cation-olefin reactions with pincer-ligated metal complexes, see: Koh, J. H.; Gagné, M. R. *Angew. Chem., Int. Ed.* **2004**, in press.
- For a recent example of an asymmetric variant using BQ see:

- Uozumi, Y.; Kyota, H.; Kato, K.; Ogasawara, M.; Hayashi, T. *J. Org. Chem.* **1999**, *64*, 1620–1625.
19. Palucki, M.; Wolfe, J. P.; Buchwald, S. L. *J. Am. Chem. Soc.* **1996**, *118*, 10333–10334.
20. Chloride-containing Pd(II)-catalyzed Wacker cyclizations are known to proceed by *exo* addition of nucleophile, while non-chloride containing catalyst can proceed by *endo* addition mechanisms, see Hayashi, T.; Yamasaki, K.; Mimura, M.; Uozumi, Y. *J. Am. Chem. Soc.* **2004**, *126*, 3036–3037.
21. The *cis*-fused bicyclic furan is known, see: Nishizawa, M.; Iwamoto, Y.; Takao, H.; Imagawa, H.; Sugihara, T. *Org. Lett.* **2002**, *2*, 1685–1687.
22. Dinorambrox and 9-*epi*-dinorambrox, see: Ohloff, G.; Giersch, W.; Pickenhagen, W.; Furrer, A.; Frei, B. *Helv. Chim. Acta* **1985**, *68*, 2002–2029.
23. We assign the *trans* configuration for entry 5 by analogy.
24. (a) Overman, L. E.; Wolfe, J. P. *J. Org. Chem.* **2002**, *67*, 6421–6429. (b) Overman, L. E. *Acc. Chem. Res.* **1992**, *25*, 352–359.
25. (a) House, H. O.; Gaa, C. P.; VanDerveer, D. *J. Org. Chem.* **1983**, *48*, 1661–1670. (b) House, H. O.; Nomura, S. G.; VanDerveer, D.; Wissinger, E. J. *J. Org. Chem.* **1986**, *51*, 2408–2416.
26. For examples of *cis* selective pinacol rearrangements, see (a) Trost, B. M.; Neilsen, J. B.; Hoogsteen, K. *J. Am. Chem. Soc.* **1992**, *114*, 5432–5434. (b) Hirst, G. C.; Howard, P. N.; Overman, L. E. *J. Am. Chem. Soc.* **1989**, *111*, 1514–1515. (c) Herrinton, P. M.; Hopkins, M. H.; Mishra, P.; Brown, M. J.; Overman, L. E. *J. Org. Chem.* **1987**, *52*, 3711–3712.
27. The stereochemistry of the major diastereomer was unambiguously determined by X-ray methods, see Ref. 17 for additional characterization on both stereoisomers.
28. For references related to the alternative oxypalladation-initiated mechanism, see: (a) Hayashi, T.; Yamasaki, K.; Mimura, M.; Uozumi, Y. *J. Am. Chem. Soc.* **2004**, *126*, 3036–3037. (b) Hosokawa, T.; Murahashi, S.-I. *Acc. Chem. Res.* **1990**, *23*, 49–54. (c) Balsells, D.; Maseras, F.; Keay, B. A.; Ziegler, T. *Organometallics* **2004**, *23*, 2784–2796. (d) Weider, P. R.; Hegedus, L. S.; Asada, H.; D'Andreq, S. V. *J. Org. Chem.* **1985**, *50*, 4276–4281.
29. Holt, D. A. *Tetrahedron Lett.* **1981**, *22*, 2243–2246.
30. Kocienski, P.; Wadman, S.; Cooper, K. *J. Org. Chem.* **1989**, *54*, 1215–1217.
31. Bottino, F.; Grazia, M. D.; Finocchiaro, P.; Fronczek, R. R.; Mamo, A.; Pappalardo, S. *J. Org. Chem.* **1988**, *53*, 3521–3529.

A practical synthesis of optically active aromatic epoxides via asymmetric transfer hydrogenation of α -chlorinated ketones with chiral rhodium–diamine catalyst

Takayuki Hamada,^a Takayoshi Torii,^a Kunisuke Izawa^a and Takao Ikariya^{b,*}

^aAminoScience Laboratories, Ajinomoto Co., Inc., 1-1, Suzuki-cho, Kawasaki-ku, Kawasaki 210-8681, Japan

^bGraduate School of Science and Engineering, Tokyo Institute of Technology and Frontier Collaborative Research Center, 2-12-1 O-okayama, Meguro-ku, 152-8552 Tokyo, Japan

Received 22 April 2004; revised 15 June 2004; accepted 15 June 2004

Available online 8 July 2004

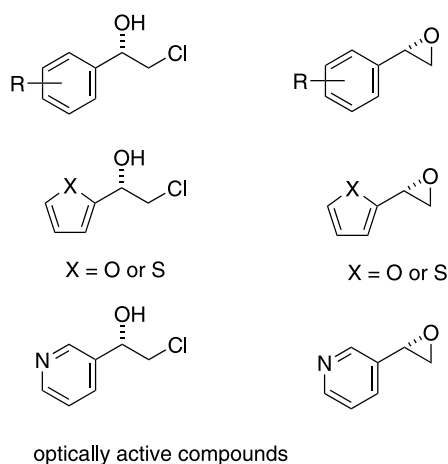
Abstract—A practical method for the synthesis of optically active aromatic epoxides has been developed via the formation of optically active α -chlorinated alcohols and intramolecular etherification. Optically active alcohols with up to 99% ee can be obtained from the asymmetric reduction of aromatic ketones with a substrate/catalyst ratio of 1000–5000 using a formic acid/triethylamine mixture containing a well-defined chiral Rh complex, Cp*RhCl[(*R,R*)-Tsdpen]. The asymmetric reduction of α -chlorinated aromatic ketones with a chiral Rh catalyst is characterized by a rapid and carbonyl group-selective transformation because of the coordinatively saturated nature of diamine-based Cp*Rh(III) hydride complexes. The outcome of the reduction is significantly influenced by the structures of the ketonic substrates as well as the hydrogen source such as formic acid or 2-propanol. Commercially available reagents and solvents can be used in this reaction without special purification. This epoxide synthetic process in either a one- or two-pot procedure is practical and particularly useful for the large-scale production of optically active styrene oxides from α -chlorinated ketones.

© 2004 Elsevier Ltd. All rights reserved.

1. Introduction

Optically active aromatic epoxides are now widely used as important synthetic intermediates for the synthesis of α 1-, β 2- and β 3-adrenergic receptor agonists.¹ This important class of compounds is readily accessible by Jacobsen's asymmetric epoxidation with (salen)Mn(III) complex^{2a,b} and kinetic resolution of racemic epoxides with cobalt–salen complexes,^{2c} in addition to some microbial approaches,³ as well as via conventional intramolecular etherification of optically active chlorinated alcohols. Although the oxidative transformation of alkenes is a straightforward procedure, a sequential transformation of α -chlorinated ketonic substrates through asymmetric reduction and intramolecular etherification is attractive because the starting carbonyl compounds are readily available. For example, optically active epoxides are readily accessible by means of asymmetric boron reduction⁴ or microbial reduction of α -halogenated ketones,⁵ followed by epoxidation of α -halogenated alcohols. However, none of the currently available chiral catalyst systems can efficiently

convert these α -halogenated ketones to optically active alcohols in a practical manner, except for some chiral Rh hydrogenation catalysts that give the product in only moderate ee.⁶



We have recently developed a highly efficient asymmetric transfer hydrogenation of aromatic ketones to the corresponding optically active alcohols catalyzed by well-defined

Keywords: Asymmetric reduction; α -Chlorinated aromatic ketone; Optically active epoxide.

* Corresponding author. Tel.: +813-573-42636; fax: +813-573-42637; e-mail address: tikariya@apc.titech.ac.jp

chiral complexes, Cp*RhCl[(*R,R*)-Tsdpen]⁷ (**1a**) and RuCl[(*R,R*)-Tsdpen](η^6 -arene) (**1b**),⁸ where Cp* = pentamethylcyclopentadienyl and TsDPEN = (1*R*,2*R*)-*N*-*p*-toluenesulfonyl-1,2-diphenylethylenediamine (Fig. 1). In particular, α -chlorinated carbonyl compounds, which cannot be efficiently hydrogenated by conventional practical hydrogenation catalysts, for example, Ru-BINAP catalysts, were found to be readily transfer-hydrogenated with these chiral complexes to the corresponding optically active chlorinated alcohols with excellent ee's.⁹ Thanks to the characteristic bifunctional properties of these chiral catalysts, functionalized aromatic ketones bearing neighboring functional groups at the α -position of the carbonyl group could be readily reduced to optically active alcohols with extremely high ee's. We describe here the details of the asymmetric synthesis of optically active epoxides through asymmetric transfer hydrogenation of α -chlorinated ketones and intramolecular etherification of the reduction products, optically active chlorinated alcohols. A mixture of formic acid/triethylamine and 2-propanol can be used as practical hydrogen sources, and the optimal hydrogen source was dependent upon the structure of the carbonyl compound.

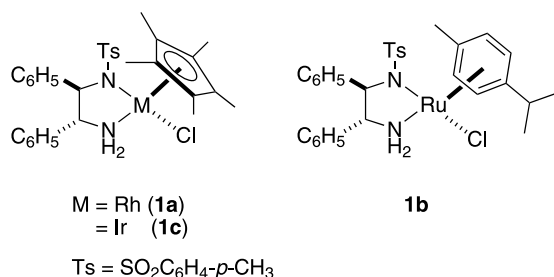


Figure 1. Chiral Rh, Ir, Ru catalysts for asymmetric transfer hydrogenation.

2. Results and discussion

2.1. Asymmetric transfer hydrogenation of α -chlorinated aromatic ketones with a formic acid/triethylamine mixture

A well-defined chiral Rh complex (*R,R*)-**1a** was found to effect the highly efficient asymmetric transfer hydrogenation of α -chloroacetophenone (**2a**) with a 5:2 formic acid/triethylamine azeotropic mixture (substrate/catalyst ratio (S/C)=1000, S/HCOOH=1/1) in a 1.0 M ethyl acetate solution at room temperature to give (*S*)- α -chlorinated alcohol (**3a**) with 97% ee and in >99% yield after 1 h. Table 1 shows some examples. The reaction proceeded equally well in various solvents, including acetonitrile, DMF, THF, toluene, CH₂Cl₂ and acetone, but not in methanol or *t*-BuOH, in which a longer reaction time was required or a lower ee was obtained. The reaction in a neat formic acid/triethylamine mixture gave unsatisfactory results in terms of enantioselectivity. A reaction temperature lower than 20 °C led to a longer reaction time and gave the product with a lower ee, and a temperature higher than 30 °C resulted in the formation of α -formyloxyacetophenone generated from the reaction of **2a** with formic acid under these conditions.

The chiral Cp*Rh complex **1a** is one of the most reactive catalysts for the asymmetric transfer hydrogenation of

Table 1. Asymmetric transfer hydrogenation of α -chloroacetophenone, **2a**, catalyzed by chiral catalysts, **1**, with a mixture of HCOOH/N(C₂H₅)₃^a

Catalyst	S/C	Temp (°C)	Solvent	Time (h)	Yield (%) ^b	ee (%) ^b	Config ^c
1a	1000	25	CH ₃ COOC ₂ H ₅	1	99	97	<i>S</i>
1b	1000	25	CH ₃ COOC ₂ H ₅	24	36 ^d	91	<i>S</i>
1c	1000	25	CH ₃ COOC ₂ H ₅	4	99	71	<i>S</i>
1a	1000	25	CH ₃ CN	1	99	93	<i>S</i>
1a	1000	25	THF	1	99	95	<i>S</i>
1a	1000	25	Acetone	1	99	96	<i>S</i>
1a	1000	25	DMF	1	99	96	<i>S</i>
1a	1000	25	CH ₂ Cl ₂	1	99	94	<i>S</i>
1a	1000	25	Toluene	1	99	92	<i>S</i>
1a	1000	25	—	1	99	89	<i>S</i>
1a	5000	25	CH ₃ COOC ₂ H ₅	2	99	96	<i>S</i>
1a	5000	20	CH ₃ COOC ₂ H ₅	5	93	71	<i>S</i>
1a	5000	30	CH ₃ COOC ₂ H ₅	2	97	92	<i>S</i>
1a	5000	40	CH ₃ COOC ₂ H ₅	8	96	81	<i>S</i>

^a The reaction of **2a** in a 0.8–1.0 M solution containing the (*R,R*)-metal catalyst (**1**) was conducted with a mixture of HCOOH and N(C₂H₅)₃ at 25 °C.

^b Unless otherwise noted, yields and ee values were determined by HPLC analysis using a Daicel Chiralcel OB-H column.

^c Configuration was determined from the sign of rotation of the isolated product.

^d Formyloxyacetophenone was formed as a main byproduct.

α -chloroacetophenones (**2a**). The reaction of **2a**, even with an S/C of 5000, under conditions otherwise identical to those described in Table 1 proceeded rapidly to give the optically active alcohol **3a** almost quantitatively with 96% ee and an initial turnover frequency (TOF) exceeding 2500 h⁻¹. The reaction rate and enantioselectivity were far superior to those obtained with the catalyst generated in situ.^{10a,b} In contrast to the Rh system, a chiral Ru complex, RuCl[(*R,R*)-Tsdpen]](*p*-cymene) (**1b**), which has a structure that is isoelectronic with **1a** and effects the asymmetric transfer hydrogenation of simple acetophenones, exhibited no remarkable activity for the reaction of **2a** with the S/C of 1000, and gave α -formyloxyacetophenone as a main product under the conditions described above. However, a decrease in the volume of the azeotropic mixture to 1 equiv. of the ketone **2a** (**2a**:HCOOH=1:1) in ethyl acetate containing 0.1 mol% chiral Ru catalyst **1b** caused an increase in the yield of desired product **3a** to 36 and 91% ee (Table 1).^{10c,d} Despite the structural similarity between the Cp*Rh and (η^6 -arene)Ru complexes, the remarkable difference in the reactivity toward α -chloroacetophenones may be attributed to the electronic properties of the central metals. An analogous Ir complex, Cp*IrCl[(*R,R*)-Tsdpen] (**1c**),⁷ exhibited reasonably high reactivity but poor enantioselectivity.

A variety of ring-substituted α -chloroacetophenones (**2b–2l**) can be transformed to the corresponding optically active secondary alcohols with high enantiomeric purities using a 5:2 formic acid/triethylamine azeotropic mixture as a hydrogen donor and the Rh catalyst **1a**, as shown in Table 2. In general, α -chloroacetophenones are more favorable substrates for transfer hydrogenation than the parent acetophenone due to thermodynamic reasons.^{8d,11} In fact, reduction of the simple acetophenone with **1a** (S/C=1000) under the same conditions gave the corresponding alcohol in only 6% yield with 91% ee after 24 h.^{8a} Noticeably, neither the rate nor the enantioselectivity are

Table 2. Asymmetric transfer hydrogenation of α -chlorinated ketones, **2**, catalyzed by chiral Rh Catalyst, **1a**, with a mixture of HCOOH/N(C₂H₅)₃^a

Substrate	R ¹	S/C	Time (h)	Yield (%) ^b	ee (%) ^b	Config ^c
2a	H	1000	1	99	97	S
2b	<i>o</i> -Cl	1000	2	81	88	S
2c	<i>m</i> -Cl	1000	2	93	95	S
2d	<i>p</i> -Cl	1000	2	90	92	S
2e	<i>o</i> -CH ₃ O	1000	2	90	95	S
2f	<i>m</i> -CH ₃ O	1000	2	90	95	S
2g	<i>p</i> -CH ₃ O	1000	2	94	94	S
2h	<i>m</i> -HO	1000	2	93	95	S
2i	<i>m</i> -CH ₃	1000	2	92	96	S
2j	<i>m</i> -CF ₃	1000	2	80	96	S
2k	<i>p</i> -MsNH	1000	2	80	97	S
2l	3',4'-OCH ₂ O	1000	2	93	98	S
2m	—	1000	2	98	59	S
2n	—	1000	2	93	58	S
2o	—	200	2	95	68	S
2p	—	1000	2	95	99	S
2q	—	1000	2	95	98	S
2r	—	500	2	95	91	S

^a The reaction of **2** in a 1.0 M CH₃COOCH₂CH₃ solution containing the (*R,R*)-Rh catalyst (**1a**) was conducted with a mixture of HCOOH and N(C₂H₅)₃ at 25 °C.

^b Unless otherwise noted, yields and ee values were determined by HPLC analysis using a Daicel Chiralcel OB or OB-H column.

^c Configuration was determined from the sign of rotation of the isolated product.

seriously affected by the electronic properties of the ring substituent. The enantiomeric excesses of the product alcohols (**3b–3l**) were generally very high (up to 97% ee). The electron-donating methoxy group on the phenyl group (**2e–2g**) did not significantly affect either the reactivity or enantioselectivity. An *o*-chloro group in acetophenone slightly decreases the enantioselectivity, possibly due to steric reasons.

The reduction of α -chloroketones bearing a conjugated C–C double (**2m, 2n**) or triple bond (**2o**) (Scheme 1), gave the corresponding products with moderate ee values of 58–68%. No reduction of the C–C double or triple bond was observed in these reactions. α -Chlorinated ketones bearing heterocyclic groups were readily reducible with the Rh

catalyst **1a** to the corresponding alcohols with excellent ee's. The reaction of furyl ketone (**2p**) or thienyl ketone (**2q**) provided the reduction product with 99% ee or 98% ee, respectively. Recently, it was reported that the reduction of α -chlorinated pyridyl ketone (**2r**) successfully proceeded to give the product with 96% ee.¹²

Similarly, the reduction of acetophenones having functional groups at the α -position in 1.0 M of ethyl acetate containing chiral catalyst and a 5:2 formic acid/triethylamine azeotropic mixture was examined.¹³ Table 3 summarizes representative results. When α -bromoacetophenone (**2s**) was used instead of α -chloroacetophenone, a side reaction gave α -formyloxyacetophenone. α -Hydroxyacetophenone (**2t**) gave a similar result as observed in a reaction of α -chloroacetophenone with the S/C of 1000. The reduction of α -methoxyacetophenone (**2u**) or α -cyanoacetophenone (**2v**), was complete with an S/C of 500 under conditions described in Table 3. The reduction of α -nitroacetophenone (**2w**) was complete with 0.1% of Rh catalyst to give the corresponding reduction product with 91% ee.^{13a} α -Benzoylacetophenone was unsuitable for this reduction.

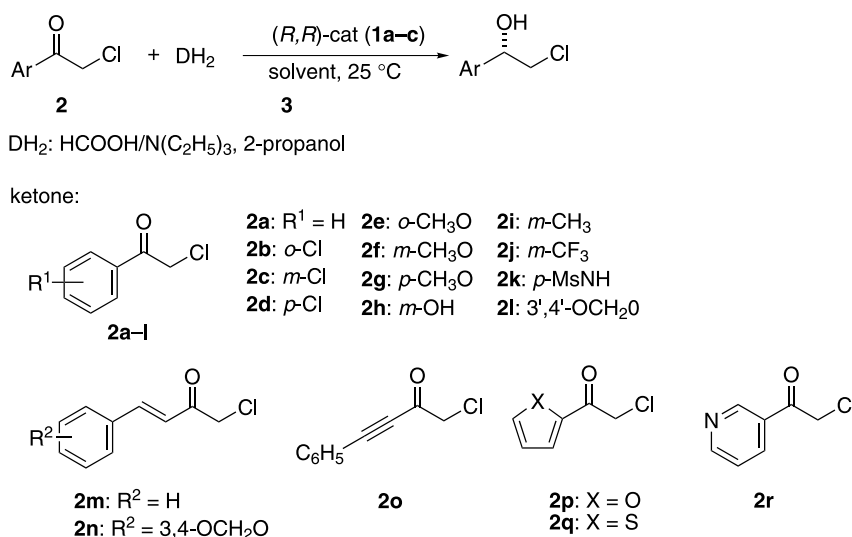
Table 3. Asymmetric transfer hydrogenation of α -substituted acetophenones (**2s–w**: PhC(=O)CH₂Y) catalyzed by chiral Rh catalyst, **1a**, with a HCOOH/N(C₂H₅)₃ mixture^a

Substrate	Y	S/C	Time (h)	Yield (%) ^b	ee (%) ^b	Config ^c
2a	Cl	5000	2	99	96	S
2s	Br	1000	1	65	10	S
2t	OH	1000	2	93	97	S
2u	OCH ₃	500	2	92	94	S
2v	CN	500	2	95	98	R
2w	NO ₂	500	2	93	95	S
2w	NO ₂	1000	4	90	91	S

^a The reaction of **2** in a 1.0 M CH₃COOCH₂CH₃ solution containing the (*R,R*)-Rh catalyst (**1a**) was conducted with a mixture of HCOOH and N(C₂H₅)₃ at 25 °C.

^b Unless otherwise noted, yields and ee values were determined by HPLC analysis using a Daicel Chiralcel OB or OB-H column.

^c Configuration was determined from the sign of rotation of the isolated product.

**Scheme 1.**

2.2. Asymmetric transfer hydrogenation of α -chlorinated aromatic ketones with 2-propanol

The outcome of the asymmetric transfer hydrogenation of **2a** with chiral Rh catalyst was influenced by the hydrogen source used. With 2-propanol, a strong base is required for the formation of an active catalyst, chiral Rh amide complex, which can react with 2-propanol to give another catalyst intermediate, chiral Rh hydride amine complex.^{8c,f} During the reversible interconversion between the amide and hydride amine complexes, the asymmetric reduction of ketones with 2-propanol can be performed.

The reaction of **2a** with the S/C of 100 with 2-propanol in the presence of a binary catalyst system, preformed Rh catalyst **1a** and *t*-C₄H₉OK, proceeded smoothly to give **3a** in 94% yield and with 98% ee after 14 h. However, an increase in the S/C ratio to 1000 caused a significant decrease in the yield due to the inherent properties of the reversible reaction with 2-propanol. Since a ternary catalyst system, [Cp**Rh*Cl₂]₂, (*R,R*)-TsDPEN, and *t*-C₄H₉OK (Rh:ligand:base=1:2:5), gave almost the same results in terms of reactivity and selectivity as the binary catalyst system, the ternary catalyst system was used to optimize the reaction conditions and to clarify the scope and limitations of the reduction with 2-propanol. The results are summarized in Table 4. The Rh catalyst strongly promoted the asymmetric reduction of α -chloroacetophenones in 2-propanol, while it showed lower reactivity toward parent acetophenone (**2x**) under the same conditions for thermodynamic reasons.^{7,8a,10d,10f} These results indicate that the catalytic performance of the Rh catalyst is completely different from that of the chiral Ru catalyst, which is an excellent catalyst for the asymmetric transfer hydrogenation of unsubstituted acetophenone.

The structure of α -chlorinated acetophenones affected the reactivity of asymmetric transfer hydrogenation in 2-propanol containing the chiral Rh catalyst. The results are shown in Table 5. The acetophenones with electron-donating alkyl (**2i**) and alkoxy (**2e–g**) groups on the aromatic ring were reducible to give the corresponding alcohols (**3e–g**, **3i**) in high yield and excellent ee. There was no substantial difference in reactivity between aromatic ring-substituted ketones at the *ortho* (**2e**), *meta* (**2f**), and *para* (**2g**) positions. Noticeably, compound **2h** bearing hydroxyl groups on the aromatic ring was also reduced

Table 4. Asymmetric transfer hydrogenation of α -chloroacetophenone, **2a**, or acetophenone, **2x**, catalyzed by chiral Rh catalyst, **1a**, with 2-propanol^a

Catalyst	Substrate	Y	Yield (%) ^b	ee (%) ^b	Config ^c
1a	2a	Cl	94	98	<i>S</i>
1b	2a	Cl	Trace	—	<i>S</i>
1c	2a	Cl	Trace	—	<i>S</i>
1a	2x	H	14	90	<i>R</i>
1b	2x	H	95	97	<i>R</i>
1c	2x	H	Trace	—	<i>R</i>

^a The reaction of **2** was conducted in a 0.1 M solution of ketone in 2-propanol at 25 °C. S/C=100.

^b Unless otherwise noted, yields and ee values were determined by HPLC analysis using a Daicel Chiralcel OB or OB-H column.

^c Configuration was determined from the sign of rotation of the isolated product.

Table 5. Asymmetric transfer hydrogenation of α -chlorinated ketones, **2**, catalyzed by chiral Rh catalyst, **1a**, with 2-propanol^a

Substrate	R ¹	Yield (%) ^b	ee (%) ^b	Config ^c
2a	H	94	97	<i>S</i>
2b	<i>o</i> -Cl	Trace	—	—
2c	<i>m</i> -Cl	Trace	—	—
2d	<i>p</i> -Cl	Trace	—	—
2e	<i>o</i> -CH ₃ O	93	96	<i>S</i>
2f	<i>m</i> -CH ₃ O	96	94	<i>S</i>
2g	<i>p</i> -CH ₃ O	96	98	<i>S</i>
2h	<i>m</i> -HO	95	99	<i>S</i>
2i	<i>m</i> -CH ₃	93	96	<i>S</i>
2j	<i>m</i> -CF ₃	Trace	—	—
2k	<i>p</i> -MsNH	Trace	—	—
2l	3',4'-OCH ₂ O	Trace	—	—
2m	—	17	92	<i>S</i>
2n	—	97	95	<i>S</i>
2o	—	Trace	—	—
2p	—	94	99	<i>S</i>
2q	—	96	98	<i>S</i>
2r	—	Trace	—	—

^a The reaction of **2** was conducted in a 0.1 M solution of ketone in 2-propanol at 25 °C. S/C=100.

^b Unless otherwise noted, yields and ee values were determined by HPLC analysis using a Daicel Chiralcel OB or OB-H column.

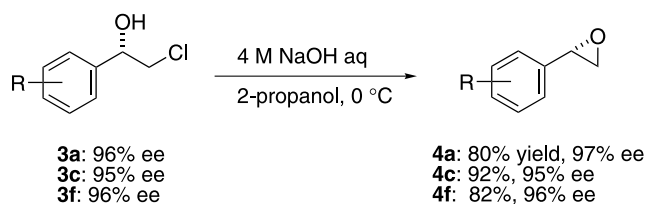
^c Configuration was determined from the sign of rotation of the isolated product.

under these reaction conditions. In contrast to the reduction with formic acid discussed above, α -chloroacetophenones bearing an aromatic ring substituents with electron-withdrawing groups, such as chloro (**2b–2d**) or trifluoromethyl (**2j**) groups, were scarcely reduced, possibly due to their strong inhibitory effect. In fact, the reaction of **2e** was retarded by an addition of 5% of **2b**, to give only 32% conversion. Compound **2b** with acidic protons might react with Rh amide to lead to the irreversible formation of catalytically inactive species.¹⁴

The reduction of 1-chloro-4-phenyl-2-butanone proceeded smoothly to give the corresponding optically active alcohol almost quantitatively with 19% ee.¹⁵ The reduction of chlorinated conjugated ketones **2n** bearing a strong electron-donating ring substituent proceeded quantitatively with good enantioselectivity. In this case, the use of 2-propanol as a hydrogen donor resulted in higher enantioselectivity than formic acid. In the reduction of aromatic heterocyclic chlorinated ketones, the electron-donating furyl (**2p**) or thienyl ketone (**2q**) were smoothly reducible to the corresponding optically active alcohols with excellent ee, as observed in the reaction of aromatic ring-substituted α -chloroacetophenone, but the electron-withdrawing pyridine (**2r**) did not give a reduced product. These results clearly show that asymmetric transfer hydrogenation of α -chlorinated aromatic ketones are delicately influenced by the structures of the ketonic substrates, and the combination of the catalyst system and hydrogen source is crucial for attaining high catalyst performance.

2.3. Epoxidation of α -chlorinated alcohols and one-pot synthesis of optically active epoxides

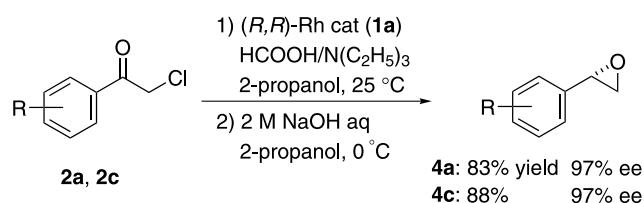
Optically active α -chlorinated alcohols **3** were readily converted by conventional procedures to optically active epoxides (**4a**, **4c**, **4f**) with excellent ee's, as shown in



Scheme 2.

Scheme 2. For example, treatment of optically active alcohol **3a** with 4 M NaOH aq. in 2-propanol afforded (*S*)-styrene oxides **4a** (97% ee) in an 80% isolated yield without loss of enantiomeric purity. In particular, *m*-chlorostyrene oxide (*S*)-**4c**, which is obtained from the reduction product (*S*)-**3c** (95% ee), is a key intermediate for the preparation of several β 3-adrenergic receptor agonist compounds.

This reductive transformation of α -chloroacetophenones to optically active epoxides was more appealing when a one-pot synthetic procedure was used. As shown in Scheme 3, sequential asymmetric reduction of **2a** or **2c** with a mixture of formic acid and triethylamine in 2-propanol containing catalyst **1a** (*S/C*=1000) for 2 h and treatment of the reaction mixture with 2 M NaOH aqueous solution at 0 °C gave optically active styrene oxide **4a** or **4c**, respectively, in an isolated yield of 80–90% with 96–98% ee in a single reactor.



Scheme 3.

3. Conclusions

We have described the successful reductive transformation of α -chlorinated ketones to optically active epoxides via asymmetric transfer hydrogenation and intramolecular etherification. The asymmetric reduction of α -chlorinated aromatic ketones with a chiral Rh catalyst is characterized by a rapid and carbonyl group-selective transformation because of the coordinatively saturated nature of diamine-based Cp*Rh hydride complexes.^{7,8,13} The neighboring chloro group at the α -position of the carbonyl group is possibly free from the metal center, leading to excellent reactivity and enantioselectivity. The outcome of the reduction is significantly influenced by the structures of the ketonic substrates as well as the hydrogen source. A simple 1:1 mixture of 98% formic acid and triethylamine can also be used instead of its azeotrope. Even commercially available reagents and solvents could be used in this reaction without special purification. This epoxide synthetic process in either a one- or two-pot procedure is particularly useful for the large-scale production of optically active epoxides.

4. Experimental

4.1. General methods

The NMR spectra were recorded in CDCl₃ with TMS (δ 0.00) as an internal standard. Infrared (IR) spectra were obtained by placing neat samples directly into the IR instrument. Enantiomer excesses of samples were determined by HPLC. Elemental analyses were performed by Tokyo Kasei Kogyo Co., Inc.

4.2. Chemical procedure

4.2.1. Preparation of α -chlorinated alcohols (2a–2r). *2-Propanol reduction system.* A mixture of **1a** (0.01 mmol) and **2a** (1.0 mmol) in 2-propanol (4.5 mL) was added to 0.1 M solution of *t*-C₄H₉OK (Rh:base:ketone=1:1:100) in 2-propanol (0.5 mL), and the mixture was stirred for 14 h at room temperature. HCl (0.5 M, 0.1 mL) was added, and the mixture was concentrated in vacuo. The residue was subjected to silica gel column chromatography to give **3a**. The ee value was determined by HPLC analysis. The absolute configuration was determined by the sign of rotation of the isolated product.

Formic acid reduction system. A mixture of α -chloroacetophenone **2a** (1.0 mmol) and catalyst **1a** (1.0 μ mol) in a 5:2 mixture of formic acid to triethylamine (0.2 mL) and ethylacetate (1.0 mL) was stirred at 25 °C for 1 h. The mixture was subjected to SiO₂ column chromatography (eluent: 20% C₂H₅OAc in hexane) to give α -chlorophenylethanol **3a**. The ee value was determined by HPLC analysis. Compounds **3a**¹⁶, **3b**¹⁷, **3c**¹⁸, **3d**¹⁷, **3g**¹⁷, **3h**¹⁷, **3i**¹⁹, **3k**¹⁶, **3l**²⁰, **3m**²¹, **3o**²² and **3r**¹² were identified by comparison to the spectral data described in the literature.

4.2.2. Large-scale preparation. 2-Chloro-*m*-chloroacetophenone **2c** (4.73 g, 25.0 mmol) was added to a solution of ethylacetate (31.3 mL) with catalyst **1a** (3.4 mg, 5.0 μ mol), formic acid (1.03 mL, 26.3 mmol) and triethylamine (3.76 mL, 26.3 mmol). The mixture was stirred at 25 °C for 2 h and washed with 2 M HCl aq. and brine. The organic layer was passed through a short SiO₂ and MgSO₄ column and concentrated to give **3c** (4.63 g, 97%). The 2-propanol solution (12.5 mL) of **3c** (4.60 g, 24.0 mmol) was treated with 4 M NaOH aq. at 0 °C for 1 h. The mixture was extracted with hexane. The organic layer was dried over MgSO₄ and concentrated to give *m*-chlorostyrene oxide **4c** (3.54 g, 96%).

4.2.3. (*S*)-2-Chloro-1-(*o*-methoxyphenyl)ethanol (3e**).** Oil; ¹H NMR (400 MHz, CDCl₃) δ 3.60–3.90 (m, 2H), 3.85 (s, 3H), 5.05–5.15 (m, 1H), 6.85–7.45 (m, 4H), ¹³C NMR (100 MHz, CDCl₃) δ 156.61, 129.60, 127.60, 121.50, 120.97, 110.83, 70.64, 55.72, 49.90; IR (neat, cm⁻¹), 3321, 1692, 1603, 1534, 1235, 1158; [α]_D²⁰ = +51.2 (*c* 2.0, CHCl₃); MS(FAB), *m/z* 186 [M]⁺. Anal. Calcd for C₉H₁₁ClO₂: C, 57.92; H, 5.94. Found; C, 57.79; H, 5.94.

4.2.4. (*S*)-2-Chloro-1-(*m*-methoxyphenyl)ethanol (3f**).** Oil; ¹H NMR (400 MHz, CDCl₃) δ 3.58–3.73 (m, 2H), 3.99 (s, 3H), 4.82 (dd, 1H, *J*=8.6, 3.6 Hz), 6.82–7.46 (m, 4H), ¹³C NMR (100 MHz, CDCl₃) δ 160.22, 142.10,

130.10, 118.77, 114.32, 112.03, 74.38, 55.67, 51.13; IR (neat, cm^{-1}), 3329, 1603, 1586, 1258, 1150, 1040; $[\alpha]_{\text{Na}}^{20} = +41.5$ (c 2.0, CHCl_3); MS(FAB), m/z 186 $[\text{M}]^+$. Anal. Calcd for $\text{C}_9\text{H}_{11}\text{ClO}_2$: C, 57.92; H, 5.94. Found; C, 57.91; H, 5.97.

4.2.5. (S)-2-Chloro-1-(*m*-trifluoromethoxyphenyl)ethanol (3j). Oil; ^1H NMR (400 MHz, CDCl_3) δ 3.42–3.91 (m, 2H), 4.94 (dd, 1H, $J=8.4, 3.4$ Hz), 7.46–7.66 (m, 4H), ^{13}C NMR (100 MHz, CDCl_3) δ 141.33, 131.58, 131.26, 130.94, 129.86, 129.85, 129.52, 129.72, 129.67, 125.60, 125.56, 123.39, 123.35, 123.31, 123.27, 123.02, 73.78, 50.84 (observed complexity due to C–F splitting); IR (neat, cm^{-1}), 3334, 1328, 1164, 1119, 1071; $[\alpha]_{\text{Na}}^{20} = +42.8$ (c 1.0, CHCl_3); MS(FAB), m/z 224 $[\text{M}]^+$. Anal. Calcd for $\text{C}_9\text{H}_8\text{ClF}_3\text{O}$: C, 48.13; H, 3.59. Found; C, 47.97; H, 3.48.

4.2.6. (S)-*trans*-4-benzo[1,3]dioxo-5-yl-1-chloro-3-buten-2-ol (3n). Oil; ^1H NMR (400 MHz, CDCl_3) δ 2.34 (brs, 1H), 3.55–3.61 (m, 1H), 3.68–3.73 (m, 1H), 4.46–4.54 (m, 1H), 5.96 (s, 2H), 6.00–6.06 (m, 1H), 6.63 (d, $J=15.9$ Hz, 1H), 6.76 (d, $J=8.0$ Hz, 1H), 6.83 (d, $J=8.0$ Hz, 1H), 6.92 (s, 1H), ^{13}C NMR (100 MHz, CDCl_3) δ 148.49, 148.08, 132.93, 130.90, 125.71, 121.96, 108.73, 106.19, 101.57, 72.75, 50.17; $[\alpha]_{\text{D}}^{20} = +15.7$ (c 0.51, CHCl_3); HRMS: Calcd for $\text{C}_{11}\text{H}_{11}\text{ClO}_3$: 226.0397, found 226.0374 (FAB).

4.2.7. (S)-2-Chloro-1-(2-furyl) ethanol (3p). Oil; ^1H NMR (400 MHz, CDCl_3) δ 2.54 (brs, 1H), 3.80–3.89 (m, 2H), 4.93–4.96 (m, 1H), 6.36–6.38 (m, 2H), 7.40–7.42 (m, 1H), ^{13}C NMR (100 MHz, CDCl_3) δ 152.95, 142.99, 110.82, 107.99, 68.43, 48.13; $[\alpha]_{\text{D}}^{20} = +23.0$ (c 0.52, CHCl_3); HRMS: Calcd for $\text{C}_6\text{H}_7\text{ClO}_2$: 146.0135, found 146.0128 (EI).

4.2.8. (S)-2-Chloro-1-(2-thienyl) ethanol (3q). Oil; ^1H NMR (400 MHz, CDCl_3) δ 2.74 (brs, 1H), 3.72–3.85 (m, 2H), 5.15–5.20 (m, 1H), 6.98–7.03 (m, 1H), 7.05–7.07 (m, 1H), 7.29–7.32 (m, 1H), ^{13}C NMR (100 MHz, CDCl_3) δ 143.58, 127.31, 125.83, 125.16, 70.71, 50.86; $[\alpha]_{\text{D}}^{20} = +28.5$ (c 0.53, CHCl_3); HRMS: Calcd for $\text{C}_6\text{H}_7\text{ClSO}$: 161.9906, found 161.9896 (EI).

4.2.9. Preparation of styrene oxides 4a–4c. The ethylacetate solution of **3a** (0.93 mmol) was treated with NaOH aqueous solution. (2 M, 10.0 mL) at 0 °C for 1 h. After usual work up procedure, styrene oxide **4a** with 96.8% ee was obtained in 83% yield. The ee value was determined by HPLC analysis using a Chiralpak AS column (250×4.6 mm). These compounds **4a**²³, **4b**²³ and **4c**²³ were identified by the spectral data described in the literature.

4.2.10. One-pot preparation of 4a. A mixture of α -chloroacetophenone **2a** (5.0 mmol) and catalyst **1a** (5.0 μmol) in a 5:2 mixture of formic acid to triethylamine (1.0 mL) and 2-propanol (6.0 mL) was stirred at 25 °C for 2 h. The mixture was cooled to 0 °C. NaOH aq. (2 M, 10.0 mL) was added to the mixture and stirred at 0 °C for 1 h. The 2-propanol layer was extracted with hexane (10 mL). The hexane solution was washed with 1 M HCl aq. (10 mL×2) and passed through a short SiO_2 column

(eluent:hexane) to give styrene oxide **4a** in 83% yield. The ee value was determined by HPLC analysis.

Acknowledgements

This work was partially supported by a Grant-in-aid from the Ministry of Education, Science, Sports and Culture of Japan (No. 14078209) and the 21st Century COE Program.

References and notes

- (a) Uehling, D. E.; Donaldson, K. H.; Deaton, D. N.; Hyman, C. E.; Sugg, E. E.; Barrett, D. G.; Hughes, R. G.; Reitter, B.; Adkison, K. K.; Lancaster, M. E.; Lee, F.; Hart, H.; Paulik, M. A.; Sherman, B. W.; True, T.; Cowman, C. *J. Med. Chem.* **2002**, *45*, 567–583. (b) CL316243: Bloom, J. D.; Dutia, M. D.; Johnson, B. D.; Wissner, A.; Burns, M. G.; Largis, E. E.; Dolan, J. A.; Claus, T. H. *J. Med. Chem.* **1992**, *35*, 3081–3084. (c) SR58611A: Cecchi, R.; Croci, T.; Boijegrain, R.; Boveri, S.; Baroni, M.; Boccardi, G.; Guimbard, J. P.; Guzzi, U. *Eur. J. Med. Chem.* **1994**, *29*, 259–267. (d) AJ9677: Kato, S.; Harada, H.; Fujii, A.; Kotai, O. JP 11255743, 1999. (e) Ro40-2148: Alig, L.; Mueller, M. EP 386603, 1991.
- (a) Palucki, M.; Pospisil, P. J.; Zhang, W.; Jacobsen, E. N. *J. Am. Chem. Soc.* **1994**, *116*, 9333–9334. (b) Palucki, M.; McCormick, G. J.; Jacobsen, E. N. *Tetrahedron Lett.* **1995**, *36*, 5457–5460. (c) Brandes, B. D.; Jacobsen, E. N. *Tetrahedron: Asymmetry* **1997**, *8*, 3927–3933.
- Matsuyama, A.; Kobayashi, Y. EP 0611826A2, 1994. (b) Tanaka, K.; Yasuda, M. *Tetrahedron: Asymmetry* **1998**, *9*, 3275–3282.
- For a review, see: (a) Wallabaum, S.; Martens, J. *Tetrahedron: Asymmetry* **1992**, *3*, 1475–1504. (b) Hett, R.; Senanayake, C. H.; Wald, S. A. *Tetrahedron Lett.* **1998**, *39*, 1705–1708. (c) Yaozhong, J.; Yong, Q.; Aiqiao, M.; Zhitang, M. *Tetrahedron: Asymmetry* **1994**, *5*, 1211–1214.
- (a) Sawa, I.; Konishi, Y.; Maemoto, S.; Hasegawa, J. WO 9201804 A1, 1992.. (b) Yasohara, Y., Sawa, I., Ueda, M., Hasegawa, J., Shimizu, A., Kataoka, M., Wada M., Kawabata, J. JP11215995, 1999.
- Devocelle, M.; Mortreux, A.; Agbossou, F.; Dormoy, J.-P. *Tetrahedron Lett.* **1999**, *40*, 4551–4554.
- Murata, K.; Ikariya, T.; Noyori, R. *J. Org. Chem.* **1999**, *64*, 2186–2187.
- (a) Hashiguchi, S.; Fujii, A.; Takehara, J.; Ikariya, T.; Noyori, R. *J. Am. Chem. Soc.* **1995**, *117*, 7562–7563. (b) Fujii, A.; Hashiguchi, S.; Uematsu, N.; Ikariya, T.; Noyori, R. *J. Am. Chem. Soc.* **1996**, *118*, 2521–2522. (c) Haack, K.-J.; Hashiguchi, S.; Fujii, A.; Ikariya, T.; Noyori, R. *Angew. Chem., Int. Ed. Engl.* **1997**, *36*, 285–288. (d) Hashiguchi, S.; Fujii, A.; Haack, K.-J.; Matsumura, K.; Ikariya, T.; Noyori, R. *Angew. Chem., Int. Ed. Engl.* **1997**, *36*, 288–290. (e) Matsumura, K.; Hashiguchi, S.; Ikariya, T.; Noyori, R. *J. Am. Chem. Soc.* **1997**, *119*, 8738–8739. (f) Noyori, R.; Hashiguchi, S. *Acc. Chem. Res.* **1997**, *30*, 97–102.
- Hamada, T.; Torii, T.; Izawa, K.; Noyori, R.; Ikariya, T. *Org. Lett.* **2002**, *4*, 4373–4376.
- (a) Palmer, M. J.; Wills, M. *Tetrahedron: Asymmetry* **1999**, *10*, 2045–2061. (b) Cross, D. J.; Kenny, J. A.; Houson, I.; Campbell, L.; Walsgrove, T.; Wills, M. *Tetrahedron:*

- Asymmetry* **2001**, *12*, 1801–1806. (c) Bayston, D. J.; Travers, C. B.; Polywka, M. E. C. *Tetrahedron: Asymmetry* **1998**, *9*, 2015–2018. (d) Kenny, J. A.; Palmer, M. J.; Smith, A. R. C.; Walsgrove, T.; Wills, M. *Synlett* **1999**, *10*, 1615–1617. (e) Ma, Y., Liu, H., Chen, L., Cui, L., Zhu, J., Deng, J **2003**, *5*, 2103–2106. (f) Blacker, A. J.; Mellor, B. J. WO 9842643, 1998. (g) Everaere, K.; Mortreux, A.; Bulliard, M.; Brussee, J.; van der Gen, A.; Nowogrocki, G.; Carpentier, J. F. *Eur. J. Org. Chem.* **2001**, *66*, 275–291. (h) Hannedouche, J.; Kenny, J. A.; Walsgrove, T.; Wills, M. *Synlett* **2002**, *13*, 263–266. (i) Palmer, M. J.; Kenny, J. A.; Walsgrove, T.; Kawamoto, A. M.; Wills, M. *J. Chem. Soc., Perkin Trans. 1* **2002**, 416–427. (j) Hannedouche, J.; Clarkson, G. J.; Wills, M. *J. Am. Chem. Soc.* **2004**, *126*, 986–987. (k) Cossy, J.; Eustache, F.; Dalko, P. I. *Tetrahedron Lett.* **2001**, *42*, 5005–5007.
11. Adkins, H.; Eloffson, R. M.; Rossow, A. G.; Robinson, C. C. *J. Am. Chem. Soc.* **1949**, *71*, 3622–3829.
12. Recently, a kg-scale reaction of (*R*)-2-amino-1-(3-pyridinyl)-ethanol was reported Duquette, J.; Zhang, M.; Zhu, L.; Reeves, R. S. *Org. Proc. Res. Dev.* **2003**, *7*, 285–288.
13. (a) Watanabe, M.; Murata, K.; Ikariya, T. *J. Org. Chem.* **2002**, *67*, 1712–1715. (b) Murata, K.; Okano, K.; Miyagi, M.; Iwane, H.; Noyori, R.; Ikariya, T. *Org. Lett.* **1999**, *1*, 1119–1121. (c) Okano, K.; Murata, K.; Ikariya, T. *Tetrahedron Lett.* **2000**, *41*, 9277–9280. (d) Koike, T.; Murata, K.; Ikariya, T. *Org. Lett.* **2000**, *2*, 3833–3836.
14. (a) Murata, K.; Konishi, H.; Ito, M.; Ikariya, T. *Organometallics* **2002**, *21*, 253–255. (b) Watanabe, M.; Murata, K.; Ikariya, T. *J. Am. Chem. Soc.* **2003**, *125*, 7508–7609. (c) Ikariya, T.; Wang, H.; Watanabe, M.; Murata, K. *J. Organomet. Chem.* **2004**, *689*, 1377–1381.
15. In the case of alkanal-*d*₁, the enantioselectivity is 24% ee; see Yamada, I.; Noyori, R. *Org. Lett.* **2000**, *2*, 3425–3427.
16. Commercially available from Aldrich.
17. Wei, Z.; Li, Z.; Lin, G. *Tetrahedron* **1998**, *54*, 13059–13072.
18. Spelberg, J. H. L.; Van Hylckama Vlieg, J. E. T.; Bosma, T.; Kellogg, R. M.; Janssen, D. B. *Tetrahedron: Asymmetry* **1999**, *10*, 2863–2870.
19. Basavaiah, D.; Reddy, G. J.; Chandrashekar, V. *Tetrahedron: Asymmetry* **2001**, *12*, 685–689.
20. Brunel, J. M.; Legrand, O.; Buono, G. *Eur. J. Org. Chem.* **2000**, *19*, 3313–3321.
21. (a) Lautens, M.; Maddess, M. L.; Sauer, E. L. O.; Ouellet, S. G. *Org. Lett.* **2002**, *4*, 83–86. (b) Schubert, T. *Berichte des Forschungszentrums Juelich* **2002**, 1–175.
22. Schubert, T.; Hummel, W.; Muller, M. *Angew. Chem., Int. Ed. Engl.* **2002**, *41*, 634–637.
23. Schaus, S. E.; Brandes, B. D.; Larrow, J. F.; Tokunaga, M.; Hansen, K. B.; Gould, A. E.; Furrow, M. E.; Jacobsen, E. N. *J. Am. Chem. Soc.* **2002**, *124*, 1307–1315.

Singlet oxygen reactions of 3-methoxy-2-pyrrole carboxylic acid *tert*-butyl esters. A route to 5-substituted pyrrole precursors of prodigiosin and analogs

Harry H. Wasserman,* Mingde Xia, Jianji Wang, Anders K. Petersen, Michael Jorgensen, Patricia Power and Jonathan Parr

Department of Chemistry, Yale University, 225 Prospect Street, New Haven, CT 06520-8107, USA

Received 27 April 2004; revised 24 May 2004; accepted 24 May 2004

Available online 17 June 2004

Dedicated with warm wishes to Professor Robert Grubbs, recipient of the Tetrahedron Prize for creativity in organic chemistry

Abstract—Reaction of the *tert*-butyl ester of 3-methoxy-2-pyrrole carboxylic acid with singlet oxygen yields a peroxidic intermediate which undergoes coupling with a range of nucleophiles to yield 5-substituted pyrroles. Among these products are α,α' -bipyrroles which serve as precursors of prodigiosin, including A-ring substituted analogues.
© 2004 Elsevier Ltd. All rights reserved.

1. Introduction

The reactions of pyrroles with singlet oxygen are of interest in connection with the widespread occurrence of pyrrole derivatives in natural products and the well-known sensitivity of these heterocyclic systems to photooxidation.^{1,2} Particular attention has been given to the role played by porphyrins in the so-called ‘photodynamic action’ the destruction of cells and tissues in the presence of light, oxygen and a sensitizing agent. These considerations have focused attention on the mechanism of pyrrole-singlet oxygen reactions leading to products of considerable interest as bioactive materials.

One of the problems in studying pyrrole photooxygenations stems from the fact that pyrrole oxidation products are usually not stable, and tend to undergo ready decomposition unless favorable conditions are present in the reaction.³ These factors include dilution, which protects against over-oxidation, and the presence of electron-withdrawing substituents. Our current studies on pyrrole photooxidation^{2,4,5} were stimulated by the availability of pyrrole derivatives having both electron-releasing substituents, attractive to the electrophilic singlet oxygen, and electron-withdrawing substituents, which help to stabilize intermediates and products.

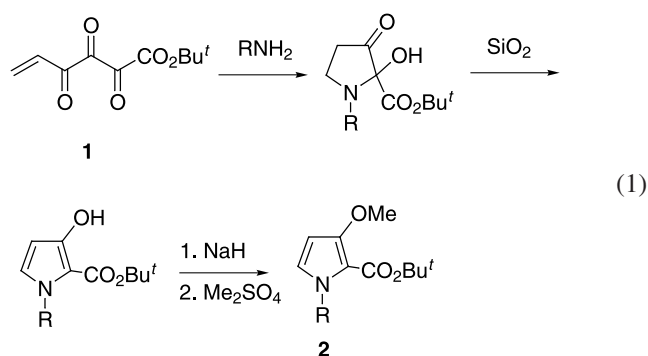
Keywords: Pyrrole; Singlet oxygen; Prodigiosin; Bipyrrole.

* Corresponding author; e-mail address: jonathan.parr@yale.edu

2. Results and discussion

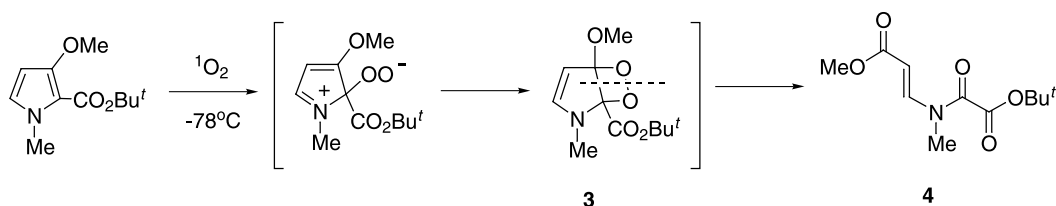
2.1. Synthesis of 5-substituted 3-methoxypyrrole 2-carboxylic acid esters

In this work, the pyrroles of special interest were the 3-methoxypyrrole 2-carboxylic acid esters **2**, readily formed by the reaction of primary amines with the

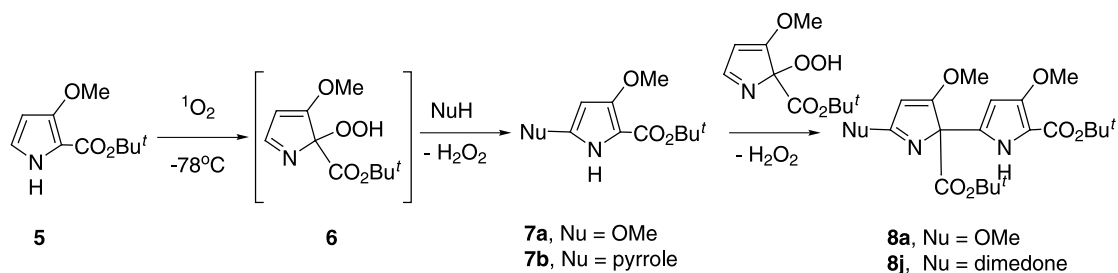


vicinal tricarbonyl ester **1** followed by methylation as shown in Eq. (1).⁶ When the oxidation reactions were carried out with pyrroles derived from primary amines such as methylamine, a mixture of products was obtained consisting mainly of the amido diester **4** (Scheme 1) resulting most probably from the cleavage of the dioxetane intermediate **3**.

With the *N*-unsubstituted pyrrole **5** formed by the reaction of the vinyl tricarbonyl **1** with ammonia, the reaction with



Scheme 1.



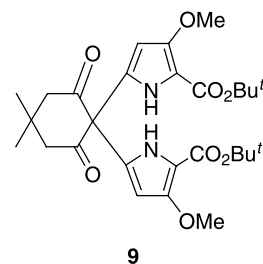
Scheme 2.

singlet oxygen in the presence of methanol took a different course, leading to the methanol adduct **7a** and the α,α' -coupling product **8a** (Scheme 2). As pictured, reaction of **5** with singlet oxygen appears to involve the formation of a transient imino hydroperoxide **6** which could then react with the nucleophile, methanol, followed by loss of hydrogen peroxide and aromatization to yield the methoxypyrrole **7a**. A second-stage addition–elimination process could then ensue generating **8a** in which two pyrrole residues are coupled in an α,α' -linkage.

In exploring the generality of this multi-step sequence particularly with respect to second-stage additions to the putative intermediate **6**, we introduced a variety of nucleophiles into the reaction of **5** with singlet oxygen.⁴ The results of this work are summarized in Table 1 showing substitution at the pyrrole 5-position. In addition to methanol (a), the nucleophiles included secondary amines, (b, c, d) pyrrole (e), imidazole (f) and β -diketones (g–k). Although singlet oxygen reactions of **5** in the presence of limited amounts of methanol yielded only **8a**, both **7a** (40%) and **8a** (22%) were obtained in the presence of higher concentrations of methanol as solvent. It appears that under the latter conditions there would be enhanced methanol competition for nucleophilic reaction with **6**.⁷ The two-stage additions to the hydroperoxide **6** involving cyclic β -diketones (Table 1, i–k) are shown in Scheme 3 using the example of dimedone as the nucleophile. The assigned structure is in complete accord with the unsymmetrical product **8j** as compared to the alternative **9**.

Compound **9** has a high degree of symmetry and would be expected to have a relatively simple ¹H NMR spectrum in accord with the presence of two equivalent pyrrole residues substituted at the quaternary carbon of dimedone. By contrast, a structure corresponding to **8j** would be expected to exhibit a more complex set of peaks consistent with the observed spectrum showing two different sets of tertiary butyl ($\delta=1.46, 1.57$), methylene ($\delta=2.40, 2.45$) and methoxy resonances ($\delta=3.80, 3.98$). Representation of **8j**

as the enol tautomer corresponds to the broad resonances of the OH proton ($\delta=9.53$) and the NH proton ($\delta=9.04$).

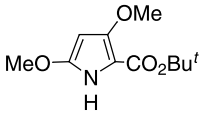
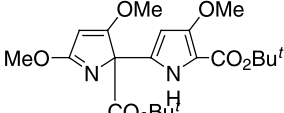
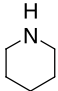
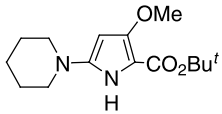
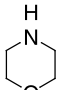
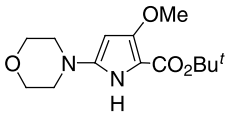
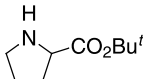
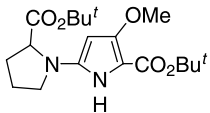
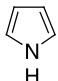
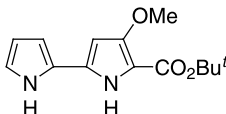
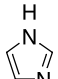
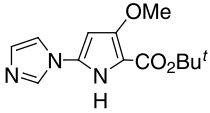
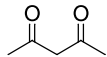
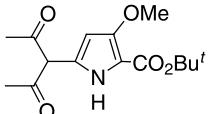
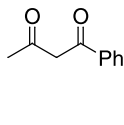
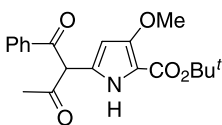
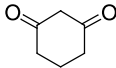
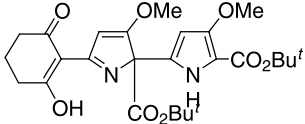
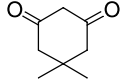
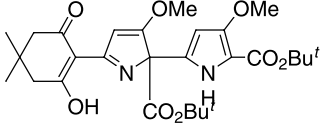
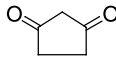
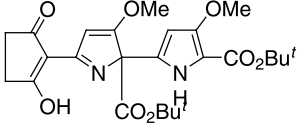


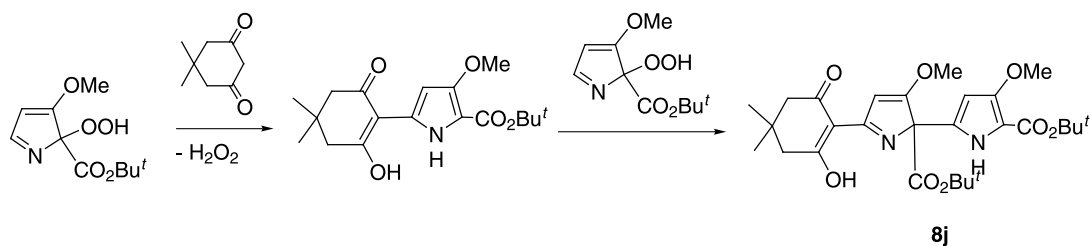
It is noteworthy that there is a difference in the outcome of the reaction of **6** with β -diketones depending on the open-chain versus cyclic nature of the nucleophile. In the case of acetylacetone ($pK_a=8.95$),¹³ the reaction yields the mono-addition product exclusively, while the cyclic β -diketones cyclohexanedione ($pK_a=5.26$), dimedone ($pK_a=4.01$) and cyclopentanedione yield only the double addition products **8(i)–(k)** (Table 1). These results can be rationalized in terms of the increased acidity of the cyclic β -diketones which will enhance the nucleophilic character of the initially-formed 5-substituted adducts, favoring the second-stage reaction. To test this idea, we used hexafluoroacetylacetone ($pK_a=5.30$)¹³ as the nucleophilic component in Scheme 3 and found that the reaction of the perfluoro analog took an entirely different direction. None of the monosubstituted product **10** was found in the reaction mixture and the only isolable product was the double-addition product **11**, identified by its characteristic proton NMR spectrum (Scheme 4).⁵ The low yield of **11** (ca. 11%) may be a consequence of side reactions such as the destruction of the initially-formed monoaddition product **10** by further reaction with singlet oxygen.

2.2. Synthesis of bipyroles related to prodigiosin

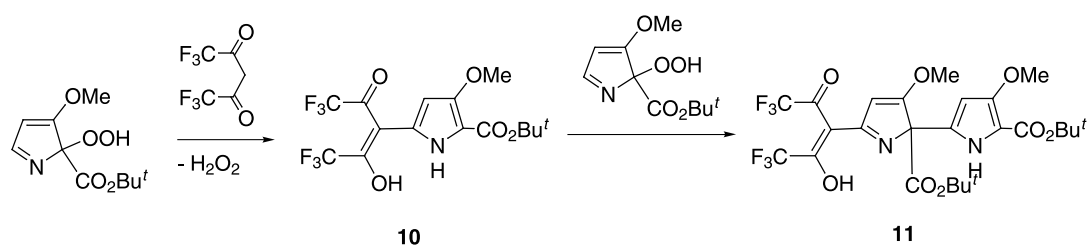
The introduction of substituents at the 5-position of 3-methoxy-2-pyrrole carboxylates may be used to form

Table 1. Photooxidation of pyrrole esters **5**. Trapping of the peroxidic intermediate with nucleophiles

Entry	Nucleophile	Monosubstitution product	Secondary addition product	Yield (%)
a	MeOH	 7a	 8a	7a , 40; 8a , 22
b				33
c				25
d				30
e		 7e		42
f				49
g				78
h				38
i				53
j				78
k				55



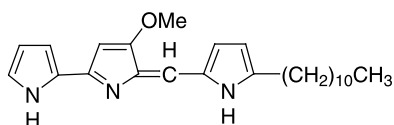
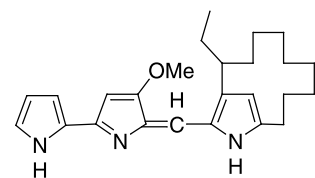
Scheme 3.



Scheme 4.

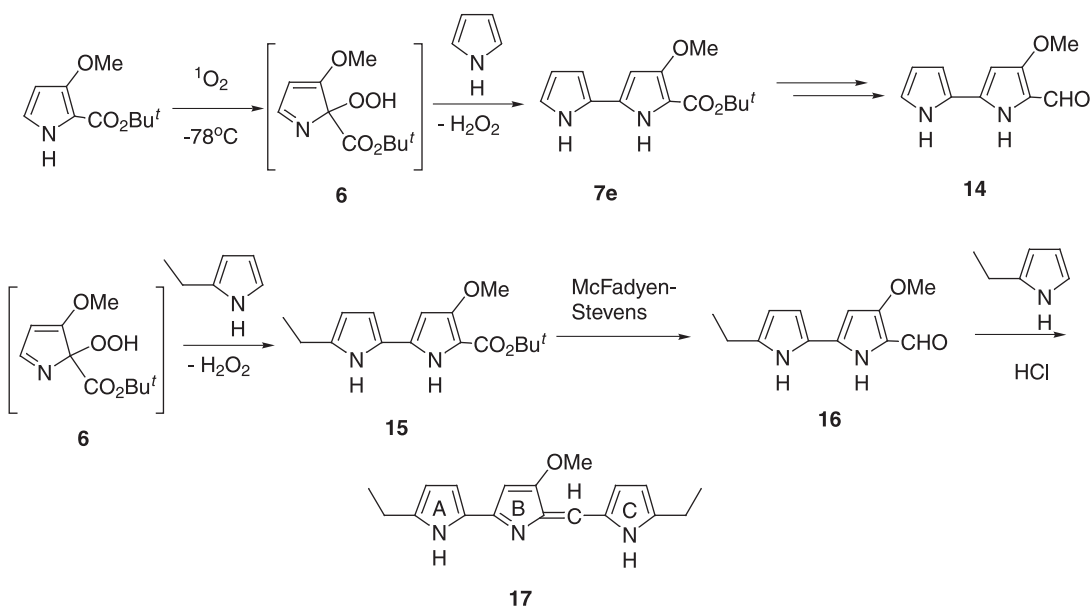
α,α' -bipyrrole derivatives which are readily convertible to tripyromethenes in the family of prodigiosins. The prodigiosins are natural products derived from *Streptomyces* or *Serratia* bacteria which have recently

received special attention because of the immunosuppressant properties exhibited by certain representatives of this family, notably the undecyl (**12**) and metacyclo (**13**) derivatives.^{10,11}

**12****13**

When pyrrole was added to the photooxidation reaction medium containing the peroxidic intermediate **6**, the α,α' -bipyrrole derivative **7e** was formed. This ester has previously been converted to the naturally-occurring aldehyde precursor **14** in a number of syntheses (Scheme 5).^{12,15,16}

Ring A analogs of prodigiosin that are not readily available through earlier routes are now accessible by this approach. Thus, the analogous A-ring substituted bipyrrole aldehyde **16** was prepared in the same way by trapping the intermediate **6** with 2-ethylpyrrole and reducing the ester to the aldehyde **16**. The next stage coupling of **16** with



Scheme 5.

ethyl pyrrole in the presence of HCl yielded the prodigiosin analog **17**.

The above synthetic procedure thus opens up the attractive possibility of employing this flexible route for sequentially coupling two substituted pyrrole units with the methoxy-pyrrole carboxylate ester core to give both A- and C-ring substituted tripyrromethenes.¹⁴

3. Experimental

3.1. General methods

All reactions were carried out in oven-dried glassware. Solvents and reagent solutions were purified according to established methods. The 3-methoxy pyrrole 2-carboxylic acid ester **5** was prepared by our procedure.² All other reagents were obtained commercially. The light source for the photooxidation was a 650 W tungsten lamp. Flash chromatography was conducted on silica gel (40–63 μm , Merck Silica Gel 60. All chromatographic purification was monitored by thin-layer chromatography (TLC) on 250 μm 60 F₂₅₄ silica-gel plates (Merck). The ¹H NMR data were collected using a Bruker AM-500 spectrometer (500 MHz) and chemical shifts are reported in ppm relative to TMS, $\delta=0$. Proton-decoupled ¹³C NMR spectra were recorded at 125 MHz. Data are reported as follows: chemical shifts in ppm downfield from TMS (δ), multiplicity (s=singlet, d=doublet, t=triplet, q=quartet, quint=quintet, m= multiplet, b=broad), coupling constants (J or $\langle J \rangle$ for an average value) in Hz, integration, and assignments. High-resolution mass spectra (HRMS) were recorded at the Mass Spectrometry Facility, Yale Medical School, Yale University. Exact molecular masses are given for the isotopes ¹H, ¹²C, ¹⁴N, ¹⁶O, ¹⁹F, ³¹P.

3.2. Experimental procedure used in the photooxidation of pyrrole **5**

3.2.1. Methanol adducts (7a) and (8a). A solution of 3-methoxy pyrrole 2-carboxylic acid ester **5** (13 mg, 0.07 mmol) and a catalytic amount of methylene blue in CH₃OH (6.6 mL) was cooled to -78°C and subjected to photooxygenation for 30 min. The solution was then concentrated and the resulting oil chromatographed (EtOAc–*n*-hexane 1:3) to yield both **7a** and **8a**. For **7a**, yield: 6 mg, 40% as a colorless oil. ¹H NMR (CDCl₃) δ : 7.68 (b, 1H, NH); 5.18 (d, $J=3.25$ Hz, 1H, pyrrole); 3.84 (s, 3H, OCH₃); 3.82 (s, 3H, OCH₃); 1.53 (s, 9H, Bu^t). ¹³C NMR (CDCl₃) δ : 174.1, 156.5, 148.7, 92.5, 79.8, 75.8, 58.1, 57.5, 27.7. HRMS: Calcd for C₁₁H₁₇NO₄: M+H⁺228.1236; found 228.1254. For **8a**, yield: 3 mg, 22% as a colorless oil. ¹H NMR (CDCl₃) δ : 9.00 (b, 1H, NH); 5.98 (d, $J=2.97$ Hz, 1H, pyrrole); 5.13 (s, 1H, pyrrole); 3.99 (s, 3H, OCH₃); 3.87 (s, 3H, OCH₃); 3.83 (s, 3H, OCH₃); 1.55 (s, 9H, Bu^t); 1.43 (s, 9H, Bu^t). ¹³C NMR (CDCl₃) δ : 178.8, 175.6, 166.6, 159.7, 152.9, 127.9, 107.3, 94.8, 92.1, 83.0, 80.1, 77.1, 59.6, 58.0, 55.0, 28.5, 27.7. HRMS: Calcd for C₂₁H₃₀N₂O₇: M+H⁺423.2136; found 423.2131.

The preparation of compounds **7(b)–(h)** and **8(i)–(k)** followed a general method, given here for **7b**.

3.2.2. Piperidine adduct (7b). A solution of **5** (10 mg, 0.051 mmol), piperidine (17 mg, 0.2 mmol) and a small amount of methylene blue in CH₂Cl₂ (10 mL) was cooled to -78°C and subjected to photooxygenation for 17 min. The solution was concentrated in vacuo and the residue purified by preparative TLC (EtOAc–*n*-hexane 1:2) to give the product as a pale solid. Yield: 13 mg, 33%. ¹H NMR (CDCl₃) δ : 7.55 (b, 1H, NH); 5.15 (d, $J=3.1$ Hz, 1H, pyrrole); 3.83 (s, 3H, OCH₃); 3.07 (m, $\langle J \rangle=5.4$ Hz, 4H, CH₂); 1.69 (m, 6H, CH₂); 1.55 (s, 9H, Bu^t). ¹³C NMR (CDCl₃) δ : 174.9, 156.0, 144.6, 100.5, 79.9, 79.4, 58.0, 48.9, 49.7, 28.8, 28.7, 25.0, 23.9. HRMS: Calcd for C₁₄H₂₄N₂O₃: M+H⁺269.1865; found 269.1859.

The following compounds were prepared according to the above method.

3.2.3. Morpholine adduct (7c). Yield: 25% as a pale yellow solid. ¹H NMR (CDCl₃) δ : 7.64 (b, 1H, NH); 5.19 (d, $J=2.9$ Hz, pyrrole); 3.82 (s, 3H, OCH₃); 3.81 (m, $\langle J \rangle=4.8$ Hz, 4H, CH₂); 3.08 (m, $\langle J \rangle=4.8$ Hz, 4H, CH₂); 1.55 (s, 9H, Bu^t). ¹³C NMR (CDCl₃) δ : 160, 143.7, 128.0, 101.2, 80.3, 79.8, 66.2, 58.1, 48.3, 28.7. HRMS: Calcd for C₁₃H₂₂N₂O₄: M+H⁺271.1657; found 271.1651.

3.2.4. Proline ester adduct (7d). Yield: 30% as a pale oil. ¹H NMR (CDCl₃) δ : 7.68 (b, 1H, NH); 4.98 (d, $J=2.6$ Hz, 1H, pyrrole); 3.98 (m, 1H, pyrrolidine); 3.67 (s, 3H, OCH₃); 3.46 (m, 1H, pyrrolidine); 3.27 (m, 1H, pyrrolidine); 2.18–2.12 (m, 4H, pyrrolidine); 1.55 (s, 9H, Bu^t); 1.47 (s, 9H, Bu^t). ¹³C NMR (CDCl₃) δ : 172.1, 165.0, 148.3, 141.6, 103.5, 82.2, 79.2, 78.1, 62.5, 58.0, 48.8, 29.9, 28.8, 28.0, 24.3. HRMS: Calcd for C₁₉H₃₀N₂O₅: M+H⁺367.2233; found 367.2229.

3.2.5. Methoxy bipyrrole ester (7e). Yield: 29% as a pale yellow solid. The product was spectroscopically identical to the known compound.¹⁶

3.2.6. Imidazole adduct (7f). Yield: 49% as a white solid. ¹H NMR (CDCl₃) δ : 9.30 (b, 1H, NH); 7.76 (s, 1H, imidazole); 7.19 (s, 1H, imidazole); 7.17 (s, 1H, imidazole); 5.93 (d, $J=2.4$ Hz, 1H, pyrrole); 3.90 (s, 3H, OCH₃); 1.57 (s, 9H, Bu^t). ¹³C NMR (CDCl₃) δ : 160.0, 152.5, 136.3, 129.9, 126.8, 118.9, 106.2, 87.4, 81.2, 58.5, 28.5. HRMS: Calcd for C₁₃H₁₇N₃O₃: M+H⁺264.1348; found 264.1342.

3.2.7. Acetylacetone adduct (7g). Yield: 70% as a white solid. ¹H NMR (CDCl₃) δ : 8.5 (b, 1H, NH); 5.79 (d, $J=2.9$ Hz, 1H); 3.86 (s, 3H, OCH₃); 1.99 (s, 6H, CH₃); 1.57 (s, 9H, Bu^t). ¹³C NMR (CDCl₃) δ : 192.8, 160.2, 153.1, 128.3, 108.4, 106.3, 98.4, 80.8, 58.2, 28.4, 23.8. HRMS: Calcd for C₁₅H₂₀NO₅: M+H⁺295.1420; found 295.1412.

3.2.8. Benzoylacetone adduct (7h). Yield: 38% as a yellow solid. ¹H NMR (CDCl₃) δ : 8.20 (b, 1H, NH); 7.42–7.20 (m, 5H, arom); 5.77 (d, $J=3.1$ Hz, pyrrole); 3.82 (s, 3H, OCH₃); 2.21 (s, 3H, CH₃); 1.54 (s, 9H, Bu^t). ¹³C NMR (CDCl₃) δ : 197.6, 184.4, 160.7, 153.3, 134.4, 131.4, 128.5, 128.4, 128.2, 128.0, 108.2, 105.1, 99.0, 80.8, 58.3, 28.6, 28.5, 25.2. HRMS: Calcd for C₂₀H₂₃NO₅: M+Na⁺380.1474; found 380.1476.

3.2.9. Cyclohexanedione adduct (8i). Yield: 53% as a pale yellow solid. $^1\text{H NMR}$ (CDCl_3) δ : 10.5 (s, 1H, OH); 9.02 (b, 1H, NH); 6.94 (b, 1H); 5.87 (d, $J=3.1$ Hz, 1H, pyrrole); 3.98 (s, 3H, OCH_3); 3.79 (s, 3H, OCH_3); 2.57 (dd, $\langle J \rangle=6.5$ Hz, 2H, CH_2); 2.52 (dd, $\langle J \rangle=6.5$ Hz, 2H, CH_2); 1.98 (dd, $\langle J \rangle=6.6$ Hz, 2H, CH_2); 1.57 (s, 9H, Bu^t); 1.47 (s, 9H, Bu^t). $^{13}\text{C NMR}$ (CDCl_3) δ : 205.9, 202.4, 175.6, 167.4, 163.3, 159.6, 152.2, 123.7, 109.7, 104.6, 95.3, 93.3, 86.2, 81.0, 71.1, 60.5, 58.3, 34.6, 33.6, 28.4, 27.7. HRMS: Calcd for $\text{C}_{26}\text{H}_{34}\text{N}_2\text{O}_8$: $\text{M}+\text{H}^+$ 503.2393; found 503.2389.

3.2.10. Dimedone adduct (8j). Yield: 78% as a pale tan solid. $^1\text{H NMR}$ (CDCl_3) δ : 10.5 (b, 1H, OH); 9.03 (b, 1H, NH); 6.95 (s, 1H, $\text{HC}=\text{C}$); 5.88 (d, $J=3.1$ Hz, 1H, pyrrole); 3.98 (s, 3H, OCH_3); 3.80 (s, 3H, OCH_3); 2.46 (s, 2H, CH_2); 2.41 (s, 2H, CH_2); 1.57 (s, 9H, Bu^t); 1.47 (s, 9H, Bu^t); 1.09 (s, 3H, CH_3); 1.08 (s, 3H, CH_3). $^{13}\text{C NMR}$ (CDCl_3) δ : 199.6, 196.9, 174.3, 170.9, 163.7, 159.6, 152.2, 124.5, 109.4, 105.1, 96.8, 95.3, 85.6, 80.8, 70.6, 60.1, 58.3, 52.8, 52.1, 30.4, 28.5, 27.8. HRMS: Calcd for $\text{C}_{28}\text{H}_{38}\text{N}_2\text{O}_8$: $\text{M}+\text{H}^+$ 531.2706; found 531.2718.

3.2.11. Cyclopentanedione adduct (8k). Yield: 55% as a pale solid. $^1\text{H NMR}$ (CDCl_3) δ : 10.1 (b, 1H, OH); 9.15 (b, 1H, NH); 6.55 (s, 1H); 5.87 (d, $J=3.1$ Hz, 1H, pyrrole); 4.01 (s, 3H, OCH_3); 3.79 (s, 3H, OCH_3); 2.57 (m, 4H, CH_2); 1.55 (s, 9H, Bu^t); 1.47 (s, 9H, Bu^t). $^{13}\text{C NMR}$ (CDCl_3) δ : 200.2, 197.3, 174.3, 171.3, 163.6, 159.6, 152.2, 124.5, 109.4, 106.2, 96.9, 95.2, 85.7, 80.8, 70.6, 60.1, 58.2, 39.0, 38.5, 28.4, 27.7, 19.4. HRMS: Calcd for $\text{C}_{26}\text{H}_{35}\text{N}_2\text{O}_8$: $\text{M}+\text{H}^+$ 503.2393; found 503.2391.

3.2.12. McFadyen–Stevens reduction forming the methoxy bipyrrole aldehyde (14). A solution of **7e** (51 mg, 0.19 mmol) was suspended in anhydrous hydrazine (4 mL) in a 10 mL round bottom flask and the apparatus was purged with argon. The flask was fitted with a reflux condenser and the reaction mixture was heated to reflux for 14 h under a balloon of argon, during which time the starting material dissolved to give a clear solution. The solution was cooled and the volatile components removed to give a light-brown oil. This oil was dissolved in pyridine (4.0 mL) and treated with a solution of TsCl (41.6 mg, 0.22 mmol) in pyridine (0.25 mL) for 30 min at room temperature. Methylene chloride (100 mL) was added to the reaction mixture and the solution was washed with water (100 mL). The aqueous phase was extracted with CH_2Cl_2 (2×100 mL) and the combined organic phases were washed with water (10 mL), dried over Na_2SO_4 and concentrated. The dark green material was dissolved in diethylene glycol (3.0 mL) and Na_2CO_3 was added. The green suspension was purged with argon and, under vigorous stirring, the mixture was lowered into a heating bath at 170°C . The color changed rapidly from green to brown. After 5 min, the heating was discontinued and after the reaction had cooled to room temperature, water (20 mL) was added. The green solution was extracted with CH_2Cl_2 (3×20 mL) and the combined organic phases were washed with water (1×5 mL) and dried over Na_2SO_4 . Removal of the volatiles gave a green solid that was chromatographed over silica (EtOAc –hexane 50:50) to give **14**. Yield: 8.4 mg, 21%. The compound was spectroscopically identical to the known material.¹⁶

3.2.13. Ethyl bipyrrole ester (15). A solution of **5** (92.3 mg, 0.47 mmol) in CH_2Cl_2 (47 mL) containing a catalytic amount of methylene blue was photolyzed for 15 min at -78°C with a steady stream of oxygen passing through the reaction mixture. The flow of oxygen was then stopped, the light turned off and 2-ethylpyrrole (0.247 g, 2.34 mmol) was added to the mixture in a single aliquot. The reaction was stirred for a further thirty minutes and then the volatiles were removed. The residue was chromatographed (EtOAc –hexane 15:85, silica gel) and the product isolated as a white powder. Yield: 33 mg, 24%. $^1\text{H NMR}$ ($\text{DMSO } d_6$) δ : 10.81 (b, 1H, NH); 10.64 (b, 1H, NH); 6.40 (m, 1H, pyrrole); 6.09 (d, $J=2.47$ Hz, 1H, pyrrole); 5.75 (m, 1H, pyrrole); 3.71 (s, 3H, OCH_3); 2.55 (q, $J=7.57$ Hz, 2H, CH_2); 1.48 (s, 9H, Bu^t); 1.18 (t, $J=7.57$ Hz, 3H, CH_3). $^{13}\text{C NMR}$ ($\text{DMSO } d_6$) δ : 159.8, 153.2, 34.9, 128.7, 122.7, 106.3, 105.8, 105.3, 90.9, 78.5, 57.6, 28.3, 20.3, 13.8. HRMS: Calcd for $\text{C}_{16}\text{H}_{22}\text{N}_2\text{O}_3$: $\text{M}+\text{H}^+$ 290.1630; found 290.1637.

3.2.14. Ethyl bipyrrole aldehyde (16). McFadyen–Stevens reduction of **15** was performed according to the method given for the reduction of **7e**. Yield: 41%. $^1\text{H NMR}$ ($\text{DMSO } d_6$) δ : 11.24 (b, 1H, CHO); 10.93 (b, 1H, NH); 9.25 (b, 1H, NH); 6.60 (m, 1H, pyrrole); 6.21 (d, $J=2.43$ Hz, 1H, pyrrole); 5.83 (m, 1H, pyrrole); 3.82 (s, 3H, OCH_3); 2.57 (q, $J=7.55$ Hz, 2H, CH_2); 1.18 (t, $J=7.55$ Hz, 3H, CH_3). $^{13}\text{C NMR}$ ($\text{DMSO } d_6$) δ : 171.1, 158.7, 136.6, 133.5, 121.9, 117.1, 108.6, 106.1, 90.4, 57.7, 20.5, 13.7. HRMS: Calcd for $\text{C}_{12}\text{H}_{14}\text{N}_2\text{O}_2$: $\text{M}+\text{H}^+$ 219.1133; found 219.1143.

3.2.15. Ethyl prodigiosin analog HCl (17). The coupling of **16** with ethylpyrrole to yield **17** was carried out under acid catalysis by known methods.^{15,16} Yield: 43%. $^1\text{H NMR}$ (CDCl_3) δ : 12.64 (b, 1H, $=\text{CH}$); 12.58 (b, 2H); 6.91 (s, 1H, pyrrole); 6.89 (dd, $J=3.69$ Hz, 2.47, 1H, pyrrole); 6.76 (dd, $J=3.53$, 2.51 Hz, 1H, pyrrole); 6.17 (d, $J=3.53$ Hz, 1H, pyrrole); 6.11 (dd, $J=3.69$, 2.10 Hz, 1H, pyrrole); 6.01 (d, $J=1.55$ Hz, 1H, pyrrole); 3.99 (s, 3H, OCH_3); 2.95 (q, $J=7.60$ Hz, 2H, CH_2); 2.80 (q, $J=7.64$ Hz, 2H, CH_2); 1.37 (t, $J=7.60$ Hz, 3H, CH_3); 1.34 (t, $J=7.64$ Hz, 3H, CH_3). $^{13}\text{C NMR}$ (CDCl_3) δ : 166.1, 152.7, 148.7, 146.8, 127.8, 125.9, 122.0, 120.9, 119.5, 114.9, 111.2, 110.3, 92.8, 58.7, 21.7, 21.6, 13.5, 13.3. HRMS: Calcd for $\text{C}_{18}\text{H}_{21}\text{N}_3\text{O}$: $\text{M}+\text{H}^+$ 296.1760; found 296.1760.

Acknowledgements

This work was supported by grants from the National Institutes of Health, the National Science Foundation and Pfizer, Inc. We thank Drs. Walter McMurray and Kathy Stone of the Yale Cancer Center Mass Spectrometry Resource for determining HRMS spectra.

References and notes

- Blum, H. R. *Photodynamic Action and Diseases Caused by Light*; Van Nostrand-Reinhold: New York, 1941.
- Wasserman, H. H.; Power, P.; Petersen, A. K. *Tetrahedron Lett.* **1996**, *37*, 6657–6659, and references cited therein.
- Wasserman, H. H.; Lipshutz, B. H. In *Singlet Oxygen*;

- Wasserman, H. H., Murray, R. W., Eds.; Academic: New York, 1979; Chapter 9.
- Wasserman, H. H.; Xia, M.; Wang, J.; Petersen, A. K.; Jorgensen, M. *Tetrahedron Lett.* **1999**, *40*, 6145–6148.
 - Wasserman, H. H.; Petersen, A. K.; Xia, M.; Wang, J. *Tetrahedron Lett.* **1999**, *40*, 7587–7589.
 - Wasserman, H. H.; Cook, J. D.; Fukuyama, J. M.; Rotello, V. M. *Tetrahedron Lett.* **1989**, *30*, 1721–1724.
 - As in many examples of pyrrole photooxidation, reaction conditions such as dilution, play an important role in determining the nature of the products. Examples of pyrrole-singlet oxygen reactions are known which normally lead to overoxidation and tar formation, but on dilution provide pure products.^{8,9}
 - Wasserman, H. H.; Liberles, A. *J. Am. Chem. Soc.* **1960**, *82*, 2086–2088.
 - de Mayo, P.; Reid, S. T. *Chem. Ind.* **1962**, 1576–1577.
 - Prodigiosin, the parent member of this group, shows potent antibacterial and cytotoxic properties although its high toxicity militates against its use as a therapeutic agent. See: Harashima, K.; Tsuchida, N.; Tanaka, T.; Nagasatu, J. *Agric. Biol. Chem.* **1967**, *31*, 481–489.
 - For a recent review of work on the synthesis of prodigiosin and other natural and unnatural tripyrromethene analogues, see Fürstner, A. *Angew. Chem., Int. Ed. Engl.* **2003**, *42*, 3582–3603.
 - The McFadyen–Stevens reduction is reliable, although inefficient because of the low (30–40%) yields. Clearly, this step needs further study in order to develop an alternative ester to aldehyde conversion.
 - Lange's Handbook of Organic Chemistry*; Dean, J. A. Ed.; 13th ed. McGraw-Hill: New York, 1985.
 - Related earlier syntheses of prodigiosin involved preparation of a substituted pyrrole and its addition to a 1,2-pyrroline followed by a dehydrogenation step¹⁵ or construction of the α,α' -dipyrrole unit from protected pyrrole-2-aldehyde by condensation with the dianion of ethylacetoacetate followed by oxidation to the tricarbonyl, dehydration and subsequent pyrrole formation by reaction with a primary amine.¹⁶
 - Rapoport, H.; Holden, K. G. *J. Am. Chem. Soc.* **1962**, *84*, 635–642.
 - Wasserman, H. H.; Lombardo, L. J. *Tetrahedron Lett.* **1989**, *30*, 1725–1728.

3,3'-Functionalized octahydro-BINOL: a facile synthesis and its high enantioselectivity in the alkyne addition to aldehydes

 Lan Liu^{a,b} and Lin Pu^{a,*}
^aDepartment of Chemistry, University of Virginia, Charlottesville, VA 22904-4319, USA

^bSchool of Chemistry and Chemical Engineering, Sun Yat-Sen University, Guangzhou 510275, People's Republic of China

Received 8 April 2004; revised 17 May 2004; accepted 19 May 2004

Available online 10 June 2004

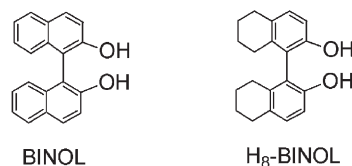
Abstract—A facile synthesis of an enantiomerically pure 3,3'-bismorpholinylmethyl H₈-BINOL ligand has been developed. This compound in combination with Et₂Zn and Ti(OⁱPr)₄ is found to catalyze the highly enantioselective reaction of phenylacetylene with aromatic aldehydes. The enantioselectivity of this catalytic process for the reactions of *ortho*-substituted benzaldehydes is significantly higher than that based on H₈-BINOL.

© 2004 Elsevier Ltd. All rights reserved.

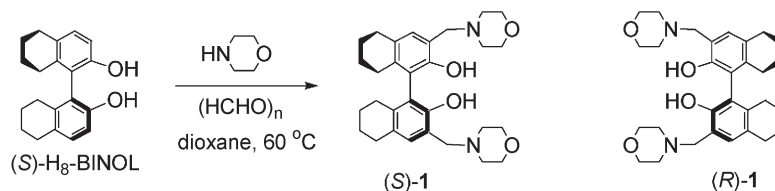
1. Introduction

Application of 1,1'-bi-2-naphthol (BINOL) and its derivatives in asymmetric catalysis has been extensively studied.^{1–3} Recently, catalysts⁴ based on the partially hydrogenated BINOL ligand, H₈-BINOL,⁵ have also been investigated. In a few cases, the partially hydrogenated BINOL has shown improved chiral induction over BINOL. This improved enantioselectivity is attributed to the increased steric interaction between the two partially hydrogenated naphthalene rings in H₈-BINOL. Considering the extremely rich chemistry of functionalized BINOLs, we envision that functionalized H₈-BINOL should also exhibit interesting properties in catalysis as well as in other applications. Especially, introduction of 3,3'-substituents to H₈-BINOL may lead to ligands of high enantioselectivity for asymmetric reactions as demonstrated by many 3,3'-substituted BINOL ligands. However, very few functionalized H₈-BINOL ligands have been synthesized and studied.^{4c–e} Herein, we report our discovery of a facile synthesis of an enantiomerically pure 3,3'-bisaminomethyl

H₈-BINOL. This compound has shown high enantioselectivity in the catalytic asymmetric alkyne addition to aromatic aldehydes, especially to the *ortho*-substituted benzaldehydes.



We conducted the reaction of the enantiomerically pure (*S*)-H₈-BINOL⁵ with paraformaldehyde and morpholine in dioxane at 60 °C.⁶ This one-pot process led to the formation of (*S*)-3,3'-bis(morpholin-4-ylmethyl)-H₈-BINOL, (*S*)-**1**, in 65% yield (Scheme 1). The specific optical rotation of (*S*)-**1**, [α]_D, was –15.5 (*c*=1.0, CHCl₃). The ¹H NMR spectrum of (*S*)-**1** gave a singlet at δ 10.37 for the two hydroxyl groups, indicating a C₂ symmetric structure probably with intramolecular hydrogen bonds between the hydroxyl groups



Scheme 1. Synthesis of the enantiomerically pure 3,3'-bismorpholinylmethyl H₈-BINOL.

Keywords: Asymmetric catalysis; H₈-BINOL; Alkyne addition; Propargylic alcohols.

* Corresponding author. Tel.: +1-4349246953; fax: +1-4349243710; e-mail address: lp6n@virginia.edu

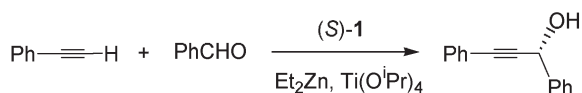
Table 1. Results for the reaction of phenylacetylene with benzaldehyde in the presence of (*S*)-**1**, Ti(OⁱPr)₄ and Et₂Zn

Entry	(<i>S</i>)- 1 (mol%)	PhCCH (equiv.)	Et ₂ Zn (equiv.)	Ti(O ⁱ Pr) ₄ (mol%)	Solvent	<i>T</i> (°C)	Yield (%)	ee (%)
1	2	4	4	100	THF (3 mL)	rt	25	81
2	5	4	4	100	THF (3 mL)	rt	64	83
3	10	4	4	100	THF (3 mL)	rt	93	83
4	20	4	4	100	THF (3 mL)	rt	95	84
5	40	4	4	100	THF (3 mL)	rt	90	85
6	20	4	4	100	CH ₂ Cl ₂ (3 mL)	rt	96	82
7	20	4	4	100	Ether (3 mL)	rt	60	84
8	20	4	4	100	Toluene (3 mL)	rt	85	84
9	10	4	4	100	THF (3 mL)	0	85	83
10	10	2	2	100	THF (3 mL)	rt	63	86
11	10	1.5	1.5	100	THF (3 mL)	rt	58	83
12	20	2	2	50	THF (3 mL)	rt	45	83
13	20	2	2	100	THF (3 mL)	rt	77	84
14	20	2	2	200	THF (3 mL)	rt	89	84
15	20	2	2	100	THF (1 mL)	rt	38	83
16	20	2	2	100	THF (6 mL)	rt	65	84

and the adjacent morpholine nitrogens. The optical purity of (*S*)-**1** was determined to be >99% by HPLC analysis on the Daicel Chiralcel OD column. The enantiomer of (*S*)-**1**, (*R*)-**1**, was also prepared by starting with (*R*)-H₈-BINOL. The specific optical rotation of (*R*)-**1**, [α]_D, was +15.5 (*c*=1.0, CHCl₃).

Compound (*S*)-**1** is an axially chiral ligand with a C₂ symmetric bis(aminoalcohol) structure. Since both chiral amino alcohols and the axially chiral BINOL compounds have exhibited excellent chiral inductions in many Lewis-acid catalyzed asymmetric reactions, (*S*)-**1** should also be potentially useful in asymmetric catalysis. We used (*S*)-**1** to catalyze the asymmetric alkynylzinc addition to aldehydes.⁷ This reaction can produce chiral propargylic alcohols that are of great utility in organic synthesis. We first explored the conditions for the reaction of phenylacetylene with benzaldehyde in the presence of (*S*)-**1**, Et₂Zn and Ti(OⁱPr)₄ (Scheme 2). As shown by the results summarized in Table 1, (*S*)-**1** catalyzed this reaction with good enantioselectivity which did not change significantly with respect to the reaction conditions. Increasing the amount of (*S*)-**1** from 2 to 40 mol% greatly increased the yield of the propargylic alcohol but not the ee (entries 1–5). Solvent and temperature also showed little effect on the enantioselectivity (entries 6–9). Decreasing the amount of Et₂Zn and phenylacetylene to 2 equiv. decreased the yield of the product (entry 10). Increasing the amount of Ti(OⁱPr)₄ from 50 to 200 mol% increased the yield (entries 12–14). Increasing or decreasing the amount of the solvent led to reduction in yield (entries 15 and 16). The configuration of the propargylic alcohol product was R as determined by comparing it with the literature.⁸

We have applied the conditions of entry 3 in Table 1 to the reaction of phenylacetylene with a variety of aldehydes and the results are summarized in Table 2. In general, (*S*)-**1** showed high enantioselectivity for the reaction of the alkyne

**Scheme 2.** Reaction of phenylacetylene with benzaldehyde catalyzed by (*S*)-**1**.

with aromatic aldehydes. Earlier, Chan and coworkers found that H₈-BINOL in combination with Ti(OⁱPr)₄ and Me₂Zn catalyzed the reaction of phenylacetylene with certain aromatic aldehydes with high enantioselectivity at 0 °C.^{4j} Under these conditions, however, the reaction of an *ortho*-substituted benzaldehyde was not very good. Using H₈-BINOL could only give 76% ee for the reaction of phenylacetylene with *o*-chlorobenzaldehyde. In contrast, the 3,3'-functionalized H₈-BINOL ligand (*S*)-**1** catalyzed the same reaction with 97% ee (entry 2, Table 2). This ligand was also found to be good for the asymmetric reaction of other *ortho*-substituted benzaldehydes with ee's in the range of 89–98% (entries 2–8, Table 2).

In summary, a novel 3,3'-functionalized H₈-BINOL has been synthesized by a one-pot reaction of H₈-BINOL with paraformaldehyde and morpholine. A preliminary study of this ligand in the asymmetric alkyne addition to aldehydes has demonstrated the potential of this ligand in asymmetric catalysis. In the presence of (*S*)-**1**, high enantioselectivity

Table 2. Asymmetric reactions of phenylacetylene with aromatic aldehydes in the presence of (*S*)-**1**, Et₂Zn and Ti(OⁱPr)₄^a

Entry	Aldehyde	Isolated yield (%)	ee (%)
1	PhCHO	93	83
2	<i>o</i> -ClPhCHO	88	97
3	<i>o</i> -MeOPhCHO	76	93
4	<i>o</i> -EtOPhCHO	83	92
5	<i>o</i> -MePhCHO	88	89
6 ^b	<i>o</i> -NO ₂ PhCHO	62	98
7	<i>o</i> -BrPhCHO	84	97
8	2,4,5-Trimethylbenzaldehyde	68	96
9	<i>m</i> -MeOPhCHO	93	86
10	<i>p</i> -BrPhCHO	86	87
11	<i>p</i> -FPhCHO	50	86
12	<i>m</i> -MePhCHO	98	91
13	<i>p</i> -MePhCHO	86	83
14	<i>p</i> -MeOPhCHO	99	85
15	1-Naphthylaldehyde	85	83
16 ^c	2,6-Dichlorobenzaldehyde	62	86
17 ^d	CH ₃ (CH ₂) ₆ CHO	76	67

^a Unless indicated otherwise, reactions were conducted by stirring (*S*)-**1**:Et₂Zn:PhCCH:Ti(OⁱPr)₄:RCHO=0.1:4:4:1:1 at room temperature in THF for 4 h.

^b 2 equiv. of Et₂Zn and 2 equiv. of PhCCH were used.

^c The reaction time was 6 h.

^d 20 mol% (*S*)-**1** was used.

has been observed for the reaction of phenylacetylene with aromatic aldehydes, especially with the *ortho*-substituted benzaldehydes. Application of this ligand to other asymmetric reactions is currently under investigation.

2. Experimental

2.1. General data

All reactions were carried out under nitrogen. Unless otherwise specified, all the reagents were purchased from Aldrich Chemical Co. and used directly. Diethylzinc (95%) was purchased from Strem. Toluene was distilled over sodium under nitrogen. Methylene chloride, diethyl ether and tetrahydrofuran were dried by passing through activated alumina columns under nitrogen. All the solvents were stored over 4 Å molecular sieves before use. Deuterated chloroform was stored over 4 Å molecular sieves before use. NMR spectra were obtained using the Varian-300 MHz spectrometer. Mass spectra were recorded either at atmospheric pressure chemical ionization (APCI) or at electrospray ionization (ESI) mode. HPLC analyses were carried out with the Waters 600 by using the Daicel Chiralcel OD column and eluting with 10% *i*-PrOH in hexane at 1.0 mL/min unless otherwise indicated, and were detected at 254 nm by the Waters 486. The optical rotations were measured on the JASCO DIP-1000 Polarimeter.

2.2. Synthesis and characterization of (S)-1

Paraformaldehyde (6.0 g, 0.20 mol) was placed in a round bottom flask equipped with a reflux condenser. Morpholine (17.6 g, 0.20 mol) was added dropwise over 0.5 h with rigorous stirring. Since this was a strongly exothermic reaction, the addition rate was adjusted in order to keep the oil bath temperature at ~60 °C. After the addition, the reaction mixture was heated at 60 °C for ca. 12 h until the solution became clear. H₈-BINOL (3.0 g, 0.010 mol) and dioxane (10 mL) were added and the solution was stirred at 60 °C for additional 8 h. The solvent was then removed by roto-evaporation. The residue was dissolved in CH₂Cl₂ (50 mL), washed with 1 M HCl (3×10 mL) and water (3×10 mL), and dried over Na₂SO₄. After roto-evaporation, the crude material was purified by using ethylacetate/hexane (3:1) to elute through a short silicon gel column. This gave (S)-1 as colorless crystals (3.3 g) in 65% yield. Mp 215.5–216.5 °C. ¹H NMR (300 MHz, CDCl₃) δ 10.37 (s, 2H), 6.73 (s, 2H), 3.83–3.57 (m, 12H), 2.72–2.13 (m, 16H), 1.72–1.56 (m, 4H). ¹³C NMR (75 MHz, CDCl₃) δ 151.71, 135.5, 128.4, 127.1, 123.6, 117.4, 66.3, 61.6, 52.5, 28.9, 26.9, 22.9, 22.8. [α]_D²⁰ = –15.5 (c=1.0, CDCl₃). Anal. Calcd for C₃₀H₃₉N₂O₄: C, 72.84; H, 8.56; N, 5.66. Found: C, 73.22; H, 8.20; N, 5.66. MS (FIA-ESI) *m/z* 493.0 (M⁺, 100).

2.3. General procedure for the phenylacetylene addition to aldehydes catalyzed by (S)-1

In a 10 mL round-bottom flask, phenylacetylene (1.0 mmol, 113 μL) was dissolved in THF (3 mL) at room temperature. Et₂Zn (1.0 mmol, 110 μL), Ti(O^{*i*}Pr)₄ (74 μL, 0.25 mmol), (S)-1 (12.3 mg, 0.025 mmol) and an aldehyde (0.25 mmol) were then added sequentially. After the resulting reaction

mixture was stirred at room temperature for 4 h, a saturated ammonium chloride solution was added to quench the reaction. The mixture was extracted with methylene chloride (3×5 mL) and the organic solution was concentrated under vacuum. The residue was purified by passing through a short silica gel column eluted with methylene chloride/hexane (1:1) which afforded the pure propargylic alcohol product.

2.3.1. 1,3-Diphenylprop-2-yn-1-ol.⁸ 86% yield. 87% ee determined by HPLC analysis. Retention time: *t*_{major} = 24.0 min and *t*_{minor} = 13.3 min.

2.3.2. 1-(2-Chlorophenyl)-3-phenylprop-2-yn-1-ol.⁹ 88% yield. 97% ee determined by HPLC analysis. Retention time: *t*_{major} = 14.0 min and *t*_{minor} = 12.0 min.

2.3.3. 1-(2,6-Dichlorophenyl)-3-phenylprop-2-yn-1-ol. 62% yield. 87% ee determined by HPLC analysis. Retention time: *t*_{major} = 12.2 min and *t*_{minor} = 8.9 min. [α]_D²⁴ = +3.67 (c=1.26, CHCl₃). ¹H NMR (300 MHz, CDCl₃) δ 7.48–7.43 (m, 2H), 7.36–7.17 (m, 6H), 6.60 (d, 1H, *J* = 10.2 Hz), 3.40 (d, 1H, *J* = 10.2 Hz). The large coupling constant observed here between the hydroxyl proton and the methine proton is probably due to the intramolecular hydrogen bond between the hydroxyl group and one of the two chlorine atoms at the 2,6-positions. This intramolecular hydrogen bond allows the hydroxyl proton and the methine proton to form an antiperiplanar conformation as shown by a PCSpartan-Semi-Empirical AM1 calculation and it significantly increases the coupling constant. ¹³C NMR (75 MHz, CDCl₃) δ 135.7, 134.7, 132.1, 130.0, 129.5, 128.9, 128.5, 122.6, 86.9, 86.5, 61.7. MS (FIA-APCI) *m/z* 258.4 (M⁺–H₂O, 100).

2.3.4. 1-(2-Nitrophenyl)-3-phenylprop-2-yn-1-ol.¹⁰ 62% yield. 98% ee determined by HPLC analysis. Retention time: *t*_{major} = 16.0 min and *t*_{minor} = 20.6. ¹H NMR (300 MHz, CDCl₃) δ 8.26–7.80 (m, 2H), 7.77–7.74 (m, 2H), 7.51–7.15 (m, 5H), 5.80 (s, 1H), 2.63 (s, 1H). ¹³C NMR (75 MHz, CDCl₃) δ 148.0, 147.6, 132.0, 130.7, 129.3, 128.7, 127.7, 124.51, 124.1, 122.0, 87.8, 87.7, 64.2.

2.3.5. 1-(2,4,5-Trimethylphenyl)-3-phenylprop-2-yn-1-ol. 68% yield. 96% ee determined by HPLC analysis. Retention time: *t*_{major} = 34.8 min and *t*_{minor} = 13.4. [α]_D²⁴ = –20.9 (c=1.38, CHCl₃). ¹H NMR (300 MHz, CDCl₃) δ 7.57–7.53 (m, 3H), 7.39–7.36 (m, 3H), 7.05 (s, 1H), 5.84 (d, 1H, *J* = 4.8 Hz), 2.95 (d, 1H, *J* = 4.8 Hz), 2.44 (s, 3H), 2.28 (s, 3H), 2.25 (s, 3H). ¹³C NMR (75 MHz, CDCl₃) δ 135.9, 134.9, 133.4, 131.4, 130.8, 127.6, 127.4, 121.8, 88.0, 85.3, 61.9, 28.9, 18.5, 17.5. MS (FIA-APCI) *m/z* 232.5 (M⁺–H₂O, 100). (The starting material contained ~7% 5-bromo-1,2,4-trimethylbenzene which could not be completely removed from the product.)

2.3.6. 1-(2-Ethoxyphenyl)-3-phenylprop-2-yn-1-ol. 83% yield. 92% ee determined by HPLC analysis. Retention time: *t*_{major} = 18.4 min and *t*_{minor} = 12.5 min. [α]_D²⁴ = +2.92 (c=1.38, CHCl₃). ¹H NMR (300 MHz, CDCl₃) δ 7.64–7.60 (m, 1H), 7.50–7.47 (m, 2H), 7.31–7.24 (m, 4H), 7.04–6.9 (m, 2H), 5.85 (d, 1H, *J* = 4.5 Hz), 4.40–4.03 (m, *J* = 6.9 Hz, 2H), 3.29 (d, 1H, *J* = 4.5 Hz), 1.51–1.46 (t, 3H),

$J=5.1$ Hz). ^{13}C NMR (75 MHz, CDCl_3) δ 156.5, 132.0, 129.9, 129.2, 128.6, 128.5, 128.3, 123.1, 121.1, 122.1, 88.7, 86.1, 64.3, 62.3, 15.2. MS (FIA-APCI) m/z 234.8 [$\text{M}^+ - \text{H}_2\text{O}$, 100].

2.3.7. 1-(2-Bromophenyl)-3-phenylprop-2-yn-1-ol.¹⁰ 84% yield. 97% ee determined by HPLC analysis. Retention time: $t_{\text{major}}=24.3$ min and $t_{\text{minor}}=20.0$ min (eluted with 5% *i*-PrOH in hexane at 1.0 mL/min). ^1H NMR (300 MHz, CDCl_3) δ 7.87–7.84 (m, 1H), 7.61–7.58 (m, 1H), 7.50–7.46 (m, 2H), 7.42–7.19 (m, 5H), 6.02 (d, 1H, $J=4.5$ Hz), 2.62 (d, 1H, $J=4.5$ Hz). ^{13}C NMR (75 MHz, CDCl_3) δ 139.7, 133.3, 132.0, 130.2, 128.9, 128.5, 128.2, 123.1, 122.5, 87.9, 87.1, 64.9.

2.3.8. 1-(2-Methoxyphenyl)-3-phenylprop-2-yn-1-ol.¹¹ 76% yield. 93% ee determined by HPLC analysis. Retention time: $t_{\text{major}}=22.1$ min and $t_{\text{minor}}=18.4$ min.

2.3.9. 1-(3-Methoxyphenyl)-3-phenylprop-2-yn-1-ol.¹¹ 93% yield. 86% ee determined by HPLC analysis. Retention time: $t_{\text{major}}=40.4$ min and $t_{\text{minor}}=21.9$ min.

2.3.10. 1-(4-Methoxyphenyl)-3-phenylprop-2-yn-1-ol.⁹ 99% yield. 85% ee determined by HPLC analysis. Retention time: $t_{\text{major}}=39.6$ min and $t_{\text{minor}}=16.8$ min.

2.3.11. 1-(4-Fluorophenyl)-3-phenylprop-2-yn-1-ol.¹¹ 50% yield. 86% ee determined by HPLC analysis. Retention time: $t_{\text{major}}=35.7$ min and $t_{\text{minor}}=11.6$ min.

2.3.12. 1-(3-Methylphenyl)-3-phenylprop-2-yn-1-ol.¹¹ 98% yield. 91% ee determined by HPLC analysis. Retention time: $t_{\text{major}}=34.4$ min and $t_{\text{minor}}=13.8$ min.

2.3.13. 1-(2-Methylphenyl)-3-phenylprop-2-yn-1-ol.¹¹ 88% yield. 89% ee determined by HPLC analysis. Retention time: $t_{\text{major}}=27.7$ min and $t_{\text{minor}}=11.8$ min.

2.3.14. 1-(4-Bromophenyl)-3-phenylprop-2-yn-1-ol.¹⁰ 86% yield. 87% ee determined by HPLC analysis. Retention time: $t_{\text{major}}=43.9$ min and $t_{\text{minor}}=12.3$ min.

2.3.15. 1-(4-Methylphenyl)-3-phenylprop-2-yn-1-ol.¹¹ 86% yield. 87% ee determined by HPLC analysis. Retention time: $t_{\text{major}}=28.6$ min and $t_{\text{minor}}=13.1$ min.

2.3.16. 1-Naphthalen-1-yl-3-phenylprop-2-yn-1-ol.¹¹ 86% yield. 87% ee determined by HPLC analysis. Retention time: $t_{\text{major}}=44.4$ min and $t_{\text{minor}}=19.8$ min.

2.3.17. 1-Phenyldec-1-yn-3-ol.⁹ 76% yield. 67% ee determined by HPLC analysis. Retention time: $t_{\text{major}}=7.6$ min and $t_{\text{minor}}=17.6$ min.

2.4. General procedure for the preparation of the racemic propargylic alcohols

All the racemic propargylic alcohols were prepared for the HPLC analysis according to the following procedure. A solution of an alkyne (0.75 mmol) in tetrahydrofuran (3 mL) in a 25 mL flask was cooled to -78 °C with a dryice/acetone bath. *n*-BuLi (1.6 M in hexanes, 0.7 mmol) was then added

and the reaction mixture was brought to room temperature and stirred for 3 h. An aldehyde (0.5 mmol) was added and the mixture was stirred for additional 8 h. The reaction was quenched with ice, and the resulting mixture was extracted with methylene chloride. After the organic solution was dried over magnesium sulfate, the solvent was removed by roto-evaporation and the residue was passed through a short silica gel column and eluted with methylene chloride/hexane (1:1) to afford the product.

Acknowledgements

L.L. thanks the support from the National Natural Science Foundation of China (Grant20202015). Partial support of this work from the National Institute of Health (R01GM58454/R01EB002037) is gratefully acknowledged.

References and notes

1. Pu, L. *Chem. Rev.* **1998**, *98*, 2405–2494.
2. Chen, Y.; Yekta, S.; Yudin, A. K. *Chem. Rev.* **2003**, *103*, 3155–3211.
3. Kočovská, P.; Vyskočil, S.; Smrčina, M. *Chem. Rev.* **2003**, *103*, 3213–3245.
4. (a) A review: Au-Yeung, T. L.-L.; Chan, S.-S.; Chan, A. S. *Adv. Synth. Catal.* **2003**, *345*, 537–555. (b) Iida, T.; Yamamoto, N.; Matsunaga, S.; Woo, H.-G.; Shibasaki, M. *Angew. Chem., Int. Ed.* **1998**, *37*, 2223–2226. (c) Reetz, M. T.; Merk, C.; Naberfeld, G.; Rudolph, J. N. G.; Goddard, R. *Tetrahedron Lett.* **1997**, *38*, 5273–5276. (d) Aeilts, S. L.; Cefalo, D. R.; Bonitatebus, P. J.; Houser, J. H.; Hoveyda, A. H.; Schrock, R. R. *Angew. Chem., Int. Ed.* **2001**, *40*, 1452–1456. (e) Schrock, R. R.; Jamieson, J. Y.; Dolman, S. J.; Miller, S. A.; Bonitatebus, P. J.; Hoveyda, A. H. *Organometallics* **2002**, *21*, 409–417. (f) Long, J.; Hu, J.; Shen, X.; Ji, B.; Ding, K. *J. Am. Chem. Soc.* **2002**, *124*, 10–11. (g) Wang, B.; Feng, X.; Huang, Y.; Liu, H.; Cui, X.; Jiang, Y. *J. Org. Chem.* **2002**, *67*, 2175–2182. (h) Chan, A. S. C.; Zhang, F.-Y.; Yip, C.-W. *J. Am. Chem. Soc.* **1997**, *119*, 4080–4081. (i) Zhang, F.-Y.; Chan, A. S. C. *Tetrahedron: Asymmetry* **1997**, *8*, 3651–3655. (j) Lu, G.; Li, X.; Chan, W. L.; Chan, A. S. C. *J. Chem. Soc., Chem. Commun.* **2002**, 172–173. (k) Waltz, K. M.; Carroll, P. J.; Walsh, P. J. *Organometallics* **2004**, *23*, 127–134.
5. Cram, D. J.; Helgeson, R. C.; Peacock, S. C.; Kaplan, L. J.; Domeier, L. A.; Moreau, P.; Koga, K.; Mayer, J. M.; Chao, Y.; Siegel, M. G.; Hoffman, D. H.; Sogah, G. D. Y. *J. Org. Chem.* **1978**, *43*, 1930–1946.
6. The reaction of 2,2'-biphenol with paraformaldehyde and morpholine was reported: Fabris, F.; Lucchi, O. D.; Lucchini, V. *J. Org. Chem.* **1997**, *62*, 7156–7164.
7. Reviews: (a) Pu, L. *Tetrahedron* **2003**, *59*, 9873–9886. (b) Pu, L.; Yu, H. B. *Chem. Rev.* **2001**, *101*, 757–824.
8. Corey, E. J.; Cimprich, K. A. *J. Am. Chem. Soc.* **1994**, *116*, 3151–3152.
9. Gao, G.; Moore, D.; Xie, R.-G.; Pu, L. *Org. Lett.* **2002**, *4*, 4143–4146.
10. Lu, G.; Li, X.; Zhou, Z.; Chan, W. L.; Chan, A. S. C. *Tetrahedron: Asymmetry* **2001**, *12*, 2147–2152.
11. Moore, D.; Pu, L. *Org. Lett.* **2002**, *4*, 1855–1857.

Regioselectivity in nickel(0) catalyzed cycloadditions of carbon dioxide with diynes[☆]

Thomas N. Tekavec, Atta M. Arif and Janis Louie*

Department of Chemistry, University of Utah, 315 South 1400 East, Salt Lake City, UT 84112-0850, USA

Received 29 March 2004; revised 27 May 2004; accepted 4 June 2004

Available online 25 June 2004

Abstract—The regioselectivity of Ni(0)-catalyzed cycloadditions of CO₂ (1 atm) with various asymmetrical diynes to afford pyrones was explored. The use of 1,3-bis-(2,6-diisopropylphenyl)-imidazol-2-ylidene (IPr) provided high regioselectivity when one terminal substituent on the diyne was a methyl group and the other was medium or large in size ($R_L=i$ -Pr, t -Bu, or TMS). In contrast, the use of a relatively small N-heterocyclic carbene, 1,3-dimesitylimidazol-2-ylidene (IMes), afforded high selectivity only when R_L was large (TMS). X-ray crystal analysis of the major isomer indicated that the relatively large R_L group was in the 3-position of the pyrone. © 2004 Elsevier Ltd. All rights reserved.

1. Introduction

The incorporation of carbon dioxide (CO₂) into organic compounds (e.g. carbohydrates) is an important chemical process used by green plants and algae for sustaining life. Although biosynthetic machinery can easily accomplish this process at ambient temperatures and pressures, chemists often resort to extreme measures to exploit its use in synthetic applications. Despite CO₂'s high thermodynamic stability and kinetic inertness, it is cheap, abundant, and relatively non-toxic, which makes it an ideal starting material.¹ Thus, the development of safe and convenient protocols that use CO₂ remains a highly investigated area of research. Although several groups have reported the use of Ni complexes as a means to activate CO₂,² a particularly interesting example is the coupling of CO₂ with a diyne to afford pyrones.^{2a,b} Pyrones are proven synthetic intermediates that serve not only as dienes in Diels–Alder reactions,³ but are also a common structural motif in many natural products.⁴

Our group recently reported the utility of Ni/imidazolylidene complexes for efficiently coupling various symmetrical diynes with CO₂ under mild conditions to produce pyrones.⁵ During the course of this investigation, it was discovered that diynes containing bulky groups (TMS,

t -butyl, etc.) at the terminal positions did not undergo cyclization. However, the use of an asymmetrical diyne, which contained a relatively bulky TMS and a relatively unhindered methyl group lead to the formation of a pyrone with high regioselectivity. Herein, we describe the scope of regioselectivity in Ni catalyzed cycloadditions of asymmetrical diynes with CO₂.

2. Results

A series of asymmetrically substituted diynes, containing one terminal methyl group and another terminal group of varying size ($R=Et$, i -Pr, t -Bu, and TMS) were prepared. To toluene solutions of each of these compounds were added 10 mol% Ni(COD)₂ and 20 mol% 1,3-bis-(1,3,5-trimethyl)-imidazol-2-ylidene (IMes, Fig. 1) and the entire reaction vessel was placed under 1 atm of CO₂. As shown in Table 1, when the steric difference between the two terminal substituents on the diyne was small (e.g. Me vs. Et), a nearly equal mixture of two pyrone regioisomers was obtained (entry 1). However, as the relative difference between the two terminal groups was increased, the regioselectivity of the reaction improved and one isomer was preferentially formed over the other. Interestingly, the use of a diyne which contained a methyl group and a very bulky TMS group afforded only one regioisomer (Table 1,

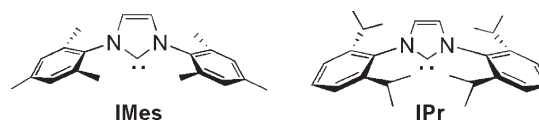
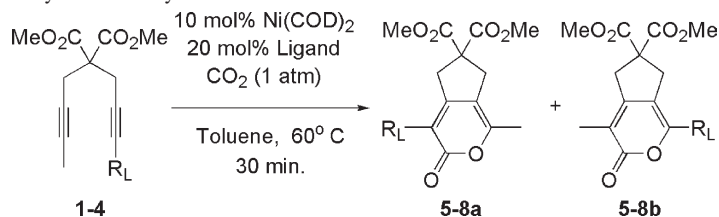


Figure 1. Imidazolylidene ligands.

[☆] Supplementary data associated with this article can be found in the online version, at doi: 10.1016/j.tet.2004.06.025

Keywords: Nickel; Carbon dioxide; N-heterocyclic carbenes; Cycloaddition; Regioselectivities.

* Corresponding author. Tel.: +1-801-581-7309; fax: +1-801-581-8433; e-mail address: louie@chem.utah.edu

Table 1. Cycloaddition with various unsymmetrical diynes

Entry	Substrate	R _L	Ligand	Product	a:b ^a	% Yield ^b
1	1	Ethyl	IMes	5	53:47	ND ^c
2	1	Ethyl	IPr	5	62:38	75
3	2	<i>i</i> -Pr	IMes	6	56:44	57
4	2	<i>i</i> -Pr	IPr	6	80:20	64
5	3	<i>t</i> -Butyl	IMes	7	64:36	ND ^c
6	3	<i>t</i> -Butyl	IPr	7	100:0	64
7	4	TMS	IMes	8	100:0	67
8	4	TMS	IPr	8	100:0	83

^a Determined by GC and ¹H NMR analysis.

^b Isolated yields (average of two runs).

^c Not determined.

entry 7). Single crystal X-ray analysis of the major isomers of entries 5 and 7 (i.e. **7a** and **8a**) revealed that the larger substituent was located at the 3-position of the pyrone ring (e.g. **7a**; Fig. 2).

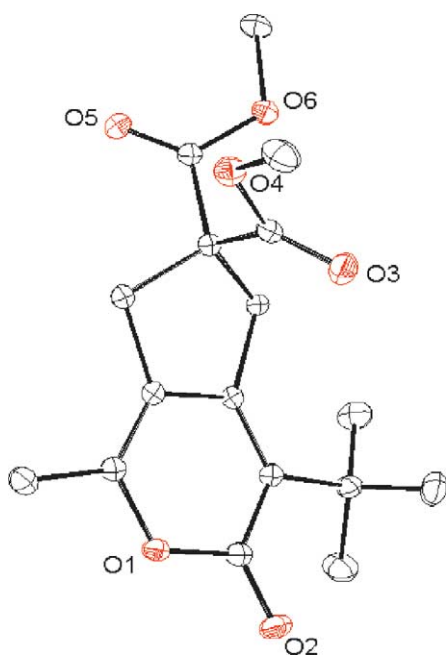
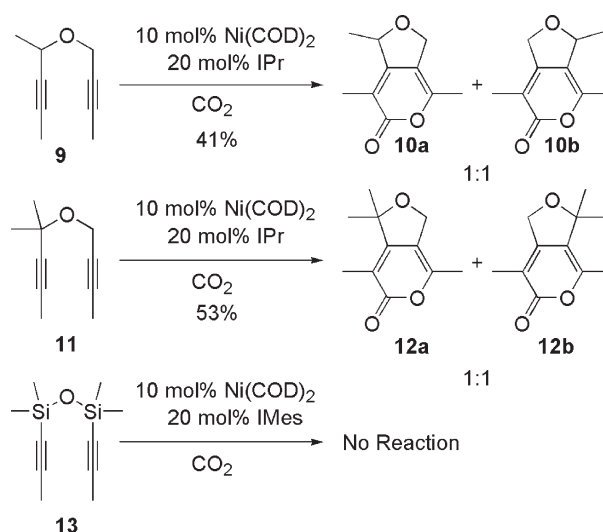


Figure 2. ORTEP representation of pyrone **7a**. Protons have been omitted for clarity

In an effort to enhance the cycloaddition's regioselectivity, a larger but electronically similar N-heterocyclic carbene ligand, 1,3-bis-(2,6-diisopropylphenyl)-imidazol-2-ylidene (IPr, Fig. 1), was used in lieu of the IMes ligand. As shown in Table 1, this ligand afforded significant improvements in regioselectivity. For example, even in cases when the difference between the terminal diyne substituents was small (Me vs. Et, entry 2 and Me vs. *i*-Pr, entry 4), a considerable excess of one regioisomer was observed.

Complete regioselectivity was observed when the bulky substituent was *t*-Bu (entry 6) or larger (TMS, entry 8).

We next explored whether regioselectivity could be influenced by varying the steric bulk of the internal tether of the diyne (Scheme 1). Diyne **9** contains an α -methyl-substituted ether which links the methyl-terminated alkynyl groups. Unfortunately, this substitution did not have any effect on the regioselectivity of the reaction as an equal mixture of both regioisomers was formed. Similar results were obtained from the cycloaddition of diyne **11** which contains an α,α -substituted ether linkage. Interestingly, no conversion was observed for disiloxane **13** using either the IPr or IMes ligands which may be due to the bulky internal substitution on both diynes.



Scheme 1. Cycloaddition of CO₂ with diynes containing sterically hindered internal linkages.

Several attempts were made to delineate electronic factors that could be influencing the regioselectivity of this reaction. Unfortunately, diynes bearing a terminal electron-withdrawing substituent (e.g. Ph or CO₂Me, Fig. 3) undergo

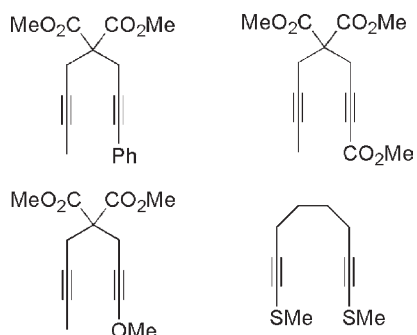


Figure 3. Diynes used for studying electronic effects in regioselective cyclizations.

side oligomerization reactions, such as alkyne trimerization, at a faster rate than cycloaddition and do not afford reasonable yields of pyrone products. Alternatively, an electron rich diyne bearing a methoxy substituent reacts under our reaction conditions, however a complex mixture of products was obtained. Diynes bearing thioethers do not undergo cycloaddition chemistry, which may be due to the incompatibility of this functional group with the nickel catalyst. We are continuing our efforts to find suitable diynes to address electronic factors on the regioselectivity of cycloaddition.

3. Discussion

We previously reported the cycloaddition of diyne **4** provides a pyrone product (**8**) as a single regioisomer.⁵ Our initial regiochemical assignment was based on a related

example of the Ni-catalyzed cycloaddition of CO₂ and diyne **14** reported by Tsuda and co-workers (Fig. 4).⁶ This assignment was based on the assumption that oxidative coupling between the sterically-unhindered alkyne and CO₂ preceded all other cycloaddition steps. Recently, X-ray analysis of pyrone **8a** revealed that the large TMS-group (and similarly, the large *t*-Bu group in pyrone **7a**, Fig. 1) was in fact at the 3-position, rather than the 6-position.⁷ These findings warranted a re-evaluation of our proposed mechanism.

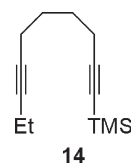
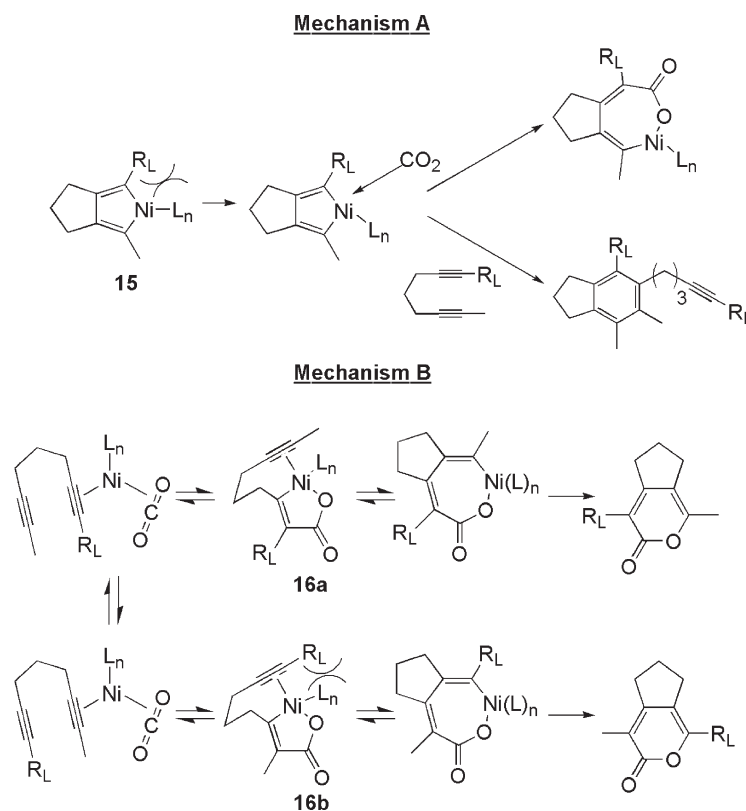


Figure 4.

A variety of Ni compounds are known to cyclotrimerize alkynes to afford aromatic products.⁸ As such, reasonable mechanisms which describe the formation of pyrones are depicted in Scheme 2. In Mechanism A, binding and cycloaddition of both alkynyl units of the diyne to the Ni center leads to a metallocyclopentadiene intermediate (**15**) which presumably is analogous to an intermediate that forms in an alkyne cyclotrimerization reaction. However, in this case, CO₂ rather than another alkyne can then insert to form a seven-member nickelacycle which then reductively eliminates to form the pyrone product. If an asymmetrical diyne is employed, then the CO₂ could insert at two distinct positions. In order to relieve steric crowding between the relatively bulky group and the ligand, CO₂ insertion into the



Scheme 2. Possible mechanisms for the cycloaddition of diynes and CO₂.

side containing the bulkier R group would be expected to be favored and afford pyrones with the bulky substituent at the 3-position (as observed in Table 1).

Although Mechanism A explains the observed regioselectivity, other data must be considered. Specifically, when unsymmetrically diynes are used as substrates, increased amounts of oligomerized products (i.e. cyclotrimerized aromatics) are formed.⁹ Thus, it is unlikely that increasing the steric crowding around the nickel center would inhibit CO₂ insertion while favoring subsequent alkyne insertion. It is more likely that both CO₂ and alkyne insertion would be inhibited.

Stoichiometric reactions⁵ have indicated that the previously proposed Mechanism B (Scheme 2) is most likely the operative pathway.¹⁰ Mechanism B involves initial binding of CO₂ followed by oxidative coupling with an alkynyl unit to afford a five-member nickelacycle intermediate (**16a** or **16b**, Scheme 2). The pendant alkynyl unit then inserts to form a seven-member nickelacycle which subsequently reductively eliminates to afford the pyrone product.

When asymmetric diynes are employed, two regioisomeric products are possible and their formation is ultimately dependent on the five-member nickelacycle intermediate. Initial oxidative coupling between the larger alkynyl unit (R_L) and CO₂ leads to the formation of nickelacycle **16a**. Subsequent insertion of the pendant alkynyl unit affords pyrones with the bulky R_L group in the 3-position (as observed as the major product in Table 1).^{2a,11} Although binding and oxidative coupling of the least sterically hindered alkynyl unit (to form **16b** and ultimately 6-substituted pyrones) is favored, subsequent insertion should be inhibited since it requires the bulky alkynyl unit to be placed adjacent to the imidazolylidene ligand. The formation of **16b** represents a catalytic sink unless oxidative coupling is reversible and can rearrange to afford **16a**. Inhibited oxidative coupling and molecular rearrangement would slow the overall rate of pyrone formation and permit the formation of side products to become competitive. Thus, Mechanism B also explains why increased amounts of oligomeric side products are observed when unsymmetrically diynes are used as substrates.

4. Conclusion

Imidazolylidene-based ligands in conjunction with a Ni(0) precursor catalyzed the reaction of CO₂ with asymmetrical diynes to afford regioisomeric mixtures of pyrones. Regioselectivity was highly dependent on the ligand employed and the size of the terminal groups on the diyne. When one alkynyl unit on the diyne was substituted with a TMS group (and the other with a relatively small methyl group), the IMes ligand afforded only one pyrone regioisomer. Improved performance was obtained with the IPr ligand as high regioselectivity were observed with diynes which contained a terminal *i*-Pr, *t*-Bu, or TMS substituent. X-ray crystal analysis indicated that the predominant regioisomer placed the relatively large substituent at the 3-position on the pyrone ring.

5. Experimental

5.1. General

All reactions were conducted under an atmosphere of N₂ using standard Schlenk techniques or in a N₂ filled glovebox. Toluene, pentane, and diethyl ether were dried over neutral alumina under N₂ using a Grubbs-type solvent purification system.¹² THF was freshly distilled from Na/benzophenone. DMF was freshly distilled from CaH₂ under reduced pressure. Anhydrous acetone was purchased and used without further purification. Ni(COD)₂ was purchased from Strem and used without further purification. The IPr and IMes ligands were prepared as previously reported.¹³ Diynes 2-but-2-ynyl-2-(3-trimethylsilylprop-2-ynyl)-malonic acid dimethyl ester (**4**),⁵ 4-but-2-ynoxy-pent-2-yne (**9**),¹⁴ 4-but-2-ynoxy-4-methyl-pent-2-yne (**11**),¹⁴ 1,1,3,3-tetramethyl-1,3-di-prop-1-ynyl-disiloxane (**13**),¹⁵ were prepared using literature procedures. Sodium hydride was thoroughly washed with pentane and dried in vacuo prior to use. All other reagents were purchased and used without further purification unless otherwise noted. ¹H and ¹³C NMR spectra of pure compounds were acquired at 300 and 75 MHz, respectively, unless otherwise noted and were referenced to residual protiated solvent. The abbreviations s, d, dd, dt, dq, t, td, q, qt, quint, sept, septt, m, brm, brt, and brs stand for singlet, doublet, doublet of doublets, doublet of triplets, doublet of quartets, triplet, triplet of doublets, quartet, quartet of triplets, quintet, septet, septet of triplets, multiplet, broad multiplet, broad triplet, and broad singlet, in that order. All ¹³C NMR spectra were proton decoupled. IR spectra were recorded on a Bruker Tensor 27 FT-IR spectrometer. HRMS were performed at the mass spectrometry facility at The University of California, Riverside. Analytical C and H combustion analyses were performed by Midwest Microlab, LLC, Indianapolis, Indiana. Crystallographic data (excluding structure factors) for compounds **7a** and **8a** have been deposited with the Cambridge Crystallographic Data Centre as supplementary publication numbers CCDC 233318 and CCDC 233319, respectively. Copies of the data can be obtained, free of charge, on application to CCDC, 12 Union Road, Cambridge CB2 1EZ, UK [fax: +44-1223-336033 or e-mail: deposit@ccdc.cam.ac.uk]. Crystal structure data and ORTEP for **7a** and **8a** and NMR spectra for **1–13** are included in the Supplementary Information as an electronic file.

5.1.1. 2-But-2-ynyl-2-pent-2-ynyl-malonic acid dimethyl ester (1). To a stirring suspension of NaH (264 mg, 11 mmol) in 25 mL THF, 2-but-2-ynyl malonic acid dimethyl ester (1.8 g, 10 mmol) was added dropwise. The resulting solution was stirred at room temperature for 1 h followed by the addition of 1-bromo-2-pentyne (1.12 mL, 11 mmol). The resulting solution was refluxed until starting material was no longer detected (monitored by TLC). The mixture was cooled to room temperature, quenched with H₂O (5 mL) and then extracted 3×10 mL diethyl ether. The collect organics were washed with brine (5 mL), dried over MgSO₄ and then concentrated in vacuo. The crude oil was purified by flash chromatography (5% EtOAc/hexanes) to yield **1** (1.83 g, 73%) as a pale yellow oil. ¹H NMR (300 MHz, CDCl₃): δ (ppm) 3.75 (s, 6H), 2.91 (brs, 4H), 2.12 (qt, *J*=7.57 Hz, 2.44 Hz, 2H), 1.76 (t, *J*=2.44 Hz, 3H),

1.08 (t, $J=7.57$ Hz, 3H). ^{13}C { ^1H } NMR (75 MHz, CDCl_3): δ (ppm) 170.7, 164.3, 155.0, 151.8, 115.9, 115.5, 59.4, 53.2, 38.6, 35.4, 17.4, 12.7. IR (neat): 2955, 1742, 1436, 1328, 1293, 1212, 1055 cm^{-1} . Anal. calcd for $\text{C}_{14}\text{H}_{18}\text{O}_4$: C, 67.18; H, 7.25, found: C, 67.29; H, 7.20.

5.1.2. 2-But-2-ynyl-2-(4-methyl-pent-2-ynyl)-malonic acid dimethyl ester (2). Prepared analogously to **1** using 2-but-2-ynyl malonic acid dimethyl ester (1.8 g, 9.5 mmol), NaH (285 mg, 12 mmol), and toluene-4-sulfonic acid 4-methyl-pent-2-ynyl ester (2.8 g, 10 mmol). The reaction mixture was purified by flash chromatography (5% EtOAc/hexanes) to yield **2** (1.7 g, 67%) as a pale yellow oil. ^1H NMR (300 MHz, CDCl_3): δ (ppm) 3.74 (s, 6H), 2.90 (m, 4H), 2.48 (septt, $J=7.08$, 2.2 Hz, 1H), 1.76 (t, $J=2.44$ Hz, 3H), 1.11 (d, $J=7.08$ Hz, 6H). ^{13}C { ^1H } NMR (75 MHz, CDCl_3): δ (ppm) 169.9, 89.6, 79.1, 73.5, 73.3, 57.5, 53.0, 23.3, 23.1, 20.6, 3.7. IR (neat): 2970, 1743, 1437, 1327, 1293, 1212, 1056 cm^{-1} . Anal. calcd for $\text{C}_{15}\text{H}_{20}\text{O}_4$: C, 68.16; H, 7.63, found: C, 67.97; H, 7.55.

5.1.3. 2-But-2-ynyl-2-(4,4-dimethyl-pent-2-ynyl)-malonic acid dimethyl ester (3). Prepared analogously to **1** using 2-but-2-ynyl malonic acid dimethyl ester (1.33 g, 7.2 mmol), NaH (30.0 mg, 9 mmol) and toluene-4-sulfonic acid 4,4-dimethyl-pent-2-ynyl-ester (2.4 g, 9.1 mmol). The reaction mixture was purified by flash chromatography (5% EtOAc/hexanes) to yield **3** (1.23 g, 62%) as a white solid. ^1H NMR (300 MHz, CDCl_3): δ (ppm) 3.74 (s, 6H), 2.88 (brs, 4H), 1.75 (brt, 2H), 1.16 (s, 9H). ^{13}C { ^1H } NMR (75 MHz, CDCl_3): δ (ppm) 170.0, 92.6, 79.1, 73.5, 73.0, 57.7, 53.1, 31.4, 27.6, 23.2, 23.0, 3.8. IR (neat): 2969, 2868, 1744, 1437, 1212, 1063, 951 cm^{-1} . Anal. calcd for $\text{C}_{16}\text{H}_{22}\text{O}_4$: C, 69.04; H, 7.97, found: C, 68.96; H, 7.96.

5.2. General [2+2+2] cycloaddition procedure

A solution of $\text{Ni}(\text{COD})_2$ and IPr or IMes is prepared and allowed to equilibrate for at least 6 h. It was previously discovered that $\text{Ni}(\text{COD})_2$ and IPr exist in equilibrium with the catalyst, $\text{Ni}(\text{IPr})_2$ and COD, and that at least 6 h is necessary to reach equilibrium.⁵ An oven-dried two-neck round-bottomed flask equipped with a magnetic stir bar, septum, gas adapter and balloon was evacuated and filled with CO_2 . A solution of diyne was added and the flask was submerged into a 60 °C oil bath. To the stirring solution, the equilibrated solution of $\text{Ni}(\text{COD})_2$ and IPr or IMes was added. The dark greenish-black reaction mixture was heated for 30 min (or until complete consumption of starting material was observed as judged by GC or TLC). The mixture was then cooled to ambient temperature, concentrated, and purified by flash chromatography on SiO_2 .

5.2.1. 4-Ethyl-1-methyl-3-oxo-3,5-dihydro-7H-cyclopenta[c]pyran-6,6-dicarboxylic acid dimethyl ester (5a) and 1-ethyl-4-methyl-3-oxo-3,5-dihydro-7H-cyclopenta[c]pyran-6,6-dicarboxylic acid dimethyl ester (5b). The general procedure was used with 2-but-2-ynyl-2-pent-2-ynyl-malonic acid dimethyl ester (**1**, 128 mg, 0.5 mmol), $\text{Ni}(\text{COD})_2$ (6.9 mg, 0.025 mmol), IPr (19.8 mg, 0.051 mmol), and 5.1 mL of toluene. The reaction mixture was purified by flash chromatography (2% $\text{Et}_2\text{O}/\text{CH}_2\text{Cl}_2$ then 4% $\text{Et}_2\text{O}/\text{CH}_2\text{Cl}_2$) to yield pyrones **5a** and **5b** in a 62:38

mixture (111.6 mg, 74%) as a white solid. ^1H NMR (300 MHz, CDCl_3): δ (ppm) 3.78 (s, 12H), 3.33 (brs, 4H), 3.27 (brm, 4H), 2.44 (app. quint, 4H), 2.16 (s, 3H), 2.00 (s, 3H), 1.21 (t, $J=7.57$ Hz, 3H), 1.11 (t, $J=7.57$ Hz, 3H). ^{13}C { ^1H } NMR (75 MHz, CDCl_3): δ (ppm) 171.1, 171.1, 164.8, 164.1, 156.8, 155.4, 154.9, 152.5, 121.8, 116.3, 116.1, 115.4, 98.8, 59.93, 59.89, 53.6, 39.0, 38.6, 35.7, 35.6, 25.3, 21.3, 17.8, 13.1, 12.7, 11.7. IR (neat): 2958, 1738, 1674, 1606, 1436, 1262, 1071, 968 cm^{-1} . HRMS(CI): calcd for $\text{C}_{15}\text{H}_{19}\text{O}_6$ (MH^+) 295.1176, obsd 295.1191.

5.2.2. 4-Isopropyl-1-methyl-3-oxo-3,5-dihydro-7H-cyclopenta[c]pyran-6,6-dicarboxylic acid dimethyl ester (6a) and 1-isopropyl-4-methyl-3-oxo-3,5-dihydro-7H-cyclopenta[c]pyran-6,6-dicarboxylic acid dimethyl ester (6b). The general procedure was used with 2-but-2-ynyl-2-(4-methyl-pent-2-ynyl)-malonic acid dimethyl ester (**2**, 105.7 mg, 0.40 mmol), $\text{Ni}(\text{COD})_2$ (11.0 mg, 0.04 mmol), IPr (31.1 mg, 0.08 mmol), and 4.0 mL of toluene. The reaction mixture was purified by flash chromatography (12% EtOAc/hexanes then 20% EtOAc/hexanes) to yield pyrones **6a** and **6b** in an 80:20 mixture (94.2 mg, 76%) as a yellow oil. ^1H NMR (300 MHz, CDCl_3): δ (ppm) 3.76 (s, 12H), 3.36 (s, 2H), 3.31 (q, $J=1.1$ Hz, 2H), 3.27 (s, 2H), 3.21 (q, $J=1.2$ Hz, 2H), 2.95 (sept, $J=7.0$ Hz, 1H), 2.72 (sept, $J=7.0$ Hz, 1H), 2.13 (t, $J=1.1$ Hz, 3H), 1.98 (brt, 3H), 1.24 (d, $J=7.0$ Hz, 6H), 1.21 (d, $J=6.87$ Hz, 6H). ^{13}C { ^1H } NMR (75 MHz, CDCl_3): δ (ppm) 171.1, 171.0, 164.6, 162.9, 159.7, 155.5, 154.1, 152.4, 125.0, 116.2, 116.0, 114.3, 59.83, 59.80, 53.4, 38.90, 38.85, 35.5, 35.2, 31.3, 28.9, 20.1, 20.0, 19.9, 17.7, 13.1. IR (neat): 2959, 1714, 1598, 1435, 1384, 1263, 1204, 1070, 1003, 940 cm^{-1} . HRMS(CI): calcd for $\text{C}_{16}\text{H}_{21}\text{O}_6$ (MH^+) 309.1333, obsd 309.1329.

5.2.3. 4-tert-Butyl-1-methyl-3-oxo-3,5-dihydro-7H-cyclopenta[c]pyran-6,6-dicarboxylic acid dimethyl ester (7a). The general procedure was used with 2-but-2-ynyl-2-(4,4-dimethyl-pent-2-ynyl)-malonic acid dimethyl ester (**3**, 129.5 mg, 0.47 mmol), $\text{Ni}(\text{COD})_2$ (12.8 mg, 0.047 mmol), IPr (36.2 mg, 0.093 mmol), and 4.7 mL of toluene. The reaction mixture was purified by flash chromatography (12.5% EtOAc/hexanes then 25% EtOAc/hexanes) to yield pyrone **7a** (96.2 mg, 64%) as a white solid. X-ray quality crystals were obtained by slow evaporation of ether from a saturated solution of **7a** in ether/cyclohexane. ^1H NMR (300 MHz, CDCl_3): δ (ppm) 3.78 (s, 6H), 3.62 (s, 2H), 3.15 (s, 2H), 2.14 (s, 3H), 1.41 (s, 9H); ^{13}C { ^1H } NMR (75 MHz, CDCl_3): δ (ppm) 171.2, 162.7, 152.7, 151.7, 127.9, 166.6, 59.7, 53.5, 41.6, 36.7, 34.4, 30.1, 17.6. IR (neat): 2956, 1712, 1674, 1562, 1435, 1264, 1209, 1104, 998 cm^{-1} . HRMS: calcd for $\text{C}_{17}\text{H}_{23}\text{O}_6$ (M^+) 323.1489, obsd 323.1486. Crystal data for $\text{C}_{17}\text{H}_{23}\text{O}_6$, $M=322.35$, monoclinic, $a=12.1818(2)$ Å, $U=3360.00(15)$ Å³, $T=150$ K, space group $P2_1/a$, $Z=8$, $\mu(\text{Mo K}\alpha) 0.096$ mm⁻¹, 13326 reflections measured, 7635 unique F^2 values used in refinement ($R_{\text{int}}=0.0218$), $R_1[4707$ with $F^2 > 2\sigma]=0.0454$, $wR_2(\text{all data})=0.1319$.

5.2.4. 1-Methyl-3-oxo-4-trimethylsilanyl-3,5-dihydro-7H-cyclopenta[c]pyran-6,6-dicarboxylic acid dimethyl ester (8a).⁵ The general procedure was used with 2-but-2-ynyl-2-(3-trimethylsilanyl-prop-2-ynyl)-malonic acid

dimethyl ester (**4**, 130.5 mg, 0.44 mmol), Ni(COD)₂ (6.1 mg, 0.022 mmol), IMes (13.5 mg, 0.044 mmol), and 4.4 mL of toluene. The reaction mixture was purified by flash chromatography (12.5% EtOAc/hexanes then 25% EtOAc/hexanes) to yield pyrone **8a** (101.3 mg, 68%) as a white solid. X-ray quality crystals were obtained by slow evaporation of ether from a saturated solution of **8a** in ether/cyclohexane. ¹H NMR (300 MHz, CDCl₃): δ (ppm) 3.78 (s, 6H), 3.37 (s, 2H), 3.21 (s, 2H), 2.16 (s, 3H), 0.30 (s, 9H). ¹³C {¹H} NMR (75 MHz, CDCl₃): δ (ppm) 171.2, 162.7, 152.7, 151.7, 127.9, 166.6, 59.7, 53.5, 41.6, 36.7, 34.4, 30.1, 17.6. Crystal data for C₁₆H₂₂O₆Si, *M*=338.43, monoclinic, *a*=12.0883(3) Å, *U*=1711.44(8) Å³, *T*=150 K, space group *P*2₁/*c*, μ(Mo Kα) 0.164 mm⁻¹, 6521 reflections measured, 3911 unique *F*² values used in refinement (*R*_{int}=0.0208), *R*₁[4707 with *F*²>2σ]=0.0386, *wR*₂(all data)=0.0994 (Fig. 5).

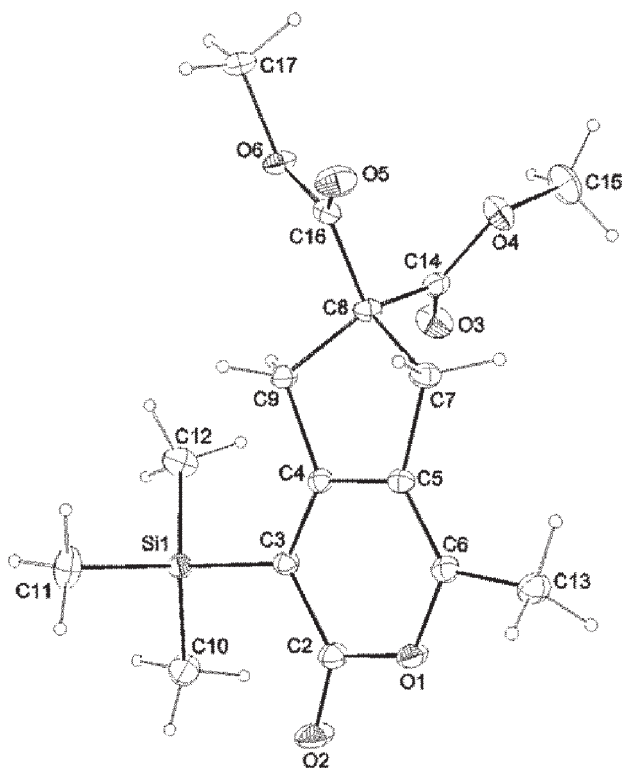


Figure 5. ORTEP representation of pyrone **8a**.

5.2.5. 1,4,7-Trimethyl-1H, 3H-furo[3,4-*c*]pyran-6-one (10a) and 3,4,7-trimethyl-1H, 3H-furo[3,4-*c*]pyran-6-one (10b). The general procedure was used with 4-but-2-ynyloxy-pent-2-yne (**9**, 75.6 mg, 0.56 mmol), Ni(COD)₂ (15.3 mg, 0.056 mmol), IPr (43.1 mg, 0.11 mmol), and 5.5 mL of toluene. The reaction mixture was purified by flash chromatography (12% EtOAc/hexanes) to yield pyrones **10a** and **10b** in ~50:50 mixture (41.3 mg, 41%) as a pale yellow oil. ¹H NMR (300 MHz, CDCl₃): δ (ppm) 5.12 (q, *J*=6.59 Hz, 2H), 4.90–4.68 (m, 4H), 1.43 (d, *J*=6.59 Hz, 6H), 2.20 (s, 3H), 2.16 (s, 3H), 2.02 (s, 3H), 1.97 (s, 3H). ¹³C {¹H} NMR (75 MHz, CDCl₃): δ (ppm) 165.0, 164.5, 158.1, 155.2, 151.0, 150.2, 120.6, 116.1, 113.2, 113.0, 78.1, 76.9, 69.4, 67.2, 21.0, 19.4, 18.1, 17.6, 13.0, 12.6. IR (neat): 2977, 2925, 1717, 1680, 1615, 1070, 1022, 863 cm⁻¹.

5.2.6. 1,1,4,7-Tetramethyl-1H, 3H-furo[3,4-*c*]pyran-6-one (12a) and 3,3,4,7-tetramethyl-1H, 3H-furo[3,4-*c*]pyran-6-one (12b). The general procedure was used with 4-but-2-ynyloxy-4-methyl-pent-2-yne (**11**, 54.9 mg, 0.21 mmol), Ni(COD)₂ (5.7 mg, 0.021 mmol), IPr (16 mg, 0.041 mmol), and 2.0 mL of toluene. The reaction mixture was purified by flash chromatography (12% EtOAc/hexanes then 15% EtOAc/hexanes then 20% EtOAc/hexanes) to yield pyrones **12a** and **12b** in ~50:50 crude mixture (79.7 mg, 53%) as a yellow solid. ¹H NMR (300 MHz, CDCl₃): δ (ppm) 4.76 (q, *J*=1.1 Hz, 2H), 4.7 (q, *J*=1.2 Hz, 2H), 2.23 (s, 3H), 2.15 (s, 3H), 2.07 (s, 3H), 1.96 (s, 3H), 1.52 (s, 6H), 1.49 (s, 6H). ¹³C {¹H} NMR (75 MHz, CDCl₃): δ (ppm) 165.4, 164.3, 160.0, 155.6, 150.9, 149.6, 123.7, 116.5, 113.0, 84.7, 83.6, 67.9, 65.3, 27.0, 25.5, 17.8, 16.8, 12.7. IR (neat): 2978, 2931, 1719, 1610, 1441, 1387, 1366, 1317, 1118, 908 cm⁻¹.

Acknowledgements

We thank the University of Utah (Seed Fund) and the PRF (Type G) for supporting this research. We also thank Dr Eduardo Véliz for technical advice and the Sigman and Keck groups for insightful discussions.

References and notes

- (a) Walther, D. *Coord. Chem. Rev.* **1987**, *79*, 135. (b) Braunstein, P.; Matt, D.; Nobel, D. *Chem. Rev.* **1988**, *88*, 747. (c) Leitner, W. *Coord. Chem. Rev.* **1996**, *153*, 257. (d) Yin, X.; Moss, J. R. *Coord. Chem. Rev.* **1999**, *181*, 27. (e) Walther, D.; Ruben, M.; Rau, S. *Coord. Chem. Rev.* **1999**, *182*, 67.
- (a) Tsuda, T.; Yoshiki, C.; Saegusa, T. *Synth. Commun.* **1979**, *9*, 427. (b) Tsuda, T.; Morikawa, S.; Sumiya, R.; Saegusa, T. *J. Org. Chem.* **1988**, *53*, 3140. (c) Takimoto, M.; Mori, M. *J. Am. Chem. Soc.* **2002**, *124*, 10008. (d) Takimoto, M.; Kawamura, M.; Mori, M. *Org. Lett.* **2003**, *5*, 2599. (e) Li, F.; Xia, C.; Sun, W.; Chen, G. *Chem. Commun.* **2003**, 2042.
- (a) Afarinkia, K.; Vinader, V.; Nelson, T. D.; Posner, G. H. *Tetrahedron* **1984**, *48*, 9111. (b) Boger, D. L.; Mullican, M. D. *J. Org. Chem.* **1984**, *49*, 4045. (c) Boger, D. L.; Brotherton, C. E. *J. Org. Chem.* **1984**, *49*, 4050. (d) Marko, I. E.; Evans, G. R.; Declercq, J. *Tetrahedron* **1994**, *50*, 4557. (e) Posner, G. H.; Lee, J. K.; White, C. M.; Hutchings, R. H.; Dai, H.; Kachinski, J. L.; Dolan, P.; Kensler, T. W. *J. Org. Chem.* **1997**, *62*, 3299.
- (a) Evidente, A.; Conti, L.; Altomare, C.; Bottalico, A.; Sindona, G.; Segre, A. L.; Logrieco, A. *Nat. Toxins* **1994**, *2*, 4. (b) Watanadilok, R.; Sonchaeng, P.; Kijjoa, A.; Damas, A. M.; Gales, L.; Silva, A. M. S.; Herz, W. *J. Nat. Prod.* **2001**, *64*, 1056.
- Louie, J.; Gibby, J. E.; Farnworth, M. V.; Tekavec, T. N. *J. Am. Chem. Soc.* **2002**, *124*, 15188.
- The data provided from Tsuda does not unambiguously establish the regiochemistry of the pyrone product obtained from the cycloaddition of diyne **14**. See ref: Tsuda, T.; Morikawa, S.; Hasegawa, N.; Saegusa, T. *J. Org. Chem.* **1990**, *55*, 2978.

7. A corrigendum has recently been submitted to *J. Am. Chem. Soc.*.
8. For an in-depth discussion of cyclotrimer side-product formation, see Tsuda, T.; Morikawa, S.; Sumiya, R.; Saegusa, T. *J. Org. Chem.* **1988**, *53*, 3140.
9. In the cycloaddition reaction with substrate **3**, a cyclotrimerized aromatic product was isolated in 18% yield. However, in reactions that typically afforded a mixture of products, the oligomers were not isolated.
10. (a) Walter, D.; Braunlich, G. *J. Organomet. Chem.* **1992**, *436*, 109. (b) Hoberg, H.; Schaeffer, D.; Burkhardt, G.; Kruger, C.; Romao, M. *J. Organomet. Chem.* **1984**, *266*, 203.
11. This is a rare example where the formation of a carbon–carbon bond adjacent to the sterically more hindered side of an alkyne is favored. For other examples, see Ref. 7 and Miller, K. M.; Luanphaisarnnont, T.; Molinaro, C.; Jamison, T. F. *J. Am. Chem. Soc.* **2004**, *126*, 4130.
12. Pangborn, A. B.; Giardello, M. A.; Grubbs, R. H.; Rosen, R. K.; Timmers, F. *Organometallics* **1996**, *15*, 1518.
13. Böhm, V. P. W.; Gstöttmayr, C. W. K.; Weskamp, T.; Herrmann, W. A. *Angew. Chem. Int. Ed.* **2001**, *40*, 3387.
14. Trost, B. M.; Rudd, M. T. *J. Am. Chem. Soc.* **2003**, *125*, 11516.
15. Moehs, P. J.; Davidson, W. E. *J. Organomet. Chem.* **1969**, *20*, 57.